LIST OF SI IONS

Numeri

VOLU

	SECTION
Management and Application o	1
Nondestructive Testing Labor	2
Field and Maintenance Tests .	3
Fundamental Testing Principle	4
Basic Test Methods . . .	5
Liquid-Penetrant Test Principl	6
Liquid-Penetrant Test Equip	7
Liquid-Penetrant Test Indica	8
Filtered-Particle Tests . .	9
Vision and Optics . . .	10
Visual Inspection Equipme	11
Optical Projectors and Con.	12
Radiation and Particle Phy	13
Electronic Radiation Sourc	14
Isotope Radiation Source	15
Radiation Detection and R	16
X-Ray Diffraction and Fluo	17
X-Ray and Isotope Gaging	18
Fluoroscopy and X-Ray Ima	19
Film Radiography . . .	20
X-Ray Film Processing .	21
Xeroradiography . . .	22
High Voltage Radiography	23
X-Ray Interpretation . . .	24
X-Ray Control of Weldments .	25
Radiation Protection . . .	26
Attenuation Coefficient Table	27

m-
che
ing
ince
ents
all
ena-
ties,
edic-
pair-
large-
all the
in a
nd data
incering
tallurgy,
cal, civil,
es a full
tions for
ucation,
offered
nental
sting,
tions,
s and
test
e of
the
ern
ish
or
k

MAI FEB 11 1980

3 1148 00650 7099

LIST OF SECTIONS

MAI OCT 13 1985

Numerical

VOLUME II

SECTION
Electrified-Particle Tests 28
Electrified-Particle Test Indications 29
Magnetic-Particle Test Principles 30
Magnetic-Particle Test Equipment 31
Magnetic-Particle Test Indications 32
Magnetic-Field Test Principles 33
Magnetic-Field Test Equipment 34
Electric Current Test Principles 35
Eddy Current Test Principles 36
Eddy Current Cylinder Tests 37
Eddy Current Tube Tests 38
Eddy Current Sphere and Sheet Tests 39
Eddy Current Test Equipment 40
Eddy Current Test Automation 41
Eddy Current Test Indications 42
Ultrasonic Test Principles 43
Ultrasonic Transducers 44
Ultrasonic Fields 45
Ultrasonic Immersion Tests 46
Ultrasonic Immersion Test Indications 47
Ultrasonic Contact Tests 48
Double-Transducer Ultrasonic Tests 49
Ultrasonic Resonance Tests 50
Natural Frequency Vibration Tests 51
Brittle-Coating Tests 52
Photoelastic-Coating Tests 53
Resistance Strain-Gage Tests 54
Index

ALPHABETICAL LIST APPEARS INSIDE BACK COVER

620.112 M16n V.2 60-16156
McMaster
Nondestructive testing handbook

kansas city public library

Books will be issued only
on presentation of library card.
Please report lost cards and
change of residence promptly.
Card holders are responsible for
all books, records, films, pictures
or other library materials
checked out on their cards.

7/31

ONE OF AN EXTENSIVE GROUP OF
REFERENCE BOOKS PUBLISHED BY
THE RONALD PRESS COMPANY

NONDESTRUCTIVE TESTING HANDBOOK

Edited for the Society for Nondestructive Testing

by

ROBERT C. MCMASTER
PROFESSOR OF WELDING ENGINEERING
THE OHIO STATE UNIVERSITY
PAST PRESIDENT
SOCIETY FOR NONDESTRUCTIVE TESTING

In Two Volumes

II

NEW YORK
THE RONALD PRESS COMPANY
1959

Copyright, ©, 1959, by
The Ronald Press Company

All Rights Reserved

No part of this book may be reproduced
in any form without permission in writing
from the publisher.

Library of Congress Catalog Card Number: 59-14660

PRINTED IN THE UNITED STATES OF AMERICA

620.112
M16n
v.2

CONTENTS

Volume II

SECTION
Electrified-Particle Tests 28
Electrified-Particle Test Indications 29
Magnetic-Particle Test Principles 30
Magnetic-Particle Test Equipment 31
Magnetic-Particle Test Indications 32
Magnetic-Field Test Principles 33
Magnetic-Field Test Equipment 34
Electric Current Test Principles 35
Eddy Current Test Principles 36
Eddy Current Cylinder Tests 37
Eddy Current Tube Tests 38
Eddy Current Sphere and Sheet Tests 39
Eddy Current Test Equipment 40
Eddy Current Test Automation 41
Eddy Current Test Indications 42
Ultrasonic Test Principles 43
Ultrasonic Transducers 44
Ultrasonic Fields 45
Ultrasonic Immersion Tests 46
Ultrasonic Immersion Test Indications 47
Ultrasonic Contact Tests 48
Double-Transducer Ultrasonic Tests 49
Ultrasonic Resonance Tests 50
Natural Frequency Vibration Tests 51
Brittle-Coating Tests 52
Photoelastic-Coating Tests 53
Resistance Strain-Gage Tests 54

Index

SECTION 28

ELECTRIFIED-PARTICLE TESTS

CONTENTS

PAGE

Principles of Test

- Development ... 1
- Advantages and limitations ... 1
    - An electrified-particle indication of a crack pattern on a porcelain-enameled sink (*f.* 1) ... 1
- Major applications ... 2
- Mechanisms of operation ... 2
    - An electrified-particle gun in operation (*f.* 2) ... 2
  - Operation on metal-backed coatings ... 2
    - A typical electrified-particle indication exhibiting two-directional stress cracks in a porcelain-enamel plate (*f.* 3) ... 3
  - Operation with liquid penetrant ... 4
- The triboelectric effect ... 4
- Electrical field conditions ... 4
- Nonconducting materials, metal-backed ... 4
    - Electrostatic situation on metal-backed ceramic material prior to application of charged powder (*f.* 4) ... 4
    - Metal-backed ceramic material after applying charged powder (*f.* 5) ... 5
    - Porcelain-enamel sample containing a crack, after charged powder is applied (*f.* 6) ... 5
    - Electrostatic situation after indication is built up (*f.* 7) ... 6
  - Limitations ... 6
- Nonconducting materials, not metal-backed ... 6
    - The electrostatic situation in glass after application of penetrant but prior to application of charged powder (*f.* 8) ... 6
  - Charge movements in penetrant ... 6
    - Effect of application of charged powder to sample shown in Fig. 8 (*f.* 9) ... 7
  - Subsurface indications ... 7
    - Effect of application of charged powder to side not containing defect (sample shown in Fig. 8) (*f.* 10) ... 7
- Thin nonconductors ... 7
- Nonconducting materials in close proximity to metals ... 8

Equipment and Materials

- Test materials ... 8
  - Powder ... 8
  - Advantages of calcium carbonate ... 8
  - Penetrant ... 8
- Test equipment ... 8
  - Powder gun ... 8
  - Gun-operating instructions ... 9
  - Technique for use of gun ... 9
  - Air supply ... 9

Control Techniques

- Electrical charging effects ... 9
  - Influence of atmospheric humidity ... 10
  - Environmental powder distribution ... 10
- Atmospheric water vapor ... 10
  - Water deposition on test objects ... 10
  - Use of heated penetrant ... 10
  - Drying part surfaces ... 11
- Excessive test-object temperatures ... 11
- Loss of indications ... 11
  - Fugitive indications ... 11
- Standard crack sample ... 11
  - Preparation of crack samples ... 11
- Bibliography ... 12

SECTION 28

ELECTRIFIED-PARTICLE TESTS

Principles of Test

DEVELOPMENT. The electrified-particle inspection method was invented by deForest and Staats in 1945 for the specific solution of a problem concerning cracks in glass bottles, too small to be seen by the naked eye. It is known as **Statiflux** (Magnaflux Corporation: method and equipment are covered by one or more of U.S. Patents 2,515,396; 2,499,466; 2,499,462; and comparable Canadian patents). During development, other uses were found which have played a more profound role in industrial nondestructive testing.

ADVANTAGES AND LIMITATIONS. The electrified-particle method works on all nonconducting materials. Representative examples are glass, nonporous ceramic materials, nonconductive plastics, and certain paint films. On some classes of **ceramic materials,** cracks are located with a sensitivity comparable to penetrant methods. However, on those materials whose surfaces are glossy or glazed, the method goes far beyond the ordinary sensitivity of all penetrant techniques. The method has the remarkable ability of enabling the

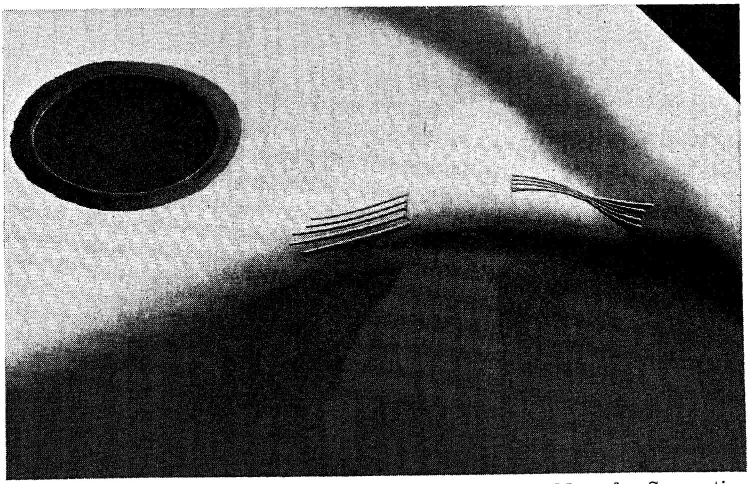

Magnaflux Corporation

Fig. 1. **An electrified-particle indication of a crack pattern on a porcelain-enameled sink.** A portion of the indication has been removed to illustrate that the actual cracks are completely invisible.

location of fine cracks which otherwise are completely invisible (as shown in Fig. 1). On such cracks, indications are built up which give **magnification factors** of approximately 30,000 to 1. An invisible defect, lying perpendicular to the surface in a transparent material does not reflect light to the human eye. According to the laws of optics, an interface of this width is less than four millionths of an inch in width.

MAJOR APPLICATIONS. The electrified-particle inspection method has three major applications: (1) on porcelain enamel, (2) on glass-to-metal seals, and (3) on various materials such as artificial teeth, glass-lined vessels, and other nonconducting materials.

MECHANISMS OF OPERATION. The method depends upon a triboelectric effect, or production of static electricity by rubbing or tearing action. Particles of **calcium carbonate** are blown through a spray gun with a special nozzle constructed of hard rubber (Fig. 2). Calcium carbonate lies higher than hard rubber in the triboelectric series and therefore becomes charged positively. While many materials exhibit this property, none become charged so readily as the particular form of calcium carbonate supplied commercially. During the initial development more than 200 varieties of calcium carbonate and other materials were tested. Only a few exhibited the property of forming clean-cut indications with little background.

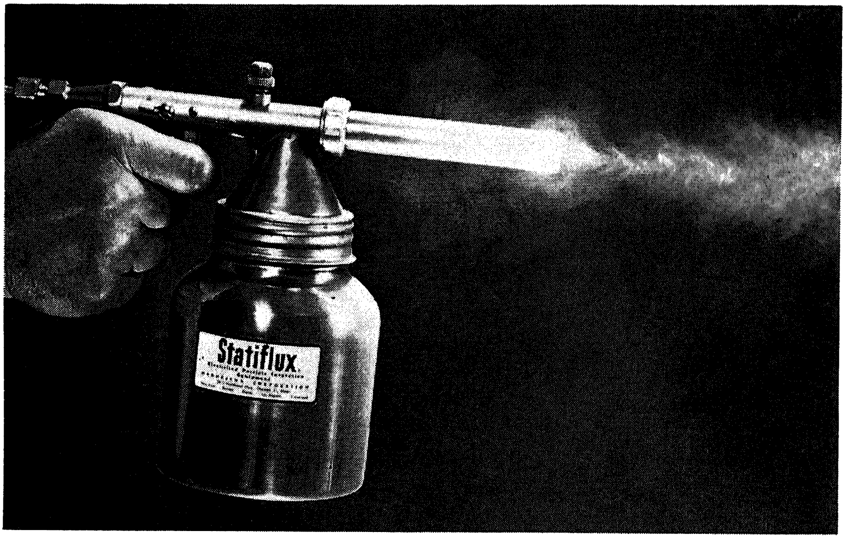

Magnaflux Corporation

Fig. 2. An electrified-particle gun in operation. Note that the positively charged particles tend to fly back to the negatively charged gun.

Operation on Metal-backed Coatings. The method has two general modes of operation. The first applies where the material to be tested is backed with metal, such as **porcelain enamel on steel.** In this instance the powder emerges from the gun charged positively and approaches the porcelain enamel. Electrons within the nonconductive glassy layer are probably attracted to the surface, but they do not enter the mechanics of the defect location. However, the electrons in the metal layer are attracted to the interface between glass and metal and set up a state of electrical strain between the interface and the surface of the porcelain enamel. When a defect is present in the glass layer, the **dielectric strength** is much lower at this point. The electrons tend to leak through the point of low dielectric strength. For all intents and purposes the crack becomes charged negatively. Since positively charged particles are attracted to negative areas, a physical indication of appreciable size will build up (Fig. 3).

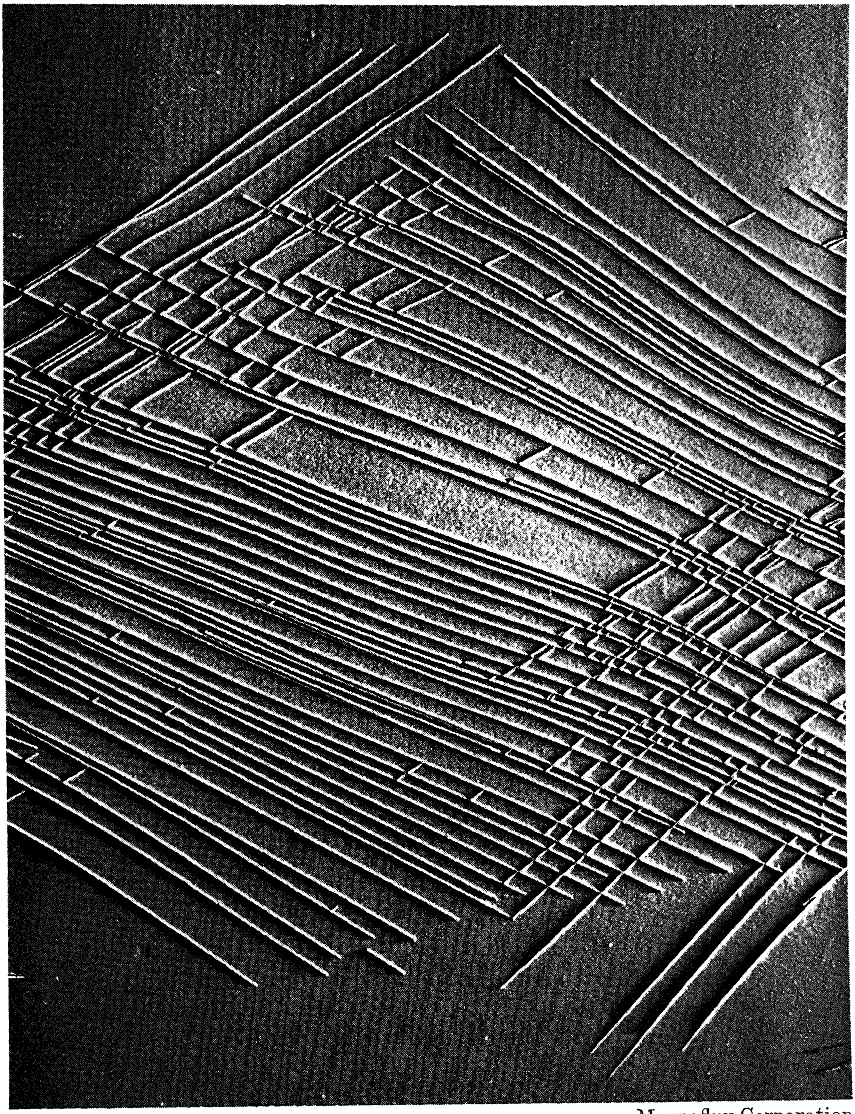

Magnaflux Corporation

Fig. 3. A typical electrified-particle indication exhibiting two-directional stress cracks in a porcelain-enamel plate.

Operation with Liquid Penetrant. The second mode of operation is used when a nonconductive surface is not backed with metal and it is impossible to locate the defect unless an electron supply is provided in back of or within the defect. This situation is handled very effectively by applying a liquid penetrant to the material. The penetrant consists of water treated with a highly active **wetting agent** and other substances which provide a good **negative-ion source.** Penetration occurs instantly on glass. After drying, charged powder is applied to the surface and an indication develops instantly. In this case the positively charged particles attract electrons within the defect.

THE TRIBOELECTRIC EFFECT. Electrification by friction or contact separation is termed **triboelectrification.** This effect can be demonstrated by the sudden separation of two contacting pieces of matter. During electrification, electrons and protons are neither created nor destroyed. They are merely separated or redistributed. It is a fundamental fact that, for every positive charge, there must be a corresponding and numerically equal negative charge developed somewhere by the same action. A **triboelectric series** is a list of substances arranged in such order that a material higher in the list is postively charged when rubbed against a material which is lower in the list. The further apart the materials are in the series, the more readily they seem to lose or gain electrons.

The electrified-particle inspection method depends upon the ease with which a specific type of **calcium carbonate** loses its electrons when placed in intimate rubbing contact with hard rubber. The powder is unique, since it appears to lose its electrons much more readily than any of several hundred varieties of materials tested. The location of these two materials at the extreme ends of the triboelectric series undoubtedly has something to do with the efficiency of the method.

ELECTRICAL FIELD CONDITIONS. When an uncharged body is brought into an electrical field, a rearrangement of the charges in the body always results. If the body is a conductor, the electrons are mobile and free to move. If the body is a nonconductor, the electrons associated with the positive nuclei in each molecule are displaced or reoriented. The electrons within the body are attracted or repelled, depending upon the electrical sign of the external field. The **movement of electrons** in various materials makes it possible to locate cracks under certain conditions. In general the method is applicable only to **nonconducting materials** or **coatings.**

NONCONDUCTING MATERIALS, METAL-BACKED. The electrostatic situation on metal-backed ceramic material, such as porcelain enamel, is substantially as shown in Fig. 4. When positively charged powder is applied to

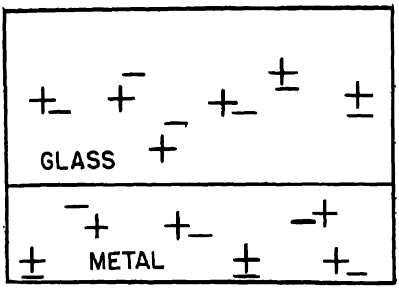

Fig. 4. Electrostatic situation on metal-backed ceramic material prior to application of charged powder.

the glass surface, the electrons in both enamel and metal tend to be attracted by the charged powder. The nonconductive enamel will allow its electrons to reorient but not to flow freely. The conductive metal permits its electrons to flow in the direction of the positive potential on the surface of the enamel, as illustrated in Fig. 5. If a crack exists in the enamel, the **dielectric strength** of the glass is much less at that point. The negative potential built up in the interface will tend to leak through and influence the field in the defect area, as shown in Fig. 6. Once this influence is established, additional positively charged particles accumulate at the defect, forming a highly visible powder indication, as shown in Fig. 7. The fact that electrons flow to the interface may be readily verified by testing the metal backing with an electroscope. When positively charged powder is applied to the glassy surface of a glass-metal combination, the metal always becomes positive.

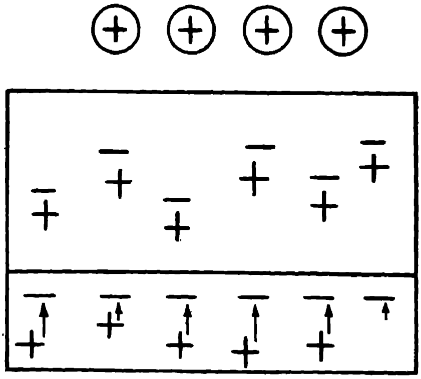

Fig. 5. Metal-backed ceramic material after applying charged powder.

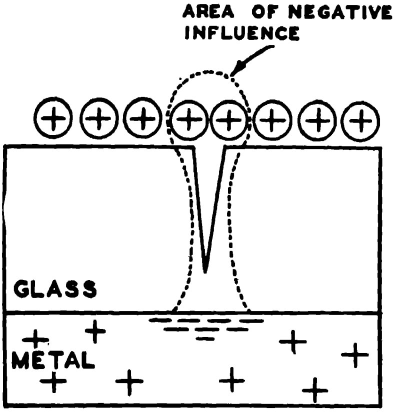

Fig. 6. Porcelain-enamel sample containing a crack, after charged powder is applied. Note leakage influence at defect.

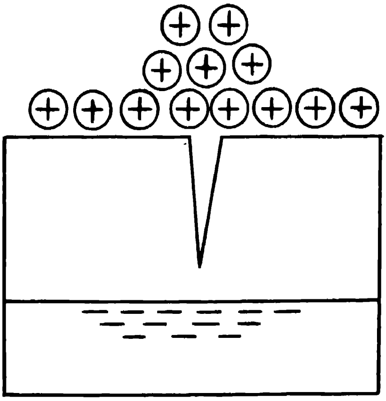

Fig. 7. Electrostatic situation after indication is built up.

Limitations. Decisive indications of cracks are sometimes difficult to form on **extremely thin, nonconducting, metal-backed materials.** Electrons in the base metal tend to leak through and influence the surface of the nonconductor to the same degree as the defect. In other words, the differential electrostatic situation is much reduced. Nonconductive coatings which have low dielectric strength tend to break down when charged powder is applied to the surface. This breakdown exhibits itself by the **formation of pinholes,** with a subsequent formation of dotlike indications.

NONCONDUCTING MATERIALS, NOT METAL-BACKED. Since glass does not have available a mobile electron source, it is necessary to provide one by introducing electrons into the crack or defect. This is accomplished by using **liquid penetrant.** The penetrant consists mainly of water, wetting agent, and other materials to provide a slight conductivity. When a glassy object is dipped into penetrant and removed and dried, the crack traps an infinitesimal quantity of penetrant (Fig. 8).

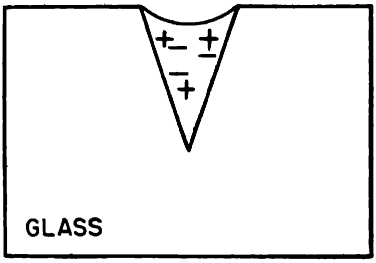

Fig. 8. The electrostatic situation in glass after application of penetrant but prior to application of charged powder.

Charge Movements in Penetrant. When positively charged particles are applied to a surface containing a crack, **negative ions** in the penetrant tend to migrate to the top of the crack. The base of the crack becomes charged positively. Since a negative field is present at the top of the crack, it will attract positively charged particles and provide a visible powder indication (Fig. 9).

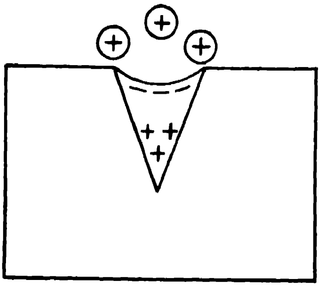

Fig. 9. Effect of application of charged powder to sample shown in Fig. 8.

Subsurface Indications. On thin materials, where a crack exists on one face and is filled with penetrant, an indication can be developed on the opposite or crack-free side. This powder indication has a fuzzy and indeterminate appearance, due to the relatively poor leakage field present. When subsurface indications are formed, the electrons will be found at the bottom of the crack, as shown in Fig. 10.

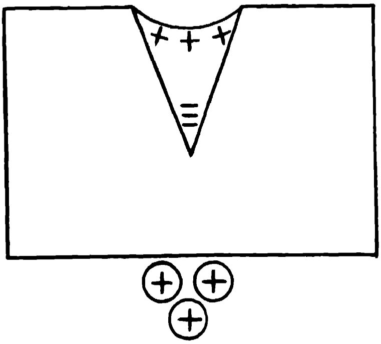

Fig. 10. Effect of application of charged powder to side not containing defect (sample shown in Fig. 8).

THIN NONCONDUCTORS. On relatively thin, nonconducting materials such as window glass, totally **invisible cracks** can be located without the use of electron-bearing penetrants. Metallic foil or powder, conductive liquids, or the human hand placed in back of or below the crack will provide the necessary electrons and influence the site of a defect. The **effect of the human hand** on thin, nonconducting materials is most interesting. When the hand is placed below and in intimate contact with glass, an outline of the hand will appear when charged powder is applied to the glass surface. When the hand or other electron-supplying materials are placed below a similar specimen containing a crack, indications will form without the aid of penetrants. To verify this effect, it is necessary to dry the glass at elevated temperatures to remove water or penetrant from the crack. Sometimes atmospheric moisture vapor will enter a crack and simulate the action of deliberately added penetrant.

NONCONDUCTING MATERIALS IN CLOSE PROXIMITY TO METALS. Some nonconductive materials have metal in close proximity or associated with a crack in glass. The electron-bearing substance may not necessarily be in back of a glassy portion, as is the case with **glass-to-metal seals.** Assuming that known cracks in the glassy portion are completely free of atmospheric vapor and water-based penetrating materials, it is frequently possible to develop indications by relying upon nearby metallic parts to supply electrons. If useful indications are not produced, penetrating materials must be used.

Equipment and Materials

TEST MATERIALS. Suitable powder and, in some cases, liquid-penetrant materials are expended during electrified-particle testing.

Powder. The powder used is a special variety of calcium carbonate commercially available in three **colors:** white, gray, and black. The gray and black powders contain a small percentage of carbon black. The amount of colorant affects the charging ability, since the higher the contamination, the lower the sensitivity. Of the three colors, white is the most sensitive; black, the least. The choice of colors available for blending is limited to those materials which tend to become charged on their own account. In addition the particles must be of the right **size and shape.** Most industrial users prefer white powder, since it is the least noticeable when left on an inspected piece. The next preference is for light-gray powder since it provides a moderate amount of contrast and is not so untidy as black. At first glance a white or gray powder indication on a white background would appear to have poor contrast and be difficult to see. However, tangentially lighted indications cast striking shadows.

Advantages of Calcium Carbonate. Many varieties of calcium carbonate tend to exhibit the electrostatic properties necessary to produce indications. **Other materials,** such as talc, ordinary household flour, and even powdered sugar, will develop usable indications when charged appropriately. Despite this, when commercially available powder is compared with other materials, the results are strikingly in its favor. It is completely safe to use, since it cannot produce silicosis and will not explode in an air mixture. It has no appreciable odor or taste and is completely nonhygroscopic. Very few other materials have all these desirable characteristics.

Penetrant. The penetrant which is commercially available is an especially safe and effective concentrate of wetting agents, water, and other materials to guarantee a slight amount of conductivity. In use, it is diluted with water. For high effectiveness, it is recommended that the penetrant be heated. Penetrant is applied by dipping, spraying, or brushing. After application it is allowed to air-dry or is wiped with paper toweling.

TEST EQUIPMENT. The electrified-particle test method requires only simple equipment for charging and applying the inspection medium.

Powder Gun. The powder gun (Fig. 2) is light and simple to use. It consists of the basic gun, cup, and charging-nozzle assembly. The **charging-nozzle assembly** is the most important element and consists of a hard-rubber insert, metal sleeve, and assembly ring. The hard-rubber insert has an extremely small bore, to assist in the development of exceptionally high electrostatic potentials. When the gun is used repeatedly in service, the bore enlarges. It should be discarded when inadequate indications are developed on standard crack samples. However, a nozzle is still usable up to the point where the bore increases to approximately 3⁄16 in. in diameter.

Gun-operating Instructions. In use, the cup is filled to half-capacity. The gasket and the top edges of the cup are carefully cleaned to assure proper seating. An **accumulation of powder on the gasket** prevents the adequate tightening of the cup to the gun. This permits air and powder leakage during use and is annoying. A small amount of lubricant applied to the threads of the cup assists in the tightening of the gun assembly.

The gun is connected to a **pressure-regulated air supply.** Air pressure is not critical and is a matter of personal preference, usually ranging from 15 to 25 p.s.i.

Two **adjusting screws** control the air supply. One is located under the trigger and controls the amount of air passing through the gun. The setting of this screw is a matter of choice. The second adjustment screw is on top of the gun (Fig. 2) and splits the air flow between cup and nozzle. When this screw is turned clockwise, it reduces the amount of powder introduced into the air stream. It generally is easier to select the desired air pressure first and then turn the adjustment knob to the point where no powder is introduced into the air stream. Using a **standard test sample,** the knob is slowly turned counterclockwise until the desired amount of powder is emitted from the nozzle. A slight shaking motion of the hand assists the gun in developing the proper powder cloud.

Technique for Use of Gun. During use, powder tends to lodge within the nozzle and on its external surfaces. After a gun has been turned off, this powder tends to break loose and blow or drop onto the test piece. This can be irritating; however, it rarely produces patterns which are mistaken for genuine defect indications. The gun should be held approximately 1 to 3 in. away from the surface and shaken gently during use. Some inspectors prefer to blow powder in short bursts rather than in one long sequence.

Air Supply. Portable air compressors can be used to develop adequate air-pressure. Pressure-regulated commercial air supplies in most industrial plants are adequate for use in spraying powder, although if not blown out occasionally, they tend to accumulate drops of water. Occasionally these droplets will ride through the line and subsequently through the gun. This has little or no effect upon the powder or the development of good indications, providing that excessive moisture is not blown directly on the test piece. Despite this, it is good practice to blow out air lines prior to use. Most commercially available devices do not provide for moisture condensation. On extremely humid days a compressor takes in moisture-laden air, compresses it, and blows moisture through the gun. When this situation is encountered, adding a **water trap** or **silica gel drier** to the line is a necessity.

Compressed-air lines may also contain **oil droplets** which originate from the lubrication of the compressor. Oil droplets entering or emerging from the powder gun have no effect upon the performance of the gun or subsequent development of indications. Excessive oil, however, may prove troublesome and untidy.

Control Techniques

ELECTRICAL CHARGING EFFECTS. Under some operating conditions, the operator will receive slight **electric shocks** from the gun or test piece during inspection. This is understandable, since the voltages developed by blowing powder through the gun may be as high as 10,000 volts. Little current is involved, so that there is little danger to the operator. However, the element of surprise may make him cautious in using the equipment. A **ground clip and wire** are provided on the gun for connection to a nearby ground. This tends to drain off the negative potential on gun and operator, thus reducing the possibility of shock. Generally speaking, little trouble is noted on this account when the operator is working on a slightly conductive floor such as concrete. Wood blocks, asphalt, or rubber covering on floors insulate the operator from ground, thus enabling him to build up a potential which may produce an electric shock. The aforementioned ground clip assists in the reduction of this potential.

Influence of Atmospheric Humidity. A shock hazard is still present despite the grounding of the gun or operator because the **test part** itself becomes charged. In dry weather it is possible for large objects to receive and hold a charge of surprisingly **high potential.** Ordinarily these will bleed off within a few seconds, but in very dry weather the potential lasts several minutes. Grounding of the object itself will help somewhat; however, if the operator knows that a shock potential exists, he can avoid touching the part for a short while.

Environmental Powder Distribution. Excessive powder may be blown and coat the operator and surrounding area. This is not hazardous, but it is a nuisance. A simple way to avoid this condition is to apply powder in a paint spray booth or near an exhaust system. Often it is convenient to use an ordinary vacuum cleaner and work with the nozzle near the spot where powder is being applied. This is particularly advantageous on large objects which are not convenient to place within a booth.

ATMOSPHERIC WATER VAPOR. Practically all materials will collect a microscopic film of moisture on their surfaces under certain atmospheric conditions. This is a natural phenomenon, and ordinarily the film is invisible and very thin. On **ceramic materials** the film appears to dissolve out soluble portions, releasing ions and rendering the surface slightly conductive. When charged powder is applied, the sample acts as though it were a metal rather than a nonconducting material.

Water Deposition on Test Objects. The amount of water deposition on materials is governed by the amount of water vapor in the air. During high temperature and humidity conditions, it is possible for much more moisture to be in the air than during cold weather. A conductive film of moisture need not interfere with effective inspection since it can be removed quite readily. When the object is warmed to slightly above room temperature, the water layer will evaporate. On large structures such as refrigerator liners, range tops, or glass-lined process vessels, this may be very awkward. Under these circumstances, commercially available **infrared lamps** can be strategically placed to warm the specific area under test.

Use of Heated Penetrant. Another useful technique for adding heat to a glass surface is to apply heated penetrant. Despite the fact that penetrant is not required in the inspection of metal-backed nonconducting materials, its use tends to help build **sharper indications.** If the penetrant is warmed to 140° F. to 150° F., the heating effect of the penetrant will serve to warm the specimen at the same time as the penetration takes place. In addition, a warm specimen is relatively easy to dry with paper towels. Once the visible moisture film is removed, heat retained by the specimen will drive off the microscopic moisture layer. The fact that a glass surface may be warm to the touch is not always sufficient evidence that the surface is dry. It is possible for glass to be exposed to sunlight and still have extensive water deposition.

Drying Part Surfaces. Troublesome water-vapor condensation can sometimes be removed by wiping the test object with fresh **paper toweling** and applying powder before a new layer deposits. Cloth toweling is not recommended because it absorbs moisture and retains it from one sample to the next. Paper toweling does not pick up atmospheric moisture vapor readily and will leave few or no fibers on the surface. **Lint, fibers, or threads** sometimes can be confused with actual indications. When used to dry surfaces, paper toweling usually is discarded rather than re-used, as is the case with cloth. Many inspectors keep paper toweling in one hand and a gun in the other. If an indication is unsatisfactory, it can be removed quickly and the test repeated. Condensation of moisture on glassy surfaces is troublesome during moist, humid weather and the summer months. In most parts of the United States, little or no trouble is experienced from September to June.

EXCESSIVE TEST-OBJECT TEMPERATURES. When test pieces are warmed in excess of 180° F., electrified particles will precipitate indiscriminately on the surface. Indications of defects will not appear. A rough gage of the correct temperature for applying powder is whether or not the hand can be placed on the sample and left in place. A temperature of 140° F. is about the maximum which the average human hand can tolerate; defects can be located at this temperature. On overheated test pieces, powder blankets the specimen and the condition is readily recognized. Normally, indications develop instantaneously and excess powder bounces off the defect-free portion of the test piece.

LOSS OF INDICATIONS. When inspecting large objects like glass-lined vessels, it is not uncommon to look back over an area which has just been processed and to locate cracks which apparently were missed. Charged powder may drift to a crack somewhat out of the field of vision, and the working area of the drift powder may be several feet in any direction from the end of the gun. Since the normal **field of precise vision** is less than a foot in diameter, it is understandable that indications can be missed.

Fugitive Indications. Sometimes an indication is fugitive. This phenomenon sometimes occurs in highly humid weather. Also, when the impingement force of charged particles is higher than the electrostatic forces, indications may refuse to stay in place. The air pressure may be reduced until the electrostatic forces are sufficiently high to overcome the physical **sandblasting effect** of the particles. Sometimes indications refuse to stay in place because the gun is held too close to the part. Conversely, if the gun is held too far away from the work, the indications become reluctant to form. Experimentation usually will indicate optimum test conditions.

STANDARD CRACK SAMPLE. It is recommended that a standard crack sample be created before any inspection work is performed. Because of the possibility that humidity may affect the inspection performance, it is necessary that a known crack sample be available to the inspector for occasional comparison. This will assist and convince the operator that the method is always operative.

Preparation of Crack Samples. Standard crack samples are easy to make. Porcelain enamel can be heated and quenched in water. This produces a system of extremely tight cracks. This same procedure can be used on most ceramic materials. A little experimentation is worthwhile, considering the importance of the inspection procedure. In many plants where inspection is performed daily, a standard crack sample is hung nearby for occasional spot comparison. In any situation where there is a possibility that no cracks will be found, it is always helpful to use the standard sample to convince the inspector that his procedure is correct.

Bibliography

For Bibliography, see section on Electrified-Particle Test Indications.

SECTION 29

ELECTRIFIED-PARTICLE TEST INDICATIONS

CONTENTS

PAGE

General Interpretation

Sensitivity of indications 1
  A transparent piece of glass containing a crack (*f.* 1) 1
  Powder indication of the crack shown in Fig. 1 (*f.* 2) 2
  The same glass sample with powder removed (*f.* 3) 2
 Comparison with liquid penetrants 3
Types of indications 3
 Indications of subsurface defects 3
  A typical subsurface defect in clear glass (*f.* 4) 3
 Faint indications 4
Pinholes 4
 Blinking indications 4
 Pinhole breakdown 5
Cracks in thin, metal-backed coatings 5
 Thin paints and resins 5
Negative indications 5
Indications on secondary surfaces 5
 Test objects immersed in oil 6
 Oil films as moisture barriers 6
 Blinking indications on secondary surfaces 6
 Precautions in explosive atmospheres 6
Indications on nonhomogeneous materials 6
False indications 6
 Powder blotting 6
 Residual powder artifacts 6
 Chemically induced artifacts 7
Loss of indications on slightly conductive materials 7

Mechanisms of Failure of Glass and Porcelain Enamels

Crack growth characteristics 7
Causes of cracking in glass 7
  Factors contributing to the growth of cracks in glass (*f.* 5) 8
Mechanisms of porcelain-enamel failure 8
 Cracks yield engineering information 8
 Direction of stress 8
 Crack formation 9
 Compression failures 9
  A porcelain-enamel failure due to compression (*f.* 6) 9
 Tension failures 9
  A tension failure on porcelain enamel (*f.* 7) 10
 Cyclic loading failures 9
  A porcelain-enamel failure, illustrating how cyclic loading contributes to failure (*f.* 8) 10

Industrial Applications

Inspection of glass containers 11
 Typical indications 11
  Rim defects in glass bottles (*f.* 9) 12
Earlier methods for inspection of coatings 11
 Brine test 11
 Limitations of brine tests 13
 Modified tesla coil test 13
Electrified-particle inspection of coatings 13
 Craze patterns 13
  Indications of a craze pattern on a typical glass-lined fitting (*f.* 10) 14
 Stress cracks 14
 Wavy cracks 14
 Pinholes 15
 Cracks through pinholes 15
 Indications from chemical residues 15
Inspection of glass-to-metal seals 15
 Effects of cracks in seals 15
  Small headers which have been removed from equipment, both having identical cracks on top and bottom (*f.* 11) 16
 Electrical leakage 16
 Intermittent faults 16
 Types of cracks 17
  Sketches of typical crack patterns on glass-to-metal seals (*f.* 12) 18
 Evaluation of cracks 17
Miscellaneous applications 17
 Porcelain teeth 17
 Terra cotta 19
  Indication of defect in glaze on terra cotta (*f.* 13) 19
 Glass lenses 20
  Indications of superficial scratches in a lens (*f.* 14) 20
 Brittle-coating tests 20
Bibliography 21

SECTION 29

ELECTRIFIED-PARTICLE TEST INDICATIONS

General Interpretation

SENSITIVITY OF INDICATIONS. The electrified-particle inspection method is a unique and powerful tool for evaluating the width of a defect in **nonconducting materials,** since it will locate cracks in clear glass which are completely invisible to the human eye. When the dimensions of a crack or interface in a transparent object become less than four millionths of an inch in width, no light is reflected because of an interference phenomenon. A simple experiment illustrates this point. Fig. 1 shows a transparent piece of glass containing a crack. The crack is visible because it reflects light to the eyes of the observer. When processed with electrified particles, a visible powder indication develops as shown in Fig. 2. The powder indication is considerably more extensive than the appearance of the crack to the eyes. If the sample is carefully bent to open the crack, the true crack length is now exposed, as seen in Fig. 3, and

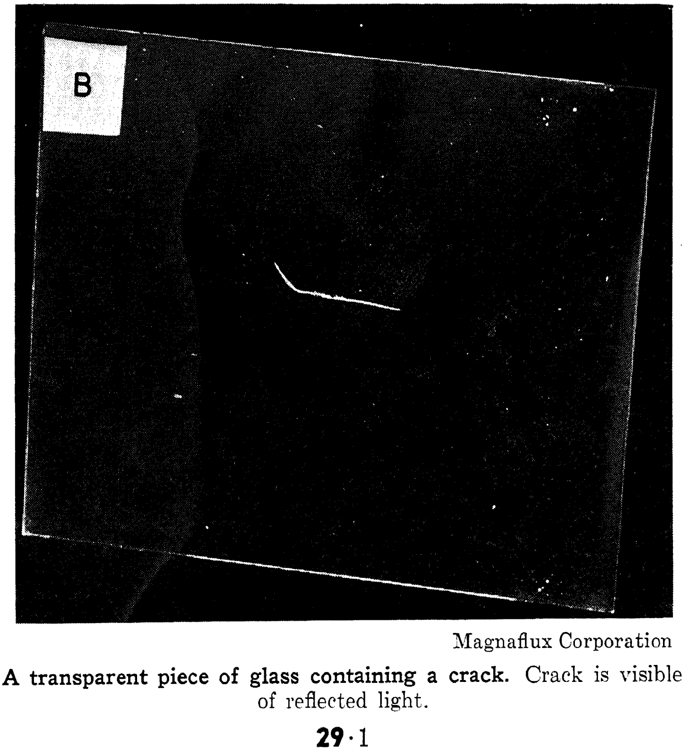

Magnaflux Corporation

Fig. 1. A transparent piece of glass containing a crack. Crack is visible because of reflected light.

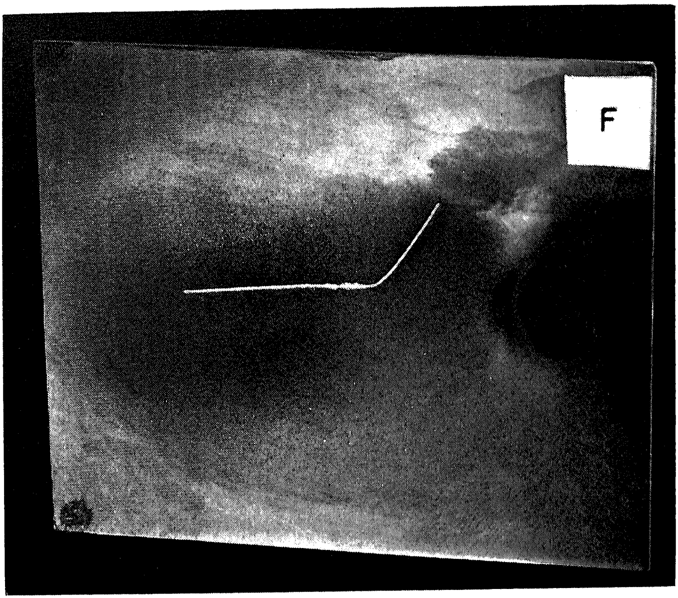

Magnaflux Corporation

Fig. 2. Powder indication of the crack shown in Fig. 1. The sample is reversed because the crack is in the opposite side.

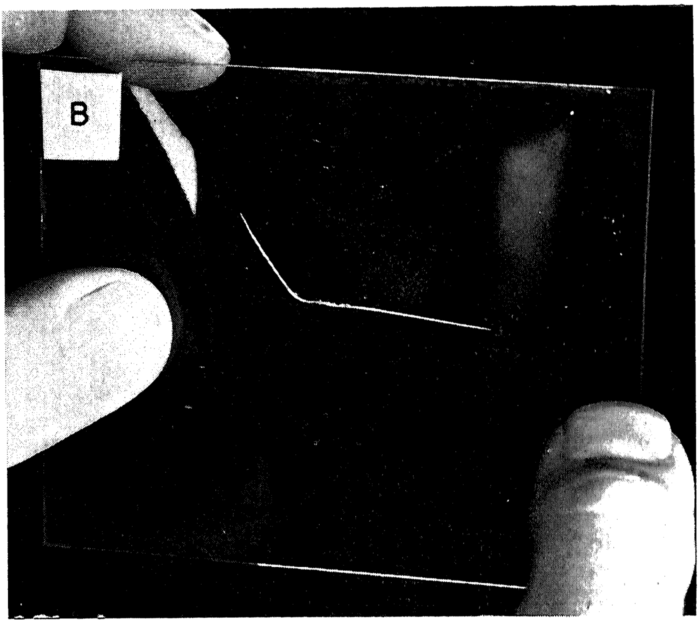

Magnaflux Corporation

Fig. 3. The same glass sample with powder removed. Sample is being bent to open the crack so that reflected light can be seen from all portions of the defect.

agrees exactly with the previous indication. This clearly illustrates the fact that cracks, which are four millionths of an inch in width or narrower, can be detected by the electrified-particle method.

Comparison with Liquid Penetrants. Other methods for detecting cracks in ceramic materials rely upon introducing **colored** or **fluorescent materials** into a crack. After excess material is removed, **blotting agents** are applied to draw the material from within the defect and make it visible (see section on Liquid-Penetrant Tests). If the material is transparent, it is possible to detect color- or fluorescence-bearing penetrant in the crack down to approximately four millionths of an inch in width. At this point the **interference phenomenon** takes place, and despite the presence of material within the crack, no reflected light will be emitted from the defect.

TYPES OF INDICATIONS. The **size of powder build-ups** on a crack is a rough indication of the size of the underlying defect. Generally, large indications indicate large defects. A wide crack may have a powder build-up which is the same size as one formed at the site of a deep defect. Therefore it is difficult to tell whether a crack is wide, exceptionally deep, or both, by the superficial appearance of an indication. Indications can be developed which are as large as ⅛ in. in width. A quick calculation will show that this is 30,000 times larger than an invisible crack in glass. This illustrates the striking magnifying ability of charged powder.

Indications of Subsurface Defects. The shape of an indication reflects some of the characteristics of a crack. **Normal indications** are almost perfectly half-cylindrical in cross-section. Cracks occurring in porcelain enamel sometimes branch out at the base of the notch, split, and form two cracks completely below

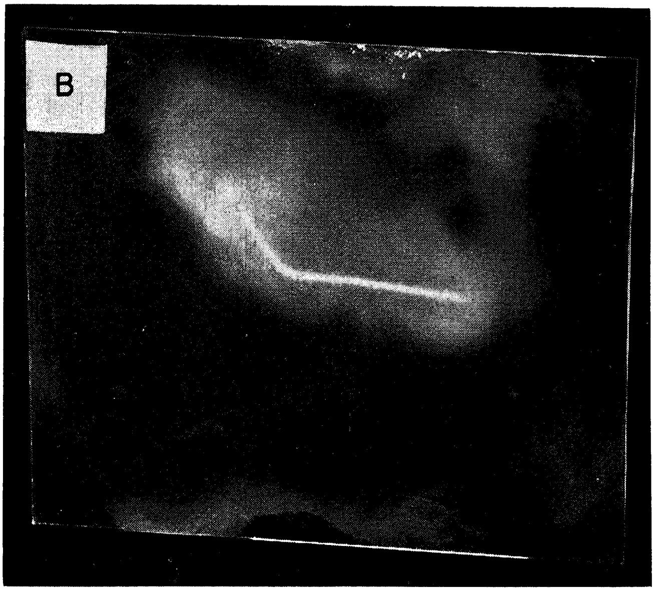

Magnaflux Corporation

Fig. 4. A typical subsurface defect in clear glass. The same piece of glass is illustrated in Fig. 1.

the surface. The indication will reflect this condition on the surface Indications of **cracks not perpendicular to the surface** appear as a shadow or as graduated powder build-ups. These usually are fuzzy and less clean-cut. Indications are broad and poorly defined on **thin specimens** where a crack is on one surface and not the other. A typical subsurface indication of a defect in glass is shown in Fig. 4. **Subsurface defects** can be located if they are not more than ¼ in. below the surface. However, due to the wide difference in dielectric properties of nonconducting materials, it is not always possible to predict the limit of this measurement. Subsurface defects, including bubbles, can be located only when a defect contains negative ions or has an electron supply nearby.

Faint Indications. It is possible to distinguish between cracks existing in relative states of tension and compression in **thermally shocked enamel.** Indications of cracks in a high state of compression lack fidelity and form hesitantly. Tight cracks provide a weak leakage field. The weaker the field, the poorer the indication.

Indications are sometimes difficult to develop on **old or weathered porcelain enamel.** It has been theorized that the difficulty is due to the infinitesimally slow dissolving of the glassy coat in **atmospheric water vapor.** The inner surfaces of cracks in glass are also affected and may encourage crystal growth. This may account for their apparent self-sealing ability and resultant faint indications. The role of atmospheric moisture vapor is extremely significant in relation to certain older porcelain enamels. When exposed to moisture vapor for prolonged periods of time, soluble portions of the coating leach out, leaving traces of moisture within the vacated voids. As **leaching** progresses, the bubble structure becomes exposed. Each of the vacated voids then may hold an infinitesimal amount of moisture. When a crack occurs in a coating of this type, it is often impossible to develop an indication, since the powder is likely to indicate the moisture in the exposed bubble structure. In this case, powder deposits as a blanket rather than as individual indications. If the sample is warmed until all moisture is driven off, indications develop in normal fashion, and the larger pores are indicated separately.

PINHOLES. Inspection for through-to-metal pinholes on metal-backed material is of real importance to the manufacturer of glass-lined process vessels and porcelain-enameled goods which are exposed to moisture or corrosive materials.

Blinking Indications. An indication of a through-to-metal defect may act mysteriously and appear to "blink." An indication will build up and blow away, whereupon a new indication will form and it, too, will blow away. This sequence usually occurs so rapidly that the indications appear to pulsate or blink. The blinking effect is caused by the build-up of positive particles directly over the breakthrough, with a resultant high negative field occurring just below in the metallic layer. When the strain between positive and negative potentials reaches a critical point, **electrical breakdown** takes place. Tiny flashes of light occur at the moment of breakdown and confirm that a spark occurred. Once the breakdown has occurred, the oncoming material forcibly removes the original indication. The initial indication is easily removed, since the electric forces which held it in place have been disposed of by the electrical breakdown. Once the indication is removed, a new one forms immediately and begins to enlarge until it reaches a critical point, whereupon it also breaks down electrically and is blown away. The indication does not always blow away completely but appears to enlarge and retract in size, giving the impression that it is pulsating. The pulsation rate may be as high as 25 c.p.s.

The blinking effect does not occur if the through-to-metal pinhole is filled with conductive material such as water or penetrant. An **exposed metallic inclusion** in the surface of a nonconducting material will act similarly. In these cases a powder indication will build up but not pulsate, since an electrical breakdown does not occur.

Pinhole Breakdown. It is possible to develop d.-c. voltages high enough to cause breakdowns of thin coatings. Many coatings contain **bubbles** which may be as large as half or more of the total coating thickness. Such things will not be indicated unless the gun is held in one place and a serious attempt made to cause a breakthrough and form an indication. A casual movement of the gun while blowing powder will rarely break down most coatings, no matter how thin they are. Breakdown usually occurs when the gun is held in one place with a steady stream of highly charged particles impinging upon the same location. The possibility of breakdown of a coating can be reduced somewhat by applying a **sheet of vinylite** over the surface in order to increase the total thickness of the dielectric film.

CRACKS IN THIN, METAL-BACKED COATINGS. The porcelain-enameling industry has exhibited a trend toward thinner coatings. As a result the incidence of cracks in commercial products appears to be much reduced, although not eliminated. As the thickness of porcelain enamel diminishes, a problem of crack interpretation arises. Generally speaking, the thinner the coating, the closer together a group of cracks will be. On **exceptionally thin coatings** (3 mils or less), cracks can occur so closely together that the respective indications tend to overlap.

Thin Paints and Resins. It is difficult to develop a sizable indication of a crack on exceptionally thin coatings without increasing the background appreciably. This effect becomes more pronounced as the dielectric strength of the coating material is reduced, as with some paints and resins. An indication forms because of an electrostatic differential between an area which contains a crack and one that does not. As the dielectric strength of the insulating material is reduced by a thinning or alteration of its electrical characteristics, the **electrostatic differential** diminishes to a point where an indication cannot form.

NEGATIVE INDICATIONS. Under certain atmospheric conditions, powder indications sometimes appear reversed. The crack is indicated by a lack of powder at the defect. The powder build-up occurs on both sides of the defect, leaving the area directly over the defect free of powder with the possible exception of a few particles. This effect rarely occurs and is extremely difficult to reproduce.

INDICATIONS ON SECONDARY SURFACES. One of the strangest effects produced by electrified particles is the formation of an indication on a secondary surface. This effect takes place when a **film of oil** or a **sheet of nonconducting vinyl** is placed directly over a cracked test piece. Indications of defects in the original surface will be reproduced on the secondary surface, although the fidelity will be somewhat reduced. The indications form hesitantly and resemble subsurface defects. It is essential that the secondary surface be in intimate contact with the surface to be inspected. This is easy to accomplish, since powder will charge the vinyl and cause it to adhere quite strongly to most materials.

Test Objects Immersed in Oil. One spectacular demonstration of the secondary-surface effect is to place a cracked porcelain-enamel sample in a vessel of light petroleum distillate. When charged powder is blown at the surface of the oil, particles will eventually migrate to the bottom of the vessel, deposit on the sample, and form indications. When oil or a sheet of nonconducting material is used as a secondary surface, it is essential that the test surface be completely free of moisture vapor, as is the case with normal inspection.

Oil Films as Moisture Barriers. Another instance where a protective coating is useful is during the testing of porcelain or ceramic coatings in the presence of excessive moisture vapor or water splashing. The object must be dried thoroughly and coated with oil prior to exposure. This will keep the surface dry and in condition to detect any cracks which occur.

Blinking Indications on Secondary Surfaces. The blinking effect described earlier occurs on a secondary surface as well as on an original surface. This phenomenon can be used to muffle electric discharges. In areas where **electric discharge** may be hazardous, it is possible to cover the specimen with vinyl sheeting and proceed with a pinhole inspection, utilizing the blinking effect. The electric discharge occurs only between the metallic layer and bottom surface of the vinyl layer. Sometimes a secondary layer is useful in preventing the unintentional puncturing of thin coatings.

Precautions in Explosive Atmospheres. The powder itself will tend to muffle electric discharges and especially so if combined with a **nitrogen pressure source** instead of compressed air. Despite these safety features, it is wise to avoid using the method in **hazardous atmospheres.**

INDICATIONS ON NONHOMOGENEOUS MATERIALS. Charged powder is attracted to materials containing free electrons and does not adhere readily to nonconducting material. Materials whose dielectric properties lie between these two extremes will attract or hold charged powder, depending upon the degree of mobility of their respective electrons. This suggests that when two materials of different dielectric properties are blended together, charged powder will adhere more strongly to materials of lower dielectric strength. This is useful in the examination of plastic materials or asphalt coatings, since it will indicate the **flow characteristics** or **distribution of blended materials.**

FALSE INDICATIONS. Indications which are not genuine occur occasionally, but usually these are due to some physical cause which can be remedied. **Moisture streaks** left from wiping cloths or toweling commonly produce false markings. However, these rarely resemble true crack indications. **Lint from cloth, rags, or felt** often resembles crack indications. When the inspector is in doubt, the indication can be pushed with a sharp point to see if it moves. Felt is the most common offender, since small fibers left on pieces resemble thermal-shock cracks.

Powder Blotting. Water or oil particles blown on specimens attract powder and resemble pinhole indications. If questionable, these can be removed and powder reapplied. False indications produced by the blotting of powder will indicate peculiarly after several seconds, since the fluid will spread.

Residual Powder Artifacts. When a surface has been sprayed with powder, it becomes positively charged. If excess powder is brushed from the surface, the remaining particles may be preferentially oriented and tend to repel freshly charged particles. The surface is charged locally so that, as the next load of charged powder is applied, it will tend to distribute itself to areas where there is the least amount of charge. The resultant images rarely resemble true indications.

Chemically Induced Artifacts. Strong acid or basic residues, and sometimes oily materials, leave streaks or peculiar markings which may be mistaken for crack indications. This is particularly true when the bubble structure of glassy coatings has been opened. Little can be done about this except to note that a true indication is always half-round, sharp, and well defined. Indications produced by such materials usually are smudged and ill defined, and do not resemble true crack indications.

LOSS OF INDICATIONS ON SLIGHTLY CONDUCTIVE MATERIALS. Glass coatings, with the exception of some high-temperature enamels, are nonconductive. The same situation exists with most resin coatings. All **silvery or black coatings** should be viewed with suspicion, however, since they may be conductive. They may contain stainless steel or aluminum bronze flakes. Black coatings invariably contain carbon. Ordinarily these materials are not considered conductive when blended with a nonconducting resinous material. However, potentials as high as 10,000-volt direct current are developed by electrified particles, and at that voltage many materials act as though they were conductive. When in doubt the inspector should always test a sample containing a known defect.

Mechanisms of Failure of Glass and Porcelain Enamels

CRACK GROWTH CHARACTERISTICS. A characteristic property of cracks in glassy materials is that they will grow under certain conditions. A crack may grow, encounter a compression area, and stop. If the **high stress area** is relieved by some external cause, the crack may start growing again and enter this zone. A stress may be incompletely relieved by the formation of an extremely small crack. Such a crack has an unpredictable growth potential, depending upon its service treatment. The direction of the crack is nearly always such that it tends to relieve locked-up stress; it depends entirely upon the **stress gradient** within the piece.

CAUSES OF CRACKING IN GLASS. The most common causes of crack growth in glass are heat, vibration, or both. Both heat and vibration generally apply cyclic loading and, when coupled with secondary causes, will cause growth. Factors contributing to the growth of cracks in glass are shown in Fig. 5. These are:

1. **Ordinary tension.** Tension stresses on the surface of a part tend to tear the glass apart.
2. **Heat via arc.** If a crack system joins two terminals or a terminal and ground where a large voltage differential exists, the ensuing breakdown develops heat within the fluid. High vapor pressures develop, thrust outward, and encourage crack growth.
3. **Random-dirt wedge.** A crack may receive dirt, and when followed by a compression loading, wedging action contributes to the growth of the crack.
4. **Crack debris wedge.** Debris from the inside of the crack may break off and drop to the bottom. When compression loading is applied, the debris acts as a wedge, and stress levels at the base of the crack increase, causing crack growth.
5. **Mismatch wedge.** If the walls of the crack do not mesh under compression loading, wedge action will be exerted, resulting in the growth of the crack.

6. **Hydrated-crystal wedge.** It is possible for water to combine with certain glass constituents and form hydrated crystals. Compression loading in combination with wedging action of the crystals will promote crack growth.
7. **Hydrated-crystal growth.** It is possible for crystal growth to occur over a long period of time and exert considerable outward thrust upon the sidewalls of the crack, causing it to split still further.

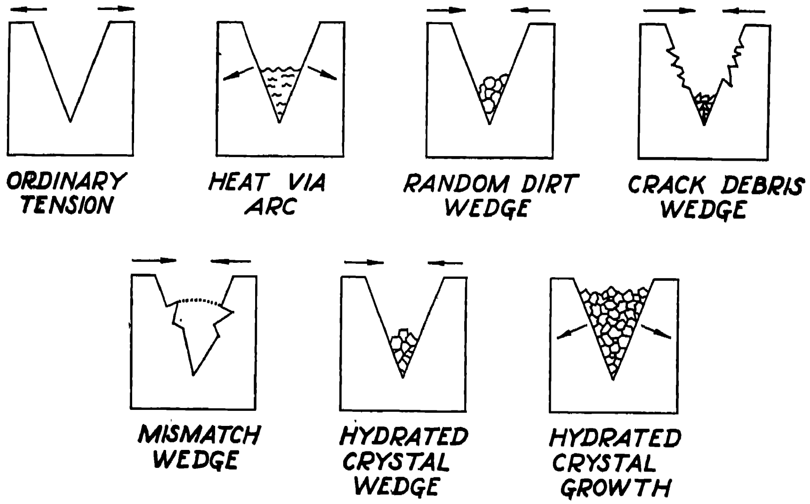

Fig. 5. Factors contributing to the growth of cracks in glass.

MECHANISMS OF PORCELAIN-ENAMEL FAILURE. Porcelain enamel, though very strong in many ways and desirable in other respects, is brittle. Despite this, it has been used widely for many years without serious difficulty. This is not so much a tribute to the ruggedness of porcelain enamel as it is to the manufacturer who has learned to design and ship his product in such a way that brittleness is overcome. Despite the success of porcelain enamel in industry and consumer fields, its inherent brittleness must always be considered in design, production, shipment, and use. For many years industry and the consumer have expected porcelain enamel to crack or fail, and neither was aware of the underlying reasons for such failure.

Cracks Yield Engineering Information. In the past few years the electrified-particle inspection method has been accepted as a reliable indicator of cracks in porcelain enamel. Further, it has been established that failures invariably occur in locations which were cracked prior to actual failure. Before this was known, **shock and impact tests** were relied upon to locate potential field failures. While some correlation can be obtained in this manner, these tests often introduce defects which lead to field failures.

Direction of Stress. Brittle materials always crack at right angles to the direction of the principal applied stress. Subsequent cracks rarely completely cross an original crack pattern. The presence of a crack pattern tells the designer that he has a **stress concentration** which may lead to more serious consequences if neglected. With the electrified-particle method, the stress-indicating cracks can be located, studied, and perhaps duplicated under controlled laboratory conditions.

Crack Formation. The formation of a crack requires the stressing of a sample to a point where compression is removed and the surface of the enamel goes into tension. When a certain point is reached, which may be prior to the yielding of the base metal, a crack will form. The crack formed in tension is visual evidence of a tension stress that reached a sufficiently high level. When load is released, the material returns to its original state, or nearly so, if the base metal has not yielded. If the inner surfaces of the crack mesh perfectly, the area at the crack is under approximately the same compression stress as the original coating. The coating, of course, does not contribute the same amount of strength in tension as it did prior to the formation of a crack.

Compression Failures. If a failed area of porcelain enamel is examined closely, it is possible to piece together the chain of events and tell how the defect occurred. When enamel is bent in compression in an unreasonable manner, it will fail in the manner shown in Fig. 6. The failure always is explosive in nature, and the amount of load must be quite high to induce failure. Relatively large areas of enamel are removed, and the edges of the failed area always have a **beveled appearance.** If the material contains a ground coat, **smooth ripples** appear.

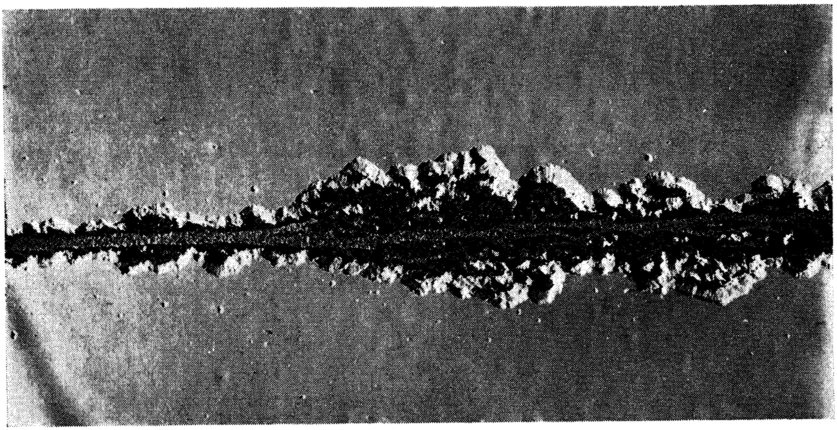

Magnaflux Corporation

Fig. 6. A porcelain-enamel failure due to compression. Note ripples in dark undercoat and the V-beveled edges of failure.

Tension Failures. Porcelain enamel, grossly bent in tension, will fail as shown in Fig. 7. Although the enamel is loose, it is usually reluctant to remove itself from the base metal. Obviously, yielding of the base metal has contributed to failure.

Exceedingly high loads are required to cause either tension or compression failures. This suggests that it is unlikely that either mild tension or compression stresses alone are responsible for field failures of porcelain enamels.

Cyclic Loading Failures. In Fig. 8 a starlike pattern was formed, with removed chips between the radial cracks. Despite the similarity to impact failure, the sample was not subjected to impact loading. This failure was artificially induced by a slow, steady loading on the reverse side until audible cracking was heard. With load still in place, the sample was processed, which verified **radial**

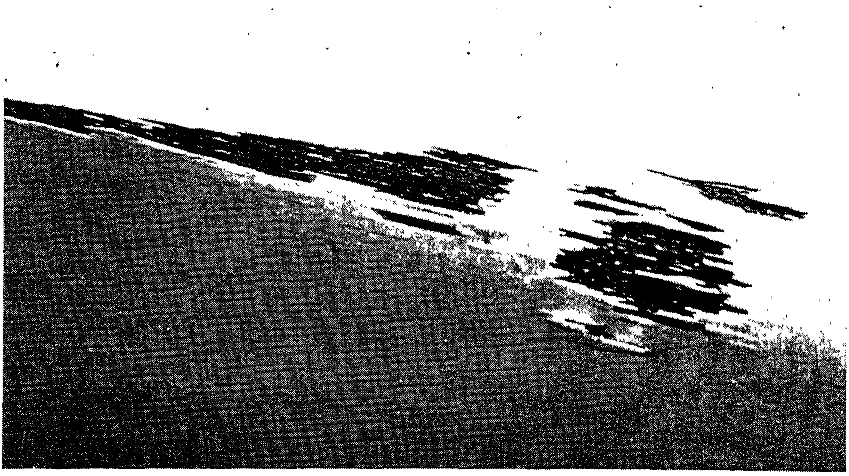

Magnaflux Corporation

Fig. 7. A tension failure on porcelain enamel. Note sharp edges of failed area and ridges in dark ground coat.

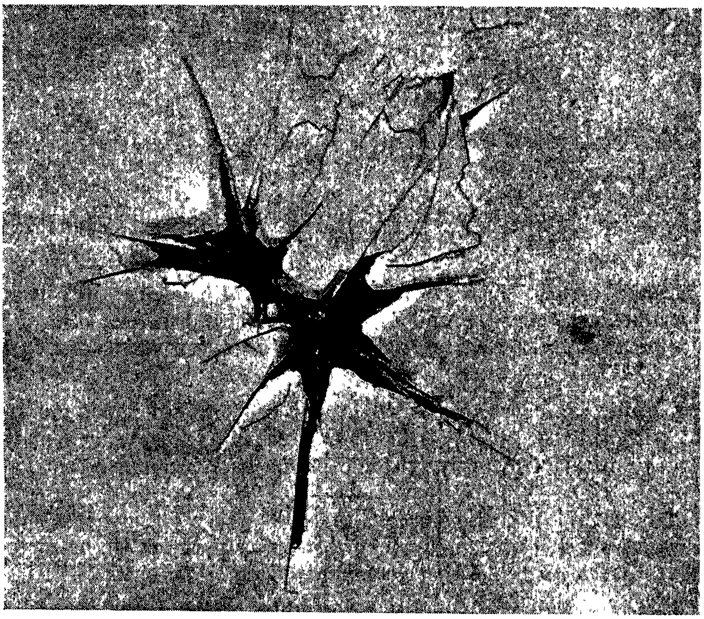

Magnaflux Corporation

Fig. 8. A porcelain-enamel failure, illustrating how cyclic loading contributes to failure. Note beveled edges indicating compression, and ridges in ground coat denoting tension.

cracking. The defective area was probed with a sharp point, and none of the enamel was found to have loosened or failed. When the load was released slowly, audible failure and removal of enamel occurred.

The simple experiment showed that removal of the enamel required a cyclic loading, with tension preceding compression. It is obvious that a crack in enamel weakens the coating to subsequent tension stress. It is not so obvious that a crack weakens the enamel to a subsequent mild compression load. Industrial tests and elaborate tests on hundreds of enamel samples have proved that many field failures can be traced to cyclic loading. In other words, failure invariably occurs after compression is applied at the site of a crack previously formed in tension. Sometimes failure occurs with the mere release of original tension. In every case, however, the failed area always shows:

1. A beveled appearance at the edges of the failed area.
2. Typical sharp ridges in the ground coat or residual ground coat.

The **ridges** are the residue of the original tension stress, and the **bevels** are an indication of compression stresses.

Several years of experience in working with porcelain enamels indicate that these are the conditions under which failure occurs. Despite this, the actual mechanism of failure is not apparent.

Industrial Applications

INSPECTION OF GLASS CONTAINERS. The electrified-particle method was developed initially for the inspection of glass bottles and containers. During its early development it was often difficult to obtain uniform test results from day to day. To overcome this, a machine was constructed which would process bottles of varying size at rates similar to a typical production line. Scores of tests were run on many types of beverage bottles manufactured by various companies.

Typical Indications. The types of indications obtained are shown in Fig. 9. Fig. 9(a) illustrates a type of defect that extends from the inside to the outside of a sealing rim on a bottle, and which constitutes a path for vacuum or pressure leakage. Another type illustrated in Fig. 9(b) does not completely cross the sealing rim. Such a crack may grow in service or repeated use. Fig. 9(c) illustrates a common defect occurring in glass containers. This type of defect sometimes results in a piece of glass dropping off inside the container. Fig. 9(d) illustrates a series of small and tiny indications of cracks which sometimes results in an explosion of a bottle during pasteurization.

EARLIER METHODS FOR INSPECTION OF COATINGS. The use of **corrosive solvents** demands great ingenuity of designers and chemists who must develop storage and processing vessels which will resist corrosion. These materials range widely in cost, availability, and effectiveness. Some of them are chemical porcelain, plastic, stainless-steel clad, glass-lined, and organic-resin coatings on steel. Inspection methods are available for most of these materials, but until the comparatively recent use of the electrified-particle inspection method, the significance of defects has not been fully recognized on glass-lined or on organic-resin-lined equipment. To understand its usefulness in this industry, it is necessary to examine other test methods.

Brine Test. The brine test involves the use of a simple **ohmmeter,** or an electrical device resembling this function. One lead of the instrument is grounded

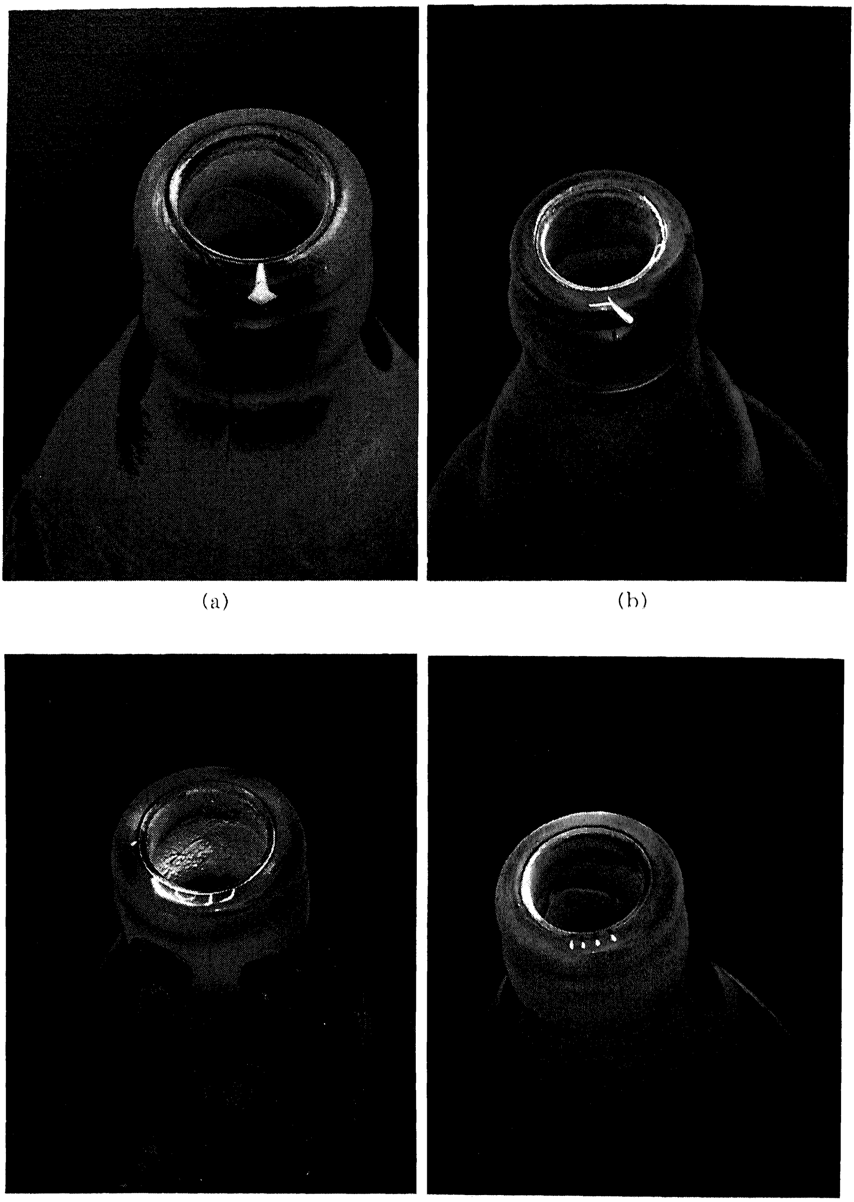

(a) (b)

(c) (d)

Magnaflux Corporation

Fig. 9. Rim defects in glass bottles. (a) Indication of a crack extending from inside to outside of a sealing rim in a beer bottle. (b) Indication of a defect which does not completely cross the sealing rim of a beer bottle. (c) Indications of cracks which may lead to chippage into the container. (d) Extremely tiny indications of cracks which are sometimes related to explosion in the pasteurization process.

to a metallic portion of the vessel. A brine-soaked sponge is attached to the tip of the other lead and swabbed over the surface of the coating. When the fluid on the end of the probe finds a **pinhole**, it rapidly penetrates into the defect and contacts base metal. A reading of lowered resistance immediately appears on the ohmmeter. The fluid completes a circuit from ohmmeter to swabbing probe to pinhole, through the fluid to metal, and from the grounded probe back to the ohmmeter. A variation on this technique is to fill the tank with a brine solution and dip one of the probes into the solution. The other probe, of course, is grounded to the base metal.

Limitations of Brine Tests. Both techniques have the disadvantage of not being able to locate a **through-to-metal pinhole** accurately. The second method is particularly disadvantageous in this respect. The probing technique is slow and tedious when inspecting extremely large vessels. It is frequently criticized because the salt water will attack the base metal at the bottom of a pinhole and produce **corrosion products** which sometimes spread below the coating. Sometimes resin coatings form **blisters** at this point and peel away from the base metal.

One serious disadvantage of the probing brine test is that it cannot always indicate the actual **breakthrough location.** When an inspector probes a long defect and encounters the end of a crack, the penetrating fluid races to the actual breakthrough, which may be several feet away. This gives a reading, and the operator will mistakenly assume that the defect is directly underneath the probe.

Modified Tesla Coil Test. Another test utilizes a device which operates on 110-volt alternating current and which resembles an old automotive induction coil. Voltages ranging between 8,000 and 45,000 volts are generated and impressed across the work by a needle protruding from one end of the device. The voltage can be varied by a control knob. As the **needle** is moved over the glass or resin lining, a high voltage spark emanates from the end of the probe and darts through a through-to-metal defect. Sometimes a **spring or chain** is placed on the end of the probe and the assembly is draped over the coating. This permits the inspection of a much larger area. In the hands of a skillful operator the Tesla coil is fairly rapid at locating pinholes and is not particularly dangerous to coatings. If the voltage is too high and the operator allows the chain or probe to dwell in one spot too long, it is possible to break down the coating and produce pinholes where none existed before.

Before the advent of the electrified-particle method, it was believed that the electric needle had the ability to locate all breakthroughs to metal. This has been disproved where a breakthrough coincides with a crack in glass linings.

ELECTRIFIED-PARTICLE INSPECTION OF COATINGS. Whenever a defect is completely through to metal, a **blinking electrified-particle indication** is produced. This is a reliable and positive way to ascertain whether or not a defect is through to metal. If a considerable length of crack is broken through, a row of round indications appears, and these blink at random. The blinking effect only occurs as the powder is being blown at the defect.

Craze Patterns. One type of crack pattern which occurs on glass-lined vessels resembles the craze sometimes found on chinaware (Fig. 10). A craze pattern usually occurs where the **coefficient of expansion of glass and base metal** are improperly matched. Years ago this type of pattern was more common than it is now. Increased knowledge and experience have enabled ceramic engineers to reduce the incidence of this type of defect. If crazing is encountered, interpretation is difficult because of the great number of defects present. So many cracks are present that the job of detecting breakthrough on each and every crack indication may be stupendous.

Despite the fact that manufacturers of glass-lined vessels rarely produce crazed coatings, there is the possibility that the user may accidentally do so. If **spalling or chipping** of the glass has already occurred, the damage can be visually observed. When the damage is not obvious, charged powder can be used to help decide whether or not to continue using the vessel.

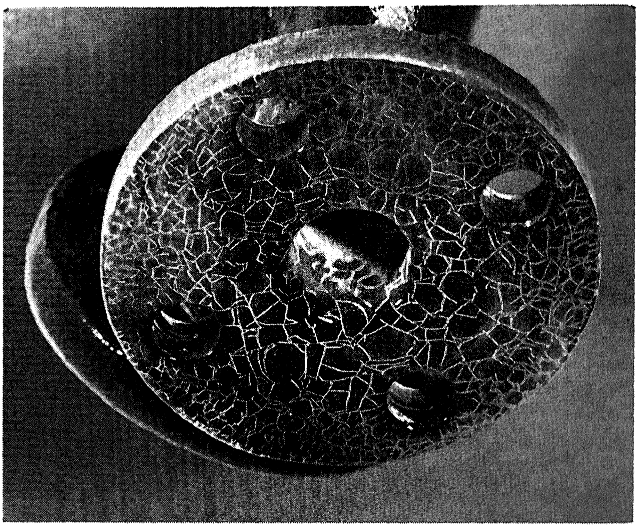

Magnaflux Corporation

Fig. 10. Indications of a craze pattern on a typical glass-lined fitting.

Stress Cracks. The most common type of crack found on glass coatings might be termed a stress crack, produced by physical **bending.** This may occur during manufacture, shipment, set-up, and in use. Such cracks are found at places of bolt-up, changes of section, or where attachments have been welded or bolted in place. They always occur perpendicular to the direction of principal stress.

Stress cracks invariably go **through to base metal** at some point in their length and for this reason are considered a serious defect. They are usually invisible to the naked eye and cannot always be found with a Tesla coil. If a defect cannot be seen, a plant inspector may assume that none is present. Thus, in service, a corrosive chemical may travel through a defect and attack the base metal, eventually causing service failure and producing disastrous results.

Wavy Cracks. Another type of defect resembles the rolling and twisting of a roller coaster. This defect does not seem to be related to any unusual applied stress and is a manufacturing rather than a user defect. The cracks may range from three to several hundred feet in length. They are smooth, curvy, and tend to wander in distinctive roller-coaster fashion. The cracks rarely cross one another. This type of crack usually occurs only on thick coats of glass such as are found on **cast-iron sanitary ware** and **glass-lined vessels.**

The roller-coaster type of crack rarely goes through to metal. Despite this, it seems wise to treat it in the same manner as a stress crack. If any portion of the defect blinks, the defect is through to metal. Little is known of the growth of either the stress or roller-coaster type of defect.

Pinholes. The occurrence of pinholes is very common in coated vessels and is considered a serious defect. After a pinhole is located, the glass is chipped away from the localized area. It is then drilled, tapped, and a tantalum or other **rare-metal plug or bolt** is threaded into the side of the vessel. A **fluorinated-plastic gasket material** is used to help complete the seal.

Cracks Through Pinholes. Sometimes a crack runs through and past a pinhole. The inspector may successfully locate the pinhole with a Tesla coil and not be aware of the fact that a crack also exists in this location. When the pinhole is repaired, the manufacturer will assume that the defect has been satisfactorily repaired. The chemical used in the vessel may enter the crack emanating from either side of the patch and work its way underneath the plugged area, producing corrosion. Eventually the plug may drop out.

If a through-to-metal pinhole is detected with charged powder, its presence can be verified by the use of a Tesla coil or a brine test. If a breakthrough occurs in a crack and is detected with the blinking effect, it may be very difficult to verify the exact location by the use of the Tesla coil or a brine test. The Tesla coil may not detect the breakthrough because it occurs within a crack. The blinking effect will not take place if brine or other conductive material is in the through-to-metal defect.

Indications from Chemical Residues. Glass-lined and other coated vessels sometimes will have other types of indications which are related to the material that was last in the tank. Very **strong acids** tend to leave residues, and it is sometimes difficult to develop good, clean-cut powder indications. Even though a tank subjected to strong acidic material has been thoroughly rinsed, there is still the possibility of developing smears and peculiar markings. This is particularly true where abrasion of the coating has occurred and the bubble structure of the coating has opened up.

Basic materials and water sometimes tend to promote healing of cracks in glass-lined vessels. Nothing seems to promote the healing of defects occurring in resin coatings. Old cracks rarely heal up completely. The indications obtained, however, may be very poor and difficult to develop.

INSPECTION OF GLASS-TO-METAL SEALS. The growth of complex electrical instrumentation in modern aircraft has emphasized the problem of maintaining the integrity of every component. As aircraft go higher and faster, the demands upon every part become more severe. During World War II a major attempt was made to eliminate high-altitude problems in electrical devices. This involved the use of hermetically sealed equipment. As the use of this type of equipment increased, problems arose involving glass-to-metal seals. Mysterious and unpredictable field failures occurred which were later traced to cracks in glass portions of the seal. The electrified-particle method has played an important role in the subsequent investigation of these failures and has aided in the development of intelligent specifications for industrial purposes.

Effects of Cracks in Seals. Many cracks in glass-to-metal seals do not go through the entire glass thickness. They do not permit **gaseous leakage** in either direction. Fig. 11 illustrates small headers which have been removed from equipment, both having identical crack patterns on top and bottom. Cracks not coincidental will not cause gaseous leakage. Any crack system which does have **coincidental cracks** on both sides of a seal should be viewed with suspicion. Despite the narrowness of cracks, they may cause **gaseous leakage** which is undetectible by crude bubble tests. The use of the mass spectrograph on such crack systems confirms the fact that through-cracks can leak.

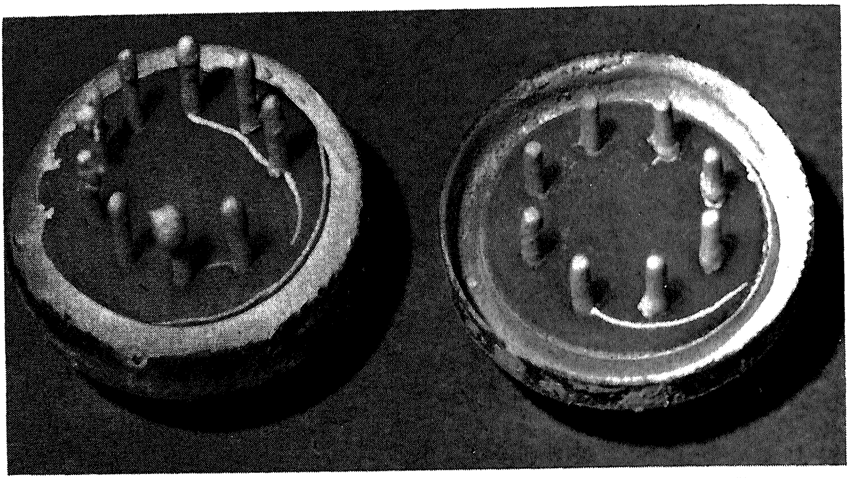

Magnaflux Corporation

Fig. 11. Small headers which have been removed from equipment, both having identical cracks on top and bottom. Note that the cracks are not coincidental.

Electrical Leakage. From some points of view, electrical leakage of a sealed component is a much more serious problem than gaseous leakage, since the failure may be abrupt and unpredictable. The designer of electrical equipment expects a certain amount of electrical leakage, depending on voltage differentials or expected atmospheric conditions. However, it is difficult to design tests to account for unpredictable crack systems.

Atmospheric conditions influence the resistance of the surface of glass. Under some conditions, moisture condenses on glass surfaces in an exceptionally thin layer. If a crack is present, moisture penetrates it readily and contributes to the over-all lowering of resistance of the seal. This fact may be verified by checking resistance with a megohmmeter before and after a crack is induced in a seal.

Intermittent Faults. One annoying thing about electrical leakage is that it may be intermittent and difficult to detect in service. If a crack contains moisture and the equipment is activated, a breakdown may occur until the **moisture within the crack** is heated by the passage of current and is driven out. When the equipment cools down, more moisture may condense on the glass surface and the sequence will be repeated. If the equipment is energized continuously, the chances of electrical breakdown are less, since the moisture is driven out and stays out as long as the equipment is warm. However, this same heat may contribute to the growth of cracks, and the situation becomes worse. Under some conditions **carbon** will deposit within cracks and provide a permanent breakdown path. This is an easier condition to locate if found in time to prevent total loss of the completed assembly.

Types of Cracks. Generally speaking, there are five types of crack patterns which appear on glass-to-metal seals. Some are caused by the assembler of the complete hermetic package. Others are caused by improper use in service. The five **classifications** shown in Fig. 12 are pictorial representations indicating only one crack of each kind, although more than one classification may occur on the same piece. They are listed in order of increasing seriousness with regard to vacuum and electrical leakage.

Fig. 12(a) shows **Type 1 cracking,** starting from the surrounding ring or terminal. The cracks are short and may not be serious unless they occur coincidentally on both sides of the seal. These cracks may grow under the conditions discussed earlier. These generally are typical manufacturing defects. The dotted lines indicate cracks on the opposite side.

Fig. 12(b) shows **Type 2 cracking,** which is comparatively rare and consists mainly of concentric circular cracks paralleling the rings or the terminals. They may be dangerous only if appearing coincidentally on top and bottom of seals.

Type 3 cracking is shown in Fig. 12(c). These cracks seem to be a typical manufacturing defect and may only be of concern if appearing coincidentally on top and bottom surfaces of headers.

Fig. 12(d) illustrates **Type 4 cracking,** typical of thermal shock. This condition sometimes is noted in new seals, but it is more commonly a result of improper soldering techniques. If the cracks are coincidental on top and bottom, gaseous leakage may occur. Electrical leakage will occur if the crack patterns are appropriately located.

Fig. 12(e) shows **Type 5 cracking,** which is the most common type of defect. It seems to be typical of processing techniques. Field repair work also may contribute to the creation of this type of defect. This can be dangerous under the same conditions mentioned for Type 4.

Evaluation of Cracks. Some manufacturing concerns inspect **hermetic seals** visually, sometimes aided by a microscope. This is time consuming, expensive, and inaccurate in locating all defects. Some companies eliminate those defective pieces containing cracks which their customers may see. Their attitude is, "What can't be seen won't hurt." Another attitude is, "We've been making these components a long time and have never received any reports of failure." Some even say, "It's impossible to eliminate defects."

The fact that a glass-to-metal seal passes through many hands before ultimately reaching its home within a complex apparatus makes it difficult to ascribe the blame for a malfunctioning piece of equipment. The failure of a single seal can contribute to the failure of a relay. This may lead to still another failure which ends in complete disaster. This chain of failures is complex in operation and difficult to trace backwards. Yet it can happen. Since the possibility of failure exists due to seemingly insignificant cracks, it is worthwhile to locate such defects, particularly since a simple method exists for their detection.

MISCELLANEOUS APPLICATIONS. Several specialized applications have been found for electrified-particle tests.

Porcelain Teeth. The relationship of cracks to the strength of porcelain teeth has been thoroughly investigated. It has been proven that **invisible defects** in porcelain teeth can contribute to failure in use. Cracks are generally formed by poor laboratory techniques rather than being formed during actual manufacturing.

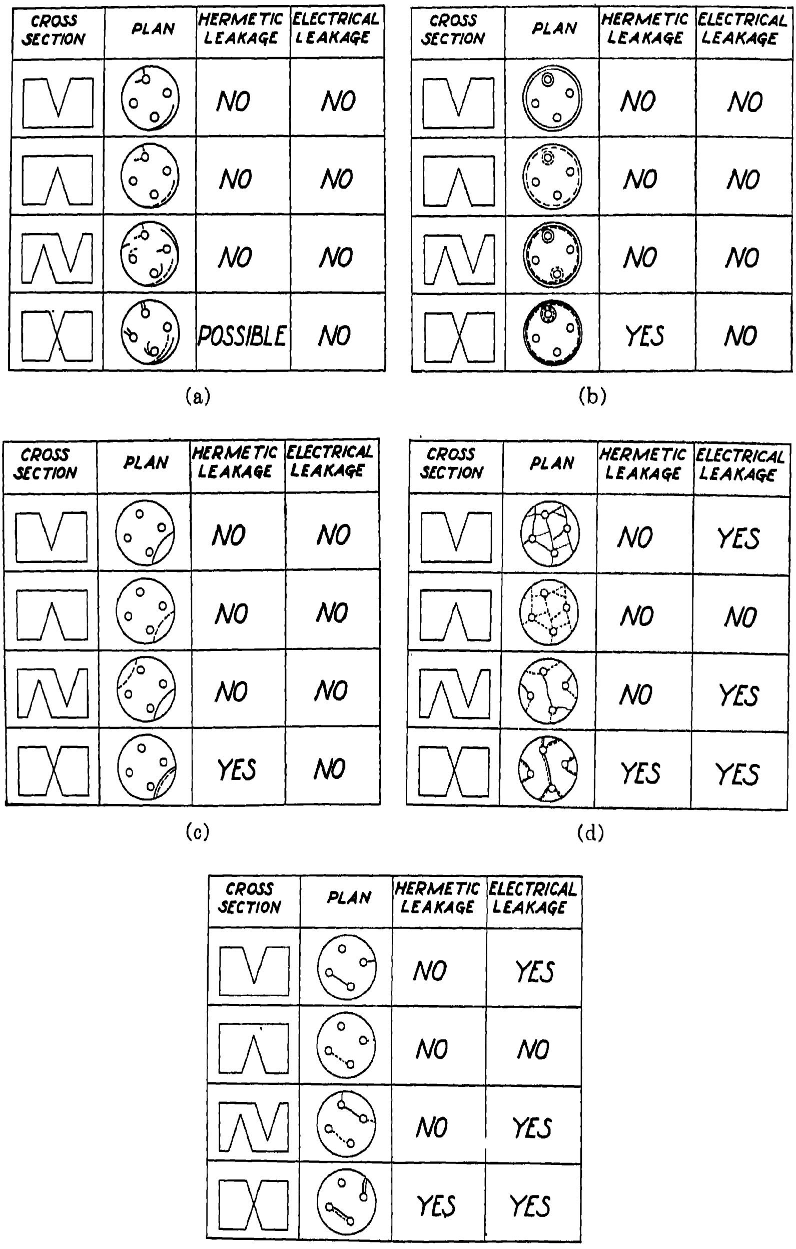

CROSS SECTION	PLAN	HERMETIC LEAKAGE	ELECTRICAL LEAKAGE
		NO	NO
		NO	NO
		NO	NO
		POSSIBLE	NO

(a)

CROSS SECTION	PLAN	HERMETIC LEAKAGE	ELECTRICAL LEAKAGE
		NO	NO
		NO	NO
		NO	NO
		YES	NO

(b)

CROSS SECTION	PLAN	HERMETIC LEAKAGE	ELECTRICAL LEAKAGE
		NO	NO
		NO	NO
		NO	NO
		YES	NO

(c)

CROSS SECTION	PLAN	HERMETIC LEAKAGE	ELECTRICAL LEAKAGE
		NO	YES
		NO	NO
		NO	YES
		YES	YES

(d)

CROSS SECTION	PLAN	HERMETIC LEAKAGE	ELECTRICAL LEAKAGE
		NO	YES
		NO	NO
		NO	YES
		YES	YES

(e)

Fig. 12. Sketches of typical crack patterns on glass-to-metal seals. (a) A typical Type 1 crack pattern. (b) A typical Type 2 crack pattern. (c) A typical Type 3 crack pattern. (d) A typical Type 4 crack pattern. (e) A typical Type 5 crack pattern.

Terra Cotta. Fig. 13 is interesting because it represents a peculiar combination of materials. The base material is porous, whereas the top surface is completely glazed and nonabsorbent. Here the defect is completely invisible to the naked eye, though successfully indicated by powder. This material always requires penetrant in order to detect cracks. The application of charged powder

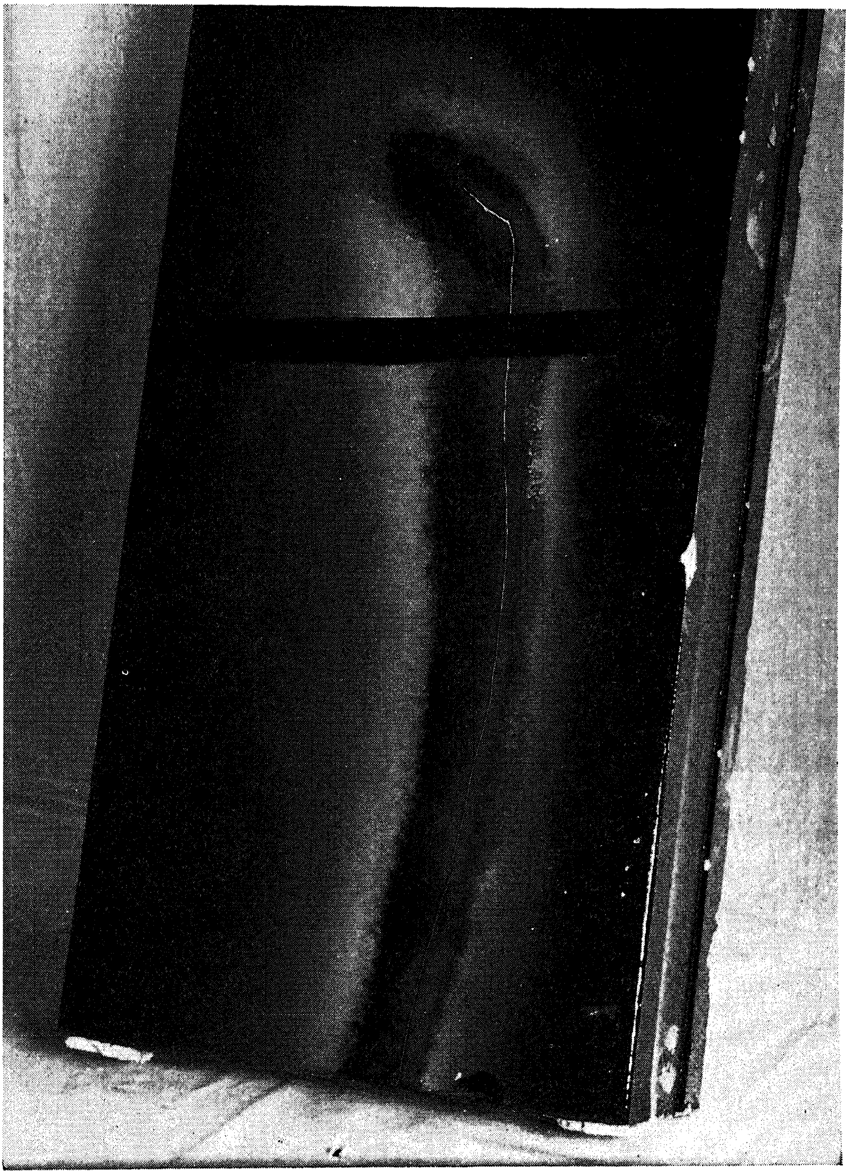

Magnaflux Corporation

Fig. 13. Indication of defect in glaze on terra cotta.

sometimes electrostatically attracts the fluid within the defect and provides blotting action in addition to the electrostatic effect. Thus a much larger crack indication is provided.

Glass Lenses. Fig. 14 shows how charged powder helps delineate superficial scratches which may not be easily visible to the human eye. Material must be given penetrant treatment and then carefully subjected to charged powder. The deepest ends of the scratches always seem to have a shadowed area in conjunction with the regular indication. The size of an indication always is dependent upon the amount of ionic attraction, which in turn is related to the depth. Thus weak indications indicate very slight defects, whereas larger indications always indicate substantially more damage.

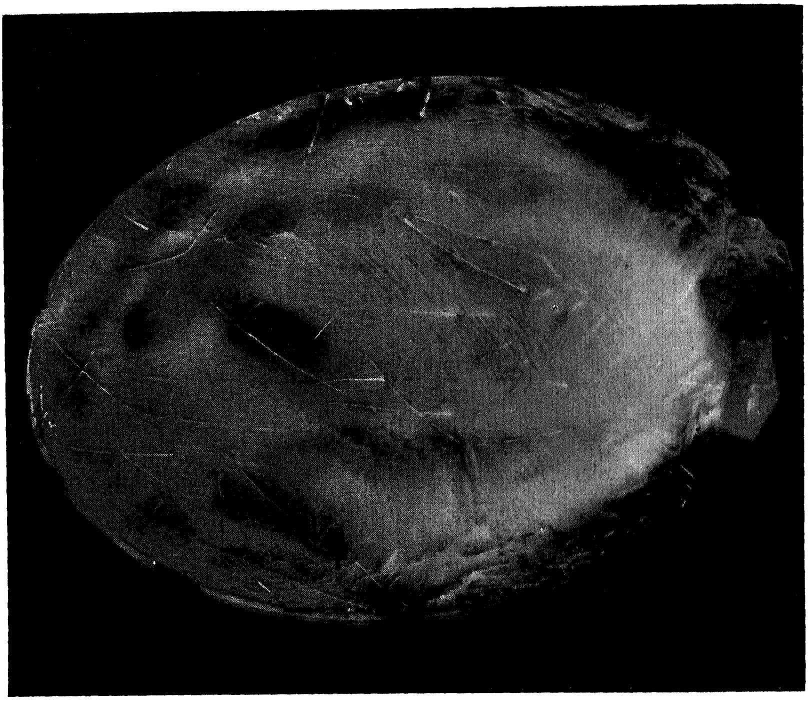

Magnaflux Corporation

Fig. 14. Indications of superficial scratches in a lens. Indications like these rarely resemble true crack indications.

Scratch indications are almost always delineated by a shadowed area at the end of a crack, and the indications are extremely difficult to keep in place during powder application. The best technique is to apply the powder in one quick burst and not to attempt to build up the indications, since they invariably blow away before an appreciable size is gained.

Brittle-coating Tests. A recent development has permitted the use of electrified particles in conjunction with the brittle-coating stress analysis method. Heretofore it has been difficult to locate cracks in the brittle coating except by essentially destructive means. Electrified-particle techniques used in conjunction with brittle-coating techniques have opened up whole new areas of experimental techniques by permitting the nondestructive location of the stress-indicating cracks in the stress-sensitive brittle coatings. (See section on Brittle-Coating Tests.)

Bibliography

Betz, C. E. "Two New Testing Methods for Ceramic Products," *Nondestructive Testing,* 7, No. 2 (1948): 22.

Cowan, R. E. "Sonic Method for Measuring Young's Modulus of Elasticity of Porcelain Enamel-Metal Composites," *Finish,* 12, No. 4 (1955): 40, 62.

Cox, J. E., and A. I. Andrews. "A Study of Hairlining," *J. Am. Ceram. Soc.,* 37 (1954): 186.

Dugger, E. "The Application of Statiflux for Nondestructive Inspection of Nonconducting Materials," *A.F. Tech. Rept.,* No. 5898 (1949).

"Electrified Particle Nondestructive Test," *Report on the State of Research and Application of Nondestructive Testing in the U.S. and Canada to the International Conference on Nondestructive Testing of Material, Brussels, Belgium, May 1955.* MP-10. Evanston, Ill.: Society for Nondestructive Testing, 1955.

Howe, E. E. "Special Techniques in Enameling," *Proc. Ann. Porcelain Enamel Inst.,* 15 (1953): 109.

Huppert, P. A. "Lithium Compounds in Porcelain Enamel Compositions," *Finish,* 4, No. 6 (1947): 18.

Hutchinson, C. "NST Testing Correlated with Shipping Performance Can Reduce Damage Losses," *Finish,* 9, No. 8 (1952): ST-5.

Jackson, H. J. "Ceramic Stress Coating," *Machine Design,* 26 (1954): 184.

McIntosh, R. O. "Hermetic Seals," *Elec. Mfg.,* 49, No. 4 (1952): 120, 328, 330, 332, 334.

McMaster, R. C. "Nondestructive Testing," 26th Edgar Marburg Lecture, *Am. Soc. Testing Materials, Proc.,* 52 (1952): 617.

McMaster, R. C., and S. A. Wenk. "Nondestructive Testing of Engineering Materials and Parts," *Materials & Methods,* 33, No. 2 (1951): 81.

Mould, R. E. "The Behavior of Glass Bottles Under Impact," *J. Am. Ceram. Soc.,* 35 (1952): 230.

Orr, S. C. "Methods for Testing for Enamel Coating Discontinuities," *Better Enameling,* 22, No. 12 (1951): 16, 31.

Petersen, F. A., T. DeForest, and H. N. Staats. "A New Method for Locating Cracks in Ceramic Materials," *Finish,* 5, No. 3 (1948): 17.

Petersen, F. A., R. A. Jones, and A. W. Allen. "A New Method for Studying Fractures of Porcelain Enameled Specimens," *J. Am. Ceram. Soc.,* 31 (1948): 186.

Pierce, J. J. "Ultramodern Supersonics and X-Rays," *Metal Progr.,* 56 (1949): 62.

Pingel, M. E. "Torsion Testing as an Aid in Process Control," *Proc. Ann. Porcelain Enamel Inst.,* 14 (1952): 139.

"Powder Finds Flaws in Liner Coatings," *Appliance Mfr.,* 1, No. 4 (1954): 1.

Singdale, F. N. "Brittle Coatings for Use in Stress Analysis Under Varying Temperature Conditions," *Nondestructive Testing,* 11, No. 6 (1953): 37.

Staats, H. N. "A New Tool for Locating Defects in Non-Conductive Coatings," *Corrosion* (in press).

———. "Detecting Cracks in Glass-to-Metal Seals," *Electronics,* 28, No. 3 (1955): 284.

———. "Gunning for Bottle Defects," *Brewers Dig.,* 30, No. 10 (1955): 58.

———. "Observations on the Nature of Cracks in Porcelain Enamel," *Am. Ceram. Soc. Bull.,* 31, No. 2 (1952): 33.

———. *Principles of Stresscoat, A Manual for Use with the Brittle Coating Stress Analysis Method.* Chicago: Magnaflux Corp., 1955. P. 19.

———. "The Testing of Ceramics," *Nondestructive Testing,* 10, No. 3 (1952): 23.

———. "Which Nondestructive Test for Finding Defects in Ceramic Parts," *Materials & Methods,* 36, No. 3 (1952): 116.

STAATS, H. N., and S. J. BARANOWSKI. "Calibrated Porcelain Enamel Coatings," *Am. Ceram. Soc. Bull.,* 35 (1956): 143.

"Symposium on Accelerated Durability Testing of Bituminous Materials," *Am. Soc. Testing Materials, Spec. Tech. Publ.,* 94 (1950).

Symposium on Electromagnetic Relays, Oklahoma Institute of Technology. Princeton, Ind.: Potter & Brumfeld, 1954. P. 13.

SECTION 30

MAGNETIC-PARTICLE TEST PRINCIPLES

CONTENTS

PAGE

Magnetic Fields

Principle of test 1
  Capabilities and limitations 1
  Operational requirements 1
  Magnetic-field principles 2
Description of magnetic fields 2
    Magnetic-field path in a horseshoe magnet (*f.* 1) 2
  Magnetized ring 2
    Magnetic-field path in a ring magnet with air gap (*f.* 2) 2
    Magnetic-field path in a closed, magnetized ring (*f.* 3) 3
  Effect of cracks in magnetized ring 3
    Magnetic particles attracted to a radial crack in a circularly magnetized part (*f.* 4) 3
  Bar magnet 3
    Straightening a horseshoe magnet results in a bar magnet (*f.* 5) 4
  Effect of cracks in magnetized bar 3
    A crack in a bar magnet creates magnetic poles which attract magnetic particles (*f.* 6) 4
Magnetization with electric current 4
  Circular magnetization 4
    Circumferential magnetic field surrounding a straight conductor carrying an electric current (*f.* 7) 4
    Circular magnetization of a test piece through which a magnetizing electric current passes (*f.* 8) 5
  Circular magnetization of solid parts 5
    Circular magnetization of typical forms of test object (*f.* 9) 5
  Circular magnetization of hollow parts 6
    Circular magnetization of cylindrical parts by use of a central current-carrying conductor (*f.* 10) 6
  Longitudinal magnetization 6
    Longitudinal or coil magnetization (*f.* 11) 7
  Coil magnetization 6
  Cable magnetization 6

Methods of Magnetization

Controlling factors 7
Alloy, shape, and condition of part 7
Type of magnetizing current 8
  Direct-current magnetization 8
  Half-wave rectified magnetizing current 8
  Alternating-current magnetization 8
Direction of magnetic field 8
  Circular magnetization 8
  Passing current through the entire part 9
  Prod magnetization of large parts 9
  Central conductor magnetization 9
  Limitations of parallel magnetization 9
  Longitudinal magnetization 9
  Important considerations in coil magnetization 10
    Coil magnetization of a wheel-like part (*f.* 12) 10
  Yoke magnetization 10
    Longitudinal magnetization of a test part by means of an external magnetizing yoke (*f.* 13) 11
Swinging-field magnetization 11

Test Procedures

Sequence of operations 11
  Continuous-field method of inspection 12
  Residual-field method of inspection 12
Value of flux density 12
  Current requirements for circular magnetization 13
  Optimum current magnitudes 13
  Current requirements for longitudinal magnetization 13
  Influence of length/diameter ratio 13
  Formula for correct ampere-turns 14
    Typical coil shot currents (amperes) for a five-turn coil (*f.* 14) 14
  Current requirements for flexible cable magnetization 14

Inspection Materials and Their Preparation

Types of magnetic particles 15
Wet bath materials 15
  Instructions for mixing the oil bath for the wet method 15
    Bath capacity of magnetic-particle equipment (*f.* 15) 16
    Required oil characteristics (*f.* 16) 16
  Bath strength 16
  Instructions for checking bath strength 16
    After 30 minutes of settling time, the bath strength is indicated by the volume of settled particles read on the scale at the bottom of the centrifuge tube (*f.* 17) .. 17

CONTENTS (*Continued*)

PAGE
  Selection of wet method paste 17
  Advantages of fluorescent particles 18
Water suspension pastes 18
Particles for the dry method 18
  Application of dry particles 18
  Mechanical powder blower 19
  Other means of applying powder 19

Special Requirements for Fluorescent Inspection

Black light requirements 19
  Influence of power supply voltage 19
  Checking light intensity 19
The inspection area 19
  Dark adaptation of inspector 20

Principles of Demagnetization

Residual magnetism 20
Reasons for requiring demagnetization 20
Causes of magnetization 20
Longitudinal and circular residual fields 21
Basic principle of demagnetization 21
  Magnetic hysteresis 21
    Typical hysteresis curve (*f.* 18) 22
  Use of diminishing a.-c. fields 22
    Diminishing hysteresis curve resulting from the alternate reversal and reduction of the applied field (*f.* 19) 23
Retentivity and coercive force 22

PAGE
Methods of demagnetization 22
  A.-c. coil demagnetization 23
    Manually operated a.-c. coil demagnetizer complete with roller carriage and automatic timing switch (*f.* 20) 24
    Alternating-current coil demagnetizer incorporated into a conveyorized unit for magnetic-particle inspection (*f.* 21) 24
  Reversing d.-c. demagnetization 25
  A.-c. circular field demagnetization 25
  A.-c. and d.-c. yoke demagnetization 25

Methods for Measuring Leakage Field Intensities

Types of measurements 25
Field indicator 26
    Typical field indicator (*f.* 22) 26
  Indications 27
  Procedure 27
Compass indicator 27
Steel-wire indicator 27
Limitations with circularly magnetized parts . 27
  Checking demagnetization 28
Demagnetization problems 28
  Shielding by magnetic shunting 28
  Small parts having a small length/diameter ratio 28
  Demagnetizing-coil field strength apparently too weak 28
  Fugitive magnetic poles 28
Bibliography 29

SECTION 30

MAGNETIC-PARTICLE TEST PRINCIPLES

Magnetic Fields

PRINCIPLE OF TEST. Magnetic-particle inspection is a nondestructive means for detecting discontinuities in ferromagnetic materials. It consists of three **basic operations:**

1. Establishing a suitable magnetic field in the test object.
2. Applying magnetic particles to the surface of the test object.
3. Examining the test-object surface for accumulations of the particles (indications), and evaluating the serviceability of the test object.

Capabilities and Limitations. The method can detect all discontinuities at the surface, and under certain conditions, those which lie completely under the surface. It depends upon the magnetic properties of the test objects and is suitable only for metallic materials which can be intensely magnetized. **Nonferromagnetic materials,** which cannot be strongly magnetized, cannot be inspected by this method. Such materials include aluminum, magnesium, brass, copper, bronze, lead, titanium, and austenitic stainless steels. With suitable **ferromagnetic materials,** magnetic-particle inspection is highly sensitive and produces readily discernible indications on the surface of the test parts. A trained inspector can, by examining the nature, location, and extent of the indications, interpret their causes and evaluate the discontinuities causing the indications.

Operational Requirements. Parts should be clean before they are subjected to magnetic-particle inspection. The ability of the method to provide indications depends upon the ability of the **magnetic particles** to move in response to leakage magnetic fields which appear at the surface of the test objects where discontinuities are present. During application the particles may be suspended in air (dry method) or in liquids such as oil or water (wet method). If parts are inspected by the wet method, all dirt, grease, oil, rust, and loose scale must be removed; otherwise it may be difficult or impossible to produce indications of discontinuities or defects. Random dirt, grease, and oil may wash from the part, contaminating the inspection liquid. Rust and loose scale may also contaminate the inspection medium or act as electrical insulators to prevent proper electrical contact for magnetization of the part. The same requirements for cleanliness apply to parts to be inspected with the dry powder technique, but in addition, the parts must be dry. **Oil, grease, or water** will cause the dry powder to stick to the surface of the test object, preventing formation of indications. **Plating on parts** will not interfere with magnetic-particle inspection, provided it is less than 0.004 in. thick. Any part made of ferromagnetic material can be inspected by the magnetic-particle method; there are no restrictions as to the shape and size of the part.

Magnetic-Field Principles. It is essential for reliable inspection that the fundamental principles of the magnetic-particle method be clearly understood, and that the method be properly applied. If improper techniques are used, some discontinuities may be missed and defective parts may be accepted by the inspector. With a useful and dependable inspection method, it is not enough to find defects; the inspector must be sure that all the defects the specific test method can reveal have been located and evaluated. For this reason the nature of magnetic fields and the basic principles of magnetic-particle inspection are described in an elementary way in the subsequent text.

DESCRIPTION OF MAGNETIC FIELDS. The magnetic-particle inspection method utilizes magnetic fields to reveal material discontinuities. **Ferromagnetism** is the property of some metals, chiefly iron and steel, to attract other pieces of iron or steel. The common horseshoe magnet will attract magnetic materials to its ends or poles. **Magnetic lines of force, or flux,** flow from the south pole through a magnet to the north pole, as shown in Fig. 1. Magnets will attract other magnetic material only where the magnetic lines of force leave or enter the magnet. When magnetic material is placed across the poles of a horseshoe magnet, the lines of force flow from the north pole of the magnet through the material to the south pole (Fig. 1). Magnetic lines of force will flow preferentially through magnetic material rather than nonmagnetic material or air.

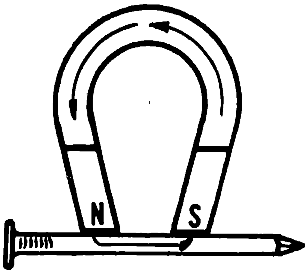

Fig. 1. Magnetic-field path in a horseshoe magnet.

Magnetized Ring. If the horseshoe magnet is bent so that its poles are close together, as shown in Fig. 2, the poles still attract magnetic materials. Iron filings or other **magnetic particles** will cling to the poles and bridge the gap between them. If the poles are fused together, the magnetic lines of force will be enclosed within the ring (Fig. 3). No external poles will exist, and magnetic

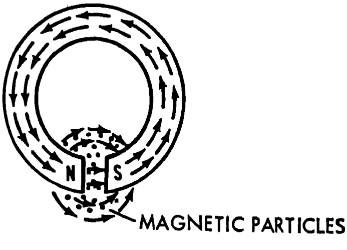

Fig. 2. Magnetic-field path in a ring magnet with air gap.

particles dusted over the ring will not be attracted to the ring even though there are magnetic lines of force flowing through it. Magnetized materials attract externally only when poles exist. A ring magnetized in this manner is said to contain a **circular magnetic field** which is wholly within the part.

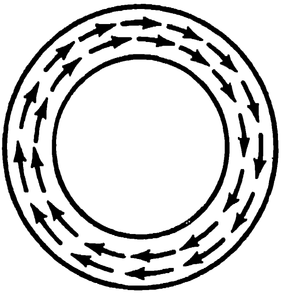

Fig. 3. Magnetic-field path in a closed, magnetized ring.

Effect of Cracks in Magnetized Ring. Any radial crack in a circularly magnetized piece will create a north and a south magnetic pole at the edges of the crack. This will force some of the magnetic lines of force out of the metal path. These are called **leakage flux.** Magnetic particles will be attracted to the poles created by such a crack, forming an **indication** of the discontinuity in the metal part (Fig. 4). This is the principle of forming magnetic-particle indications by means of **circular magnetization.**

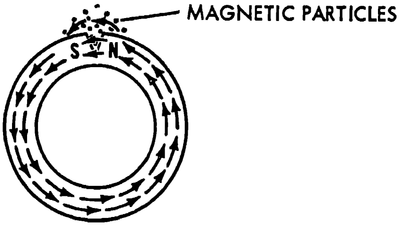

Fig. 4. Magnetic particles attracted to a radial crack in a circularly magnetized part.

Bar Magnet. When a horseshoe magnet is straightened, it becomes a bar magnet. A bar magnet has **poles** at each end. Magnetic lines of force flow through the bar from the south pole to the north pole (Fig. 5). Magnetic particles are attracted to any location where flux lines emerge and particularly to the ends of the magnet where the concentration of flux lines is greatest. Since the magnetic lines of force within a bar magnet run the length of the bar, it is said to be **longitudinally magnetized** or to contain a **longitudinal field.**

Effect of Cracks in Magnetized Bar. A crack in a bar magnet (Fig. 6) distorts the magnetic lines of force and creates poles on either side of the crack. These poles will attract magnetic particles to form an **indication of the crack.** The strengths of poles formed at a crack depends on the number of magnetic lines of force interrupted. A crack at right angles to the magnetic lines of force

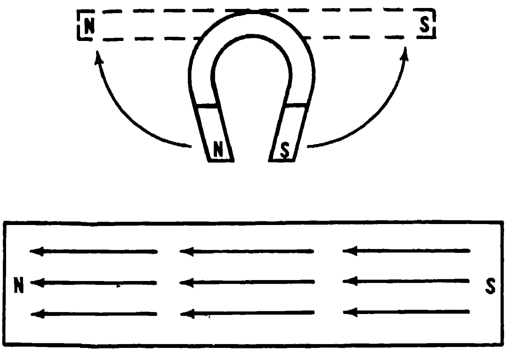

Fig. 5. Straightening a horseshoe magnet results in a bar magnet. Lines of magnetic flux pass through the magnet from its south to its north pole.

interrupts more lines of force and creates stronger poles than a crack more nearly parallel to the lines of force. **Indications of maximum size** are formed when the magnetic lines of force are at right angles to discontinuities.

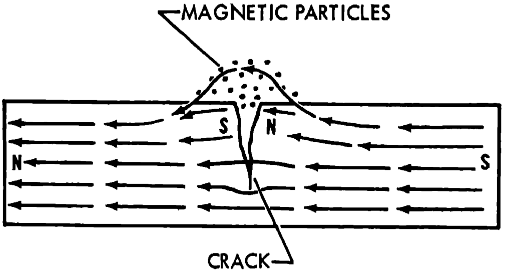

Fig. 6. A crack in a bar magnet creates magnetic poles which attract magnetic particles.

MAGNETIZATION WITH ELECTRIC CURRENT. Electric currents are used to create or induce magnetic fields in magnetic materials. Since it is possible to alter the directions of magnetic fields by controlling the direction of the magnetizing current, the arrangement of current paths is used to induce the magnetic lines of force so that they are at right angles to a discontinuity in the test object.

Circular Magnetization. Electric current passing through any straight conductor such as a wire or bar creates a **circular magnetic field** around that conductor, as shown in Fig. 7. The magnetic lines of force are always at right angles to the direction of the current which induces the magnetic field.

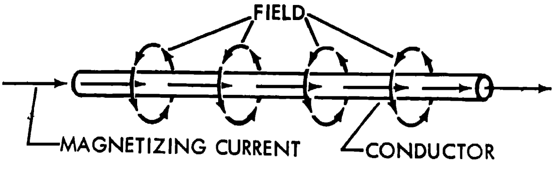

Fig. 7. Circumferential magnetic field surrounding a straight conductor carrying an electric current.

To remember the direction taken by magnetic lines of force around a conductor, imagine that the conductor is grasped with the right hand so that the thumb points in the direction of the current flow. The fingers then point in the direction taken by the magnetic lines of force in the magnetic field surrounding the conductor. This is known as the **right-hand rule.** When a conductor of electric current is a magnetic material, the passage of current induces a magnetic field in the conductor as well as in surrounding space. A piece magnetized in this manner is said to have a **circular field** or to be **circularly magnetized** (Fig. 8).

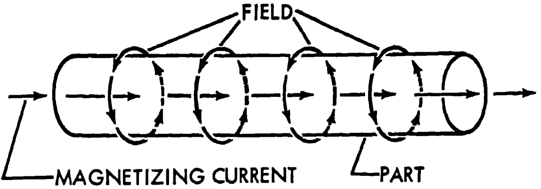

Fig. 8. Circular magnetization of a test piece through which a magnetizing electric current passes.

Circular Magnetization of Solid Parts. To induce a circular field in a part, current is passed through the part, as shown in Fig. 9(a). This sets up a circular

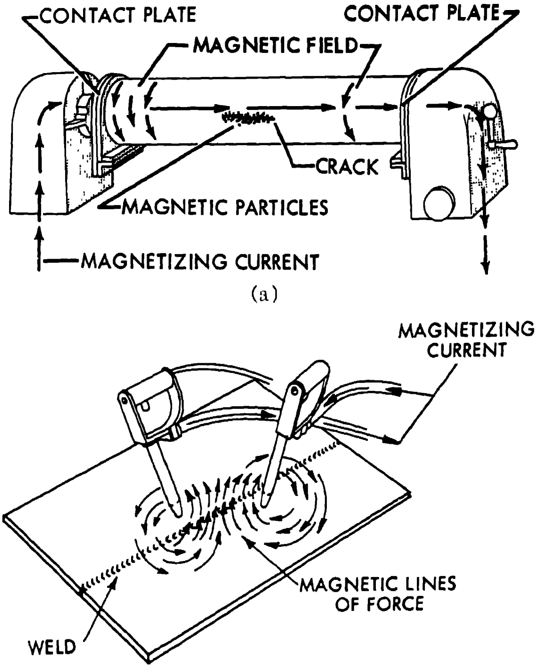

Fig. 9. Circular magnetization of typical forms of test object. (a) Circular magnetization of test object by passing electric current through part from machine contact plates. (b) Production of localized circular field in part by passing electric current between contact prods.

magnetic field in the part, which creates poles on both sides of any **crack or discontinuity** parallel to the length of the part. These poles will attract fine magnetic particles and form an indication of the discontinuity. It is also possible to induce a circular field in localized areas of the part by using **cables and prods** or contacts to pass current through the area being inspected [Fig. 9(b)].

Circular Magnetization of Hollow Parts. With hollow or tubelike parts the inside surfaces may be as important to inspect as the outside. When such parts are circularly magnetized by passing the magnetizing current through the part, a satisfactory magnetic field is not produced on the inside surface. Since a magnetic field surrounds a current-carrying conductor, it is possible to induce a satisfactory magnetic field by sliding the part on to a **central copper bar or conductor** (Fig. 10). Passing current through the bar induces a circular magnetic field on both inside and outside cylindrical surfaces of the tubelike part.

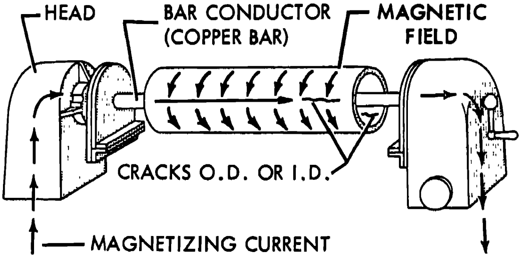

Fig. 10. Circular magnetization of cylindrical parts by use of a central current-carrying conductor.

Longitudinal Magnetization. Electric current can also be used to create a **longitudinal magnetic field** in magnetic materials. When electric current is passed through a **coil** of several turns, a magnetic field is established lengthwise or longitudinally within the coil (Fig. 11). The nature and direction of this field are the result of the field around the conductor which forms the turns of the coil. Application of the right-hand rule to the conductor at any point in the coil illustrated in Fig. 11(a) shows that the field within the coil is lengthwise, as indicated.

Coil Magnetization. When magnetic material is placed within a coil, the magnetic lines of force created by the electric current concentrate themselves in the part and induce a longitudinal magnetic field as indicated in Fig. 11(b). Inspection of a cylindrical part with longitudinal magnetization is shown in Fig. 11(c). With a **transverse discontinuity** in the part, magnetic poles are formed on both sides of the crack. These poles will attract magnetic particles to form an indication of the discontinuity. A comparison of Fig. 11(c) with Fig. 9(a) shows that in both cases a magnetic field has been induced in the part which is at right angles to the defect. This is the most desirable condition for reliable inspection.

Cable Magnetization. Parts too large to fit in a fixed coil can be magnetized longitudinally by making a coil of several turns of **flexible cable.** The use of **portable magnetizing equipment** with cables and prods has immeasurably broadened the use of magnetic-particle inspection, since there is no limit to the size of the part which can be inspected in this manner. It may be necessary to magnetize and inspect small areas sequentially, to cover a large surface area with **prod magnetization.**

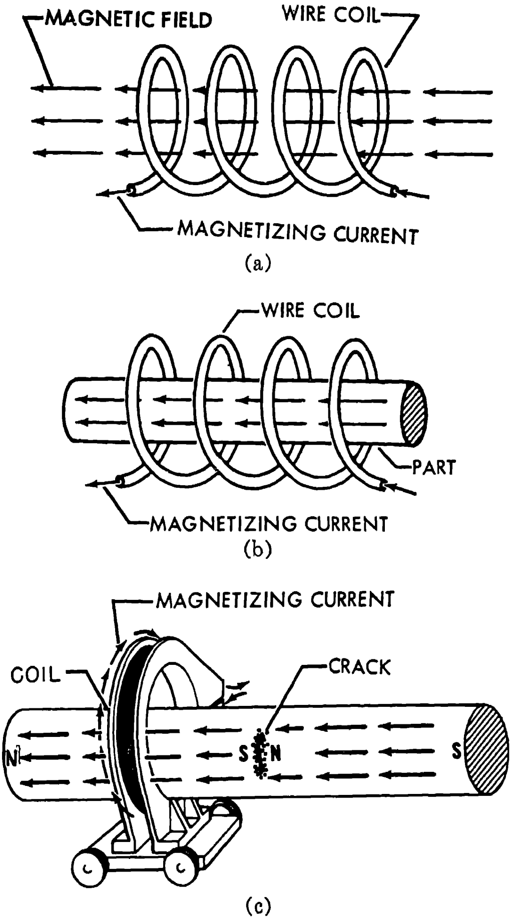

Fig. 11. Longitudinal or coil magnetization. (a) Longitudinal magnetic field within a current-carrying magnetizing coil. (b) Longitudinal magnetization of test object with coil. (c) Typical arrangement of coil and test object for longitudinal magnetization.

Methods of Magnetization

CONTROLLING FACTORS. Five factors must be considered in selecting the method of magnetization: (1) alloy, shape, and condition of part; (2) type of magnetizing current; (3) direction of magnetic field; (4) sequence of operations; and (5) value of flux density.

ALLOY, SHAPE, AND CONDITION OF PART. The particular alloy, heat treatment, cold working, and other factors determine the **permeability** of a part, i.e., the ease with which it can be magnetized. It is necessary to consider the nature of the alloy in connection with selection of the sequence of operations and the value of **flux density** or **magnetic-field intensity.** These, in turn, affect selection of the magnetization method. The size and shape of the part determine the most practical method of magnetization with the available equipment. The condition of the part, especially the **surface condition,** influences the selection of the magnetization method. Surface conditioners such as Dulite, Parkerizing, and lacquer coatings are poor electrical conductors, and therefore it is impossible to pass magnetizing current through such coatings. If parts so treated can be adequately magnetized in a coil or with a central conductor, they can be inspected without removing such coatings.

TYPE OF MAGNETIZING CURRENT. Many types of magnetizing current can be used, of which only one is best for each type of inspection.

Direct-Current Magnetization. Direct current (d.c.) obtained from storage batteries was first believed to be the most desirable current to use, since direct current penetrates more deeply into test specimens than alternating current. The big disadvantage of **storage batteries** as a source of current is that there is a definite limit to the magnitude and duration of current which can be drawn from the battery before recharging. Battery maintenance is costly and can become a source of trouble. Direct current obtained through **dry-plate rectifiers** from a.-c. power lines is similar to battery current and has the advantage of permitting an almost unlimited number of magnetizing current "shots." Current obtained by passing three-phase alternating current through special rectifiers is called **three-phase rectified alternating current.** It is most commonly used in wet horizontal units for any general magnetic-particle inspection and is equal to direct current.

Half-Wave Rectified Magnetizing Current. Half-wave rectified alternating current is the most effective current to use for the detection of subsurface and surface defects when **dry magnetic particles** are used. This type of current is produced by rectifying single-phase alternating current. Half-wave rectified current imparts a very noticeable pulse to the particles. This gives them mobility and aids in the formation of indications.

Alternating-Current Magnetization. Alternating current (a.c.) at line frequency is the most effective current to use for the **detection of surface discontinuities,** particularly fatigue cracks. It is important that a.-c. inspection equipment be built to include proper current controls. An advantage of a.-c. inspection is the ease with which parts so inspected can be demagnetized.

DIRECTION OF MAGNETIC FIELD. Of the five factors involved in determining inspection techniques, the most critical is the direction of the magnetic field. The proper orientation of the magnetic field in the part, in relation to the direction of the defect, is a more important factor than the magnitude of the magnetizing current. For reliable inspection the magnetic lines of force should be at right angles to the defect to be detected. If the magnetic lines of force are parallel to the defect, there will be little magnetic leakage at the defect. If any indication is formed, it is likely to be extremely small or indefinite.

Circular Magnetization. The magnetizing method which is easiest to control in most parts is circular magnetization. This is the method in which the magnetizing current is passed directly through the part, setting up circular magnetic lines of force at right angles to the direction of current flow.

Passing Current Through the Entire Part. When the parts can be placed between the contact plates of stationary magnetic-particle inspection equipment, this is the best way to magnetize the part circularly (see section on Magnetic-Particle Test Equipment). Care should be taken to clamp the part firmly between the soft lead **contact plates.** Enough surface area of the part must make contact with the plates to permit passage of the magnetizing current without burning the part. As the area of surface contact decreases, the probability of burning increases. On irregular parts it is helpful to use **copper-braid contact pads** between the part and plates, to prevent overheating. When inspecting parts with irregular cross-section, it may be necessary to magnetize circularly with a low current to inspect the thin areas, and then devise some method of passing a higher current through the heavier section for inspection of that area.

Prod Magnetization of Large Parts. When the part is too big to fit into available stationary equipment, or if only portable equipment is available, then the part or areas of the part can be circularly magnetized by either of two methods. One method is to use **prod contacts** with cables to transmit the magnetizing current from the source to the part [see Fig. 9(b)]. Prods are attached to the ends of the cables so that magnetizing current can be passed through the part or through an area of the part. **Portable equipment** should have a remote control switch to enable the operator to turn the current on and off while moving the prods or viewing the work. **Contact clamps** can be used with cables instead of prods, particularly when the parts are relatively small in diameter. Tubular structures can be inspected by positioning the clamps so that the current passes through the suspected area and along the line of suspected discontinuities.

Central Conductor Magnetization. When a circular magnetic field is set up in a tubular part by passing current through the tube itself, a satisfactory field is not induced on the inside surface of that tube. If the part is hollow or has holes through which a central conductor can be passed, it is best to induce a circular magnetic field in that part by passing the magnetizing current through the conductor. Circular magnetization with a central conductor has the following **advantages** over passing current through the part itself:

1. It induces a field on the inside diameter of the part, permitting inspection of inner as well as outer surfaces.
2. Direct electrical contact is not made with the part, thereby eliminating the likelihood of burning.
3. Several parts, like washers or nuts, can be suspended on the same conductor and inspected in groups.

Limitations of Parallel Magnetization. The magnetic principle underlying circular magnetization with a central conductor is based on the fact that there is a circular magnetic field surrounding any electrical conductor. Knowing this fact, some operators have assumed that they can induce a circular field in a part by placing it next to instead of around a conductor. This is not true. Some field is induced in the part by such a procedure, but since a portion of the path of the magnetic flux is in air and some through the part, the field in the part is greatly reduced, distorted, and unevenly distributed. This procedure is sometimes called "parallel" magnetization. It is not dependable and should not be used.

Longitudinal Magnetization. A longitudinal field can be induced in a part by placing the part in a fixed current-carrying coil, mounted either on the rails of a stationary unit or attached by cables to a portable unit. The **effective magnetic field** induced in a part by a coil extends from 6 to 9 in. beyond either end of the coil. If the part is long, it will be necessary to magnetize and inspect it in sections along the length of the piece. Longitudinal magnetization with portable equipment is accomplished by wrapping current-carrying cable in coil fashion around the part.

Important Considerations in Coil Magnetization. To induce an adequate longitudinal magnetic field with a coil, the long dimension of the part should be at least twice as great as its short dimension, and the long axis of the part should be parallel to the coil axis. This is especially true in the case of **irregularly shaped parts,** since the shape of the part affects the direction of the induced field. Take, for example, the case of a wheel-like part. If such a part is placed in a coil, as illustrated in Fig. 12, a field will be induced in the white areas of the part in such a direction that **radial defects** would create indications. However, radial cracks in the shaded areas of the part will be parallel (or nearly so) to the induced magnetic field, so that few or no indications will be formed. To indicate radial defects in the shaded areas, it would be necessary to rotate the part through 90 deg. and remagnetize it. The detection of radial cracks in a part of this type is more positively and rapidly done by the use of a central conductor.

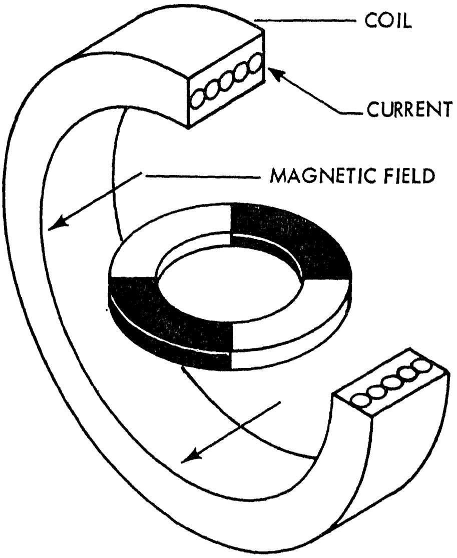

Fig. 12. Coil magnetization of a wheel-like part. Radial defects will be indicated only in **white** areas shown. To reveal radial defects in the **dark** areas, the part must be rotated through 90 deg. and remagnetized.

Yoke Magnetization. A longitudinal magnetic field can be induced in a part, or in an area of a part, by means of a yoke. A **yoke** is a C-shaped piece of soft magnetic material, either solid or laminated, around which is wound a coil carrying the magnetizing current (Fig. 13). When a part is placed across the opening of the C-shape and the coil is energized, the part completes the path of the magnetic lines of force. This sets up a longitudinal field in the part between the ends of the C-shape. **Permanent magnet yokes** can also be used to create a magnetic field.

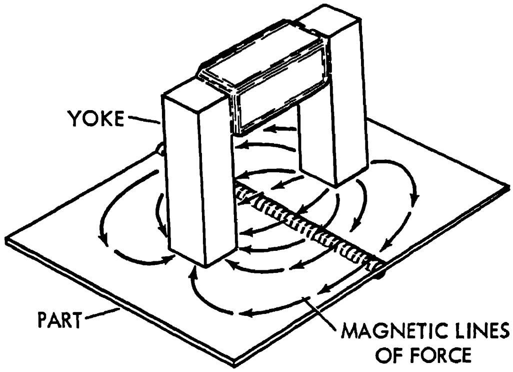

Fig. 13. Longitudinal magnetization of a test part by means of an external magnetizing yoke.

SWINGING-FIELD MAGNETIZATION. For complete inspection for defects oriented in different directions in a part, **two or more magnetizations** and inspections are necessary. First the part should be circularly magnetized and inspected; then, longitudinally magnetized and inspected. Usually the part should finally be demagnetized. If the shape of the part is complicated, it may be necessary to use more than the two magnetizing operations to be sure that all areas have been properly magnetized.

Defects are shown best when they are at right angles to the magnetic lines of force. Also, the effective field induced by a coil on a long part extends only 6 to 9 in. beyond either end of the coil; therefore a long part, say, 3 ft. long, should be given at least two magnetizing shots along its length.

On certain parts it is possible, by using specially designed equipment, to apply two or more magnetizing currents simultaneously to the part in order to find defects in all directions. This creates a so-called swinging field. Such equipment shortens inspection time considerably, but application of the technique is critical and it should be used only under close control and observation by qualified personnel. Inspection employing swinging fields can be performed best on equipment designed for this purpose and for specified test objects.

Test Procedures

SEQUENCE OF OPERATIONS. The magnetic field is strongest while magnetizing current is flowing. When the current is cut off, the field drops to a lower value, its residual strength. If the part is of hard steel with a high carbon content, the **residual magnetic field** existing after current ceases to flow will be relatively strong but still weaker than when current was flowing. If the material is soft steel, the residual field will be too weak to attract particles and indicate cracks or defects. For **greatest sensitivity** the particles should be present on the part and under the influence of the magnetic field while magnetizing current is flowing.

Continuous-Field Method of Inspection. When the particles are applied to the part while the magnetizing current is flowing, the technique is known as the continuous method. With the **wet continuous method,** the inspection bath is liberally applied to all surfaces of the part, care being taken to be sure that all surfaces are wet. The instant that the bath stream is removed from the part, the **magnetizing shot** is applied. This ensures that the particles will be on the part while the current is flowing, so they can be attracted to any leakage fields created by discontinuities. If wet bath is applied during or after the magnetizing shot, there is a possibility that the force of the bath stream may wash away lightly held indications. For this reason the shot should always be given immediately after the bath flow is stopped.

When the **dry continuous method** is used, the part is magnetized by using prods, clamps, or a coil. While the current is flowing, powder is applied in a light cloud to magnetized areas. **Excess powder** is blown off with a light air stream. After excess powder is removed, magnetizing current is shut off. It is important that powder be applied as a light cloud and not simply dumped on the surface. The operator should watch the inspected area carefully as the powder is being applied, since it is usually easy to see indications form even before excess powder is removed. If the current flow is stopped before the excess powder is blown off, it is possible that **lightly held indications** will be removed.

Residual-Field Method of Inspection. When the residual field left in parts is high, it may be sufficiently strong to form adequate indications. However, residual fields are always weaker than magnetic fields present when magnetizing current is flowing. Consequently inspection with the residual method will not be so sensitive as the continuous method. When using the **wet residual method,** the length of time that the part is covered by the inspection bath is of importance. Long exposure of a magnetized part to the wet bath increases the build-up of magnetic particles forming the indication. It is usually difficult to indicate **subsurface defects** when using the residual method. This fact is sometimes used to determine whether an indication is showing a defect on the surface or beneath the surface. To determine this, the indication formed by the continuous method is wiped off, and the bath or powder is reapplied. If the indication returns, it usually means a surface discontinuity.

VALUE OF FLUX DENSITY. The strength of the magnetic field induced in a part is often referred to as the flux density. The proper value of flux density, or strength of field, must be determined for each part. Factors which affect the strength of field include the test-object size, shape, and material. **Field strength** is one of the factors which determine the success of magnetic-particle inspection. A field that is either too weak or too strong will create too little or too much leakage at discontinuities. However, the direction of the magnetic field is more important than the flux density.

The behavior of the magnetic particles on the surface of a part during magnetization provides an excellent indication of the strength of the induced magnetic field or of the amount of magnetizing current being used. This is particularly true when dry powder is used, but it is also noticeable with the wet method. With dry powder **a field that is too strong** will frequently cause particles to adhere tightly to the surface and hinder their mobility. In fact it may sometimes prevent their moving to a defect and may cause them to actually stand on end, parallel to the lines of force. On the other hand, when no pattern is observable while the current is applied, it is frequently an indication that **insufficient magnetizing current** is being used. The use of over-strong magnetic fields may not only mask sought-for defects but may also produce strong leakage fields at projections, off-sets, corners, or angles. This may cause an excessive number of particles to adhere at such locations. Removal of these accumulations may be so difficult as to require special cleaning operations, even after demagnetization.

Usually, observing the **particle pattern,** particularly where it can be easily observed (as with dry powders), is as satisfactory a guide to proper flux density as is the ammeter reading.

Current Requirements for Circular Magnetization. Only enough current should be used to show the indications of sought-for defects. If the magnetizing current is too strong, it may bring out things which are not important to the inspection. The best gage of magnetizing current strength is to **retest sample parts** with typical indications which can be checked from time to time.

Optimum Current Magnitudes. It is difficult to assign arbitrary current values for a certain size of part. The value for optimum results is affected by the **magnetic characteristics of the metal, shape and configuration of the part,** and the **type and severity of discontinuities** which are present. The current values used for overhaul inspection should be lower than those used when inspecting for subsurface discontinuities, since in the overhaul of most equipment, only fatigue or other surface cracks are usually sought. The **recommended current value** for the inspection of new aircraft parts during or just after manufacture is from 600 to 800 amp. per linear inch of section thickness when circularly magnetized with direct current. Inspection of other parts may require as little as 400 amp. per inch; optimum value for a part should be determined by experimentation. For example, using these standards, if a cylindrical part is 1 in. in diameter, one should pass from 600 to 800 amp. through it. The **length of the part** does not affect this determination except that the electrical resistance of a long part may reduce the current magnitude. If the part is 2 in. in diameter, 1200 to 1600 amp. should be used for magnetization. If exceptionally **heavy accumulations of particles** occur, particularly at abrupt changes in section, the current should be reduced. The proper direction of the magnetizing current and concentration of particles are as critical for reliable inspection as the magnitude of the magnetizing current. This does not mean that the magnitude of magnetizing current is not important, but rather that there are other factors which are equally important.

Current Requirements for Longitudinal Magnetization. Extensive laboratory tests confirmed by mathematical analyses have recently provided a sound basis for determining the proper current to be used when a part is to be longitudinally magnetized in a coil. This replaces the older and unreliable rule of thumb which has been in wide use previously. For example, a current of 1000 amp. through a five-turn coil creates a magnetizing force of 5000 ampere-turns.

Influence of Length/Diameter Ratio. For reliable **d.-c. coil magnetization (longitudinal),** the part to be magnetized should be shaped so that its length is at least two or three times as great as its diameter. This relationship is referred to as the **length/diameter, or *l/d*, ratio.** Knowing the *l/d* ratio and the number of turns in the coil, it is possible to determine accurately the required current for coil shots, providing the following conditions are met:

1. Cross-sectional area of part is not greater than one-tenth the area of the coil opening.

2. Part or section of part to be magnetized is no more than 18 in. long.
3. Part is held against the inside wall of coil and not positioned in center of coil.
4. Part has an l/d ratio between 2 and 15.
5. Part is positioned in coil with its long axis parallel to the applied field (coil axis).

Formula for Correct Ampere-Turns. If all the above conditions are met, then the formula for determining correct number of ampere-turns can be stated as

$$\text{Ampere-turns} = \frac{45{,}000}{l/d} \tag{1}$$

To use the formula, the l/d ratio is reduced to a number and divided into 45,000. The result will be the number of ampere-turns necessary to magnetize the part properly. The number of ampere-turns obtained should then be divided by the number of turns in the coil to give the correct current in amperes. These calculations apply only to parts not exceeding 18 in. in length. For **parts longer than 18 in.**, the same calculation is used, but a separate magnetizing shot is given for each 18 in. of its length. An example of the calculation of the coil shot for a part 8 in. in length and 2 in. in diameter is

$$l = 8, d = 2$$

Therefore

$$l/d = 8/2 = 4$$

$$\text{Ampere-turns} = 45{,}000/4 = 11{,}250$$

If the coil has five turns, then

$$\text{Magnetizing current} = 11{,}250/5 = 2{,}250 \text{ amp.}$$

Fig. 14 shows other examples.

Part Length (in.)	Part Diameter (in.)	l/d Ratio	Ampere-Turns Required	Amperes Required
8	4	2	22,500	4500
12	3	4	11,250	2250
12	2	6	7,500	1500
16	2	8	5,625	1125
10	1	10	4,500	900
18	1½	12	3,750	750
14	1	14	3,214	643

Fig. 14. Typical coil shot currents (amperes) for a five-turn coil.

Current Requirements for Flexible Cable Magnetization. The correct flux density is easier to determine when using portable equipment because it is possible, with the use of prods or clamps for circular magnetization, to vary the current setting on the equipment and also the space between the prods. Too heavy a particle accumulation between the points of contact is called **banding.** Banding indicates that the field strength is too great and should be reduced by lowering the current setting on the equipment or by increasing the space between the prods. On **large parts** the use of from 600 to 800 amp. with a prod spacing of from 6 to 8 in. is found to be most effective.

A **longitudinal field** is usually created with portable equipment by wrapping a cable around the part. The effective field strength is measured in ampere-turns and is the product of the current and the number of turns. When using d.c., the more turns of cable, the stronger the field, but with a.c. there is a limit to the number of turns which will increase the flux density. Three to five turns is generally the best number. Since the **effective field of a coil** extends only 6 to 9 in. beyond either end of the coil, long parts require several successive shots along the part. If the powder accumulation on the ends of a longitudinally magnetized part is too heavy, it may prevent good inspection. Such heavy accumulations indicate that the current should be reduced.

Inspection Materials and Their Preparation

TYPES OF MAGNETIC PARTICLES. Two classes of magnetic particles are available, depending upon the vehicle or carrying agent used. The wet method particles use a liquid vehicle; the dry method particles are borne by air. These particles are not ordinary iron filings but are made of carefully selected magnetic materials of proper size, shape, magnetic permeability, and retentivity. They are colored to give good color contrast with the surface being inspected. The **wet particles** are best suited for the detection of fine surface discontinuities such as fatigue cracks. They are commonly used in stationary equipment where the bath can be used until contaminated. It is possible to use wet particles in field operations with portable equipment, but care must be taken to agitate the bath constantly. This means that the spray applicator used to apply the bath should be shaken regularly to keep the particles in suspension. **Dry particles** are most sensitive for use on very rough surfaces and for detecting defects beneath the surface. They are usually used with portable equipment. Reclaiming and re-using dry particles is not recommended.

WET BATH MATERIALS. The particles used in the wet method are ground in oil and are obtained from the manufacturer as a thick paste. The paste must be completely dispersed in a liquid bath of proper consistency, color, and flash point. **Magnetic paste** for the wet method is available in black-, red-, and fluorescent-particle coatings. These pastes are equally sensitive in most applications for forming indications at areas of magnetic leakage. The selection of a particular **paste color** depends upon the visibility or contrast of the paste on the part and the required inspection speed. Magnetic particles are available for suspension in vehicles other than oil. It is extremely important that these particles be used in accordance with manufacturers' recommendations and in equipment designed for their use.

Instructions for Mixing the Oil Bath for the Wet Method. Cleanliness of the equipment and bath is vital for reliable inspection. Special attention should be given to cleanliness as well as accuracy in proceeding with the following steps:

1. Before mixing a new bath, the equipment should be cleaned thoroughly. Remove and clean agitator pipe. Clean other pipes in the unit and the tank, pump, and strainer.
2. Weigh or measure paste into a clean container. Measure out 1½ oz. per gallon of oil.
3. After tank and hose have been thoroughly cleaned, close all drain cocks and add oil in quantities recommended by the equipment manufacturer. This amount varies with different suppliers. Fig. 15 may be used as a guide. The oil used in preparing the bath should be a light, well-refined petroleum distillate

Equipment Length, Maximum Possible Distance Between Contact Plates (in.)	Gallons of Oil To Be Used
48	8
54	10
72	12
96	15
144	25

Fig. 15. Bath capacity of magnetic-particle equipment.

of low sulfur content, should be treated for odor, and should have a relatively high flash point. It should have the characteristics indicated in Fig. 16. Excessive viscosity makes it more difficult to form indications. If the flash point is too low, a distinct fire hazard exists. If the color is incorrect, the oil may mask fine indications. If the sulfur content is too high, the odor at the inspection station will be disagreeable, and contact with the oil may cause excessive irritation to the skin of the operator.

Viscosity [kinematic at 100° F. (38° C.)]	3 centistokes (max.)
Flash point (tag closed cup)	135° F. (57° C.) (min.)
Initial boiling point	390° F. (199° C.) (min.)
End point	500° F. (260° C.) (max.)
Color (Saybolt)	Plus 25
Low sulfur available (Copper test: ASTM—D129-52)	

Fig. 16. Required oil characteristics.

4. Add a little oil from the tank to the paste in the container and mix thoroughly. Continue to add oil to the container and stir until a thin mixture is obtained.
5. Turn on pump motor in equipment and pour paste and oil mixture from container into the equipment tank. Run pump for several minutes, rinsing out any sediment from the container with the hand hose.
6. Test for proper bath strength and adjust as necessary.

Caution: Never add magnetic paste directly from the can into the equipment tank. Always mix paste with oil in a separate clean container. Paste added directly from its shipping can to inspection equipment will not disperse in the bath and can clog the system and make inspection unreliable. Wet-method bath for use in spray applicators should also be mixed with care. The mixing and storing container should be kept clean. Always stir or shake thoroughly before filling the spray applicator.

Bath Strength. The number of magnetic particles per gallon of fluid in the inspection bath is called its strength or **concentration.** If the bath strength is not at the proper level, inspection cannot be reliable. Even when the proper processing techniques are used with the correct amount of magnetizing current, no indications will form if a sufficient concentration of particles is not present in the bath. If there are too many particles in the bath, indications may be masked.

The **usable limits of bath concentration** are very broad, but for consistent results the bath strength should be the same at all times. Deep cracks will usually form good indications with a light bath strength, but a heavier particle concentration will show up fine defects better. The bath concentration which will best detect all defects should be determined and maintained constant. The bath strength should be checked daily.

Instructions for Checking Bath Strength. Check the bath strength every day as follows:

1. Let pump motor run for several minutes to agitate a normal mixture of particles and oil.
2. Flow the bath mixture through hose and nozzle for a few moments to clear hose.
3. Fill a 100-c.c. centrifuge tube to the 100-c.c. line with fluid from the inspection bath.
4. After 30 min., read the volume of the settled particles on the scale at bottom of centrifuge tube. For black or red paste the reading should be from 1.5 to 2.0 c.c., while for fluorescent paste the reading should be from 0.2 to 0.4 c.c., as indicated in Fig. 17. Do not include dirt particles in centrifuge tube readings.
5. If reading is higher than allowable, add oil to bath. Repeat centrifuge tube test if in doubt about the bath strength after making addition.

The bath should be changed regularly, once each week in production or up to once a month if it is not contaminated or if inspection volume is low.

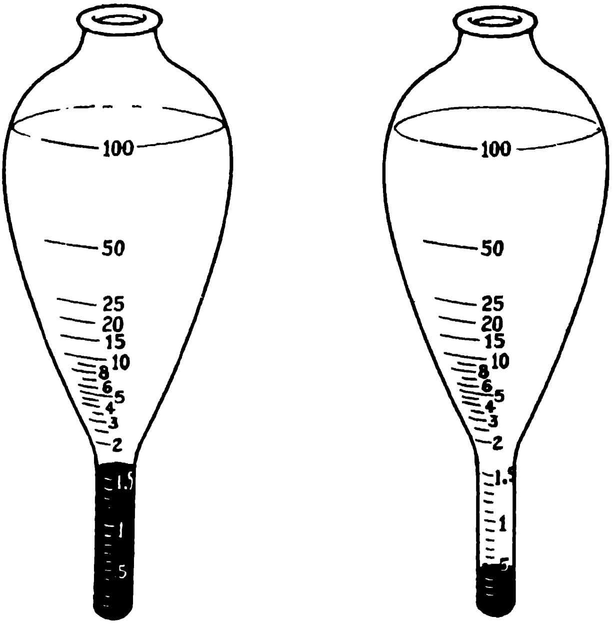

Fig. 17. After 30 min. of settling time, the bath strength is indicated by the volume of settled particles read on the scale at the bottom of the centrifuge tube. For black or red pastes the reading should be from 1.5 to 2 c.c. For fluorescent paste the reading should be from 0.2 to 0.4 c.c. for proper particle concentration.

Selection of Wet Method Paste. Since the particles available for the wet method are equally sensitive in most applications, the selection depends upon the type of particles which provide greatest contrast to the surface inspected.

Black- or red-paste indications are viewed under ordinary light. Adequate daylight is optimum. The **fluorescent-paste particles** must be viewed under near-ultraviolet, or "black light," of adequate intensity, and the equipment or inspection area must be darkened to cut off normal light.

Advantages of Fluorescent Particles. The main advantage of fluorescent particles is increased visibility. In some experiments fluorescent-magnetic indications have been found to be 100 times more easily visible than black- or red-particle indications. This increased visibility permits a lighter concentration of paste in the fluorescent magnetic-particle bath. Since fluorescent particles are easily visible, it takes fewer to form an indication, and it is easier to detect weak leakage fields. Fluorescent particles are ideal on **threaded parts and coil springs.** With threaded parts there is frequently a leakage field at the thread root which may attract particles that mask or cover true defects. Since there are fewer fluorescent particles in the bath, this masking effect is reduced considerably. Coil springs are difficult to inspect because of their shape. Care must be taken to view all surfaces. When fluorescent particles are used on coil springs, indications attract the attention of the inspector.

For **high speed and high volume inspection,** fluorescent indications permit inspection speeds as much as six to ten times those possible when particles are viewed under white light.

WATER SUSPENSION PASTES. Red, black, and fluorescent pastes are available for suspension in water. It is extremely important that these particles be used in accordance with manufacturers' recommendations and in equipment designed for their use. The use of water reduces the fire hazard present with oil suspensions and also reduces probabilities of dermatitis. The fluorescent paste for use with water is extremely sensitive for fine discontinuities and produces a minimum of background fluorescence.

The disadvantages of water suspensions should be considered before using them. Water may corrode the inspection equipment as well as the parts inspected. Sometimes water suspensions do not readily wet the part and some areas may not get any magnetic particles. Wetting agents are added to offset this condition, but excessive additives may cause foaming. It is more difficult to keep a water bath at optimum balance and to maintain the correct viscosity. Evaporation and freezing are factors that must be considered. The possibility of water damage to electrical components is the reason that water suspensions should be used only in equipment built for that purpose.

PARTICLES FOR THE DRY METHOD. The particles used in the dry method are in the form of a powder. They are available with red, black, gray, and fluorescent coatings. The magnetic properties and particle size are similar in all colors, making them equally efficient. The choice of powder is then determined only by which powder will give the best contrast on the test objects.

Application of Dry Particles. Dry particles depend upon air to carry them to the surface of the part, and care must be taken to apply them correctly. The particles should float to the inspected surface as gently as possible and not be thrown against it forcibly. As they float to the magnetized surface, the particles are free to be influenced by magnetic leakage fields and form indications. **Powder forcibly applied** is not equally free to be attracted by leakage fields. Rolling a magnetized part in powder or pouring the powder on the part is not recommended. When dry particles are used, it is important to watch the magnetized area as the particles are applied to it, when the indications can be seen to form.

Mechanical Powder Blower. One of the best ways to apply dry powder is by specially designed, mechanical powder-blowers. The air stream of such blowers is of the low velocity necessary to apply a cloud of powder to the test area. Mechanical blowers can also deliver a light stream of air to blow off excess powder gently.

Other Means of Applying Powder. Powder can also be applied with small **rubber spray bulbs** or **shakers.** In all cases of powder application it is important that a gentle cloud of powder be applied to the area being inspected.

Special Requirements for Fluorescent Inspection

BLACK LIGHT REQUIREMENTS. The fluorescent coating on the magnetic particles is most brilliant when viewed under near-ultraviolet light of sufficient intensity, of a specific **wavelength** (3650 Å). This wavelength is between the visible and ultraviolet in the spectrum and is usually considered as noninjurious to the skin or eyes. Illumination must be of proper intensity and wavelength, or the effectiveness of the inspection will be greatly reduced. The approved **light source** for producing black light is a 100-watt, reflector-spot-type of **mercury-vapor bulb.** This bulb operates from 110-volt, 60-cycle, single-phase, alternating current and requires a special transformer. A special **filter** is fastened to the front of the mercury-vapor bulb to absorb visible light and to pass only light of the proper wavelength required for inspection. **Cracked or broken filters** should be replaced immediately. The filter and face of the bulb should be cleaned regularly so that dust and dirt do not reduce transmission of black light.

Influence of Power Supply Voltage. Lamps used in black lights are very sensitive to fluctuations in power line voltage, and frequently a small percentage of **line voltage drop** may cause the bulb to be extinguished. It is recommended that the circuits which supply the black lights have a constant voltage. If necessary a **constant-voltage transformer** should be used in the circuit.

Checking Light Intensity. As a general rule, black lights of the recommended type emit light of sufficient intensity for average inspection as long as they still function. **Black light intensity** of 90 to 100 foot-candles is suitable for the detection of all indications. This intensity is obtained with a normal 100-watt, reflector-spot, mercury-vapor bulb at a distance of 15 in. from the face of the bulb. If indications are heavy and broad, a light intensity of 20 to 25 foot-candles may be sufficient.

The **test for light intensity** should be made with a Weston Sight Light Meter No. 703, Type 3 (unfiltered), equipped with a 10X multiplier disc or equivalent. To measure intensity, the bulb should be equipped with a regular black-light filter. Care should be taken to see that bulb and filter are clean. To read the light intensity correctly, the meter should face the light source at the distance normally used for inspection.

THE INSPECTION AREA. When using fluorescent particles, the inspection area should be free from **random fluorescent materials,** since these are likely to confuse the inspector. The operator may experience clouding of vision if black light is permitted to shine directly or reflect into the eyeball. This **cloudy sensation in the eye** disappears when such illumination ceases. Because it is a somewhat disagreeable sensation, it is desirable to arrange the lights in the inspection area so that neither direct nor reflected light shines into the inspector's eyes.

Dark Adaptation of Inspector. For best results with fluorescent particles, the inspection should be done in a darkened area. The darker the area of inspection, the more brilliant the indication. Dark adaptation from bright, white light to levels necessary for reliable fluorescent magnetic inspection may require several minutes. The inspector should become adapted to the darkened area before starting inspection. He should also avoid going from the dark booth to lighted areas and back again without allowing sufficient adaptation time.

Principles of Demagnetization

RESIDUAL MAGNETISM. Parts fabricated from ferromagnetic material retain a certain amount of residual magnetism (or remanent field) after exposure to a magnetizing force. The **magnitude of field retained** by a part is dependent upon the

1. Magnetic characteristics of the particular material.
2. Strength of applied magnetizing force.
3. Direction of magnetization (longitudinal or circular).
4. Geometry of the part.

Demagnetization of ferromagnetic material in industry is limited to reducing the degree of magnetization to an acceptable level, since **complete demagnetization** is usually impractical.

REASONS FOR REQUIRING DEMAGNETIZATION. Careful consideration should be given to whether or not parts require demagnetization. There are four basic reasons for requiring demagnetization.

1. When subsequent machining or an arc-welding operation is to be performed on the part, a strong residual field in the part may interfere. The field may attract and hold chips or particles to the surface of the part and adversely affect surface finish or cutting action. In arc welding, the presence of strong residual fields may deflect the arc.
2. Subsequent operation of the part may be impaired if its leakage field is excessive. The attraction of chips or particles to rotating parts may cause malfunctions, especially with bearings and bearing surfaces. Strong residual fields are a source of excessive friction between moving parts; for instance, between a piston and cylinder wall.
3. The leakage fields emanating from a part may interfere with instrumentation. Even slightly magnetized aircraft parts may cause the magnetic compass of an airplane to read erroneously.
4. The presence of a residual field may hamper removal of chips or particles during subsequent cleaning operations.

Unless at least one of the above rules is applicable, demagnetization may be unnecessary.

CAUSES OF MAGNETIZATION. A ferromagnetic part can become magnetized in many ways, such as the following:

1. The earth's magnetic field can impart a fairly strong residual field to many parts. This usually occurs when a part is shocked or vibrated while its long axis is parallel to the earth's field. Such residual magnetization may become quite significant for long parts subjected to severe vibrations in service. The intensity (horizontal component) of the earth's field in the United States is

approximately 0.2 oersted, equivalent to the field intensity at the center of a five ampere-turn coil, 12 in. in diameter.

2. Frequently parts become magnetized when subjected to an electric arc-welding operation.
3. Parts are purposely magnetized in magnetic-particle inspection.
4. Parts operating or stored in close proximity to high-current electric circuits often acquire residual magnetization.
5. Accidental contact with the pole of a permanent magnet or other highly magnetized objects may produce a residual field in a part.
6. Magnetic chucks are another source of residual fields. Strong residual fields may be left if a part is removed from the chuck before the demagnetizing cycle has been completed. Sometimes the method of demagnetizing the chuck may be inadequate and leave the part partially magnetized.
7. Low-frequency induction heating can induce very strong residual fields in a part.

LONGITUDINAL AND CIRCULAR RESIDUAL FIELDS. The existence of a residual field is much more evident on parts magnetized in the **longitudinal direction.** This is due to the relatively high concentration of external fields (lines of magnetic flux entering and leaving the part) associated with longitudinally magnetized parts. These conditions of magnetization are easily detected by indicating devices and by the attraction of other magnetic parts or particles. Therefore this type of residual field is usually most objectionable; however, it is also the most responsive to demagnetization.

Unlike longitudinal residual fields, the circular residual field exhibits little or no external evidence of its existence. The field is almost entirely confined to the part itself, depending somewhat upon part geometry and method of magnetization. For example, if current has passed through a homogeneous piece of ferromagnetic bar stock having a circular cross-section, the resulting residual field is, for all practical purposes, undetectible without altering the bar in some manner. Virtually no **leakage fields** emanate from its surface, since the magnetic flux path is closed upon itself within the part. The **internal residual field** is much stronger than if the part had been magnetized longitudinally by a coil (or solenoid) having comparable field intensity. Since there is very little leakage flux associated with circular fields, they are not so objectionable as longitudinal residual fields. **Demagnetization** of a circularly magnetized part can be very difficult. Reorientation of the circular field into a longitudinal field before demagnetization may be advantageous in some instances.

BASIC PRINCIPLE OF DEMAGNETIZATION. Ferromagnetic materials retain a certain amount of residual magnetism after being subjected to a magnetizing force. When the magnetic domains of a ferromagnetic material have been oriented by a magnetizing force, some domains remain so oriented until an additional force in the opposite direction causes them to return to their original random orientation. This force is commonly referred to as **coercive force.**

Magnetic Hysteresis. This is graphically illustrated by the **hysteresis curve** of Fig. 18. It may be assumed from Fig. 18 that the residual field (B_r) could be reduced to zero simply by subjecting the residually magnetized material to a field intensity equal to H_c in the opposite direction of magnetization. Theoretically this is a valid assumption, but it is not a practical method of demagnetization. It is not practical because H_c is a variable which is dependent upon a number of **factors,** such as the type of material, geometry of the part, homogeneity, hardness, and the intensity of the field which originally magnetized the part. However, a slight modification of this method does make it quite practical.

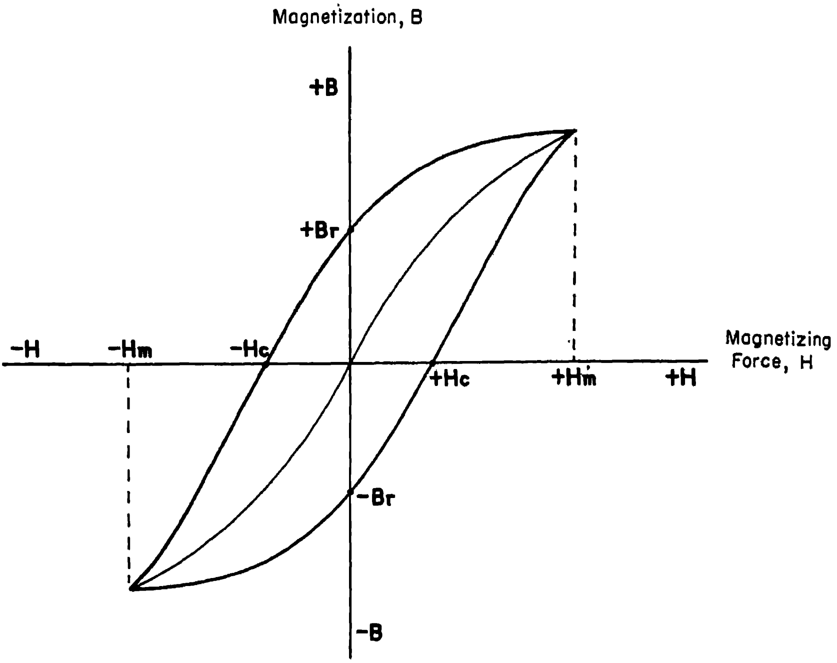

Fig. 18. Typical hysteresis curve.

Use of Diminishing A.-C. Fields. The coercive force H_c is always less than the magnetizing force H_m. Therefore, if a part is subjected to a magnetizing force initially greater than H_c, which is alternately reversed in direction while being gradually reduced in magnitude, H_c and B_r will also be reduced in magnitude. Both H_c and B_r will eventually approach zero, as shown in Fig. 19. **Intentionally overshooting** H_c with each reversal can eliminate the guesswork associated with the theoretically possible, single-shot demagnetizer. This principle is the basis for practically all demagnetizing methods used today.

RETENTIVITY AND COERCIVE FORCE. As a general rule, high coercive forces are associated with harder materials and low coercive forces with softer materials. Therefore **hard materials** usually offer more resistance to demagnetization and require more intense demagnetizing fields than softer materials. The fact that a part retains a strong residual field (B_r) is not necessarily indicative of a high coercive force (H_c), since some materials retain appreciable residual fields and yet are very easily demagnetized. On the other hand, some materials which retain only a relatively weak residual field can be extremely difficult to demagnetize because of their high coercive force.

METHODS OF DEMAGNETIZATION. Practically all demagnetizing methods in use today are based upon a common procedure. This is the application of a magnetizing force of sufficient intensity to overcome the initial coercive force (H_c), and which is alternately reversed in direction and gradually reduced in magnitude. There is one exception which should be mentioned. A part can be demagnetized by raising its temperature above the **Curie point** (approximately

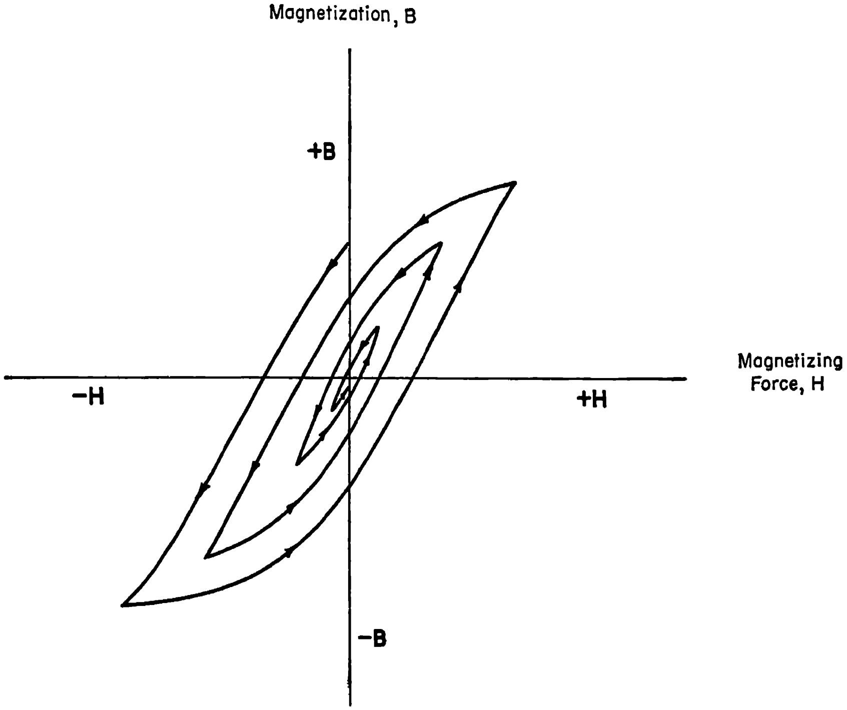

Fig. 19. Diminishing hysteresis curve resulting from the alternate reversal and reduction of the applied field.

1200° F. to 1600° F., depending upon the particular material). Although this method will probably result in the most thorough demagnetization, it leaves much to be desired in the way of convenience and practicability.

A.-C. Coil Demagnetization. An a.-c. coil is the most common method of demagnetization. The coil is usually designed to operate at line voltage and frequency (usually 60 c.p.s.). When a part is placed in the coil, it is subjected to a reversing field due to the cyclic action of the current. The magnitude of the field can be gradually reduced by slowly withdrawing the part from the coil, or the part can be held stationary while the coil is being withdrawn. The coil should not be de-energized until the part has been withdrawn to a position beyond the influence of the coil field. This method is advantageous for high production rates, since a properly designed coil can be energized continuously while a steady stream of parts is conveyed through the coil opening. Typical a.-c. coil demagnetizers are shown in Figs. 20 and 21.

Modified versions of this method are sometimes employed. The reduction in field intensity is often obtained by reducing the current to the coil in a predetermined manner while the part remains within the coil until the current has been reduced to zero. Current control is achieved by various means, such as a saturable reactor or an autotransformer in conjunction with a tap switch.

The a.-c. coil method is sometimes ineffective on large parts, due to lack of penetration, since the a.-c. magnetic field is confined fairly well to the surface

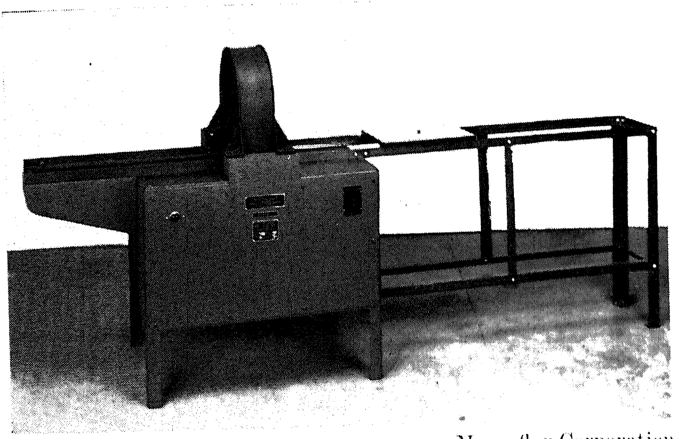

Magnaflux Corporation

Fig. 20. Manually operated a.-c. coil demagnetizer complete with roller carriage and automatic timing switch.

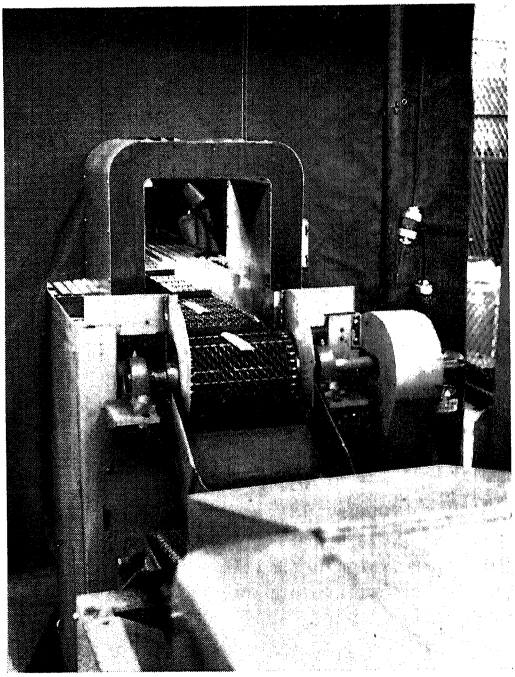

Magnaflux Corporation

Fig. 21. Alternating-current coil demagnetizer incorporated into a conveyorized unit for magnetic-particle inspection.

of the part by the currents induced within the part itself. The higher the frequency, the more pronounced the skin effect.

To minimize the **effects of the earth's field,** particularly with long parts, the demagnetizing coil should be oriented with the central axis pointing east and west. Normally, best results are obtained if the long axis of the part is parallel to the coil axis.

Reversing D.-C. Demagnetization. In demagnetization with reversed direct current, the desired magnetic field is obtained by means of a coil or passage of current through the part itself. The direct current is alternately reversed in direction and reduced in amplitude. If a coil is used, the part is left in the coil until the demagnetizing cycle has been completed. This method provides **deep penetration** and is usually very effective on parts that are difficult to demagnetize. Usually, ten reversals and reductions in current will provide satisfactory results. However, more reliability can be attained by utilizing a greater number of reversals and reductions in current (approximately 30).

A.-C. Circular Field Demagnetization. Demagnetizing with an a.-c. circular field is similar to the a.-c. coil method, in that the field reversal is provided by the cyclic nature of the current. However, in this case, the desired field is obtained by passing current through the part. The magnitude of the current is systematically reduced to zero by some suitable device. This method is usually employed on rather large parts, just after they have been inspected by the magnetic-particle method. Some inspection units have **built-in devices for the systematic reduction of current,** and it is found to be convenient to demagnetize bulky parts before they are removed from the unit.

A.-C. and D.-C. Yoke Demagnetization. Yokes are used primarily for demagnetizing small parts having very high coercive forces. They are C-shaped and are usually designed for demagnetization of a specific type of part. Some a.-c. yokes are similar in operation to the a.-c. coil method whereby the part is passed between the pole faces (maximum field intensity) and then withdrawn. A modified version of this is a **solenoidal electromagnet** which is light enough to be passed over the surface of a part; however, its effectiveness is limited to a few special cases.

Direct-current yokes are usually based upon the reversing d.-c. method; however, some designs utilize a damped oscillation to obtain the required reversing and diminishing field. The oscillation is derived from a circuit containing capacitance, inductance, and resistance. Design of the circuit is usually based upon a specific part. In general, d.-c. yokes probably provide the deepest penetration of any method.

Methods for Measuring Leakage Field Intensities

TYPES OF MEASUREMENTS. Leakage field intensities can be measured by quantitative or comparative methods. Quantitative measurements usually involve the use of instruments, such as D'Arsonval-type meter movements, in conjunction with search coils or probes (see section on Magnetic-Field Test Principles). Such instruments are often classified as laboratory equipment and require competent laboratory personnel for their operation. As a general practice, leakage field intensities are measured by the comparative method. A few of the methods employed are discussed in the subsequent text.

FIELD INDICATOR. The field indicator, a pocket instrument, is used to determine the relative intensity of leakage fields emanating from a part. The construction of a typical field indicator is shown in Fig. 22, and the theory of operation is quite simple. As indicated in Fig. 22, an elliptically shaped, soft-iron vane is attached to a pointer which has pivot points in top and bottom bearings. A rectangularly shaped, permanent magnet is mounted in a fixed position directly above the soft-iron vane. Since the soft-iron vane is under the influence of the magnet, it will align its long axis to correspond with the direction of the leakage field of the magnet. In so doing, the vane becomes magnetized and has a magnetic pole induced at each end of its long axis. On the end of the vane, which is below the south pole(s) of the magnet, a north pole will be induced. Correspondingly, a south pole will be induced at the other end of the vane, below the north pole of the magnet.

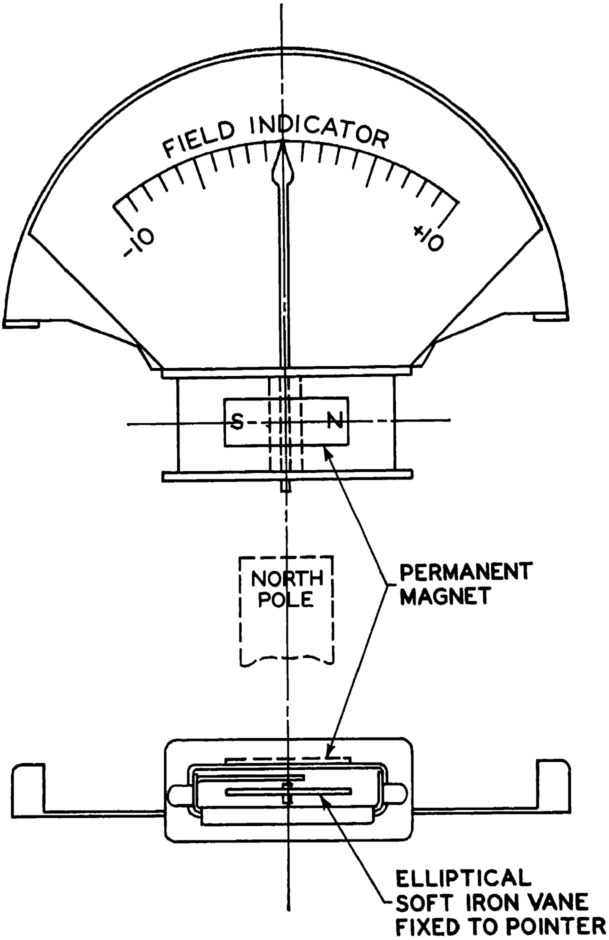

Fig. 22. Typical field indicator.

Indications. The pointer normally points to zero on the graduated scale, in the absence of external fields. When the magnetic north pole of a magnetized part is moved close to the pivot end of the pointer, the south pole of the vane will be attracted toward the part. The pointer will consequently move in the plus direction. The restraining torque is provided by the tendency of the vane to remain aligned with the leakage field of the permanent magnet.

Procedure. The relative intensity of a leakage field is measured by bringing the field indicator to the part and noting the deflection of the pointer. The edge of the field indicator case at the pivot end of the pointer should be closest to the part being investigated. For small parts it is sometimes advisable to place the instrument face up on a **nonferrous surface** and then slide the part up to the instrument. The required degree of demagnetization is usually specified as a **maximum field indicator reading** (perhaps 2.0 divisions). The readings obtained with a field indicator are relative units. However, having once determined the maximum allowable field, the field indicator can be used as a convenient comparator.

COMPASS INDICATOR. A compass is sometimes used for indicating the presence of external leakage fields. A compass is placed upon a nonmagnetic surface and a magnetized part (aligned due east and west) is moved slowly toward the east or west side of the compass case. The presence of an external leakage field from the part will cause the compass needle to deviate from its normal north-south alignment. However, demagnetized parts will cause the needle to deviate from its normal position if the compass case is not approached from an easterly or westerly direction. The theory of operation is very similar to that for the field indicator, the compass needle being a permanent magnet with a magnetic pole at either end. Restraining torque is provided by the tendency of the needle to align itself with the earth's north-south magnetic field. The sensitivity will depend upon the type of compass.

STEEL-WIRE INDICATOR. A piece of **iron or steel tag wire** can be fashioned into a fairly good detector when nothing else is available. By forming a loop at one end of a piece of tag wire approximately 6 in. long, it can be suspended from a second wire supported in the horizontal plane. The part in question is then brought into contact, near the free end of the vertically suspended wire. The presence of leakage fields will cause the wire to deviate from its normal vertical position as the part is slowly withdrawn in a horizontal direction. Care must be taken to demagnetize the vertically suspended wire between each test. Small pieces of tag wire about 1 in. long are sometimes used to indicate the presence of leakage fields. The piece of demagnetized wire is placed upon a horizontal nonmagnetic surface and the part in question is placed on top of it. If the piece of tag wire can be lifted off the surface as the part is slowly raised, the leakage fields are excessive.

LIMITATIONS WITH CIRCULARLY MAGNETIZED PARTS. It might be noted that all the methods mentioned pertain to the measurement or comparison of **external leakage fields** rather than internal residual fields. As mentioned before, circularly magnetized parts may possess strong residual fields with the (virtual) absence of any leakage fields. However, some circularly magnetized parts may exhibit objectionable leakage fields because of their geometry or method of magnetizing, such as an **off-center central-conductor shot.** The leakage fields from such parts may be very weak and defy detection without the aid of special equipment. Nevertheless, demagnetization may be required to prevent the attraction and holding of fine magnetic particles to the surface of the part.

Checking Demagnetization. Since circularly magnetized parts can be very difficult to demagnetize, merely going through the usual demagnetization operation does not necessarily mean that a part has been demagnetized. Some means of determining the effectiveness of the demagnetizing method should be employed. Similar parts that have been scrapped can prove to be very helpful in such situations. By magnetizing and demagnetizing them in the proposed manner, effectiveness of demagnetizing methods can in many cases be determined by sectioning the part at right angles to the known direction of magnetization. In so doing, the path of the circular residual field is interrupted, and any residual field will now be easily detectible in the form of a leakage field. For example, the **demagnetization of a bearing race** magnetized with a central-conductor shot can be checked by breaking or cutting the ring-shaped part into two pieces. The presence of a residual field will be evident in the form of leakage fields at all four exposed ends.

DEMAGNETIZATION PROBLEMS. Several situations listed here may prove helpful when demagnetization of parts becomes problematical.

Shielding by Magnetic Shunting. Whenever possible, a part requiring demagnetization should be demagnetized before being assembled with other parts. Occasionally demagnetization of a part is attempted after it has become part of an **assembly** and is adjacent to or surrounded by other magnetic materials. In such cases, the demagnetizing field may very well be shunted through the adjacent material rather than through the desired part, and demagnetization will be ineffective. **Small parts** should not be passed through a demagnetizing coil in bundles or heaped in baskets for the same reason. The parts in the center will be shielded from the demagnetizing field by the outer layer of parts. **Magnetic baskets or containers** may be objectionable for the same reason.

Small Parts Having a Small Length/Diameter Ratio. A demagnetizing field may be inadequate for small parts having a length-to-diameter (l/d) ratio less than three to one (3:1). This situation can usually be corrected by increasing the l/d ratio by the addition of **ferromagnetic pole pieces** at either end of the part. Pole pieces should be at least 6 in. long and approximately the same diameter as the part. With pole pieces at both ends, the part is passed through the demagnetizing coil in the usual manner. For large lots of such parts it is sometimes convenient to pass the parts through the demagnetizing coil, end to end in chain fashion.

Demagnetizing-Coil Field Strength Apparently Too Weak. The field intensity of a coil is a function of the coil diameter as well as of the applied ampere-turns. In general, the smaller the coil diameter, the more intense the field for the same applied ampere-turns. Therefore, the use of a smaller diameter coil of the same ampere-turn rating or greater may be advantageous. However, passing the part through the coil as close as possible to the inside wall may be all that is required, since the field intensity is greater there than at the center.

Fugitive Magnetic Poles. Occasionally attempts to demagnetize a part will result in chasing magnetic poles from one location on the part to another. This may be due to the particular geometry of the part or its orientation with respect to the demagnetizing field. This situation can usually be alleviated by **rotating the part** while it is within the influence of the demagnetizing field. In particular, ring-shaped parts such as bearing races can be rolled through an a.-c. coil to obtain the desired results.

The mere fact that a part has been passed through an a.-c. coil, or subjected to some other method of demagnetization, does not necessarily mean that the part has been suitably demagnetized. The results obtained by any method should be carefully evaluated before concluding that a given method is applicable to the particular part in question.

Bibliography

CAINE, J. B. "Magnetic Particle Inspection Standards," *Foundry,* 83, No. 12 (1955): 84.

CATLIN, F. S. "Testing Methods Valuable in Improving Casting Design," *Foundry,* 85, No. 3 (1957): 168.

CLARKE, J. E., R. A. PETERSON, and T. J. DUNSHEATH. "Automatic Inspection of Pipe," *Welding Engr.,* 36, No. 2 (1951): 38.

COX, R., and W. A. GARDNER. "Maintenance Is Key to Service Fleet Success," *Drilling,* 12, No. 5 (1951): 54.

DOANE, F. G., and C. E. BETZ. *Principles of Magnaflux.* 3d ed. Chicago: Photopress, 1948.

GILBERT, L., and W. B. BUNN. "Inspection Techniques for Quality Welding," *Welding J.,* 32 (1953): 614.

KELLY, S. G., JR. "New Magnetic Particle Testing Technique Speeds Inspection of Ferrous Parts," *Materials & Methods,* 33, No. 6 (1951): 66.

"Magnetic Particle Inspection," *Welding Handbook.* 3d ed. New York: American Welding Society, 1950. P. 957.

McCABE, J. L., and B. HIRST. "Use of Tap Water in Magnetic Particle Inspection," *Metal Progr.,* 70, No. 1 (1956): 77.

McCUTCHEON, D. M. "Testing, Inspection and Quality Control," *Metal Progr.,* 68, No. 3 (1955): 141.

MIGEL, H. "Magnetic Particle, Penetrant and Related Inspection Methods As Production Tools for Process Control," *Steel Processing,* 41 (1955): 86.

"Standardization Aids Weld Inspection of Tractors," *Welding Engr.,* 42, No. 4 (1957): 47.

THOMAS, W. E. "Economic Factors of Nondestructive Testing," *Nondestructive Testing,* 11, No. 4 (1953): 9.

———. "Magnaflux Inspection," *Proc. 29th Ann. Conv. Automotive Engine Rebuilders Assoc.,* May 7-9, 1951.

WILSON, T. C. "Nondestructive Testing of Refinery Equipment," *Petrol. Engr.,* 27, No. 7 (1955): C-16.

WOLDMAN, N. E. "Some Notes on Fatigue Failures in Aircraft Parts," *Iron Age,* 162, No. 24 (1948): 97.

SECTION 31

MAGNETIC-PARTICLE TEST EQUIPMENT

CONTENTS

PAGE

Selection of Equipment

- Range of available types 1
- Equipment selection considerations 1

Manual Inspection Equipment

- Small, low current units 2
  - Hand-held yoke 2
    - Hand-held electromagnetic yoke kit for magnetic particle inspection (*f.* 1) 3
  - Portable a.-c. prod and cable magnetizing unit 3
    - Magnetic particle crack detector with accessories in built-in tool box (*f.* 2) 4
  - Small kit for cable magnetizing 3
  - Medium unit for cable magnetizing 3
    - Medium cable magnetizing unit (*f.* 3) 5
- Medium and heavy duty equipment 4
  - Medium service a.-c. and half-wave unit .. 4
    - Combination a.-c. and half-wave magnetizing unit (2000-amp. output) (*f.* 4) 6
    - Ratings of a.-c. and half-wave units (*f.* 5) 6
  - Heavy-duty a.-c. half-wave unit with automatic demagnetizer 6
    - Combination a.-c. and half-wave magnetizing unit, 3000-amp. type with 30-point demagnetizing current control (*f.* 6) 7
  - Three-phase rectifier d.-c. unit 7
- Stationary equipment 7
  - Horizontal wet-method a.-c. units 8
  - Horizontal wet-method a.-c. units with automatic demagnetizer 9
    - Heavy-duty a.-c. wet-method magnetic particle inspection unit, for parts up to 96 in. long (*f.* 7) 8
  - Horizontal wet-type d.-c. units 9
  - Horizontal wet-type d.-c. units for very heavy parts 9
    - Horizontal d.-c., wet-method magnetic-particle inspection unit providing both longitudinal and circular magnetization, with 30-point demagnetizing switch (*f.* 8) 9
- Wheel-mounted wet-method units 10

Mechanized Inspection Equipment

- Semi-automatic inspection equipment 10
- Single-purpose semi-automatic equipment 10
  - Gas-turbine compressor blade test 10
    - Three-shot semi-automatic magnetic particle inspection unit (*f.* 9) 11
  - Conveyorized compressor blade test 11
    - Conveyorized magnetic-particle inspection unit providing three magnetizing shots at one station (*f.* 10) 12
  - Automatic inspection of steering spindles .. 12
  - Aircraft engine cylinder inspection 12
- Multi-purpose semi-automatic equipment 12
  - Automotive forgings test 12
    - Conveyorized magnetic-particle inspection unit providing head shot, coil shot, or both, as required (*f.* 11) 13
  - Conversion of hand-operated units 13
  - Inspection of automotive steering parts 13
- Fully-automatic, magnetic-particle test equipment 14
  - Photoelectric white-light scanner automatically locates and marks defective areas revealed by magnetic particles (*f.* 12) 14
- Equipment selection 15
- Demagnetizers 15
- Bibliography 15

SECTION 31

MAGNETIC-PARTICLE TEST EQUIPMENT

Selection of Equipment

RANGE OF AVAILABLE TYPES. More than fifty different varieties of standard magnetic-particle test equipment are available for industrial use. Over one hundred special-purpose types are used, and new designs are continually being developed to meet new needs. This variety in equipment for different uses, materials, methods, and techniques of magnetic-particle testing has developed because of wide industrial use and the flexibility inherent in the method. Over 3000 plants in hundreds of industrial groups that make or utilize magnetic materials, parts, or machinery in the United States currently employ magnetic-particle inspection.

EQUIPMENT SELECTION CONSIDERATIONS. Considerations involved in selection of magnetic-particle inspection equipment include:

1. **Type of magnetizing current.**
   - a. Alternating current (a.c.).
   - b. Direct current (d.c.).
   - c. Half-wave rectified current (h.-w.d.c.).
   - d. Multiple magnetizations (combination currents).
   - e. Permanent magnets.
2. **Location and nature of testing.**
   - a. Portable equipment. Portable magnetic-particle inspection equipment is taken to the inspection site. It is used to test large castings and weldments, assembled or welded structures, or parts of assemblies tested without disassembly.
   - b. Fixed equipment. Large or small test parts are brought to a fixed inspection station by conveyor, by plant truck, or by hand.
   - c. Production line. Inspection is part of the production line operation. Parts can be tested at any stage of manufacture, and handling can be automatic, semi-automatic, or manual. Either percentage sampling or 100 percent inspection may be done at one or more locations along the production line.
   - d. High volume, single part. Where parts of only one design are manufactured in high volume, specialized testing equipment may be best for minimum testing cost per part. An example is testing of automotive connecting rods at rates up to 2800 per hour on a two-shift basis.
   - e. High volume, various parts. In many plants, inspection of a variety of sizes and designs of parts results in very high volume on a single piece of test equipment. Eight, ten, or twenty different parts may be inspected on one piece of testing equipment in lots of several thousand each, at rates of several hundred or several thousand per hour.
   - f. Low volume, varying design and size of test objects. This test situation is similar to the preceding case (e), but volumes may be much lower. Also, in production job shops, the variety of part designs and sizes may be much greater, up to several hundred different parts.

   g. Combinations providing flexibility for changing conditions. Some test needs vary from time to time between two or more situations. For example, percentage production inspection may be carried out until excessively numerous defects are located. Then 100 percent testing is used until the cause of defects is again under control. Testing equipment in such situations must meet various needs.

3. **Test materials used.**
   a. Wet bath, visible.
   b. Wet bath, fluorescent.
   c. Dry powder applied manually or automatically.
4. **Purpose of test.**
   a. Maximum sensitivity. Maximum sensitivity inspection is used for parts which are extremely critical, whose failure would endanger human life or cause failure or breakdown of an entire equipment assembly. For such parts, 100 percent reliability must be assured, and maximum sensitivity may be required on all areas of the part.
   b. Controlled intermediate sensitivity. Over-inspection is to be avoided on many normal industrial products or consumer goods. In many cases very fine defects need be located only in limited, highly stressed areas on the parts. In some cases defects in one direction are serious, while those in another direction are of no consequence.
   c. Minimum sensitivity. In some parts of low critical nature or of heavy structure, only very severe cracks need be located. Here sensitivity and application of the test must be controlled to avoid over-inspection and over-rejection.
5. **Area inspected.**
   a. Entire part. For very critical parts that carry high stress, or where stresses and loads have not been thoroughly evaluated, the entire part often requires inspection. The inspection equipment must permit positive inspection at lowest possible operating cost.
   b. Selected areas. On many industrial parts only small areas carry a high stress and often in only one direction. The inspection, then, is applied only where needed.

For each test situation, one type of equipment is best suited to achieve the required test at lowest cost per piece. Several types of magnetic-particle inspection equipment are described in this section, including most of those in widest use.

Manual Inspection Equipment

Approximately twenty standard sizes of portable magnetic-particle inspection equipment are in use. They vary from small hand-held yokes which consist of permanent magnets or electromagnets energized from 115-volt, a.-c. lines to large, 10,000-amp., heavy-duty power units used for the inspection of large castings, weldments, or forgings. For purposes of economy to the user, equipment is not built for continuous operation at the maximum amperage rating. For example, a 1000-amp. rated unit may have around 400-amp. rating for continuous duty, although 1000 amp. can be delivered for a short duty cycle.

SMALL, LOW CURRENT UNITS. Small, low-cost portable equipment types include power supplies for **prod** and **cable magnetization.**

Hand-held Yoke. The hand-held, electromagnetic yoke shown in Fig. 1 supplies a high intensity, unidirectional magnetizing field between the poles when placed on a magnetic part and energized. It operates from 115-volt, 60-c.p.s. a.-c. lines on less than 6 amp. It can be used with d.c. from a 12-volt automotive battery, drawing 12 amp. This yoke is primarily used (1) to detect surface cracks of moderate to large size, as in gray iron; (2) for locating cracks in welds or castings; and (3) for locating fatigue cracks during overhaul of large assemblies.

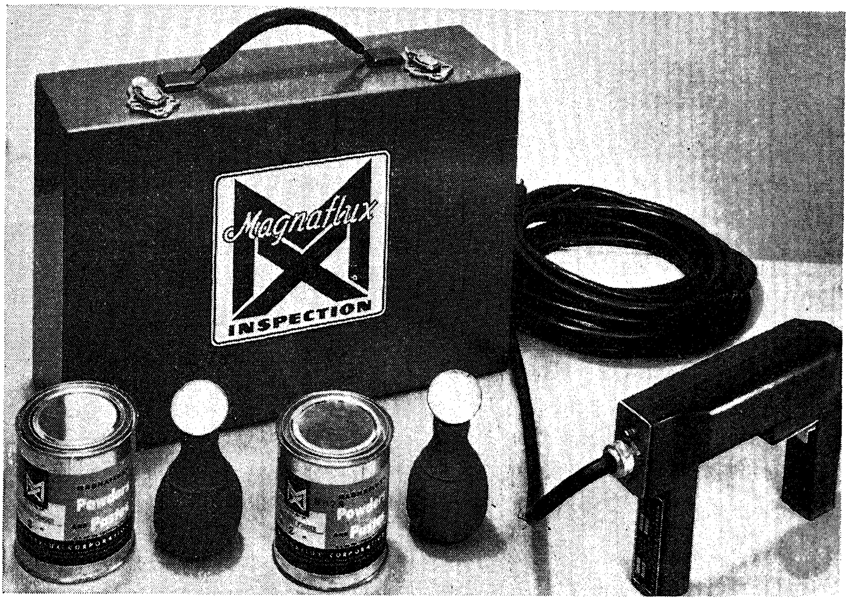

Magnaflux Corporation

Fig. 1. Hand-held electromagnetic yoke kit for magnetic-particle inspection.

Portable A.-C. Prod-and-Cable Magnetizing Unit. European developments have led to a small, portable, a.-c. magnetizing unit for prod and cable magnetization, as shown in Fig. 2. The compact kit includes a **tapped transformer** for control of magnetizing current magnitude, cables with **prod terminals, meter** to indicate current magnitude, and accessories. The prods may be coupled with a special fitting for cable magnetization. A **field strength indicator** included with the kit is intended for checking field strengths on the surface of test objects, to aid in determining optimum magnetizing currents.

Small Kit for Cable Magnetizing. Another small cable magnetizing unit supplies a.-c. magnetizing currents up to 500 amp. for intermittent use, when operated from a 115-volt, 60-c.p.s., a.-c. line. Parts are magnetized with **prods** or **cable coils.** Magnetizing fields are adequate to indicate fatigue and other surface cracks in shafts, beams, or machine parts up to several inches in diameter. **Dry powder** or **magnetic-particle baths** are normally used with this equipment.

Medium Unit for Cable Magnetizing. A medium cable unit supplies up to 500 amp. of magnetizing current when operated from 115-volt a.c. (Fig. 3). Both half-wave rectified and a.-c. magnetizing currents are available, and use of either is at the option of the operator. Magnetization can be done by cable coils or through prods. The unit illustrated can supply a continuous output of

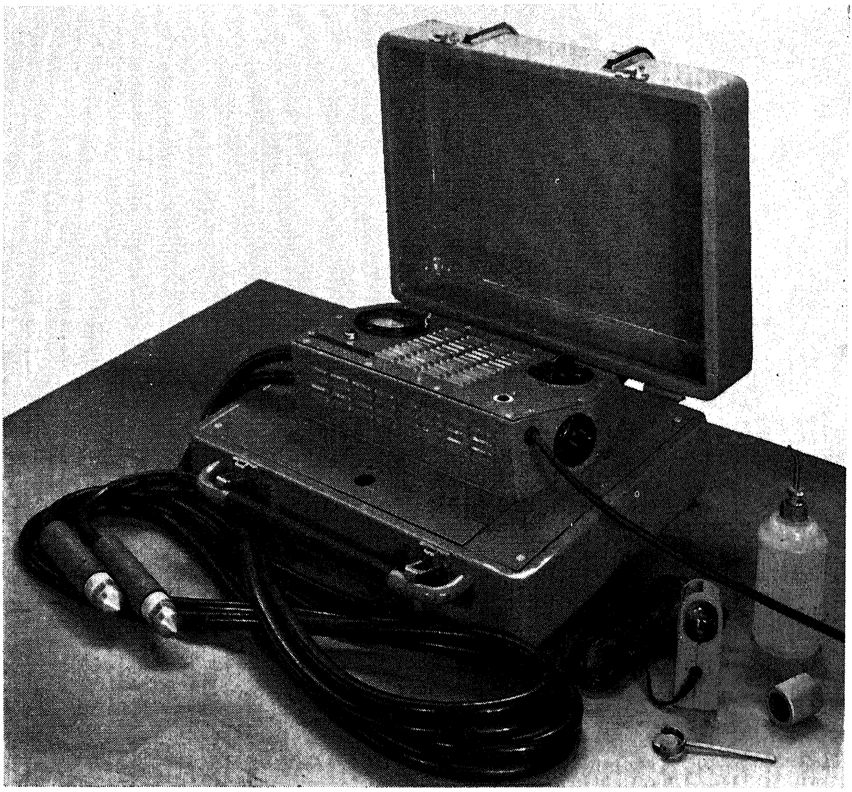

Röntgen Technische Dienst

Fig. 2. Magnetic-particle crack detector with accessories in built-in tool box.

500 amp. through 30 ft. of magnetizing cable; it is ruggedly built for general shop or field use in maintenance inspection.

MEDIUM AND HEAVY DUTY EQUIPMENT. Higher-current units supply 1000 to 10,000 amp. of a.c., d.c., or half-wave rectified magnetizing current. In inspection of medium-sized weldments and castings, the equipment most widely used supplies a.c. or half-wave current at the option of the operator. Sensitivity may be controlled to reveal only surface cracks with a.c., or surface cracks and subsurface defects with half-wave current. The very high amperage units provide up to 10,000 amp. for over-all magnetization of medium to large castings and forgings.

All equipment rated above 500 amp. operates from either 220- or 440-volt, single-phase or three-phase, a.-c. supply lines. The **input current requirements** will depend in part upon the duty cycle required, the magnetizing amperage drawn, and electrical characteristics of the magnetizing circuit. For mobile operation, gasoline generator units are used to supply 220- or 440-volt a.c. to magnetic-particle test units.

Medium Service A.-C. and Half-Wave Unit. Widely used, portable units supply a.-c. or half-wave magnetizing currents of 1000 to 2500 amp., selected

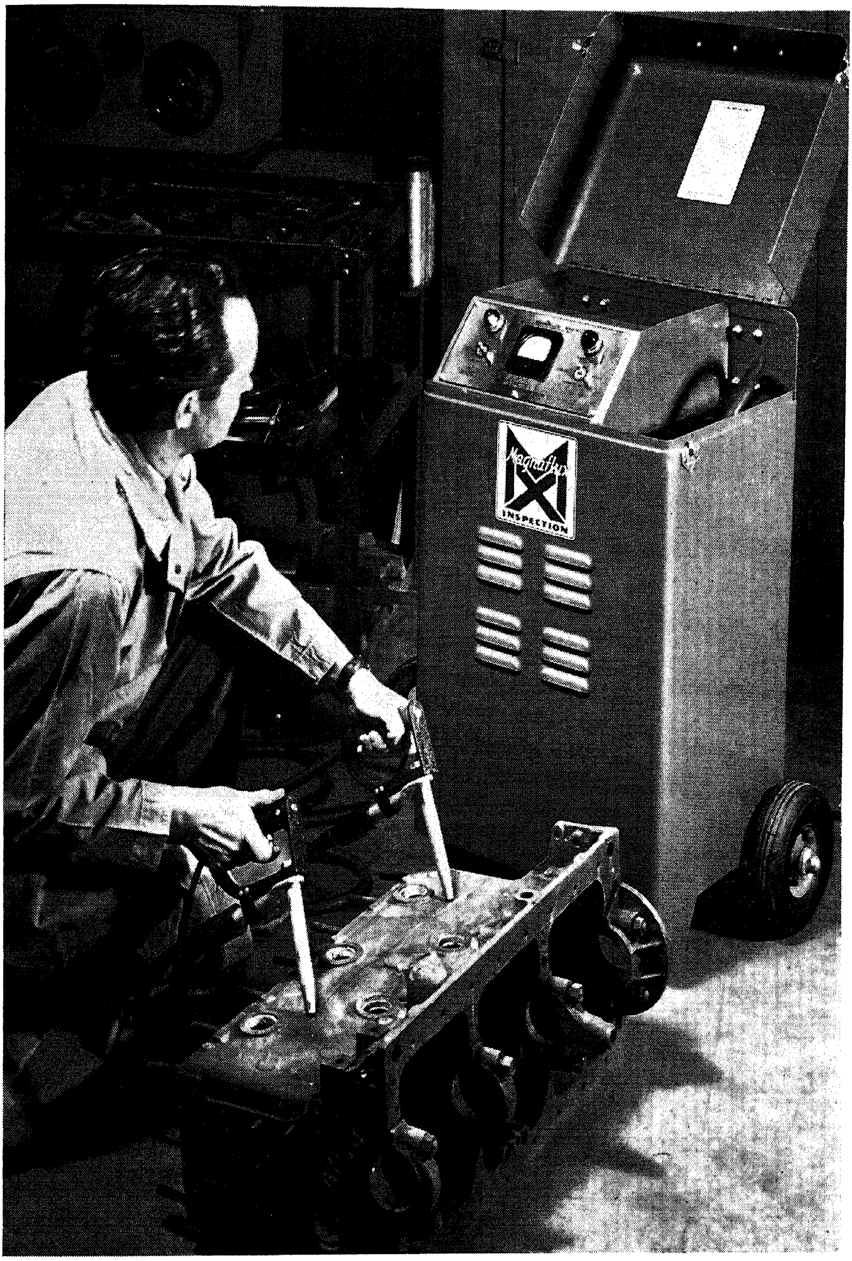

Magnaflux Corporation

Fig. 3. Medium cable magnetizing unit.

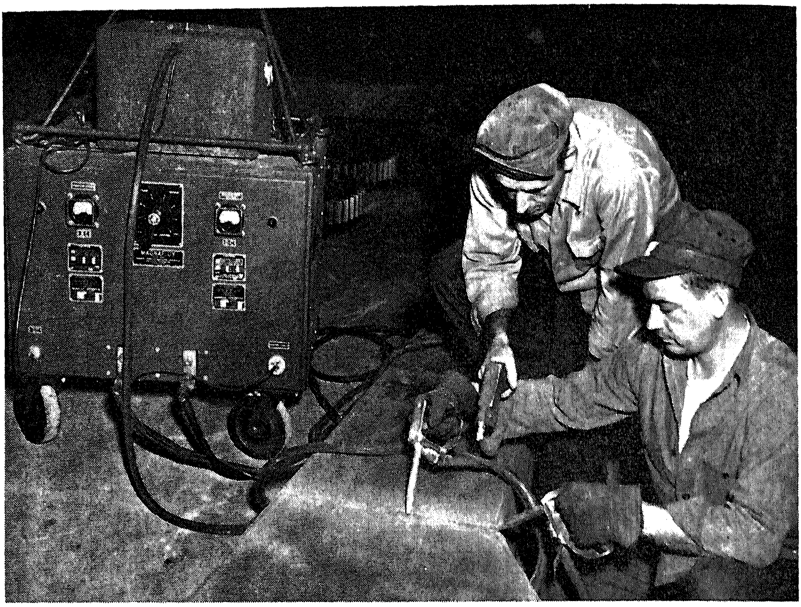

Magnaflux Corporation.

Fig. 4. Combination a.-c. and half-wave magnetizing unit (2000-amp. output).

by the operator (Fig. 4). These medium-service units are representative of several in the low end of the high current group of **heavy industrial portable units.** Powered by either 220- or 440-volt, 50- to 60-c.p.s. lines, the two units supply magnetizing currents as shown in Fig. 5. Where tests are to be made with long leads at distances of 80 to 100 ft. from the unit, the unit supplies only 450 amp. This is usually less than is required for inspection of heavy weldments or castings. Current selection is made with an eight-point switch on both units.

Nominal Unit Rating (amp.)	Magnetizing Current Output	Output Amperes		
		Maximum	Continuous	Long Lead Test
2000	A.C.	2500	500	450
	H.-W. D.C.	2000	1000	450
3000	A.C.	3000	600	800
	H.-W. D.C.	3000	1250	800

Fig. 5. Ratings of a.-c. and half-wave units.

Heavy-Duty, A.-C., Half-Wave Unit with Automatic Demagnetizer. The heavy-duty unit shown in Fig. 6 is similar to the 3000-amp., medium service unit, but it has a heavier duty electrical system and provides a 30-point, automatic, motor-driven, step-down switch for demagnetization of large, irregularly shaped parts or frames. The switch also provides much closer control of magnetizing

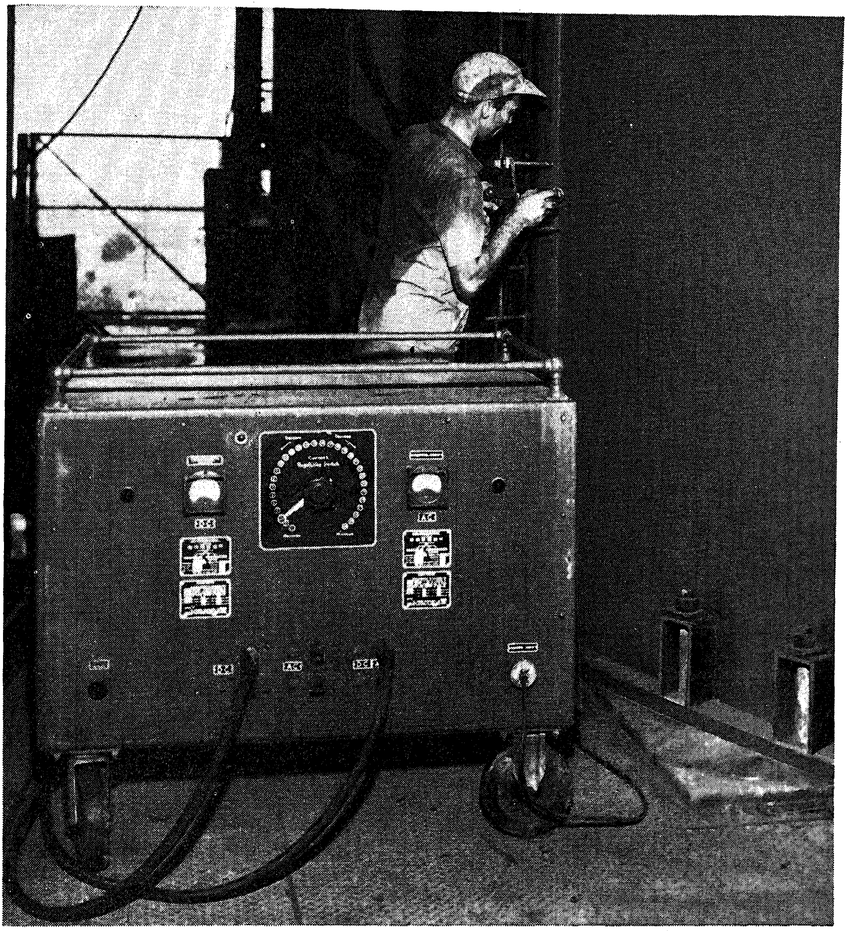

Magnaflux Corporation

Fig. 6. Combination a.-c. and half-wave magnetizing unit, 3000-amp. type with 30-point demagnetizing current control.

current magnitudes. This unit supplies high current through long leads and is commonly used where heavy weldments, castings, or large structures are inspected at distances of 100 ft. or more from the unit.

Three-Phase Rectifier, D.-C. Unit. The high-current d.-c. magnetizing unit supplies three-phase rectified current. It requires a 220- or 440-volt, three-phase supply. Maximum output is 5000 amp.; the continuous rating, 2000 amp. A particular advantage of this unit is a 30-point, **motor-driven, tap switch** which automatically reverses the polarity of the d.c. and steps it down in regular decrements. This provides effective demagnetization of parts of complex shape, such as large crankshafts.

STATIONARY EQUIPMENT. Hand-operated, stationary, horizontal, wet-method equipment is widely used for **small manufactured parts.** This type probably accounts for about 75 percent of the magnetic-particle inspection units currently in use in the United States.

Stationary units normally contain a built-in tank with a pump which agitates the wet particle bath and pumps inspection fluid through a hand-held hose for application to test objects. A part is clamped within the **magnetizing coil** between the copper contact faces of the head and tail stocks. At the operator's option, the parts can be magnetized circularly with current between the heads, or longitudinally with current through the coil; or both, if desired. The **dual magnetization** can be sequential on any unit or may be simultaneous on multiple magnetization equipment. While the part is magnetized, the operator applies the liquid inspection medium and then views the surface for indications. Most units are provided with inspection hood and black lights so that the fluorescent magnetic-particle inspection medium can be used. This increases the speed of inspection and reduces the possibility of missing an indication. The most common multiple-purpose, horizontal, wet-method stationary units are described in detail here.

Horizontal, Wet-Method, A.-C. Units. The smallest horizontal wet-method units are electrically identical. They supply 600-amp., a.-c., continuous magnetizing current or a maximum of 2700 to 3000 amp. of intermittent magnetizing current. The 54-in. unit accepts parts up to 54 in. long; the longest unit, parts up to 96 in. long. Current is controlled by a nine-point tap switch. The units can be operated from 220- or 440-volt, a.-c., 50- to 60-c.p.s. power. The **bath-agitation system** and **tanks** are built into the unit, with a hose to apply in-

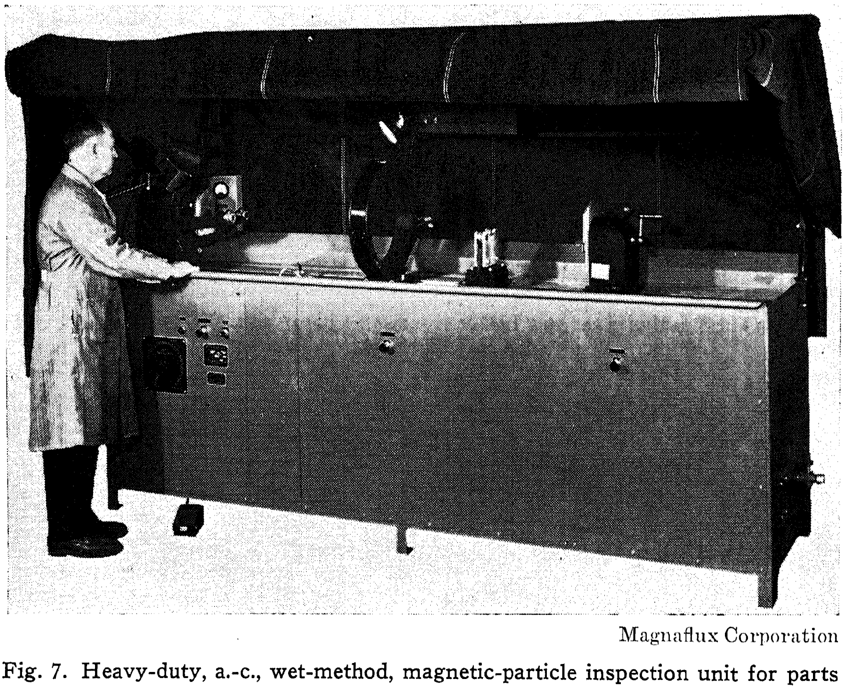

Magnaflux Corporation

Fig. 7. Heavy-duty, a.-c., wet-method, magnetic-particle inspection unit for parts up to 96 in. long. Unit equipped with hood, black lights, and 30-point demagnetizing switch.

spection medium to the test part. The units are equipped with hoods and black lights for normal use with fluorescent particles in industrial manufacture or overhaul inspection. Since this is an a.-c. unit, parts may be demagnetized with the magnetizing coil on the unit itself if required.

Horizontal, Wet-Method, A.-C. Units with Automatic Demagnetizer. Fig. 7 shows a typical a.-c. unit with 3000-amp. maximum magnetization current which accepts parts up to 96 in. long. A smaller unit accepts parts up to 54 in. long. A special advantage of this type of horizontal, wet-type, a.-c. equipment is the 30-point tap switch which provides both close current control for magnetization and **automatic step-down demagnetization** cycles for complex parts. This equipment can be operated from 220- or 440-volt, 50- to 60-c.p.s., a.-c. supplies and is sometimes built for 25-c.p.s. operation or for special voltage supplies. Magnetizing coils of various sizes are available. This equipment is commonly used with **wet fluorescent magnetic-particle tests**

Horizontal, Wet-Type, D.-C. Units. Units supplying d.-c. magnetizing currents are available in horizontal, wet-type equipment and can be equipped with hoods. The shorter unit accepts parts up to 54 in. long and supplies d.c. (full-wave, rectified a.c.) up to 4500 amp. The longer equipment accepts parts up to 96 in. long and supplies maximum d.-c. magnetizing currents of 5500 amp. These units are representative of many similar types in wide use for subsurface and surface inspection of **aircraft parts.**

Horizontal, Wet-Type, D.-C. Units for Very Heavy Parts. Fig. 8 shows a large, horizontal, wet-type unit for heavy castings, forgings, and welded struc-

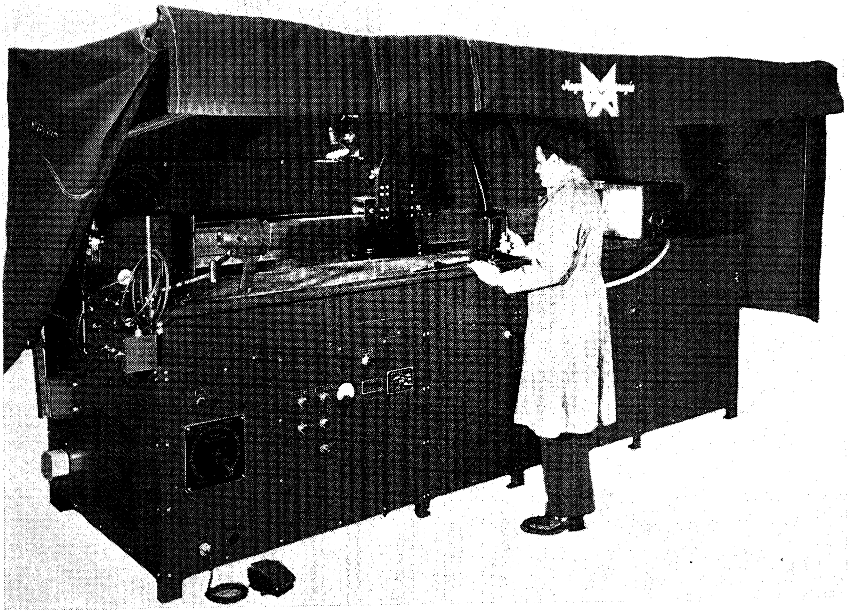

Magnaflux Corporation

Fig. 8. Horizontal, d.-c., wet-method, magnetic-particle inspection unit providing both longitudinal and circular magnetization, with 30-point demagnetizing switch.

tures. These are set on the stainless grille during testing. Both longitudinal and circular magnetization are available. Maximum test-object capacities are: weight, 1200 lb; length, 108 in.; and maximum diameter, 24 in. Direct-current magnetization is supplied intermittently up to 5000 or 5500 amp., or at 2000 amp. continuously. A 30-point, automatic-reversing, d.-c. tap switch is provided for demagnetization of parts in place on the unit.

WHEEL-MOUNTED, WET-METHOD UNITS. Analogous to the horizontal units are movable stationary units (mounted on wheels) which can be used in one location and quickly rolled to another. Small parts can be run at production rates of several thousand per hour. An air compressor is built in. Most units operate on 220- or 440-volt a.c. When moved in the plant, they require only electrical connection to be operational. Electrically they are built to meet Joint Industry Conference design specifications. For high speed operation, a built-in, automatic, magnetizing cycle is provided with head clamping and magnetization actuated by a foot switch.

Mechanized Inspection Equipment

SEMI-AUTOMATIC INSPECTION EQUIPMENT. Several score of types of almost completely automatic magnetic-particle inspection units are used in hundreds of plant locations. Inspection processing is carried out automatically on parts carried by a **continuous conveyor.** Loading and unloading may be manual or automatic. The inspector is required to view the parts as they pass on the conveyor and must only see and react to readily visible indications. Parts bearing indications are diverted for later evaluation and salvage or rejection. Accepted parts remain on the conveyor and pass through an **automatic demagnetizing coil** before being discharged from the unit. This equipment permits rapid, low-cost inspection, where slower inspection may not be worth its cost.

Applications of such inspection include automobile and truck steering parts, connecting rods, many types of bolts, and similar mechanical parts. Similar automatic handling and operation is used on such critical parts as aircraft gas-turbine blades, where volume is very high and it is desirable to inspect at several stages of manufacture. Semi-automatic equipment may be special purpose or multi-purpose.

Semi-automatic processing paces the inspection rate much better than human operators. It also standardizes and controls the processing steps themselves. Thus, fully reproducible test results are achieved on every part tested, independent of human operator variations.

SINGLE-PURPOSE SEMI-AUTOMATIC EQUIPMENT. Semi-automatic equipment can be custom designed for inspection of one type of part.

Gas-Turbine Compressor Blade Test. The three-shot, multiple-magnetization, gas-turbine compressor blade inspection unit shown in Fig. 9 applies **circular magnetization** through the blade and through the dove tail, and also **coil longitudinal magnetization** of the blade, all during a single operating cycle. It is jigged for automatic blade handling and automatically applies a gentle dip-in bath. Magnetizing currents are applied during part removal and drain-off, for maximum sensitivity to detect very fine defects. This unit illustrates how special equipment is developed to provide a very special technique required for highest sensitivity, in moderate to high volume rates (600 parts per hour) with no damage to the delicate blades.

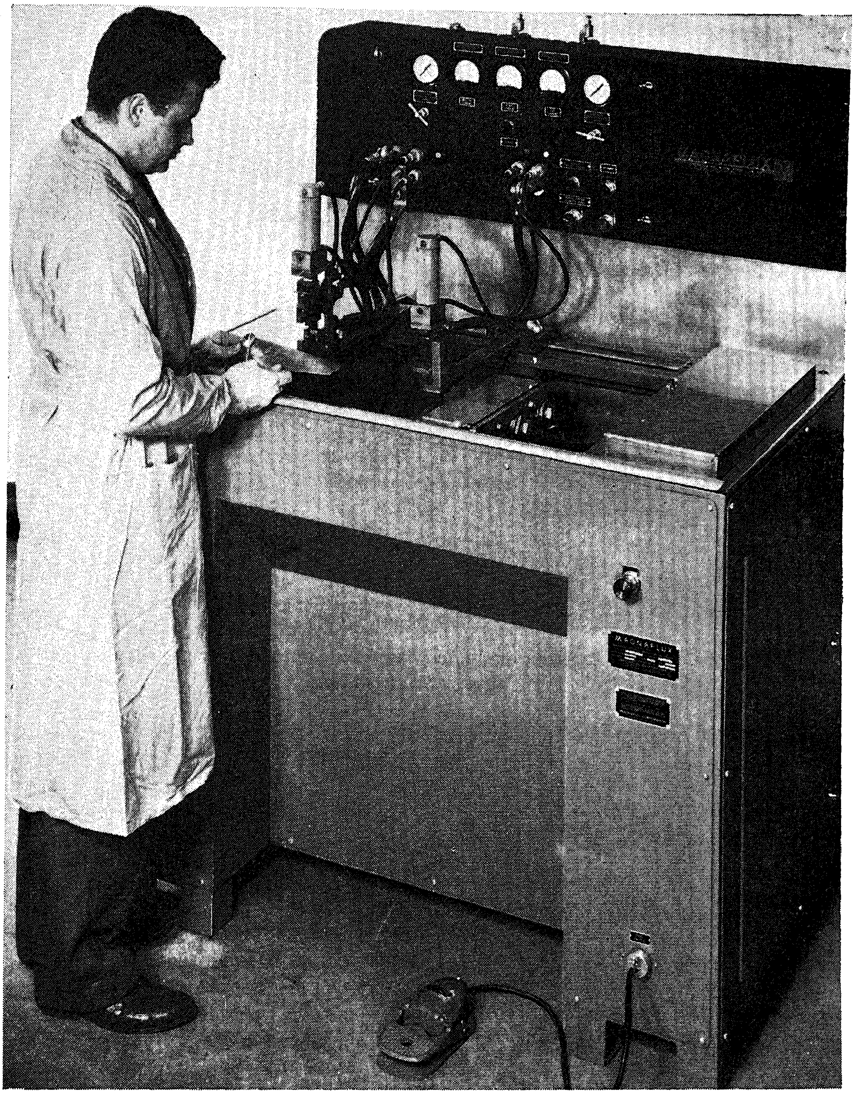

Magnaflux Corporation

Fig. 9. **Three-shot, semi-automatic, magnetic-particle inspection unit.**

Conveyorized Compressor Blade Test. The three-shot, multiple-magnetization, gas-turbine compressor blade conveyorized unit shown in Fig. 10 applies three magnetizing shots at one station, with automatic bath application as the blades pass through. Up to six inspectors can be used at maximum inspection rates of 2400 parts per hour. Thus an all-direction inspection and high sensitivity control are achieved through automatic operation, eliminating human process errors.

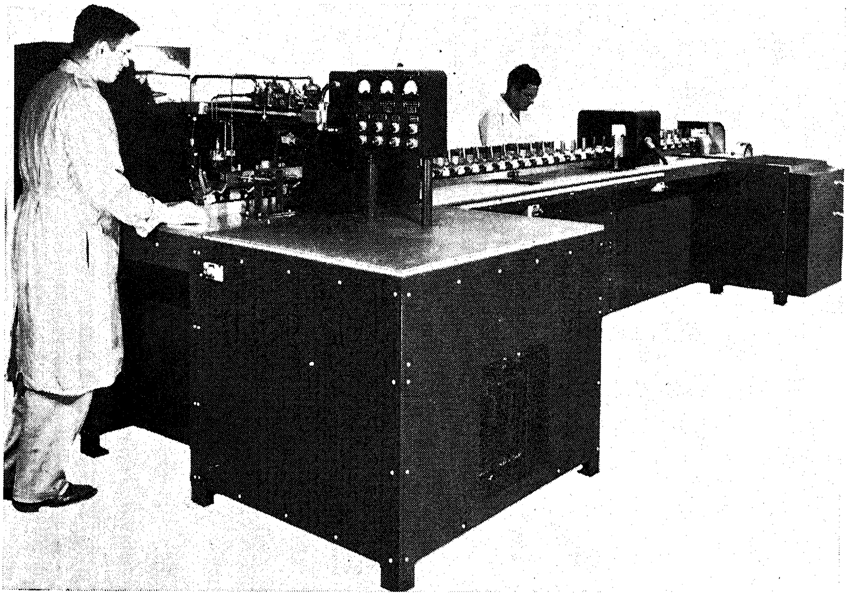

Magnaflux Corporation

Fig. 10. Conveyorized magnetic-particle inspection unit providing three magnetizing shots at one station.

Automatic Inspection of Steering Spindles. Steering spindles are automatically inspected on an **indexing turntable unit.** This unit was developed for testing a single type of spindle assembly at a rate of 650 units per hour. It provides two head shots from the end of the spindle through the two arms and a separate coil shot. Alternating-current magnetization is used with water-suspended, fluorescent magnetic-particle wet bath. It is fully automatic, with automatic demagnetization and automatic conveyor unloading.

Aircraft Engine Cylinder Inspection. Aircraft cylinders are semi-automatically inspected with a d.-c. multiple magnetizing unit which processes the entire inside diameter and the exposed outside diameter of surfaces of the steel cylinder liner. This equipment uses central conductor and coil magnetization, with automatic bath application. The aircraft cylinders enter by **roller conveyor** and are up-ended on a **rotating table support.** Upon actuation, all clamping, magnetizing, bath operations, and 30-point step-down demagnetization following the magnetizing cycle are completed automatically.

There are many other special-purpose units designed and widely used in such applications as railroad axle inspection and jet compressor overhaul tests.

MULTI-PURPOSE SEMI-AUTOMATIC EQUIPMENT. Similar parts of differing sizes and shapes may be handled on multi-purpose equipment.

Automotive Forgings Test. Various automotive forgings are inspected on a versatile conveyorized unit which provides head shot, coil shot, or both, as required for individual parts, at rates up to 900 to 1200 parts per hour (Fig. 11). The two magnetizations are separate. The head shot may be applied by hand, which then permits rapid circular magnetization of parts of various shapes

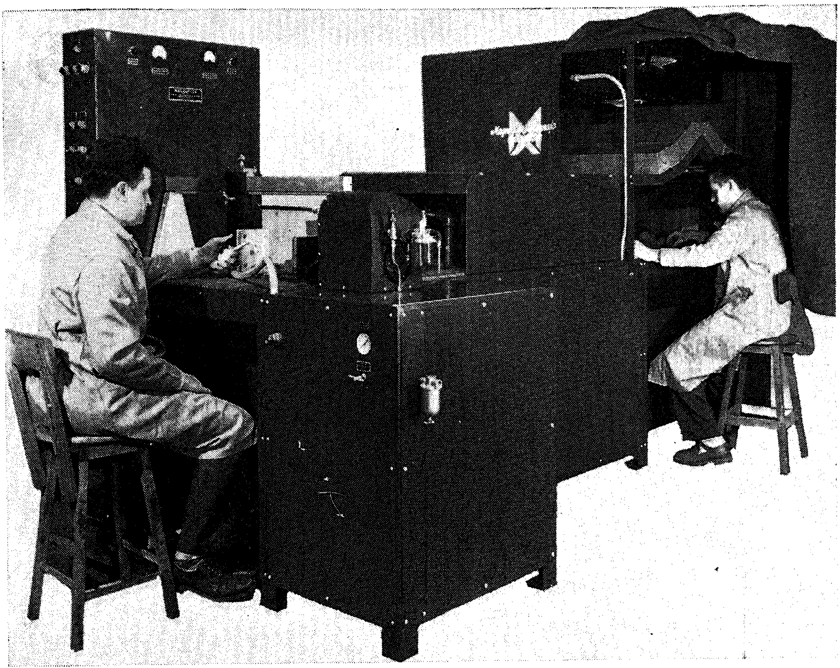

Magnaflux Corporation

Fig. 11. Conveyorized magnetic-particle inspection unit providing head shot, coil shot, or both, as required.

or sizes up to 28 in. long. Bath application can be by hand or automatic for the circular shot. For the longitudinal magnetization the part is dropped on the mesh conveyor belt and automatically carried through coil magnetization and bath application. On **rough-surfaced parts,** such as forgings, one indication is applied on top of the other, with a single inspection further down the conveyor under the black light in the hood. Then the conveyor carries the part through automatic demagnetization and ejects it into tote bins or onto a take-away conveyor.

Conversion of Hand-operated Units. Auxiliary conveyorized units permit conversion of existing standard hand-operated units to **semi-automatic operation** at less cost than a complete automatic or semi-automatic unit. Circular magnetization is applied on the standard unit where the part is magnetized and bath applied. The part is then placed on the auxiliary unit conveyor. The auxiliary unit carries the part through automatic coil magnetization and bath application, if longitudinal magnetization is required, and then presents the part to the inspectors. After this, the conveyor carries the parts through automatic demagnetization and ejects them.

Inspection of Automotive Steering Parts. A general purpose, longitudinal-shot unit was developed to handle large forged truck and bus-steering parts of many designs and shapes, weighing up to 40 lb. each. It handles the full production of assorted designs at one plant. Longitudinal magnetization (with automatic bath application) is the only direction of inspection applied, since only transverse defects are serious on these parts. Inspection is by fluorescent magnetic-particle bath, and automatic demagnetization is provided.

FULLY AUTOMATIC, MAGNETIC-PARTICLE TEST EQUIPMENT. In recent years equipment has been developed which uses photoelectric or television viewing of indications to replace the human inspector. This is applicable on an automatic basis to parts with simple shapes or to continuous simple areas, such as the longitudinal weld on seam-welded pipe. On large pipe, **white-light scanning** is used. For smaller tubes, equipment is designed to use fluorescent indications, with black-light scanning.

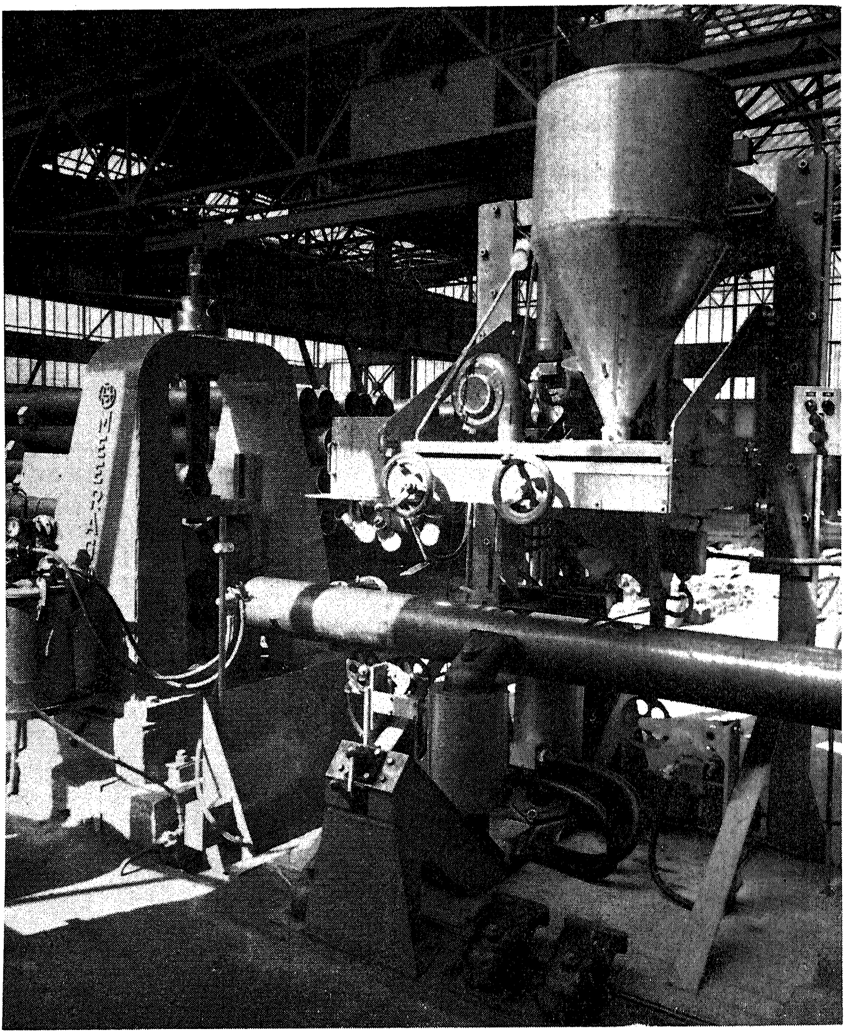

Magnaflux Corporation

Fig. 12. Photoelectric white-light scanner automatically locates and marks defective areas revealed by magnetic particles.

Fig. 12 shows an automatic white-light scanner in operation at a steel mill which makes large-diameter welded line pipe. The unit automatically magnetizes the weld area as the pipe passes, applies a special black, dry powder, and blows off and reclaims excess powder. A white strip is applied to the weld area before the pipe enters the unit. Thus the indication is a black line on a white background, and as it passes under the illuminated photoelectric scanner, the crack indication is automatically viewed and detected. When a defect is detected, an **automatic paint spray** marks the section of the pipe for later repair.

EQUIPMENT SELECTION. To meet an inspection need, magnetic-particle test equipment should be selected from the available models or the many variations by special design. Considerations governing this selection include:

1. Minimum inspection cost, per piece tested.
2. Inspection rate requirements.
3. Flexibility in use.
4. Sensitivity requirements.

It is desirable to investigate carefully and select the best equipment to achieve the test requirements when a magnetic-particle test is introduced or test conditions change. Thus maximum results may be obtained with minimum total cost.

DEMAGNETIZERS. Often demagnetizers are required after a magnetic-particle test to remove fields resulting from the test itself or from other magnetizing operations, such as holding with magnetic chucks. For this need, various heavy-duty industrial demagnetizers and procedures have been developed. Demagnetizers have small- or large-diameter coils, as required by part size. They can be **hand operated** or **automatic** and can operate **intermittently** or **continuously.** On semi-automatic units the demagnetizer is commonly integral with the test unit and automatically demagnetizes parts as they pass by on the conveyor.

The best demagnetizer is selected on the basis of part size, complexity of shape, hardness or magnetic retentivity of test objects, and degree of demagnetization required. In selecting magnetic-particle test equipment, this supplemental need may or may not exist but should be considered (see section on Magnetic-Particle Test Principles for further details).

Bibliography

BARTH, V. C. "C. & N.W. Intensifies Inspection of Equipment Parts," *Ry. Mech. Engr.*, 123 (1949): 556.

"Black Lighting Trouble Spots," *Ties* (January, 1954).

CLARKE, J. E., R. A. PETERSON, and T. J. DUNSHEATH. "Automatic Inspection of Pipe," *Welding Engr.*, 36, No. 2 (1951): 38.

DOANE, F. G., and C. E. BETZ. *Principles of Magnaflux.* 3d ed. Chicago: Photopress, 1948.

"Fully Mechanized Automatic Handling Features Pipe Inspection Unit," *Steel Equipment and Maintenance News* (December, 1956).

"Move the Part and Save the Time," *Solar Blast* (May, 1955).

SMITH, O. G. "Magnetic Particle Technique Makes Billet Inspection Positive and Efficient," *Iron Age,* 175, No. 18 (1955): 99.

"Take Magnetic Inspection Afield," *Construction Methods and Equipment* (July, 1954).

THOMAS, W. E. "Economic Factors of Nondestructive Testing," *Nondestructive Testing,* 11, No. 4 (1953): 9.

VAN MANEN, M. H. "Portable Magnetic Particle Equipment," *Southern Power & Ind.* (October, 1955).

SECTION 32

MAGNETIC-PARTICLE TEST INDICATIONS

CONTENTS

PAGE

Interpretation Guide

- Phases of inspection 1
  - Need for training 1
  - Required information 1
- Classification of indications 1
  - Surface discontinuities 1
    - Dry magnetic-particle indications of a transverse quench crack and longitudinal seam in a railroad locomotive spring (*f.* 1) 2
    - Wet magnetic-particle indication of a seam in a diesel-engine wrist pin (*f.* 2) 2
  - Subsurface discontinuities 2
    - Comparison of wet- and dry-method indications of subsurface defects at varying depths (*f.* 3) 3
- Checking indications 3
  - Checking by residual method 4
  - Checking with magnifying glass 4
- Indications of nonmetallic inclusions 4
  - Characteristics of inclusions in hot-worked materials 4
  - Typical examples of inclusions 6
    - Dry magnetic-particle indications of nonmetallic inclusions in a jack screw (*f.* 4) 4
  - Nonplastic inclusions 6
    - Magnetic-particle indication of nonplastic subsurface inclusion (*f.* 5) 5
- Indications of surface seams 6
    - Magnetic-particle indication of a longitudinal seam in a rolled steel bar (*f.* 6) 6
- Indications of cooling cracks 7
    - Magnetic-particle indication of a cooling crack of varying depth (see Fig. 8) (*f.* 7) 7
    - Cross-sections showing crack depths at locations marked on bar of Fig. 7 (*f.* 8) 7
- Indications of laminations 7
- Indications of forging laps 7
    - Forging lap in a propeller-shaft lock nut (*f.* 9) 8
- Indications of forging bursts and flakes 9
    - Magnetic-particle indications of forging bursts in upset forging (*f.* 10) 9
- Indications of gas porosity 9
    - Dry magnetic-particle indications of subsurface gas porosity (blow holes) in a cast steel flange (*f.* 11) 10
- Indications of incomplete weld penetration 10
    - Dry magnetic-particle indication (arrow) of incomplete penetration in a fillet weld in a marine structural weldment (*f.* 12) 11
- Indications of heat-treat cracks 11
    - Magnetic-particle indication of a quench crack under a bolt head (see Fig. 14) (*f.* 13) 12
    - Cross-section, after deep etching, of quench crack in bolt head, similar to that shown in Fig. 13 (*f.* 14) 13
- Indications of grinding, plating, or etching cracks 11
    - Wet-method magnetic-particle indications of grinding cracks in a crankshaft (*f.* 15) 14
- Indications of fatigue cracks 12
  - Characteristics of fatigue cracks 13
    - Magnetic-particle indication of a fatigue crack propagating from an oil hole on inside of a hollow crankshaft (*f.* 16) 15
  - Development of fatigue cracks 14
    - Progressive fracture showing typical "fatigue crescents" (*f.* 17) 16
- Nonrelevant indications 14
  - Effect of overmagnetization 14
  - Geometric effects 15
    - Nonrelevant magnetic-particle indications of interior splines of hollow shaft (*f.* 18) 17
  - Recognition of nonrelevant indications 15
  - Magnetic writing 17
- Permanent records of magnetic-particle indications 18
  - Lacquer fixing of indications 18
  - Tape transfer of indications 18
  - Photography of indications 18
  - Fluorescent indication photography 18

Nondestructive Supplemental Tests

- Reasons for supplemental tests 19
- Direct surface inspection 19
  - Checking indications by residual magnetization 19
- Surface inspection with magnifiers 19
  - Cleaning surface 20
  - Inspection glasses 20
  - Binocular microscope 20
- Probing methods 21
  - Filing 21
    - File cut applied to a crack in bar stock (*f.* 19) 21
  - Grinding 22
  - Chipping 22

CONTENTS (*Continued*)

PAGE
Removal of defects 22
  Repair by welding 22
  Flame gouging 22

Destructive Supplemental Tests

Reasons for destructive tests 22
Fracturing 23
  Fracturing by hammering 23
    Two rail-joint bars with fracture completed through fatigue crack (*f.* 20) 23
  Fracturing in mechanical testing machines .. 23
  Fracturing after blueing by heating 23
  Fracturing after chilling 24
Sawing 24
Trepanning or core drilling 24
Sectioning with cut-off wheels 24
  Effects of overheating while cutting 24
Examination of cut surface 24
    Spring sectioned on cut-off wheel (*f.* 21) . 25

PAGE
  Belt sanding 25
  Etching 25
  Types of etching 25
  Deep etching or macro-etching 25
    Persulphate-etched section of a double-Vee butt weld (*f.* 22) 26
  Persulphate etching 26
  Etching of ingots or coarse castings 26
  Etch cracking 26
    Etching cracks in a twist drill (*f.* 23) 27
  Tempering before etching 26
  Etching technique and equipment 26
  Acid etching 27
    Deep-etched section of a forging, showing flow lines (*f.* 24) 28
Metallographic examination 28
  Preparation of specimen 28
  Examination of nonetched specimens 29
  Examination of etched specimens 29
Utility of tests 29
Bibliography 29

MAGNETIC-PARTICLE TEST INDICATIONS

Interpretation Guide

PHASES OF INSPECTION. Magnetic-particle inspection involves three phases. The first phase includes the mechanical processes necessary to create suitable accumulations of magnetic particles at discontinuities, i.e., the **formation of indications.** The second phase is the **interpretation** of the condition in the part which has caused the formation of the indication. The third is the **evaluation** of the seriousness of the cause of the indication as it can affect the use of the part and the disposition of the part: whether it need be scrapped, can be reworked, or used as it is.

Need for Training. The **evaluation of indications** and of the discontinuities which cause them, as well as determining the disposition of the part, should be done by individuals whose knowledge of metals and engineering principles enables them to make a sound decision. **Decisions**, or **specifications** enabling others to make such decisions, should be made by skilled and trained men.

Required Information. In most cases it is possible for an experienced inspector to tell, from the location and appearance of a magnetic-particle indication, what condition in the part has caused the accumulation of magnetic particles. Such an appraisal can be made accurately only if the history of the part, its metallurgical composition, method of formation, and processing are known.

CLASSIFICATION OF INDICATIONS. Magnetic-particle indications fall into three broad classes:

1. Surface discontinuities.
2. Subsurface discontinuities.
3. Nonrelevant magnetic disturbances.

Each class possesses characteristics which generally make its recognition possible.

Surface Discontinuities. Surface discontinuities produce sharp, distinct patterns which are usually held tightly to the surface of the part. This is particularly true of the sharp, close-lipped **surface defects** which are difficult to see and are most objectionable.

Fig. 1 illustrates typical **surface crack indications.** This helical spring of a railroad locomotive contains a transverse quenching crack and a longitudinal seam. Both are clearly shown by sharp, clean-cut, and tightly adherent dry-powder indications. Fig. 2 shows a **seam** in a wrist pin inspected with the wet method. The closely held, compact particle pattern has some height and in some cases enough "build-up" to cast a shadow.

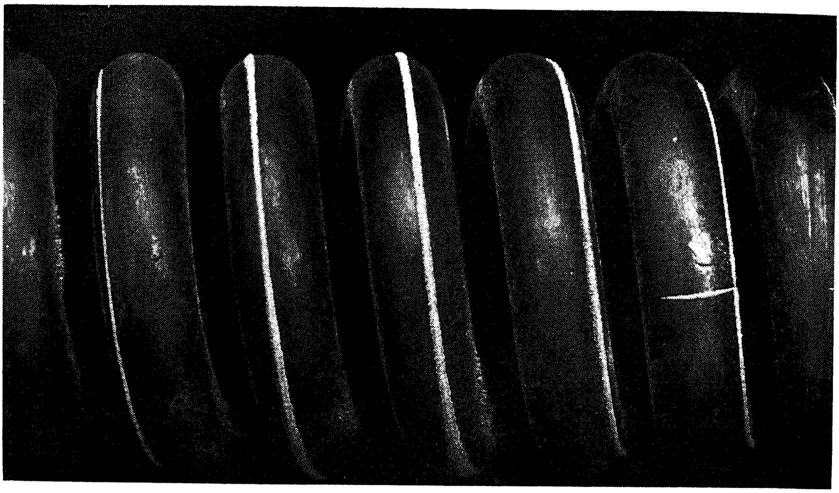

Magnaflux Corporation

Fig. 1. Dry magnetic-particle indication of a transverse quench crack and longitudinal seam in a railroad locomotive spring.

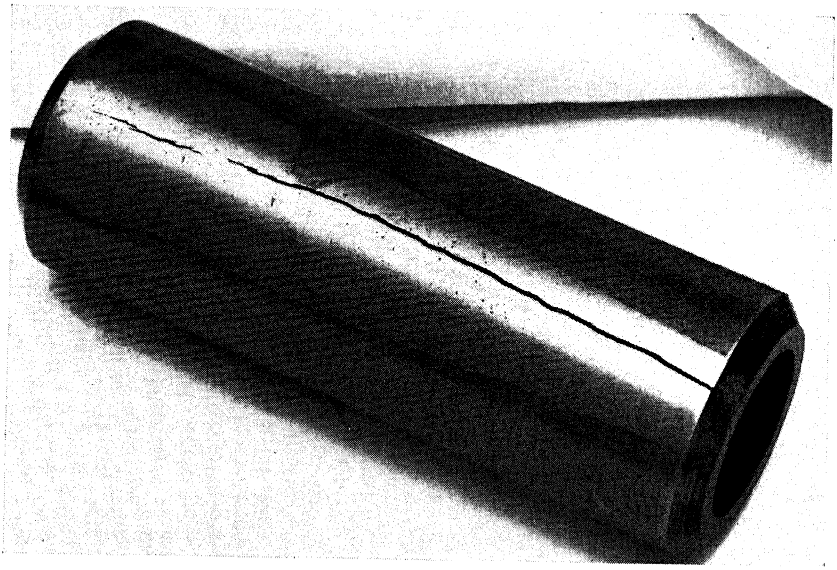

Magnaflux Corporation

Fig. 2. Wet magnetic-particle indication of a seam in a diesel-engine wrist pin.

Subsurface Discontinuities. Fig. 3 clearly illustrates two important effects observed in magnetic-particle inspection. These indications are those of holes drilled at varying depths beneath the surface of a steel part. The indications near the left end of each strip show the artificial defect closest to the surface, and each successive indication to the right is over a deeper defect. This clearly

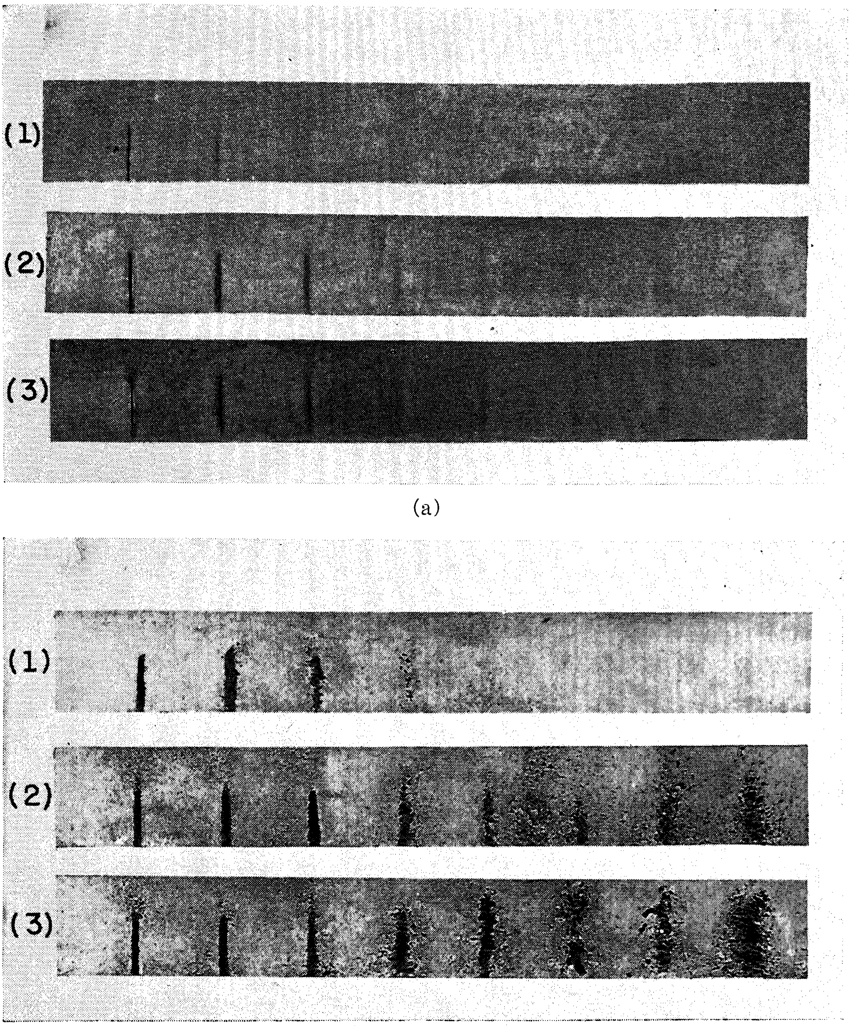

(a)

(b)

Magnaflux Corporation

Fig. 3. Comparison of wet- and dry-method indications of subsurface defects at varying depths. From left to right, subsurface holes were drilled at increasing depths. (a) Indications obtained with wet method, continuous magnetization: (1) 500 amp., (2) 1000 amp., (3) 2000 amp. (b) Indications obtained with dry magnetic powder, continuous magnetization: (1) 500 amp., (2) 1000 amp., (3) 2000 amp.

shows that the indications become broader and fuzzier as the discontinuity causing them lies deeper beneath the surface. The results of this test also show that the dry powder is much more sensitive than wet particles for subsurface defects.

CHECKING INDICATIONS. It is usually easy to determine whether the discontinuity is surface or subsurface. First, the **appearance of the indication** itself may be all that an experienced operator needs to make a decision. Second, wiping away a part of the indication allows a close examination of the area. Often some **surface irregularity** appears, although its exact nature may not be clear. If there is no surface irregularity under the indication, it is very likely that its cause is completely beneath the surface.

Checking by Residual Method. A reapplication of magnetic particles permits one to observe whether the indication readily reappears. This is actually an attempt to reproduce the indication by the residual method. The residual method is always less sensitive than the continuous method. It is obvious that if the original indication was produced by the continuous method, the manner in which the indications reappear will give some notion as to the severity and extent of the discontinuity. Sometimes the reproduction of an indication by the residual method is used as a criterion for rejection on certain types of parts.

Checking with Magnifying Glass. A small hand glass with a magnification power of 2 to 7 diam. is a great aid for inspectors. With such a glass it is possible first to examine the indication in detail, and later, after wiping away the indication, to see material surface conditions. The majority of **surface cracks and seams** can be seen with a low-power glass, provided the exact area has been previously indicated by the line of magnetic particles. If no surface discontinuity is visible under the indication after thorough cleaning, the conclusion that the discontinuity is subsurface may be justified.

INDICATIONS OF NONMETALLIC INCLUSIONS. The subsurface discontinuity most commonly found with magnetic-particle inspection is the nonmetallic inclusion. Even though it is found most frequently, it is often of little significance in determining the usefulness of the part. When such inclusions occur in **areas of high stress** or in certain special locations or directions, they may be cause for rejection. But it is incorrect to call them "defects" without reservation, for they occur in all steels and are not defects unless they reduce the strength of the part. For this reason it is important to be able to recognize and appraise the true importance of the indications of such nonmetallic inclusions (sometimes called **stringers**). Usually they are very fine and are revealed with magnetic-particle inspection only when they occur near the surface. They are more likely to be shown on highly finished surfaces inspected by the wet method and at high magnetization levels.

Characteristics of Inclusions in Hot-worked Materials. The indications are usually straight and parallel to the **rolling direction** on rolled products. On

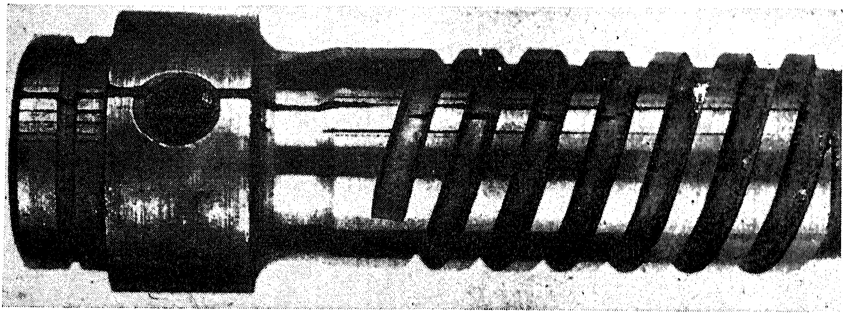

Magnaflux Corporation

Fig. 4. Dry magnetic-particle indications of nonmetallic inclusions in a jack screw.

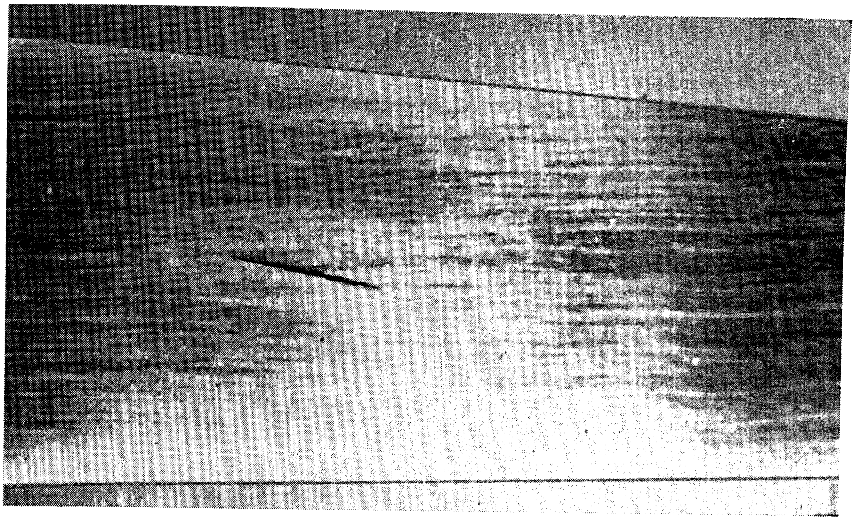

(a)

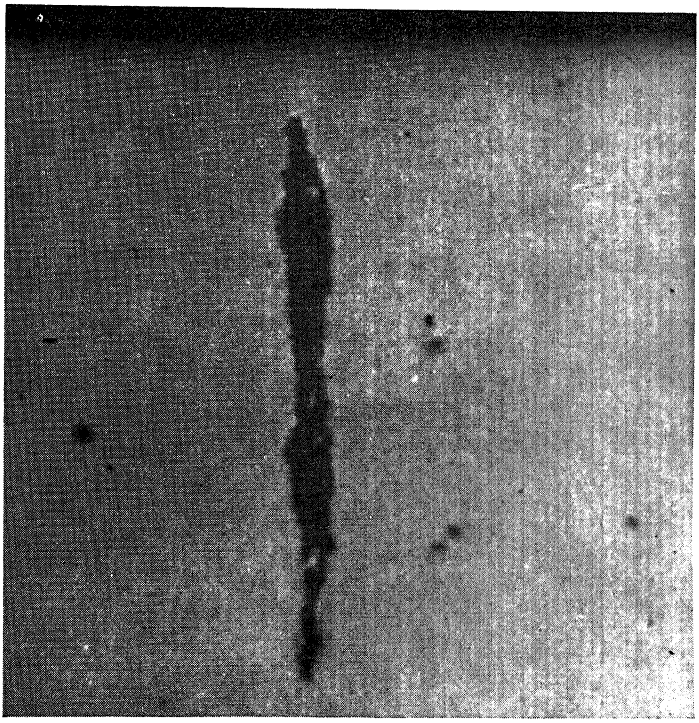

(b)

Magnaflux Corporation

Fig. 5. Magnetic-particle indication of nonplastic subsurface inclusion. (a) Indication is not parallel to grain flow in forging. (b) Section through forging beneath indication, showing inclusion at 100× magnification.

forgings, they parallel **flow lines** which may be curved. Because they show only when near the surface but are distributed throughout the cross-section, **inspection before machining** is not helpful, and if inclusions are considered cause for rejection, parts should be inspected after surface finishing.

Typical Examples of Inclusions. Fig. 4 shows a jack screw machined from a rolled bar. The nonmetallic inclusions were not visible without magnetic-particle inspection. The **straightness of the indications** is important, as is the fact that different inclusions were brought near the surface in the complex machining of the part.

Nonplastic Inclusions. A subsurface condition which is much more likely to be dangerous is the presence of a nonmetallic inclusion which was not plastic at the temperature of the rolling or forging. This may be a **fragment of hard refractory,** and since it is not plastic, it remains large and may be unfavorably located near the surface. Fig. 5(a) shows an indication of such a nonplastic inclusion. It is not a stringer because it is not parallel to the grain flow in the forging. It is subsurface because its indication is slightly fuzzy and because the surface of the material shows no discontinuity when the indication is removed. When this part was sectioned and microscopically inspected, as shown in Fig. 5(b), the inclusion was shown to be quite large and and at right angles to the surface.

INDICATIONS OF SURFACE SEAMS. Surface seams in rolled bars result from cracks or other **surface defects in the billets** from which they are rolled or from some **defect introduced into the rolling operation** itself. The great elongation of the metal draws out such surface defects into long, straight seams, usually closely parallel to the direction of rolling. Fig. 6 shows an indication of such a seam in a rolled bar. Seams are recognizable by their straightness and because they are at the surface and are roughly parallel to the direction of rolling.

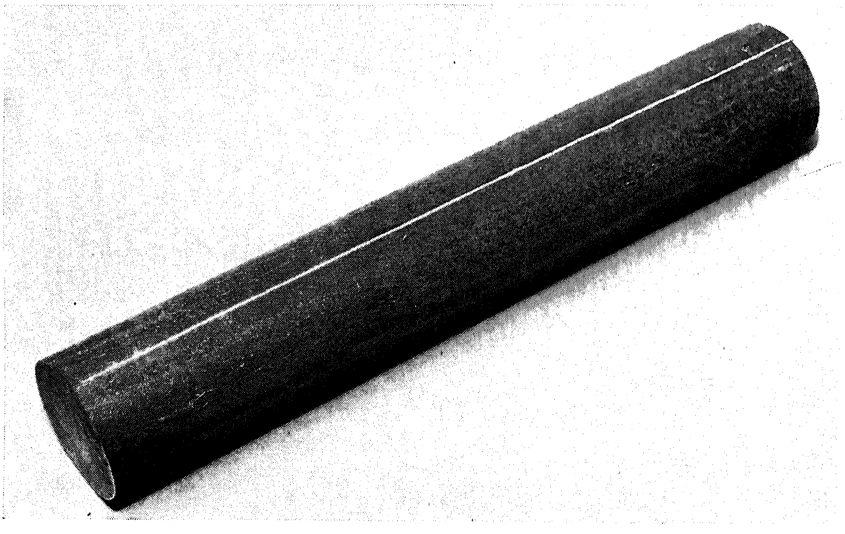

Magnaflux Corporation

Fig. 6. Magnetic-particle indication of a longitudinal seam in a rolled steel bar.

INDICATIONS OF COOLING CRACKS. Cooling cracks which occur in rolled bars are similar to seams but usually differ in appearance in some respects. Fig. 7 shows an indication of a cooling crack. It is sharp, well defined, and adherent, but it deviates somewhat from the rolling direction. The **depth of the crack** varies, as indicated by the heaviness of the indication. Fig. 8 shows sections through the 2½-in. bar shown in Fig. 7. This illustrates how the appearance of an indication may vary with the depth of the crack causing that indication. When all the variables of the method are controlled, the amount of the **powder build-up** can be used to judge the depth of the crack.

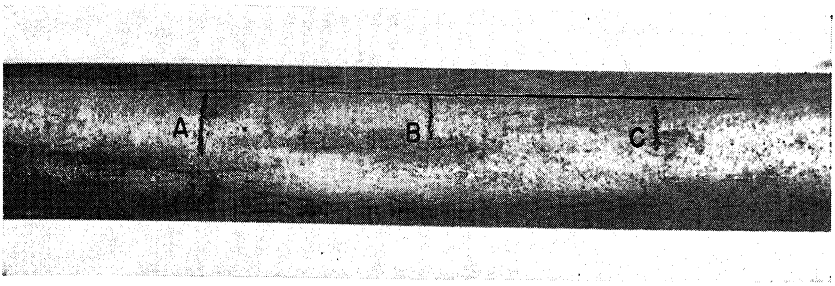

Magnaflux Corporation

Fig. 7. Magnetic-particle indication of a cooling crack of varying depth (see Fig. 8).

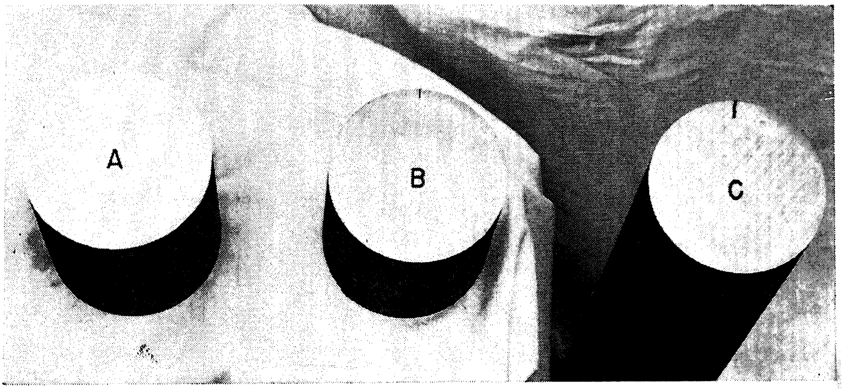

Magnaflux Corporation

Fig. 8. Cross-sections showing crack depths at locations marked on bar of Fig. 7.

INDICATIONS OF LAMINATIONS. Laminations in plate or sheet are formed in a manner similar to seam formation in bars. Since laminations are parallel to the surface, they cannot be detected with magnetic-particle inspection except at an edge or at a hole cutting through the lamination.

INDICATIONS OF FORGING LAPS. Forging laps are irregular in contour, are generally at right angles to the direction of metal flow, and often

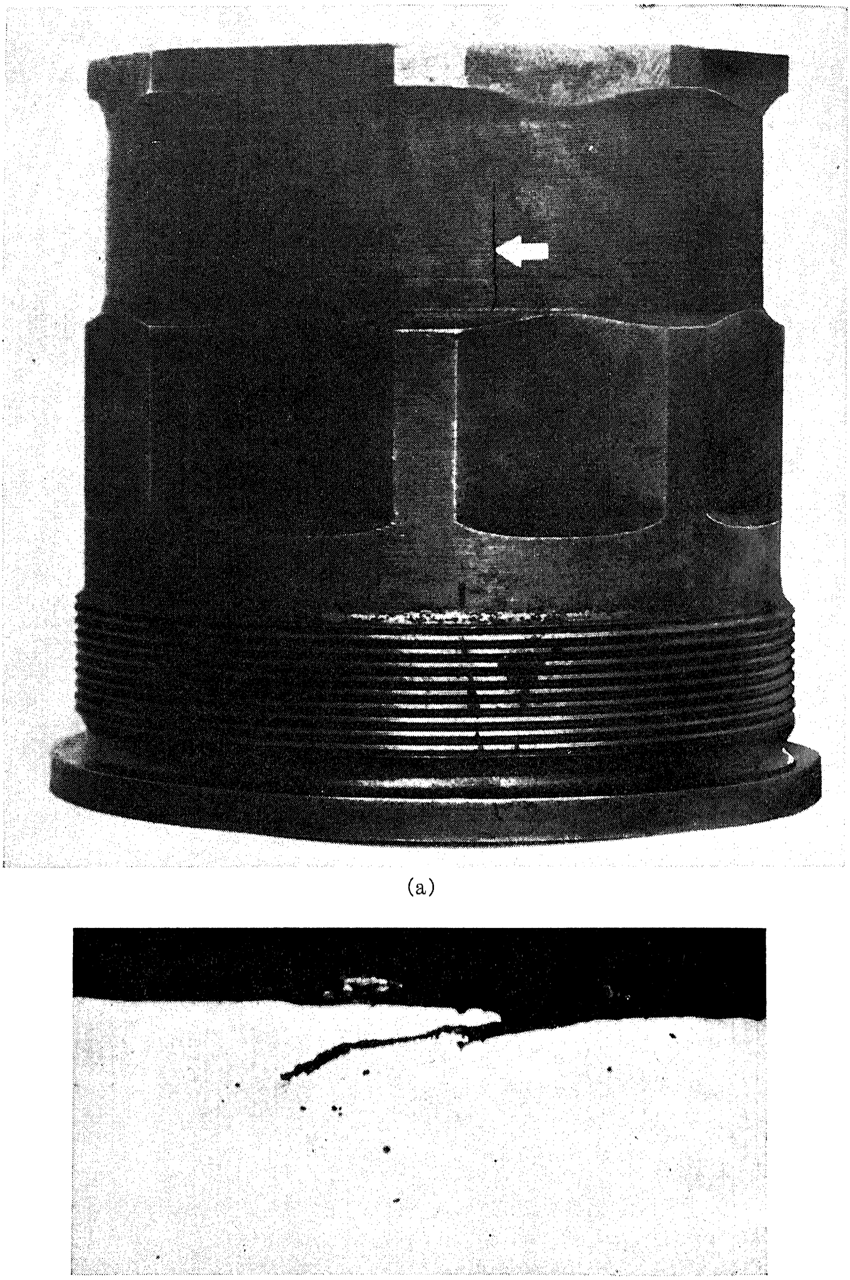

(a)

(b)

Magnaflux Corporation

Fig. 9. Forging lap in a propeller-shaft lock nut. (a) Magnetic-particle indication shown by white arrow. (b) Cross-section through forging lap of (a), magnified 100×, no etch.

occur at an acute angle to the surface. This last condition usually results in a fairly **weak leakage field.** For this reason indications of forging laps are often not well defined. Fig. 9(a) shows a forging lap and Fig. 9(b) a section through the lap, magnified 100×, which clearly shows the angle of the lap to the surface. **Destructive tests** must often be employed to confirm the inspectors' judgment or to determine the exact nature of a defect. **Sectioning** through the indication is extremely useful. Often **deep-etching** the surface of the cross-section brings out grain flow and gives important information as to the cause of the defect.

INDICATIONS OF FORGING BURSTS AND FLAKES. Forging a metal or alloy at too low a temperature may produce bursts, i.e., ruptures which may be wholly internal or which may occur at the surface, as shown in Fig. 10.

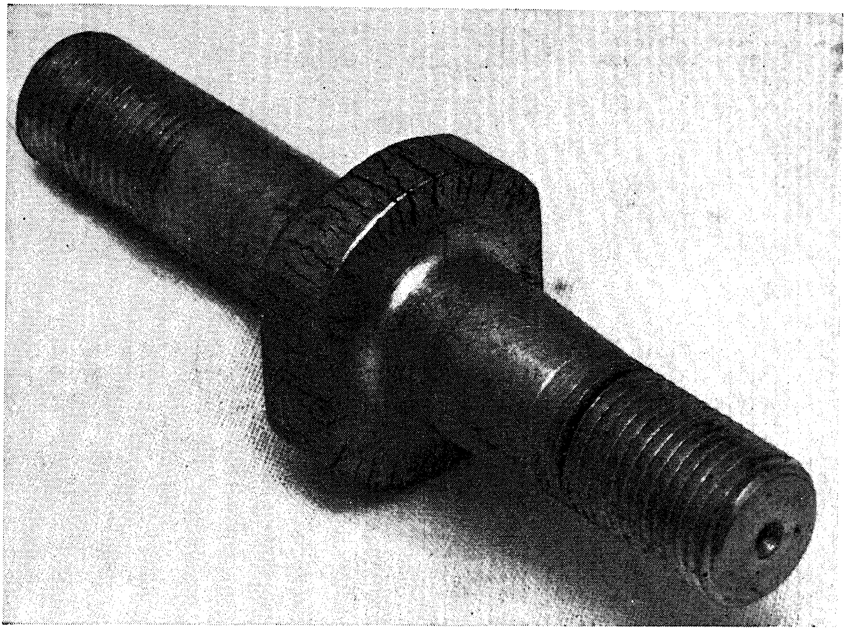

Magnaflux Corporation

Fig. 10. Magnetic-particle indications of forging bursts in upset forging.

When masses of metal are cooled too rapidly through a certain temperature range, they are subject to **internal ruptures** called "flakes." **Dissolved gases** coming out of solution in this temperature range contribute to this occurrence. Steels of certain composition are more susceptible to flaking than others.

INDICATIONS OF GAS POROSITY. Porosity in castings, caused by gases trapped in the solidification of the molten metal, can sometimes be located with magnetic-particle inspection. **Subsurface blow holes** in a cast steel flange are shown in Fig. 11. These indications were brought out with d.-c. magnetizing and dry powder. **Thermal cracks** in castings caused by unequal shrinkage can be shown with magnetic-particle inspection.

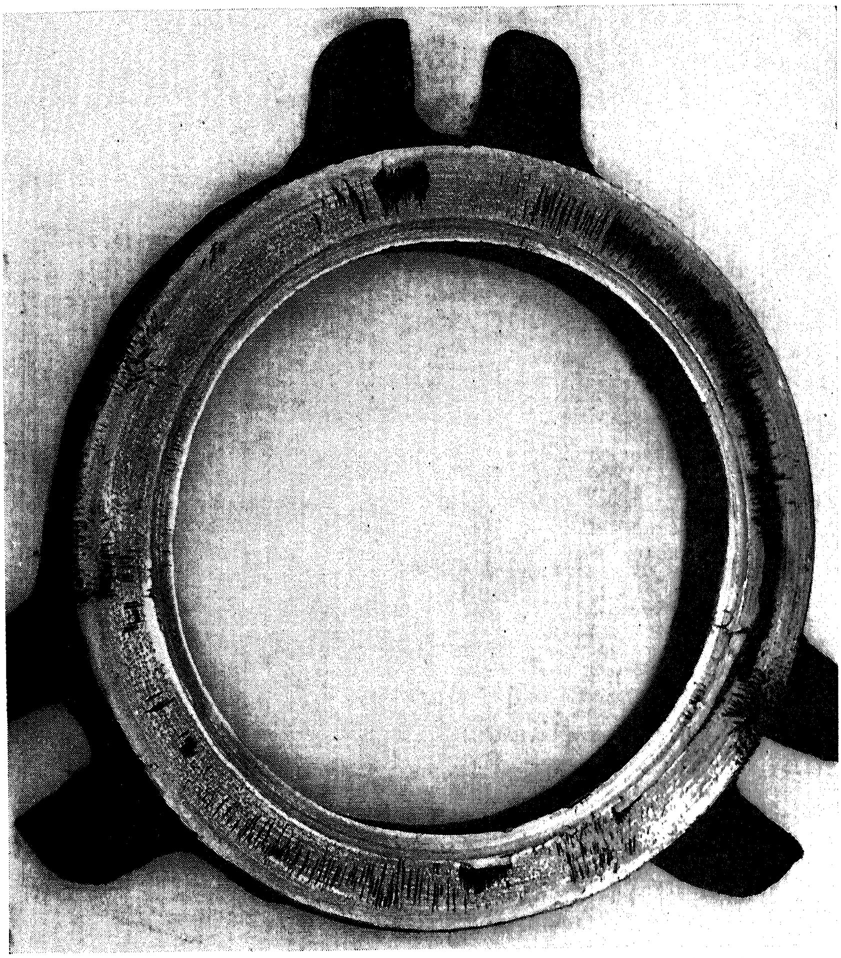

Magnaflux Corporation

Fig. 11. **Dry magnetic-particle indications of subsurface gas porosity (blow holes) in a cast steel flange.**

INDICATIONS OF INCOMPLETE WELD PENETRATION. Magnetic-particle inspection is used extensively on welds. It is possible to find **porosity, slag inclusions, shrink cracks, inadequate penetration, and incomplete fusion.** The indication pointed out by the arrow in Fig. 12 is broad and fuzzy, which is typical of a **subsurface discontinuity.** It is caused by lack of penetration at the root of the fillet weld. It may not represent a defect if 100 percent penetration is not needed in this part. This indication was brought out by half-wave magnetizing current and dry powder. Such a fuzzy indication may mask a serious **defect at the surface,** such as a fine shrink crack. However, if a.-c. is substituted for d.-c. magnetization, only these surface conditions will be revealed. Equipment used for weld inspection should be capable of producing

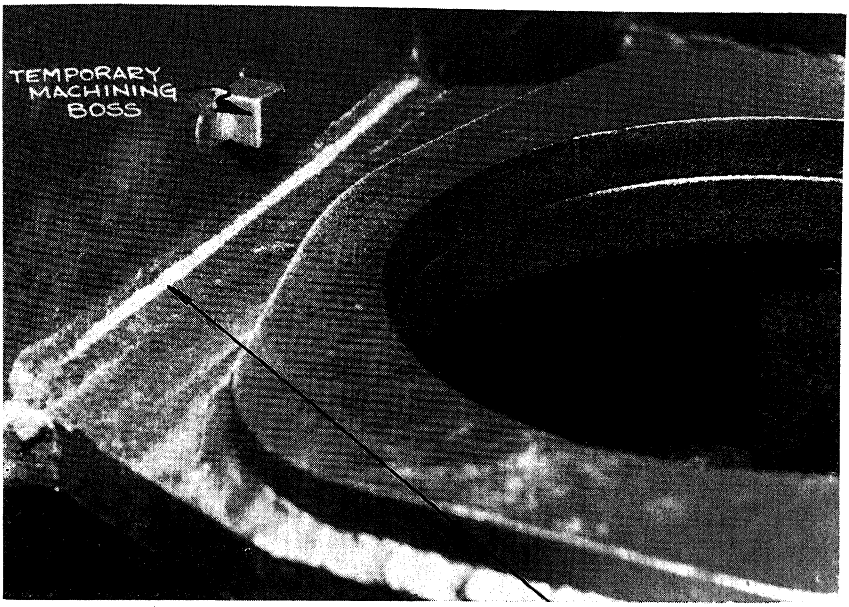

Magnaflux Corporation

Fig. 12. Dry magnetic-particle indication (arrow) of incomplete penetration in a fillet weld in a marine structural weldment.

both half-wave and a.-c. current, to enable the operator to detect either surface or subsurface discontinuities.

INDICATIONS OF HEAT-TREAT CRACKS. Cracks caused by faulty heat-treat processing are readily found with magnetic-particle inspection. Such cracks may occur during either the heating or quenching cycle and may be an enlargement of a condition existing in the part from some previous operation. Heat-treat cracks which are created by the quench cycle **(quench cracks)** usually are to be found at sharp changes of section, which cause unequal cooling rates, or at fillets or notches which act as stress-concentration points. The indication under the head of the bolt in Fig. 13 is caused by a quench crack. A similar indication can be produced by a fold in the **upsetting operation.** Fig. 14 shows a deep etch of a section through an indication similar to that shown in Fig. 13. Since the flow lines show no distortion—in fact the crack cuts directly across the flow lines—it is evident that the crack was introduced, after the upsetting, in the heat-treating operation. The destructive testing performed on this bolt demonstrates how laboratory techniques can increase the value of magnetic-particle inspection.

INDICATIONS OF GRINDING, PLATING, OR ETCHING CRACKS. One of the most prolific sources of trouble in highly finished precision parts is cracking caused by faulty grinding operations. **Grinding cracks** are often critical because they usually occur on surfaces which will be highly stressed. They are very fine and sharp and usually occur at right angles to the direction of grinding. Fig. 15(a) shows a typical example of grinding cracks which usually are found in groups or families, although occasionally a single

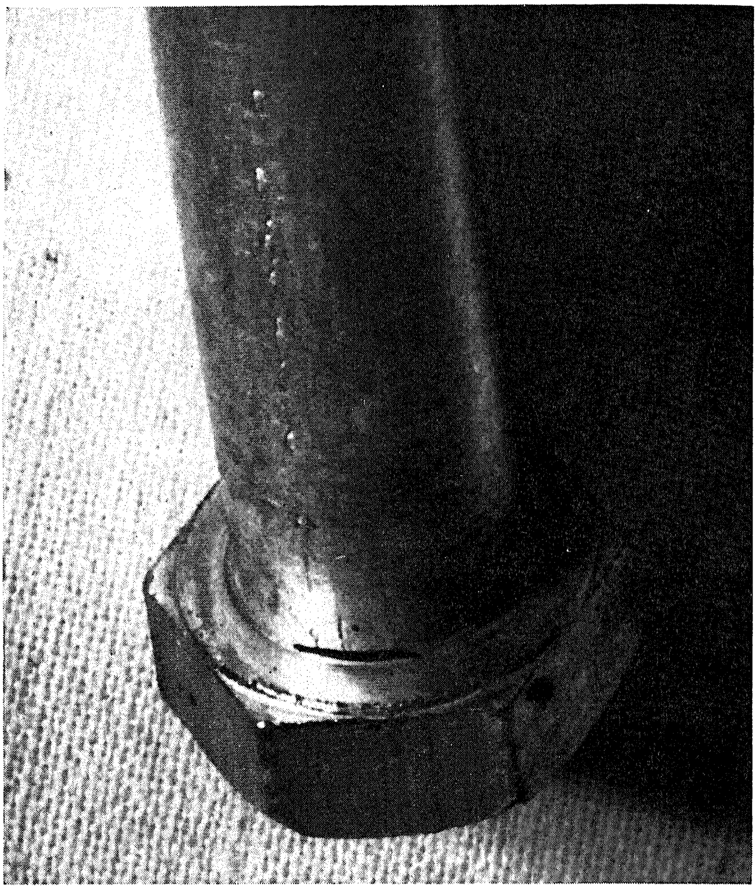

Magnaflux Corporation

Fig. 13. Magnetic-particle indication of a quench crack under a bolt head (see Fig. 14).

grinding crack may be found on a part. Fig. 15(b) shows a section through a grinding crack at 100×. This crack had an actual depth of 0.021 in.

Plating cracks or **etching cracks** are found only in areas where high residual stresses remain from some previous process, such as hardening. When such parts are plated, that operation may cause those stresses to crack the surface.

INDICATIONS OF FATIGUE CRACKS. Fatigue cracks are produced in service under **repeated stress reversals** or **stress variations.** A crack almost invariably starts at a highly stressed surface and propagates through the section until failure results. A fatigue crack will start more readily where design or surface conditions provide a point of **stress concentration.** Sharp fillets, poor surface finish, seams, grinding cracks—all act as stress raisers and assist in the start of fatigue cracking.

All magnetic-particle inspection to eliminate seams, inclusions, cooling cracks, laps, bursts, porosity, heat cracks, and grinding cracks is for the purpose of

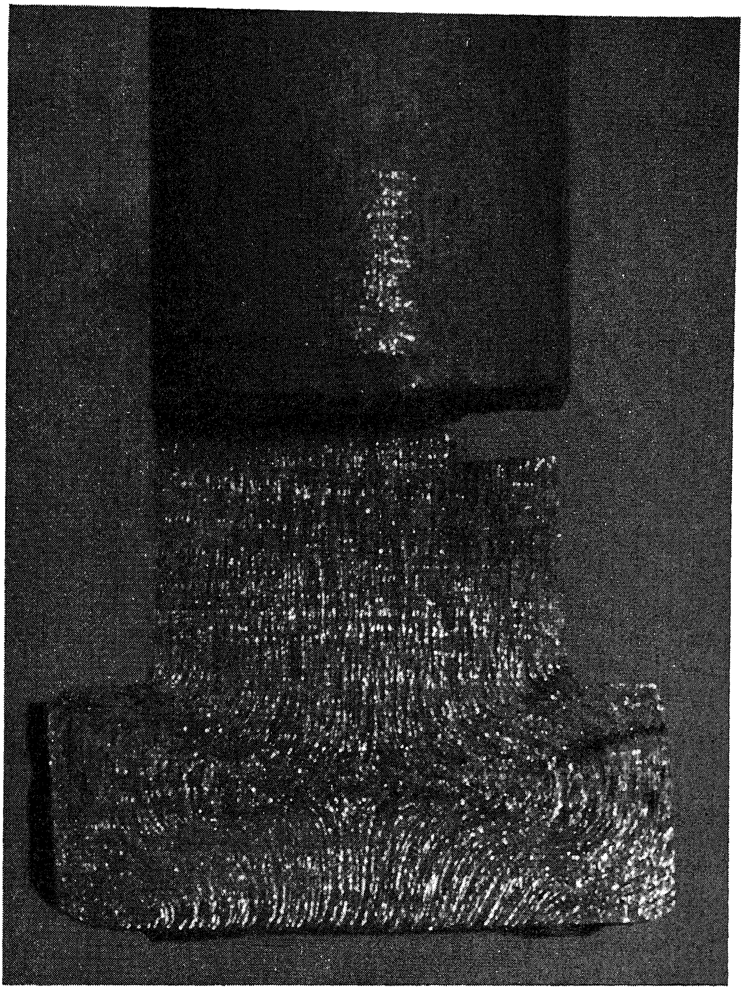

Magnaflux Corporation

Fig. 14. Cross-section, after deep etching, of quench crack in bolt head, similar to that shown in Fig. 13. Note the crack propagation across forging flow lines.

preventing fatigue or service failure after the part goes into service. Consistent and studied use of magnetic-particle inspection, as well as other nondestructive tests in a well-planned **preventive-maintenance program,** can in many cases reduce service failure from fatigue to practically zero.

Characteristics of Fatigue Cracks. Fatigue cracks occur only in parts that have been in service. They are, with few exceptions, **surface cracks** and can therefore be found by using **a.-c. current for magnetization.** They are sharp, close-lipped, and occur in a direction transverse to the direction of local stress. They are seldom perfectly straight but usually "wander" a bit from a straight line. Fig. 16 shows a fatigue crack in a crankshaft. A close examination of this

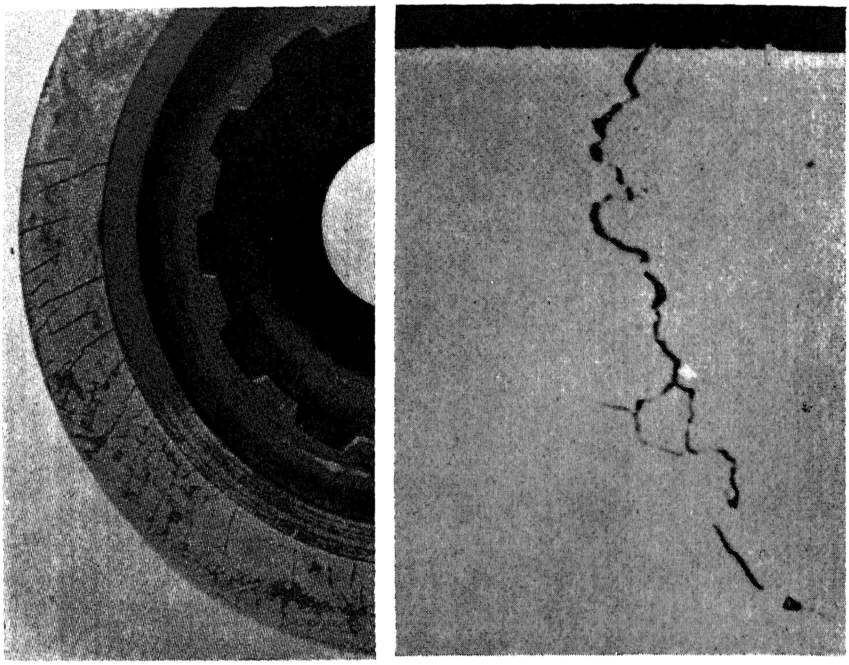

Magnaflux Corporation

(a) (b)

Fig. 15. Wet-method magnetic-particle indications of grinding cracks in a crankshaft. (a) Crankshaft assembly magnified approximately 1¼ times. (b) Cross-section through typical grinding crack with a depth of approximately 0.021 in. (Magnification 100×, no etch.)

crack showed that it started at the oil hole on the inside of the hollow shaft. The burr from drilling the hole had not been smoothed away, leaving small, sharp irregularities which served as **stress raisers.**

Development of Fatigue Cracks. Since a fatigue crack, once started, progresses through a cross-section, sometimes very slowly, it is sometimes referred to as a **progressive fracture.** The faces of such a crack are smooth and show typical "oyster shell" markings, or **fatigue crescents.** When complete fracture occurs, the last part of the section to break shows a rougher face. Fig. 17 shows the progression of a fatigue crack.

NONRELEVANT INDICATIONS. One last group of indications is extremely important in any consideration of interpretation. These are nonrelevant indications. The term "false indications" is not an accurate one for this group because they are caused in almost all cases by an accumulation of magnetic particles held to a particular area by a **leakage field.** With nonrelevant indications the leakage fields are caused by conditions which have no bearing on the suitability of the part for service and are therefore nonrelevant to the proper evaluation of the part.

Effect of Overmagnetization. Perhaps the most commonly found nonrelevant indication is the particle adherence due to local poles, i.e., leakage fields at **sharp**

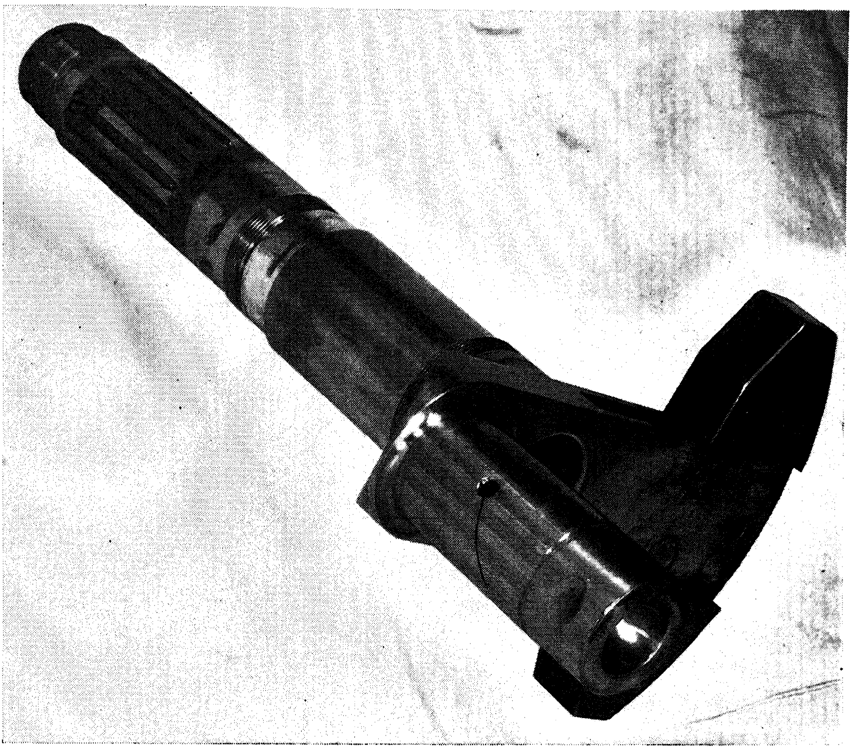

Magnaflux Corporation

Fig. 16. Magnetic-particle indication of a fatigue crack propagating from an oil hole on inside of a hollow crankshaft. The burr left from drilling served as a fatigue nucleus.

edges or at the **ends of parts** longitudinally magnetized. The presence of such patterns is often caused by overmagnetization.

Geometric Effects. A **constriction in the metal path** through which the magnetic field must pass may cause the field to be forced out of the part, creating poles which will attract particles. In Fig. 18 the splines on the inside of the hollow shaft create a particle pattern or nonrelevant indication on the outside surface. The field is crowded out by the reduced metal path at the base of the splines. Similar crowding at the inside corners of sharp fillets or at the root of threads may cause the same type of nonrelevant indication.

Recognition of Nonrelevant Indications. Nonrelevant indications can usually be recognized when:

1. Given the same magnetizing technique, indications appear on all parts and in the same locations.
2. Indications always can be related to some feature of construction or cross-section which accounts for such a leakage field by a constriction in the metal path.
3. Indications seldom appear, to an experienced inspector, like indications of actual discontinuities.

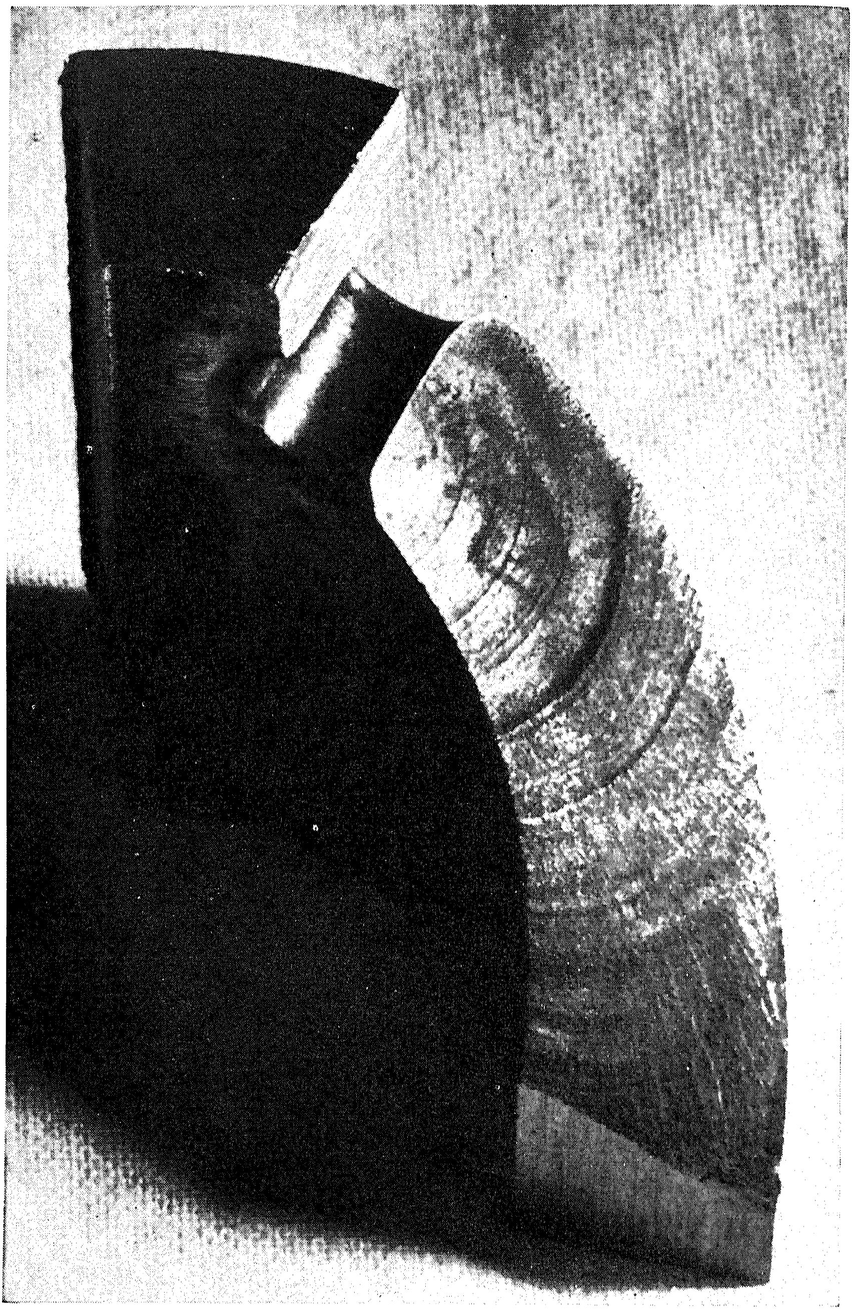

Magnaflux Corporation

Fig. 17. Progressive fracture showing typical "fatigue crescents."

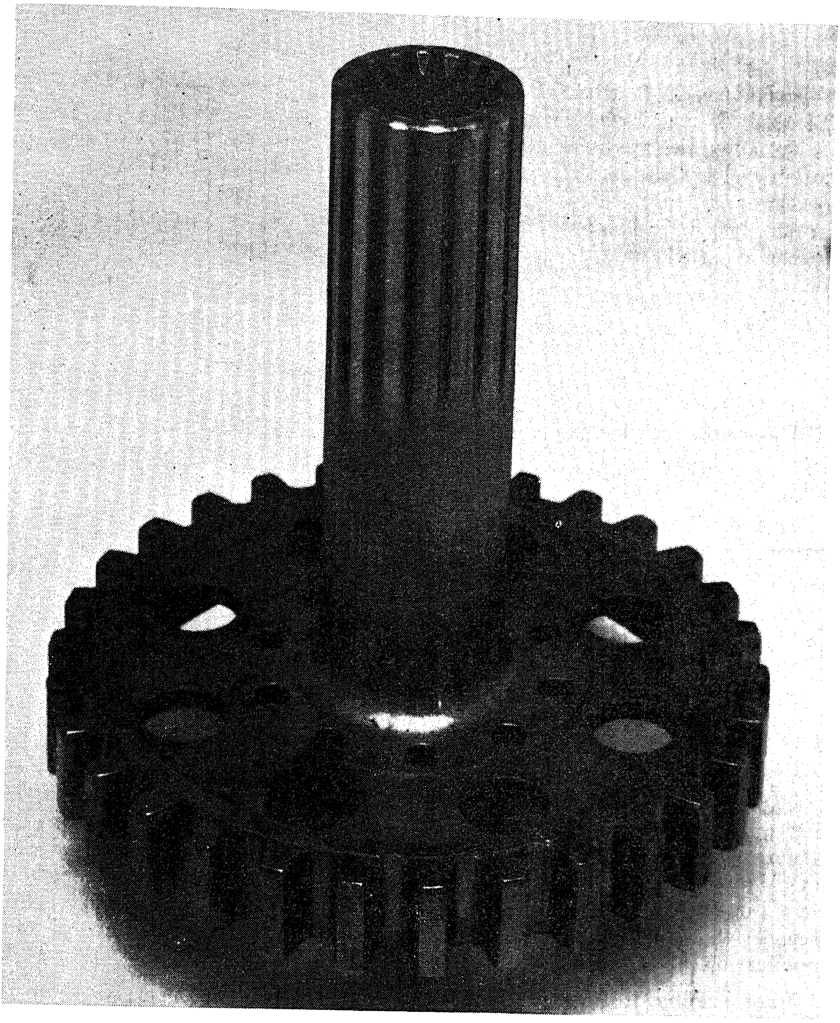

Magnaflux Corporation

Fig. 18. Nonrelevant magnetic-particle indications of interior splines of hollow shaft.

Magnetic Writing. Another type of nonrelevant magnetization indication is caused by the creation of local poles set up by contact between a hardened part and another piece of magnetized material. A **magnetized part** may produce poles on an unmagnetized part. Poles may also be produced on a circularly magnetized part by **contact with unmagnetized steel.** This type of nonrelevant indication is known as magnetic writing and can be recognized because the indication is poorly delineated and loosely held and usually runs in haphazard directions.

Nonrelevant indications are sometimes found at borders of **local areas of cold working** of a part or along the **weld line** in the parent metal, where the heat of welding has changed the permeability of the metal. Particle patterns will frequently be found at the boundary of the change of permeability.

PERMANENT RECORDS OF MAGNETIC-PARTICLE INDICATIONS. Magnetic-particle inspection is a rapid method in which indications of discontinuities are quickly formed on the part and remain there for interpretation and evaluation. There is no need to study an oscilloscope screen or to develop and study a negative and then relate that evidence to the part or area in question. It is, however, sometimes desirable to make a permanent record of magnetic-particle indications. There are four ways that permanent records can be made:

1. Lacquer-fixing of indication on part.
2. Transparent-tape fixing of indication on part.
3. Transfer of indication onto record sheet.
4. Photography.

The simplest visible record is a **sketch of the part** showing the location and extent of the indications. On large parts it is sometimes sufficient to sketch only the critical area.

Lacquer-fixing of Indications. If the part itself is to be preserved, the indication can be fixed permanently by using a transparent lacquer which should be thinned somewhat and applied by spraying or gently flowing over the indication. Before applying lacquer, the surface must be dry. If the indication was formed with the wet method, the vehicle used in making the bath must be allowed to dry before lacquering. **Drying of the indication** can be accelerated by heat or by gently flowing on a volatile solvent.

Indications can also be fixed on a part by covering with **pressure-sensitive transparent tape.** While this is faster than using lacquer, it may be difficult to get a smooth fit if the surface is irregular.

Tape Transfer of Indications. Transparent tape can also be used to lift indications from a part and transfer them to a permanent record sheet or card. Before using this method to transfer powder indications, it is essential that excess dry powder be blown off. **Wet-method indications** should not be transferred until the surface is dry. Tape transfers of indications are usually slightly broader than the original indications because of the **flattening effect of tape application.**

Photography of Indications. Photographs of indications can also be taken for record purposes. Enough of the part should be shown to make it possible to recognize the part and the position of the indication. It is also helpful to include a ruler or some familiar object in the photograph, to show relative size. Care must be taken to avoid **highlights and reflections** on highly polished parts, since they may make the indication less outstanding.

Fluorescent Indication Photography. Photography of fluorescent indications calls for special photographic techniques but, with practice, excellent results can be obtained. Fast panchromatic film is preferred. Pictures are taken in a darkened room with at least two 100-watt black lights positioned at a distance which gives evenly distributed illumination of the area being photographed. Sometimes better results are obtained by using white light during part of the exposure to record a faint outline of the part. **Exposure time** may vary from 20 min. to 1 hr., and a better result is usually obtained by using either a G (orange) or K2 (yellow) filter. When photographing highly reflective surfaces, the use of **polarizing filters** may improve results but longer exposure times will be needed with such filters. **Random fluorescence** on the part will reduce the contrast of the indication and the background and should be removed before photographing. Excessively high magnetizing currents may create a generally fluorescent background which can be reduced by reprocessing the part, using lower current values. Fluorescent oil or finger marks can be removed with solvents.

Nondestructive Supplemental Tests

REASONS FOR SUPPLEMENTAL TESTS. In specific, difficult problems of interpretation, various confirming tests help in determining the nature of discontinuities which produce magnetic-particle indications. Knowledge of what to look for is indispensable to intelligent interpretation of indications. On the other hand, the ability to recognize magnetic-particle indications of discontinuities, so as to identify them definitely, depends equally on actual experience with **indications of typical discontinuities.** To gain such experience, one must actually identify sufficient cases to be acquainted with the kinds of indications produced by various discontinuities. Therefore, various supplemental tests are needed. These tests often involve cutting up a typical specimen to see what the discontinuity really is and where it is located.

Many confirming tests are simple and can be performed with limited laboratory or testing equipment. Others require specialized equipment and experience involving use of testing laboratories and methods of metallographical investigation.

DIRECT SURFACE INSPECTION. Often an indication cannot be satisfactorily accounted for within the inspector's experience, and no decision can be made regarding such indications without supplemental tests. However, each test improves the inspector's knowledge and makes it easier to identify similar indications later.

Some of the simplest tests are almost instinctively applied when an indication appears. For instance, when one observes **magnetic-particle build-up,** one almost automatically wipes it off the surface to see what may lie underneath. Sometimes some sort of surface irregularity appears immediately under the indication, though its exact nature may not be clear.

Checking Indications by Residual Magnetization. Usually the powder or liquid bath is reapplied to determine if the indication readily reappears. This is first tried without demagnetizing or remagnetizing; that is, one attempts to reproduce the indication by the **residual method.** Since the residual method is always less sensitive than the continuous method, the manner in which the residual indication reappears helps to indicate its severity and extent. As a matter of fact, this criterion of reproduction by residual magnetization is made the basis of acceptance or rejection on many aircraft engine parts under the recommended practice of the U.S. Navy, Bureau of Aeronautics. Often it is worthwhile to demagnetize the part and repeat the test from the start to confirm the indication.

SURFACE INSPECTION WITH MAGNIFIERS. Most inspectors carry a small hand glass with magnifications from 2 to perhaps 7 diam. Examining the indication under low-power magnification often helps the inspector to form an opinion as to its cause. Such a magnified view may show that the **powder build-up** is dense and tightly packed, as from a sharp discontinuity lying at or just under the surface. Powder somewhat spread out and loosely packed would indicate a discontinuity farther below the surface; or it could mean that the indication is due to some nonrelevant condition. Again, wiping away part of the indication and looking just under it with a low-powered glass may reveal a **surface condition** responsible for the powder pattern. The majority of surface cracks and seams can be seen with a low-power glass after they have been located by magnetic-particle inspection.

Cleaning Surface. If the surface being examined is scaled, rusted, or covered with a thin coat of paint, examination with a low-power hand glass is often facilitated by using **fine emery paper** to clean the surface where the indication appears. Such cleaning clears away surface material which may obstruct a view of the crack itself. Sometimes a new application of powder over the clean surface will be helpful. Sometimes an indication appears on a **rough-machined surface** where the roughness of the surface itself may obscure the crack even though the magnetic particles clearly indicate its presence. Here again, smoothing of the surface with emery paper (this time perhaps somewhat coarser so that some actual surface metal is removed) makes it possible to see the crack with a low-power glass.

Inspection Glasses. Most inspection-department equipment includes large-diameter, low-power, magnifying glasses set on stands with some sort of lamp to illuminate the specimen (see section on Visual Inspection Equipment). Such glasses are extremely useful, not only for examination of particular specimens but often in the course of routine inspections as well. The nature of the parts or the character of the defects sought may make such low-power magnification of the surface helpful in seeing the indication in the first place. These glasses usually have a magnification of about 4 diam. but provide a large viewing area so that a considerable portion of the surface can be seen at one time.

Binocular Microscope. Often a surface crack may be extremely fine or closed at the surface, so that it cannot be seen with low-power magnifying glasses. An extremely useful piece of supplemental equipment for the inspector, therefore, is a binocular microscope which permits examination of surfaces at higher magnification (see section on Visual Inspection Equipment). Binocular microscopes are easy to use and do not require a skilled technician. These microscopes come mounted on stands for bench use, but **special mounting supports** are also provided which permit the microscope to be swung out on an arm at any desired height so that large and irregularly shaped pieces can be examined. The principal requirement for such examinations, in addition to the microscope itself, is good light. Since the area which can be magnified and observed at one time is much smaller than that examined with lower-power lenses, better light on the surface is proportionately more important.

Binocular microscopes of this type are fitted with various lenses to permit **magnification ranges** from 10 to about 32 diam. Such magnifications make nearly all surface discontinuities visible, although, again, some surface preparation may be necessary. Such **surface preparation** may involve cleaning with emery cloth or smoothing with a file or coarse emery. Sometimes light etching of the surface is useful. Of course, if none of these methods of surface examination reveals a surface discontinuity which will account for the magnetic-particle indication, and the indication persists after the surface is smooth and clean, the presumption is that the discontinuity is below the surface. Interpretation of **subsurface discontinuities** may be confirmed by the appearance of the powder particles when examined under one or another of these magnifying devices. These surface examinations are usually the first step in the identification of a discontinuity and damage the part in no way.

PROBING METHODS. Often information beyond that revealed by microscopic surface examination of a discontinuity is required. Various simple methods of probing the **depth and extent of a discontinuity** are available and are frequently used.

Filing. One of the simplest probing methods is the use of either a triangular or flat file, used cornerwise. Usually one selects a point where the appearance of the powder pattern suggests that the discontinuity is most severe and cuts across the indication with the file. Such cutting, of course, will quickly show whether the indication is caused by a very shallow surface condition or whether it penetrates appreciably into the metal. The file cut is usually continued until the **bottom of the crack or seam is** reached or until the cut has gone to such a depth that it becomes apparent the defect is severe enough to warrant rejection of the piece. Checking the seam or crack at the file cut by **reapplying magnetic powder** or liquid indicates whether or not the cut has gone to the bottom of the defect, as shown by Doane and Betz, Principles of Magnaflux, in Fig. 19.

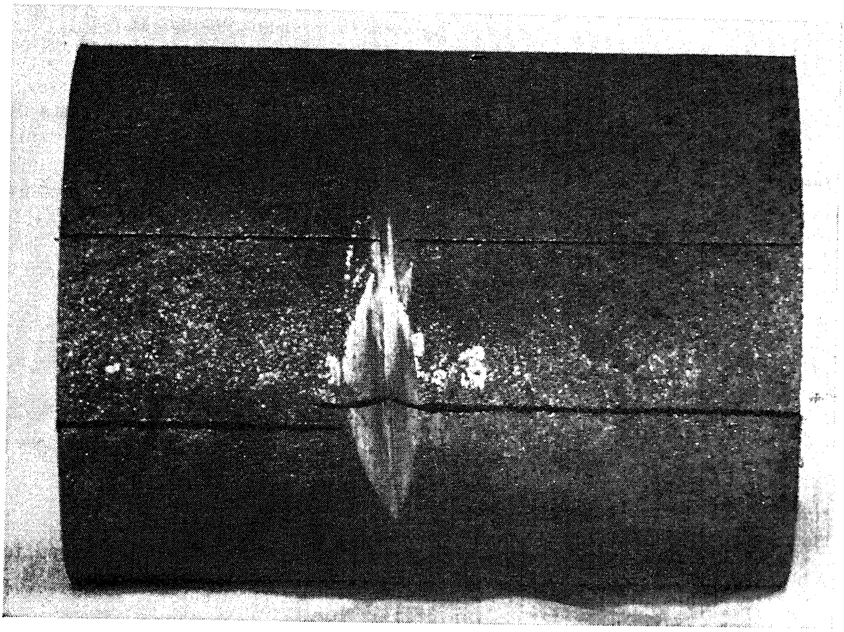

Fig. 19. File cut applied to a crack in bar stock. Crack is shown with magnetic particles.

The **file method of inspection for seams** in hot-rolled bars, particularly alloy and tool steel bars, is common practice in all mills. It is sometimes the only means of inspection and serves as an aid to the eye of the inspector where magnetic-particle inspection is not being used to locate seams. The file method of checking may, of course, be used on any surface. However, **filing on finished parts** may destroy usefulness for service. On some parts, such depth probing may determine whether the defect can be removed by finish machining or grinding.

Grinding. A similar test for determining depth and extent of surface discontinuities is obtained by grinding the surface at the indication. For this purpose a **flexible-shaft grinding wheel** is often used. Another very useful tool is the **small hand grinder**, provided with a number of specially shaped grinding heads which permit grinding down at the location of the crack with a minimum removal of metal beyond that strictly local to the crack. Such grinding methods permit exploring a crack over a greater length more readily than by filing.

In the **inspection of small forgings,** for instance, it is common practice to investigate indications of forging laps with the grinding wheel. **Shallow laps** are usually ground out entirely, so that the objectionable condition is completely removed from the part. Caution must be exercised to determine that the area ground has sufficient tolerance to permit grinding.

Chipping. An additional method for probing the depth of surface seams or cracks is by chipping. Chipping either by hand or by power hammer, using properly shaped chipping tools, is much faster than grinding and cuts more quickly to the bottom of deep cracks. Chipping methods are most commonly used on **welds, castings, and forgings,** not only that the inspector may determine the actual depth of the defect but also in **preparation for salvaging.**

In such chipping operations, the **split chip test** is also useful. This merely involves observation of the manner in which the chip comes away from the chisel as the cut proceeds either along or across the crack. If the crack extends completely through the chip being removed, the chip would, of course, separate into two parts. When the cut extends below the bottom of the crack, the chip will not separate. A **magnetic-particle check,** however, is a sure safeguard.

REMOVAL OF DEFECTS. Grinding and chipping methods often serve the double purpose of determining the extent of the defect and at the same time removing the defect from the part. **Forgings** are commonly ground to remove entirely a discontinuity which does not penetrate below the minimum dimensional tolerance of the part. Frequent rechecking with magnetic particles is used to ensure complete removal of such defects.

Repair by Welding. In case of large castings, forgings, and heavy welds, a crack may be chipped out and the cavity filled with weld metal if the operation is carried out with suitable precautions. For the purpose of such **salvage,** it is essential that the crack be entirely removed. A magnetic-particle check of the bottom of the chip groove is necessary to ensure that no trace of the crack remains before welding is begun.

Flame Gouging. In the particular case of castings, removal of the defect before welding may be accomplished by flame gouging. By suitable manipulation of the cutting torch, metal may be very rapidly removed in a defective area. By watching the surface of the metal under the flame before actual cutting commences, it is often possible to observe the presence of a surface crack. However, magnetic-particle checking before welding is again a safe precaution.

Destructive Supplemental Tests

REASONS FOR DESTRUCTIVE TESTS. To derive the maximum possible information concerning a questioned indication, numerous useful tests involve complete destruction of a part. Such tests, of course, cannot be regularly applied in the course of routine inspection, but they are invaluable to the inspector who is attempting to improve his own knowledge of the nature of defects occurring in the products for which he is responsible. Such tests also are frequently used after a part has been rejected because of an indication, in order to confirm the judgment of the inspector making the rejection. This, of course, again leads to increased knowledge to aid further decisions.

FRACTURING. One of the easiest destructive confirming tests is to break the part or attempt to break it through the discontinuity. Usually preliminary tests have shown that the indication is caused by a surface crack or discontinuity of some sort.

Fracturing by Hammering. The part may be placed in a vise in such a manner that the metal on one side of the crack is held firmly. The rest of the piece projects from the vise so that when struck heavy blows with a hammer, it will tend to break at the crack. Such procedures usually work best on **hard parts,** although they are sometimes applied with good results on relatively soft materials (Fig. 20).

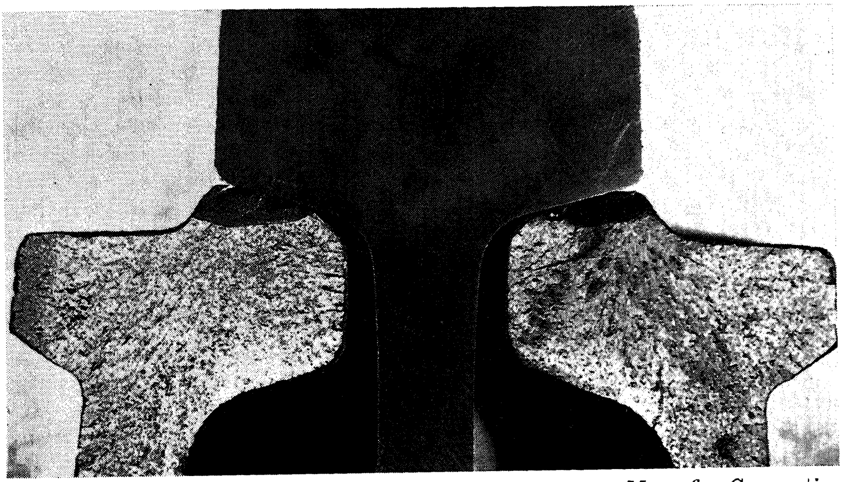

Magnaflux Corporation

Fig. 20. Two rail-joint bars with fracture completed through fatigue crack.

Fracturing in Mechanical Testing Machines. Another way of completing the fracture, if the section is too large to handle by the hammer and vise method, is to put the part in a large testing machine and apply a load in such fashion that the part tends to break at the crack. Such methods are particularly effective in the case of **fatigue cracks** or in the case of **heat-treat and grinding checks.**

Fracturing After Blueing by Heating. Sometimes the value of a test can be increased by heating the part before fracturing to a sufficiently high temperature so that the surface becomes blued. When fracture at the crack is completed, the original face of the crack itself will appear dark, while the fracture produced at the time of breaking will be bright.

Fracturing After Chilling. To facilitate fracturing, particularly on small parts, the part may be chilled in dry ice and then fractured immediately. At temperatures far below 0° F., most steels, even those which may be relatively soft at ordinary temperatures, become brittle enough to break easily.

SAWING. Often it is desirable to examine a **cross-section of the crack or discontinuity.** Various methods are used for sectioning a part. If the material is soft, the easiest procedure is to saw across the crack to obtain a view of the depth and direction of the crack in a cross-section. This may be done with a hand or power hacksaw or with a slotting saw on a milling machine.

TREPANNING OR CORE DRILLING. When large forgings, castings, or other bulky parts are being investigated, a complete section is difficult or costly to make. It is simpler to remove a piece of metal by various methods so as to include a cross-section of the crack for its entire depth. **Slotting saws,** chisels, and various ingenious methods are sometimes necessary to get such a piece out of the larger part. One rather easy technique is to use a **core drill.** This is a circular hollow cutter which drills a core about an inch in diameter. Cores may extend to any required depth. This method of cutting a section (often called "trepanning") is extensively used in the investigation of **welds in heavy plate.**

SECTIONING WITH CUT-OFF WHEELS. Usual sawing methods are either too slow and difficult or cannot be used at all to make a cross-sectional cut on **very hard materials** because the saws are not so hard as the part itself. In this case, sectioning by means of the **high-speed abrasive wheel or disc** is easy. The disc revolves at very high speeds and is quite thin, often only 1/16 in. thick. It is made up of a fine abrasive cutting material molded into shape with hard rubber or plastic which preferably should not be brittle. A **brittle wheel** might break if a deep cut were being made and the part not carefully fed. Such a cutting device should never be used unless it is fully guarded to minimize **danger to the operator** if breakage does occur, nor should the part ever be hand fed against the wheel. Many such cutting wheels are provided with a mechanical feed.

Effects of Overheating While Cutting. Great care must be taken to avoid overheating of the part during this cutting operation. Heating at the cut is very rapid, and even slight local temperature increases may cause the **crack** being investigated to extend beyond its original length or depth. Such heat may also change the **structure of the metal,** which may be a matter of importance. Frequently it is necessary to remove the specimen and cool it under water or adopt other means to keep the cut cool. Some wheels operate under water. This probably is the best technique, although some, which are also very good, apply a **constant stream of water** to the cut.

EXAMINATION OF CUT SURFACE. Some cut cross-sections can be examined without further treatment, either directly with a glass or microscope or by the application of magnetic particles after suitable magnetization (Fig. 21). More often, however, it is better to smooth the surface of the cut in some manner. This can sometimes be done by using a flat file held crosswise of the work so that, by grasping the ends of the file with both hands, the back-and-forth motion will produce a perfectly flat and relatively **smooth surface.** This may be followed by **polishing** with emery cloth which may be wrapped around the file and applied with similar motion. Alternatively, the emery can be laid on a flat surface and the cross-section laid against it and smoothed by a back-and-forth motion.

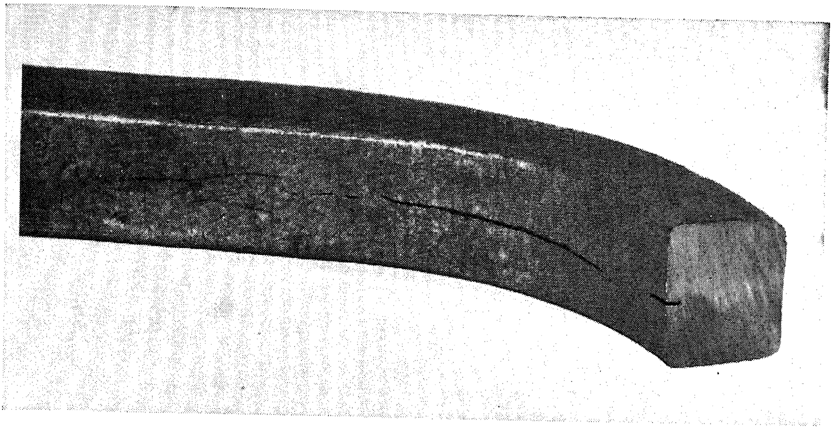

Magnaflux Corporation

Fig. 21. Spring sectioned on cut-off wheel. No surface preparation. Depth of crack on section is shown with magnetic particles.

Belt Sanding. Draw filing and emery polishing are usually best done in a direction transverse to the crack. The belt sander can be used as a substitute for draw filing. This is especially useful for a hard part. In this case the **emery or carborundum cloth** moves in the form of an endless belt across a solid, flat backing surface. The face of the section of the part should be held firmly against the surface of the moving belt. This produces the same effect as the hand motion on the flat emery cloth but can be done more rapidly and with less effort. By using successively finer grades of cloth, a surface which is flat and free of coarse scratches can be obtained. After such preparation, magnetic particles may be applied, or the depth and contour of the crack may be examined under the binocular microscope.

Etching. Acids or other etching reagents can be used to obtain information with respect to discontinuities, either on the original surface of a part or on a cut cross-section. "Etching" is the term applied to the process of attacking the surface under examination by means of acids or other chemical reagents. Such **etching materials** eat out the surface but not uniformly. For instance the edges of a crack will be more rapidly attacked than the flat surface adjoining these edges. The result is that the surface opening of the crack is exaggerated, often making a very fine crack easily visible to the eye. Minute **variations in composition** of the metal also affect the rate of attack of the etching material. **Grain boundaries** or **flow lines** indicating the grain flow in the metal in rolling or forging can be brought out in relief.

Types of Etching. Etching can be conducted in various ways for various purposes, and the technique varies widely, depending on the information sought. The purpose of etching may be to bring out the coarse structure or surface characteristics of the metal. In this case it is referred to as **macro-etching.** Etching designed to bring out microscopic grain structure and characteristics of the metal is referred to as **micro-etching.**

Deep Etching or Macro-etching. Macro-etching is most frequently applied as a **severe acid attack** (often called "deep etching") for the purpose of bringing out **flow lines** and exaggerating **cracks and segregated areas.** In this case,

acid etching reagents are used. When the purpose of the etch is to show **grain structure,** a solution of **ammonium persulfate** is used instead of acids. Such an etch applied to a cross-section through a weld will reveal the boundary of the weld area and distinguish between base metal and weld metal, as shown by Doane and Betz, Principles of Magnaflux, in Fig. 22.

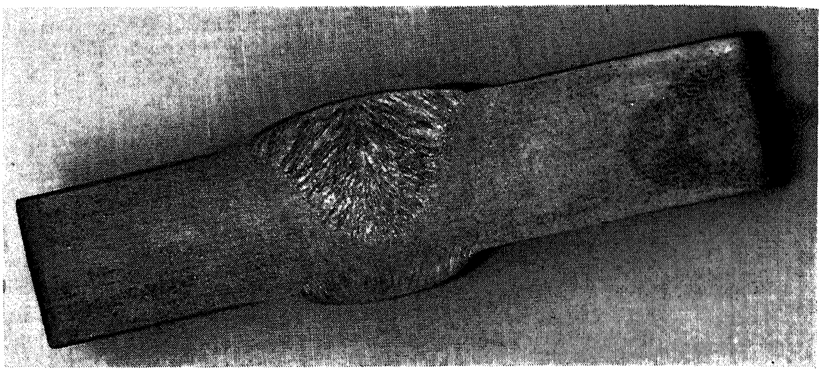

Fig. 22. Persulfate-etched section of a double-Vee butt weld.

Persulfate Etching. Persulfate etching is carried out with a 10 to 20 percent solution of ammonium persulfate in water. This solution is used cold and swabbed on the surface to be etched with a cotton swab. Etching proceeds quite rapidly, and when complete to the desired point, the surface is washed, dried, and lacquered.

Etching of Ingots or Coarse Castings. Persulfate etching on a cross-section of an ingot or a nonheat-treated casting will show the **coarse casting structure** resulting from relatively slow freezing of the molten metal. The use of etching methods to reveal the presence of cracks in surfaces is of long standing. Before the advent of magnetic-particle inspection, it was much more commonly used than at present as a method of locating surface cracks in suspected areas.

Etch Cracking. If a hardened part is to be etched, one precaution must be consistently kept in mind. **Heat-treated or ground articles** which have not been thoroughly stress-relieved by tempering or drawing contain **residual stresses** to such an extent that if the surface fibers of the metal are attacked by etching reagents, these stresses may cause cracks to appear in the surface as the stresses relieve themselves. Such cracking (often spoken of as "etch cracking") appears on the etched surface (as shown by Doane and Betz, Principles of Magnaflux, in Fig. 23) and is often indistinguishable from cracks which may have been present before etching.

Tempering Before Etching. Failure to recognize this occurrence has often led to false conclusions regarding the presence of cracks in such articles. If, therefore, the surface of a **highly hardened part** is to be etched as a means of confirming the presence of cracks or of investigating cracks revealed by magnetic-particle test, the specimen should first be freed of **residual stresses** by heating to temperatures which probably need not exceed 700° F., cooling slowly, and then submitting to the etching reagent.

Etching Technique and Equipment. Surfaces to be etched may or may not require preliminary preparation. They should, at least, be free of **oil and grease.**

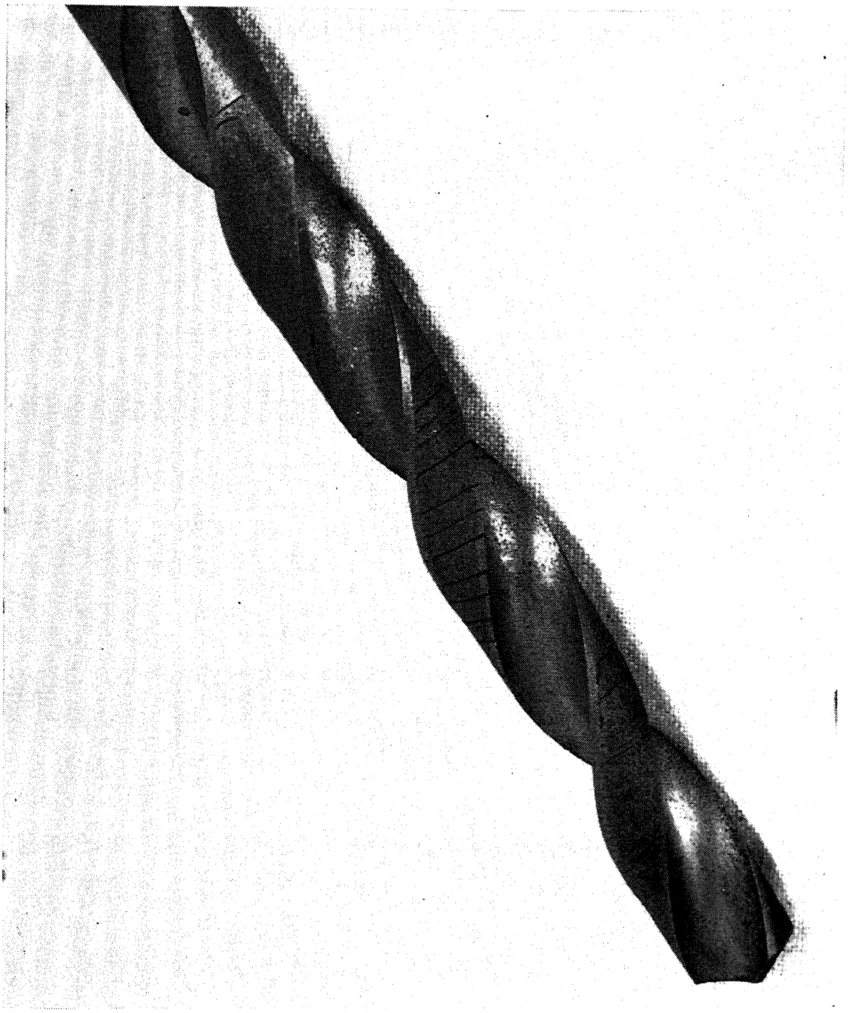

Fig. 23. Etching cracks in a twist drill.

Scale or other **corrosion products** usually need not be removed prior to deep etching, since the acid itself dissolves or removes scale and rust and exposes the etched surface without additional help. Cut surfaces should be relatively smooth, and usually some sort of dressing, as described previously, is desirable.

Acid Etching. Deep etching for **grain flow** (illustrated by Doane and Betz, Principles of Magnaflux, in Fig. 24) requires a less smooth surface than persulfate etching for structure. The usual **deep etching reagent** consists of equal parts of commercial hydrochloric acid and water and is used hot at a temperature of from 160° F. to 175° F. Sufficient attack on most steels can be obtained in 15 to 45 min. with this technique. The same reagent can be used cold, but in that case several hours may be required to complete the etch.

Another **acid mixture** that is considered satisfactory for such etching is a mixture of 38 percent by volume of commercial hydrochloric acid, 12 percent of concentrated sulfuric acid, and 50 percent of water. **Caution:** Concentrated sulfuric acid can cause severe burns and must be handled with great care. It is important to add the sulfuric acid to the cold mixture, rather than vice versa, to avoid the danger of spattering. Temperature and etching time are approximately the same as for the hydrochloric-acid mixture. The etching should be carried out in glass or porcelain vessels. Since the **fumes from the process** are corrosive, care must be taken that such fumes do not damage metallic equipment in the laboratory. When etching is complete, the specimen is washed under hot running water and scrubbed with a stiff brush. It is usually a good plan then to wash the etched surface with dilute ammonia to neutralize any **remaining acid,** after which scrubbing in hot water is repeated. The part should then be dried rapidly and protected from rusting by the application of a thin, clear lacquer.

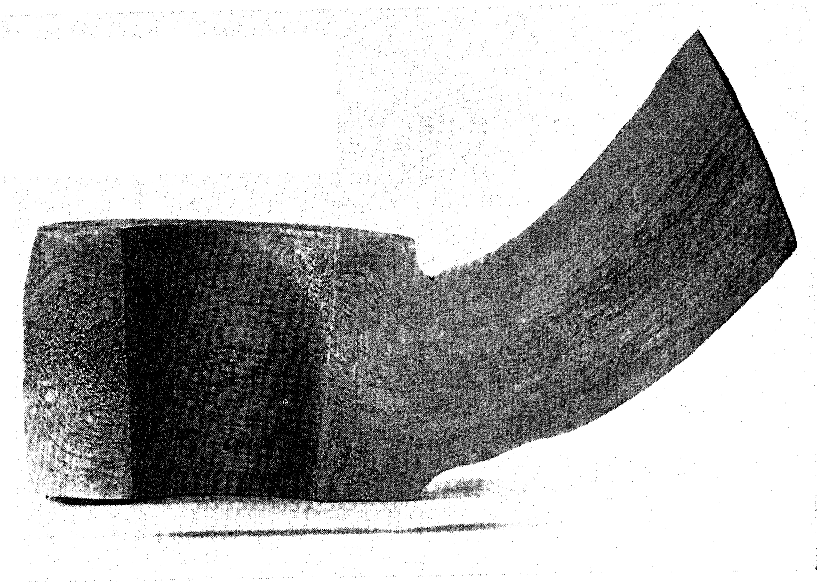

Fig. 24. Deep-etched section of a forging, showing flow lines.

METALLOGRAPHIC EXAMINATION. Often a great deal of information as to the character and origin of a crack or other discontinuity which has produced a magnetic-particle indication can be obtained by examining sections at much higher magnification than provided by the usual binocular microscope. Satisfactory microscopic examination requires very special equipment and special skill and training on the part of the person who undertakes such investigations. Usually this is a job for a metallurgical laboratory, but the methods employed are of general interest.

Preparation of Specimen. Specimens for examination under the microscope should be small and must, of necessity, be free of all **surface scratches** which could interfere with proper observation of the surface at high magnification. A section is usually cut across the crack or over a questionable area. Special care must be exercised, particularly if the cutting-off disc is used, so that **local heat**

does not change the metal structure or the extent of the crack at the section. The cross-section is (1) brought to a flat surface on the belt sander or coarse polishing wheel, (2) polished on succeeding grades of emery of increasing grain fineness, and finally (3) polished to a scratch-free surface on special polishing wheels employing fine polishing materials such as rouge, magnesium oxide, and alumina.

Examination of Nonetched Specimens. Properly polished specimens are usually examined under a microscope at **magnifications** of 50 to 200 diam. Microscopes must be provided with special methods of illuminating this surface, since at high magnification the lens must be extremely close to the metal surface. The character and extent of cracks and other discontinuities, as well as large and small nonmetallic inclusions, can be studied by such examination. Most **metallurgical microscopes** are provided with camera attachments so that typical portions of the surface can be photographed at high magnifications (see section on Visual Inspection Equipment).

Examination of Etched Specimens. Much additional information can be obtained from specimens by etching their surfaces and examining under magnifications of 100 diam. or more. Such etching differs greatly from macro-etching.

The **most common etching fluid,** especially for carbon steels, is a mixture of 5 parts of nitric acid to 100 parts of alcohol. The reagent is called **"nital."** It reveals grain structure and carbon distribution in plain carbon steels and most steels of low alloy content. Numerous other etching reagents are used for various steels and for various purposes. Micro-etching requires considerable skill and experience and is often done in only a second or two. In examining a cracked specimen after micro-etching, information may be obtained as to (1) whether the crack has followed grain boundaries or cut across them, (2) whether the edges of the crack have been oxidized with a resultant loss of carbon in the layers of metal immediately adjoining the crack, (3) whether there is a decarburized surface layer of metal that may have affected the start of a fatigue crack, and much other information along similar lines. The interpretation of structure is the field of the **trained metallurgist.**

UTILITY OF TESTS. The supplemental tests just described are for the most part simple and require equipment usually already available in most plants. All the equipment, with the exception of metallurgical microscopes and polishing facilities, is relatively inexpensive and can be readily obtained if not available. In the utilization of the results of nondestructive testing for defects, such tests are obviously of great value, since they confirm the **inspector's judgment** in interpreting such results and build up his **experience in diagnosing trouble.**

Often much **more elaborate tests** and **experimental programs** are well worthwhile for the purpose of determining definitely the reason for the occurrence of certain defects. Such tests can lead more positively to design, material, or process improvement. The **avoidance of defects,** rather than their mere location, should be the goal of all nondestructive testing of this type.

Bibliography

Allen A. H. "Improved Tools Expedite Magnetic Particle and Penetrant Inspection," *Metal Progr.*, 65, No. 1 (1954): 161.

Baxter, L. E. "Magnetic Particle Inspection of Welds," *Can. Welder*, 46, No. 6 (1955).

"Black Light Finds Flaws in Axles," *Mod. Railroads,* (January, 1949).

Caine, J. B. "What's Wrong With Castings," *Foundry,* 79, No. 6 (1951): 106, 267.

Catlin, F. S. "Nondestructive Sample Testing for Cracks Aids Heat Treating," *Metal Treating,* (March–April, 1956).

"Checking Equipment Parts Saves Time and Money at Dewey Cement Plant," *Pit and Quarry,* (February, 1954).

Cover, H. T. "How the PRR Uses Non-destructive Testing," *Ry. Age,* 135, No. 26 (1953): 48.

Dehn, G. L. C. "Magnaflux for Quality Control of Pipe-Line Welds," *Welding J.,* 32 (1953): 721.

———. "Magnetic Particle Inspection in the Oil Industry," *Drilling Contractor,* (April, 1950).

DeVries, A. J. "Productive Inspection Assures Quality and Reduces Scrap," *Chicago Midwest Metalworker,* (January, 1956).

Doane, F. G., and C. E. Betz. *Principles of Magnaflux.* 3d ed. Chicago: Photopress, 1948.

"Double Inspection Assures 'Safe Service' Castings," *Iron Age,* 178, No. 1 (1956): 67.

Geist, C. M. "Magnetic Particle Inspection," *Nondestructive Testing,* 10, No. 3 (1951–1952): 27.

Harrer, J. R. "Greater Acceptance of Welding Through the Use of Inspection Methods," *Welding J.,* 36 (1957): 252.

"Latest Improvements in Diesel Overhaul," *Southern Power & Ind.,* (October, 1949).

Lee, F. E. "Fleet Shop Detective," *Fleet Owner* (October, 1949).

Lindgren, A. R. "Complete Weld Check Setup Prevents Leaks on Indiana Line," *Gas,* 29 (1953): 132, 134, 136, 138.

Love, J. L. "The Value of Scientific Inspection," *Proc. 27th Ann. Conv. Automotive Engine Rebuilders Assoc.,* (May 19–21, 1949).

MacPherson, J. R., and A. H. Prucknicki. "Detecting Flaws in Traction Gears," *Ry. Locomotives and Cars,* 125, No. 12 (1955): 66.

Maradudin, A. P. "Quality Control of the Fabrication of High Yield-Strength Pipelines," *Gas,* 25, No. 8 (1949): 77.

McParlan, J. L. "How Nondestructive Testing Aids Power Station Maintenance," *Power Eng.,* 61, No. 3 (1957): 57.

Oye, L. J. "Nondestructive Testing of Structures," *Welding J.,* 33 (1954): 223.

Patterson, N. C. "Armco Avoids Accidents with Lifting Inspection Program," *Power Eng.,* 59, No. 11 (1955): 80.

Peterson, R. S. "Engineering Life Savers," *Speed Age,* (April, 1950): 18.

Platt, D. M. "How Magnetic Particle Inspection Aids Maintenance at Camas," *Paper Trade J.,* 138, No. 20 (1954): 98.

Robinson, A. "Magnetic Particle Inspection of Jet Engine Parts," *Nondestructive Testing,* 10, No. 3 (1951–1952): 19.

Simkins, M. K. "Parts Inspection Pays in Three Ways," *Com. Car J.,* (October, 1953).

Skeie, K. "Increased Foundry Profits Through Non-destructive Testing," *Trans. Am. Foundrymen's Soc.,* 63 (1955): 730.

Smith, O. G. "Magnetic Particle Technique Makes Billet Inspection Positive and Efficient," *Iron Age,* 175, No. 18 (1955): 99.

Sweet, J. W. "Weldment Inspection in Aircraft Construction," *Nondestructive Testing,* 10, No. 2 (1951): 34.

Thomas, W. E. "Economic Factors of Nondestructive Testing," *Nondestructive Testing,* 11, No. 4 (1953): 9.

Totaro, S. C. "Nondestructive Tests Check Forging Quality, Spot Equipment Troubles," *Iron Age,* 174, No. 7 (1954): 117.

"Tracking Down Cracks and Hidden Flaws," *Bus Transportation,* (August, 1950).

Upson, F. A. "Magnaflux Inspection of Welded Storage Tanks," *Welding J.,* 29 (1950): 27.

Viglioni, J. "Fatigue Strength of Bolts Reduced by Longitudinal Flaws," *Prod. Eng.,* 28, No. 3 (1957): 203.

Wenk, S. A., and H. M. Banta. "A New Nondestructive Test for Corrosion Fatigue Cracks in Drill Pipe," *Oil Gas J.,* 50, No. 2 (1951): 90.

SECTION 33

MAGNETIC-FIELD TEST PRINCIPLES

CONTENTS

PAGE

Magnetic-Field Probes

Types of probes 1
Foerster probe arrangements 1
    Probe arrangements used for various problems (*f.* 1) 2
  Longitudinal field probe 1
  Field difference (gradient) probe 1
  Tangential gradient probe (tangential component) 2
  Tangential gradient probe (normal component) 2
  Astatic magnetometer probe 2
  Tape or gap probe 2
Probe-coil operation 2
  A.-c. hysteresis loop 3
    Magnetization curve of a ferromagnetic material (*f.* 2) 3
  Hysteresis loop with d.-c. bias 3
Circuit for measuring d.-c. magnetic fields .. 3
    Circuit arrangement for measuring d.-c. magnetic field (*f.* 3) 4
    Derivation of secondary-voltage wave forms for the field probe arrangement (*f.* 4) 5
  Secondary voltage 4
  Second harmonic voltage 4
Circuit for measuring field difference 6
    Derivation of secondary-voltage wave forms for the gradient (*f.* 5) 7
  Secondary voltage 7
  Accuracy of field gradient measurements 8
Design of instruments 8

Probe-Type Magnetic Field Meters

Precision magnetic-field meter 8
  Circuit arrangement 9
    Block diagram of the electric circuit of the field meter (*f.* 6) 9
  Meter calibration 9
  Types of pick-up probes 9
  Measurements of uniform fields 10
  Measurements of nonuniform fields 10
  Cancellation of earth's field 10
  Field gradient measurements 10

PAGE

  Tape-probe measurements 10
  Tape test technique 11
  Tape transport 11
  Recording instruments 11

Hall-Generator Magnetic Field Meters

Hall generators 11
    Hall generator element used for static magnetic-field measurements (*f.* 7) 12
  Materials for Hall-effect probes 11
  Measurement of tangential field strength .. 12
  Hall detector probes 12
    Arrangements of Hall probe measurement heads (*f.* 8)............................ 13
Use of Hall detector instruments 14
  Measurement of strong magnetic fields 14
    Arrangement of Hall generator with compensation of the Hall voltage by a potentiometer arrangement, for sensitive comparison of strong magnetic fields (*f.* 9) 14

Application In Magnetic-Particle Testing

Surface field strength measurements 14
  Surface flux density 15
  Demagnetization by free poles 15
    Distribution of magnetic field in a complicated test part, showing the demagnetizing action of free magnetic poles (*f.* 10) 15
  Intensity of demagnetization 15
  True field strength 16
  Calculation of demagnetization factor 16
  Determining true field strength 16
The field recorder method 16
  Field distribution on magnetized camshaft . 17
    Distribution of the true field strength (H_t) on a camshaft at a coil field (H_a) of 190 oersteds (*f.* 11) 17
  Measuring impulse fields 17
References 17
Bibliography 18

SECTION 33

MAGNETIC-FIELD TEST PRINCIPLES

Magnetic-Field Probes

TYPES OF PROBES. During recent years there has been a great increase in use of magnetic-field instrumentation. The following **static magnetic-field measurement methods** are now used in industry:

1. The rotating coil.[1]
2. The oscillating coil.[2]
3. The second-harmonic magnetometer (Foerster probe).[3]
4. The impedance variation of bismuth wires in magnetic fields.[4]
5. The Hall generator.[5]
6. The deflection of an electron beam in vacuum.
7. Nuclear resonance.[6]

A method using the **Hall generator** has recently led to several new measurement methods and promising applications in nondestructive testing.[7] These developments are a result of the recent discovery of new substances with an unusually large Hall effect and a low temperature sensitivity.[8] In the field of nondestructive testing in European industry, the method utilizing the **Foerster probe**[9] is especially successful because of the small probe dimensions and its high sensitivity.

FOERSTER PROBE ARRANGEMENTS. The heart of the Foerster device is a pair of specially constructed probes having cores of high-permeability material that saturates at a relatively low flux density. For some types of instrumentation utilizing the Foerster probe, the two cores with their associated coils are mounted in separate probes. In other cases the two cores are mounted in fixed positions with respect to each other in the same probe. Fig. 1 summarizes probe-coil arrangements used for various problems.

Longitudinal Field Probe. The arrangement shown in Fig. 1(a) is used to measure the static magnetic-field component along the longitudinal axis of the probe coil. This arrangement finds applications in **geophysics** and **ship degaussing.** The same arrangement, in miniaturized form, is used to determine true field strength on the surface of magnetically soft material and to evaluate effects of **static screening.**

Field Difference (Gradient) Probe. The arrangement shown in Fig. 1(b) measures field differences independently of average field strength. Designed in miniaturized forms, it measures the **field gradient.** Practical applications include:

1. Iron search instrument.
2. Detection of ferromagnetic impurities.
3. Astatic coercive-force measurements.

4. Wall-thickness meters for nonferrous materials.
5. Local hardness measurements.

Tangential Gradient Probe (Tangential Component). Fig. 1(c) illustrates the probe-coil arrangement for measurement of the tangential component of the tangential field gradient. This arrangement serves for:

1. Measurement of the tangential component in the point-pole method.
2. Local coercive-force measurement.
3. Nondestructive determination of the magnetic anisotropy of sheets.

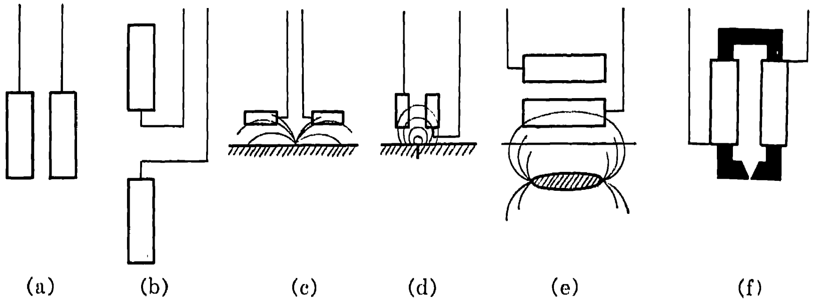

Institut Dr. Foerster

Fig. 1. Probe arrangements used for various problems. (a) General field strength measurement (geophysics, ship measurements, etc.). (b) Field difference measurement (iron search instrument, astatic coercive-force measurement arrangement, pole searcher, wall thickness meter for nonferrous materials). (c) Tangential component of the tangential gradient (local coercive-force measurement, nondestructive determination of the magnetic anisotropy). (d) Normal component of the tangential gradient (crack testing, coercive-force measurement with double-point method). (e) Tangential component of the normal gradient (astatic magnetometer). (f) Gap probe for the measurement of the state of magnetization in small zones (sound-tape measurement).

Tangential Gradient Probe (Normal Component). Fig. 1(d) presents the arrangement for measurement of the normal component of the tangential field gradient. This arrangement is used for:

1. Crack testing.
2. Local coercive-force measurement with the double-pole method.
3. Wall-thickness measurements on ferromagnetic materials.

Astatic Magnetometer Probe. The probe arrangement of Fig. 1(e), for measurement of the tangential component of the normal gradient, is used in the astatic magnetometer for determination of sample magnetization.

Tape or Gap Probe. Fig. 1(f) illustrates the gap probe for measurement of the magnetization in small zones having an extent of a few microns. This method is used in industry for the measurement of **magnetic tapes** and **magnetic recorder wires.**

PROBE-COIL OPERATION. Each probe core carries a **primary** and **secondary winding.** In some cases the primary coils are connected in series opposition. At any instant the alternating-current (a.-c.) field due to the first primary coil acts in the opposite direction to that of the second coil. The two secondary coils are connected in series so that the two secondary voltages add. Conversely, the primary coils may be connected in series adding and the secondary coils in series opposing.

A.-C. Hysteresis Loop. Fig. 2(a) shows the magnetization curve of a ferromagnetic material (solid line). The magnetization curve is assumed to be free from hysteresis, which means that the magnetic induction B is zero when the field strength H is zero. When an alternating current is applied to a coil containing the ferromagnetic material, the magnetization field strength H varies symmetrically about the zero axis [Fig. 2(b)]. When a direct-current (d.-c.) magnetic field (for example, the earth's field) is applied to the core material in addition to the a.-c. field, the curve is displaced horizontally along the H axis to the position shown by the dotted line.

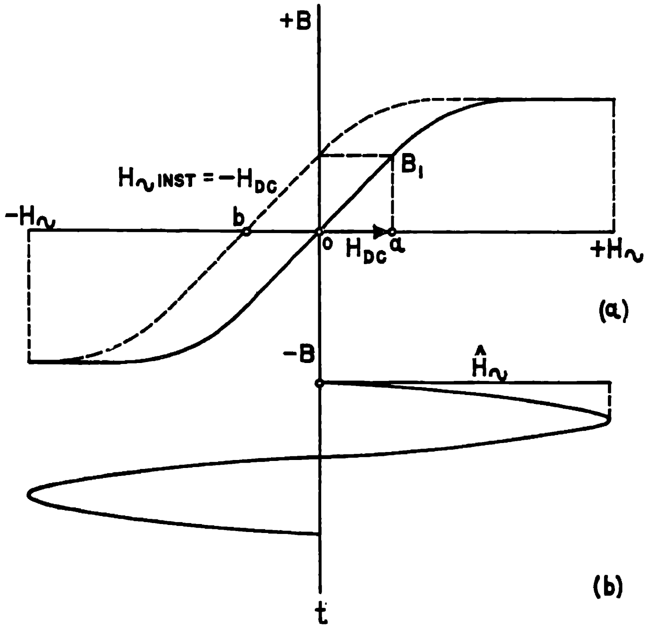

Fig. 2. Magnetization curve of a ferromagnetic material.

Hysteresis Loop with D.-C. Bias. Let $H_{\text{d.c.}}$ be the simultaneous d.-c. field. When the a.-c. field passes through zero, the induction B has not yet reached zero because the field $H_{\text{d.c.}}$ is still applied to the coil. The field $H_{\text{d.c.}}$ corresponds to an induction B_1 [see Fig. 2(a)]. The entire field H, and consequently the induction B, equals zero only when the instantaneous value of the a.-c. field is equal and opposite to the d.-c. field (point b). That is, under the action of the d.-c. field, the (dotted) **magnetization curve** in Fig. 2 is displaced by an amount $H_{\text{d.c.}}$ in the horizontal direction from zero, opposite to the direction of the field.

CIRCUIT FOR MEASURING D.-C. MAGNETIC FIELDS. Fig. 3 shows an arrangement of two cores, K_1 and K_2, each having a magnetization coil through which magnetizing current flows. The magnetization coils are wired so that at any instant, the **magnetizing field strength** at K_1 is equal in magnitude to but opposite in direction from that at K_2. Fig. 4(a) shows the two **magnetization loops** plotted on the same graph. If a d.-c. field, $H_{d.c.}$, is applied so that it has the same direction in both strips, the magnetization curve of K_1 is displaced from zero to b, and the magnetization curve of K_2 is displaced in the opposite direction from zero to a. Fig. 4(b) shows the sum of the two displaced curves, $B_1 + B_2$. In the absence of a d.-c. field, the sum $B_1 + B_2$ is zero because of the opposite magnetization of the two loops. However, under the influence of a d.-c. field, a horizontal displacement of both curves results. The sum $B_1 + B_2$ is then different from zero.

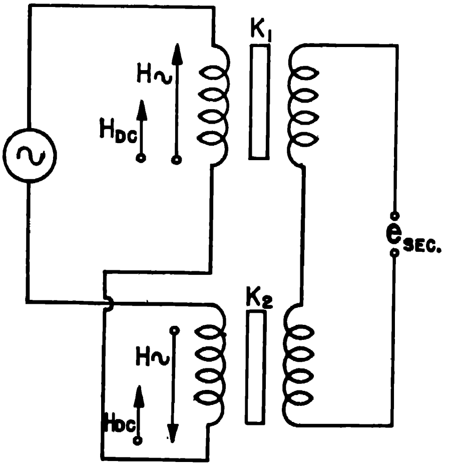

Institut Dr. Foerster

Fig. 3. Circuit arrangement for measuring d.-c. magnetic fields.

Secondary Voltage. The secondary voltage e_{sec} at the terminals of the two secondary coils in Fig. 3 is

$$e_{sec} = \frac{d}{dH}(B_1 + B_2)\frac{dH}{dt} \tag{1}$$

$$e_{sec} = \frac{d}{dt}(B_1 + B_2) \tag{2}$$

Fig. 4(d) shows the secondary voltage which appears under the influence of the d.-c. field.

Second Harmonic Voltage. Fig. 4(d) indicates that the frequency of the secondary voltage contains a strong second harmonic component. When the sum $B_1 + B_2$ goes through half a period, the secondary voltage goes through its full period. The dependence of the secondary voltage on the d.-c. field to be measured can be analytically investigated. The time variation of the secondary voltage, Fig. 4(d), can be expanded as a Fourier series,[10] and closed expressions can be obtained for the fundamental wave and harmonics.

The development of the afore-mentioned mathematical process is very involved, so only the final results are given here. The second harmonic component of the

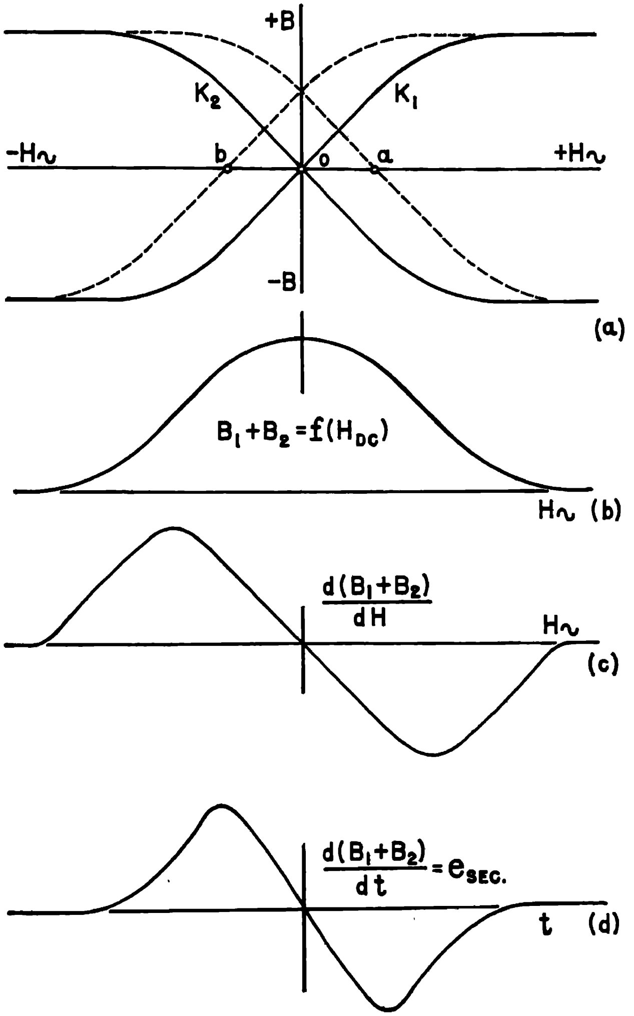

Fig. 4. Derivation of secondary-voltage wave forms for the field probe arrangement.

secondary voltage can be filtered out of the spectrum. This component can be used to measure the d.-c. field. The **maximum amplitude** e_2 is

$$\hat{e}_2 = 2\pi f w_2 F \mu_\Delta \hat{H}_\sim \left[\frac{4}{\pi} \sin\left(2\frac{H_s}{\hat{H}_\sim}\right) \frac{\cos\left(2\frac{H_s}{\hat{H}_\sim} \cdot \frac{H_K}{H_s}\right)}{1-\left(\frac{4}{\pi}\frac{H_s}{\hat{H}_\sim} \cdot \frac{H_K}{H_s}\right)^2} \right] \left[\sin\left(2\frac{H_{\mathrm{d.c.}}}{\hat{H}_\sim}\right) \right] \qquad (3)$$

where w_2 = the number of secondary turns on the probe coil (Fig. 3).
f = the magnetization current frequency.
F = the cross-sectional area of the probe-coil core.

μ_A = the initial relative permeability of the coil core (slope of the straight portion of the curve where it passes through zero induction). This value is dependent upon the ratio (l/d) or form permeability.
H_s = the saturation field strength (the intersection of the continuation of the straight portion of the loop with the saturation magnetization line).
H_K = the bending field strength which results from the approximation of the hysteresis curve by an extension of its straight-line portion to H_s.
$\hat{H}_\sim$ = the maximum amplitude of the magnetization field strength.
$H_{\text{d.c.}}$ = the d.-c. field to be measured.

For a given curve shape for the core (H_s, H_K, μ_A), as well as a specific magnetization field strength $\hat{H}_\sim$, at the location of the probe core, the term

$$\frac{4}{\pi}\sin\left(2\frac{H_s}{\hat{H}_\sim}\right)\frac{\cos\left(2\frac{H_s}{\hat{H}_\sim}\cdot\frac{H_K}{H_s}\right)}{1-\left(\frac{4}{\pi}\frac{H_s}{\hat{H}_\sim}\cdot\frac{H_K}{H_s}\right)^2}=h_2 \tag{4}$$

can be combined as a constant h_2. Investigation has shown that the value of the expression h_2 is relatively insensitive to changes in the ratios of H_K/H_s and $H_s/\hat{H}_\sim$.

Therefore the voltage generated by the field probes is

$$e_2 = B\sin\left(2\frac{H_{\text{d.c.}}}{\hat{H}_\sim}\right) \tag{5}$$

where the constant B contains the operational and constructional data of the probe coil as well as the magnetic characteristics of the core. The magnetization field strength $\hat{H}_\sim$ should be much greater than the highest d.-c. field strength, $H_{\text{d.c.}}$, to be measured, so that

$$\sin\left(\frac{2H_{\text{d.c.}}}{\hat{H}_\sim}\right) = \sin\,\theta \cong \theta$$

can be replaced by the angle θ. The result is that the secondary voltage increases linearly with the d.-c. field strength to be measured; i.e.,

$$\hat{e}_2 = AH_{\text{d.c.}} \tag{6}$$

The proportionality between the d.-c. field strength and the secondary voltage generated by the probe coil is an essential characteristic of the **field-strength meter.** Fig. 3 shows the arrangement of the two probe coils for field-strength measurement. Note the opposing directions of the primary windings (magnetization windings) as well as the similar winding sense of the secondary windings.

CIRCUIT FOR MEASURING FIELD DIFFERENCE. It is a remarkable characteristic of this field instrumentation method that the field-strength meter is converted into a **difference-field meter** simply by turning one probe coil into the opposite direction. The latter indicates only the difference in field strength at the locations of the two probe coils, independently of the d.-c. field strength.

For difference-field measurements, the primary winding of one of the probe coils shown in Fig. 3 is reversed, without changing the balance of the circuit. The magnetization direction H_t is now the same in both halves of the probe coil, while the secondary windings are connected in phase opposition. If a uniform d.-c. field is superimposed on the a.-c. field and is parallel to it at the location of the two probe coils, the horizontal curve-displacement depicted in Fig. 2 occurs in the same direction in both loops [Fig. 5(a)]. In this case $B_1 - B_2$ equals zero under the influence of a uniform d.-c. field [Fig. 5(b)]. As soon as a field difference appears between the two probe coils, however, the displacement of the two curves will be of different magnitude [Fig. 5(c)]. A field difference,

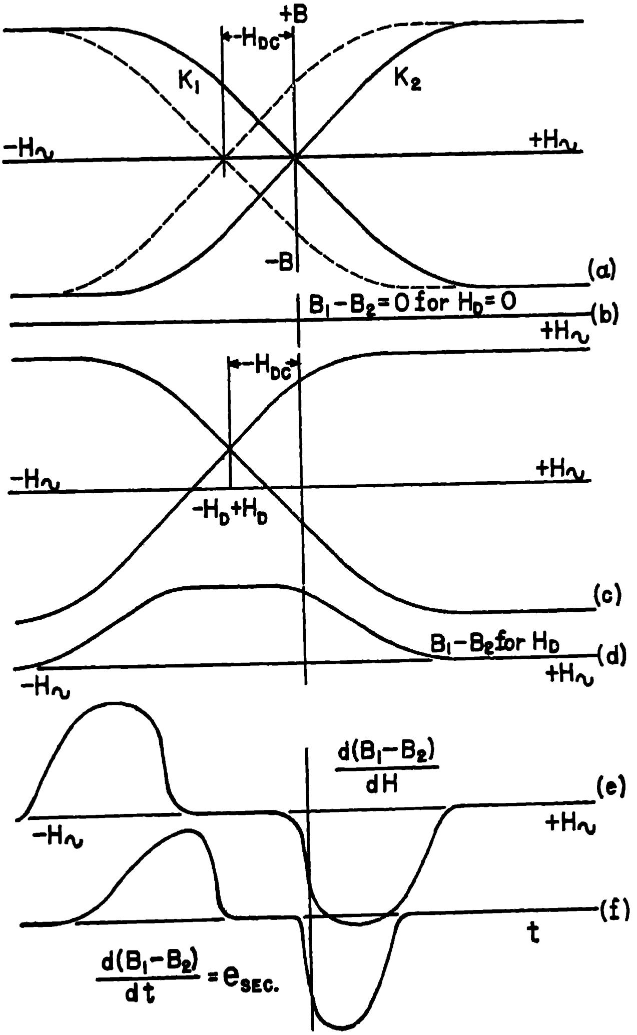

Fig. 5. Derivation of secondary-voltage wave forms for the gradient.

$2H_D$, causes the curve K_1 to be displaced by an amount H_D to the left. The cross-over point of the two curves, measured from the zero reference of $H_{\sim\text{inst.}}$ equals $-H_{\text{d.c.}}$.

Secondary Voltage. Therefore, under the influence of a nonuniform field, a difference magnetization appears, as shown in Fig. 5(d). The derivative of this difference magnetization [Fig. 5(e)] results in a voltage in the secondary coil, as shown in Fig. 5(f). In the field-difference meter, the **second harmonic component** is again filtered out of this voltage. The **voltage** $\hat{e}_2$ of the field-strength difference meter is

$$\hat{e}_2 = 2\pi f w_2 F \mu_A \hat{H}_{\sim} h_2 \cdot \cos\left(2\frac{H_{\text{d.c.}}}{\hat{H}_{\sim}}\right) \sin\left(2\frac{H_D}{\hat{H}_{\sim}}\right) \tag{7}$$

Accuracy of Field Gradient Measurements. Eq. (7) agrees with Eq. (3) except for one term. Instead of the d.-c. field strength $H_{\text{d.c.}}$, the **difference field strength** H_D appears. Only the term cos $(2H_{\text{d.c.}}/\hat{H}_{\sim})$ shows that the difference-field indication depends on the d.-c. field $H_{\text{d.c.}}$ in which the field-difference measurement takes place. However, Eq. (7) shows that the field-difference indication may be obtained independently of the d.-c. field if the a.-c. field excitation is chosen considerably larger than the d.-c. field strength $H_{\text{d.c.}}$. The expression $\cos(2H_{\text{d.c.}}/\hat{H}_{\sim})$ will then be very nearly unity. For example, if the a.-c. field amplitude reacting on the probe-coil cores is chosen ten times larger than the **earth's field**, the error which appears in a difference-field measurement because of the simultaneous action of the earth's field is below 0.5 percent. In case of a twenty-fold a.-c. field amplitude, the error caused by a d.-c. field decreases to 0.1 percent. This means that difference-field (field gradient) measurements, which are carried out in the direction of the earth's field and perpendicular to it, differ by not more than 0.1 percent in the two cases.

In case of a large a.-c. field amplitude,

$$\sin\left(\frac{2H_D}{\hat{H}_{\sim}}\right) \cong \frac{2H_D}{\hat{H}_{\sim}}$$

so that, for the voltage generated from the difference-field measurement arrangement, a nearly linear relationship with the difference field strength exists; i.e.,

$$\hat{e}_2 = AH_D \tag{8}$$

DESIGN OF INSTRUMENTS. The complete theory of the field and difference-field measurement methods[10] provides data for optimum **probe-coil dimensioning** at a given oscillator power and at a chosen oscillator frequency for various requirements. These requirements include (1) measurement of a maximum d.-c. field (or difference field) at a desired linearity, and (2) independence of the difference-field measurement from the environmental d.-c. field.

If the probe pair is arranged as shown in Fig. 1(a), the absolute value of the d.-c. field strength is indicated by means of an **instrument deflection** which is proportional to the field strength. The alternate arrangement of the probe pair shown in Fig. 1(b) gives an indication of the field difference between the two probe halves, independent of the ambient d.-c. field. In each case only the field component or the field difference along the longitudinal axis of the probe is indicated.

Probe-Type Magnetic-Field Meters

PRECISION MAGNETIC-FIELD METER. One example of equipment making use of magnetic-field probes is the precision magnetic-field meter. Direct measurement can be made of weak magnetic fields (10^{-5} to 10^{-1} oersted for one scale division, or 0.001 to 1.0 oersteds for full-scale deflection). Direct-current field-measuring instruments for field strengths up to 1000 oersteds have been developed which use this principle. Field strength is indicated on a large precision **mirror-scale microammeter** with an error of less than 1 percent.

Circuit Arrangement. Fig. 6 shows a block diagram of the electric circuits of the field meter and the difference-field meter. A **stabilized oscillator** serves as an excitation current source for the probes. The second harmonic component of the secondary voltage in the probe is filtered out and amplified in a selective amplifier. **Rectification** of the a.-c. voltage output from the amplifier takes place in a phase detector. Contrary to standard detectors, north-south and south-north field polarities are indicated by opposite deflections of the meter from its zero center position. The **control voltage** necessary for the phase detector is obtained from the oscillator by means of a transformer followed by a frequency doubler. Through the use of phase detection, the operation is independent of small **hysteresis variations in the core strips.** In addition, exact linearity is obtained down to zero signal, while in a standard rectifier nonlinearity exists for small values of signal.

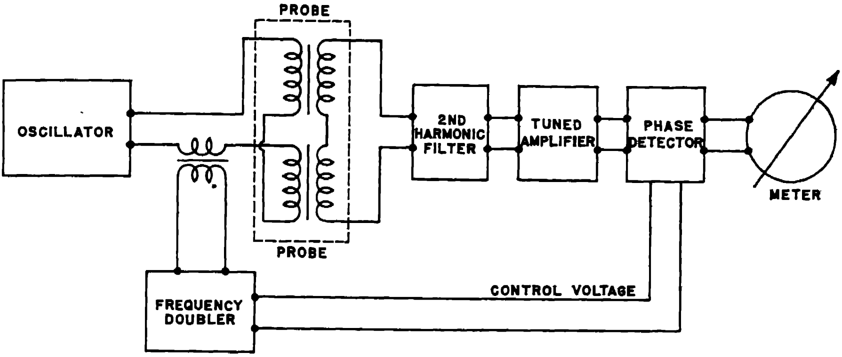

Institut Dr. Foerster

Fig. 6. Block diagram of the electric circuit of the field meter.

Meter Calibration. Calibration of this equipment is checked by depressing a push button on the front panel. This introduces a controlled amount of d.-c. current into the secondary windings of the probes. This current produces a magnetic field which is measured by the instrument. If the meter needle does not deflect from zero to the full-scale mark, the calibration control should be adjusted until the proper value is obtained. This calibration procedure is applicable only when the field probes are being used.

Types of Pick-up Probes. Four types of pick-up probes may be used with the instrument:

1. The **field probe** is the principal pick-up device used. Its use is explained in detail later. The indicating meter of the instrument is direct-reading in millioersteds for this pick-up device only.
2. The **microprobe** is the smallest of the pick-up devices used with the equipment. It is intended to be used in locations where the larger size of the field probes prevents their use. The microprobe has one-tenth the sensitivity of the field probe.
3. The **gradient probe** contains two tiny sensing elements arranged to indicate the differences in field strength between them. The instrument is not direct-reading, but readings are repetitive. A calibration curve can be obtained by placing the probe in fields of known gradient.

4. The **tape probe** is intended for static measurements of the field on magnetic tape and wire. Tape or wire is placed in the channel of the probe assembly, in contact with the pick-up device. The gap in the pick-up device is 0.002 in. wide. The readings are relative, since the instrument is not calibrated in absolute units for use with this probe.

Measurements of Uniform Fields. The operation of the meter with the field probes is quite simple. Suppose it is desired to measure the field at the center of a **solenoid coil** which is considerably larger than the probes. With the solenoid coil current turned off, both field probes are placed inside the solenoid at the measurement point. The field probes should be side by side, pointing in the same direction and parallel with the field, as shown in Fig. 1(a). If the field of the solenoid alone is desired, the effect of the earth's field must be eliminated. To do this, the solenoid is turned until the probes point approximately east or west, so that the field meter reads zero in the appropriate range. When current is applied to the solenoid, the field meter will indicate the absolute value of the field acting on its probes.

Measurements of Nonuniform Fields. If one probe is turned 180 deg., as shown in Fig. 1(b), the reaction of one probe is canceled by an equal and opposite reaction in the other probe. This probe arrangement results in a zero meter reading in uniform fields. In nonuniform fields the meter reads one-half the difference in field between the two probes. This suggests that this probe arrangement could be used to measure **field gradients.**

Cancellation of Earth's Field. Two probes can be arranged to cancel out the earth's field. One probe is placed inside the solenoid producing the unknown field. The other is placed far enough from the solenoid so that the effect of the solenoid field is negligible. This second probe is oriented experimentally to zero the field meter, with the solenoid current turned off. The instrument calibration should be checked, as described previously, with the probes in position. Upon turning on the solenoid current, the field meter will read one-half the magnitude of the unknown field. However, this method should not be used to compensate for unwanted fields stronger than five times the earth's field. **Partial saturation** of the probes may result, causing errors in the readings obtained.

Field Gradient Measurements. The gradient probe contains two sensing elements, positioned so as to be equivalent to the arrangement shown in Fig. 1(d). The readings obtained with this probe are proportional to one-half the difference in field (field gradient) between the two probes. The probe should be oriented so that the field is parallel with the probe axis for gradient indications. The readings obtained are relative unless the instrument is calibrated by placing this probe in a field with a known gradient. In this case the magnitude of the calibrating field should be about the same as the field to be explored, to avoid saturation effects.

In some applications it is desirable to explore the surface of steel samples for **leakage fields.** Hard wear plates are provided on the end of the probe to facilitate sliding the probe along the surface of samples.

Tape-Probe Measurements. The tape probe [sketched in Fig. 1(f)] should be fastened to a wooden work table, by means of nonmagnetic screws in the screw holes provided, before using it for precise measurements. All tools or other articles made of steel, iron, or other magnetic material must be removed from the vicinity of the probe. The meter is adjusted to read zero by means of the knob on the probe assembly. This knob controls the position of a small **per-**

manent magnet which balances out the effect of the earth's field on the probe. This adjustment should be made first at a low sensitivity setting of the range switch and repeated as the range switch is advanced to the desired sensitivity.

Tape Test Technique. The tape or wire sample is placed in contact with the pole pieces of the pick-up in the channel of the probe [see Fig. 1(f)]. The gap is 0.002 in. wide. The highest frequency that can be measured on the tape is a function of the speed at which the signal was recorded on the tape. Readings obtained are directly proportional to the field strength of the magnetic recording on the tape, but the field meter is not calibrated directly in oersteds for this probe. With the aid of the probe, the linearity of modulation of the tape can be investigated for any signal strength ranging from the very low to the highest.

Tape Transport. It may be convenient to use an automatic tape-transport device and a recording oscillograph in this application. A tape speed of 0 to 2.5 in. per minute is recommended.

Recording Instruments. Two jacks are provided on the back of the field meter for connecting a **recorder.** Both these terminals are at a potential of 195 volts with respect to chassis. Accidental shorting of one of these jacks to chassis may damage the front panel meter. Standard banana plugs fit the instrument jacks. A switch connected with one jack disconnects the front panel meter while the recorder is connected.

Two types of recorders are suitable. **Recording galvanometers** (without electronic amplifiers) having a zero-center scale, a d.-c. resistance of about 1500 ohms, and a current sensitivity of 50-μa full scale are suitable. No connection should be made to the chassis when using a recording instrument of this type.

Recorders using **electronic amplifiers** with a push-pull, high-impedance input are also suitable. The shunt resistance from each jack terminal to ground should be about 1 megohm or higher. The recorder should have a sensitivity of about 75-mv. full scale.

The **speed of response** of the field meter is much faster (about 1 msec.) when used with a recorder than when used with the front panel meter.

Hall-Generator Magnetic-Field Meters

HALL GENERATORS. In 1879 Hall discovered that a flat conductor, carrying a longitudinal component of electric current I and penetrated perpendicularly to its largest surface by a magnetic field H, exhibits a potential difference U_H at its narrow sides (A, A'). (See Fig. 7.) The following equation holds true for the **Hall voltage,** U_H:

$$U_H = R_H\left(\frac{I \cdot H}{t}\right) \tag{9}$$

where R_H = a material constant, known as the Hall coefficient.
I = the current through the Hall conductor.
H = the magnetic d.-c. field strength perpendicular to the largest surface.
t = the thickness of the Hall plate.

Materials for Hall-Effect Probes. A material is especially suited for the measurement of d.-c. magnetic fields if it has

1. A large Hall coefficient.
2. Good electrical conductivity.
3. A low dependence of the Hall coefficient and the electrical conductivity upon temperature.

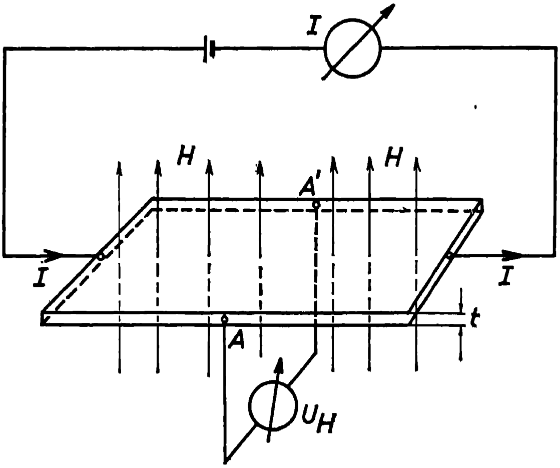

Fig. 7. Hall generator element used for static magnetic-field measurements.

Semi-conductor combinations such as indium-antimony (InSb) and indium-arsenic (InAs) discovered recently[5] fulfill these requirements especially well. In miniaturized form these Hall generators permit the point measurement of magnetic d.-c. fields in fractions of 1 oersted up to the highest producible field strengths.

Measurement of Tangential Field Strength. The Hall generator method is especially well suited for the determination of the tangential field strength, that is, the true field strength during magnetization of a test part, because of the small dimension of the measurement probe. For **complicated test parts** such as crankshafts, measurement of the tangential field strength with the Hall microgenerator determines the density B of the lines of force in a test part.

In **magnetic-particle testing,** this field strength is proportional to the magnetic crack-leakage flux. An induction of 11,000 gausses reportedly corresponds to a true field strength of 157 oersteds (i.e., 125 ampere-turns per centimeter) for most steels. To determine the tangential surface field strength (true field strength), a Hall microprobe is placed on the surface of the test object during magnetization. Thus one can directly determine whether the field strength is adequate for magnetic-particle inspection.

As far as convenience of measurement is concerned, the Hall-generator method surpasses the field recorder method (see The Field Recorder Method in this section). Furthermore it is insensitive to the opposing field ($-N \cdot I$) which appears after magnetization and which can alter the indications of the field recorder method in case of hard magnetic materials (see True Field Strength in this section).

Hall Detector Probes. A hand-held measurement head has been designed whose Hall generator can be attached to the handle in each of three directions for various d.-c. field measurement problems. Fig. 8(a) illustrates the positioning of the head for measuring the **surface field strength** of a circularly magnetized part. Fig. 8(b) shows the procedure for measuring **true field strength** in a longitudinally magnetized test object. Positioning to measure the **true circular field strength** on the inside surface of a tube is shown in Fig. 8(c).

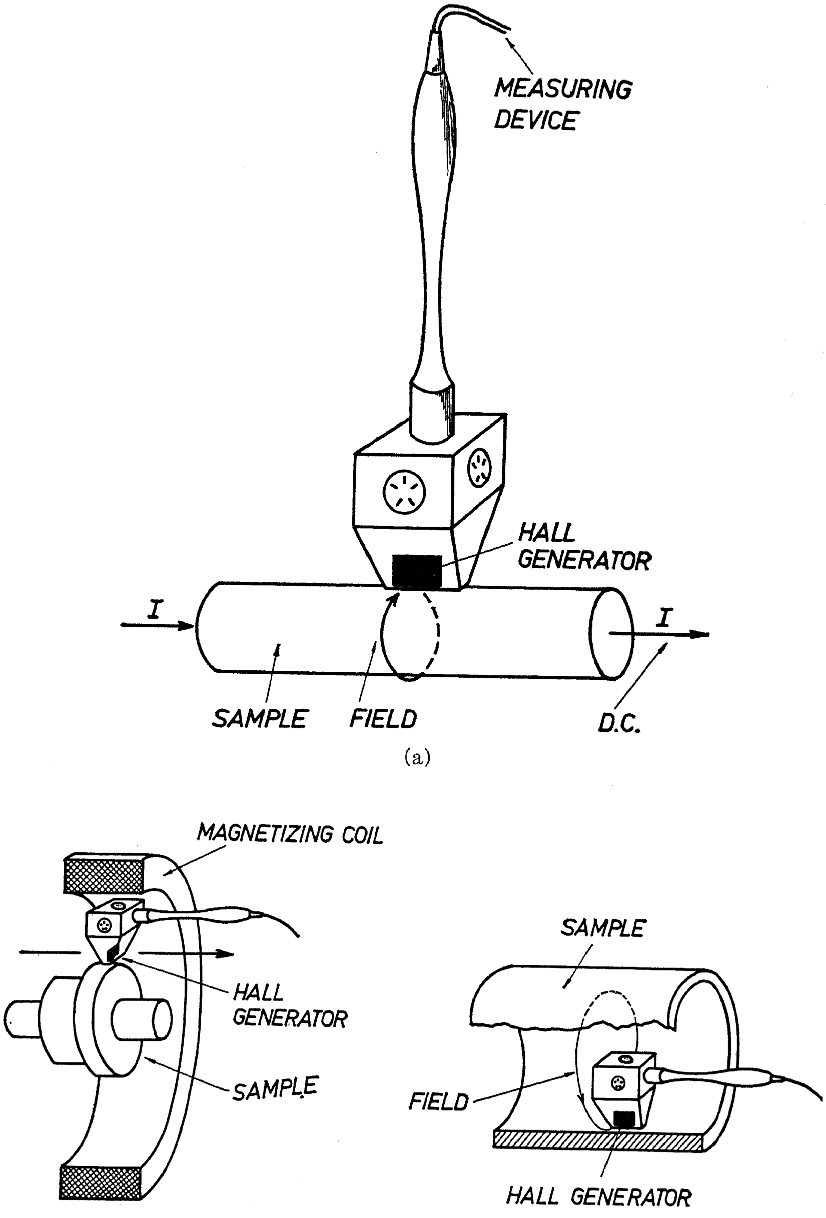

(a)

(b)

(c)

Institut Dr. Foerster

Fig. 8. Arrangements of Hall probe measurement heads. (a) Arrangement for measurement of surface field strength in a circular field produced by a longitudinal current. (b) Arrangement for determination of true longitudinal field strength within a coil. (c) Arrangement for determination of true circular field strength inside of tube.

USE OF HALL DETECTOR INSTRUMENTS. Various types of instrumentation are available for d.-c. magnetic-field measurement with Hall generators. One small instrument is easy to carry and operates from self-contained batteries. Its most sensitive measurement range is 200 oersteds. Its least sensitive measurement range is 10,000 oersteds for full-scale deflection. A larger instrument has a maximum sensitivity of 0.5 oersted for 100 scale divisions, which can be reduced, in ten sensitivity steps, to 20,000 oersteds for 100 scale divisions. It has a cathode-ray tube which serves for the simultaneous measurement of a.-c. fields superimposed on the d.-c. fields and which indicates the form and magnitude of magnetization impulses.

Measurement of Strong Magnetic Fields. The Hall generator method is especially well suited for the measurement of high magnetic-field strengths of several thousand oersteds. In a potentiometer arrangement (Fig. 9) the Hall voltage U_H which appears at a specific d.-c. field is suppressed to zero by displacement of the potentiometer slide. If the sensitivity of the instrument is then increased by a factor of 10 or 100, deviations from the original d.-c. field for which the potentiometer slide was calibrated can be measured with a ten- to hundred-fold increase in sensitivity. This method can be used to compare strong magnetic fields at different locations.

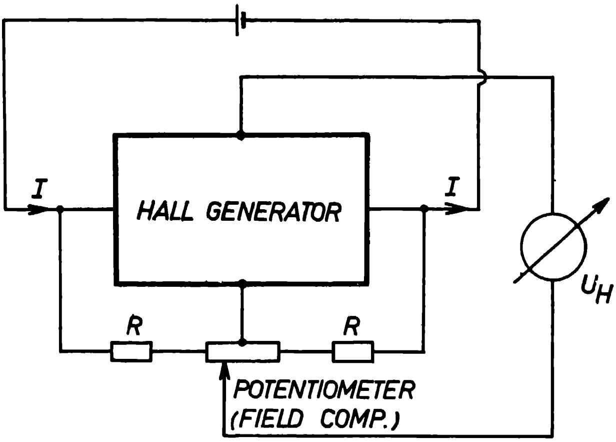

Institut Dr. Foerster

Fig. 9. Arrangement of Hall generator with compensation of the Hall voltage by a potentiometer arrangement, for sensitive comparison of strong magnetic fields.

Application in Magnetic-Particle Testing

SURFACE FIELD STRENGTH MEASUREMENTS. In magnetic-particle tests, the test objects are often magnetized with a direct current or a static magnetic field. To develop **crack indications,** the density of the magnetic lines of force (induction B) in the surface of the test object must exceed a minimum value so that ferromagnetic powder particles will gather at the crack. The magnetic-particle indications are a result of the **crack-leakage flux.** This flux is proportional to the flux density, B, in the surface of the specimen.

Surface Flux Density. The magnetic flux density B in the surface of a test object is

$$B = \mu H_t \tag{10}$$

Here μ is the **material permeability** and H_t is the **true tangential field strength** in the surface of the test part. The permeability μ is known approximately for steels of various types and heat treatments. It is necessary only to determine the field strength H_t to obtain the flux density B.

Demagnetization by Free Poles. It is extremely difficult to determine the surface field strength, especially for complicated parts such as crankshafts. The **true surface field strength,** H_t, of the test object can differ by a factor of 10 or 100 from the applied field strength H_a. The coil field strength can be calculated from the magnetizing current and the coil factor of the magnetizing coil. This condition is of special significance in magnetic-particle tests.

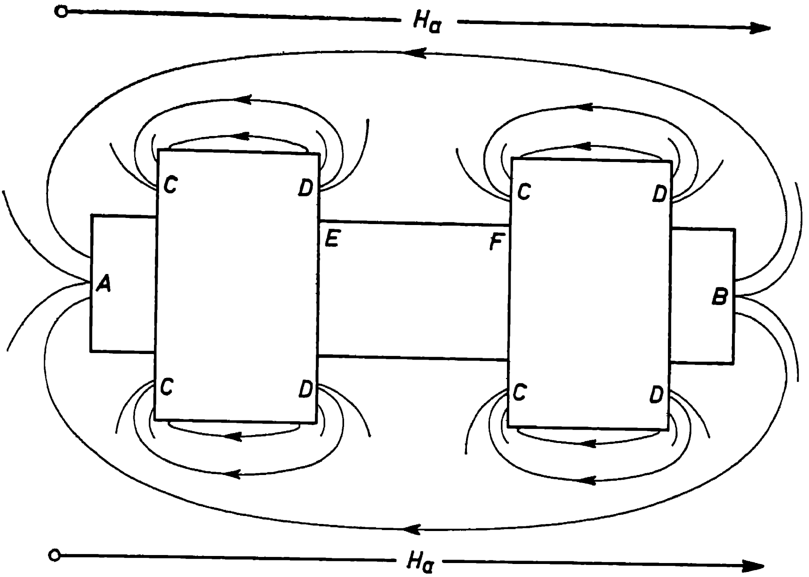

Fig. 10. Distribution of magnetic field in a complicated test part, showing the demagnetizing action of free magnetic poles.

For example, Fig. 10 shows a specimen with two thick sections (C–D). It is assumed to be magnetized within a coil of field strength H_a. At ends A and B and in areas C and D of the two thick sections, free magnetic poles appear as a result of magnetization. It is well known that magnetic lines of force exist between two opposite magnetic poles; for example, A and B or C and D. These lines of force pass from one pole to the other, both through the air and through the test part. Lines of force emerging from the induced magnetic poles oppose and weaken the externally applied magnetic field H_a, as indicated in Fig. 10.

Intensity of Demagnetization. Lines of force resulting from free magnetic poles and reacting on the original magnetic field H_a become denser

1. As the magnetization I of the test part increases.
2. As the distance between the free poles decreases.

As is indicated in Fig. 10, the lines of force emerging from the magnetic poles A and B weaken the original field H_a less than those emerging from the more closely spaced poles C and D. The longer air path, AB, has a greater reluctance to the returning lines of force than the shorter path, CD.

True Field Strength. The true field strength H_t is the difference between the coil field strength H_a and the reverse field strength H_p resulting from the free poles; i.e.,

$$H_t = H_a - H_p \tag{11}$$

The field strength resulting from the free poles is calculated to be

$$H_p = NI \tag{12}$$

From Eqs. (11) and (12),

$$H_t = H_a - NI \tag{13}$$

Here, I is the magnetization of the test part. The demagnetizing pole strength is proportional to the magnetization I. N is the so-called **demagnetizing factor.** N becomes larger as the test part becomes shorter, i.e., as the distance AB becomes smaller. For a complicated test part, demagnetization increases as poles C and D get closer together.

Calculation of Demagnetization Factor. The demagnetizing factor N can be calculated exactly only for the rotation ellipsoid.[11] Empirical values are known for cylindrical bodies.[11] When the demagnetizing factor N is known, even approximately, the true field on the surface of the test part can be calculated from Eq. (13). If the permeability μ is known, the density B of the lines of force can be calculated from Eq. (10). This flux density B must reach a specific minimum value if cracks are to be indicated with the magnetic-particle method. McClurg has discussed these relationships thoroughly.[12]

Determining True Field Strength. Calculation of the true field strength H_t is impossible for complicated bodies like that of Fig. 10 because the demagnetizing factor N varies from point to point. However, the true tangential field strength H_t on the surface and directly below the surface is constant on either side of the boundary between the material and air. Thus, if it is possible to measure the **true tangential field strength** in the air close to the surface of the test part, then the true field strength H_t on and immediately below the surface can be assumed to be identical. With this field strength and the approximate permeability μ, the flux density can be obtained from Eq. (10).

The field strength in air due to the leakage flux of a crack is proportional to the magnetic field strength in the crack. The field strength in the crack is also identical with the flux density B in the test part. With complicated shapes of specimens or **closely spaced demagnetizing poles,** the field strength must be measured closer to the surface to obtain the true field strength H_t on the surface. The **highest surface field strength** H_t exists at the location of the smallest specimen diameter (for example, at EF in Fig. 10). At these points the direction of the lines of force from the poles C and D have the same direction as the field strength H_a (see arrow direction).

THE FIELD RECORDER METHOD. By means of the "field recorder method" it is possible to measure the field strength closer than 0.0004 in. to the surface of the test part. This is done by placing a 0.0004 in. thick, ¼ × ¼-in. piece of special magnetic alloy with characteristics similar to "magnetic recording tape" on the surface of the test object. After magnetization this recorder strip retains a residual magnetization proportional to the highest field attained during magnetization.

Field Distribution on Magnetized Camshaft. The residual magnetization of the strip is measured with a field-measurement instrument and microprobe to determine H_t. Fig. 11 illustrates the field strength distribution obtained with this method on a complicated camshaft. The magnetizing-coil field strength H_a was 190 oersteds. The field strength distribution H_t of the camshaft is noted at several points directly on the surface and is indicative of the field in the surface. The fact that the true field strength for complicated test parts varies to such an extent from point to point can be determined readily with the "field recorder method" or by means of the Hall-generator probe instrument.

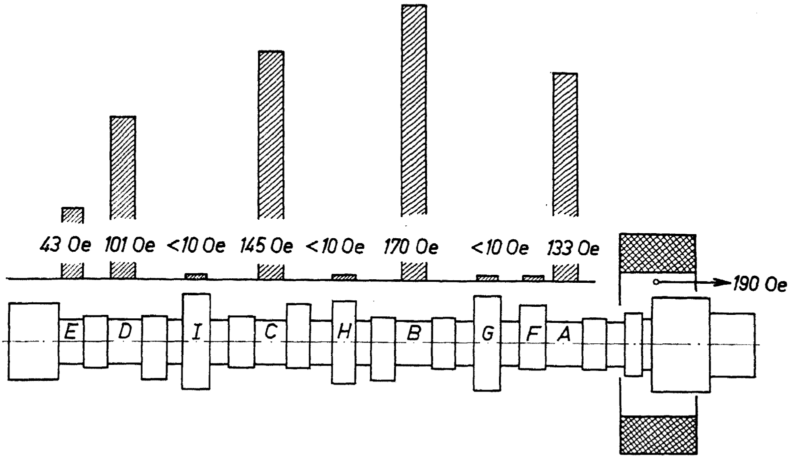

Institut Dr. Foerster

Fig. 11. Distribution of the true field strength (H_t) on a camshaft at a coil field (H_a) of 190 oersteds.

Measuring Impulse Fields. In the "field recorder method," the period of the field reaction on the recorder tape can be less than 10^{-3} sec. Thus the maximum field strengths obtained with impulse magnetization can be determined readily. For example, the field recorder method has been used to measure **lightning currents,** since the magnetic field of the peak lightning current leaves a residual magnetization in recorder tapes at various locations. In the United States these magnetic recording elements are known as **surge crest ammeters.**

References

1. Wills, M. S. "A Rotating Coil Fluxmeter," *J. Sci. Instr.,* 29 (1952): 374.
2. Kiesskalt, S. "Aus der Praxis der zerstoerungsfreien Schweissnahtpruefung (Nondestructive Testing of Welded Seams)," *Autogene Metallbearbeitung,* 27 (1934): 65.
3. Foerster, F. "A Method for the Measurement of D.C. Fields and D.C. Field Differences and Its Application to Nondestructive Testing," *Nondestructive Testing,* 13, No. 5 (1955): 31.

4. Dewar, J., and J. A. Fleming. "On the Electrical Resistivity of Bismuth at the Temperature of Liquid Air," *Proc. Roy. Soc. London*, 60 (1896–1897): 72.
5. Barlow, H. E. M. "Hall Effect in Semi-Conductors," *Elec. Rev.*, 155 (1954): 848.
6. Block, F. "Nuclear Induction," *Phys. Rev.*, 70 (1946): 460; Block, F., W. W. Hansen, and M. Packard. "The Nuclear Induction Experiment," *Phys. Rev.*, 70 (1946): 474.
7. Foerster, F. "The Application of Hall Generators for Nondestructive Testing," *Z. Metallk.* (In press.)
8. Welker, H. "Neue Werkstoffe mit grossem Hall-Effekt und grosser Widerstandsaenderung im Magnetfeld (New Materials with Great Hall Effect and Great Change of Resistance in the Magnetic Field)," *Elektrotech. Z.*, 76 (1955): 513.
9. Foerster, F. "Ein Verfahren zur Messung von magnetischen Gleichfeldern und Gleichfelddifferenzen und seine Anwendung in der Metallforschung und Technik (A Method for the Measurement of Steady Magnetic Fields and Differences of Steady Fields and Its Application to Metallurgical Research and Industry)," *Z. Metallk.*, 46 (1955): 358.
10. *Zerstoerungfreie Werkstoffpruefung mit elektrischen und magnetischen Verfahren (Nondestructive Material Testing with Electrical and Magnetic Methods).* Berlin, Goettingen, Heidelberg: Springer-Verlag. (In press.)
11. Bozorth, R. M. *Ferromagnetism.* 2d ed. New York: D. Van Nostrand Co., Inc., 1953. Pp. 846, 847, 849.
12. McClurg, G. O. "Theory and Application of Coil Magnetization," *Nondestructive Testing*, 13, No. 1 (1955): 23.

Bibliography

Borowik, A. "Ferromagnetic Metals. Identification and Measurement of Internal Stresses, Part 1. Magnetic Tests," *Iron and Steel*, 21 (1948): 3, 39.

Bozorth, R. M., and J. M. Williams. "Effect of Small Stresses on Magnetic Properties," *Rev. Mod. Phys.*, 17 (1945): 72.

Brown, R. J., and J. H. Bridle. "A New Method of Sorting Steels," *Engineer*, 176 (1943): 442.

Diamond, M. J. "Hardness Tester Sorts Auto Engine Parts," *Electronics*, 27, No. 12 (1954): 160.

Foerster, F. "Nouveaux procédés d'essai électronique nondéstructif des matériaux (New Procedures for the Electronic Nondestructive Testing of Materials)," *Métaux (Corrosion-Inds.)*, 26 (1951): 497.

———. "Theoretische und experimentelle Grundlagen der elektromagnetischen Qualitaetssortierung von Stahlteilen, IV. Das Restfeldverfahren (Theoretical and Experimental Foundation of the Electromagnetic Quality Sorting of Steel Parts. IV. The Residual Field Method)," *Z. Metallk.*, 45 (1954): 233.

Foerster, F., and G. Zizelmann. "Die schnelle zerstoerungsfreie Bestimmung der Blechanisotropie mit dem Restpunktpolverfahren (The Rapid Nondestructive Determination of Sheet Anisotropy with the Residual Point Pole Method)," *Z. Metallk.*, 45 (1954): 245.

Foerster, F., and K. Stambke. "Magnetische Untersuchungen innerer Spannungen, I. Eigenspannungen beim Recken von Nickeldraht (Magnetic Investigations of Internal Stresses, I. The Internal Stress of Nickel Wire During Stretching)," *Z. Metallk.*, 33 (1941): 97.

Hainz, R. "Beispiel einer Einfuehrung der elektromagnetischen Sortierverfahren in die Fertigung von Dieseleinspritzpumpen und duesen (Example of the Use of Magnetic Sorting in the Production of Components for Diesel Injection Pumps and Nozzles)," *Z. Metallk.*, 45 (1954): 238.

Kehoe, W. K. "Magnetic Testing to Control Quality of Ferrous Alloy Parts," *Gen. Elec. Rev.*, 47, No. 4 (1944): 59.

Miekiejohn, W. H. "A Non-Destructive Magnetic Hardness Tester," *Electronic Inds. and Instrumentation*, 1, No. 10 (1947): 14, 45.

ORTHEIL, J. "Kritische Betrachtungen der magnetischen Sortierung von Stahlteilen in der Massenfertigung (Critical Considerations of Magnetic Sorting of Steel Parts in Mass Production)," *Z. Metallk.*, 45 (1954): 243.

SANFORD, R. L. "An Alternating-Current Magnetic Comparator, and Testing of Tool-Resisting Prison Bars," *J. Research Natl. Bur. Standards,* 16 (1936): 563.

SECTION 34

MAGNETIC-FIELD TEST EQUIPMENT

CONTENTS

PAGE

Coercive-Force Tests

- Advantages of magnetic tests 1
- Applications in metallurgical tests 1
  - Advantages of measuring coercive force and permeability 1
  - Technique of measuring coercive force 1
- Coercive-force meter 2
    - Block diagram of equipment for measurement of coercive force of materials (*f.* 1) 2
    - Coercive-force measurement equipment (*f.* 2) 3
  - Compensation of earth's field 3
  - Range of applications 3
- Measurement of magnetic-material properties 4
- Coercive-force measurements at high temperature 4
    - High-temperature magnetometer arrangement for indication of true magnetization and true field strength (*f.* 3) 4
- Automatic sorting of production parts by coercive force 5
  - Residual magnetization as a measure of coercive force 5
    - Magnetization loop of a short production part (*f.* 4) 6
  - Measuring residual magnetization with external probes 5
  - Automatic sorting arrangement 6
    - Arrangement for automatic sorting of production parts by residual field values and (for many alloys) hardness (*f.* 5) .. 7
  - Advantages of automatic sorting by coercive force 6
- Applications of sorting by coercive-force tests 7
  - Ball bearings 7
  - Control of hardness of tempered parts 7
  - Hardened steel parts 7
  - Tempered castings 8
    - Statimat graph of the frequency distribution of annealed cast parts (*f.* 6).. 8
  - Electrical relay parts 8

Point-Pole Tests

- The point-pole method 9
- Measuring anisotropy in sheet materials 9
  - Probe and magnet arrangement used to determine grain orientation of sheet steel (*f.* 7) 9
  - Polar diagram of magnetic field about a point pole for various types of steel sheet (*f.* 8) 10
- Hysteresis loss of electrical steel sheets 10
- Internal stress in structural steel 10
- Analysis of carbon content 11
  - Point-pole indication as a function of the carbon content for carbon steel (*f.* 9) .. 11
- Sorting mixed stocks 11
  - Frequency distribution in a lot of two mixed alloys, obtained in a steel plant (*f.* 10) 12
  - Sorting of two similar alloys with an expanded measurement scale (*f.* 11) 12
- Hardness testing 13
  - Relation between point-pole indication and mechanical hardness of centrifugally cast tubes (*f.* 12) 13
- Depth of case hardening 13
- Other applications 13
- Scale expansion with compensating magnet 14
- Double-pole tests 14
  - Difference-probe arrangement for magnetization with a pot magnet (double-pole pole) to suppress influence of the earth's field (*f.* 13) 14

Thickness Tests

- Probe measurement of nonmagnetic wall thickness 15
  - Probe array with permanent magnet for wall thickness measurement of nonferrous metals (independent of wall material) (*f.* 14) 15
  - Scale expansion 15
  - Cast nonferrous parts 16
  - Automotive piston heads 16
  - Large wall thickness 16
- Multiple-point measurements of wall thickness 16
  - Sheet and plate thickness measurements .. 16
    - Multiple thickness-measurement device with simultaneous indications on the screen of a cathode-ray tube (*f.* 15) ... 16
  - Continuous-sheet thickness measurements .. 17
- Hall-generator measurement of wall thickness 17
  - Arrangement of Hall probe for measurement of wall thickness (*f.* 16) 17

CONTENTS (*Continued*)

PAGE

Sheet thickness meter 17
Nonferromagnetic-coating thickness meter . 17
Arrangement of permanent magnet with Hall generator for measurement of thickness of nonferromagnetic layers of iron and steel (*f.* 17) 18
Eccentricity of a conductor in insulating covering 18
Probe arrangement for direct representation of position of conductor in an insulating covering (*f.* 18) 19
Feedback control 19
Measurement of the eccentricity of tubes 19
Field within an eccentric tube carrying current 19
Arrangement for measuring the eccentricity of a nonferrous metal tube by measuring the magnetic field inside the tube produced by a current in the tube wall (*f.* 19) 20

PAGE

Other Applications

Crack depth measurement 20
Effect of crack on path of current (*f.* 20) 21
Determination of iron impurities in nonmagnetic material 21
Arrangement for rapid, continuous measurement of iron content in nonferromagnetic materials (*f.* 21) 22
Detecting ferrous material in packaged foods 22
Iron in nonferrous scrap 22
Iron core-wire in nonferrous castings 22
Unexploded blasting cartridges 22
Survey markers 23
Buried, unexploded bombs, pipelines, cable boxes 23
Liquid-level control 23
Flow meters 23
Detecting movement of nonferrous materials 23
References 23

SECTION 34

MAGNETIC-FIELD TEST EQUIPMENT

Coercive-Force Tests

ADVANTAGES OF MAGNETIC TESTS. Static magnetic field tests have found many applications in nondestructive testing in recent years for the following reasons:

1. Test indications are representative of the entire cross-section of the test object and are related to important material characteristics.
2. Static field methods used in defect testing have a greater depth of penetration than varying fields, since skin effect is absent.
3. Wall thickness indications for nonferromagnetic materials are independent of the electrical properties of the test object.

APPLICATIONS IN METALLURGICAL TESTS. The use of modern electronic techniques has increased considerably in industrial measurement, test, and control techniques for metallurgical tests. However, the well-known classical measurement methods are still widely applied. The metallurgist measures the physical properties of his material for various reasons. First the measurement serves to identify or determine the application of the material. For example, the **specific electrical conductivity** of materials used for electric circuits or the coercive force of **materials used for permanent magnets** can be determined. Second, and this represents the predominating case, the measurement can provide a means of observing metallurgical processes such as **transformations, age-hardening effects, ordering processes, aging, and other phenomena.**

Advantages of Measuring Coercive Force and Permeability. The physical factors with the greatest variation range in ferromagnetic materials are coercive force and permeability. Most physical properties such as conductivity, density, or elasticity will change by a factor of only 10 to 100 over the entire metallurgically interesting range, whereas the variation in coercive force and permeability is about 10^5. In permeability measurements, the **shape of the test sample** enters decisively into the result, but the coercive force represents a factor which can be measured independently of shape. Therefore a rod or small grindings of a given material will give, without recalculation, the same measured values. In addition, by suitable instrumentation, the coercive force can be measured as a function of temperature more readily than any other factor.

Technique of Measuring Coercive Force. Coercive force is defined as the **demagnetization field strength** H_c required to bring about the disappearance of the **magnetization intensity** J or the **residual induction** B in a material, following saturation. Therefore the measurement process consists of increasing the field strength in a material to saturation, followed by a reversal in field strength back to zero. The sample then has a residual magnetization. If a field of reversed polarity with increasing strength is applied to the sample, magnetic induction will decrease to zero. The strength (in oersteds) of the opposing field at which the magnetic moment passes through zero is the **coercive force** H_c.

COERCIVE-FORCE METER. Fig. 1 shows the block diagram of a commercially available instrument designed to measure the coercive force with high accuracy in a few seconds. A variable transformer, in conjunction with a rectifier and filter circuit, supplies direct current to the magnetic coil. The current is continuously variable by means of a knob on the front panel of the equipment (see Fig. 2). By turning this control once from zero to full scale and back again, the sample is magnetized to saturation and returns to the residual field point. The field meter now shows a deflection corresponding to the **residual magnetization** of the sample. By throwing the current-reversing switch from the "magnetizing" to "measuring" position and turning the variable control transformer once more, a field appears whose direction is opposite to the original saturation field. This opposing field is now increased by means of the variable transformer until the deflection caused by the sample magnetization passes through zero. At this moment the absolute value of coercive force appears on the calibrated, precision, coercive-force meter.

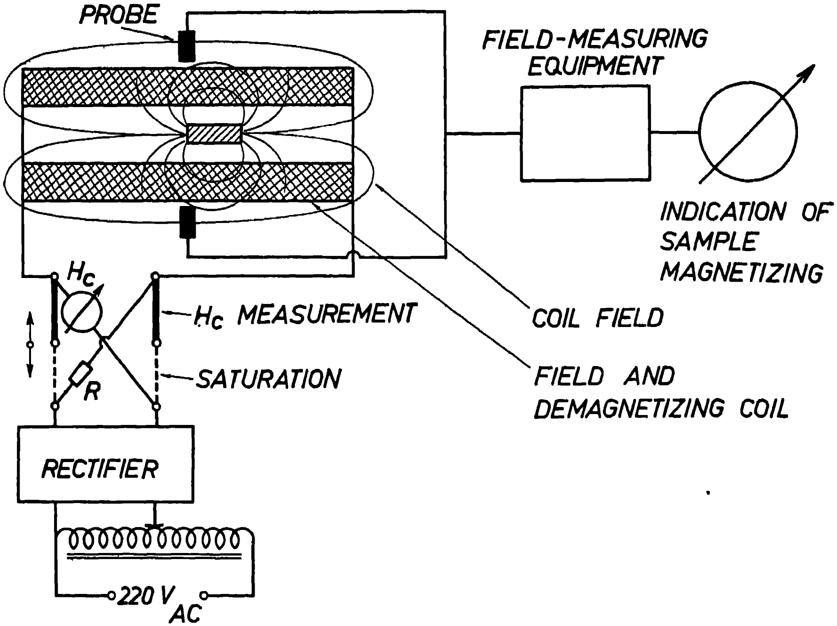
PROBE
FIELD-MEASURING EQUIPMENT
INDICATION OF SAMPLE MAGNETIZING
COIL FIELD
FIELD AND DEMAGNETIZING COIL
Hc
Hc MEASUREMENT
SATURATION
R
RECTIFIER
220 V AC

Institut Dr. Foerster

Fig. 1. Block diagram of equipment for measurement of coercive force of materials.

Operation of the equipment depends on the use of **high-sensitivity field probes** in conjunction with a magnetic-field meter. The probes are aligned so that the lines of force from the magnetizing field coil cannot influence the field probes. However, as shown in Fig. 1, the lines of force emanating from the sample are measured, and thus the magnetic-field strength in the sample may be measured directly and independently of the field in the main magnetization coil. The complete set-up is illustrated in Fig. 2.

Compensation of Earth's Field. Additional precautions must be taken when measuring the coercive force of very soft magnetic materials. The effect of the earth's magnetic field will cause a considerable error at lower levels of measurement. Compensation of this field at the sample location in the coil may be done with the same equipment and will completely eliminate this extraneous effect.

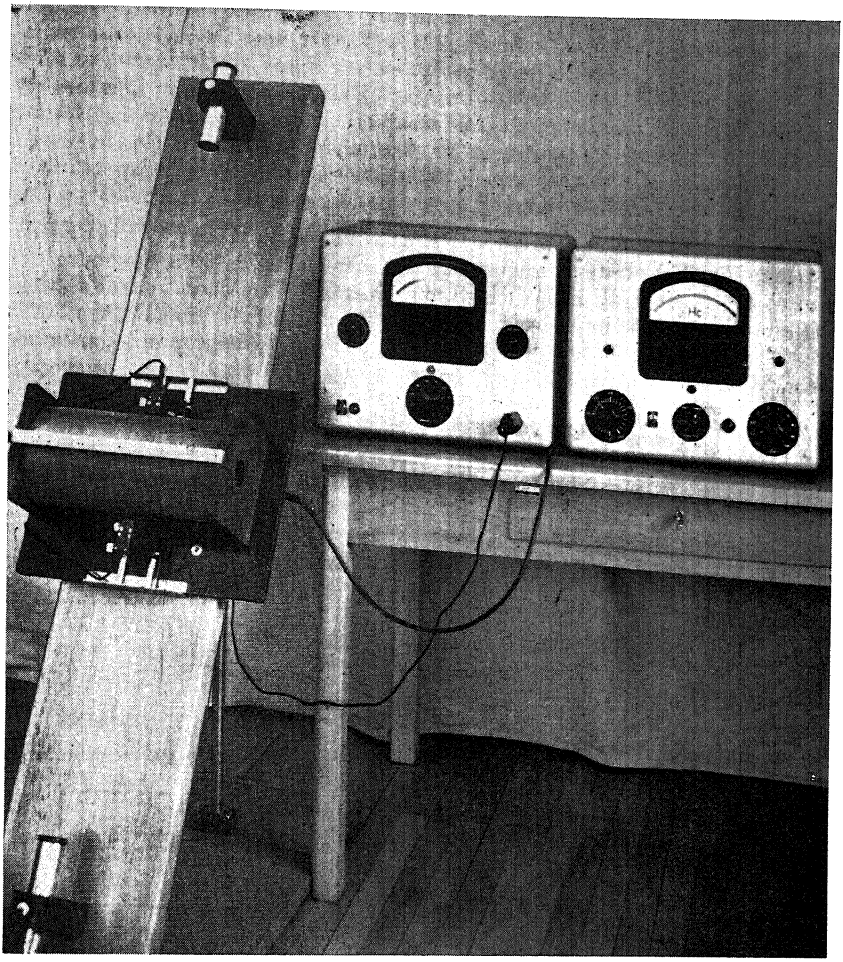

Institut Dr. Foerster

Fig. 2. Coercive-force measurement equipment.

Range of Applications. The sensitivity of the probe-coil method for measuring coercive force is so great that accurate results may be obtained even in the case of austenitic steels and nonferrous metals with small ferromagnetic additions. Relay parts or hard metal parts may be sorted according to coercive-force values.

MEASUREMENT OF MAGNETIC-MATERIAL PROPERTIES. Magnetic properties, such as coercive force, saturation flux density, remanence, permeability, or hysteresis loss, permit nondestructive determination of important mechanical and metallurgical conditions. For example, coercive force aids in evaluating the **quality of tungsten carbide,** since coercive force increases, in accordance with Néel's theory,[1] as the cobalt is more finely distributed in the tungsten carbide. A fine distribution of cobalt is required for high wear resistance. Many hard metals produced in Europe are tested with the coercive-force meter with Foerster probes.[2] Measurement of magnetic-saturation flux density indicates material properties such as **residual austenite content** and **ferrite content.** A universal arrangement for determining the entire d.-c. hysteresis loop as a function of temperature is especially suited to practical application.[3] It measures the true field strength inside the test object.

COERCIVE-FORCE MEASUREMENTS AT HIGH TEMPERATURE. Fig. 3 illustrates a magnetizing coil surrounding an oven containing the test object. A specimen is selected with a dimension ratio whose specific demagnetization factor N is known. Desirable shapes include the cylinder with cone-shaped ends or the rotation ellipsoid. In this arrangement, probes for measurement of magnetization intensity of the test object are placed outside the magnetizing coil. Thus, by using an oven in the magnetizing coil, this arrangement can be used for measurement of the variation of coercive force with temperature. Coercive force is a sensitive indicator of metallurgical changes such as conversion, precipitation, and age hardening[4] in the test specimen. The lines of force emerging from the specimen are detected by two d.-c. field-measurement probes, P_1 and P_2. The field strength resulting from the test body at probe P_1 is proportional to the magnetization $4\pi I$ of the specimen. The distance of probe P_1 from

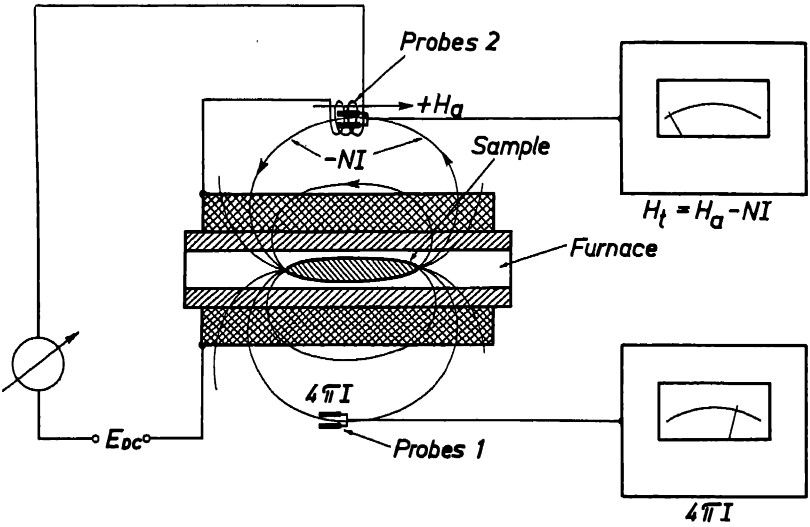

Institut Dr. Foerster

Fig. 3. High-temperature magnetometer arrangement for indication of true magnetization and true field strength.

the specimen is adjusted initially so that the ratio of the field strength at the location of the probe P_1 to the magnetization $4\pi I$ in the test body is exactly 1:10,000. Thereafter, all field strengths measured at the probe P_1 need only be multiplied by 10,000 to obtain the magnetization inside the test specimen.

Probe P_2 is located within an auxiliary coil energized by the same current as the magnetizing coil. Thus the field generated in the auxiliary coil is proportional to the field H_a of the magnetizing coil at the test specimen. The field resulting from magnetization of the specimen reacts simultaneously on probe P_2. The distance of probe P_2 from the test body is fixed so that the field strength resulting from the magnetization, $4\pi I$, of the test body is $-N \cdot I$. Thus two fields, namely, H_a and $N \cdot I$, react on the probe P_2. These two fields oppose each other. Together they give the true field strength $H_t = H_a - N \cdot I$. The two meters in Fig. 3 show the true magnetization and the true field strength of the specimen, respectively. The test specimen can be heated above the **Curie point** in the furnace within the coils.

AUTOMATIC SORTING OF PRODUCTION PARTS BY COERCIVE FORCE.[4,5,6] The coercive force is the most important magnetic characteristic of test materials. It is related to significant mechanical and metallurgical properties such as **hardness, tensile strength, depth of case, alloy content** (especially **carbon content**) and **aging conditions.** These properties can be nondestructively determined in many cases by measuring the coercive force. However, before magnetic sorting methods are used, extensive experiments are needed to check the relationship between the coercive force and the significant properties, such as hardness or tensile strength. It is essential that no reversal appear in the function relating hardness to coercive force. Such reversals can appear with several alloys, especially after repeated heat treatment. However, coercive-force measurement requires three steps:

1. Saturation.
2. Reduction of the magnetization force H to zero.
3. Increase of the opposing field until the magnetization is reduced to zero.

This requires so much time that it is unsuitable for production sorting.

Residual Magnetization as a Measure of Coercive Force. The residual magnetic field which remains after saturation magnetization is approximately proportional to the coercive force for normal production test parts.[7] Short production parts do not exhibit the typical material permeability μ. Instead, they exhibit a greatly reduced **form-permeability** μ_F. This is a function only of the ratio of specimen length to diameter (l/d). It is a result of the strong demagnetization caused by free magnetic poles. For cylindrical parts the apparent form-permeability μ_F is [8,9]

$$\mu_F = 6\frac{l}{d} - 5 \tag{1}$$

However, the permeability is generally given as the increase of the magnetization, $4\pi I$, with the field strength H, so that from the triangle of Fig. 4 we have

$$\tan\phi = \mu_F = \left(\frac{4\pi I_r}{H_c}\right) \tag{2}$$

Measuring Residual Magnetization with External Probes. The residual magnetization $4\pi I_r$ generates a magnetic field H_r outside the test specimen. This external field H_r is proportional to the residual magnetization I_r. It is a function

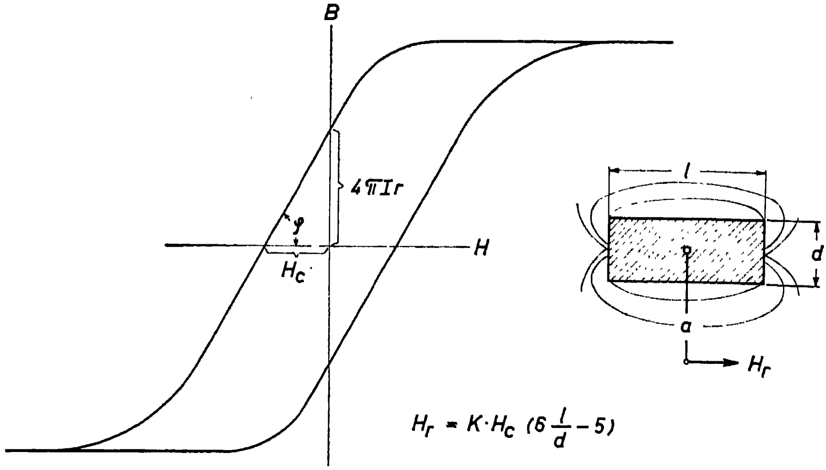

Fig. 4. Magnetization loop of a short production part (length, l; diameter, d). Note the proportionality between coercive force and the residual field of the test object.

of the distance a of the probes from the test part and the length l of the test part only. From Eqs. (1) and (2), the residual field H_r measured by the probe is

$$H_r = K(4\pi I_r) = KH_c\left(6\,\frac{l}{d} - 5\right) \tag{3}$$

The constant K is calculated from the distance a of the probe from the test object and the length l of the test object. The exact calculation is presented by Foerster.[7]

Eq. (3) indicates the proportionality between the field measured with the probe and the coercive force of the test specimen. It is the basis of several fully automatic sorting instruments.

Automatic Sorting Arrangement. Fig. 5 illustrates such an automatic sorter schematically. The test parts are fed to the conveyor belt at specific intervals. They then pass through the magnetizing coil. At a specific distance beyond the coil, they pass the probe. The latter measures the residual field (proportional to the coercive force) within 1/1000 sec. Gates are electronically controlled to sort test parts according to their coercive-force values. These values are related to specimen hardness, tensile strength, carbon content, or other factors.

An **astatic arrangement of four probes**[7] can be used to eliminate the influences of the **earth's magnetic field** and **inexact centering of test parts** on the conveyor belt. Test indications are independent of the **speed of parts** passing the probe. This has lead to a very simple test arrangement. Test parts are placed in an inclined groove, slide through the magnetizing coil, pass the probe, and are automatically sorted according to their hardness range. Just before entering their particular containers, parts pass through a demagnetizing coil to remove residual fields which may affect subsequent machining operations.

Advantages of Automatic Sorting by Coercive Force. Automatic coercive-force sorting has three significant advantages:

1. Low sensitivity to test-object dimensions and shape.
2. Uniform response to the entire cross-section of test objects.
3. High sorting speed.

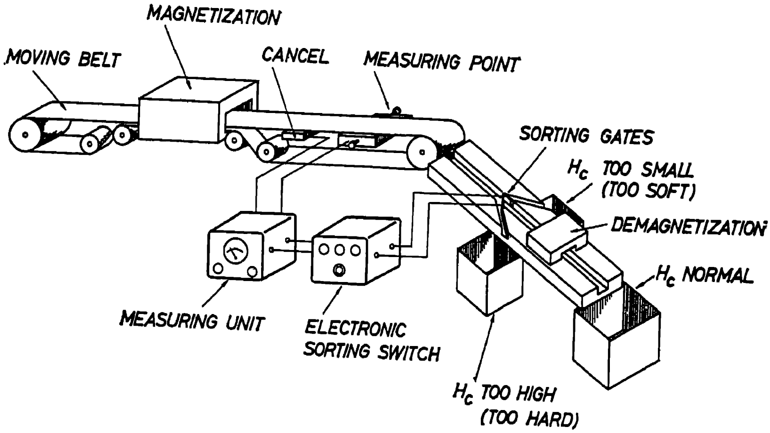

Institut Dr. Foerster

Fig. 5. Arrangement for automatic sorting of production parts by residual field values and (for many alloys) hardness.

APPLICATIONS OF SORTING BY COERCIVE-FORCE TESTS. Coercive-force tests are used in many European countries for sorting screws, bolts, nuts, pin bearings, rollers, balls, ball-bearing rings, drills, and other parts. For example, producers of **wrist pins** use this method for their finished products. In the testing of ball-bearing steels, the magnetic-sorting method shows a greater resolution of the structural variations than do **mechanical hardness tests.** In addition, the measurement of the average properties over the entire volume of each test object is more reliable than the point-by-point mechanical hardness testing.

Ball Bearings. For example, a well-known ball-bearing plant daily tests 100,000 bearing pins and a corresponding number of rollers and ball-bearing rings. Automatic feeding of parts permits high test speeds unattainable with mechanical hardness tests. Such automatic sorting is especially well suited for 100 percent inspection.

Control of Hardness of Tempered Parts. Other industries test vital automotive parts[10] subject to high wear, to attain uniform tempering. Before the change-over from mechanical hardness testing of each individual part to the much faster electronic testing, one plant made comparison tests between mechanical and magnetic hardness testing on 40,000 parts from various heats. This extensive test showed that the deviation between mechanical and electrical determinations of the hardness lay within the normal variation of Rockwell hardness measurements. Individual mechanical tests could not have given more exact results than the much faster nondestructive sorting by hardness values.

Hardened Steel Parts. In the magnetic sorting of high quality diesel motor parts[11] subject to high wear (such as injection pumps and nozzle needles), it was proved statistically that a considerable increase was obtained in the **average service life.** Material structure could be kept to much **closer tolerances** as a result of the residual-field measurement. Mechanical hardness testing obviously could not be applied to 100 percent of production.

Tempered Castings. In tempered cast parts,[12] it is important to control carbon content. Excessive carbon results in a poor machineability; insufficient carbon results in difficulties in the threading dies. The material is too soft, or it "smears."

Residual fields remaining after magnetization of tempered cast parts corresponds exactly to the carbon content; so, tempered cast parts are sorted automatically according to the mechanical **machineability.** The results of sorting

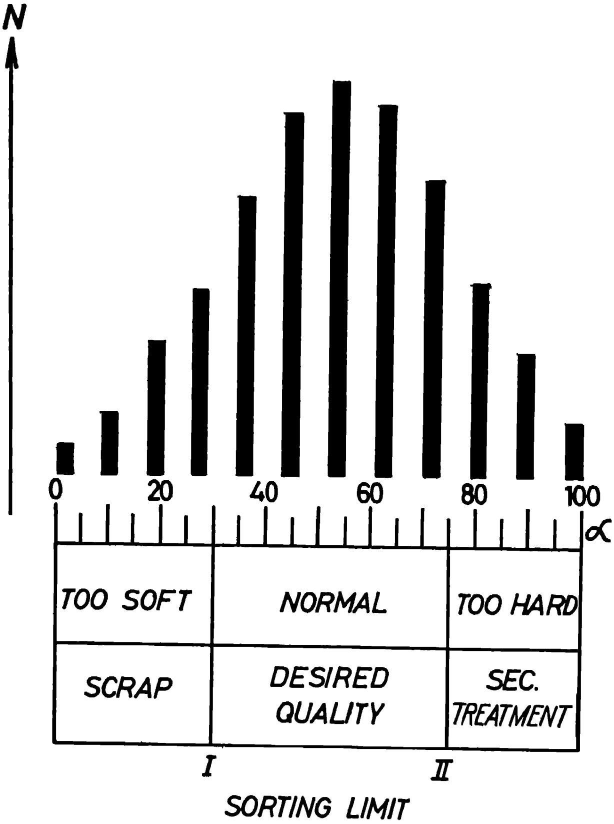

Institut Dr. Foerster

Fig. 6. Statimat graph of the frequency distribution of annealed cast parts. Sorting limit between 30 and 75 scale divisions.

are easily observed with the Statimat instrument, a newly developed method for the automatic indication of statistical distributions. The twelve indicating channels of this instrument show the statistical frequency distribution of measured properties such as hardness, tensile strength, machineability, or carbon content. Fig. 6 shows the Statimat graph resulting from sorting of **tempered cast parts** for machineability.

Electrical Relay Parts. In the examples previously discussed, measurement of coercive force was only an auxiliary means for indicating hardness. European plants in the electrical industry are also using magnetic-sorting instruments for production sorting of relay parts into various coercive-force groups. Coercive force represents an important characteristic of relay parts. Excessively high coercive force leads to **erratic relay operation.**

Point-Pole Tests

THE POINT-POLE METHOD. In cases of strong demagnetization (for example, of short production parts), the residual magnetic field remaining after previous saturation is proportional to the coercive force. This important relationship between residual field and coercive force[13] is valid both in case of magnetization of entire test parts and for local point-pole magnetization.[14]

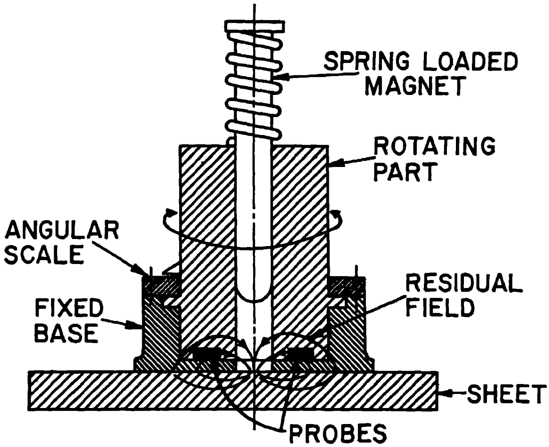

Institut Dr. Foerster

Fig. 7. Probe and magnet arrangement used to determine grain orientation of sheet steel.

If a test object is brought into brief contact with the suitably contoured point of a permanent magnet, a **residual magnetic pole** remains in the test object. The larger the demagnetization factor *N*, the more exact the proportionality between the pole's residual field and coercive force. The surface of a test part (mathematically described as an infinitely large half-plane) has an especially strong demagnetizing action on the point pole. This corresponds to a large **demagnetization factor.** Consequently the requirement for proportionality between point-pole strength and coercive force is fulfilled. The residual field strength indicates the coercive force at the point pole.

A series of measurements on sheets, machine parts, and forgings has confirmed this proportionality between the point-pole indication, obtained with the probe, and the local coercive force.[13]

MEASURING ANISOTROPY IN SHEET MATERIALS. A combination of a rod magnet with a probe arrangement, as shown in Fig. 7, is used for determination of the anisotropy of sheets. Pushing the spring-loaded magnet down onto the sheet surface will cause a point magnetic pole to appear on the sheet surface. The tangential component of the point-pole field is measured by the difference probe pair. The deflection of the meter connected to the pair is proportional to the coercive force at the location of the point pole. This permits quick and nondestructive sorting of sheets by coercive-force values. These measurements indicate certain engineering properties such as **elasticity** or **deep-drawing ability.** If the probe pair is rotated around the point pole, a constant deflection of the meter will be obtained only in case of **isotropic material.**

Fig. 8 is a **polar diagram** of the instrument deflection for various sheets. Here all maximum deflections are normalized to the same value. This method is of importance in the electrical industry where **grain-oriented sheets** are used, as well as in the sheet-metal industry where too heavy an orientation leads to undesirable **lobe-formation** during deep drawing.

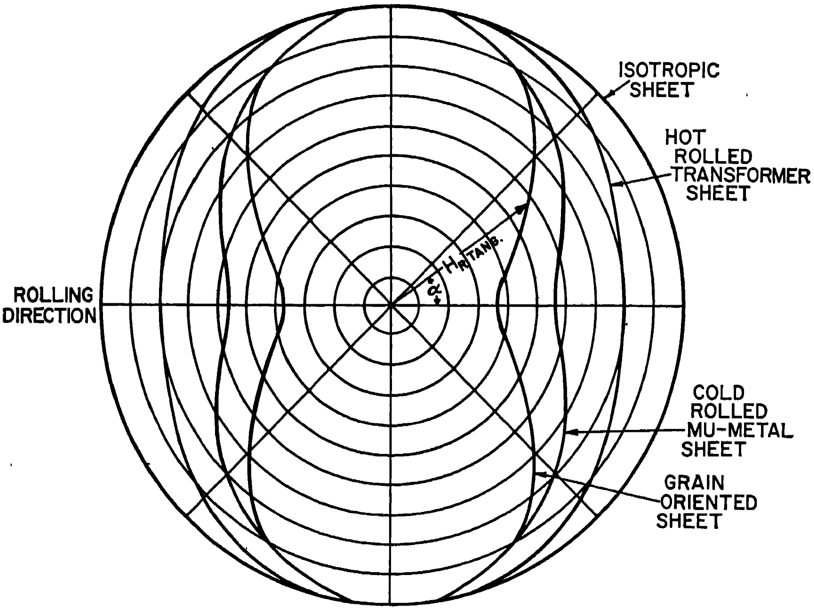

Fig. 8. Polar diagram of magnetic field about a point pole for various types of steel sheet.

Hysteresis Loss of Electrical Steel Sheets. The point-pole method is used extensively in sorting of electrical steel laminations. Generally the hysteresis loss of electrical sheets increases with coercive force, i.e., with widening of the hysteresis loop. Thus the point-pole strength of electrical sheets represents the static component of the wattage loss. This hysteresis loss is measured very simply.

Internal Stress in Structural Steel. An especially important application of the point-pole method is the nondestructive determination of internal stress in steel structures. Normally, structural steels do not exhibit **magnetic anisotropy.** Under tensile or compressive stress, anisotropy results in the material. This causes a deformation of the circle. The internal stress is determined from the ratio of maximum to minimum deflection and the calibration for the corresponding steels. Thus the point-pole method has possible uses as a nondestructive method for instantaneous determination of the magnitude and direction of internal stresses. The **stress direction** is indicated by the direction of maximum deformation of the circle.

ANALYSIS OF CARBON CONTENT. On large machine parts the point-pole method tests the uniformity of heat treatment or of carburized or induction-hardened layers. In steel plants, large pieces of steel are tested for carbon content. Fig. 9 illustrates the relationship of the point-pole instrument indication (H_c) to carbon content. The band width in Fig. 9 indicates the accuracy of the magnetic carbon analysis with the point-pole method.

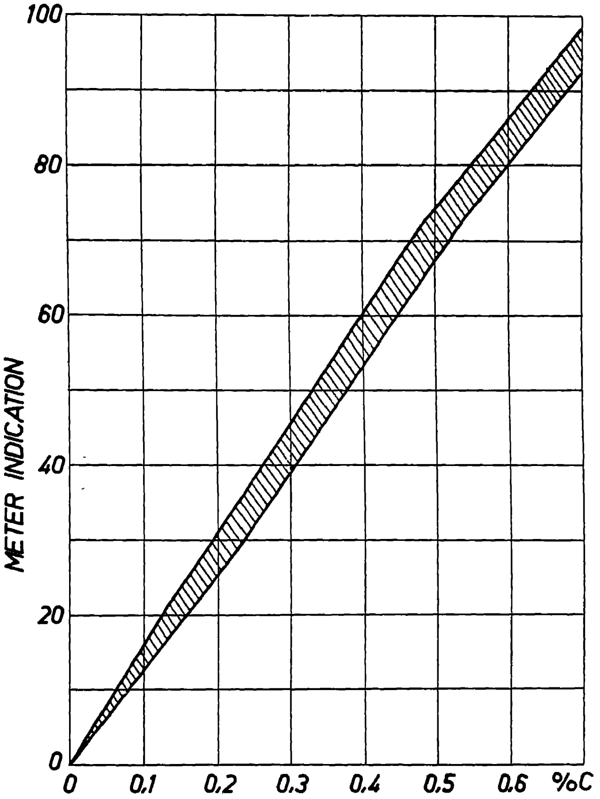

Fig. 9. Point-pole indication as a function of the carbon content for carbon steel.

Sorting Mixed Stocks. The point-pole method can also be used to sort **semi-finished steel parts** into various alloy groups, as long as their coercive-force values are sufficiently distinguishable. Frequently a point-pole measurement at the ends of bars in stock piles is sufficient to separate mixed alloys.

Fig. 10 illustrates the frequency distribution of indications from point-pole sorting of mixed lots of C1040 and C1060 steel rods.[15] The spread from 30 to 40 scale divisions for the C1040 steel is a result of slight variations in the carbon

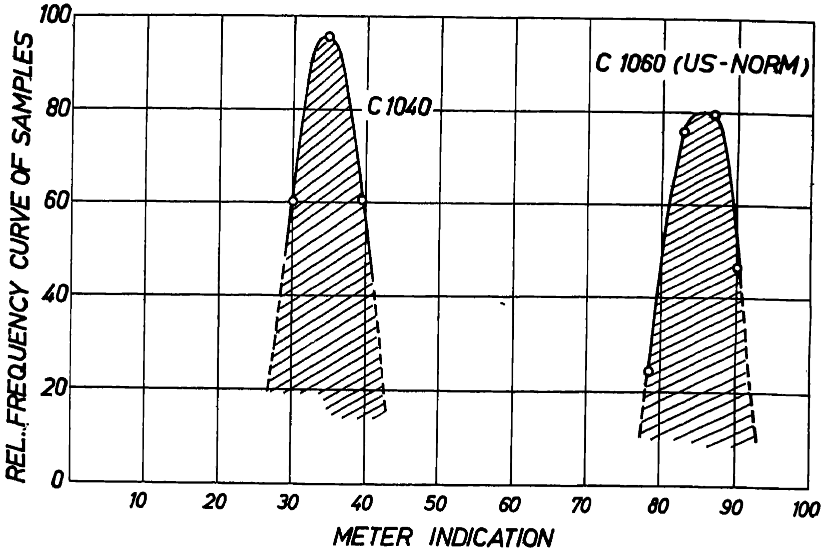

Fig. 10. Frequency distribution in a lot of two mixed alloys, obtained in a steel plant.

content from various heats. Fig. 10 shows reliable separation of both steels, as indicated by the large distance between their indications.[16] The test data of Fig. 10, obtained by counting, are found automatically by testing with the Statimat instrument. Generally, two alloys can be separated if at least one channel remains empty between the distributions of the two alloy groups. Fig. 11 illustrates

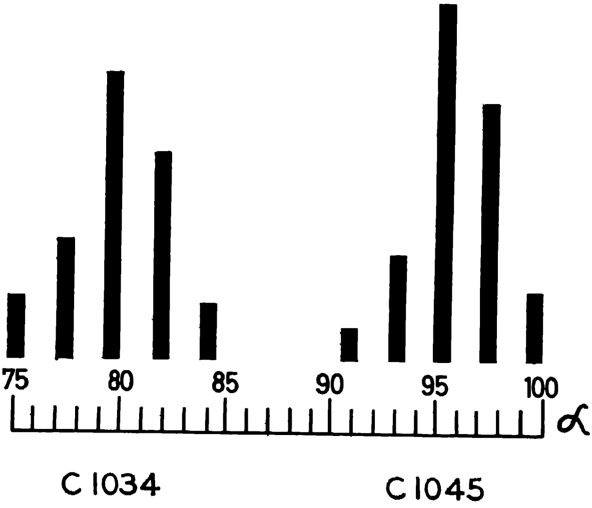

Fig. 11. Sorting of two similar alloys with an expanded measurement scale. Feasibility of reliable separation is indicated by empty sorting channels between the two frequency groups.

the distribution of indications for two similar alloys (C1034, C1045), obtained with an expanded measurement range. The empty **indication channels** indicate that reliable sorting is possible.

Hardness Testing. The point-pole method can be used for rapid sorting of **centrifugally cast tubes** for surface hardness. Foerster shows the relation between the meter indication and the mechanical hardness of centrifugally cast tubes in Fig. 12.[6] This relationship must first be established experimentally with control samples whose alloy content, heat treatment, and microstructure are held constant. Hardness is indicated nondestructively and quickly after pressing down the rod-shaped permanent magnet.

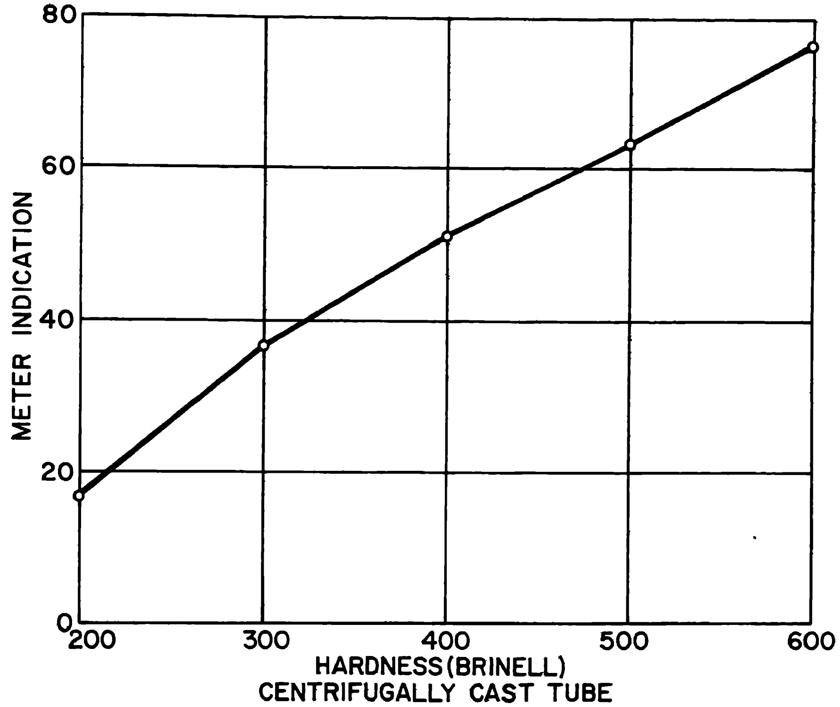

Fig. 12. Relation between point-pole indication and mechanical hardness of centrifugally cast tubes.[6]

Depth of Case Hardening. Another application of this method is the local determination of the case depth on crankshafts and other machine parts. Since the static field method has greater penetration depth than the a.-c. field method, much heavier **case depth** and **induction-hardened layers** can be measured. The point-pole method can generally be used even on parts with large dimensional variations.

Other Applications. Small parts and fine cast iron (for example, in the sewing machine industry) are normally cast in a cluster. By measuring only a section of this cluster, the quality of a number of test parts is determined simultaneously. The **fine cast method** uses carbon-arc furnaces, and occasionally carbon particles falling into the melt increase the carbon content undesirably. Such cast parts are easily detected by their excessive coercive force and high point-pole indications.

Another application is hardness sorting of **textile spindle tips.** A point pole is induced in the spindle tip with a permanent magnet of suitable shape. The pole strength is proportional to the mechanical hardness of the outer tip. The method permits indirect hardness measurements at locations not accessible to mechanical hardness testing; for example, at the base of a ⅛-in. diam. **injection-nozzle hole** of a diesel engine.[11]

Scale Expansion with Compensating Magnet. The probe method permits convenient expansion of the measurement scale. This is done with an adjustable compensation magnet near the upper gradient probe. The unused portion of the scale from 0 to 75 scale divisions is suppressed to obtain the results shown in Fig. 11. Only indications above 75 scale divisions result in deflections. If a higher sensitivity is selected, the range between 75 and 100 scale divisions can be expanded to cover the entire scale.

DOUBLE-POLE TESTS. A double magnetic pole[6] produced with a **pot magnet** is used with the gradient probe (tangential gradient of the normal component) for tests on **magnetized parts** or tests in the presence of other **interfering fields.** Fig. 13 illustrates the pole form and probe arrangement for the double residual-pole test. The lines of force of the residual pole caused by the pot magnet at the first probe are opposite in direction to those at the second probe. This field distribution is measured by the gradient probe. Magnetization of the entire rod (caused, for example, by the earth's field) creates magnetic lines of force having the same direction at each probe. The gradient probe is insensitive to such fields.

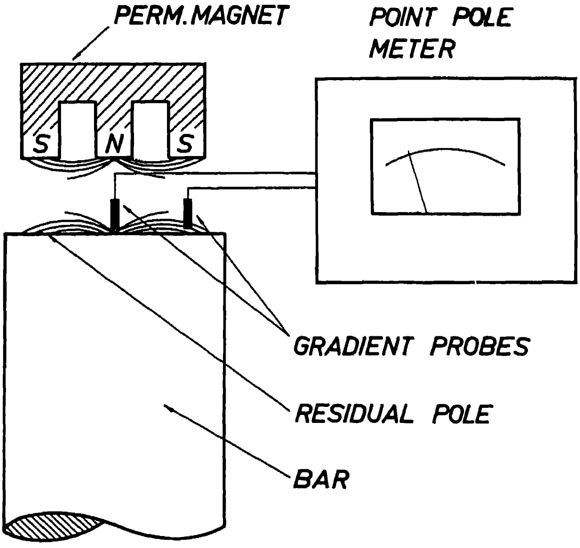

Institut Dr. Foerster

Fig. 13. Difference-probe arrangement for magnetization with a pot magnet (double-pole pole) to suppress influence of the earth's field.

Thickness Tests

PROBE MEASUREMENT OF NONMAGNETIC WALL THICKNESS.[6] The gradient probe shown in Fig. 14 is not affected by the earth's field (normal gradient of the normal component). If it is placed on one side of a wall while a small permanent magnet is held on the opposite side, the field strength at the probe is a function only of the distance from magnet to probe. The measurement is not a function of the characteristics such as electrical conductivity of the wall material, as are alternating field methods which have been suggested for this purpose.[17] The **indication scale** is identical for all nonferrous metals as well as for glass, plastic, or wood.

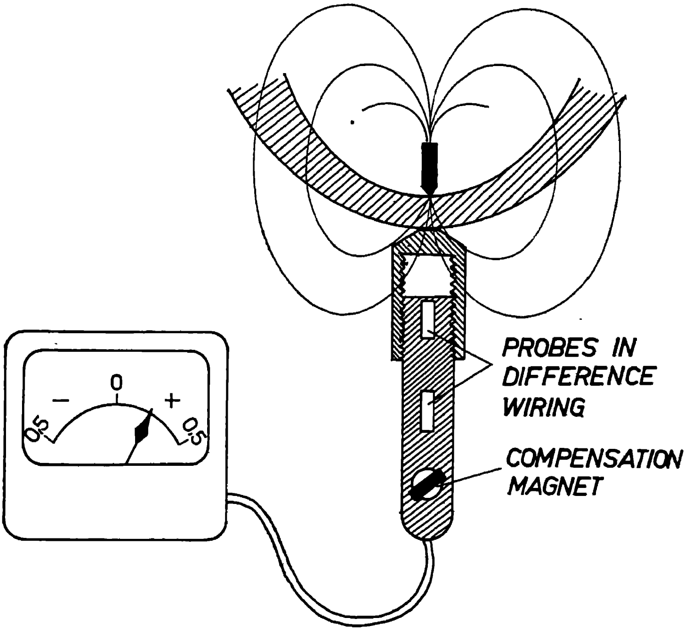

Institut Dr. Foerster

Fig. 14. Probe array with permanent magnet for wall thickness measurement of nonferrous metals (independent of wall material).

Scale Expansion. Expansion of the thickness indication scale into a desired range is often convenient. The field of the main permanent magnet is compensated at the probe with a small, adjustable magnet in the probe head. The "required" value is centered to $H = 0$ on the wall thickness scale. Thus, by selecting a suitable sensitivity, a ±1/10-, ±1/100-, or ±1/1000-in. deviation from the required value results in a full-scale deflection.

The probe with difference coils (Fig. 14) contains a screw cap which can be adjusted in or out for the desired **measurement range.** The instrument uses the same scale for various thickness ranges. By adjusting the cap, the distance from magnet to probe for the selected required value is always the same.

Cast Nonferrous Parts. For wall thickness measurement of cast nonferrous parts, the probe is placed outside the test part (Fig. 14). The very small permanent magnet, mounted on a flexible wire, can be inserted even into complicated hollow bodies.[18]

Automotive Piston Heads. An automatic instrument has been devised for sorting automotive piston heads into various thickness groups. The difference probe is held lightly against the bottom side of the piston by a spring. As soon as the center of the piston is below the permanent magnet, the magnet is pressed down against the piston head. At the same instant the light beam of the instrument indicates the piston thickness. A **color marker,** triggered by photocells on the instrument scale, marks the piston according to its thickness group.

Large Wall Thickness. Wall thicknesses far above 100 in. are measured with large permanent magnets (for example, 1 × 4 in.). The probe method is used in **mining** to measure the thickness of walls remaining between two galleries drilled from opposite sides.

MULTIPLE-POINT MEASUREMENTS OF WALL THICKNESS. Probe-and-magnet wall thickness measurement devices are relatively small and are independent of the **rigidity requirements** of a mechanical caliper. This method is especially suitable for multiple measurements where numerous points are measured simultaneously.

Sheet and Plate Thickness Measurements. Fig. 15 illustrates a ten-point wall thickness measurement device for nonferrous metal, wood, glass, plastic, and similar materials. The probes are pressed lightly by springs against the bottom of the surface to be measured. The permanent magnets are located opposite the probes, on the top surface. These magnets can be conveniently lowered to the surface to be measured by an electromagnetic device. With **electronic scanning** of all measurement points, indications appear simultaneously on a cathode-ray tube. This display shows deviations from standard values and indicates the shape of the test object.

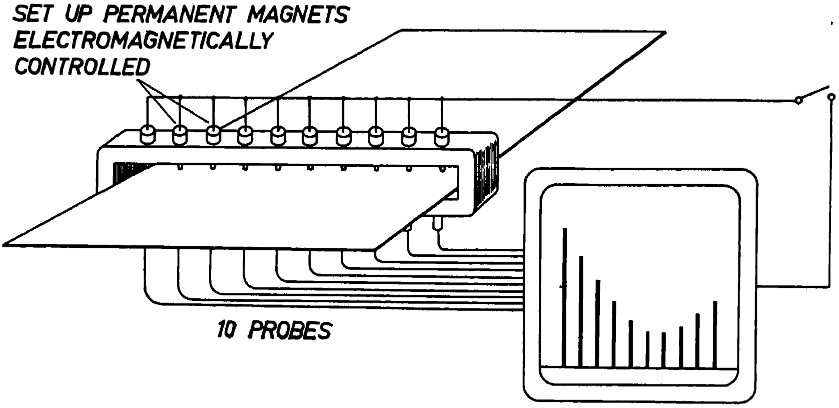

Institut Dr. Foerster

Fig. 15. Multiple thickness-measurement device with simultaneous indications on the screen of a cathode-ray tube.

Continuous-Sheet Thickness Measurements. The method is also suitable for a continuous operation in which the individual thickness indications and the cross-section of the test object appear continuously as a luminous picture on the screen. Thicknesses which exceed or fall below the tolerance trigger a signal. Methods using a **roller guide** for the probes and magnets are used in the linoleum and plastic industry. The thickness of the material to be tested is recorded during production.

Test indications are entirely independent of the rigidity of the supporting fixture which carries the probes and the small permanent magnets (Fig. 15). Continuous thickness measurements on flat nonferrous materials can be carried out far from the edge without constructing an especially rigid fork to carry the probe and the magnet.

HALL-GENERATOR MEASUREMENT OF WALL THICKNESS. Fig. 16 illustrates the application of the Hall generator for the wall thickness measurement of ferromagnetic material from one side.[19] A **pot-shaped yoke magnet** magnetized by direct current is placed on the wall whose thickness is to be measured. The Hall generator is placed in the induced flux of the center leg. When the yoke magnet is placed on the wall, the increase in magnetic flux is proportional to the product of wall thickness and saturation magnetization of the wall material. For many materials, such as **deep-drawing sheets, boiler walls,** and **boiler tubes,** the saturation magnetization is constant, so that the instrument deflection can be calibrated directly in wall thickness.

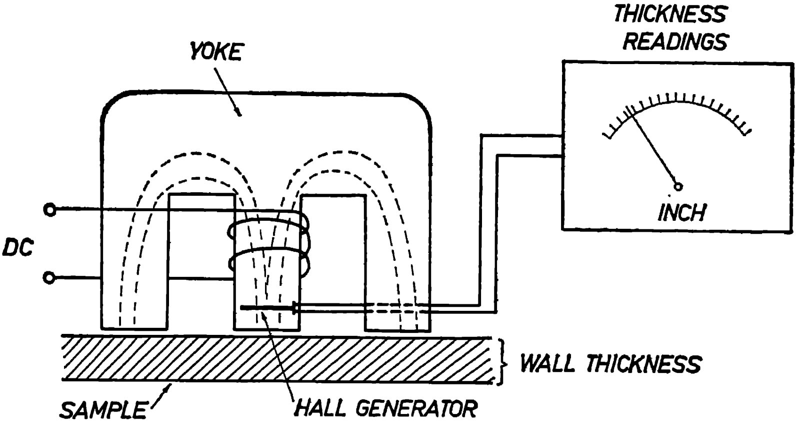

Institut Dr. Foerster

Fig. 16. Arrangement of Hall probe for measurement of wall thickness.

Sheet Thickness Meter. By means of the electrical compensation, a small portion of the thickness range can be represented on the measurement scale. A sheet thickness meter with Hall generator is used for automatic sheet-metal thickness sorting. Adjustable **microphoto cells,** providing a maximum of 30 sorting groups, are located on the scale of the light-beam galvanometer for adjustment of the desired thickness in each sorting group.

Nonferromagnetic-coating Thickness Meter. Another application of the Hall generator is the measurement of thickness of nonferromagnetic coatings on a **ferromagnetic base.** A series of instruments is available for coating thickness measurements. These measure the force required to lift a permanent magnet from the surface of the layer to be measured. A greater lifting force indicates a stronger magnetic induction in the tip of the permanent magnet.

With the miniaturized Hall probe it is possible to measure the magnetic induction in the tip of the permanent magnet. The indicating instrument of Fig. 17 can be calibrated directly in wall thickness values.

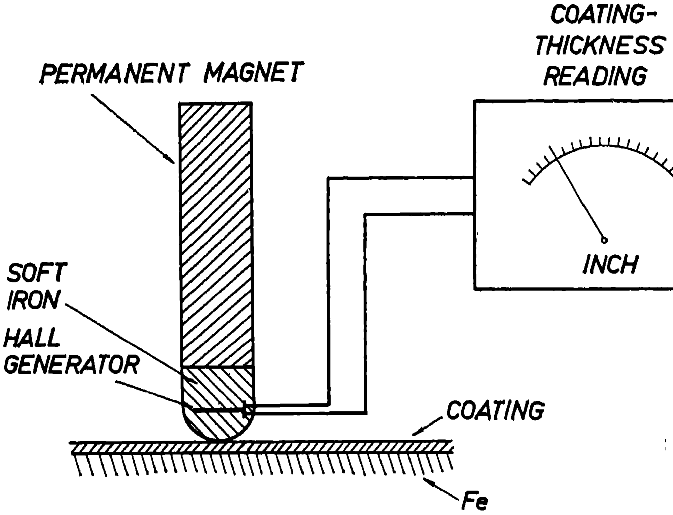

Institut Dr. Foerster

Fig. 17. Arrangement of permanent magnet with Hall generator for measurement of thickness of nonferromagnetic layers of iron and steel. The density of the lines of force in the tip is measured by means of the Hall generator.

ECCENTRICITY OF A CONDUCTOR IN INSULATING COVERING. If current flows in a conductor, a **ring-shaped magnetic field** appears, surrounding the conductor. The field strength H is

$$H = \frac{0.2I}{R} \tag{4}$$

where H = the field strength in oersteds.
I = the current through the conductor, in amperes.
R = the distance in centimeters from the center of the conductor to the point at which the field strength is to be measured.

The displacement of the conductor from its concentric position is measured with a suitable probe arrangement moved by means of small rollers on the insulated conductor. Fig. 18 illustrates the arrangement with which the position of the conductor in its covering is indicated on a cathode-ray tube screen.

The direct current flowing through the conductor generates a magnetic field H at the probe array. The **probe array** is constructed so that no indication is obtained when the conductor is centered with reference to the probes. With an eccentric conductor, the field reaction on the difference-probe pairs, P_1-P_2 and P_3-P_4, will no longer cancel. By connecting probes P_1 and P_2 (which measure the horizontal deviation of the conductor from its concentric position) to the horizontal plates and probes P_3 and P_4 to the vertical plates, the position of the beam of the cathode-ray screen indicates the position of the conductor in the insulating cover. If the eccentricity of the conductor in the insulating cover exceeds a specific value, the beam moves out beyond the **tolerance circle** on the screen.

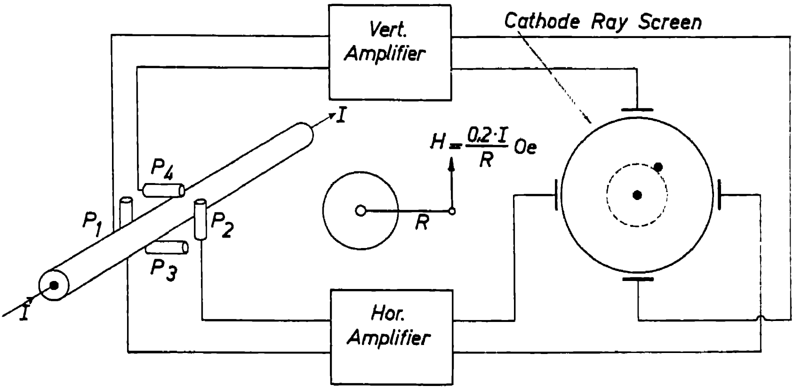

Institut Dr. Foerster

Fig. 18. Probe arrangement for direct representation of position of conductor in an insulating covering.

Feedback Control. The voltages produced by the probes can be used to guide the conductor back to its concentric position by means of a suitable control mechanism. The direct current which flows through the conductor is simultaneously used for the sensitivity control of the probe amplifier. In this way the eccentricity measurement is independent of the magnitude of the direct current through the conductor. A similar arrangement can be used to determine the eccentric position of the metallic core in covered welding electrodes.

MEASUREMENT OF THE ECCENTRICITY OF TUBES. If direct current passes through the wall of a concentric tube, the static magnetic field outside the tube will be exactly the same as though the current were concentrated in a central conductor within the tube. The inside of a concentric tube is entirely free of magnetic field.

Field Within an Eccentric Tube Carrying Current. In an eccentric tube with nonuniform wall thickness, a completely **homogeneous magnetic field strength,** $H_{\text{ecc.}}$, appears. As shown in Fig. 19, this field is perpendicular both to the tube axis and to the line connecting the point of minimum wall thickness with that of maximum wall thickness.

The **eccentricity** e in the tube results in a field $H_{\text{ecc.}}$ calculated as

$$H = \frac{0.2eI}{R_1^2 - R_2^2} \tag{5}$$

Here e, as indicated in Fig. 19, is the displacement of the center point of the inside wall of the tube with respect to the center point of the outer wall of the tube. In a concentric tube, both center points coincide ($e = 0$), and

R_1 = the outside radius.
R_2 = the inside radius of the tube.
I = the current in amperes which flows parallel to the tube axis.

By using two probe pairs placed perpendicular to each other and connected to the deflection plates of the cathode-ray tube, the magnitude and direction of eccentricity of a tube can be read directly from the screen.

Eccentricity in wall thickness of tubes can also be determined by measuring the **radial component of the field strength** outside the tube. In a concentric tube the radial component of field strength is always zero. In this case the magnetic lines of force are concentric circles around the tube, perpendicular to the direction of the radius. However, the radial surface field strength for an eccentric tube is never zero.

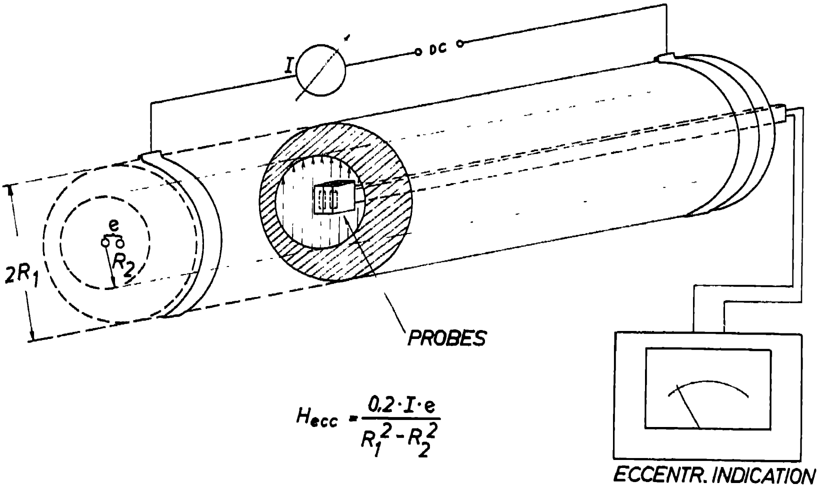

Institut Dr. Foerster

Fig. 19. Arrangement for measuring the eccentricity of a nonferrous metal tube by measuring the magnetic field inside the tube produced by a current in the tube wall.

Foerster has described the mathematical derivation of the field distribution of an eccentric tube[20] and has presented examples of nondestructive eccentricity measurement on other production parts.

Other Applications

CRACK DEPTH MEASUREMENT. The small dimensions of the **Hall microprobe** make possible the measurement of the magnetic leakage flux of cracks on the surface of test objects. Thus, the Hall probe can be used for the experimental verification of theoretical calculations[21] for the magnetic leakage flux over cracks.

Fig. 20(a) illustrates the arrangement of the Hall probe for crack depth measurement. The crack lies between the two contacts which apply a direct current to the test part. The Hall microprobe is located directly above the crack so that the magnetic d.-c. field is perpendicular to the largest surface of the Hall crystal. The instrument connected with the Hall probe indicates the magnetic-field strength generated by the direct current. In the absence of a crack, Fig.

20(b), the main portion of the current flows directly below the surface. Zero crack depth corresponds to a specific d.-c. field strength at the location of the Hall probe for this current distribution. The Hall voltage at zero crack depth can be compensated by means of a compensation voltage E_0 obtained from the d.-c. circuit across a resistor R. If a crack is present, the d.-c. current path is forced deeper into the test part. However, the greater length of the current path results in a weakening of the magnetic d.-c. field. This weakening increases with crack depth. Thus it seems practical for crack depth applications to determine the magnetic field instead of the potential difference above the crack. The non-contacting Hall probe requires much lower currents and eliminates interference caused by thermoelectric forces.

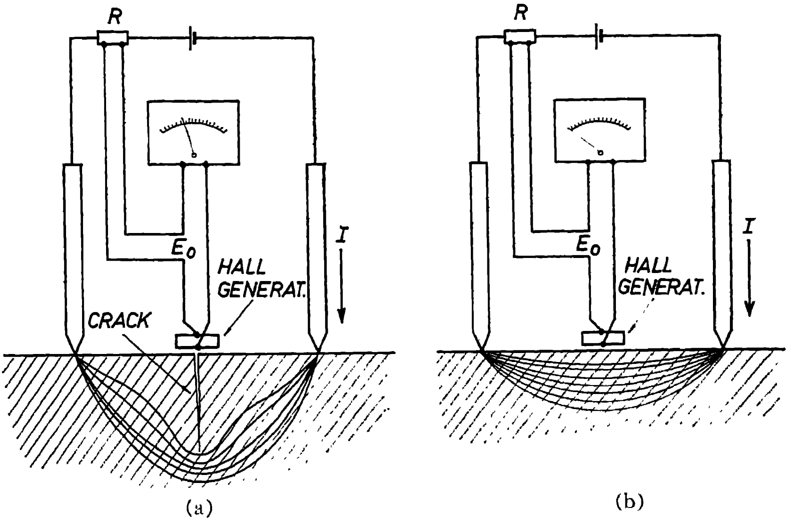

(a) (b)

Institut Dr. Foerster

Fig. 20. Effect of crack on path of current. (a) Current path around crack. (b) Current path without a crack.

DETERMINATION OF IRON IMPURITIES IN NONMAGNETIC MATERIAL. For many applications it is important that a material be as free as possible of magnetic impurities. For example, an iron-free material is required for the construction of electrical measurement instruments, such as compass housings. Fig. 21 illustrates a simple arrangement for the quantitative determination of very small amounts of free, **undissolved iron** in small, rod-shaped test samples. The arrangement utilizes a Foerster probe at a specific distance above a strong permanent magnet. The field of the large permanent magnet is compensated at the probe by a small permanent magnet whose distance above the probe is adjustable. In the absence of a test object, the probe indicates zero field strength. If a specimen is brought into the field, a large measurement effect appears, even in case of low iron impurities. This permits quantitative determination of the **iron content.** The instantaneous indication of iron content permits continuous operation as rods and tubes pass between the probe and the permanent magnet.

Detecting Ferrous Material in Packaged Foods. Induction methods for detection of iron contamination cannot be used with metal-foil wrapped packages. However, the **static magnetic-field test** can be applied.[6] The packages pass through the field of a permanent magnet for sorting. The probe is placed in an astatic gradient arrangement independent of the earth's field and perpendicular to the field of the permanent magnet. For example, **iron-wire particles** weighing less than 10^{-3} gram produce additional lines of force detectible by the probe. These can be utilized for the automatic elimination of contaminated packages.

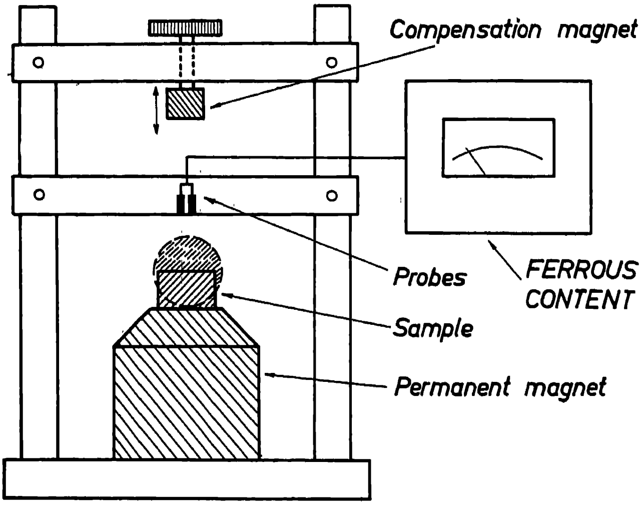

Institut Dr. Foerster

Fig. 21. Arrangement for rapid, continuous measurement of iron content in nonferromagnetic materials.

Iron in Nonferrous Scrap. Specially designed search instruments are used to locate compact iron parts in scrap packages. In tightly pressed nonferrous metal scrap, the presence of iron parts is disadvantageous. These iron parts can be detected from the outside with a special search instrument.

Iron Core-Wire in Nonferrous Castings. In the casting of complicated nonferrous castings, it frequently happens that **iron core-wires** or **chills** sometimes remain inside the cast bodies. These later cause difficulties. These wires are easily located with a small model of the search instrument.

Unexploded Blasting Cartridges. In the following example, the word "nondestructive" is of special significance because it does not refer to test parts but to people. In mining and in construction of tunnels, large numbers of blasting cartridges are placed and simultaneously detonated. Occasionally a cartridge does not explode. A worker may later accidentally explode an unfired cartridge, resulting in injuries or death. One European country which has to construct an especially large number of tunnels and power plants is considering equipping all blasting cartridge with small magnets. These would be pulverized during the explosion. As soon as a detonation of many cartridges occurred, the blast-off wall would be scanned with a gradient probe, which operated independently of the earth's field but reacted to the field of the small magnets. Each unexploded cartridge would be immediately indicated on the gradient probe instrument by a flashing signal lamp.

Survey Markers. Another application of the gradient probe is in geodesy. In the measurement of **land boundaries,** markers are posted to record the survey. These, however, can be displaced as time passes. If a sealed glass tube containing a permanent magnet the size of a pencil is buried at a depth of 3 ft., the exact location can be identified within an accuracy of 1 in. with a simple gradient-probe instrument on the ground surface.

Buried, Unexploded Bombs, Pipelines, Cable Boxes. Most European countries use search instruments with Foerster probes for the location of iron parts such as **dud bombs** in the ground. These instruments are also used to locate **hidden pipelines.** The Telephone and Telegraph Division of the German Federal Postal Department uses these search instruments to relocate buried cable boxes.

LIQUID-LEVEL CONTROL. The combination of the d.-c. probe with a small permanent magnet has numerous other measurement possibilities. The liquid level in a closed container can easily be observed and controlled by using a small permanent magnet sealed in a glass tube as a float. The approach of this magnet to the built-in gradient-probe array can be quantitatively indicated on the outside of the container. Liquid level is indicated not only at a predetermined limit but over the entire measurement range. Probe signals can be used for control of the liquid level.

Flow Meters. Another application is the measurement of the speed of flow of a liquid in a closed tube. A small turbine wheel placed in this tube carries a small permanent magnet. The wheel rotates in proportion to the **speed of flow.** The reaction of the permanent magnet on the probe outside the tube continuously indicates the number of rotations of the wheel. The small permanent magnet reacts on the probe even through iron tubes. The speed of rotation measures the speed of flow. **Electronic integrating counters** can measure the total amount of liquid passing the measuring point.

DETECTING MOVEMENT OF NONFERROUS MATERIALS. If a probe is located in the field of a rod-shaped permanent magnet so that lines of force of the magnet are perpendicular to the probe, no field strength is indicated by the probe. However, as soon as a sheet of nonferromagnetic metal is moved between the probe and the magnet, the lines of force of the permanent magnet are apparently carried along because of the well-known eddy current effect. In consequence the probe is no longer perpendicular to the lines of force. The field strength measured while a metallic body moves between the probe and the magnet is proportional to the thickness of the metallic body, its electrical conductivity, and its speed. With this arrangement it is possible to obtain large deflections from movements of 1/1000 in. per second.

References

1. Néel, L. "Nouvelle théorie du champ coercitif (New Theory of the Coercive Field)," *Physica*, 15 (1949): 225.
2. Foerster, F. "New Measuring Methods." *Ind. Anzeiger*, 77 (1955): 220.
3. ———. "An Astatic Magnetometer for the Determination of Properties and its Temperature Dependence," *Arch. tech. Messen.* (in press).

4. **Foerster**, F. "Die schnelle und genaue Messung der Koerzitivkraft (A Quick and Accurate Measurement of the Coercive Force)," *Arch. tech. Messen.*, Lfg. 254 (1957): 65; Lfg. 255 (1957): 87.
5. ———. "A Method for the Measurement of D. C. Fields and D. C. Field Differences and its Application to Nondestructive Testing," *Nondestructive Testing*, 13, No. 5 (1955): 31.
6. ———. "Ein Verfahren zur Messung von magnetischen Gleichfeldern und Gleichfelddifferenzen und seine Anwendung in der Metallforschung und Technik (A Method for the Measurement of Steady Magnetic Fields and Differences of Steady Fields and its Application to Metallurgical Research and Industry)," *Z. Metallk.*, 46 (1955): 358.
7. ———. "Theoretische und experimentelle Grundlagen der elektromagnetischen Qualitaetssortierung von Stahlteilen, IV. Das Restfeldverfahren (Theoretical and Experimental Foundation of the Electromagnetic Quality Sorting of Steel Parts, IV. The Residual Field Method)," *Z. Metallk.*, 45 (1954): 233.
8. **Borsorth**, R. M. *Ferromagnetism*. 2d ed. New York: D. Van Nostrand Co., Inc., 1953. Pp. 846, 847, 849.
9. **McClurg**, G. O. " Theory and Application of Coil Magnetization," *Nondestructive Testing*, 13, No. 1 (1955): 23.
10. **Ortheil**, J. "Kritische Betrachtungen der magnetischen Sortierung von Stahlteilen in der Massenfertigung (Critical Considerations of Magnetic Sorting of Steel Parts in Mass Production)," *Z. Metallk.*, 45 (1954): 243.
11. **Hainz**, R. "Beispiel einer Einfuehrung der elektromagnetischen Sortierverfahren in die Fertigung von Dieseleinspritzpumpen und -duesen (Example of the Use of Magnetic Sorting in the Production of Components for Diesel Injection Pumps and Nozzles)," *Z. Metallk.*, 45 (1954): 238.
12. **Foerster**, F. "Nouveaux procédés d'essai électronique nondestructif des matériaux (New Procedures for Electronic Nondestructive Testing of Materials)," *Métaux (Corrosion-Inds.)*, 26 (1951): 497.
13. **Foerster**, F., and G. **Zizelmann**. "Die schnelle zerstoerungsfreie Bestimmung der Blechanisotropie mit dem Restpunktpolverfahren (The Rapid Nondestructive Determination of Sheet Anisotropy with the Residual Point Pole Method)," *Z. Metallk.*, 45 (1954): 245.
14. ———. "The Quality Sorting of Sheets with Electrical and Magnetic Methods," *Blech*, 1 (1952): 1.
15. **Michalski**, A. "Nondestructive Testing with the Magnetic Leakage Field Method," *Z. Metallk.* (in press).
16. **Foerster**, F. "New Methods of the Quality Control from the Viewpoint of Automation," *Tech. Mitt.*, (April, 1957).
17. **Colten**, R. B. "Noncontacting Gages for Nonferrous Metals," *Electronics*, 29, No. 3 (1956): 171.
18. **Schneider**, **Ph.**, and P. **Dekker**. "Die Wandstaerkemessung von Leichtmetallgusstellen mit dem Sondenkawimeter nach Dr. Foerster (The Measurement of Wall Thickness with the Foerster Kawimeter)," *Metall*, 3 (1949): 321.
19. **Foerster**, F. "The Application of Hall Generators for Nondestructive Testing," *Z. Metallk.* (in press).
20. ———. *Zerstoerungsfreie Werkstoffpruefung mit elektrischen und magnetischen Verfahren* (Nondestructive Material Testing with Electrical and Magnetic Methods). Berlin, Goettingen, Heidelberg: Springer-Verlag (in press).
21. ———. "Theoretical and Experimental Foundation of the Leakage Field," *Z. Metallk.* (in press).

SECTION 35

ELECTRIC CURRENT TEST PRINCIPLES

CONTENTS

PAGE

Measurement of Wall Thickness and Crack Depth

Principle of test 1
Test development 1
Test requirements 1
Applications and limitations 1
Test equipment 2
Schematic illustration of equipment used in direct-current conduction testing of wall thickness and crack depth (*f.* 1) 2
Electrodes 2
Electrode spacing 2
Current source 2
Potential measurement 2
Selection of components 3
Preparatory measurement procedure 3
Electrode spacing 3
Surface preparation 3
Electrode contact 3
Wall thickness measurement procedure 3
Crack depth measurement procedure 3

Interpretation of Test Indications

Flat plate thickness 4
Electrode arrangement 4
Calibration curves for case of four-electrode array on an infinite plate (*f.* 2) 5
Thickness-potential relation 4
Thin-plate modification 4
Calibration 4
Edge corrections 5
Values of K' for equally spaced array ($B/A = 1$) near an edge of a semi-infinite plate[2] (*f.* 3) 6
Positioning electrodes near edges 5
Temperature control 7
Thickness of curved walls 7
Crack depth indications 7
Long perpendicular surface cracks 7
Calibration curves for equally spaced array on "ideal" crack in finite thickness plate (*f.* 4) 7
Short perpendicular surface cracks 9
Calibration curves for finite-length cracks having rectangular shapes in semi-infinite medium (*f.* 5) 8
Calibration curves for finite-length cracks having circular shapes in a semi-infinite medium (*f.* 6) 8
Other crack conditions 9

PAGE

Guide to Proper Application of Test Method

Wall thickness measurement 9
Selecting electrode spacing 9
Selecting current magnitude 9
Corrosion wall-thinning 9
Crack depth measurement 10
Selecting electrode spacing 10
Selecting current magnitude 10
Forging cracks 10
Wall thickness measurement with square electrode array 10
Sensitivity of square array of electrodes 11
Crack propagation study 11

Tests of Railroad Rails

Principle of test 11
The magnetic field 11
Magnetic field surrounding current-carrying conductor (*f.* 7) 12
Effect of a change in conductor cross-section 11
Induced electromotive force 12
Magnetic field around sound rail 12
Magnetic field about a current-carrying railroad rail (*f.* 8) 13
Magnetic field around defective rail 12
Searching coil reactions 13
Rail test equipment 13
Rail detector car (*f.* 9) 14
Main rail-current generator 13
Main brush carriages 13
Main brush carriage of rail detector car (*f.* 10) 14
Third brush carriages 13
Third-brush carriage which supplies pre-energizing current (*f.* 11) 15
System for providing magnetizing current to main brush carriage and to third brush carriage (pre-energizing current) of rail detector car (*f.* 12) 15
Detector unit carriage 16
Searching units 16
Power supplies 16
Amplifiers 16
Pen unit 17
Rail detector car multiple-channel tape-recording unit (*f.* 13) 16
Detector car tape 17

CONTENTS *(Continued)*

PAGE

- Paint guns 19
- Hand test equipment 19
  - Hand test equipment for determining exact location, size, and type of rail defects (*f.* 14) 17
- Personnel requirements 20
- Interpretation of indications 20

PAGE

- Typical defects detected 20
  - Typical rail defects (*f.* 15) 18
- Interpretation procedures 20
- Classification of defects 20
- Marking defects in rail 21
- References 21
- Bibliography 22

SECTION 35

ELECTRIC CURRENT TEST PRINCIPLES

Measurement of Wall Thickness and Crack Depth

PRINCIPLE OF TEST. If four electrodes are placed in contact with an electrically conducting object of resistivity ρ (ohm-centimeter), and a current I (amperes) is passed between two of the electrodes, a potential V (volts) will be produced between the other two electrodes such that,

$$\frac{V}{I} = K\rho \tag{1}$$

Here, K is a constant having the units of length (centimeter) and depending only upon the geometry of the electrode arrangement and the geometry of the object. For a fixed electrode arrangement and one material, an observed change in the ratio V/I will therefore represent a change in geometry of the part. This is the basic principle used for the nondestructive measurement of wall thickness and crack depth by the **direct-current conduction method.**

Test Development. Thornton and Thornton[7,8] used four-point electrodes for measuring the wall thickness (from one side only) of a large variety of plates, pressure vessels, boiler tubes, ship hulls, and castings. During the course of this work they discovered that a surface crack interposed between the electrodes caused anomalous readings, and thereafter they employed the method for **crack detection.**[6] Other workers [3,4,5] used this principle to detect cracks, and some efforts were made to devise a **calibration technique** for crack depth measurement. The method was finally developed[1] to a point where crack depths can be measured with fair accuracy in many cases.

Test Requirements. Both wall thickness and crack depth determinations depend upon the existence of **homogeneous and isotropic electrical resistivity** within the test object. Fortunately, to the accuracy required in most cases, this is true for most metallic materials. The need to make electrical contact at four points and to measure very small potentials (about 30 μv.) constitute the main **difficulties** of the measurements. The principal **advantage** is that only one material property, the resistivity, enters into the measurement. This simplifies interpretation of test indications.

Applications and Limitations. The direct-current test method can be used for wall thickness measurements from one side only, where other techniques may not be applicable. **Edge effects** and other **calibration difficulties** tend to limit the usefulness of the method, but these can usually be overcome. The technique is very useful for crack depth measurement and is often the only method available. Its greatest field of application is to single cracks previously delineated by visual observation, magnetic-particle, or penetrant techniques. The method cannot be easily applied in continuous inspection problems, due to the difficulty in balancing out changing **thermal electromotive forces** at the contacting electrodes.

TEST EQUIPMENT. The basic equipment for measuring wall thickness or crack depth is the same and is shown schematically in Fig. 1. Contact is made to the metal through the four electrodes, C_1, C_2, P_1, and P_2, mounted either in a single **insulating head** (Fig. 1), or in two separate heads, as used by Thornton.[8]

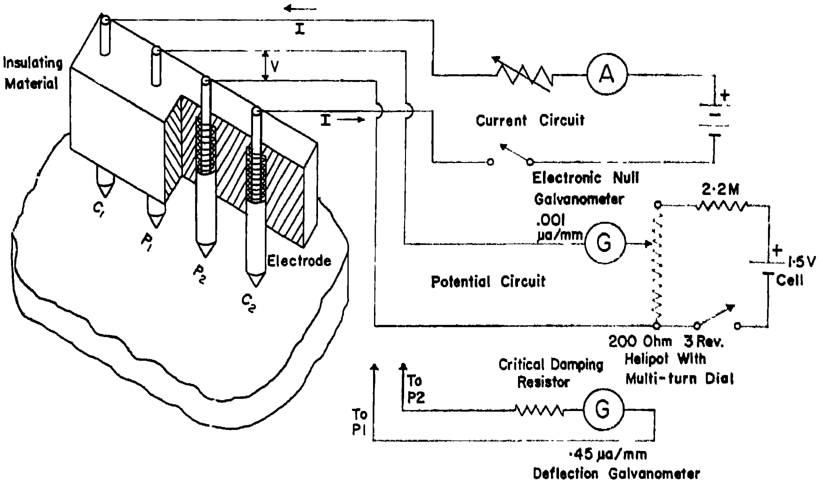
I
V
I
Insulating Material
C_1
P_1
P_2
C_2
Electrode
A
+
Current Circuit
Electronic Null Galvanometer
.001 μa/mm
G
2·2M
+
1·5V Cell
Potential Circuit
200 Ohm 3 Rev. Helipot With Multi-turn Dial
Critical Damping Resistor
To P2
To P1
G
·45 μa/mm Deflection Galvanometer

Dept. of Mines and Technical Surveys (Canada)

Fig. 1. Schematic illustration of equipment used in direct-current conduction testing of wall thickness and crack depth.

Electrodes. The electrodes are spring-loaded to facilitate contact on uneven or curved surfaces. A convenient **electrode material** is hardened drill steel which will retain a sharp point.

Electrode Spacing. The electrode spacings depend upon the application. Large spacings (½ in. or greater) are generally used in measuring thickness. Small spacings (¼ in. and less) are commonly used for crack depth measurement. Unequal spacings are often used in wall thickness measurement, but equal spacings give best results in crack depth measurement.

Current Source. The current I is passed through the metal between current electrodes C_1 and C_2. It is supplied from a **battery** or other **d.-c. source** capable of delivering up to 10 amp., depending upon the application. The current is controlled by a **rheostat** and read on an **ammeter.**

Potential Measurement. The potential V is measured either by a **potentiometric circuit** consisting of a 1½-volt battery, dropping resistor, voltage divider, and null galvanometer; or more simply (but less accurately) by measuring the deflection produced on a **moving-coil galvanometer.** With either system, potentials of about 30 to 100 μv. must be measured. Readings which are proportional to I and V are quite adequate, since changes in the V/I ratio are always used in determining thicknesses or crack depth.

Selection of Components. It is difficult to assign fixed values to the electrical components in the current circuit of Fig. 1 because they depend somewhat upon the spacing and the material. However, once the **electrode geometry** has been decided upon from considerations of sensitivity and range, the current required to produce 30 μv. can be calculated, and the rheostat and battery values can be found. In the potential circuit in Fig. 1, values are assigned to the components which are satisfactory for measuring 30 μv. or greater. Instruments can be designed to cover a wide range of commonly occurring values and can also be made to read directly in inches of wall thickness or crack depth by calibrating either the potential-measuring device (constant-current method) or the ammeter (constant-potential method).

PREPARATORY MEASUREMENT PROCEDURE. The preparatory steps given here are used in advance of each calibration and test measurement described later.

Electrode Spacing. Select a suitable electrode spacing for the particular problem at hand (see Guide to Proper Application of Test Method, in this section).

Surface Preparation. Prepare the surface of calibration and test specimens so that electrical contact will be made at all electrodes. **Freshly machined surfaces** need no preparation, and **mildly oxidized surfaces** can be prepared easily by rubbing with emery cloth. For **corroded or scaled surfaces** a convenient method is to scribe a heavy mark on the surface in the line where the electrodes are to be placed. Punch marks at each electrode have also been used.

Electrode Contact. Apply the electrodes to the surface and make a steady contact. If the electrode head is hand-held, it should be designed so that the head itself can rest against the metal as the electrodes are pushed upward. A magnet attached to the head is useful for magnetic materials. Clamping or weighting of the electrode head may also be used.

WALL THICKNESS MEASUREMENT PROCEDURE. To measure wall thickness, after the preparatory steps proceed as follows:

1. Energize the potential circuit, keeping the current circuit open. Balance out the thermal e.m.f. produced between potential electrodes P_1 and P_2 or possibly from other points in the potential circuit. This can be done either with a bucking-out circuit or more simply by adjusting the zero on the galvanometer.
2. Apply a current I and measure V, the potential produced by this current flow (or some reading proportional to V) on the calibration specimen of known thickness and the same resistivity as the specimen.
3. Repeat measurement steps 1 and 2 on the specimen of unknown thickness, using either the same current as in the calibration procedure (constant current method), or the same potential (constant potential method).
4. Obtain the thickness from the ratio $V_{\text{test}}/V_{\text{cal.}}$ (or $I_{\text{test}}/I_{\text{cal.}}$) and a calibration chart (see Interpretation of Test Indications, in this section).

A variation in this method[8] utilizes six electrodes. It permits measurement of wall thickness on **material of unknown resistivity.** A calibration plate of known thickness is not required.

CRACK DEPTH MEASUREMENT PROCEDURE. The crack is delineated either visually or by some other method such as magnetic-particle or liquid-penetrant inspection. Two surface areas, one over the crack and the other remote from the crack, are prepared as described previously. **Measurement steps** are:

1. Apply the electrodes and make a steady contact on the surface of sound metal remote from the crack on the specimen to be tested. For deep cracks the nearest electrode should be at least five times the electrode spacing A away from the crack. Balance out the thermal e.m.f. as described in step 1 under Wall Thickness Measurement Procedure, in this section.
2. Apply a current I and measure V, the potential in this remote calibration area.
3. Place the electrode array centrally over the crack and at right angles to it, balance out the thermal e.m.f., and measure I or V, using either the same current or the same potential as before.
4. Obtain the crack depth from the $V_{\text{crack}}/V_{\text{normal}}$ (V_c/V_n) ratio or the $I_{\text{crack}}/I_{\text{normal}}$ ratio, or from other observed geometry such as the thickness of the part or the calibration data (see Crack Depth Indications, in this section).

Interpretation of Test Indications

FLAT PLATE THICKNESS. The simplest case of interpretation, where this method is most usefully employed, is that of measurements on flat plates having lateral dimensions about ten times the thickness or greater. The analytical solution to the problem has been established, and calibration curves can be readily obtained for this case.

Electrode Arrangement. In the schematic diagram in Fig. 2, four electrodes are placed in line, contacting an infinite slab of homogeneous, isotropic material having a resistivity ρ (ohm-centimeter) and a thickness T (centimeter). The potential electrodes P_1 and P_2 are separated by a distance B (centimeter), while spacings C_1P_1 and P_2C_2 are both equal to A (centimeter).

Thickness-Potential Relation. If a current I (amperes) is passed through the material between C_1 and C_2, and the potential V (volts) is measured between P_1 and P_2, it can be shown that

$$K' = \frac{2\pi AV}{\rho I} = \frac{2B}{A+B} + \frac{A}{T}\left[M\left(\frac{A+B}{2T}\right) - M\left(\frac{A}{2T}\right)\right] \tag{2}$$

Here M is a function calculated and tabulated by Uhlir.[2] The above relation is plotted in Fig. 2 with K' as ordinate, T/A as abscissa, and B/A as a family parameter. For particular electrode spacings other than those plotted in Fig. 2, the calibration data can be calculated, using the tables for M given by Uhlir.[2]

Thin-Plate Modification. For thin plates Eq. (2) becomes

$$K' = \frac{2\pi AV}{\rho I} = \frac{A}{T}\left[2\log_e\left(\frac{A+B}{A}\right)\right] \tag{3}$$

This formula holds within 1 percent for $T/A \leq 0.5$. In this case it can be seen that V/I is inversely proportional to the thickness T. Utilizing an array such that T/A is less than 0.5 simplifies interpretation considerably, since in that case Eq. (3) holds. The potential V is inversely proportional to T if the constant current method is used, or I is directly proportional to T if the constant potential method is used.

Calibration. Knowing the electrode spacings, the pertinent calibration curve can be chosen. A reading taken upon a plate of known thickness establishes the scale factor by which readings can be converted to values of K'. Then subse-

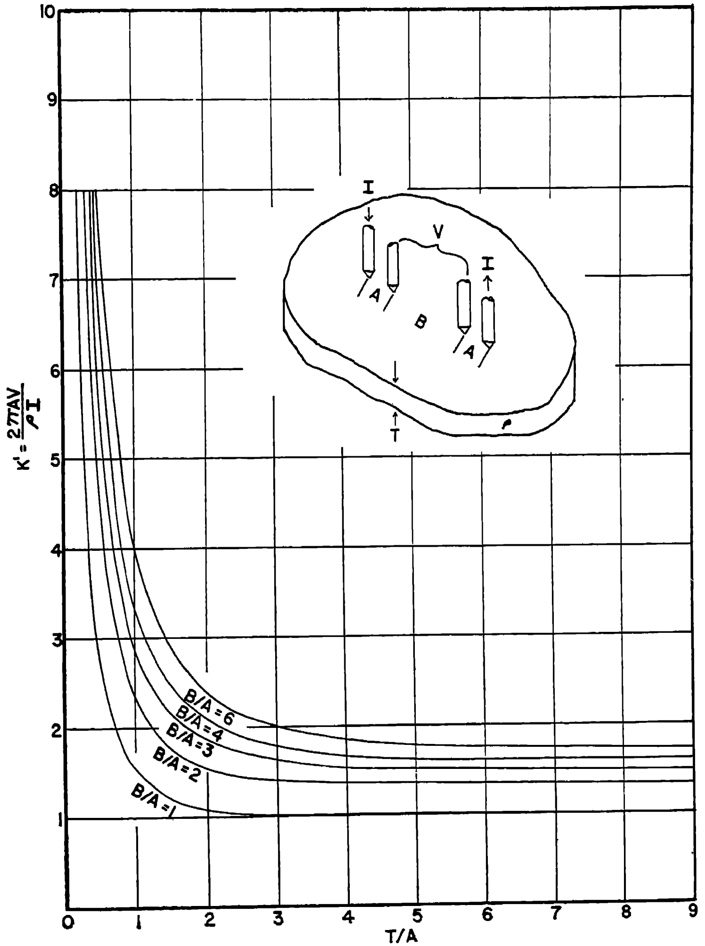

Dept. of Mines and Technical Surveys (Canada)

Fig. 2. Calibration curves for case of four-electrode array on an infinite plate.

quent readings on plates of the same material but of unknown thicknesses can be converted to K' values and hence to thickness.

Edge Corrections. It is not always possible to utilize spacings large enough with respect to the thickness to produce the condition $T/A \leqq 0.5$, due to edge effects. Fig. 3 (Uhlir[2]) shows the effect of edge distance on K' of an equally spaced electrode array ($B/A = 1$) for the two cases of (1) the array placed parallel to an edge, and (2) the array placed perpendicular to an edge. Here L is the distance from the nearest electrode to the edge of the plate. The equal spacing between adjacent electrodes in the straight-line array is identified as A. The ratio of edge distance to electrode spacing is L/A.

Positioning Electrodes Near Edges. Comparison of values of K' obtained for finite L/A with those obtained for infinite L/A (no edge effect) shows that

	Array Parallel to Edge (L = distance from line of array to edge)					Array Perpendicular to Edge (L = distance from nearest electrode to edge)					
(L/A)	0	0.5	1	5	10	0	0.5	1	5	10	∞
T/A											
10	2.002	1.52	1.19	1.004	1.002	1.450	1.133	1.060	1.004	1.002	1.001
1	3.009	2.45	1.98	1.534	1.512	2.033	1.730	1.638	1.522	1.510	1.504
0.2	13.863	11.51	9.28	7.078	6.969	9.282	8.047	7.599	7.022	6.960	6.932
0.1	27.726	23.03	18.56	14.156	13.938	18.563	16.094	15.198	14.043	13.920	13.863

Dept. of Mines and Technical Surveys (Canada)

Fig. 3. Values of K' for equally spaced array ($B/A = 1$) near an edge of a semi-infinite plate.[2]

smaller corrections are necessary for the array placed perpendicular to an edge. For this case L/A should be greater than 5 if no correction is to be made without incurring errors greater than 1 percent.

Temperature Control. Care should be taken to ensure that the test plate and the calibration plate are at the same temperature. The resistivity increases with temperature and will change the readings accordingly.

Thickness of Curved Walls. The determination of wall thicknesses can also be carried out for other than flat plates. In general the theoretical solution for the current flow and potential distribution in these cases is not known. Interpretation must be based on experimentally established **calibration curves.** It is not necessary to use the test material to obtain calibration curves, provided the calibration material and the test material obey Ohm's law.

CRACK DEPTH INDICATIONS. Crack depths are most readily evaluated for surface cracks perpendicular to the exposed surface.

Long Perpendicular Surface Cracks. The first case to be considered is an **ideal surface crack** of depth D, whose plane is perpendicular to the surface of a slab of thickness T. The crack length is assumed long in comparison with its depth. Fig. 4 illustrates this case and gives the calibration curves V_c/V_n plotted against D/A, with T/A as the family parameter. These curves were established experimentally,[1] using mercury as the metal and a bakelite strip as the "crack." They can be used to determine the crack depth for this case. Equally spaced electrodes are used throughout this analysis.

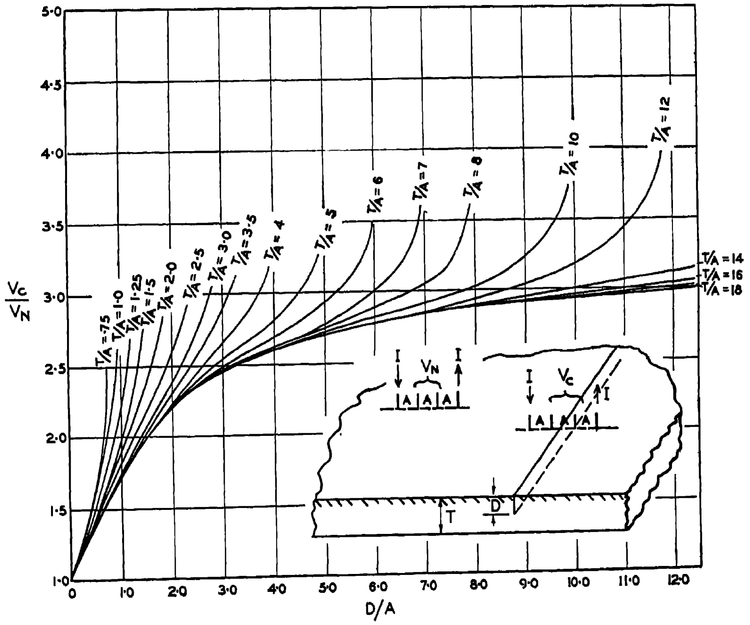

Dept. of Mines and Technical Surveys (Canada)

Fig. 4. Calibration curves for equally spaced array on "ideal" crack in finite thickness plate.

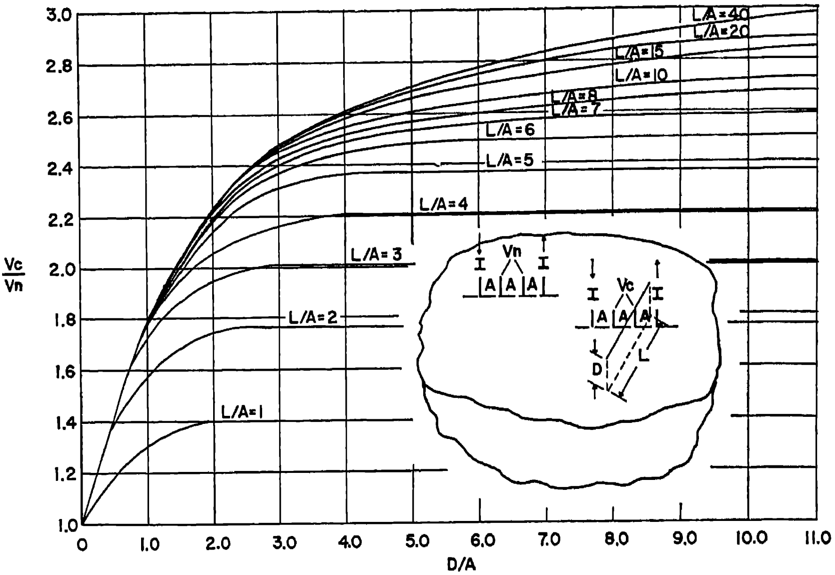

Dept. of Mines and Technical Surveys (Canada)

Fig. 5. Calibration curves for finite-length cracks having rectangular shapes in semi-infinite medium.

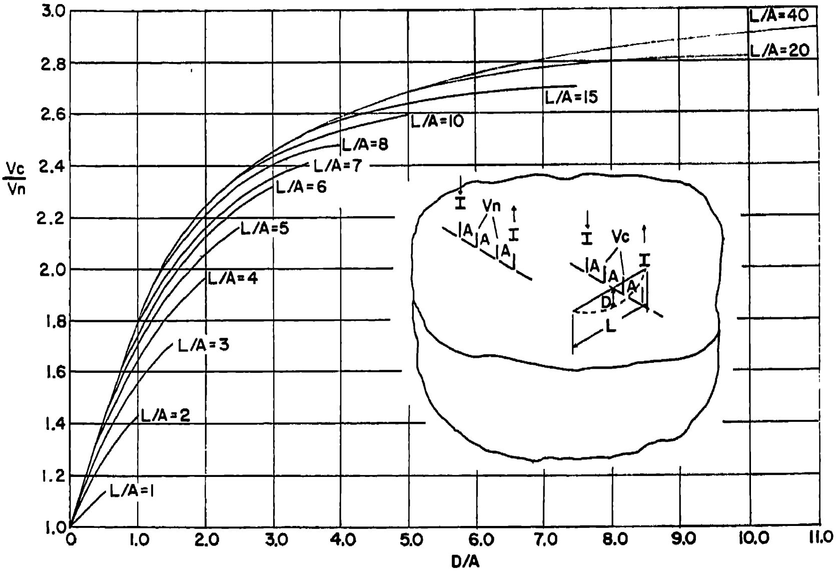

Dept. of Mines and Technical Surveys (Canada)

Fig. 6. Calibration curves for finite-length cracks having circular shapes in a semi-infinite medium.

Short Perpendicular Surface Cracks. In practice, many cracks are not long in comparison with their depth but have a finite length, and sometimes their shapes are irregular. Two cases of **finite-length cracks** have been investigated:

1. Rectangular cracks having a constant depth over their entire length.
2. Cracks of circular shape having their maximum depth D at the center of their lengths.

These two cases, along with the calibration data (also established by the bakelite-strip-in-mercury technique), are illustrated in Figs. 5 and 6. In these graphs L/A is the family parameter, and all the results apply to cases where material thickness T is large with respect to electrode spacing A. For a given value of V_c/V_n obtained from readings on a finite-length crack, these two graphs permit the placing of approximate limits on the actual depth. By assuming the existence of a rectangular crack, a smaller depth will be indicated than that for a circular crack.

In practice it is often possible to choose such a spacing A that one will be operating on the envelope curve of each of the sets of curves given in Figs. 4, 5, and 6. This is discussed more fully under Guide to Proper Application of Test Method, in this section.

Other Crack Conditions. The preceding discussion does not strictly apply to cracks which are not at right angles to the surface nor to cracks on curved surfaces. However, where the angle of inclination is not excessive or where the surface curvature is not too great, quantitative results can still be obtained. **Nonsurfacing cracks** can be detected with this technique, but analysis of crack depth is not generally possible.

Guide to Proper Application of Test Method

WALL THICKNESS MEASUREMENT. The first step in applying the direct-current test technique to a specific measuring problem is to choose the **electrode spacing** which covers the range of thicknesses to be encountered and which provides sufficient sensitivity to obtain the required accuracies.

Selecting Electrode Spacing. For best sensitivity, T/A should be less than 0.5, but unfortunately this sometimes makes A too large to be practical without making sizeable corrections due to edge effects. The curves in Fig. 2 and Eq. (3) permit calculation of the best spacing for the problem. Another consideration is that this method samples an area roughly circular in shape and encompassing all the electrodes.

Selecting Current Magnitude. Having determined the spacing, the **current** required to produce a value for V of at least 30 μv. should be calculated from Eq. (2) or (3). Provision should be made to supply this current with smooth control over the required range. Larger currents are required for good conductors such as copper, aluminum, or brass than for poorer conductors such as alloy steel.

Corrosion Wall-Thinning. As an example, consider the problem of measuring corrosion thinning on mild **steel hull plates** which are nominally ½ in. thick and whose thicknesses are to be measured from one side only to an accuracy of ±1/64 in. or ±3 percent. As a trial spacing, assume $A = 1$ in. $(T/A = 0.5)$ and $B/A = 1$. A comparison of K' calculated from Eq. (3) and the value from Eq. (2) shows that they do not differ by 1 percent (2.77 and

2.78). Therefore, with this spacing, I would be proportional to T with the constant voltage method. A 3 percent change in thickness would give a 3 percent change in meter reading, which would be quite readable. However, assuming a value of ρ equal to 15×10^{-6} ohm-cm., it can be shown by Eq. (3) that a current of 11.5 amp. is required to produce a potential of 30 μv. This current could be provided, but if a current less than 10 amp. were desirable, a value of 2 for B/A would increase K' to 4.40 and reduce the current requirement to about 7 amp. The latter choice of electrode spacing would sample a larger area but would be subject to larger edge effects. For this spacing, a rheostat providing smooth control over the range from 8 to about 4 amp. (assuming a reduction in thickness of 50 percent) should be chosen.

CRACK DEPTH MEASUREMENT. For best results in measuring crack depths, the electrode spacing A should be chosen so that the minimum crack depth of interest produces a value of V_c/V_n of 1.1 or greater. This can be done by reference to Figs. 4, 5, and 6.

Selecting Electrode Spacing. Except for cracks with small lengths L, the spacing A should be about ten times the crack depth. Generally speaking, if readings of V_c/V_n larger than about 2 are obtained on a crack, the accuracy of the result will be lowered, and a larger spacing should be used.

Selecting Current Magnitude. Once the spacing is established, the current I which will produce 30 μv. for V_n can be obtained from Fig. 2 (for the case $B/A = 1$) and the value of ρ for the material under test. If the material is thick, $T/A > 3$, the current can be found with sufficient accuracy from the formula

$$I = 2\pi A \frac{V}{\rho} \tag{4}$$

Forging Cracks. As an example, consider cracks in forgings whose depths must be established to determine the possibility of removing them by machining. Suppose that the maximum allowable machining is ⅛ in. A convenient electrode spacing, A, for this case is 5⁄32 in. (0.156 in.), which permits using ⅛-in. drill steel for electrodes. For this spacing a crack depth D of ⅛ in. produces a value of V_c/V_n of about 1.6, which would be a convenient operating point. If the material were an alloy steel with a resistivity ρ equal to 40×10^{-6} ohm-cm., Eq. (4) shows that a current I of 1.9 amp. would produce the required potential of 30 μv. for V_n. If the constant current method is employed, facility to supply 2 amp. with fine control over a small range (to allow for variations in contact resistance) and facilities for measuring potentials up to about 100 μv. should be provided. The potential circuit shown in Fig. 1 would be satisfactory for this purpose.

This technique can also be used as a **crack detector** where only small areas of a part are suspected of being defective. When used in this manner, it is useful to know that an array placed so that only one electrode is over the crack will result in a reading for V less than V_n, as has been shown analytically for the case of very deep cracks.[1]

WALL THICKNESS MEASUREMENT WITH SQUARE ELECTRODE ARRAY. A special application of this method to wall thickness measurements is to place four electrodes in the form of a square instead of in line; the two current electrodes are on one side of the square, and the two potential electrodes are on the other.[9] The measuring apparatus is essentially the same as for the in-line array.

Sensitivity of Square Array of Electrodes. The sensitivity of this array to thickness changes can be calculated from the formula

$$\frac{2\pi AV}{I_p} = 2 - \sqrt{2} + \frac{A}{T}\left[M\frac{A}{\sqrt{2}T} - M\left(\frac{A}{2T}\right)\right] \tag{5}$$

Here A is the electrode spacing along the sides of the square. It can be shown that for the same value of A, this expression is always less than the value of K' given by Eq. (2); i.e., the square electrode array is always less sensitive than the in-line array. However, it does have a smaller edge-correction factor for the same spacing than an equally spaced in-line array.

CRACK PROPAGATION STUDY. The detection and measurement of edge cracks is an application requiring special treatment. A particular example is the study of the rate of propagation of cracks in the trailing edges of **turbine blades during thermal cycling.** The location of the cracks can be readily determined by using knife-edge electrodes with a small spacing (say, 0.075 in.) and by plotting voltage/current readings for consecutive probe positions. Then, placing the probe symmetrically over each crack in turn, the depth can be determined from the V_c/V_n ratio and a calibration curve.

A theoretical curve has been derived for the two-dimensional case, and good agreement has been obtained with an experimental calibration using a thin brass plate with **machined edge cracks.** Subsequent cleaning of the blades, followed by measurement of the cracks with a traveling microscope, gave results within 20 percent of those determined from the V_c/V_n ratios and the curve. The cracks were markedly asymmetrical, however, and although the mean of the microscope readings was taken in each case, this was obviously only an approximation. It is considered that better agreement would probably be obtained by using a calibration made under conditions more closely simulating those of the turbine blade.

Tests of Railroad Rails

PRINCIPLE OF TEST. The electric current method of rail testing can be described briefly as follows:

1. A heavy current is passed through the rail to be tested, thus establishing a strong magnetic field around the rail.
2. Searching coils are moved through the established magnetic field at a fixed rate and distance above the rail.
3. Electromotive-force pulses from the coils are recorded. These are the result of changes in the magnetic field around the rail at points where internal defects cause deflection of the electric current path.

The Magnetic Field. Whenever a current is passed through an electrical conductor, a magnetic field is set up surrounding that conductor. This magnetic field can be considered as a region composed of concentric lines of force, each of which is perpendicular to the axis of the conductor. The intensity or strength of the magnetic field, measured by the degree of concentration of lines of force, is greatest at the surface of the conductor and decreases as distance from the conductor increases. Fig. 7(a) is a conventional representation of the magnetic field around a sound circular conductor.

Effect of a Change in Conductor Cross-Section. If the cross-section of the circular conductor shown in Fig. 7(a) is altered to a semi-circle, the magnetic field assumes the shape shown in Fig. 7(b). When the conductor returns to its original circular shape, the magnetic field is restored to its original position and shape.

Induced Electromotive Force. If a coil is moved through a magnetic field so as to cut a changing number of lines of force, an electromotive force (e.m.f.) is induced in the coil and is measurable as a voltage output. If the same coil is moved through an unchanging magnetic field at a constant speed, no e.m.f. is developed. If a coil moves along the length of a circular conductor at a constant speed and constant distance from its center, no e.m.f. is developed until it reaches the point where the cross-section diminishes to a semi-circle. At that point it would cut a decreasing number of lines of force and an e.m.f. would be induced. The e.m.f. is induced slightly before the coil passes the actual change in cross-section, since the current path is deflected downward. When the conductor again becomes circular in cross-section, an e.m.f. of opposite polarity is generated, since the coil then cuts an increasing number of lines of force.

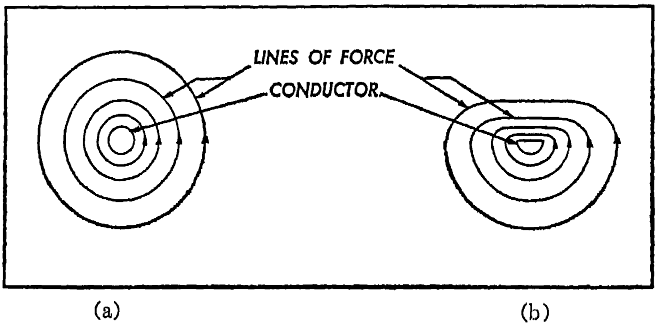

Fig. 7. Magnetic field surrounding current-carrying conductor. (a) Magnetic field around circular conductor. (b) Magnetic field around semi-circular conductor, simulating a defect in circular cross-section conductor.

Magnetic Field Around Sound Rail. In the Sperry system of rail testing,[9] current is introduced into the rail head and sets up a magnetic field approximately as shown in Fig. 8. The field thus established remains constant in both strength and shape as long as both (1) the effective cross-section of the rail and (2) the test current remain constant. The lines of force pass not only through the air around the rail but also through the rail as they seek the path of least reluctance in completing their circuits.

Magnetic Field Around Defective Rail. Any defect in a rail reduces the cross-sectional area by an amount equal to the transverse area of that defect. This is due to the inability of low voltage current to jump the gap presented by the defect. The current is forced into the sound portions of the rail in order to flow around the defect and then fans out once more after passing the defect.

The change in direction and density of the current as it flows around a defect is accompanied by a corresponding change in the direction and position of the magnetic field around the defective portion of the rail. Since the magnetic field is always perpendicular to the axis of the current path, transverse deflection of the current as it flows past a defect causes the magnetic lines of force to be displaced proportionately.

Searching Coil Reactions. The reaction of searching coils to a change in the direction of the magnetic field is dependent to some extent upon their positions relative to the magnetic field. This factor permits some coils to move closer to a defect before being affected by the changing magnetic field than others whose axes are arranged in a different direction. Similarly, some coils, by virtue of their position with respect to the rail, are affected only by magnetic-field changes caused by **defects in the field side** of the rail head; others, only by **gage side changes**; and still others, only by **longitudinal defects.** The efficiency and thoroughness of rail testing is based upon the application of this selective principle.

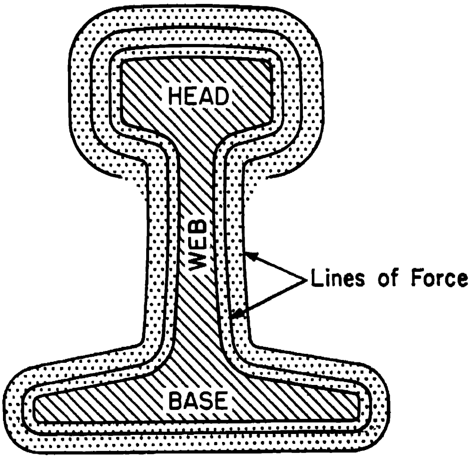

Fig. 8. Magnetic field about a current-carrying railroad rail.

RAIL TEST EQUIPMENT. The **rail detector car** developed and used by the Sperry Rail Test Service is shown in Fig. 9. Its equipment components and their functions are described in the subsequent text. Such cars test about 50 miles of track per day.

Main Rail-Current Generator. The main rail-current generator and its accessories provide a controllable current, possessing the proper characteristics, which can be introduced into rails to set up the magnetic field necessary for testing.

Main Brush Carriages. The main brush carriages provide the means of introducing the output of the rail-current generator into the rails to be tested (Fig. 10). The forward cluster of each main brush carriage also provides a path for the introduction of a pre-energizing current into the rail.

Third Brush Carriages. The third brush carriages (Fig. 11) are used to provide a return path for the pre-energizing current which was introduced into the rail through the leading brushes of the main carriages. In operation, the third brush carriages are held against the rail by a pneumatic pressure system. These carriages operate in unison with the corresponding main brush carriages (see Fig. 12).

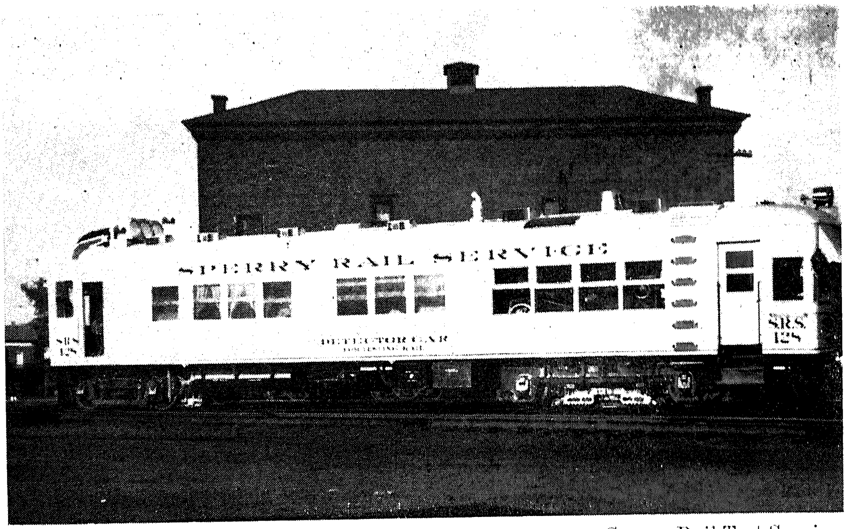

Sperry Rail Test Service

Fig. 9. Rail detector car.

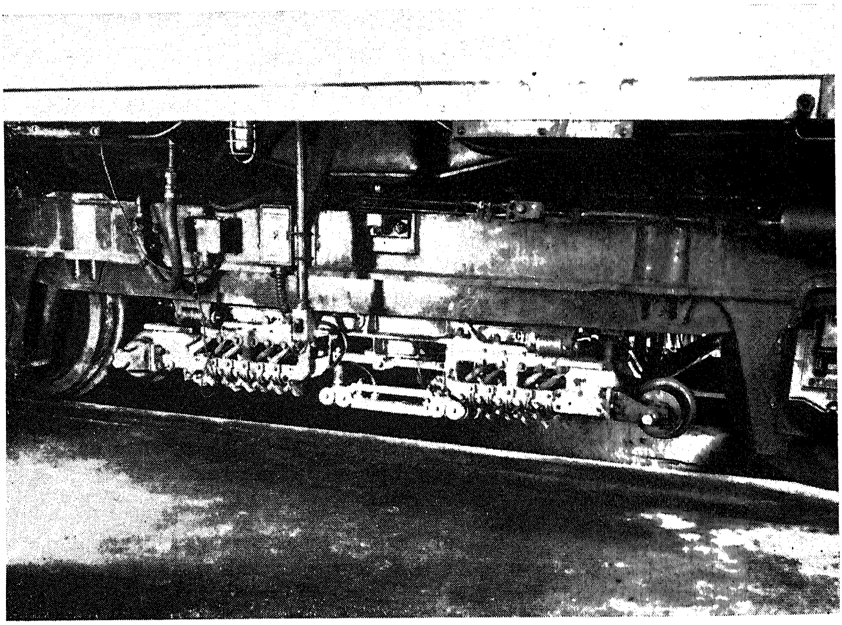

Sperry Rail Test Service

Fig. 10. Main brush carriage of rail detector car.

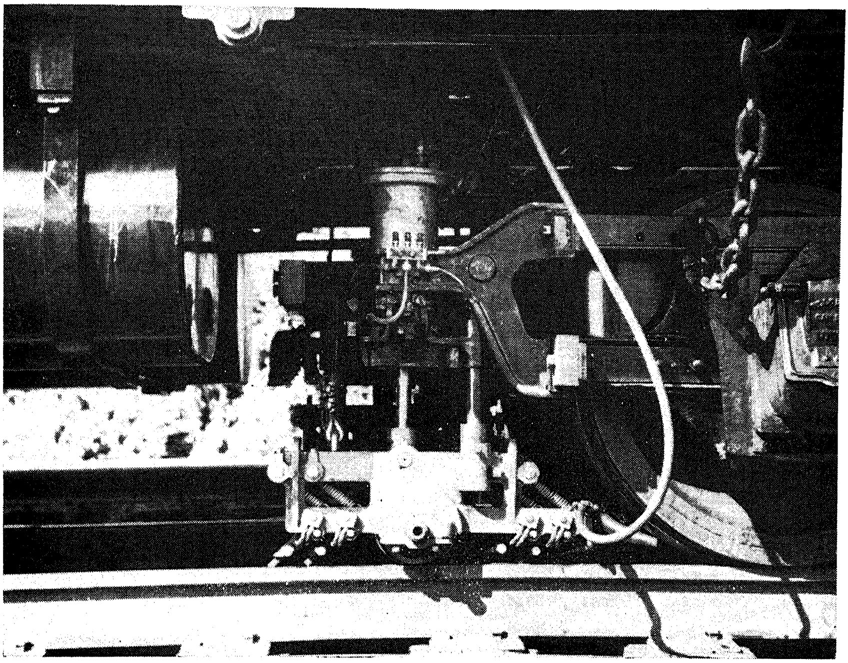

Sperry Rail Test Service

Fig. 11. Third-brush carriage which supplies pre-energizing current.

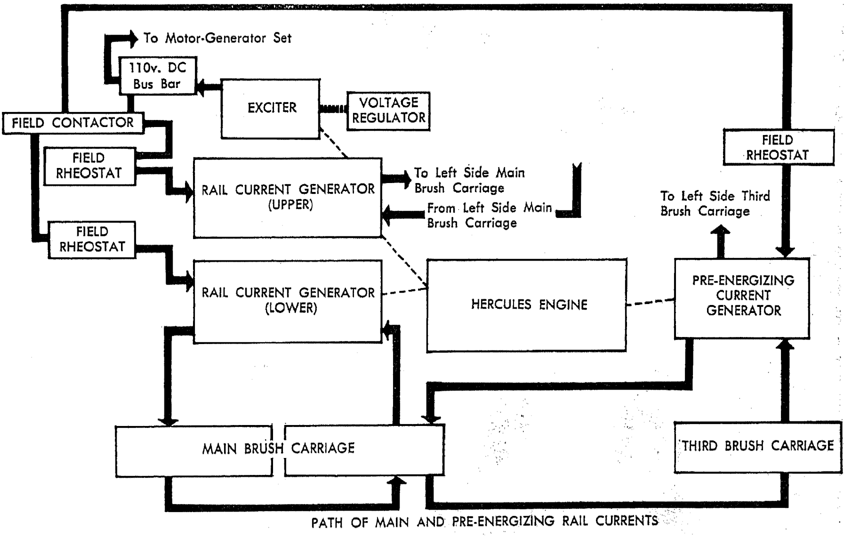
To Motor-Generator Set
110v. DC Bus Bar
EXCITER
VOLTAGE REGULATOR
FIELD CONTACTOR
FIELD RHEOSTAT
RAIL CURRENT GENERATOR (UPPER)
To Left Side Main Brush Carriage
From Left Side Main Brush Carriage
FIELD RHEOSTAT
To Left Side Third Brush Carriage
FIELD RHEOSTAT
RAIL CURRENT GENERATOR (LOWER)
HERCULES ENGINE
PRE-ENERGIZING CURRENT GENERATOR
MAIN BRUSH CARRIAGE
THIRD BRUSH CARRIAGE
PATH OF MAIN AND PRE-ENERGIZING RAIL CURRENTS

Sperry Rail Test Service

Fig. 12. System for providing magnetizing current to main brush carriage and to third brush carriage (pre-energizing current) of rail detector car.

Detector Unit Carriage. The function of the detector carriage is to carry the searching units at a fixed distance and in a fixed position above the running surface of the rail. Means are provided for adjusting this distance when necessary. One detector unit carriage is suspended from each main brush carriage.

Searching Units. The function of each searching unit is to produce an electrical impulse or signal every time it passes over a defect in the rail being tested. This **defect signal** initiates operation of the indicating units of the detection equipment. Each searching unit contains several sets of coils arranged in pairs and positioned effectively to cover the entire magnetic field about the rail. The axis and winding of the various coils are designed so that a defect will be detected by at least one set of coils. This arrangement permits **preliminary interpretation,** or classification, of the indicated defect by consideration of the coils involved in initiating the pen response.

Power Supplies. An engine-driven generator provides a source of filtered alternating current at a constant 115 volts for the detection equipment. Power packs provide the voltages necessary for the proper operation of the amplifiers, relays, and other detection equipment.

Amplifiers. Amplifiers increase the signal strength from searching unit coils to operate relays controlling the indicating units of the detector equipment. The amplifiers operate conventionally except that **selective filtering action** is used to improve response. The amplifier outputs are fed to a series of sensitive relays which in turn actuate pens on the operator's recording tape. These relays and

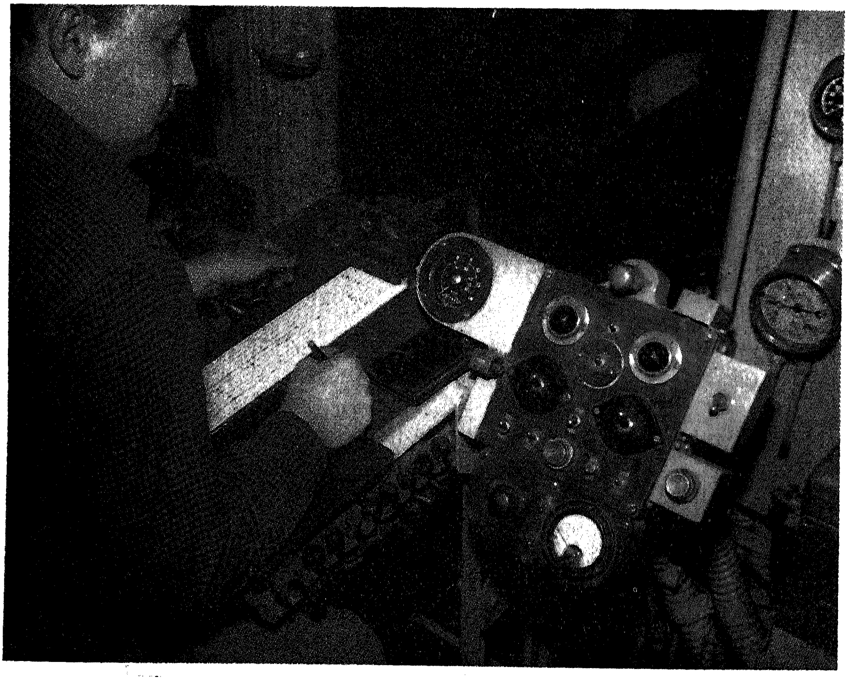

Sperry Rail Test Service

Fig. 13. Rail detector car multiple-channel tape-recording unit.

associated circuitry are interconnected so that improper functioning of any portion of the detection circuit will be indicated on the record tape. **Sensitivity of the amplifier** is normally set to respond to signals caused by defects having an effective transverse area of 10 percent or more of the cross-sectional area of the rail head.

Pen Unit. The pen unit provides a visible indication on the detector car tape of signals from the various coils of the searching units. One pen provides a visible warning when the rail current drops below the operating standard. A land mark pen is used to inscribe the **land mark code** and a **time interval marker.** The indicating pens for both sides of the track are grouped together in a single pen unit mounted on a recording table (Fig. 13).

Detector Car Tape. The detector car tape provides a visual indication of defects and rail conditions found by the detection equipment at the time of test. This facilitates interpretation by the operator of the pen indications and rail surface. The table which supports the tape, tape drive, and pen unit is located in front of the middle rear window in the rear compartment of the rail test car (Fig. 13). The unit consists of a working surface, tape guide, pen unit mounting and tape drive mechanism. The tape is driven by a power take-off from the rear axle. A 1⁄16-in. movement of the tape corresponds to 1-ft. movement along the track.

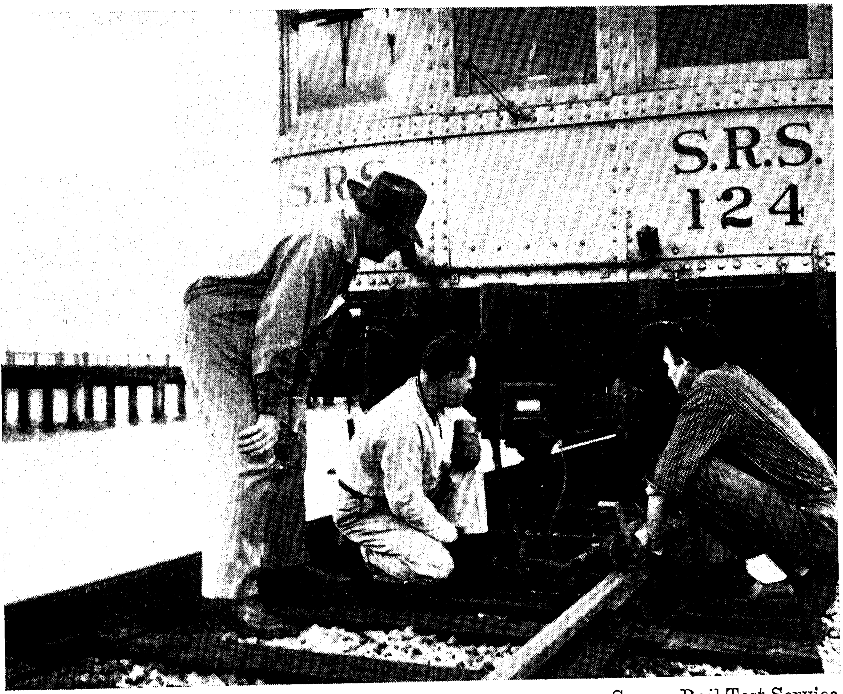

Sperry Rail Test Service

Fig. 14. Hand test equipment for determining exact location, size, and type of rail defects.

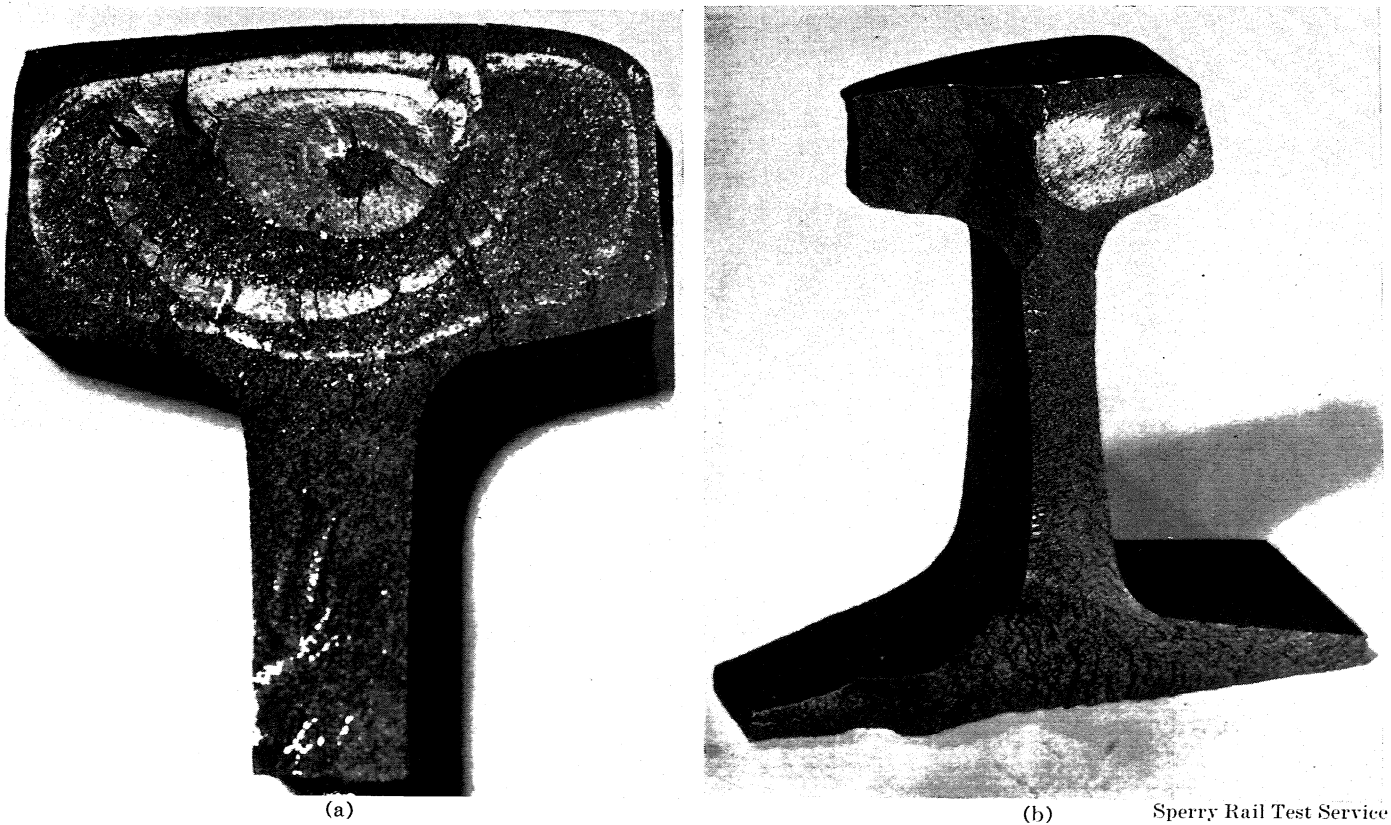

(a) (b) Sperry Rail Test Service

Fig. 15. Typical rail defects. (a) Transverse fissure (note fatigue crack growth rings). (b) Detail fracture (hot tear).

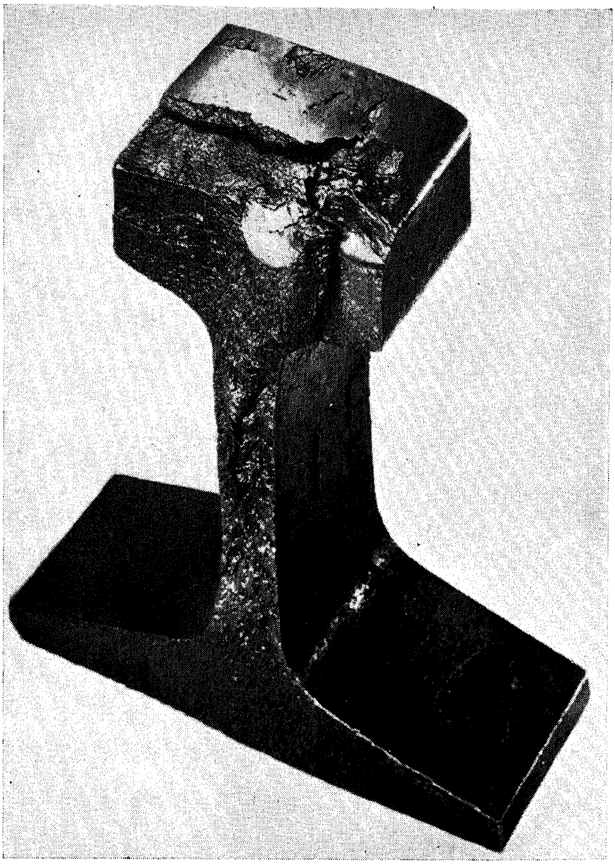

(c) Sperry Rail Test Service

Fig. 15. (Continued.) (c) Engine burn fracture.

Paint Guns. Paint guns provide a visible indication on the inside of the rail web at any point where the magnetic field is distorted sufficiently to cause an indication on the tape. The **paint marks** are used to locate suspected sections of rails when interpreting the cause of the indication. Two paint guns are mounted on each brush carriage adjacent to the front end of the searching unit and point at the center of the web on the inside of the rail. Each gun is connected by piping to a pressurized paint tank.

Hand Test Equipment. Hand test equipment provides a means of determining the exact location, size, and type of defects. Hand testing is based on the **potential rise principle** rather than on the magnetic induction principles discussed earlier.[10] The hand contactor is placed on the rail close to the paint mark indicating the location of a possible defect (Fig. 14). If a transverse separation is present, the deflection of the current will cause an increased difference in potential to exist between the two sides of the separation. When the **hand contactor** is moved along the rail and its two **spring contacts** enter the area directly above the separation, the rise in potential at that point (directly above the defect) will cause a corresponding rise in the millivoltmeter reading. The rise confirms the presence of the defect. The amount of rise indicates the size of the defect. The rate of rise indicates the general type of defect. By the use of this equipment, defects are finally and accurately pinpointed to within ⅜ in.

PERSONNEL REQUIREMENTS. The standard detector car crew consists of a chief operator assisted by two operators. The chief operator is in full charge of the car and is responsible, through a supervisor in a specified territory, to the operating manager.

During testing, there are three **operating stations** manned by (1) a tape operator, (2) an examining operator, and (3) a driving operator. **Testing speed** varies from 6 to 12 miles per hour, depending on rail conditions. Potentially dangerous areas are indicated on a continuously moving detector car tape and may require verification by the tape operator.

INTERPRETATION OF INDICATIONS. In both new and old rail the extent and **development of progressive fractures** from microscopic irregularities is of great concern. The location and size of these defects determine the capacity of the rail to withstand the stresses imposed upon it in service. Each year, approximately 150,000 miles of track are tested by Sperry induction cars, which locate approximately 50,000 defects. Since 1928 this method has been used for inspection of more than 3 million miles of rail, equivalent to 600 million tons of steel. More than 1½ million defective rails, equivalent to 2 million tons of steel, have been marked for removal.

Typical Defects Detected. Typical rail defects detected are shown in Fig. 15. More than half the defects detected are classified as **transverse defects,** and one-third as **vertical split heads**; the balance are **horizontal split heads** and miscellaneous.

Interpretation Procedures. One problem that confronts the interpreter is to distinguish indications caused by **harmless surface defects** or track structures from those caused by dangerous internal separations or defects in the rail. Three procedural steps assist him in making his decision:

1. **Visual examination** from the cars of the condition of the rail in the immediate vicinity of the paint mark which corresponds to the pen indication to be interpreted.
2. **Ground examination** of the rail at the point where the indication occurred. This method becomes necessary when the indication cannot be verified from the car. The pen indication provides a clue as to what to look for and where to look for it. By examining the rail at close range, external signs of an internal defect may often be found and the cause of the indication thus verified.
3. **Hand testing** must be used when the visual inspections fail to reveal the cause of the indication. Hand testing is also used when the operator doubts that a visible surface defect is the true cause of the indication. In many cases an internal defect has been found directly below the surface defect.

Classification of Defects. After an indication has been verified as being the result of an internal defect, it is necessary to decide what kind and what size defect is present. This process is called "classification." In classification, as in interpretation, the operator must make use of a number of sources of information to determine the type of defect that has been found.

The **pen indication** gives the first clue to the nature of the defect. Although all defects of a given type will not cause identical pen indications, the operator will soon learn to associate certain combinations of pen responses with certain defects.

The second and most important factor used in classifying a defect is the **visual appearance of the rail,** seen either from the car or from the ground, at the point where the indication occurred. With the exception of transverse defects that have not progressed to the surface, most defects develop certain recognizable characteristics. Experience is the best teacher in developing the ability to recognize such visible characteristics.

Hand testing is the third factor in determining the proper classification of a verified defect. With the exception of longitudinal defects, each general type of defect will produce different meter reactions when a hand test is made. By carefully observing the meter reaction in relation to the position of the hand contactor on the rail, the operator can classify the defect as to size. A hand test, made to classify a visible defect, provides more exact knowledge of the size and location of that defect.

Marking Defects in Rail. Each rail containing a verified internal defect is marked by yellow crayon with the following information for the guidance of the contracting railroad's maintenance personnel:

1. Type or types of defects detected.
2. Estimated size of transverse separation, if present (except in the case of engine burn fractures).
3. Serial number of defect. If two or more defects are found in one length of rail, the serial number is marked below the most serious defect.
4. Location or longitudinal extent of the defect.

References

1. Buchanan, J. G., and R. C. A. Thurston. "The Measurement of Crack Depths by the Direct-Current Conduction Method," *Nondestructive Testing*, 14, No. 5 (1956): 36, 43.
2. Uhlir, A. "The Potentials of Infinite Systems of Sources and Numerical Solutions of Problems in Semiconductor Engineering," *Bell System Tech. J.*, 34 (1955): 105.
3. Jackson, L. R., H. M. Banta, R. C. McMaster, and T. P. Nordin. "Electric Current Conduction Tests, Fifth Progress Report on Nondestructive Testing of Drill Pipe," *Drilling Contractor* (August, 1948): 68.
4. Armour, A. M. "Eddy Current and Electrical Methods of Crack Detection," *J. Sci. Instr.*, 25 (1948): 209.
5. Hirst, G. W. C. "Apparatus for an Electrical Determination of the Depth of Transverse Cracks or Fissures in Magnetizable Circular Prisms," *J. Inst. Engrs. Australia*, 19 (1947): 145.
6. Thornton, B. M. "The Detection of Cracks in Castings by an Electrical Method," *Foundry Trade J.*, 68 (1942): 277.
7. Thornton, B. M., and W. M. Thornton. "On Testing the Wall Thickness of Castings," *Foundry Trade J.*, 65 (1941): 253.
8. ———. "The Measurement of the Thickness of Metal Walls From One Surface Only, by an Electrical Method," *Proc. Inst. Mech. Engrs.*, 140 (1938): 349.
9. Sperry, E. A. (To Sperry Development Co.) "Fissure Detector for Metals." U.S. Patent No. 1, 820, 505, (Aug. 25, 1931).
10. ———. (To Sperry Products, Inc.) "Fissure Detector for Steel Rails." U.S. Patent No. 1, 804, 380, (May 5, 1931).

Bibliography

BARNES, W. C., and H. W. KEEVIL. "Method and Apparatus for Detecting Flaws in Rails." U.S. Patent No. 2, 410, 803, (Nov. 12, 1946).

CAMPBELL, J. E., H. O. MCINTIRE, and G. K. Manning. "Summary Report on the Examination of Rails Which Contain Detail Fractures to Joint Contact Committee on Rails of American Railroads and American Iron and Steel Institute and Committee on Rails of American Railway Engineering Association," *Am. Ry. Eng. Assoc. Bull.,* 51 (1950): 608.

CRAMER, R. E. "Investigation of Failures in Railroad Rails," *Am. Ry. Eng. Assoc. Bull.,* 51 (1950): 543.

FRICKEY, R. E., and C. W. MCKEE. (To Welding Service, Inc.) "Method and Apparatus for Detecting Flaws in Rails." U. S. Patent No. 2, 388, 683, (Nov. 13, 1945).

KEEVIL, H. W. "Method and Apparatus for Detecting Flaws in Metallic Bodies." U.S. Patent No. 2, 089, 967, (Aug. 17, 1937).

MANNING, G. K. "Summary Report on the Examination of Shelled Rails to Joint Contact Committee on Rails of Association of American Railroads and American Iron and Steel Institute," *Am. Ry. Eng. Assoc. Bull.,* 50 (1949): 542.

MCBRIAN, R., C. J. CODE, C. B. BRONSON, G. F. HAND, J. G. RONEY, and A. A. SCHILLANDER. "Rail Failure Statistics," *Am. Ry. Eng. Assoc. Bull.,* 51 (1950): 550.

Rail Defect Manual 4. Danbury, Conn.: Sperry Rail Test Service, 1949.

SPERRY, E. A. "Non-Destructive Detection of Flaws," *Iron Age,* 122 (1928): 1214.

SECTION 36

EDDY CURRENT TEST PRINCIPLES

CONTENTS

PAGE

Basic Principles

Principle of test 1
    Typical arrangements of probe coil and test object (*f.* 1) 2
  Test coil characteristics 1
    Representation of test coil characteristics on impedance plane (*f.* 2) 3
Development of basic principles 8
    Summary of eddy current test problems solved by Institut Dr. Foerster (*f.* 3) .. 4

Effective Permeability

Assumptions used in analysis 9
Determination of effective permeability 10
    Schematic drawing of test object in "feed-through" test coil with primary (excitation) and secondary (pick-up) windings (*f.* 4) 10
  Empty coil voltage 10
  Influence of test object 11
    Schematic representation of magnetic-field conditions with test object in test coil (*f.* 5) 11
  Secondary coil voltage with test object 11
    Simplified representation of magnetic conditions within test object in test coil (*f.* 6) 12
  General case of a cylindrical test object 12
  Limit frequency, f_g 13
Effective permeability as a function of frequency ratio 13
    Variation in effective permeability (*f.* 7) .. 14
    Tabular listing of values of effective permeability (*f.* 8) 15
  Sample calculations for effective permeability and secondary coil voltage 13
Test object smaller than secondary coil diameter 16
    Test coil containing a test object of smaller diameter, *d* (*f.* 9) 17
  Secondary coil voltages 16
  Complex permeability plane 17
    Parameter as a function of complex permeability (*f.* 10) 18
  Correction for ferromagnetic test object ... 19
Impedance characteristics of a single test coil 19
    Arrangement of cylindrical test object in a single test coil (*f.* 11) 19
  Normalized coil characteristics 20
  Example of nonferromagnetic test object .. 20
  Three complex planes for eddy-current test data 20
References 21

SECTION 36

EDDY CURRENT TEST PRINCIPLES

Basic Principles

PRINCIPLE OF TEST. In many eddy current (or electromagnetic induction tests), the test object is placed in the varying magnetic field of a coil or an array of conductors carrying an alternating current (a.c.). The a.-c. magnetic field induces **eddy currents** in the test object. These eddy currents, in turn, produce an additional a.-c. magnetic field in the vicinity of the test object. Fig. 1(a) illustrates conditions for a coil placed on the surface of a test object. The vector H_p represents the **primary a.-c. field** of the test coil, whereas H_s indicates the **secondary a.-c. field** resulting from eddy currents in the test object. Fig. 1(b) represents conditions for the arrangement in which the test coil surrounds the test object. In each case two a.-c. magnetic fields are superimposed. The magnetic field near the test coil is modified if a test object is present. Other arrangements of eddy current test coils are summarized in Fig. 3 of this section. Coil shapes include: solenoid coils, inside coils, hand-probe coils, fork-shaped coils, and special coil shapes for specific test objects. (The illustrations in this section and those following on eddy current tests are from the Institut Dr. Foerster, except where otherwise indicated.)

Test Coil Characteristics. In general the test coil is characterized by two **electrical impedance** quantities:

1. The inductive reactance $X_L = 2\pi fL$, where f is the frequency of the a.-c. field in cycles per second (c.p.s.) and L is the self-inductance of the coil.
2. The ohmic resistance R.

It is common practice to plot the reactance X_L as ordinate and resistance R as abscissa in the **impedance plane.** In this way the test coil impedance Z is represented by a point P, formed by two perpendicular components, $X_L = 2\pi fL = \omega L$, and R, on the impedance plane. In the absence of a test object, the **empty test coil** has a characteristic impedance with coordinates $X_{L_0} = \omega L_0$ and R_0, shown on the impedance plane by the **empty point** P_0 of Fig. 2. If a test object is placed in the field of the test coil, the original field of the empty test coil is modified by the superimposed field of the eddy currents. This field modification has exactly the same effect as would be obtained if the characteristics of the test coil itself had been changed. The influence of the test object can be described by a variation in test coil characteristics. The **apparent impedance** of the "empty" coil represented by P_0 is displaced to P_1 (corresponding to new values of reactance ωL_1, and resistance R_1) under the influence of the test object (see Fig 2).

The magnitude and direction of the displacement of the apparent impedance from P_0 to P_1 under the influence of the test object are functions of the properties

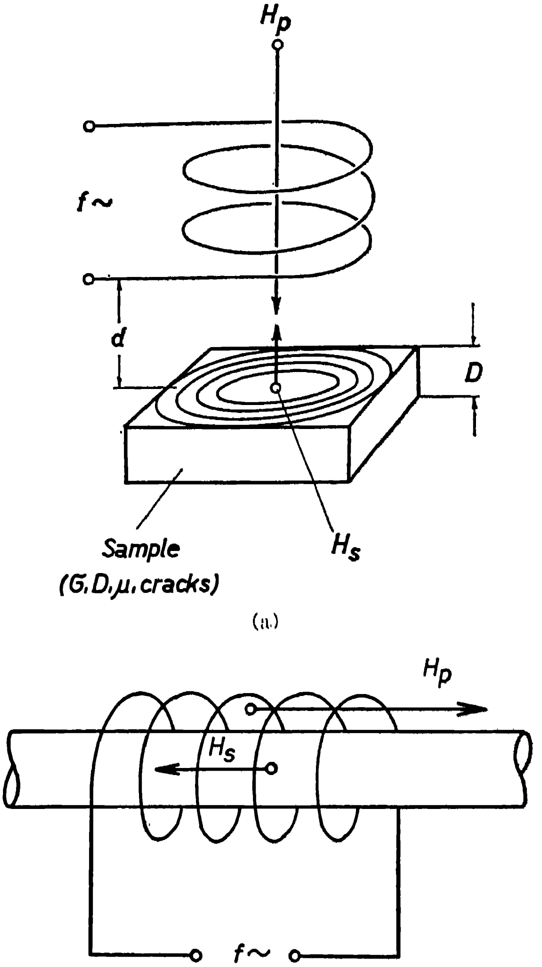

(a)

(b)

Institut Dr. Foerster

Fig. 1. Typical arrangements of probe coil and test object. (a) Probe coil above flat surface of a metallic test object. (b) Test object within a cylindrical test coil.
H_p = primary field of coil in absence of test object.
H_s = secondary field created by eddy currents in test object.

of the test object and of the characteristics of the instrumentation. **Significant properties of the test object** include:

1. Electrical conductivity (σ).
2. Dimensions (such as diameter of rods).
3. Magnetic permeability (μ).
4. Presence of discontinuities such as cracks or cavities.

Significant instrument characteristics include:

1. Frequency of the a.-c. field of the test coil.
2. Size and shape of the test coil.

3. Distance of test coil from test object (coupling between the coil and the specimen).

The influence of several **physical properties of the test specimen** upon the impedance characteristics of the probe coil can be calculated for various test frequencies in certain cases. Often it is possible to determine from the impedance change (distance P_0 to P_1), and frequently to measure quantitatively and independently of each other, not only the conductivity, dimensions, and magnetic permeability of the test object but even the magnitude and direction of cracks. The **optimum frequency** for a specific test problem is determined by theory or by experiment and provides the highest sensitivity obtainable with eddy current methods for detection of:

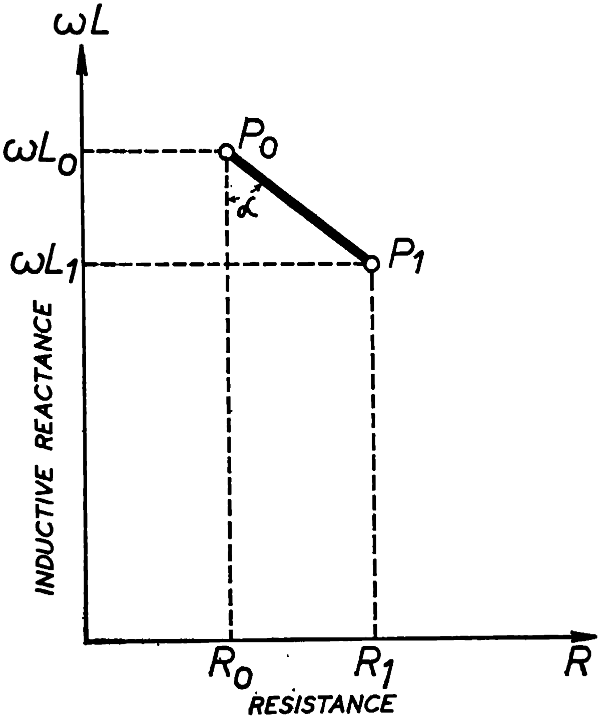

Fig. 2. Representation of test coil characteristics on impedance plane. Point P_0 = impedance of coil in absence of test object. Point P_1 = impedance of test coil with test object.

1. Variations in electrical conductivity, used in sorting alloys.
2. Variations in test-object diameter, used in dimensional control.
3. Cracks.

Indications are obtained, without electrical contact with the test object, in extremely short **time intervals,** such as 1/1000 sec. Physical properties measured include: alloy, heat treatment, hardness, depth of case, surface decarburization, magnitude of defects, and dimensions.

Methods of Testing of Solid Cylindrical Parts

Specimen Conditions	Shape of Coil	Test Arrangement	Properties Measured	Test Conditions Determined by
Uniform Material	Solenoid Coil	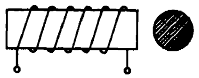	Diameter, Permeability, Conductivity	Mathematical Calculation
Uniform Material	Fork-Shaped Coil	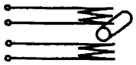	Diameter, Permeability, Conductivity	Mathematical Calculation
Material With Defects	Solenoid Coil	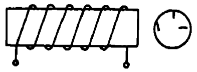	Shape, Size, Depth, Length, Position of Cracks	Model Test
Material With Defects	Fork-Shaped Coil With Probe Coils	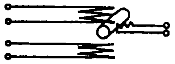	Defects	Model Test
Two-Layer Materials (Plated Cylinders)	Solenoid Coil	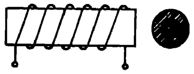	Diameter, Conductivity of Each Layer	Mathematical Calculation

(a)

Methods of Testing of Hollow Tubular Parts

Specimen Conditions	Shape of Coil	Test Arrangement	Properties Measured	Test Conditions Determined by
Uniform Material	Solenoid Coil	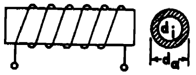	Inner Diameter, Outer Diameter, Conductivity, Permeability	Mathematical Calculation
Material With Defects	Solenoid Coil	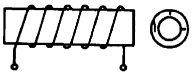	Shape, Width, Depth, Length, Position of Defects	Model Test
Two-Layer Materials (Plated Tubes)	Solenoid Coil	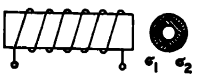	Inner Diameter, Layer Diameter, Outer Diameter, Conductivity of Each Layer	Mathematical Calculation
Eccentricity of Wall Thickness	Solenoid Coil	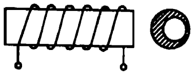	Eccentricity, Inner Diameter, Outer Diameter, Conductivity	Model Test
Uniform Material	Inside Coil	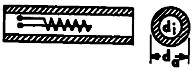	Inner Diameter, Outer Diameter, Conductivity	Mathematical Calculation

(c)

Fig. 3. Summary of eddy current test problems solved by Institut Dr. Foerster.

Applications and Equipment For Tests of Solid Cylindrical Parts

Specimen Conditions	Shape of Coil	Application	Material	Instrument Designation		Refs.
				European Type	American Type	
Uniform Material	Solenoid Coil	Quality control, classification for component, hardness, tensile strength and dimensions	Iron and Steel	Magnatest Q	Magnatest FS 300	26
			Nonferrous Metals	Sigmaflux Multitest	Magnatest FW300 Magnatest FS 200	26,43,45, 48,53,85
Uniform Material	Fork-Shaped Coil	Quality control Conductivity Testing	Steel			
			Nonferrous Metals			
Material With Defects	Solenoid Coil	Defect detection	Iron and steel	Magnatest D		3,80–82
			Nonferrous Metals	Bar and Wiretester Multitest	Magnatest FW200 Magnatest FW400 Magnatest FS 200	11,18,32, 43,48,53, 63,85
Material With Defects	Fork-Shaped Coil With Probe Coils	Defect detection, cracks, overlaps, soft spots	Nonferrous Metals and Steel	Durometer		35
Two-Layer Materials (Plated Cylinders)	Solenoid Coil	Plating thickness, case depth, decarburization, diffusion	Nonferrous Metals	Multitest	Magnatest FS200	21,32,36
			Steel	Magnatest Q Multitest	Magnatest FS300 Magnatest FS200	4,21,34

(b)

Applications and Equipment For Tests of Hollow Tubular Parts

Specimen Conditions	Shape of Coil	Application	Material	Instrument Designation		Refs.
				European Type	American Type	
Uniform Material	Solenoid Coil	Quality control, classification for alloy components, conductivity test, hardness and tensile strength	Nonferrous Metals	Sigmaflux Multitest	Magnatest FW300 Magnatest FS200	11,32,48
			Steel	Magnatest Q Multitest	Magnatest FS300 Magnatest FS200	18,21
Material With Defects	Solenoid Coil	Defect detection	Nonferrous Metals	Bar and Wiretester Multitest	Magnatest FW200 Magnatest FW400 Magnatest FS 200	11,32,43, 48,53, 63,85
			Steel	Magnatest D Multitest	Magnatest FS200	31,80, 81,82
Two-Layer Materials (Plated Tubes)	Solenoid Coil	Plating thickness, diffusion	Nonferrous Metals	Multitest	Magnatest FS200	27,32,36
			Steel	Multitest	Magnatest FS 200	4,21,34
Eccentricity of Wall Thickness	Solenoid Coil	Eccentricity and Shrinkage	Nonferrous Metals	Multitest Sigmaflux	Magnatest FS 200 Magnatest FW300	32,48
			Steel	Multitest Magnatest Q	Magnatest FS200 Magnatest FS300	32,48
Uniform Material	Inside Coil	Inner Defects	Nonferrous Metals	Sigmaflux Multitest	Magnatest FW300 Magnatest FS 200	17

(d)

(Reference numbers refer to references listed in section on Eddy Current Test Indications.)

Methods of Testing of Spherical and Ellipsoidal Parts

Specimen Conditions	Shape of Coil	Test Arrangement	Properties Measured	Test Conditions Determined by
Ellipsoid of Uniform Material	Solenoid Coil	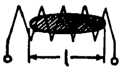	Diameter, Length, Permeability, Conductivity	Mathematical Calculation
Ball of Uniform Material	Solenoid Coil	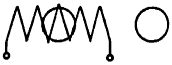	Diameter, Permeability, Conductivity	Mathematical Calculation
Ball with Defects	Solenoid Coil	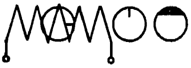	Diameter, Cracks, Permeability, Conductivity	Model Test
Ball with Defects	Fork-Shaped Coil	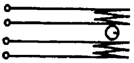	Defects	Model Test

(e)

Methods of Testing of Sheets and Plates

Specimen Conditions	Shape of Coil	Test Arrangement	Properties Measured	Test Conditions Determined by
Uniform Material	Hand Probe Coil on One Side of Specimen	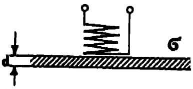	Thickness, Conductivity	Model Test
Uniform Material	Fork-Shaped Coils on Both Sides of Specimen	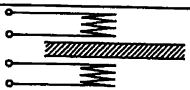	Thickness, Conductivity	Mathematical Calculation
Two-Layer Identical Nonferrous Material With Spacing	Hand Probe Coil on One Side of Specimen	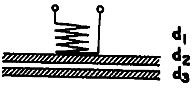	Thickness of Each Layer, Separation Between Layers	Model Test
Nonferrous Plated Materials	Hand Probe Coil on One Side of Specimen	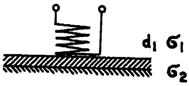	Plating Thickness, Conductivity of Each Material	Model Test
Nonferrous Plating on Ferromagnetic Material	Hand Probe Coil on One Side of Specimen	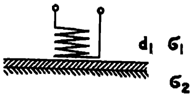	Plating Thickness, Conductivity of Each Material	Model Test
Material With Defects	Hand Probe Coil on One Side of Specimen	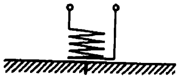	Depth of cracks, Shrinkage, Porosity	Model Test

(g)

Fig. 3. (Continued.)

Applications and Equipment For Tests of Spherical and Ellipsoidal Parts

Specimen Conditions	Shape of Coil	Application	Material	Instrument Designation		Refs.
				European Type	American Type	
Ellipsoid of Uniform Material	Solenoid Coil	Quality control of short pieces	Steel			34
Ball of Uniform Material	Solenoid Coil	Quality control (Alloy content, hardness)	Steel and Nonferrous Metals	Multitest	Magnatest FS200	39,85
Ball with Defects	Solenoid Coil	Defect detection	Steel and Nonferrous Metals	Multitest	Magnatest FS200	85
Ball with Defects	Fork-Shaped Coil	Defect detection, cracks, soft spots	Steel	Crack Detector for Balls		18

(f)

Applications and Equipment For Tests of Sheets and Plates

Specimen Conditions	Shape of Coil	Application	Material	Instrument Designation		Refs.
				European Type	American Type	
Uniform Material	Hand Probe Coil on One Side of Specimen	Quality control, conductivity test, alloy composition, hardness, porosity, wall thickness measurement	Nonferrous Material	Sigmatest	Magnatest FM 100	7,9,11, 12,15,30, 61,66,71
			Steel	Magnatest Q	Magnatest FS300	65
Uniform Material	Fork-Shaped Coils on Both Sides of Specimen	Thickness measurement of foils sheet and strips (square resistivity)	Nonferrous Metals	Sheet and foil Gage Square Resistivity Meter	Magnatest FT 200 Magnatest FT 100	33,36
Two-Layer Identical Nonferrous Material With Spacing	Hand Probe Coil on One Side of Specimen	Separation of Layers, Spalled Coatings	Nonferrous Metals	Multitest	Magnatest FS200	32
Nonferrous Plated Materials	Hand Probe Coil on One Side of Specimen	Thickness measurement of conductive, nonferrous layers on nonferrous base	Nonferrous Metals	Argentometer	Magnatest FT600	20,36,40, 59,60
Nonferrous Plating on Ferromagnetic Material	Hand Probe Coil on One Side of Specimen	Thickness measurement of metal coating on iron or steel (tin layers on sheets)	Tin Plate			42
Material With Defects	Hand Probe Coil on One Side of Specimen	Defect detection, cracks, shrinkages, porosity	Nonferrous Metals	Sigmatest Defektometer	Magnatest FM100	30

(h)

(Reference numbers refer to references listed in section on Eddy Current Test Indications.)

Methods of Testing of Plates With Insulating Layers				
Specimen Conditions	**Shape of Coil**	**Test Arrangement**	**Properties Measured**	**Test Conditions Determined by**
Insulated Coating on Nonferrous Metal	**Hand Probe Coil on One Side of Specimen**	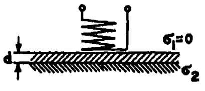	**Thickness of Insulating Coating**	**Model Test**
Nonferrous Metal on Insulating Material	**Hand Probe Coil on One Side of Specimen**	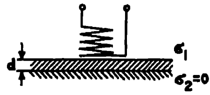	**Thickness, Conductivity of Metallic Layers**	**Mathematical Calculation**

(i)

Fig. 3. (Continued.)

Because of its versatility, the eddy current test method is finding increased **industrial use,** particularly in fully automatic test units. Some ten million parts such as rods, tubes, and automotive parts are tested daily in Europe by this method at the present time. This increase in use, particularly in recent years, is based upon extensive theoretical and experimental developments which have established the fundamental principles underlying this test method. These principles indicate the capabilities and limitations, as well as the practical applications of the method, both for existing and new test problems.

DEVELOPMENT OF BASIC PRINCIPLES. The basic principles underlying eddy current test methods were developed in two ways. First, those test problems amenable to **mathematical analysis** were calculated quantitatively on the basis of reasonable assumptions concerning test-object shape and material properties. Cases included in this group, for example, were:

1. The cylinder with single and multiple layers.[48]
2. The tube with single and multiple layers.[48]
3. The sphere.[39]
4. The rotation ellipsoid.
5. The probe coil inside the tube.
6. The pick-up coil for testing thin metallic layers.[33]
7. The fork coil used for noncontacting thickness measurement, or the measurement of resistance per unit square, for metal foils and laminations.[33]
8. The cylinder within a fork coil (with the direction of the field perpendicular to the axis of the cylinder).

The first four items in the preceding list refer to the case of a test object within a cylindrical probe coil (a "feed-through" coil).

In the second group of test problems, exact mathematical solutions of eddy current effects were impossible because of the boundary conditions involved. However, a **similarity law** applicable to eddy current problems makes it feasible to obtain quantitative information by means of measurements on models. These **model test** data can then be applied to practical test objects whose dimensions, electrical conductivity, and relative magnetic permeability are given. Included in this group are cases such as:

1. The cylinder or tube with cracks, cavities, or other discontinuities of any given shape and position.[43]
2. The eccentric tube.

Applications and Equipment For Tests of Plates with Insulating Layers

Specimen Conditions	Shape of Coil	Application	Material	Instrument Designation		Refs.
				European Type	American Type	
Insulated Coating on Nonferrous Metal	Hand Probe Coil on One Side of Specimen	Thickness measurement of insulated coating on nonferrous metals	Nonferrous Metals	Isometer	Magnatest FT 400	20,33,36, 40,46
Nonferrous Metal on Insulating Material	Hand Probe Coil on One Side of Specimen	Thickness measurement of conductive nonferromagnetic coatings (square resistivity)	Nonferrous Metals	Equivalent silver coating-thickness meter		20,33,36, 60,64

(j) Institut Dr. Foerster

(Reference numbers refer to references listed in section on Eddy Current Test Indications.)

3. The sphere containing cracks.
4. Pick-up coil tests of thick metal plates with variations in material electrical conductivity, plate thickness, and distance of the coil from the plate surface.[30]
5. Pick-up coil tests of crack depth and location in plate or cylinder.[30]

The first three items in the list refer to the case of a test object within a concentric coil ("feed-through" coil).

The **typical problems solved** are shown schematically with their test arrangements in Fig. 3 (a)–(j). Numerous other nondestructive test problems can be related to these standard cases which have already been evaluated.

Effective Permeability

ASSUMPTIONS USED IN ANALYSIS. The concept of effective permeability considerably simplifies the analysis of eddy current test arrangements. It will be illustrated by the example of a long, **cylindrical test object** magnetized within a **cylindrical coil** carrying alternating current. The following assumptions are made for this example:

1. The test coil produces an essentially uniform magnetizing field, H_0, throughout the cross-section within it.
2. The test object is infinitely long, i.e., end effects are neglected.
3. The test object is cylindrical in shape, of constant diameter d.
4. The electrical conductivity σ and the magnetic permeability μ of the test object are constant, both throughout its volume and with varying states of magnetization.
5. Initially it is assumed that the test object fills the test coil. Later, the case of smaller test objects which incompletely fill the coil are considered.
6. The varying states of magnetization, resulting from the shielding effects of eddy currents which oppose the magnetizing field, can be represented by means of an "effective permeability," $\mu_{\text{eff.}}$, which compensates for varying conditions within the test object.
7. The magnetizing field is assumed sinusoidal and of a single frequency. The effects of harmonic frequency components generated by nonlinear characteristics of the test object are ignored. Thus the test coil can be characterized by "impedances" similar to those used in analysis of linear a.-c. circuits.
8. The effects of magnetic hysteresis, shown to be of small magnitude in comparison with the effects of eddy currents in the test object, are neglected.

DETERMINATION OF EFFECTIVE PERMEABILITY. Fig. 4 illustrates schematically the most widely used arrangement for eddy current testing. A **primary coil,** carrying an a.-c. current of frequency f, generates the primary a.-c. magnetic field H_0. The **secondary coil** is located inside the primary coil. The secondary coil is characterized by its number of turns, n, and the average area of the opening within the winding, $\pi D^2/4$, where D is the diameter of the secondary coil. The material to be tested, such as a wire, tube, rod, or equivalent, passes through the center of the concentric primary and secondary windings.

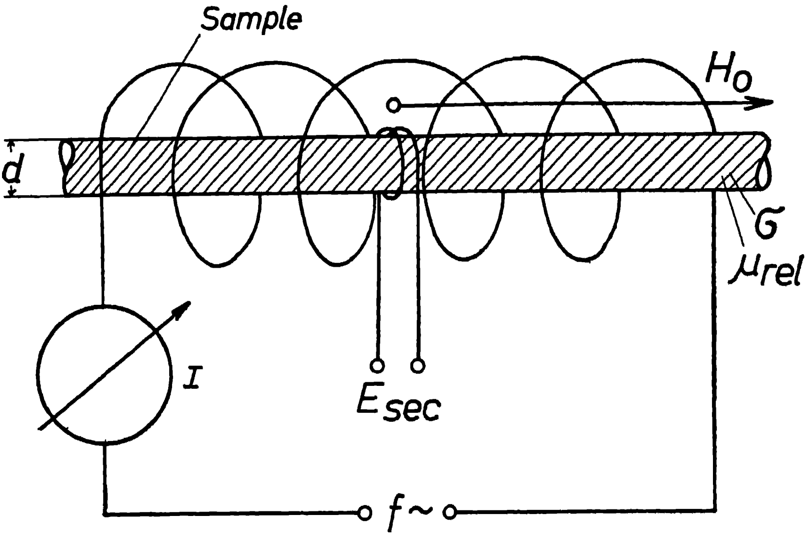

Institut Dr. Foerster

Fig. 4. Schematic drawing of test object in "feed-through" test coil with primary (excitation) and secondary (pick-up) windings.

Empty Coil Voltage. The basic problem in eddy current testing is to obtain valid information concerning the test material from the **secondary coil voltage,** $E_{sec.}$. The method becomes quantitative and useful only by exact analysis of how test-object conditions influence the secondary voltage, so that physical properties can be determined from test indications. In the absence of a test object, the voltage appearing across the terminals of the secondary coil is calculated to be:

$$E_{sec.} = (2\pi f)(n)\left[\frac{\pi D^2}{4}\right](\mu_{rel.})H_0 \times 10^{-8} \quad \text{volts} \qquad (1)$$

where f = test excitation frequency, c.p.s.
$\pi D^2/4$ = area within secondary coil.
D = diameter of secondary coil.
n = number of turns in secondary coil.
$\mu_{rel.}$ = relative magnetic permeability (approximately 100 for iron, Fe, equal to unity for aluminum, copper, and other nonferromagnetic metals and alloys).
H_0 = excitation field strength inside the test coil, in oersteds.

In the absence of a test object, the density of magnetic lines of force measured in gausses in the air within the test coil is numerically equal to the exciting field strength H_0, measured in oersteds, of the primary coil.

Influence of Test Object. If a test object such as a metal rod is inserted within the coil, eddy currents are induced within it by the primary a.-c. field. The test object acts like a short-circuited winding of an air-core transformer. The eddy currents, in turn, generate a magnetic field which tends to weaken the primary magnetic field H_0 within the test object. The resultant field-weakening decreases the secondary coil voltage $E_{\text{sec.}}$, in accordance with Eq. (1).

The weakening of field strength within the test object by the action of the eddy currents can be described in two ways. The first, which corresponds to physical reality, is illustrated schematically in Fig. 5. The **field strength outside the test object** corresponds to the field H_0 resulting from the primary coil (not shown).

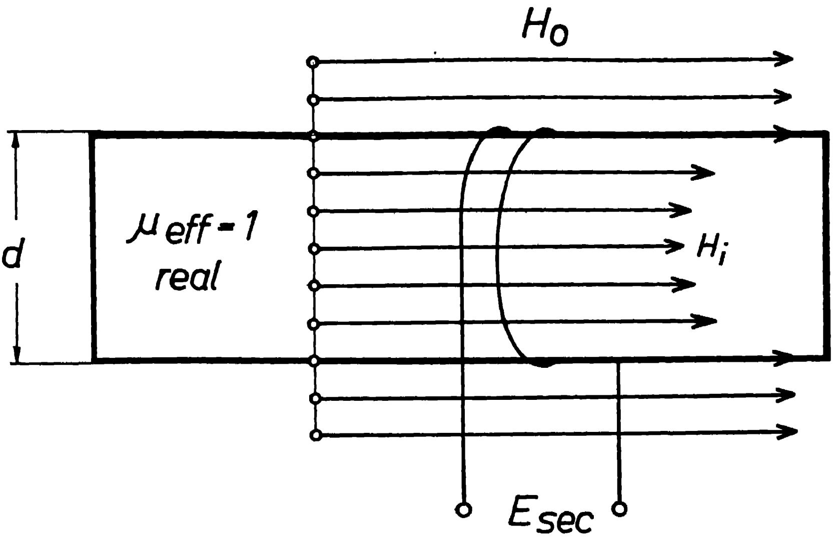

Fig. 5. Schematic representation of magnetic-field conditions with test object in test coil.

Within the test object, the field strength H_i is weakened by the effect of the eddy currents and decreases in intensity toward the center as a consequence of **skin effect.** An additional effect (not shown in Fig. 5) is a **phase displacement** of the a.-c. magnetic-field strength associated with this decreased field intensity. This phase displacement (in time) occurs to an increasing extent toward the center of the test object.

Secondary Coil Voltage with Test Object. To calculate the secondary coil voltage, $E_{\text{sec.}}$, by Eq. (1) would require that the test object be divided into an infinite number of cylindrical elements, each of area dF and field strength H_i (which would vary from area element to area element both in magnitude and phase angle). The secondary voltage $E_{\text{sec.}}$, would be calculated from the summation of the products of the area and the **actual field strength** within each cylindrical element, as follows:

$$E_{\text{sec.}} = [(2\pi f)(n)\,\mu_{\text{rel.}} \times 10^{-8}] \sum_{v=1}^{v=\infty} H_v d_v \qquad (2)$$

where H_v = actual magnetic-field strength within element v.
d_v = cross-sectional area of element v.

As an alternative to this complex representation, the test condition can be indicated more simply as shown in Fig. 6. Here it is assumed that the applied field strength H_0 is uniform and undisturbed over the entire cross-section of the test object. However, it is assumed that the test object can be assigned an **effective permeability**, $\mu_{\text{eff.}}$, which is (1) constant over the entire cross-section of the test object, and (2) a complex number with a magnitude smaller than unity. The computed secondary voltage $E_{\text{sec.}}$, is the same whether one uses the summation of area elements of Eq. (2) or the assumed constant field strength H_0 multiplied by the fictitious **complex material constant** $\mu_{\text{eff.}}$. The latter assumption leads to an expression for the secondary voltage as follows:

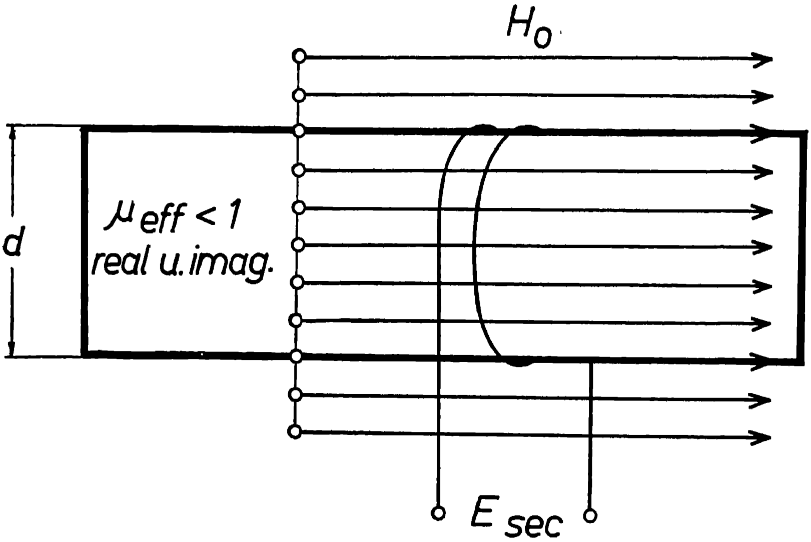

Fig. 6. Simplified representation of magnetic conditions within test object in test coil, assuming an effective permeability less than unity and a constant field strength H_0.

$$E_{\text{sec.}} = (2\pi f)(n)(\pi d^2/4) \times 10^{-8}(\mu_{\text{rel.}})(\mu_{\text{eff.}})H_0 \qquad (3)$$

General Case of a Cylindrical Test Object. Extensive mathematical calculations have been made for the effective permeability $\mu_{\text{eff.}}$ for the general case of a cylinder consisting of several layers of various conductivities and thicknesses, as functions of:

1. Electrical conductivity, σ, of the test object.
2. Relative magnetic permeability, $\mu_{\text{rel.}}$, of the test object.

3. Diameter of the test object, d.
4. Test frequency, f.

The homogeneous cylinder or rod of uniform material results as a special case of the general computation.[48] In the calculation of the effective permeability, the following expression occurs as the **argument A of the Bessel functions:**

$$A = \frac{f\mu_{\text{rel.}}\sigma d^2}{5066} \tag{4}$$

where f = frequency of the primary exciting field, c.p.s.
σ = electrical conductivity of test material, meter/ohm-mm.^{2}.
d = diameter of test object, cm.
$\mu_{\text{rel.}}$ = relative permeability of test material (approximately 100 for iron, unity for aluminum).

Limit Frequency, f_g. Fortunately the **test frequency,** f, can always be selected so that the factor A in Eq. (4) will be equal to unity. This frequency at which $A = 1$ for given values of σ, d, and $\mu_{\text{rel.}}$, is called the **limit frequency f_g.** Substituting this limit frequency f_g for the frequency f in Eq. (4), and taking factor $A = 1$, the expression can be solved for f_g as follows:

$$f_g = \frac{5066}{\mu_{\text{rel.}}\sigma d^2} \quad \text{c.p.s.} \tag{5}$$

If test frequencies are selected so that the **frequency ratio** $f/f_g = 1,2,3 \ldots$, the quantity A in Eq. (4) also assumes the values $A = 1,2,3 \ldots .$

Effective Permeability as a Function of Frequency Ratio. Since the effective permeability $\mu_{\text{eff.}}$ is a function only of the magnitude of the quantity A in Eq. (4), considerable simplification is attained if $\mu_{\text{eff.}}$ is expressed as a function of the frequency ratio f/f_g, i.e., as a **multiple of the limit frequency f_g** of Eq. (5). Fig. 7 shows computed values of $\mu_{\text{eff.}}$ (both real and imaginary components) for the case of the **solid cylindrical test object.**[48] This curve gives values for $\mu_{\text{eff.}}$, as a function of the frequency ratio f/f_g, in the **complex effective permeability plane.** Points corresponding to multiples of the limit frequency f_g are marked on the curve throughout the range from $f/f_g = 0$ (at the top) to $f/f_g = \infty$ (at the bottom). In this curve the **real component of μ_{eff}** is plotted vertically, while the **imaginary component** is plotted horizontally. Fig. 8 lists precise values for $\mu_{\text{eff.}}$ corresponding to points marked in the curve of Fig. 7.

Sample Calculations for Effective Permeability and Secondary Coil Voltage. Since the data of Figs. 7 and 8 form the basis of **eddy current tests of cylindrical objects,** the calculation of $\mu_{\text{eff.}}$ and the determination of the secondary coil voltage $E_{\text{sec.}}$ from Eq. (3) will be illustrated by a practical example. Let us assume a **copper rod** of diameter $d = 1$ cm., with electrical conductivity $\sigma = 50.6$ meter/ohm-mm.^{2}, and a relative magnetic permeability $\mu_{\text{rel.}} = 1$. The limit frequency f_g is calculated to be $f_g = 100$ c.p.s., from Eq. (4). If the rod is placed in a coil excited at a frequency of 100 c.p.s., the frequency ratio f/f_g is unity. Under these conditions the copper rod exhibits an effective permeability, $\mu_{\text{eff.}}$, corresponding to $f/f_g = 1$ in Figs. 7 and 8. From Fig. 8 it is found that $\mu_{\text{eff.(real)}} = 0.9798$ and $\mu_{\text{eff.(imag.)}} = 0.1216$. However, if one were now to select a measurement frequency of 1000 c.p.s., the ratio f/f_g would be 10. In this case Fig. 8 gives the **components of the effective permeability** as $\mu_{\text{eff.(real)}} = 0.4678$ and $\mu_{\text{eff.(imag.)}} = 0.3494$.

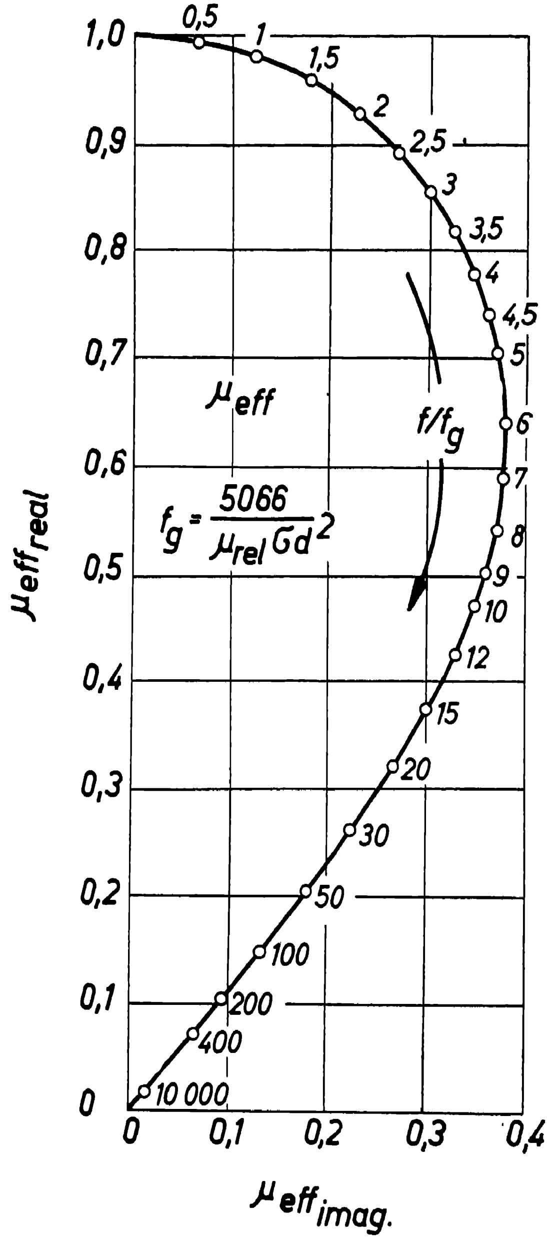

Institut Dr. Foerster

Fig. 7. Variation in effective permeability μ_{eff}. with frequency ratio f/f_g, plotted in the complex permeability plane.

f/f_g	$\mu_{\text{eff.(real)}}$	$\mu_{\text{eff.(imag.)}}$
0.00	1.0000	0.0000
0.25	0.9989	0.0311
0.50	0.9948	0.06202
1	0.9798	0.1216
2	0.9264	0.2234
3	0.8525	0.2983
4	0.7738	0.3449
5	0.6992	0.3689
6	0.6360	0.3770
7	0.5807	0.3757
8	0.5361	0.3692
9	0.4990	0.3599
10	0.4678	0.3494
12	0.4202	0.3284
15	0.3701	0.3004
20	0.3180	0.2657
50	0.2007	0.1795
100	0.1416	0.1313
150	0.1156	0.1087
200	0.1001	0.09497
400	0.07073	0.06822
1,000	0.04472	0.04372
10,000	0.01414	0.01404

Institut Dr. Foerster

Fig. 8. Tabular listing of values of effective permeability $\mu_{\text{eff.}}$ for specific values of frequency ratio f/f_g, from Fig. 7.

The **voltage induced** in a one-turn secondary winding ($n = 1$), for $H_0 = 1$ oersted, can be computed from Eq. (3) for a frequency $f = 100$ c.p.s. Since this is equal to the limit frequency, $f_g = 100$, the frequency ratio $f/f_g = 1$. In this case the **real component of secondary voltage** is

$$E_{\text{sec.(real)}} = 0.600 \times 10^{-6} \text{ volt}$$

and the **imaginary component** is

$$E_{\text{sec.(imag.)}} = 4.83 \times 10^{-6} \text{ volt}$$

In accordance with the terminology of electrical engineering, the real component of voltage results from multiplying Eq. (3) by the imaginary component of the effective permeability; hence

$$E_{\text{real}} = 2\pi f n (\pi d^2/4) \mu_{\text{rel.}} \mu_{\text{eff.(imag.)}} H_0 \times 10^{-8} \text{ volt} \tag{6a}$$

The imaginary component of voltage is similarly obtained by multiplying by the real component of the effective permeability; hence

$$E_{\text{imag}} = 2\pi f n (\pi d^2/4) \mu_{\text{rel.}} \mu_{\text{eff.(real)}} H_0 \times 10^{-8} \text{ volt} \tag{6b}$$

These **basic eddy current test equations** permit computation of the components of secondary voltage for various test-object materials and dimensions. The steps involved are:

1. Substitute the numerical values of test-object electrical conductivity σ, relative magnetic permeability $\mu_{\text{rel.}}$, and dimensional constant d into Eq. (5) to determine the limit frequency f_g.

2. Divide the operating test frequency f by the limit frequency f_g to obtain the frequency ratio f/f_g.
3. Use this frequency ratio and Figs. 7 or 8 to obtain the components of the effective permeability $\mu_{\mathrm{eff.}}$.
4. Calculate the components of secondary coil voltage by substituting these values of effective permeability into Eqs. (6, a and b).

For all **nonferromagnetic materials,** the value of $\mu_{\mathrm{rel.}} = 1$ is used in Eq. (6, a and b).

Values of $\mu_{\mathrm{rel.}}$ for ferromagnetic materials are obtained from experience or by tests on the specific material. To illustrate the procedure, the secondary voltage components will be calculated for a **ferromagnetic test object** for which:

Electrical conductivity $\sigma = 10$ meter/ohm-mm.^{2}
Diameter $d = 1$ cm.
Relative permeability $\mu_{\mathrm{rel.}} = 100$.

The secondary coil will be assumed to be a one-turn winding ($n = 1$). The primary coil field strength is taken as 1 oersted ($H_0 = 1$). For a larger number of turns or higher field strength, this calculated voltage would be multiplied by the corresponding factors. The limit frequency f_g is found from Eq. (5) to be 5.07 c.p.s. If the test frequency is $f = 50$ c.p.s., one obtains

$$f/f_g = 10 \text{ (approx.)}$$

$$\mu_{\mathrm{eff.(real)}} = 0.47$$

$$\mu_{\mathrm{eff.(imag.)}} = 0.35$$

The secondary coil voltage components obtained from Eq. (6) are

$$E_{\mathrm{real}} = 86.6 \times 10^{-6} \text{ volt}$$

$$E_{\mathrm{imag.}} = 116.4 \times 10^{-6} \text{ volt}$$

TEST OBJECT SMALLER THAN SECONDARY COIL DIAMETER. In the preceding examples, it was assumed that a test object of diameter d completely filled a secondary coil with the inside diameter D, so that $d = D$. In practice, however, the coil diameter D must be considerably larger than the test object diameter d, so that the test object can pass through the secondary coil freely and without contacting it at high test speeds. Fig. 9 illustrates a cross-section of a secondary coil enclosing a smaller test object. The **annular air space** between the test object and the coil has an area of

$$A_{\mathrm{air\ ring}} = (\pi/4)(D^2 - d^2)$$

and permeabilities of

$$\mu_{\mathrm{rel.}} = 1 \qquad \mu_{\mathrm{eff.}} = 1 \text{ (a real number only)}$$

Secondary Coil Voltages. The primary magnetizing field H_0 produces two **components of voltage** in the secondary coil. The first component, contributed by the field in the annular air space, is purely imaginary (since $\mu_{\mathrm{eff.}}$ is real); hence

$$E_{\mathrm{sec.(air\ ring)}} = 2\pi f n(\pi/4)(D^2 - d^2)H_0 \times 10^{-8} \text{ volt} \tag{7}$$

The second component, contributed by the presence of the test object, is a complex number:

$$E_{\mathrm{sec.(test\ object)}} = 2\pi f n(\pi/4)d^2\mu_{\mathrm{rel.}}\mu_{\mathrm{eff.}}H_0 \times 10^{-8} \text{ volt} \tag{8}$$

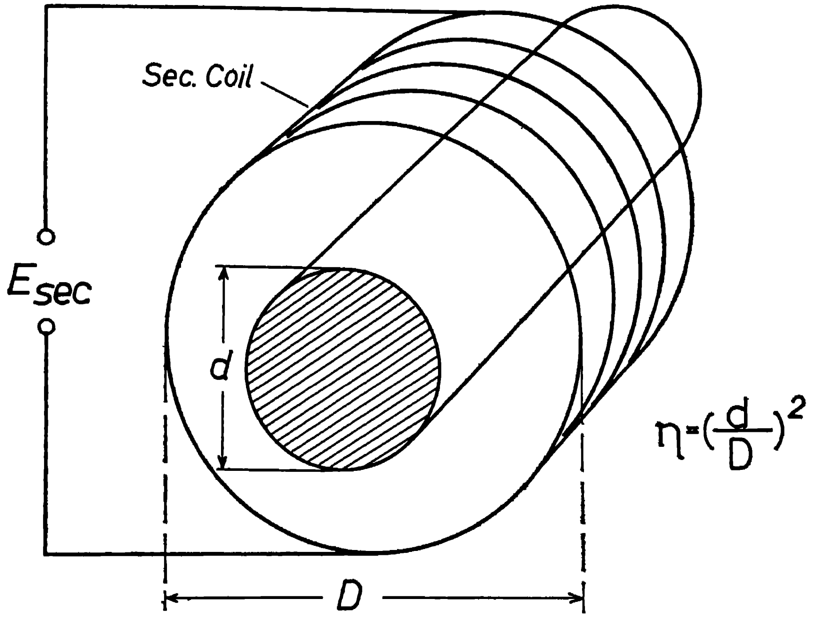

Fig. 9. Test coil containing a test object of smaller diameter *d*, partially filling the coil.

The **total secondary coil voltage** is obtained by the vectorial addition of the components of Eqs. (7) and (8); hence

$$\begin{aligned} E_{\text{sec.(total)}} &= E_{\text{sec.(air ring)}} + E_{\text{sec.(test object)}} \\ &= 2\pi fn(\pi D^2/4)\,[1 - (d/D)^2 + (d/D)^2\mu_{\text{rel}}\,\mu_{\text{eff.}}]H_0 \times 10^{-8}\text{ volt} \end{aligned} \tag{9}$$

The ratio $(d/D)^2$ indicates the fraction of the secondary coil area filled by the test object. This is known as the **fill factor,** η, for the coil; i.e.,

$$\eta = (d/D)^2 \tag{10}$$

In the absence of a test object $(d = 0)$, the term within the brackets in Eq. (9) becomes unity. For the empty coil the secondary coil voltage becomes

$$E_0 = 2\pi fn(\pi D^2/4)H_0 \times 10^{-8}\text{ volt} \tag{11}$$

In the general case in which a **nonferromagnetic test object** partially fills the test coil, the coil voltage can be expressed as

$$E = E_0(1 - \eta + \eta\mu_{\text{eff.}}) \tag{12}$$

The parenthesized expression, $(1 - \eta + \eta\mu_{\text{eff.}})$, in Eq. (12) is an important and useful parameter. By multiplying it by the voltage E_0 of the empty coil, one obtains the secondary voltage with a test object within the coil.

Complex Permeability Plane. Fig. 10 shows values of the parenthetical expression from Eq. (12), plotted on the complex permeability plane for two fill factors, as

$\eta = 1$ (The test object completely fills the test coil.)
$\eta = ½$ (The cross-sectional area is only one-half the area within the secondary winding of the test coil.)

For $\eta = 1$, the parenthetical expression has the same value as $\mu_{\text{eff.}}$. Figs. 7 and 8 apply for $\eta = 1$. The outermost curve in Fig. 10 is thus identical with the curve of Fig. 7. For the case in which $\eta = \frac{1}{2}$, the **steps involved in using** Fig. 10 are

1. Plot the value of $(1 - \eta) = 0.5$ along the ordinate in Fig. 10, i.e., in the direction of $\mu_{\text{eff.(real)}}$. Here the term $(1 - \eta)$ corresponds to the contribution of the annular air ring and is not influenced by the properties of the test object. With an infinitely high test frequency, $\mu_{\text{eff.}} = 0$ (from Fig. 8). In this case only the air ring influences the value of the parenthetical expression in Eq. (12). The parenthetical expression then reduces to $(1 - \eta)$.
2. The value of the complex permeability $\mu_{\text{eff.}}$ multiplied by the fill factor η is then plotted vectorially from the end of the vector $(1 - \eta)$ at point B. For example, the $\eta\mu_{\text{eff.}}$ value for $f/f_g = 4$ is plotted in Fig. 10 as line BA.
3. The total value of the parenthetical expression in Eq. (12) is now given by the vector from the origin O to the point A (distance OA). Its real and imaginary components can be read from the coordinates of Fig. 10.

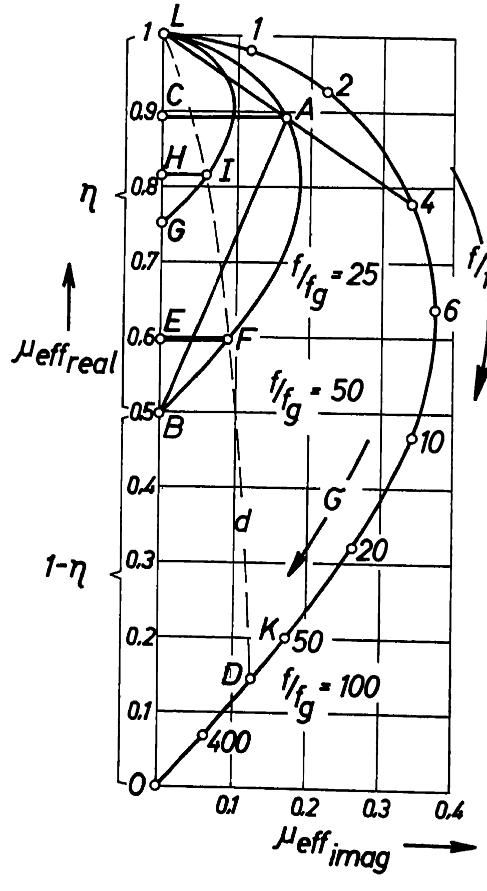

Fig. 10. Parameter $(1 - \eta + \eta\mu_{\text{eff.}})$ as a function of complex permeability $\mu_{\text{eff.}}$, for fill factors $\eta = 1$ and $\eta = \frac{1}{2}$.

Summary. In Fig. 10:

Distance OB represents the term $(1-\eta)$
Distance BA represents the term $\eta\mu_{\text{eff.}}$
Distance BC represents the product $\eta\mu_{\text{eff.(real)}}$
Distance CA represents the product $\eta\mu_{\text{eff.(imag.)}}$
Distance OA represents the entire parameter $(1-\eta+\eta\mu_{\text{eff.}})$

Correction for Ferromagnetic Test Object. If a ferromagnetic test cylinder with the relative magnetic permeability $\mu_{\text{rel.}}$ is placed in the test coil of Fig. 9, it is necessary to modify Eq. (12) as follows:

$$E = E_0(1-\eta+\eta\mu_{\text{rel.}}\mu_{\text{eff.}}) \qquad (13)$$

IMPEDANCE CHARACTERISTICS OF A SINGLE TEST COIL. The impedance characteristics of a single test coil (see Fig. 11) can be determined with the aid of the preceding development. In the absence of a test object, the **empty coil** of Fig. 11 is characterized by an impedance whose components are

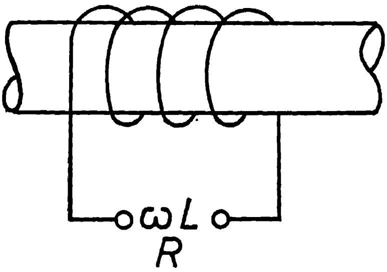

Fig. 11. Arrangement of cylindrical test object in a single test coil characterized by an inductive reactance ωL and an ohmic resistance R.

ωL_0 = inductive reactance (empty coil).

R_0 = ohmic resistance (empty coil).

The **self-inductance** of a cylindrical coil with no test object is

$$L_0 = K(n^2A/l) \qquad (14)$$

where K = constant.
A = average coil area.
n = number of series turns in coil winding.
l = coil length.

When a portion of the coil area is filled by a cylindrical test object of diameter d, conductivity σ, and relative permeability $\mu_{\text{rel.}}$, the self-inductance L is calculated by analogy to Eq. (13) as

$$L = L_0(1-\eta+\eta\mu_{\text{rel.}}\mu_{\text{eff.(real)}}) \qquad (15)$$

The **voltage drop due to self-inductance** E_L is given by the product of the coil current I and the inductive reactance ωL; thus

$$E_L = I(2\pi fL) = I(\omega L) \qquad \text{(imag.)}$$

The **voltage drop due to ohmic resistance** in the test coil is given by the product of the coil current by the resistance

$$E_R = IR \qquad \text{(real)}$$

In Eqs. (6) through (12), the excitation field strength of a current-carrying coil

$$H_0 = k(nI)$$

where k is a constant, n is the number of magnetizing turns, and I is the current through the coil.

Normalized Coil Characteristics. The voltages induced in a test coil containing a test object are said to be "normalized" when they are divided by the inductive reactance component of voltage, E_{L_0}, of the same coil when empty (see Eq. 11). The **normalized imaginary component of coil voltage** becomes

$$\frac{E_{\text{imag.}}}{E_{L_0}} = \frac{\omega L}{\omega L_0} = [1 - \eta + \eta\mu_{\text{rel.}}\mu_{\text{eff.(real)}}] \qquad (16a)$$

The **normalized real component** of coil voltage becomes

$$\frac{E_{\text{real}}}{E_{L_0}} = \frac{R - R_0}{\omega L_0} = [\eta\mu_{\text{rel.}}\mu_{\text{eff.(imag.)}}] \qquad (16b)$$

These equations indicate that the curves of Fig. 10 apply to either

1. The normalized secondary coil voltage components, or
2. The normalized values of the inductive reactance $(\omega L/\omega L_0)$ and the resistance $(R - R_0)/\omega L_0$ of a single test coil.

The **normalized resistance** (real) and the **normalized inductive reactance** (imag.) of the test coil are the components of its **"normalized" impedance.**

Example of Nonferromagnetic Test Object. In the case of nonferromagnetic test materials such as stainless steel, copper, or aluminum, $\mu_{\text{rel.}} = 1$. If the test cylinder entirely fills the test coil (fill factor $\eta = 1$), Eqs. (16 a and b) reduce to

$$\mu_{\text{eff.(real)}} = \frac{\omega L}{\omega L_0} = \frac{E_{\text{imag.}}}{E_0} \qquad (17a)$$

$$\mu_{\text{eff.(imag.)}} = \frac{R - R_0}{\omega L_0} = \frac{E_{\text{real}}}{E_0} \qquad (17b)$$

Three Complex Planes for Eddy Current Test Data. Thus the effective permeability represented in Figs. 7 and 8 is identical to the secondary voltages and coil data normalized to the empty coil values. Fig. 7 equally well represents three valuable forms of eddy current test data as follows:

1. The **complex permeability plane,** showing components of $\mu_{\text{eff.}}$ (real and imaginary).
2. The **complex impedance plane,** showing the components of the normalized impedance (real and imaginary).
3. The **complex plane of secondary coil voltages** normalized to the "empty coil" value.

For example, the impedance plane will be referred to in later discussions of test methods using a bridge arrangement of primary coils only. On the other hand, test arrangements with both primary and secondary coils will be referred to the complex voltage plane. Eqs. (17 a and b) indicate that both test arrangements are described by the same equations.

The **effective permeability,** obtained from Eq. (5) or Figs. 7 or 8, is a fundamental factor in all eddy current tests. It is used to obtain information on physical properties or discontinuities in test objects.

References

Reference numbers in this section refer to the references at the end of the section on Eddy Current Test Indications.

SECTION 37

EDDY CURRENT CYLINDER TESTS

CONTENTS

PAGE

Conductivity, Permeability, and Diameter of Cylindrical Test Objects

- Assumptions used in analysis 1
- Separation of effects of conductivity and diameter (nonmagnetic cylinder) 1
  - Variation of conductivity σ 2
- Characteristics of the complex impedance or voltage planes 2
    - Complex impedance and voltage planes for various fill factors (nonferromagnetic materials) (*f.* 1) 3
  - Selection of frequency for separation of diameter and conductivity variations 2
  - Effect of high test frequencies 3
  - Effect of low test frequencies 3
  - Effect of variation in fill factor 4
  - Determination of limit frequency f_g 4
  - Quantitative test indications 4
- Separation of effects of conductivity, diameter, and relative magnetic permeability (ferromagnetic cylinders)[28] 4
    - Complex impedance and voltage planes for ferromagnetic cylinders with various relative permeabilities (*f.* 2) 5
  - Advantage in crack detection 5
  - Effect of changes in cylinder diameter 6
  - Effect of changes in electrical conductivity . 6
  - Effects of magnetic hysteresis 6
  - Separation of variable parameters 6

Field Strength and Eddy Current Distribution in Cylinders [48]

- Field strength distribution 6
    - Amplitude and phase angle of field strength distribution within a metallic cylinder (*f.* 3) 7
- Eddy current distribution 8
    - Amplitude and phase angle of eddy current distribution within a metallic cylinder (*f.* 4) 8
  - Examples of eddy current distributions 9
    - Magnitudes of field strength and eddy current density as functions of radial position in cylinder (*f.* 5) 9
  - Penetration depth 9
    - The penetration depth P at which field strength and eddy current density are $1/e = 37$ percent of surface values, as a function of frequency ratio (*f.* 6) 10
  - Control of eddy current magnitudes 10
- The similarity law in eddy current testing 10
  - Application to detection of discontinuities .. 11
  - Application to model tests 11
- Experimental verification of mathematical calculations 11
    - Mercury model for experimental verification of field strength and eddy current distribution in cylindrical test object (*f.* 7) 12
    - Comparison between calculated and experimentally determined field strength distribution in mercury model cylinder (*f.* 8) 12
- Model tests as a basis for quantitative tests of discontinuities 13
    - Model arrangement for simulating any given discontinuity in the mercury cylinder (*f.* 9) 13
    - Electric circuit used in model tests with mercury cylinder (*f.* 10) 13
    - Summary of types of discontinuities in cylindrical specimens studied in mercury model tests (*f.* 11) 14

Test Coil Arrangements for Feed-through Testing

- Classification of feed-through coil arrangements 15
    - Arrangements for test coils for feed-through tests (*f.* 12) 16
- Complex voltage or impedance plane for feed-through coils 15
    - Complex voltage and impedance planes for test coil arrangements of Fig. 12 (*f.* 13) 17
  - Single primary test coil 15
  - Primary and secondary coil arrangement 17
  - Bridge arrangement of test coils 17
  - Differential or self-comparison arrangements 18

Tests for Cracks in Solid Cylinders

- Cracks in nonferrous cylindrical test objects . 18
    - Impedance variations caused by surface and subsurface cracks in nonferromagnetic cylinders, at a frequency ratio $f/f_g = 5$ (*f.* 14) 19
    - Impedance variations caused by surface and subsurface cracks in nonferromagnetic cylinders, at a frequency ratio $f/f_g = 15$ (f. 15) 20

CONTENTS (*Continued*)

PAGE

- Impedance variations caused by surface and subsurface cracks in nonferromagnetic cylinders, at a frequency ratio $f/f_0 = 50$ (*f.* 16) 21
- Impedance variations caused by surface and subsurface cracks in nonferromagnetic cylinders, at a frequency ratio $f/f_0 = 150$ (*f.* 17) 22
- Test coil voltages 19
  - Differential test coil arrangement containing sound and defective cylindrical test specimens (*f.* 18) 22
- Suppression of variations in cylinder diameter 21
- Frequency selection for surface crack detection 23
  - Changes in effective permeability $|\Delta\mu_{eff.}|$ caused by surface cracks of various depths in nonferromagnetic cylinders (*f.* 19) 23
  - Changes in component of effective permeability $|\Delta\mu_{eff.}|$ perpendicular to direction of diameter changes, caused by surface cracks of various depths in nonferromagnetic cylinders (*f.* 20) 24
- Frequency selection for subsurface crack detection 24
  - Changes in effective permeability $|\Delta\mu_{eff.}|$ caused by subsurface cracks of 30 percent crack depth at various distances below the surface of nonferromagnetic cylinders (*f.* 21) 25
  - Changes in component of effective permeability $|\Delta\mu_{eff.}|$ perpendicular to direction of diameter changes, caused by subsurface cracks of 30 percent crack depth at various distances beneath outer surface of nonferromagnetic cylinder (*f.* 22) 26

Cracks in ferromagnetic cylinders 25

- Suppression of variations in cylinder diameter 25
  - Changes in component of effective permeability $|\Delta\mu_{eff.}|$ perpendicular to the direction of diameter and relative permeability changes, caused by surface cracks of various depths in ferromagnetic cylinders (*f.* 23) 27
- Frequency selection for crack detection 26

Quantitative measurement of crack depths 27

- Experimental determination of frequency ratio f/f_0 27
  - Variation of angle α with frequency ratio f/f_0 or product σd^2 in nonferromagnetic cylinder (*f.* 24) 28
- Crack evaluation with comparison specimen 28
  - Explanation of complex plane conditions for comparison specimen test arrangement (*f.* 25) 29
- Conductivity or diameter evaluation with comparison specimen 30
- Instrument sensitivity calibration 30
- Quantitative crack-depth calculations 31
  - Quotient $Q = \Delta\mu_{eff.}$/(absolute value) as a function of frequency ratio f/f_0 for surface cracks of various depths in nonferromagnetic cylinders (*f.* 26) 30
- Computing crack depth from instrument indication 32
  - Quotient $Q = \Delta\mu_{eff.}$/(absolute value) as a function of crack depth, for various frequency ratios, f/f_0, with nonferromagnetic cylinders (*f.* 27) 31

Applications of Test Instruments

Operation of test instruments 32

  - Simplified schematic diagram of eddy current test instrument for quantitative measurement of crack effects, conductivity effects, and diameter effects in nonferrous cylinders (*f.* 28) 32
- Analysis of screen patterns 33
  - Characteristics of elliptical screen pattern, resulting from sinusoidal deflection voltages displaced in phase angle, on eddy current test instrument (*f.* 29) 33
- Adjustment of the phase shifter 34
- Instrument sensitivity characteristics 35
  - Impedance variations (amplitude and phase) for a 1 percent variation of conductivity (*f.* 30) 34
  - Impedance variations (amplitude and phase) for a 1 percent variation in diameter (*f.* 31) 35
  - Variation in effective permeability $\Delta\mu_{eff.}$, for 1 percent conductivity variation in nonferromagnetic cylinder (*f.* 32) 36
  - Variation in effective permeability $\Delta\mu_{eff.}$, for 1 percent diameter variation in nonferromagnetic cylinder (*f.* 33) 36

Quantitative measurements of conductivity or diameter effects 35

  - Quotient $Q = \Delta\mu_{eff.}$/(absolute value), for 1 percent conductivity variation in nonferromagnetic cylinder (*f.* 34) 37
  - Quotient $Q = \Delta\mu_{eff.}$/(absolute value), for a 1 percent diameter variation in nonferromagnetic cylinder (*f.* 35) 37
- Conductivity measurement 36
- Diameter measurement 38
- Setting tolerance limits 38
- Detecting cracks independently of diameter variations 38
  - Component of quotient $Q = \Delta\mu_{eff.}$/(absolute value), perpendicular to diameter direction in effective permeability plane (*f.* 36) 39
- Crack evaluation with diameter variations 39

References 39

SECTION 37

EDDY CURRENT CYLINDER TESTS

Conductivity, Permeability, and Diameter of Cylindrical Test Objects

ASSUMPTIONS USED IN ANALYSIS. The influence of test-object electrical conductivity σ, magnetic permeability $\mu_{rel.}$, and diameter d will be explored for the case of a long, cylindrical test object within a **cylindrical test coil arrangement,** with the same basic assumptions listed in the preceding section for the analysis of effective permeability. These test-object properties influence the value of the **characteristic function**; i.e.,

$$1 - \eta + \eta\mu_{rel.}\mu_{eff.}$$

used in calculating coil impedance characteristics (Eqs. 13, 15, 16, and 17 in the section on Eddy Current Test Principles) or secondary coil voltages. This function contains all the **basic factors which influence eddy current tests** where:

1. The **effective permeability** $\mu_{eff.}$ is determined by the frequency ratio f/f_g.
2. The **limit frequency** f_g is a function of the physical properties of the test object, including conductivity σ, permeability $\mu_{rel.}$, and diameter d.
3. The **test frequency** f is a characteristic of the test instrument.
4. The **fill factor** η is determined by the diameter of the test object, d, and the inside diameter of the test coil, D.

Fortunately for the development of a number of practical eddy current test instruments, the electrical conductivity σ appears only in the term $\mu_{eff.}$ of the characteristic function. (See Eq. 5 in the section on Eddy Current Test Principles.) On the other hand, the test-object diameter d influences both the effective permeability $\mu_{eff.}$ and the fill factor η.

SEPARATION OF EFFECTS OF CONDUCTIVITY AND DIAMETER (NONMAGNETIC CYLINDER). To illustrate the possibilities for separation of the effects of variations in electrical conductivity from those of test-object diameter, the case of a nonferromagnetic cylinder will be considered. The test object will be assumed to be an **aluminum rod** (with a conductivity $\sigma = 35$ meter/ohm-mm.^{2}, a diameter $d = 1.2$ cm., a magnetic permeability $\mu_{rel.} = 1$) which entirely fills the test coil so that fill factor $\eta = 1$. The limit frequency f_g is calculated from Eq. (5), Eddy Current Test Principles, to be $f_g = 100$. The test frequency of the instruments is assumed to be $f = 10{,}000$ c.p.s., so that the frequency ratio $f/f_g = 100$.

From the outermost curve of Fig. 10 in the section on Eddy Current Test Principles (which applies for $\eta = 1$), the point $f/f_g = 100$ (point D) is selected in order to obtain the secondary voltage of the test coil normalized to the "empty coil" value (see Eq. 16, Eddy Current Test Principles). Now suppose that the aluminum rod is ground down from its original diameter (1.2 cm.) to 0.85 cm.

From Eq. (5), Eddy Current Test Principles, the frequency ratio f/f_g is now 50. From Eq. (10) in the same section, the fill factor η is calculated as 0.5.

To compute the new position on the impedance plane corresponding to the **reduced bar diameter** (see Fig. 10 in the section on Eddy Current Test Principles):

1. The value $(1 - \eta) = 0.5$ is measured along the ordinate. This distance OB corresponds to the **influence of the annular air ring** upon the secondary coil voltage.
2. The components of the product $\eta\mu_{eff.}$ (where $\eta = 0.5$ and the components of $\mu_{eff.}$ are found in the section on Eddy Current Test Principles from Fig. 8 for $f/f_g = 50$) are plotted vectorially from point B. The real component $(BE) = 0.5 \times 0.20$ is plotted along the ordinate axis. The imaginary component $(EF) = 0.5 \times 0.18$ is plotted parallel to the abscissa.
3. The **characteristic function** corresponding to the reduced bar diameter is represented by point F on the complex voltage plane. The vector OB represents the term $(1 - \eta)$, the vector BF corresponds to the term $\eta\mu_{eff.}$, and their vector sum OF corresponds to the entire characteristic function $(1 - \eta + \eta\mu_{eff.})$.

Thus, the reduction of bar diameter from 1.2 to 0.85 cm. has displaced the normalized secondary voltage (or the normalized impedance values) from point D to point F.

If the diameter of the aluminum rod is still further decreased to 0.6 cm., the new frequency ratio f/f_g will equal 25, and the fill factor η will equal 0.25. In the complex plane of Fig. 10 in the section on Eddy Current Test Principles, the distance OG corresponds to the term $(1 - \eta) = 0.75$. Addition of the components of $\eta\mu_{eff}$ for $f/f_g = 25$ locates point I for the characteristic function for the aluminum rod of 0.6-cm. diam.

Variation of Conductivity σ. If the electrical conductivity of the original 1.2-cm. diam. aluminum rod had been reduced from its original value of $\sigma = 35$ to a new value of $\sigma = 17.5$ (for example, **by heating**), point D on the outermost curve of Fig. 10 in the section on Eddy Current Test Principles would be displaced from the value corresponding to $f/f_g = 100$ to the point K whose $f/f_g = 50$ (see Eq. 5, Eddy Current Test Principles). Thus, conductivity variations take place in a different direction from diameter variations in the complex impedance or voltage planes. This introduces the possibility (later discussed in more detail) of separating conductivity variations (used, for example, in sorting alloys) from diameter changes.

CHARACTERISTICS OF THE COMPLEX IMPEDANCE OR VOLTAGE PLANES. Fig. 1 shows curves of the characteristic function on the complex impedance or voltage plane for fill factors of $\eta = 1$, 0.75, 0.50, and 0.25. Various frequency ratios f/f_g are marked on the various fill-factor curves. The **directions of conductivity variations** are indicated by arrows labeled with σ. The **directions of diameter variations** are shown by arrows labeled d. The characteristics discussed here and illustrated by Fig. 1 are used as a basis for several eddy current instruments to be described later.

Selection of Frequency for Separation of Diameter and Conductivity Variations. At low test frequencies, where f/f_g takes on low values, the characteristic function is represented by points near the top of the curves of Fig. 1. Here the angle between the directions of diameter and conductivity variations decreases considerably, and the separation of these points is difficult. The separation of diameter and conductivity effects is better where the angle between the two variations is greater. For best results it is desirable to work at frequency ratios f/f_g larger than 4.

Effect of High Test Frequencies. At high test frequencies, where the f/f_g ratio is of the order of 10 or greater, the characteristic function is represented by points on the lower halves of the curves of Fig. 1. As the frequency ratio approaches infinity (very high test frequencies), the direction of changes due to diameter variations approaches the vertical, the direction of the self-induction or of the imaginary component of secondary coil voltage. On the other hand, variations in electrical conductivity σ cause displacements at an angle of about 45 deg. to the abscissa in the complex plane.

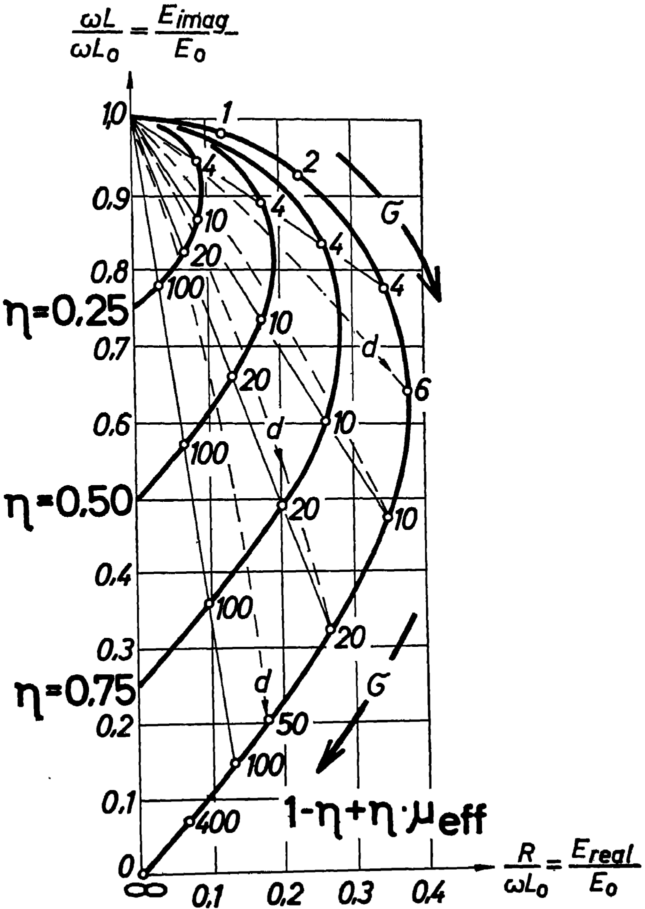

Institut Dr. Foerster

Fig. 1. Complex impedance and voltage planes for various fill factors (nonferromagnetic materials).

Effect of Low Test Frequencies. For very small f/f_g ratios, the direction of diameter changes approaches the direction of changes in resistance (parallel to the abscissa). This is the direction of the real component of voltage, E_{real}. As f/f_g becomes smaller (near the tops of the curves), the directions of changes in apparent test coil resistance R and test-object conductivity σ approach each other.

Effect of Variation in Fill Factor. Lines connecting the point at which $\mu_{\text{eff.}} = 1$ (top left of impedance plane) to specific f/f_g points on the curve for fill factor $\eta = 1$ intersect the curves for all other fill factors at exactly the same f/f_g values. In other words, a straight line drawn from the point for $\mu_{\text{eff.}} = 1$ shows the effect of variation in fill factor at a constant test frequency.

Determination of Limit Frequency f_g. The straight lines connecting points of various fill factors for a given test frequency also permit **evaluation of an eddy current test without detailed coil data.** The angle ϕ between the ordinate axis and the straight line corresponding to a specific f/f_g ratio is independent of the fill factor η; that is, independent of the test coil data. Consequently the f/f_g ratio for the test object can be determined simply by measuring only the angle ϕ. Since an instrument normally operates at a specific frequency f, the limit frequency f_g is given by the angle ϕ. The diameter of the test cylinder can be easily measured with a caliper. Thus, with the aid of Eq. (5), Eddy Current Test Principles, and the values of f_g and d, the value of the electrical conductivity σ can be obtained quantitatively without specific coil data.

Quantitative Test Indications. Practical eddy current test instruments to be described later have the following capabilities. They

1. Read directly the product σd^2 (electrical conductivity times square of cylinder diameter).
2. Indicate quantitatively, for each sensitivity step, the effect of 1 percent variation in electrical conductivity or in diameter.
3. Show crack depths of specific magnitudes, such as 5, 10, or 20 percent of the cylinder diameter.

SEPARATION OF EFFECTS OF CONDUCTIVITY, DIAMETER, AND RELATIVE MAGNETIC PERMEABILITY (FERROMAGNETIC CYLINDERS).[28] Eq. (16), Eddy Current Test Principles, used in the analysis of the response of the test coil to nonferrous cylinders, can be modified to show the entirely different effect of ferromagnetic test materials. The **relative magnetic permeability** of ferromagnetic materials is normally far greater than unity ($\mu_{\text{rel.}} >> 1$). When the fill factor η is not too small, the term $(1 - \eta)$ can often be neglected in comparison with the much larger term $\eta\mu_{\text{rel.}}\mu_{\text{eff.}}$. In consequence Eqs. (16 a and b) may be modified for this case as follows:

$$\frac{E_{\text{imag.}}}{E_0} = \frac{\omega L}{\omega L_0} \cong \eta\mu_{\text{rel.}}\mu_{\text{eff.(real)}} \quad \text{(approx.)} \tag{1a}$$

$$\frac{E_{\text{real}}}{E_0} = \frac{R}{\omega L_0} \cong \eta\mu_{\text{rel.}}\mu_{\text{eff.(imag.)}} \quad \text{(approx.)} \tag{1b}$$

Fig. 2 shows the **complex impedance plane** for the case in which a ferromagnetic test cylinder entirely fills the test coil (fill factor $\eta = 1$). This curve differs from preceding curves in that the values of $\mu_{\text{eff.(real)}}$ and $\mu_{\text{eff.(imag.)}}$ are increased by the factor $\mu_{\text{rel.}}$.

The **effective permeability components,** $\mu_{\text{eff.(real)}}$ and $\mu_{\text{eff.(imag.)}}$ depend only upon the value of the frequency ratio; thus

$$\frac{f}{f_g} = \frac{f\mu_{\text{rel.}}\sigma d^2}{5066} \tag{2}$$

In Eq. (1), the factor $\eta\mu_{\text{rel.}} = (d^2/D^2)\mu_{\text{rel.}}$ appears in the same manner as in Eq. (2); i.e., as the product of the relative permeability and the square of the test-object diameter. Because they are associated together in this manner, variations in $\mu_{\text{rel.}}$ and d appear in the same direction on the impedance plane (Fig. 2).

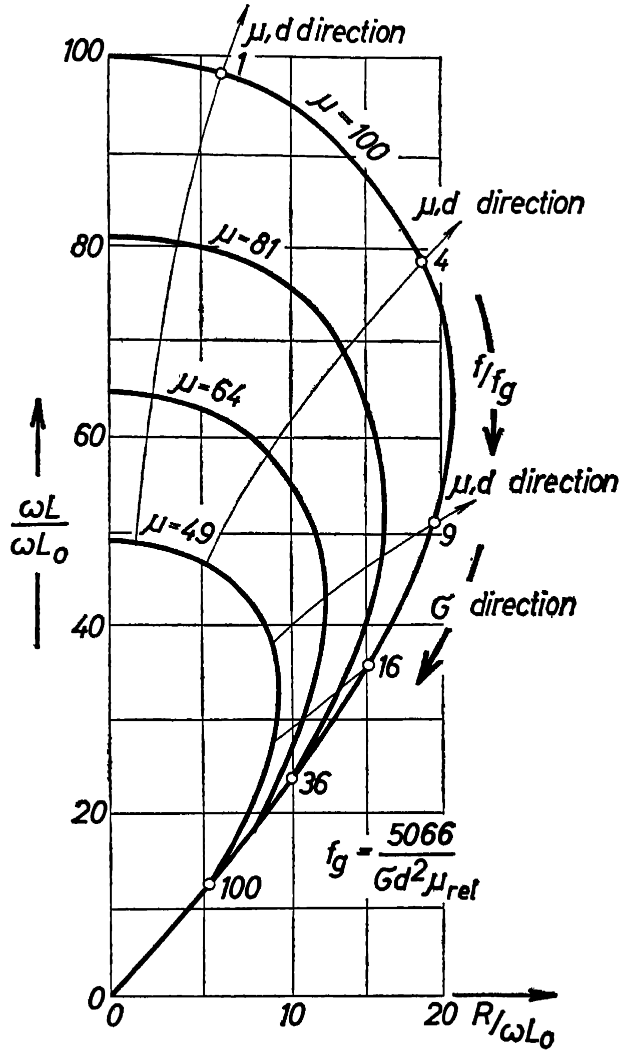

Institut Dr. Foerster

Fig. 2. Complex impedance and voltage planes for ferromagnetic cylinders with various relative permeabilities (fill factor $\eta = 1$).

Consequently it is impossible to distinguish whether a change in this direction is caused by a permeability or by a diameter effect.

Advantage in Crack Detection. Fortunately, in surface crack testing of steel, for example, the common direction of diameter and permeability changes on the impedance plane is at a relatively large angle to the direction of changes caused by cracks in test cylinders. Thus the interfering effects of variations in diameter and permeability can be separated from the indications of surface cracks. Such permeability variations can arise from conditions such as internal stress following straightening. They are often very annoying difficulties in eddy current tests of steel parts.

Effect of Changes in Cylinder Diameter. With nonferromagnetic materials, an increase in cylinder diameter resulted in a decrease in the effective permeability (see Fig. 1). However, an opposite effect is obtained with ferromagnetic materials in the useful range (see Fig. 2) of measurements ($0 < f/f_g < 200$). Here the increase in the quantity of magnetic material in the test coil (which increases the secondary voltage) outweighs the weakening of the field by eddy currents (which tends to reduce the secondary voltage).

Effect of Changes in Electrical Conductivity. In the impedance or voltage plane of Fig. 2, the direction of changes in electrical conductivity σ is identical to the direction of changes in effective permeability with variations in frequency ratio f/f_g. Conductivity changes can be separated from the effects of changes in diameter or permeability most effectively in the upper half of the impedance plane of Fig. 2, where the angle between the conductivity direction and the direction of diameter and permeability changes is greatest. For f/f_g ratios less than 15, changes in conductivity (which are a function of **alloy content** and of **structural conditions related to hardness**) can be measured independently of the effects of permeability changes due to **mechanical stress after cold-working** such as drawing or straightening. Such measurements can also be made independent of the effects of the diameter variations always present in commercial parts.

Effects of Magnetic Hysteresis. Magnetic hysteresis effects add to the horizontal or real component of the apparent impedance of the test coil, in the direction of $\mu_{\mathrm{eff.(imag.)}}$ of Fig. 2. However, this component is always small in comparison with the component due to eddy currents and will be neglected in this discussion.

Separation of Variable Parameters. The preceding observations indicate the degree of separation feasible, at any given test frequency and for a given coil diameter (fill factor η), of the variables:

1. Effects of electrical conductivity σ.
2. Effects of magnetic properties $\mu_{\mathrm{rel.}}$.
3. Effects of geometrical properties (diameter of cylinder d).

The direction of changes of the apparent impedance of the test coil indicates which effect was responsible for the impedance variations. Instruments have been developed for the continuous testing of nonferrous wires and rods, for example, which measure electrical conductivity and diameter directly with an accuracy of 1 percent while samples pass through the test coil rapidly and without contacting it (see section on Eddy Current Test Equipment).

Field Strength and Eddy Current Distribution in Cylinders [48]

FIELD STRENGTH DISTRIBUTION. The distributions of magnetic-field strength and of eddy current density within the cylindrical test object placed in the a.-c. field of the test coil determine the **depth sensitivity** of the test method. The formulas given in the literature for the field strength penetration depth apply only for **very high frequency ratios**, where the Bessel functions can be approximated by means of exponential functions. However, the range of high f/f_g ratios is of little interest in eddy current nondestructive tests. At high test frequencies the sensitivity to conductivity and crack effects is reduced considerably, whereas the sensitivity to diameter changes increases considerably. To obtain the **true field strength** and **eddy current distributions** within the test

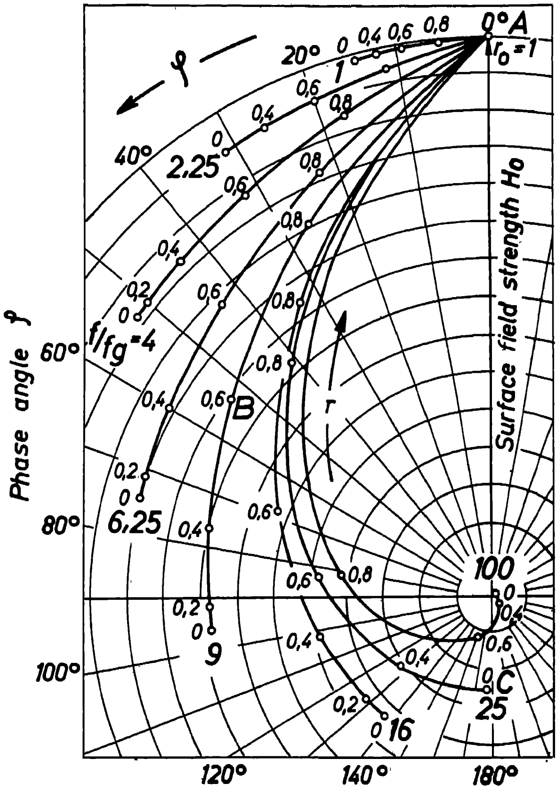

Fig. 3. Amplitude and phase angle of field strength distribution within a metallic cylinder. Curves show various frequency ratios f/f_g. Numbers on curves show fraction of cylinder radius from surface ($r = r_0$).

cylinder, the f/f_g ratio must be calculated by Eq. (5), Eddy Current Test Principles, for the test object. This ratio characterizes its physical properties of electrical conductivity σ, relative magnetic permeability $\mu_{\text{rel.}}$, and diameter d, as well as the test frequency f.

Fig. 3 shows the field strength distribution within **cylindrical specimens** for various frequency ratios. The vector from the zero point of the coordinate system to the point $r_0 = 1$ corresponds in magnitude and direction to the field strength directly at the surface of the test cylinder (the **external field strength**). Numbers along the curves indicate **radial location** in the cylinder, in fractions of the cylinder radius. For example, the value of 0.6 corresponds to a point at a radius of 60 percent of the distance from the center line to the outer surface r_0 of the cylinder. Such a point would lie beneath the cylinder surface by a distance corresponding to 20 percent of the **diameter** of the cylinder ($2r_0$). For low multiples of the limit frequency f_g (small frequency ratios f/f_g), the field strength suffers a **phase displacement** toward the center of the cylinder. At high frequencies, in addition to the phase displacement, the field strength also diminishes rapidly toward the center of the specimen.

EDDY CURRENT DISTRIBUTION. Fig. 4 illustrates the distribution of **eddy current density** from the surface to the interior of the cylinder, in fractions of the specimen radius, for various frequency ratios. The current density values given in this figure correspond to an external field strength of 1 oersted in the test coil. **Defects or discontinuities** within the cylindrical specimen can be detected only when the eddy currents are interrupted or deflected by the discontinuity. In contrast to the field strength, the eddy current density always disappears at the center of the cylinder. Thus **discontinuities which lie exactly along the center line** (such as central piping) cannot be detected. The depths at which discontinuities can be detected beneath the surface will be described quantitatively later.

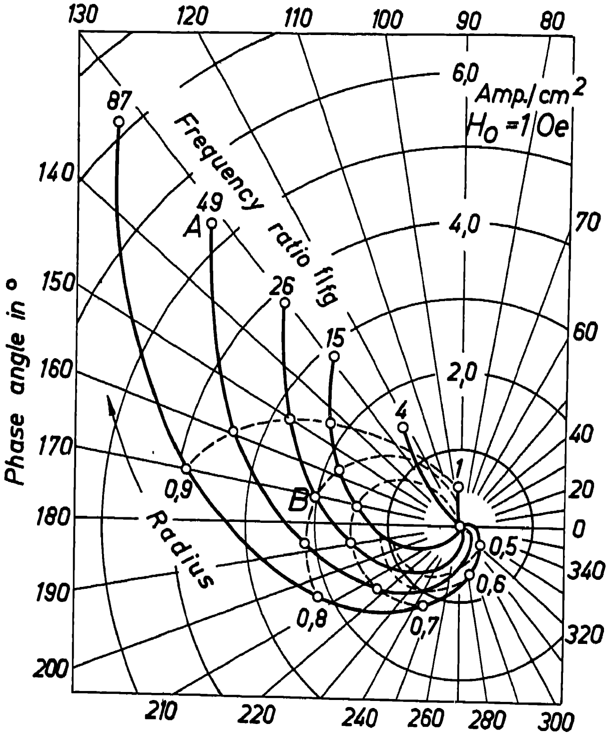

Fig. 4. Amplitude and phase angle of eddy current distribution within a metallic cylinder. Curves show various frequency ratios f/f_g. Numbers on curves show fraction of cylinder radius from outer surface (r_0).

Examples of Eddy Current Distributions. Fig. 5 shows the absolute magnitudes of eddy current and field strength distributions (without regard to phase angles) at whole multiples of the limit frequency throughout the cross-section of the cylinder. Its use will be explained by means of an example. Assume that the test object is a **cylindrical rod of an aluminum-magnesium-copper alloy** whose electrical conductivity $\sigma = 20$ meter/ohm-mm.^{2} and whose diameter $d = 1.6$ cm. The limit frequency is calculated from Eq. (5), Eddy Current Test Principles, as $f_g = 100$. At a test frequency of 10,000 c.p.s. $= 100\ f_g$, the field strength is practically zero at 0.3 of the radius from the center line, while at 0.9 of the radius, the field strength is decreased to approximately one-half of the external field strength.

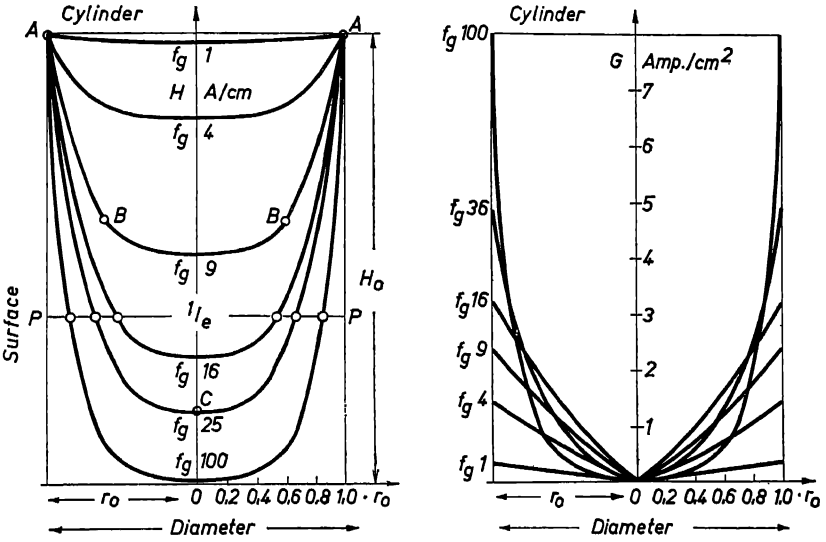

Fig. 5. Magnitudes of field strength and eddy current density as functions of radial position in cylinder, for various frequency ratios f/f_g.

Penetration Depth. The penetration depth P is generally defined as the depth below the surface at which the field strength has decreased to $1/e = 36.8$ percent of the surface field strength. This value is shown in Fig. 5 by the line PP. Thus the penetration depth can be obtained in fractions of cylinder radius for each f/f_g ratio. The frequency ratio f/f_g is calculated by Eq. (5), Eddy Current Test Principles, from the physical constants of the test object and the test frequency. Fig. 6 shows the penetration depth P as a function of the frequency f/f_g. It indicates that for frequency ratios $f/f_g < 13$, the **field strength in the center of the cylinder** is greater than 36.8 percent of the surface field strength. In this case the penetration depth P is greater than the cylinder radius r_0. In Fig. 6 the solid curve labeled H shows the penetration depth P of the **magnetic field strength** H. The solid curve labeled G denotes the penetration depth of the **eddy current density.** The dotted curve gives the theoretical penetration depth for both field strength and eddy current density as calculated from the common approximation formula.

In Fig. 5 it is evident that the eddy current densities at a distance of $0.3r$ from the center of the cylinder are the same at $100\ f_g$ as at $1\ f_g$. However, the eddy

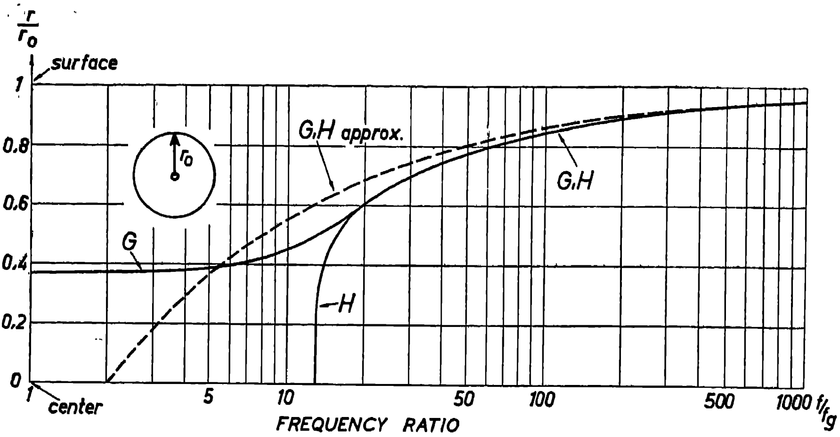

Fig. 6. The penetration depth P at which field strength and eddy current density are $1/e = 37$ percent of surface values, as a function of frequency ratio f/f_g. Solid curve H shows field strength. Solid curve G shows eddy current density. Dotted curve shows penetration depth calculated by approximation formula. Frequency ratio, f/f_g.

current density at the surface of the cylinder is 20 times larger than at 1 f_g. Consequently the **response to surface cracks** is greatly reduced at low f/f_g ratios (low test frequencies) because of the low eddy current density at the surface.

Control of Eddy Current Magnitudes. Fig. 4 shows the amplitude of eddy current densities for various frequency ratios and radial positions in the cylinder. In this case, with an applied field strength of 1 oersted (produced by the coil in the absence of the test object), the current density at the surface of the cylinder would amount to 7.7 amp./cm.^{2}. If the magnetizing field strength were increased to 100 oersteds, the eddy current density would also increase a hundredfold. Thus Fig. 4 makes it possible to determine at each test frequency the **permissible field strengths** which do not exceed practical limits beyond which the test objects would be heated by excessive eddy current density. A **temperature rise during testing** could result in changes in electrical conductivity in the test object, which might result in erroneous test indications.

THE SIMILARITY LAW IN EDDY CURRENT TESTING. The effect of the test object upon the test coil is determined entirely by the ratio of the test frequency f to the limit frequency f_g, as indicated by Eqs. (5) and (16), Eddy Current Test Principles. As indicated in Fig. 7 in the section on Eddy Current Test Principles, the **critical eddy current parameter** $\mu_{\text{eff.}}$, the effective permeability, is determined entirely by the magnitude of the frequency ratio f/f_g. Similarly it is indicated in Figs. 3 and 4 here that the **geometrical distributions of field strengths and of eddy current densities** within the test cylinder are functions only of f/f_g. These conditions lead to the fundamental similarity law for eddy current tests, as follows:

> The effective permeability, as well as the geometrical distributions of the field strength and eddy current densities, is the same for two different test objects if the frequency ratio f/f_g, is the same for each test object.

From Eq. (5), Eddy Current Test Principles, it is evident that this **condition of similarity** is met if

$$f_1\mu_{rel.1}\sigma_1 d_1^2 = f_2\mu_{rel.2}\sigma_2 d_2^2 \tag{3}$$

where the subscripts 1 and 2 refer to the properties of test objects 1 and 2, respectively.

For example, this similarity law indicates that:

1. An aluminum cylinder with an electrical conductivity $\sigma = 35$ meter/ohm-mm.^{2}, with the diameter $d = 10$ cm., whose limit frequency $f_g = 1.45$ c.p.s., tested at a frequency of 145 c.p.s., so that $f/f_g = 100$.

exhibits the same effective permeability and geometrically similar distributions of field strength and eddy current density as:

2. A thin iron wire with an electrical conductivity $\sigma = 10$ meter/ohm-cm.^{2}, a relative peremability $\mu_{rel.} = 100$, with a diameter $d = 0.01$ cm., whose limit frequency $f_g = 50{,}660$ c.p.s., tested at a frequency of 5.07 Mc. per second, so that f/f_g also equals 100.

Application to Detection of Discontinuities. The similarity law provides a basis for the experimental determination of the effects upon the apparent impedance of the test coil of **cracks having a specific depth, shape, and location.** Although the influence of the physical properties and dimensions of cylindrical test objects could be determined mathematically, it is not possible to calculate the effects of defects having specific depth, shape, and location, upon the apparent impedance of the test coil. The similarity law, applied to discontinuities in the material, states:

> Geometrically similar discontinuities (such as cracks with specific depth and width measured in percentage of cylinder diameter) will result in the same eddy current effects and in the same variation of the effective permeability if the f/f_g ratio is the same.

Thus a crack of 0.0005-cm. depth in a tungsten wire of 0.01-cm. diam. would result in the same variation in effective permeability as a crack of 0.5-cm. depth in an aluminum cylinder of 10-cm. diam., or also a crack of 0.005-cm. depth in an iron wire of 0.1-cm. diam., if, for all three examples, the same f/f_g value were chosen by means of a suitable selection of test frequencies.

Application to Model Tests. If model measurements are once made with **artificial discontinuities** for the entire f/f_g range, to determine the variation of effective permeability as a function of crack depth, crack shape, and crack location, the similarity law indicates that:

> The variations in the effective permeability caused by discontinuities obtained by model measurements can be transferred quantitatively to any given test object of cylindrical shape.

This technique will be discussed later.

EXPERIMENTAL VERIFICATION OF MATHEMATICAL CALCULATIONS. The similarity law can be used in experimental verification of the preceding mathematical indications which are basic in eddy current testing. For these tests a **glass cylinder filled with mercury,** with a field test coil wound on the outer surface of the cylinder, can be used (Fig. 7). The field strength within the metallic mercury cylinder is measured by a very small **microcoil** which is moved along the radius of the cylinder by means of a micrometer. The a.-c. field strength measured by the microcoil appears as a voltage across the coil. This **signal voltage** is split into two components by two phase-controlled amplifiers. The two components of the voltage are then applied to the deflection plates of a cathode-ray tube. The **screen display** of the cathode-ray tube reproduces the field strength plane (see Fig. 3), including both phase and amplitude. This arrangement permits direct experimental reproduction of the field strength distributions calculated by means of Bessel functions.

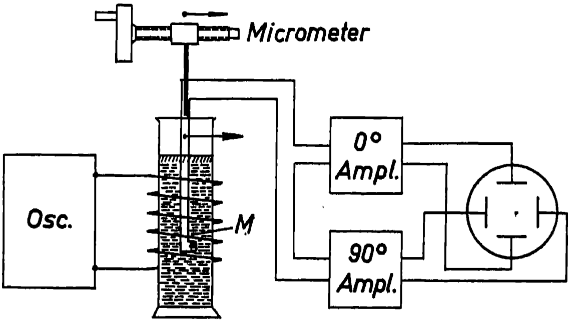

Institut Dr. Foerster

Fig. 7. Mercury model for experimental verification of field strength and eddy current distribution in cylindrical test object.

Fig. 8 shows the **results of field strength measurements** as a function of the radial position of the probe coil in the mercury tube. The experimental points are plotted as small circles, whereas the calculated results are shown as smooth curves. The high degree of correlation between experimental points and calculated values indicates the reliability of the mathematical calculations.

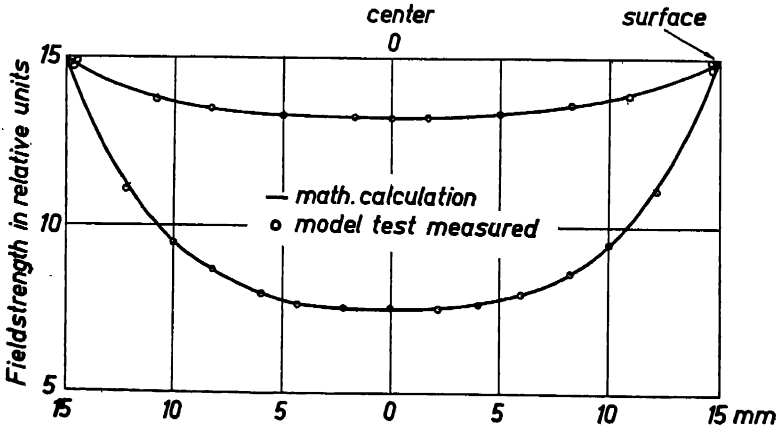

Institut Dr. Foerster

Fig. 8. Comparison between calculated (solid lines) and experimentally determined (o) field strength distribution in mercury model cylinder; for two test frequencies.

MODEL TESTS AS A BASIS FOR QUANTITATIVE TESTS OF DISCONTINUITIES. Mercury is an ideal material for measurements of the effects of discontinuities because any given discontinuity can be easily represented by the insertion of a suitable shape of insulating material. Fig. 9 illustrates the **model test arrangement.** A coil is wound on a glass cylinder. **Insulating bodies** of any desired shape can be inserted within the mercury-filled glass tube. The position of these insulating bodies, representing **artificial defects or discontinuities,** can be changed accurately with the aid of micrometer drives. During insertion of the artificial discontinuities, the mercury can be emptied from the glass cylinder by means of a movable storage reservoir.

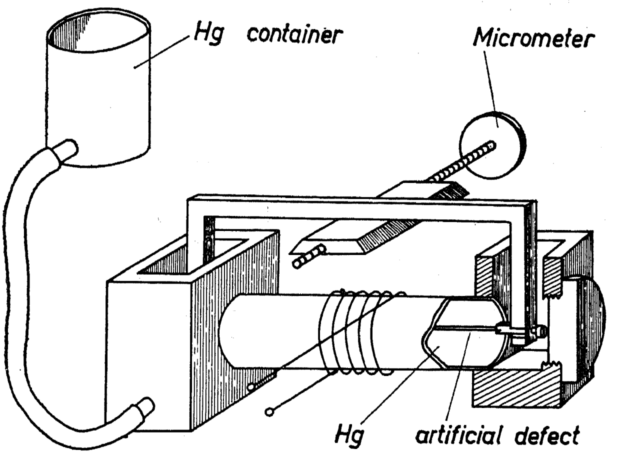

Institut Dr. Foerster

Fig. 9. Model arrangement for simulating any given discontinuity in the mercury cylinder.

Fig. 10 shows the **electric circuit** used for precise measurement of the effects of cracks on the apparent impedance of the test coil throughout a wide frequency range. The bridge arrangement, fed by a variable-frequency generator, contains

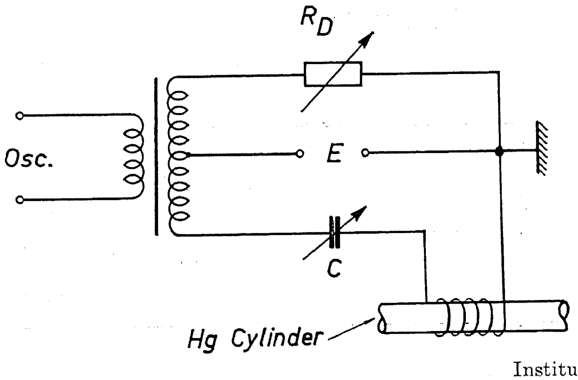

Institut Dr. Foerster

Fig. 10. Electric circuit used in model tests with mercury cylinder.

a precision resistance decade in one arm and a precision capacitance decade in series with the mercury-filled test coil in the other arm. If the variable capacitance and resistance arms are balanced so that zero voltage appears at the input to the amplifier in the diagonal arm of the bridge, the following relations exist:

1. The reactance of the test coil, $\omega L = 2\pi f L$, is equal to the capacitive reactance of the decade capacitor, $1/\omega C$, where f is the test frequency.
2. The resistance of the test coil, R, is equal to the resistance of the variable resistor decade, R_D.

The corresponding values for the test coil without mercury are ωL_0 and R_0 (empty coil values). From Eqs. (16, a and b), Eddy Current Test Principles, the mercury-filled cylinder, prior to insertion of insulating discontinuities, is described by

$$\frac{\omega L}{\omega L_0} = 1 - \eta + \eta\mu_{\text{eff.(real)}} \tag{4a}$$

$$\frac{R - R_0}{\omega L_0} = \eta\mu_{\text{eff.(imag.)}} \tag{4b}$$

If a discontinuity of specific magnitude, location, and shape is simulated in the mercury by the insertion of a piece of plastic, a voltage appears across the diagonal of the measurement bridge of Fig. 10. This voltage is again adjusted to

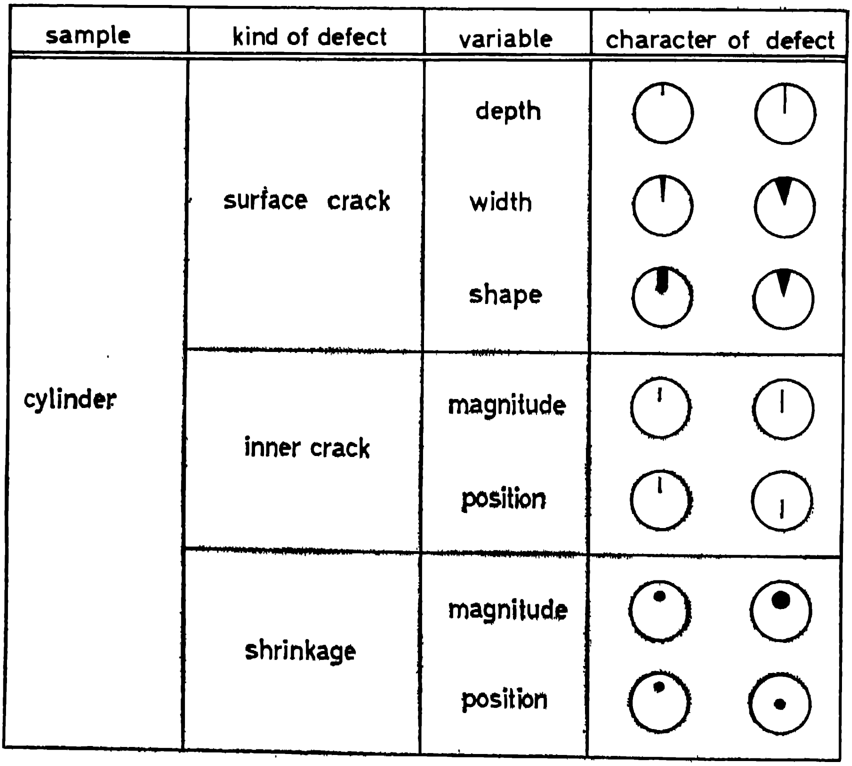

Institut Dr. Foerster

Fig. 11. Summary of types of discontinuities in cylindrical specimens studied in mercury model tests.

zero by varying the capacitive and resistive arms of the bridge, to obtain values of C_{crack} and R_{crack}. The variation of the effective permeability $\Delta\mu_{\text{eff.}}$, resulting from the presence of the crack, is calculated by means of the following relations:

$$\Delta\,\mu_{\text{eff.(real)}} = \frac{C_0}{\eta}\left[\frac{(C_{\text{crack}} - C)}{C(C_{\text{crack}})}\right] \tag{5a}$$

$$\Delta\,\mu_{\text{eff.(imag.)}} = \frac{\omega C_0}{\eta}(R_{\text{crack}} - R) \tag{5b}$$

In addition to the known fill factor for the coil arrangement, Eqs. (5, a and b) contain only factors measured very exactly with the precision condenser and resistor of the bridge circuit. Fig. 11 illustrates the scope of a program of more than 50,000 measurements to determine the influence of given discontinuities upon the effective permeability of cylindrical specimens over the entire range of frequency ratios. Once obtained, these results can be transferred to any given material and test cylinder in accordance with the similarity law. The results of these model measurements indicate if and how discontinuities with specified shape, depth, and location will be indicated by eddy current tests.

Test Coil Arrangements for Feed-through Testing

CLASSIFICATION OF FEED-THROUGH COIL ARRANGEMENTS. Various coil arrangements are used in the field in eddy current testing where cylindrical test objects are inserted into the coil for measurement. Coil types include:

1. Single primary coil, Fig. 12(a).
2. Primary and secondary coils, Fig. 12(b).
3. Bridge arrangement of two primary coils, Fig. 12(c).
4. Bridge arrangement of two primary and two secondary coils, Fig. 12(d).
5. Comparison arrangement of two primary coils, Fig. 12(e).
6. Differential arrangement of two primary and two secondary coils, Fig. 12(f).

With these various coil arrangements, quantitative measurements can determine:

1. The absolute value of electrical conductivity σ.
2. Phase and amplitude variations caused by diameter or conductivity variations or by a surface crack of specific depth.

These quantitative measurements are possible even if the coil data (fill factor η) or the electrical conductivity σ of the test cylinder are unknown.

COMPLEX VOLTAGE OR IMPEDANCE PLANE FOR FEED-THROUGH COILS. Fig. 13 shows the apparent impedance plane, or the complex voltage plane, for the various coil arrangements of Fig. 12. It is constructed for the assumed case in which the fill factor $\eta = 0.75$ and the frequency ratio $f/f_g = 9$. As indicated previously, the same complex plane diagram applies whether:

1. The ordinate represents the normalized inductive reactance, $\omega L/\omega L_0$, and the abscissa represents the normalized coil resistance $R/\omega L_0$, or
2. The ordinate represents the imaginary component of the normalized coil voltage, $E_{\text{imag.}}/E_0$, and the abscissa represents the real component of the normalized coil voltage, E_{real}/E_0.

Single Primary Test Coil. Fig. 12(a) shows the very simple case in which the test coil consists of a single primary winding. In this case, the vector OP_0 of Fig.

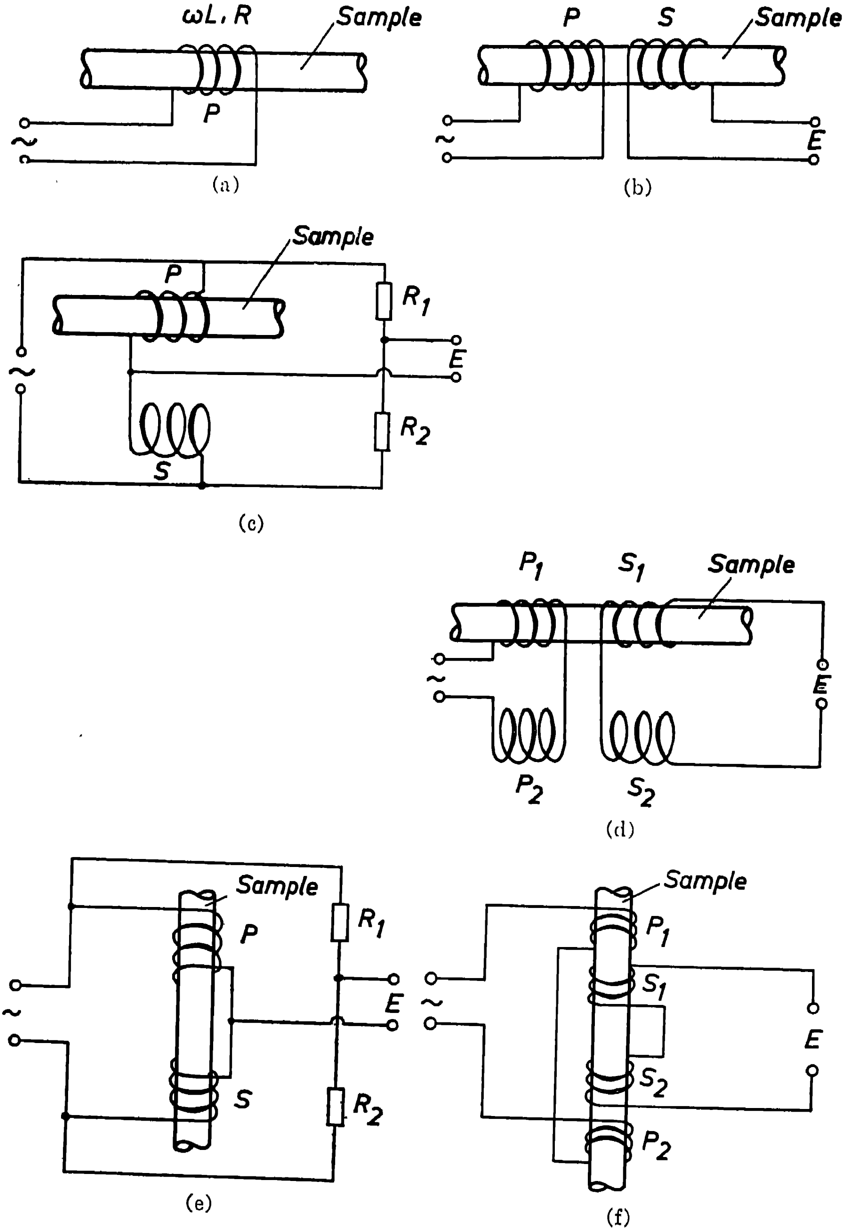

Institut Dr. Foerster

Fig. 12. Arrangements for test coils for feed-through tests. (a) Single primary test coil. (b) Primary and secondary coil. (c) Bridge circuit of two primary coils. (d) Bridge circuit with two primary and two secondary coils. (e) Self-comparison arrangement of two primary coils. (f) Self-comparison arrangement of two primary and two secondary coils.

13 represents the **apparent impedance** of the empty coil or the complex voltage across the empty coil. When the test cylinder is inserted, the new apparent impedance vector OP appears across the coil.

Primary and Secondary Coil Arrangement. For the primary and secondary coil arrangement of Fig. 12(b), the distance OP_0 in Fig. 13 represents the **secondary coil voltage** in the absence of the test object. The vector OP represents the secondary coil voltage with the test cylinder inserted into the coils.

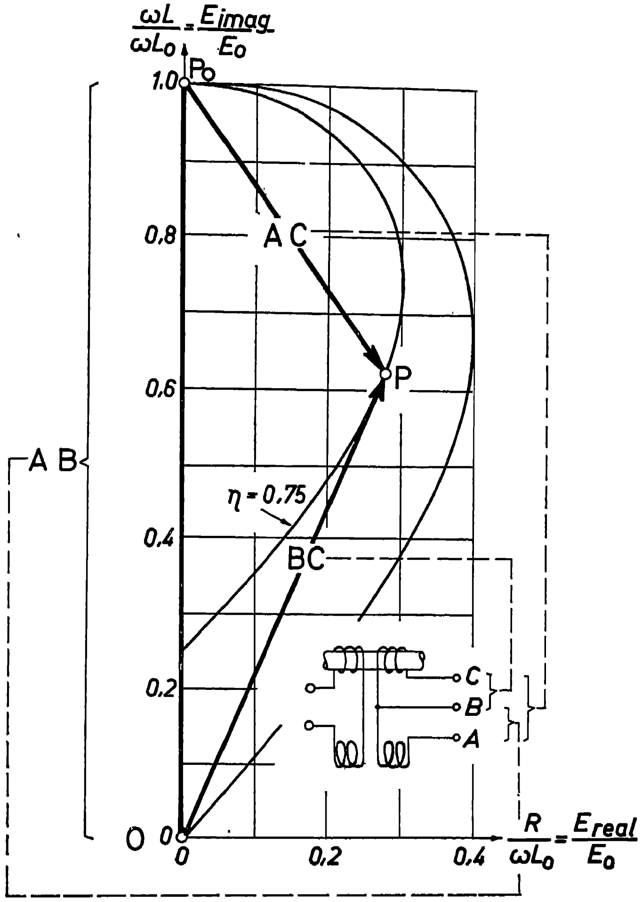

Fig. 13. Complex voltage and impedance planes for test coil arrangements shown in Fig. 12. Fill factor $\eta = 0.75$. Frequency ratio $f/f_g = 9$. Relative permeability $\mu_{\text{rel.}} = 1$.

Bridge Arrangements of Test Coils. In the bridge arrangements with two primary coils [Fig. 12(c)] or two primary and two secondary coils [Fig. 12(d)], no voltage appears across the diagonal of the bridge circuit or across the **differentially connected secondary coils** in the absence of the test cylinder. The bridge is balanced, or the two secondary coil voltages cancel each other in the "empty state." When the test cylinder is inserted into either of these coil arrangements, the voltage vector P_0P appears in Fig. 13.

If another test cylinder with the same physical properties is now inserted into the second (empty) coil, the voltage across the bridge terminals, or at the output of the differentially connected secondary coils, disappears. If the physical properties (for example, the conductivity) of one test specimen vary from those of the comparison specimen, their effective permeabilities will also differ. In this case a voltage difference will appear across the terminals of the bridge of Fig. 12(c) or the secondary coils of Fig. 12(d). This **voltage difference, ΔE,** will be related to the difference in effective permeabilities, $\Delta\mu_{\text{eff.}} = \mu_{1\,\text{eff.}} - \mu_{2\,\text{eff.}}$, as follows:

$$\Delta E = E_0(\mu_{1\text{eff.}} - \mu_{2\text{eff.}})\eta = E_0(\eta)(\Delta\mu_{\text{eff.}}) \tag{6}$$

where η is the fill factor of the coil and E_0 the coil voltage in the absence of the test object. But to draw conclusions concerning the **physical cause of the signal voltage** in this case, the following information must be determined in advance:

1. The fill factor η of the coil and test cylinders.
2. The effective permeability $\mu_{\text{eff.}}$ of the test cylinder.
3. From these, the frequency ratio f/f_g used in the test.

The variation in effective permeability caused by a specific conductivity, diameter, or crack effect is a function of the specific frequency ratio used in the test, which in turn depends upon the effective permeability of the test cylinder. With known values for σ, $\mu_{\text{rel.}}$, and d, the **frequency ratio** f/f_g can be determined from Figs. 7 or 8 in the section on Eddy Current Test Principles.

Differential or Self-Comparison Arrangements. In the bridge arrangements of Figs. 12(c) and (d), the second test cylinder served only for compensation of the fundamental voltage (P_0P) of Fig. 13. The test coil arrangements of Figs. 12(e) and (f), on the other hand, employ a different portion of the same cylindrical test object as a **standard of comparison.** This is often called a "self-comparison" arrangement. In this case a voltage appears at the output terminals of the coils only if the **local effective permeability of the test cylinder** differs at the locations of the first and second test coils. If the test cylinder is inserted into only one of the two coils, the voltage (P_0P) of Fig. 13 will again appear at the coil output terminals.

This "self-comparison" arrangement is often used in **crack-test instruments,** since the crack depth normally varies from location to location along the test cylinder. (Note, however, that a long, uniform crack is indicated only at its ends and not along the uniform, continuous portions.) Variations in physical properties (such as conductivity, relative magnetic permeability, and diameter) from one test cylinder to another have no effect with these coil arrangements, since their influence on the effective permeability is compensated by the differential connections of the double test coils. **Slowly varying physical properties** in the test cylinders are also suppressed if the two self-comparison coils are close to each other. The fact that cracks of constant depth cannot be indicated is a limitation of the self-comparison test method, which will be discussed later in more detail.

Tests for Cracks in Solid Cylinders

CRACKS IN NONFERROUS CYLINDRICAL TEST OBJECTS. Figs. 14 through 17 show apparent impedance variations resulting from cracks of various depths and radial locations in nonferromagnetic cylinders for frequency ratios of 5, 15, 50, and 150. The frequency ratio $f/f_g = 5$ is particularly useful, since it permits **detection of surface and subsurface cracks with the same sensitivity.**

As indicated in Eq. (17), Eddy Current Test Principles, the components of the effective permeability are equal to those of the apparent impedance or those of the secondary coil voltage if the fill factor $\eta = 1$. Point O in Fig. 14 corresponds to the case of a **nonferromagnetic cylinder without a crack.** This point O appeared on the effective permeability curve of Fig. 7 in the section on Eddy Current Test Principles at the location marked $f/f_g = 5$. Thus Fig. 14 represents the area near $f/f_g = 5$ in Fig. 7 (section on Eddy Current Test Principles) but on a considerably enlarged scale. Figs 15, 16, and 17 are corresponding enlargements of the areas near f/f_g ratios of 15, 50, and 150 in Fig. 7 (section on Eddy Current Test Principles). Figs. 14 through 17 permit direct determination of secondary coil voltages corresponding to **surface or subsurface cracks at specific depths and locations.**

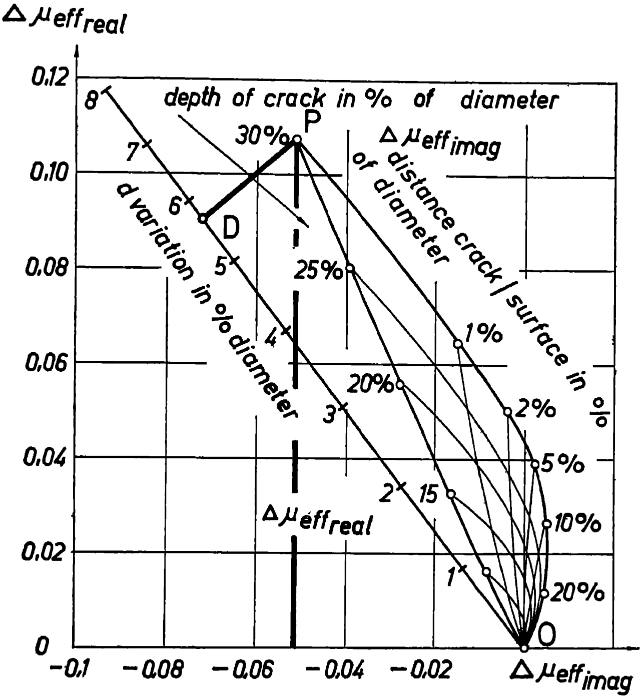

Institut Dr. Foerster

Fig. 14. Impedance variations caused by surface and subsurface cracks in nonferromagnetic cylinders, at a frequency ratio $f/f_g = 5$.

Test Coil Voltages. Fig. 18 illustrates a pair of test coil units consisting of two primary and two secondary coils. When a nonferromagnetic cylinder free from cracks is placed through both coils, no voltage appears at the output terminals of

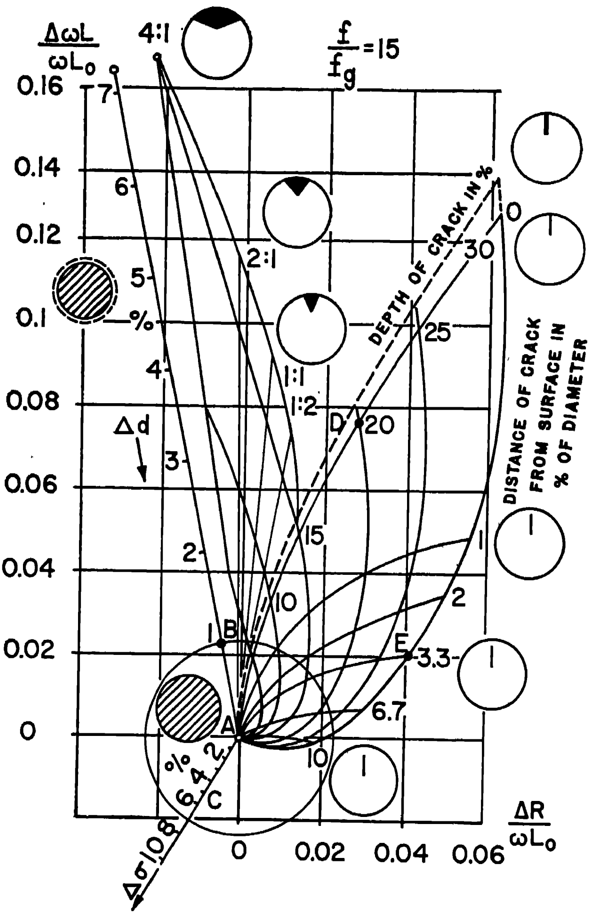

Institut Dr. Foerster

Fig. 15. Impedance variations caused by surface and subsurface cracks in nonferromagnetic cylinders, at a frequency ratio $f/f_g = 15$.

the secondary coils. However, as soon as a crack appears in one of the two test coil locations, the differential voltage ΔE appears. **The normalized components of the crack signal voltage** are

$$\frac{E_{\text{imag.}}}{E_0} = \eta[\Delta\mu_{\text{eff.(real)}}] \tag{7a}$$

and

$$\frac{E_{\text{real}}}{E_0} = \eta[\Delta\mu_{\text{eff.(imag.)}}] \tag{7b}$$

Here E_0 is the voltage of the empty secondary coil, and η is the fill factor of the secondary coil (see Eq. 10, Eddy Current Test Principles). The factors $\Delta\mu_{\text{eff.(real)}}$

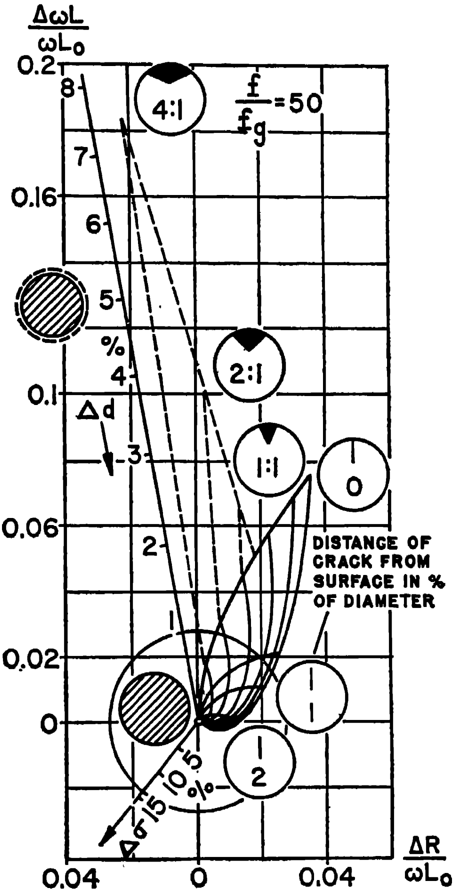

Institut Dr. Foerster

Fig. 16. Impedance variations caused by surface and subsurface cracks in nonferromagnetic cylinders, at a frequency ratio $f/f_g = 50$.

and $\Delta\mu_{\text{eff.(imag.)}}$ are shown as coordinates in Fig. 14. For a surface crack of 30 percent depth, point P has coordinates of

$$\Delta\mu_{\text{eff.(real)}} = 0.11$$

$$\Delta\mu_{\text{eff.(imag.)}} = -0.05$$

These factors, when inserted in Eqs. (7, a and b) for a given crack, indicate the corresponding test coil voltages for this crack.

Suppression of Variations in Cylinder Diameter. Particular attention is directed to those components of the variation in effective permeability which are perpendicular to the direction of diameter variations in the complex impedance plane. Those physical effects of the test object which produce displacements in the impedance plane in the same direction as changes in cylinder diameter cannot be

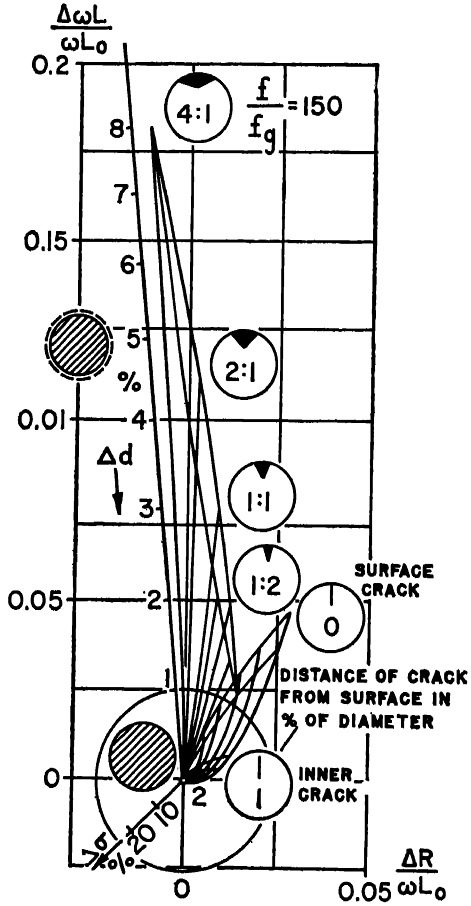

Institut Dr. Foerster

Fig. 17. Impedance variations caused by surface and subsurface cracks in nonferromagnetic cylinders, at a frequency ratio $f/f_g = 150$.

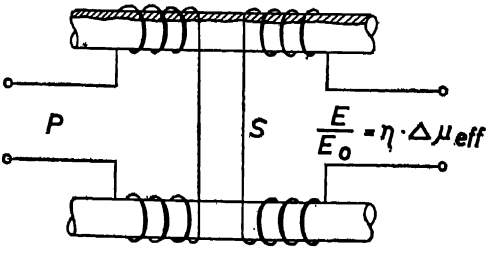

Institut Dr. Foerster

Fig. 18. Differential test coil arrangement containing sound and defective cylindrical test specimens.

separated from the ever-present **interfering variations in diameter.** However, as will be shown later, these interfering diameter effects can be entirely suppressed if test indications can be limited to those which are perpendicular to the direction of diameter variations in the impedance plane. For example, in Fig. 14, the vector *PD* represents the **change in effective permeability or apparent impedance normal to the diameter direction** for a crack of 30 percent depth, tested at a frequency ratio $f/f_g = 5$.

Frequency Selection for Surface Crack Detection. Fig. 19 presents an evaluation of the impedance plane data of Figs. 14 through 17. The ordinates represent the values of the effective permeability variations $|\Delta\mu_{\text{eff.}}|$ resulting from surface cracks. The abscissae show the frequency ratio f/f_g. Various **crack depths** are shown by different curves. For example, the data for 30 percent crack depth correspond to the distance *OP* in Fig. 14 for $f/f_g = 5$.

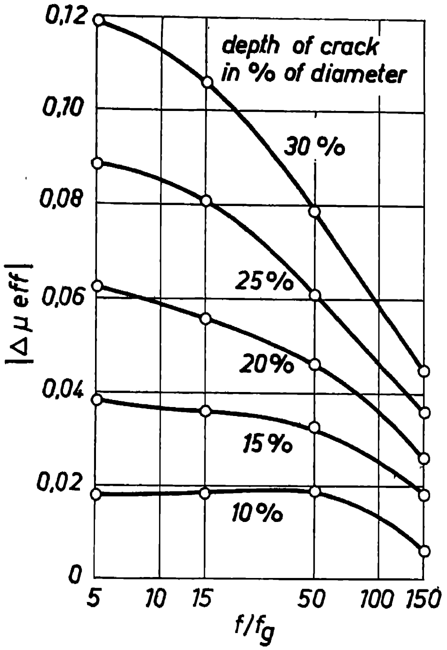

Fig. 19. Magnitude of changes in effective permeability $|\Delta\mu_{\text{eff.}}|$, caused by surface cracks of various depths in nonferromagnetic cylinders, as a function of frequency ratio, f/f_g.

Fig. 20 illustrates the magnitudes of **surface crack signals** in a test **instrument which suppresses the interfering influence of diameter variations.** Here the ordinates represent only the component of the change in effective permeability perpendicular to the direction of diameter changes on the complex impedance planes. Thus, for the evaluation of surface cracks in nonferromagnetic cylinders, independently of variations in cylinder diameter, the **optimum frequency range** as indicated in Fig. 20 is for f/f_g ratios between 10 and 50.

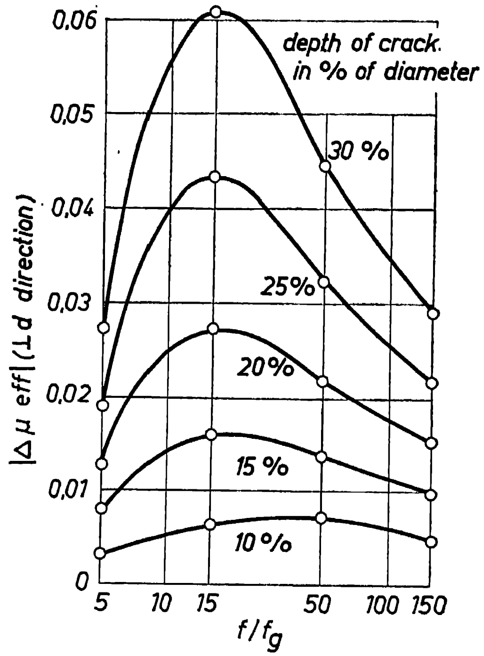

Fig. 20. Magnitude of changes in component of effective permeability $|\Delta\mu_{eff.}|$ perpendicular to direction of diameter changes, caused by surface cracks of various depths in nonferromagnetic cylinders, as a function of frequency ratio f/f_g.

Frequency Selection for Subsurface Crack Detection. Fig. 21 provides a similar evaluation for subsurface cracks in nonferromagnetic cylinders. A crack depth of 30 percent of the cylinder diameter is taken as an example in this illustration. However, families of curves for any other specific crack depths can be derived from these model curves. The ordinates in Fig. 21 represent magnitudes of effective permeability variations $|\Delta\mu_{eff.}|$ resulting from subsurface cracks. The abscissae indicate the depth of cracks from the outer surface of the cylinder, in percentage of cylinder diameter. A crack with zero-percent distance is a surface crack. The great decrease in magnitude of crack signals with increasing depth from the surface, particularly at high frequency ratios, is clearly indicated in Fig. 21.

Fig. 22 is analogous to Fig. 20 in that it shows only the component of the change in effective permeability whose direction is perpendicular to the direction of diameter variations in the complex impedance plane. Thus Fig. 22 corresponds to the magnitudes of crack signals obtained in instruments which suppress diameter variations. The curve for $f/f_g = 5$ is important. It illustrates that in the range of this f/f_g value, crack indications on instruments which suppress diameter variations are practically independent of the distance of the crack below the surface of the test cylinder, provided this distance is not excessive. This fortunate independence of depth in the crack indication results from the fact that variations in effective permeability for subsurface cracks result in phase rotations in the complex impedance plane into the direction perpendicular to the diameter variations. Thus the component of $|\Delta\mu_{eff.}|$ perpendicular to the diameter direc-

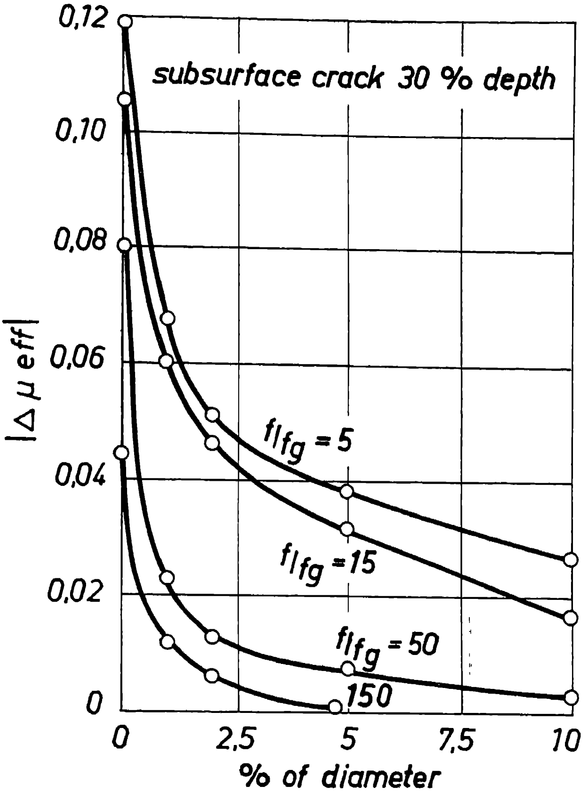

Fig. 21. Magnitude of changes in effective permeability $|\Delta\mu_{eff.}|$ caused by subsurface cracks of 30 percent crack depth at various distances below the surface of nonferromagnetic cylinders. Frequency ratios shown on curves. Distance below surface given in percentage of cylinder diameter.

tion remains practically constant with increasing distance of cracks beneath the surface, whereas the magnitude of $\Delta\mu_{eff.}$ itself decreases considerably, as shown in Fig. 21. Consequently the **optimum test frequencies** for subsurface crack detection correspond to frequency ratios f/f_g which lie between 4 and 20.

CRACKS IN FERROMAGNETIC CYLINDERS. The methods for analysis of cracks in nonferrous cylinders can be extended to the case of ferromagnetic cylinders, at least in so far as the magnitude of the variation in effective permeability (see Fig. 19) is concerned. For a ferromagnetic cylinder the **signal voltage components** of Eqs. (7, a and b) need only be multiplied by the relative permeability $\mu_{rel.}$ to apply to the ferromagnetic cylinder. For example, if $\mu_{rel.}$ equals 100, the **secondary voltage signal** resulting from the presence of a specific crack is 100 times larger than for the nonferromagnetic cylinder, provided both tests have been made at the same frequency ratio f/f_g.

Suppression of Variations in Cylinder Diameter. The directions of diameter variations are entirely different for ferrous and nonferrous materials in the com-

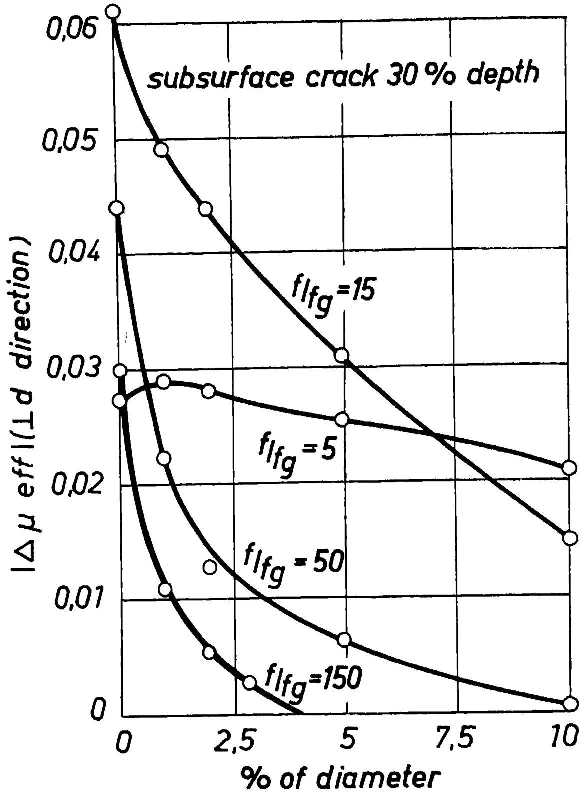

Fig. 22. Magnitude of changes in component of effective permeability $|\Delta\mu_{\text{eff.}}|$ perpendicular to direction of diameter changes, caused by subsurface cracks of 30 percent crack depth at various distances beneath outer surface of nonferromagnetic cylinder. Frequency ratios shown on curves. Distance below surface given in percentage of cylinder diameter.

plex impedance plane (compare Figs. 1 and 2). Fig. 23 shows the component of the variation in effective permeability, perpendicular to the direction of diameter variation, for ferromagnetic cylinders whose relative magnetic permeability $\mu_{\text{rel.}} >> 1$.

Frequency Selection for Crack Detection. In contrast to the situation with nonferrous cylinders, the directions of diameter and of crack effects form a large angle with each other at low frequency ratios in the complex impedance and voltage planes. Therefore, to separate crack and diameter effects for steel cylinders, the **optimum frequencies** correspond to f/f_g ratios of less than 10. However, for ratios of $f/f_g < 10$, the **interfering effects of both diameter and permeability variations** (such as result from cold working or straightening) have the same direction, perpendicular to the direction of crack effects. Thus these two interfering effects are simultaneously separated from the indications of cracks in crack-detection instruments. The preceding observations refer only to the fundamental wave. Effects caused by the appearance of harmonics **(hysteresis loops)** will be discussed in subsequent sections.

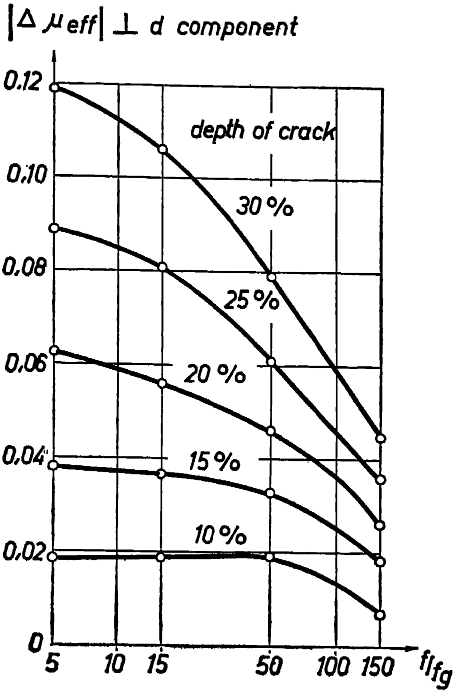

Fig. 23. Magnitude of changes in component of effective permeability $|\Delta\mu_{eff.}|$ perpendicular to the direction of diameter and relative permeability changes, caused by surface cracks of various depths in ferromagnetic cylinders, as a function of frequency ratio f/f_g.

QUANTITATIVE MEASUREMENT OF CRACK DEPTHS. Extensive crack model tests have made it possible to measure crack depths quantitatively and to calibrate eddy current test instruments in terms of crack depth and location. Alternatively, the test instruments can be used to measure variations in diameter or electrical conductivity or the value of the electrical conductivity by itself.

Experimental Determination of Frequency Ratio f/f_g. The frequency ratio f/f_g can be determined experimentally, even with a **fixed-frequency test instrument.** When a cylindrical test specimen is inserted into the measurement coils of Fig. 12(d), for example, the voltage vector P_0P appears in the complex voltage plane of Fig. 13. This voltage vector is characterized both by its magnitude and by the angle α, which the new vector P_0P makes with the voltage vector OP_0 of the empty test coil. Fig. 24 shows the relationship between the angle α and the frequency ratio f/f_g for the case of **nonferromagnetic cylinders.** If the test instrument has a fixed operating frequency, say, 1000 c.p.s. (1 kc.), the f/f_g scale of the instrument can be replaced by a scale reading in terms of the **product σd^2 of the electrical conductivity and the square of the cylinder diameter.** In the case of a cylinder of unknown conductivity, the diameter can be measured with a caliper, and the **conductivity** can be determined directly from the angle α and Fig. 24. This measurement of conductivity is independent of the properties of the test coil or fill factor η.

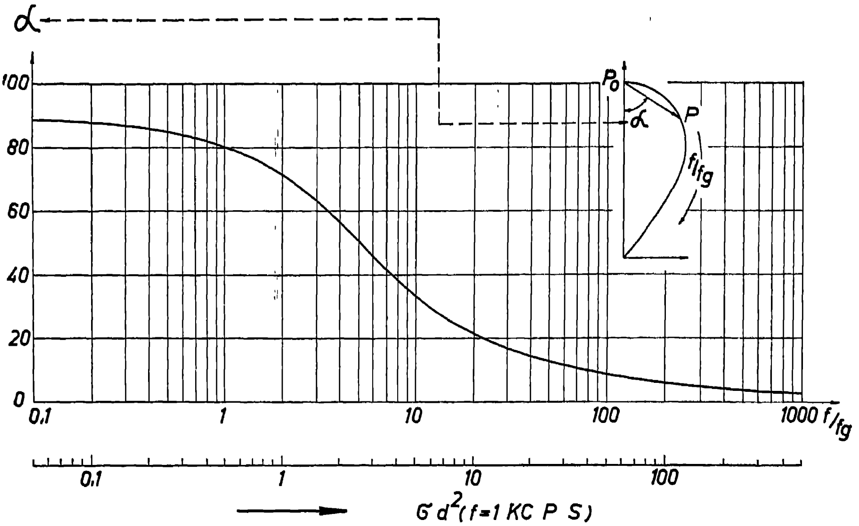

Fig. 24. Variation of angle α with frequency ratio f/f_g or product σd^2 in nonferromagnetic cylinder.

Crack Evaluation with Comparison Specimen. In normal testing with a comparison standard specimen, the standard (crack-free) specimen is placed in one of the two test coils and the unknown specimen in the other coil. The comparison standard serves to compensate the voltage P_0P of the unknown cylinder (see Fig. 25). If the two cylinders are equivalent, the differential connection of the secondary coils causes the two vector voltages P_0P and PP_0 to cancel each other, so that the **output voltage** is zero. However, if the unknown specimen contains a crack, the output voltage vector of its test coil will change from PP_0 to CP_0, for example (see Fig. 25). Now the voltage vectors of the crack-free standard (P_0P) and the cracked specimen (CP_0) no longer cancel. Instead, a complex voltage signal, $\Delta E/E_0 = PC$, appears at the terminals of the differentially connected secondary coils.

If the test cylinders do not fill the test coils but have, for example, a **fill factor** $\eta = 0.75$, the following important relationship is obtained from the similar triangles of Fig. 25:

$$\frac{P_0P}{P_0P_1} = \eta, \qquad \frac{PC}{P_1C_1} = \eta \tag{8}$$

where point P_1 lies on the curve for $\eta = 1$. Here the vector P_1C_1 corresponds to the variation in effective permeability, $\Delta\mu_{\text{eff.}}$, caused by a crack, as described previously (see Fig. 14). These **crack effects** are shown in Figs. 14 to 17 for a fill factor $\eta = 1$. It follows from Eq. (8) that

$$PC = \eta(\Delta\mu_{\text{eff.(crack)}}) \qquad P_0P = \eta(P_0P_1) \tag{9}$$

From Eqs. (8) and (9), one obtains

$$\frac{PC}{P_0P} = \frac{\Delta\mu_{\text{eff.(crack)}}}{P_0P_1} \tag{10}$$

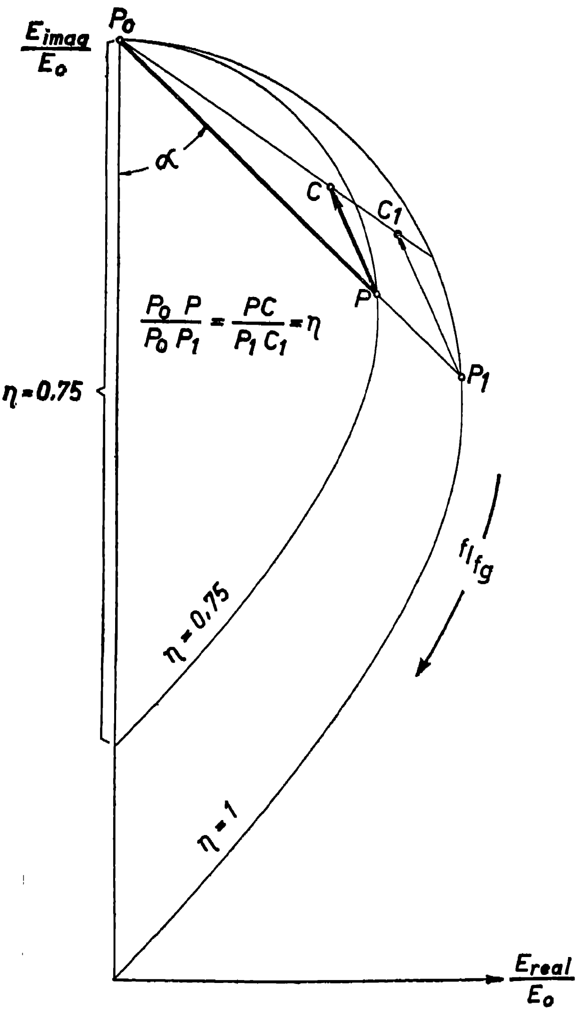

Fig. 25. Explanation of complex plane conditions for comparison specimen test arrangement.

The vector P_0P represents the voltage which appears when one coil contains a cylinder with the fill factor η while the other coil is empty. (This quantity is known in European literature as the **absolute value** of the test cylinder.) From Eq. (10), the **unknown fill factor of the coil** can be determined from the quotient of the measured effect (for example, the variation PC caused by a crack) and the "absolute value" (vector P_0P). The variations in effective permeability found in **crack model tests** (Figs. 14 to 17), divided by the magnitude of the vector P_0P (connecting P_0 to the corresponding f/f_g point P_1 on the $\eta = 1$ curve), correspond to the ratio of the measured effect (PC) to the "absolute value" (P_0P), both measured by the test instrument.

Conductivity or Diameter Evaluation with Comparison Specimen. A similar technique is used in analysis of conductivity or diameter variations. The $\Delta\mu_{\text{eff.}}$ values (from Fig. 1) are divided by the distance from point P_0 to the corresponding f/f_g values on the $\mu_{\text{eff.}}$ curve of Fig. 13 (i.e., by the "absolute value").

Instrument Sensitivity Calibration. Eddy current test instruments (such as those manufactured by the Institut Dr. Foerster in Reutlingen, West Germany) can be equipped with a **sensitivity switch** indicating what percentage of the "absolute value" (P_0P) corresponds to a 1-in. deflection on the cathode-ray screen

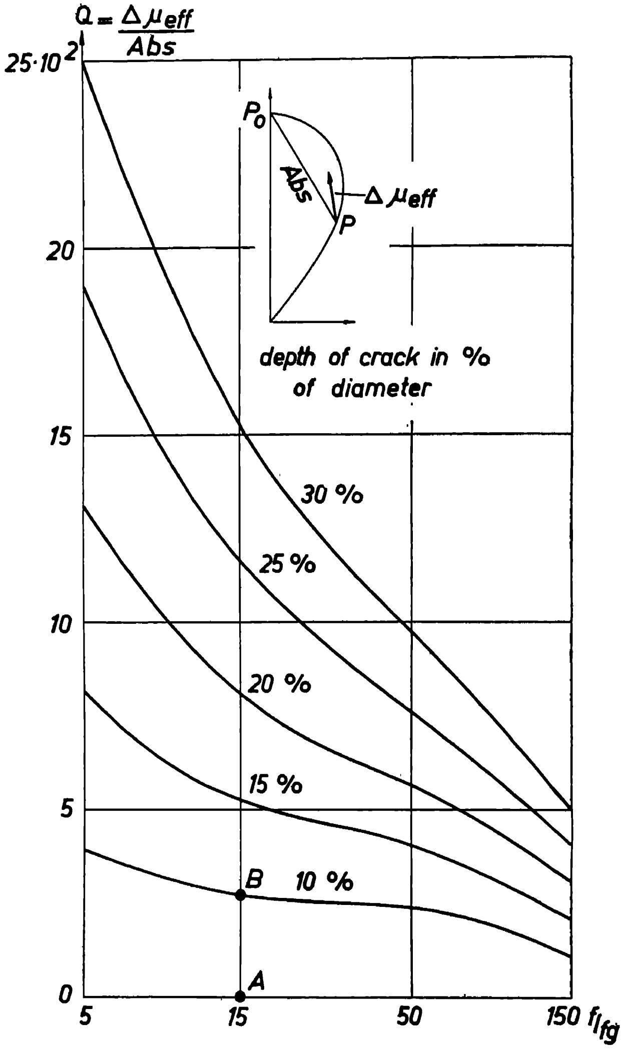

Fig. 26. Quotient $Q = \Delta\mu_{\text{eff.}}/(\text{absolute value})$ as a function of frequency ratio f/f_g for surface cracks of various depths in nonferromagnetic cylinders. Crack depth in percentage of cylinder diameter.

for any given sensitivity step. The frequency ratio f/f_g can also be read from the **phase-shifter** of the instrument through a method described later. These calibrations make the test method quantitative in measuring test-object properties.

Quantitative Crack-Depth Calculations. Fig. 26 can be used as an example for calculating crack depth in nonferromagnetic cylinders from the data of Fig. 19. The ordinate in Fig. 26 corresponds to the ratio

$$Q = \frac{\Delta\mu_{\text{eff.}}}{\text{(absolute value)}}$$

of the variation in effective permeability to the "absolute value" (vector P_0P). Fig. 26 shows **curves for Q for cracks** having depths of 10, 15, 20, 25, and 30 percent of the cylinder diameter.

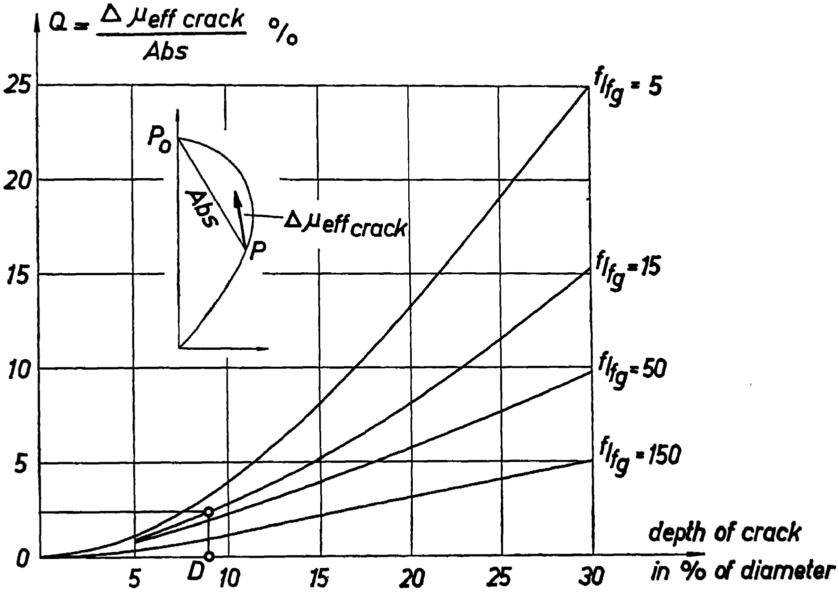

Fig. 27. Quotient $Q = \Delta\mu_{\text{eff.}}/$(absolute value) as a function of crack depth, for various frequency ratios f/f_g, with nonferromagnetic cylinders.

To calculate the **deflection corresponding to a crack of 10 percent depth,** for example, at a given instrument sensitivity setting, the steps are:

1. The frequency ratio f/f_g of the test object is determined from the f/f_g scale (phase shifter) of the test instrument. (For this example assume that the value read is $f/f_g = 15$.)
2. Determine Q (percentage ratio of $\Delta\mu_{\text{eff.}}$ to the "absolute value") from Fig. 26. (For the assumed 10 percent crack depth, the ordinate at point B indicates that $Q = 2.9$ percent.)
3. Determine the sensitivity setting of the test instrument from the sensitivity control knob setting. (For example, the knob may indicate $N = 2$ percent per inch, in which case a deflection of 1 in. on the cathode-ray screen corresponds to 2 percent of the "absolute value.")

4. To obtain the deflection corresponding to a 10 percent crack depth at this sensitivity setting, divide the value of Q by N. (Thus a crack of 10 percent depth would be indicated by a deflection of $Q/N = 2.9/2 = 1.45$ in.)

Computing Crack Depth from Instrument Indication. In normal testing, a deflection appearing on the screen of the test instrument must be converted into crack depth. Fig. 27 is used for this **conversion.** The steps involved are:

1. Read the instrument deflection. (For example, an unknown crack may be indicated by a deflection $A = 2.5$ in. when the sensitivity control setting is $N = 1$ percent per inch and the phase-shift control indicates a frequency ratio $f/f_g = 15$.)
2. Multiply the deflection A by the sensitivity setting N. (In this case, $N \times A = (1\%/\text{inch}) \times (2.5\text{ in.}) = 2.5\%$ of the "absolute value.")
3. On Fig. 27 find the intersection of the ordinate ($Q = 2.5\%$) with the crack-depth curve (for $f/f_g = 15$). Read the corresponding crack depth on the abscissa scale. (In this example point D corresponds to a crack depth $D = 9\%$.)

The preceding explanation applies to surface cracks in nonferrous cylinders. The **position and depth of subsurface cracks** may be established also.[42]

Applications of Test Instruments

OPERATION OF TEST INSTRUMENTS. Fig. 28 shows a simplified **circuit diagram** for a typical ellipse-method eddy current instrument (Sigmaflux or Wire Crack test instrument developed by Institut Dr. Foerster). An oscillator feeds the two pairs of test coils (P_1S_1, P_2S_2) with the magnetizing field current. The secondary windings of the test coils act on the amplifier. The amplifier sensitivity control N indicates the percentage of the "absolute value" corresponding to a 1-in. deflection on the cathode-ray screen. The amplifier output acts on the vertical deflection plates of the cathode-ray tube. The primary magnetizing field current acting through transformer T induces a secondary voltage whose phase angle corresponds to the phase angle of the voltage of a secondary test coil in the

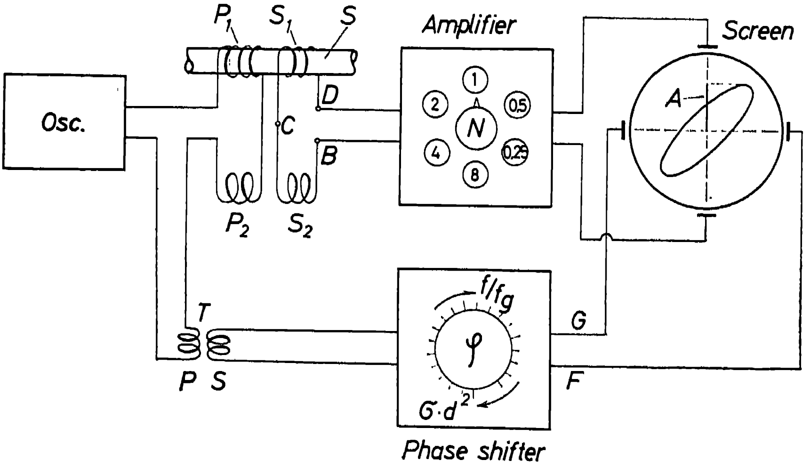

Institut Dr. Foerster

Fig. 28. Simplified schematic diagram of eddy current test instrument for quantitative measurement of crack effects, conductivity effects, and diameter effects in nonferrous cylinders.

absence of a test object. The secondary voltage of the transformer T is applied to a precision phase-shifter whose phase angle is indicated exactly. The output voltage FG of the phase shifter is applied to the horizontal deflection plates of the cathode-ray oscilloscope.

Analysis of Screen Patterns. Before a cylindrical test specimen S is placed in test coil P_1S_1, no voltage is applied to the vertical plates of the oscilloscope. A horizontal straight line appears on the screen. Insertion of the test specimen produces a voltage on the vertical plates. This voltage is proportional to the vector P_0P of Fig. 29. It has the phase angle α, measured between the horizontal and vertical deflection voltages, if the phase-shifter is adjusted to 0 deg. (the direction of the normalized inductive reactance $\omega L/\omega L_0$). Two sinusoidal voltages of single frequency, displaced in phase by the angle α, form an **ellipse on the cathode-ray screen.** The character of the ellipse has special significance in eddy current testing.

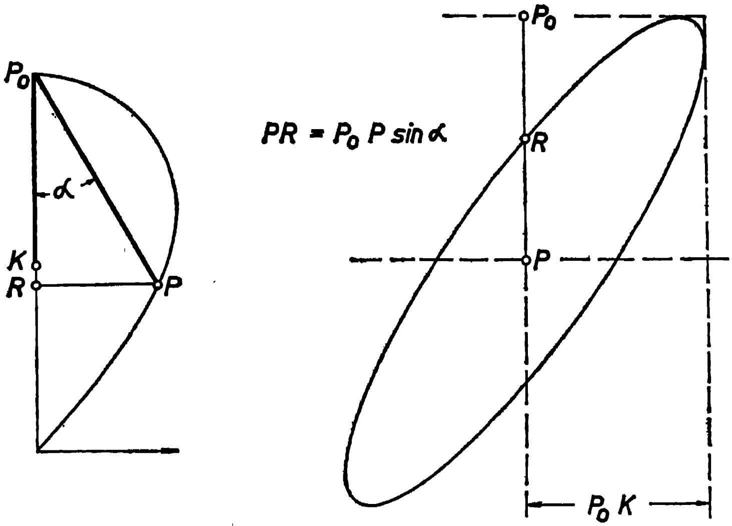

Fig. 29. Characteristics of elliptical screen pattern, resulting from sinusoidal deflection voltages displaced in phase angle, on eddy current test instrument.

Fig. 29 serves to explain the most important **characteristics of the elliptical screen pattern.** The vector voltage P_0P appears as the maximum vertical deflection of the ellipse when a test cylinder is inserted into the measurement coil of Fig. 28. The maximum horizontal deflection of the ellipse has the amplitude P_0K. The vertical section PR from the screen center to the upper side of the ellipse is of special significance. This is the component of the vertical measurement voltage perpendicular to the direction of the horizontal base voltage. It permits **separation of diameter and crack effects.** When the voltage at the horizontal plates lies exactly in the diameter direction (on the effective permeability plane), **diameter effects** acting on the vertical plates can appear on the screen only as inclined straight lines. (This corresponds to no phase displacement between the vertical and horizontal deflection voltages.) In this case, widening or **splitting of the ellipse** (PR in Fig. 29) cannot occur. Thus the splitting (PR), if it appears in the test indications, can be caused only by **cracks or conductivity variations.**

The components of crack and conductivity effects which lie perpendicular to the direction of diameter changes on the effective permeability plane (see Fig. 14) are significant for separation of diameter effects from quantitative measurements of crack and conductivity effects.

Adjustment of the Phase Shifter. The elliptical screen pattern which appears when the test cylinder is inserted into the test coil shows two important characteristic factors, as follows:

1. The magnitude of the "absolute value" of the specimen (vector P_0P).
2. The angle α.

With these factors known, Fig. 24 can be used to determine the frequency ratio f/f_g, and at a given test frequency f, the product σd^2 of the electrical conductivity and the square of the cylinder diameter.

The angle α is adjusted with the precision phase shifter until the ellipse changes into a straight line. The phase-shifter angle at which the ellipse disappears can be determined exactly. The scale of the phase shifter in Fig. 24 is calibrated in terms of the product σd^2 for a test frequency of 1000 c.p.s. When the phase shifter is adjusted to convert the ellipse to a straight line, the frequency ratio f/f_g and the product σd^2 can be read directly from its scale. By measuring the cylinder diameter with a caliper, the electrical conductivity can be determined.

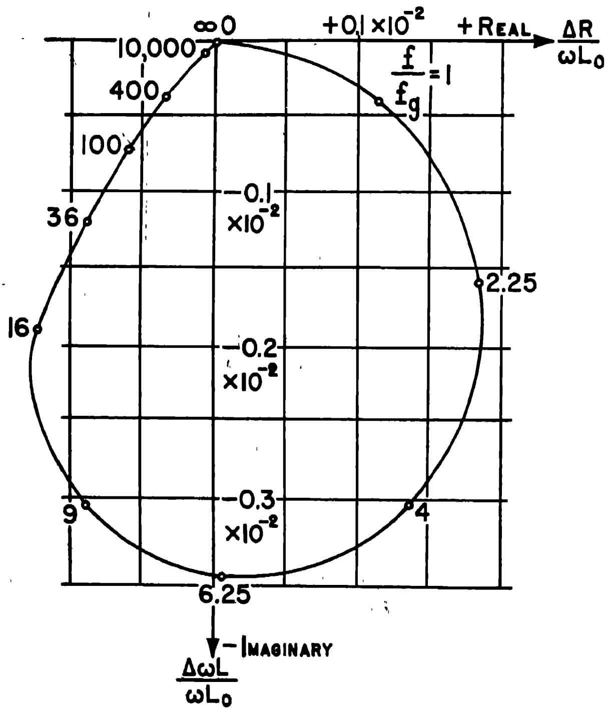

Fig. 30. Impedance variations (amplitude and phase), for a 1 percent variation of conductivity, as a function of frequency ratio f/f_g. Nonmagnetic materials ($\mu = 1$).

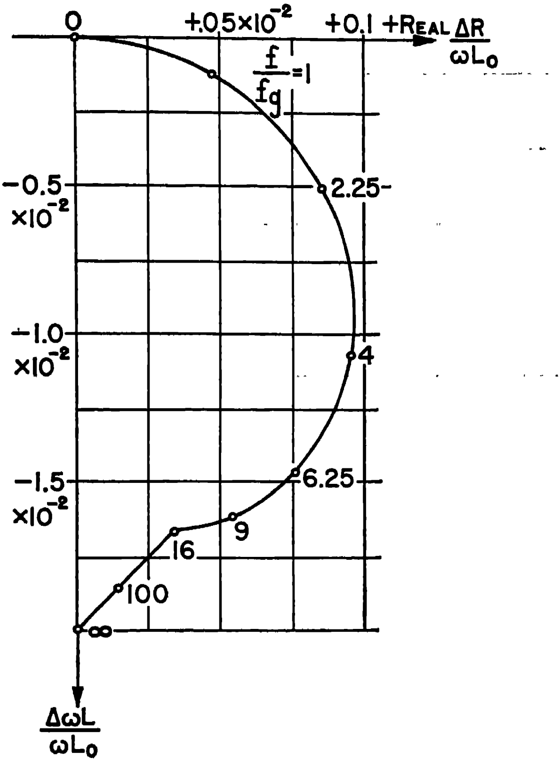

Fig. 31. Impedance variations (amplitude and phase), for a 1 percent variation in diameter, as a function of frequency ratio f/f_g. Nonmagnetic material ($\mu = 1$).

Instrument Sensitivity Characteristics. Figs. 30 and 31 show **sensitivity diagrams for conductivity and diameter effects.** These diagrams show the variations in effective permeability or complex impedance when conductivity or diameter of the test cylinder vary by 1 percent. Figs. 32 and 33 show the amplitude of the variations in effective permeability for these 1 percent changes. The **secondary coil voltage change, ΔE,** resulting from an M-percent change in conductivity or diameter effect is

$$\frac{\Delta E}{E_0} = \eta M[\Delta\mu_{\text{eff.}(1\%)}] \tag{11}$$

where η is the fill factor of the test coil (see Eq. 10, section on Eddy Current Test Principles), E_0 is the voltage of the empty coil (BC in Fig. 28), and $\Delta\mu_{\text{eff.}(1\%)}$ is shown as a function of f/f_g in Figs. 32 or 33 for 1 percent variations in conductivity or diameter.

QUANTITATIVE MEASUREMENTS OF CONDUCTIVITY OR DIAMETER EFFECTS. Unknown conductivity or diameter effects can be measured quantitatively, even with unknown fill factors, with calibrated eddy current instruments. The variation in effective permeability $\Delta\mu_{\text{eff.}}$ can be ob-

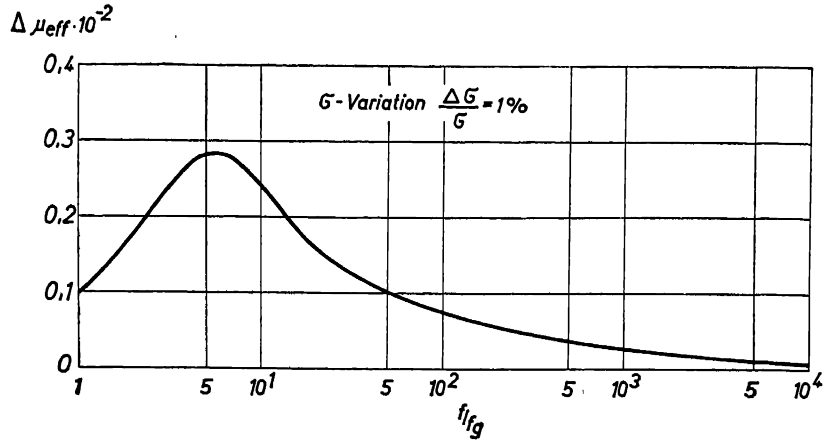

Fig. 32. Variation in effective permeability $\Delta\mu_{\text{eff.}}$, for 1 percent conductivity variation in nonferromagnetic cylinder, as a function of frequency ratio f/f_g.

tained from Figs. 32 and 33. Figs. 34 and 35 show the quotient $Q = \Delta\mu_{\text{eff.}}/$(absolute value) as a function of f/f_g for 1 percent diameter or conductivity effects. The example here will illustrate the quantitative measurement of a given conductivity or diameter variation even when fill factor, specimen conductivity, and test frequency are all unknown.

Conductivity Measurement. When an unknown test cylinder is inserted into one of the two test coils connected in series opposition, an ellipse appears on the screen of the cathode-ray tube, as described earlier in this section. The precision phase shifter of Fig. 28 is adjusted until the ellipse forms a straight line. The f/f_g

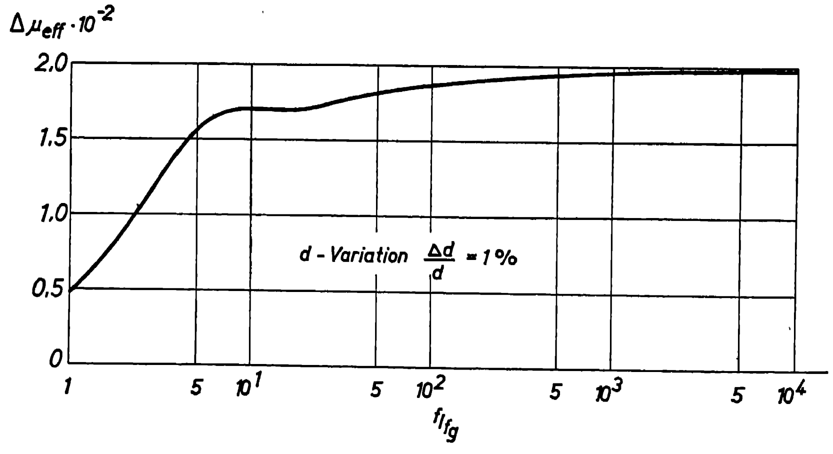

Fig. 33. Variation in effective permeability $\Delta\mu_{\text{eff.}}$, for 1 percent diameter variation in nonferromagnetic cylinder, as a function of frequency ratio f/f_g.

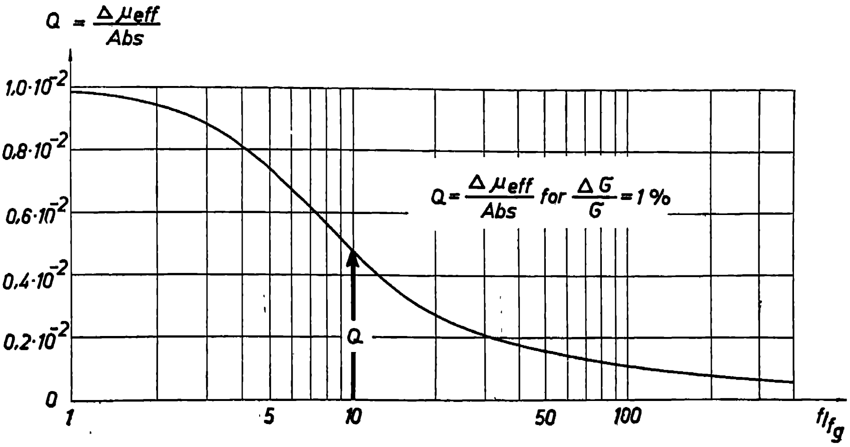

Fig. 34. Quotient $Q = \Delta\mu_{\text{eff.}}$/(absolute value), for 1 percent conductivity variation in nonferromagnetic cylinder, as a function of frequency ratio f/f_g.

ratio is obtained from the resultant phase angle and Fig. 24. When another test specimen is inserted into the second coil, the voltage output of the opposed secondary coils again becomes zero. Now assume that a conductivity variation occurs during testing, resulting in a beam deflection A of 1.5 in. If the sensitivity knob of the instrument is set at $N = 4\%$ per inch, a 1-in. deflection corresponds to 4 percent of the "absolute value" (P_0P in Figs. 13 and 25). Thus the measured effect has a magnitude of $A \times N = (1.5) \times (4) = 6$ percent of the "absolute value." Suppose that the phase shifter now indicates a frequency ratio $f/f_g = 10$. From Fig. 34 the corresponding value of Q is found to be 0.47 percent for a 1 percent

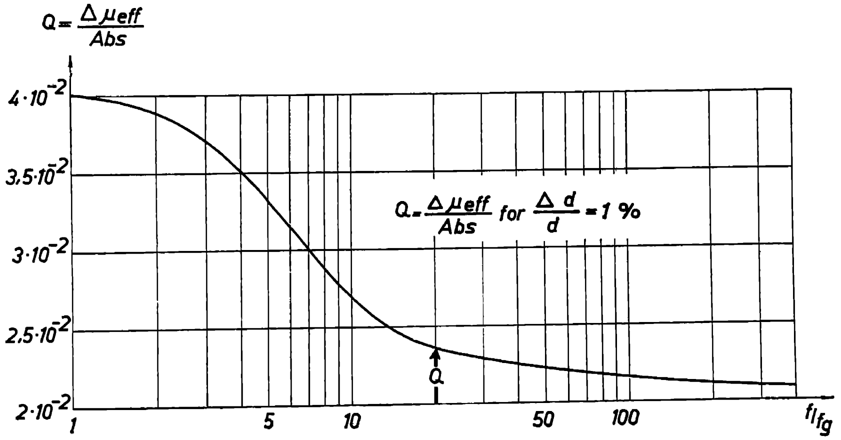

Fig. 35. Quotient $Q = \Delta\mu_{\text{eff.}}$/(absolute value), for a 1 percent diameter variation in nonferromagnetic cylinder, as a function of frequency ratio f/f_g.

variation in conductivity. Thus the **variation in conductivity** is found to be $(6)/(0.47) = 12.6\%$ in this example. More generally,

$$\frac{\Delta\sigma}{\sigma}(\%) = \frac{AN}{Q} \tag{12}$$

where $\Delta\sigma/\sigma(\%)$ = percentage change in electrical conductivity.
A = deflection of beam (in inches) caused by the conductivity variation.
N = instrument sensitivity setting (given in percentage of the "absolute value" for 1-in. beam deflection).
Q = quotient read from Fig. 34 for the f/f_g ratio shown on the phase shifter.

Diameter Measurement. The magnitude of a diameter variation can be measured in the same manner as a conductivity variation. When the cylinder diameter varies from that of the reference standard, the cathode-ray beam is again deflected in the test instrument. If the deflection $A = 2.5$ in. at a sensitivity setting $N = 2\%$ per inch, the diameter effect is $N \times A = (2) \times (2.5) = 5\%$ of the "absolute value." Suppose that the phase shifter indicates the frequency ratio to be $f/f_g = 20$. Fig. 35 indicates that a diameter variation of 1 percent at $f/f_g = 20$ results in a measurement effect of $Q = 2.35$ percent of the "absolute value." The **diameter effect** for the example in question is calculated to be

$$\frac{\Delta d}{d}(\%) = \frac{5.00}{2.35} = 2.14\%$$

In the general case,

$$\frac{\Delta d}{d}(\%) = \frac{AN}{Q} \tag{13}$$

where $\Delta d/d(\%)$ = percentage change in cylinder diameter.
A = measured deflection on screen of eddy current test instrument, caused by a diameter effect.
N = instrument sensitivity setting (given in percentage of the "absolute value" for 1-in. beam deflection).
Q = quotient read from Fig. 35 for the f/f_g ratio shown on the phase shifter.

Setting Tolerance Limits. If tolerances are specified for conductivity or diameter variations, the beam deflections corresponding to these tolerance limits can be established for each sensitivity setting of the test instrument. Suppose that the specified tolerance for conductivity or diameter is T percent. The **beam deflection corresponding to this tolerance percentage** is then

$$A = \frac{TQ}{N} \tag{14}$$

where Q = the quotient taken from Figs. 34 or 35 for the f/f_g ratio indicated on the phase shifter.

For eddy current instruments equipped with signaling or automatic sorting devices, the **sorting limits** can be adjusted as indicated above for a specified conductivity tolerance (alloy sorting), hardness tolerance, or diameter tolerance, for each sensitivity step, in accordance with Eq. (14).

Detecting Cracks Independently of Diameter Variations. In practical testing, crack effects and diameter variations often appear simultaneously (for example, in tungsten and molybdenum wires). In this case the **crack depth** can still be determined quantitatively by means of the ellipse-analysis method (see Analysis of Screen Patterns in this section and Fig. 29). If the voltage on the horizontal deflection plates of the cathode-ray tube is adjusted precisely in phase angle to the direction of diameter variations (see Fig. 14), the **intersection of the ellipse with the vertical center line** (*PR* in Fig. 29) represents the component of the crack signal perpendicular to the diameter direction on the complex permeability plane of Fig. 14. Fig. 36 represents the component of the quotient Q, perpendicular to the diameter direction (Fig. 27), as a function of frequency ratio f/f_g. It provides a means of **quantitative crack evaluation** even when diameter variations are present in the test cylinder. This is true even though the eddy current effects, $\Delta\mu_{\text{eff.}}$, of **diameter variations** can be many times larger than those resulting from crack effects.

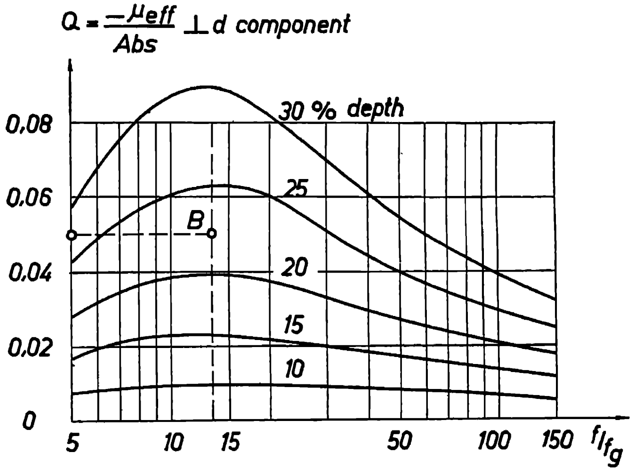

Fig. 36. Component of quotient $Q = \Delta\mu_{\text{eff.}}/$(absolute value), **perpendicular to diameter direction in effective permeability plane, as a function of frequency ratio** f/f_g. Curves show crack depths independently of cylinder diameter variations. Crack depths in percentage of diameter of nonferrous cylinder.

Crack Evaluation with Diameter Variations. The evaluation of cracks in the presence of diameter variations will be illustrated by means of an example. When a crack is present in the test cylinder, an ellipse will appear upon the screen of the indicating instrument. The voltage applied to the horizontal deflection plates is selected to conform with the direction of diameter variations. The vertical intercept (*PR* in Fig. 29) is read as $A = 1.25$ in., for example. Suppose that the sensitivity control indicates $N = 4\%$ per inch of "absolute value." The product $AN = 0.05$. The frequency ratio, indicated by the phase shifter, is $f/f_g = 13$. The coordinates of $Q = 0.05$ and $f/f_g = 13$ (point B in Fig. 36) correspond to a crack depth of 22 percent.

References

Reference numbers in this section refer to the references at the end of the section on Eddy Current Test Indications.

SECTION 38

EDDY CURRENT TUBE TESTS

CONTENTS

PAGE

Tests of Thin-Walled Tubes

- Significant characteristics of tubes 1
- Thin-walled nonferrous tubes 1
  - Complex impedance or voltage plane 1
    - Curve of effective permeability $\mu_{eff.}$ as a function of frequency ratio f/f_g for thin-walled, nonferromagnetic tube filling the test coil (*f.* 1) 2
  - Construction of frequency ratio scale 3
  - Sample calculations for effective permeability and secondary coil voltage 3
  - Direct computation of components of effective permeability from frequency ratio, f/f_g 3
  - Effect of changes in outside diameter of tube (with proportional changes in tube wall thickness) 3
    - Normalized apparent impedance plane for thin-walled, nonferromagnetic tubes with varying outside diameters and a constant ratio of inside to outside diameter (*f.* 2) 4
  - Effect of changes in outside diameter of tube (with inside diameter held constant) ... 4
    - Normalized apparent impedance plane for thin-walled, nonferromagnetic tubes with varying outside diameters and fixed inside diameter, and constant conductivity σ (*f.* 3) 5
- Thin-walled ferromagnetic tubes 6
- Sensitivity of tests of thin-walled tubes 6
    - Sensitivity diagram for eddy current tests of thin-walled tubes (*f.* 4) 6
  - Maximum test sensitivity 6
  - Experimental determination of frequency ratio f/f_g 7
    - Variation of angle α with frequency ratio f/f_g, or product $(\sigma d_i W)$, in nonferromagnetic tube (*f.* 5) 7
  - Cracks in thin-walled tubes 7
  - Frequency selection for crack detection 7

Tests of Thick-Walled Tubes

- Thick-walled nonferrous tubes 8
    - Range of variation of effective permeability for thick-walled, nonferrous tubes (shown by shaded area) (*f.* 6) 8
  - Effect of variations in inside diameter (with outside diameter held constant) 8
    - Complex permeability or impedance plane for nonferromagnetic tubes of various wall thicknesses (*f.* 7) 9
  - Sample calculation for variation of inside diameter 10
  - Effect of variations in electrical conductivity 10
  - Effect of variations of outside diameter (with ratio of inside to outside diameter held constant) 10
    - Complex impedance or permeability plane for nonferromagnetic tubes with wall thickness of 20 percent of outside tube radius as outside diameter d_a of tube varies (*f.* 8) 11
  - Maximum test sensitivity 12
  - Calculation of frequency ratio, f/f_g, for maximum test sensitivity 12
    - Frequency ratios f/f_g for optimum test sensitivity in thick-walled tubes with various ratios of wall thickness W to outside radius r_a (*f.* 9) 12
- Cracks in nonferromagnetic tubes 12
  - Quantitative evaluation of crack depths 12
    - Apparent impedance plane showing effects of cracks for four different tube wall thicknesses, at a frequency ratio $f/f_g = 5$, for nonferromagnetic tubes (*f.* 10). 13
    - Apparent impedance plane showing effects of cracks for four different tube wall thicknesses, at a frequency ratio $f/f_g = 15$, for nonferromagnetic tubes (*f.* 11) 13
    - Apparent impedance plane showing effects of cracks for four different tube wall thicknesses, at a frequency ratio $f/f_g = 50$, for nonferromagnetic tubes (*f.* 12) 14
    - Apparent impedance plane showing effects of cracks for four different tube wall thicknesses, at a frequency ratio $f/f_g = 150$, for nonferromagnetic tubes (*f.* 13) 14
  - Characteristics of crack evaluation curves .. 14

Eddy Current Tests of Tubes With Internal Test Coil

- Applications of internal probes 15
- Internal probe test arrangements 15
    - Test coil inside cylinder (*f.* 14) 15
  - Heavy-walled tubes 15
    - Arrangement for measuring the screening effect of tubes (*f.* 15) 16
    - Decrease of field strength upon insertion of tube between coils of Fig. 15, for

CONTENTS (*Continued*)

PAGE

- copper, brass, and stainless steel tubes of 0.8-in. outside diameter and 0.040-in. wall thickness (*f.* 16) 16
- Evaluation of thin-walled nonferromagnetic tubes 17
- Evaluation of thick-walled nonferromagnetic tubes 17
  - Apparent impedance diagram of test coil inside heavy-walled nonferrous tube (*f.* 17) 18
- Separation of material properties and inside corrosion thinning 17
- Maximum test sensitivity 17
- Evaluation of medium-thickness tube walls 17

Penetration Depth Limitations

- Significance of penetration depth 19
  - Penetration depths for different instrument sensitivities (10^{-2}, 10^{-3}, 10^{-4}, and 10^{-5}) as a function of frequency ratio f/f_g (*f.* 18) 19
  - Significance of instrument sensitivities 19
  - Limitations in detection of concentric cavities 20
  - Determination of secondary coil voltages with tubes 20
  - Magnetic permeability limitations on depth penetration 20
    - Relative magnetic permeability of a carbon steel as a function of external magnetic-field strength (*f.* 19) 20
  - Limitations in use of high magnetizing field strengths 21
    - Penetration depths for carbon steel tubes of 0.040, 0.080, and 0.120 in. wall thickness (*f.* 20) 22
  - Shielding tests at 50-c.p.s. frequency 21
  - Shielding tests at 5-c.p.s. frequency 22

Tests of Small Diameter Tubing

- Principle of test 23
- Impedance plane characteristics 23
  - Impedance plane for coil encircling nonferromagnetic metal tubes (*f.* 21) 24
  - Controlling factors 24

PAGE

- Types of coil systems 25
  - Test coil configurations for eddy current testing of small-diameter tubing (*f.* 22) 25
  - Sensitivity and signal discrimination 26
  - Differential coil system 26
  - Absolute coil system 26
  - Tube-feeding mechanism 27
    - Encircling-coil assembly and feed mechanism for tubing inspection (*f.* 23) 27
- Instrumentation 27
- Resistive-component sensing instruments 28
  - Resistance-loss test indications as a function of tubing wall thickness with f/f_c as a parameter (*f.* 24) 28
- Flaw sensitivity 29
  - Eddy current signal trace and photomicrograph of defective ¼ × 0.049-in. Hastelloy tubing (*f.* 25) 29
  - Detection of intergranular corrosion 30
    - Eddy current signal trace and photomicrograph of intergranular corrosion on inside surface of Nimonic tubing (*f.* 26) 30
    - Eddy current signal trace and photomicrographs of defective 3/16 × 0.025-in. Inconel tubing (*f.* 27) 32
  - Sensitivity to small discontinuities 31
  - Wall thickness and tube diameter 31
  - Frequency selection 31
    - Comparison of resistive and reactive component signal traces with actual dimensional variations in a 0.220 × 0.025-in. Inconel tube (*f.* 28) 33
- The surface probe-coil system 35
  - Coil holder assembly 36
    - Eddy current probe coil and holder for scanning small-diameter tubing (*f.* 29) .. 34
  - Control of coil-to-tube spacing 36
    - Inspection of tubing with an eddy current probe (*f.* 30) 35
  - Advantages of probe-coil system 36
    - Probe-coil eddy current B-scan photographs (*f.* 31) 37
- Limitations in test automation 37
- Selection of signal-display system 38
  - Eddy current signals from defective 3/16 × 0.025-in. Inconel tubing (*f.* 32) 38
- Application areas 39
- References 39

SECTION 38

EDDY CURRENT TUBE TESTS

Tests of Thin-Walled Tubes

SIGNIFICANT CHARACTERISTICS OF TUBES. The use of metallic tubes in industry is increasing continuously. Typical applications include the construction of boilers and heat exchangers, reactors, refrigerating systems, chemical and oil refining plants, and many process industries. Therefore nondestructive testing of large quantities of tubular products for discontinuities, eccentricity, wall thickness, alloy, hardness, and other properties is an especially important problem. However, additional difficulties are encountered in eddy current testing of tubes, since additional factors, not present in testing solid cylinders, influence tube tests. Among the **characteristics** and **possible discontinuities** which must be considered in **tube testing** are:

1. The electrical conductivity σ.
2. The relative permeability of ferromagnetic materials.
3. The outside diameter $d_a = 2r_a$, where r_a is radius.
4. The inside diameter $d_i = 2r_i$, where r_i is radius.
5. Wall thickness $W = (d_a - d_i)/2 = r_a - r_i$.
6. Subsurface cracks of specific depth, C_i (in percentage of wall thickness).
7. Outside-wall surface cracks of specific depth, C_a (in terms of wall thickness).
8. Inside-wall surface cracks of specific depth, C_m (in percentage of wall thickness).

Eccentricity, in percentage of the wall thickness, is given as the ratio of the thinnest wall thickness $W_{\text{min.}}$ to the nominal wall thickness W of the concentric tube; i.e.,

$$\text{Eccentricity } (\%) = \frac{W_{\text{min.}}}{W} \times 100$$

THIN-WALLED NONFERROUS TUBES. The thin-walled tube is an especially clear example for introducing the mathematical treatment of the eddy current problem. Its calculations can be carried out with elementary formulas. The two components of the **effective permeability,** or **apparent impedance** of the test coil in which the tube is placed, can be expressed by closed solutions. The simple mathematical relationships for the thin-walled tube are derived from the rather complicated system of formulas applicable to the tube with a given wall thickness.

Complex Impedance or Voltage Plane. The basic curve for the effective permeability (shown for the solid metallic cylinder in Fig. 7 of the section on Eddy Current Test Principles) becomes an exact semi-circle with diameter $d = 1$ for the thin-walled tube which entirely fills the test coil, $\eta = 1$ (Fig. 1). The **argument,**

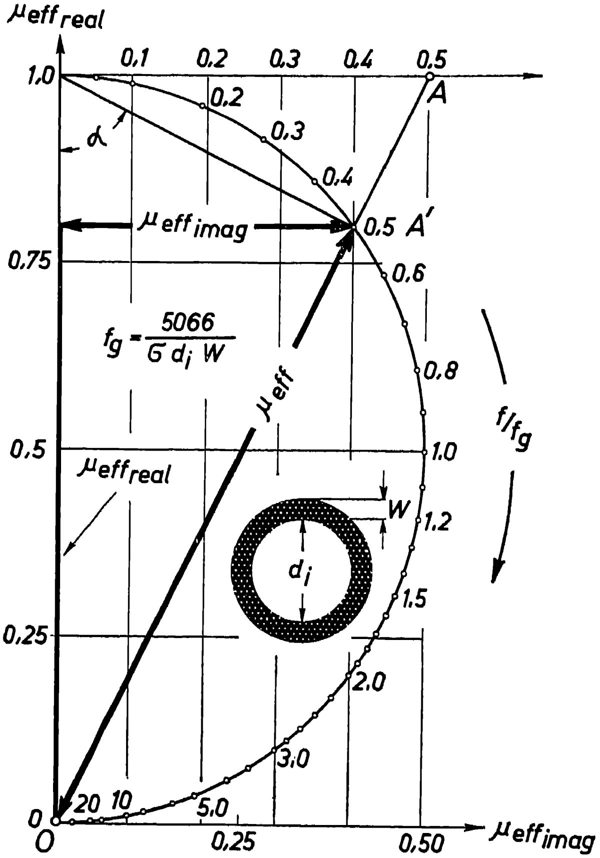

Institut Dr. Foerster

Fig. 1. Curve of effective permeability $\mu_{eff.}$ as a function of frequency ratio f/f_g for thin-walled, nonferromagnetic tube filling the test coil ($\eta = 1$).

A, of the basic function for calculation of eddy current behavior in thin-walled tubes, appears as the product

$$A = \frac{f \mu_{rel.} \sigma d_i W}{5066} \tag{1}$$

where f = test frequency, c.p.s.
σ = electrical conductivity, meter/ohm-mm.^{2}.
d_i = inside diameter of tube, cm.
W = wall thickness of tube, cm.

[Compare with Eq. (4), Eddy Current Test Principles, for the solid cylinder.]

If, as in the case of the solid cylinder, the test frequency f is selected so that the argument A in Eq. (1) equals unity, this frequency is called the **limit frequency** f_g for the tube; i.e.,

$$f_{g(\text{tube})} = \frac{5066}{\mu_{rel.} \sigma d_i W} \tag{2}$$

[Compare with Eq. (5), Eddy Current Test Principles, for the solid cylinder.]

Construction of Frequency Ratio Scale. The f/f_g scale is determined by a simple geometrical construction on the semi-circle of effective permeability for the thin-walled tube (Fig. 1). A linear horizontal scale is constructed from the ordinate point $\mu_{\text{eff.(real)}} = y = 1$, and values $x = 0.1$, 0.2, etc., are marked on this horizontal scale. A straight line drawn from the origin O of the effective permeability coordinates to any given point on this horizontal scale will intersect the semi-circle at the corresponding f/f_g point. For example, the line drawn from O to $A = 0.5$ in Fig. 1 intersects the semi-circle at $f/f_g = 0.5$ (point A'). Similarly a straight line drawn from O to any point N of the horizontal scale at $y = 1$ will intersect the semi-circle exactly at the point where $f/f_g = N$.

Sample Calculations for Effective Permeability and Secondary Coil Voltage. As an example, consider a thin-walled tube of **stainless steel** for which the electrical conductivity $\sigma = 2$ meter/ohm-mm.^{2}, relative magnetic permeability $\mu_{\text{rel.}} = 1$, inside diameter $d_i = 2.5$ cm., and wall thickness $W = 0.1$ cm. From Eq. (2) the limit frequency is calculated to be $f_g = 10{,}000$. If the test frequency is also taken as 10,000 c.p.s., the frequency ratio $f/f_g = 1$. From Fig. 1 the components of the effective permeability are found to be $\mu_{\text{eff.(real)}} = 0.5$ and $\mu_{\text{eff.(imag.)}} = 0.5$.

The two components of the **apparent impedance of the test coil,** or of the **secondary coil voltage** in coil arrangements such as shown in Fig. 12(c) and (d) in the section on Eddy Current Cylinder Tests, are

$$\frac{\omega L}{\omega L_0} = \frac{E_{\text{imag.}}}{E_0} = 1 - \eta\mu_{\text{eff.(real)}} \tag{3a}$$

$$\frac{R}{\omega L_0} = \frac{E_{\text{real}}}{E_0} = \eta\mu_{\text{eff.(imag.)}} \tag{3b}$$

where $\eta = (d_a/d_o)^2$ = fill factor of coil.
d_a = outside diameter of tube.
d_o = average diameter of test coil.

Eqs. (3) for the thin-walled tube are comparable to Eq. (16), Eddy Current Test Principles, for the solid cylinder.

Direct Computation of Components of Effective Permeability from Frequency Ratio, f/f_g. With thin-walled tubes the components of effective permeability $\mu_{\text{eff.}}$ can be calculated directly from the frequency ratio f/f_g by the simple formula

$$\mu_{\text{eff.(real)}} = \frac{1}{1 + (f/f_g)^2} \tag{4a}$$

$$\mu_{\text{eff.(imag.)}} = \frac{f/f_g}{1 + (f/f_g)^2} \tag{4b}$$

where

$$f/f_g = \frac{f\sigma d_i W}{5066}$$

for the thin-walled, nonferrous tube (see Eq. 2). These components of $\mu_{\text{eff.}}$ can be inserted into Eq. (3) to obtain the normalized apparent impedance components or the normalized components of secondary coil voltage. In this way the response of the test coil to the thin-walled tube can be calculated quantitatively by means of closed formulas.

Effect of Changes in Outside Diameter of Tube (with Proportional Changes in Tube Wall Thickness). If the ratio (d_i/d_a) of inside to outside tube diameter is held constant while the outside tube diameter varies, the changes in effective permeability are as shown in Fig. 2. The outermost curve of Fig. 2 corresponds to the semi-circle of Fig. 1, for which the fill factor $\eta = 1$. The curves of Fig. 2 correspond to those for the solid cylinder shown in Fig. 1, in the section

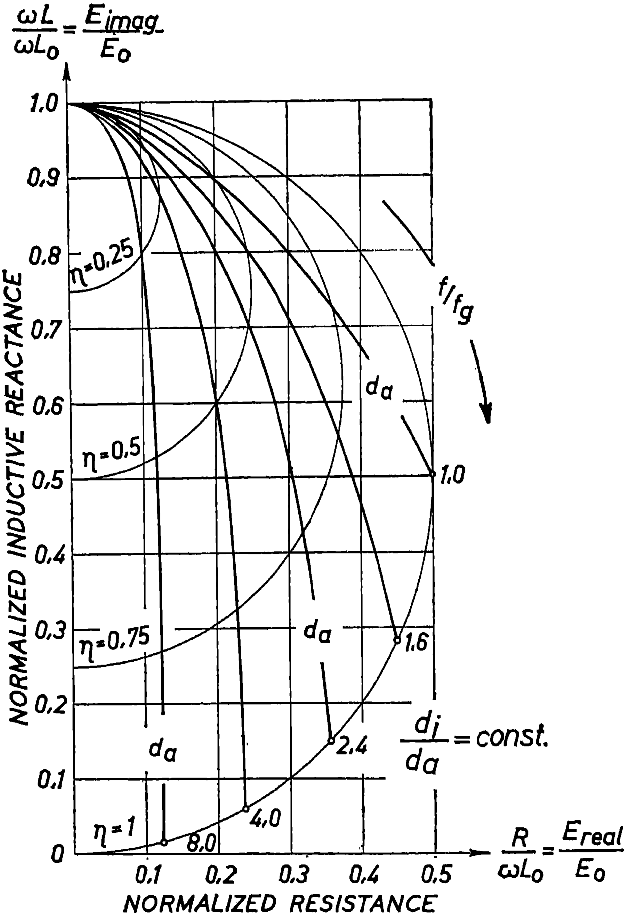

Institut Dr. Foerster

Fig. 2. Normalized apparent impedance plane for thin-walled, nonferromagnetic tubes with varying outside diameters and a constant ratio of inside to outside diameter (d_i/d_a = constant).

on Eddy Current Cylinder Tests. Variations of electrical conductivity σ, inside diameter d_i, and wall thickness W at constant outside diameter d_a are also indicated by these curves.

Effect of Changes in Outside Diameter of Tube (with Inside Diameter Held Constant). If the outside diameter of the tube decreased while the inside diameter was held constant, a very small reduction in outside diameter would result in a large decrease in tube wall thickness W. Fig. 3 shows the apparent impedance plane for this case. For example, suppose that the wall thickness $W = 10\%$ and the inside tube radius is 90 percent of the outside tube radius. If the outside diameter now decreases by 5 percent while the inside diameter

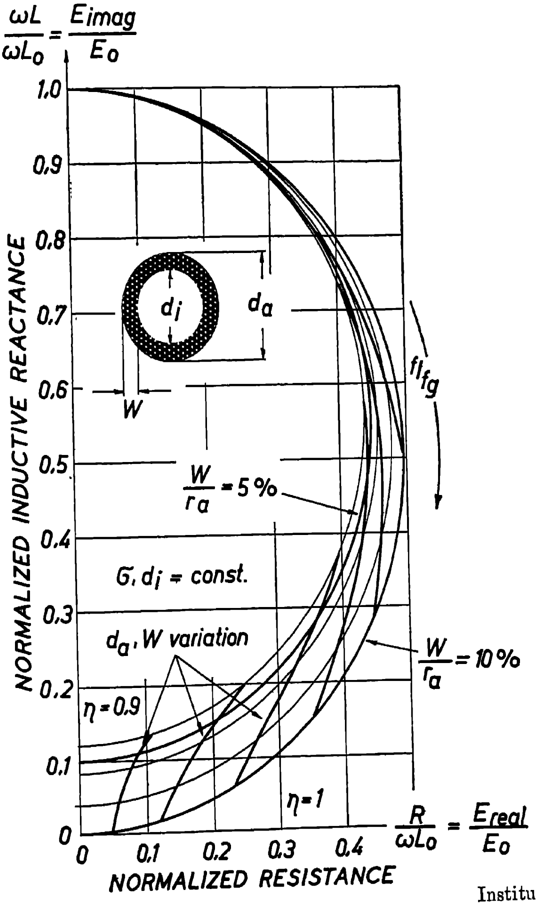

Institut Dr. Foerster

Fig. 3. Normalized apparent impedance plane for thin-walled, nonferromagnetic tubes with varying outside diameters, fixed inside diameter, and constant conductivity σ.

remains constant, the wall thickness will be reduced by 50 percent. However, a decrease of the wall thickness factor W in Eq. (2) to one-half its original value reduces the frequency ratio f/f_g to one-half of its original value. But the outside diameter decrease (by 5 percent) must also be considered. Consequently the impedance variation lies on the curved line connecting the original f/f_g point on the permeability curve for fill factor $\eta = 1$ to the point corresponding to one-half of this f/f_g value on the permeability curve for $\eta = 0.9$. (A decrease of 5 percent in diameter corresponds to a decrease in fill factor of approximately 10 percent, since $\eta = (d/D)^2$, where d is test-object diameter and D is coil diameter, from Eq. 10, Eddy Current Test Principles.) Thus, if either wall thickness or electrical conductivity varies while outside diameter remains constant, the apparent impedance or secondary coil voltage varies along the curved lines labeled "d_a, W variation" in Fig. 3.

THIN-WALLED FERROMAGNETIC TUBES. The preceding development referred to nonferromagnetic tubes for which $\mu_{rel.} = 1$. For a ferromagnetic tube for which $\mu_{rel.} >> 1$, the procedure is developed in the same manner as in Eqs. (1, a and b), in the section on Eddy Current Cylinder Tests, for the solid cylinder. However, with thin-walled steel tubes, only the volume of the tube wall contributes to the magnetization. These relationships for ferromagnetic tubes are treated more thoroughly in the literature.[42] The characteristics of ferromagnetic tubes tested at high field strengths, where the relative permeability varies with the field strength, will be discussed more thoroughly subsequently in this section under Limitations in Use of High Magnetizing Field Strengths.

SENSITIVITY OF TESTS OF THIN-WALLED TUBES. Fig. 4 indicates the variations in effective permeability resulting from 1 percent changes in tube characteristics such as electrical conductivity σ, relative magnetic permeability $\mu_{rel.}$, inside diameter d_i, or wall thickness W. If σ, $\mu_{rel.}$, or the product $(d_i \times W)$ vary by 1 percent, the magnitude and direction of the change in effective permeability are given by the vector from the origin O to the f/f_g point on the circle corresponding to the specific tube (see Eq. 2).

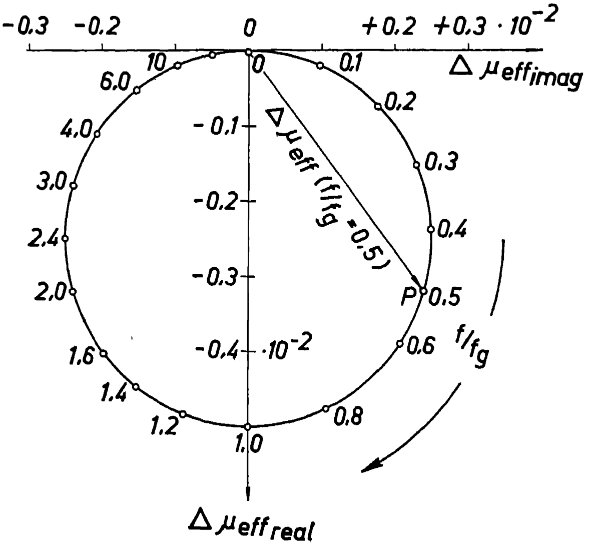

Fig. 4. Sensitivity diagram for eddy current tests of thin-walled tubes. Vector OP indicates direction and magnitude of variation in effective permeability for 1 percent variations of conductivity σ, inside diameter d_i, or wall thickness W.

Maximum Test Sensitivity. In accordance with a general law in the theory of eddy current testing, maximum test sensitivity is attained at that point on the effective permeability curve where the imaginary component (along the horizontal or x-axis) $\mu_{\mathrm{eff.(imag.)}}$ goes through a maximum. In Fig. 1, for example, this maximum lies at $f/f_g = 1$. The corresponding point is shown at the bottom of the circle in Fig. 4. At maximum sensitivity ($f/f_g = 1$), a 1 percent variation in conductivity or in the product ($d_i \times W$) results in 0.5 percent variation in the effective permeability. This variation occurs in the vertical direction along the vector from the point $f/f_g = 0$ to the point for $f/f_g = 1$ in the $\mu_{\mathrm{eff.(real)}}$ direction (see Fig. 4). Fig. 4 indicates the magnitude and direction of apparent impedance variation caused by a change in tube characteristics (σ, d_i, or W) in the apparent impedance plane.

Experimental Determination of Frequency Ratio f/f_g. The frequency ratio f/f_g can be determined experimentally, even with a fixed-frequency test instrument. The procedure is similar to that presented earlier for solid cylinders (see Fig. 24 of the section on Eddy Current Cylinder Tests.) Fig. 5 shows the relation between the angle α and the frequency ratio f/f_g, for the case of nonferromagnetic tubes. From this curve and known values of test frequency f, wall thickness W, and inside diameter d_i, the electrical conductivity of the tube material can be determined directly from Eq. (2).

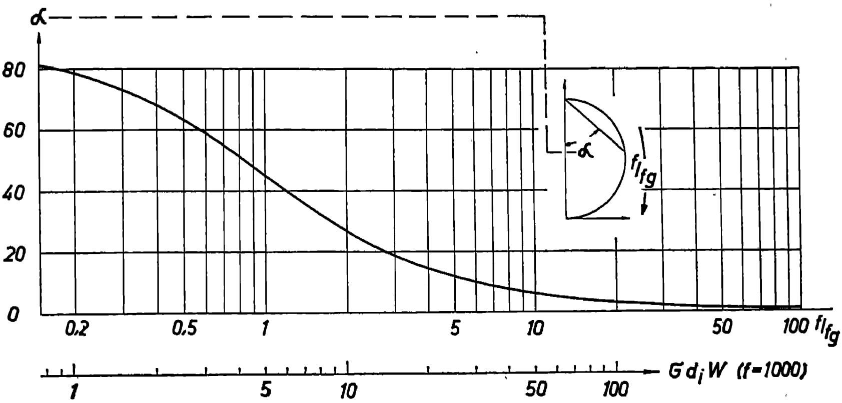

Fig. 5. Variation of angle α with frequency ratio f/f_g, or product ($\sigma d_i W$), in nonferromagnetic tube.

Cracks in Thin-walled Tubes. Cracks in thin-walled tubes have the same eddy current effect as a decrease in the wall thickness W. Thus, **outside cracks** produce variations in effective permeability which lie in the same direction on the complex permeability plane as a decrease in outside diameter d_a, with inside diameter held constant (see Fig. 3). **Inside cracks** produce variations in the same direction as a decrease of wall thickness with constant outside diameter. Thus, inside cracks are indicated by variations toward smaller f/f_g values along the semi-circles in the permeability plane of Fig. 2.

Frequency Selection for Crack Detection. In crack testing of thin-walled tubes, the crack sensitivity curve corresponds in general to Fig. 4. Thin-walled tubes should be tested for cracks, alloy, or wall thickness at **frequency ratios** between $f/f_g = 0.4$ and $f/f_g = 2.4$. These limits correspond to a decrease from maximum test sensitivity of $1/\sqrt{2}$, or 71 percent.

Tests of Thick-Walled Tubes

THICK-WALLED NONFERROUS TUBES. The characteristics of a test coil containing a thick-walled tube lie between those for a thin-walled tube (semi-circles of Fig. 1) and those of a solid cylinder (Fig. 7 in the section on Eddy Current Test Principles). The shaded area in Fig. 6 shows the range of effective permeability within which all variations in tube properties occur.

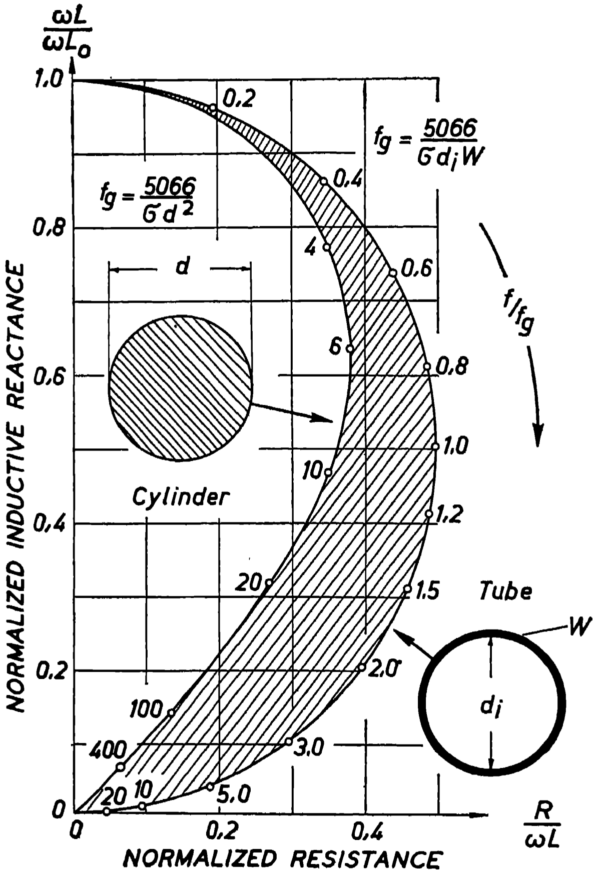

Institut Dr. Foerster

Fig. 6. Range of variation of effective permeability for thick-walled, nonferrous tubes (shown by shaded area). Variations in conductivity, inside diameter, and wall thickness occur in this range when outside diameter is held constant.

Effect of Variations in Inside Diameter (with Outside Diameter Held Constant). To illustrate the case of inside diameter variations, assume that a test cylinder is initially solid. The effective permeability or apparent impedance values for the test coil lie along the curve of Fig. 7 (of the section on Eddy Current Test Principles) at the f/f_g value calculated from Eq. (5) in the same section. Now suppose that successively larger holes are drilled along the longitudinal axis of the tube. The inside diameter d_i increases, while the wall thickness W decreases.

For a given thin-wall thickness, the permeability curve of Fig. 1 is applicable. When the wall thickness is reduced to zero ($W = 0$), the effective permeability falls at $\mu_{\text{eff.(real)}}$ or $\omega L/\omega L_0 = 1$ (top left of Fig. 1). In the absence of the test object, this point corresponds to the effective permeability of the coil when empty.

Fig. 7 shows the paths followed by effective permeability for four solid cylinders with frequency ratios of $f/f_g = 4$, 9, 25, and 100, as **wall thickness** varies from that of the solid cylinder ($W = d_a/2$) to zero (empty test coil). The electrical

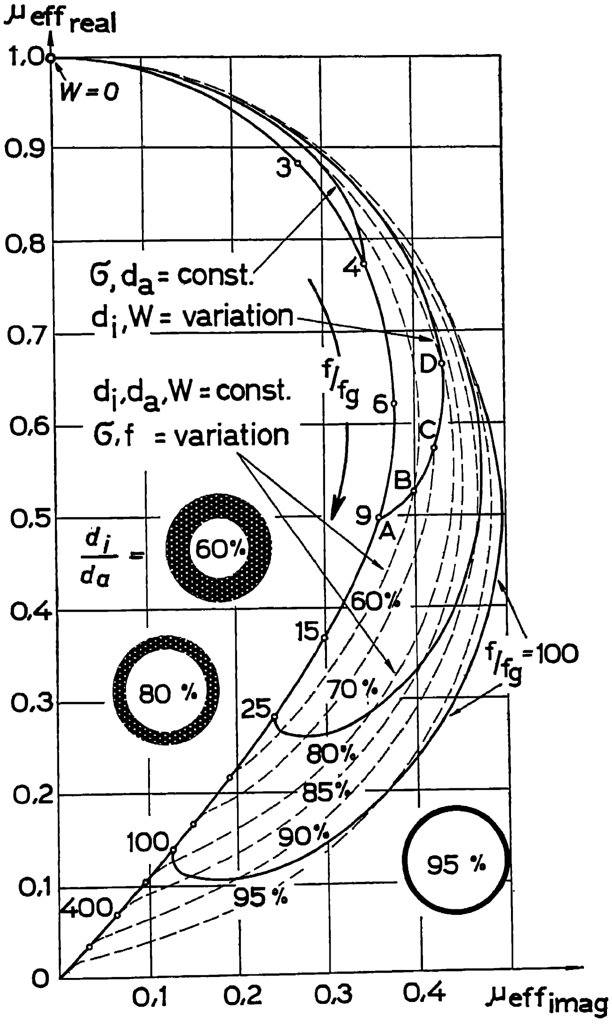

Institut Dr. Foerster

Fig. 7. Complex permeability or impedance plane for nonferromagnetic tubes of various wall thicknesses. Solid curves represent variations of inside diameter d_i and wall thickness W, with constant conductivity and outside wall diameter. Dashed curves indicate conductivity or frequency variations with constant tube geometry.

conductivity σ and outside diameter d_a are assumed constant for these curves, while only inside diameter d_i and wall thickness W vary. To simplify the presentation, the f/f_g value for the solid cylinder is taken for the entire curve extending from solid cylinder to empty coil conditions. Only the inside diameter varies along these curves for specific f/f_g ratios. The **ratios of inside diameter to outside diameter,** $d_i/d_a = r_i/r_a$, in percentages, are marked on these dashed curves.

Sample Calculation for Variation of Inside Diameter. To obtain the effective permeability or apparent impedance of the test coil for the thick-walled tube, the steps are:

1. Calculate the f/f_g ratio for the solid cylinder from Eq. (5), Eddy Current Test Principles.
2. Select the tube curve in Fig. 7 which starts at this f/f_g value on the curve for the solid cylinder and ends at the point where $\mu_{eff.(real)} = 1$ for wall thickness $W = 0$ (at upper left of Fig. 7).
3. Find the point which corresponds to the diameter ratio d_i/d_a, for the tube in question, along the selected curve.
4. The real and imaginary components of the effective permeability of this point on Fig. 7 are inserted into Eqs. (16, a and b), Eddy Current Test Principles, to determine the components of the apparent impedance of the test coil containing the thick-walled tube.

For example, point A in Fig. 7 corresponds to a solid cylinder with a frequency ratio $f/f_g = 9$. If this cylinder is drilled out until the inside diameter is 60 percent of the outside diameter, the effective permeability is given by point B. Point C corresponds to a diameter ratio $d_i/d_a = 70\%$; and point D corresponds to 80 percent.

Effect of Variations in Electrical Conductivity. Dashed curves in Fig. 7 connect points with the same diameter ratio, $d_i/d_a = r_i/r_a$, between the various f/f_g curves. For example, at $d_i/d_a = 95\%$, the wall thickness is 5 percent of the outside radius r_a of the tube. The frequency ratio f/f_g increases along these curves, corresponding to changes in either the electrical conductivity or the test frequency.

Effect of Variations of Outside Diameter (with Ratio of Inside to Outside Diameter Held Constant). Fig. 8 shows the apparent impedance plane for tubes with varying outside diameter d_a for the special case in which **wall thickness** W is 20 percent of the outside radius ($W/r_a = 20\%$). The **diameter ratio,** d_i/d_a, is constant, as well. The apparent impedance for this case is obtained by combining data from Figs. 7 and 8. The solid curves of Fig. 7 show the effects of varying the ratio of d_i to d_a. The family of curves of Fig. 8 shows the effect of the **variations in fill factor** η, which correspond to various outside diameters in relative units. Since $\eta = (d_a/D)^2$, where d_a is the outside diameter of the tube and D is the inside diameter of the test coil, the **fill-factor curves** represent outside diameters as follows:

$d_a = 1$ $\eta = 1$
$d_a = 0.9$ $\eta = 0.81$
$d_a = 0.8$ $\eta = 0.64$

and so forth.

The outermost curve of Fig. 8, labeled "$\eta = 1$," corresponds to the curve for d_i/d_a of Fig. 7. In Fig. 8 the **directions of diameter and conductivity effects** are clearly indicated. The d_a curves form large angles with the σ curves, so that diameter and conductivity variations are readily separated from each other.

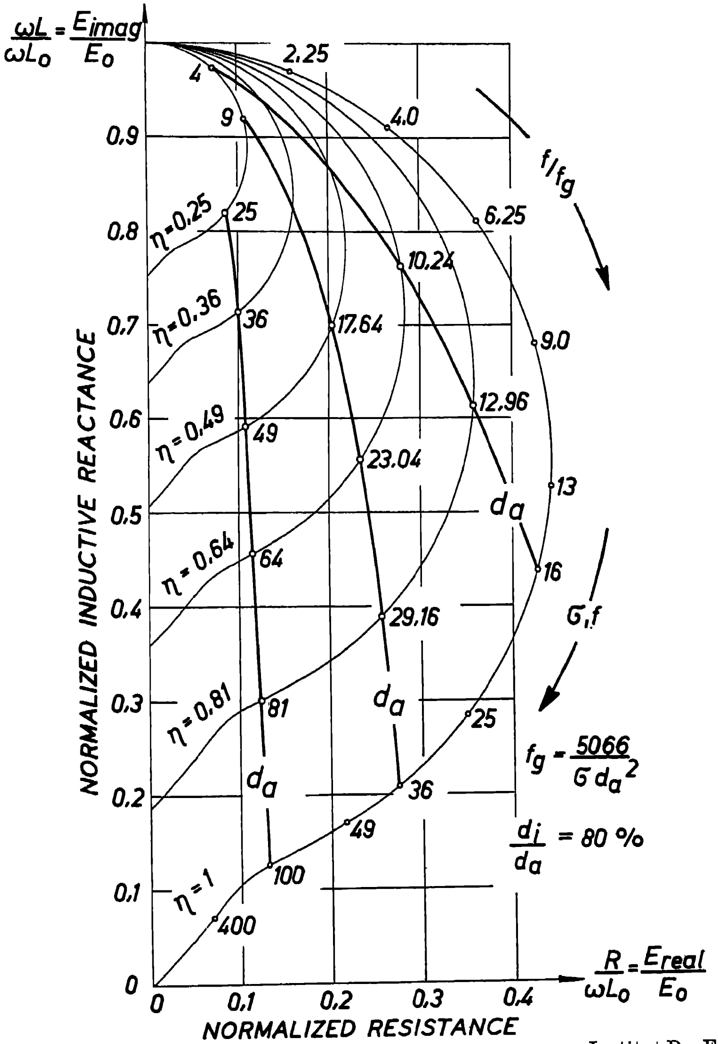

Institut Dr. Foerster

Fig. 8. Complex impedance or permeability plane for nonferromagnetic tubes with wall thickness of 20 percent of outside tube radius as outside diameter d_a of tube varies. Curves labeled d_a correspond to variations of outside diameter. Variations of electrical conductivity or test frequency are indicated along f/f_g curves.

The f/f_g ratio for the solid cylinder, from Eq. (5), Eddy Current Test Principles, is used for the thick-walled tubes in Fig. 7, where conductivity σ and outside diameter d_a were assumed to be constant while wall thickness W varied from $d_a/2$ (solid cylinder) to zero (empty coil). Each curve in Fig. 7 which starts at a specific f/f_g value for the solid cylinder and ends at the empty value (upper left) for $W = 0$ crosses the curve for $d_i/d_a = 80$ percent at one point. These points were used to plot the curve for $\eta = 1$ (outermost curve of Fig. 8) for $d_i/d_a = 0.8$.

Maximum Test Sensitivity. The maximum test sensitivity for effects of conductivity, wall thickness, and cracks occurs where the real component of apparent impedance, $R/\omega L_0$, or of normalized secondary coil voltage, E_{real}/E_0, reaches a maximum. In the case shown in Fig. 8, this occurs near $f/f_g = 13$ (right extremity of f/f_g curve for $\eta = 1$). Thus, if a tube with 20 percent wall thickness is to be tested, the **frequency ratio** f/f_g for a solid cylinder of the same material (with the same electrical conductivity σ) and the same outside diameter d_a should be in the vicinity of 13.

Calculation of Frequency Ratio, f/f_g, for Maximum Test Sensitivity. The frequency ratio f/f_g for optimum sensitivity in tube tests is calculated, from Eq. (5), Eddy Current Test Principles, for the solid cylinder, and Eq. (2) of this section, for the thin-walled tube as

$$(f/f_g)_{\text{solid cylinder}} = \frac{2}{(1 - W/r_a)(W/r_a)} \qquad (5)$$

For the thick-walled tube of Fig. 8, where $W/r_a = 0.8$, the f/f_g ratio calculated from Eq. (5) is found to be $f/f_g = 12.5$. This correlates well with the maximum deflection to the right in Fig. 8. The maximum test sensitivity thus lies exactly at $f/f_g = 12.5$ (previously estimated from the curve to be near 13).

Fig. 9 tabulates frequency ratios for optimum test sensitivities for various ratios of wall thickness W to outside tube radius r_a. If the tube wall is not too thin, this optimum f/f_g ratio can be varied from 0.7 to 1.4 times the optimum without decreasing test sensitivity below 80 percent of the optimum.

W/r_a	f/f_g, Cyl. Opt.	f/f_g, Range
0.4	8.35	6–12
0.3	9.5	7–14
0.2	12.5	9–18
0.1	22.2	15–30
0.05	42	30–60
0.02	100	70–140
0.01	200	140–280

Fig. 9. Frequency ratios f/f_g for optimum test sensitivity in thick-walled tubes with various ratios of wall thickness W to outside radius r_a.

CRACKS IN NONFERROMAGNETIC TUBES. Since the complexity of boundary conditions prevents exact mathematical solution of the problem of tubes containing cracks, data were obtained by means of extensive **model experiments.** The mercury model technique (see Figs. 7 to 10 of the section on Eddy Current Cylinder Tests) was used to determine the influence of outside-surface, inside-surface, and subsurface cracks of various depths over a wide frequency range. Thousands of individual measurements were needed to account for the effects of tube wall thickness and material conductivity upon crack indications.

Quantitative Evaluation of Crack Depths. Only a small portion of the extensive crack-effect studies can be reproduced here. Figs. 10 to 13 show the **influence of cracks at various locations and of various depths,** for various tube wall thicknesses, and for frequency ratios of $f/f_g = 5$, 15, 50, and 150, respectively. The analysis procedure is similar to that used previously for analysis of cracks in

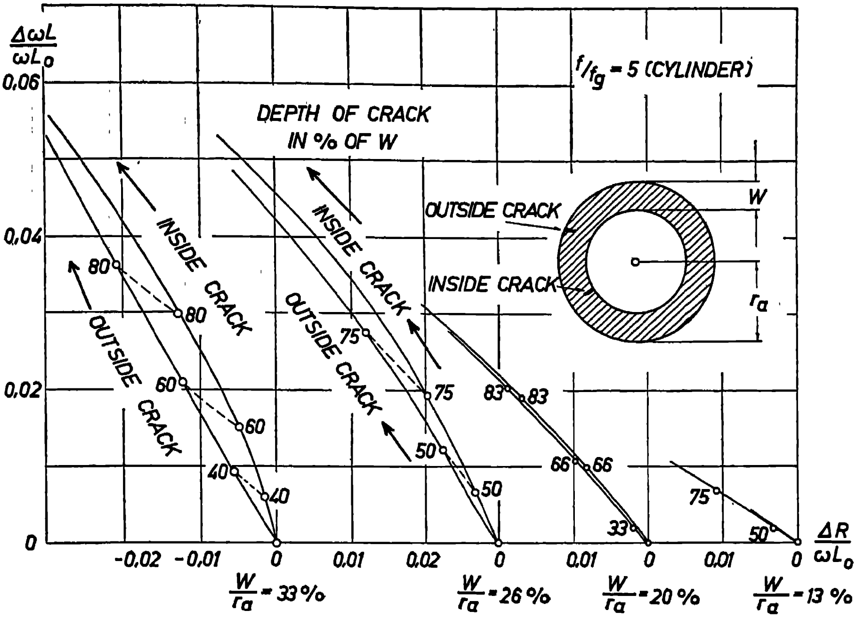

Fig. 10. Apparent impedance plane showing effects of cracks for four different tube wall thicknesses, at a frequency ratio $f/f_g = 5$, for nonferromagnetic tubes.

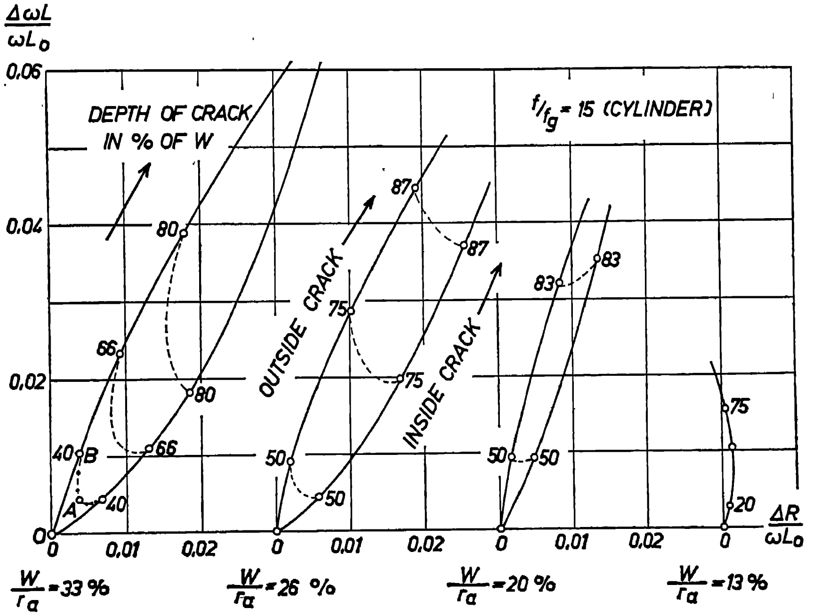

Fig. 11. Apparent impedance plane showing effects of cracks for four different tube wall thicknesses, at a frequency ratio $f/f_g = 15$, for nonferromagnetic tubes.

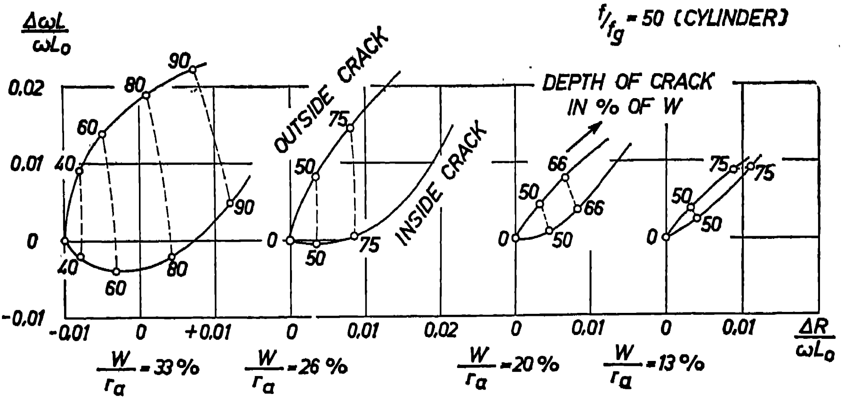

Fig. 12. Apparent impedance plane showing effects of cracks for four different tube wall thicknesses, at a frequency ratio $f/f_g = 50$, for nonferromagnetic tubes.

solid cylinders. A family of curves is obtained for each f/f_g value for the solid cylinder, showing the apparent impedance values for various crack depths and locations. From these, a new family of curves is obtained for each tube wall thickness. Figs. 10 to 13 show such families of **crack curves** for the following wall-thickness ratios: $W/r_a = 33\%$, 26%, 20%, and 13%. Here, W is the wall thickness and r_a is the outside tube radius $r_a = d_a/2$.

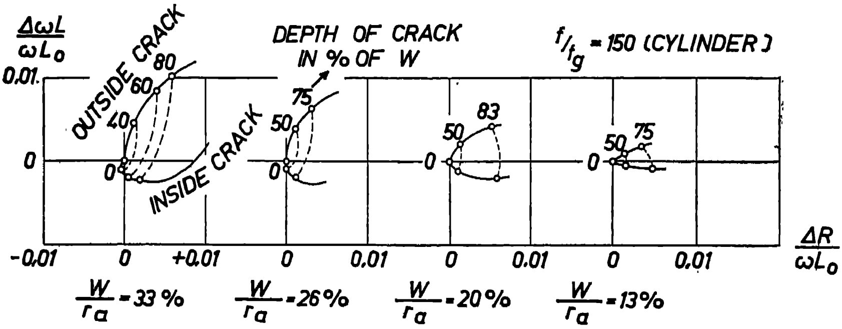

Fig. 13. Apparent impedance plane showing effects of cracks for four different tube wall thicknesses, at a frequency ratio $f/f_g = 150$, for nonferromagnetic tubes.

Characteristics of Crack Evaluation Curves. With higher frequency ratios and thicker tube walls, the **phase displacement** between field strength of outside and inside tube surfaces increases. For W/r_a ratios of only 13 percent (curves on right of Figs. 10 and 11), no phase displacement exists in the impedance curves for outside and inside surface cracks. It is also interesting to note from Fig. 11 that the **influence of a subsurface crack** (which reaches neither inside nor outside tube surfaces) is slightly smaller than for a surface crack of the same depth (compare distances OA and OB). (This is analogous to the accumulation point of a stream of water. A board placed transversely to the stream direction in the center of the stream causes less current resistance that does the same board at the edge of the stream.)

The **response to a crack-free tube** can be determined from Fig. 7 for specific f/f_g ratios for the solid cylinder [calculated from Eq. (5) of the section on Eddy Current Test Principles, the tube material properties, and W/r_a ratio]. Figs. 10 to 13 are plotted to scale so that the **components of relative permeability,** $\Delta\mu_{\text{eff.}}$, obtained from these curves can be inserted into Eqs. (7, a and b), of the section on Eddy Current Cylinder Tests, to obtain the voltage variations ΔE of the test coil, in response to the cracks.

Eddy Current Tests of Tubes with Internal Test Coil

APPLICATIONS OF INTERNAL PROBES. There are numerous eddy current test problems in which the test coil is located within the test object. For example, large numbers of tubes are required for boilers, condensers, coolers, and heat exchangers in oil refineries, steam power plants, chemical plants, and sugar refineries. Such installations usually consist of large numbers of tubes located close together and enclosed in a vessel so that their external surfaces are not accessible. These tubes can be tested only by inserting the test coil into the tubes from the **tube header or other access points.** In other cases it becomes necessary to test **deep, small-diameter drilled holes** in large metal parts (for discontinuities, segregation, corrosion, or other conditions) by inserting the test coil within the hole.

Another important problem is the **internal testing of thick-walled tubes** which, although their external surfaces are accessible, do not permit detection of dangerous inside-surface cracks because their heavy wall thickness limits the eddy current penetration depth. This situation arises in cases of **stress corrosion** in the chemical industry, for example.

INTERNAL PROBE TEST ARRANGEMENTS. Fig. 14 illustrates a test coil of diameter d placed within a tube of inside diameter D_i. To calculate how the coil characteristics vary with test object characteristics, such as (1) inside diameter of tube, D_i, (2) tube wall thickness, W, (3) electrical conductivity σ of tube material, (4) relative magnetic permeability $\mu_{\text{rel.}}$ of tube material, three distinguishing cases must be considered:

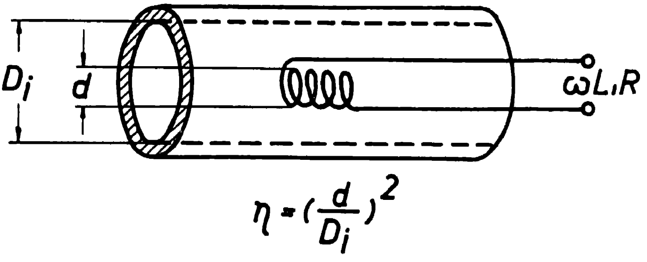

Fig. 14. Test coil inside cylinder.

1. The thin-walled tube, ($W << D_i$).
2. The tube with medium wall thickness.
3. The heavy-walled tube.

Heavy-walled Tubes. Fig. 15 can be used to illustrate the definition of the **limit between medium and heavy-tube wall thicknesses.** In Fig. 15 the in-

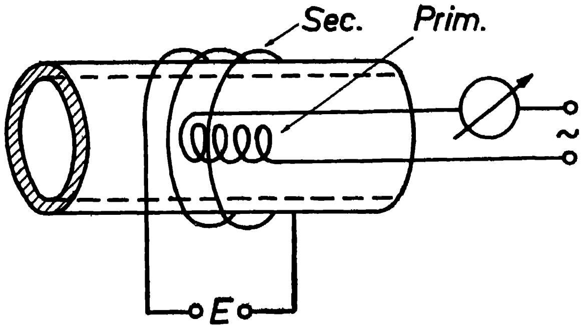

Institut Dr. Foerster

Fig. 15. Arrangement for measuring the screening effect of tubes.

ternal coil is connected to a source of alternating current and serves to establish an a.-c. magnetizing field. The external coil serves as a secondary winding. If the tube in Fig. 15 is removed from the coil system, the a.-c. field of the internal primary coil induces a voltage E_0 in the external secondary winding. If the tube is again placed between the primary and secondary coils of Fig. 15, a reduced voltage E appears across the secondary coil terminals. Fig. 16 shows the experimentally determined ratio of the voltage E, obtained with a tube in place, to the voltage E_0 of the empty coil system, as a function of test frequency. Curves are presented for three tubes, of **copper, brass, and stainless steel,** each with an outside diameter $d_a = 0.8$ in. and a wall thickness $W = 0.040$ in. Whether a tube is considered heavy-walled or medium-walled depends upon the **test frequency,** as illustrated by Fig. 16. If less than 10 percent of the magnetizing field of the

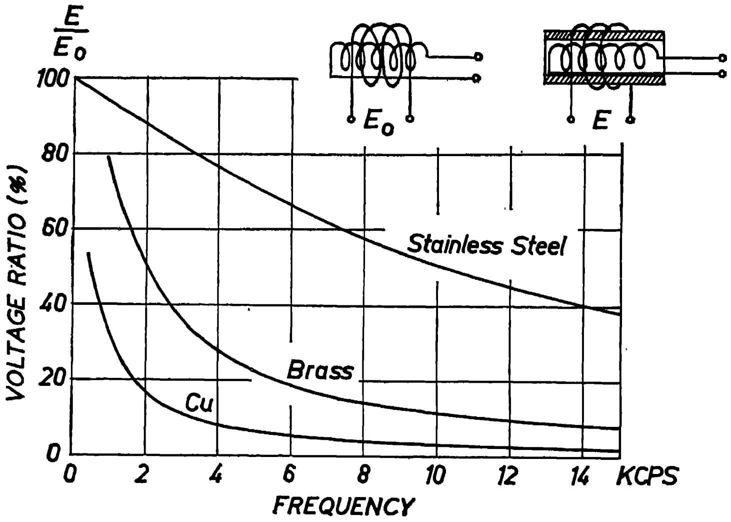

Institut Dr. Foerster

Fig. 16. Decrease of field strength upon insertion of tube between coils of Fig. 15, for copper, brass, and stainless steel tubes of 0.8-in. outside diameter and 0.040-in. wall thickness.

inside primary coil penetrates the tube and is indicated by secondary coil voltage, the tube is considered to be heavy-walled. Thus the copper tube with wall thickness of 0.040 in., tested at frequencies exceeding 3000 c.p.s. (3 kc.), as well as the brass tube at frequencies above 11 kc., appear to be thick-walled.

Evaluation of Thin-walled Nonferromagnetic Tubes. The evaluation of thin-walled, nonferromagnetic tubes is attained through the use of Figs. 1 to 4, which apply also for the testing of thin-walled tubes with an inside coil. The **apparent impedance of the test coil** is the same, whether the test coil is placed directly inside the inner surface or directly on the outer surface of a thin-walled tube. In both cases the lines of magnetic flux are present within the tube material, so that the field of the short-circuited eddy currents has the same reaction on the inside coil as on the outside coil.

Evaluation of Thick-walled Nonferromagnetic Tubes. The thick-walled tube, on the other hand, has an entirely different reaction. A **limit frequency** f_g is defined, as with the solid cylinder, by equating to unity the argument of the mathematical function describing the problem. For the inside coil and thick-walled tube, the limit frequency is defined as

$$f_g = \frac{5066}{\sigma D_i^2 \mu_{\text{rel.}}} \tag{6a}$$

and the **frequency ratio** f/f_g as

$$f/f_g = \frac{f \sigma D_i^2 \mu_{\text{rel.}}}{5066} \tag{6b}$$

where σ = electrical conductivity of tube material, meter/ohm-mm.^{2}.
$\mu_{\text{rel.}}$ = relative magnetic permeability of tube material.
D_i = inside diameter of tube, cm.

Before insertion in the tube, the test coil exhibits the apparent impedance values ωL_0 and R_0. After insertion, these values change to ωL and R. Fig. 17 shows the **normalized impedance components** for various frequency ratios f/f_g and four different fill factors $\eta = (d/D_i)^2$. The **apparent impedance curve** for the fill factor $\eta = 1$ is identical with the effective permeability. The ordinate $\omega L/\omega L_0$ corresponds to the real component, and the abscissa $(R - R_0)/\omega L$ to the imaginary component of the **effective permeability.**

Separation of Material Properties and Inside Corrosion Thinning. When the material conductivity or relative permeability characteristics vary, while the inside diameter D_i of the tube remains constant, the apparent impedance values of the test coil move along the f/f_g curves. In the case of **variation of the inside diameter of the tube** caused, for example, by corrosion wall-thinning, the apparent impedance of the test coil moves along the D_i curves of Fig. 17. Thus a **corrosion effect** (variation in D_i) lies in a different phase direction in the apparent impedance plane than does a variation in material characteristics from tube to tube. Consequently, corrosion effects can be measured with the inside test coil independently of tube material properties.

Maximum Test Sensitivity. The greatest indication sensitivity for conductivity σ, relative permeability $\mu_{\text{rel.}}$, and crack effects lies at test frequencies for which the **frequency ratio** f/f_g is in the range from 1.5 to 12.

Evaluation of Medium-Thickness Tube Walls. The theory of the inside coil with medium-thickness tube walls, in which inside as well as outside cracks influence the coil indications, is discussed more thoroughly in the literature.[42]

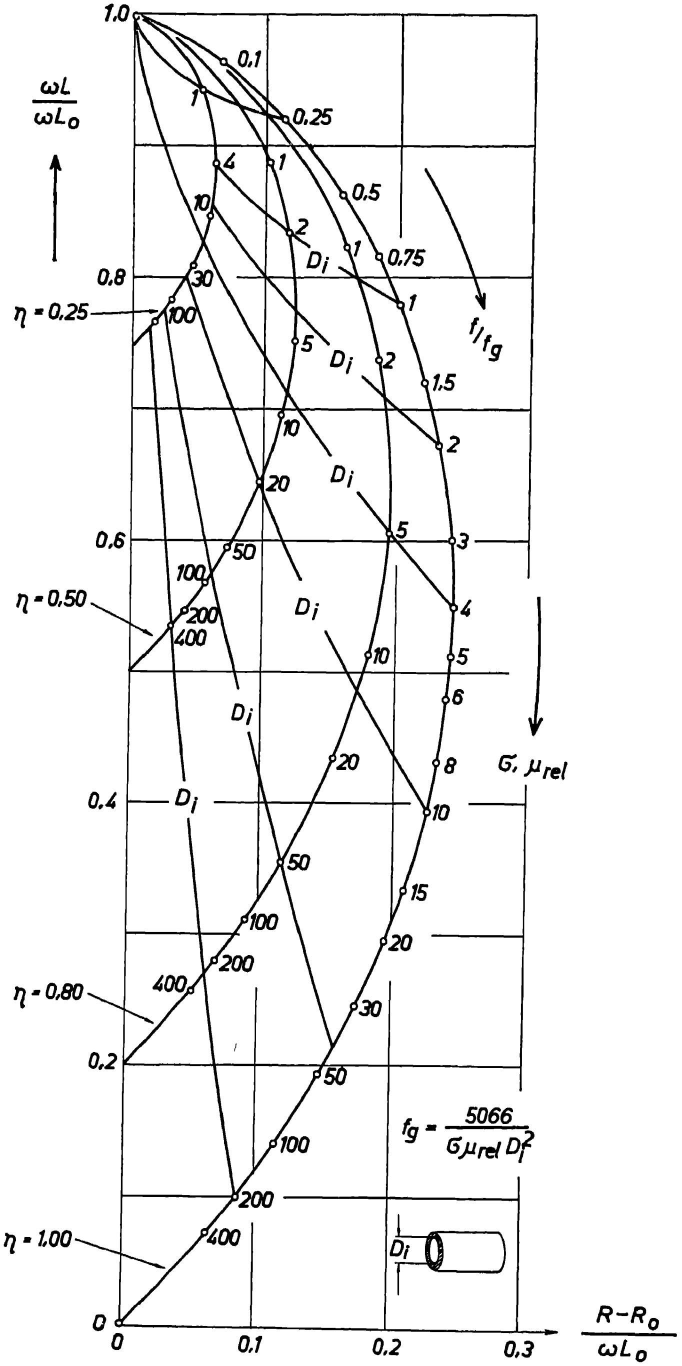

Fig. 17. **Apparent impedance diagram of test coil inside heavy-walled nonferrous tube,** for various fill factors η. Institut Dr. Foerster.

Penetration Depth Limitations

SIGNIFICANCE OF PENETRATION DEPTH. Quantitative calculation of the effective permeability values of tubes with a given wall thickness permits determination of the penetration depth, a fundamental factor in eddy current testing. The calculation indicates the maximum tube wall thickness detectible. If a tube is placed in the field of the test coil instead of a solid cylinder, the calculation indicates at what **diameter ratio** (D_i/D_a) the difference in effective permeability between the solid cylinder and the tube is sufficiently large to produce reliable test indications.

Depending upon the **sensitivity of the test instrument,** it is able to "see" more or less deeply into the inside of the cylinder. Fig. 18, based upon an exact calculation of the difference in permeability between cylinder and tube, indicates to what extent the center of the cylinder can be drilled out before the test instrument can detect the variation from the apparent impedance of the solid cylinder. This **maximum detectible wall thickness** is a function of the frequency ratio and of the sensitivity of the test instrument. Fig. 18 shows curves for fill factor $\eta = 1$, corresponding to four different instrument sensitivities.

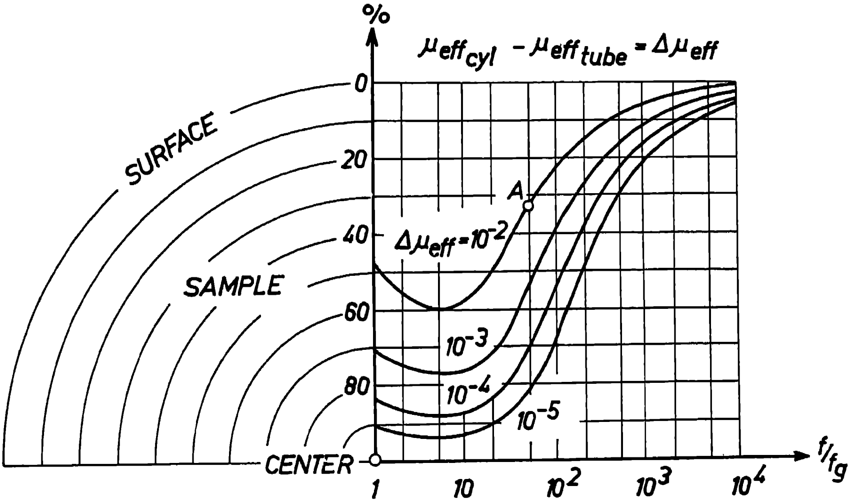

Fig. 18. Penetration depths for different instrument sensitivities (10^{-2}, 10^{-3}, 10^{-4}, and 10^{-5}) as a function of frequency ratio f/f_g.

Significance of Instrument Sensitivities. An instrument sensitivity of 10^{-2} or 10^{-5}, for example, means that a variation of 10^{-2} or 10^{-5} in effective permeability (as described by Fig. 7 of the section on Eddy Current Test Principles) is still clearly visible in the instrument indication. Since Fig. 18 applies for **fill factor** $\eta = 1$, the variation in effective permeability must be twice as large to be detectible for a fill factor $\eta = \frac{1}{2}$. Fig. 18 indicates the penetration depth for a wide range of **frequency ratios** f/f_g for instrument sensitivities of 10^{-2}, 10^{-3}, 10^{-4}, and 10^{-5}. Alternatively, Fig. 18 indicates how far the central cavity in a cylinder can increase before it is just detectible at specific instrument sensitivity and f/f_g values. It shows the relative **insensitivity of eddy current methods to concentric cavities.**

Limitations in Detection of Concentric Cavities. Even in the **most favorable case,** with $f/f_g = 6.25$ and an instrument sensitivity as high as 10^{-5}, the central 6 percent of the diameter of a cylinder cannot be inspected with eddy current measurements. With an instrument sensitivity of 10^{-3}, even with the most favorable frequency ratio of $f/f_g = 6.25$, the central 23 percent of the cylinder diameter cannot be inspected. However, in most cases, discontinuities such as **cracks and cavities which influence serviceability** have an eccentric location and are more easily determined.

Determination of Secondary Coil Voltages with Tubes. To calculate the variation in test coil voltage when a tube rather than a solid cylinder is present, the $\Delta\mu_{\text{eff.}}$ values from Fig. 18 are inserted into Eq. (7).

$$\Delta E/E_0 = \eta(\Delta\mu_{\text{eff.}}) \tag{7}$$

The $\Delta\mu_{\text{eff.}}$ values on the curves of Fig. 18 are determined, of course, by the available instrument sensitivities. When voltage values have been calculated for a specific instrument sensitivity by means of Eq. (7), Fig. 18 can be used to obtain penetration depths in percentages of the outside radius of the cylinder.

Magnetic Permeability Limitations on Depth Penetration. Ferromagnetic test materials are subject to a phenomenon which generally causes considerable decrease in the effective depth of penetration of eddy current measurements. Fig. 19 shows the relative magnetic permeability $\mu_{\text{rel.}}$ as a function of the magnetizing

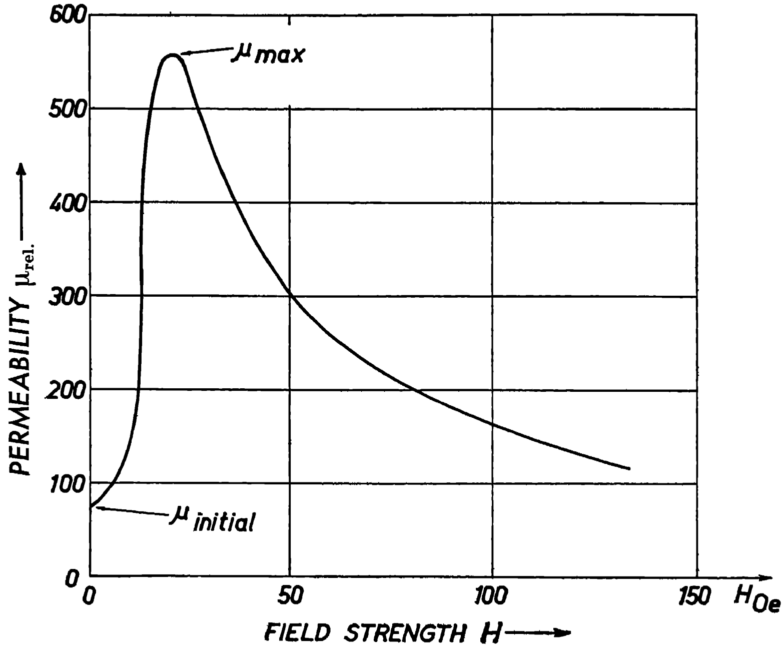

Fig. 19. Relative magnetic permeability, $\mu_{\text{rel.}}$ of a carbon steel as a function of external magnetic-field strength. Note rapid increase in initial permeability with increasing field strength.

field strength for a typical carbon steel. At low field strengths the ferromagnetic material normally shows a very small **initial permeability,** $\mu_{\text{init.}}$. As the field strength is increased, the relative permeability increases greatly and eventually reaches the high **maximum permeability,** $\mu_{\text{max.}}$. At still higher magnetizing field strengths, the permeability values decrease more slowly.

The theory of penetration depth, as summarized in Figs. 3, 4, 5, and 6 in the section on Eddy Current Cylinder Tests, indicates that **penetration depth** decreases with increases in the product ($D^2\sigma\mu$) of the square of cylinder diameter, electrical conductivity, and relative magnetic permeability. Thus Fig. 19 would appear to indicate that it would be practical to work with very low field strengths, to take advantage of the very low initial permeability. If this were feasible, it might permit a greater penetration depth and better indication of subsurface cracks. However, the **use of weak field strengths** is impossible because of the influence of inhomogeneous stresses caused, for example, by the process of straightening rods and tubes, which influence the magnetic characteristics of the test material. The initial permeability is especially changed by **inhomogeneous mechanical stress conditions.** In consequence, various initial permeability values appear from point to point, in accordance with previous deformations, in the testing of rods or tubes.

Limitations in Use of High Magnetizing Field Strengths. The known decrease of field strength toward the inside of the cylinder (see Fig. 5 of the section on Eddy Current Cylinder Tests) appears also in the use of higher a.-c. magnetizing field strengths. As soon as the field strength within the cylinder approaches the value at which the maximum permeability occurs, a large and rapid decrease occurs in field strength as a result of the increasing product ($D^2\sigma\mu$). At **test frequencies of 60 c.p.s.,** even with high external field strengths, field strength values corresponding to the maximum permeability are obtained immediately below the surface of the cylinder or tube. This **layer of maximum permeability** offers considerable resistance to deeper penetration of the a.-c. field. Fig. 20 presents experimental proof of the existence of this condition, which becomes quite important in nondestructive **testing of iron and steel.**

In the experiments used to provide the data of Fig. 20, three steel tubes with low carbon content were prepared with diameters of 1.2 in. and wall thicknesses of 0.040, 0.080, and 0.120 in. Cylindrical plugs were made to fill the entire interior volume of each tube. First, the three plugged tubes, whose physical behavior is the same as that of solid cylinders, were inserted into the test coil and resulting test coil voltages were measured. Then the cylindrical core of each tube was removed, and the test repeated. The voltages obtained with the empty tubes, expressed in percentages of the voltages of the filled cylinders, were plotted as the ordinates in Fig. 20.

Shielding Tests at 50-C.p.s. Frequency. Fig. 20 shows the differences in voltages between the solid cylinder and the hollow tube as a function of external field strength (measured in terms of magnetizing amperes). In tests made at **low field strengths** and 50 c.p.s., removal of the cylindrical core from the 0.040-in. wall tube resulted in 38 percent voltage variation (see point A, Fig. 20). As field strengths were increased toward the condition of maximum relative permeability, the influence of the core decreased. When the **maximum permeability** was reached, the influence of the core was only 3.5 percent (see point B). The **effect of the core** was reduced tenfold because of the decrease in penetration depth as magnetization increased from the initial permeability conditions at low field strengths to the maximum permeability condition. At still higher field strengths, the relative permeability decreases. The penetration depth increases above the maximum permeability condition of magnetization, so that the effect of the core is again more distinct.

Shielding Tests at 5-C.p.s. Frequency. At the low test frequency of 5 c.p.s., the **penetration depth** is greater than at 50 c.p.s. Removal of the cylindrical core from the 0.040-in. wall tube results in an 80 percent voltage variation at low field strengths. In the **initial permeability range**, the influence of the core is about twice as great at 5 c.p.s. as at 50 c.p.s. With tubes of greater wall thickness, the difference in penetration depth between 5- and 50-c.p.s. test frequencies is considerably larger.

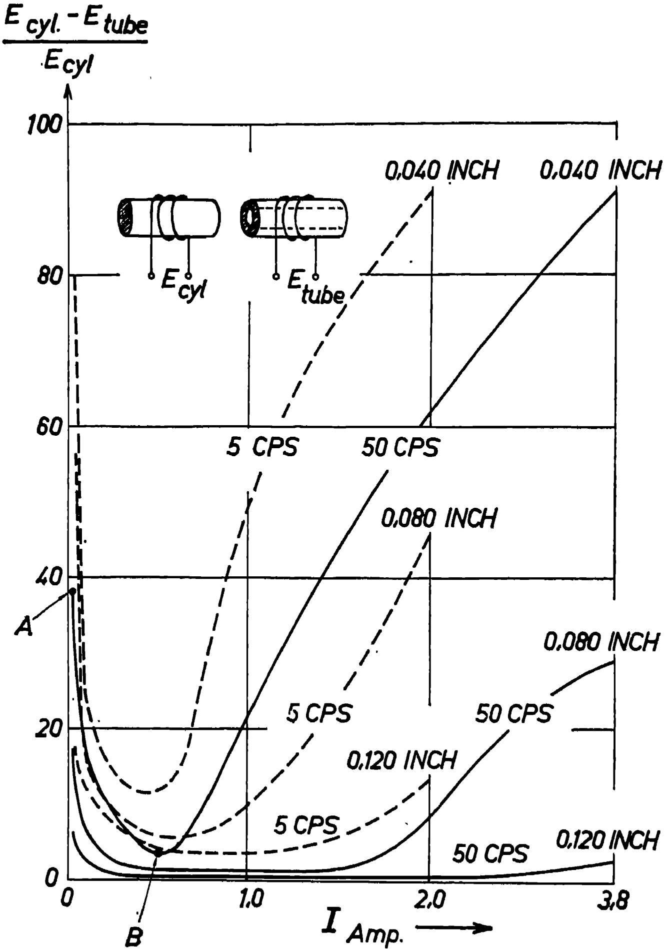

Institut Dr. Foerster

Fig. 20. **Penetration depths for carbon steel tubes of 0.040, 0.080, and 0.120 in. wall thickness,** 1.2-in. diameter, at 5 and 50 c.p.s.

At **medium field strengths** (corresponding to a magnetizing current of 1.5 amp. in Fig. 20), changing from 50 to 5 c.p.s. increases the influence of the core, by a ratio of 16:1, with tubes of 0.080-in. wall thickness. With even greater wall thicknesses, the **superiority of 5-c.p.s. test frequencies** in increasing the penetration depth is even more obvious. The relatively low penetration depths of eddy current tests of ferromagnetic materials makes them most suitable for **detection of surface discontinuities** only, for the reasons discussed above.

Tests of Small Diameter Tubing

PRINCIPLE OF TEST. Electromagnetically induced, alternating, eddy current flow is a method of determining the quality of small-diameter, nonferromagnetic, metallic tubing. Fluctuations in the field of an exciting coil system are produced by variations in eddy current flow in a tube moved relative to the coil. In general, two distinctly different effects on the field of the coil are produced by **eddy current flow**:

1. The flow of induced current through a metal part of finite resistivity produces a **power loss.** This must be supplied by the exciting field, which in turn must be supplied from the alternating current feeding the exciting coil. Thus the exciting coil impedance must have a resistive component whose magnitude depends upon the power loss in the metal.
2. The field of the induced current opposes the exciting field, decreasing the field flux of the exciting coil. The **inductance** of the exciting coil (the ease with which it produces magnetic flux) is reduced by an amount depending upon the induced current magnitude. The reactive component of the exciting coil impedance is reduced accordingly.

As the tube moves through the coil, fluctuations occur in both the resistive and reactive components of the coil impedance. These correspond to variations in the magnitude, phase, and distribution of the induced eddy currents.

IMPEDANCE PLANE CHARACTERISTICS. The "impedance-plane" curves of Fig. 21 show variations in amplitude and phase of impedance for a test coil encircling a cylindrical metal tube. Here the amplitude and phase values are resolved into two quadrature components, the reactive and resistive components. These values are normalized to the pure reactive impedance of the coil in the absence of the metal tube. The frequency ratio f/f_c permits this plot to be used for **tubing** of any conductivity, diameter, and wall thickness. The quantity f_c is a **characteristic frequency** defined by the relationship

$$f_c = \frac{2}{\pi \mu \gamma D_p^2} \qquad (8)$$

where μ = permeability, henries/meter, ($4\pi \times 10^{-7}$ for nonmagnetic material).
γ = conductivity, mhos/meter.
D_p = outside diameter of part, meters.

The plot of Fig. 21 was made for a ratio of part diameter to coil diameter, $\nu = D_p/D_c = 1$, and four different values of f/f_c. The dotted curve is for varying f/f_c ratios, the heavy dashed lines show the effect of varying outside diameter, and the solid lines show the effect of varying wall thickness. These curves differ considerably in shape from those representing the impedance of a coil encircling a solid rod. The **wall thickness** of the tube is as important in influencing the impedance of the coil as are the conductivity and outside diameter of the tube.

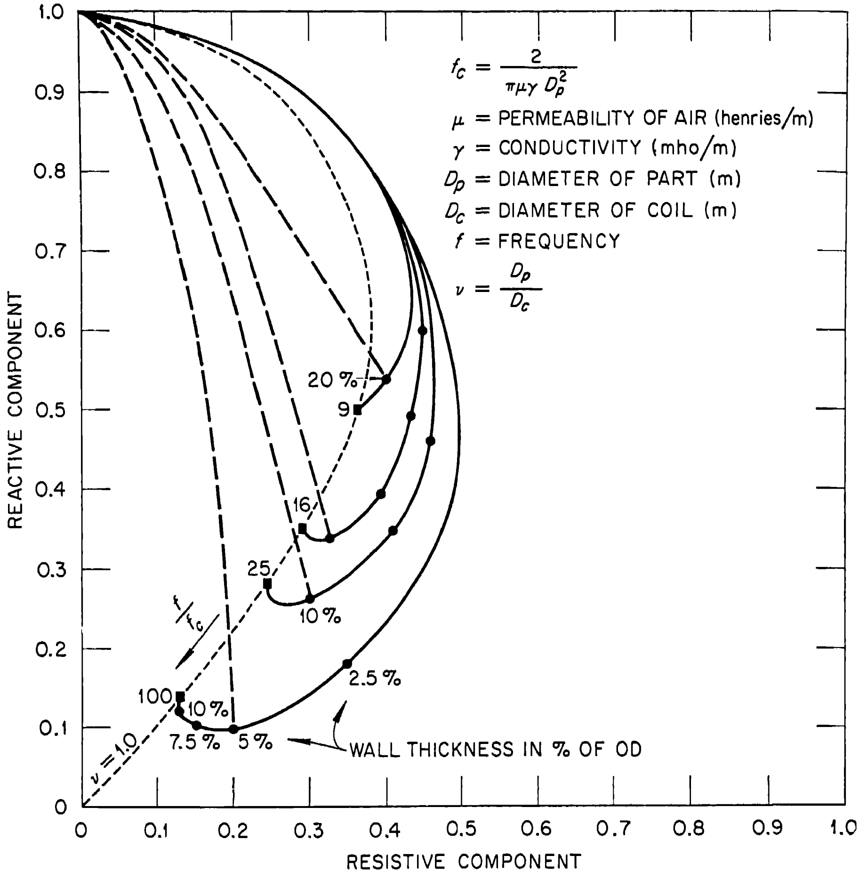

Oak Ridge Nat'l. Lab.

Fig. 21. Impedance plane for coil encircling nonferromagnetic metal tubes.

Controlling Factors. The alteration of the field produced by the induced eddy currents is a function of

1. The frequency of the exciting current.
2. The electrical conductivity and magnetic permeability of the tube.
3. The physical dimensions of the tube and its location in the field.
4. The presence and location of discontinuities or "inhomogeneities" within the tube wall.

Since the **mechanical and thermal history** of the tube influence its electrical conductivity and, in the case of the austenitic stainless steels, its magnetic permeability, they also influence the field of the coil. **Mechanical, metallurgical, or chemical variations** within the tube, as it moves through the coil, affect the coil impedance. The numerous sources of signals from this type of test place a large burden of interpretation upon the inspector.

The exact nature of the signals obtained and their interpretation depend entirely upon the type of coil system and instrumentation used. In addition the manner in which signals are displayed and the method used to move the tube through the coil system are exceedingly important in the interpretation.

TYPES OF COIL SYSTEMS. Fig. 22 shows three basic coil systems used on **small-diameter tubing.**

1. Encircling, or "feed-through," coils.
2. Inside-probe, or "bobbin," coils.
3. Surface probe coils.

Also illustrated for each case is the use of both "absolute" measurements (without a direct reference) and differential methods. The **encircling-coil system** is more common because of its ease of utilization and relatively high inspection speeds. The mechanical difficulties involved in the application of **bobbin coils** are considerable, particularly in the case of long lengths of very small-diameter tubing. Despite this, their use may be warranted for inspection of the bore of heavy-wall tubing or duplex tubing. The **surface probe coil** is not in general use for inspection of small-diameter tubing because of inherent mechanical problems and slow inspection speeds. Its high sensitivity to small discontinuities and definitive ability, however, are very attractive for critical inspection and will be considered in detail later.

The use of **single and double coil arrangements** is also illustrated in Fig. 22. In the case of the double encircling-coil system, the a.-c. excitation is applied to

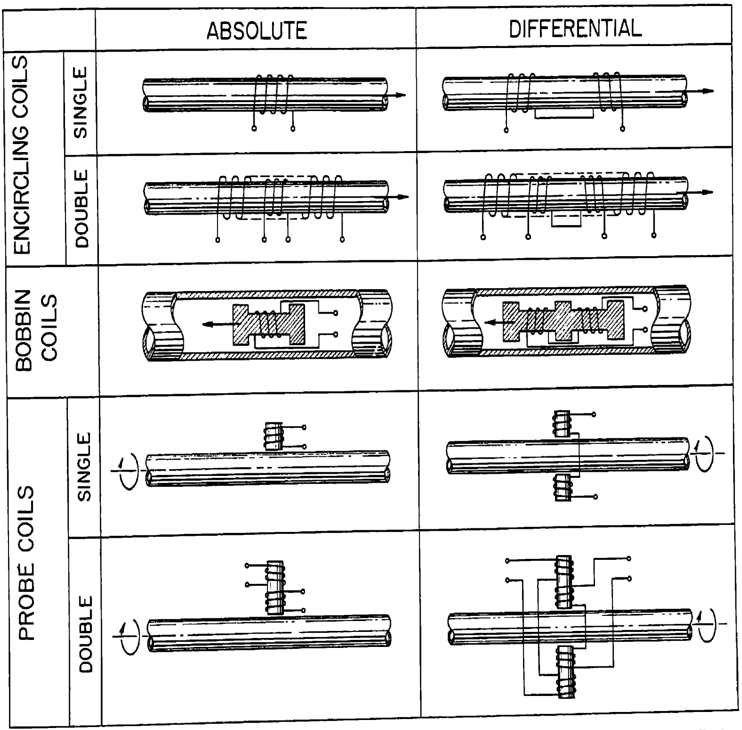

Oak Ridge Nat'l. Lab.

Fig. 22. Test coil configurations for eddy current testing of small-diameter tubing.

the outer coil, and the voltage induced in the inner "pick-up" coil is examined. The advantage of this arrangement is that the pick-up coil may have a very small dimension in the longitudinal direction and thus be sensitive to very short discontinuities. At the same time the exciting field in the vicinity of the pick-up coil may be made almost a geometrically perfect cylinder of flux parallel to the axis of the coil and of uniform density in absence of the tube. This is done by the use of an elongated exciting coil. The double-coil system does not appear to offer a great practical advantage over the single-coil system with a large ratio of outside diameter of tube to effective coil diameter, since the effect of field distortion in the vicinity of the tube wall produced by the use of a thin single coil is small.

Sensitivity and Signal Discrimination. In employing an encircling coil to inspect tubing, the problem is more than one of sensitivity to **variations in the tube.** As suggested previously, the eddy currents will, in general, be influenced by all possible variations occurring in the tube. By exercising a little ingenuity, several instrument types can be contrived which will have a very sensitive response to these variations. The problem is one of separation and classification of these variations by their nature and extent. More specifically, it is desirable to distinguish signals resulting from **dimensional variations** from those resulting from **discontinuities** in the tubing. In addition, it would be advantageous to separate outside-surface from inside-surface discontinuity signals and also to separate the effects of wall-thickness and diameter changes.

Differential Coil System. One approach to the problem of distinguishing between signals from discontinuities and those resulting from dimensional variations is the use of the differential-coil system illustrated in Fig. 22. In this scheme, signals from coils encircling two adjacent sections of the tube are subtracted. **Dimensional variations** generally occur more slowly as a function of tube lengths than do the discontinuities, and if the two coils are closely spaced, the signals from the dimensional variations tend to be eliminated. Several disadvantages and limitations are imposed by the use of this technique. If the system is successful, the dimensional signals are completely eliminated from the test indications instead of being separated for observation or monitoring. An additional **absolute coil** must be used to obtain the dimensional information when it is desired.

If the differential system is to be insensitive to dimensional variations, the two coils must be very close together. All **drawn tubing** contains a **periodic variation in both wall thickness and diameter,** varying in magnitude within a period of 2 to 8 in., depending upon the material, tube size, and the drawing and annealing practices used. Thus, if the two coils are not close together, the dimensional signals may be added rather than subtracted. Assuming that the coils are in proximity, there is a further and more serious **disadvantage:** A signal produced by this system measures only the size of a discontinuity when the length of the discontinuity is less than the distance between the coils. For discontinuities longer than this distance, the signal measures the size of the leading and trailing edges of the discontinuity over a length equal to the coil spacing, and the rate of change with respect to tube length at all intermediate points. Thus signals from such a system may be very difficult to interpret, even to the extent of being misleading.

Absolute Coil System. The absolute encircling-coil system does not inherently distinguish between dimensional variations and discontinuities. However, the resultant signals usually can be identified separately if the signal is recorded as a function of tube length, as will be illustrated later.

Tube-feeding Mechanism. Interpretation of signals from encircling-coil systems is often hampered by **spurious signals** caused by the **wobble of the tubing** in the coil. A tube-feeding mechanism, such as that illustrated in Fig. 23 has been very effective in eliminating such spurious signals. In this system the testing coil is wound on a laminated-plastic **guide tube,** having a length approximately equal to ten tubing diameters. The tube under inspection slides inside this guide tube. The coil assembly is then supported by very light springs so that it can move freely with the tube.

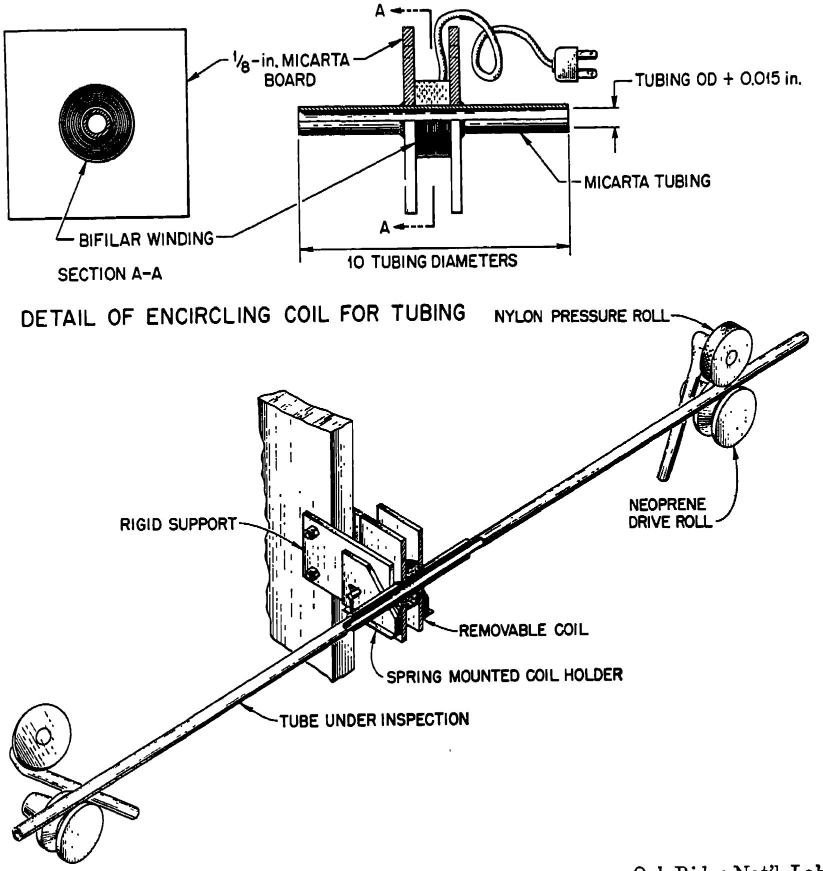

Oak Ridge Nat'l. Lab.

Fig. 23. Encircling-coil assembly and feed mechanism for tubing inspection.

INSTRUMENTATION. Four basic types of measurements can be applied to the inspection of small-diameter tubing:

1. Measurement of the change in magnitude of the total impedance of the testing coil, regardless of the phase.
2. Measurement of only the resistive component of the coil impedance (core loss).
3. Measurement of only the reactive component of the testing-coil impedance.
4. Phase-sensitive measurements which separate the resistive and reactive components of the coil impedance.

Regardless of the type of instrumentation used, signals from the test coil behave primarily as indicated by the impedance plane of Fig. 21. Of the four basic instrument types, those employing **phase-sensitive detectors** have gained the greatest popularity, since two forms of information are obtained rather than one. For example, refer to the impedance plot of Fig. 21 and consider a tube having a wall thickness of 10 percent of its diameter. If a frequency is chosen such that $f/f_c = 25$, the effects of varying diameter and varying wall thickness are separated in phase by approximately 90 deg. Thus, by employing phase-sensitive detectors, it is possible simultaneously to obtain separate signals for varying wall thickness and varying diameter. However, to attain a 90-deg. separation between the effects of varying diameter and varying wall thickness, two conditions must be obtained.

1. The operating frequency must be varied according to the square of the tube diameter and with the first power of the tube conductivity.
2. The f/f_c ratio must be varied as the percentage of wall thickness varies.

This illustrates the inadequacy of fixed-frequency, phase-sensitive, inspection instruments.

RESISTIVE-COMPONENT SENSING INSTRUMENTS. Instruments which measure only one component on the impedance plane of Fig. 21, and those which measure the total vector magnitude of a change on the impedance plane, can be used to advantage in the inspection of tubing. An example of this is the use of an instrument which measures only the **resistivity component** of changes in the testing-coil impedance. Fig. 24 is a plot of the instrument reading (at a reduced sensitivity) as a function of tube-wall thickness, with the ratio f/f_c as a parameter. This read-out is a distorted inverse measure of the resistive components on the impedance plane of Fig. 21. The **nonlinear characteristic** of this instrument near the zero or "quench" of the oscillator causes the read-out to be distorted. It also accounts for the high sensitivity of the instrument.

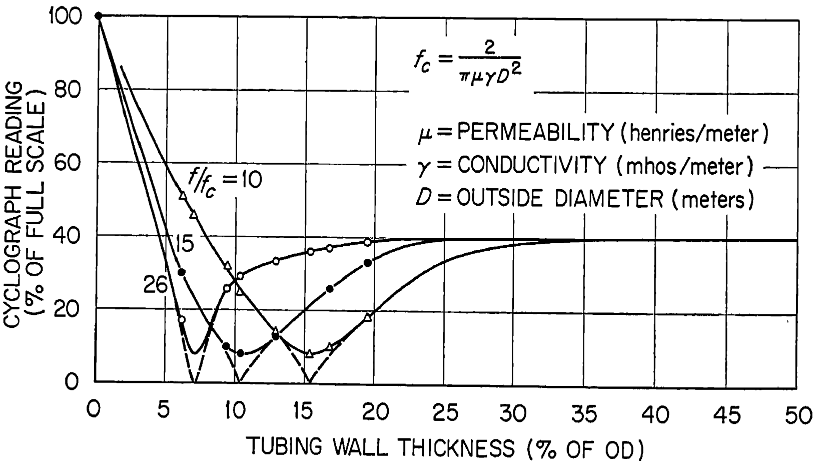

Oak Ridge Nat'l. Lab.

Fig. 24. Resistance-loss test indications as a function of tubing wall thickness with f/f_c as a parameter.

FLAW SENSITIVITY. The optimum outside diameter and inside diameter flaw sensitivity is obtained for a value of f/f_c which causes the curve to peak for a value of wall thickness near that of the tubing to be tested. This is the condition of **maximum power loss** or core loss in the tube. In general, discontinuities within the tube wall cause indications similar to those from reductions in wall thickness. Therefore **operating points** are selected just to the left of negative peaks in the curves of Fig. 24. Discontinuities, wall-thickness reductions, and diameter reductions then cause positive **deflections in the instrument** read-out, whereas increases in the wall thickness or diameter, or foreign-metal pick-up, cause negative deflections. Although the signals obtained from this system are not

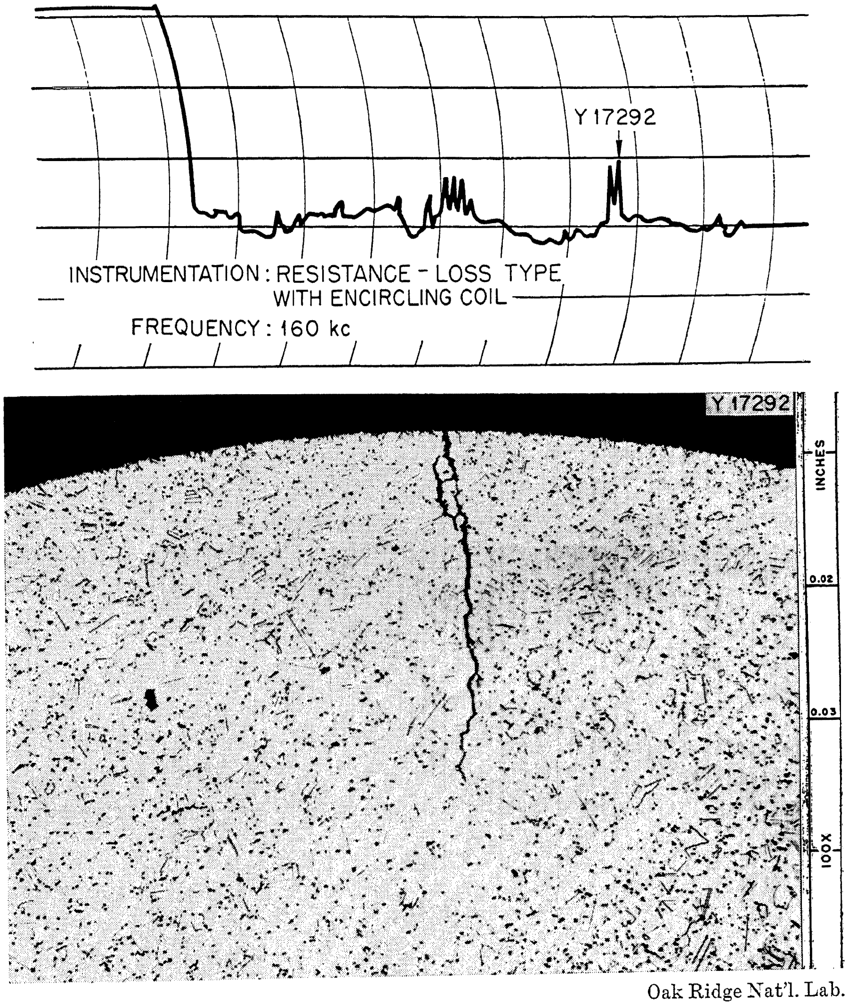

Oak Ridge Nat'l. Lab.

Fig. 25. Eddy current signal trace and photomicrograph of defective ¼ × 0.049-in. Hastelloy tubing.

definitive in themselves, interpretation can be enhanced by recording the signals as a function of tube lengths. Signals due to relatively **large discontinuities** are usually very easily separated from those resulting from dimensional variations in the tube because of their large amplitude and very abrupt nature. This is illustrated by the sharp positive spikes in the trace of Fig. 25, caused by an outside radial crack of 0.036-in. depth in a 1/4 × 0.049-in. Hastelloy B tube.

Detection of Intergranular Corrosion. Intergranular attack on the inner surface of tubing produces signals similar to the indications illustrated in Fig. 26,

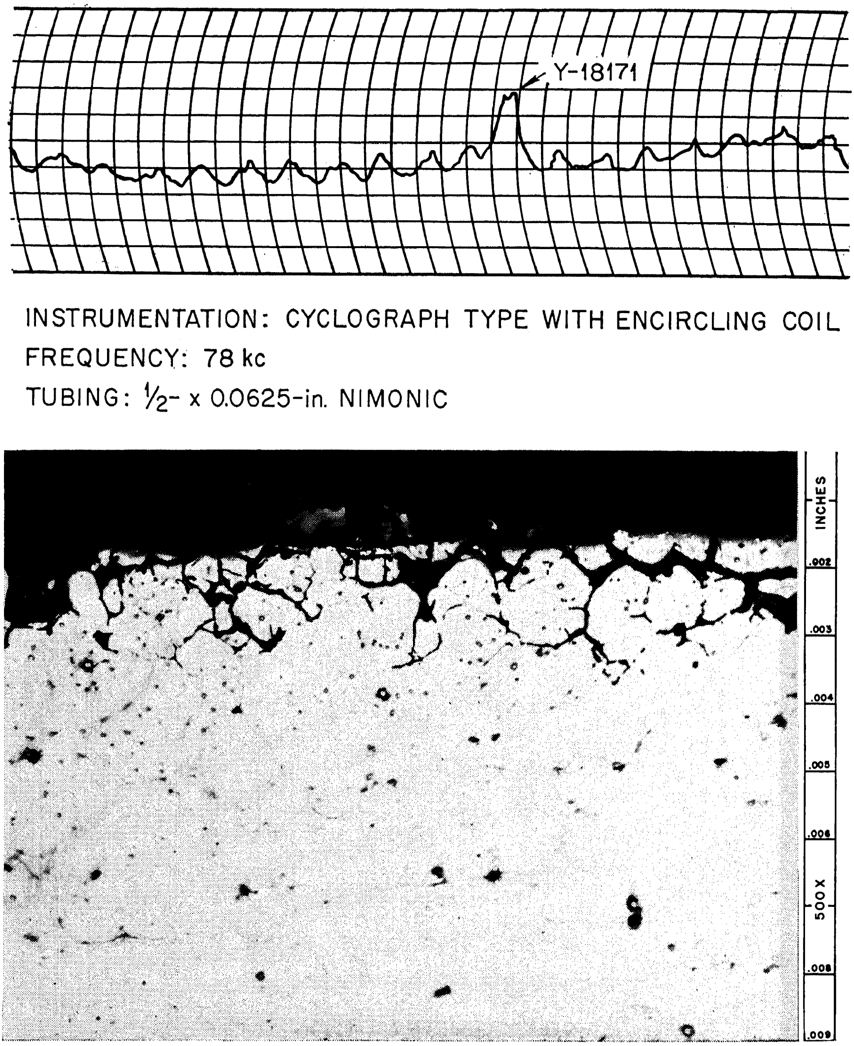
Y-18171
INSTRUMENTATION: CYCLOGRAPH TYPE WITH ENCIRCLING COIL
FREQUENCY: 78 kc
TUBING: 1/2- x 0.0625-in. NIMONIC
INCHES
.002
.003
.004
.005
.006
500X
.008
.009

Oak Ridge Nat'l. Lab.

Fig. 26. Eddy current signal trace and photomicrograph of intergranular corrosion on inside surface of Nimonic tubing.

which appear less sharp than signals caused by cracks. The indicated signal was produced by the 0.002-in. deep, corrosive condition shown in the photomicrograph. The smaller signals appearing on the trace were produced by dimensional variations and less severe conditions of intergranular attack. **Foreign metallic particles** are sometimes found embedded in the inside wall of redrawn small-diameter tubing. These bodies are usually picked up from tools used in manufacturing of the tubing and generally have a high magnetic permeability; hence, they are very easily detected by eddy currents in a nonferromagnetic tube. Fig. 27 shows a photomicrograph of two such pick-up areas on the inside wall of a 3⁄16 × 0.025-in. Inconel tube, and the corresponding eddy current trace. The presence of these areas is indicated by the two sharp negative spikes. These spikes are in the opposite direction to those caused by the cracks of Fig. 25 and the intergranular attack shown in Fig. 26. The **smooth cyclic variations** in this trace are due to dimensional variations in the tube.

Sensitivity to Small Discontinuities. The signal traces shown in Fig. 27 indicate a limitation imposed by the use of the encircling coil for the detection of very small discontinuities. A defect cannot be resolved if the signal it produces is small compared with the signals from all other variations, including dimensional variations, observed as the tube is moved through the coil. The **maximum practical test sensitivity** which may be achieved with this type of test is the detection of discontinuities which

1. Have lengths comparable to, or longer than, that of the coil.
2. Have depths of 5 percent or more of the wall thickness.

The sensitivity to average dimensional changes and to relatively large areas of intergranular attack is, of course, much greater than this, as has been shown in the previous illustrations.

Wall Thickness and Tube Diameter. In many critical uses of small-diameter tubing, the physical dimensions of the tubing are important. In such cases, the consumer must be able to determine the conformity of the tube to the **required dimensional tolerance range.** The only promising approach to a fast, accurate, continuous gaging of tube dimensions is that of the encircling-coil, eddy current method.

The difficulty encountered in utilizing an instrument measuring only resistance losses in this application is that signals due to both diameter and wall thickness, in addition to signals from the other variables previously mentioned, appear together in the single channel read-out. Furthermore, all encircling-coil tests are inherently more sensitive to diameter changes than to wall-thickness changes, due to the attenuation of the eddy current density as a function of depth. Therefore the difficulty in interpreting the diameter and wall-thickness signals in the single channel read-out is further increased. Although it is theoretically possible to use phase-sensitive instruments to separate these effects, available fixed-frequency instruments of this type are insufficiently versatile to allow the wall thickness and diameter signals to be separated for any appreciable range of diameter, wall thickness, or material. An experimental instrument has been developed which is variable in frequency over a very wide range. It circumvents the frequency dependence of phase-balance and detector circuits by employing an indirect method of measuring the reactive and resistive components of the test coil impedance.

Frequency Selection. The operating frequencies usually selected for use do not give 90-deg. separation between the effects of changing diameter and wall

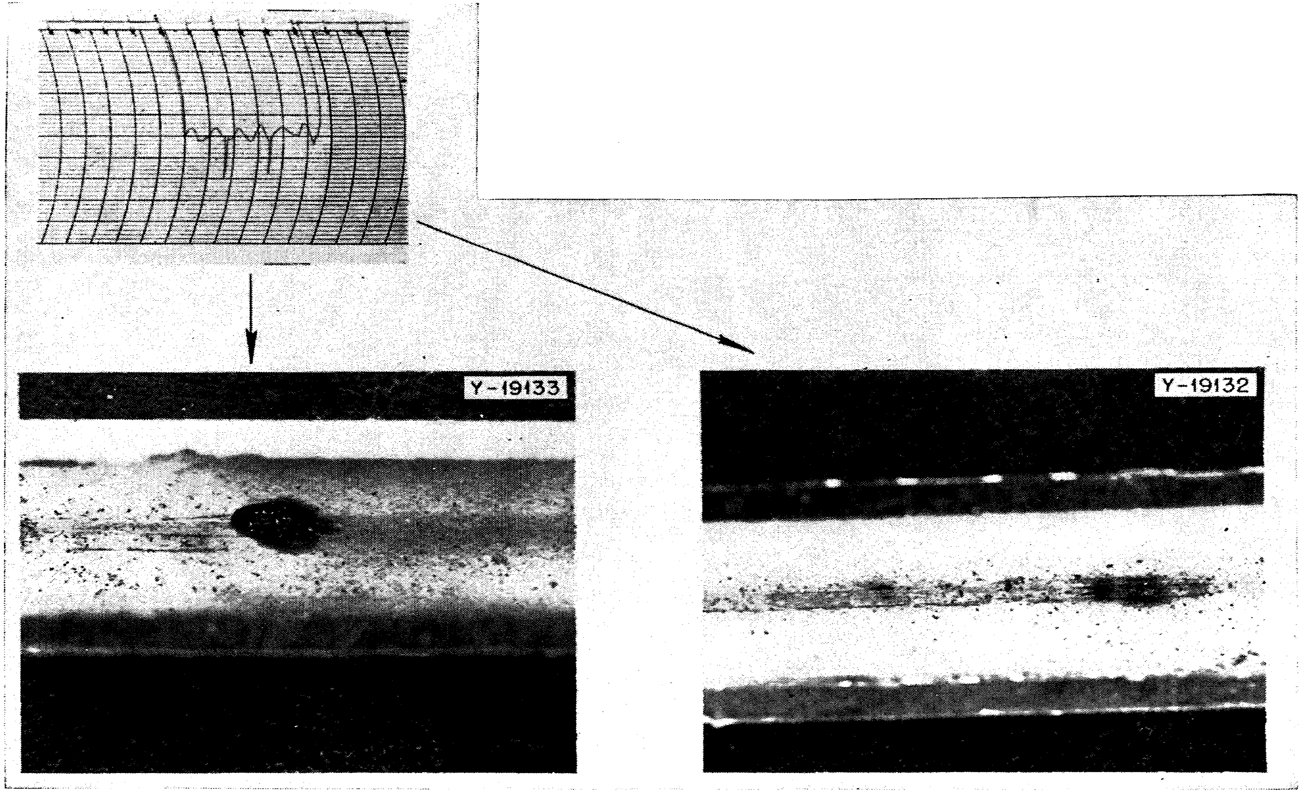

Oak Ridge Nat'l. Lab.

Fig. 27. Eddy current signal trace and photomicrographs of defective $\frac{3}{16} \times 0.025$-in. Inconel tubing.

thickness. The use of high frequencies to produce 90-deg. separation results in undesirably high **attenuation of the eddy current density** at the inside surface. Use of lower frequencies yields operating points near the resistive peak of the impedance plane of Fig. 21. Because of the resultant lower attenuation, considerable improvement is obtained in the sensitivity to defects on the inner surface, but at the expense of less phase separation between outside and inside diameter effects. An operating point is thus selected for a particular tube, such that small changes in wall thickness produce little or no change in the resistive components

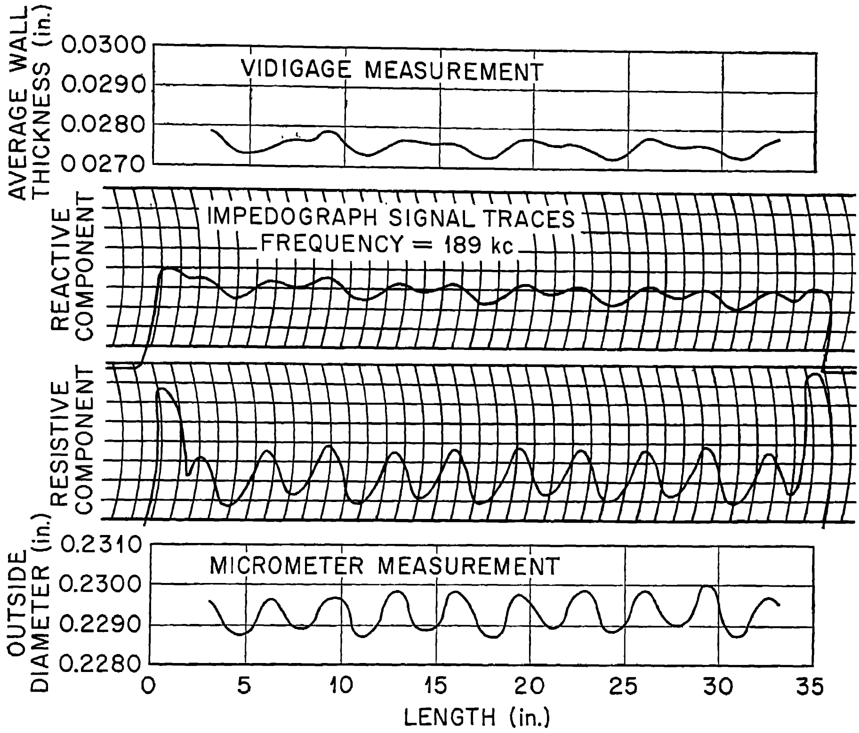

Oak Ridge Nat'l. Lab.

Fig. 28. Comparison of resistive and reactive component signal traces with actual dimensional variations in a 0.229 × 0.025-in. Inconel tube.

but produce maximum change in the reactive component. Thus **changes in the outside diameter** produce impedance variations at an angle oblique to both resistive and reactive components. These produce signals in both the resistive and reactive channels. The controls of the resolving bridges provided in the instrument can then be adjusted until one channel responds primarily to variation in diameter and the other primarily to variation in wall thickness. **Small defects on the inner wall** of the tubing cause impedance excursions which are nearly in phase with those from wall-thickness variations. **Small defects on the outer surface** cause excursions which are nearly in phase with those from diameter variations. Therefore small inside defects appear on the same channel with wall-thickness variation and small outside defects appear on the same channel

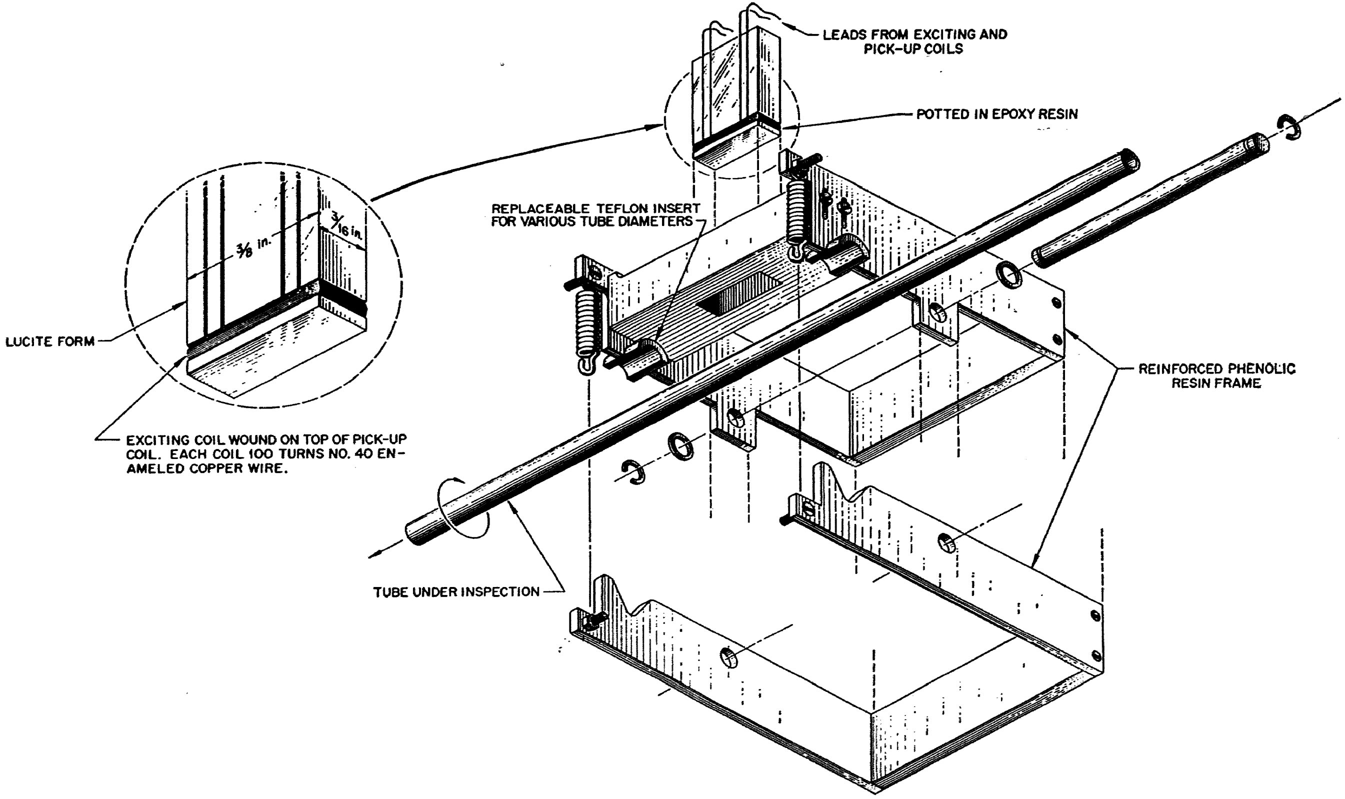
LEADS FROM EXCITING AND PICK-UP COILS
POTTED IN EPOXY RESIN
REPLACEABLE TEFLON INSERT FOR VARIOUS TUBE DIAMETERS
3/8 in.
3/16 in.
LUCITE FORM
EXCITING COIL WOUND ON TOP OF PICK-UP COIL. EACH COIL 100 TURNS NO. 40 ENAMELED COPPER WIRE.
REINFORCED PHENOLIC RESIN FRAME
TUBE UNDER INSPECTION

Oak Ridge Nat'l. Lab.

Fig. 29. Eddy current probe coil and holder for scanning small-diameter tubing.

with diameter variation. **Gross defects** cause very large impedance excursions at some phase angle between the effects of varying diameter and wall thickness; thus the large resultant defect signal is present in both channels.

The ability of this system to distinguish between diameter and wall-thickness variations is illustrated in Fig. 28. The signal traces are recordings from the two signal channels for two 35-in. lengths of 0.229 × 0.025-in. Inconel tubing which were previously stretched to accentuate their dimensional variation. Above the traces are shown plots of the average wall thickness as measured with the ultrasonic-resonance thickness gage. Plots of the average outside diameter, as measured with mechanical micrometers, are shown below the traces. It is readily seen that close correlation exists between the instrument signal and the other independent measurements. These traces were made on the 0.229 × 0.025-in. Inconel tubing at a linear **tube speed** of approximately 1 f.p.s., and at an operating frequency of 189 kc., for which $f/f_c = 15$.

THE SURFACE PROBE-COIL SYSTEM. From the standpoint of interpretability, the probe-coil system illustrated in Fig. 22 is very attractive. In such a system the probe mechanically scans the tube surface in a helical pattern. Sig-

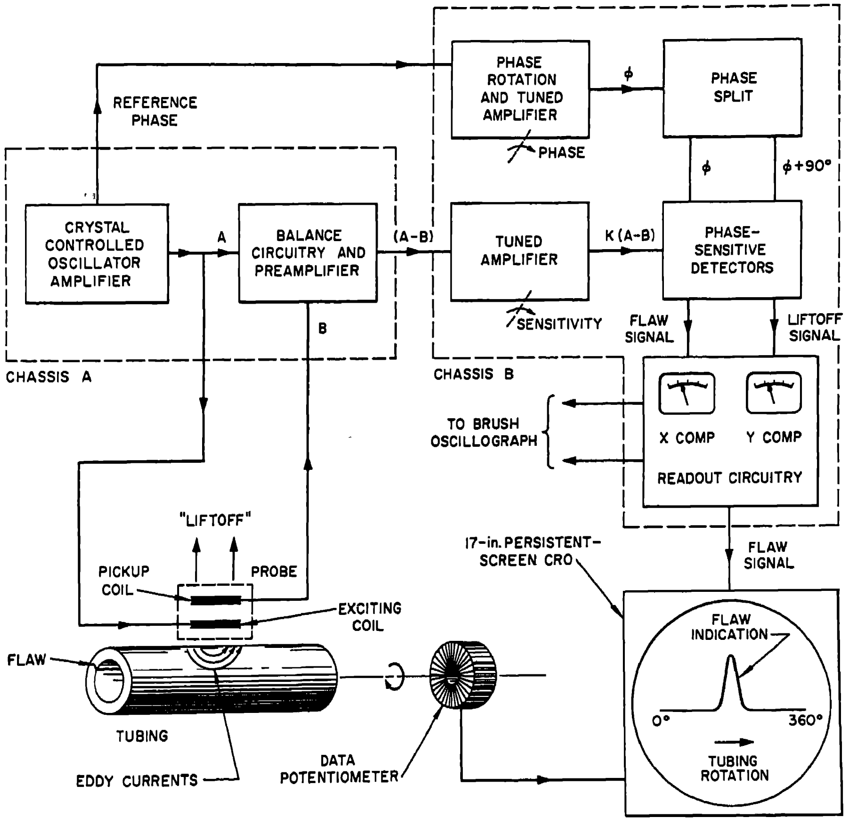

Oak Ridge Nat'l. Lab.

Fig. 30. Inspection of tubing with an eddy current probe.

nal variations are displayed on a **persistent-screen oscilloscope** as a function of tube rotation. The advantage of the probe coil is its inherent ability to be definitive. Because it is a surface probe, it is not affected by changes in diameter. **Changes in wall thickness** are indicated by changes in the signal level, which is a function of the position along the tube but independent of the tube rotation. **Eccentricity** is indicated by changes in the signal level, which varies slowly as a function of tube rotation. **Discontinuities** within the wall of the tube, because of their abrupt nature, cause sharp indications in the pattern.

Coil Holder Assembly. The probe coil and holder assembly illustrated in Fig. 29 are typical of those which have been constructed and successfully utilized. **Probe coils** as small as 1⁄16-in. diam. have been constructed and found to be very sensitive to minute defects. This small size results in very slow scanning rates. Therefore **elongated probes** must be utilized, although the sensitivity to minute discontinuities is reduced in proportion to the increased length. The coil mounting is spring-loaded to hold the coil face in contact with the tube surface of the tube. **Replaceable inserts** allow the mechanism to be used for a range of tube diameters.

Control of Coil-to-Tube Spacing. The difficulty with the probe-coil system is that even with a very carefully designed coil-holding mechanism, **wobble of the tubing** does occur, and the output signal varies with the coil-to-tube spacing. These signals sometimes look like those obtained from cracks. To obtain a first-order discrimination against wobble or **lift-off signals,** an instrument has been built which utilizes phase-sensitive detectors, as illustrated in the block diagram of Fig. 30. In this system the probe is composed of two coils: the exciting coil, fed by alternating current of constant amplitude, and the pick-up coil, placed in proximity to the exciting coil. The voltage from the pick-up coil is compared with that from adjustable balance circuits in the instrument. The difference is amplified and detected in phase-sensitive circuits in which the reference phase is continuously variable. Thus, lift-off signals can be eliminated from one of the detector channel outputs, leaving only signals from defect or wall-thickness changes. Such a system has three major **undesirable features:**

1. The phase of the lift-off signals varies with the amount of the lift-off. The phase-control adjustment which eliminates the lift-off signal of one magnitude will not, in general, remove the lift-off signal of a different magnitude.
2. Discrimination against signals from lift-off will, in general, result in discriminating against signals from very small discontinuities on the outside surface of the tube.
3. Successful operation of these circuits depends upon choice of a test frequency according to the wall thickness and tube material, such that phase separation between lift-off signals and wall thickness signals approaches 90 deg.

The difficulties are also encountered with phase-sensitive detectors in instrumentation employing encircling coils.

Advantages of Probe-Coil System. Despite difficulties encountered in the application of the probe-coil system, its superior **definitive abilities** and **ease of signal interpretation** cannot be overemphasized. The typical oscilloscope patterns shown in Fig. 31 demonstrate the ease with which signals obtained from this system can be interpreted. This method is mechanically difficult and is inherently a much slower method than that of the encircling coil. However, its superior definitive abilities can more than offset its disadvantages in many inspection applications.

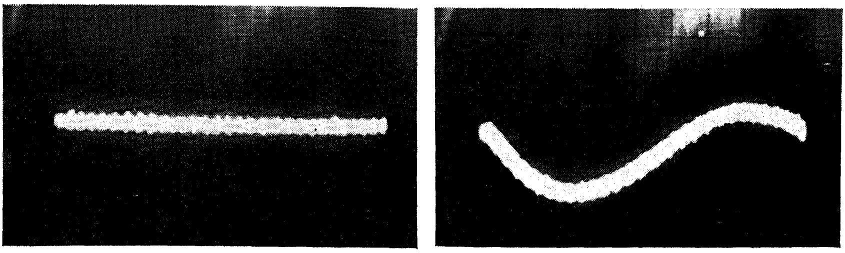

(a) No indication of defects.

(b) Indication of tube wall eccentricity.

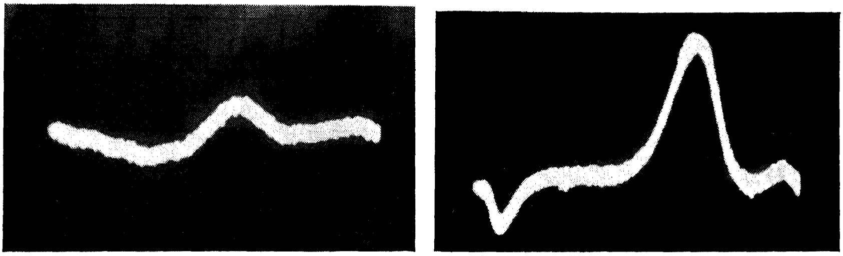

(c) Indication of small defect.

(d) Indication of large defect.

Oak Ridge Nat'l. Lab.

Fig. 31. Probe-coil eddy current B-scan photographs.

LIMITATIONS IN TEST AUTOMATION. The techniques and instrumentations of eddy current methods presently employed for small-diameter tubing have not yet advanced to the level of automation. Eddy current testing cannot be made fully automatic until the method can be standardized to give, at least, semi-quantitative indications of defect depth and length. The **problem of standardization** will be very difficult because:

1. Every variation in the tubing may produce indications which obscure or confuse the defect indication.
2. If the signals are differentiated, either in terms of time or distance, the signal amplitude will be dependent on the rate of change rather than on the defect size.
3. The sensitivity of the test to a given defect is dependent on the selected test conditions, since these test parameters describe a position on the impedance plane, as shown in Fig. 21.
4. The density of the induced currents decreases with depth into the tube wall. Hence, similar defects at the inner and outer surfaces of the tube wall give signals of different amplitudes. Eddy current tests will be difficult to standardize unless the location of the defect can be determined.
5. The impedance change caused by a defect is a change in both amplitude and phase. These changes are dependent not only on the type of defect but also on the defect location in the tube wall.

The complexities of the eddy current method make automation difficult unless the inspection is intended to locate only large flaws. For more **critical inspection applications,** the method requires inspectors with the experience and judgment of trained engineers to separate and evaluate the signals from the large number of possible variables. Furthermore, present-day eddy current instrumentation available for use on small-diameter tubing is not sufficiently versatile to provide the inspector with adequate information in a form that is readily interpretable.

SELECTION OF SIGNAL-DISPLAY SYSTEM. Regardless of the instrumentation used in a given eddy current test, the type of signal display system utilized is of primary importance in determining signal interpretability. Experience has indicated that interpretation can be greatly enhanced by introducing **positional intelligence** into the signal-display system. This is illustrated in Fig. 32, which compares indications caused by a gross crack found in a length of $\frac{3}{16} \times 0.025$-in. Inconel tubing inspected by both the probe-coil method and the encircling-coil method. A cross-section of the crack is shown in Fig. 32(c). The

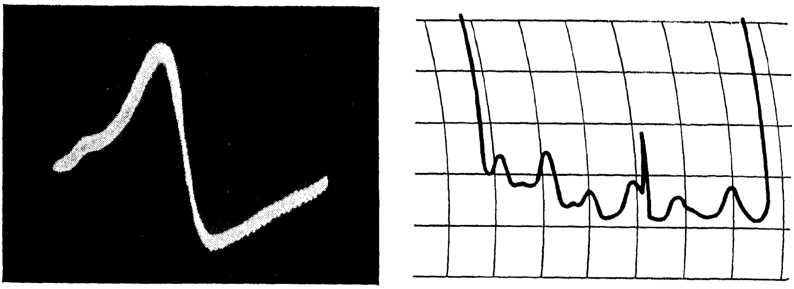

(a) Probe-coil eddy current B-scan frequency, 200 kc.

(b) Encircling-coil eddy current trace frequency, 200 kc.

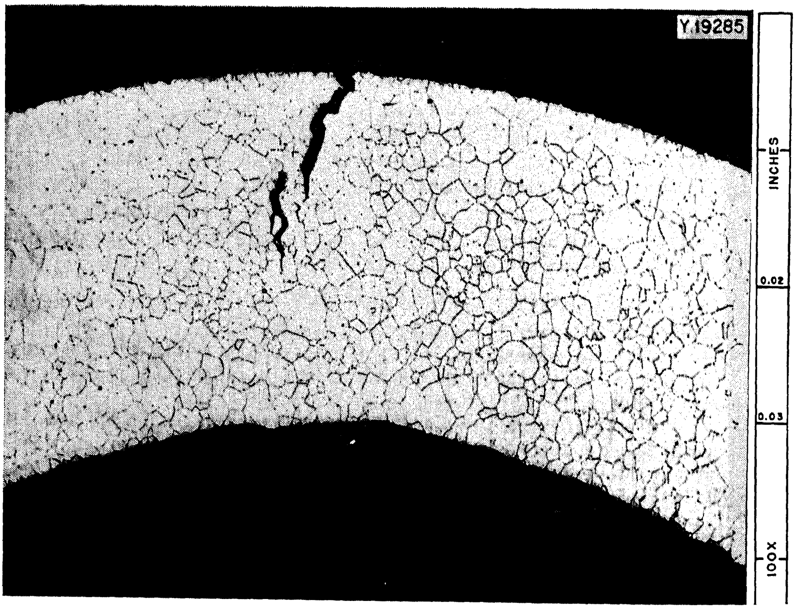

(c) Cross-section of crack in tube. Oak Ridge Nat'l. Lab.

Fig. 32. Eddy current signals from defective $\frac{3}{16} \times 0.025$-in. Inconel tubing.

trace from the encircling-coil test is shown in Fig. 32(b) and indicates the presence of the crack by the sharp upward spike. The trace from the probe coil for the same defect is shown in Fig. 32(a). In both cases the amplitude of the signal from the crack was not large enough, compared with the other signals obtained from dimensional variations in the tube, for reliable detection. When displayed either as a function of tube length or tube rotation, however, the sharpness of the signals was sufficient to allow the detection and interpretation to be made easily and quickly.

APPLICATION AREAS. At their present stage of development, eddy current techniques can, if properly utilized, perform valuable inspection on small-diameter tubing. For the detection of gross defects in commercial-grade tubing, the encircling-coil technique is the fastest and most effective nondestructive test which exists today. The **inspection of premium-quality tubing** for critical applications by this method allows:

1. High-speed detection of intergranular corrosion on the inside surface.
2. The detection of foreign metal pick-up on the inside surface.
3. High-speed continuous gaging of the dimensions of the tubing.

None of these inspections can be accomplished by any other method.

References

Reference numbers in this section refer to the references at the end of the section on Eddy Current Test Indications.

SECTION 39

EDDY CURRENT SPHERE AND SHEET TESTS

CONTENTS

PAGE

Eddy Current Tests of Spheres

Significance of spherical test objects 1
Determination of the limit frequency f_g 1
Effective permeability, $\mu_{eff.}$, of the sphere .. 3
  Effective permeability for a sphere of high relative magnetic permeability, $\mu_{rel.}$ (*f.* 1) 2
Normalized impedance and secondary voltages for a sphere 3
  Sphere in various test coil arrangements (*f.* 2) 3
Characteristics of the complex voltage or impedance plane 4
  Apparent impedance diagram for a short, circular test coil containing a sphere (*f.* 3) 5
 Effect of changes in fill factor η 4
 Effect of variations in conductivity and relative permeability 4
 Separation of diameter changes 4
 Effect of extending test coil length 4
 Effect of low test frequency or high relative permeability 4
Shape permeability and demagnetization factor 4
 Demagnetization factor N for a sphere 6
 Effect of variation in relative permeability of material 6
  Apparent impedance diagram for a short, circular coil containing a sphere, for fill factor $\eta = 1$ and relative magnetic permeabilities $\mu_{rel.} = 50, 5, 2,$ and 1 (*f.* 4) 7
 Shape permeability for short cylinders 6
 Short cylinder with axis transverse to axis of test coil 6
Computing effective permeability 7
 Computing initial points of apparent impedance curves 7
 Prolate ellipsoids 8
Apparent impedance curves for short cylinder or ellipsoid 8
Complex voltage and impedance planes for nonferromagnetic spheres 8
  Complex impedance or voltage plane for circular coil with nonferromagnetic sphere (*f.* 5) 9
 Application to small metallic impurities in nonmetallic test objects 10
Crack testing of spheres 10
  Three main positions of cracks in spheres, relative to the direction H of the a.-c. magnetizing field (*f.* 6) 10
 Apparent impedance plane for spheres with cracks 11
  Apparent impedance plane of a test coil containing spheres free from cracks (open-circle points) and with cracks (black dots) (*f.* 7) 12
 Determination of fill factor η 11
 Field strength and eddy current distribution in spheres 11

Eddy Current Tests of Sheets and Foils

Applications of sheet and foil tests 12
Principle of fork coil tests 12
  Arrangement of a fork coil system consisting of a primary magnetizing coil and a secondary pick-up coil between which a flat metallic sheet, M, is located (*f.* 8) 13
Transmission coefficient T 13
 Limit frequency f_g 13
 Independence of test-object position in forked coil 14
Plane of complex transmission coefficient T ... 14
  Complex plane of transmission coefficient T, for a flat metallic sheet, as a function of frequency ratio f/f_g (*f.* 9) 15
 Analysis of the complex T plane 14
 Similarity law for tests of flat conductors .. 14
 Reaction of eddy current field 14
 Maximum test sensitivity 15
  Sensitivity diagram for indication of effects of conductivity, thickness, and magnetic permeability variations in flat sheet materials (*f.* 10) 16
Tests for conductivity and thickness of flat conductors 16
 Differential circuit arrangement 17
  Circuit for measuring the product of conductivity and thickness of flat metallic sheets by frequency adjustment (*f.* 11) 17
 Determining the product of conductivity and thickness of metallic sheets 17
 Application of calibrated RC oscillator 18
  Arrangement for measuring the thickness of flat metallic sheets with a calibrated RC oscillator (*f.* 12) 18
 Direct indication of thickness of metallic sheets and foils 18
 Direct measurement of resistance per unit square 18
 Control of film resistance during metal deposition 19
  Differential arrangement for the measurement of resistance per unit square for thin metallic foils (*f.* 13) 19
References 19

SECTION 39

EDDY CURRENT SPHERE AND SHEET TESTS

Eddy Current Tests of Spheres

SIGNIFICANCE OF SPHERICAL TEST OBJECTS. The basic theory for spheres placed in the electromagnetic field of an eddy current test coil is important for several reasons. Most **production test parts,** such as bolts and bearing rollers, are relatively short. In these cases the **demagnetizing influence** of the ends of the test part becomes more obvious. The assumptions used in the analysis of the infinitely long cylinder in a test coil providing a homogeneous field are no longer applicable. The sphere is the more typical case for the short production part. Because of its symmetrical form, the case of the sphere is approachable with exact mathematical calculations. The results so obtained for the sphere can then be related to other short production parts, and several important characteristics of the behavior of the short part in the a.-c. magnetic field can be derived.

Another application of the basic methods for analysis of the sphere is in the detection of small **ferromagnetic or nonferromagnetic impurities in a nonmetallic substance** such as paint or food products. The theory provides exact formulas for the measurement voltage caused by a small metallic particle passing through the **metal detection coil.** This voltage is a function of the particle diameter, electrical conductivity, and magnetic permeability, as well as of the test frequency and the coil size.

DETERMINATION OF THE LIMIT FREQUENCY f_g. To calculate the effect of a sphere in an a.-c. electromagnetic field, **Maxwell's equations** are transformed into spherical coordinates. The solution of these differential equations involves the usual **boundary conditions:**

1. Continuity of the tangential components of the electric and magnetic field strengths.
2. Continuity of the normal component of the magnetic induction, leading to solutions in the form of hyperbolic functions.

As discussed in the section on Eddy Current Cylinder Tests, a **limit frequency** f_g is defined as the frequency at which the argument of the functions used for the calculation becomes equal to unity. In the case of the sphere this is the **argument of the hyperbolic functions.** The following equation holds for the limit frequency f_g of the sphere:

$$f_g = \frac{5066\,\mu_{\text{rel.}}}{\sigma B^2} \tag{1}$$

where σ = electrical conductivity of material in sphere, meter/ohm-mm.^{2}.
B = diameter of the sphere, cm.
$\mu_{\text{rel.}}$ = relative magnetic permeability of material in sphere.

In the case of nonmagnetic materials, $\mu_{\text{rel.}} = 1$.

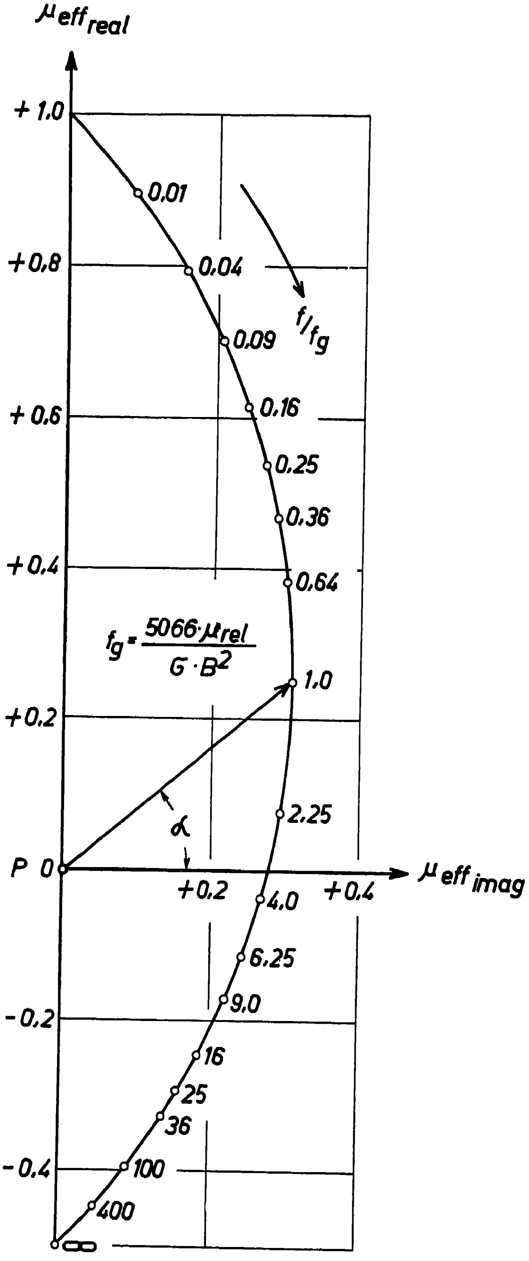

Institut Dr. Foerster

Fig. 1. Effective permeability for a sphere of high relative magnetic permeability, μ_{rel}.

EFFECTIVE PERMEABILITY, $\mu_{\text{eff.}}$, OF THE SPHERE. An effective permeability $\mu_{\text{eff.}}$ introduced for the sphere is similar to that used previously in analysis of cylinders. Its real and imaginary components are obtained from Fig. 1. The effective permeability of the sphere is obtained by calculating the **frequency ratio** f/f_g from

$$f/f_g = \frac{f\sigma B^2}{5066\,\mu_{\text{rel.}}} \tag{2}$$

where f is the test frequency. These f/f_g ratios are shown along the curve of Fig. 1. The **real and imaginary components** of the effective permeability are read from the coordinates of these points. For example, if $f/f_g = 1$, these components appear as

$$\mu_{\text{eff.(real)}} = +0.25$$

and

$$\mu_{\text{eff.(imag.)}} = +0.31$$

NORMALIZED IMPEDANCE AND SECONDARY VOLTAGES FOR A SPHERE. Fig. 2 shows coil arrangements used for testing of spheres and short production parts. Fig. 2(a) shows an arrangement of a single test coil whose impedance components are ωL and R. Fig. 2(b) shows an arrangement with primary and secondary coils, for which the secondary coil voltage components are $E_{\text{imag.}}$ and E_{real}. The normalized components of impedance and secondary voltage for this case are

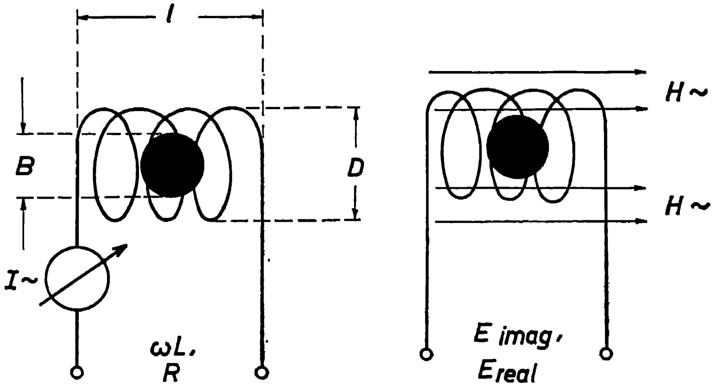

(a) (b)

Fig. 2. Sphere in various test coil arrangements. (a) Sphere in a single test coil. (b) Sphere in a coil arrangement of a primary coil (not shown here) and a secondary coil (shown).

$$\begin{aligned}\frac{\omega L}{\omega L_0} = \frac{E_{\text{imag.}}}{E_0} &= 1 + \left(\frac{2(B/D)^3}{\sqrt{1+(l/D)^2}}\right)\mu_{\text{eff.(real)}} \\ &= 1 + \left(\frac{2(\eta)^{3/2}}{\sqrt{1+(l/D)^2}}\right)\mu_{\text{eff (real)}}\end{aligned} \tag{3a}$$

$$\begin{aligned}\frac{R-R_0}{\omega L_0} = \frac{E_{\text{real}}}{E_0} &= \left(\frac{2(B/D)^3}{\sqrt{1+(l/D)^2}}\right)\mu_{\text{eff.(imag.)}} \\ &= \left(\frac{2(\eta)^{3/2}}{\sqrt{1+(l/D)^2}}\right)\mu_{\text{eff.(imag.)}}\end{aligned} \tag{3b}$$

where B/D is the ratio of the sphere diameter B to the coil diameter D. As in the case of the cylinder, the coil fill factor η is defined as $\eta = (B/D)^2$. The expression $\sqrt{1 + (l/D)^2}$ takes the **coil dimensions** into account, where l is the length of the coil.

For the **short, circular coil** where $l << D$, the denominators in Eqs. (3) become unity. An extension of the length of the test coil merely decreases the influence of the sphere upon the coil impedance, since with a long coil a portion of the coil is not affected by the insertion of the sphere. For example, in a coil whose length l is equal to its diameter D, so that $(l/D) = 1$, the influence of the sphere is $1/\sqrt{2} = 71$ percent of the effect for a short, circular coil.

CHARACTERISTICS OF THE COMPLEX VOLTAGE OR IMPEDANCE PLANE. Fig. 3 shows the test coil characteristics as a function of the frequency ratio f/f_g, calculated from Eqs. (3). It illustrates the influence of the characteristics of the sphere (diameter B, conductivity σ, and relative permeability $\mu_{\text{rel.}}$) and of the test frequency f on the normalized impedance or secondary coil voltage. It also illustrates the variation in coil characteristics (inductive reactance ωL and coil resistance R) when the **diameter of the sphere** decreases from the value $(B/D) = 1$ (at which the sphere entirely fills the test coil) to smaller diameters.

Effect of Changes in Fill Factor η. Fig. 3 shows curves for a number of values of fill factor $\eta = (B/D)^2$. The bending of the sphere diameter curves (labeled B) with decreasing sphere diameters results from the simultaneous variation in the frequency ratio f/f_g [see Eq. (2)] when the sphere diameter B becomes smaller.

Effect of Variations in Conductivity and Relative Permeability. Variations in the conductivity and permeability of the sphere, as well as variations in the test frequency, result in displacements in the ωL and R values along the f/f_g direction of the circular arcs. Especially interesting is the fact that with **infinitely high values of relative permeability,** the impedance ratio is always $f/f_g = 0$. Thus, at any test frequency, but with infinitely high permeability, the same apparent impedance results as for $f/f_g = 0$.

Separation of Diameter Changes. The relatively large angles between the directions of the diameter curves (B) and the curves for changes in conductivity or permeability (σ, $\mu_{\text{rel.}}$) in Fig. 3 indicate the degree to which diameter variations for spheres can be separated from material property variations.

Effect of Extending Test Coil Length. As indicated by Eqs. (3), an extension in the length l of the test coil has the same effect as a decrease in the fill factor η, without influencing the frequency ratio f/f_g. Lengthening the test coil to twice the coil diameter ($l = 2D$) results in the same fill-factor curve in Fig. 3 as a decrease in sphere diameter from $(B/D) = 1$ to $(B/D) = 0.76$ [see Eqs. (3)].

Effect of Low Test Frequency or High Relative Permeability. Fig. 1, showing the effective permeability values of the sphere for any given frequency ratio, is accurate only for large values of relative permeability ($\mu_{\text{rel.}} \geqq 100$). For **very small frequency ratios** (static case) or for very large relative permeability values, the normalized inductive reactance, $\omega L/\omega L_0 = 3$ for fill factor $\eta = 1$.

SHAPE PERMEABILITY AND DEMAGNETIZATION FACTOR. Generally, in short production parts, the apparent or **shape permeability,** $\mu_{\text{app.}}$, is considerably smaller than the relative permeability of the test material because

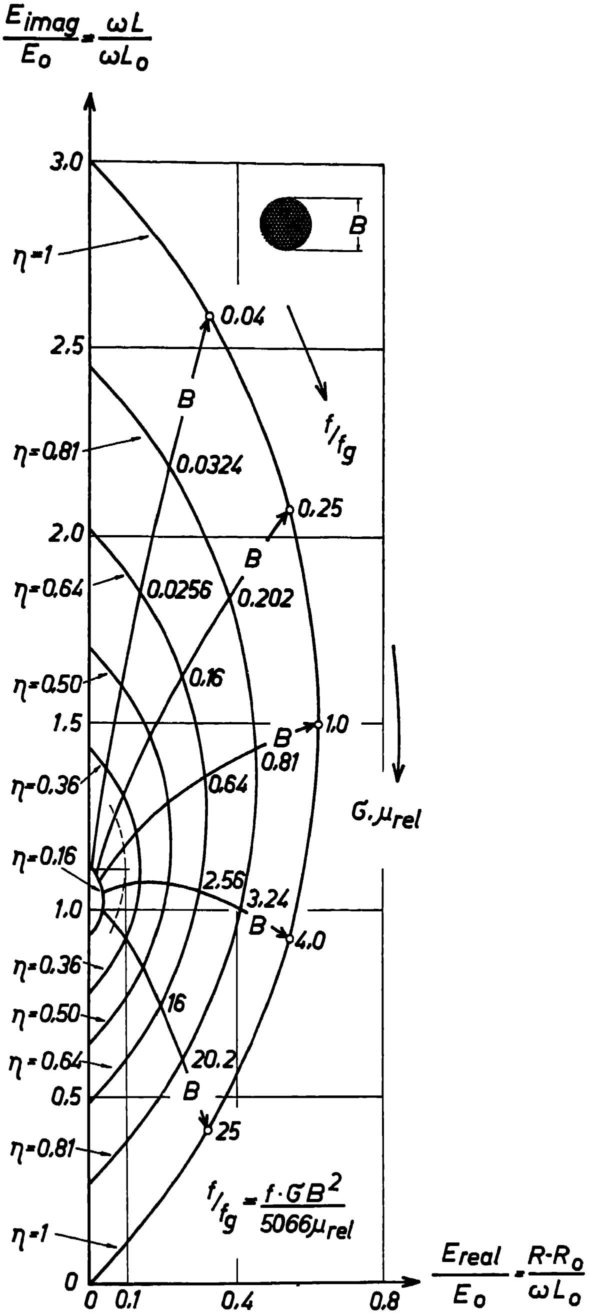

Institut Dr. Foerster

Fig. 3. Apparent impedance diagram for a short, circular test coil containing a sphere.

of the high demagnetization effects. [See Eq. (1) in the section on Magnetic-Field Test Equipment for discussion of shape or form permeability effects.] In general,

$$\mu_{\text{app.}} = \frac{4\pi}{N} \tag{4}$$

where N is the so-called **demagnetization factor,** which becomes larger as the length-to-diameter ratio of the test part becomes smaller.

Demagnetization Factor N for a Sphere. For a sphere, the demagnetization factor is

$$N = 4\pi/3$$

so that the apparent permeability [from Eq. (4)] is $\mu_{\text{app.}} = 3$. Now the **self-induction of a coil** is proportional to the permeability of its core. Thus, if the sphere has an apparent permeability of 3, the self-induction of the small, circular coil shown in Fig. 2 must be three times larger when the sphere is present, (at $f/f_g = 0$, the static case) and fill factor $\eta = 1$, than without a sphere within the coil. Thus, as shown in Fig. 3, the normalized inductive reactance $\omega L/\omega L_0 = 3$.

Effect of Variation in Relative Permeability of Material. Fig. 4 illustrates curves for the apparent impedance of the test coil for four different values of relative magnetic permeability of the test material. The curve for $\mu_{\text{rel.}} = 1$ applies for **nonferromagnetic spheres**; for example, of stainless steel. The difference in the apparent impedance curves for small relative permeability values is especially obvious for **low frequency ratios** f/f_g. For values of $\mu_{\text{rel.}} > 5$ and f/f_g values exceeding unity, the apparent impedance curves all coincide (lower half of outermost curve in Fig. 4). Thus the calculations of effective impedance are exact down to the very low permeability value of $\mu_{\text{rel.}} = 5$, corresponding, for example, to **permanent magnets or to tungsten carbide.**

Shape Permeability for Short Cylinders. As previously indicated, the apparent impedance curve for the short test coil, for which $l << D$ and $\eta = 1$, starts at $f/f_g = 0$ at the value of the apparent shape permeability for the sphere with $\mu_{\text{app.}} = 3$, namely, $\omega L/\omega L_0 = 3$. The shape permeability for a short test cylinder can be obtained from Eq. (4) and the demagnetization factor N. **Values of demagnetization factors** N given by Bozorth,[6] can be used for cylinders with different length-to-diameter ratios. For example, the value given for the demagnetization factor N is 3.4 for a short cylinder whose length is equal to its diameter ($l/D = 1$). From this, the apparent permeability $\mu_{\text{app.}} = 3.7$ is calculated from Eq. (4). The apparent impedance curve for such a short cylinder starts at $\omega L/\omega L_0 = 3.7$ at $f/f_g = 0$, as shown in Fig. 4.

Short Cylinder with Axis Transverse to Axis of Test Coil. If the short cylinder is turned so that its longitudinal axis is perpendicular to the coil axis while within the coil, its **apparent permeability** decreases from 3.7 to 2.0. The **demagnetizing factor** N of the cylinder perpendicular to its longitudinal axis is calculated as $N = 2\pi$. Substituting this value in Eq. (4) gives the value of $\mu_{\text{app.}} = 2$. The normalized reactance of the test coil also changes from $\omega L/\omega L_0 = 3.7$ to $\omega L/\omega L_0 = 2$ as the short cylinder turns from the longitudinal to the transverse position within the coil. Thus an **inexact positioning** of the cylinder in the longitudinal axis of the coil can cause considerable variation in the apparent impedance. This positioning must be carefully controlled in eddy current testing of **roller-shaped test objects.**

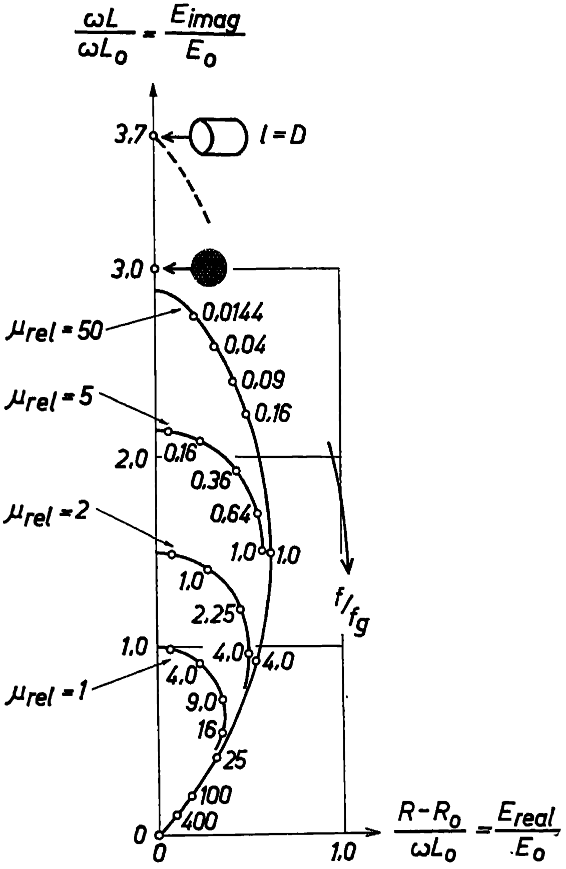

Institut Dr. Foerster

Fig. 4. Apparent impedance diagram for a short, circular coil containing a sphere, for fill factor $\eta = 1$ and relative magnetic permeabilities $\mu_{\text{rel.}} = 50, 5, 2,$ and 1. Dashed curve is initial portion of curve for a cylinder with $l/D = 1$.

COMPUTING EFFECTIVE PERMEABILITY. The components ωL and R of the apparent impedance of the test coil are obtained by Eqs. (3) from:

1. The test coil dimensions (l, D).
2. The coil fill factor η.
3. The components of effective permeability, $\mu_{\text{eff.(real)}}$ and $\mu_{\text{eff.(imag.)}}$.

The **effective permeability components** can be taken from Fig. 1 for any given frequency ratio f/f_g of the sphere. The **components of the apparent impedance** are derived from the effective permeability values and are shown in Fig. 3.

Computing Initial Points of Apparent Impedance Curves. The initial point of the apparent impedance curve corresponds to the frequency ratio $f/f_g = 0$, the static case. For fill factor $\eta = 1$,

$$\left(\frac{\omega L}{\omega L_0}\right)_{(f/f_g=0)} = \mu_{\text{app}}. \tag{5}$$

From Eqs. (3a) and (5), the initial point of the effective permeability curve at $f/f_g = 0$ is generally found to be

$$[\mu_{\text{eff.(real)}}]_{(f/f_g=0)} = (\mu_{\text{app.}})/2 - 0.5 \tag{6}$$

According to McClurg,[70] the approximate relationship for the **apparent permeability of a cylindrical body** of length l and diameter D, where $2 < (l/D) < 10$, is

$$\mu_{\text{app.}} = 6(l/D) - 5 \tag{7}$$

Thus the initial point of the apparent impedance curve for **short cylinders** is calculated to be

$$[\mu_{\text{eff.(real)}}]_{(f/f_g=0)} = 3(l/D) - 3 \tag{8}$$

No approximation formula exists for computing the apparent permeability for short cylinders with length/diameter ratios between 1 and 2. In this case Eq. (4) can be used for the calculation if the demagnetizing factor N is taken from Bozorth's curves[6] for any given l/D ratio for the cylinder.

Prolate Ellipsoids. For prolate ellipsoids with ratios of major to minor diameters between 1 and 10, Foerster[29] has derived the following **approximation formula:**

$$\mu_{\text{app.}} = 3(l/D) \tag{9a}$$

where l is the large axis and D the small axis of the ellipsoid. From this approximation the **initial point** for the effective permeability curve at $f/f_g = 0$ is obtained as

$$[\mu_{\text{eff.(real)}}]_{(f/f_g=0)} = 1.5(l/D) - 0.5 \tag{9b}$$

Either Eq. (6) or Eqs. (9) is used for calculating initial points, depending upon whether the shape of the short test object more nearly approximates a cylinder or an ellipsoid.

Apparent Impedance Curves for Short Cylinder or Ellipsoid. To calculate the normalized reactance $\omega L/\omega L_0$ of the test coil containing either a short cylinder or ellipsoid at $f/f_g = 0$, the approximation formulas [Eqs. (7) or (9a)] are inserted into Eq. (5). Since the apparent impedance curves for short cylinders and short ellipsoids are similar (see Fig. 3), the **behavior of short production parts** in the a.-c. field can be estimated. However, an exact calculation for the short cylinder in the a.-c. field is not possible because the magnetization is not homogeneous over the length of the cylinder and decreases toward the ends as a result of the demagnetization. As the **demagnetizing influence of the ends of the cylinder** diminishes, however, the apparent permeability more closely approaches the relative permeability of the material. Under these conditions the apparent impedance curves of Fig. 4 tend to approach the curves for the infinitely long, solid cylinder shown in Fig. 2 of the section on Eddy Current Cylinder Tests.

COMPLEX VOLTAGE AND IMPEDANCE PLANES FOR NONFERROMAGNETIC SPHERES. The performance of the test coil containing a nonferromagnetic sphere is of special interest, since it approximates its behavior with short nonferromagnetic objects. This situation is intermediate between the case of the long, solid cylinder and that of the sphere. The impedance or complex voltage plane for a test coil containing a nonferromagnetic sphere is computed from Eqs. (3) and the apparent impedance values for $\mu_{\text{rel.}} = 1$ in Fig. 4. Fig. 5 shows the resultant family of curves. These are very similar to the curves for the infinitely long cylinder given in Fig. 2 of the section on Eddy Current Cylinder

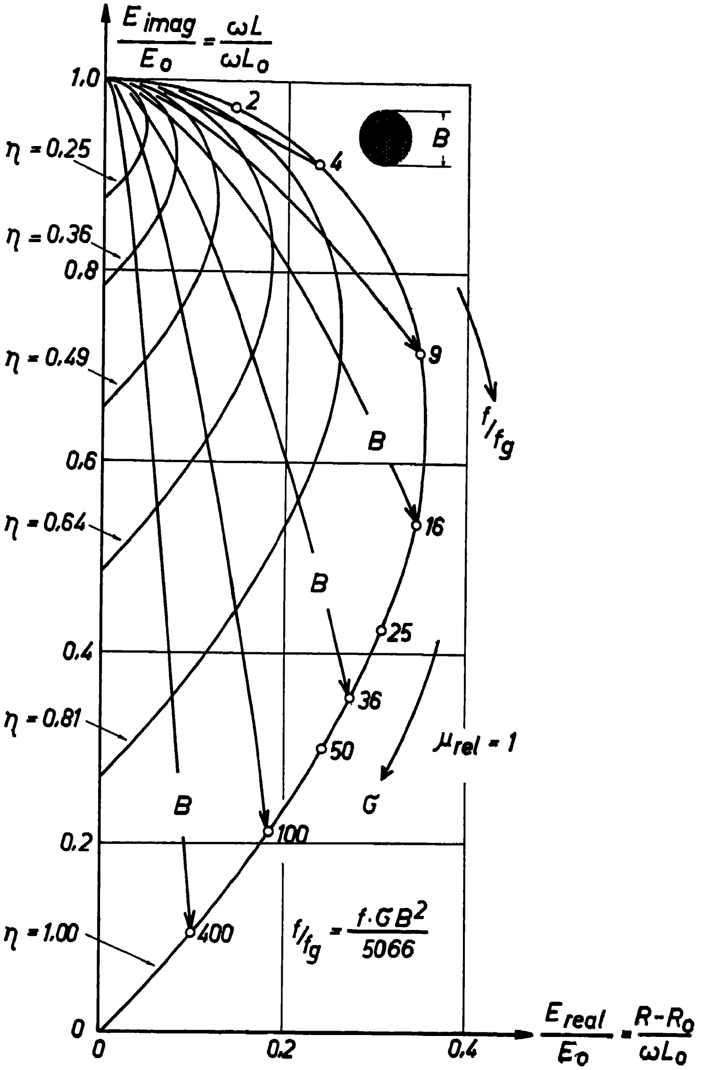

Institut Dr. Foerster

Fig. 5. Complex impedance or voltage plane for circular coil with nonferromagnetic sphere. Direction B corresponds to increasing sphere diameter.

Tests, although the path of the apparent impedance curve of Fig. 5 in this section is not identical with that of Fig. 2.

Eq. (5) of the section on Eddy Current Test Principles, and Eq. (1) of this section for the limit frequency f_g are the same for the nonferromagnetic sphere and the nonferromagnetic cylinder ($\mu_{rel.} = 1$). Fig. 5 shows that the same variations in apparent impedance are obtained for the sphere at an f/f_g ratio approximately twice as high as for the cylinder. By comparing the test specimen with a reference standard in differentially connected test coils (the so-called absolute method), the quantitative **measurement of the electrical conductivity** is possible by means of Fig. 5.

Application to Small Metallic Impurities in Nonmetallic Test Objects. The preceding theory of the influence of the sphere on the apparent impedance or secondary voltage of the test coil can be used to compute the effects resulting when an a.-c. coil is used to search for metallic impurities (assumed to be sphere-shaped) in nonmetallic substances. If the smallest voltage variation which can just be indicated is known for the test coil, the **minimum detectible impurity size** can be calculated in terms of:

1. The test coil size (diameter D and length l).
2. The properties of the spherical impurity (conductivity σ and relative permeability $\mu_{rel.}$).
3. Fig. 1 for ferromagnetic sphere-shaped impurities.
4. Fig. 5 for nonferromagnetic sphere-shaped impurities.

CRACK TESTING OF SPHERES. The influence of cracks in spheres was determined experimentally, since complicated boundary conditions made mathe-

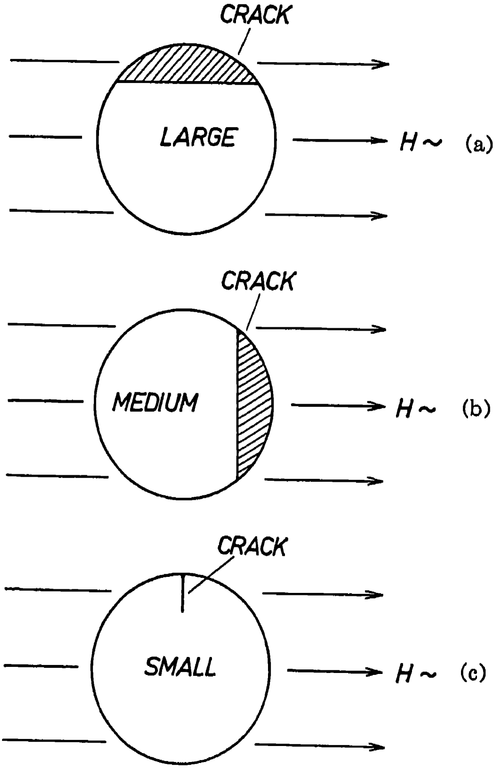

Fig. 6. Three main positions of cracks in spheres, relative to the direction H of the a.-c. magnetizing field. (a) Large, position for greatest crack indication sensitivity. (b) Medium, position for medium crack indication sensitivity. (c) Small, position for minimum crack indication sensitivity.

matical solutions impossible. **Surface cracks** in spheres can have three main positions, depending upon the location of the crack in the a.-c. field of the test coil (see Fig. 6). These positions are:

1. Long dimension of crack paralleling direction of magnetizing field, Fig. 6(a), producing a large test indication.
2. Short dimension (depth) of crack paralleling direction of magnetizing field, Fig. 6(b), producing an intermediate test indication.
3. Crack transverse to direction of magnetizing field, Fig. 6(c), producing minimum test indication.

In the **optimum crack position,** which produces a large test indication, the crack surface is perpendicular to the equatorial plane. The lines of force of the primary magnetizing field are parallel to the length of the crack. The **equatorial plane** is the one having the greatest eddy current density, which explains the large sensitivity of crack indications. In the intermediate position, Fig. 6(b), the crack surface in a region of medium eddy current density is perpendicular to the eddy current pole axis. When the crack is in the **least-detectible position,** Fig. 6(c), the plane of the crack is parallel to the direction of eddy current flow. Here it has no reaction upon the eddy currents and produces no weakening of the eddy current density.

Apparent Impedance Plane for Spheres with Cracks. Fig. 7 shows a small portion of the apparent impedance plane of Fig. 3, showing variations found experimentally as a result of cracks in spheres. The apparent impedance values of several **crack-free spheres** are shown by open circles in the dotted rectangle near the bottom of the graph. The slight variations of the positions of these points (open circles) result from the small **degree of anisotropy** found in the spheres (probably a consequence of the **grain orientation** in the section of rod from which the spheres were made). Varying the position of crack-free spheres in the test coil had very little effect upon the external impedance of the test coil.

The indications obtained from spheres containing cracks are shown by solid black dots in Fig. 7. At the bottom of the graph, within the dotted rectangle, are black dots corresponding to tests of spheres with **cracks in the position of minimum detectibility** [see Fig. 6(c)]. However, if the crack in a sphere is brought into the **position of medium sensitivity** [see Fig. 6(b)], its indications appear near the middle portion of the curves of Fig. 7, as noted by "Medium." With cracks oriented into the **optimum test position** [see Fig. 6(a)], the test indications are changed considerably, as shown by the black dots near the top of the curves of Fig. 7. The "empty value" of the impedance, ωL_0, of the test coil in the absence of a test sphere corresponds to the point $\omega L/\omega L_0 = 1$ in Fig. 3. Thus cracks in spheres result in an increase of the **normalized reactance** along the apparent impedance curves of Fig. 3 or 7.

Determination of Fill Factor η. The fill factor $\eta = (B/D)^2$ can be determined for spherical test objects, as follows: Suppose that the impedance coordinates in Fig. 3 for a test coil containing a sphere are, as shown by the light coordinate lines, $\omega L/\omega L_0 = 1.11$ and $(R - R_0)/\omega L_0 = 0.1$. These coordinates indicate that the fill factor $\eta = 0.3$ because the (dashed) apparent impedance curve for $\eta = 0.3$ intersects the point given by these coordinates.

Field Strength and Eddy Current Distribution in Spheres. The distribution of field strength and eddy current densities on the surface and within the interior of spheres, as well as the quantitative influence of crack conditions, will be discussed more thoroughly in the literature.[42]

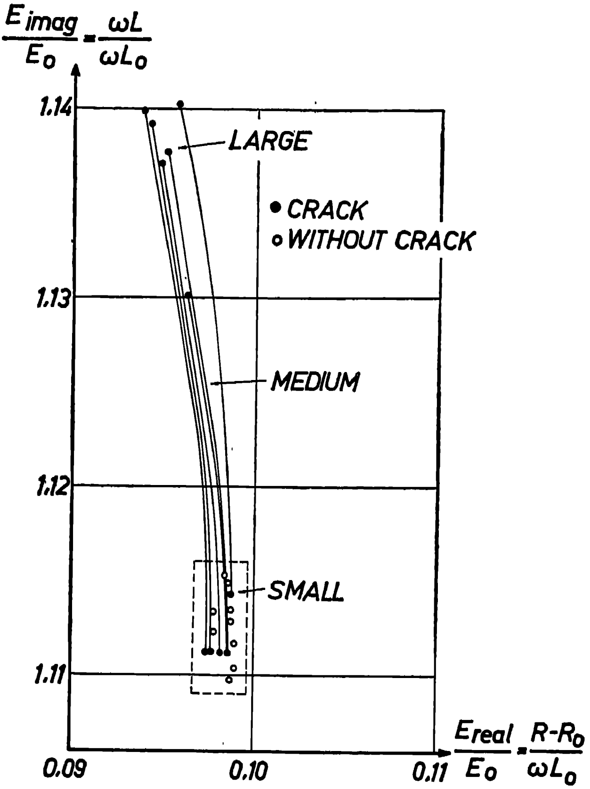

Fig. 7. Apparent impedance plane of a test coil containing spheres free from cracks (open-circle points) and with cracks (black dots).

Eddy Current Tests of Sheets and Foils

APPLICATIONS OF SHEET AND FOIL TESTS. An important field of application for the eddy current test method is in **noncontacting measurements** of the thickness, electrical conductivity, and magnetic permeability of flat metallic sheets, foils, and surface films. These techniques have been developed for direct measurement of the electrical conductivity and for the quantitative measurement of corrosion attack upon sheet materials. Instruments utilizing these test methods are described in the section on Eddy Current Test Equipment.

PRINCIPLE OF FORK COIL TESTS. Fig. 8 shows the arrangement of the fork coil for tests of sheet materials. A generator sends an alternating current (a.c.) of frequency f through the primary or magnetizing coil. The test material is placed between the primary coil and a secondary or pick-up coil. The field of the primary coil at the secondary coil location, at a distance A from the primary coil, induces an a.-c. voltage in the secondary coil. In the absence of the intervening test sheet, the secondary voltage is E_0. As soon as a metallic sheet M is inserted between the coils, the primary magnetizing field produces **eddy currents in the sheet** whose fields are superimposed upon the weakened fields of the primary coil. Thus, the insertion of the metallic layer M between the primary and secondary coils changes the original primary field at the location of the secondary coil. As a result of the **screening action of the metal sheet,** a new a.-c. voltage, E_M, appears across the terminals of the secondary coil.

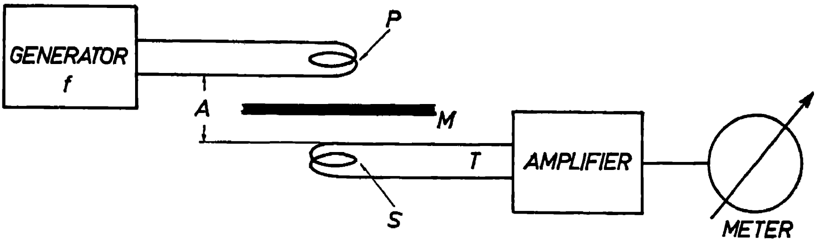

Institut Dr. Foerster

Fig. 8. Arrangement of a fork coil system consisting of a primary magnetizing coil and a secondary pick-up coil between which a flat metallic sheet, *M*, is located.

Transmission Coefficient *T*. The ratio of the secondary coil voltage E_M, with the test sheet inserted, to the "empty coil" voltage E_0 in the absence of the test object is termed the transmission coefficient T. This transmission coefficient is a function of:

1. The electrical conductivity σ of the metallic sheet.
2. The relative magnetic permeability $\mu_{rel.}$ of the sheet.
3. The thickness D of the metallic sheet.
4. The test frequency f.
5. The distance A of the primary coil from the secondary coil.

Similarity laws, analogous to those developed for the case of solid cylindrical test objects (see Similarity Law in Eddy Current Testing in the section on Eddy Current Cylinder Tests), illustrate the relations between these controlling variables and the transmission coefficient, $T = E_M/E_0$.

Limit Frequency f_g. The theory of the forked coil was solved mathematically as a boundary-value problem, using **Maxwell's equations.** The solution of the differential equations had to satisfy the following **boundary conditions:**

1. Continuity of the tangential components of electric and magnetic-field strengths.
2. Continuity of the normal component of the magnetic induction through the metallic surfaces.

The extensive calculations, which cannot be discussed further here, again resulted in a limit frequency, f_g, chosen by equating to unity the argument of the function which appeared in the calculation of the transmission coefficient T. The **limit frequency** for the case of a flat conductor within the forked coil is

$$f_g = \frac{2534}{\sigma D \mu_{rel.} A} \qquad (10a)$$

and the **frequency ratio** f/f_g is

$$f/f_g = \frac{f \sigma D \mu_{rel.} A}{2534} \qquad (10b)$$

where σ = electrical conductivity of sheet material, meter/ohm-mm.^{2}.
D = thickness of flat metallic conductor, cm.
$\mu_{rel.}$ = relative magnetic permeability of flat metallic sheet.
A = distance (cm.) of the primary coil from the secondary coil (a fixed constant of the test instrument in most cases).

It should be noted that the factor A, representing the **geometry of the coil arrangement** (see Fig. 8), is contained in the expression for the limit frequency [Eq. (10a)]. This is contrary to the situation in the case of the solid cylinder and the hollow tube in the feed-through coil arrangement, where the limit frequency was independent of the specific coil arrangements. This dependency upon A can be used to advantage in computing the **"lift-off" effect** of the test coil, described in the literature.[42]

Independence of Test-Object Position in Forked Coil. The distance A between primary and secondary coils appears in Eq. (10), but the distance of the metallic sheet from the coils does not appear. As indicated by theory, the influence of the metallic layer upon the secondary coil characteristics is independent of the position of the metallic layer between the two coils.

PLANE OF COMPLEX TRANSMISSION COEFFICIENT T. The transmission coefficient consists of two **components,** a real component, T_{real}, and an imaginary component, $T_{\text{imag.}}$. These are plotted on a complex plane in the same manner as the components of the effective permeability for the cylinder and tube. Various **frequency ratios** are noted along the transmission-coefficient curve of Fig. 9, which shows the characteristics of $T = E_M/E_0$ as obtained by extensive calculations. With zero sheet thickness (no material within the forked coil), the frequency ratio $f/f_g = 0$, and the transmission coefficient $T = T_0 = 1$ (a real number).

Analysis of the Complex T Plane. To illustrate the use of the complex plane of the transmission coefficient T, assume that the test object is an **aluminum foil** with the following characteristics:

1. Thickness, $D = 10\mu = 0.001$ cm.
2. Electrical conductivity, $\sigma = 38$ meter/ohm-mm.^{2}.
3. Relative magnetic permeability, $\mu_{\text{rel.}} = 1$.

The distance of the primary coil from the secondary is assumed to be 10 cm. The **limit frequency** is calculated from Eq. (10) as $f_g = 6660$ c.p.s. If the test frequency is chosen as 6660 c.p.s., the **frequency ratio** $f/f_g = 1$. In this case the vector representing the transmission coefficient T for the foil extends from the origin to the point at which $f/f_g = 1$ on the curve of Fig. 9. Before insertion of the foil into the test coil system, the vector representing the transmission coefficient T_0 extended from the origin to the point $T_0 = +1$, along the vertical (real) axis. Upon insertion of the test material, the **transmission coefficient vector** underwent both a shift in phase and a reduction in amplitude to 87.5 percent of its initial value. This change was caused by the field of the eddy current induced in the foil.

If the test frequency for the preceding foil test had been selected as $f = 66{,}600$ c.p.s., the vector representing the transmission coefficient T would have extended from the origin to the point where $f/f_g = 10$ on the curve of Fig. 9. Thus, from Eq. (10) and Fig. 9, the influence upon secondary coil voltage can be determined for any given metal thickness, electrical conductivity, and magnetic permeability.

Similarity Law for Tests of Flat Conductors. The similarity law for eddy current testing of flat conductors states:

> Any given metallic material and any given flat sheet thickness result in the same transmission coefficient T if the test is made at the same frequency ratio f/f_g as given by Eq. (10).

Reaction of Eddy Current Field. The reaction field of the eddy currents in a test sheet is superimposed upon the original field, $T_0 = 1$, of the test coils in the absence of the test object. The effect of the eddy current field is described by the vector W in the complex plane of Fig. 9. Thus the undisturbed primary field (described by vector T_0) and the eddy current field (described by vector W) act simultaneously upon the secondary coil. Their vector difference is the vector T. Inversely, by adding the vector representing the field acting upon the secondary coil when a test object is present (vector T) to the secondary field in the metal plate (vector W), one obtains the undisturbed primary field (vector $T_0 = 1$).

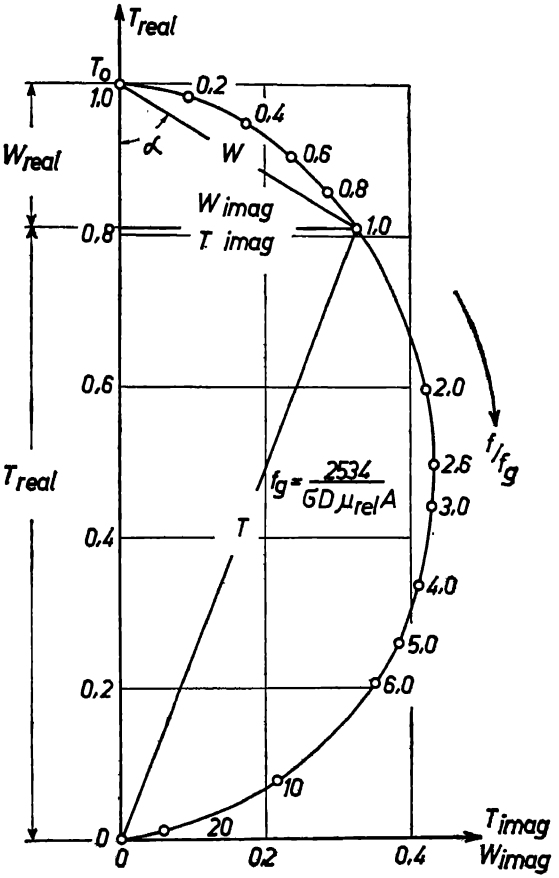

Institut Dr. Foerster

Fig. 9. Complex plane of transmission coefficient T, for a flat metallic sheet, as a function of frequency ratio f/f_g.

Maximum Test Sensitivity. The highest indication sensitivity for the metallic sheet in the forked coil arrangement is determined, as a function of the electrical conductivity and thickness of the test sheet, in a manner analogous to the determination for optimum test sensitivities for cylinders and tubes, presented previously. Fig. 10 shows the **sensitivity diagram for the fork-coil test method.** The line connecting the origin O to a specific f/f_g value on the curve represents the variation ΔT in the transmission coefficient (shown as ΔW in Fig. 10) for 1 percent variation in conductivity or thickness in the test material. As in all eddy current problems, the **maximum indication sensitivity** occurs at the maximum of the imaginary component of T, corresponding to the **maximum eddy current loss.** In Fig. 10 this point is located at $f/f_g = 2.75$, at the bottom of the circle.

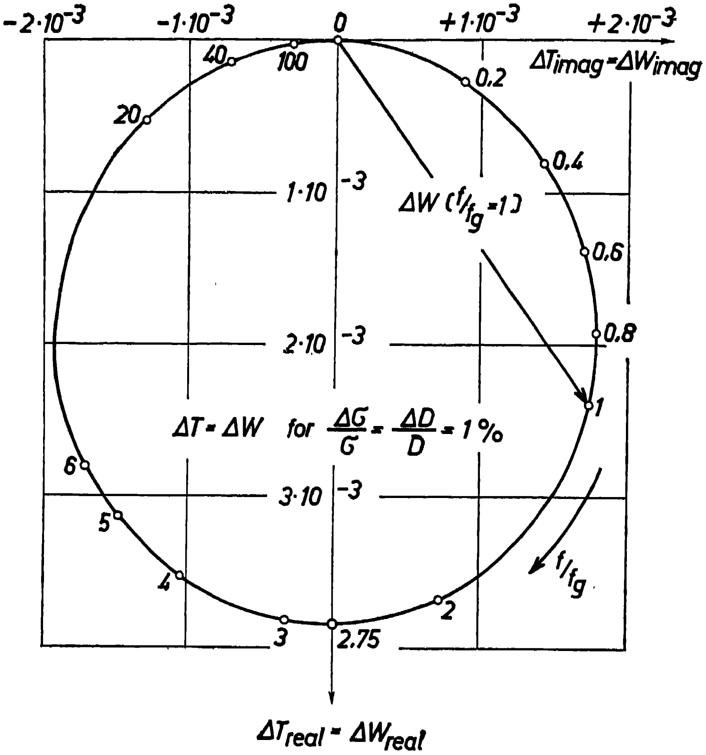

Fig. 10. Sensitivity diagram for indication of effects of conductivity, thickness, and magnetic permeability variations in flat sheet materials. Vector diagram shows variation of transmission coefficient, $\Delta T = \Delta W$, for a variation of 1 percent in test object conductivity or thickness.

For this frequency ratio, a conductivity or thickness variation of 1 percent corresponds to a variation of 3.85×10^{-3} in the transmission coefficient T. At this point of optimum sensitivity, the direction of the T variation is parallel to the real axis (vertical direction) in Fig. 9 (the direction from $f/f_g = 2.6$ to $f/f_g = 3.0$ in Fig. 9).

TESTS FOR CONDUCTIVITY AND THICKNESS OF FLAT CONDUCTORS. The sensitivity diagram of Fig. 10 provides a basis for a method of determining the magnitude of the **product (σD) of conductivity and thickness** of flat metallic sheets. In this arrangement the scale of the indicating meter has the same calibration (in percentage of the deviation factor σD) for both positive and negative variations and is independent of the specific values of conductivity and thickness for the metal sheet.

Differential Circuit Arrangement. Fig. 11 shows the circuit used for measuring the magnitude of the product σD, which is described in European literature as the **"absolute measurement method."** A variable-frequency generator feeds the primary magnetizing coil P, which acts identically upon the two similar secondary coils S_1 and S_2. The voltages induced in secondary coils S_1 and S_2 are separately amplified, and after rectification, are connected in series opposition as d.-c. voltages. To **calibrate the test instrument,** the switch at the input to the second amplifier is turned to C (calibration). In the absence of a test object between the primary P and secondary coil S_1, the amplifier output voltages must be identical, and the indicating meter will show zero. As shown in Fig. 9, the distance T from the origin to the $f/f_g = 2.75$ point (where highest measurement sensitivity is attained) amounts to 68 percent of the "empty coil" voltage $T_0 = 1$ (no test object). To measure the product σD of a metallic sheet or foil between P and S_1, the input switch of the second amplifier is turned to M (measurement), which decreases the voltage from S_2 to 68 percent of its true magnitude.

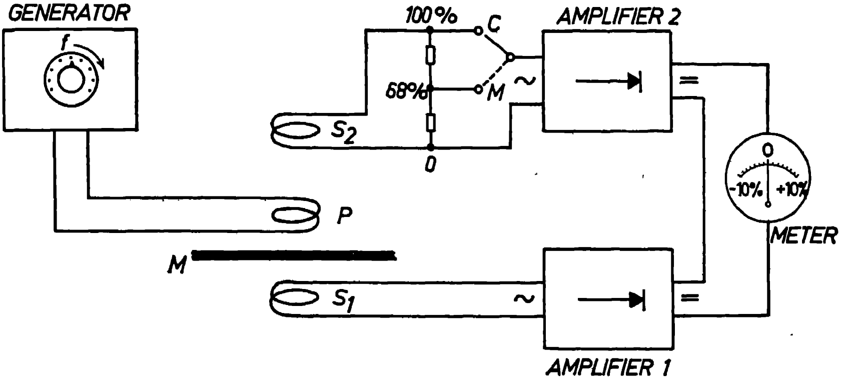

Institut Dr. Foerster

Fig. 11. Circuit for measuring the product of conductivity and thickness of flat metallic sheets by frequency adjustment.

Determining the Product of Conductivity and Thickness of Metallic Sheets. Insertion of a metallic sheet between the coils P and S_1 of the instrument shown in Fig. 11 causes the output voltage of secondary coil S_1 to diminish. If the oscillator feeding the primary coil is varied in frequency until the indicating meter shows a zero deflection, the amplitude of the field of the primary coil at the location of the secondary coil S_1 is also decreased to exactly 68 percent. The **transmission coefficient** T now corresponds to the line connecting the origin to the point at which $f/f_g = 2.75$ in Fig. 9. The magnitude of T is now 68 percent of $T_0 = 1$. In this way one has selected the frequency which provides the **maximum indication sensitivity** (see Fig. 11) for conductivity and thickness variations. At this point, $f/f_g = 2.75$, Eq. (10) indicates that

$$\sigma D = \left(\frac{7000}{A}\right)\left(\frac{1}{f}\right) \tag{11}$$

The **instrument constant** A (the effective distance from the primary to the secondary coil) can be determined with a metal foil (for example, of aluminum) of known conductivity and thickness from Eq. (11). The determination of the product σD by Eq. (11) is based upon a frequency measurement which can be carried out with high accuracy.

Application of Calibrated *RC* Oscillator. A calibrated resistance-capacitance (*RC*) oscillator can be used as the generator in the system shown in Fig. 12. As is well known, the **frequency** of such an oscillator is inversely proportional to the resistance *R* and the capacitance *C* of the *RC* network. In this case, as indicated by Eq. (11), the **product σD** is proportional to the resistance *R* of the oscillator (if a fixed capacitance *C* is employed).

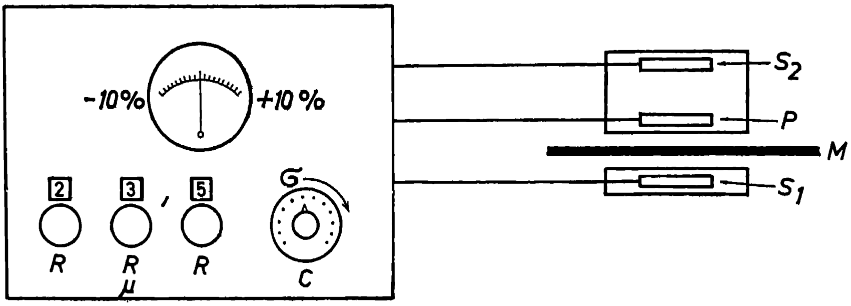

Institut Dr. Foerster

Fig. 12. Arrangement for measuring the thickness of flat metallic sheets with a calibrated *RC* oscillator. Thickness is read directly from the scales of three decade resistances. Variations of electrical conductivity with alloy or temperature are compensated with the capacitance *C*.

Direct Indication of Thickness of Metallic Sheets and Foils. The capacitance *C* of the oscillator in the system shown in Fig. 12 can be adjusted to correspond with the electrical conductivity σ of the material being inspected. **Variations in alloy or in temperature** during testing can thus be adjusted with the capacitor. If the resistance variation is made with precision decade resistors, the thickness can then be indicated directly by the settings of the decade resistance. The calibration of the indicating meter in terms of the **percentage deviation in sheet thickness** remains constant, since all tests are made at the same frequency ratio $f/f_g = 2.75$ on the transmission-coefficient curve of Fig. 9, without regard to the individual values of conductivity or thickness of the test material.

Direct Measurement of Resistance per Unit Square. In many measurements of conducting films, resistance is measured per unit square. The **resistance per unit square,** $R_\square$, is defined as the electrical resistance between two opposite edges of a square of conducting film, and is given in units of ohms per unit square. (The dimensions of the square are of no significance in this measurement.) Eq. (10), applied to the resistance per unit square, indicates that the **limit frequency** is

$$f_g = 2.5 \times 10^{7} \, (R_\square / A) \qquad (12a)$$

and the **frequency ratio** is

$$f/f_g = 4 \times 10^{-8} \, (fA/R_\square) \qquad (12b)$$

where A = distance between primary and secondary coil.
$R_\square$ = resistance per unit square of conducting film.

Control of Film Resistance During Metal Deposition. To illustrate an application of the fork-coil eddy current test of resistance per unit square, consider the problem of continuous observation of the vacuum vapor-deposition **process of making condenser foils.** In this case the resistance per unit square, $R_\square$, of the metallized paper is of interest. Fig. 13 shows the schematic circuit diagram of a measuring instrument designed for direct, continuous indication of the resistance per unit square during the process of **metal deposition in vacuum.**

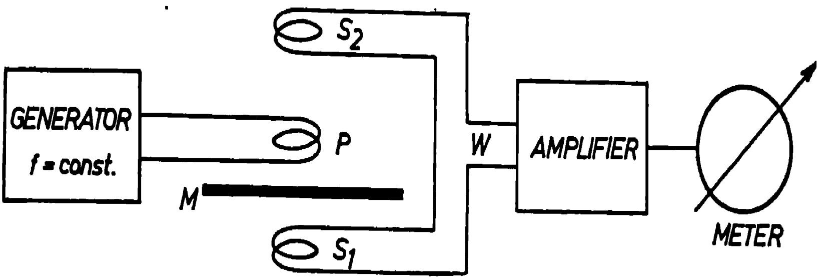

Institut Dr. Foerster

Fig. 13. Differential arrangement for the measurement of resistance per unit square for thin metallic foils.

A fixed-frequency oscillator energizes the primary coil P, which acts on the two balanced secondary coils S_1 and S_2 so that their induced voltages cancel. With no metallic layer between P and S_1, the indicating meter shows no deflection. The **oscillator frequency** is selected so that the test will be carried out at very low f/f_g ratios ($f/f_g < 0.4$) in the range of interest. In this range the vector W of Fig. 9 is proportional to $1/R_\square$, as shown by the approximation formula for small f/f_g ratios. As a result of this simple relationship, the indicating meter of the resistance-per-unit-square test instrument in Fig. 13 can be calibrated without a sample.

Instruments developed for production control of **rolling processes** and for control of **metal deposition processes** for foils or condenser paper in industry are described in the section on Eddy Current Test Equipment.

References

Reference numbers in this section refer to the references at the end of the section on Eddy Current Test Indications.

SECTION 40

EDDY CURRENT TEST EQUIPMENT

CONTENTS

PAGE

Impedance-Magnitude Tests

Classification of eddy current test equipment 1
- Types of test coils 1
- Test coil circuit arrangements 1
- Impedance-plane response characteristics 4
- Type of presentation of test indications 4
- Identification of eddy current test instruments 4
  - Classification of eddy current instruments for measuring material properties and discontinuities (*f*. 1) 2
- Principle of operation of impedance-magnitude tests 5
  - Simplified diagram of impedance-magnitude test instrument, showing primary and secondary coil connections, with comparison standard test specimen (*f*. 2) 5
  - Simplified diagram of impedance-magnitude test instrument, with bridge circuit and two primary coils, with comparison standard test specimen (*f*. 3) 6
- Test indications 5
- 20-Mc. tungsten wire test 6
- Balancing of test bridges 6
  - Circuit for balancing an eddy current test bridge in both ωL and R directions (*f*. 4) 7
- Limitations of impedance-magnitude tests. 7

Reactance Magnitude Tests

Principle of operation 7
- Frequency of oscillations 7

Frequency variations resulting from conductivity changes in nonferromagnetic test cylinders 8
- Sample calculation of frequency variation resulting from 1 percent conductivity change 9
  - Relative frequency variation, caused by 1 percent variation in electrical conductivity of a nonferromagnetic test cylinder, as a function of frequency ratio f/f_g for four coil fill factors, $\eta = 1.0$, 0.75, 0.5, and 0.25 (*f*. 5) 9

Frequency variations resulting from diameter changes in nonferromagnetic test cylinders 10
- Relative frequency variation, $\Delta f/f$ caused by a 1 percent variation in test-object diameter, as a function of frequency ratio f/f_g (*f*. 6) 10

Frequency variations resulting from cracks in nonferromagnetic test cylinders 11
- Frequency variations, caused by surface cracks of depth equal to 10 percent of diameter of nonferromagnetic cylinders placed in test coils of oscillator circuits, as a function of frequency ratio f/f_g (*f*. 7) 11
- Frequency variations, caused by surface cracks of depth equal to 20 percent of diameter of nonferromagnetic cylinders placed in test coils of oscillator circuits, as a function of frequency ratio f/f_g (*f*. 8) 12
- Frequency variations, caused by surface cracks of depth equal to 30 percent of diameter of nonferromagnetic cylinders placed in test coils of oscillator circuits, as a function of frequency ratio f/f_g (*f*. 9) 13

Test frequency selection 11
- Frequency selection for temperature compensation 12
- Calculating frequency ratios for temperature compensation 13

Radiofrequency crack detector 14

Limitations of reactance magnitude tests 14

Feedback-controlled Impedance Tests

Principle of operation 15

Circuit analysis 15
- Basic oscillator circuit used in feedback-controlled impedance, eddy current test method (*f*. 10) 15
- Amplitude of oscillations 16
- Condition for no test indication 16
- Direction on impedance plane for no test indication 17
  - Impedance plane for feedback-controlled impedance test method (*f*. 11) 17
- Direction on impedance plane for maximum test indications 18

Response characteristics of the cyclograph 18
- Cyclograph-response impedance plane 18
  - Impedance plane for feedback-controlled impedance tests showing direction of conductivity σ, diameter d, crack effects (black areas), and test measurement directions C (*f*. 12) 19

Response characteristics of the Sedac instrument 18

CONTENTS (*Continued*)

PAGE

- Response characteristics of the Zijlstra instrument ... 19
- Response characteristics of the Cornelius instrument ... 20
- Suppression of undesired test effects ... 20

Cathode-Ray Tube Vector Point Tests

- Principle of operation ... 20
  - Electric circuit ... 20
    - Wiring diagram of Foerster Multitest instrument with automatic sorting device (American designation: Magnatest FS-200) (*f.* 13) ... 21
  - Calibration ... 21
  - Test indications ... 22
    - Impedance plane displays of the vector-point test instrument (Foerster Multitest) (*f.* 14) ... 22
  - Sorting ... 22
- Applications ... 23

Cathode-Ray Tube Ellipse Tests

- Principle of operation ... 23
    - Wiring diagram for Foerster ellipse method test instrument (*f.* 15) ... 24
  - Phase rotation ... 23
  - Impedance-plane analysis of ellipse patterns ... 24
    - Impedance plane showing diameter direction *EOC* and crack direction *OA* (*f.* 16) ... 25
    - Analysis of impedance-plane measurement effects from elliptical screen patterns (*f.* 17) ... 25
  - Separation of crack and diameter effects ... 26
- Sigmaflux eddy current test instrument ... 26
  - Meter indications ... 26
  - Sigmaflux test equipment ... 27
    - Ellipse test instruments (*f.* 18) ... 27
    - Test coils for ellipse test instruments (*f.* 19) ... 28
- Applications of the ellipse test method ... 28

Linear Time-Base Tests

- Principle of operation ... 29
  - Circuit analysis ... 29
    - Wiring diagram of linear time-base test instrument (*f.* 20) ... 29
  - Calibration ... 30
  - Slit analysis technique ... 30
    - Screen image of linear time-base test instrument, with sinusoidal signals (*f.* 21) ... 31
    - Section of complex voltage plane showing vector voltages *OA* and *OB* of Fig. 21 (*f.* 22) ... 32
  - Impedance-plane analysis of slit values ... 32
    - Complex voltage plane of test coil, containing a ferromagnetic test cylinder, for a fixed test frequency of 5 c.p.s. (*f.* 23) ... 33
  - Sample calculations for iron rod ... 32
- Crack depth analysis ... 35
    - Analysis of Magnatest Q screen patterns and impedance plane characteristics (*f.* 24) ... 34

PAGE

  - Self-comparison crack depth tests ... 35
    - Response of difference-coil method to surface cracks in cylindrical test objects (*f.* 25) ... 36
  - Combined absolute and comparison tests ... 36
  - Secondary coil voltage signals ... 36
  - Selection of test frequency ... 37
- Applications ... 38
    - Test coils for Foerster Magnatest Q instruments (American designation, Magnatest FS-300) (*f.* 26) ... 37

Suppression of Undesired Effects

- Significance of undesired effects in test indications ... 38
- Phase-controlled rectifier method ... 38
    - Basic circuitry of the phase-controlled rectifier (*f.* 27) ... 38
  - In-phase operation ... 39
    - Analysis of operation of phase-controlled rectifier (*f.* 28) ... 40
  - Out-of-phase operation ... 39
  - Operation at intermediate phase angles ... 39
  - Suppression of undesired signals ... 39
  - Suppression of undesired harmonics ... 41
    - Analysis of harmonics in signal voltage (*f.* 29) ... 41
  - Condition for suppression of nth harmonic ... 42
- Resonant circuit impedance variation test ... 42
    - Circuit for complete suppression of undesired effects such as "lift-off" effect by partial compensation of voltage across a condenser in the resonance circuit (*f.* 30) ... 42
    - Vector relations in the circuit of Fig. 30 (*f.* 31) ... 43
  - Circle diagram ... 43
  - Suppression of lift-off effects ... 44
    - Impedance plane showing "lift-off" direction *ABC*, with conductivity σ and crack directions (*f.* 32) ... 44
  - Crack detection ... 45
- Applications of suppression techniques ... 46
  - Crack-depth tests ... 47
    - Defectometer probe-coil instrument for detection of cracks and crack-depth measurement on both ferromagnetic and nonferromagnetic materials (*f.* 33) ... 45
    - Deflection on the Defectometer instrument of Fig. 33 above the cross-section of a sound (left) and a cracked piston head (right) (*f.* 34) ... 45
  - Porosity test ... 47
    - Defectometer indication of porosity in the cross-section of a light metal block (*f.* 35) ... 46
  - Cracks within drilled holes ... 47
    - "Crack detector" for light-alloy compressor blades (*f.* 36) ... 47
  - Tests for thickness of nonmetallic layers ... 47
    - Eddy current instrument for the measurement of the thickness of insulating layers (Foerster Isometer) (*f.* 37) ... 48
- References ... 48

SECTION 40

EDDY CURRENT TEST EQUIPMENT

Impedance-Magnitude Tests

CLASSIFICATION OF EDDY CURRENT TEST EQUIPMENT. The theory developed and presented in the preceding sections on eddy current tests provides data on the optimum test conditions, test frequency, variations in measured quantities, suppression of undesired influences, and related parameters for various test problems in the field of eddy current testing. However, many eddy current test instruments were developed on an empirical basis before this theory was available. In consequence their designs sometimes deviate considerably from the optimum indicated by theory for specific test problems. The many different design variations are indicated in the classifications of **eddy current instrument characteristics** which are discussed in the subsequent text.

Types of Test Coils. The most common types of test coils used in eddy current test equipment are:

1. **Feed-through coils,** in which test objects such as rods, tubes, extruded or rolled shapes, wire, and other production parts are passed through a hole within the test coil.
2. **Inside test coils,** which are inserted within cavities such as the interior of hollow tubes or drilled holes.
3. **Probe coils,** which are placed on the surfaces of test objects.
4. **Forked coils,** through whose arms test objects such as sheets, foils, metallized paper, and similar conducting materials pass during tests.

Test Coil Circuit Arrangements. Test coils are connected to the electronic test instruments in various circuit arrangements which produce varying measurement effects, as follows:

1. Resonance-circuit methods, in which the test coil is part of a resonant circuit within the test instrument.
2. Time-differentiated resonance methods, in which a resonance coil is connected to a circuit with time differentiation to suppress slowly changing variations in the test objects.
3. Differential arrangements with a comparison coil (called the "absolute coil" method in European literature). In these the measurement voltage from the coil containing the unknown test object is compensated by that from a second coil containing a standard test object.
4. Time-differentiated comparison arrangements, utilizing comparison coils, but with time differentiation in the indicating circuit to suppress slowly changing variations in the test objects.
5. Self-comparison differential coil methods, in which one portion of the test object is compared with another portion of the same test object.
6. Time-differentiated self-comparison methods, in which the output of a differential coil system is subjected to time differentiation in the indication circuit so

Name of Instrument or Commercial Designation	Types of Test Coils	Test Coil Circuit Arrangements	Impedance-Plane Response Characteristics	Types of Presentation of Test Indications	Typical Industrial Applications
Schirp[78, 79]	Feed-through	Bridge circuit	Impedance-magnitude	Meter	Tests of tubes
Mathes[69]	Feed-through	Bridge circuit	Impedance-magnitude	Meter	Aluminum alloys
Brown & Bridle[8]......	Feed-through	Bridge circuit	Impedance-magnitude	Cathode-ray tube	Steel sorting
Salford Bridge[2]	Feed-through	Bridge circuit	Impedance-magnitude	Cathode-ray tube	Tungsten wires
Radio-Frequency Crack Detector	Feed-through	Oscillators	Reactance-magnitude	Meter	Crack detection
Plant & Manual[74]	Feed-through	Oscillators	Reactance-magnitude	Meter	Stainless tubes
Cyclograph	Feed-through	Feedback oscillator	Feedback-controlled impedance	Cathode-ray tube	Alloy sorting
Sedac	Surface probe	Feedback oscillator	Feedback-controlled impedance	Meter	Crack and seam depth tests
Zijlstra	Feed-through	Feedback oscillator	Feedback-controlled impedance	–	Tungsten wires
Cornelius	Feed-through	Feedback oscillator	Feedback-controlled impedance	Meter	Cracks in rod and tube
Foerster Multitest (Magnatest FS-200)..	Feed-through and special types	Differential coil comparison	Impedance vector analysis	Vector point on cathode-ray tube	Production parts
Foerster Wire Crack Test Instrument (Magnatest FW-200).	Feed-through	Differential coil comparison	Ellipse analysis of impedance vector	Ellipse on cathode-ray tube	Cracks in wires

Foerster Rod Crack Test Instrument (Magnatest FW-400) .	Feed-through	Differential coil comparison	Ellipse analysis of impedance vector	Ellipse on cathode-ray tube	Cracks in rods
Foerster Sigmaflux (Magnatest FW-300) .	Feed-through	Differential coil comparison	Ellipse analysis of impedance vector	Ellipse on cathode-ray tube	Alloy sorting Hardness sorting Crack testing Dimensional tests
Foerster Magnatest Q (Magnatest FS-300) . .	Feed-through	Differential coil comparison	Linear-time-base analysis	Sinusoidal curves on cathode-ray tube (slit analysis technique)	Carbon content Crack depth analysis Alloy sorting
Foerster Sigmatest (Magnatest FM-100) .	Probe coil	Resonant-circuit impedance variation	Conductivity response with lift-off suppression	Meter	Alloy sorting and electrical conductivity measurement
Foerster Defectometer. .	Probe coil	Resonant-circuit impedance variation	Conductivity response with lift-off suppression	Meter	Crack detection and crack-depth measurement
Foerster Crack Detector for Light-Alloy Blades	Internal rotating probe coil unit	Resonant-circuit impedance variation	Conductivity response with lift-off suppression	Cathode-ray tube and meter	Detection of cracks in small drilled holes
Foerster Isometer	Probe coil	Resonant-circuit impedance variation	Conductivity response with lift-off suppression	Meter	Measuring thickness of insulating layers

Fig. 1. Classification of eddy current instruments for measuring material properties and discontinuities.

that only effects with a rapid time variation of the impedance difference are indicated.

Impedance-Plane Response Characteristics. Discriminating circuits used in eddy current test instruments vary with respect to those characteristics of impedance-plane changes to which they respond. Various methods include:

1. Impedance magnitude methods, which indicate only the magnitude of variations in the total impedance Z, regardless of the phase angle or direction in which it occurs on the impedance plane. (See section on Eddy Current Cylinder Tests for explanation of the characteristics of impedance planes for eddy current tests.)
2. Inductive-reactance magnitude methods, which indicate only the magnitudes of changes in inductive reactance, ωL, without regard to changes in the resistive component of the total impedance. In many of these methods, changes in reactance are detected by changes in the frequency of tuned circuits containing the test coils.
3. Feedback-controlled impedance methods, which are also sometimes designated as core-loss or loss-sensing methods. In these methods the phase angle or ratio L/R of the inductance to the resistance of the test coil circuit influences the feedback factors of self-excited oscillator circuits.
4. Impedance vector analysis methods, which indicate both the magnitude and phase angle (or direction on the impedance plane) of impedance variations.
5. Methods which suppress the indications of undesired or insignificant test object effects.

Type of Presentation of Test Indications. Various methods are used to present eddy current test indications to the observer or to automatic selection or control devices. Among these are:

1. Direct meter indication with pointer-type instruments.
2. Meter indication with phase-controlled rectifier.
3. Cathode-ray tube indicators, showing a generalized representation of the test indications.
4. Cathode-ray tube point method, in which the apparent impedance plane is represented by the screen of the cathode-ray tube, and measured values appear as a luminous point on the screen.
5. Cathode-ray tube ellipse method, in which the measurement effect reacts on the vertical deflection plates of a cathode-ray tube, and a reference voltage, whose direction on the impedance plane can be selected at will, is applied to the horizontal deflection plates.
6. Linear time-base method, in which the measurement effect influences the vertical deflection of the cathode-ray beam. Here a linear saw-tooth timing voltage, whose phase position can be selected at will, is applied to the horizontal deflection plates.
7. Time-slit selection method, in which a specific instant or phase-angle point is selected in the sinusoidal signal or control voltage, and measured values at that time instant only are indicated or evaluated.

Identification of Eddy Current Test Instruments. The preceding classifications can be used to explain the basic principles of operation of eddy current test instruments, as shown in Fig. 1. **Commercial designations** are included to aid in identification of these particular instrument types. The following discussion of eddy current test equipment will be devoted to those types whose performance can be described in terms of their impedance plane characteristics, since these characteristics are intimately related to the nature and operation of the tests. Only those methods which are widely used in industry or show promise of increased future acceptance are discussed in detail.

Principle of Operation of Impedance-Magnitude Tests. Eddy current test instruments that indicate only the magnitude of variations in the total impedance of the test coil were widely used in the past. Their principle of operation is indicated in the diagram of Fig. 2. An alternating current (a.c.) flows through two primary coils. One coil contains the unknown part to be tested, while the other contains a comparison or reference standard specimen. If both test specimens are identical, no voltage appears at the terminals of the secondary coils, since these are connected in series opposition and therefore their voltages cancel. A difference voltage appears across the secondary terminals if the unknown test object deviates in any of its properties from those of the reference standard. The **test response** may be caused by variations in test-object conductivity, magnetic permeability and dimensions, or by the presence of cracks or other discontinuities. The bridge circuit arrangement of Fig. 3 can also be used for measuring the magnitude of impedance variations, in place of the arrangement shown in Fig. 2.

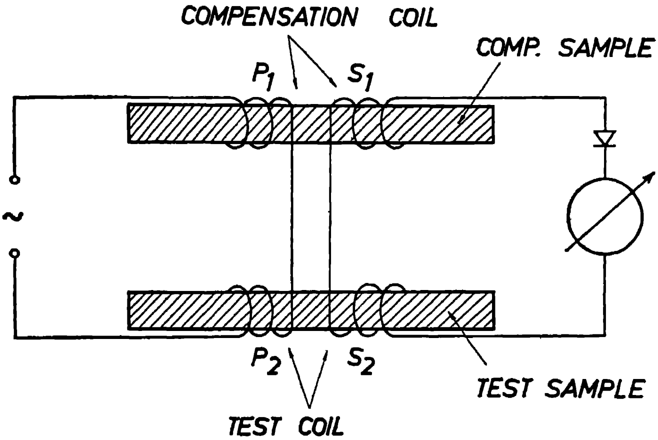

Institut Dr. Foerster

Fig. 2. Simplified diagram of impedance-magnitude test instrument, showing primary and secondary coil connections, with comparison standard test specimen.

Test Indications. The various methods for measuring the magnitude of impedance variations are also distinguished by the type of indication of the difference voltages. Schirp,[78, 79] Mathes,[69] and others indicate the difference voltage by means of a meter. Brown and Bridle [8] display the variations of the two secondary coils by the deflection of the beam of a cathode-ray tube. In the "Magnetic Sorting Bridge" of the Salford Electrical Instrument Company,[2] a horizontal line appears on the screen of a cathode-ray tube when the unknown test object and the standard are the same. If the test specimen deviates from the reference standard specimen, the cathode-ray beam is also deflected vertically by a distance which corresponds to the degree of variation between the test specimen and the standard. The deflection is proportional to the magnitude of the variation between the sample and the standard. However, it is not possible to identify a given factor in the screen display with an individual property of the test material. The reference voltage applied to the horizontal deflection plates is fixed in apparent impedance direction, which makes an impedance analysis impossible.

20-Mc. Tungsten Wire Test. A bridge similar to that shown in Fig. 3 was used by O'Dell[73] for the indication of **splitting in tungsten wires.** However, its test frequency was 20 megacycles (Mc.) per second. Thus, in practice, only surface cracks could be found. In addition, at this high test frequency, the sensitivity for crack indications is very low compared to the sensitivity of the indication to diameter variations. For tungsten wire of 2-mm. thickness, the limit frequency $f_g = 7000$ c.p.s. [see Eq. (5) in the section on Eddy Current Test Principles for the definition of the limit frequency for solid cylinders]. A test frequency of 20 Mc. is 2860 times this limit frequency. Here the **crack sensitivity** is only 4 percent of that for a test frequency which is six times the limit frequency.

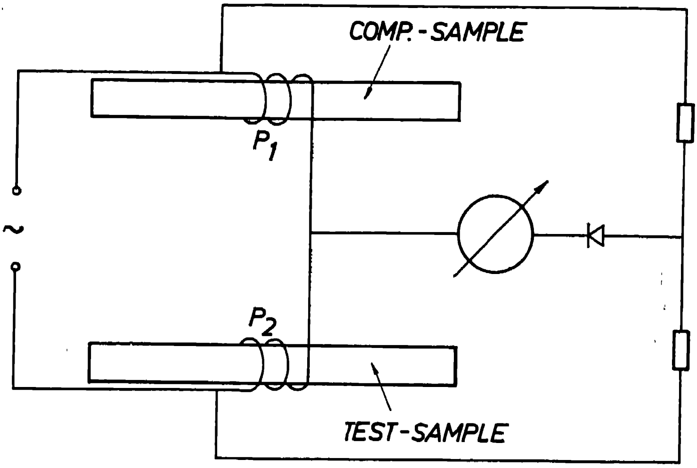

Institut Dr. Foerster

Fig. 3. Simplified diagram of impedance-magnitude test instrument, with bridge circuit and two primary coils, with comparison standard test specimen.

Model tests and the similarity law for eddy current tests indicate that at a frequency of 20 Mc., a surface crack of 10 percent depth in 2-mm. tungsten wire is indicated with the same sensitivity as a diameter variation of only 0.15 percent. However, since tungsten wire is usually swaged, which results in **diameter variations** of 2 to 3 percent, there is considerable difficulty in separating dangerous cracks from harmless diameter variations.

Balancing of Test Bridges. Various eddy current bridge test methods are distinguished not only by differences in the presentation of indications but also in the methods used for bridge balancing. It is impossible to wind test coils and compensation coils so exactly alike that no residual difference voltage appears. Thus it is necessary to balance **residual bridge voltages** by means of additional circuitry. Balancing can be entirely eliminated in simple bridges such as that developed by Brown and Bridle,[8] for example, and in the "Ferrometer" and "Magnetrie" bridges of French construction. Other bridges can be balanced for variations in the reactance direction by means of a resistor. The bridge used by Schirp and Mathes[78] permits balancing of both the reactance and the resistive components. Fig. 4 shows a schematic diagram of this bridge. The reactance control balances variations in the ωL direction, while the resistance control balances variations in the R direction.

Limitations of Impedance-Magnitude Tests. All impedance-magnitude eddy current tests similarly indicate desired effects, such as conductivity variations or crack effects, and undesired effects, such as minor diameter variations. These **allowable tolerances in diameters** of semi-finished products are the reason why methods which indicate only the magnitude of apparent impedance variations are often unsuccessful in practice. The dimensional tolerances far outweigh, in their eddy current response, the effects of **variations in electrical conductivity** which are often used in sorting alloys. For example, at a frequency ratio of $f/f_g = 100$, the effect of a 1 percent diameter variation is 20 times as strong as the effect of a 1 percent conductivity variation. However, a 1 percent diameter variation is well within commercial tolerance and is insignificant, whereas a 20 percent variation in conductivity can be highly significant in some instances.

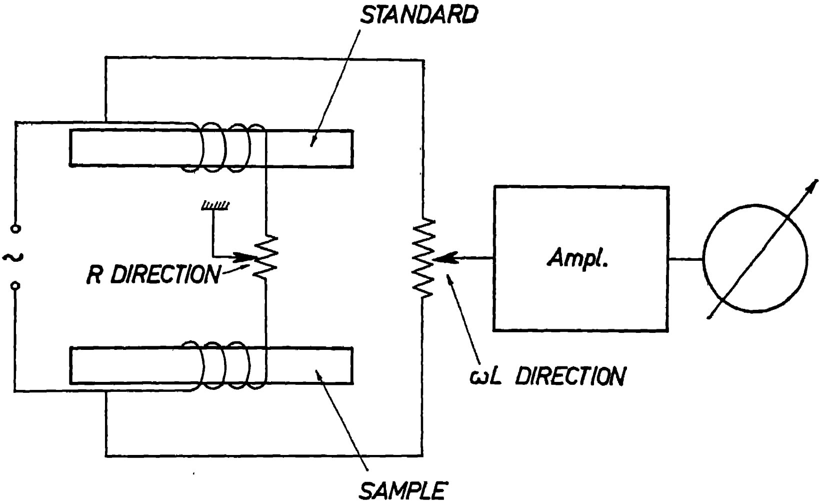

Institut Dr. Foerster

Fig. 4. Circuit for balancing an eddy current test bridge in both ωL and R directions.

Reactance Magnitude Tests

PRINCIPLE OF OPERATION. Another series of eddy current test methods utilizes variations of the fundamental frequency of an oscillatory electrical circuit whose inductance is determined in part or entirely by the test coil. The fundamental frequency of an oscillatory circuit is a function of its self-inductance, but (to a first approximation) is not significantly influenced by its resistance R. Consequently all physical effects of the test object which cause a change in the reactance of the test coil can be indicated. (See section on Eddy Current Test Principles for an explanation of inductance variations resulting from test-object properties.)

Frequency of Oscillations. Methods in which oscillation frequency is influenced by the test coil are widely used in eddy current test devices. The quantitative theory of this method indicates, for any given test material or test frequency, the change in oscillator frequency resulting from 1 percent variations in conductivity or diameter or from a crack of given depth. For an oscillator circuit consisting of a self-inductance L (henries) and a capacitance C (farads), the fundamental frequency f (c.p.s.) is

$$f = \frac{1}{2\pi\sqrt{LC}} \tag{1}$$

The **self-inductance** L of the test coil has been derived [see Eq. (15) in the section on Eddy Current Test Principles] as

$$L = L_0\,[1 - \eta + \eta\mu_{\text{rel.}}\mu_{\text{eff.(real)}}] \tag{2a}$$

where L_0 = self-inductance of the test coil in the absence of a test object.
η = coil fill factor.
$\mu_{\text{rel.}}$ = relative magnetic permeability of test material.
$\mu_{\text{eff.(real)}}$ = real component of the complex effective permeability.

The effective permeability $\mu_{\text{eff.}}$ is a function of the frequency ratio

$$f/f_g = \frac{f\sigma\mu_{\text{rel.}}d^2}{5066} \tag{2b}$$

where f_g = limit frequency.
f = test frequency, c.p.s.
σ = electrical conductivity of test material, meter/ohm-mm.^{2}.
d = diameter of test cylinder, cm.

(See Effective Permeability in the section on Eddy Current Test Principles for an explanation and quantitative values for these parameters.)

FREQUENCY VARIATIONS RESULTING FROM CONDUCTIVITY CHANGES IN NONFERROMAGNETIC TEST CYLINDERS. The relative frequency variation, $\Delta f/f$, can be determined for given variations in test-object conductivity, relative magnetic permeability, or dimensions, as well as from the presence of specific surface or subsurface cracks. For eddy current tests whose oscillator frequency is influenced by the test coil, only the real component of the effective permeability, $\mu_{\text{eff.(real)}}$, need be considered, since only this component influences the frequency. In this case the frequency variation caused by a 1 percent variation in the electrical conductivity of the test material amounts to

$$\Delta f/f = (-\eta/200)\,\frac{Re\,[1 + (J_1^2/J_0^2) - \mu_{\text{eff.}}]}{[(1-\eta)/\mu_{\text{rel.}}] + \eta\mu_{\text{eff.(real)}}} \tag{3}$$

where $\Delta f/f$ = relative frequency variation of the oscillatory circuit whose self-inductance is produced by the test coil when the electrical conductivity of the test object in the coil varies by 1 percent.
η = fill factor of coil = d^2/D^2 (for a solid cylinder).
d = diameter of test cylinder.
D = diameter of test coil.
J_1 = Bessel function of first order $\left(\text{Argument } A = \dfrac{f\mu_{\text{rel.}}\sigma d^2}{5066}\right)$.
J_0 = Bessel function of zero order $\left(\text{Argument } A = \dfrac{f\mu_{\text{rel.}}\sigma d^2}{5066}\right)$.
$\mu_{\text{eff.}}$ = effective permeability.

(Values for the effective permeability are shown in Figs. 7 and 8 of the section on Eddy Current Test Principles for specific frequency ratios f/f_g.) Note that the effective permeability $\mu_{\text{eff.}}$ is a complex number, so that

$$|\mu_{\text{eff.}}| = \sqrt{[\mu_{\text{eff.(real)}}]^2 + [\mu_{\text{eff.(imag.)}}]^2}$$

Values of the Bessel functions J_1 and J_0 for given frequency ratios are found from Bessel function tables.

Sample Calculation of Frequency Variation Resulting from 1 Percent Conductivity Change. Fig. 5 shows an evaluation of the frequency variations of Eq. (3) as a function of frequency ratio f/f_g for four different coil fill factors η.

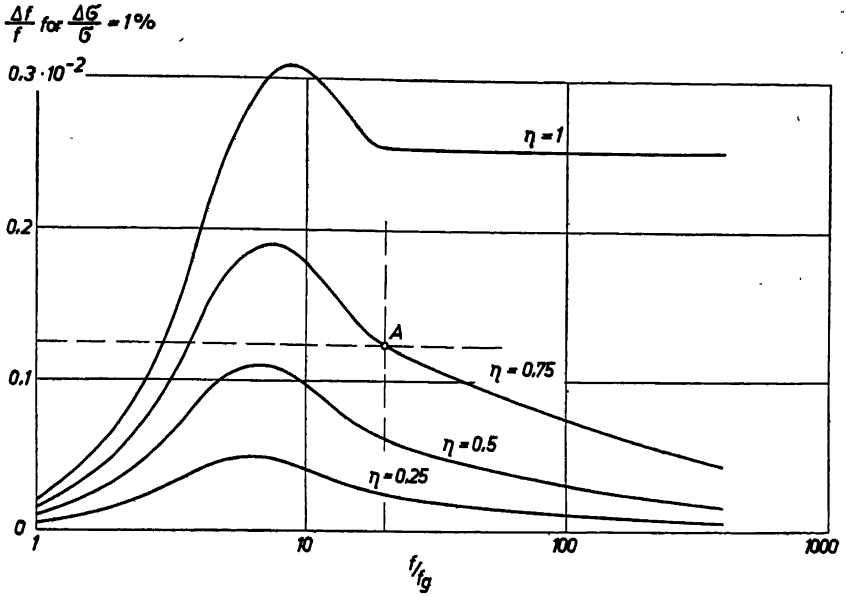

Fig. 5. Relative frequency variation, caused by 1 percent variation in electrical conductivity of a nonferromagnetic test cylinder, as a function of frequency ratio f/f_g for four coil fill factors, $\eta = 1.0, 0.75, 0.5$, and 0.25. Frequency variation given in percentage of test frequency.

These frequency variations correspond to variations of 1 percent in test material conductivity for the case of solid nonferromagnetic cylinders. To illustrate the use of these curves, suppose, for example, that an aluminum rod has the following characteristics:

Diameter, $d = 1$ cm.
Electrical conductivity, $\sigma = 35$ meter/ohm-mm.^{2}.
Relative magnetic permeability, $\mu_{\text{rel.}} = 1$.

Assume that this rod is inserted into the test coil and that the frequency of the oscillator circuit is adjusted to $f = 2860$ c.p.s. by varying the tuning capacitor. The frequency ratio f/f_g now equals 20 (approximately), from Eq. (2b). If the fill factor $\eta = d^2/D^2 = 0.75$ for the specific test coil in use, point A in Fig. 5 is selected. The corresponding ordinate is about 0.12×10^{-2}. This value of $\Delta f/f$, multiplied by the test frequency $f = 2860$ c.p.s., corresponds to a frequency variation of 3.44 c.p.s. This frequency variation is the consequence of a change of 1 percent in the electrical conductivity of the aluminum rod, which could possibly result from a temperature variation of 2.5° C.

FREQUENCY VARIATIONS RESULTING FROM DIAMETER CHANGES IN NONFERROMAGNETIC TEST CYLINDERS. The frequency variations caused by a 1 percent change in the diameter of a nonferromagnetic test cylinder placed in the test coil of an oscillator circuit are given by

$$\Delta f/f = (-\eta/100)\,\frac{[(\mu_{\text{rel.}} - 1)/(\mu_{\text{rel.}})] + [Re(J_1^2/J_0^2)]}{[(1-\eta)/(\mu_{\text{rel.}})] + \eta\mu_{\text{eff.(real)}}} \tag{4}$$

The symbols are explained below Eq. (3). The terms $Re(J_1^2/J_0^2)$ and $\mu_{\text{eff.(real)}}$ depend upon the specific frequency ratio f/f_g used in the test.

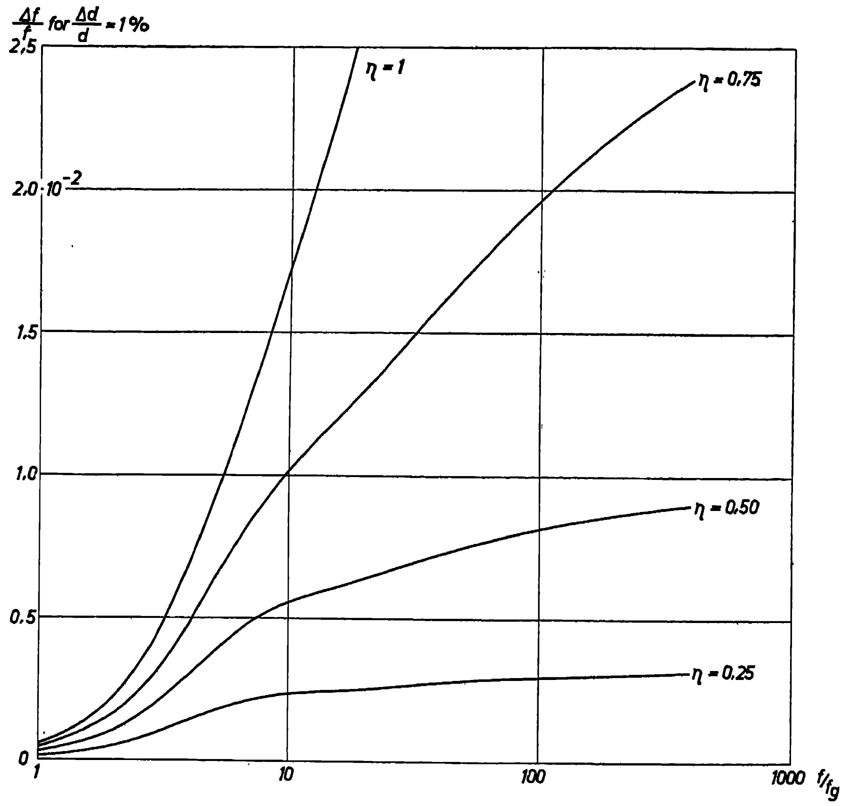

Fig. 6. Relative frequency variation, $\Delta f/f$, caused by 1 percent variation in test-object diameter, as a function of frequency ratio f/f_g. Curves are shown for four different coil fill factors η, corresponding to Fig. 5.

Fig. 6 shows frequency variations computed from Eq. (4) as a function of frequency ratio f/f_g and coil fill factor η. At a frequency ratio of $f/f_g = 10$ and a coil fill factor $\eta = 0.75$, for example, a diameter variation of 1 percent causes a frequency variation of 1 percent. At a frequency ratio of $f/f_g = 100$, with the same 1-cm. diam. aluminum rod whose properties were listed earlier, the frequency variation caused by 1 percent diameter change is 20 times as great as that caused by a 1 percent change in conductivity.

FREQUENCY VARIATIONS RESULTING FROM CRACKS IN NONFERROMAGNETIC TEST CYLINDERS. Cracks in test cylinders which form the core of test coils in oscillator circuits also influence the frequency variations in such test instruments. The variation in effective permeability, $\Delta\mu_{\text{eff.}}$, caused by **surface and subsurface cracks in nonferromagnetic test cylinders** has been determined quantitatively. (See Figs. 14 to 17, inclusive, in section on Eddy Current Cylinder Tests.) Similar determinations have been made for **outside surface, inside surface, and subsurface cracks in tubes.** (See Figs. 10 to 13 in section on Eddy Current Tube Tests.) Only the real component, $\Delta\mu_{\text{eff.(real)}}$, of the variation in effective permeability due to cracks causes a frequency variation in oscillator test instruments. The quantitative relationship between the crack effect, $\Delta\mu_{\text{eff.(real)}}$, and the resultant variation in oscillator frequency, $\Delta f/f$, is

$$\Delta f/f = \frac{-(1/2)\mu_{\text{eff.(real)}}}{(1/\eta\mu_{\text{rel.}}) + \mu_{\text{eff.(real)}}} \tag{5}$$

Here the term $\mu_{\text{eff.(real)}}$ is the real component of the effective permeability for the specific frequency ratio f/f_g at which crack tests are made. (The values for $\mu_{\text{eff.(real)}}$ are given for various frequency ratios for solid test cylinders in Figs. 7 and 8 of the section on Eddy Current Test Principles.)

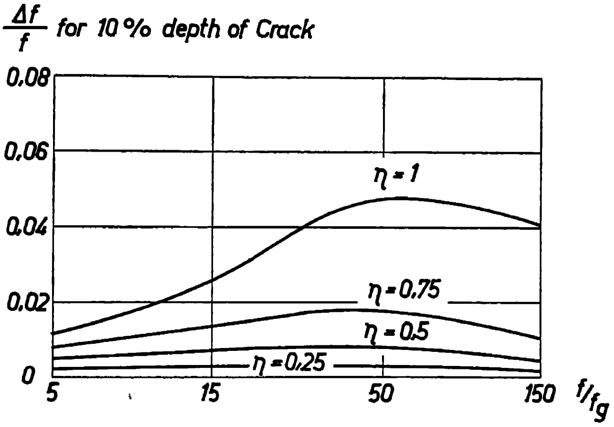

Fig. 7. Frequency variations, caused by surface cracks of depth equal to 10 percent of diameter of nonferromagnetic cylinders placed in test coils of oscillator circuits, as a function of frequency ratio f/f_g. Curves are shown for coil fill factors $\eta = 1.0$, 0.75, 0.50, and 0.25.

Figs. 7, 8, and 9, based on Eq. (5), show the relative frequency variations, resulting from **cracks of various depths in nonferromagnetic test cylinders,** as a function of frequency ratio f/f_g. As shown in Fig. 9, a crack having a depth equal to 30 percent of the cylinder diameter, tested as a frequency ratio $f/f_g = 50$, causes the same frequency variation as either a 2.4 percent change in cylinder diameter or a 36 percent change in material conductivity.

TEST FREQUENCY SELECTION. Eq. (5) can be used not only for the case of solid metallic cylinders but also in the same manner to calculate the frequency variations resulting from cracks in tubes and spheres and from surface

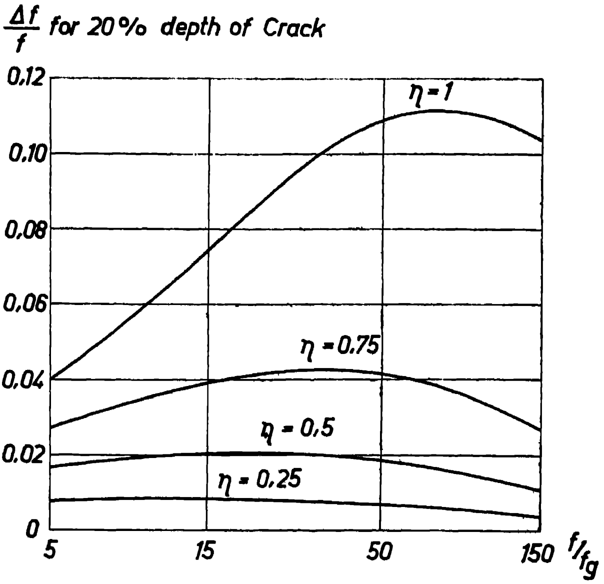

Fig. 8. Frequency variations, caused by surface cracks of depth equal to 20 percent of diameter of nonferromagnetic cylinders placed in test coils of oscillator circuits, as a function of frequency ratio f/f_g. Curves are shown for coil fill factors $\eta = 1.0$, 0.75, 0.50, and 0.25.

cracks in metallic sheets. (Curves showing the variations in effective permeability for these cases are presented in the preceding sections on eddy current tests.) Figs. 5 through 9 permit calculation of the frequency variations resulting from various conductivity, dimensional, and crack effects for any test frequency and coil fill factors. Fig. 5 shows that the maximum test sensitivity for specific **conductivity effects,** at which the largest frequency variations result, is attained at frequency ratios f/f_g between 4 and 10. Fig. 6 indicates that maximum sensitivity to **diameter changes** in nonferromagnetic cylinders increases steadily with increasing frequency ratios f/f_g. Figs. 5 and 6 are used to obtain an important result which can be applied to measurement of intergranular corrosion effects by an eddy current method (see the section on Eddy Current Test Indications).

Frequency Selection for Temperature Compensation. The heating of a metal rod results in an increase in its diameter. As indicated in Fig. 6, this results in a decrease of oscillator frequency. However, at the same time, the higher temperature results in a decrease in electrical conductivity which, in turn, increases the self-inductance. As indicated in Fig. 5, this results in an increase of the oscillator frequency. Now, for example, the **temperature coefficient of expansion** of aluminum is approximately 200 times smaller than the temperature coefficient of electrical conductivity. Consequently one can select the frequency ratio f/f_g so high that the frequency response to dimensions becomes 200 times as great as the frequency response to conductivity changes. Thus, for any given temperature coefficients of expansion and conductivity, a frequency ratio is available at which the frequency influence of the conductivity variation and the diameter variation during heating or cooling compensate each other. At the fre-

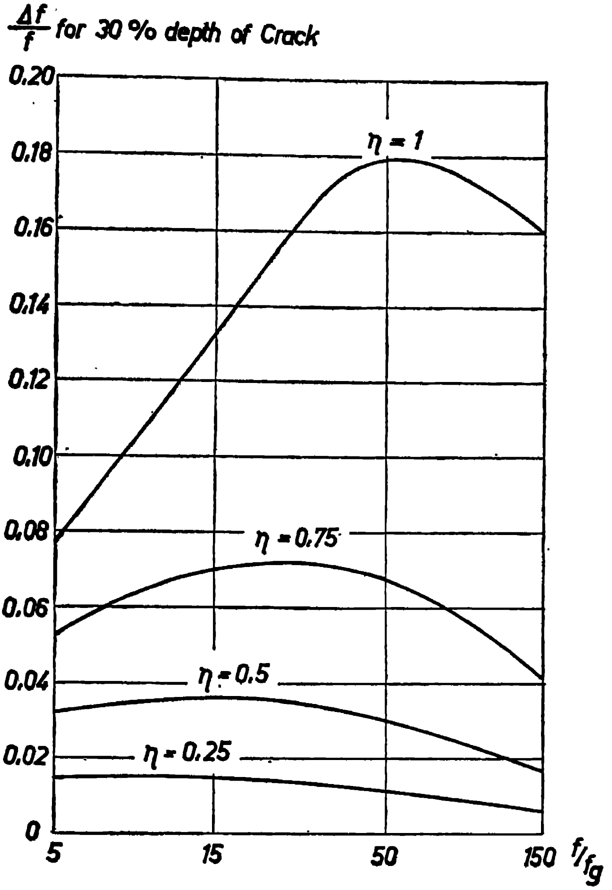

Fig. 9. Frequency variations, caused by surface cracks of depth equal to 30 percent of diameter of nonferromagnetic cylinders placed in test coils of oscillator circuits, as a function of frequency ratio f/f_g. Curves are shown for coil fill factors $\eta = 1.0, 0.75, 0.50$, and 0.25.

quency ratio where test response is independent of temperature, **diameter variations** as small as, for example, 10^{-5}, possibly caused by corrosion, can be measured with an extremely high sensitivity, independently of temperature variations.

Calculating Frequency Ratios for Temperature Compensation. For a given test cylinder diameter d and electrical conductivity σ, it is possible to calculate the frequency ratio f/f_g at which the frequency influence of the expansion is compensated by the frequency influence of electrical conductivity. For a **nonferromagnetic test cylinder** with a temperature coefficient of electrical conductivity α and a temperature coefficient of expansion β, this frequency ratio is

$$f/f_g = (\alpha/\beta)^2/8 \qquad (6a)$$

The limit frequency f_g is a function of test cylinder diameter and conductivity [see Eq. (2b)], so that this relation can be written as

$$f_i = \frac{634}{\sigma d^2}(\alpha/\beta)^2 \qquad (6b)$$

where f_i is the **temperature-invariant test frequency** at which the conductivity influence and the diameter influence due to temperature variations compensate one another. This frequency is selected, for example, to measure corrosion effects of **external and intergranular corrosion** (which reduces cylinder diameter) with extremely high sensitivity independent of temperature variations.

RADIOFREQUENCY CRACK DETECTOR. The "Radiofrequency Crack Detector" (Salford Electrical Instrument Co.) operates at test frequencies between 50 kc. and 5 Mc. In its operation, two transmitters feed a mixer tube which reproduces the difference frequency of the two transmitters. If the frequencies of the transmitters are equal, the difference frequency disappears. As noted previously, all apparent impedance effects which have a component in the inductive reactance (ωL) direction can be converted into a frequency effect. If one of these effects, such as a variation in conductivity, permeability, or diameter, or the presence of cracks, causes the frequency of the transmitter containing the test object in its oscillator coil to vary, a difference frequency appears at the output of the mixer tube. After rectification this output appears as a meter indication. The mixer tube operates on a resonant circuit. This causes the instrument deflection to be proportional to the difference frequency and thus to the variation of the reactance (ωL) of the test coil. A similar arrangement is used by Plant and Manual [74] to detect **defects in thin-walled stainless steel tubes.**

LIMITATIONS OF REACTANCE MAGNITUDE TESTS. Variations in effective permeability caused by surface cracks have a specific component in the reactance direction on the complex plane. (See, for example, Figs. 14 through 18 in the section on Eddy Current Cylinder Tests.) Unfortunately, however, variations in diameter of test cylinders also produce variations in the reactance direction. Since **semi-finished industrial parts,** as already noted, are subject to certain allowable diameter variations, it is impossible to distinguish between crack effects and diameter variations with reactance magnitude tests. At 15 times the limit frequency, a crack of 5 percent depth causes the same reactance effect as a diameter variation of 1 percent (see Fig. 15 in the section on Eddy Current Cylinder Tests). However, for some applications, a crack of 5 percent depth is undoubtedly a serious defect.

The **diameter variations corresponding to 5 percent crack depth** in their reactance variations, for nonferromagnetic cylinders, are as given in the accompanying table.

Frequency Ratio, f/f_g, of Test Frequency to Limit Frequency	Diameter Variation Corresponding to 5 Percent Crack Depth (Percent)
15	1
50	0.47
100	0.33
300	0.22
1000	0.112
3000	0.062

Here the frequency ratio f/f_g is computed from the physical properties of the test cylinder and the test frequency [see Eq. 2(b) in this section]. For example, at test frequencies of 1000 times the limit frequency, a diameter variation of approximately 0.1 percent causes the same variation in inductive reactance as a crack of 5 percent depth. Thus, frequency-response tests that operate at high multiples of the limit frequency are limited to detection of surface cracks with extremely accurately ground test objects and do not approach the optimum test sensitivity. The disadvantage of eddy current tests in which oscillator frequency is influenced by the test coil lies generally in the fact that it is impossible to separate desirable measurement effects (such as material conductivity or presence of cracks) from less significant effects such as trivial **diameter variations** which produce larger test indications. Of all effects present on the impedance plane, only the components in the inductive reactance direction are indicated.

Feedback-controlled Impedance Tests

PRINCIPLE OF OPERATION. Several eddy current test methods have a common feature in that the test coil forms the self-inductance of a feedback oscillator circuit. In these tests the ratio of the inductance to the resistance of the test coil influences the feedback factor of a self-excited oscillator circuit. Such tests are sometimes described as **loss-sensing tests,** since energy losses in the test object tend to damp out the oscillations. Commercial test instruments in this class include:

1. The Cyclograph.
2. The Sedac instrument.
3. The Cornelius instrument.
4. The Crack-Test instrument by Zijlstra.

Since the Cyclograph is well known in the United States, the theory underlying its operation and that of other instruments in this group will be discussed in relation to impedance-plane effect indications.

CIRCUIT ANALYSIS. Each of the instruments in the preceding list can be related to the basic circuit shown in Fig. 10. The test coil represents the self-

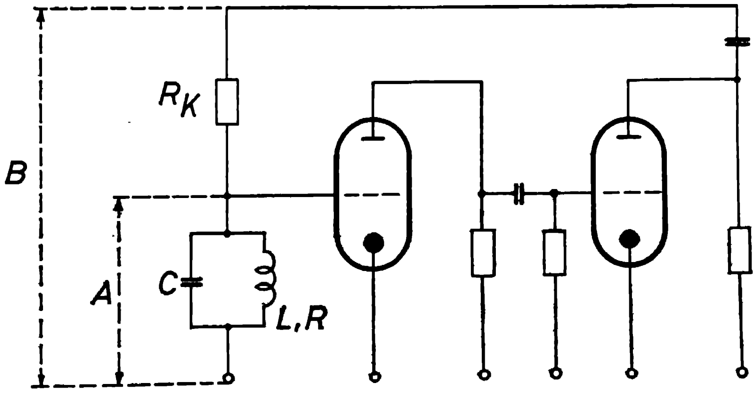

$$K \approx \frac{1}{R_K} \cdot \frac{L}{C \cdot R} \qquad K \cdot V = 1$$

Fig. 10. Basic oscillator circuit used in feedback-controlled impedance, eddy current test method.

inductance of the oscillator circuit and at the same time determines the **feedback factor.** The feedback voltage is fed back to the oscillator through the ohmic resistance R_K. Oscillations are self-excited in the circuit arrangement of Fig. 10 when the feedback requirement

$$KV = 1$$

is fulfilled. Here K is the feedback factor and V is the amplification factor of the oscillator tube circuit. From Fig. 10 the feedback factor K is given by

$$K = A/B$$

For example, if the amplification factor of the oscillator tube circuit is $V = 100$, undamped oscillations are excited as soon as K equals or exceeds 1/100. The **self-excited oscillation** always occurs at the natural frequency of the oscillating circuit, composed of the capacitance C, the resistance R, and the self-inductance L. Since the oscillating circuit always operates at the resonance point, it represents the equivalent of an ohmic resistance of magnitude L/CR. Thus the feedback factor K for the circuit of Fig. 10 is

$$K = A/B = \frac{L/CR}{R_K + (L/CR)} \approx \frac{1}{R_K}(L/CR) \tag{7a}$$

Since R_K is normally much larger in magnitude than L/CR, the latter can be neglected to a first approximation in the denominator of Eq. (7a).

Amplitude of Oscillations. The amplitude A of the self-excited oscillations of the circuit of Fig. 10 increases in a certain range in proportion to the feedback factor K. Thus this amplitude can be approximated by

$$A \propto K \propto (1/R_K C)(L/R) \tag{7b}$$

The factors C and R_K are fixed for a specific test object. Therefore the amplitude of self-excited oscillations for the circuit of Fig. 10 is a function only of the ratio L/R. Consequently it is easily understood that all physical effects of test objects which cause a variation of impedance in which the ratio L/R remains constant cannot be indicated with feedback-controlled, impedance oscillator test methods of the type illustrated in Fig. 10.

Condition for No Test Indication. The amplitude A of the self-excited oscillation remains constant, $(\Delta A/A = 0)$, for a variation of self-inductance ΔL and of resistance ΔR if the following condition is fulfilled:

$$\frac{L + \Delta L}{R + \Delta R} = \frac{L}{R} \tag{8}$$

In other words, if a variation ΔL in the self-inductance L and a variation ΔR in the resistance R occur simultaneously and are such that the ratio $(L + \Delta L)/(R + \Delta R)$ after the impedance variation remains equal to the ratio L/R before the impedance variation, no change occurs in the amplitude of the self-excited oscillation. Consequently no indication of such an effect occurs in the feedback-controlled impedance test method. From Eq. (8) it follows that the condition for no change in indicated amplitude of oscillations also can be written as

$$\Delta L/\Delta R = L/R \qquad \text{for } \Delta A/A = 0 \tag{9}$$

The test coil of the feedback-controlled impedance test method has two functions. The ratio L/R determines the amplitude of oscillations, whereas the factor L alone determines the frequency of the self-excited oscillation. If the self-inductance L

increases by 1 percent, the frequency f, and thus the factor $\omega = 2\pi f$, decrease by ½ percent in accordance with Eq. (1). The result is an increase in the product ωL, or inductive reactance, by ½ percent.

Direction on Impedance Plane for No Test Indication. The condition upon the components of the impedance variation ($\Delta\omega L$ and ΔR), for which the amplitude A of the self-excited oscillations remains constant despite changes in test object properties,

$$\frac{\Delta\omega L}{\Delta R} = \frac{\omega L}{2R} \tag{10}$$

is obtained from Eqs. (1) and (9). Eq. (10) indicates the direction of impedance variations on the complex impedance plane which have no influence upon the amplitude of the self-excited oscillation, and which therefore cannot be indicated with a feedback-controlled, impedance test method.

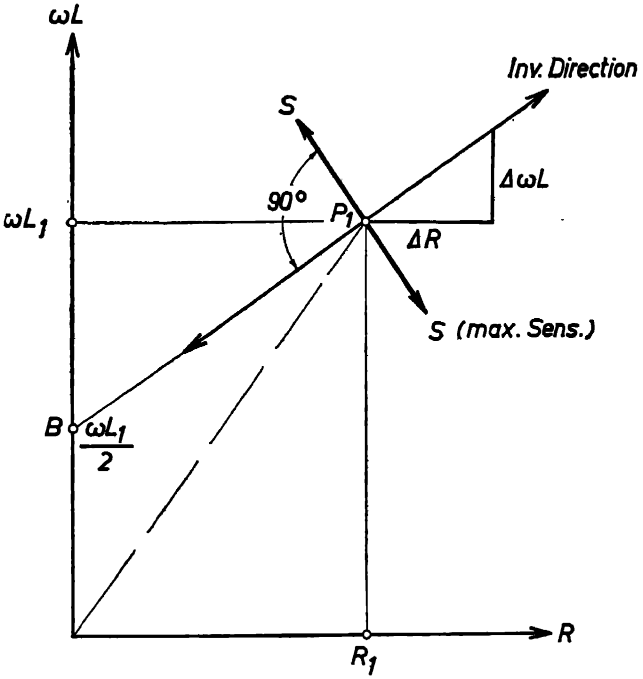

Fig. 11. Impedance plane for feedback-controlled impedance test method. The insensitive direction is parallel to line BP_1. The sensitive direction is parallel to line SS. Test indications result only from impedance variations parallel to the sensitive direction SS.

This impedance variation direction (corresponding to no change in oscillation amplitude) is given on the impedance plane of Fig. 11 by a straight line drawn from the point B ($\omega L_1/2$ on the ordinate axis) to the point P_1 (corresponding to the impedance values ωL and R). An impedance variation $\Delta\omega L$ and ΔR plotted in the direction of line BP_1 fulfills the requirements of Eq. (10). Such an impedance variation causes no change in the oscillation amplitude. Consequently such a change is not indicated by feedback-controlled impedance tests.

Direction on Impedance Plane for Maximum Test Indications. On the other hand, impedance variations in the SS direction on the impedance plane of Fig. 11, normal to the line BP_1, cause a maximum variation in oscillation amplitude. The condition for this direction of **maximum test sensitivity** is obtained from Eq. (10), in accordance with the laws of analytic geometry, as

$$\frac{\Delta\omega L}{\Delta R} = -\frac{2R}{\omega L} \quad \text{for } \Delta A/A = \text{max.} \tag{11}$$

The maximum sensitivity direction SS calculated from Eq. (11) represents the general direction of test measurements. In the case of impedance variations caused by physical effects such as variations in conductivity, permeability, or diameter or crack effects in the test object, the variation in any given direction is split into two components. The component parallel to the direction of line BP_1 in Fig. 11 has no effect upon test indications. Only the component parallel to the sensitive direction SS causes a change in test indications.

RESPONSE CHARACTERISTICS OF THE CYCLOGRAPH.

The effect M measured by the test indications of the Cyclograph in response to a test coil impedance variation of

$$\Delta Z = \sqrt{(\Delta\omega L)^2 + (\Delta R)^2}$$

is given by

$$M_{\text{Cyclograph}} \approx \Delta A/A \approx \left[\sqrt{(\Delta\omega L)^2 + (\Delta R)^2}\right] \cos\phi \tag{12}$$

Here the angle ϕ is the direction between the sensitive direction SS in Fig. 11 [as given by the condition of Eq. (11)] and the direction of the actual impedance variation ΔZ. The manner in which the Cyclograph indicates a variation in conductivity, dimensional, or crack effects in a cylinder, tube, sphere, or sheet at any test frequency is given by Eq. (12) and the theoretical characteristics of the impedance planes given previously. (See section on Eddy Current Cylinder Tests for detailed analysis of impedance-plane response to various test-object characteristics.)

Cyclograph-Reponse Impedance Plane. Fig. 12 shows the impedance plane and the directions of conductivity, diameter, and crack effects for nonferromagnetic materials. The **measurement direction** C of the Cyclograph is plotted as solid lines intersecting the f/f_g curves, in accordance with the conditions of Eq. (11). Only test object effects which have an impedance component in the sensitive measurement direction of the Cyclograph cause an indication, in accordance with Eq. (12). Fig. 12 shows that conductivity and diameter as well as crack effects cause an indication effect because all these effects have a larger or smaller component in the direction of Cyclograph sensitivity. Thus **suppression of the influence of cylinder diameter** is not possible for nonferrous test objects in the Cyclograph indications. On the other hand, Fig. 2, in the section on Eddy Current Cylinder Tests, shows that the direction of diameter changes for ferromagnetic materials can be made perpendicular to the sensitive direction of the Cyclograph by selecting a specific test frequency (a specific ωL value).

RESPONSE CHARACTERISTICS OF THE SEDAC INSTRUMENT.

The Sedac instrument is designed to indicate the **depth of seams and cracks.** With this instrument, a point in the impedance plane can be reached by selecting a suitable test frequency at which the direction of the **undesired "lift-off" effect** is perpendicular to the sensitive S direction on the impedance plane given by Eq. (11). To do this, the test coil data (L, R) and the test frequency are selected

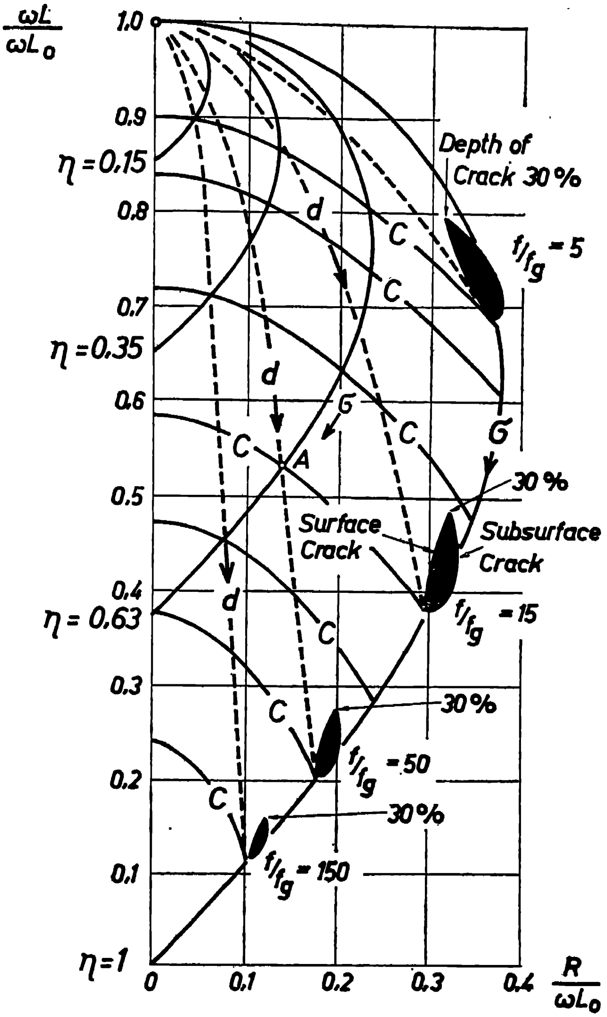

Institut Dr. Foerster

Fig. 12. Impedance plane for feedback-controlled impedance tests showing direction of conductivity σ, diameter d, crack effects (black areas), and test measurement directions C.

so that Eq. (10) applies for the "lift-off" effect. Experience indicates that this condition is met for ferromagnetic materials in the vicinity of 10-kc. test frequencies.

RESPONSE CHARACTERISTICS OF THE ZIJLSTRA INSTRUMENT. Zijlstra[88] uses the feedback-controlled impedance test principle for the detection of cracks in metallic wires, particularly fused-in lead wires through glass envelopes. However, lead wires of tungsten and molybdenum in particular exhibit considerable thickness variations, since their thickness is reduced by means of swaging. It has previously been shown how cracks appear in the impedance plane and how their effects compare with those of thickness variations (see preceding sections on eddy current tests). As theory indicates, thickness variations far outweigh crack effects in their influence upon the L/R ratio in feedback-controlled impedance tests. The **separation of serious cracks** from insignificant variations in dimensions does not seem feasible in theory. Actually, as Zijlstra[88] points out at the end of his paper, this method can also be used to detect changing wire thicknesses. However, at high f/f_g ratios, a diameter increase reacts upon the L/R ratio exactly like a small surface crack, and thus it affects instrument indications.

The Zijlstra instrument operates with a frequency of 5.6 Mc. and is used for wires of 0.7 to 2.5-mm. diam. A test frequency of 5.6 Mc. represents about 400 times the limit frequency for a 1.5-mm. diam. tungsten wire. At this frequency the defect sensitivity is considerably lower than at 10 times the limit frequency.

RESPONSE CHARACTERISTICS OF THE CORNELIUS INSTRUMENT. The Cornelius test instrument[16] (Wickman Co., England) also utilizes the feedback-controlled impedance method. The inventor indicates application fields for the instrument, including measurement of hardness, geometrical dimensions, cracks, thickness of insulating layers, and electrical conductivity. All these effects influence the apparent impedance of the test coil, and thus the amplitude of the self-excited oscillations. However, separation of the various effects in a "one-dimensional" test indication is impossible in principle. Variations in several factors usually occur in practical testing.

SUPPRESSION OF UNDESIRED TEST EFFECTS. With feedback-controlled impedance tests, it is possible to suppress certain undesired effects, such as **dimensional variations** in the test object or the **lift-off effect** of the test coil. To do this, the test frequency is selected so that the requirements of Eq. (10) are met for the small impedance variations caused by an undesired effect. However, the test frequency indicated by Eq. (10) for suppressing undesirable effects need not be identical with the optimum test frequency for the specific test problem. Impedance vector-analysis methods, described next, can usually be better adapted to test problems requiring suppression of such effects.

Cathode-Ray Tube Vector Point Tests

PRINCIPLE OF OPERATION. Variations in physical properties such as the conductivity, permeability, or discontinuities in test objects are represented by specific magnitudes and directions of changes in the apparent test coil impedance. (See preceding sections on eddy current tests for details of these changes.) The **Multitest instrument** permits the impedance plane of the test coil to be represented quantitatively upon the screen of a cathode-ray tube. Impedance values calculated from theory for given test-object conductivities and diameters appear as luminous points on this screen.

Electric Circuit. Fig. 13 shows the block diagram of a Multitest instrument. An oscillator, *1*, feeds two primary windings, P_1 and P_2, of two test coils. Oppositely connected secondary coils, S_1 and S_2, are connected to two **compensators,** *3* and *4*. Compensator *3* serves for compensation of imaginary voltages corresponding to the inductive reactance, ωL, direction on the impedance plane. Compensator *4* compensates the real component of the voltage corresponding to the resistance, R, direction on the impedance plane. These compensators permit the operator to move the **field of view** on the screen of the cathode-ray tube (in the imaginary ωL and the real R directions) to any point on the complex impedance or voltage planes. The result is analogous to moving the field of view of a microscope by operating the mechanical stage which carries the object under inspection.

Compensators *3* and *4* obtain their voltages from the transformers T_1 and T_2 through which the primary magnetizing coil current flows. The amplifier *2* amplifies the compensated signal voltages from the test coils. Its function is analogous to the magnification adjustment of a microscope; at very high amplifications only a very small portion of the impedance plane is represented on the cathode-ray screen.

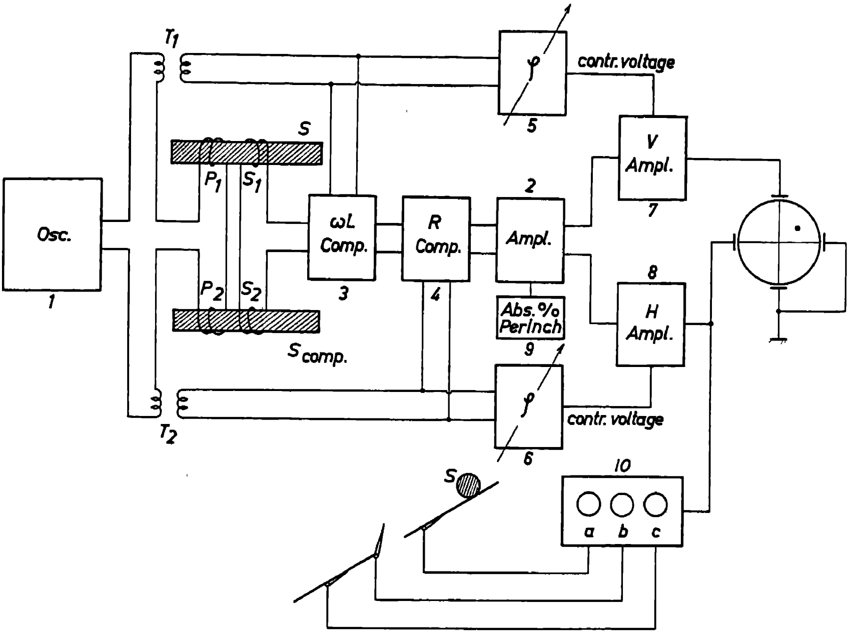

Institut Dr. Foerster

Fig. 13. Wiring diagram of Foerster Multitest instrument with automatic sorting device (American designation: Magnatest FS-200).

Calibration. The amplifier *2* has ten sensitivity steps. The amplification doubles with each higher step, so that the area of the impedance plane shown on the screen is reduced to one-fourth. At the highest step (No. 10), the **impedance plane area** shown on the screen is 10^{-6} of that shown at the lowest sensitivity step (No. 1). Only a very small portion of the impedance plane is shown at the highest step, but here a change of only 10^{-5} in conductivity or diameter effects is readable in the beam deflection. A **calibration ring,** calibrated in terms of percentage of "absolute value," indicates the percentage of the "absolute value" corresponding to 1-in. deflection. This permits quantitative measurements not dependent upon the selection of the test coil, and the comparison of test results from differing test conditions.

Test Indications. The output of amplifier *2* is applied to the horizontal and vertical deflection amplifiers *7* and *8* of the oscilloscope. Amplifier *8* for horizontal deflection is designed to amplify only signal components corresponding to a specific, selected direction in the impedance plane. The vertical deflection amplifier *7* responds to signal components in the direction perpendicular on the impedance plane to the direction selected for the horizontal deflection. (The method is described in this section under Suppression of Undesired Effects.)

Actually, the deflection amplifiers *7* and *8* contain **phase-controlled rectifiers.** The control voltage from a phase-shifter, *5*, controls the response of the vertical deflection amplifier *7*. Similarly the phase-controlled rectifier in the horizontal amplifier *8* obtains its control voltage from phase shifter *6*. The control voltages from these two **phase shifters** are always at 90 deg. from each other. The phase angle of the phase shifters can be controlled arbitrarily without changing their 90-deg. phase displacements from each other.

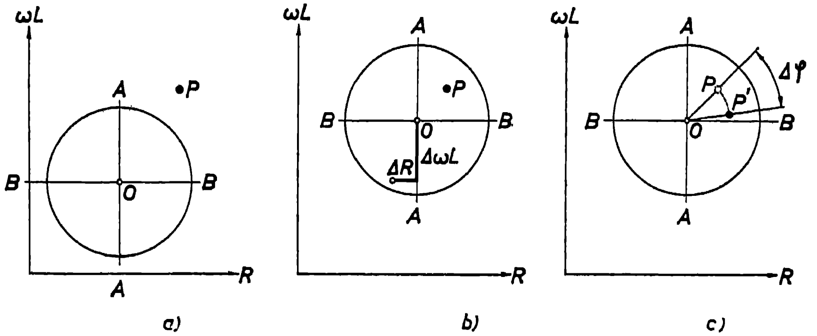

Fig. 14. Impedance plane displays of the vector-point test instrument (Foerster Multitest). (a) Impedance plane showing circular field of view on cathode-ray screen. (b) Displacement of field of view with compensators to bring point P into field of view. (c) Rotation of point P to P' through the angle ϕ by means of phase shifters *5* and *6* in Fig. 13.

Fig. 14(a) shows the impedance plane with the section represented on the cathode-ray screen within the circle. Let O be the center of the screen. This point O can be displaced in the vertical direction by adjusting the ωL compensator *3*. It is displaced horizontally by means of the R compensator *4*. For example, to bring the test point P onto the screen, the ωL compensator is displaced by $\Delta\omega L$ and the R compensator by ΔR, as shown in Fig. 14(b). Adjustment of the phase shifters *5* and *6* moves point P on a circular path through an angle $\Delta\phi$ at constant radius from O. The angle POP' is identical with the phase displacement of the phase shifters. In this way any desired direction on the impedance plane can be selected for representation along the horizontal axis of the oscilloscope.

Sorting. The horizontal deflection voltage controls the automatic sorter *10* (see Fig. 13). **Sorting gates** are opened automatically whenever the horizontal deflection voltage exceeds selected magnitudes (a, b, c, etc.). Since the horizontal deflection voltage direction can be selected at will to correspond with any desired direction in the impedance plane, it is possible to suppress undesired effects, such as diameter variations in sorting for alloy, or conductivity variations when sorting for dimension. To do this, the phase shifters *5* and *6* are displaced so that the direction of undesired effects is perpendicular to the direction of the horizontal-deflection amplifier signals, and such effects are then represented by vertical deflections only. Since the automatic sorter responds only to horizontal deflection signals, the undesired effects are suppressed in the sorting operation.

In sorting tests, a normal and acceptable test object is placed in test coils P_1 and S_1 (see Fig. 13). The resultant secondary coil output voltage is largely compensated by a **compensation specimen,** $S_{\text{comp.}}$, which is then placed in test coils P_2 and S_2. The residual voltage from the differentially connected secondary coils is next compensated (by compensators *3* and *4*) so that the beam rests at the center point O of the cathode-ray screen, with the normal test object in P_1S_1.

If, for example, the test objects are to be sorted for **conductivity variations,** the normal test object in coils P_1S_1 is removed and its diameter varied by filing or grinding (a decrease of 0.5 to 1 percent in diameter is sufficient). The specimen with reduced diameter is again inserted into test coil P_1S_1. The beam of the cathode-ray tube then moves away from the screen center O as a result of the variation in impedance caused by the decrease in diameter. The position of the cathode-ray beam is now adjusted by means of phase shifters *5* and *6* until it rests on the vertical center line through O. The undesired-dimension variation direction now lies perpendicular to the horizontal deflection used for sorting. Consequently the dimensional variations no longer influence the sorting operation. However, the position of the beam, as shown upon the screen, indicates all impedance variations, from whose magnitude and direction the causes can often be determined by impedance-plane analysis. (See preceding sections on eddy current tests.)

APPLICATIONS. The Multitest method, which produces a point indication on the cathode-ray screen for each test object, is especially well suited for testing of **production parts.** Test objects such as spheres, rollers, pins, and other production parts can fall freely through the test coil at very high speeds (four to five small parts per second). The very high **test sensitivity** permits sorting of watch springs weighing only 10^{-3} grams (for ladies' wrist watches) according to the so-called **thermoelastic coefficient.** In some cases, parts must be tested at a specific point, as in hardness tests of the tips of drills or sewing machine needles. For these applications the Multitest instrument test coil is equipped with an electronically controlled stop which holds the test object in the desired position for about 1/100 sec. The sorting gate is then reset by the approach of the next test object. (Additional applications of Multitest methods are described in the section on Eddy Current Test Indications.)

Cathode-Ray Tube Ellipse Tests

PRINCIPLE OF OPERATION. In many respects the equipment for the ellipse test method is similar to that used in the vector point method. As shown in Fig. 15, the test coils, the ωL and R compensators, and the vertical amplifier correspond to the components of the Multitest instrument of Fig. 13. In the ellipse method, however, the amplified voltage from the secondary test coils acts directly upon the vertical deflection plates of the cathode-ray oscilloscope. The voltage applied to the horizontal deflection plates corresponds to the primary magnetizing current in the test coils and is taken from this current through transformer T_2.

Phase Rotation. The phase of the horizontal deflection voltage can be turned to any desired direction on the impedance plane by means of the **phase shifter** *5*. The voltage output of the phase shifter *5* is amplified by the horizontal deflection amplifier 7. The output of this amplifier is applied both to the horizontal plates and to the 90-deg. phase shifter 8. This 90-deg. phase shifter produces the control voltage for the phase-controlled rectifier 9. The output of rectifier 9 indicates only the component of the test-coil signal voltage which is perpendicular on the impedance plane to the voltage direction of the signal applied to the horizontal deflection plates. The signal used for sorting or for marking of defective test objects is also influenced only by this component of the vertical voltage which is perpendicular to the horizontal deflection voltage.

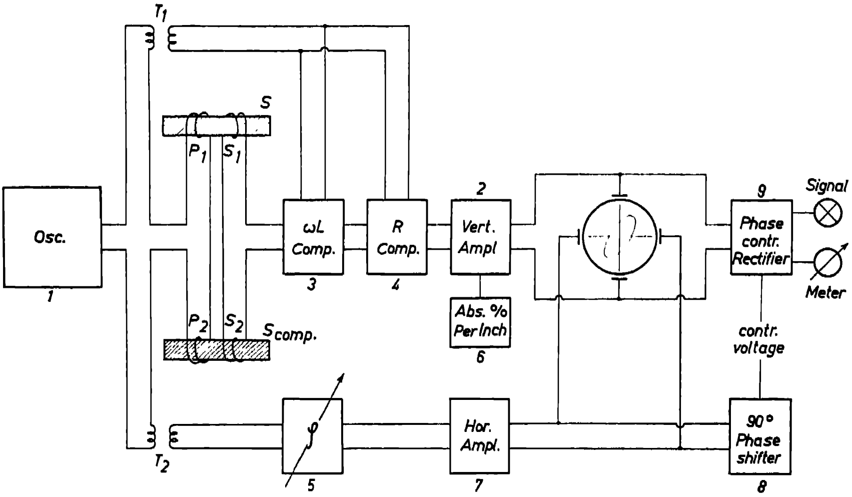

Institut Dr. Foerster

Fig. 15. Wiring diagram for Foerster ellipse method test instrument. Wire Crack Test Instrument (FW-200); Rod Crack Test Instrument (FW-400); Sigmaflux Instrument (FW-300).

Impedance-Plane Analysis of Ellipse Patterns. Various physical effects shown by displacements on the impedance plane (such as variations in dimensions, conductivity, permeability, or crack conditions) are indicated by the shapes of the elliptical patterns on the screen of the cathode-ray oscilloscope. Fig. 16 shows the impedance plane with the **direction of diameter variations** shown by the line *EOC* and the **direction of crack effects** assumed to be *OA*. If the voltage *OC* is applied to the horizontal deflection plates, a horizontal trace of length *COC′* (Fig. 17) appears on the screen as long as no voltage is applied to the vertical deflection plates.

Suppose that the voltage *OE* (Fig. 16), corresponding to an increase in test-object diameter is now applied to the vertical deflection plates. In this case an inclined line such as *E′ OE″* (Fig. 17) appears in the cathode-ray tube display. A straight-line trace results because two voltages having the same phase displacement which are applied simultaneously to the two sets of deflection plates of a cathode-ray oscilloscope always produce a straight-line trace. In this inclined line *E′ OE″*, the horizontal half-amplitude *OC* corresponds to the magnitude of vector *OC* in Fig. 16.

The vertical half-amplitude *OE* in Fig. 17 represents the magnitude of vector *OE* in Fig. 16. However, if a crack effect is present, as represented by vector *OA*

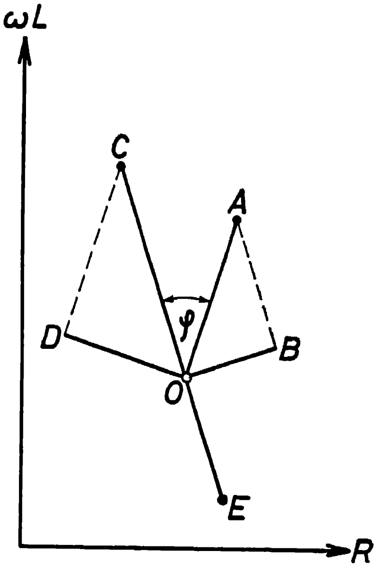

Fig. 16. Impedance plane showing diameter direction *EOC* and crack direction *OA*.

in Fig. 16, the voltages applied to horizontal and vertical deflection plates differ in phase. In this case the cathode-ray tube pattern is an ellipse, as traced in Fig. 17.

The relationships given here are important in analysis of elliptical screen patterns. The vertical half-amplitude *OA* of the ellipse in Fig. 17 corresponds to the magnitude of the vector *OA* resulting from a crack effect in the impedance plane of Fig. 16. If the horizontal deflection reference voltage *COC′* is shorted out by means of a short-circuit button, the distance *OA* appears as a vertical trace on

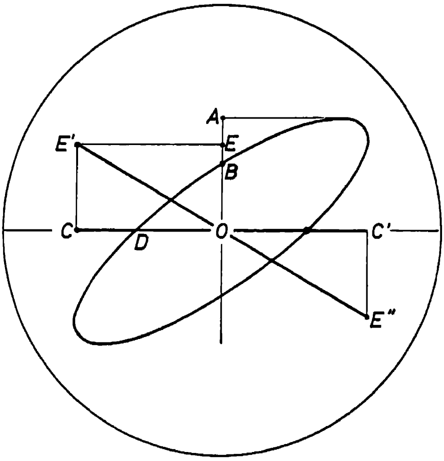

Fig. 17. Analysis of impedance-plane measurement effects from elliptical screen patterns.

the cathode-ray oscilloscope (CRO) screen. The labels on the elliptical display of Fig. 17 are defined as follows:

$OC = b$ = reference voltage in the diameter direction.
$OA = c$ = signal corresponding to a crack effect.
ϕ = phase angle between direction of crack effect and direction of diameter variations (reference voltage) in Fig. 16.
OB = component of crack signal perpendicular to the diameter direction in Fig. 16. $OB = OA \sin \phi$.
OD = component of reference voltage OC perpendicular to direction of crack effect in Fig. 16. $OD = b \sin \phi$.
OE = increase in diameter of test object.

Separation of Crack and Diameter Effects. The important feature of the elliptical pattern is the intersection of the ellipse with the vertical axis (direction OA). The vertical intercept (line OB) or **opening of the ellipse** is proportional to the crack component perpendicular to the diameter direction in the impedance plane of Fig. 16. Diameter effects, as previously noted, cannot cause an opening of the ellipse. If diameter and crack effects appear simultaneously, as is often the case in practical testing, the opening of the ellipse always corresponds to the crack effect, independently of the diameter variations.

The magnitudes of the components of crack effects perpendicular to the diameter direction on the impedance plane have been determined as a function of crack depth and frequency ratio f/f_g. (For example, see Fig. 36, in the section on Eddy Current Cylinder Tests, for curves for the case of nonferromagnetic test cylinders.) These components of the crack effect perpendicular to the diameter direction are represented by the opening OB of the elliptical screen patterns.

SIGMAFLUX EDDY CURRENT TEST INSTRUMENT. Fig. 15 shows the **electrical block diagram** of the Sigmaflux instrument of the Institut Dr. Foerster (American designation: Magnatest FW-300). It is a typical example of the ellipse test method. An oscillator sends an a.-c. magnetizing current through the pair of primary coils P_1 and P_2. The residual secondary voltage, with test objects in the coils, is compensated to zero by means of the **complex compensators** *3* and *4*, is amplified, and then is applied to the vertical deflection plates. These compensators are energized from the primary coil current through transformer T_1. A voltage, which also originates from the magnetizing primary coil current energizing transformer T_2, is applied to the **phase shifter.** The output voltage of this phase shifter *5* is applied, after amplification, to the horizontal deflection plates and also to the input of the 90-deg. phase shifter *8*. The 90-deg. phase shifter provides a control voltage to the **phase-controlled rectifier** *9*.

Meter Indications. If the phase shifter *5* in Fig. 15 is adjusted so that the horizontal deflection voltage corresponds to the diameter direction of the impedance plane of Fig. 16, **diameter variations** appear as inclined straight lines on the cathode-ray tube display (as previously noted). The secondary coil voltage applied to the vertical deflection plates is also applied to the phase-controlled rectifier *9*, which obtains its control voltage from phase shifter *8*. The indicating instrument or meter of the instrument shown in Fig. 15 reads zero in case of diameter variations such as are shown by a straight line on the tube screen. Only signal voltages which have a component in phase with the 90-deg. control signal from phase shifter *8* are amplified by the phase-controlled rectifier *9*. Since this reference voltage is displaced 90 deg. in phase from diameter-direction voltages, diameter effects cannot be amplified by amplifier *9*.

The meter in Fig. 15 shows only components perpendicular to the diameter direction in the impedance plane of Fig. 16; that is, parallel to the vector *OB*. The meter indication thus corresponds to the opening *OB* of the ellipse in Fig. 17. The signal used for **sorting** or **marking defective parts** is likewise influenced only by defects and not by diameter effects.

Sigmaflux Test Equipment. Fig. 18 shows the Sigmaflux instrument widely used in European industry for defect testing, conductivity measurements, sorting of alloys, dimensional testing, and in fully automatic test units. Fig. 19 shows the wide range of **test coil types,** of varying dimensions, used with these ellipse test

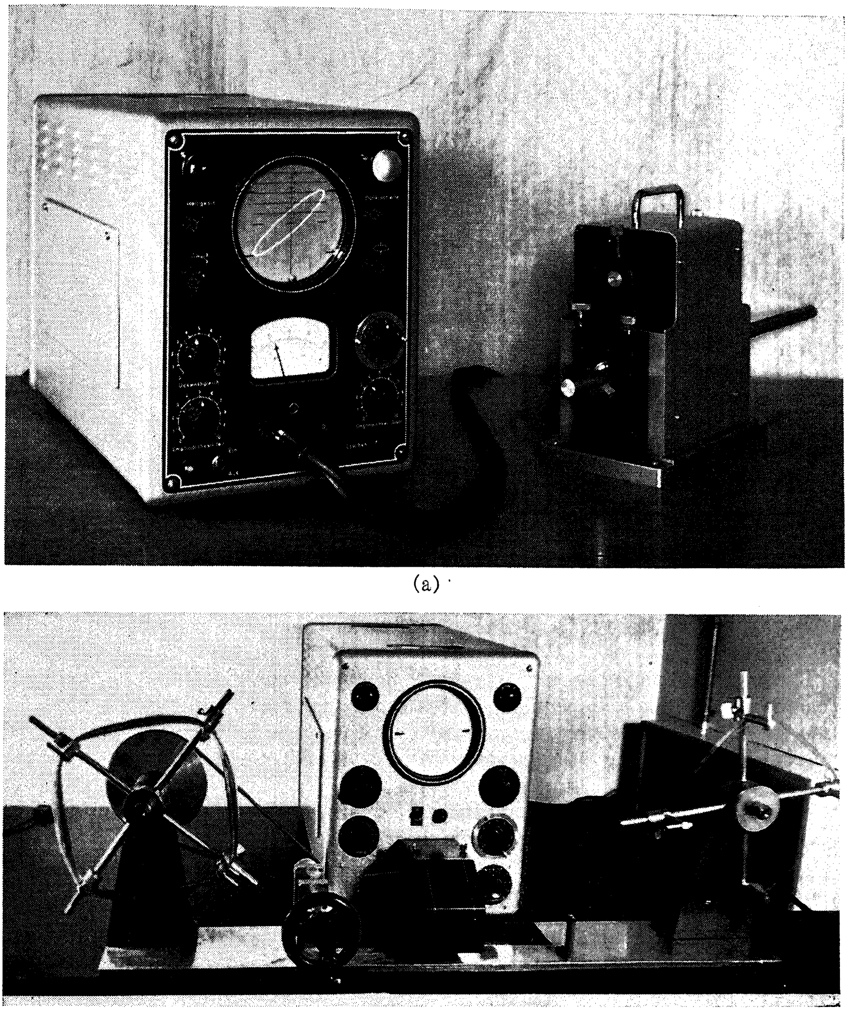

(a)

(b)

Institut Dr. Foerster

Fig. 18. Ellipse test instruments. (a) Sigmaflux eddy current test instrument (American designation: Magnatest FW-300). (b) Foerster wire crack-test instrument (American designation: Magnatest FW-200).

instruments in testing of semi-finished parts in industry. The upper row of coils in Fig. 19 shows complete coil assemblies. The center row shows coil inserts for the self-comparison difference coil method in which one section of the test object is compared electrically with another section of the same test object. The lower row of coils shows the inserts for tests with a separate comparison specimen, the so-called absolute method.

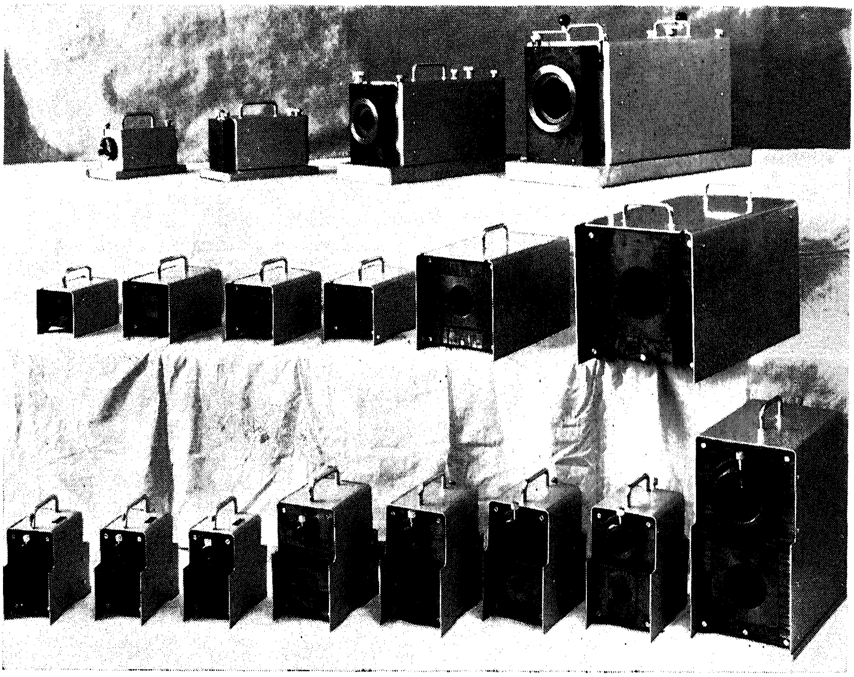

Institut Dr. Foerster

Fig. 19. Test coils for ellipse test instruments.

The **coil holders** shown in the top row in Fig. 19 contain devices which continuously adjust the coil opening to match the diameter of the test parts. In addition these coil holders contain a device consisting of a light source, optics, and microphotocell which assures that the electronic components will be inactive unless the **light beams** are interrupted at both ends of the coil by a test piece extending entirely through the coil. The **coil inserts** are of the plug-in variety which automatically make electrical contact when inserted into the coil holders.

APPLICATIONS OF THE ELLIPSE TEST METHOD. The ellipse test method is used with **feed-through coils** for the following applications:

1. Alloy sorting of semi-finished metallic parts (such as rods, tubes, and wires) by electrical conductivity measurements, as in sorting mixed lots.
2. Hardness sorting of age-hardenable light-metal alloys.
3. Control of the uniformity of hardening of semi-finished parts quenched immediately after extruding.
4. Testing of rods, tubes, and wires for surface and subsurface cracks.
5. Measurement of the diameter of rods, tubes, and wires without direct contact and independent of test-object material.

The **diameter range** of the ellipse test method extends from 0.41 to 100 mm. Since the conductivity range of most test parts lies between the approximate limits of 1 and 60 meters per ohm-mm.^{2}, the corresponding range of limit frequencies extends from $f_g = 1$ to $f_g = 3 \times 10^6$. For testing of small or very short discontinuities in test parts, a time selection circuit can be used to indicate only rapid variations and to suppress **slowly varying effects.** Commercial forms of ellipse test instruments include a wire crack-test unit, a rod crack-test unit, and the Sigmaflux instrument (American designations are the Magnatest FW-200, 400, and 300, respectively).

Linear Time-Base Tests

PRINCIPLE OF OPERATION. In the cathode-ray tube vector-point and ellipse test methods described previously, only the fundamental frequency of the a.-c. magnetization was used to produce test indications. This fundamental frequency appears alone in the output signal from the test coils in tests of materials whose relative magnetic permeability is a constant, independent of the field strength of the test coil. However, in **ferromagnetic test-object materials,** the relative magnetic permeability $\mu_{\text{rel.}}$ is more or less a function of the magnetizing field strength. (For example, see Fig. 19 in the section on Eddy Current Tube Tests.) The nonlinear magnetization curve of ferromagnetic materials causes odd **harmonic frequencies,** such as the third, fifth, and seventh harmonics of the fundamental frequency, to appear in the output voltage of the secondary test coils. Even harmonics appear only if a direct-current (d.-c.) field reacts upon the test object in addition to the alternating-current (a.-c.) field, or if the test object exhibits a preferential direction of magnetization as a consequence of a previous d.-c. magnetization. By contrast, the linear time-base eddy current test method is especially well suited for the analysis of mixtures of fundamental and harmonic frequencies in test signals. In this method the harmonic frequencies play an important role in the interpretation of the test indications. (Examples of applications of this test method are given in the section on Eddy Current Test Indications.)

Circuit Analysis. Fig. 20 shows the block electrical diagram for a linear time-base eddy current test instrument (the Foerster Magnatest Q instrument; Amer-

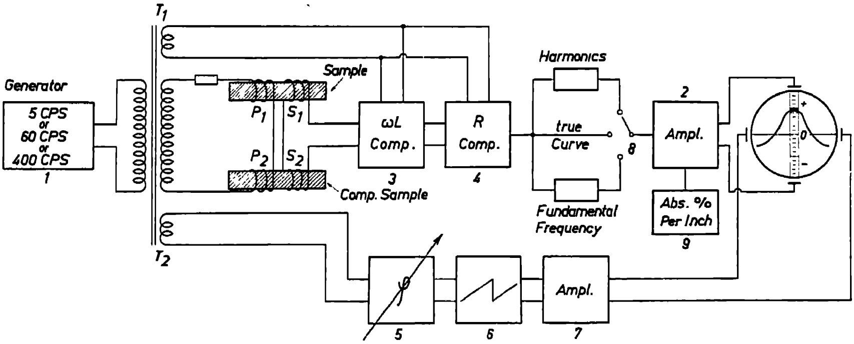

Institut Dr. Foerster

Fig. 20. **Wiring diagram of linear time-base test instrument.** (Foerster Magnatest Q; American designation, Magnatest FS-300.)

ican designation, Magnatest FS-300). The two primary coils, P_1 and P_2, are energized from an adjustable current regulator having sinusoidal output frequencies of 5, 60, or 400 c.p.s. The residual voltages from the differentially connected secondary coils of the comparison coil system are compensated to zero for normal test specimens by means of the **complex compensators** *3* and *4*. The operating voltages for these complex compensators are obtained from the magnetizing field-current regulator through transformer T_1.

The voltage which results from a variation in the conductivity, permeability, dimensions, or discontinuities of an unknown test object in test coils P_1S_1 is amplified in amplifier *2* and applied to the vertical deflection plates of a cathode-ray oscilloscope. Another voltage from the magnetizing field-current regulator is applied through transformer T_2 to the **phase shifter** *5*. By adjusting this phase shifter, this voltage can be turned to any desired direction in the impedance plane. The sinusoidal output voltage of the phase shifter is next converted into a saw-tooth wave form by the saw-tooth generator *6*. This voltage, after amplification in amplifier *7*, is applied to the horizontal deflection plates of the oscilloscope to provide a linear, **horizontal sweep signal.** When a signal is applied from the secondary test coils to the vertical deflection plates, a sinusoidal curve (which can contain harmonics) appears on the screen. This curve can be displaced horizontally to any desired position by means of the phase shifter *5*. The interesting portion of the curve can be moved to the center of the screen, where a **reading slit** is located, for quantitative evaluation.

Calibration. The signal amplifier *2* is provided with a calibration control which indicates, for any given sensitivity step, the percentage of the "absolute value" corresponding to 1-in. beam deflection. The **absolute value** is defined as the voltage effect produced by the test object in the absence of a compensating test object in the comparison test coil. This sensitivity indication is independent of both the selection of the test coil type and of the particular test object employed. This indication of the absolute value for each sensitivity step on the Magnatest Q instrument is especially significant in **quantitative interpretation** of test indications.

Test indications corresponding to the depth of case-hardened layers, mechanical hardness, carbon content, edge decarburization, or other factors can be given in terms of the percentage of absolute value. This percentage is independent of the specific instrument, test coil, and test object involved. Consequently test indications, obtained in different plants at various times on test objects of differing dimensions and in various sizes of test coils, can be compared with each other. (Examples of quantitative evaluation of test indications are presented in the section on Eddy Current Test Indications.)

Slit Analysis Technique. The switch *8* (Fig. 20) in the test coil signal circuit permits application to the vertical deflection plates of one of three **signals:**

1. The true secondary coil voltage signal.
2. The fundamental frequency only of the signal voltage.
3. The odd harmonics of the signal voltage.

The choice depends upon the nature of the testing problem. A choice also exists in selection of the **test frequency** between 5, 60, and 400 c.p.s. The 5-c.p.s. frequency increases the applicability of the method considerably because of the greater penetration depth of eddy currents at this low frequency. (Applications of each frequency and signal selection are discussed in the section on Eddy Current Test Indications.)

A **slit** is provided in the center of the cathode-ray tube screen for quantitative analysis of signal wave forms. The interesting portion of the signal wave form can be moved to the slit by means of the **phase shifter.** Fig. 21 shows the CRO screen with a sinusoidal signal of amplitude *OA* selected in phase with the voltage from the phase shifter (solid curve). Here the amplitude *OA* corresponds to the vector *OA* on the impedance plane of Fig. 22, corresponding to a measurement effect. The instantaneous value of this signal voltage at the vertical center slit is zero. Now, if a measurement effect perpendicular to the base direction *OA* appears on the impedance plane (for example, vector *OB*), the wave form displayed on the CRO screen corresponds to the dashed curve in Fig. 21. Its amplitude at the slit is *OB* and is designated as the slit value *M*. In general,

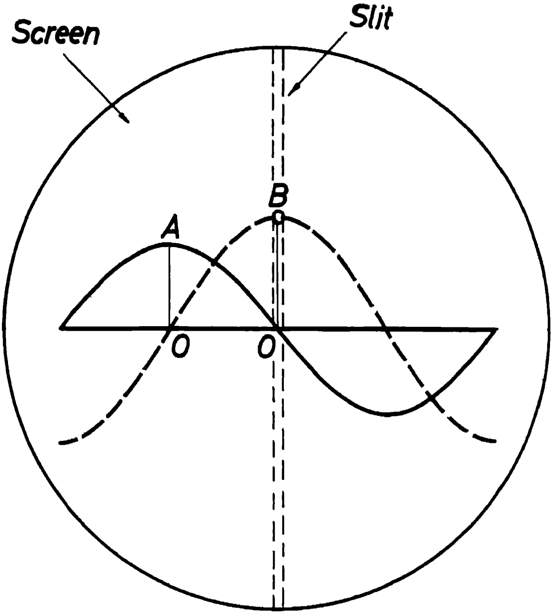

Fig. 21. Screen image of linear time-base test instrument, with sinusoidal signals.

$$M = A \sin \phi \tag{13}$$

where *A* is the amplitude of the measurement effect and ϕ is the angle between the measurement effect and the base voltage on the impedance plane (Fig. 22).

The **linear horizontal sweep** of the oscilloscope is synchronized with the base voltage or output of the phase shifter. The beam starts from the left side of the screen at the zero point ($\phi = 0$) of the base voltage and travels linearly to the right side during one cycle ($\phi = 360°$), retraces rapidly, and repeats this sweep procedure. The **slit value** *M* therefore indicates the component of a given measurement effect which is perpendicular to the direction of the base voltage on the impedance plane. Thus the slit value *M* is identical to the opening of the ellipse in the elliptical presentation (see Fig. 17).

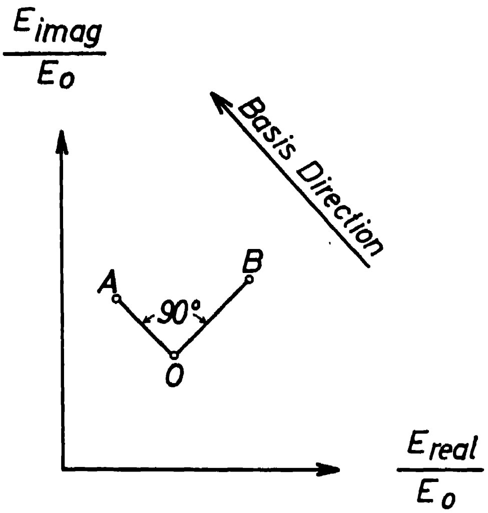

Fig. 22. Section of complex voltage plane showing vector voltages *OA* and *OB* of Fig. 21.

Impedance-Plane Analysis of Slit Values. The complex voltage plane for a ferromagnetic test cylinder is shown in Fig. 23. This diagram differs from preceding impedance-plane illustrations where points along the curves were identified in terms of the frequency ratio f/f_g, defined by

$$f/f_g = \frac{f\sigma\mu_{rel.}d^2}{5066}$$

Here, the curves are labeled for the specific test frequency of 5 c.p.s. in terms of the product $\sigma\mu_{rel.}d^2$, where

σ = electrical conductivity of test material in meter/ohm-mm.^{2}.
$\mu_{rel.}$ = relative magnetic permeability (usually between 10 and 500 for ferromagnetic materials used in industry).
d = diameter of cylindrical test object, cm.

Fig. 23 shows curves for two values of relative permeability, $\mu_{rel.} = 50$ and $\mu_{rel.} = 100$.

The directions of **variations in relative permeability** and in **diameter** coincide (as indicated in Fig. 2 in section on Eddy Current Cylinder Tests). **Variations in conductivity** occur along the heavy curves for various $\mu_{rel.}$ values. The **effects of surface cracks** of 30 percent depth are shown by arrows at four points where the product $\sigma\mu_{rel.}d^2$ assumes the values of 5,000, 15,000, 50,000, and 150,000.

Sample Calculations for Iron Rod. Assume that an iron rod has the following characteristics:

Electrical conductivity, $\sigma = 10$ meter/ohm-mm.^{2}.
Relative permeability, $\mu_{rel.} = 100$.
Diameter, $d = 2$ cm.

In this case, the product

$$\sigma\mu_{rel.}d^2 = 4000$$

Assuming that the test cylinder fills the test coil, the coil fill factor $\eta = 1$. The test point is shown at C on the outer curve of Fig. 23. Here the normalized imaginary component of the test coil voltage $E_{\text{imag.}}/E_0 = 77.4$, the ordinate of point C. E_0 is the secondary test coil voltage in the absence of a test object. Thus, inserting the ferromagnetic cylinder into the test coil increases the imaginary component of its output voltage by 77.4 times the signal voltage available with the coil empty. The real component (abscissa) of point C is $E_{\text{real}}/E_0 = 34.5$.

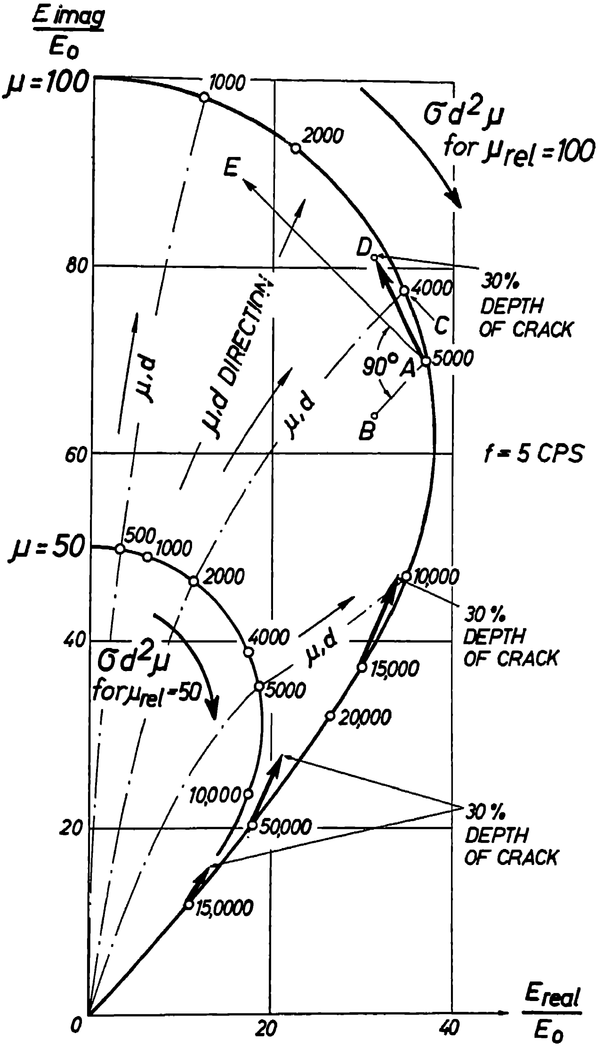

Institut Dr. Foerster

Fig. 23. Complex voltage plane of test coil, containing a ferromagnetic test cylinder, for a fixed test frequency of 5 c.p.s. Values of product ($\sigma\mu_{\text{rel}}.d^2$) shown on curves. Coil fill factor $\eta = 1$.

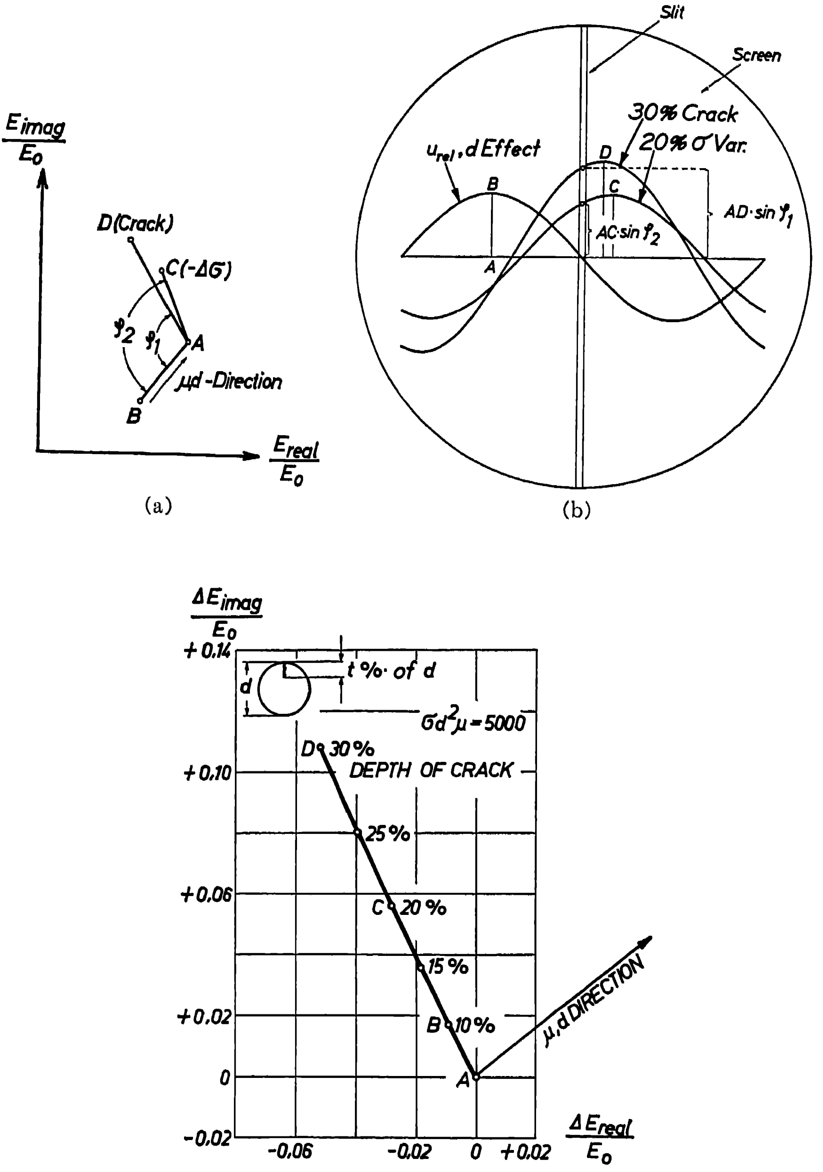

(a) (b)

(c)

Institut Dr. Foerster

Fig. 24. Analysis of Magnatest Q screen patterns and impedance plane characteristics. (a) Enlargement of area around point *A* in complex voltage plane of Fig. 23, showing directions of diameter and permeability variations (vector *AB*), crack effects (vector *AD*), and conductivity effects (vector *AC*). (b) Screen indications corresponding to vector effects of Fig. 24(a) for Foerster Magnatest Q instrument. (c) Enlarged portion of the impedance plane of Fig. 23, showing crack effects along line *AD* and direction of diameter and permeability variations.

Suppose now that the phase direction *AB* (corresponding to variations of permeability or diameter) is selected for the **base voltage** to which the horizontal sweep of the instrument is synchronized. In this case all variations in diameter or magnetic permeability which appear in the signal voltage on the CRO screen have no influence upon the signal at the slit. Hence the wave form passes through zero at the slit, and the **slit value** *M* equals zero.

If, however, a physical effect such as a **variation in carbon content** of the iron rod causes its electrical conductivity to increase from $\sigma = 10$ to $\sigma = 12.5$, the test point moves from point *C* (where the product $\sigma\mu_{\text{rel.}}d^2 = 4000$) to point *A* (where the product $\sigma\mu_{\text{rel.}}d^2 = 5000$). The direction of vector *CA* in Fig. 23 lies almost perpendicular to the direction of diameter and permeability changes. Thus the conductivity variation is indicated sensitively by the slit method, with relatively little interference from variations in diameter or permeability. The vector *AD*, corresponding to the effect of a crack of 30 percent depth, also has a large component in the direction *AE*, perpendicular to the base voltage. Thus **crack effects and conductivity variations** are indicated similarly and cannot be separated effectively under this test condition.

CRACK DEPTH ANALYSIS. In the complex voltage plane of Fig. 24(a), various physical effects for the test object (ferromagnetic cylinder), including

1. The diameter and permeability effect (vector *AB*),
2. The conductivity effect (vector *AC*), and
3. The crack effect (vector *AD*) for a 30 percent depth of crack

are replotted from Fig. 23. These vectors are transferred to the **Magnatest Q screen pattern** in Fig. 24(b). An amplification factor of unity has been selected in the transfer from Fig. 24(a) to Fig. 24(b) so that the distance *AB* on the screen pattern is equal to the distance *AB* on the complex voltage plane. Fig. 24(c) shows an enlargement of a portion of the complex voltage plane for the case in which the product $\sigma\mu_{\text{rel.}}d^2 = 5000$. **Crack effects** are shown along the line *AD*. Distance *AB* corresponds to a 10 percent crack depth, *AC* to a 20 percent crack depth, and so on, according to the crack depth scale plotted along line *AD*. The direction of diameter and permeability effects is also indicated.

Self-Comparison Crack Depth Tests. In the Magnatest Q method described earlier, the voltage of the test coil containing the unknown test object is always compensated (approximately to zero) by means of the compensation coil containing the reference-standard test object. However, the Magnatest D method utilizes the **technique of self-comparison** in which one portion of the test rod is electrically compared with another portion of the same test rod. [See Fig. 12(f) in the section on Eddy Current Cylinder Tests for an illustration of this arrangement.] Fig. 25(a) shows a test rod with a crack which increases in depth from 0 to 30 percent of the rod diameter, passing through a pair of differentially connected secondary test coils, S_1 and S_2. If coils S_1 and S_2 are both over **defect-free portions** of the test rod, the net secondary voltage equals zero. However, if a crack of 10 percent depth [point *B* in Fig. 25(a)] moves into coil S_1 while the portion of the rod within coil S_1 is still free from defects, a signal voltage appears across the terminals of the secondary coils. This voltage corresponds to the vector *AB* in Fig. 24(c) . The corresponding test indication is shown as *AB* in Fig. 25(b). As the rod progresses through the coils, the secondary coil S_1 will contain the point *B* (of 10 percent crack depth) when coil S_2 contains point *C* (of 20 percent crack depth). At this instant the difference voltage is given by the vector *BC* in

Fig. 24(c) and indicated as *BC* in Fig. 25(b). As the rod proceeds until the **uniform crack depth** of 30 percent lies within both test coils, no difference voltage appears at the terminals of the test coils, and the indication returns to zero, as shown in Fig. 25(b).

Thus the difference test method indicates only the **variations in crack depth.** Therefore a crack having a constant depth cannot be indicated. However, **shallow cracks** normally vary continuously in their depth; they usually begin and end several times over the entire length of a rod. Only in the case of **stress cracks** or of a seam-welded tube which has completely burst open along the seam will the defect progress through the entire length at a constant depth.

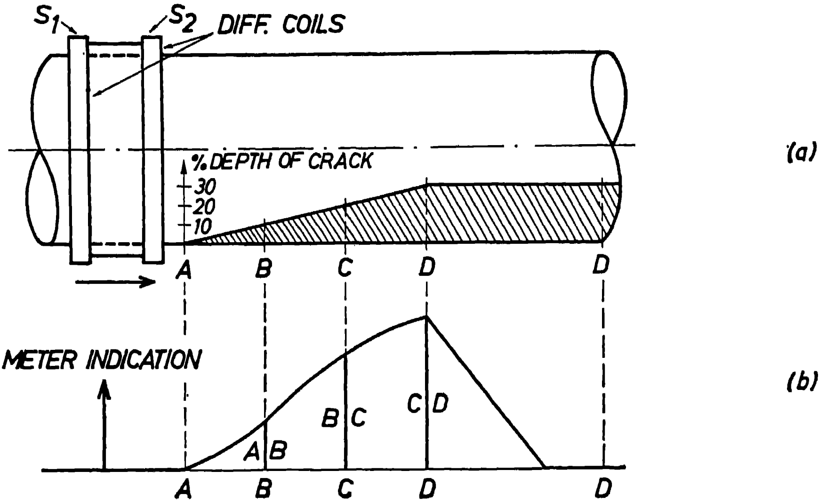

Fig. 25. Response of difference-coil test method to surface cracks in cylindrical test objects. (a) Metallic rod with surface crack depth increasing from 0 to 30 percent of diameter. (b) Test indication or "slit value *M*" on cathode-ray screen as crack passes test coils.

Combined Absolute and Comparison Tests. The crack test method, using difference coils for self-comparison on the same test specimen, can be combined with the "absolute method," in which the unknown test rod is compared with a reference standard rod. With this combination, **cracks of constant depth** can also be indicated, since small quality variations in alloy, lot, heat treatment, and so on, from rod to rod are outweighed by the effects of deep cracks. However, for detection of **fine cracks,** it is necessary to use only the difference method (Magnatest D), in which one point of the rod is compared electrically with another point of the same rod. This follows because variations in physical constants can be considerably greater than the effects caused by fine cracks.

Secondary Coil Voltage Signals. The magnitude of the coil voltage M, appearing at the slit in the cathode-ray screen in **response to a crack,** is

$$M = E_0 \eta \mu_{\text{rel.}} (\Delta \mu_{\text{eff.}}) \sin \phi \tag{14}$$

where E_0 = voltage of a single secondary coil in the absence of a test object.
η = coil fill factor = $(d/D)^2$.
d = diameter of test cylinder.
D = diameter of test coil.
$\mu_{rel.}$ = relative magnetic permeability of test-object material.
$\Delta\mu_{eff.}$ = variation in effective permeability caused by the crack (see distance AD in Fig. 23).
ϕ = phase angle between direction of diameter and permeability variations, and direction of crack effects, on the complex voltage plane [see Fig. 24(a)].

In the difference test method, $\Delta\mu_{eff.}$ corresponds to the difference voltage of the two secondary coils resulting from the crack effects (see Fig. 25).

Selection of Test Frequency. Fig. 23 shows that the angle between the direction of permeability and diameter effects and the direction of crack effects decreases as the product $\sigma\mu_{rel.}d^2$ becomes larger. Thus the possibility of **separating serious crack effects** from insignificant dimensional and permeability effects is diminished at higher frequency ratios f/f_g. Consequently, lower test frequencies would be preferred for this application. Fig. 23, of course, refers to the funda-

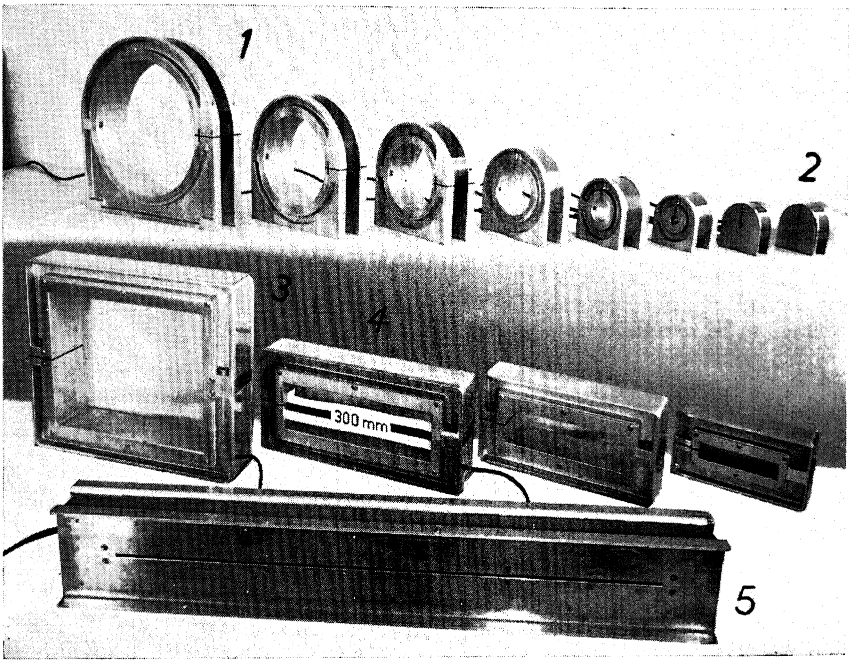

Institut Dr. Foerster

Coil 1 = 300-mm. diam.
Coil 2 = 1-mm. diam.
Coil 3 = square cross-section, 400 × 400 mm.
Coil 4 = rectangular cross-section, 300 × 100 mm.
Coil 5 = rectangular cross-section for sheet metal, 6 × 1100 mm.

Fig. 26. Test coils for Foerster Magnatest Q instruments (American designation, Magnatest FS-300).

mental test frequency. The influence of test-object properties upon harmonic frequencies is described in the literature.[42]

APPLICATIONS. Fig. 26, showing **test coils** for Magnatest Q instruments, illustrates the wide range of test-object dimensions tested with this instrument in European industry. The **diameter range of the test coils** extends from 1 to 400 mm. Coils with rectangular cross-sections are used for **steel blocks** and similar test objects. Entire **metal sheets** are tested with the large slit coils. The Magnatest Q instrument is the magnetic-quality test instrument most widely used in European steel industry. The practical application as well as the interpretation of the test results obtained with this instrument will be discussed in the section on Eddy Current Test Indications.

Suppression of Undesired Effects

SIGNIFICANCE OF UNDESIRED EFFECTS IN TEST INDICATIONS. In the practical test instruments developed during the past 20 years, various methods, as appropriate to specific test problems, are used for the suppression of undesired effects.[23, 44, 45] The basic theory for nondestructive testing with eddy current methods has shown that it is essential to suppress undesired effects in test indications. For example, dimensional effects and "lift-off" effects are frequently considerably greater in magnitude than desired effects, such as crack effects and conductivity effects. Two methods which will now be described are the phase-controlled rectifier and a resonance test system.

PHASE-CONTROLLED RECTIFIER METHOD. The Multitest instrument of Fig. 13 and the Sigmaflux instrument of Fig. 15 employ an arrangement which is termed a "phase-controlled rectifier." This system indicates only those components of the test coil voltage which have the same phase direction as the so-called **control voltage.**

Fig. 27 shows a simple **design** of the phase-controlled rectifier. The resistors R_1 through R_4, together with the rectifiers r_1 and r_2, form a bridge circuit. The voltage to be measured, E_M, is applied to one diagonal of the bridge, while the control voltage $E_{\text{contr.}}$ is applied to the other bridge diagonal. The control voltage,

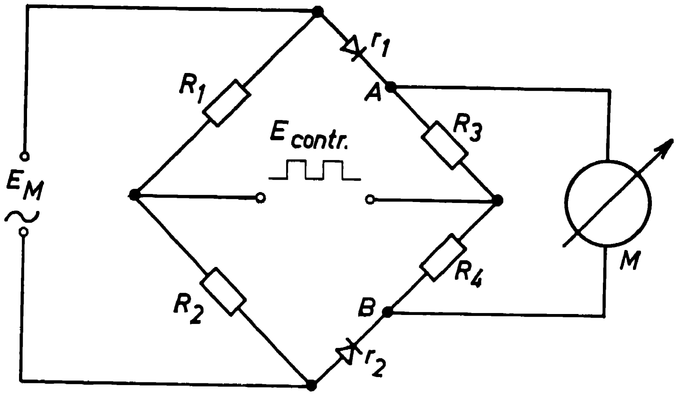

Institut Dr. Foerster

Fig. 27. Basic circuitry of the phase-controlled rectifier. E_M = measurement voltage. $E_{\text{contr.}}$ = control voltage.

assumed to be of **rectangular wave shape,** causes a current $I_{\text{contr.}}$ to flow through the two **rectifiers** r_1 and r_2 during those half-cycles when the control voltage is in the forward direction of the rectifier. In the other half-cycle, the two rectifiers r_1 and r_2 do not conduct, since the voltage $E_{\text{contr.}}$ is in the reverse direction of the rectifier. However, the current $I_{\text{contr.}}$ does not result in a deflection of the meter M, since in the absence of a measurement voltage, points A and B exhibit the same potential because of the symmetrical bridge circuit. Thus the control voltage turns the two rectifiers r_1 and r_2 into two switches. They are "closed" when the current $I_{\text{contr.}}$ flows in the forward direction of the rectifier. They are "open," i.e., they block the current, when the control voltage is in the reverse direction of the rectifier.

In-Phase Operation. Therefore, the measurement voltage E_M is applied to the meter M only during the **positive half-cycle,** while the control voltage operates in the forward direction of the rectifier. When the control voltage is in-phase with the measurement voltage, the results shown in Fig. 28(a) are obtained. From point F to G, i.e., during a half-cycle, the measurement voltage of amplitude A is applied to the instrument. During the next half-cycle, the measurement voltage at the instrument is turned off, as discussed previously. Thus, during the entire cycle FH, the **average current** passing through the instrument corresponds to the vertically shaded area over FG. This operation is repeated during the next cycle.

Out-of-Phase Operation. Fig. 28(b) shows the conditions with a **phase displacement** of 90 deg. between measurement and control voltage. The measurement voltage at the meter is now between the points L and M, so that the current through the meter corresponds to the shaded area between L and M. However, the meter M is a direct-current instrument which averages the positive and negative portions of the wave form. The **mean current value** in Fig. 28(b) equals zero because of the equally great positive and negative currents. With a phase displacement of 90 deg. between the measurement and control voltage, the control voltage is suppressed in the indication of the meter. The **deflection of the meter** M for the in-phase condition corresponds to the mean value HB plotted in Fig. 28(a), since the area under the sine curve from F to G is equal to the area $(FH) \times (HB)$.

Operation at Intermediate Phase Angles. With a general phase displacement of angle ϕ between control and measurement voltage, the **mean current value** through the meter is

$$I_M = \left(\frac{E_{M(\text{max.})}}{R}\right)\left(\frac{1}{\pi}\right)\cos\phi \tag{15}$$

Here $E_{M(\text{max.})}$ is the maximum amplitude of the measurement voltage and R is the resistance of the meter plus that of the rectifier in the forward direction.

Suppression of Undesired Signals. An undesired effect can be suppressed if one selects a **control voltage** which is perpendicular to the direction of this undesired effect in the impedance plane or complex voltage plane. All other effects which are not in the direction of the undesired effect are indicated according to their components in the direction of the control voltage; i.e., according to their components perpendicular to the direction of the undesired effect.

The influence of various effects such as conductivity, diameter, permeability, or crack effects on the impedance or complex voltage plane of the test coils has been described in the preceding sections on eddy current tests. From these discussions, one can see easily which effects can be separated from each other in the indication. For a metallic test rod in **alloy sorting,** for example, one selects the control voltage perpendicular to the diameter direction. On the contrary, to register the **dimensions of wires,** independent of the material, the control voltage is selected perpendicular to the conductivity direction. An eddy current instrument with two phase-controlled rectifiers (the so-called **σ-D instrument**) has been developed to measure the variation of the specific electrical conductivity and the diameter, independently of each other. It can be used, for example, during tensile tests on metal rods.

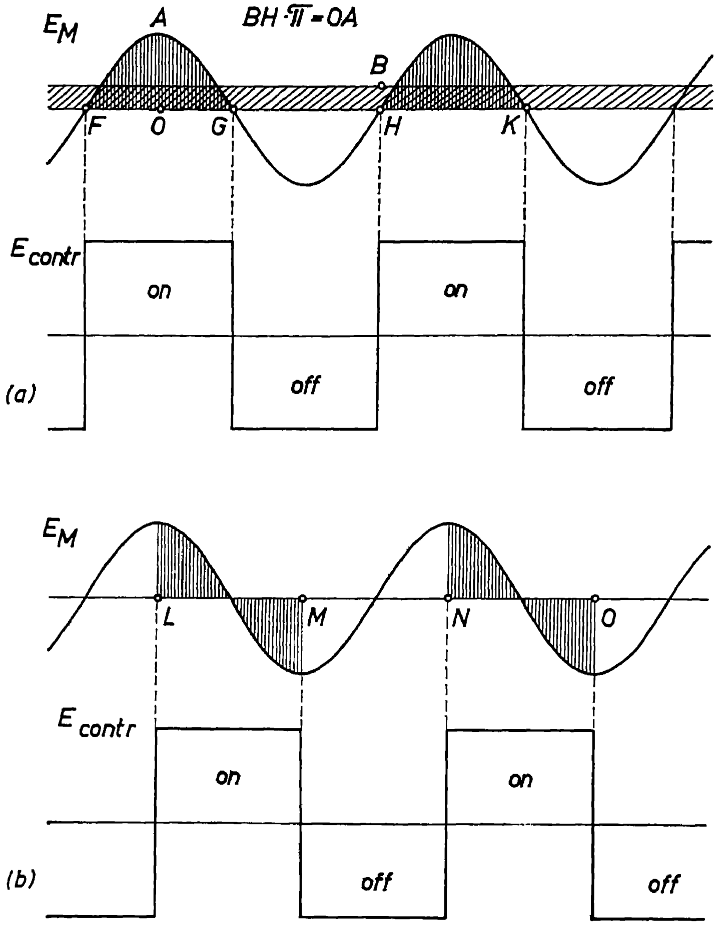

Fig. 28. Analysis of operation of phase-controlled rectifier. (a) Measurement voltage E_M and control voltage $E_{contr.}$ are in phase. Current flowing from the phase-controlled rectifier through the instrument M corresponds to the area under the sine wave from F to G. The height HB is the arithmetic average value. (b) A 90-deg. phase displacement between the control voltage and E_M. The average value of the area from L to M equals zero; i.e., there is no meter indication.

Suppression of Undesired Harmonics. In Fig. 28 the effective duration of the control voltage *FG* or *LM* was assumed to be 180 deg.; i.e., a half-cycle. There are several problems in **testing of ferromagnetic materials** in which it is possible to suppress specific undesired effects, which appear in the harmonic frequencies, by selecting an effective duration of the control voltage which is less than a half-period (180 deg.). Fig. 29(a) shows a **distorted voltage,** observed frequently in induction testing of ferromagnetic objects, which consists of a fundamental and a third harmonic frequency. Fig. 29(b) shows the fundamental frequency and the third harmonic plotted separately by Fourier analysis.

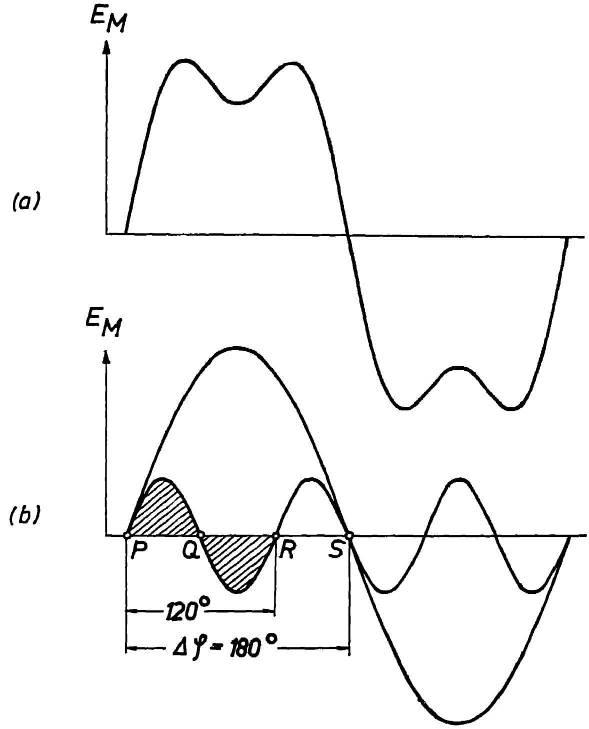

Fig. 29. Analysis of harmonics in signal voltage. (a) Composite wave consisting of the fundamental frequency and third harmonic, appearing in the testing of ferromagnetic materials. (b) Fundamental frequency and third harmonic separated by Fourier analysis.

If the control voltage in the circuit of Fig. 27 acts from point *P* to *S*, the **fundamental frequency** is reproduced. In the third harmonic, the area extends above *PQ* and below *QR*, so that only the area above *RS* (i.e., one-third of the entire effect) is reproduced. Generally, the phase-controlled rectifier circuit responds to the *n*th harmonic with $1/n$ of the amplitude, as long as the effective width of the control voltage is exactly a half-cycle (180 deg.) of the fundamental frequency.

By selecting a different effective width for the control voltage, one can entirely **suppress undesired harmonics** in the indication of the phase-controlled rectifier. For example, if one selects not 180 deg. but 120 deg. as the effective width of control voltage corresponding to the distance *PR* in Fig. 29(b), a full cycle of the third harmonic always lies in this effective range. Thus, with an effective control voltage interval of 120 deg., the positive and negative areas of the third harmonic always cancel each other in the indication. In this case the third harmonic is suppressed entirely, independent of the phase position of the control voltage.

Condition for Suppression of *n*th Harmonic. In general, the nth harmonic is suppressed in the indication of the phase-controlled rectifier if the effective width $\Delta\phi$ of the control voltage is selected from the following values:

$$\Delta\phi = \frac{360°}{n}(m) \tag{16}$$

$$m = 1, 2, 3 \cdots \left(\frac{n-1}{2}\right)$$

For example, to suppress the seventh harmonic ($n = 7$), Eq. (16) indicates the value of the effective width $\Delta\phi$ of the control voltage as $\Delta\phi = (360/7)(1)$, $(360/7)(2)$, and $(360/7)(3)$. For an effective width $\Delta\phi$ of the control voltage, the current at the fundamental frequency is

$$I_M = \left(\frac{E_{M(\text{max.})}}{R}\right)\left(\frac{1}{\pi}\right)(\cos\phi)\left(\sin\frac{\Delta\phi}{2}\right) \tag{17}$$

Here ϕ is the angle between the measurement voltage and the control voltage, and $\Delta\phi$ is the effective width of the control voltage. Inserting 180 deg. for $\Delta\phi$ in Eq. (17) results in Eq. (15). In general, Eq. (17) permits

1. The suppression of specific undesired effects in the impedance plane by the selection of the phase angle ϕ of the control voltage.
2. In addition, for materials whose permeabilities depend upon magnetizing field strengths, the suppression of specific harmonics by the selection of the effective width $\Delta\phi$.

RESONANT CIRCUIT IMPEDANCE VARIATION TEST. Another method, developed in 1947,[30] permits complete suppression of an undesired factor in the impedance plane; for example, the "lift-off" effect at coil distances from zero to infinity.

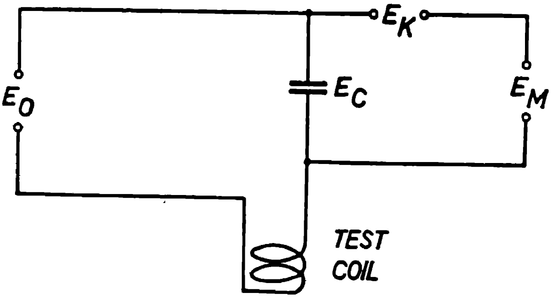

Institut Dr. Foerster

Fig. 30. Circuit for complete suppression of undesired effects such as "lift-off" effect by partial compensation of voltage across a condenser in the resonant circuit. E_0 = voltage of an oscillator. E_K = compensation voltage. E_M = measurement voltage. E_c = voltage across condenser.

Fig. 30 shows a resonant circuit, consisting of the test coil with impedance values ωL and R, in series with the capacitance C. The current I through the oscillating circuit is

$$I = \frac{E_0}{\sqrt{R^2 + [\omega L - (1/\omega C)]^2}} \tag{18}$$

As soon as $\omega L = 1/\omega C$, the maximum current in the resonance circuit is

$$I_{(\max.)} = \frac{E_0}{R} \tag{19}$$

The resistance R can be expressed by the vector OA in Fig. 31, which shows a section of the impedance plane. At point O on the ωL axis, it is assumed that $\omega L = 1/\omega C$. If the resonant circuit is detuned by $\Delta\omega L$, due to a variation of the reactance, the resonance current is

$$I = \frac{E_0}{\sqrt{R^2 + (\Delta\omega L)^2}} \tag{20}$$

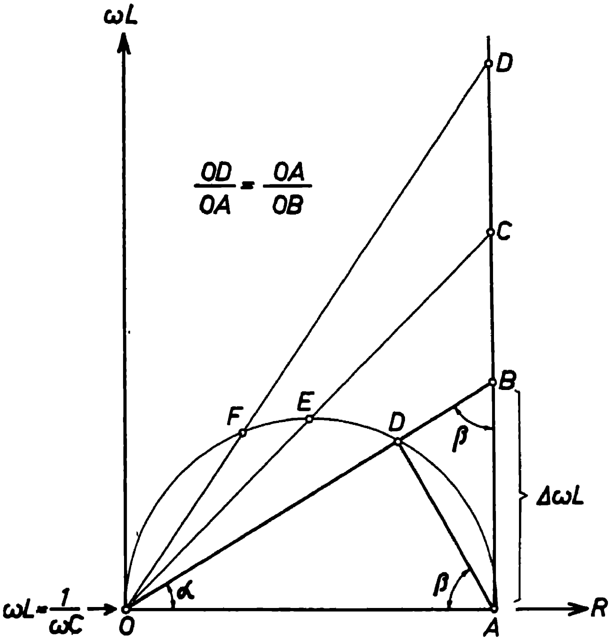

ωL
D
$\frac{OD}{OA} = \frac{OA}{OB}$
C
B
F
E
D
β
ΔωL
α
β
$\omega L = \frac{1}{\omega C}$
O
A
R

Fig. 31. Vector relations in the circuit of Fig. 30.

Circle Diagram. By using the inversion method, one can construct the current in the resonance circuit for any given ωL value. The **inversion method** is explained by Fig. 31. The triangle OAB is similar to the triangle ODA because the three angles of the triangle are equal. Thus $OD/OA = OA/OB$; i.e., $OD = (OA)^2/OB$. The line OB intersects the half-circle at D, where the distance OD is inversely proportional to the distance OB. At the same time $OE = (OA)^2/OC$ and $OF = (OA)^2/OD$. The distance OB is identical to the expression $OB = \sqrt{R^2 + (\Delta\omega L)^2}$ in Fig. 31. From Eq. (20) the **current in the resonant circuit** of Fig. 30 is proportional to the distance OD, OE, or OF when the resonance circuit is detuned by the distance $\Delta\omega L = AB$, AC, or AD, respectively. In other words the graphic representation of the current in the resonant circuit is the half-circle shown above the resistance in the impedance plane at the resonance point $\omega L = 1/\omega C$.

Suppression of Lift-off Effects. Fig. 32 shows the impedance plane with lift-off, crack, and conductivity directions designated. The point *A* represents the impedance of the probe coil placed on the test body. Suppose now that the resonant circuit is not tuned to resonance according to the ωL value *G* in Fig. 32, but to the point *O*, where *OA* is selected perpendicular to the impedance direction of the undesired effect. In this case the half-circle *ADEG* represents the locus of the current in the resonant circuit of Fig. 31 while the coil is lifted from the test object. When the impedance value of the test coil, while being lifted, changes along the lift-off effect curve *ABC,* the current of the resonant circuit passes through the values *OA*, *OD,* and *OE.*

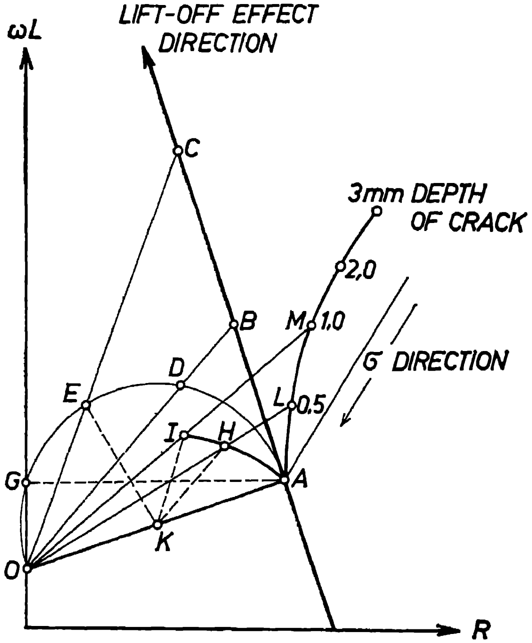

Institut Dr. Foerster

Fig. 32. Impedance plane showing "lift-off" direction *ABC*, with conductivity σ and crack directions.

Point *K* (i.e., the center point of the half-circle of diameter *OA*) is always the same distance from the points *A*, *D*, and *E*. In the resonant circuit of Fig. 30, a **compensation voltage** E_K (corresponding to the distance *OK* in Fig. 32) is added to the voltage drop across the condenser E_C. Under these conditions the lift-off can be entirely suppressed in the measurement voltage E_M because the measurement voltage rotates around the point *K*, with constant amplitude (*KA*, *KD*, *KE*). However, with a crack (for example) having a depth of 0.5 mm. (point *L*) or of 1 mm. (point *M*), the amplitude of the resonant current is calculated from the relations: $OH = (OA)^2/OL$ and $OI = (OA)^2/OM$. Thus cracks *L* and *M* result in a reduction of the measurement voltage E_M of the resonant circuit of Fig. 30, corresponding to the distances *KH* and *KI*, respectively, in Fig. 32.

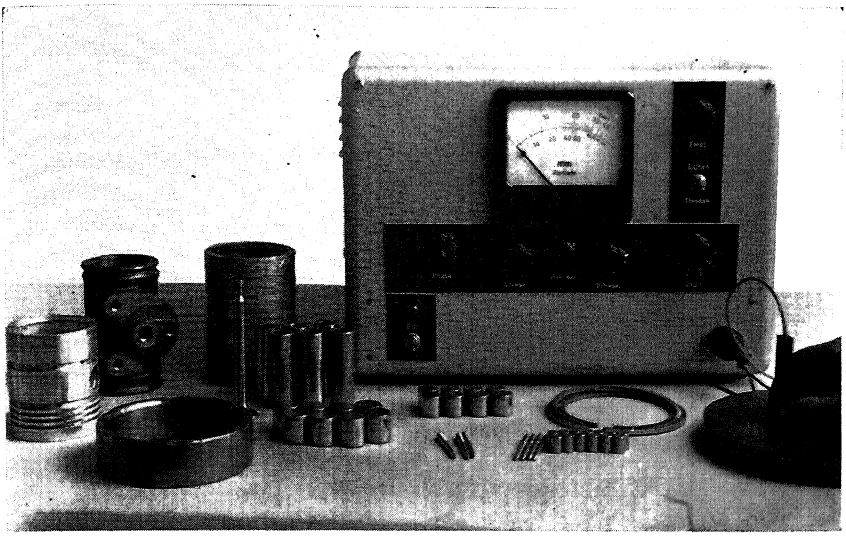

Institut Dr. Foerster

Fig. 33. Defectometer probe-coil instrument for detection of cracks and crack-depth measurement on both ferromagnetic and nonferromagnetic materials.

Crack Detection. Compensation of the lift-off effect (or any other undesired effect) has a strange measurement consequence. As one places the test coil on the specific metal (point *A*, Fig. 32) or removes it entirely, the measurement voltage does not react at all. As soon as a crack is present in the metal below the test coil, however, an indication is obtained. Thus it is possible to move the test coil rapidly and without special care over the surface of a metal. An effect can be expected only when the test coil moves over a crack.

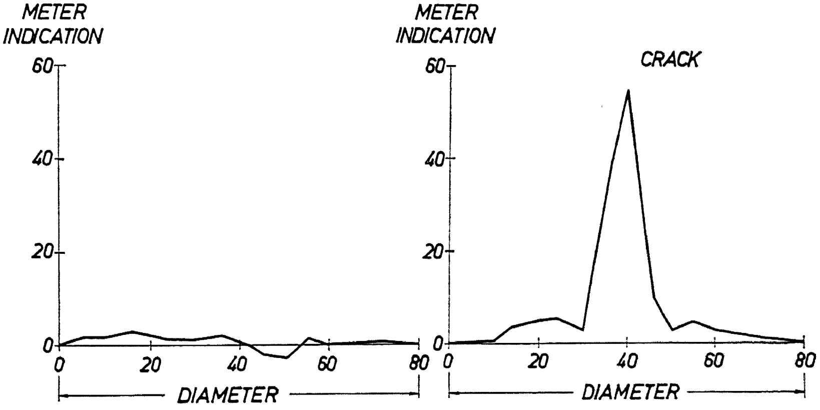

Fig. 34. Deflection on the Defectometer instrument of Fig. 33 above the cross-section of a sound (left) and a cracked piston head (right).

APPLICATIONS OF SUPPRESSION TECHNIQUES. The possibilities described here for suppressing undesired effects in the impedance plane are but two examples from a number of methods used in eddy current test instruments. In the **Sigmaflux instrument** (American designation, Magnatest FW-300), the influence of the test-object dimension is suppressed by means of a phase-controlled rectifier of special construction. In the instrument for measuring the diameter of wires which pass rapidly through the test coil, the influence of material conductivity is eliminated.

In the **Sigmatest probe-coil instrument** (American designation, Magnatest FM-100) for conductivity measurements independent of test-object shape, the lift-off effect of small coil distances is suppressed. The deflection of the indicating meter of the Sigmatest instrument, plotted as a function of the distance from the coil to the metal surface, is a cosine curve.[30] As is well known, the cosine value changes only very slightly at small arguments, which has the effect of suppressing the lift-off effect.

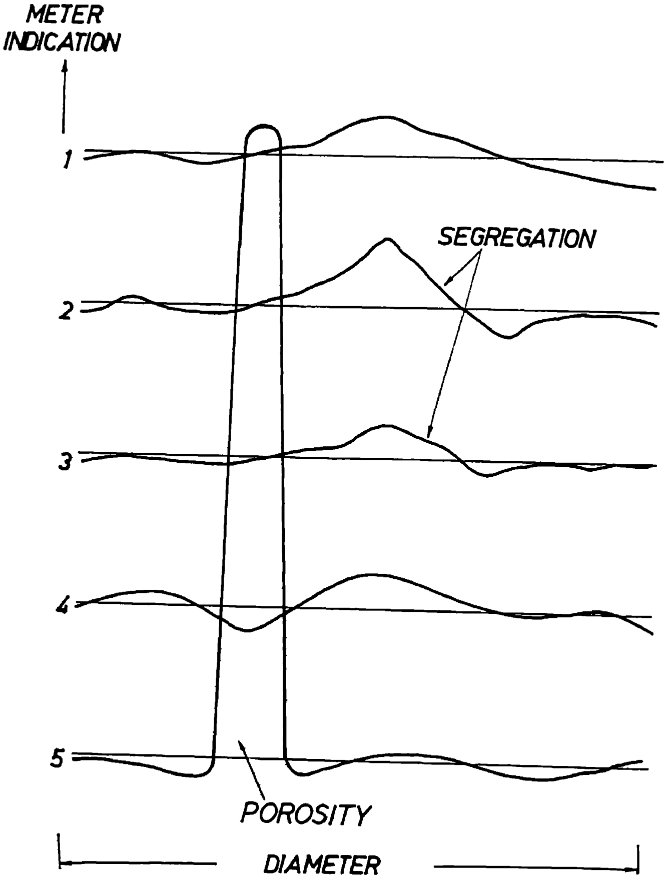

Fig. 35. Defectometer indication of porosity in the cross-section of a light metal block.

Crack-Depth Tests. In the **Defectometer,** shown in Fig. 33, the suppression of the lift-off effect is obtained by means of a new principle. The Defectometer was especially developed for crack detection and crack-depth measurement. For example, it is used in the nonferrous metal industry for detection and measurement of cracks in rods, pressed parts, and pistons. Fig. 34 shows the deflection curve of the Defectometer above the cross-sections of a sound and of a defective **piston rod.** The small deflections above the sound rod are caused by segregation; i.e., by conductivity variations.

Porosity Test. Fig. 35 shows the influence of porosity in **light metal blocks.** The curves *1* to *5* show the deflection of the Defectometer instrument while the probe coil passes over five cross-sections of a light metal block. The lift-off effect of the test coil is entirely suppressed. The presence of porosity is indicated by a large deflection.

Cracks Within Drilled Holes. The semi-automatic crack test instrument of Fig. 36 was developed for the detection of cracks in small drilled holes; for example, within pinholes in **turbine blades.** The turbine blade rotates on the measurement table. The scanning **microprobe coil,** which is perpendicular to the inside surface of the hole, is moved in the longitudinal direction of the hole. This results in a spiral scanning of the inside hole surface. This method does not react to distance variations between coil and metal. A defect is indicated by a signal. This instrument for **testing for inside cracks** has proved successful for numerous test parts. A correlation of defect indication and defect size was obtained for even the smallest size of cracks.

Tests for Thickness of Nonmetallic Layers. A number of examples can be given from the field of nondestructive testing with eddy current methods in which a method could be adapted for industrial use only after the suppression of one or several undesired effects. The **Isometer** (American designation, FT-400), shown

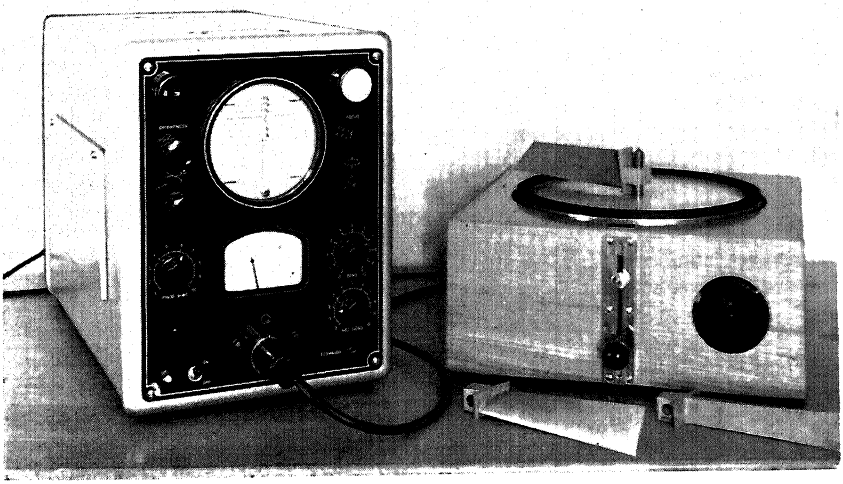

Institut Dr. Foerster

Fig. 36. "Crack detector" for light-alloy compressor blades.

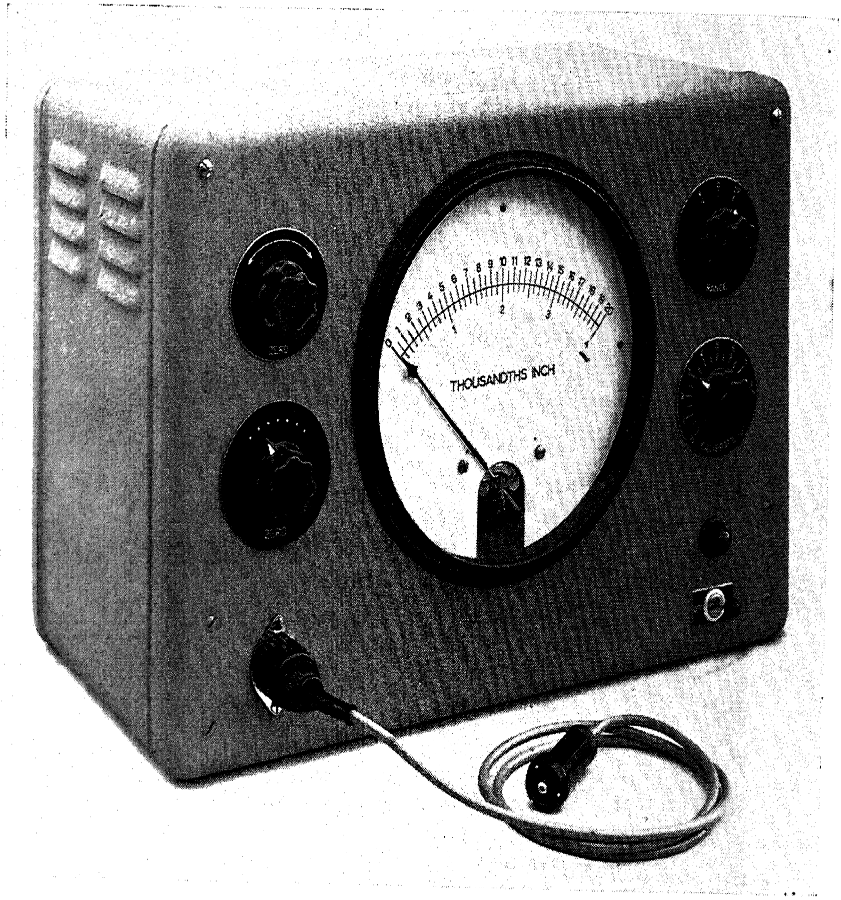

Institut Dr. Foerster

Fig. 37. Eddy current instrument for the measurement of the thickness of insulating layers (Foerster Isometer).

in Fig. 37, is an example of an instrument which applies this principle to the measurement of the **thickness of insulating layers.** However, the suppression of these undesired effects was possible only after the effects of various significant factors on the impedance of the test coil were determined quantitatively (see section on Eddy Current Sphere and Sheet Tests).

References

Reference numbers in this section refer to the references at the end of the section on Eddy Current Test Indications.

SECTION 41

EDDY CURRENT TEST AUTOMATION

CONTENTS

PAGE

Industrial Test Applications

- Significance of test speed 1
- Automatic testing with the Multitest instrument 1
  - Applications 2
    - Three automatic Multitest sorters for sorting drills by hardness values, with electromechanical positioning of test parts in the test coil (*f.* 1) 1
    - Fully automatic unit for sorting watch springs according to the thermoelastic coefficient, with automatic calibration-checking device and statistical-evaluation instrument (*f.* 2) 2
    - Examples of test objects sorted with the Multitest instrument for hardness, alloy, heat treatment, or defects (*f.* 3.) 3
- Handling of test parts 2
- Automatic control 3
    - Noncontacting foil-thickness meter with automatic feedback control of rolls (*f.* 4) 4
  - Metallizing of condenser paper 4
    - Vacuum metallizing unit with control of metal-layer thickness by means of the square resistance meter (*f.* 5) 4
- Automation of the Magnatest Q test 5
  - Sorting heat-treated forgings 5
    - Three Magnatest Q curves of forged parts (*f.* 6) 5
    - Bands formed by a large number of Magnatest Q curves resulting from forged parts in the conditions *A*, *B*, and *C* of Fig. 6 (*f.* 7) 6
  - Selecting test conditions 6
  - Establishing sorting limits 6
  - Speed of testing 6
  - Adjusting sorting limits 7
    - Magnatest Q picture of group *C* from Fig. 7 at four times higher sensitivity (*f.* 8) 7
- Automation of sorting and quality control data 7
    - Block diagram of the automatic Magnatest Q instrument (*f.* 9) 8
  - Handling of large parts 8
  - Conveyorized systems 8
    - Automatic Magnatest Q unit with conveyor belt (*f.* 10) 9

PAGE

- Other automation applications 8
    - A number of Magnatest Q units in operation for 100 percent quality control in a large European steel plant (*f.* 11) 10
  - Automation of crack testing 10
  - Magnetic-analysis equipment 11
    - Zuschlag magnetic-analysis crack test instrument with conveyor for semifinished parts (*f.* 12) 11

Automation of Statistical Quality Control

- Significance of statistical test data 12
- Automatic statistical control indicator 12
    - Statimat used for automatic recording of statistical distribution during nondestructive testing (*f.* 13) 12
  - Statistical records of alloy or carbon content 13
    - Statistical distributions obtained for alloys (*f.* 14) 13
  - Automatic sorting systems 13
    - Automatic unit for sorting into 13 groups during nondestructive tests (*f.* 15) 14
  - Ball-bearing tests 14
    - Two automatic instruments for rapid production-sorting of balls for defects (*f.* 16) 15
    - Magnatest Q picture of test parts of ball-bearing steel (*f.* 17) 15
  - Other applications 17
    - Magnatest Q spread bands for chain bushings with various depths of case, together with frequency distribution of case depths (*f.* 18) 16
    - Multitest point picture with Statimat picture (*f.* 19) 16
  - Evaluation of statistical information 18
  - Quality figure for continuous test materials 18
- Combined automatic tests 19
    - Automatic tester for sorting defective ball-shaped test bodies and simultaneous sorting into 12 dimensional groups which deviate from each other by 40 μin. (*f.* 20) 18
- References 19

EDDY CURRENT TEST AUTOMATION

Industrial Test Applications

SIGNIFICANCE OF TEST SPEED. Eddy current methods are distinguished from other nondestructive test methods by their unusually high test speeds. This lends itself readily to automation of the test processes. Most of the Foerster test instruments discussed in the section on Eddy Current Test Equipment can operate fully automatically in industry. In the subsequent text the automation of several test processes is discussed.

AUTOMATIC TESTING WITH THE MULTITEST INSTRUMENT. Possibilities for the automation of the Multitest method have been pointed out previously. (See Fig. 13 in the section on Eddy Current Test Equipment.) Production parts, such as balls, needles, or rollers, slide or roll freely at high speed through the test coil. The maximum measurement value which occurs when the part passes the coil center requires only about 1/1000 sec. for the control of the corresponding sorting gates. Fully automatic units have been developed for **sorting balls for cracks.** Some of these units sort with a speed of more than 10,000 parts per hour. Such parts are passed freely through the test coil when the maximum measurement value in the coil center is sufficient. However, there are many parts which have to be tested at a specific point; for example, drills at their hardened tips or sewing-machine needles at the needle tip. For this purpose, electronically controlled devices were developed which fix the test part at a specific point in the coil for about 1/10 sec.

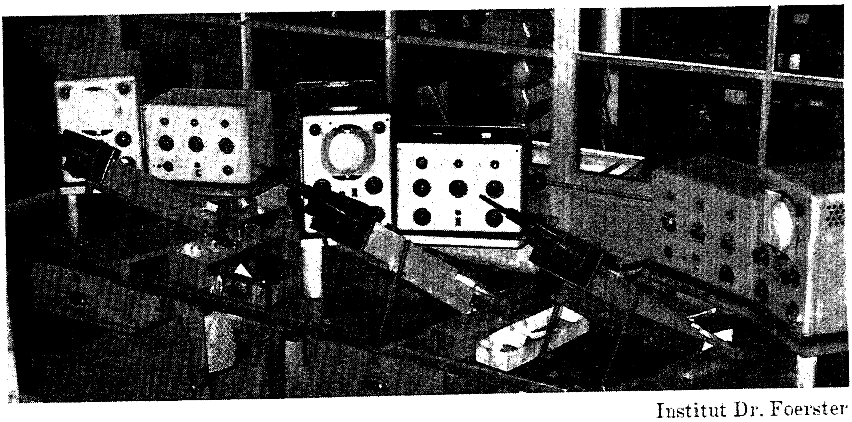

Institut Dr. Foerster

Fig. 1. Three automatic Multitest sorters for sorting drills by hardness values, with electromechanical positioning of test parts in the test coil.

Applications. Fig. 1 shows three automatic Multitest sorters which sort the main portion of the production in a large European drill factory into three **hardness groups.** Here, by means of an electromechanical-positioning feature, only the tips of the drills are measured. **Pressed, light-metal parts** are sorted automatically in the same manner for hardness, since, for age-hardened aluminum alloys, a linear relationship exists between the electrical conductivity and the hardness. Furthermore, automatic Multitest devices serve for sorting **arc-light carbons** according to the thickness of the copper plating. Metal parts are sorted for cracks, and steel parts for heat treatment and cracks.

Fig. 2 shows a fully automatic unit for **sorting watch springs** according to the so-called thermoelastic coefficient. The zero point of the instrument is automatically checked during each rotation of the conveyor belt. The **thermoelastic coefficient** (which indicates how many seconds per day a watch will be fast or slow at a 1° C. temperature variation) has a linear relationship to the magnetic property measured by the Multitest instrument. The automatic sorter sorts the watch springs into three quality groups. An electrical device subdivides the test results into 12 groups. Each of the 12 groups controls a channel of the **statistical evaluation instrument** shown in Fig. 2. This instrument automatically indicates the frequency distribution curve for the thermoelastic coefficient during sorting and permits the production quality to be observed at a glance. Fig. 3 shows a selection of production parts (against a centimeter rule) which are automatically sorted for quality with the Multitest instrument.

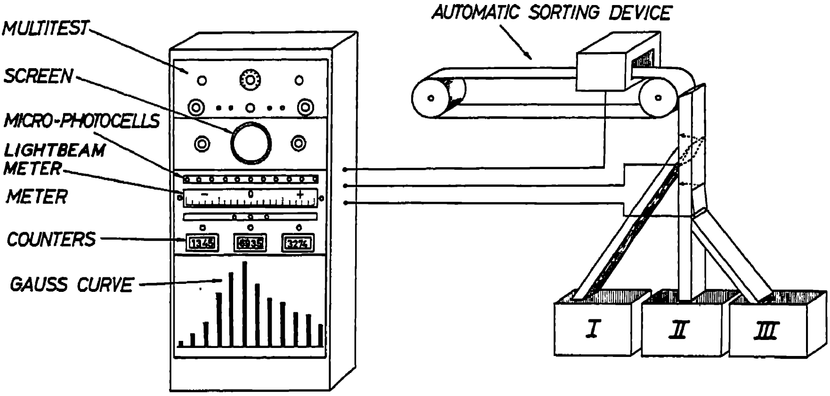

Institut Dr. Foerster

Fig. 2. Fully automatic unit for sorting watch springs according to the thermoelastic coefficient, with automatic calibration-checking device and statistical-evaluation instrument.

HANDLING OF TEST PARTS. An automatic conveyor belt is used in most of the instruments for the automation of alloy sorting and crack testing of nonferrous and ferrous **metal rods.** Test parts are passed through the coil on the belt at a constant speed. When a defect appears, a color marking is usually applied to the specific point with the aid of a spray gun. In several automatic units, two color markings (red and white) are used to indicate the beginning and the end of a defect by different colors.

In the **difference-coil method,** defects having a constant depth are not indicated. Only variations of the crack depth are shown, as is well known. However, the beginning and the end of a crack are indicated by a measurement effect in an opposite phase position. This is used to control the color marking with corresponding colors. By means of the different colored markings at the beginning and end of a defect, it is possible, especially in the case of long rods, to cut out defective pieces. The defective rods are pushed out on the "waste" side after they have passed the test coil. In some cases this is accomplished by compressed air control; in other cases, by means of a magnetic **ejector**; and in still others, by a motor-driven ejector.

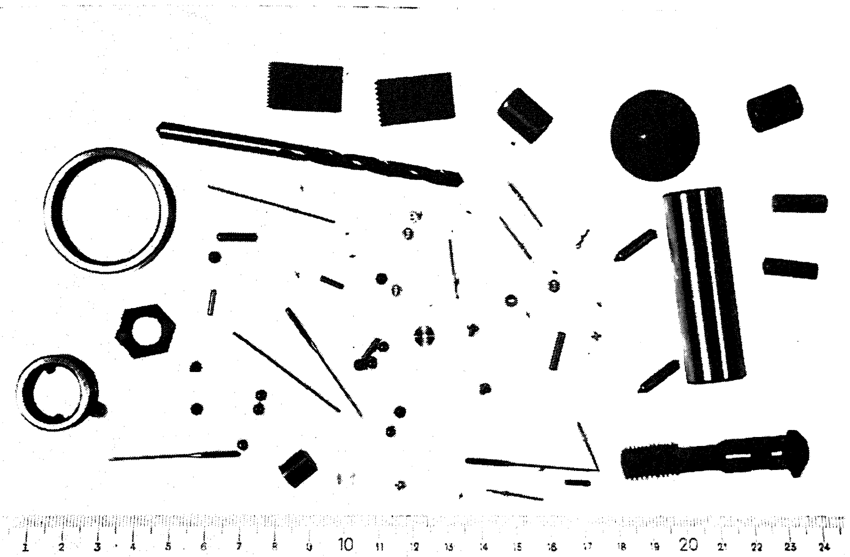

Institut Dr. Foerster

Fig. 3. Examples of test objects sorted with the Multitest instrument for hardness, alloy, heat treatment, or defects.

In several units the test parts are put through the coil of the crack test instrument, as well as through the coil of the Sigmaflux alloy-testing instrument, to eliminate cracked and mixed materials at the same time. Still other designs permit dimensional measurements.

AUTOMATIC CONTROL. The theory of thickness measurement of nonferrous metal foils and layers has been discussed in the section on Eddy Current Sphere and Sheet Tests. Fig. 4 shows a **foil-thickness meter** whose light beam galvanometer is equipped with microphotocells. These photocells can be moved arbitrarily to any tolerance value on the scale of the instrument. When the light-beam indicator exceeds or falls short of the previously adjusted tolerance value of the thickness meter, the adjusting motor of the rolling mill is automatically energized until the foil thickness reaches the required value. Another photocell, located at or within the required value, again turns off the adjusting motor. Therefore the automatic foil-thickness measurement instrument contains

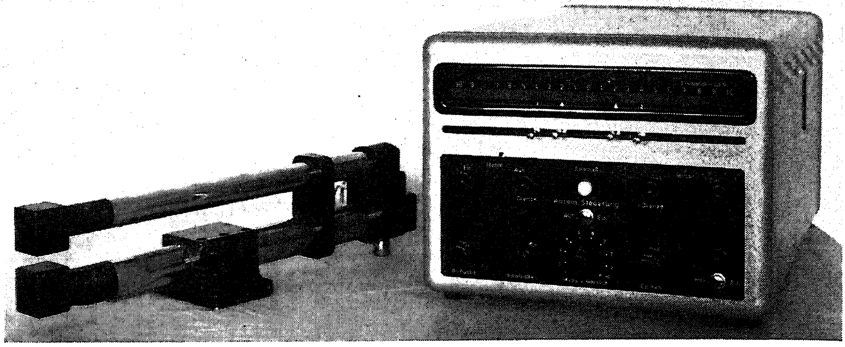

Institut Dr. Foerster

Fig. 4. Noncontacting foil-thickness meter with automatic feedback control of rolls.

four photocells which can be arbitrarily adjusted for upper and lower tolerance limit control.

Metallizing of Condenser Paper. The metallizing of condenser paper in vacuum is controlled in a similar manner. The paper with the metal layer passes at high speed in vacuum through the **fork coil arrangement** without direct con-

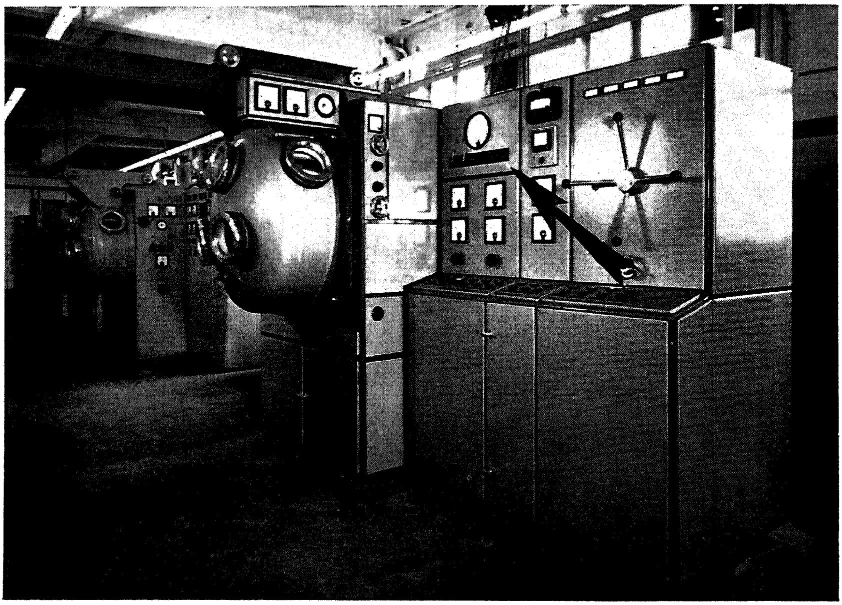

Institut Dr. Foerster

Fig. 5. Vacuum metallizing unit with control of metal-layer thickness by means of the square resistance meter (shown by arrow).

tact. The **resistance per unit square** of the condenser paper is indicated directly in ohms on the "square resistance" meter. The nondestructively measured square resistance value controls the metallizing process. This is one example of how a nondestructive test instrument takes over control of production processes in large industrial plants. Fig. 5 shows a large vacuum metallizing unit in an American plant in Europe. Here the square resistance meter (indicated by arrow) is built into the instrument panel.

AUTOMATION OF THE MAGNATEST Q TEST. With the Magnatest Q test method, the range with the best possibility of separation of the interesting effect (for example, tensile strength, depth of case, or alloy variation) can be moved to the screen center where the reading slit is located. In the prior discussion of the **linear time-base method,** it was shown that the slit value represents the measurement effect perpendicular to the base voltage. If one selects the direction of the undesired effect (for example, diameter or permeability effect) in the complex voltage plane as the base voltage, the undesired effect is eliminated in the slit value.

With a new electronic method utilizing a special **electron-beam-deflection tube,** only the slit value is used in automation of the Magnatest Q instrument. This signal controls the electrical-sorting mechanism and a statistical evaluation instrument. Only the instantaneous value of the Magnatest Q curve, exactly in the screen center, is used.

Sorting Heat-treated Forgings. Fig. 6 shows three Magnatest Q curves for a forged part in the conditions: *A*, hard-forged; *B*, annealed and quenched; *C*, tempered to 65 to 80 kg./mm.^{2}. The curve *B* is adjusted to zero (horizontal

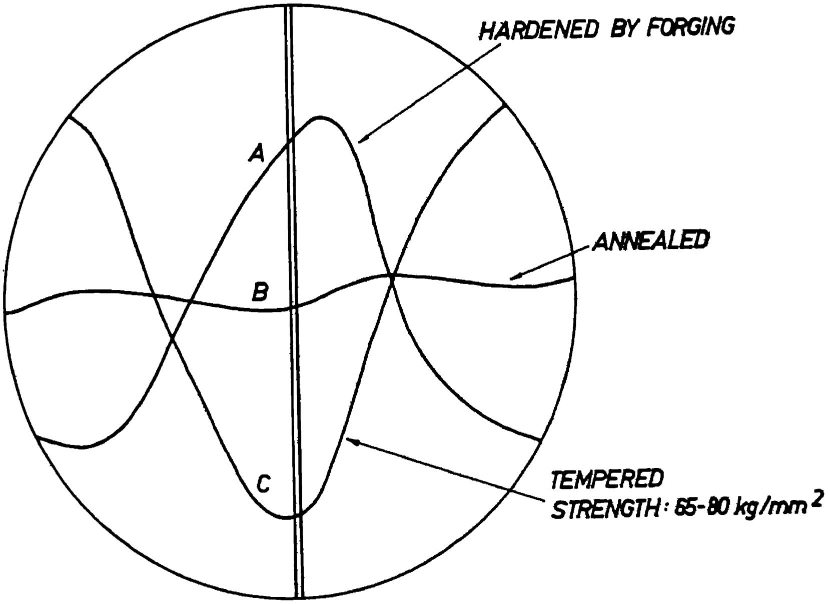

Fig. 6. Three Magnatest Q curves of forged parts. Conditions: *A*, hard-forged; *B*, annealed and quenched; *C*, tempered for 65 to 80 kg./mm.^{2} tensile strength.

straight line) by means of the compensators in the instrument. If, for example, 3000 forged parts are tested in the conditions *A*, *B*, and *C*, the entire curves of one condition result in a **spread band** as shown in Fig. 7.

Selecting Test Conditions. The main problem of Magnatest Q testing is selecting the test conditions such as field strength, frequency, and number of the harmonics, to avoid overlapping of the spread bands of conditions which have to be separated from each other. By selecting the phase direction in the voltage or impedance plane, the screen picture can be moved so that the point with the largest vertical separation of the individual bands can be moved into the reading slit in the screen center.

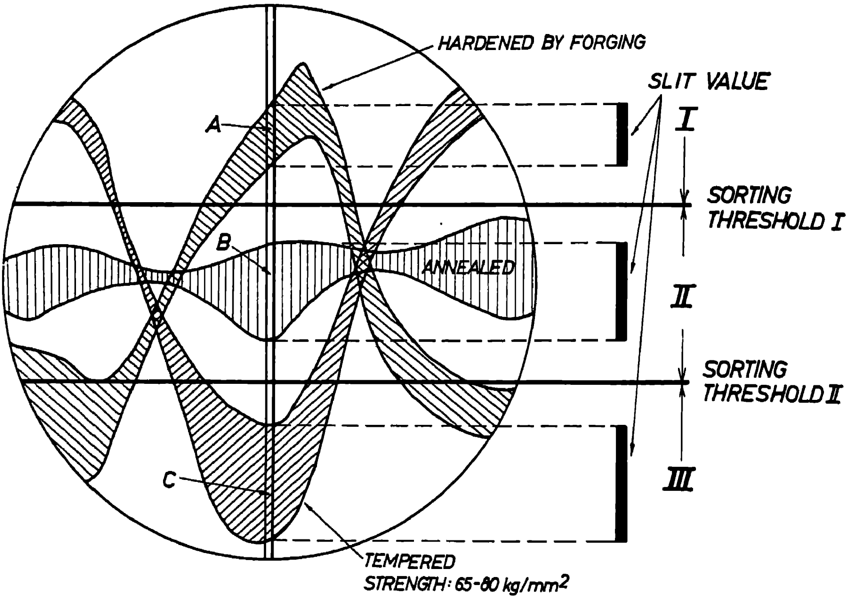

Fig. 7. Bands formed by a large number of Magnatest Q curves resulting from forged parts in the conditions *A*, *B*, and *C* of Fig. 6. Sorting limits are indicated for optimum separation of the three conditions, *A*, *B*, and *C*.

Establishing Sorting Limits. The sorting limits plotted in Fig. 7 are arbitrarily adjustable in vertical direction. In each case they are adjusted in the center of the space between the bands which are separated from each other. The slit values of the three bands, between which the sorting limits are placed, are shown to the right in Fig. 7. The slit is used for **electronic control of the sorting gates.** All slit values which fall in ranges I, II, or III open the corresponding sorting gates I, II, or III in the equipment sketched in Fig. 9.

Speed of Testing. One cycle of the test frequency is sufficient to open the corresponding sorting gate while the test part passes through the test coil on the conveyor belt. This amounts to 0.2, 0.017, or 0.0025 sec., depending on the frequency of the Magnatest Q instrument used (5, 60, or 400 c.p.s.). Since only one cycle is needed to control the automatic sorter, this slit method provides the highest test speed that can be obtained with a 5-, 60-, or 400-c.p.s. method.

Adjusting Sorting Limits. By arbitrarily adjusting the sorting limits, this automatic sorter can be very quickly adapted to specific test problems. For example, the band *C* (tempered to 65 to 80 kg./mm.^{2}) in Fig. 7 can be moved to the screen center of the Magnatest Q instrument by means of the compensators.

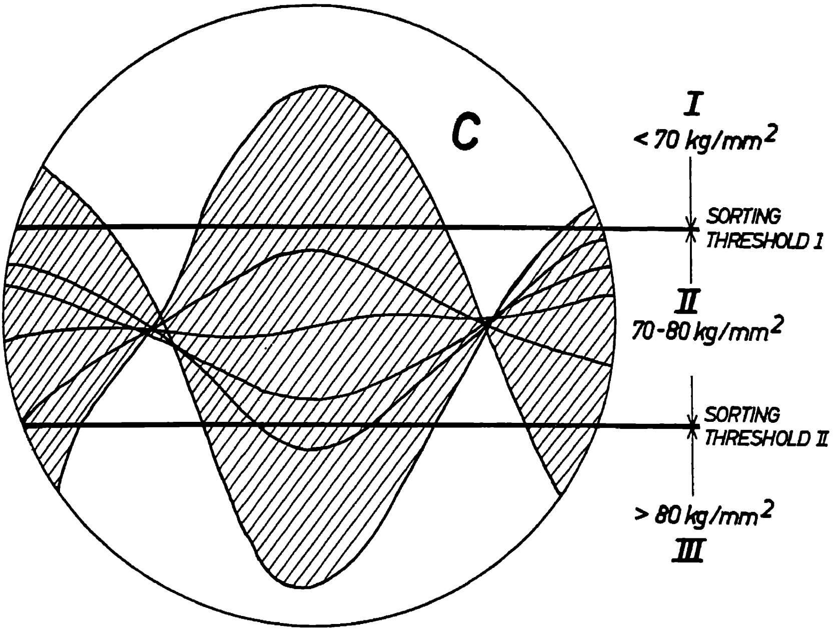

Fig. 8. Magnatest Q picture of group *C* from Fig. 7 at four times higher sensitivity. The nodal point of group *C* has been moved to the screen center to permit sorting by tensile strength values.

By turning the sensitivity knob, for example, to four times higher sensitivity, the spread of band *C* will become four times as wide. By a suitable adjustment of the sorting limits, one can now sort the group *C* into the following three tensile strength groups:

Group I (tensile strength lower than 70 kg./mm.^{2}),
Group II (tensile strength between 70 and 80 kg./mm.^{2}), and
Group III (tensile strength greater than 80 kg./mm.^{2}).

Fig. 8 shows the Magnatest Q screen picture with a sensitivity four times higher than that shown in Fig. 7. The group *C* from Fig. 7 is moved to the screen center by means of the compensators.

AUTOMATION OF SORTING AND QUALITY CONTROL DATA. Fig. 9 shows schematically the automation device for the Magnatest Q instrument. The test part passes through the test coil on the conveyor belt. When the part enters the coil, the position of the sorting gate is reset from the previous position. The **visual indicator** *A* shows the test-part curve, while the **electronic slit** *B* utilizes only the instantaneous value in the center of the reading slit. The electronic slit controls the **sorting gates** within one cycle, triggers at the same time the colored **signal lamp** which corresponds to the sorting group, counts the test part, and steps up the **counter** for the specific sorting group. Thus the electronic slit not only carries out automatic sorting; it also gives numerical data for quality control, including the entire number of parts tested and the number of test parts in groups I, II and III. Since the counters can be returned to zero only by means of special keys, one is able to retain, for example, the quality test results obtained during a night shift.

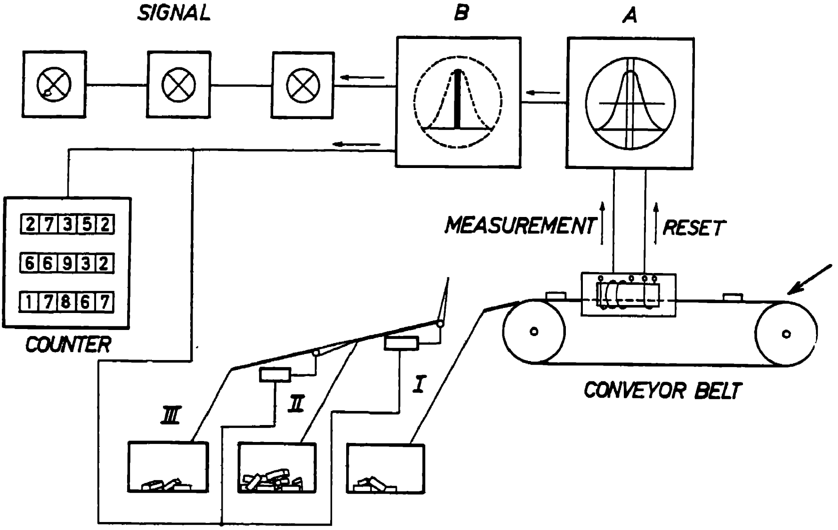

Institut Dr. Foerster

Fig. 9. Block diagram of the automatic Magnatest Q instrument.

Handling of Large Parts. For larger test parts which are difficult to transport on a conveyor belt, the electronic slit method can be used to reduce **human error.** Lamps are clamped to the corresponding containers for the three or more groups of test parts. These light up, according to the test group, so that the operator merely places the test part in the corresponding container indicated by the lamp.

Conveyorized Systems. Fig. 10 shows an automatic Magnatest Q unit with a conveyor belt. The hourly rate of testing lies between 3000 and 8000 parts, depending on the size of the test part. The conveyor belt is suitable for test parts whose maximum value during passage through the coil is representative of the test part. However, some parts such as drills with soft shafts, complicated forged parts, and certain screws require testing at a specific point or in a specific position in the coil. Use is then made of **automatic tilting or moving coils** in which the test parts are maintained in the coil in a specific position during testing. After the test the coil is tilted by a motor, and the test part slides through the sorting gate into the container which corresponds to its quality.

OTHER AUTOMATION APPLICATIONS. Other automatic instruments utilizing the Magnatest Q test process will sort, for example, long spring

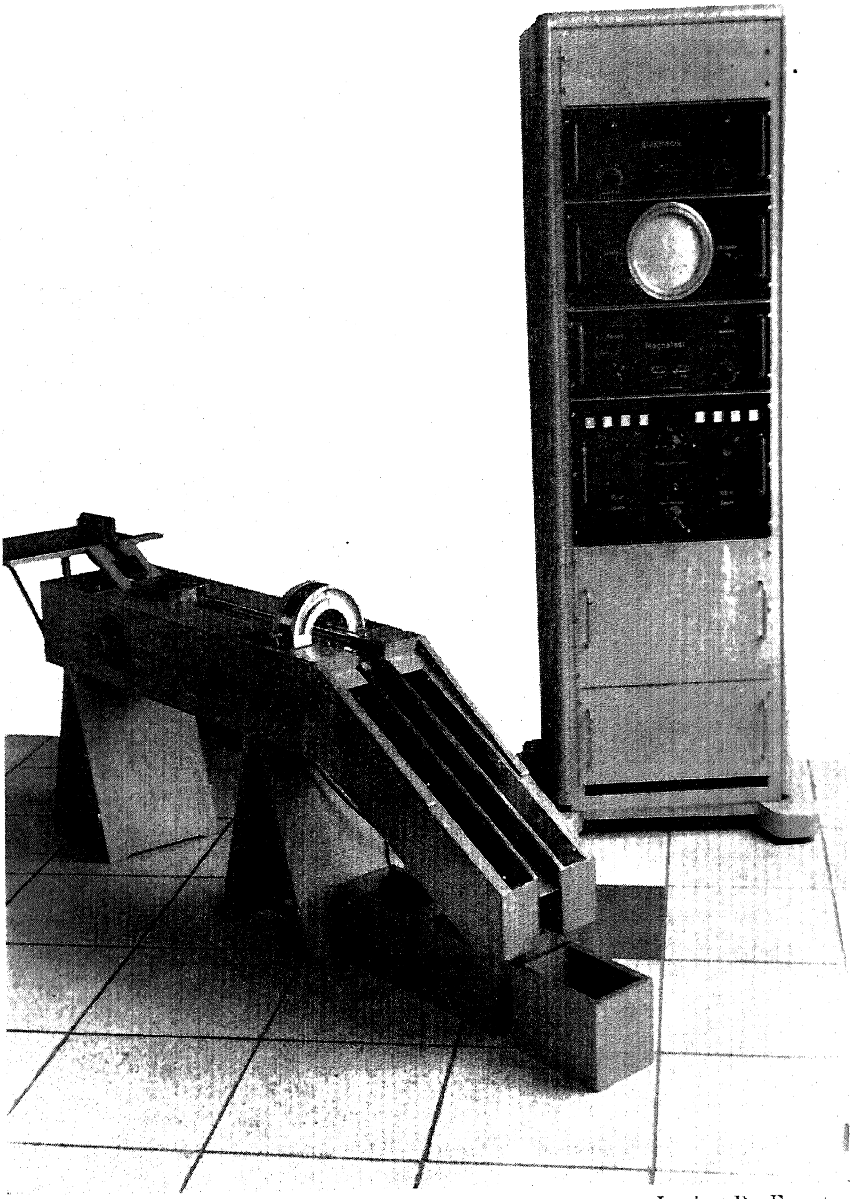

Institut Dr. Foerster

Fig. 10. Automatic Magnatest Q unit with conveyor belt.

rods into three hardness groups, or in the testing of spheres and rollers, will sort out parts which are too soft after heat treatment. In **sorting production parts,** it is always advisable to adjust the automatic equipment to the test part. An automatic sorting instrument which must sort large forged parts as well as small rollers, etc., necessarily has low efficiency. The significance of production sorting of steel parts with eddy current methods, in the steel industry, can be seen in Fig. 11, which shows a number of Magnatest Q instruments (indicated by arrows) for 100 percent quality control, in operation at the same time in a large European steel plant. The Magnatest Q instrument is the most widely used eddy current test instrument in European industry, evidencing the great desire for automation of the test process.

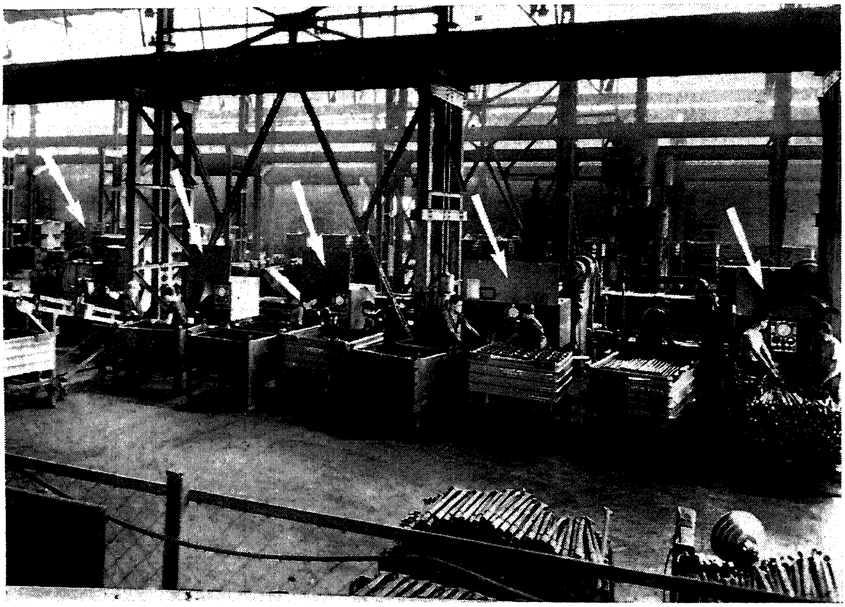

Institut Dr. Foerster

Fig. 11. A number of Magnatest Q units in operation for 100 percent quality control in a large European steel plant.

Automation of Crack Testing. The Magnatest D instrument for steel crack testing is automated in much the same manner as the Magnatest Q instrument. However, it is equipped with difference coils instead of the absolute coils which are used in the Magnatest Q instrument. The defects in the rods are marked with **color-spray devices.** A time delay, which is adjusted to the speed of the semifinished parts, assures that the rod is only marked with paint when the defective location has reached the point of the paint marker. The beginning and the end of the defect are marked in different colors.

European industrial users of this crack-test instrument state that cracks with depths even as small as 1 percent of the rod diameter can be found.[80] However, steel types with strong **magnetic-permeability variations** (heavy straightening stresses) are less suited for eddy current testing. Fig. 23 in the section on Eddy

Current Test Equipment indicates how permeability effects (mechanical stresses) can be separated in the indication from crack effects. However, when permeability effects caused by **inhomogeneous mechanical stresses** greatly outweigh the crack effect, separation of crack signals from the much greater permeability effect is very difficult. By means of a special test-coil design which was developed from exact field-distribution calculations, the defect sensitivity was considerably increased, while the so-called **fluttering effect** of the test rod was brought to zero.

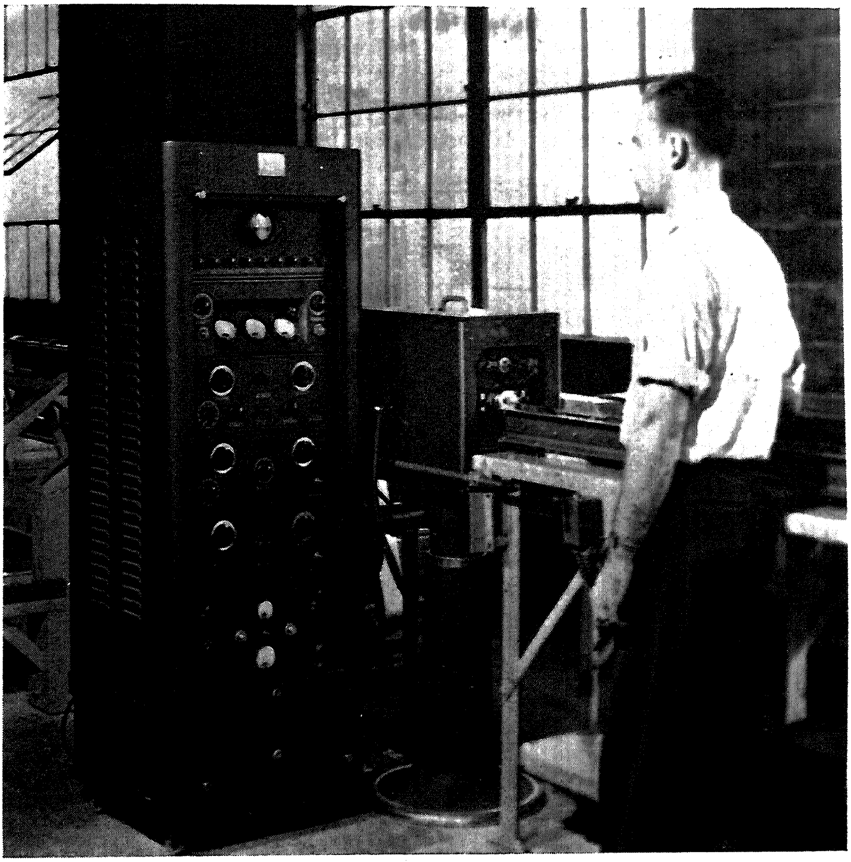

Magnetic Analysis Corp.

Fig. 12. ***Zuschlag*** **magnetic-analysis crack test instrument with conveyor for semi-finished parts.**

Magnetic-Analysis Equipment. Fig. 12 shows the American crack-test instrument which was developed by Zuschlag of the Magnetic Analysis Corporation.[89] Zuschlag's work in the development of the basic apparatus for the **slit methods** was of great merit. The instrument shown in Fig. 12 serves for simultaneous testing for cracks and mixed alloys. The conveyor can be seen behind the instrument. Defective rods are pushed out on the "waste" side.

Automation of Statistical Quality Control

SIGNIFICANCE OF STATISTICAL TEST DATA. Since eddy current sorting methods are outstanding because of their test speed, they are especially suited to production parts. In this application statistical evaluation of the test results gains steadily in importance because the quality of a product is characterized by the statistical frequency distribution of measured values such as hardness, depth of case, or type of alloy. A large **spread in hardness values** for a product, for example, indicates an error in the hardening process. An especially large spread in the eddy current test indications for the same parts before hardening indicates alloy differences or heat variation.

AUTOMATIC STATISTICAL CONTROL INDICATOR. Fig. 13 illustrates the **Statimat** which can be connected to the various automatic sorters to

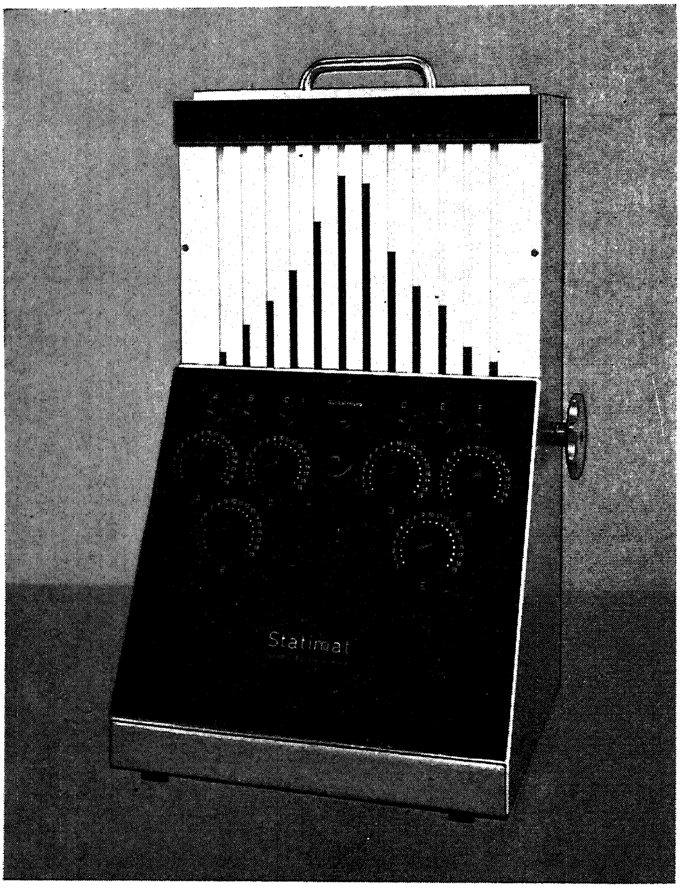

Institut Dr. Foerster

Fig. 13. Statimat used for automatic recording of statistical distribution during nondestructive testing.

indicate statistical distributions during sorting; for example, of carbon content, depth of case, tensile strength, hardness, magnitude of cracks, and other characteristics. As soon as the indicating line of a sorting channel reaches the upper limit (selected, for example, as 100 parts or 1000 parts), the statistical distribution can be automatically determined, after which all indicator lines are returned to zero for the next test run. The Statimat also contains a number of **preselector knobs** to provide a signal (for example, for turning off a production machine). For instance these operate if the waste at specific sorting channels exceeds a specific percentage of the total number of test parts.

Statistical Records of Alloy or Carbon Content. Fig. 14 illustrates the statistical records which can be obtained. Fig. 14(a) shows the distribution of the carbon content in one heat of a carbon steel. Fig. 14(b) illustrates the statistical distribution of the carbon content for two **mixed heats** of the same alloy. Two clearly indicated, maximum Gaussian curves correspond to the slightly shifted carbon content in the two heats. Fig. 14(c) shows the statistical distribution for two different alloys. The Gaussian curves do not indicate any overlapping. Thus Fig. 14(c) clearly illustrates the reliable sorting possibility of these two alloys. Fig. 14(d) illustrates the corresponding statistical distribution in eddy current sorting of three alloys which can be reliably separated.

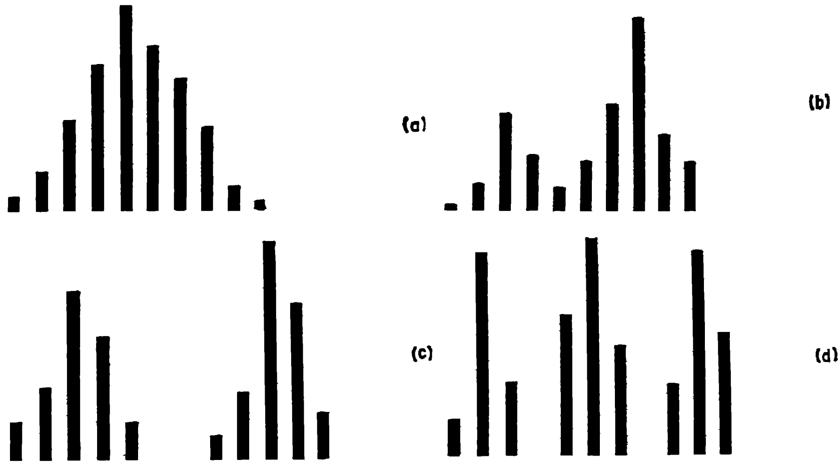

Fig. 14. Statistical distributions obtained for alloys. (a) Statistical distribution of the carbon content in one heat of a carbon steel (horizontal axis, C content; vertical axis, number of test parts with a specific C content). (b) Statistical distribution of carbon contents for two mixed heats of the same alloy. (c) Statistical distributions for two different alloys with satisfactory separation. (d) Statistical distributions in the eddy current sorting of three alloys with satisfactory separations.

Automatic Sorting Systems. Fig. 15 illustrates an automatic instrument for sorting into 13 groups. It is used increasingly for nondestructive-sorting processes, for dimensional sorting, and for combinations of both methods. The measurement factor (depth of case, hardness, carbon content, or dimension) is converted into a light deflection whose position can be read on the large scale in Fig. 15. New microphotocells whose light-sensitive area is less than 10^{-3} sq. in. are located below the scale.

During automatic sorting, this **light indicator** passes a specific number of microphotocells while moving from off-scale to the measured value. The number of cells passed determines the sorting group. While the light indicator passes a microphotocell, an electric impulse is created by the cell. Thus the corresponding sorting group is clearly indicated by the number of impulses obtained (i.e., photocells passed by the light indicator). The number of photocell impulses electronically counted opens the corresponding **sorting gate.** The 13 sorting limits can be easily adjusted by hand to any desired value. For example, in automatic eddy current **sorting of sheet materials according to thickness,** all sorting limits can be moved so close together that an eddy current sheet-thickness sorting with 13 tolerance groups, each of 0.0004-in. width, is obtained. This has proved to be very satisfactory in industry.

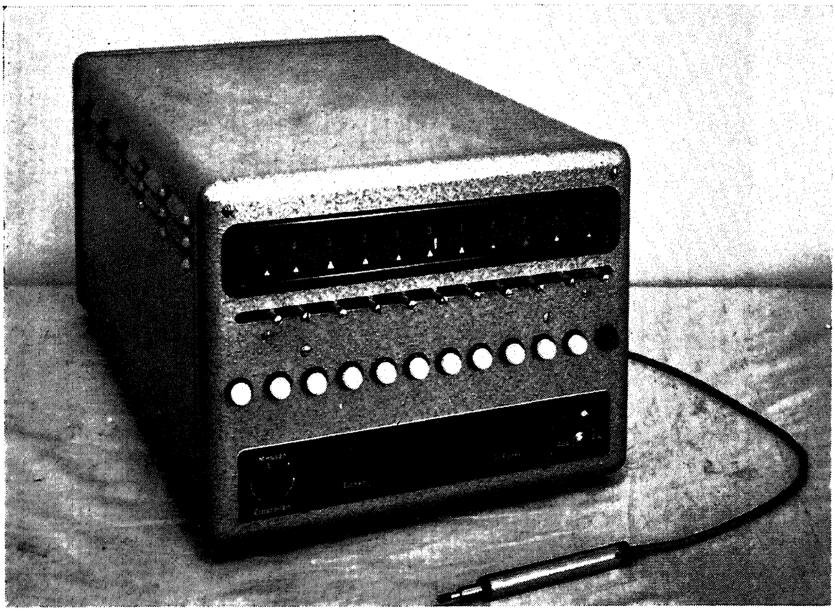

Institut Dr. Foerster

Fig. 15. Automatic unit for sorting into 13 groups during nondestructive tests.

Ball-Bearing Tests. The largest part of the balls produced by a well-known European ball-bearing plant pass through the two eddy current test arrangements shown in Fig. 16 to be tested for **cracks.** The test speed lies between one and five balls per second, depending on the size. The balls roll freely through the test coil and are tested for cracks in 1 msec.

Fig. 17 shows the Magnatest Q picture of test parts made of ball-bearing steel. Several specific screen patterns are shown on the left. The mechanically measured **hardness values** corresponding to a specific value are indicated to the right of the Magnatest Q patterns. The Statimat picture is shown on the right side of

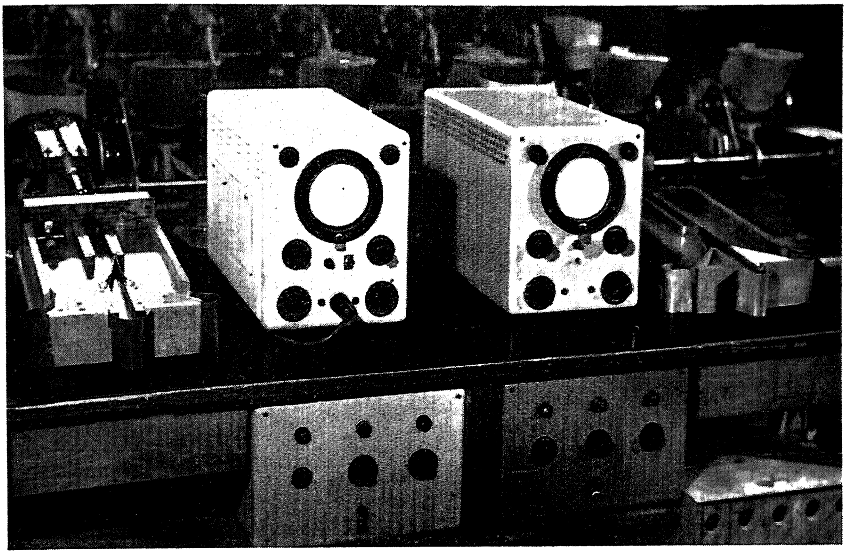

Institut Dr. Foerster

Fig. 16. Two automatic instruments for rapid production-sorting of balls for defects.

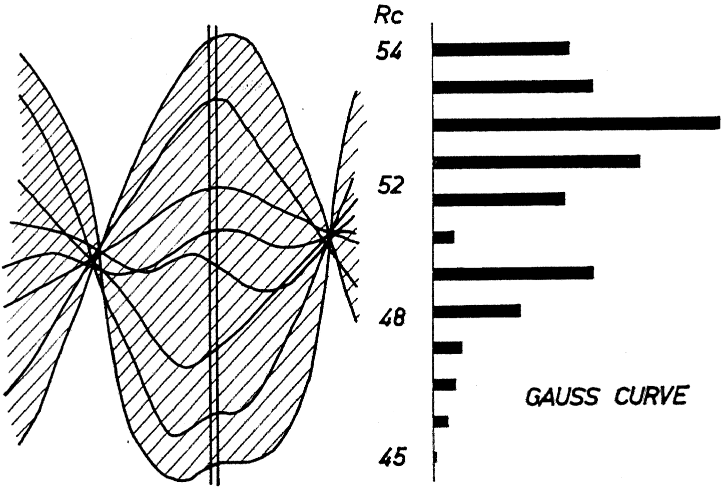

Fig. 17. Magnatest $\not{Q}$ picture of test parts of ball-bearing steel. Hardness values given for corresponding slit values (left). Frequency distribution of hardness values shown by Statimat instrument (right).

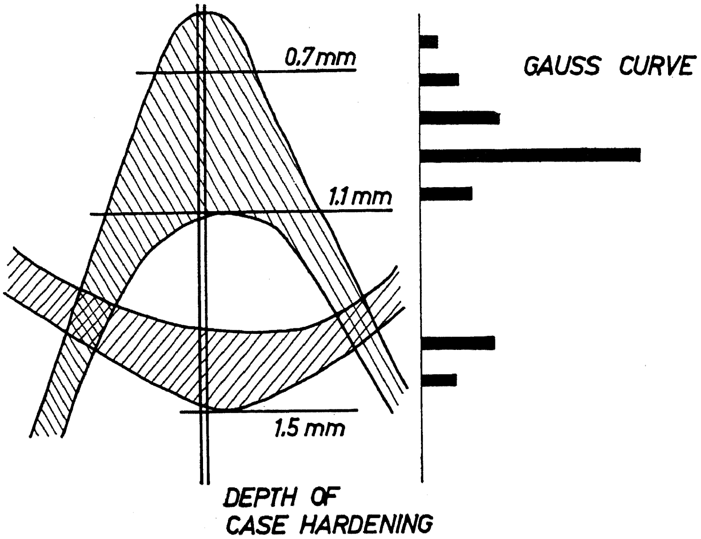

Fig. 18. Magnatest Q spread bands for chain bushings with various depths of case, together with frequency distribution of case depths.

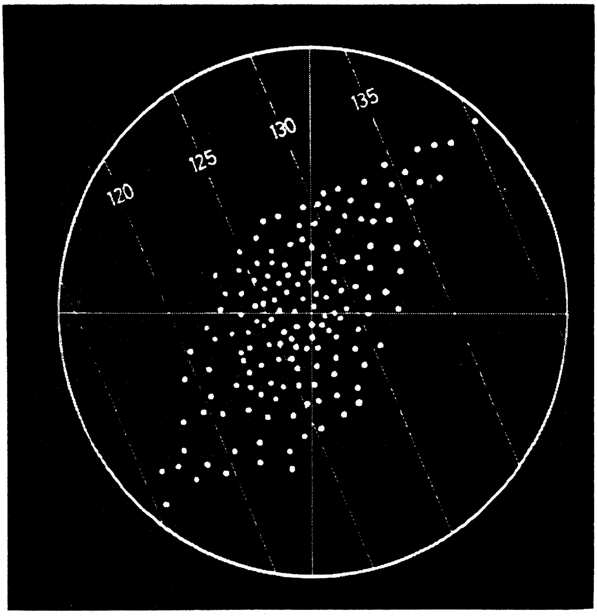

(a)

Fig. 19. Multitest point picture with Statimat picture. (a) Actual Multitest point picture of pressed parts of AlCuMg, with plotted hardness values. (b) Multitest picture of (a), turned so that the hardness direction is in the horizontal sorting direction. Statimat picture of frequency distribution of hardness values is shown below.

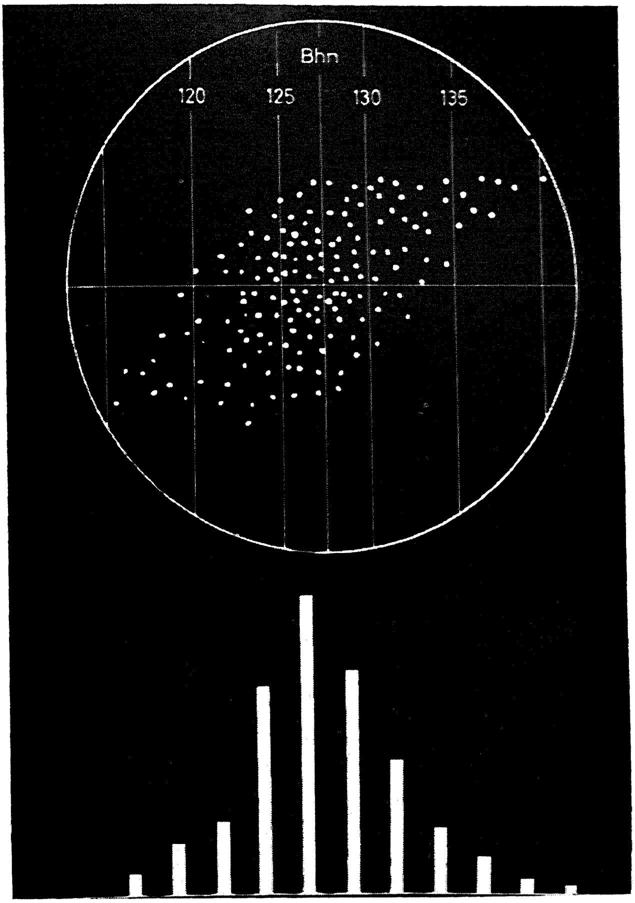

(b) Institut Dr. Foerster

Fig. 19. (Continued.)

the figure. The frequency distribution of the test parts with specific hardness values is also illustrated. The hardness value, 53 Rc., appears most frequently as shown by the Statimat picture.

Other Applications. Fig. 18 shows the Magnatest Q band for chain bushings with various **depths of case hardening.** The depth-of-case frequency distribution (Statimat picture), obtained automatically, is illustrated to the right. The largest number of test parts has a depth of case in the vicinity of 1 mm.

In testing with the Multitest instrument, the Statimat picture gives all important information concerning the quality of a product. Fig. 19(a) shows the Multitest point picture of a number of AlCuMg pressed parts. In Fig. 19(b) the point picture is turned, by means of the phase shifter 5 shown in Fig. 13 of the section on Eddy Current Test Equipment, so that the hardness direction is in the horizontal sorting direction. The frequency distribution of the hardness values obtained with the Statimat instrument is shown below the Multitest picture.

Evaluation of Statistical Information. In general, one can see that the Statimat picture obtained automatically in nondestructive quality-sorting of production parts gives important information concerning the quality of the production. Trouble in a production run is indicated directly in the Gaussian curve on the Statimat instrument. One can frequently draw conclusions as to the cause from the deviation from the "normal Gaussian curve." Depending on whether (1) a displacement of the maximum of the Gaussian curve appears, (2) the Gaussian curve, at a constant position of the maximum, increases in width, or (3) several maximum points appear, one obtains important information concerning the type of trouble in the production process.

Quality Figure for Continuous Test Materials. A different statistical quality number is used in testing for defects such semi-finished parts as rods, tubes, and

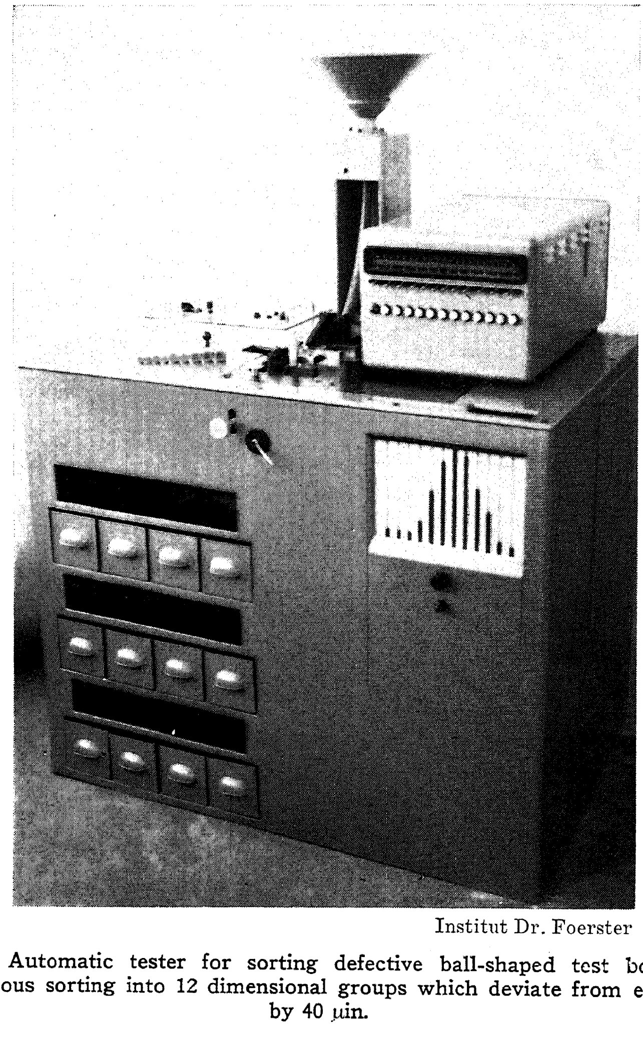

Institut Dr. Foerster

Fig. 20. Automatic tester for sorting defective ball-shaped test bodies and simultaneous sorting into 12 dimensional groups which deviate from each other by 40 μin.

especially wires. By indicating the number of meters of semi-finished parts tested and by electronically counting the defects which have appeared in this length, the **quality number Q** of the tested material can be defined as

$$Q = \frac{\text{number of meters}}{\text{number of defects}} \tag{1}$$

Thus the quality number gives the average number of meters per defect which have appeared. The characterization of the quality by means of a number is important, especially for wires in which defective sections cannot be cut out.

COMBINED AUTOMATIC TESTS. It can be expected that the automation of nondestructive test processes will expand in the future. The test parts must be brought to the instrument by means of a transport mechanism in all automatic-sorting operations. In this case it is desirable to combine into a **chain of tests** the various quality tests such as crack testing, dimension testing, roughness testing, form testing, testing for eccentricity, and testing of the depth of a case layer. Fig. 20 shows a combination automatic tester in which ball-shaped bodies are tested simultaneously for cracks and dimension. After the crack-testing operation, in which defective parts are sorted out, the test parts pass the dimension-testing station and are sorted automatically into 12 groups which deviate from each other by $1\mu = 40\ \mu$in.

The Gaussian curve of the dimensions of the test parts is obtained automatically during the sorting process. The form of the Gaussian curve permits one to draw important conclusions concerning the production process. The automatic instrument shown in Fig. 20 can be used to obtain the statistical distribution of the **degree of sphericity** of the test parts. For this purpose, the test parts which were sorted into a specific sorting channel and which may still exhibit diameter variations of 1μ ($40\ \mu$in.) are sorted once more. One now obtains a Gaussian curve with a steep slope within the limits of three adjacent sorting channels. This is a result of a certain lack of sphericity of the test parts, since their diameters can vary, depending upon the specific point at which they were measured. By repeating the sorting of test parts from one diameter group, a certain number of test parts will fall in the neighboring channels as a consequence of their lack of sphericity.

This principle of the determination of quality variations around the circumference of a test body can also be applied advantageously in nondestructive-sorting processes (for example, for detecting soft spots in spheres). Methods such as these are especially helpful in meeting the increasing industrial demand for 100 percent, nondestructive, quality testing and sorting.

References

Reference numbers in this section refer to the references at the end of the section on Eddy Current Test Indications.

SECTION 42

EDDY CURRENT TEST INDICATIONS

CONTENTS

PAGE

Range of Test Applications

Significance of test method 1
  Significance of electrical conductivity 1
  Significance of hysteresis loop characteristics 1
  Significance of impedance characteristics .. 2
Noncontacting dimensional controls 2
    Diameter variations of a rod of nonferrous metal, recorded while the rod is passed without contact through the Foerster Sigmaflux instrument (American designation, Magnatest FW-300) (*f.* 1) 2
Measurement of electrical conductivity with a feed-through coil 3
  Light alloys 3
  Tungsten wires 6
    Wavy fiber texture of a tungsten wire, caused by excessively large steps in the swedging process (*f.* 2) 3
Crack testing with feed-through coils 6
    Indications of the ellipse method, including test samples with decreasing diameter and surface and subsurface cracks with increasing depth (*f.* 3) 4
Defects in tungsten and molybdenum wire .. 6
    Schematic representation of typical defects in tungsten rods, as detected with the Foerster wire-crack test instrument (American designation, Magnatest FW-200) (*f.* 4) 7
    Microsections of tungsten rods and wires corresponding to the schematic drawings of defects in Fig. 4 (*f.* 5) 8
    Microsections from the tungsten and molybdenum industry (*f.* 6) 9

Conductivity Measurements

Application of the probe coil method 10
Probe coil test procedure 11
    Testing rods of mixed alloys by applying the probe coil of Foerster Sigmatest to the rod ends (*f.* 7) 11
Control of copper castings 12
    Decrease in conductivity of copper, caused by various impurities (*f.* 8) 12
  Phosphorus content 12
  Oxygen content 13
    Variation of the conductivity during deoxidation of a copper melt[9] (*f.* 9) 13
  Electrical conductivity 13
Control of aluminum castings 14
    Influence of metallic additives on the conductivity of aluminum (*f.* 10) 14
  Silicon content 14
  Determination of segregation 14
    Conductivity variation caused by segregation in a cast block of AlCuMg alloy (*f.* 11) 15
Testing of mixed alloys 15
    Electrical conductivity values for various American alloys (*f.* 12) 17
  Austenitic stainless steels 15
Indirect hardness measurements 18
    Relationship between conductivity and hardness in cold age-hardened alloys (*f.* 13) 18
  Control of heat treating 19
    Conductivity and hardness of sheets of an AlCuMg alloy (*f.* 14) 19
  Quench-hardened parts 19
    Indications of a soft spot in sheet (*f.* 15) 20
  Titanium alloys 21

Hysteresis-Loop Tests

Quality testing of ferromagnetic materials ... 21
  Correlation problems 21
Precision determination of hysteresis loops .. 21
    Standard test object for investigating the ferromagnetic properties of a material on the Foerster Ferrograph (*f.* 16) 22
    Device for magnetizing standard ring samples with axial current and measurement of the field strength with the air ring coil (*f.* 17) 22
    Screen picture of the Ferrograph with calibration of *B* and *H* scales (*f.* 18) .. 23
Determination of static hysteresis loop 23
    Superimposed hysteresis loop of standard ring sample of Fig. 16 and sample from the same material but with a $\sqrt{2}$ larger wall thickness (*f.* 19) 24
  Correction for eddy current effects......... 24
Analysis of hysteresis loop patterns 25
  Effects of internal stress 25
    Family of hysteresis loops of a normal sample of C1015 cold-drawn carbon steel (*f.* 20) 26
    Family of hysteresis loops of the normal sample from Fig. 20 but stress-relief annealed (*f.* 21) 26
  Effects of annealing 25

CONTENTS *(Continued)*

PAGE

- Superimposed loops of the sample from Fig. 21, but carburized for 1 hr. at 900° C. in a C-atmosphere (loop with higher magnetization values) and quenched (loop with smaller magnetization values and higher coercive force) (*f.* 22) ... 27
- Effects of carburization ... 28
  - Superimposed magnetization loops of two normal samples with various hardness (*f.* 23) ... 27
- Predicting mechanical and structural characteristics ... 28
- Internal stress in mangetostrictive materials ... 28
  - Influence of tensile stress on the magnetization loop of a hard nickel wire (*f.* 24) ... 28

Comparator Bridge Tests

- Principle of operation ... 29
  - Magnatest Q pictures derived from the difference in the magnetization loops (*f.* 25) ... 30
- Magnatest Q sorting ... 31
  - Recording test results ... 32
    - Magnatest Q picture of cobalt alloys having similar alloy contents (*f.* 26) ... 32
  - Range of test applications ... 33
- Setting up Magnatest Q instrument ... 33
  - Adjustment of the Magnatest Q screen picture for optimum test conditions (*f.* 27) ... 34
  - Sensitivity calibration ... 33
  - Compensation adjustments ... 33
  - Spread band characteristics ... 33
    - Magnatest Q curve and spread band of C1015 carbon steel and a free-cutting steel (*f.* 28) ... 36
- Selecting optimum test conditions for sorting alloys ... 33
  - Separation of three different alloys ... 34
    - Magnatest Q picture of three alloys, 3415, 5115, and free-cutting steel with 0.22C, with an optimum screen utilization (*f.* 29) ... 36
    - (a) Spread bands of a large number of rods of C1034, C1045, and 5140 steels. (b) Spread bands of unfinished piston rods of C1015 and 5115 steels (*f.* 30) ... 37
  - Use of harmonics in separating similar alloys ... 34
  - Sorting mixed lots ... 35
    - Separation of C1034, C1045, and C1075 carbon steels and free-cutting steel with 0.1 percent C (*f.* 31) ... 38
- Testing billet materials ... 35
  - Separation of hot-rolled billets of 5132, C1075, 5140, and 6150 steels (*f.* 32) ... 39
  - Spread bands of hot-rolled billets of 60 × 60 mm. cross-section, of E52 100 steel, a wrought heat-resisting steel for valves, and C1034 and C1015 carbon steels (*f.* 33) ... 40
  - Use of low field strengths ... 38
    - Spread bands of rolled billets of the two spring steel alloys A and B (see analysis) (*f.* 34) ... 41
    - Spread bands of the alloys of Fig. 34, but with an eight times lower field strength (*f.* 35) ... 42

PAGE

- Optimum utilization of screen area ... 39
  - Spread bands of 5140, C1045, and 3115 steels with optimum screen utilization (*f.* 36) ... 43
  - Spread bands of the two alloys E4132H and 5132, which differ by only 0.23 percent Mo (*f.* 37) ... 44
- Influence of test frequency ... 40
  - Spread bands of the five alloys, C1015, C1034, 5115, free-cutting steel with 0.1 percent C, and free-cutting steel with Mn, at a test frequency of 60 c.p.s. (*f.* 38) ... 45
  - At a test frequency of 5 c.p.s., a separation of the five alloys from Fig. 38 is possible at the dashed vertical line (*f.* 39) ... 45
- Tests of wire samples ... 41
  - Spread bands of C1045, C1034, and 5140 steels at 60 c.p.s. (*f.* 40) ... 46
  - Satisfactory separation of the three steels with strong inhomogeneous stresses from Fig. 40, at a test frequency of 5 c.p.s. (*f.* 41) ... 46
- Advantages of low frequency ratios ... 42
  - Complex voltage plane of the Magnatest Q coil which contains a test body with the diameter d, the electrical conductivity σ, and the permeability μ_{rel}. (*f.* 42) ... 47
  - Angle between the conductivity direction and the diameter-permeability direction, as a function of the f/f_g ratio (*f.* 43) .. 48
- Permeability effects at high frequency ratios ... 42
- Effects of inhomogeneous internal stresses . 43
- Influence of field strength ... 44
  - Spread bands with a test frequency of 60 c.p.s., corresponding to Fig. 40 but taken with a higher test field strength (*f.* 44) ... 48
  - Spread bands corresponding to Fig. 44 but with a test frequency of 5 c.p.s. (*f.* 45) ... 49
- Effects of straightening ... 47
  - Spread bands of the 4140 and 5140 alloy steels at a test frequency of 60 c.p.s. (*f.* 46) ... 49
  - Spread bands of 4140 and 5140 alloy steels of Fig. 46 at a test frequency of 5 c.p.s. (*f.* 47) ... 50
- Effects of stress relief by annealing ... 50
  - Spread bands of 4140 and 5140 alloy steels at a test frequency of 60 c.p.s. after stress-relief annealing (*f.* 48) ... 51
  - Spread bands of annealed 4140 and 5140 alloy steels of Fig. 48, but with a test frequency of 5 c.p.s. (*f.* 49) ... 51
- Separation of drawn, annealed, and tempered carbon steel ... 52
  - Spread bands of C1034 carbon steel for three conditions: cold-drawn, annealed, and tempered (*f.* 50) ... 52
  - Three spread bands of C1034 steel for three tensile strength groups: 74,500 to 79,000, 83,000 to 87,500, and 90,000 to 100,000 p.s.i. (*f.* 51) ... 53
  - Evaluation of Fig. 51, showing measured tensile strength values as a function of the Magnatest Q slit value (*f.* 52) ... 54
- Slit indications for quantitative measurements ... 53

CONTENTS (*Continued*)

PAGE

Sorting for tensile strengths 54
(a) Spread band of C1036 carbon steel at various tensile strength steps. (b) Results of Magnatest Q sorting (*f.* 53) ... 55
Forged parts 54
Sorting for tensile strength of support levers of tempered C1040 carbon steel (*f.* 54) 56
Sorting of the parts from Fig. 54 for tensile strength, where the small journal of the support lever is in the test coil (*f.* 55) 56
Testing of large crankshafts for correct metallurgical condition of the journals (*f.* 56) 57
Screen picture of drop-forged parts of C1034 carbon steel hardened (bottom curve) and annealed for various tensile strengths (*f.* 57) 57
Hardness testing of ball and roller bearings 58
Spread bands of ball-bearing steel (ball-bearing rings) hardened and annealed at various temperatures (*f.* 58) 58
Measurement of case depth on case-hardened production parts 58
Magnatest Q spread bands of case-hardened valve stems, which were case-hardened for 8, 12, and 16 hr. to obtain various depths of case (*f.* 59).......... 59
Use of probe and yoke coils 59
Valve stems 59
Magnatest Q spread bands of valves with various depths of case (*f.* 60) 60
Applications in materials research 60
Aging of Thomas steel 60
Results of age-hardening experiments on Thomas steel (*f.* 61) 61
Plastic flow of steel during tensile tests . .. 60

Crack Testing of Steel

Principle of operation 61
Separation of crack and stress effects 61
Analysis of screen patterns 62
Multiple-exposure picture of curves appearing on screen when a rod with inhomogeneous stresses passes through the test coil of the Magnatest D instrument (*f.* 62) 62
Multiple-exposure picture of a rod with cracks (*f.* 63) 63
Interpretation of crack indications 62
Indications of sound rod 62
Analysis of sound test rod (*f.* 64) . . 64
Indications of defective rod 63
Analysis of cracked rod (*f.* 65) 65
Indications of fine crack 68
Analysis of fine crack (*f.* 66) 66
Indications of short defects 68
Analysis of short discontinuities (*f.* 67).. 67
Crack-test equipment installation 69
Special applications of eddy current methods 69
References 69

SECTION 42

EDDY CURRENT TEST INDICATIONS

Range of Test Applications

SIGNIFICANCE OF TEST METHOD. The basic theory of eddy current testing and design measures used in the test instruments have been discussed in the preceding sections on eddy current tests. By the means described in these sections the **eddy current method** was developed to a quantitative measurement method which permits the magnitude of an effect to be determined from the test indication. In the same manner in which the electrical conductivity of a material can be obtained from the indication of a Thomson bridge and the dimensions of a test rod, the value of the specific conductivity of a material can be determined from the indication of an eddy current instrument, from the test frequency and the diameter of the test cylinder. (See sections on Eddy Current Test Principles and on Eddy Current Cylinder Tests for a more complete discussion of theory and methods of measurement.)

If slight variations of the conductivity or the diameter of the test body have to be detected, the **sensitivity** and **accuracy** of the eddy current method is far superior to the normal, classical bridge methods. Even a variation of 10^{-5} in the diameter or electrical conductivity results in a noticeable deflection. The significance of the eddy current method is especially obvious if one realizes that these measurement values are obtained without direct contact while the test object passes through the test coil at high speed. The physical material properties, such as electrical conductivity, permeability, coercive force, and magnetic saturation, which are determined by the eddy current method, characterize the test part in many ways.

Significance of Electrical Conductivity. The electrical conductivity is an important indication of the condition of nonferrous metals; for example, of the **purity of unalloyed metals.** The magnitude of the electrical conductivity is of significance especially for the electrical industry. For **age-hardenable aluminum and titanium** alloys, the electrical conductivity is a measure of hardness. **Mixed alloys** can often be sorted by conductivity measurements. **Segregation effects** can frequently be indicated by the curve of the conductivity over an entire metal block.

Significance of Hysteresis Loop Characteristics. For ferromagnetic alloys the characteristic values of the hysteresis loop give important information concerning the composition and the structural condition. Relationships between the magnetic and the mechanical properties of materials were discovered long ago. By 1889 Hughes had applied a magnetic method for **separating hard and soft steel parts** from each other.[57] Three years earlier, Ryder applied for an American patent for the determination of **carbon content** in iron by measuring the permeability.[76] The American Society for Testing Materials established a Committee on Magnetic Analysis in 1917. The work of this committee was concerned with:

1. Testing steel qualities.[10]
2. Testing of ball-bearing races.[77]
3. Testing of the relationship between mechanical and magnetic behavior of cast iron.[86]

Significance of Impedance Characteristics. However, only modern electronic techniques can subject electrical and magnetic properties of materials to 100 percent, nondestructive quality sorting. Only recently has it been possible to resolve the influence of the electrical and magnetic material properties on the impedance characteristics of a test coil whose electromagnetic field reacts on the test object. The eddy current methods permit one to obtain, for an unknown test object and an unknown test coil, the frequency ratio f/f_g and the number N, the percentage of the "absolute value" per inch of instrument deflection. If the instrument frequency is known, then one obtains the value of the electrical conductivity directly from $f/f_g = f\sigma d^2/5066$. Furthermore, as a result of the basic analyses given in the preceding sections on eddy current tests, one can state (for each sensitivity step of the instrument) how large the **instrument deflection** is for a conductivity variation of 1 percent, a diameter variation of 1 percent, and for a crack of a given depth. These characteristics make the instruments discussed in the section on Eddy Current Test Equipment a quantitative measurement method.

NONCONTACTING DIMENSIONAL CONTROLS. Fig. 1 shows diameter variations of a rod of an AlCuMg alloy, which were recorded with the Sigmaflux instrument (American designation, Magnatest FW-300). Diameters of the rod measured with a micrometer are plotted below the recorded curve. The

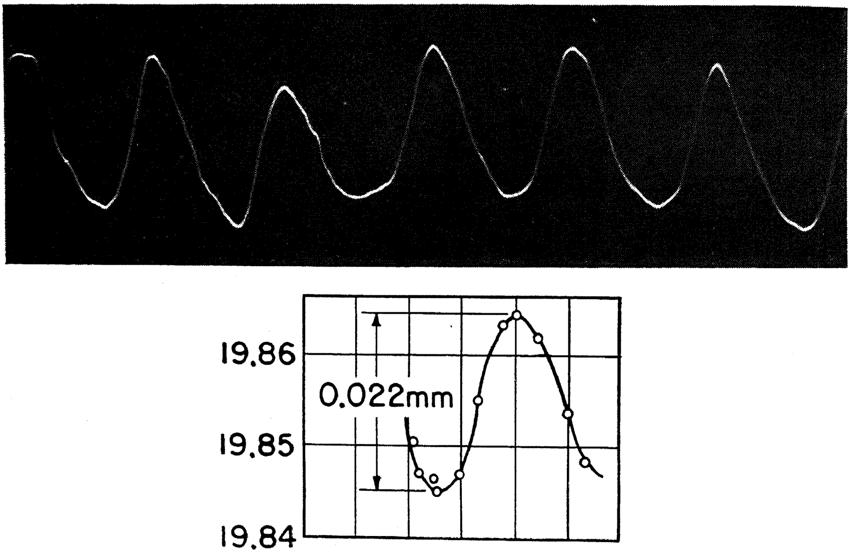

Institut Dr. Foerster

Fig. 1. Diameter variations of a rod of nonferrous metal, recorded while the rod is passed without contact through the Foerster Sigmaflux instrument (American designation, Magnatest FW-300).

measurement results obtained with the eddy current method can be checked by means of micrometer measurements in each case.

The nondestructively obtained recorder curves of the **diameter of semi-finished parts** which originated from various metal plants permit an accurate identification of the producer. Each producer has its special dimensional characteristics, which permit one to draw conclusions concerning the production process. The recording of the dimension of a wire during drawing continuously and quantitatively indicates the **wear of drawing tools.** For tungsten and molybdenum wires with ground surfaces, **periodic diameter variations** resulting from incomplete grinding processes are clearly indicated by the eddy current method. In **tensile testing** of metal rods, the cross-sectional variation during elongation of the rod can be measured quantitatively with high sensitivity by the eddy current method. The Poisson ratio is obtained from the elongation and decrease in cross-section. Production parts can be sorted according to dimension with the Multitest instrument, independent of the material.

With the inside coil one can quantitatively determine the inside diameter of the tube without dependence on the test material. The **detection of corrosion** on the inside diameter of a tube using an inside coil gives the same indication as an increase in tube inside diameter.

MEASUREMENT OF ELECTRICAL CONDUCTIVITY WITH A FEED-THROUGH COIL. The Sigmaflux instrument (American designation, Magnatest FW-300) is used for the sorting of semi-finished parts for electrical conductivity and thus for alloy. There are relatively few nonferrous alloys whose conductivities overlap, so that in most cases the conductivity is representative for the alloy (see Fig. 12).

Light Alloys. In the continuously quenched aluminum and magnesium alloys, soft spots can appear in the semi-finished parts as a result of faulty water flow, steam bubbles, etc. These areas can be detected satisfactorily because of their conductivity variations. Measurement of electrical conductivity while wire or rod

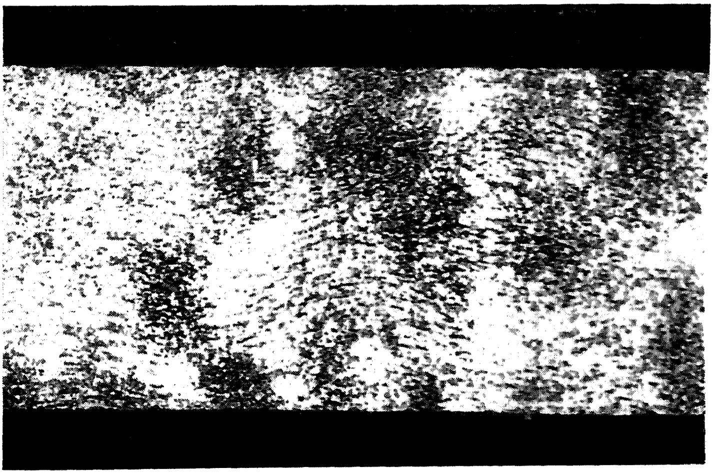

Institut Dr. Foerster

Fig. 2. Wavy fiber texture of a tungsten wire, caused by excessively large steps in the swedging process.

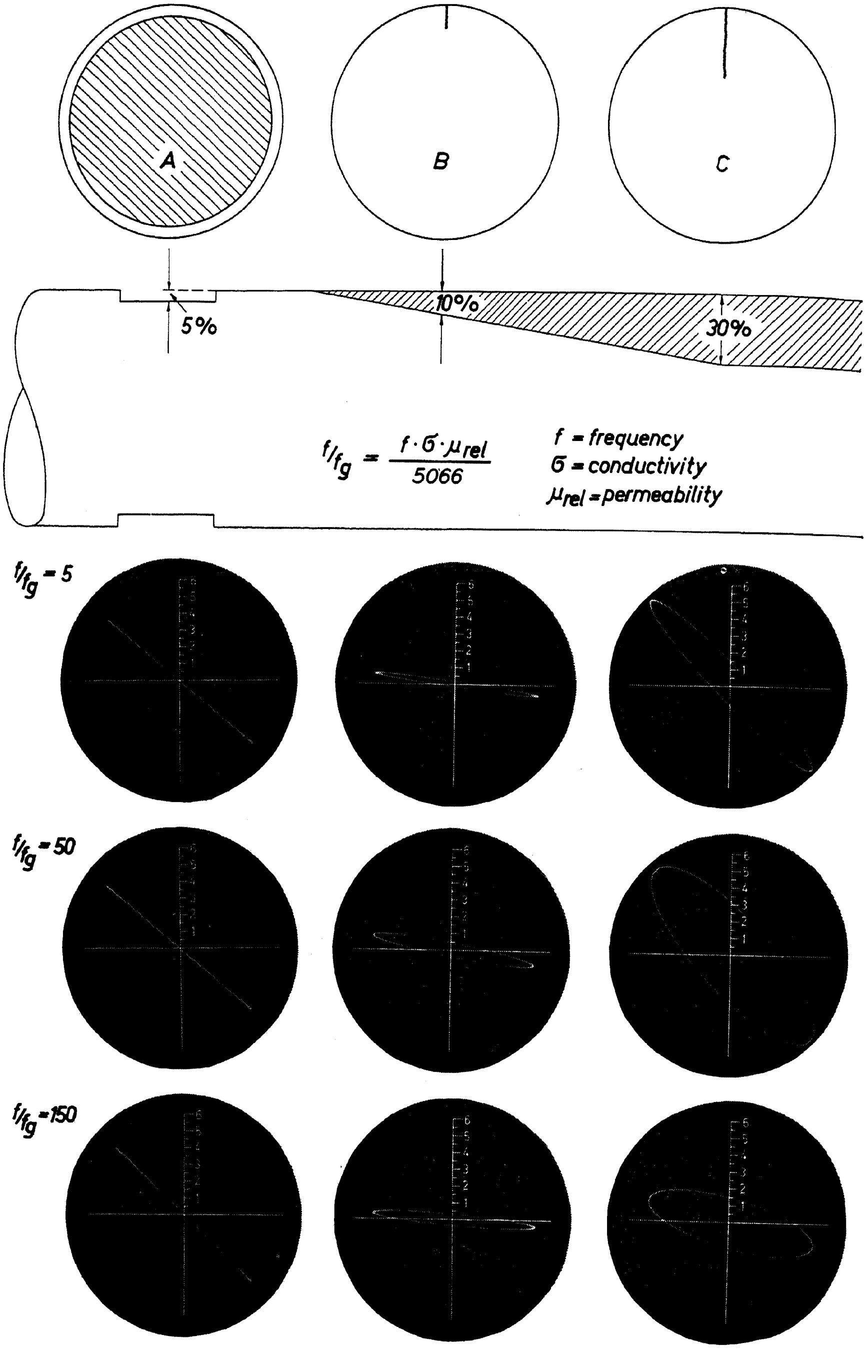

Fig. 3. Indications of the ellipse method, including test samples with decreasing

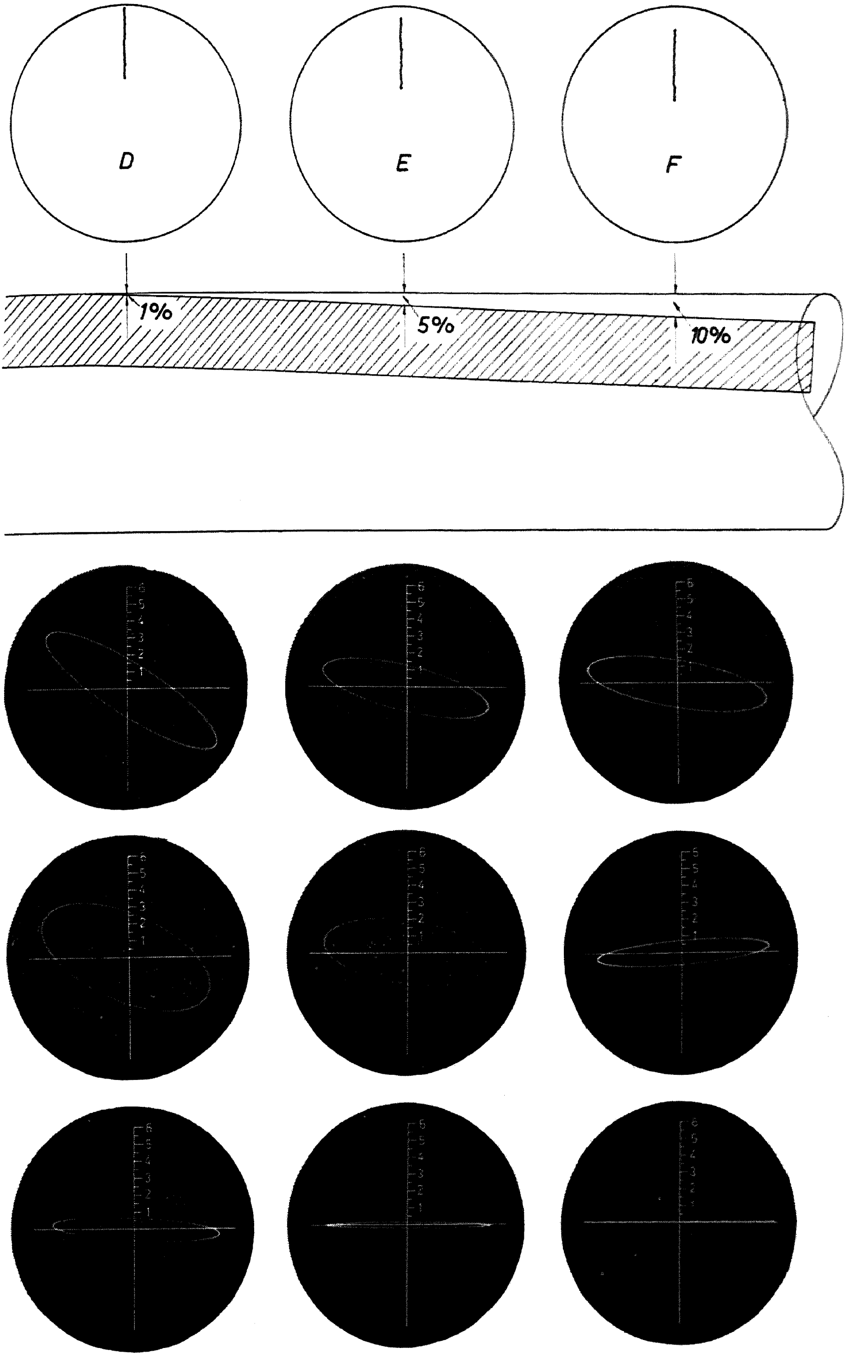

Institut Dr. Foerster

diameter and surface and subsurface cracks with increasing depth.

passes through the test coil often gives valuable clues concerning the production process. For example, rods made of cold age-hardened aluminum alloys frequently show a characteristic conductivity curve along the rod. This was found to be due to a temperature decrease along the rod during age-hardening, resulting in an undesirable hardness curve.

Tungsten Wires. In 100 percent testing of tungsten wire production, periodic conductivity variations appeared along the wire from time to time, as was determined by Keil [63]. These were indicated by a periodic opening of the straight line into an ellipse on the screen of the wire-crack test instrument. Fig. 2 shows a microsection of such a wire with a periodic conductivity variation. This was caused by the **wavy fiber texture** which resulted from excessively large steps in the swedging process or by unsuitably formed swedging jaws. The material was not uniformly distributed along the wire shown in Fig. 2. This is not an actual physical discontinuity; however, such material with a wavy fiber texture is undesirable for **electrical contacts,** since burning off under the action of sparking is influenced by the condition of the fiber texture with reference to the contact surfaces.[62] Fig. 2 is an example of how nonuniformities in the production process, which normally would not be discovered, are easily determined through nondestructive measurement of an important material factor.

CRACK TESTING WITH FEED-THROUGH COILS. Fig. 3 shows a cylinder with a local diameter decrease of 5 percent and a surface crack which increases in depth from 0 to 30 percent (percentage of the cylinder diameter). This crack disappears beneath the surface so that it finally lies 10 percent below the surface. The photographs of the **ellipse test** screen picture show the diameter decrease and the cracks with various depths and locations; below these the various effects are indicated in the ellipse method at $f/f_g = 5$, 50, and 150. The horizontal voltage is selected in the direction of the diameter so that diameter variations are represented by an inclined straight line. Fig. 3 shows that **cracks below the surface** can no longer be indicated at high f/f_g values. Furthermore it illustrates that subsurface cracks with increasing depth below the surface result in a horizontally lying ellipse, which can even tip in the opposite direction (for example, a crack of 30 percent depth, 5 percent below the surface).

The crack representation of Fig. 3 is used in the ellipse method for a given f/f_g value, along with the instrument scale deflection, to determine the depth and location of the discontinuity. It should be pointed out that the adjusted sensitivity is only 1/100 of the maximum sensitivity of the test instrument in Fig. 3. Even cracks having a depth of 1 percent of the diameter will result in an ellipse which can be readily evaluated at maximum sensitivity.

DEFECTS IN TUNGSTEN AND MOLYBDENUM WIRE. Fig. 4 shows schematically the types of gross defects in W and Mo wire which were detected over a period of years by Keil and Meyer [63] with the **wire-crack test instrument.** The defects (a), (b), and (c) are **compacting defects.** During the compacting of the metal powder before sintering, the compacting form sometimes yields and springs back after the compacting die is released. This causes the formation of **hairline cracks** in the compacted body. These cracks cannot be welded in the subsequent finishing process. Such cracks can appear along the lower edge of the die or can proceed diagonally from one edge to the other of the compacted part. In the latter case, the cracks are distorted into S-shapes during the **swedging process** [Fig. 4(b)]. Fig. 4(d) shows a lap on the rod surface. An erroneous sequence in dimensions of swedging jaws and too low swedging tempera-

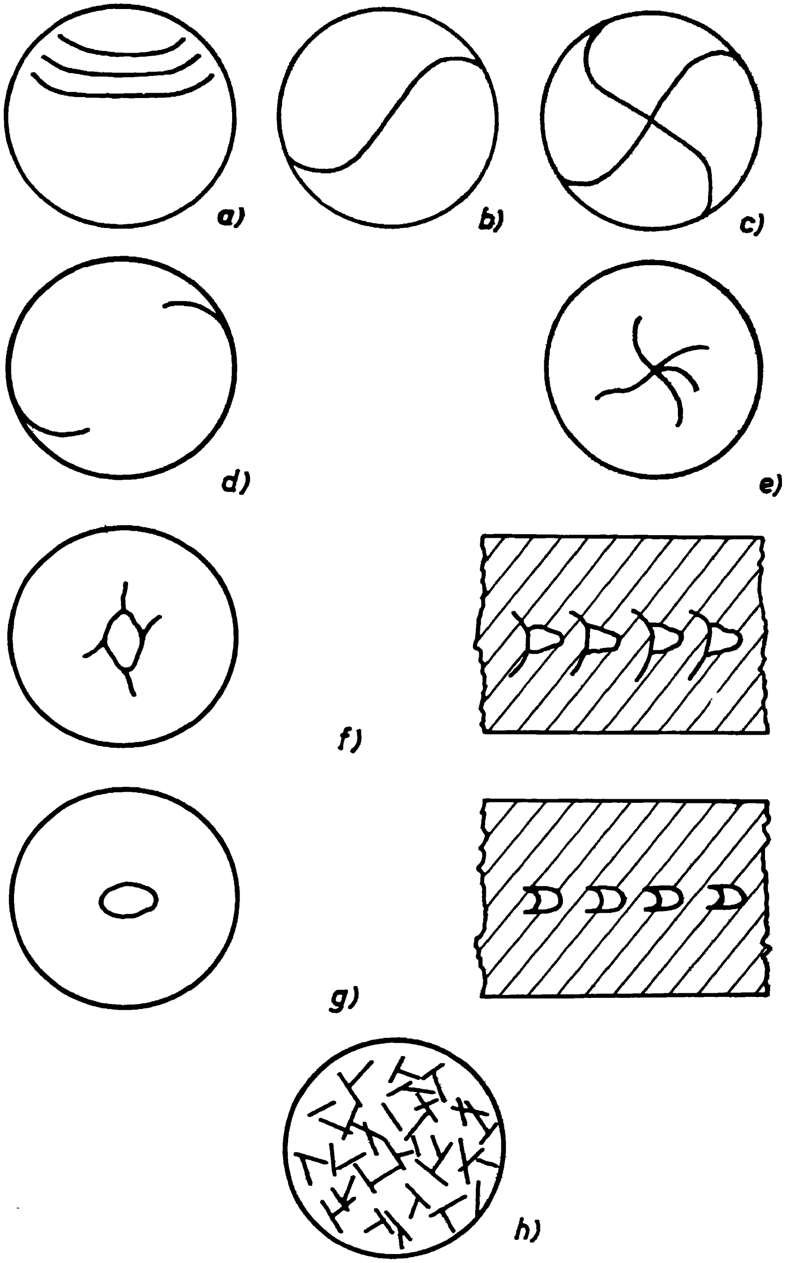

Fig. 4. Schematic representation of typical defects in tungsten rods, as detected with the Foerster wire-crack test instrument (American designation, Magnatest FW-200). (a, b, c) Compacting defects. (d) Surface lap. (e) Core splitting caused by low swedging temperature or excessive steps in the dimensions of the swedging jaws. (f) Cavities caused by incorrect swedging procedure. (g) Cavities caused by melting channels. (h) Grinding cracks.

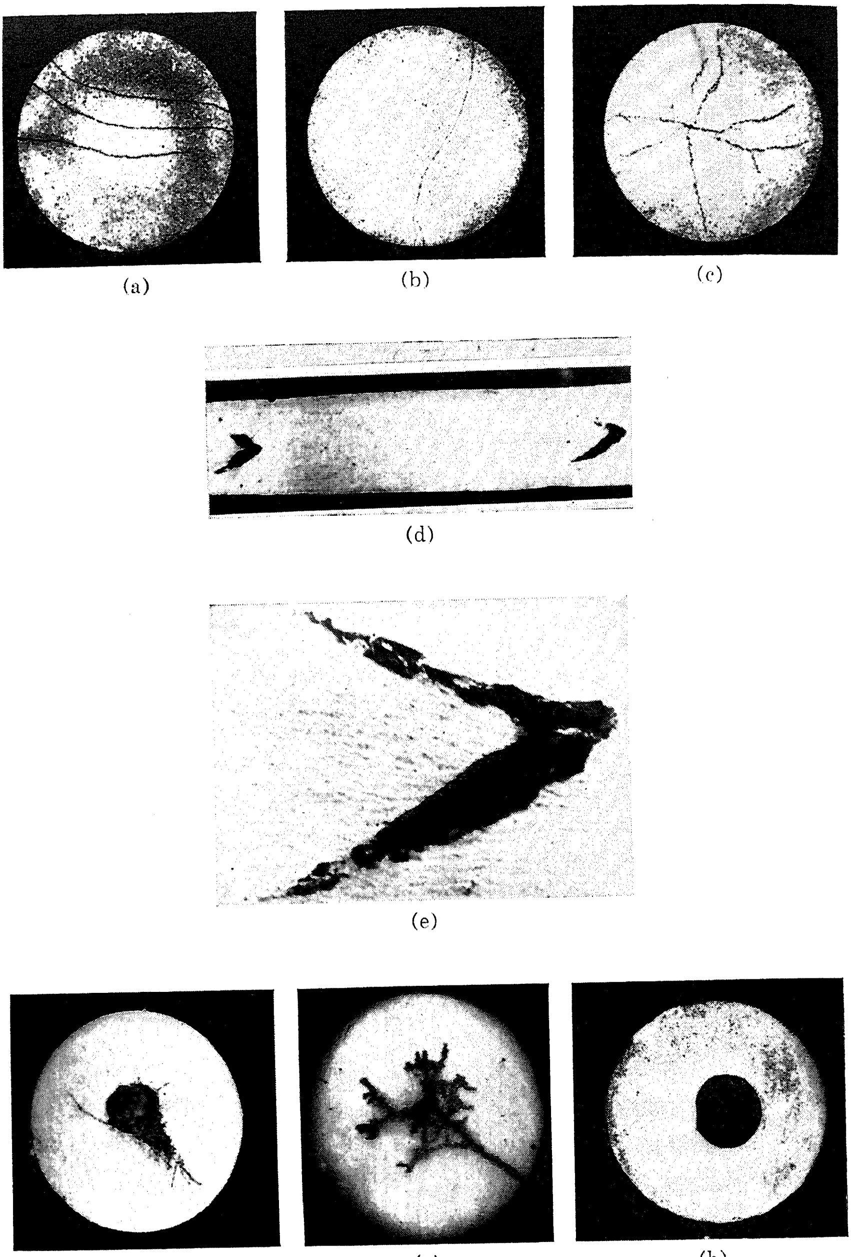

(a) (b) (c)

(d)

(e)

(f) (g) (h)

Institut Dr. Foerster

Fig. 5. Microsections of tungsten rods and wires corresponding to the schematic drawings of defects in Fig. 4. (a, b, c) Compacting defects. (d, e, f) Defects caused by too heavy swedging. (g) Defect originating from a central flaw, caused by too heavy swedging. (h) Internal melting channel.

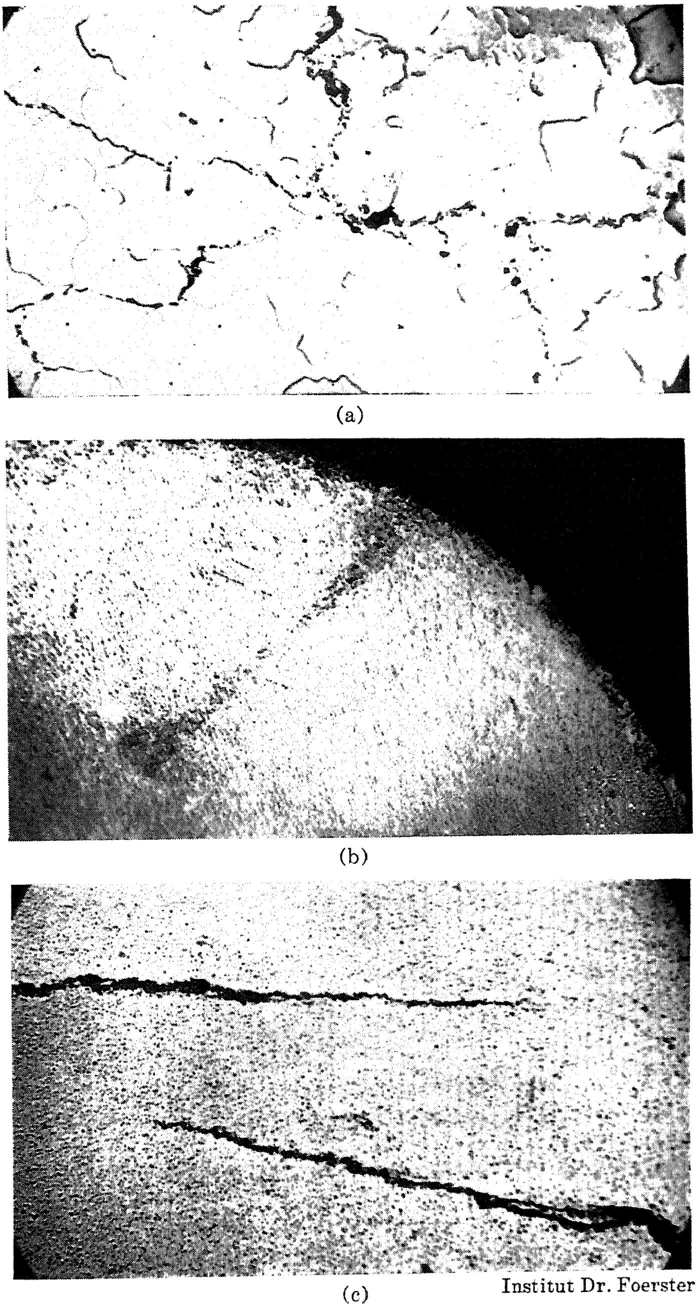

(a)

(b)

(c)

Institut Dr. Foerster

Fig. 6. Microsections from the tungsten and molybdenum industry. (a) Defective structure with holes. (b) Weak spot where a crack originates which appears during finishing of the wire in the melting furnace. (c) Cracks caused by compacting defects before sintering.

tures lead to splitting inside the rod, as shown schematically in Fig. 4(e). In extreme cases, cavities can appear according to Fig. 4(f.) Sometimes channels of local melting appear during **final sintering** and are deformed during swedging into a string of cavities, as in Fig. 4(g). The typical characteristic discontinuity caused by the swedging process, shown in Fig. 4(f), is a smooth (melted) inside surface of the cavity.

Small netlike cracks sometimes appear on **finished electrical contacts** made from material which was found to be free of defects when the rod was tested with the wire-crack test instrument. These cracks can be detected on the finished contacts by the Defectometer with probe coil. These defects are caused in the final finishing steps, either during cutting off the contact buttons or during grinding of their surfaces with insufficient cooling [see Fig. 4(h)].

Fig. 5 shows several microsections of tungsten rods and wires as proof of the defects shown schematically in Fig. 4. The natural defects in Figs. 5(a), (b), and (c) correspond to the schematic drawings of Figs. 4(a), (b), and (c). Figs. 5(d), (e), and (f) illustrate defects caused by too heavy swedging; these correspond to Fig. 4(e). Fig. 5(g) shows a crack which proceeds radially from a flaw located in the core to the outside surface. The crack itself extends along the rod even though its cause is localized in the core. Fig. 5(h) shows a defect with smooth inside surface which resulted from a melted channel and was caused during final sintering of the tungsten rod [compare with Fig. 4(g)]. Fig. 6 shows microsections of tungsten rods taken from a paper by Gromodka[53], who has employed the Foerster wire-crack test instrument in the production of tungsten and molybdenum wire. Fig. 6(a) shows a defective structure with holes through which air can enter into the vacuum envelopes for which these tungsten wires are used as **sealed-in lead wires.** Fig. 6(b) shows a defect which does not yet appear as an actual material separation but which, however, will burst open in the melting furnace during finishing of the wire. Fig. 6(c) shows the usual splits which appear as a result of **compacting defects** before sintering. The preceding Figs. 3 to 6 are examples of how, by means of 100 percent nondestructive crack testing, defects are not only sorted out but also how, by means of a systematic evaluation of the defect phenomena, the defect causes can be discovered and thus be largely eliminated from the production process.

The Sigmaflux eddy current instruments and the rod-crack test instrument have been used in various branches of the European metal industry for systematic defect analyses in other materials. Rods, wires, tubes, and shapes of materials such as copper, aluminum, light metal alloys, brass, bronze, German silver, and stainless steel have been tested with these instruments. Important shipments of semi-finished parts are frequently given 100 percent tests in the European metal industry.

Conductivity Measurements

APPLICATION OF THE PROBE COIL METHOD. The probe coil method for conductivity measurement of metals of all shapes was introduced to industry in 1939. Before the suppression of the lift-off effect of the test coil in the instrument indication, this method could be used for smooth metal surfaces only in rare cases. After the suppression of the lift-off effect in 1941,[44, 45] the application range of the Sigmatest instrument increased rapidly. By 1944 many hundreds of these probe coil instruments, which contained only one electronic tube, were used in industry. Today, the Sigmatest instrument in its improved design is the most widely used eddy current method in industry.

The Sigmatest probe coil instrument is used in industry for the following tests:

1. Determination of the electrical conductivity of parts, made of copper, aluminum and their alloys, for the electrical industry and determination of the degree of purity of metals.
2. Sorting of mixed metallic alloys.
3. Hardness measurement on alloys whose hardness exhibits an unequivocal relationship with the electrical conductivity.

PROBE COIL TEST PROCEDURE. For a conductivity test the probe coil is placed on the part to be tested, as shown in Fig. 7, which results in a deflection of the pointer on the meter. The large **conductivity scale** of the test instrument is calibrated in conductivity units, i.e., either in meter per ohm-mm.^{2} or in percentage IACS (International Annealed Copper Standard). The control knob is adjusted until the pointer of the indicating instrument rests at the zero point in the center of the scale. Now the absolute value of the electrical conductivity can be read directly on the large conductivity scale. Thus the electrical conductivity can be measured within a few seconds. Only a flat surface on the part, of 0.4-in. maximum diameter, is required to be accessible.

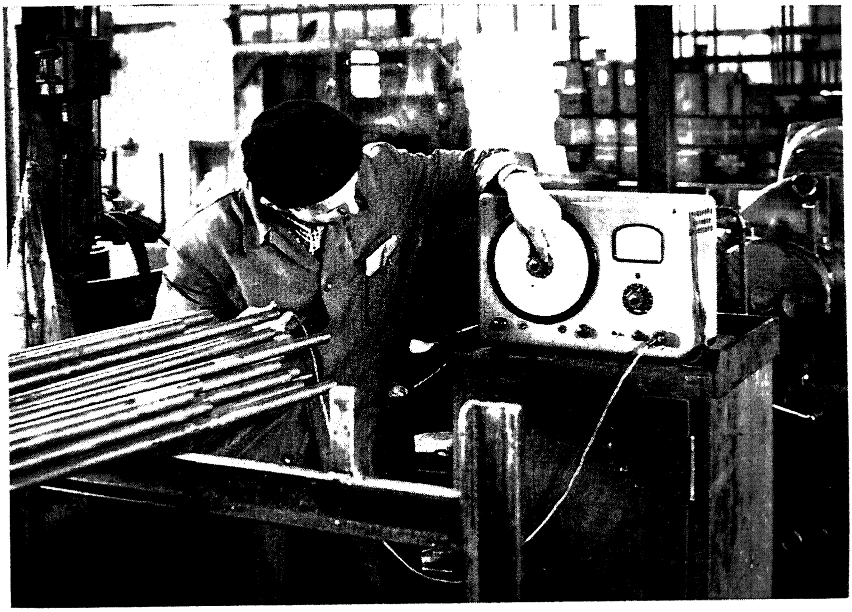

Institut Dr. Foerster

Fig. 7. Testing rods of mixed alloys by applying the probe coil of Foerster Sigmatest to the rod ends.

In addition to determination of the electrical conductivity, the deflection method is used for the rapid sorting by conductivity (i.e., for hardness, purity, alloy). For this the pointer of the meter is adjusted to zero for the average value of the interesting conductivity range. When the electrical conductivity deviates from this average value, a deflection is obtained either in the positive or negative direction, according to the increase or decrease in conductivity from the value which results in a zero deflection. By means of the sensitivity control, one can select the sensitivity so that a specific deflection (for example, ten scale divisions) is obtained, in case of an electrical conductivity variation of 1, 5, or 10 percent IACS. Sorting can be carried out rapidly because one will observe only the deflection of the meter when the probe coil is placed on the part, which requires approximately 1 sec. Thus it is possible to sort production parts according to conductivity with a speed of about 1500 to 3000 measurements per hour, obtaining the conductivity value for each individual part.

If one selects a low sensitivity, the entire conductivity range can be contracted on the scale of the zero meter. This is of significance, for example, for a **rapid scrap sorting** when alloys which cover a very large conductivity range must be separated from each other and sorted according to alloy groups.

In **hardness testing** the sensitivity can be adjusted so that a positive or negative deflection of one scale division corresponds to a hardness variation of one Brinell unit, for example.

CONTROL OF COPPER CASTINGS. The determination of the electrical conductivity is of special significance to the producers of copper or aluminum wire conductors. The minimum permissible **conductivity of copper wires** in the annealed and hard-drawn conditions is specified by the electrical industry. To maintain these values, the copper must be free of additives. The great influence of small amounts of other metals on the conductivity of copper was investigated and has been reported in numerous papers.[58] Fig. 8 shows the decrease in conductivity of copper as a result of various impurities. The Sigmatest instrument saves time and money in testing the degree of purity of metals, since the conductivity can be determined on small solidified samples of the melt, while the melt itself is still in the refining furnace.

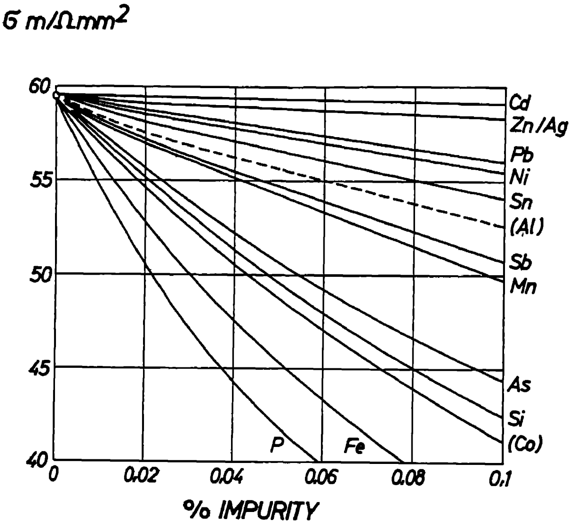

Fig. 8. Decrease in conductivity of copper, caused by various impurities.

Phosphorus Content. A specific phosphorus content is desirable in order to obtain a satisfactory pourability of copper for casting. Soft copper, before the addition of phosphorus, has a conductivity between 51 and 55 meters per ohm-mm.², while the conductivity decreases to between 49 and 41 meters per ohm-mm.² after a phosphorus addition of between 0.018 to 0.038 percent. This can be determined within a short time with the test coil instrument on small **melt samples.** The testing, including taking of the liquid sample, requires only 2 to 3 min. Thus phosphorus can be added to the liquid melt until the desired conductivity is obtained. This method is not limited to copper casting only but can also be used for alloys which contain a high amount of copper; for example, **conductive bronze** with tin, silicon, or cadmium, and lead-bronze.

Oxygen Content. Furthermore the probe coil instrument of Fig. 7 is used for the purely operational determination of the oxygen content in **oxidizing melting of copper,** since the conductivity of copper decreases with increasing oxygen content.[9] After completion of the oxidizing melting period, the melter has an approximate idea of the oxygen content, and he can measure the amount of reducing agents to be added from the result of the conductivity measurement of the sample drawn out from the melt. Fig. 9 shows the conductivity increase after deoxidation and the conductivity decrease following further phosphorus-copper additions. The conductivity values (ordinate of Fig. 9) give indications of possible impurities, so that corrections can be made before casting. The progress of the melting-loss of the additives which are to be removed can be controlled by drawing samples continuously during the refining process.

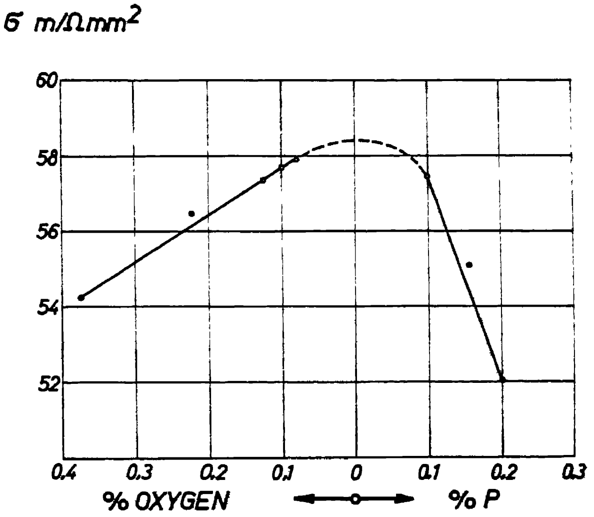

Fig. 9. Variation of the conductivity during deoxidation of a copper melt.[9]

Electrical Conductivity. The Sigmatest instrument is also used for the testing of highly conductive copper rings for squirrel-cage induction motors. For these rings the customer requires a conductivity of 98 percent IACS (56.8 meters per ohm-mm.²). The fulfilment of the requirement can be determined nondestructively within seconds on finished **squirrel-cage motors.**

In British plants, copper blocks (melted in their own plants as well as in other plants) are tested for conductivity with the Sigmatest in order to eliminate those which do not meet the British specifications for copper conductivity.[51] It is of significance that the test speed of 100 blocks in 3 min. is limited only by the transport of the block sections.

CONTROL OF ALUMINUM CASTINGS. The degree of purity of aluminum can be tested analogously. Fig. 10 shows the influence of metallic additives on the **conductivity of aluminum.** Even in aluminum foundries there exists a desire to test the cast block for its suitability for use in wires made according to the technical requirements for minimum conductivity. The Sigmatest permits the determination of the conductivity instantly on drawn samples of very small dimensions. In this manner the conductivity can be determined on analysis samples drawn during casting. In order to produce a uniform reference structure, these materials are precipitation-hardened for 4 hr. at 350° C.

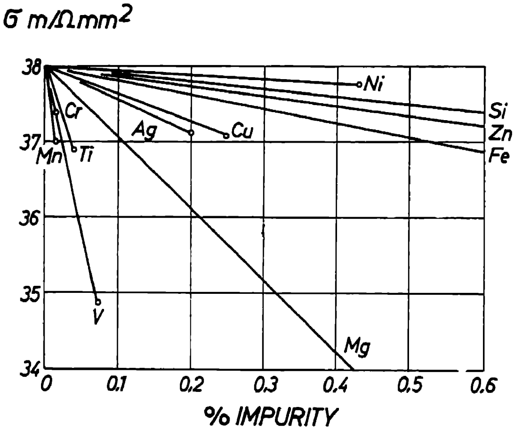

Fig. 10. Influence of metallic additives on the conductivity of aluminum.

Such conductivity measurements were carried out in a plant on a large number of aluminum samples drawn from the melts, and the conductivity values so obtained were compared with the conductivity of both **pressed wires** and **hard-drawn wires.** It was thus determined that the conductivity of the cast metal in the heterogeneous state was lower than that for pressed and precipitation-hardened wires from this block, by only 0.2 meter per ohm-mm.² maximum. By means of these results, one can draw conclusions from the measurements on cast analysis samples concerning the electrical conductivity of the wires produced later.

Silicon Content. Impurities in aluminum often include iron and silicon. The conductivity of aluminum is influenced only slightly by iron because of its low solubility.[72] Silicon, however, which is soluble to 1.65 percent in aluminum at the **eutectic temperature** (578° C.), results in a large decrease in conductivity from pure aluminum. In the range above 0.15 percent silicon, an approximately linear relationship exists between concentration and conductivity. Therefore the Sigmatest is used in industry continuously for the testing of the degree of purity of aluminum.[83]

Determination of Segregation. Fig. 11(a) shows the variation in conductivity as a result of segregation in a cast block of AlCuMg alloy. The test was carried out after the rough surface had been removed, in order to have a sufficiently flat test surface for the Sigmatest coil. During scanning of the cross-section, a picture of the segregation zone was obtained. A subsequent chemical analysis showed that the conductivity curve was influenced essentially by the **copper segregation,** Fig. 11(b). In any case, the Sigmatest instrument is a simple means of determining the extent of segregation by scanning a block only once.

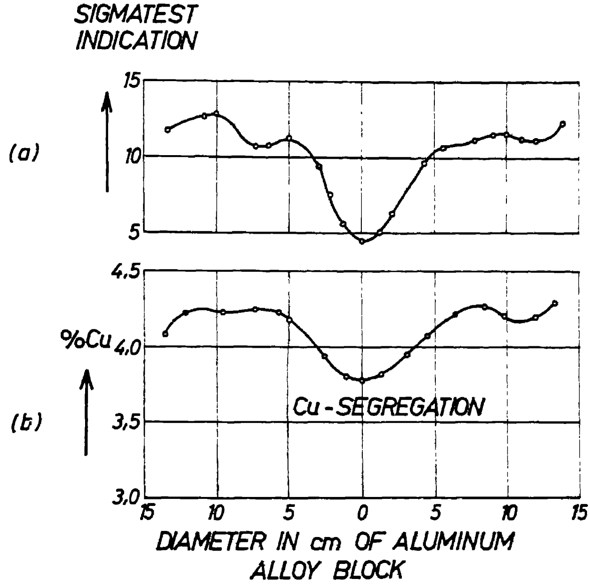

Fig. 11. Conductivity variation caused by segregation in a cast block of AlCuMg alloy. (a) Variation in conductivity due to segregation. (b) Percentage of copper segregation.

TESTING OF MIXED ALLOYS. Various alloys can be separated reliably with the Sigmatest when the mixed materials exhibit differences in conductivities. The conductivities of numerous alloys are given in Fig. 12. For each metal, and especially for each alloy, a specific **spread range** exists which is caused by impurities in pure metals; in alloys, by the permissible variation in the percentage content of the alloy elements.

Because of the large number of different alloys, the same conductivity values sometimes appear for different materials. In such cases other characteristics can be used for separation. In **scrap sorting,** the color, type of finish, and appearance of fractured pieces are additional characteristics. In doubtful cases, the specific gravity and the corrosion test, or the hardness, give an indication. For heavy metals, only special brass and bronzes may exhibit the same conductivity, while there are several overlaps for light metal alloys.

Austenitic Stainless Steels. Recently, Sigmatest instruments have been increasingly used for the sorting of austenitic steels (stainless steels). For this purpose a Sigmatest was developed with a conductivity range of from 0.5 to 6 meters per ohm-mm.^{2}. The absolute value of the conductivity can be determined for stainless steel only when the material is not magnetic; i.e., when the **permeability**

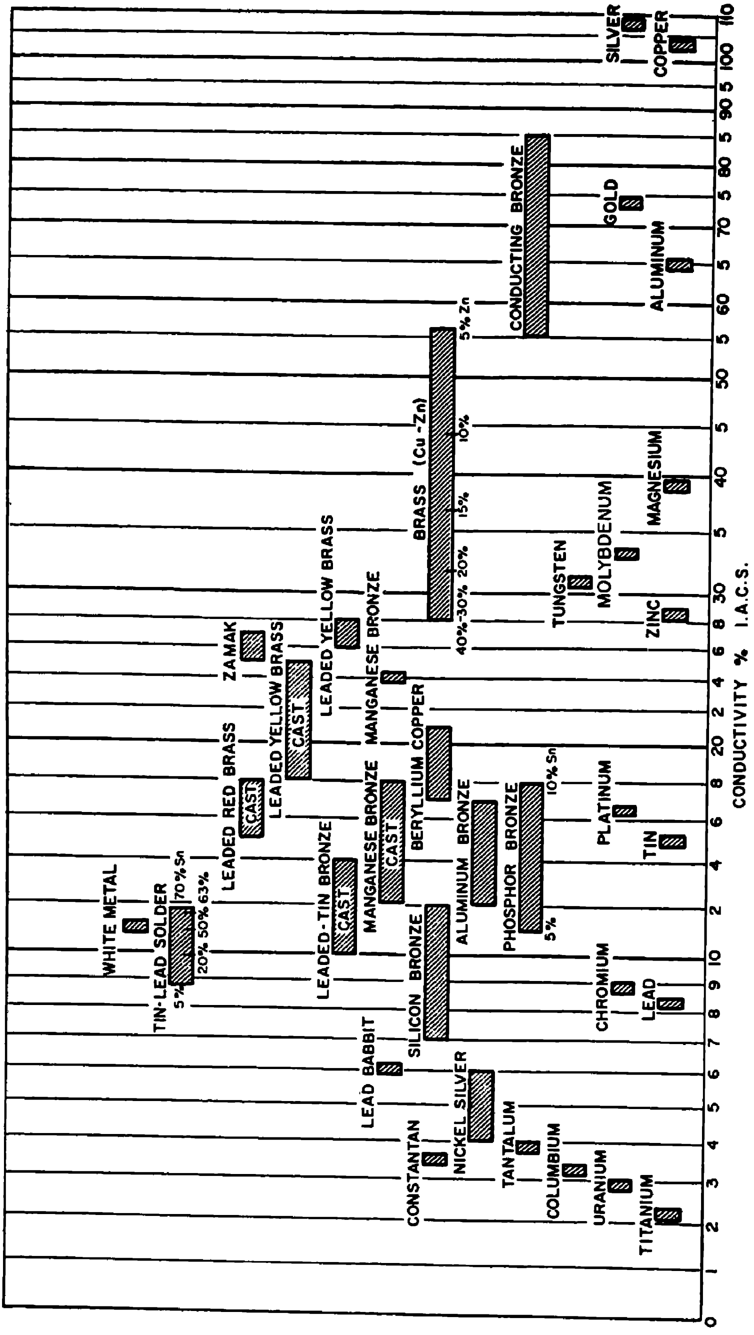
SILVER
COPPER
CONDUCTING BRONZE
GOLD
ALUMINUM
5% Zn
BRASS (Cu-Zn)
10%
15%
20%
40%-30%
MAGNESIUM
MOLYBDENUM
TUNGSTEN
ZINC
LEADED YELLOW BRASS
ZAMAK
LEADED YELLOW BRASS CAST
MANGANESE BRONZE
LEADED RED BRASS CAST
BERYLLIUM COPPER
MANGANESE BRONZE CAST
LEADED-TIN BRONZE CAST
ALUMINUM BRONZE
PHOSPHOR BRONZE
10% Sn
5%
PLATINUM
TIN
WHITE METAL
TIN-LEAD SOLDER
70% Sn
63%
50%
20%
5%
SILICON BRONZE
CHROMIUM
LEAD
LEAD BABBIT
NICKEL SILVER
CONSTANTAN
TANTALUM
COLUMBIUM
URANIUM
TITANIUM
0
1
2
3
4
5
6
7
8
9
10
2
4
6
8
20
2
4
6
8
30
5
40
5
50
5
60
5
70
5
80
5
90
5
100
110
CONDUCTIVITY % I.A.C.S.

(a)

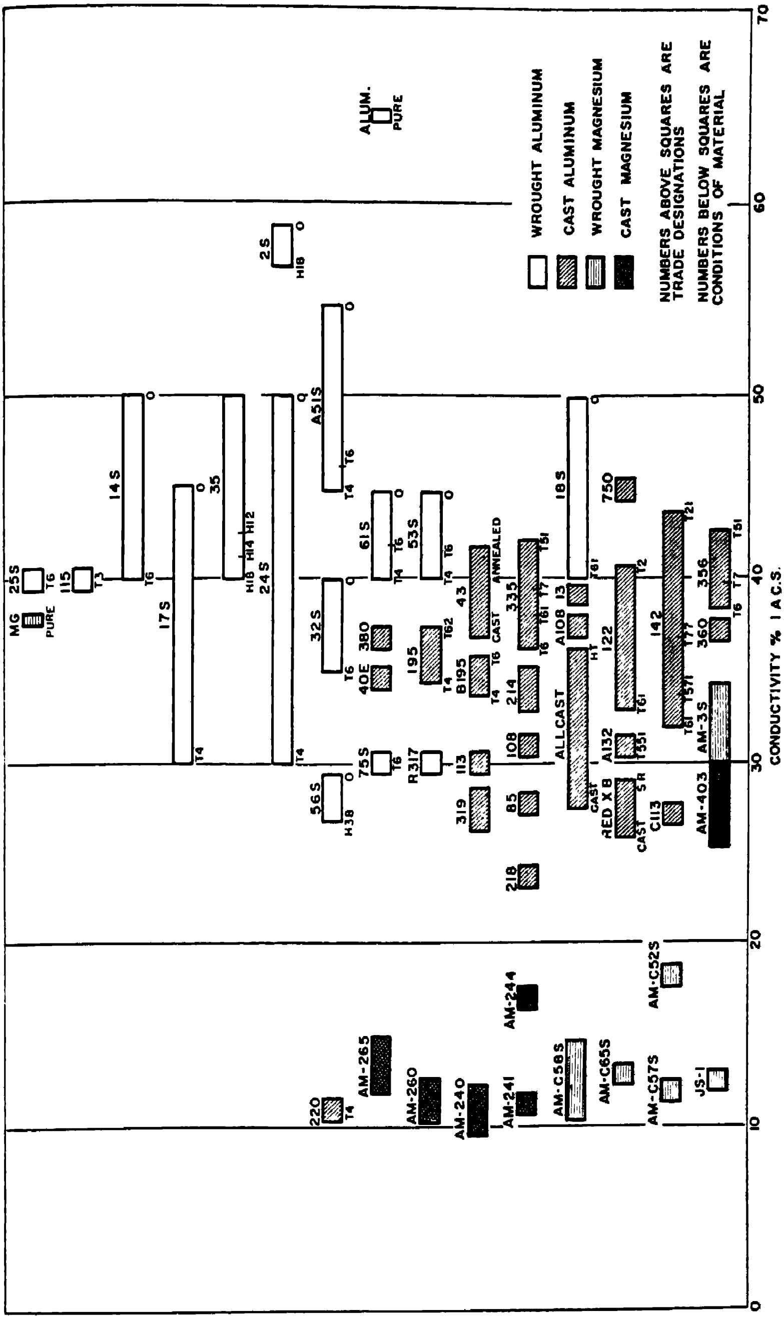

(b)

Magnaflux Corporation

Fig. 12. Electrical conductivity values for various American alloys. (*a*) Conductivity of various metals and alloys. (*b*) Conductivity of aluminum and magnesium alloys.

equals one or very nearly one. As was discussed in the theory of the probe coil method, the product of conductivity and permeability plays a decisive role. Therefore an exact measurement of the conductivity at high permeability values is no longer possible. However, since the absolute value of the conductivity is of little interest in sorting, the method has become increasingly popular, especially since it separates the strong magnetic alloys from each other very sensitively.

A large American plant uses this instrument to separate various types of high-temperature and austenitic steels from each other. **Testing of mixed lots** is carried out only in rare cases with the absolute method, i.e., by reading the actual conductivity value on the calibrated scale. Most testing of mixed materials is done with the much faster relative method, by observing the deflections on the zero meter. In these tests the sensitivity is decreased so that the measurement values of all interesting materials are still on the scale of the instrument. For **low-conductivity materials** such as graphite or carbon, a special Sigmatest instrument has been developed with a correspondingly low conductivity range.

INDIRECT HARDNESS MEASUREMENTS. The conductivity of age-hardened aluminum alloys has, according to theoretical principles, an unequivocal relationship to the hardness.[66] Thus indirect hardness measurement with the Sigmatest has become a widely used method. For the **age-hardenable alloys** of the types AlCuMg, AlMgSi, and AlMgZn in the technically interesting range of the cold age-hardenable state, there is a proportionality between hardness and conductivity. Consequently mechanical hardness tests can be replaced by a conductivity measurement. Vosskuehler[84] has clarified these relationships with the Sigmatest for the seawater-proof AlMg alloys. Fig. 13 shows how the conductivity of AlMgSi, AlCuMg, and AlMgZn alloys decreases with increasing hardness. The hardness measurement with the Sigmatest instrument has gained in significance especially in the testing of light-metal pressed parts. The test speed is many times higher than that of the Brinell test, even when more modern rapid measurement methods are used. In one metal plant, thousands of man-hours were saved by the use of only one Sigmatest instrument.

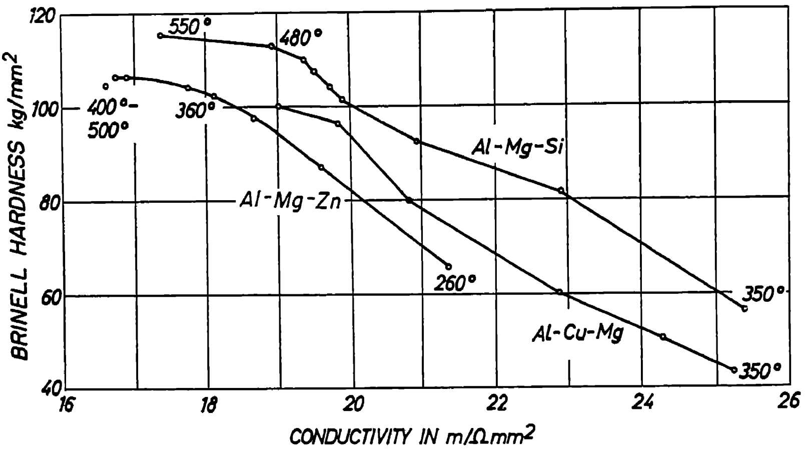

Fig. 13. Relationship between conductivity and hardness in cold age-hardened alloys.

Hardness testing is carried out with the Sigmatest instrument exclusively by the relative method. The tolerance range is adjusted on the zero meter of the instrument by means of two test parts whose hardness has been mechanically measured. The calibration is carried out for each alloy by means of two test parts with various hardnesses of each alloy to be tested.

Control of Heat Treating. Indirect hardness measurement with the eddy current instrument is used also with **overheated parts, or parts quenched at high temperature.** These can be eliminated as a result of their low conductivity. Fig. 14 shows how the conductivity of thin sheets steadily decreases with increasing quenching temperature, whereas the Brinell hardness (as well as the tensile strength and the yield point) peaks at some temperature and decreases for higher quenching temperature, so that an unequivocal relationship between the hardness and structure condition is no longer possible. Furthermore one can see in Fig. 14 that the **Brinell hardness values** spread considerably more than the conductivity values on the Sigmatest instrument. The **spread range** is indicated by the shaded area around each curve. The conductivity value measured over a specific area is more representative of the condition of the alloy than the hardness value obtained on a very small area. With Sigmatest testing, one can maintain the range of the specified **quenching temperature** (505° C. to 520° C.) and the specified hardness (125 to 145 kg. per mm.²) much more accurately than by measuring the Brinell hardness.

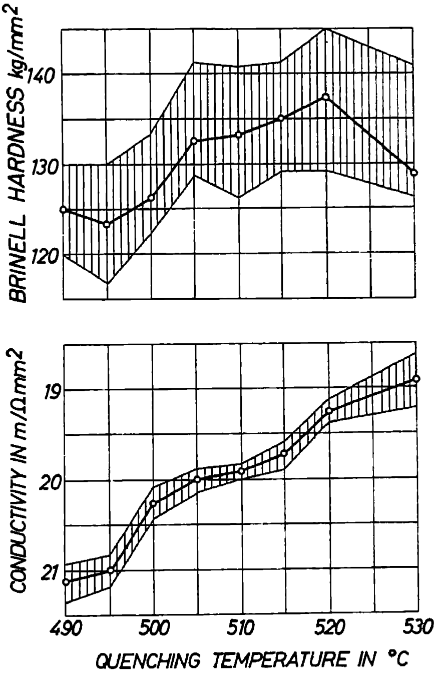

Fig. 14. Conductivity and hardness of sheets of an AlCuMg alloy.

Quench-hardened Parts. The Sigmatest is also used for controlling the uniformity of hardness on semi-finished parts (rods, sheets, extruded shapes, and tubes). When numerous semi-finished parts are quenched simultaneously, so-called **soft areas** appear occasionally if the parts are not submerged uniformly in the bath. The same defect can appear on extruded shapes which are quenched immediately after extrusion. For the separation of the extruded parts, the press-feed is turned off, and a heterogeneous area forms between the quenched portion and the portion remaining still hot. Also, an area with strongly varying hardness, as well as formation of steam bubbles, can appear because of a variable water supply.

For **testing of extruded shapes**, a search coil is moved along the extrusion. Testing the entire length of 15 meters requires less time than a single Brinell impression. A special probe coil was developed to detect soft spots quickly on large metal surfaces such as sheets. Fig. 15(a) shows the diagram which results when the probe coil moves over the sheet, where no special steps were taken for the

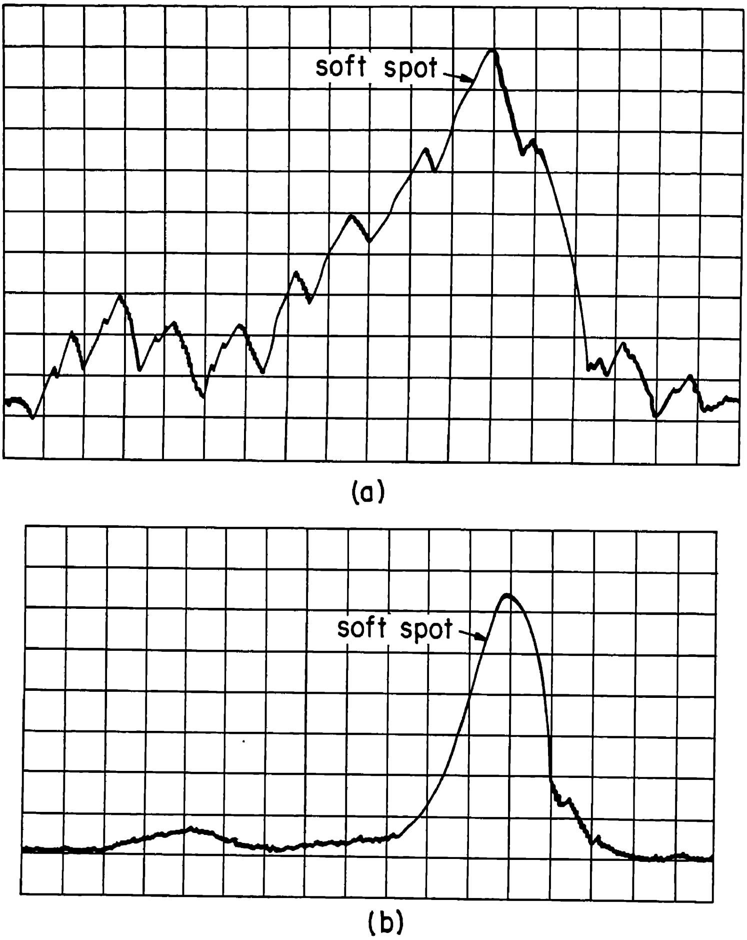

Fig. 15. Indications of a soft spot in sheet. (a) Without suppression of the lift-off effect. The periodic deflections are caused by irregular movement of the wheels of the traveling coil. (b) With suppression of the lift-off effect.

suppression of the lift-off effect. On the other hand, Fig. 15(b) shows how the large deflections are suppressed by the lift-off effect, so that only the alloy conditions such as structure or soft spots are indicated.

Titanium Alloys. Recently the Sigmatest instrument has proved successful in the hardness testing of titanium alloys, since an unequivocal relationship also exists between the electrical conductivity and the Brinell hardness.

Hysteresis-Loop Tests

QUALITY TESTING OF FERROMAGNETIC MATERIALS. The magnetic behavior of a ferromagnetic material is characterized by its magnetization curve. It is of significance that the various factors of the magnetization loop, such as saturation, remanence, coercive force, and permeability, are influenced in a different manner by the material properties such as alloy composition, structure, and internal stress.

The **magnetic saturation** is mainly a function of the chemical composition and the crystal structure, while the **coercive force,** the most important magnetic characteristic factor in eddy current testing of materials, is influenced by the following material properties:

1. Internal stress and magnetostriction.
2. Number, magnitude, and distribution (degree of dispersion) of foreign bodies embedded in or between ferromagnetic crystals.
3. Crystal energy and size of the ferromagnetic crystals.

The magnetostriction, crystal energy, saturation magnetization, and Curie point are independent of the structural condition; i.e., these factors are among the **structure-insensitive factors.** However, the coercive force, the permeability, and the Rayleigh constant are influenced by internal stress and the structural condition. Therefore, these factors belong to the **structure-sensitive magnetic characteristic factors.** The magnetic behavior depends to a larger degree on the selection of the initial materials, and the melting, foundry, rolling, and annealing processes, than any other characteristic.

Correlation Problems. From the many effects which influence the magnetic characteristic values, those which are of interest (for example, hardness or carbon content) have to be filtered out during testing by means of suitable devices. The problem of nondestructive testing with eddy current methods consists in drawing conclusions concerning properties, such as hardness, tensile strength, and the alloy content, from the magnetic and electrical values of the test body. Thus, it is necessary to investigate the following questions:

1. Which relationships exist between the mechanical properties (hardness, tensile strength, etc.), the metallurgical properties (for example, carbon content or structure), and the magnetic properties of the material?
2. How are the magnetic material values indicated in the eddy current sorting method?
3. How can test conditions be created so that specific desired properties have an optimum indication, while undesired properties are suppressed?

PRECISION DETERMINATION OF HYSTERESIS LOOPS. For the systematic investigation of the relationships of metallurgical and technological material properties, a method has been developed for the representation without distortion of the hysteresis loop of steel samples which one can easily produce from standard semi-finished parts. As is well known, only the infinitely long sample or the ring sample without magnetic poles permits representation of the hysteresis loop without distortion. After many experiments, the **tube-ring sample** shown in Fig. 16 was used as a **standard sample** (normal sample) for magnetic investigations. The sample of Fig. 16 can be produced easily on a lathe from a short piece of bar stock. For magnetizing, this sample is placed on a conducting rod (Fig. 17) which in turn is placed in a high-current fixture and through which currents flow with amplitude adjustable up to 5000 amp. at 60 c.p.s. Thus a circular magnetization without free poles is produced in the sample. The sample contains a winding for measurement of the induction. At the same time a ring coil is placed over the high-current rod for the measurement of the field strength.

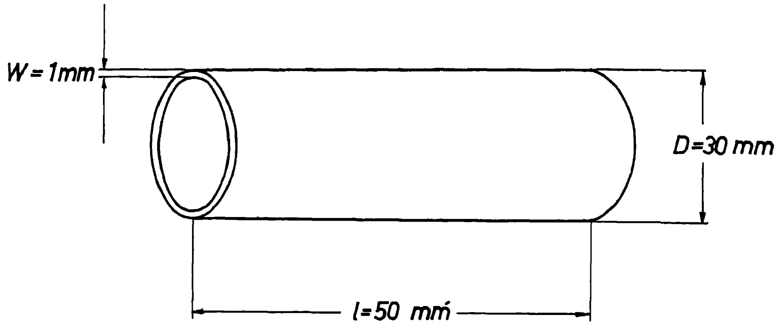

Fig. 16. Standard test object for investigating the ferromagnetic properties of a material on the Foerster Ferrograph.

The entire **distortion-free magnetization loop** appears on the screen of the

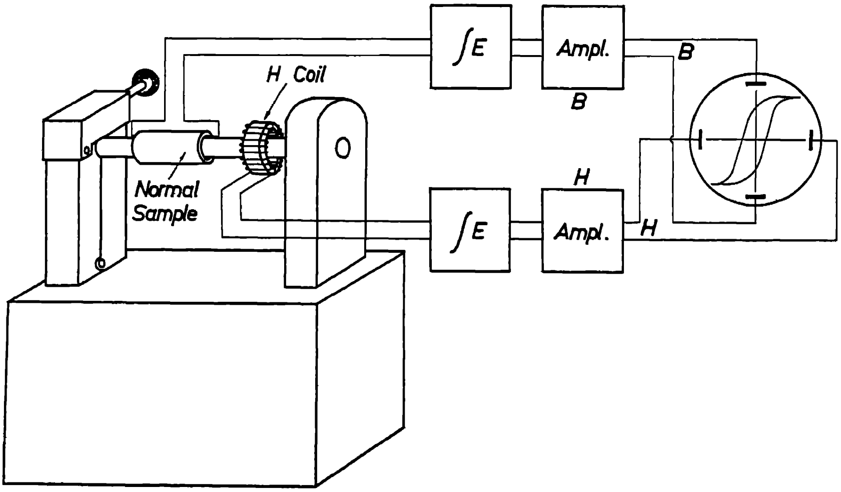

Institut Dr. Foerster

Fig. 17. Device for magnetizing standard ring samples with axial current and measurement of the field strength with the air ring coil.

Ferrograph (Fig. 18). The Ferrograph was developed especially for magnetic material investigations.[22] It possesses ten sensitivity steps on the B and H channels. For each sensitivity step, the calibration factor appears for the B channel,

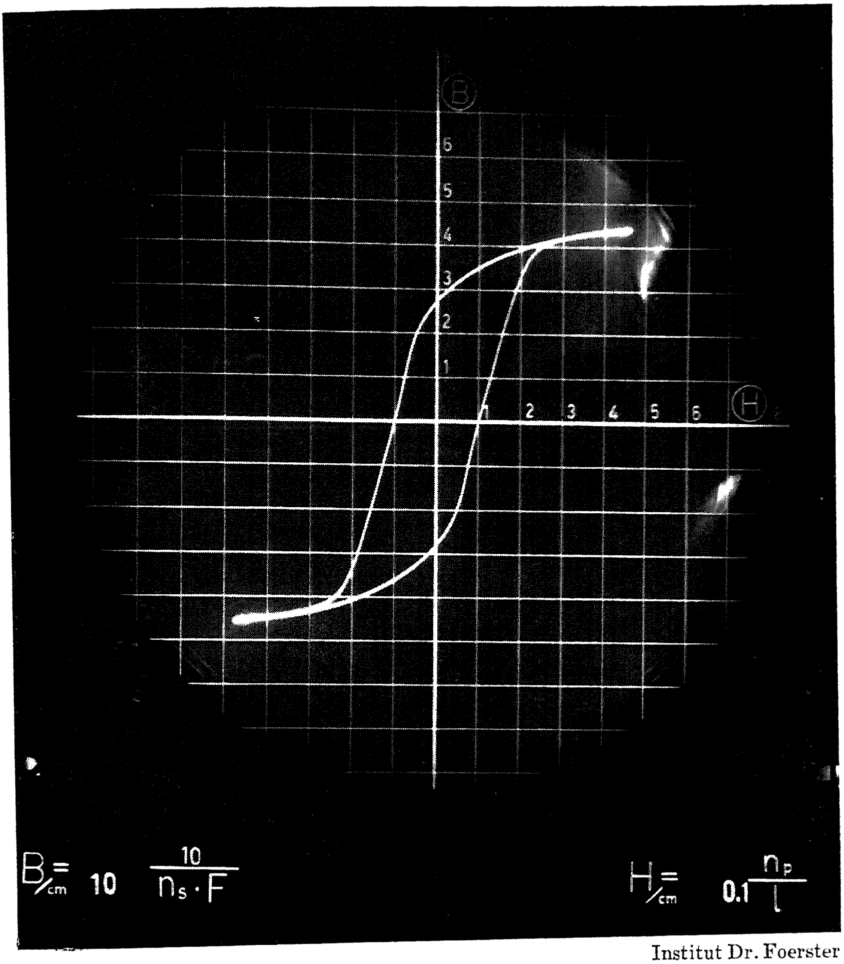

Institut Dr. Foerster

Fig. 18. Screen picture of the Ferrograph with calibration of B and H scales.

gauss per centimeter in the vertical, and for the H channel, oersted per centimeter in the horizontal. Thus, as shown in Fig. 18, all interesting data necessary for the evaluation appear in the photograph of the screen picture.

DETERMINATION OF STATIC HYSTERESIS LOOP. The static hysteresis loop at 0 c.p.s. can be obtained from the 60-c.p.s. dynamic loop in the following manner: Two **ring samples,** one right next to the other, are cut from the same rod. The dimensions of the **standard sample** (diameter D_n, length L_n and wall thickness W_n) are taken according to Fig. 16, while for the second sample the following dimensions are selected: $L = L_n/\sqrt{2} : W = W_n\sqrt{2}$. The portion of the area of the hysteresis loop which results from eddy currents (the dynamic component) increases, according to the theory of eddy currents, with the square of the wall thickness W. Thus the sample whose wall thickness is larger by $\sqrt{2}$ results in a doubling of the eddy current component of the hysteresis loop with reference to the standard sample. Fig. 19 shows superimposed screen picture of the standard sample and the sample having a $\sqrt{2}$ times larger wall thickness.

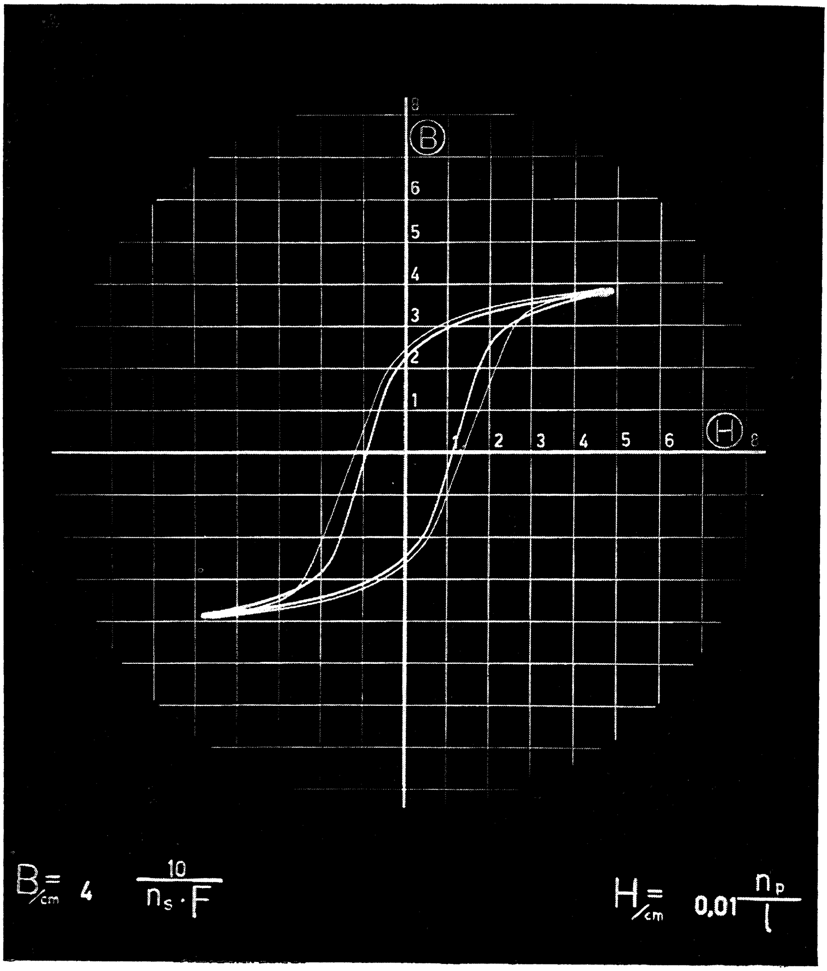

Institut Dr. Foerster

Fig. 19. Superimposed hysteresis loop of standard ring sample of Fig. 16 and sample from the same material but with a $\sqrt{2}$ larger wall thickness.

Correction for Eddy Current Effects. The portion of the area of the hysteresis loop due to eddy currents in the sample, with the $\sqrt{2}$ times larger wall thickness, is twice as large as that for the standard sample. Thus the difference between the two hysteresis areas, i.e., the area between the inside and the outside loop, represents the portion of the area due to eddy currents in the standard sample (the inside loop).

The **area** A_n of the hysteresis loop of the standard sample is given by

$$A_n = H_L + E_L \tag{1}$$

where H_L is the hysteresis loss of the static loop at $f = 0$ c.p.s. and E_L is the eddy current loss. For the sample with the $\sqrt{2}$ times greater wall thickness, a doubling of the portion of the area of the hysteresis loop results, due to eddy currents. Thus, the area of the hysteresis loop of this sample results in

$$A = H_L + 2E_L \tag{2}$$

By subtracting Eq. (1) from Eq. (2), Eq. (3) is obtained:

$$A - A_n = E_L \tag{3}$$

i.e., the strip between the inside loop and the outside loop represents the **eddy current component** of the area of the inside loop. Thus, if the strip between the inside and outside loop is subtracted from the inside loop, so that the horizontal distance of the outside loop from the inside loop is always decreased toward the inside, the static magnetization loop at $f = 0$ c.p.s. is obtained. Thus the influence of the electrical conductivity of the material on the hysteresis loop can be determined separately.

ANALYSIS OF HYSTERESIS LOOP PATTERNS. With the aid of the standard sample, the effect of the various influential factors of the hysteresis loop is illustrated by a large number of screen pictures. In the subsequent text the influence of the carbon content, the hardening process, and the internal stresses on the magnetization loop of steel will be explained by means of a qualitative description. At the same time the field strengths which permit an especially good separation of the individual material properties will be indicated.

Effects of Internal Stress. Fig. 20 shows a family of hysteresis loops for a standard sample of cold-drawn C-1015 carbon steel, while Fig. 21 illustrates the family of hysteresis loops after **annealing** to remove internal mechanical stresses. In addition to the decrease of the coercive force, it is clear that the greatest variations in the degree of magnetization of the sample, with and without stresses, appear at low field strengths. This behavior is typical, so that stresses (for example, caused by the straightening process) always result in an especially large influence on the magnetization values at low field strengths; i.e., below one-half the coercive force. At a field strength corresponding to ½ horizontal unit, the ratio of the magnetization of the stress-free sample to that of a sample with internal stresses is 5:1. Therefore, in the quality sorting of materials which also exhibit **inhomogeneous stresses** (as caused by straightening), it is necessary to work at field strengths which are higher than the coercive force.

Effects of Annealing. Fig. 22 shows the loops, photographed one on top of the other, of the standard sample of C1015 in the following conditions:

1. Annealed in C-atmosphere at 900° C. for 1 hr. and slowly cooled (upper curve).
2. Annealed in C-atmosphere at 900° C. for 1 hr. and quenched.

The recarburized and slowly-cooled sample already shows a large increase in the **coercive force,** as compared with Fig. 21. For the quenched sample, a further increase in coercive force is observed, plus the great permeability decrease.

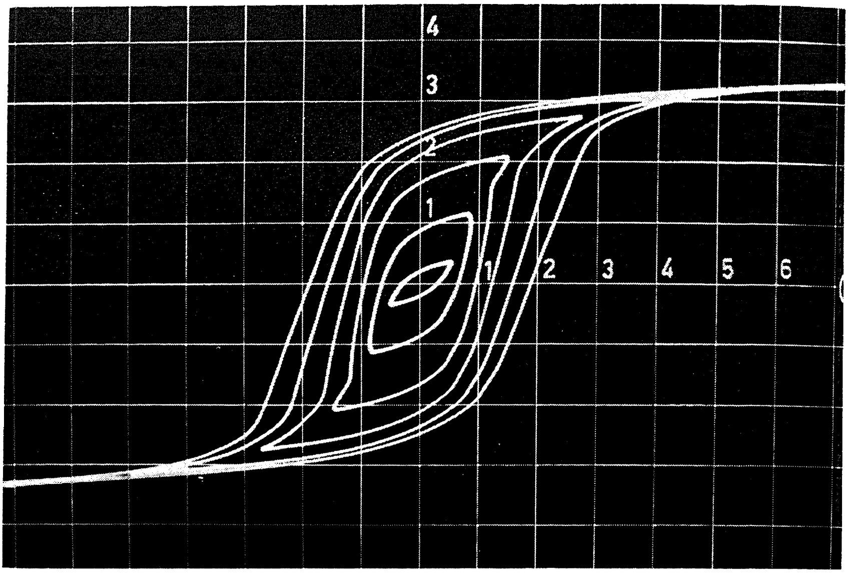

Institut Dr. Foerster

Fig. 20. Family of hysteresis loops of a normal sample of C1015 cold-drawn carbon steel.

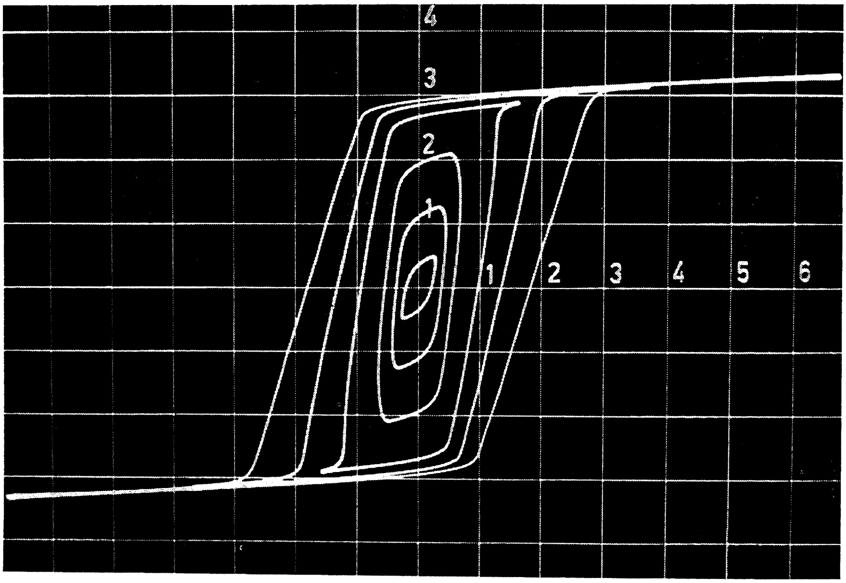

Institut Dr. Foerster

Fig. 21. Family of hysteresis loops of the normal sample from Fig. 20 but stress-relief annealed.

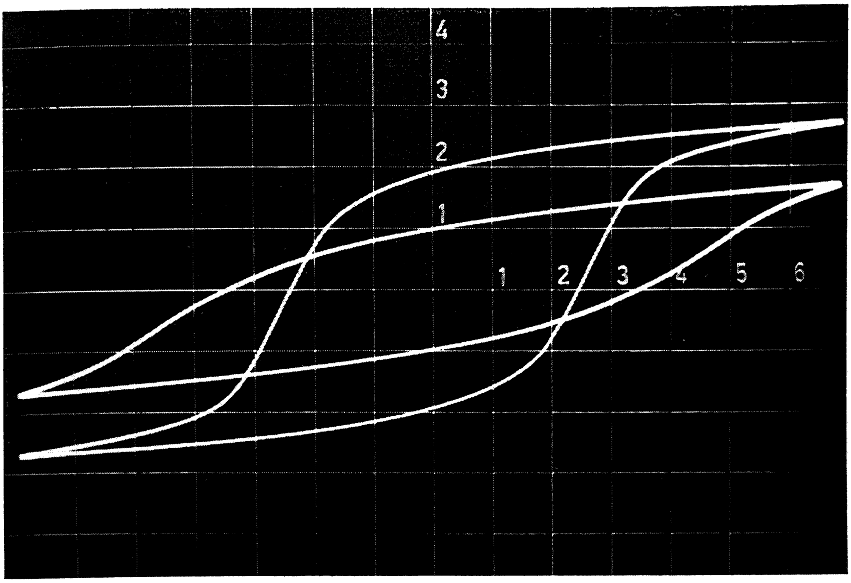

Institut Dr. Foerster

Fig. 22. Superimposed loops of the sample from Fig. 21, but carburized for 1 hr. at 900° C. in a C-atmosphere (loop with higher magnetization values) and quenched (loop with smaller magnetization values and higher coercive force).

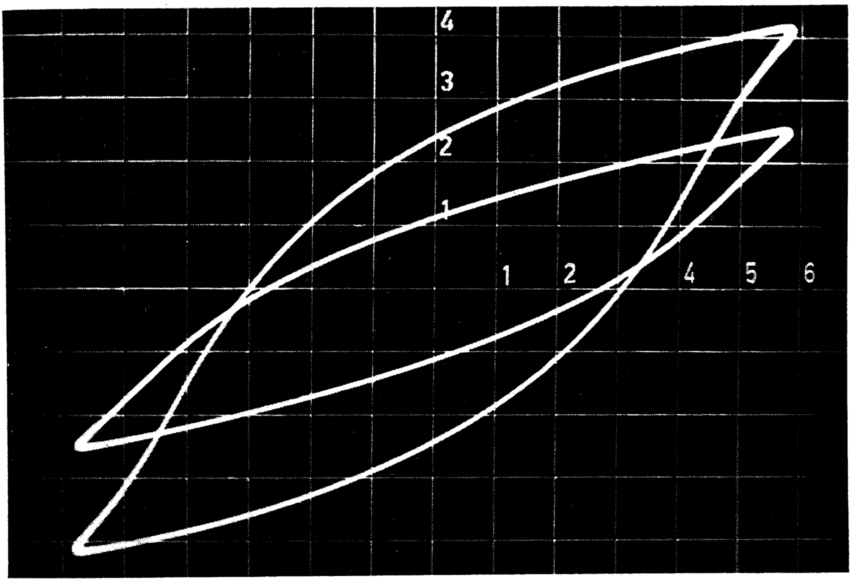

Institut Dr. Foerster

Fig. 23. Superimposed magnetization loops of two normal samples with various hardness. The samples were carburized 1 and 3 hr. at 900° C. and then quenched. The field strength was selected so that the hardness variations were represented optimally by means of the magnetization amplitude.

Effects of Carburization. Fig. 23 shows the standard sample at the field strength for optimum **separation of hardness variations** in the following conditions:

1. Carburized at 900° C. for 1 hr. and quenched (upper curve).
2. Carburized at 900° C. for 3 hr. and quenched.

The lower curve shows a greater hardness because of the higher carbon concentration.

Predicting Mechanical and Structural Characteristics. The preceding four examples illustrate how cold-forming, variation of the carbon content, and hardness variations result in a considerable variation in magnetic properties. These great influences on the magnetic properties caused by mechanical and metallurgical effects meet the necessary requirements for **eddy current quality sorting.** This eddy current quality control is useful because it is possible to draw conclusions concerning the mechanical and metallurgical properties of the material from the variations of the electromagnetic properties.

Internal Stress in Magnetostrictive Materials. Internal mechanical stresses have a pronounced influence on the magnetization loop. This influence becomes

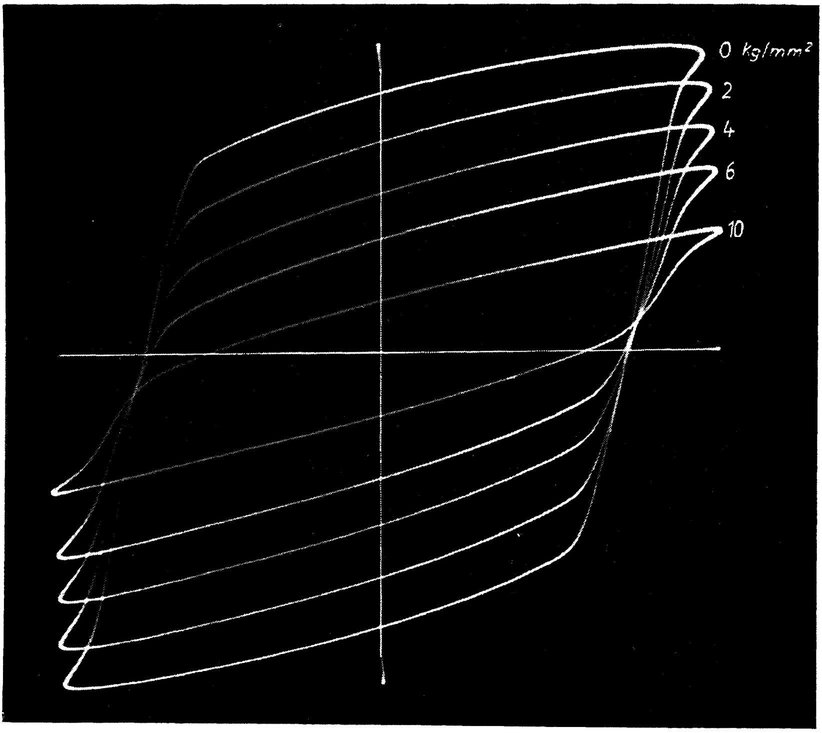

Institut Dr. Foerster

Fig. 24. Influence of tensile stress on the magnetization loop of a hard nickel wire. The loop with the highest magnetization value corresponds to the wire without tensile stress. The loops shown below correspond to a tensile stress of 2, 4, 6, and 10 kg. per mm.^{2}.

larger with higher values of magnetostriction. Fig. 24 shows the effect of tensile stress on the magnetization loops of a **hard nickel wire** which is loaded to 0, 2, 4, 6, and 10 kg. per mm.^{2}. Under tension the magnetization values of nickel decrease greatly (negative magnetostriction). The investigation of the variation of the magnetic values as a result of tension has led to a quantitative method of measuring the internal stresses. The build-up of internal stresses has been observed quantitatively by means of the stretch and drawing processes, and the decrease of internal stresses by means of the annealing process.[4, 49]

Comparator Bridge Tests

PRINCIPLE OF OPERATION. The use of the hysteresis difference loop for nondestructive quality testing of steel was suggested in 1939.[22] Today, this difference method is used in various comparator bridges. However, it is evident that the hysteresis loop, or the difference loop, is not an optimum representation of the magnetic material values for the purpose of quality sorting. In the subsequent test the Magnatest Q picture will be discussed as an improved representation of magnetic and electrical material characteristic values.

Fig. 25(a) shows the two magnetization loops of the **carbon steels** C1015 (inside loop) and C1034 (outside loop), photographically superimposed. The vertical magnetization M is measured by the integration of the measurement voltage E at the secondary difference coil.

$$M = \int E\, dt \tag{4}$$

is plotted above the field strength H and is indicated in Fig. 25 by $f(H)$.

Fig. 25(a) was obtained by inserting two steel samples (C1015 and C1034) in the secondary coil S_1, one after the other, as indicated in the sketch of the secondary coil. In Fig. 25(b) the rod of the steel C1015 is inserted in S_1, and after the sample is removed from S_1, the steel sample C1034 is inserted in S_2. This results in opposite directions for the two hysteresis loops. Fig. 25(c) shows the difference of the two loops of Fig. 25(b), obtained by placing the two steel samples in S_1 and S_2 at the same time. Increasing the amplification by a factor of 4 results in Fig. 25(d). Figs. 25(c) and (d) represent an important characteristic step of the eddy current sorting method: By using two equal or similar steel samples in the two secondary coils, only a slight difference appears; this is then amplified to attain the desired resolution.

A time-dependent representation of the magnetization difference is selected instead of the field-dependent representation in Fig. 25(e). Thus the representation becomes unequivocal because only one magnetization value belongs to each abscissa value, in contrast to the previous pictures. In Fig. 25(f), the time derivative of the magnetization difference is represented, instead of the time-dependent magnetization, by means of elimination of the integration.

Figs. 25(e) and (f) describe entirely different properties of the magnetization loop. Fig. 25(e) represents the difference of the magnetization value of the two test bodies placed in S_1 and S_2 as a function of time, while Fig. 25(f) represents

$$\frac{dM_1}{dt} - \frac{dM_2}{dt} = f(t) \tag{5}$$

This can be expressed as follows:

$$\frac{dM_1}{dH}\left(\frac{dH}{dt}\right) - \frac{dM_2}{dH}\left(\frac{dH}{dt}\right) = f(t) \tag{6}$$

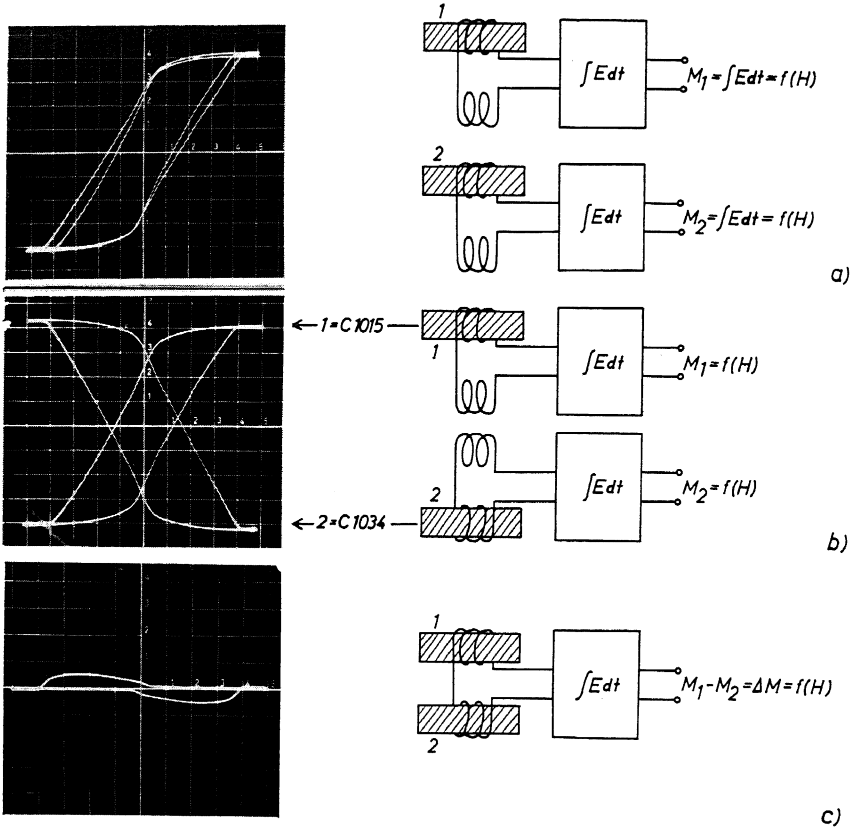

Fig. 25. Magnatest Q pictures derived from the difference in the magnetization loops. (a) Superimposed magnetization loops of C1015 and C1034 carbon steels. (b) Sample C1015 in coil 1, and after removal of sample C1015, sample C1034 in coil 2. (c) Difference of magnetization loops of the C1015 and C1034 samples as a

The two expressions dM_1/dH and dM_2/dH represent the **differential permeability** of the magnetization loops. Thus Fig. 25(f) represents the difference of the permeability value of the two test bodies S_1 and S_2 multiplied by the factor dH/dt. By multiplying by dH/dt, the difference of the permeability of the two samples is distorted according to a cosine curve. At small angles, the cosine is nearly unity, so that the permeability difference is represented undistorted. However, the distortion of the permeability difference according to a cosine curve is meaningless in quality sorting.

If the curve of Fig. 25(f) is electrically differentiated with respect to time, so that

$$\frac{d^2\,\Delta M}{dt^2} = f(t) \tag{7}$$

then essentially only the variations in the curvature (second derivative) of the magnetization loops of the two samples in S_1 and S_2 are represented, merely multiplied by the factor d^2H/dt^2.

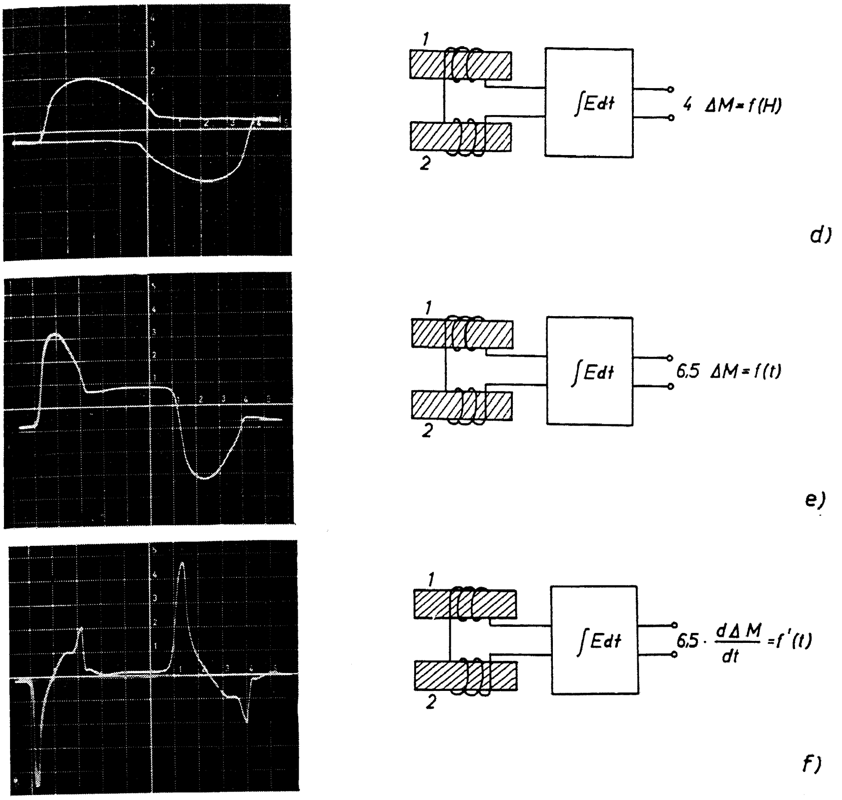

Institut Dr. Foerster

function of the field strength. (d) Same as in (c) but at a four times greater amplification of the magnetization difference. (e) Unequivocal representation of the magnetization difference from (d) above a linear time scale. (f) Time differential quotient of the magnetization difference from (e) above a linear time scale.

MAGNATEST Q SORTING. With Magnatest Q curves, either the magnetization variations, the permeability variations, or the variations of the curvature of the hysteresis loop of the test body with reference to a standard are indicated, depending on the selection of the representation.

The **influence of the test field strength** must also be considered. Test bodies with homogeneous mechanical deformation can be tested at low field strengths. Because of the low initial permeability, the penetration depth is then greater, so that edge decarburization or soft spots have little influence. Large permeability variations can be evident for **mechanically deformed parts,** such as rods which have passed through a straightening machine. Therefore it is practical to use a high field strength with integrated measurement voltage (magnetization difference).

In addition to the field strength and the type of representation, the frequency can also be adapted to the test problem. For many problems, a frequency of 5 c.p.s. is superior to 60 c.p.s. It provides at the same time a flexible theoretical interpretation of the frequency influence on the analysis possibility of the eddy current quality testing.

Recording Test Results. Considerable numbers of test results were gathered in recent years by distributing among many hundreds of users the printed **transparent paper charts** for the screen of the Magnatest Q instrument. Permanent records of the test results can be obtained quickly with the aid of these transparent paper charts by tracing screen patterns with various colors, so that the suitability of the test method for a specific test problem can be observed at a glance.

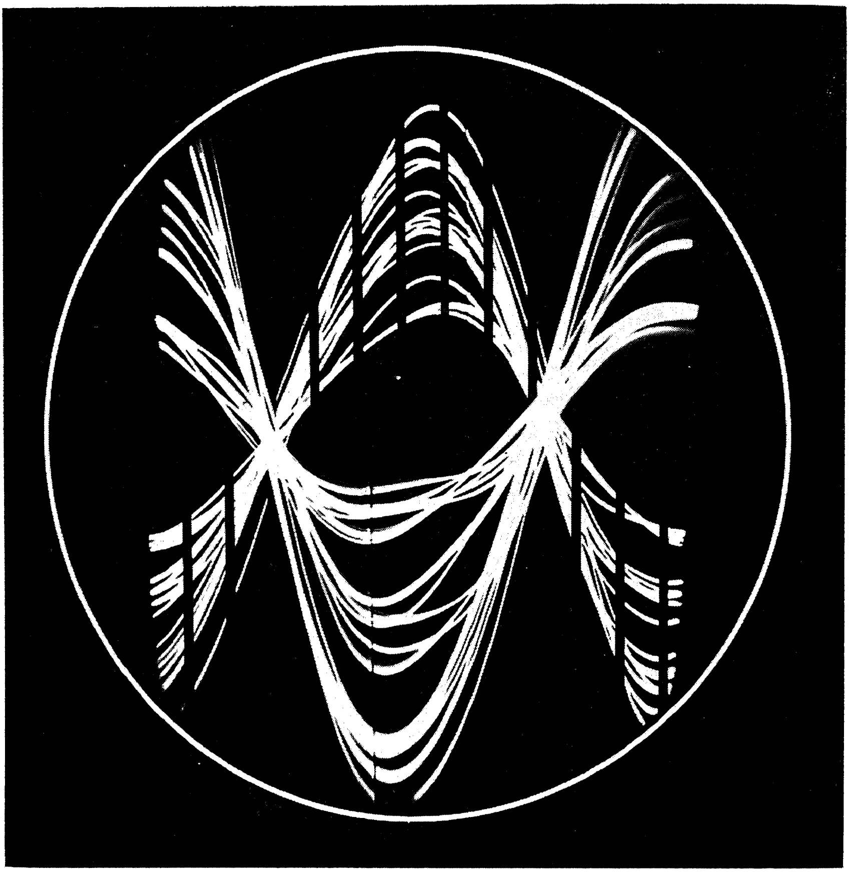

Institut Dr. Foerster

Fig. 26. Magnatest Q picture of cobalt alloys having similar alloy contents. One alloy is identified in the picture by a grid.

Another way of recording test results in easily observable manner is by photographing the various screen patterns. For example, in investigating how two alloys, A and B, can be separated in the Magnatest spread band, a **transparent disc with a grid** is placed in front of the screen while the curves of the alloy A are taken, so that the curves in the photograph are interrupted in a characteristic pattern. With the aid of discs with various grids, one can easily differentiate between the curves of the various alloys. Fig. 26 shows the curves of two cobalt alloys which are very similar in their alloy contents and which are clearly distinguished from each other through the grid pattern present in one set of curves.

Range of Test Applications. The Magnatest Q pictures given in the subsequent discussions represent a small selection from large numbers of test results obtained from industry. The following **test problems** are treated:

1. Sorting of rod material according to alloy.
2. Sorting of rolled billets according to alloy.
3. Sorting of small parts according to alloy and condition.
4. Sorting for heat treatment and structural conditions, and thus sorting according to hardness, tensile strength, etc.
5. Sorting for depth of case and edge decarburization.
6. Sorting with special coils.

SETTING UP MAGNATEST Q INSTRUMENT. Fig. 27 indicates schematically the optimum adjustment of the test instrument. Suppose that two alloys, A and B, are to be separated from each other. First, a sample of the alloy A is inserted in the test coil. The pattern of Fig. 27(a) will appear on the screen. The sensitivity is selected so low that the entire curve of A_1 of sample appears on the screen.

Sensitivity Calibration. The maximum of this curve A_1 is brought, by means of an adjustment on the instrument, to a specific indication height called the **absolute value.** In this way, for all sensitivity positions of the sensitivity knob, the sensitivity is indicated in percentage of this absolute value. This makes it possible, independent of the specific instrument, the specific coil, and the specific material, to relate the information to the absolute value of the material. Thus results obtained at various locations can be easily compared with each other.

Compensation Adjustments. Next, a sample of the alloy A is inserted in each of the two difference coils. The solid curve A_1, appears on the screen at a higher sensitivity [see Fig. 27(b)]. If sample A_1 is now replaced by a sample B_1 of the alloy B, then the interrupted curve B_1 appears as in Fig. 27(b). Now, after the sample B_1 is again replaced by the sample A_1, the compensator is adjusted so that curve A_1 becomes a horizontal straight line, as shown in Fig. 27(c). In the next step, Fig. 27(d), the curve B_1 is displaced by operating the phase shifter, so that the maximum lies in the center of the screen. In Fig. 27(e) the curve A_1 is symmetrically displaced toward the bottom, with reference to the curve B_1, by means of the compensator. Now, in Fig. 27(f), the amplifier sensitivity is increased so that the screen is fully utilized.

Spread Band Characteristics. Fig. 28 shows curves for rods of C1015 **carbon steel** and for **free-cutting steel.** The spread band around the two curves is plotted from the results when 1000 rods of each material are fed through the coil. Thus the spread band gives the variations which can result from segregation effects, internal stresses, inhomogeneous deformations, and edge decarburization effects within one heat.

SELECTING OPTIMUM TEST CONDITIONS FOR SORTING ALLOYS. The main problem of the Magnatest Q testing is to select the following test conditions: sensitivity, type of indication, frequency, field strength, and phase position, as well as the compensation adjustment so that no overlap appears

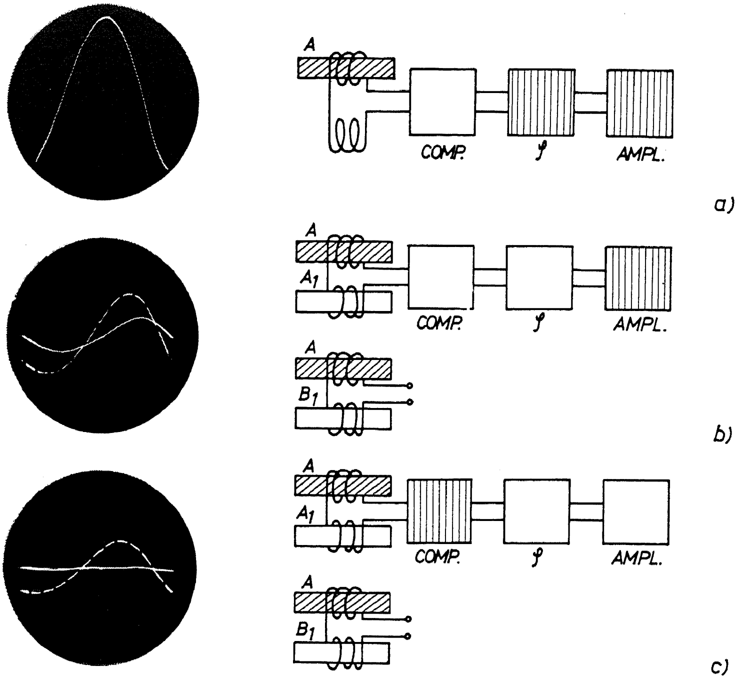

Fig. 27. Adjustment of the Magnatest Q screen picture for optimum test conditions. (a) Adjustment of the absolute value. (b) Curve A_1 and curve B_1 (interrupted) at a sensitivity eight times higher than in (a). (c) Curve A_1 adjusted to a horizontal line by means of the compensators. (d) Maximum of curve B_1 (inter-

for alloys which vary only slightly in their contents. The optimum adjustment was selected for Fig. 28 so that the spread bands are **symmetric.** The largest variations between the two spread bands are on the vertical center line of the screen (reading slit of the Magnatest Q instrument).

Separation of Three Different Alloys. Fig. 29 shows the optimum representation of the separation possibility of three different alloys. The alloy spread bands are moved so that the maximum separation between bands is at the vertical center line of the screen, and by means of the compensation controls, the curves are moved so that the screen is fully utilized. Fig. 29 shows the optimum adjustment for the three alloys 3415, 5115, and free-cutting steel with 0.22 percent C. The Magnatest Q picture in Fig. 30(a) shows the three alloys C1034, C1045, and 5140. The spread bands of the alloys C1034 and C1045 are very close at the point of the best possible separation, since both alloys are close with reference to their carbon content.

Use of Harmonics in Separating Similar Alloys. One can see, even in Fig. 30(a), that related alloys have similar characteristic curves. The alloy 5140 distinguishes itself in a characteristic manner from the curves of the two other carbon steels. Fig. 30(b) shows the separation possibilities for the alloys C1015 and 5115. The curves, which were obtained on unfinished **piston rods,** clearly

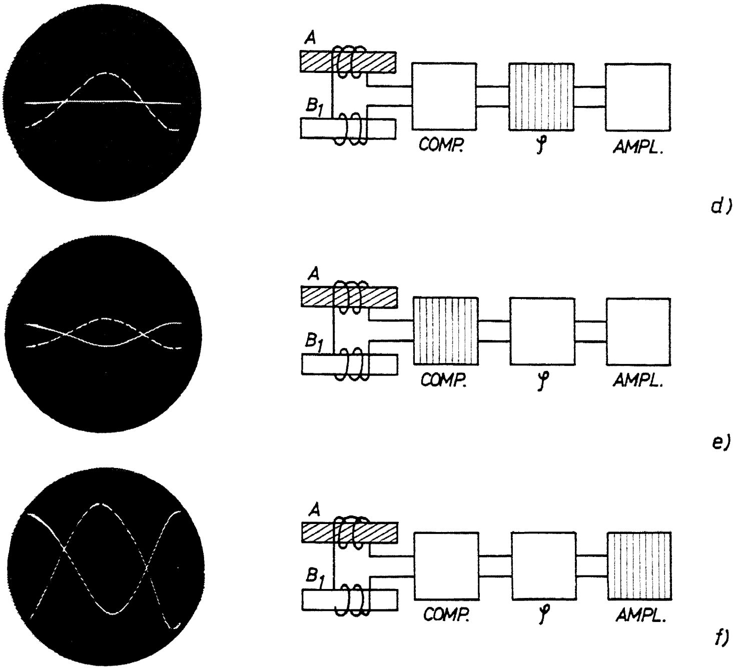

Institut Dr. Foerster

rupted line) moved to the screen center with the aid of the phase shifter. (e) A_1 and B_1 symmetrically displaced toward the top and the bottom by means of the compensators. (f) Four times increase of sensitivity, providing full utilization of screen picture with optimum separation in the screen center.

show that the two alloys distinguish themselves essentially in the **harmonics,** while the amplitude of the fundamental wave is almost equal. This is a typical case in which a better separation possibility for the alloys is given by favoring the harmonics.

Sorting Mixed Lots. In general, the problem of sorting mixed alloys is to detect, in a mass of test parts of one alloy, a part of the mixed alloy. Occasionally, however, it happens that a series of mix-ups occurs at the same time, and these have to be sorted with the Magnatest Q into their correct alloy groups. Fig. 31 is an example for the **separation of four different alloys,** C1034, C1045, C1075, and free-cutting steel with 0.1 percent C. It is shown that the separation in the center vertical (reading slit) is incomplete because an overlapping between the alloys C1045 and C1075 is evident. If, however, the Magnatest Q picture is adjusted by means of the phase shifter so that the dashed line is in the screen center, then all four alloys are satisfactorily separated from each other.

TESTING BILLET MATERIALS. The mixed material previously discussed pertained to semi-finished rods. In the subsequent text, mix-ups of rolled billet material with square cross-sections of 60 × 60 mm. are discussed. The **hot-rolled, semi-finished parts** are generally considered homogeneous and uniform with reference to their structure. Thus, difficulties which appear because of the

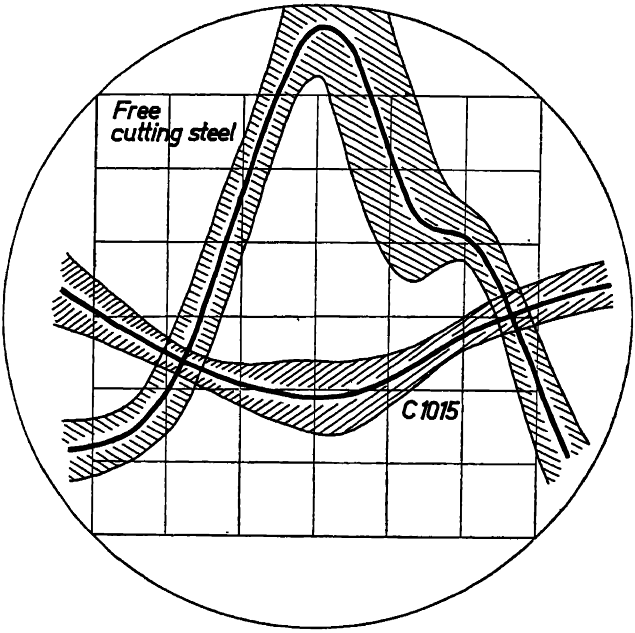

Fig. 28. Magnatest Q curve and spread band of C1015 carbon steel and a free-cutting steel.

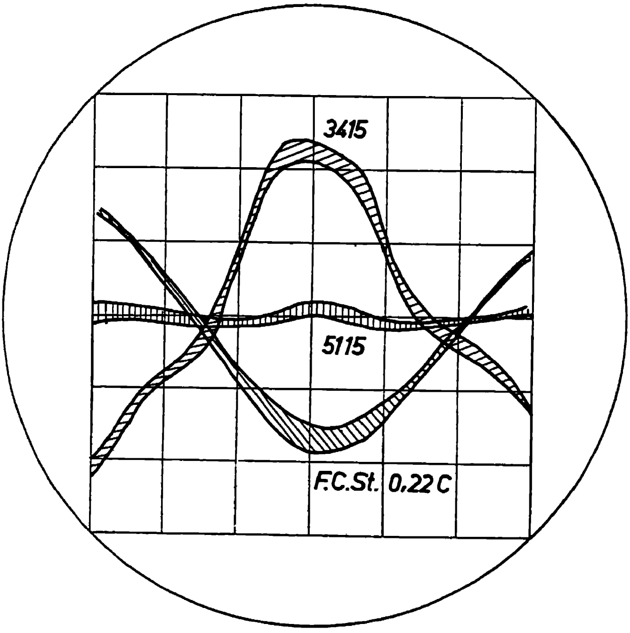

Fig. 29. Magnatest Q picture of three alloys, 3415, 5115, and free-cutting steel with 0.22C, with an optimum screen utilization.

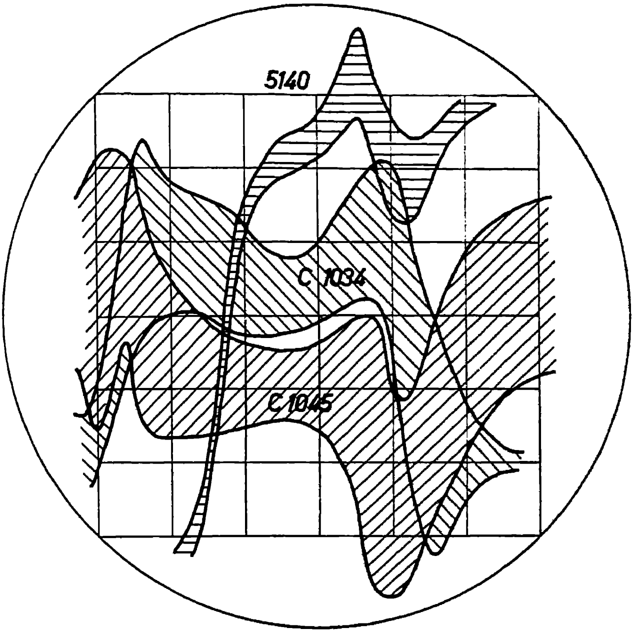

(a)

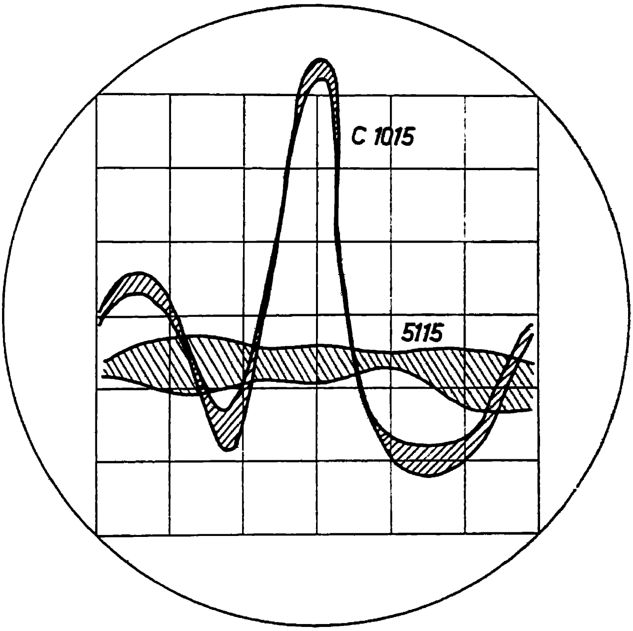

(b)

Fig. 30. **(a) Spread bands of a large number of rods of C1034, C1045, and 5140 steels. (b) Spread bands of unfinished piston rods of C1015 and 5115 steels.** A better separation is obtained by favoring the harmonics.

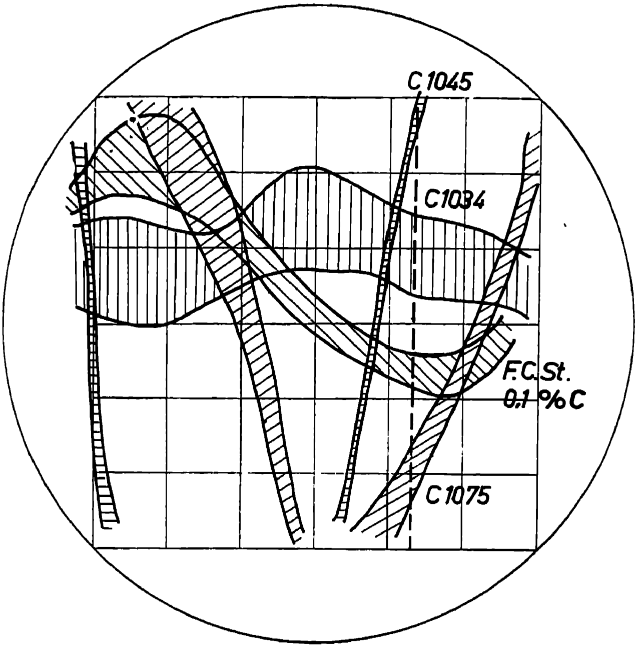

Fig. 31. Separation of C1034, C1045, and C1075 carbon steels and free-cutting steel with 0.1 percent C. Separation of all four alloys is possible at the dashed vertical line.

permeability variations due to cold working are not to be expected. Fig. 32 shows the Magnatest Q spread bands of the alloys 5132, C1075, 5140, and 6150. As can be seen, the four alloys can be satisfactorily separated with the selected optimum adjustment which was carried out according to the schematic shown previously. All spread bands are separated far from each other, and the spread ranges are relatively small because of the homogeneous condition. It is of significance that the two **chromium steels,** 5132 and 5140, which are very similar in their alloy content, can be separated from each other without difficulty. A billet of the C1075 steel is used as a **compensation sample.**

Fig. 33 shows the test results for the four steels C1015, C1034, E52 100, and a wrought heat-resisting steel, which can be satisfactorily separated. For optimum adjustment, the spread band of the compensation sample is moved far enough to the top so that the screen is fully utilized.

Use of Low Field Strengths. Fig. 34 shows the spread bands of two **spring steel alloys,** A (55 Si 7) and B (65 Si 7) which lie close together in their alloy content (see analysis). In this figure the two alloys are illustrated in two different heats each, so that relatively wide spread bands are obtained. However, these can be clearly distinguished, especially if worked at very low field strengths, as in Fig. 35. In Fig. 35 the field strength is only one-eighth of that of the preceding figure.

The influence of the **field strength** on the possibility of separation is of special importance in complicated cases. A very low field strength acts like a lower fre-

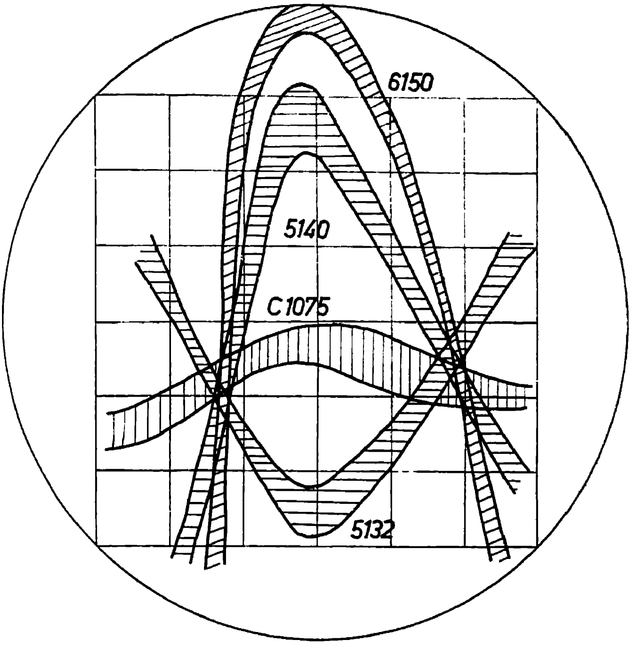

Analysis A

Material	C	Si	Mn	P	S	Cr	V
C1075	0.76	0.37	0.67	0.025	0.027		
5132	0.35	0.32	0.65	0.021	0.028	0.99	
5140	0.40	0.36	0.76	0.025	0.016	1.10	
6150	0.51	0.29	0.97	0.021	0.017	1.05	0.10

Fig. 32. Separation of hot-rolled billets of 5132, C1075, 5140, and 6150 steels.

quency, since at low field strengths the material appears only in its very low initial permeability. Thus, according to the theory of eddy currents, the f/f_g value becomes smaller. However, at small f/f_g values, the separation between conductivity, permeability, and diameter effects is considerably better than at higher f/f_g values. In the range of small f/f_g values, the conductivity direction is almost perpendicular to the diameter and permeability direction on the impedance plane.

Since the billets are not very exact in their dimensions, it is practical to select the field strength so that the f/f_g value is kept small by means of the low initial permeability. In this way the **conductivity effects,** which are essentially responsible for an alloy separation, can be separated satisfactorily from permeability and diameter effects.

Optimum Utilization of Screen Area. Fig. 36 shows another example with the steels C1045, 5140, and 3115. The C1045 steel serves as a **compensation**

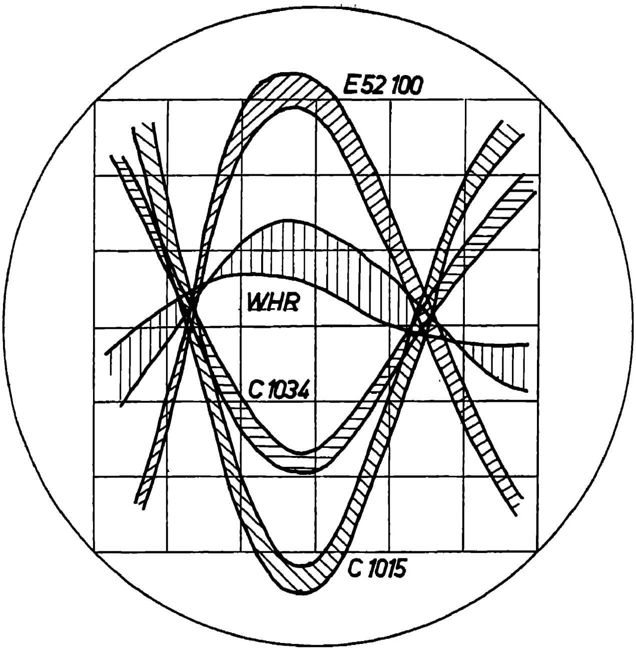

Analysis B

Material	C	Si	Mn	P	S	Cr
C1015	0.13	0.37	0.52	0.016	0.019	
C1034	0.37	0.36	0.61	0.012	0.027	
WHR	0.74	0.26	0.28	0.018	0.022	0
E52 100	1.04	0.32	0.28	0.011	0.026	1.07

Fig. 33. Spread bands of hot-rolled billets of 60 × 60 mm. cross-section, of E52 100 steel, a wrought heat-resisting steel for valves, and C1034 and C1015 carbon steels.

sample. Again the curve of this compensation sample is moved to the bottom until the three spread bands are distributed nearly symmetrically over the screen of the Magnatest Q instrument, so that an optimum utilization of the screen is assured. If one were to adjust the spread band of the C1045 steel in the horizontal, then the spread band of the alloy 5140 would fall outside the screen. Fig. 37 shows the separation of two very close alloys, E4132H and 5132, which are distinguished from each other by only 0.23 percent Mo.

INFLUENCE OF TEST FREQUENCY. For a number of applications, a frequency of 5 c.p.s. gives better results than a higher frequency in Magnatest Q tests. Fig. 38 shows that the separation of these similar alloys is not possible with 60 c.p.s., since no range is available at which the spread bands of these alloys

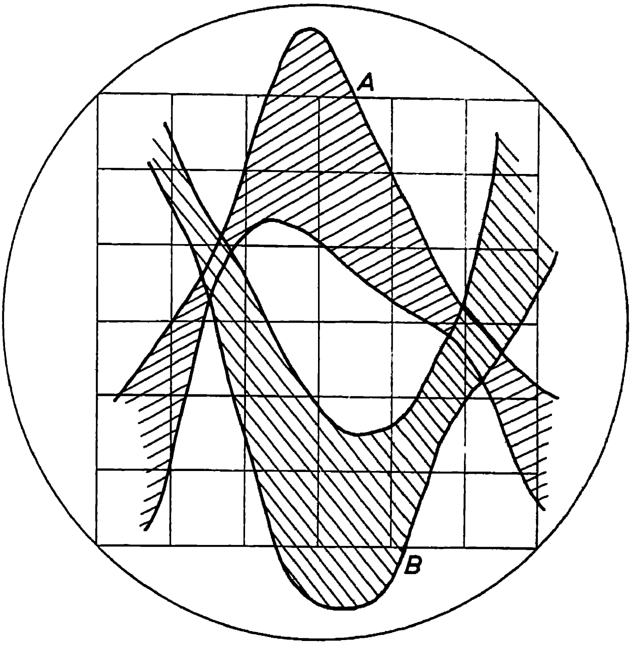

Analysis C

Material	C	Si	Mn	P	S
A	0.55	0.170	0.80	0.012	0.024
B	0.62	0.159	0.83	0.020	0.027

Fig. 34. Spread bands of rolled billets of the two spring steel alloys A and B (see analysis).

are distinguishable from each other. Wherever one alloy distinguishes itself from the other, still other alloys fall together at the same phase point. However, Fig. 39 shows the same alloys sorted at 5 c.p.s. Here, it can be clearly seen that the better **resolution** is at the lower test frequency, which is especially obvious in this difficult borderline case. At the location of the dashed line, all five alloys can be reliably separated from each other.

Tests of Wire Samples. The following example shows an especially interesting case: In the continuous **testing of mixed wires,** one piece was cut from each roll, then straightened by hammering, and tested with the Magnatest Q for mix-up. Fig. 40 shows the three steels, C1045, C1034, and 5140, tested with a frequency of 60 c.p.s. It is clearly seen that there is no point at which the three alloys can be separated from each other. The spread bands of the individual alloys always overlap in certain phase ranges. However, when tested with 5 c.p.s., as in Fig. 41, a range appears in which a satisfactory separation of the spread bands of the three steels is possible.

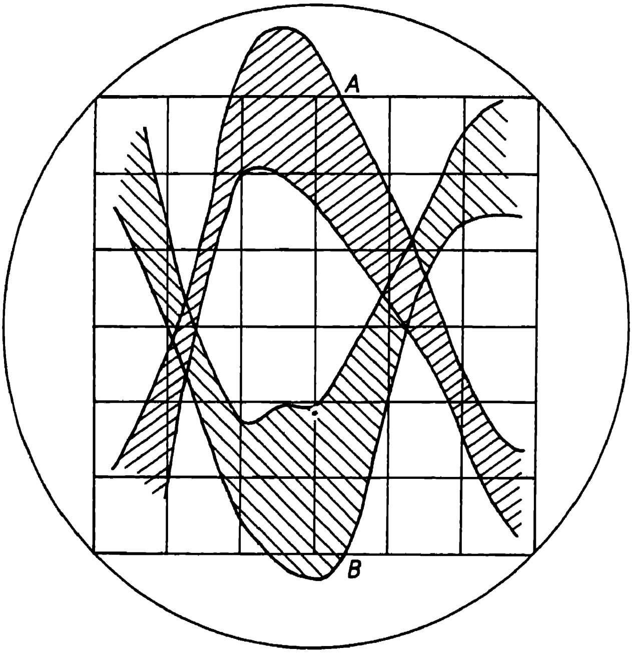

Fig. 35. **Spread bands of the alloys of Fig. 34, but with an eight times lower field strength.**

Advantages of Low Frequency Ratios. It is of interest to note why, in the aforementioned cases of similar alloys and of alloys in which internal stresses were induced by means of straightening, a separation can be carried out considerably better with 5 c.p.s. than with 60 c.p.s.

Fig. 42 represents the **complex voltage plane** of the Magnatest Q coils containing a sample with a specific conductivity, specific diameter, and specific permeability. From the formula given in Fig. 42, one can calculate the ratio of the measurement frequency f to the limit frequency f_g. It can be seen that at small f/f_g values ($f/f_g < 10$), the conductivity direction is almost perpendicular to the diameter and permeability direction. When permeability and conductivity effects are to be separated from each other, one must work at small f/f_g values. The larger the f/f_g value, the smaller the angle between the conductivity, the permeability, and the diameter direction. At higher f/f_g values (for example, above 10), a separation of the effects becomes more and more difficult.

Fig. 43 shows the angle between the direction of **diameter and permeability changes,** and the conductivity direction, as a function of the ratio f/f_g. The more nearly the angle between σ and ($\mu_{\text{rel.}}, d$) approaches 90 deg., the better the analysis possibility. In the vicinity of 180-deg. angles between σ and ($\mu_{\text{rel.}}, d$), the influence of **internal stresses** can no longer be separated from conductivity effects.

Permeability Effects at High Frequency Ratios. At high f/f_g values, the effect of conductivity variations on the Magnatest Q indication can be canceled by means of corresponding permeability variations because both effects have

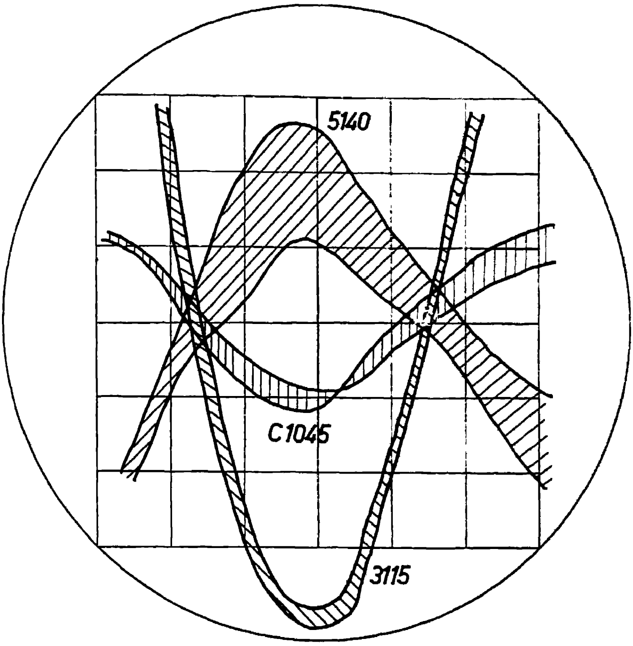

Analysis

Material	C	Si	Mn	P	S	Cr	Ni
C1045	0.42	0.36	0.70	0.020	0.025		
5140	0.40	0.29	0.73	0.028	0.024	1.04	
3115	0.12	0.29	0.55	0.012	0.012	1.49	1.60

Fig. 36. Spread bands of 5140, C1045, and 3115 steels with optimum screen utilization.

approximately the same direction. However, at small f/f_g values ($f/f_g < 10$), an unequivocal separation of the effects is possible. Fig. 38 illustrates a difficult case in which similar alloys cannot be separated at 60 c.p.s. but can be separated at 5 c.p.s. This results from the fact that the various alloys are distinguished from each other in their electrical conductivity. However, at 60 c.p.s. the conductivity effects are overlapped by simultaneous permeability effects, so that a separation is no longer possible. On the contrary, at 5 c.p.s. the f/f_g value of the sample is lowered so that the conductivity forms a large angle with the permeability direction. Here the spread bands of the individual alloys can be separated in a wide phase range.

Effects of Inhomogeneous Internal Stresses. Fig. 40 showed test results on wire ends cut from wire rolls and straightened by means of hammering. This resulted in a strong **inhomogeneous deformation**. Heavy internal stresses were present, causing relatively large permeability variations. These **permeability**

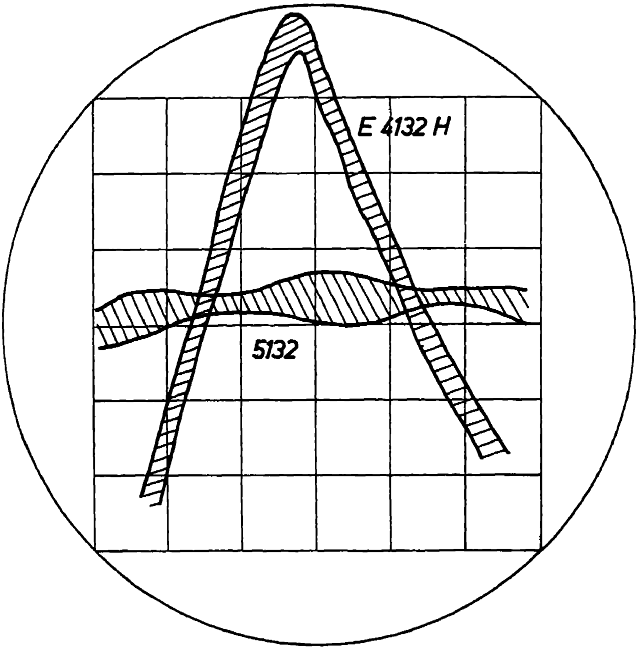

Analysis

Material	C	Si	Mn	P	S	Cr	Mo
E4132H	0.33	0.30	0.66	0.016	0.024	0.90	0.23
5132	0.33	0.27	0.70	0.016	0.012	0.97	

Fig. 37. Spread bands of the two alloys E4132H and 5132, which differ by only 0.23 percent Mo.

variations prevented a separation of the three alloys at 60 c.p.s., since these permeability variations are very nearly in the conductivity direction at 60 c.p.s. Under these conditions the **conductivity effects,** in which the three alloys are easily distinguishable from each other, cannot be separated from the permeability variations resulting from internal stresses. At 5 c.p.s., however, the conductivity direction is different from the permeability direction. Therefore a phase range is available in which the three alloys can be satisfactorily separated from each other because of the conductivity variations. These two examples are typical of a number of applications of the 5 c.p.s. Magnatest Q. It is significant that the reasons for a better analysis possibility with the low frequency are given by the theory of eddy currents.

INFLUENCE OF FIELD STRENGTH. Figs. 44 and 45 show the spread bands from the samples of Figs. 40 and 41 but taken, however, at a higher field strength. As is well known, permeability variations caused by **inhomogeneous internal stresses** have a greater effect at low field strengths. At higher field strengths, the stress influence disappears more and more in the harmonics. At a

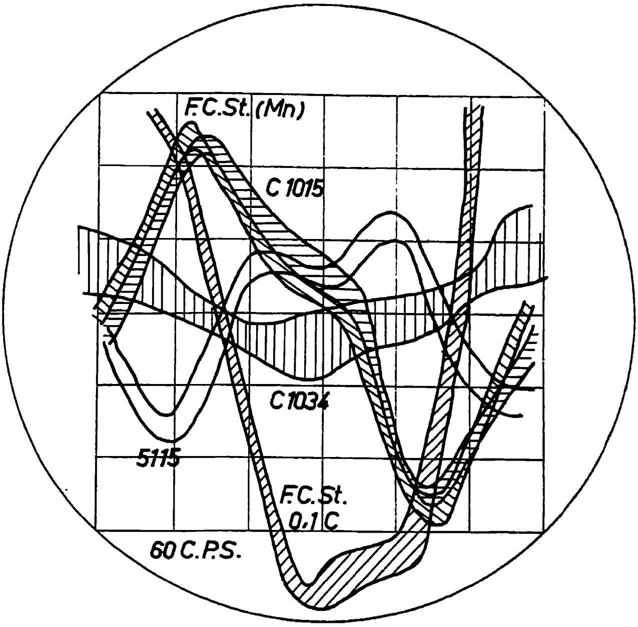

Fig. 38. Spread bands of the five alloys, C1015, C1034, 5115, free-cutting steel with 0.1 percent C, and free-cutting steel with Mn, at a test frequency of 60 c.p.s. There is no phase point available at which all five alloys can be separated.

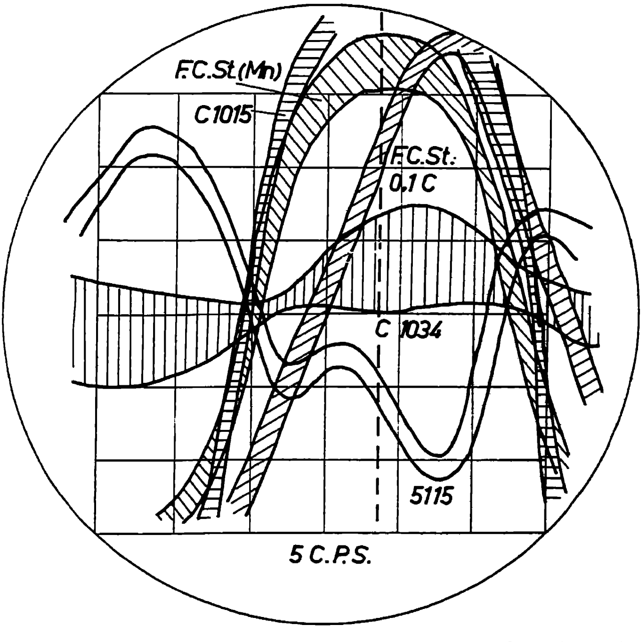

Fig. 39. At a test frequency of 5 c.p.s., a separation of the five alloys from Fig. 38 is possible at the dashed vertical line.

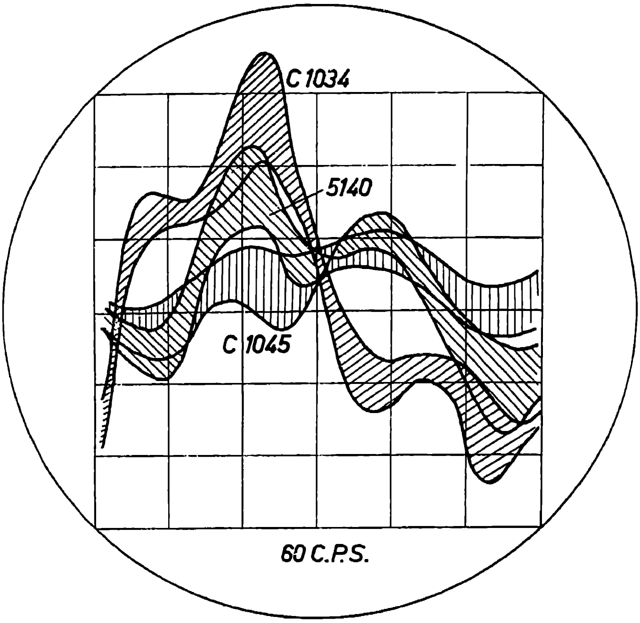

Fig. 40. Spread bands of C1045, C1034, and 5140 steels at 60 c.p.s. For the test, the test parts are cut from a wire roll and straightened by hammering. Because of strong inhomogeneous stresses, separation of the three alloys is not possible at any phase point.

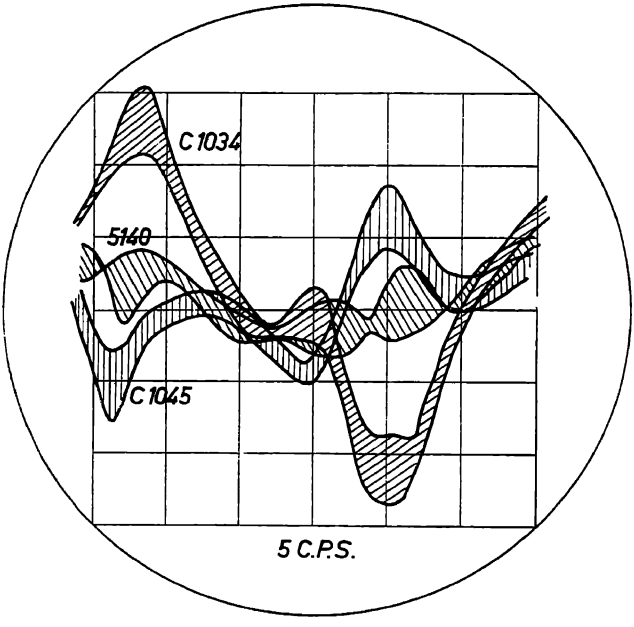

Fig. 41. Satisfactory separation of the three steels with strong inhomogeneous stresses from Fig. 40, at a test frequency of 5 c.p.s.

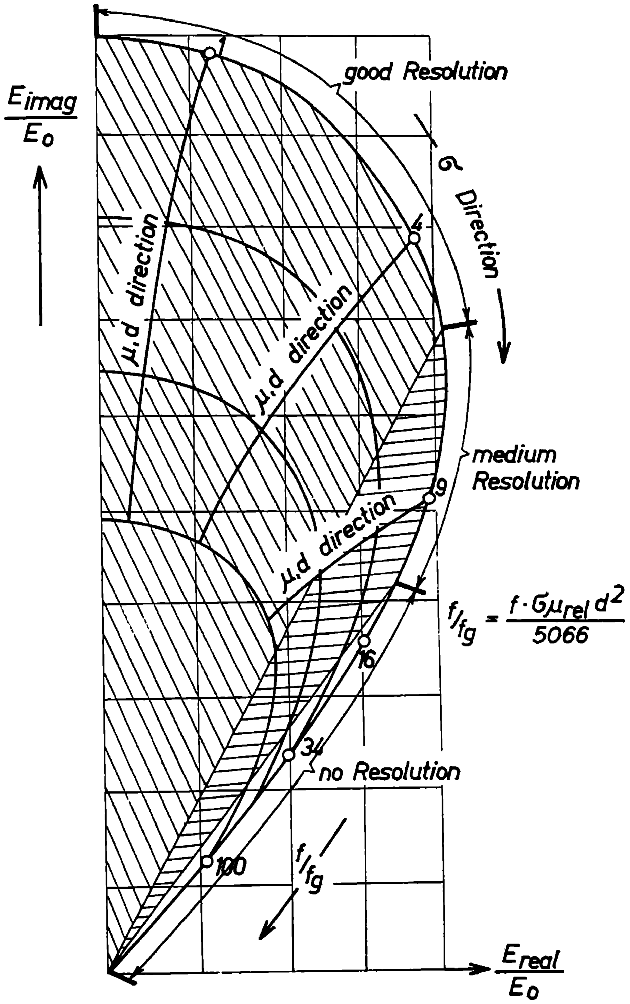

Institut Dr. Foerster

Fig. 42. Complex voltage plane of the Magnatest Q coil which contains a test body with the diameter *d*, the electrical conductivity σ, and the permeability μ_{rel}.

low field strength, according to Fig. 40, no phase range is available in which the three alloys can be separated because of the strong inhomogeneous deformation of the test parts. At higher field strengths (Fig. 44) a phase range, although small, appears around the vertical dashed line, making possible a separation of the three alloys. If both a high field strength and a low frequency are used (Fig. 45), then a wide phase range with a good separation possibility is obtained.

EFFECTS OF STRAIGHTENING. The following four Magnatest Q pictures represent an especially interesting example. In all four pictures the spread bands of the two alloys 5140 and 4140 are present. The test objects were

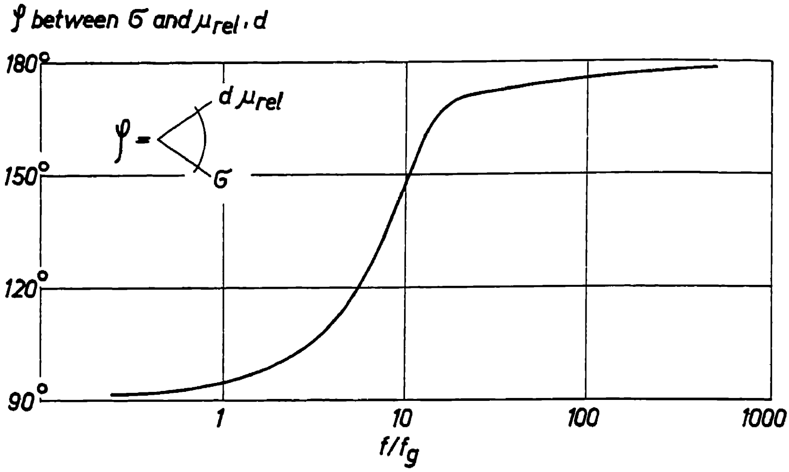

Fig. 43. Angle between the conductivity direction and the diameter-permeability direction, as a function of the f/f_g ratio.

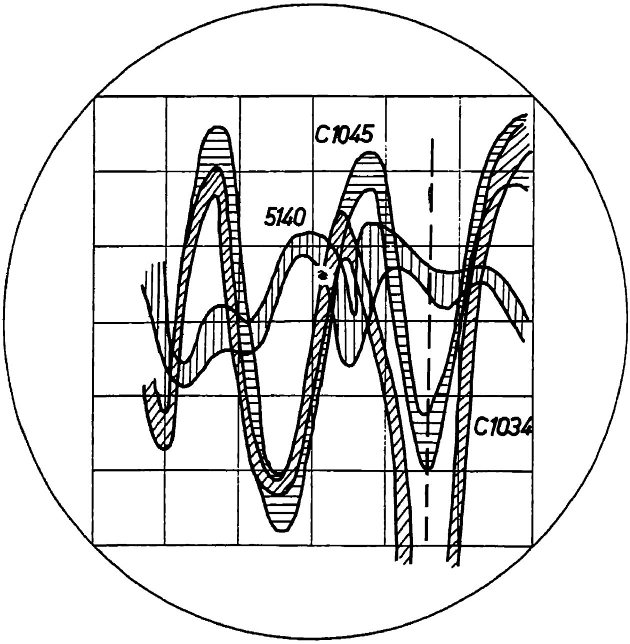

Fig. 44. Spread bands with a test frequency of 60 c.p.s., corresponding to Fig. 40 but taken with a higher test field strength.

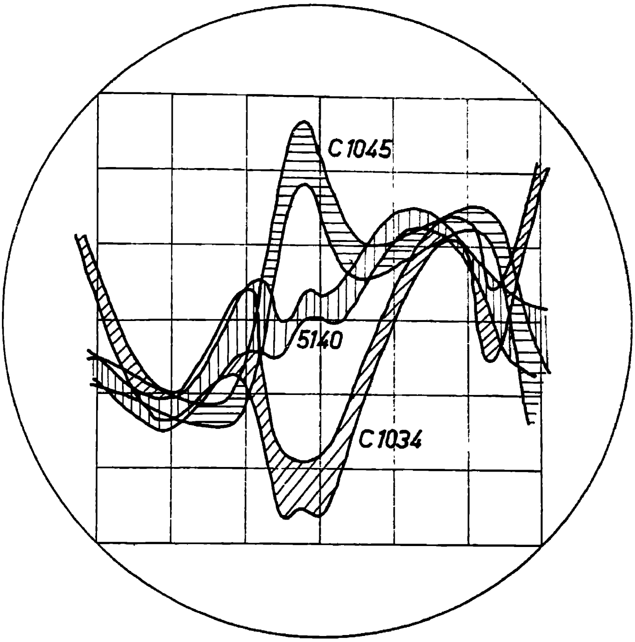

Fig. 45. Spread bands corresponding to Fig. 44 but with a test frequency of 5 c.p.s.

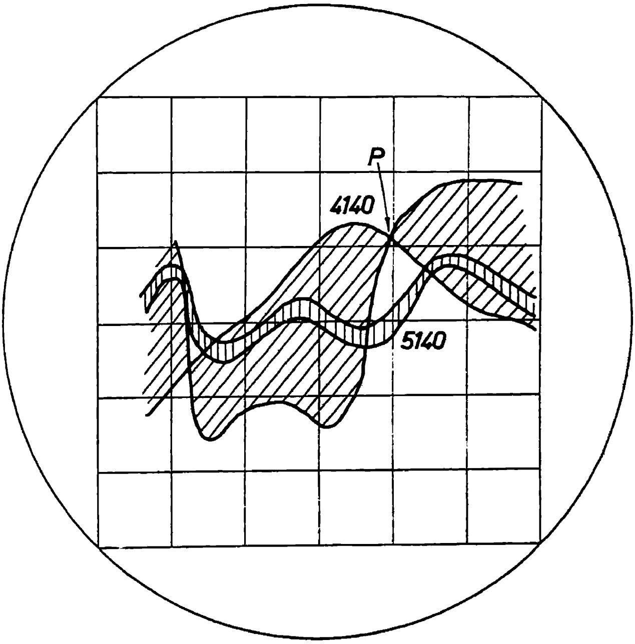

Fig. 46. Spread bands of the 4140 and 5140 alloy steels at a test frequency of 60 c.p.s. The test objects were straightened by means of hammering.

again cut from wire rolls and straightened by means of hammering in order to induce strong internal stresses. As can be seen in Fig. 46, the test is almost impossible at 60 c.p.s., since only a very small phase range is available in which the spread bands of the two alloys separate. At 5 c.p.s. (Fig. 47), however, a wide phase range with a good separation possibility is available. The reason is a decrease of the f/f_g value of the test object by using the lower frequency of 5 c.p.s., where the conductivity direction is nearly perpendicular to the diameter and permeability direction, so that conductivity effects can be separated from inhomogeneous permeability effects caused by straightening stresses.

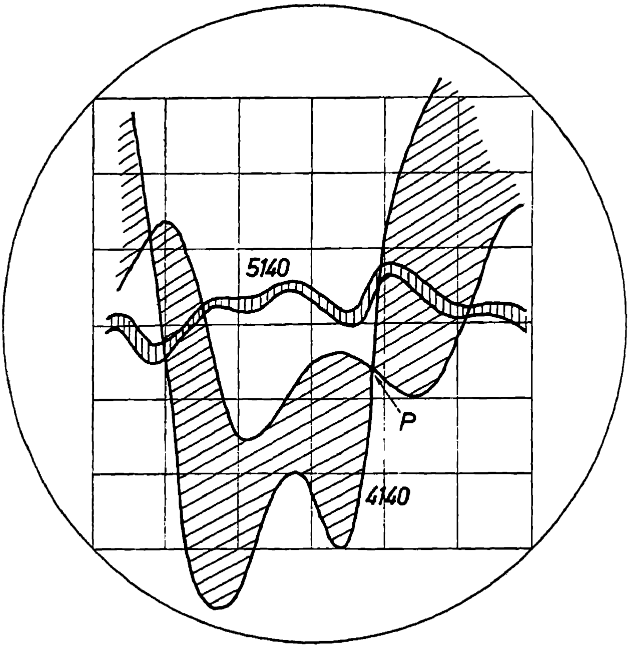

Fig. 47. Spread bands of 4140 and 5140 alloy steels of Fig. 46 at a test frequency of 5 c.p.s.

Of interest is the single point *P* of the spread band from the alloy 4140, at which all Magnatest curves intersect. This point is an additional characteristic of a specific alloy.

EFFECTS OF STRESS RELIEF BY ANNEALING. The spread bands of samples shown previously in Figs. 46 and 47 are again illustrated in the two Figs. 48 and 49, but after annealing in order to stress-relieve the material. Thus it is possible that a good separation will occur between 4140 and 5140 even at 60 c.p.s. However, the spread band of the 4140 alloy is relatively wide. This picture clearly shows that a separation of the two alloys at 60 c.p.s. in Fig. 46 is impossible only because of the strong inhomogeneous stresses; i.e., because of permeability variations. After annealing, the permeability values are approximately equal, so that a separation is also possible at 60 c.p.s.

However, Fig. 49 shows that a separation at 5 c.p.s., also in the annealed condition, is considerably more favorable. The spread band of the alloys to be

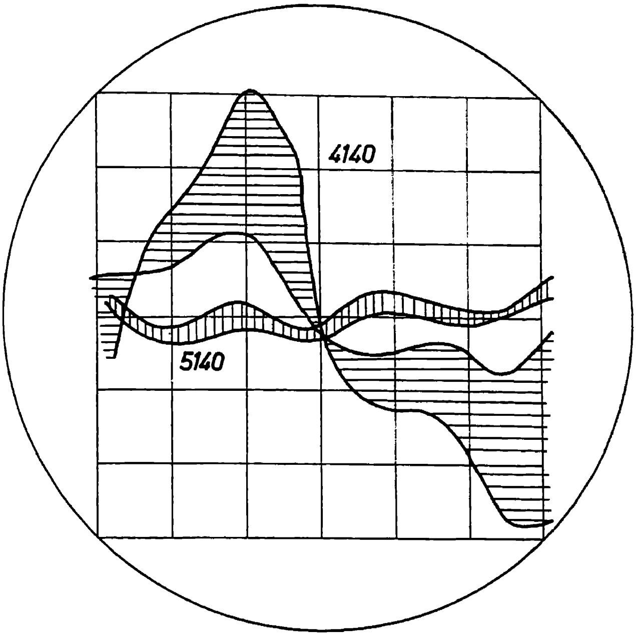

Fig. 48. Spread bands of 4140 and 5140 alloy steels at a test frequency of 60 c.p.s. after stress-relief annealing.

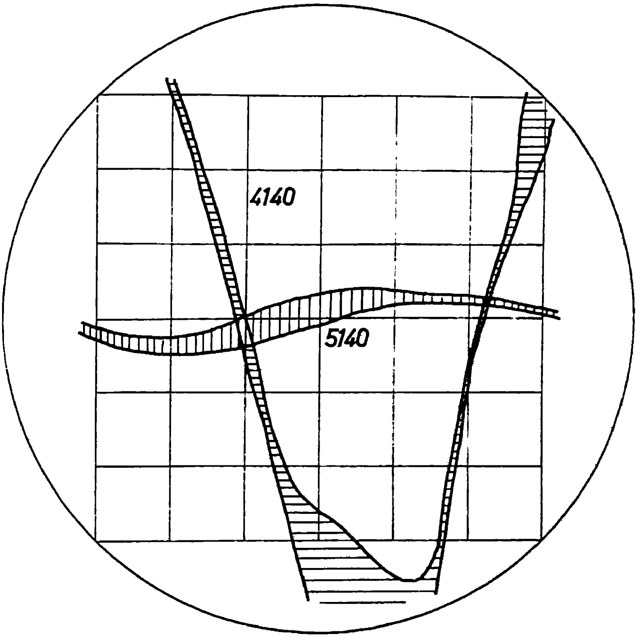

Fig. 49. Spread bands of annealed 4140 and 5140 alloy steels of Fig. 48, but with a test frequency of 5 c.p.s.

separated is generally smaller at 5 c.p.s. because the surface of the material has more influence at 60 c.p.s. than at 5 c.p.s. Thus, slight **edge decarburization** in the wire increases the spread band width, whereas at 5-c.p.s. test frequency, a relatively higher penetration depth exists. At 5 c.p.s. a measurement value is obtained which is representative of a large portion of the test body volume. Therefore, variations in the surface, such as edge decarburization and soft spots, are less noticeable at 5 c.p.s. than at 60 c.p.s.

Separation of Drawn, Annealed, and Tempered Carbon Steel. It is also of interest to investigate the influence of the thermal and mechanical treatment of ferromagnetic material on the Magnatest Q picture. Fig. 50 shows the spread bands of the steel C1034 in three conditions: drawn, annealed, and tempered. The picture clearly shows the great influence of the type of treatment on the magnetic properties. The electrical values vary only slightly between the three conditions.

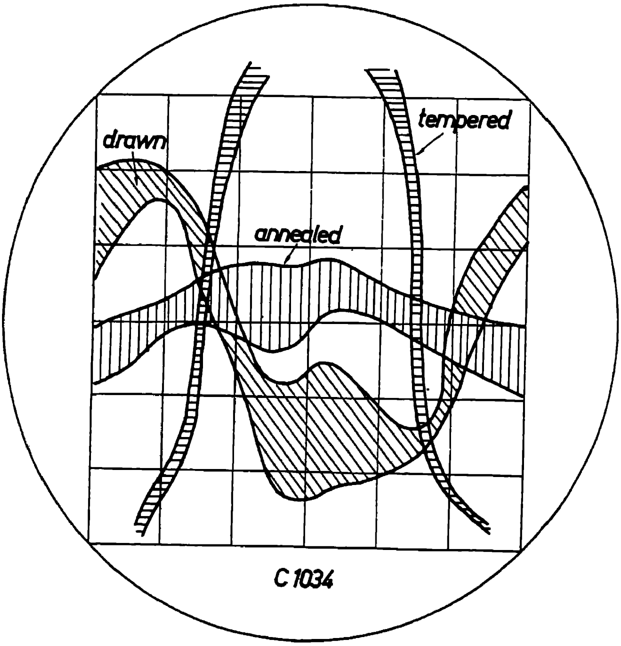

Fig. 50. Spread bands of C1034 carbon steel for three conditions: cold drawn, annealed, and tempered.

A laboratory investigation was made in a large automobile plant for the purpose of determining the influence of the heat treatment and thus the tensile strength of automotive parts on the picture of the Magnatest Q instrument.[4] A large number of guiding sleeves of the material C1034 served as experimental specimens (these guiding sleeves consist of tube sections; length, 76 mm.; outside diameter, 42 mm.; and inside diameter, 30 mm.). The test parts were subjected to various heat treatments so that three different ranges of tensile strength were obtained.

For the test parts of the first group, which after a normal **annealing** (1½ hr. at 860° C.) were uniformly cooled in the furnace for 12 hr., the tensile strength values were between 74,500 and and 79,000 p.s.i. Groups 2 and 3 were cooled after the same annealing in still air or by means of air circulation so that the test parts of group 2 had a tensile strength range between 83,000 and 87,500 p.s.i., and those of group 3 had a spread range between 90,000 and 100,000 p.s.i.

Fig. 51 shows the three spread ranges for the three tensile strength groups of the test parts, whose heat treatment was described above. In Fig. 52 the measured tensile strength values for the three groups, with various cooling periods, are plotted as a function of the slit value on the screen of the Magnatest Q. The three tensile strength groups are clearly separated from each other, and it is shown that the slit values give an even better differentiation of the heat treatment condition than the tensile strengths which are obtained by means of ball impression at only one point, while the magnetic values are obtained as an average over a larger volume.

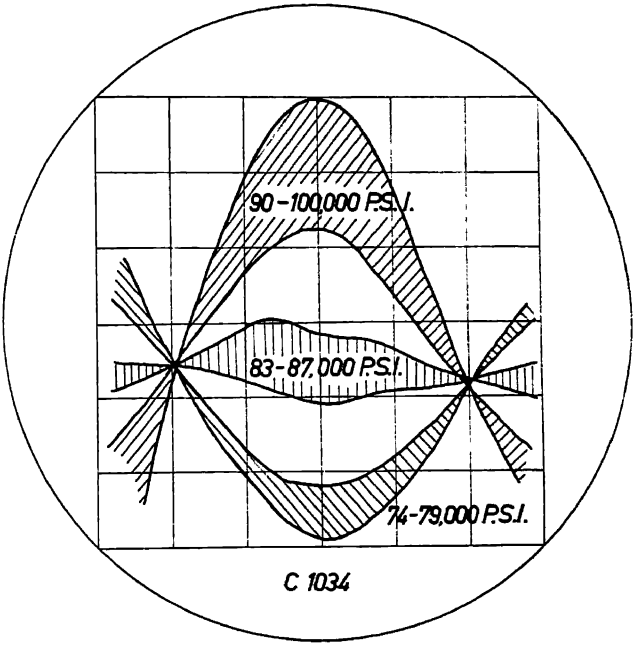

Fig. 51. Three spread bands of C1034 steel for three tensile strength groups: 74,500 to 79,000, 83,000 to 87,500, and 90,000 to 100,000 p.s.i. The three tensile strength groups were obtained by cooling periods of different duration.

SLIT INDICATIONS FOR QUANTITATIVE MEASUREMENTS. Figs. 51 and 52 are an example of an essential characteristic of the Magnatest Q instrument. On one hand, it gives an entire curve with its specific characteristic for a specific material or material condition. On the other hand, quantitative measurement values from the entire curve can be read as a result of the introduction of the slit value. Thus the picture screen fulfills two functions: First, it represents the entire curve with all the characteristics of a two-dimensional picture. Second, the screen of the Magnatest Q instrument fulfills at the same time the functions of a measurement instrument with pointer indication. In general, for an **optimum analysis possibility,** two characteristics of the test instruments are required: two-dimensional representation of a characteristic curve, as well as the possibility of indicating specific measurement values.

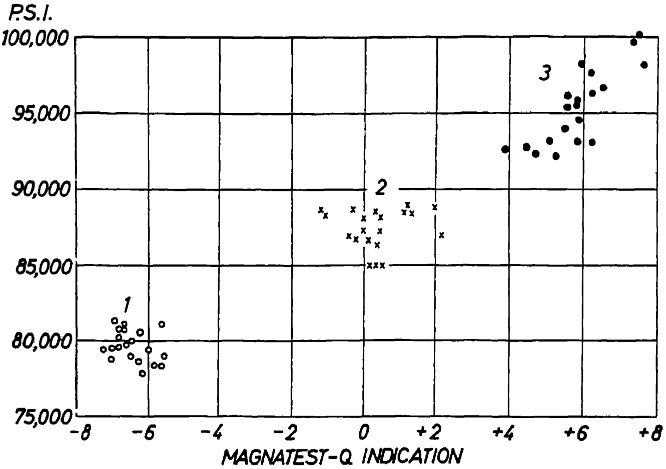

Fig. 52. Evaluation of Fig. 51, showing measured tensile strength values as a function of the Magnatest Q slit value. The values obtained electromagnetically give a higher resolution of structure variations than hardness measurement.

SORTING FOR TENSILE STRENGTHS. Fig. 53(a) shows another example of the separation of automotive parts according to tensile strength values. From a number of tubes of C1036 material, all parts were to be rejected, for reasons of machinability, whose tensile strength was above 115,000 p.s.i. Test parts having a tensile strength higher than 115,000 p.s.i. have caused excessive wear of the finishing machines. The Magnatest Q instrument sorted the test parts into four groups, which are given in Fig. 53(a).

An annealed part with a tensile strength of 100,000 p.s.i. served as **compensation test body.** The Magnatest sorted four groups with the following tensile strengths: 107,000 to 113,000 p.s.i., 113,000 to 115,000 p.s.i., 116,000 to 120,000 p.s.i., and 122,000 to 129,000 p.s.i. Fig. 53(b) shows the result, which is typical for the application of the test instrument for the sorting of parts with excessive hardness. Such experiments with technological proof of the eddy current test results serve for the calibration of the test instrument for 100 percent sorting.

Forged Parts. The following example (Fig. 54) was obtained for forged parts. Testing for tensile strength is especially successful here. In the finishing of support levers, difficulties were encountered in a plant because of **excessive tool wear,** since the tensile strength limits of 115,000 p.s.i. were occasionally exceeded. The support lever tested has two **journals** which were separated from each other by a distance of 200 mm. With a suitable Magnatest Q coil, it was possible to determine the tensile strength values of the two journals separately. Figs. 54 and 55 give the tensile strength values from the same test part, measured at the large

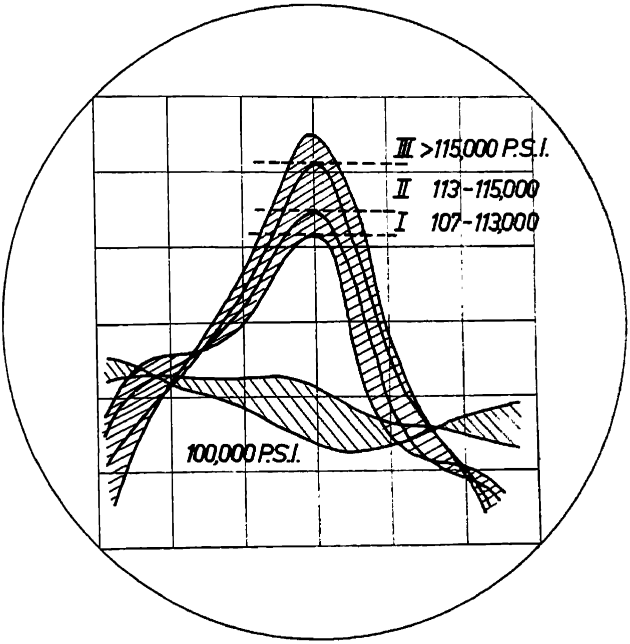

(a)

Group	I	II	III	IV
Number tested	106	60	40	1
Measured tensile strength in p.s.i.	107,000–113,000	113,000–115,000	116,000–120,000	122,000–129,000
Remarks	Usable	Usable	Too hard	Too hard

(b)

Fig. 53. (a) Spread band of C1036 carbon steel at various tensile strength steps. Rejection of all parts having a tensile strength of 115,000 p.s.i. (above the dashed horizontal line) is possible. **(b) Results of Magnatest Q sorting.**

journal (Fig. 54) and at the small journal (Fig. 55). Figs. 54 and 55 are an example of the possibility of testing specific zones separately, which is of special importance on complicated test parts.

Fig. 56 shows the testing of **large crankshafts.** Because of the considerable weight of these test parts, the test coil is placed on the journals, which are thus tested for the correct metallurgical condition.

Fig. 57 also shows results of tests on **drop forgings** of the alloy C1034 at various heat treatment conditions. The curve with the largest peak at the bottom corresponds to the hardened condition, while the other spread bands correspond to conditions of the forged parts which were annealed for various tensile strength ranges. The spread bands in Fig. 57 cover the tensile strength range of from 86,000 to 130,000 p.s.i.

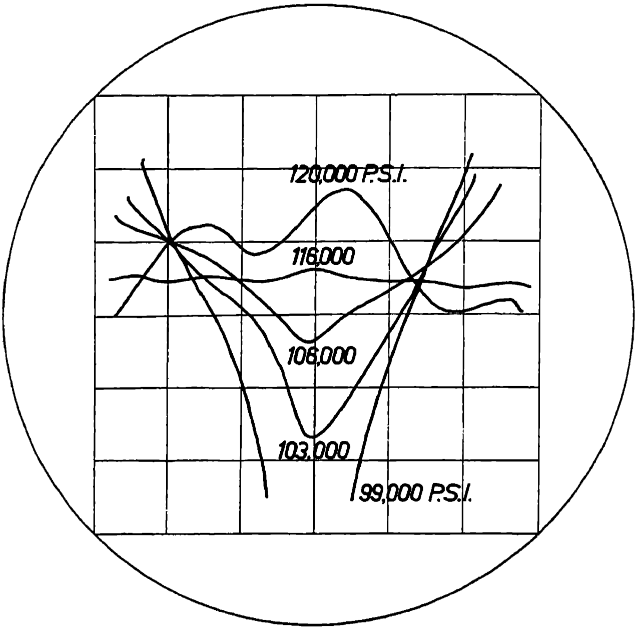

Fig. 54. Sorting for tensile strength of support levers of tempered C1040 carbon steel. The test coil contains the large journal of the support lever.

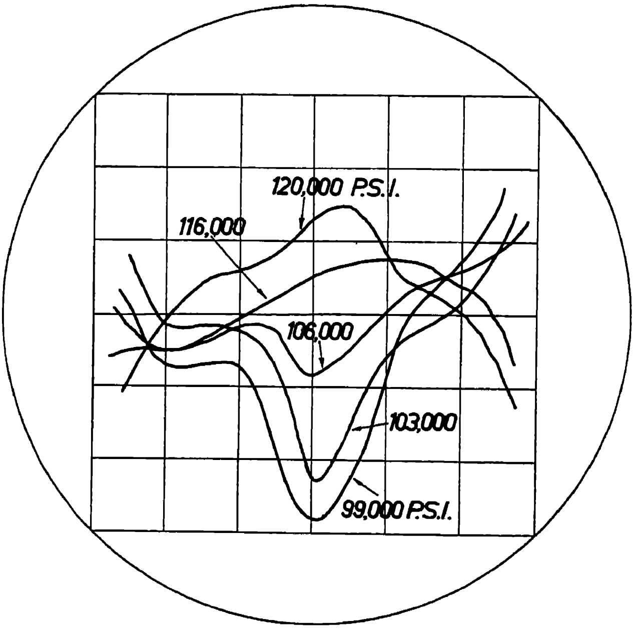

Fig. 55. Sorting of the parts from Fig. 54 for tensile strength, where the small journal of the support lever is in the test coil. Example of testing only a portion of a production part.

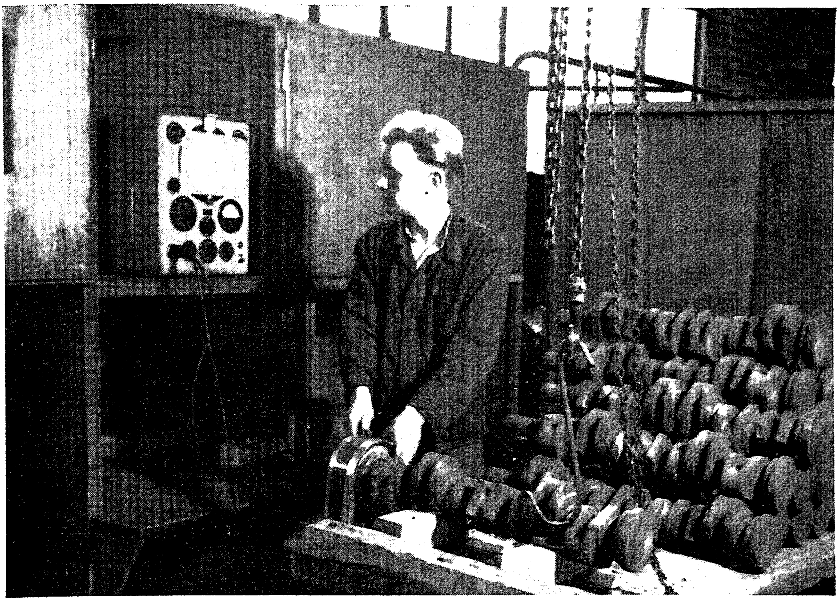

Institut Dr. Foerster

Fig. 56. Testing of large crankshafts for correct metallurgical condition of the journals.

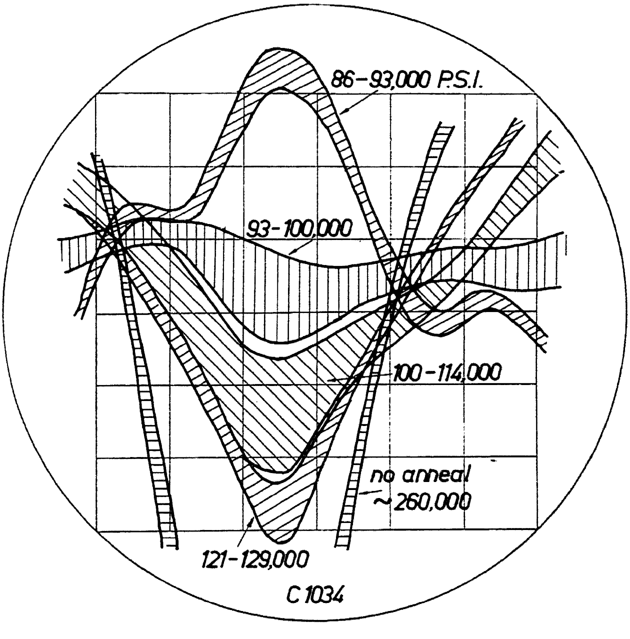

Fig. 57. Screen picture of drop-forged parts of C1034 carbon steel hardened (bottom curve) and annealed for various tensile strengths.

HARDNESS TESTING OF BALL AND ROLLER BEARINGS. The Magnatest Q instrument is also used in the ball-bearing industry for the sorting of ball-bearing rings, rollers, and balls according to **heat treatment** condition. Fig. 58 shows the spread bands of ball-bearing rings which were tempered and annealed for various hardnesses. The curve with the peak at the bottom corresponds to the annealed condition. **Ball-bearing steels** in general result in small spread bands for the various conditions, so that the eddy current sorter provides a higher accuracy than hardness test methods. The speed of hardness testing of items such as ball bearing rings is between 4000 and 8000 pieces per hour. The test parts are transported through the test coil at a specific distance from each other by means of a transport belt.

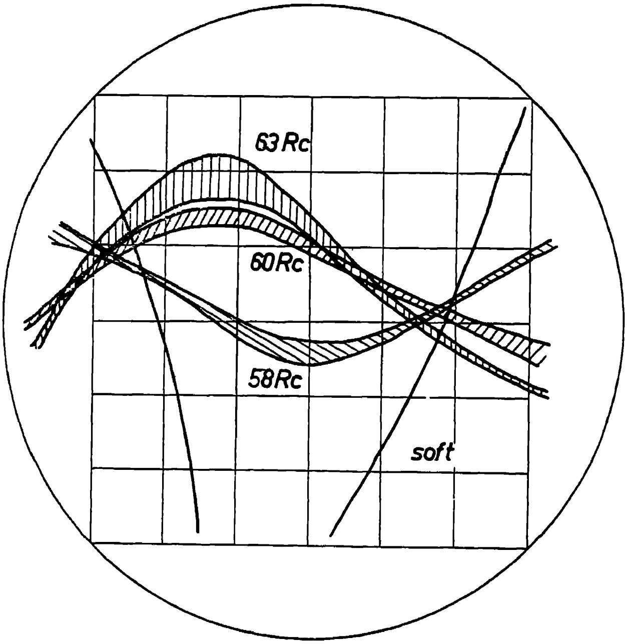

Fig. 58. Spread bands of ball-bearing steel (ball-bearing rings) hardened and annealed at various temperatures. Bottom curve corresponds to the annealed condition.

The Magnatest Q is also used for the sorting of hard and soft balls which pass through the coil in close succession in an endless chain. If a soft ball appears between the hard balls, the sorting gate is triggered, and in addition to the soft ball, several hard balls will fall into the rejection group. At the end the soft balls are retested and separated from the hard balls. Here, of course, an extremely high test speed is obtained.

MEASUREMENT OF CASE DEPTH ON CASE-HARDENED PRODUCTION PARTS. The Magnatest Q is used in many plants for the measurement of the depth of case. Fig. 59 shows the Magnatest Q spread bands of case-hardened **valve stems** which were annealed in a carbon atmosphere for 8, 12, and 16 hr. Case depths of 0.6, 0.9, and 1.6 mm. were obtained. In sorting for case depths, it is relatively simple to adjust the sorting limits so that all test parts with too little or too much case depth will be rejected. For case depths up to approximately 1.5 mm., the frequency of 60 c.p.s. can be used. For greater case depths (which, for example, are common in crankshafts), a frequency of 5 c.p.s. is necessary.

Use of Probe and Yoke Coils. Besides the test coil into which the test part is inserted for testing, yoke and probe coil arrangements are used more and more in connection with the Magnatest Q instrument. In this case the test coil is placed on the test part. Thus it is possible to measure the magnetic and thereby the mechanical and metallurgical properties at a specific point. In large European automobile plants, the case depth at specific points on the **intake valves** for automobiles is tested with the aid of yoke coils. Another application of the point measurement is the **testing for constant case depths** on large machine parts.

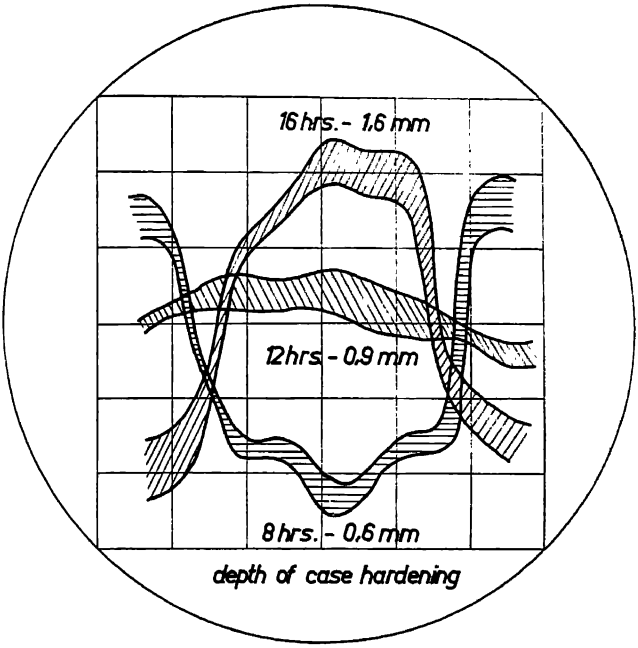

Fig. 59. Magnatest Q spread bands of case-hardened valve stems, which were case-hardened for 8, 12, and 16 hr. to obtain various depths of case.

Valve Stems. Finally, Fig. 60 shows the satisfactory differentiation of the case depth on valve stems, obtained with the Magnatest Q method. It can be seen in Fig. 60 that case-depth variations of 0.1 mm = 4/1000 in. have a considerable influence on the indication, so that sorting in increments of 1/10-mm. case depth is entirely possible. If one considers that this test is possible on fully automatic Magnatest Q equipment within a fraction of a second, then one realizes the saving of time which is connected with such a nondestructive test of an important factor of the test object.

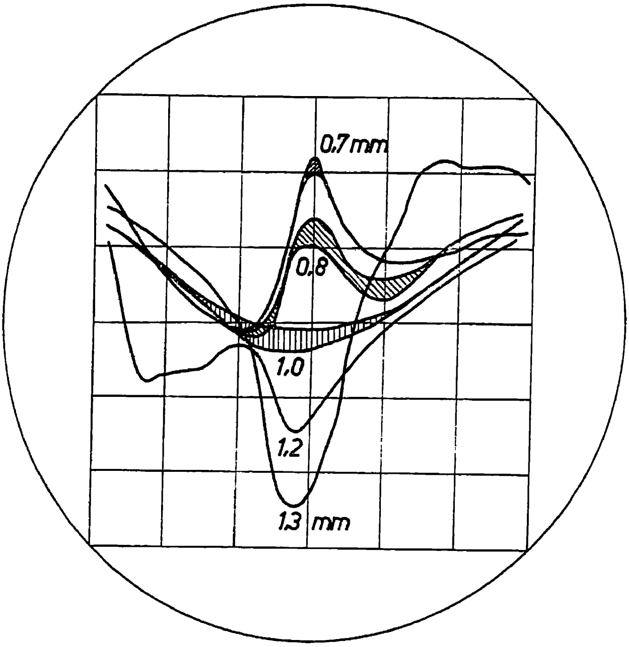

Fig. 60. Magnatest Q spread bands of valves with various depths of case. Resolution better than 4/1000-in. depth of case.

APPLICATIONS IN MATERIALS RESEARCH. As mentioned at the beginning of this section, the examples discussed previously represent only a small selection of numerous test results obtained in many hundreds of European plants with this widely used eddy current method. In addition to being used in nondestructive material testing, the Magnatest Q is also used for many problems in nondestructive material research.

Aging of Thomas Steel. Because of the unusually high sensitivity of the electromagnetic difference method represented by the Magnatest Q, it is possible to notice slight variations during tensile tests or during aging with a sensitivity which far exceeds that of any other method. Fig. 61 shows the results of aging experiments on Thomas steel.[54] In the curve *A*, the Thomas steel was normalized with 0.06 percent C and 0.018 percent N, and quenched in water from 680° C. and precipitated at 110° C. It can be seen that even after 2 hr., a characteristic beginning of the precipitation is noticeable by means of the variation of the Magnatest Q values. In Fig. 61 the slit values of the Magnatest curve of the test body are plotted as a function of time. In curve *B* the same Thomas steel was stretched by 5 percent and precipitated at 100° C. It is clearly shown how the nitrogen segregation is sensitively indicated by the magnetic measurement method. In Fig. 61 the selected test sensitivity is only one-twentieth of the maximum sensitivity of the instrument.

Plastic Flow of Steel During Tensile Tests. Additional experiments were carried out to clarify the behavior of steel during tensile tests, where even far below the yield point an **irreversible deformation** must appear, which is indi-

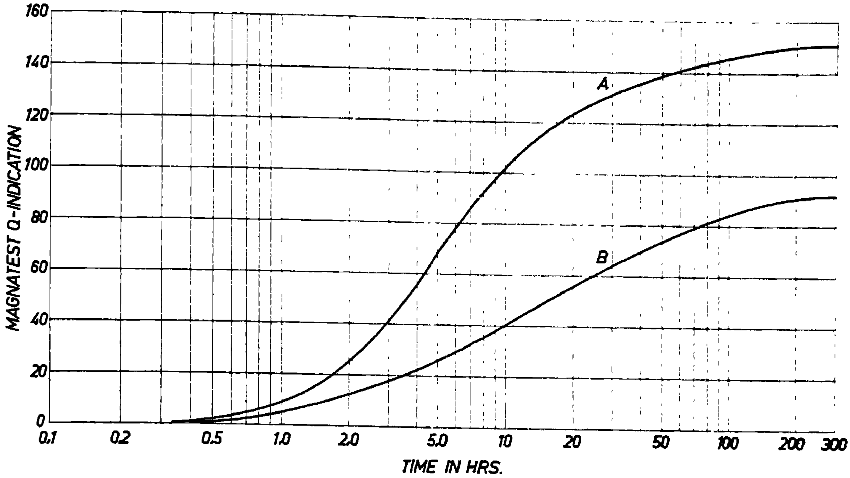

Fig. 61. Results of age-hardening experiments on Thomas steel. Curve *A* shows Thomas steel with 0.06 percent C and 0.018 percent N, normalized and quenched in water from 680° C., then aged at 110° C. The slit values of the Magnatest Q are plotted against time. Curve *B* shows Thomas steel stretched by 5 percent and aged at 100° C. Nitrogen segregation during aging causes the variation of the Magnatest Q values.

cated by the magnetic values. It was demonstrated early that the magnetic difference method is the most sensitive method with which to determine the beginning of the first **plastic flow.**[47]

Crack Testing of Steel

PRINCIPLE OF OPERATION. The Magnatest D has also been used in crack testing of semi-finished steel parts. The Magnatest D operates on a principle similar to that of the Magnatest Q. However, it uses a difference coil for electromagnetic self-comparison of two different portions of the same test object. For crack testing, a considerably higher **field strength** is used than for quality tests, which were discussed in the preceding text. The analysis of the Magnatest D curve picture on the screen of the cathode-ray tube shows that the **internal stress effects** which appear in rods after a straightening process are indicated in a specific phase range. **Cracks,** however, appear in a different phase range, so that the two effects can be separated from each other. In general, the amplitude of screen patterns caused by stress effects, i.e., variations of the permeability, are not noticeably greater than effects which are caused by cracks.

SEPARATION OF CRACK AND STRESS EFFECTS. In the theory of crack testing (see preceding sections on eddy current tests), it was explained why crack effects and stress effects appear at different points on the screen. By means of the phase shifter, the curve on the cathode-ray tube is displaced so that the stress effect has a zero point at the slit in the center of the screen. Thus effects which appear in this slit are caused by cracks. By electronic means the deflections in the slit in the screen center are converted into a signal in which the beginning and the end of the crack are indicated differently. As is well known, the **differ-**

ence method indicates only variations of the crack depth. In other words, no quantitative data concerning the crack depth are available. However, since a crack, with the exception of very rare cases, is subject to continuous depth variations, an indication of this variation effect is usually given. The beginning of a crack results in a deflection on the screen in the opposite direction from that for the end of the crack because the difference coil measures first the increasing crack and then the decreasing crack.

ANALYSIS OF SCREEN PATTERNS. In the exact investigation of the effects of cracks and stresses on the screen picture of the Magnatest D instrument, individual photographs of specific characteristic effects are made first. Then the **technique of multiple exposures** is used. Here the shutter of the camera remains open as the rod proceeds through the test coil, so that all curves which appear on the screen are recorded by the camera. Fig. 62 shows the entirety of all curves which appear on the screen when internal stresses are present, while Fig. 63 shows the multiple-exposure picture of a cracked rod. It is clearly visible that maxima of the indicating effect appear at several points. (The theory for these tests was given in the preceding sections on eddy current tests.)

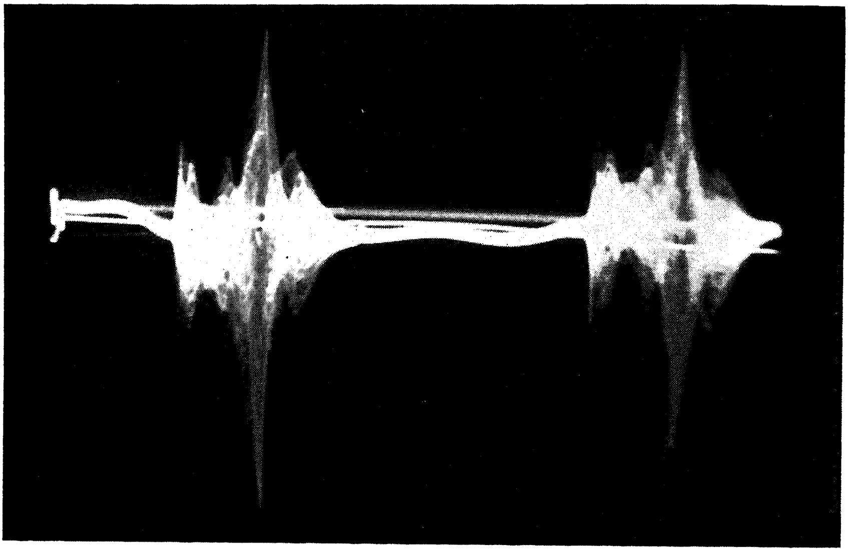

Institut Dr. Foerster

Fig. 62. Multiple-exposure picture of curves appearing on screen when a rod with inhomogeneous stresses passes through the test coil of the Magnatest D instrument.

INTERPRETATION OF CRACK INDICATIONS. Several characteristic examples of cracks in steel are illustrated by means of curve pictures on the screen of the Magnatest D, as well as fracture pictures and microsections of the test objects.

Indications of Sound Rod. Fig. 64(a) shows the multiple-exposure picture of a sound rod. In this picture the camera shutter remained open over the entire

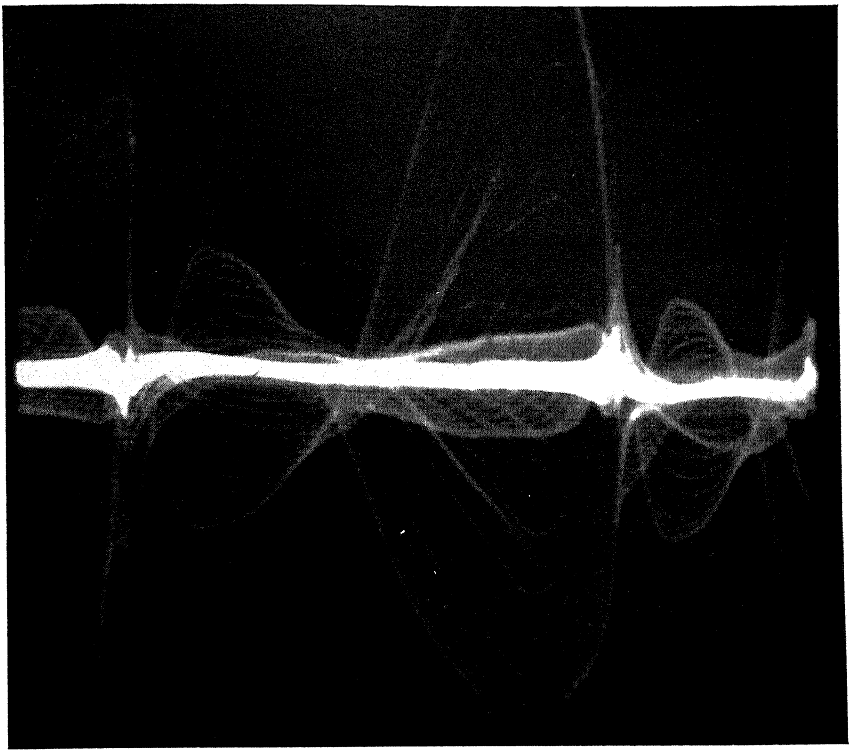

Institut Dr. Foerster

Fig. 63. Multiple-exposure picture of a rod with cracks.

length of the rod. Fluctuations appear only at the peaks, which are caused by **internal stresses.** Fig. 64(b) shows a screen picture of a specific point on the rod (single exposure). It shows that the spread band in the center portion of the curve, which normally indicates the crack effect, is very narrow. Fig. 64(c) illustrates the confirmation for this picture. The fracture shows no defect indications, even under the microscope. Fig. 64(d) shows the microsection etched according to Oberhofer. The **segregation structure** appears clearly in the cross-section of the test body. Fig. 64(e) shows an edge section of the unetched microsection where one can see an accumulation of **nonmetallic inclusions**; these, however, do not influence the screen picture. Fig. 64(f) shows the microsection etched with HNO_3, which indicates no interruptions.

Indications of Defective Rod. Fig. 65(a), however, shows a **multiple-exposure picture** of a rod with a defect. The multiple-exposure curves in the center of the field, which were obtained while the rod passed through, clearly indicate a defect. Fig. 65(b) shows the **single-exposure picture** at the largest defect variation, i.e., the largest deflection of the curves in Fig. 65(a). Fig. 65(c) shows the fracture in the plane of the largest defect variation. One can clearly see the **crack** which was opened by the fracturing; this, however—and it is essential to point this out—is not visible on the surface in its continuation. The

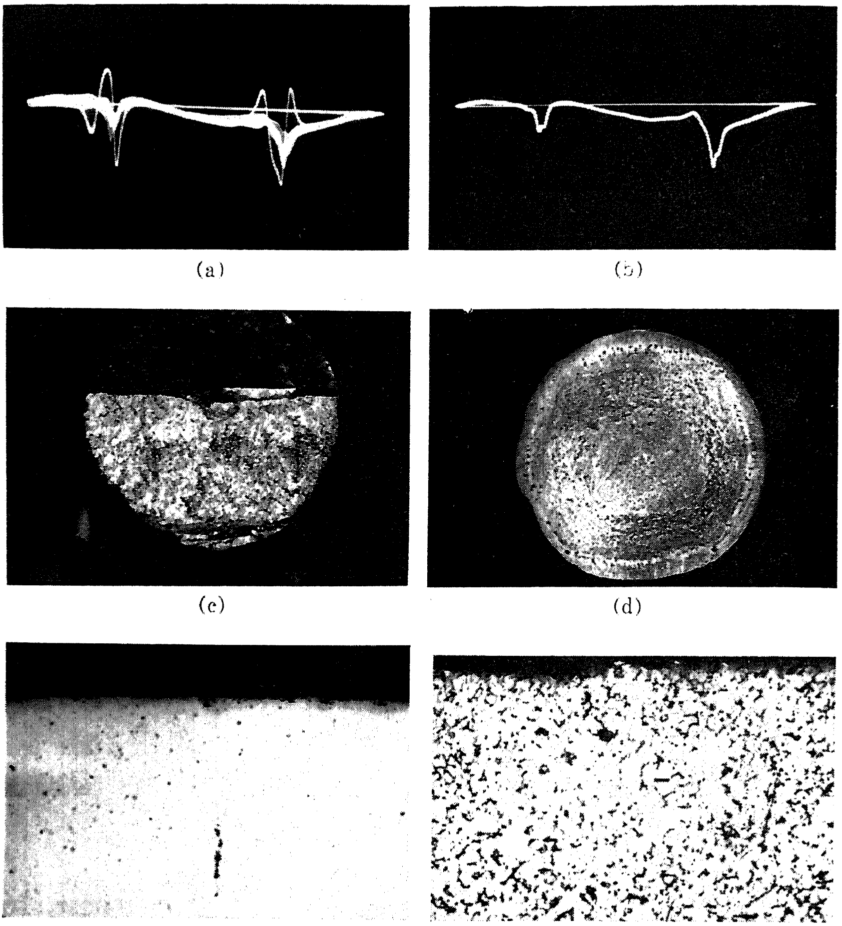

(a) (b)

(c) (d)

(e) (f)

Institut Dr. Foerster

Fig. 64. Analysis of sound test rod. (a) Multiple-exposure picture of a defect-free rod. (b) Single exposure of the Magnatest D curve at a specific point of the rod. (c) Picture of the rod fracture. No defects are detectible. (d) Etching picture according to Oberhofer for a clear illustration of the *P* and *S* segregation in the rod cross-section. (e) Microsection, unetched (100×). (f) Microsection, etched (100×).

short portion, in which the crack came to the surface, caused the indication of the maximum defect variation. Fig. 65(d) shows the microsection etched according to Oberhofer. The upper portion of the picture shows **ray-shaped subsurface voids,** of which the one in the center nearly reaches the rod surface. Fig. 65(f) shows the defect at 100× magnification. Fig. 65(h) shows the etched microsection at a 100× magnification. Even at a 30× magnification, the full size of the void is not visible. However, the 100× magnification shows that the crack, which is continuous to the rod surface, also passes through somewhat larger **nonmetallic inclusions.**

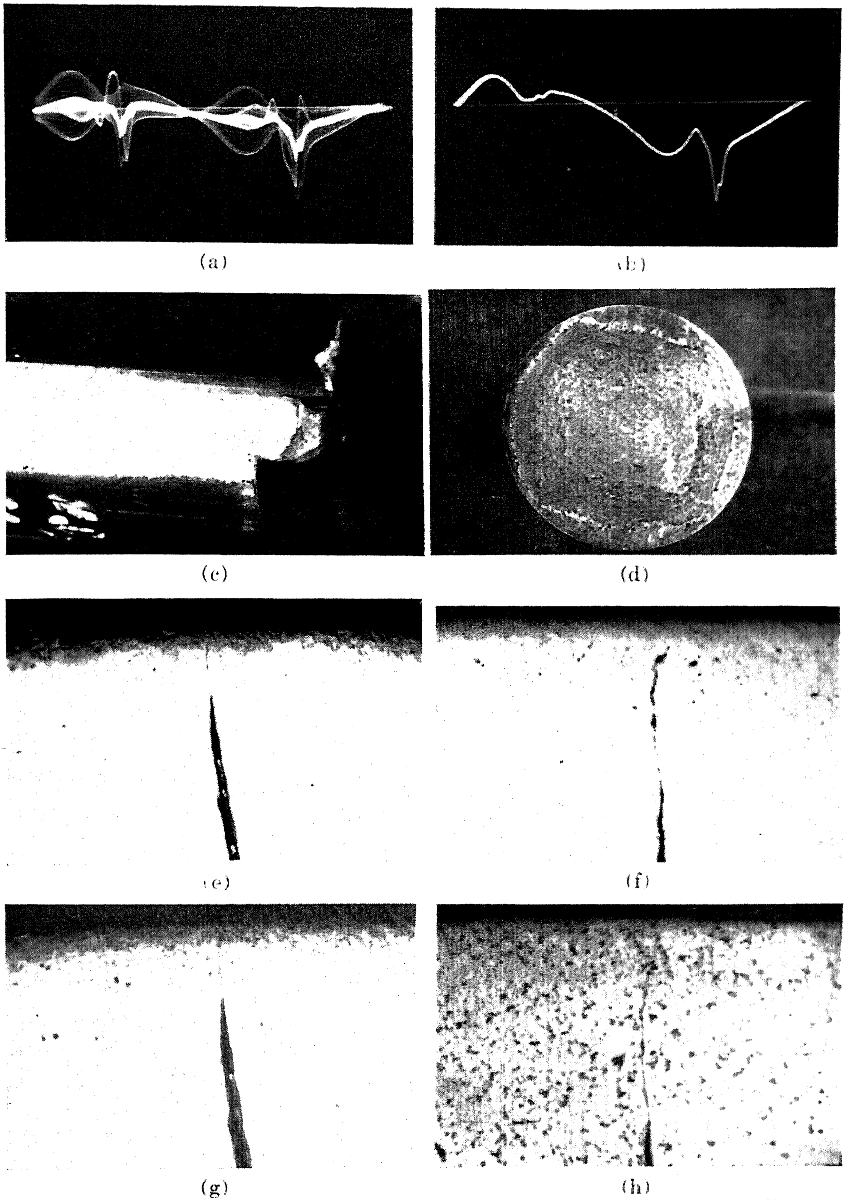

(a) (b) (c) (d) (e) (f) (g) (h)

Institut Dr. Foerster

Fig. 65. Analysis of cracked rod. (a) Multiple-exposure picture of a steel rod with one defect. (b) Single exposure at the largest defect variation. (c) Fracture picture of the point of the rod which corresponds to the curve in picture (b). Clear representation of the crack which was opened by fracturing. (d) Etching picture according to Oberhofer for the representation of the *P* and *S* segregation. (e) Unetched fine-section (30×). (f) Unetched fine-section (100×). (g) Etched section (40×). (h) Etched section (100×). Crack runs along several nonmetallic inclusions to the surface.

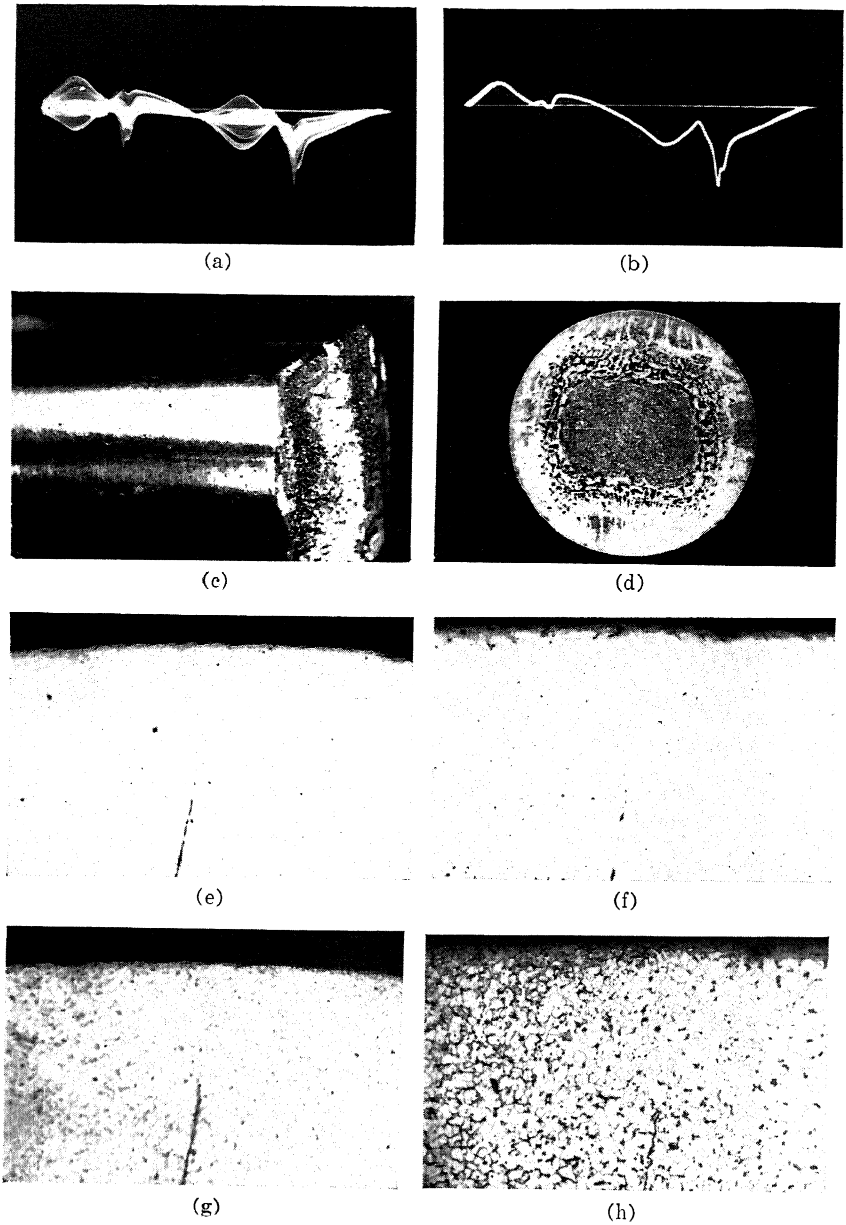
(a) (b) (c) (d) (e) (f) (g) (h)

Institut Dr. Foerster

Fig. 66. Analysis of fine crack. (a) Multiple-exposure picture of a crack, taken with the camera shutter open. (b) Largest defect variation as single exposure. (c) Fracture picture in the plane of the rod which produced the single exposure (b). (d) Etching picture according to Oberhofer for the representation of the P and S segregation in the cross-section. (e, f) Unetched fine-section (30× and 100×). (g, h) Etched fine-section (30× and 100×).

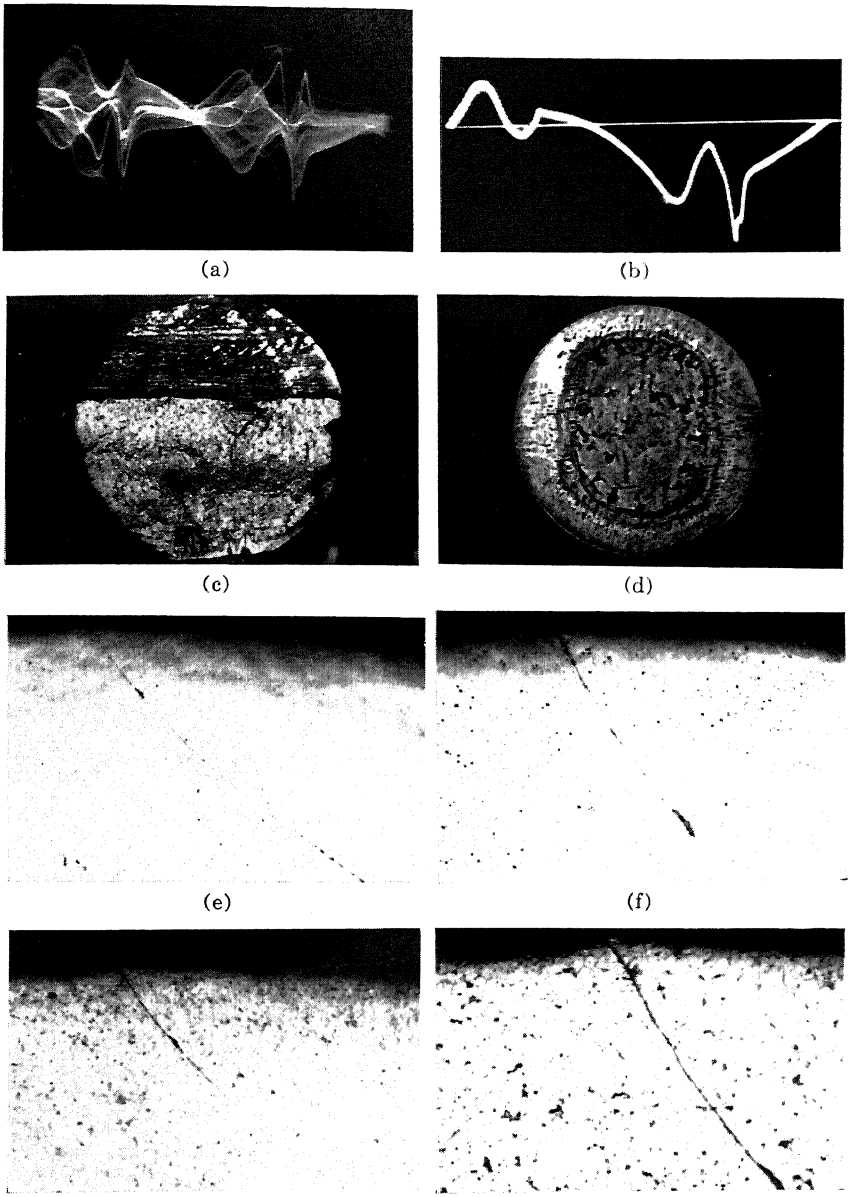

(a) (b)

(c) (d)

(e) (f)

(g) (h)

Institut Dr. Foerster

Fig. 67. Analysis of short discontinuities. (a) Multiple-exposure picture of a steel rod with several short defects. (b) Single exposure of the largest defect variation from (a). (c) Fracture picture, showing inclined, incoming crack on the left side. (d) Etching picture according to Oberhofer. Because of the low magnification, the crack is not visible. (e, f) Unetched fine-section (30× and 100×). (g, h) Etched fine-section (30× and 100×).

Indications of Fine Crack. Fig. 66(a) shows a multiple-exposure picture which again points unequivocally to a defect. Fig. 66(c) shows the fracture in the plane of the largest defect variation and clearly shows the indicated defect in the upper portion. Fig. 66(d) shows the microsection etched according to Oberhofer. However, the defect indicated in Fig. 66(b) is not visible with this magnification. Fig. 66(e) shows the unetched fine-section at a 30× magnification. Here, also, it is a case of an **elongated void** which was opened up to the external skin of the rod by the straightening operation. Fig. 66(f) shows the same defect at a 100× magnification. Fig. 66(g) shows the fine-section etched with NHO_3 at a 30× magnification, while Fig. 66(h) shows the same section at a 100× magnification.

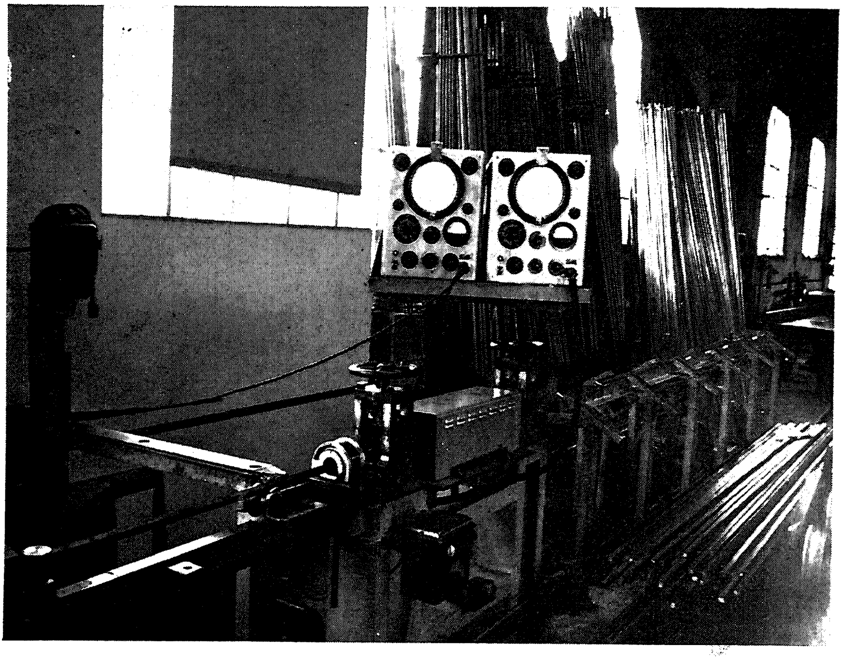

Institut Dr. Foerster

Fig. 68. **Automatic unit in a steel plant for simultaneous quality testing of semi-finished steel parts for mixed alloys and defects.**

Indications of Short Defects. Fig. 67(a) shows the multiple-exposure picture of a rod with several defect variations. It can be concluded from the structure of the multiple-exposure pattern that several short defects exist in the rod. The beginning of an individual defect is indicated by an upward turn of the curve, and the end of the defect by a downward turn of the curve. Fig. 67(b) shows the largest defect variation, i.e., the greatest amplitude in the crack-sensitive phase range, as a stationary picture. Fig. 67(c) shows the fracture which is placed in the plane of the greatest defect variation. An inclined, incoming **crack** is visible on the left side of the fracture. Fig. 67(d) again shows the microsection etched according to Oberhofer. In this picture the defect is not visible because of the low magnification. Fig. 67(e) shows the unetched fine-section at a 30× magnification. The inclined, incoming crack is clearly visible. Fig. 67(f) shows the same section at a 100× magnification. Fig. 67(g) shows the etched fine-section at a 30× magnification, and Fig. 67(h) at a 100× magnification. The defect curve in all microsections is as clear as the indication form of the Magnatest D curve picture.

Crack-Test Equipment Installation. Figs. 63 through 67 illustrate the comparison of crack indications shown on the screen of the Magnatest D instrument with the results obtained metallographically on the defects. These examples represent a small selection from extensive research material collected during recent years. **By systematic analysis of defects** found with the Magnatest D instrument, the cause from which these defects originated could be determined, as for the tungsten wires previously discussed. The pictures are taken from a paper by Sprungmann[81] describing industrial experience with crack testing in a rolling mill, using the Magnatest D instrument. Fig. 68 shows the units used there.

SPECIAL APPLICATIONS OF EDDY CURRENT METHODS. As discussed, the various eddy current methods for nondestructive testing have found wide application for test and research purposes. A few practical applications of scientific and technical investigations are listed here. The following methods, which are carried out with the instruments described in the previous sections, are of practical significance:

1. Noncontacting measurement of the electrical conductivity at high temperatures (taking of temperature-conductivity-diagrams of alloys; control of the sintering process at high temperatures).
2. Measurement of the thickness of an intercrystalline corrosion layer.
3. Determination of the diffusion speed of two metals as a function of temperature.
4. The nondestructive measurement of the corrosion rate under the action of the corroding medium.
   a. For rod-shaped samples.
   b. For flat samples.
5. Electronic indication of a metallurgical condition diagram on the screen of a cathode-ray tube.
6. Noncontacting measurement of the magnetic property variations at high temperatures.
7. Noncontacting measurement of the eccentric position of a conductor in an insulating coating.
8. Control of the metallizing process of metal paper.
9. Method for noncontacting measurement of heating of sewing needles during sewing.
10. Quantitative determination of the magnitude and type of internal stress in ferromagnetic materials.

The methods listed here are discussed more thoroughly in the literature.[42]

The application and interpretation examples given in this section represent only a small portion of the entire application range of the eddy current method. If it is considered that these methods exceed most other nondestructive test methods in test speed, then it is realized that these test methods are excellently suited to control the quality of metal products by means of 100 percent tests.

References

1. Allen, J. W., and R. B. Oliver. "Inspection of Small-Diameter Tubing by Eddy-Current Method," *Nondestructive Testing*, 15, No. 2 (1957): 104.
2. Bates, L. F., and N. Underwood. *B.I.S.R.A.*, *Rept. No.* MG/EG 82 (1948).

3. Beuse, H., and H. Koelzer. "Erfahrungen mit der magnetinduktiven Pruefung von Stabstahl auf Risse (Experience with the Magnetic Testing of Steel Rods for Cracks)," *Arch. Eisenhuetenw.*, 23 (1952): 363.
4. ———. "Industrielle Erfahrungen mit dem Magnatest-Q-Geraet (Industrial Experiences with the Magnatest Q Instrument)," *Z. Metallk.*, 45 (1954): 677.
5. Blanderer, G. "Erkennung und Sortierung von Metallproben (Identification and Sorting of Metal Samples)," *Z. Erzbergbau Metallhuetenw.*, 5 (1952): 257.
6. Bozorth, R. M. *Ferromagnetism.* 2d ed. New York: D. Van Nostrand Co., Inc., 1953. P. 847.
7. Breitfeld, H. "Die zerstoerungsfreie Pruefung von Metallen mit dem magnetinduktiven Tastspul-Geraet (Nondestructive Testing of Metals with the Magneto-Inductive Probe Coil Instrument)," *Metall*, 9 (1955): 14. [Sigmatest]
8. Brown, R. J., and J. H. Bridle. "A New Method of Sorting Steels," *Engineer*, 176 (1943): 442.
9. Bunge, G. "Betriebliche Anwendung eines Tastspulgeraetes bei Nichteisen-Metallen (Industrial Application of the Probe Coil Instrument on Nonferrous Metals)," *Z. Metallk.*, 45 (1954): 205. [Sigmatest]
10. Burrows, C. W., and F. P. Fahy. "Magnetic Analysis as a Criterion of the Quality of Steel and Steel Products," *Am. Soc. Testing Materials, Proc.*, 19, Pt. II (1919): 5.
11. Cannon, W. A., Jr. "Industrial Application of Eddy Current Testing," *Nondestructive Testing*, 11, No. 5 (1953): 30. [Sigmatest, Sigmaflux]
12. ———. "Practical Conductivity Measurement for the Electrical Industry," *Nondestructive Testing*, 13, No. 6 (1955): 32. [Sigmatest]
13. Cavanagh, P. E., and T. Wlodek. "Magnet Stress Analysis," *Am. Soc. Testing Materials, Spec. Tech. Publ.*, 85 (1949): 123.
14. Cornelius, J. R. "Electronic Inspection," *Aircraft Production*, 10 (1948): 52.
15. Coscrove, L. A. "Quality Control Through Nondestructive Testing with Eddy Currents," *Nondestructive Testing*, 13, No. 5 (1955): 13.
16. "Electronic Comparators, An Important Development in Testing Equipment," *Automobile Engr.*, 37 (1947): 206; "Electronic Comparators, Some Applications of Cornelius Equipment," *ibid.*, 271.
17. Foerster, F. "Die automatische Sortierung von Massenteilen nach Rissen mit einem werkstoffunabhaengigen Verfahren (The Automatic Sorting of Production Parts for Cracks with a Material-Independent Method)," *Z. Metallk.* (in press)
18. ———. "Die Automatisierung der zerstoerungsfreien Qualitaetspruefung mit dem Magnatest-Q (The Automation of Nondestructive Quality Testing with the Magnatest Q)," *Z. Metallk.* (in press)
19. ———. "Einfuehrung in die Grundlagen der Wirbelstromrisspruefung von Halbzeug (Introduction to the Foundation of Eddy Current Crack Testing of Semi-Finished Parts)," *Z. Metallk.* (in press)
20. ———. "Grundlagen und Praxis der Dickenmessung duenner Metallischichten (Principle and Practice of the Thickness Measurement of Metal Layers)," *Z. Metallk.* (in press)
21. ———. "Die magnetische und elektromagnetische Sortentrennung von Stahlhalbzeug und Massenteilen (The Magnetic and Electromagnetic Sorting of Semi-finished Steel Production Parts)," *Arch. Eisenhuettenw.*, 25 (1954): 383. [Magnatest Q and Multitest]
22. ———. "Ein Messgeraet zur schnellen Bestimmung magnetischer Groessen (An Instrument for the Rapid Determination of Magnetic Quantities)," *Z. Metallk.*, 32 (1940): 184.
23. ———. "Neuartige Geraete zur zerstoerungsfreien Werkstoffpruefung (New Instruments for Nondestructive Material Testing)," *Z. wirtsch. Fertigung*, 4 (1941). [Metallotest]
24. ———. "Neuere Verfahren zur zerstoerungsfreien Werkstoffpruefung (Newer Methods for Nondestructive Material Testing)," *Berg- u. Huettenmaennische Monats.*, 95 (1950): 284.

25. FOERSTER, F. "Ein neues Verfahren zur Automatisierung der statistischen Qualitaetskontrolle in der zerstoerungsfreien Werkstoffpruefung (A New Method for the Automation of the Statistical Quality Control in Nondestructive Material Testing)," *Z. Metallk.* (in press) [Statimat]

26. ———. "Non-Destructive Electronic Sorting of Metals for Physical Properties," *Am. Soc. Testing Materials, Spec. Tech. Publ.*, 145 (1953): 89. [Multitest]

27. ———. "Nouveaux procédés d'essai électronique non destructif des matériaux (New Procedures for the Electronic Nondestructive Testing of Materials)," *Métaux (Corrosion-Inds.)*, 26 (1951): 497.

28. ———. "Theoretische und experimentelle Grundlagen der elektromagnetischen Qualitaetssortierung von Stahlhalbzeug und Stahlteilen, I. Die magnetinduktiven Verfahren bei alleiniger Beruecksichtigung der Grundwelle (The Theoretical and Experimental Foundation of the Electromagnetic Quality Sorting of of Semi-Finished Steel Production Parts, I. The Magneto-Inductive Method with the Exclusive Consideration of the Fundamental Wave)," *Z. Metallk.*, 45 (1954): 206. [Magnatest Q]

29. ———. "Theoretische und experimentelle Grundlagen der elektromagnetischen Qualitaetssortierung von Stahlteilen, IV. Das Restfeldverfahren (Theoretical and Experimental Foundation of the Electromagnetic Quality Sorting of Steel Parts, IV. The Residual Field Method)," *Z. Metallk.*, 45 (1954): 233.

30. ———. "Theoretische und experimentelle Grundlagen der zerstoerungsfreien Werkstoffpruefung mit Wirbelstromverfahren, I. Das Tastspulverfahren (Theoretical and Experimental Basis for Nondestructive Material Testing with Eddy Current Methods, I. The Pickup Coil Method)," *Z. Metallk.*, 43 (1952): 163. [Sigmatest]

31. ———. "Theoretische und experimentelle Grundlagen der zerstoerungsfreien Werkstoffpruefung mit Wirbelstromverfahren, VII. Die magnetinduktive Risspruefung von Stahl (Theoretical and Experimental Basis for the Nondestructive Material Testing with Eddy Current Methods, VII. The Magneto-Inductive Crack Testing of Steel)," *Z. Metallk.*, 45 (1954): 221. [Magnatest D]

32. ———. "Theoretische und experimentelle Grundlagen der zerstoerungsfreien Werkstoffpruefung mit Wirbelstromverfahren, IV. Praktische Wirbelstromgeraete mit Durchlaufspule zur quantitativen zerstoerungsfreien Werkstoffpruefung (Theoretical and Experimental Basis for the Nondestructive Material Testing with Eddy Current Methods, IV. Practical Eddy Current Instruments with Feed-Through Coil for the Quantitative Nondestructive Material Testing)," *Z. Metallk.*, 45 (1954): 180. [Sigmaflux, Wire-Crack Test Instrument, Multitest]

33. ———. "Theoretische und experimentelle Grundlagen der zerstoerungsfreien Werkstoffpruefung mit Wirbelstromverfahren, VI. Die beruehrungsfreie Messung der Dicke und Leitfaehigkeit von metallischen Oberflaechenschichten, Folien und Blechen, 1. Teil: Theoretische Grundlagen (Theoretical and Experimental Basis for the Nondestructive Material Testing with Eddy Current Methods, VI. The Contact-free Measurement of the Thickness and Conductivity of Metallic Surface Layers, Foils and Sheets, Pt. 1. Theoretical Basis)," *Z. Metallk.*, 45 (1954): 197.

34. ———. "Theoretische und experimentelle Grundlagen des Magnatest Q Geraetes (Theoretical and Experimental Foundation of the Magnatest Q Instrument)," *Z. Metallk.* (in press)

35. ———. "Das Wirbelstromverfahren als quantitatives Pruef- und Messverfahren der zerstoerungsfreien Werkstoffpruefung (The Eddy Current Method as a Quantitative Test and Measurement Method for Nondestructive Material Testing)," *Z. Metallk.* (in press)

36. ———. "Wirbelstromverfahren zur zerstoerungsfreien Werkstoffpruefung von Metallen (Eddy Current Methods for Nondestructive Material Testing of Metals)," *Aluminium*, 30 (1954): 511. [The methods discussed in this article include Sigmatest, Sigmaflux, Crack Tester, Layer Thickness Meter, Wall Thickness Meter.]

37. Foerster, F. "Wirtschaftliche Gesichtspunkte bei der zerstoerungsfreien Werkstoffpruefung (Economic Considerations in Nondestructive Material Testing)," *Z. Metallk.*, 44 (1953): 346.

38. ———. "Wirtschaftliche Gesichtspunkte der zerstoerungsfreien Werkstoffpruefung (Economical Considerations in Nondestructive Material Testing)," *Industrieblatt*, 54, No. 9 (1954).

39. ———. "Die zerstoerungsfreie elektronische Sortierung von Metallen nach physikalischen Eigenschaften (The Nondestructive Electronic Sorting of Metals According to Physical Properties)," *Schweiz. Arch. angew. Wiss. u. Tech.*, 19 (1953): 57. [Multitest]

40. ———. "Die zerstoerungsfreie Messung der Dicke von nichtmetallischen und metallischen Oberflaechenschichten (Nondestructive Measurement of the Thickness of Nonmetallic and Metallic Surface Layers)," *Metall*, 7 (1953): 320.

41. ———. "Die zerstoerungsfreie Messung der Dicke von nichtmetallischen und metallischen Oberflaechenschichten (The Nondestructive Measurement of the Thickness of Nonmetallic and Metallic Surface Layers)," *Jahrbuch Oberflaechentech.* (1954).

42. ———. *Zerstoerungsfreie Werkstoffpruefung mit elektrischen und magnetischen Verfahren* (Nondestructive Material Testing with Electrical and Magnetic Methods). Berlin, Goettingen, Heidelberg: Springer-Verlag. (in press)

43. Foerster, F., and H. Breitfeld. "Theoretische und experimentelle Grundlagen der zerstoerungsfreien Werkstoffpruefung mit Wirbelstromverfahren: V. Die quantitative Risspruefung von metallischen Werkstoffen (Theoretical and Experimental Basis for the Nondestructive Material Testing with Eddy Current Methods, V. Quantitative Crack Testing of Metallic Materials)," *Z. Metallk.*, 45 (1954): 188.

44. ———. "Die zerstoerungsfreie Pruefung von Leichtmetall mit Hilfe einer Tastspule (The Nondestructive Testing of Light Metal by Means of a Pickup Coil)," *Aluminium*, 25 (1943): 253. [Sigmatest]

45. ———. "Zerstoerungsfreie Pruefverfahren auf elektrischer Grundlage (Nondestructive Material Testing on an Electrical Basis)," *Aluminium*, 25 (1943): 130.

46. ———. Zerstoerungsfreie Werkstoffpruefung mit Wirbelstromverfahren, II. Praktische Ergebnisse und industrielle Anwendungen des Tastspulverfahrens (Nondestructive Testing of Materials with Eddy Current Methods, II. Practical Results and Industrial Application of the Pickup Coil Method)," *Z. Metallk.*, 43 (1952): 172. [Sigmatest]

47. Foerster, F., and K. Stambke. "Magnetische Untersuchungen innerer Spannungen, I. Eigenspannungen beim Recken von Nickeldraht (Magnetic Investigations of Internal Strain, I. Internal Stress During the Stretching of Nickel Wire)," *Z. Metallk.*, 33 (1941): 97. "II. Eigenspannungen bei duesengezogenem Nickeldraht (Internal Stress in Nickel Wire Extruded Through a Nozzle)," *ibid.*, 104.

48. ———. "Theoretische und experimentelle Grundlagen der zerstoerungsfreien Werkstoffpruefung mit Wirbelstromverfahren, III. Verfahren mit Durchlaufspule zur quantitativen zerstoerungsfreien Werkstoffpruefung (Theoretical and Experimental Basis for the Nondestructive Material Testing with Eddy Current Methods, III. Feed-Through Coil Method for Quantitative Nondestructive Material Testing)," *Z. Metallk.*, 45 (1954): 166.

49. Foerster, F., and H. Wetzel. "Zur Frage der magnetischen Umklappvorgaenge in Eisen und Nickel (On the Question of Magnetic Reversals in Fe and Ni)," *Z. Metallk.*, 33 (1941): 115.

50. Gerlach, W. "Magnetische Verfahren zur Werkstoffpruefung (Magnetic Method for Material Testing)," *Z. Tech. Physik*, 15 (1934): 467.

51. Gilmour, C. M. "Non-Destructive Testing," *Metal Ind.* (London), 85 (1954): 229.

52. Graef, H. "Die zerstoerungsfreie Qualitaetspruefung von grossen Schmiedeteilen

mit dem Magnatest-Q (Nondestructive Quality Testing of Large Forged Parts with the Magnatest Q)." *Z. Metallk.* (in press)

53. Gromodka, E. "Zerstoerungsfreie Pruefung von Wolfram- und Molybdaen-Draehten mit Hilfe des Drahtrisskawimeters (Nondestructive Testing of Tungsten and Molybdenum Wires with the Aid of the Wire Crack Kawimeter)," *Metall*, 5 (1951): 335. [Wire-Crack Test Instrument]
54. Hennig, R. "Ueber die Anwendung magnetischer Differenzverfahren, insbesondere bei der Untersuchung von Aushaertungs- und Reckalterungsvorgaengen sowie waehrend elastischer und plastischer Verformung (Concerning the Application of the Magnetic Difference Method, Especially in the Investigation of Age-Hardening and Recrystallization Processes as Well as During Elastic and Plastic Deformation)," *Diplomarbeit der Technischen Hochschule Aachen*, (1953).
55. Hochschild, R. "Eddy Current Testing by Impedance Analysis," *Nondestructive Testing*, 12, No. 3 (1954): 35, 51. [Multitest, Sigmatest]
56. ———. "The Theory of Eddy-Current Testing in One (Not-So-Easy) Lesson." *Nondestructive Testing*, 12, No. 5 (1954): 31.
57. Hughes, D. E. "On an Induction Balance," *Phil. Mag.*, [5] 8 (1879): 50.
58. Kayser, O., F. Pawlek, and K. Reichel. "Die Beeinflussung der Leitfaehigkeit reinsten Kupfers durch Beimengungen (The Influence of Impurities on the Conductivity of Purest Copper)," *Metall*, 8 (1954): 532.
59. Keil, A. "Anwendung von Wirbelstromverfahren in einem Metallwerk (Application of the Eddy Current Methods in a Metal Plant)," *Z. Metallk.* (in press) [Sigmatest, Wire-Crack Test Instrument, Equivalent Layer Thickness Meter]
60. ———. "Leitfaehigkeitsmessungen an galvanisch erzeugten Metallfolien (Conductivity Measurement on Galvanically Produced Metal Foils)," *Metalloberflaeche*, 9 (1955): 81(A). [Equivalent Layer Thickness Meter]
61. Keil, A., and C. L. Meyer. "Die Anisotropie der elektrischen Leitfaehigkeit einiger gesinterter Kontaktwerkstoffe (The Anisotropy of Electrical Conductivity of Some Sintered Contact Materials)," *Z. Metallk.*, 45 (1954): 119. [Sigmatest]
62. ———. "Der Einfluss des Faserverlaufes auf die elektrische Verschleissfestigkeit von Wolfram-Kontakten (The Influence of the Direction of the Fibers on the Electrical Corrosion-Resistance of Tungsten Contacts)," *Elektrotech. Z.*, 72 (1951): 343.
63. ———. "Die zerstoerungsfreie Risspruefung von Wolframstaeben nach dem Wirbelstromverfahren (Nondestructive Crack Testing of Tungsten Rods According to the Eddy Current Method)," *Z. Metallk.*, 45 (1954): 194. [Wire-Crack Test Instrument]
64. Keil, A., and G. Offner. "Ueber die Pruefung von Metallbelaegen auf Isolierstoffen mit einem Wirbelstromverfahren (Concerning the Testing of Metal Layers on Insulating Materials with an Eddy Current Method)," *Z. Metallk.*, 45 (1954): 200. [Equivalent Layer Thickness Test]
65. Koch, W. "Industrielle Anwendungen des elektromagnetischen Qualitaetspruefgeraetes in der stahlerzeugenden und stahlverbrauchenden Industrie (Industrial Application of the Electromagnetic Quality Test Instrument in the Steel-Producing and Steel-Consuming Industry)," *Z. Metallk.* (in press) [Magnatest Q]
66. Koester, W., and H. Breitfeld. "Haerte und Leitfaehigkeit kalt ausgehaerteter Aluminium-Legierungen (Hardness and Conductivity of Cold-Hardened Aluminum Alloys)," *Z. Metallk.*, 35 (1943): 163.
67. Matthaes, K. "Abnahmepruefung von Aluminium-Legierungen mit den elektroinduktiven Pruefgeraeten von Dr. Schirp (Receiving Testing of Aluminum Alloys with the Electroinductive Test Instruments by Schirp)." *Aluminium*, 25 (1943): 106.
68. ———. "Erfahrungen bei der zerstoerungsfreien Werkstoffpruefung (Experience with Nondestructive Material Testing)," *Metall*, 5 (1951): 544.

69. Matthaes, K. "Magnetinduktive Stahlpruefung (Magnetoinductive Testing of Steel)," *Z. Metallk.*, 39 (1948): 257.
70. McClurg, G. O. "Theory and Application of Coil Magnetization," *Nondestructive Testing*, 13, No. 1 (1955): 23.
71. Nachtigall, E. "Die elektrische Leitfaehigkeit von Aluminium (The Electrical Conductivity of Aluminum)," *Aluminium*, 30 (1954): 529. [Sigmatest]
72. Nowotny, H., W. Thury, and H. Landerl, "Die Bestimmung von Silicium in Reinaluminium mittels elektrischer Leitfaehigkeitsmessung (The Determination of Si in Pure Aluminum by Means of Conductivity Measurement)," *Z. anal. Chem.*, 134 (1951): 241. [Sigmatest]
73. O'Dell, D. T. "Apparatus for the Detection of Splits in Tungsten Wire," *J. Sci. Instr.*, 20 (1943): 147.
74. Plant, W. R., and C. Manual. "Eddy Current Testing of Capillary Tubing," *Am. Soc. Testing Materials, Spec. Tech. Publ.*, 223 (1958).
75. Robinson, I. R. "Magnetic and Inductive Nondestructive Testing of Material," *Metal Treatment*, 16 (1949): 12.
76. Ryder, C. M. "Devices for Testing Carbonization of Metals," U.S. Patent No. 185,647 (1876).
77. Sanford, R. S., and M. F. Fischer. "Application of Magnetic Analysis to the Testing of Ball Bearing Races," *Am. Soc. Testing Materials, Proc.*, 19, Pt. II (1919): 68.
78. Schirp, W. "Die magnetinduktive Pruefung von Rohren (The Magneto-Inductive Testing of Tubes)," *Elektrotech. Z.*, 60 (1939): 857. "Neue magnetinduktive Pruefgeraete fuer Halbzeuge aus Nichteisenmetallen (New Magnetoinductive Testing Apparatus for Semi-Finished Material of Nonferrous Metals)," *ibid.*, 64 (1943): 413.
79. ———. "Zerstoerungsfreie Werkstoffpruefung mit Hilfe elektronischer Verfahren (Nondestructive Material Testing with the Aid of Electronic Methods)," *Elektropost*, 8/9 (1954): 234.
80. Sprungmann, K. "Betriebliche Erfahrung der Wirbelstrom-Risspruefung bei Stahlhalbzeug (Industrial Experience with Eddy Current Testing of Semi-finished Steel)," *Z. Metallk.*, 45 (1954): 227. [Magnatest D]
81. ———. "Industrielle Erfahrungen der Risspruefung von Stahlhalbzeug mit dem Magnatest D (Industrial Experience with the Magnatest D in the Crack Testing of Semi-finished Steel Parts)," *Z. Metallk.*, (in press)
82. ———. "Die Risspruefung von Stahlhalbzeug mit dem Magnatest D (The Crack Testing of Semi-finished Steel Parts with the Magnatest D)," *Z. Metallk.* (in press)
83. Staats, H. N. "Conductivity—Now a Useful Nondestructive Testing Tool," *Materials and Methods*, 38, No. 4 (1953): 124. [Sigmatest]
84. Vosskuehler, H. "Zerstoerungsfreie Pruefung der Al-Mg-Zn-Legierung Hy 43 auf magnetinduktivem Wege (Nondestructive Testing of an Al-Mg-Zn Alloy Hy 43 with a Magnetoinductive Method)," *Metall*, 3 (1949): 247, 292.
85. Wieland, F., and F. Rosche. "Elektronische Fehlersortierung mit dem Multitest-Geraet (Electronic Defect Sorting with the Multitest Instrument)," *Z. Metallk.*, 45 (1954): 231. [Multitest]
86. Williams, S. R. "The Magnetic-Mechanical Analysis of Cast Iron," *Am. Soc. Testing Materials, Proc.*, 19, Pt. II (1919): 130.
87. Zeppelin, H. von. "Betriebliche Schnellbestimmung und Aenderung des Phosphorgehaltes in Schmelzen von Kupfer und Kupferlegierungen (Rapid Industrial Determination and Change of Phosphorus Content in Metals of Copper and Copper Alloys)," *Giesserei*, 38 (1951): 51. [Sigmatest]
88. Zijlstra, P. "Die Pruefung von Draehten aus Wolfram und Molybdaen auf Risse (The Testing of Tungsten and Molybdenum Wires for Cracks)," *Philips Tech. Rev.*, 11 (1949): 12.
89. Zuschlag, T. "Magnet Analysis Inspection in the Steel Industry," *Am. Soc. Testing Materials, Spec. Tech. Publ.*, 85 (1949): 113.

SECTION 43

ULTRASONIC TEST PRINCIPLES

CONTENTS

PAGE

Basic Methods of Ultrasonic Inspection

Transmission and reflection techniques 1
Basic testing methods (*f.* 1) 2
Ultrasonic test systems 1
Ultrasonic frequency ranges 1
Ultrasonic stress ranges 1
Applications of ultrasonic techniques 2
Advantages of ultrasonic tests 2
Limitations of ultrasonic tests 2
Development of tests 3
Early industrial applications 3
Recent improvements 3

Generation of Ultrasonic Vibrations

Ultrasonic sources 4
Ultrasonic transducer types 4
Typical transducer characteristics 4
Properties of thickness-mode transducer elements (*f.* 2) 4
Activity constant 4
Resolving power and sensitivity 5
Additional design requirements 5
Typical search units (*f.* 3) 6
Straight-beam contact units 5
Straight-beam faced units 5
Angle-beam contact units 5
Immersion units 7
Contoured or focused units with acoustic lenses 7
Standard ratings 7
Search unit frequencies and sizes most commonly used (*f.* 4) 7
Special units 7

Ultrasonic Wave Propagation Characteristics

Assumptions 9
Wavelength 9
Acoustic properties of materials (*f.* 5) ... 8
Velocity 9
Principal wave velocities in solids (*f.* 6).. 9
Calculation of acoustic velocities 10
Relationships between ultrasonic velocities and the elastic constants of isotropic solids (*f.* 7) 10
Relationship of velocity ratios to Poisson's ratio (*f.* 8) 11
Impedance 12

PAGE
Effects at plane interfaces 12
Reflection 12
Percentage ultrasonic reflection coefficients for normally incident plane waves at interfaces between various materials (*f.* 9) 13
Transmission through thin plates 14
Transmission through thin plate (*f.* 10) .. 14
Resonance thickness measurements 15
Refraction 15
Refraction and mode conversion at plane interface (angular incidence) (*f.* 11).... 16
Mode conversion 17
Mode conversion by reflection at plane interface (*f.* 12) 16
Angular and amplitude relationships 18
Amplitude ratio of reflected-to-incident longitudinal waves (*f.* 13) 17
Amplitude ratio of reflected-to-incident shear waves (*f.* 14) 18
General cases of angular incidence 19
Longitudinal waves in water incident on steel (*f.* 15) 19
Longitudinal waves in steel incident on water (*f.* 16) 20
Shear waves in steel, vibrating in plane of incidence, incident on water (*f.* 17) .. 21
Refraction analyzer (*f.* 18) 22
Refraction data (*f.* 19) 23
Beam spread (*f.* 20) 24
Diffraction 21
Attenuation 22
Attenuation sources and relationships (*f.* 21) 25
α', attenuation (db. cm.)^{29} (*f.* 22) 26
Disturbing influences 24

Basic Instrumentation and Techniques

Classification of equipment 26
Through-transmission techniques 27
Equipment 27
Types of through-transmission systems (*f.* 23) 27
Defect detectibility 27
Limitations 28
Advantages 28
Applications 28
Techniques using amplitude and transit-time indication 28
Time measurement systems.................. 28
Equipment 28

CONTENTS (*Continued*)

PAGE
- Basic pulse-reflection system (*f.* 24) 29
- A-scan presentation 29
  - Functional diagram of pulse-reflection A-scan equipment (*f.* 25) 30
- Techniques 30
  - Basic testing methods (*f.* 26) 31
- Distance or time scale markers 30
- Limitations 31
  - Testing distance obscured by pulse (interface signal or initial pulse) (*f.* 27) 32
- Sensitivity 31
- Alternative arrangements 32
- Special features 33
- B-scan presentation 33
  - B-scan presentation (*f.* 28) 34
  - Equipment 33
  - Defect detectibility 33
  - Alternative arrangements 34
- C-scan presentation 34
  - Equipment 34
    - C-scan presentation (*f.* 29) 35
  - Alternative arrangements 34
  - Gated systems 35
- Techniques using transducer loading effects .. 35
  - Equipment 36
    - Manual resonance system (*f.* 30) 36
    - Automatic resonance system (*f.* 31) 36
  - Resonant frequencies 36
  - Thickness measurements 37
  - Alternative arrangements 37

Calibration Problems

- Need for calibration 37
- Basic considerations 37
- Major parameters 38
  - Parameters affecting signals in ultrasonic pulse-reflection technique (*f.* 32) 38
  - Operator-controlled parameters 39
  - Parameters controlled by inspection problems 39
- Evaluation of parameters 39
  - Basic types of test blocks used for calibration (*f.* 33) 40
  - Amplitude-distance data for standard contact search units (*f.* 34) 41
  - Beam profile variation with distance (*f.* 35) 41
  - Comparative amplitude-distance data, contact test (*f.* 36) 42
  - Comparative amplitude-distance data, contact tests (*f.* 37) 43
  - Comparative amplitude-distance data; immersed tests for four materials (*f.* 38) 44
  - Reflections from immersed steel spheres (*f.* 39) 45
  - Amplitude versus area calibration data (*f.* 40) 46
  - Calculated signal-amplitude ratios in immersed testing of various metals (*f.* 41) 46
  - Test conditions for Fig. 41 (*f.* 42)..... 47

Ultrasonic Test Features

- Testing applicability 47
- Advantages 47
  - Mechanical testing 47
  - Instantaneous indication 47
  - Volume scanning 47
  - Versatility 47
  - Safety and convenience 48
  - Wide applicability 48
  - Sensitivity and directivity 48
  - Portability 48
  - Ease of operation 48
  - High development 48
  - Wide acceptability 48
- Capabilities 48
  - Established applications 48
  - Applications proved feasible 49
  - Potential applications 49
- Limitations 49
  - Defect detectibility 49
  - Coupling and scanning 50
  - Economics 50
- Criteria for successful inspection 50
- References 50

SECTION 43

ULTRASONIC TEST PRINCIPLES

Basic Methods of Ultrasonic Inspection

TRANSMISSION AND REFLECTION TECHNIQUES. Ultrasonic inspection is usually performed by one of two basic methods. A beam of ultrasonic energy is directed into the specimen and (1) the energy transmitted through it is indicated or (2) the energy reflected from areas within it is indicated. Inspection is accomplished because the ultrasonic beam travels with little loss through homogeneous material except when it is intercepted and reflected by discontinuities in the elastic continuum. Fig. 1 illustrates two basic techniques applied to internal flaw detection. In Fig. 1(a), the flaw is detected by the decrease of transmitted energy at the receiver; in Fig. 1(b) it is detected by energy reflected to the receiver.

ULTRASONIC TEST SYSTEMS. A complete ultrasonic inspection system consists of the **basic components** shown in Fig. 1, including:

1. Electrical signal generator, *G*.
2. Transmitting transducer, or "search unit."
3. Couplant to transfer acoustic energy to specimen.
4. Test specimen.
5. Couplant to transfer acoustic energy to receiver.
6. Receiving transducer, or "search unit."
7. Electrical indicator, *I*.

Component design and arrangement will depend primarily upon which specific characteristics of ultrasonic wave propagation are utilized for detection and measurement of specimen properties. The phenomena involved may include:

1. Velocity of wave propagation.
2. Beam geometry (focusing field pattern or dual-transducer systems).
3. Energy transfer (reflection, refraction, or mode conversion).
4. Energy losses (scattering, absorption).

Ultrasonic Frequency Ranges. Ultrasonic inspection utilizes high-frequency mechanical vibrations for nondestructive testing of materials. Most commercial ultrasonic testing is done at frequencies between 1 and 25 megacycles per second (Mc.). However, applications exist for frequencies as low as 25 kilocycles per second (kc.) and as high as 200 Mc. Various ultrasonic inspection techniques and instruments have been developed to beam ultrasonic energy directly through test objects. **Low-frequency resonance methods** (see section on Natural Frequency Vibration Tests), in which the entire specimen is caused to vibrate at sonic frequency, should not be confused with ultrasonic methods whose probing beam is usually restricted to a small fraction of the specimen.

Ultrasonic Stress Ranges. All mechanical testing methods involve similar phenomena described by the fundamental laws of mechanics and acoustics. The various methods differ primarily in the frequency and magnitude of the stresses developed in the test material. Sonic and ultrasonic nondestructive tests employ low-amplitude stresses which do not permanently affect the specimen. **Destructive mechanical tests,** such as static physical tests and forced-vibration fatigue testing, usually involve high-amplitude stresses. These may cause heating, nonlinear effects, permanent deformation, and eventual rupture of the sample.

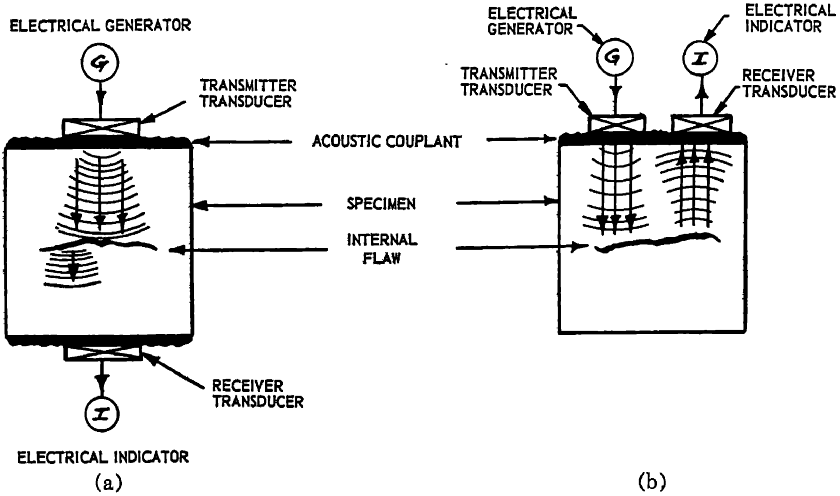

Fig. 1. Basic testing methods. (a) Flaw detected by decrease of energy at receiver. (b) Flaw detected by energy reflected to receiver.

Applications of Ultrasonic Techniques. Because ultrasonic techniques are basically mechanical phenomena, they are particularly adaptable to the determination of structural integrity of engineering materials. Their principal applications consist of:

1. Flaw detection.
2. Thickness measurement.
3. Determination of elastic moduli.
4. Study of metallurgical structure.
5. Evaluation of the influence of processing variables on the specimen.

Advantages of Ultrasonic Tests. The desirable features of ultrasonic tests include:

1. High sensitivity, permitting detection of minute defects.
2. Great penetrating power, allowing examination of extremely thick sections.
3. Accuracy in the measurement of flaw position and estimation of flaw size.
4. Fast response, permitting rapid and automated inspection.
5. Need for access to only one surface of the specimen.

Limitations of Ultrasonic Tests. Test conditions which may limit the application of ultrasonic methods usually relate to one of the following factors:

1. Unfavorable sample geometry; for example, size, contour, complexity, and defect orientation.
2. Undesirable internal structure; for example, grain size, structure porosity, inclusion content, or fine, dispersed precipitates.

Development of Tests. The possibility of utilizing ultrasonic waves for nondestructive testing was recognized in the 1930's in Germany by Mulhauser,[1] Trost,[2] Pohlman,[3] and in Russia by Sokoloff,[4] all of whom investigated various continuous wave techniques. **Flaw detection equipment** was eventually developed, based on the principle of ultrasonic energy interception by a gross flaw in the path of the beam. This technique later became known as the **through-transmission method.** An ingenious transmission system developed by Pohlman produced shadow-like images of internal flaws.[5] Later, several transmission-type flaw detectors were marketed.

During this early period, efforts were also made to employ reflected as well as transmitted ultrasonic waves. These were intended to overcome certain limitations of the earlier methods, especially the necessity of requiring access to both specimen surfaces. No practical method was found, however, until Firestone invented apparatus utilizing **pulsed ultrasonic wave trains** to obtain reflections from minute defects.[6, 7] This development, which he called the "Supersonic Reflectoscope," was aided by the rapid growth of electronic instrumentation techniques. It led during the 1940's to the marketing of practical ultrasonic flaw detectors in the United States and abroad. In the same period, ultrasonic test equipment was developed independently by Sproule in England[8] (see the section on Double-Transducer Ultrasonic Tests). As with early industrial X-ray equipment, the first instruments were for the most part considered to be laboratory tools and were installed in metallurgical research departments.

Early Industrial Applications. Production applications were soon found, and ultrasonic inspection was applied to critical **quality control** problems. Among the outstanding early applications was the inspection of the first jet-engine rotor forgings for internal flaws[9] (see section on Ultrasonic Immersion Test Indications). In the meantime, fundamental and applied research continued and many significant contributions were made. Firestone and his associates at the University of Michigan investigated transducer mechanisms,[10] polarized sound using shear waves,[11] applications of Rayleigh or surface waves,[12] the Raybender for variable-angle inspection,[13] the delay column or "schnozzle" for close-to-surface inspection,[14] a pulsed-resonance method for thickness measurement,[15] and a variety of Lamb or "plate" wave techniques.[16] Other developments included a frequency-modulated resonance thickness gage by Erwin,[17, 18] improved immersed inspection systems by Erdman,[19, 20] and several ultrasonic visualization or flaw-plotting techniques by Sproule,[21] Erdman,[22] Wild and Reid,[23] Howry,[24] and others. (See Pringle[25] and Smack.[26])

Recent Improvements. Recent developments relate primarily to one or more of the following:

1. High speed, automated inspection systems.
2. Improved instrumentation for greater resolution of flaw indications.
3. Better data presentation.
4. Simpler interpretation.
5. Studies of fine changes in metallurgical condition.
6. More detailed analyses of the acoustic phenomena involved.

During the same period those concerned directly with application of ultrasonic inspection techniques made contributions toward its utilization and to the establishment of procedures and standards, particularly in the aircraft, electrical, and nuclear energy fields.

Generation of Ultrasonic Vibrations

ULTRASONIC SOURCES. Mechanical vibrations for measurement, analysis, or test purposes are generated by **electromechanical transducers,** i.e., elements having the ability to transform electrical into mechanical energy, and vice versa. For ultrasonic inspection at frequencies above 200 kc., **piezoelectric transducers** are used. These employ materials which generate electric charges when mechanically stressed, and conversely, become stressed when electrically excited. Transducer elements suitably mounted for inspection work are commonly called **search units, crystals,** or **probes.** (See section on Ultrasonic Transducers for details of transducer materials, construction, and characteristics.)

ULTRASONIC TRANSDUCER TYPES. Transducer materials[27, 28, 29] having the best characteristics for search units are (1) natural quartz crystals, (2) lithium-sulfate monohydrate crystals, and (3) polarized polycrystalline ceramics such as fired barium titanate. Transducer elements which operate as **thickness expanders** are widely used. These produce motion similar to that of an oscillating piston and generate compressional waves in the specimen. For special studies requiring **transverse waves,** crystal cuts can be used which produce shear motion. If maximum sensitivity is required, the element is electrically driven at its fundamental resonant frequency.

TYPICAL TRANSDUCER CHARACTERISTICS. The properties of typical 1-Mc. transducer elements are given in Fig. 2.[30] Values for other frequencies, f, or areas, A, can be found by using the relationship:

Thickness: $$t = t_1/f \tag{1}$$

Capacitance: $$c = c_1 \times f \times A \tag{2}$$

where t = thickness, in.
t_1 = 1-Mc. thickness, in.
f = frequency, Mc.
c = capacitance, μμf.
c_1 = unit capacitance, μμf/in.^{2}.
A = area, in.^{2}.

Material	Wave	Thickness, t_1 ($f = 1$ Mc.)	Capacitance, c_1 (Area = 1 in.^{2})	Activity Constants*	
				S_T	S_R
X-cut quartz	Longitudinal	0.1126 in.	9 μμf	1	1
Y-cut quartz	Transverse	0.084 in.	14 μμf	–	–
Lithium sulfate	Longitudinal	0.100 in.	22 μμf	8	3
Ceramic titanate	Longitudinal	0.1 in.	2000 μμf	25	2

* Determined experimentally for typical search unit assemblies.

Fig. 2. Properties of thickness-mode transducer elements.

Activity Constant. Activity constants indicate approximate sensitivities of elements as acoustic transmitters, S_T, and receivers, S_R, as compared with X-cut quartz. The absolute magnitudes are dependent upon the mechanical loading on front and back faces of the transducer, the nature of the applied electric signal, and the effective electrical impedances involved.

Resolving Power and Sensitivity. The resolving power of a search unit is directly proportional to its **band width** (Δf), which is primarily a function of the damping produced by the mechanical loading on its faces. Conversely, the number of cycles required for crystal vibration to reach full amplitude when driven by constant a.-c. supply voltage is given by its **mechanical Q** (the reciprocal of band width expressed in percentage). Typical measured values of Δf and Q determined experimentally for 1-Mc. ultrasonic immersion search units (i.e., with a water load on front face) are given in the accompanying table.[27, 30]

Transducer	Backing	Δf(Mc.)	Q
Quartz	Air	0.06	17
Quartz	Phenolic	0.16	6
Quartz	Loaded epoxy	0.25	4
Barium titanate	Phenolic	0.1	10
Barium titanate	Loaded epoxy	0.25	4
Lithium sulfate	Loaded epoxy	>0.3	<3

Since the sensitivity of a given system increases directly with the Q of its components (search unit, pulser, and electrical amplifier), a compromise to achieve the optimum sensitivity-resolution product is desirable. System Q's of 3 to 10 are typical in commercial pulsed-wave-train flaw detectors. For a given Q, resolution increases directly with system frequency.

Additional Design Requirements. In the design of practical search units for various applications, additional requirements to be considered include:

1. Mechanical: contact area, wear resistance, waterproofing, and connectors.
2. Electrical: voltages, wave shapes, capacity, and grounding.
3. Acoustic: noise level, beam divergence, and face plates.

Construction of four principal types of **search unit assemblies** is shown in Fig. 3.

Straight-Beam Contact Units. Straight-beam contact search units, whose construction is shown in Fig. 3(a), have one face of the crystal exposed to contact the work. These units are widely used in the 0.5- to 10-Mc. frequency range and can generally be used on any reasonably flat surface which is electrically conductive. Typical variations in construction include spring mounting and curved crystals.

Straight-Beam Faced Units. Fig. 3(b) shows the construction of straight-beam faced units. These employ thin **wear plates** to prevent crystal breakage and to protect the front electrode which provides internal grounding. Facings of quartz, metal, plastic, and rubber have been used. Applications include testing of **rough surfaces** and **electrical nonconductors.** For rapid testing of large plate, a special unit employing a moving plastic belt between the crystal and specimen has been developed.

Angle-Beam Contact Units. Angle-beam search units, which direct the beam away from normal incidence toward selected areas within a specimen, use a wedge between the crystal and sample [Fig. 3(c)]. Various **wedge materials** have been used, the most successful being methacrylate resin.[31] Particularly useful units are available which utilize shear or surface waves produced by refraction and mode conversion.[32] Most of the commercial angle-beam units operate in the 1- to 5-Mc.

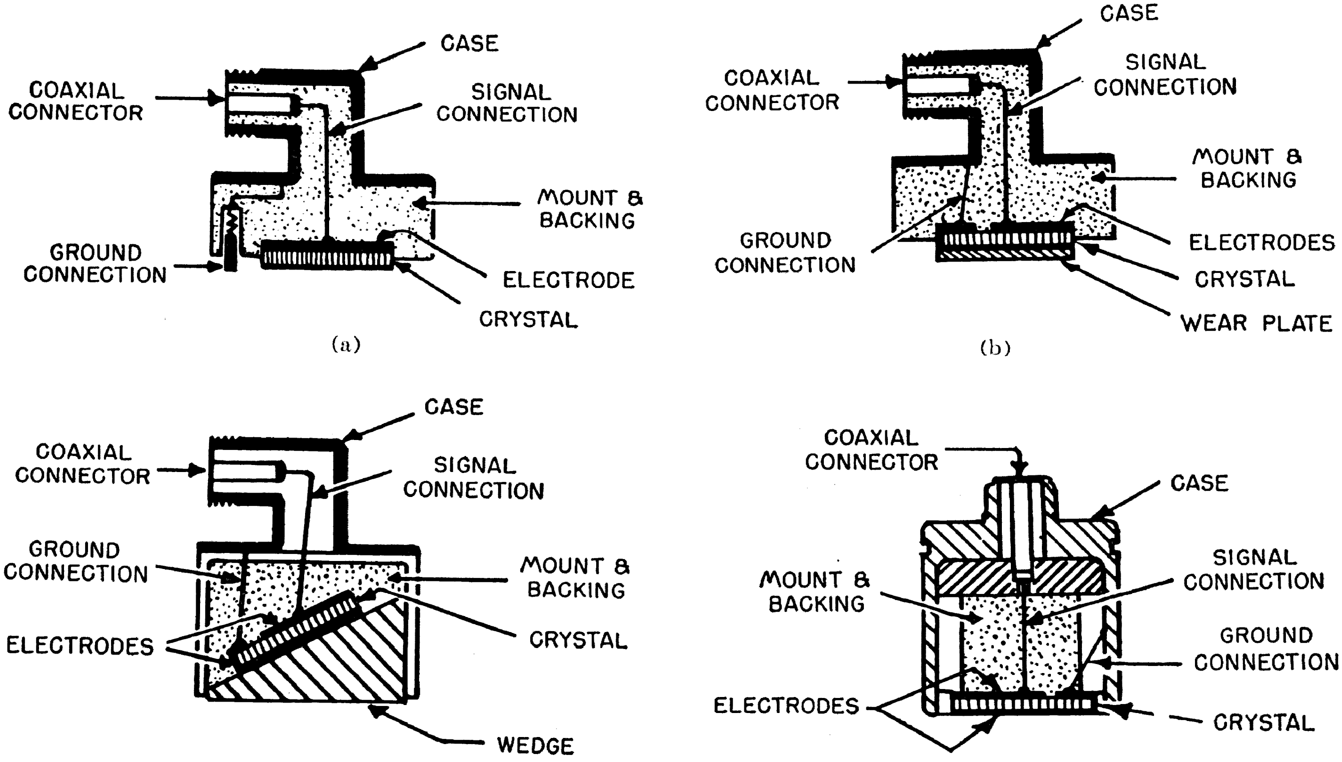

(a) (b) (c) (d)

Sperry Products, Inc.

Fig. 3. Typical search units. (a) A straight-beam contact search unit. (b) A straight-beam faced unit. (c) Angle-beam search unit. (d) Immersion search unit.

range. Special types include **curved shoes** for pipe inspection[33] and **variable-angle units** for axle testing.[34]

Immersion Units. Search units used in immersion testing are separated from the test object by a couplant of considerable thickness [Fig. 3(d)]. (See section on Ultrasonic Immersion Tests for details of ultrasonic immersion techniques.) The crystal mounting must be thoroughly waterproofed and a grounding electrode must be provided on the front face. Search units are available for all standard test frequencies within the range from 200 kc. to 25 Mc.

Contoured or Focused Units with Acoustic Lenses. The addition of acoustic lens elements to the front face of immersion search units makes possible the focusing of ultrasonic beams. **Cylindrical curvatures** permit focusing the sound energy to enter cylindrical surfaces normally or along a line focus. **Spherical lens curvatures** focus the sound at a point. (See section on Ultrasonic Transducers for further characteristics and applications of acoustic lens systems.)

Standard Ratings. The frequencies and sizes of search units most commonly employed for industrial inspection are shown in Fig. 4. **Off-frequency operation** is sometimes used, particularly at very high frequencies where thick crystals are frequently driven at multiple odd harmonics.

Frequency (Mc.)	Crystal * Thickness (in.)	Diameter ** of Active Area (in.)			
		Type			
		Contact	Faced	Angle Beam	Immersed
0.2	0.5	–	–	–	3
0.5	0.2	1⅛, 2	–	1 × 1	1⅛
1.0	0.1	¾, 1⅛	1⅛	1 × 1	¾, 1⅛
2.25	0.05	¾, 1⅛	¾, 1⅛	½ × ½, 1 × 1	¾, 1⅛
5.0	0.02	¾, 1⅛	¾	½ × ½, 1 × 1	⅜, ¾. 1⅛
10	0.01	¾	–	–	⅜, ¾
15	0.007	–	–	–	⅜
20	0.006	–	–	–	⅜
25	0.005	–	–	–	⅜

* Approximately correct for X-cut quartz, lithium sulfate, and titanate ceramics.

** Round crystals are generally accepted as industry standards except in angle-beam units, for which square or rectangular elements are preferred.

Fig. 4. Search unit frequencies and sizes most commonly used.

SPECIAL UNITS. For applications requiring nonstandard units, various special styles, sizes, and frequencies have been developed, including:

1. Dual crystals, common holder.
2. Large crystals, 1 × 4 in. and larger.
3. Mosaics, three or more crystals.
4. Small crystals, ⅛-in. diam. and less.
5. High frequency, up to 50 Mc. (fundamental).
6. Alternate crystal materials: lithium sulfate, fired titanate ceramics.
7. Sandwich and "tandem" arrangements.
8. Y-cut crystals for shear wave generation.

Material	Velocity [(cm./sec.) × 10^5]				Acoustic Impedance (ρV_L) (gram/cm.^{2}-sec.)	Wave-length, λ (cm. at 1 Mc.)	Density, ρ (gram/cm.^{3})	References
	V_O	V_L	V_T	V_R				
Metals								
Aluminum 2SO	5.10	6.35	3.10	2.90	1.72 × 10^6	0.635	2.71	65 (V_O found in 64)
Aluminum 17ST	5.08	6.25	3.10	2.79	1.75	0.625	2.80	64
Beryllium	12.75	12.80	8.71	7.87	2.33	1.28	1.82	64
Brass (Naval)	3.49	4.43	2.12	1.95	3.61	0.443	8.1	35 (V_R—64)
Bronze, Phosphor (5%)	3.43	3.53	2.23	2.01	3.12	0.353	8.86	64
Copper	3.71	4.66	2.26	1.93	4.18	0.466	8.9	35 (V_R—64)
Lead, pure	1.20	2.16	0.70	0.63	2.46	0.216	11.4	35 (V_R—64)
Lead, antimony (6%)	1.37	2.16	0.81	0.74	2.36	0.216	10.90	64
Magnesium (Am35)	5.00	5.79	3.10	2.87	1.01	0.579	1.74	65 (V_O—64)
Mercury	...	1.42	...	...	1.85	0.142	13.00	64
Molybdenum	5.45	6.29	3.35	3.11	6.35	0.629	10.09	65 (V_O—64)
Nickel	4.79	5.63	2.96	2.64	4.95	0.563	8.8	35 (V_R—64)
Inconel (wrought)	5.08	7.82	3.02	2.79	6.45	0.782	8.25	64
Monel (wrought)	4.52	6.02	2.72	1.96	5.31	0.602	8.83	64
Silver-nickel (18%)	3.83	4.62	2.32	1.69	4.03	0.462	8.75	64
Steel	5.17	5.85	3.23	2.79	4.56	0.585	7.8	35 (V_R—64)
Stainless 302	4.90	5.66	3.12	3.12	4.55	0.566	8.03	64
Stainless 410	5.03	7.39	2.99	2.16	5.67	0.739	7.67	64
Titanium (Ti 150A)	5.08	6.10	3.12	2.79	2.77	0.610	4.54	64
Tungsten	4.60	5.18	2.87	2.65	9.98	0.518	19.25	65 (V_O—64)
Nonmetals								
Air	...	0.33	...	...	0.00033	0.033	0.001	35
Oil, transformer	...	1.38	...	...	0.127	0.138	0.92	64
Plastic (acrylic resin)	...	2.67	1.12	...	0.32	0.264	1.18	35
Quartz (natural)	...	5.73	...	...	1.52	0.573	2.65	64
Water	...	1.49	...	...	0.149	0.149	1.00	64
Fused quartz	...	5.93	3.75	3.39	1.30	0.593	2.20	65
Pyrex	...	5.57	3.44	3.13	1.24	0.557	2.23	65
Plate glass	...	5.77	3.43	3.14	1.45	0.577	2.51	65
Ice	3.28	3.98	1.99	...	0.40	0.398	1	35

Fig. 5. Acoustic properties of materials. All values in the Velocity columns are to be multiplied by 10^5. All values in the Acoustic Impedance column are to be multiplied by 10^6, including the value for air.

Ultrasonic Wave Propagation Characteristics

ASSUMPTIONS. The major effects encountered in practical ultrasonic inspection can be predicted with reasonable accuracy by making the following simplifying assumptions:

1. The ultrasonic beam consists of plane wave fronts.
2. Elastic moduli are independent of stress amplitude, frequency, and direction.
3. When frequency is a parameter, particle motion is continuous and sinusoidal.

These conditions are generally valid for ultrasonic materials inspection unless extremely short or very large amplitude pulses are employed.

WAVELENGTH. Wavelength, λ, a parameter useful for describing certain characteristics of transducers, beam geometries, and modes of propagation, is related to oscillation frequency and velocity of propagation as follows:

$$\lambda = v/f \qquad (3)$$

where λ = wavelength, cm. (in., ft., etc.).
v = velocity, cm./sec. (in./sec., ft./sec., etc.).
f = frequency, c.p.s.

Values of λ in several common materials at 1 Mc. are given in Fig. 5 for the longitudinal mode.

VELOCITY. Several possible modes of vibration can propagate in solids. In general, pulse-time techniques indicate the **wave packet or "group" velocity.** This velocity is independent of sample geometry when the cross-section is very large compared with beam area and wavelength. The **principal wave velocities** encountered in solids at ultrasonic frequencies are given in Fig. 6.

Symbol	Nomenclature	Conditions	Particle Motion	Single-valued
V_O	Thin rod	Small diameter bar	Compound	Yes
V_L	Longitudinal	Extended media	Longitudinal	Yes
V_T	Shear	Extended media	Transverse	Yes
V_R	Rayleigh surface	Semi-infinite free surface	Compound	Yes
V_{P_n}	Lamb or "plate"	Thin sheet	Compound	No

Fig. 6. Principal wave velocities in solids.

Longitudinal waves are dilational or nondistortional, while shear waves involve only distortion and are polarized. V_L is sometimes called the compressional, plate, or bulk wave velocity (not to be confused with plate waves in thin sheets or bulk waves in fluids). By definition, V_L, V_T, and V_R are independent of frequency. In objects where one or more dimensions approach a wavelength, various **phasing effects** can occur. In thin sheet and small tubing, for example, various Lamb or "plate" waves are encountered which have intermediate values of V_{P_n}, varying with the test conditions.[12]

Calculation of Acoustic Velocities. To calculate absolute values, a consistent set of units must be used. For example, in c.g.s. units: moduli (Y,μ), dynes/cm.^{2}; density ρ, gram/cm.^{3}; velocity V, cm./sec. Formulas for computing these velocities from the density and appropriate elastic "constants," as well as their interrelationships, are given in Fig. 7. Like elastic moduli, velocities can be interrelated as functions of Poisson's ratio (σ) only. Their ratios are shown in convenient form in Fig. 8.

Velocity Formulas

(a) $V_O = \sqrt{\frac{Y}{\rho}}$ Thin-rod velocity

(b) $V_L = \sqrt{\frac{Y}{\rho}\frac{(1-\sigma)}{(1+\sigma)(1-2\sigma)}} = \sqrt{\frac{K+(3/4\mu)}{\rho}}$ Longitudinal velocity

(c) $V_T = \sqrt{\frac{Y}{\rho}\frac{1}{2(1+\sigma)}} = \sqrt{\frac{\mu}{\rho}}$ Shear velocity

Velocity Ratio Equations

(d) $\frac{V_O}{V_L} = \sqrt{\frac{(1+\sigma)(1-2\sigma)}{(1-\sigma)}}$

(e) $\frac{V_T}{V_L} = \sqrt{\frac{1-2\sigma}{2(1-\sigma)}}$

(f) $\frac{V_R}{V_T} = \frac{0.87+1.12\sigma}{1+\sigma}$ Bergmann approximation

Poisson's Ratio Formulas

(g) $\sigma = \frac{1-2(V_T/V_L)^2}{2-2(V_T/V_L)^2}$

(h) $\sigma = 1 - \frac{8-8a^2}{8a^2-8a^4+a^6}$ where $a = \frac{V_R}{V_T}$

Elastic Constants Formulas

(i) $\mu = V_T{}^2\rho$

(j) $Y = V_O{}^2\rho = V_L{}^2\rho\frac{(1+\sigma)(1-2\sigma)}{1-\sigma}$

(k) $Y = 2\mu(1+\sigma) = 3K(1-2\sigma) = \frac{9K\mu}{\mu+3K}$

Key to Symbols Used:

V_O = thin rod velocity, cm./sec.
V_L = longitudinal wave velocity, cm./sec.
V_T = transverse wave velocity, cm./sec.
V_R = Rayleigh or surface wave velocity, cm./sec.
Y = Young's modulus of elasticity, dynes/cm.^{2}.
μ = shear modulus of elasticity, dynes/cm.^{2}.
σ = Poisson's ratio.
ρ = density, grams/cm.^{3}.
K = bulk modulus, dynes/cm.^{2}

Fig. 7. Relationships between ultrasonic velocities and the elastic constants of isotropic solids.

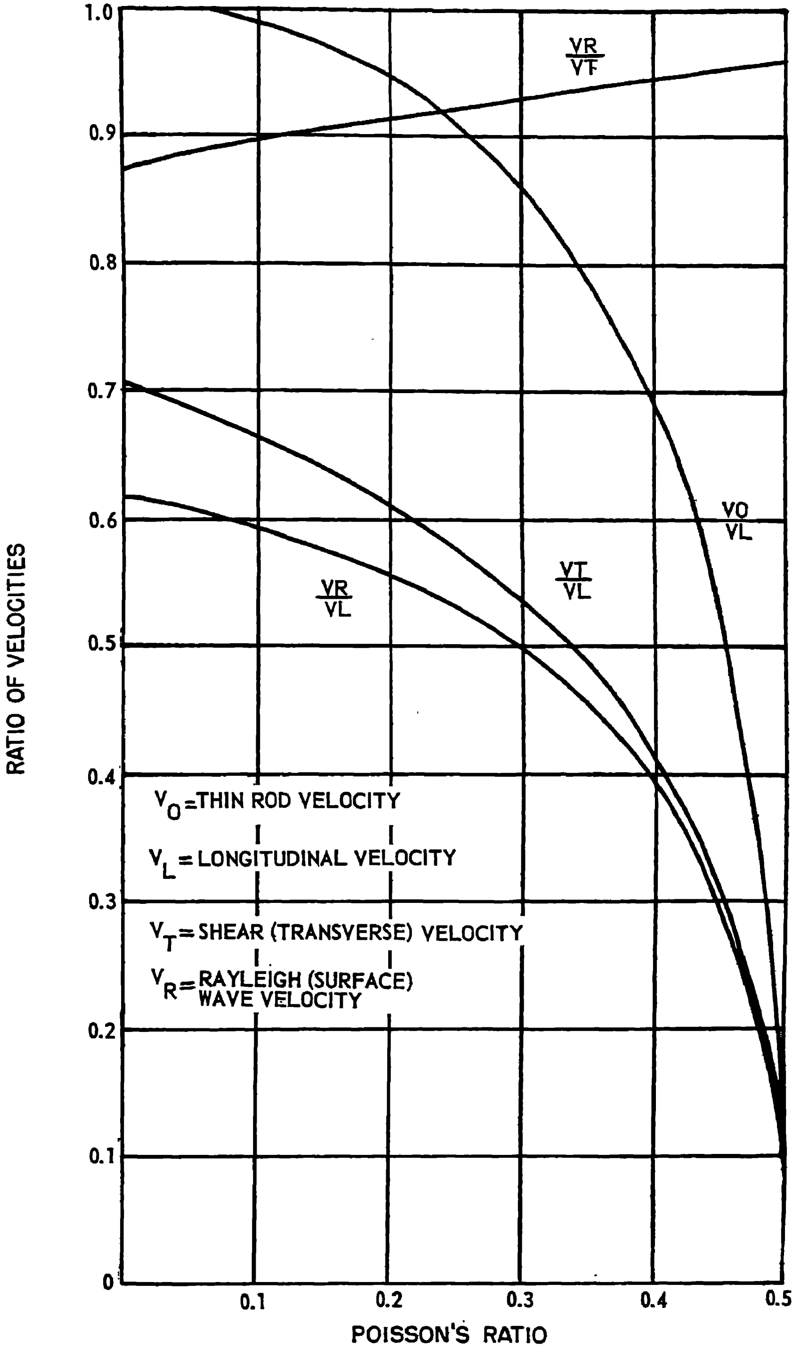

Fig. 8. Relationships of velocity ratios to Poisson's ratio.

While precise measurement of ultrasonic velocities is possible with present instrumentation, values within a few percent are usually adequate for inspection problems. One exception is the determination of elastic moduli by velocity measurements, which may require high accuracy for both velocity and density data to achieve the precision desired.

IMPEDANCE. Another useful parameter of a material is its impedance, or more accurately, its characteristic acoustic impedance, Z, which is defined as the product of density ρ and wave velocity v (usually longitudinal). Impedance is then given by

$$Z = \rho v \quad \text{gram/cm.}^2\text{-sec.} \tag{4}$$

where ρ = density, gram/cm.^{3}.
v = velocity, cm./sec.

Fig. 5 gives representative velocity, wavelength, and acoustic impedance data for typical materials encountered in ultrasonic inspection work.

EFFECTS AT PLANE INTERFACES. Ultrasonic inspection techniques depend upon the principle that the propagation of an ultrasonic beam is influenced by the acoustic properties of the media in which it is propagating. Variations can produce (1) reflection, (2) refraction, (3) mode conversion, and (4) diffraction of the beam, or various combinations of these effects.[35, 36] With extended plane interfaces and the assumptions given previously, the beam intensity relationships can be calculated. In addition, attenuation of the beam with distance results from losses in common materials, the magnitude being determined experimentally. The values obtained for beam intensity are stated in units of either energy or power. Relative amplitudes of the **particle velocity, displacement,** and **pressure** in a given medium can be obtained by taking the square root of the energy ratios. These can be related to indications on ultrasonic flaw detectors. Since these employ piezoelectric transducers, linear amplifiers, and proportional display systems, their indications are proportional to amplitude or to square root of intensity. For **nonidealized conditions,** complete analysis of all the effects involved is difficult and is all too often neglected, with consequent errors in ultrasonic test interpretation. Typical of such factors are surface roughness, specimen curvature, structure variations, irregular defect shapes, and nonuniform beam characteristics. (See section on Ultrasonic Fields for analyses of these factors.)

Reflection. The percentage of incident energy reflected when a beam encounters an abrupt change of medium depends upon (1) impedance "mismatch" Z_1/Z_2 and (2) angle of incidence. At **normal incidence** (the simplest case), the ratio between reflected beam intensity W_r and incident intensity W_i is given by the **reflection coefficient** R, where

$$R = \frac{W_r}{W_i} = \left(\frac{Z_2 - Z_1}{Z_2 + Z_1}\right)^2 = \left(\frac{r - 1}{r + 1}\right)^2 \tag{5}$$

The ratio between transmitted beam intensity W_t and incident intensity W_i is given by the **transmission coefficient** T as

$$T = \frac{W_t}{W_i} = \frac{4Z_2Z_1}{(Z_2 + Z_1)^2} = \frac{4r}{(r + 1)^2} \tag{6}$$

The sum of the reflection and transmission coefficients is unity; i.e.,

$$R + T = 1 \tag{7}$$

In the preceding relations we define

$$Z_1 = \rho_1 V_1 \quad \text{(medium 1)}$$

$$Z_2 = \rho_2 V_2 \quad \text{(medium 2)}$$

$$r = Z_2/Z_1$$

The **impedance ratio** Z_2/Z_1, or mismatch factor r, is a convenient base for plotting the intensity relationships. This ratio is of the order of magnitude of 20 for liquids to metals (possibly 80 percent reflection) and about 100,000 for gases to metals (virtually 100 percent reflection).

		Medium 2												
Medium 1	Z*	Aluminum	Steel	Nickel	Copper	Brass	Lead	Mercury	Glass	Quartz	Polystyrene	Bakelite	Water	Oil
Aluminum	1.70	0	21	24	18	14	3	1	2	0.3	50	42	72	74
Steel	4.56		0	0.2	0.3	1	9	16	31	27	77	76	88	89
Nickel	4.95			0	0.8	2	12	19	34	29	79	75	89	90
Copper	4.18				0	0.2	7	13	19	22	75	71	87	88
Brass	3.92					0	5	10	23	16	73	68	86	87
Lead	2.46						0	1	9	8	62	55	79	80
Mercury	1.93							0	4	1	8	6	75	76
Glass	1.80	$\frac{W_r}{W_i} \times 100\%$							0	0.8	40	32	65	67
Quartz	1.52									0	46	17	68	71
Polystyrene	0.29										0	1	12	17
Bakelite	0.36											0	18	23
Water	0.15												0	0.6
Oil (xformer)	0.13													0

* (gm./cm.^{2}-sec.) × 10^6.

Fig. 9. Percentage ultrasonic reflection coefficients for normally incident plane waves at interfaces between various materials.

Reflection coefficients (times 100 percent) **for typical conditions** which might be encountered in practice are given in Fig. 9.[35] The proportion of transmitted energy can then be easily found by Eq. (7). Intimate molecular contact or "wetting" of interface surfaces is assumed.

Eqs. (5), (6), and (7) can be used to determine the results of passing the beam through any **number of interfaces,** provided the layers are thick compared with the length of the wave trains employed so that interferences between the effects of successive interfaces are avoided. Possible applications include comparison of test blocks of different materials, evaluation of bonding conditions, and calibration of instruments. To avoid errors, it is preferable to utilize energy relationships only and to determine amplitude ratios at the transducer as a final step. Angular incidence introduces additional effects described later; however, for very small angles of incidence as sometimes used in flaw size or orientation studies, the same general results are obtained. For two media having unequal impedances but equal velocities, the angles of reflection and of refraction would equal the angle of incidence, with all angles from the normal being equal. Any differences in acoustic velocities between adjacent media produce refraction and possible mode conversion, as described subsequently.

Transmission Through Thin Plates. When the thickness of a layer becomes less than the length of the wave train propagating through it, interferences occur which violently affect the various amplitudes involved. Long wave trains can approximate a steady state or **continuous wave condition**, producing confusing results. Conversely, such resonance effects can be used effectively to measure

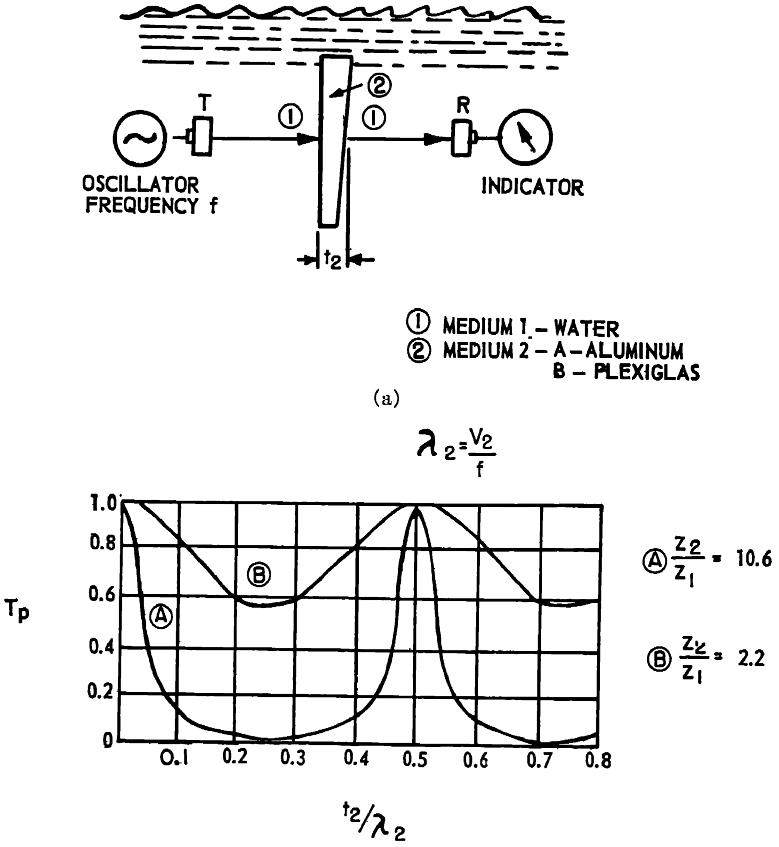

(a)

(b)

Fig. 10. Transmission through thin plate. (a) Schematic of testing set-up. Item 1 is the water medium. Item 2 is the plate, either aluminum or Plexiglas. Other items are: t_2, sample thickness; T, transmitter; R, receiver. (b) Relative transmission curves. For curve A, $Z_2/Z_1 = 10.6$; for curve B, $Z_2/Z_1 = 2.2$, where T_p is thickness of plate.

sample thickness, detect unbonding, or determine velocity. Several commercial instruments have been developed for such purposes. **Interferences** occur whenever multiple reflections within a layer cause superposition of waves having different time relationships. The magnitude and direction of the interference effects depend upon the phase angles. The effects are largest when:

1. Attenuation losses are low.
2. Layer thicknesses approach a few wavelengths or less.
3. Surfaces are impedance "mismatched" to give poor coupling.
4. Provision is made for adjusting or "tuning" the frequency of the transmitted waves.

The effect is illustrated by Fig. 10, which shows the **transmission through a thin solid sheet,** bounded on either side by a liquid, as a function of sample thickness. In terms of sample thickness t_2 and wavelength λ_2 within it, and neglecting losses, the relative transmission is given by

$$\frac{W_t}{W_i} = T_p = \frac{1}{1 + \frac{1}{4}\left(r - \frac{1}{r}\right)^2 \sin^2 \frac{2\pi t_2}{\lambda_2}} \qquad (8)$$

where $r = Z_2/Z_1$
$\lambda_2 = V_2/f$

Transmission maxima are repeated at thicknesses of integral half-wavelengths; and minima, at odd quarter-wavelengths. A simple adaptation of this technique can be used to measure velocity and attenuation in plastic sheet.[37, 38]

Resonance Thickness Measurements. A technique for measuring thickness from one side of an object, utilizing the resonance effect with pulsed wave trains, has been described.[12] The search unit can contact the work piece or be separated by a water column. Either constructive or destructive interference can be used, depending upon the sharpness of the tuning desired. The method can be used effectively for **detection of unbonded areas** in adhesive-cemented structures.

Resonance instruments designed primarily for thickness determination are usually tunable continuous-wave systems which indicate the loading of the transducer by the sample. Instrumentation details are given in the section on Ultrasonic Resonance Tests.

REFRACTION. When an ultrasonic beam is incident other than normally upon an interface between two materials having unequal sound velocities, the transmitted beam will assume a new direction of propagation, given by the angle of refraction. In the most general case, additional beams may be generated by **mode conversion** (see Fig. 11).

The **angular relationships for plane-wave propagation** are given by an equation known in optics as **Snell's law:**

$$\frac{\sin \phi_1}{V_1} = \frac{\sin \phi_2}{V_2} = \frac{\sin \phi_3}{V_3} \qquad (9)$$

The equation gives a necessary, although not sufficient, condition for the existence of transmitted or reflected beams at any angle. **Critical angles** can be determined by Eq. (10), beyond which no transmitted or reflected beam of a stated velocity can exist.

$$\phi_1 \geqq \sin^{-1}(V_1/V_2) \qquad (10)$$

$$V_2 > V_1$$

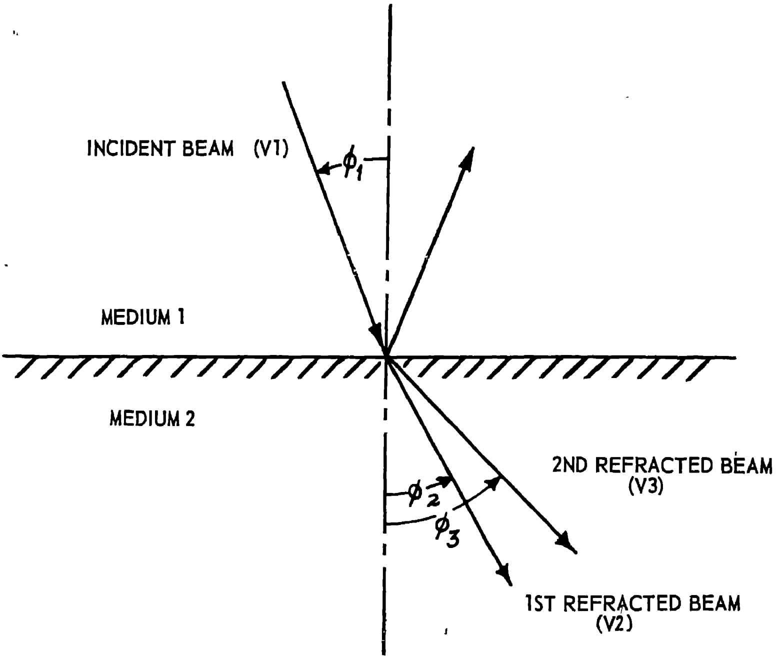

Fig. 11. Refraction and mode conversion at plane interface (angular incidence).

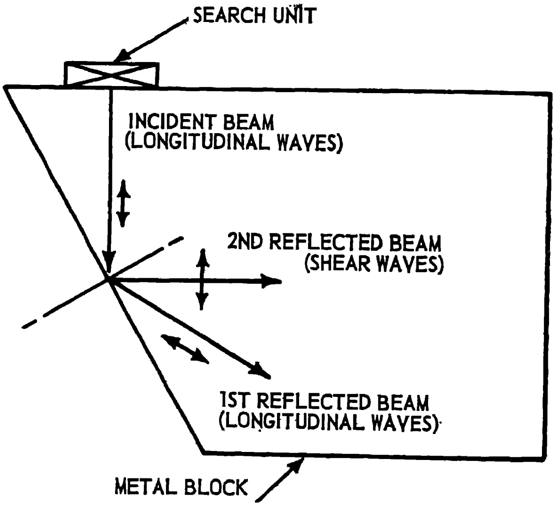
SEARCH UNIT
INCIDENT BEAM (LONGITUDINAL WAVES)
2ND REFLECTED BEAM (SHEAR WAVES)
1ST REFLECTED BEAM (LONGITUDINAL WAVES)
METAL BLOCK

Fig. 12. Mode conversion by reflection at plane interface.

Since no energy values are given, the intensities of the refracted beams or of those generated by mode conversion must be determined by other relationships.

MODE CONVERSION. In an extended medium, acoustic energy propagates in three **principal modes**: as longitudinal, shear, or surface waves. Each propagates at a characteristic velocity for a specific material. When a beam strikes an interface between materials of different acoustic velocity or impedance properties, at other than normal incidence, some energy may be converted to other modes of vibration during reflection or refraction. A simple example is reflection of an incident longitudinal beam on a free surface within a solid, such as the steel block of Fig. 12. Since a negligible amount of energy leaves the steel because of the extreme mismatch to air, the reflection must be total. However, to satisfy all **continuity conditions**, two reflected beams exist. One beam consists of longitudinal waves and the second of shear (transverse) waves, polarized as shown in Fig. 12. At

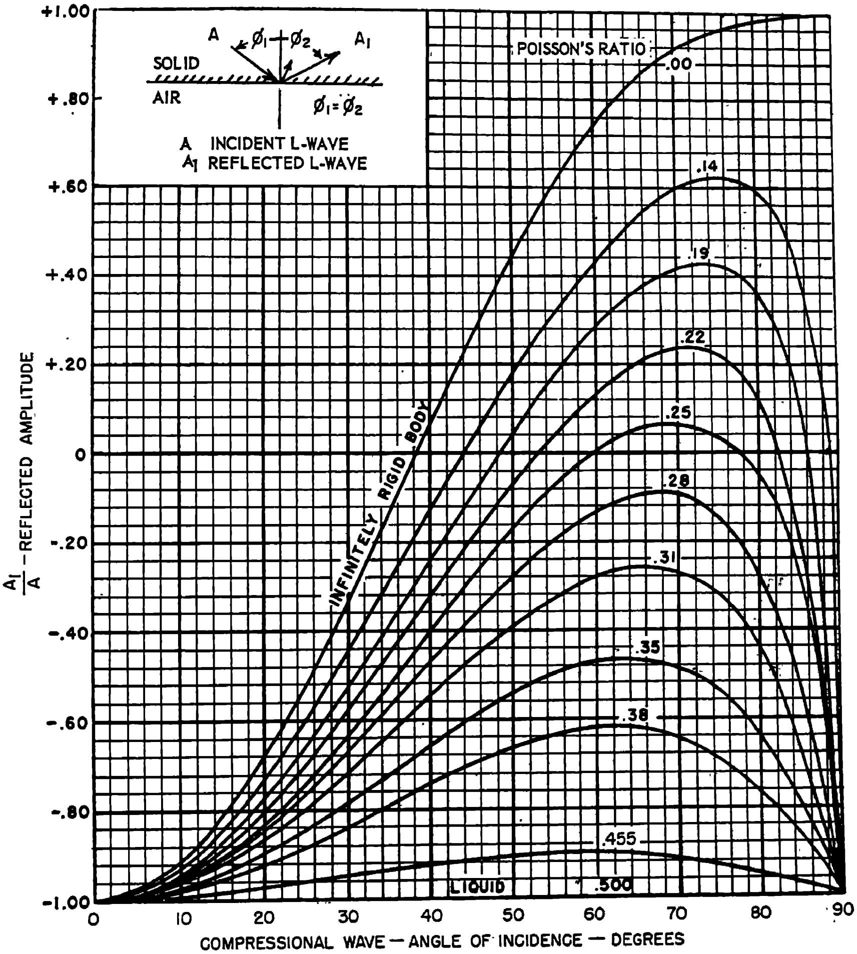

Fig. 13. Amplitude ratio of reflected-to-incident longitudinal waves.

large or glancing angles of incidence, the conversion to shear waves is almost total. In practical testing, this condition frequently occurs as a result of beam spread and produces so-called ghost and subsidiary indications.[12]

Angular and Amplitude Relationships. Angular relationships are uniquely given by the reflection equivalent of Snell's law. However, computation of the energy values requires a set of continuity equations known as **Knott's equations.**[39, 40] For a solid-to-air (free surface) condition, these reduce to functions of Poisson's ratio only and can be conveniently shown graphically. The amplitude ratio between incident and reflected beams as a function of angle for various Poisson's ratios is shown in Figs. 13 and 14.[41] Critical angles for minimum, maximum, or total conversion can be found from these curves of angular incidence.

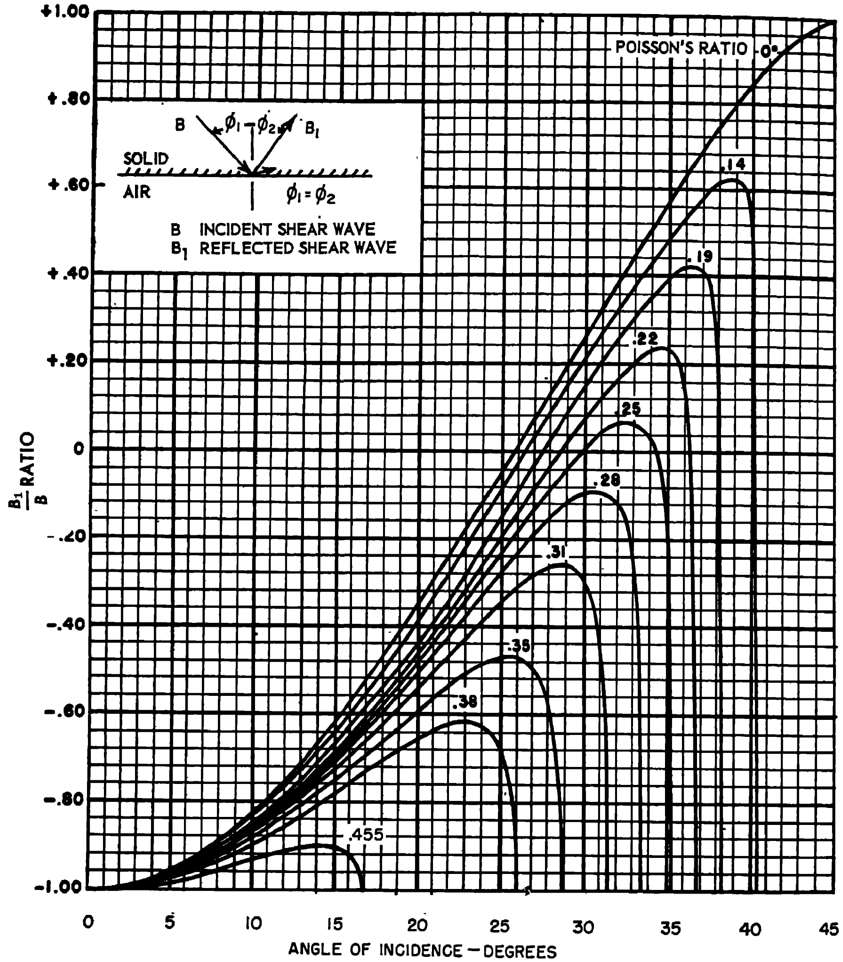

Fig. 14. Amplitude ratio of reflected-to-incident shear waves.

General Cases of Angular Incidence. In addition to the simpler interface conditions of normal incidence between two media and the angular reflection at a free surface, several more complicated but important cases of angular incidence arise in practice as follows:

1. Liquid to solid: incident longitudinal wave only.
2. Solid to liquid:
   - a. Incident longitudinal wave.
   - b. Incident shear wave.
   - c. Incident surface wave (rare).
3. Solid to solid:
   - a. Incident longitudinal wave.
   - b. Incident shear wave.
   - c. Incident surface wave.

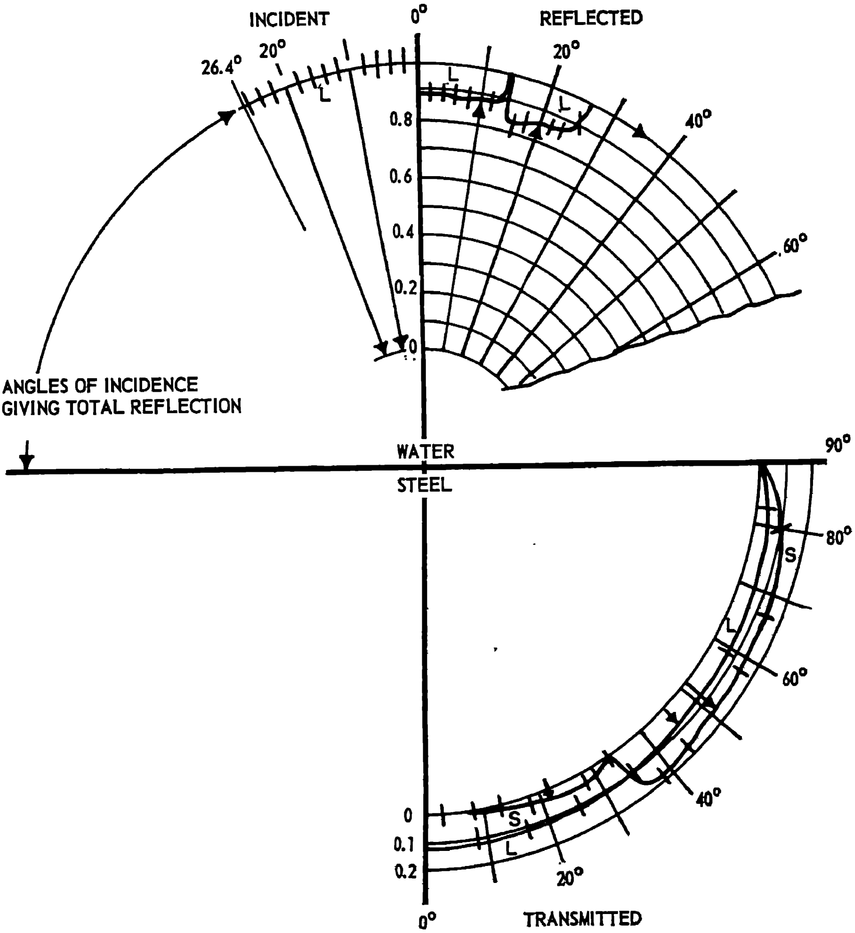

Fig. 15. Longitudinal waves in water incident on steel. Power in entire reflected and transmitted beams.

In each case the reflected and transmitted beams may include both longitudinal and shear types unless (1) critical angles are exceeded or (2) the medium is a nonviscous liquid which can support only longitudinal waves.

In ultrasonic testing, two relations are usually of interest: first, that giving intensity of the beam entering the specimen; and second, that describing the beam returning to the search unit. Any case can be solved by the use of Knott's equations, provided all the parameters, including the densities and elastic constants of the media involved, are accurately known. A few specific cases, including **water-steel**, have been completely worked out.[13] The results are shown graphically in Figs. 15, 16, and 17.

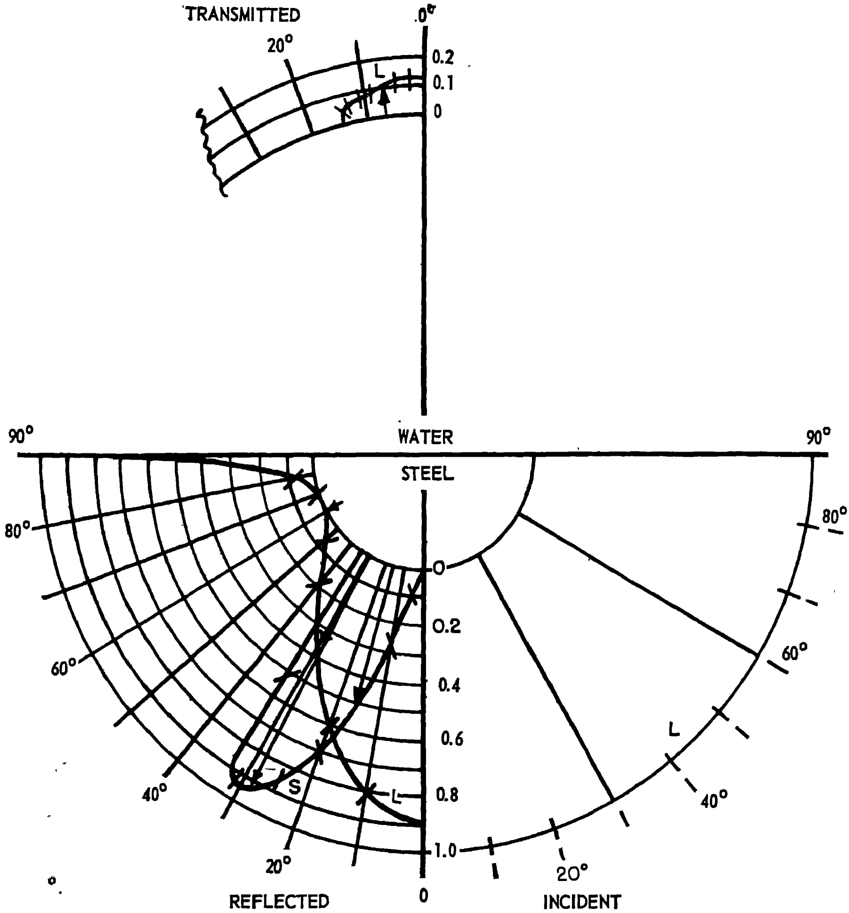

Fig. 16. Longitudinal waves in steel incident on water. Power in entire reflected and transmitted beams.

The equations for any specific system can also be solved experimentally with a device similar to the optical refractometer. **Refraction analysis equipment**[42] developed especially for investigating plastic wedges is shown in Fig. 18. Reasonably close correlation with theory has been obtained, even though additional effects such as couplant and beam spread are introduced by test conditions. Amplitude and angle data for Lucite and steel are shown in Figs. 19(a) and (b), respectively. Optimum wedge angles for various applications can be determined

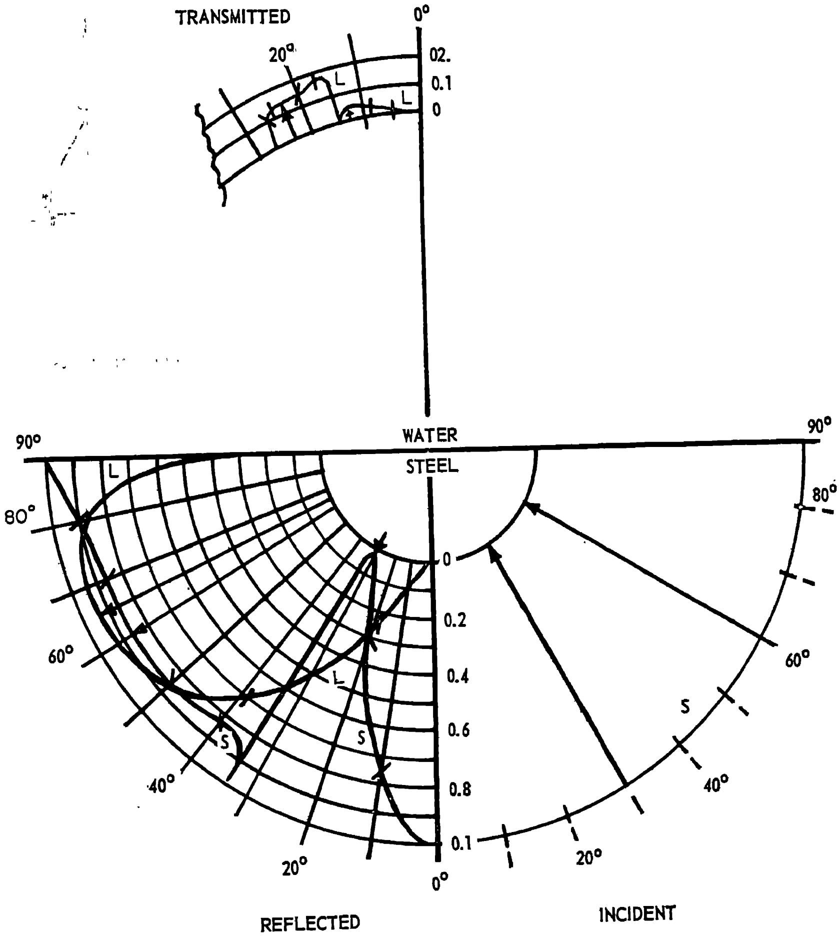

Fig. 17. Shear waves in steel, vibrating in plane of incidence, incident on water. Power in entire reflected and transmitted beams.

from such data. The experimental approach has certain advantages. Actual test conditions can be closely approximated, including all principal variables. By using a second crystal as a receiver, the amplitude of the transmitted signals and the beam spread can be measured, as shown in Fig. 20.

DIFFRACTION. When a plane wave of infinite cross-section passes through an aperture, the emerging beam diverges and also has nonplanar wave fronts.

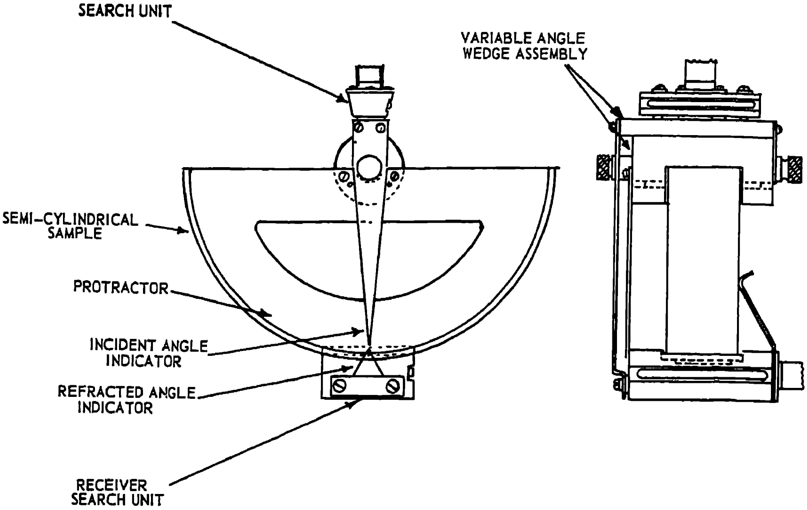

Sperry Products, Inc.

Fig. 18. Refraction analyzer.

These effects result from **wave interference** or diffraction, as in optics. Similarly the beam pattern from a transducer of finite area or the reflection from a small discontinuity will have a diffraction pattern. (The theory of this phenomenon and some of its practical implications are discussed in the section on Ultrasonic Fields.) A complete analytical solution of a typical flaw detection situation is usually impractical because of complex geometry and phasing conditions encountered. Three important effects can be described qualitatively:

1. Transducer beam spread.
2. Beam profiles.
3. Defect reflection factors.

Their importance in practical ultrasonic inspection cannot be overestimated. They relate to instrument calibration, flaw evaluation, optimizing scanning paths, and explanation of spurious reflections. In particular it is necessary to understand the characteristics of the ultrasonic beam referred to as the "near field" and "beam profile" effects (see section on Ultrasonic Transducers).

ATTENUATION. Elementary plane-wave theory usually assumes no transmission losses other than interface effects. However, **energy losses** do occur in all materials to some extent and must be considered in certain aspects of ultrasonic inspection.[27, 29, 35, 43] For plane-wave propagation, the attenuation constant α is given by

$$\frac{I_2}{I_1} = e^{-2\alpha} \tag{11}$$

where α = attenuation constant, nepers per unit distance (e.g., cm.).

$\frac{I_2}{I_1}$ = ratio of intensities at two points a unit distance apart.

$I_1 > I_2$

Alternate forms sometimes used and their conversions are:

$$\alpha' = 8.68\alpha \quad \text{(db./cm.)}$$

$$A_1 = \lambda\alpha \quad \text{(nepers/wavelength)}$$

$$A = 8.68\lambda\alpha \quad \text{(db./wavelength)}$$

The **attenuation** α is a difficult quantity to measure accurately, particularly in solid materials, such as the common structural metals, at the test frequencies usually employed, i.e., 1 to 10 Mc. The over-all result usually observed includes **other loss mechanisms** such as beam spread, field effects, couplant mismatch, transducer loading, or sample geometry. These factors cannot be isolated without special techniques and equipment.[28, 29, 44]

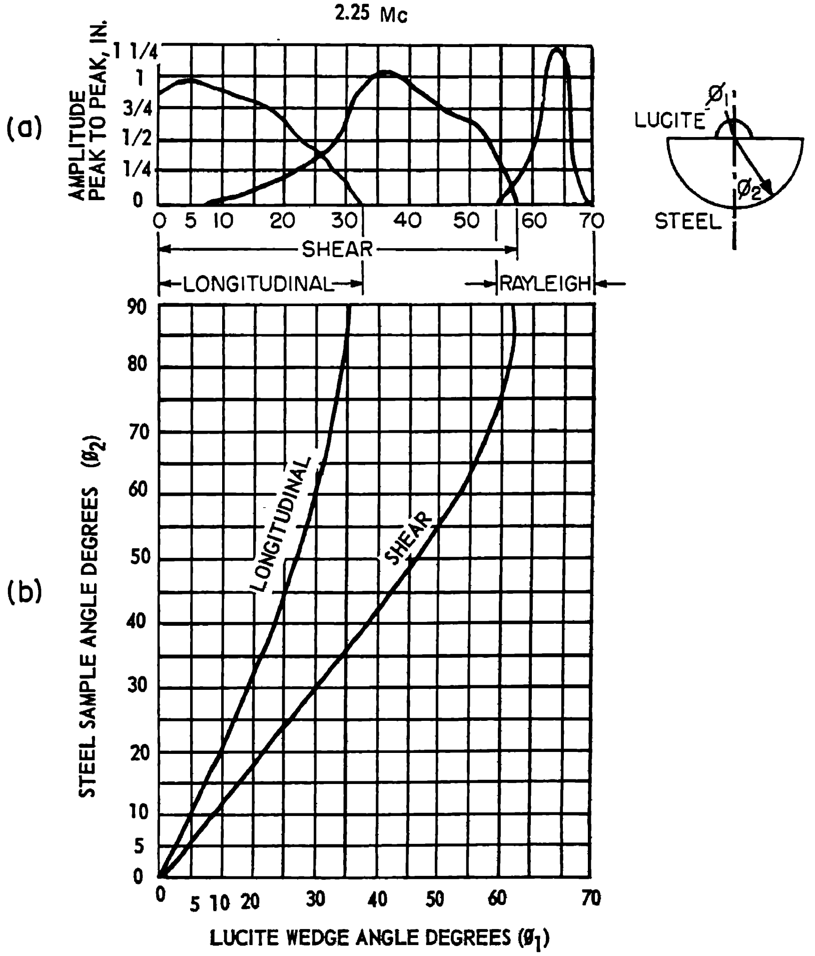

Sperry Products, Inc.

Fig. 19. Refraction data. (a) Amplitude data. (b) Angle data.

For most flaw detection work it is helpful to know the approximate "penetrability" of the specimen in terms of a similar reference sample of a known material. Large **differences in attenuation** are indicated as sizable changes in the reflection obtained from the far face of a flat specimen, i.e., its "back reflection."[7, 45] The technique is therefore commonly known as the **loss-of-back-reflection method** and is sometimes used to show unrefined grain structure in forgings. In such materials an attenuation increase is usually accompanied by a noticeable rise in random reflections or **noise** from scattering surfaces, probably caused by larger grain faces, excessive porosity, or numerous inclusions. These **interfering reflections** usually limit the upper frequency that can be used practically for testing a given material. Quantitative studies of attenuation phenomena offer many potentialities both in theoretical and applied fields. Some of the interrelationships of interest are shown in Fig. 21.[46]

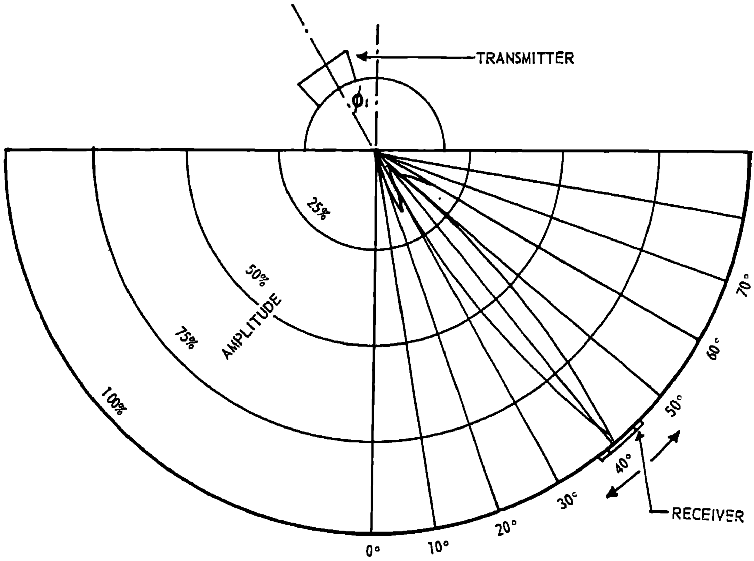

Sperry Products, Inc.

Fig. 20. Beam spread. Amplitude of refracted shear wave as a function of receiver angle.

Measured values of **attenuation in some typical materials,** extracted from several publications, are shown in Fig. 22 with their probable frequency relationships.[29]

DISTURBING INFLUENCES. The conditions encountered in practical inspection may depart from those of plane-wave theory in several aspects. This makes it quite difficult to predict quantitatively the amplitudes of the various signals obtained from given specimens. The **major effects** relate to one or more of the following:

1. Beam spread due to finite transducer size.
2. Attenuation of beam due to such causes as scattering and damping.
3. Beam nonuniformity due to field effects.

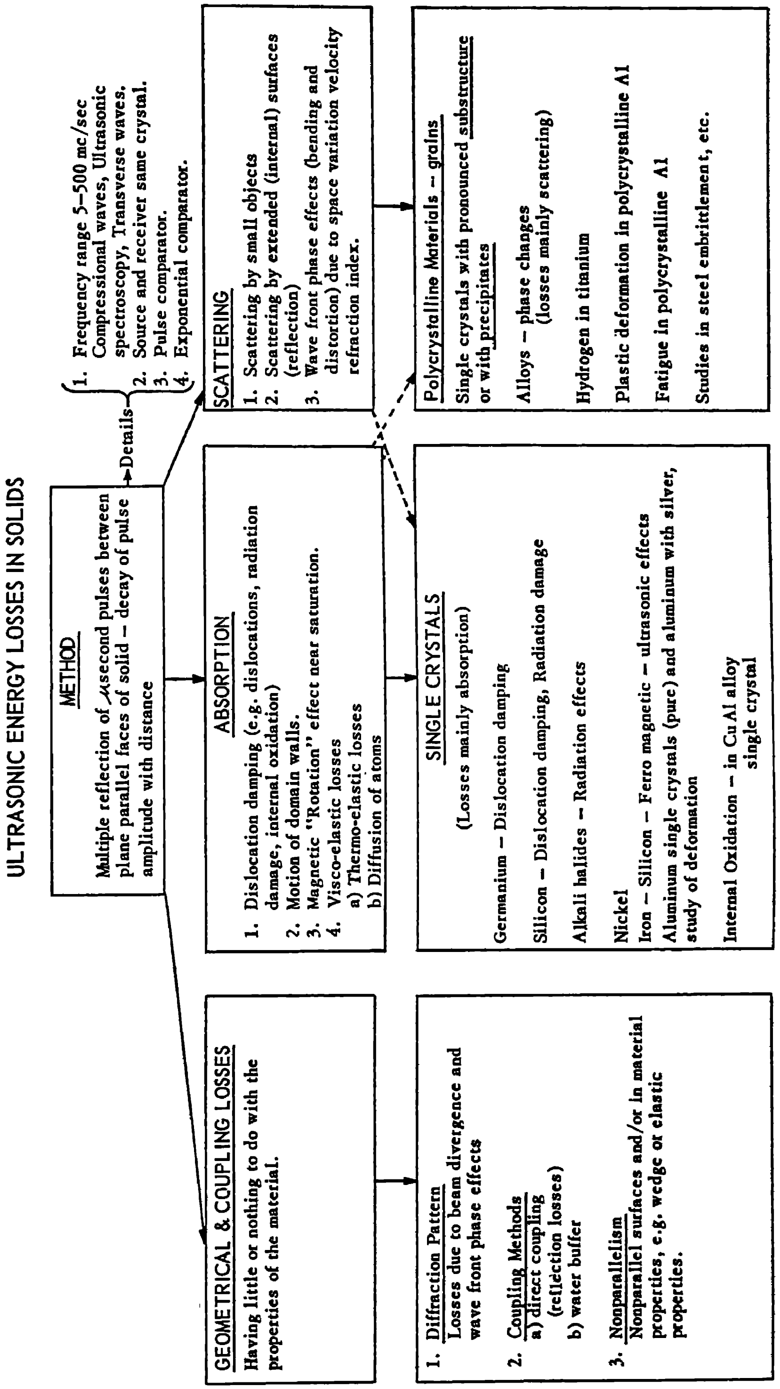
ULTRASONIC ENERGY LOSSES IN SOLIDS
METHOD
Multiple reflection of μsecond pulses between plane parallel faces of solid – decay of pulse amplitude with distance
Details
1. Frequency range 5–500 mc/sec Compressional waves, Ultrasonic spectroscopy, Transverse waves.
2. Source and receiver same crystal.
3. Pulse comparator.
4. Exponential comparator.
GEOMETRICAL & COUPLING LOSSES
Having little or nothing to do with the properties of the material.
ABSORPTION
1. Dislocation damping (e.g. dislocations, radiation damage, internal oxidation)
2. Motion of domain walls.
3. Magnetic "Rotation" effect near saturation.
4. Visco-elastic losses
a) Thermo-elastic losses
b) Diffusion of atoms
SCATTERING
1. Scattering by small objects
2. Scattering by extended (internal) surfaces (reflection)
3. Wave front phase effects (bending and distortion) due to space variation velocity refraction index.
1. Diffraction Pattern
Losses due to beam divergence and wave front phase effects
2. Coupling Methods
a) direct coupling (reflection losses)
b) water buffer
3. Nonparallelism
Nonparallel surfaces and/or in material properties, e.g. wedge or elastic properties.
SINGLE CRYSTALS
(Losses mainly absorption)
Germanium – Dislocation damping
Silicon – Dislocation damping, Radiation damage
Alkali halides – Radiation effects
Nickel
Iron – Silicon – Ferro magnetic – ultrasonic effects
Aluminum single crystals (pure) and aluminum with silver, study of deformation
Internal Oxidation – in Cu Al alloy single crystal
Polycrystalline Materials – grains
Single crystals with pronounced substructure or with precipitates
Alloys – phase changes (losses mainly scattering)
Hydrogen in titanium
Plastic deformation in polycrystalline Al
Fatigue in polycrystalline Al
Studies in steel embrittlement, etc.

Fig. 21. Attenuation sources and relationships.

4. Transducer loading by couplant or specimen.
5. Defect reflection factor related to such factors as shape, size, surface, and impedance.
6. Masking "noise" from normal discontinuities.
7. Instrumentation variables.

Considerable experimental work and some analytical study have been applied to isolate and evaluate the parameters involved. (Some of the effects are discussed in the sections on Ultrasonic Transducers and Ultrasonic Fields.)

Material	Frequency (Mc.)				
	1.0	2.5	5	10	25
Aluminum, 17ST (0.13 mm. grain)	–	<0.01	0.02	0.12	1.06
Aluminum, 17ST (0.23 mm. grain)	<0.01	0.02	0.07	0.26	0.86
Glass, Corning 012	0.02	0.06	0.12	0.24	0.6
Lucite	1.5	3.5	7	–	–
Magnesium (0.21 mm. grain)	–	–	–	0.4	1.34
Magnesium (2.0 mm. grain)	–	–	–	0.4	0.6
Neoprene, GN	9	22	–	–	–
Polystrene	0.8	1.6	3.5	–	–
Quartz, fused	–	<0.007	0.01	0.02	0.07
Carbon tetrachloride	0.05	0.36	1.44	5.7	36
Kerosene	0.01	0.06	0.25	1.0	6.2
Water, distilled	0.002	0.016	0.063	0.25	1.56
Air (dried)	1.7	11	40	170	–

Fig. 22. α', **Attenuation (db./cm.).**[29]

In general, existing theory is not directly applicable to solution of the conditions encountered in practice. Its refinement to provide for all the variables involved is probably unwarranted. Beyond the effects which can be correlated with plane-wave and elementary transducer theory, an **empirical approach** will probably be necessary for some time, particularly with respect to those variables affected by the frequency of the ultrasonic waves involved. For these reasons, **calibration of inspection equipment** for critical applications is usually performed experimentally with a set of test blocks simulating the range of conditions expected (material, distance, defect type and size, etc.), as described in this section and in the section on Ultrasonic Immersion Tests.

Basic Instrumentation and Techniques

CLASSIFICATION OF EQUIPMENT. Equipment for ultrasonic inspection of solid materials usually falls within one of three categories, based on the parameter indicated:

1. Amplitude of transmitted energy only.
2. Amplitude and transit time of transmitted or reflected energy.
3. Loading of transducer by specimen.

Other arbitrary subdivisions are possible, and in some techniques, combination effects must be considered.

THROUGH-TRANSMISSION TECHNIQUES. Transmission systems using only amplitude information depend on the principle that certain specific changes in the sample will produce significant changes in the intensity of an ultrasonic beam passing through it.[35]

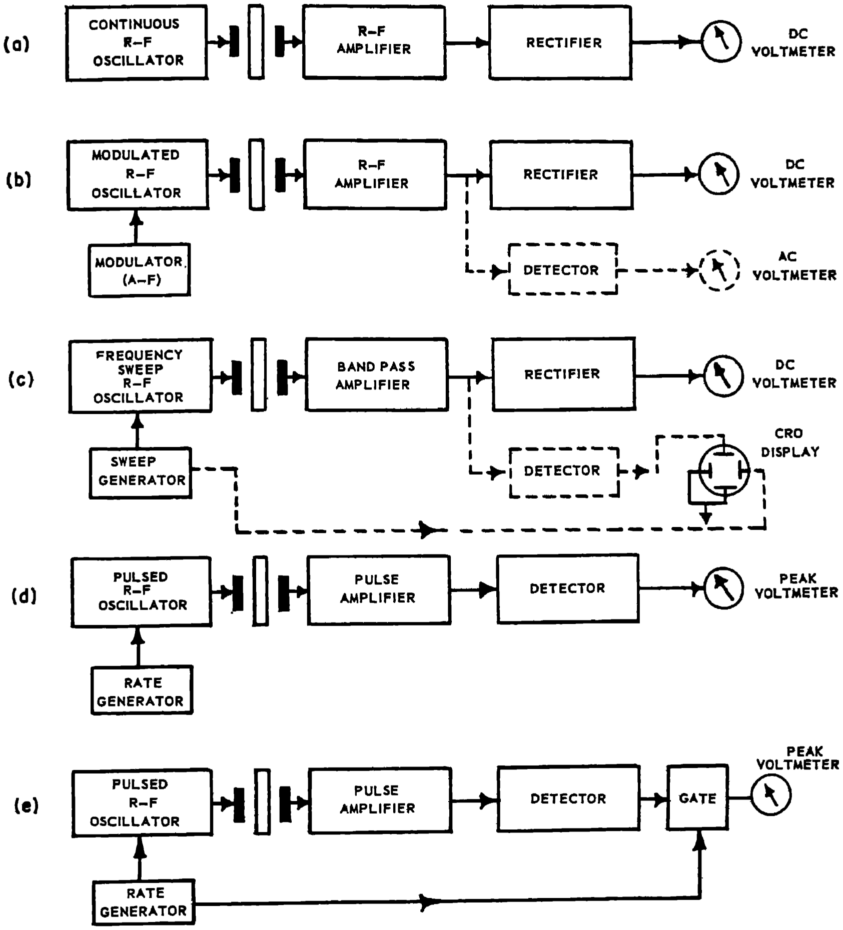

Fig. 23. Types of through-transmission systems.

Equipment. Structurally, the equipment need consist only of a sound source, receiver, sample, and suitable couplant, as shown in Fig. 23. Usually, however, a **scanning mechanism** and **recording or alarm device** are required, since the ultrasonic beam area is likely to be much smaller than that of the sample cross-section.

Defect Detectibility. As in any "shadow-casting" situation,[47] the defect detectibility of this system depends principally on:

1. The ratio of defect area to beam size.
2. The separation between defect and the transducers.

Limitations. In addition to these limitations, other problems may be involved, such as spurious signals from **multi-path reflections,** amplitude variations due to minor **geometry changes,** undesirable **resonances** of sample or couplant, and direct electrical **cross-talk** between transducers. If contact coupling is used, **pressure effects** are large. If sample immersion is used, **standing waves** can sometimes occur when continuous waves interfere after reflection. To minimize such variables, the electric signal applied to the transducer is usually frequency-modulated (wobbulated) or else pulsed (chopped). In this way resonances are averaged out and standing waves are reduced. Several possible configurations of such equipment are shown diagrammatically in Fig. 23(a) through (e).

Advantages. Advantages of the method include simplicity of equipment, ease of interpretation, and noncritical sample alignment. Although this was the earliest known method, only a few of the several thousand ultrasonic inspection installations now in world use are known to employ the transmission technique. A large percentage of these are **modified pulse-time instruments.** Where optimum results are desired, it is usually preferable to employ a **gated pulse-time system** adapted to transmission indication. This retains the basic simplicity of a transmission test without the disadvantages of nongated systems.

Applications. The principal applications described in the literature relate to detection of the following flaws:

1. Lack of bonding in clad fuel elements.[48, 49]
2. "Cupping" in drawn stock.[50]
3. Flaws in grinding wheels.
4. Laminations in rubber tires.[51]

TECHNIQUES USING AMPLITUDE AND TRANSIT-TIME INDICATION.

The most versatile techniques for ultrasonic inspection of solid materials involve measurement of two parameters simultaneously:

1. The amplitude of signals obtained from any internal discontinuities.
2. The time required for the beam to travel between specific surfaces and these discontinuities.

Time Measurement Systems. Three basic time-modulated measurement systems can be used: (1) pulse time, (2) frequency modulated (FM), and (3) resonance or phasing. Each has certain advantages and limitations. However, at the present time almost all instruments used for the detection of small defects are pulse-time devices, while most thickness-measurement units use resonance. FM techniques have been limited to special applications.[20] Most resonance equipment also employs the technique of indicating the loading of the transducer by the work piece.

Equipment. The basic components of a **pulse-time flaw detector** [7] are shown in Fig. 24. Similar techniques are employed in some radar and depth-sounding equipment, although the problems relating to interpretation, resolution, and frequency range may be very different. A short electric pulse is generated and applied to the electrodes of the search unit. This produces a short train of ultrasonic waves which are coupled into the specimen. **Timing circuits** then measure the intervals between the transmittal of the initial pulse and the reception of signals from within the specimen. This cycle is repeated at regular periods so that an essentially continuous indication is obtained. The **pulse repetition rate** is made low enough so that reverberations within the specimen decay completely between pulses. Several types of instrumentation are possible, depending principally on the methods of timing and indicating. Many application techniques can also be used, depending on the number and style of search units employed, the frequency range covered, and the means for coupling or scanning. In addition, numerous variations and combinations of circuit components can be incorporated into the equipment. However, only those in common use will be described. A convenient breakdown of basic types relates primarily to the **method of presenting flaw information,**[25] as shown in the table here.

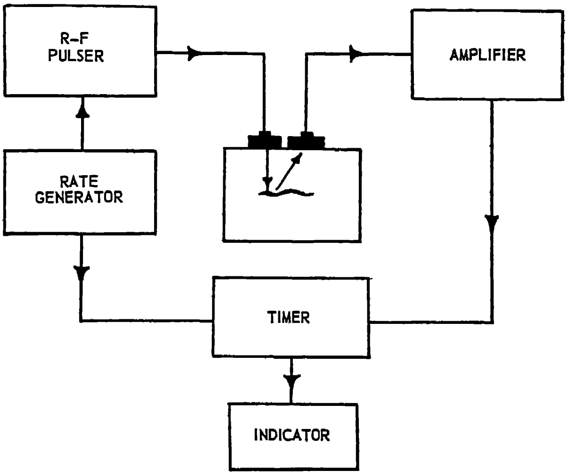

Fig. 24. Basic pulse-reflection system.

Type	Means of Presentation	Indicates Principally
A scan	CRO screen	Flaw depth and amplitude of flaw signal.
B scan	CRO screen	Flaw depth and flaw distribution in cross-sectional view.
C scan	CRO screen	Flaw distribution in plan view.
Gated systems	Electrical signal for alarm, marker, facsimile, or chart recorder	Determined by technique.

A-Scan Presentation. Most instruments in use have a basic A-scan presentation of the type shown in Fig. 25. The horizontal base line on the cathode-ray (CRO) tube screen indicates **elapsed time** (from left to right) and the vertical deflection shows **signal amplitudes.** For a given ultrasonic velocity in the specimen, the sweep can be calibrated directly in terms of distance or depth. Conversely, when the dimensions of the sample are known, the **sweep time** can be used to determine ultrasonic velocities from which elastic moduli can be calculated. The **signal amplitudes** represent the intensities of transmitted or reflected beams. These may be related to flaw size, sample attenuation, beam spread, and other factors.

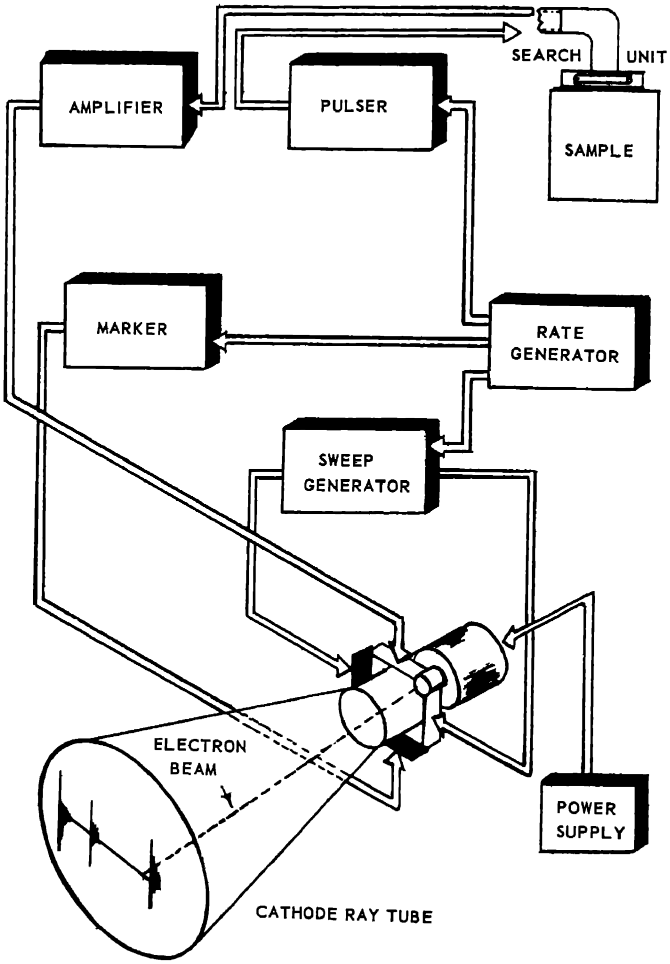

Sperry Products, Inc.

Fig. 25. Functional diagram of pulse-reflection A-scan equipment.

Techniques. As shown in Fig. 26, several techniques can be used. These include through-transmission or reflection, single or double search-unit systems, and contact or immersion coupling. Other possibilities include angle-beam and surface-wave techniques using single or dual search units, and various combinations of methods. In the United States, **single search-unit operation** is used for most reflection-testing applications, as represented by Fig. 26(c), (d), and (e). The **two-transducer technique** is more widely used in Great Britain and Europe. (See section on Double-Transducer Ultrasonic Tests.)

Distance or Time Scale Markers. To permit easy reading of flaw depth, scale markers are usually provided. These can be adjusted, using test blocks, so that each space represents some desired distance in the material (such as 1 in.). The

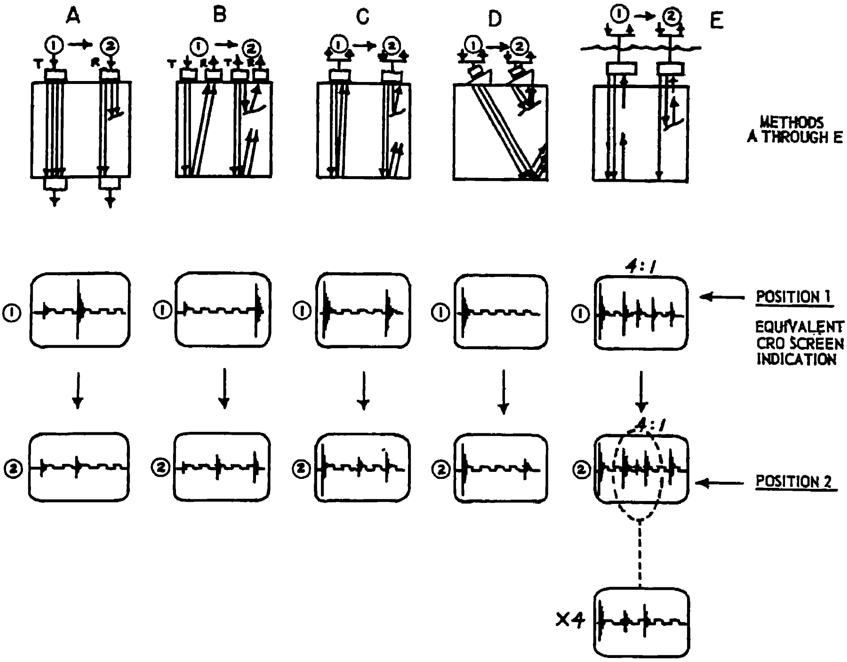

Fig. 26. Basic testing methods.

time intervals for markers or sweep length can also be computed from the known velocities in the materials of interest. The values in the table here are approximately correct for the **total reflection time in typical materials.**

Materials	Longitudinal Waves	Shear Waves
Liquids	40 μsec./in.	–
Plastics	20 μsec./in.	40 μsec./in.
Metals	10 μsec./in.	20 μsec./in.

Limitations. A wave train consisting of 10 cycles at 1 Mc. in a metal occupies 1 in. of sweep time. It will partially obscure any flaw-reflection indications occurring at the same instant. Similarly, if the amplifier circuits have a recovery period of 10 μsec. after a large signal, as much as 1 in. of material may be hidden.

The **transducers** and **amplifiers** used in typical systems tend to "ring" or to "stretch" the signals even when the initial pulse contains only a single cycle. The resolution of such systems, i.e., the ability to detect a small signal immediately after a large one, is limited to about 5 to 10 cycles, depending upon the absolute signal amplitudes involved. Values of **wave-train length in aluminum** for standard test frequencies and several pulse periods are given in Fig. 27.

Sensitivity. The absolute sensitivity required varies greatly with the application. In practical testing, the sensitivity of **commercial instruments** is usually adequate to detect the smallest defects of structural concern such as cracks, inclusions and porosity, although other limitations such as resolution may exist. Reasonable amplifier linearity is desirable for calibration and flaw comparison purposes. **Reading accuracies** of 1 part in 20 are usually sufficient, since discrepancies due to other variables such as coupling and alignment predominate. **Precision markers** or high sweep linearity are ordinarily not required for flaw detection, although one or the other may be necessary for accurate thickness or velocity measurements. In some cases precision markers are provided as special accessories.

Pulse Frequency (Mc.)	Pulse Length in Cycles		
	1	5	10
0.2	0.59 in.	2.95 in.	5.90 in.
0.5	0.24	1.18	2.36
1	0.12	0.59	1.18
2¼	0.053	0.26	0.52
5	0.024	0.12	0.24
10	0.012	0.06	0.12
15	0.008	0.04	0.08
20	0.006	0.03	0.06
25	0.005	0.02	0.05
50	0.002	0.01	0.02

Fig. 27. Testing distance obscured by pulse (interface signal or initial pulse). Thickness of a material in **inches** having a velocity of 2.36×10^5 in./sec. (6×10^5 cm./sec.) equivalent to pulses of various lengths and frequencies in echo testing.

Alternative Arrangements. Among the possible alternative **constructions for circuit components** are the following:

1. **Synchronizer** (rate generator)
   a. Pulse repetition rate: fixed at 60 c.p.s., 400 c.p.s., etc. Adjustable (fixed range). Stepped (with sweep range). Variable (50 c.p.s. to 1000 c.p.s.).
   b. Locking signal: line voltage (or harmonic); internal.
2. **Pulser**
   a. Wave shape: impulse, spike, gated sine wave, damped wave train, etc.
   b. Type: tunable, impedance matched, variable amplitude, etc.
   c. Circuit: thyratron, hard tube, pulsed oscillator.
3. **Amplifiers**
   a. Type: tuned radio-frequency, wide band, superheterodyne.
   b. Response: linear, sharp cut-off, logarithmic, etc.
   c. Sensitivity: time variable (TVG) or constant.
   d. Controls: gain, input attenuation, reject, variable band width, etc.
4. **Signal Display**
   a. Type: RF wave train, video.
   b. Source: RF output, IF output, rectified (envelope), differentiated video, etc.
5. **Sweep**
   a. Type: logarithmic, high linearity, conventional.
   b. Delay: adjustable, automatic, none.
   c. Expansion: fixed, adjustable, related to sweep.

6. **Markers**
   a. Type: fixed scale on CRO, precision electronic, adjustable square wave, movable step mark, etc.
   b. Source: crystal oscillator, adjustable multi-vibrator, precision integrator, etc.
   c. Display: superimposed on signals, alternate sweep, separate trace, intensity modulated, etc.

7. **Signal Gates**
   a. Types: amplitude proportional, fixed level alarm.
   b. Output: D-C level, modulated, rectangular wave at PRR, pulse stretched, etc.

8. **System**
   a. Frequency range: single, selectible, continuous tuning; low (50–200 kc.); intermediate (200 kc.–5 Mc.); high (5–25 Mc.).

Special Features. Special instrument features required for some applications may include the following:

1. Provision for two-crystal operation.
2. Interference elimination circuitry.
3. Compensation for long search-unit cables.
4. Stabilization for extreme line-voltage changes.
5. Exponential calibrator for attenuation measurements.
6. Exceptional portability for field use.
7. Remote indicators.
8. Extended frequency range (for example, above 100 Mc.).
9. Ultra-high resolution.

B-SCAN PRESENTATION. When the shape of large flaws or their distribution within a sample cross-section is of interest, the B-scan display can be useful. In addition to the basic components of the A-scan unit, provision must be made for these additional functions:

1. Intensity modulation or brightening of the CRO spot in proportion to the amplitude of the flaw signal.
2. Deflection of the CRO trace in synchronism with the motion of the search unit along the sample.
3. Retention of the CRO image by use of a long-persistence phosphor.

A system for producing a **section view in rectangular coordinates** is shown in Fig. 28. Other possible scanning procedures for specific applications are described in the literature.[22, 23, 24, 52]

Equipment. Often a B-scan display is used in conjunction with A-scan inspection or as an attachment to standard A-scan equipment. Therefore the design criteria depend greatly on that equipment and the application. Where **high-speed scanning** is required, the longer persistence of the B-scan display may be an advantage to the operator.

Defect Detectibility. The effectiveness of the B scan in showing flaw detail depends upon the relationship of flaw size, beam area, and wavelength. Optimum results are obtained with larger flaws, smaller crystals, and higher frequencies. For other conditions, **beam-sharpening techniques** such as focusing and electronic contrast enhancement may be required.

Alternative Arrangements. Presentations similar to the B scan, but not employing CRO displays, have also been used. One form uses a matrix of small neon lamps somewhat in the manner of an animated billboard.[30] It has high brightness and permanent memory but very limited resolution. To provide reasonable detail for display of flaw distribution, several hundred lamps were used. In certain applications, photographic film or chart recorders have been used for image formation.[21]

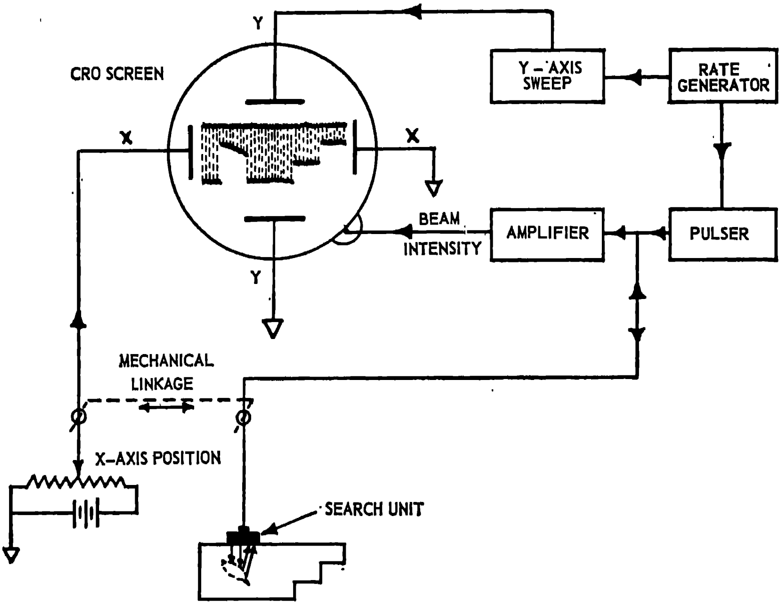

Fig. 28. B-scan presentation.

C-SCAN PRESENTATION. By synchronizing the position of the CRO spot with the search-unit scanning motion along two coordinates, a **plan view of the sample** can be developed similar to the common PPI (plan position indicator) radar display.[25, 52]

Equipment. In addition to the circuitry required for a B scan, provision must be made for eliminating unwanted signals such as the initial pulse, interface echo, or back reflection, which would obscure internal flaw signals. An **electronic gate** is used to render the display circuits sensitive only for the short intervals of sweep time when signals from the desired depth range occur, as shown in Fig. 29. Because of the relatively long period required to scan a large area, conventional CRO tubes do not have adequate persistence for practical ultrasonic C scans. **Chart recorders, facsimile techniques,** and the newer **memory tubes** have been found more satisfactory. Each has certain limitations in the detail that can be displayed, the maximum scanning speed, size of plot, and other factors.

Alternative Arrangements. In certain cases hybrid systems which present some information both as to flaw size and location have been used with some sacrifice in flaw shape and position detail.[53] The C-scan display can also be developed with through-transmission techniques and appropriate scanning and indicating methods.[48, 54]

Gated Systems. The necessity of gating or selecting certain portions of the sweep period for a C-scan display was mentioned previously. In general, gating provisions are required for all automatic systems which alarm, mark, record, chart, or otherwise replace visual interpretation. Such gating circuits may be built into the flaw detector or supplied as separate attachments.

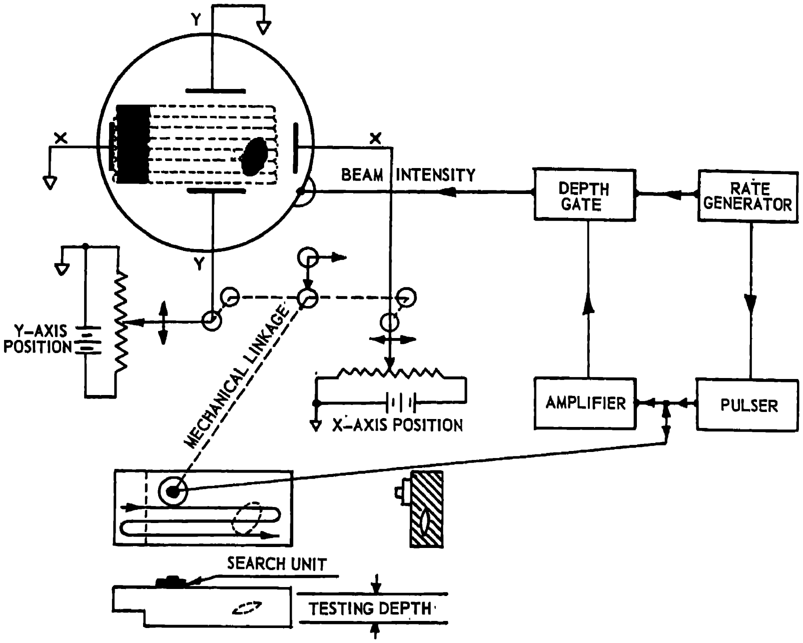

Fig. 29. C-scan presentation.

Commercial **recording attachments, or monitors,** usually provide at least two gates, one to indicate the presence of flaws within the sample and the second to show a decrease of back reflection. Some units provide **additional flaw gates** so that two or more alarm levels can be set or so that different depth increments can be examined.[25, 26, 55]

If the cross-section of the specimen varies during the scanning cycle in an automatic test, the gating periods must be simultaneously adjusted, a technique known as **programming.** In addition, other functions such as sensitivity, search-unit angle, and recorder speed may have to be controlled. One system intended for the inspection of large gun tubes having a variable cross-section uses a **pre-set program** controlled by stepping relays which are in turn set by the location of the search unit in the gun tube.[56] One installation developed for the automatic inspection of contoured jet engine forgings employs a punched tape to control each of the six variables involved.[53]

TECHNIQUES USING TRANSDUCER LOADING EFFECTS. The most common instruments utilizing transducer-loading effects are those which employ resonance effects to indicate sample thickness.

Equipment. The basic system is shown in Fig. 30. By the proper selection of components, it is possible to tune through one or more resonances from which the sample thickness can be determined.[17, 27, 57]

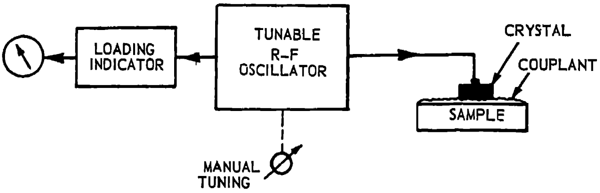

Fig. 30. Manual resonance system.

A more elaborate system which automatically sweeps the frequency and displays thickness indications on a CRO screen is shown in Fig. 31. (Typical instruments and their uses are described in the section on Ultrasonic Resonance Tests.) Calibration is usually performed experimentally with known samples, although appropriate frequency-thickness scales can be calculated. The crystal, couplant, and sample comprise a composite transducer whose electrical impedance can be calculated as a function of frequency.[58] At resonance the impedance becomes minimum, causing an increase of loading on the source.

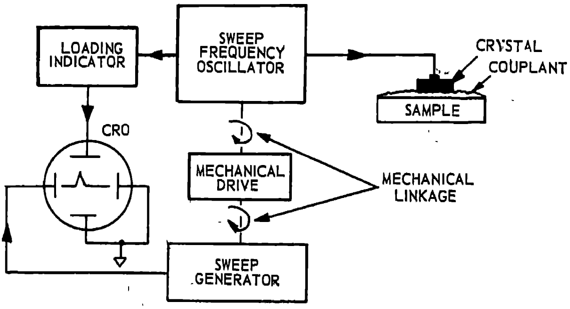

Fig. 31. Automatic resonance system.

Resonant Frequencies. The lowest resonant frequency of the system, f_1, is given approximately by the following conditions, provided the crystal is operated near its fundamental frequency:

$$t \cong \frac{\lambda_1}{2} \tag{12}$$

$$f_1 \cong \frac{v}{2t} \tag{13}$$

where t = thickness.
$\lambda_1 = v/f_1$.
f_1 = lowest resonant frequency.
v = longitudinal velocity.

Certain conditions may produce spurious signals giving irrelevant indications.

An infinite series of **higher-order harmonic resonances** is also possible, as given by

$$t = \frac{n\lambda_n}{2} \tag{14}$$

$$f_n = \frac{nv}{2t} \tag{15}$$

where $\lambda_n = \lambda_1/n$.
$n = 1, 2, 3$, etc.
f_n = successive resonances.
v = longitudinal velocity.
t = thickness.

Conversely, by measuring the frequencies of two successive harmonics, that of the fundamental can be obtained as

$$f_1 = f_{(n+1)} - f_n = \Delta f \tag{16}$$

Thickness Measurements. Test-object thickness is given by

$$t = \frac{v}{2f_1} = \frac{nv}{2f_n} = \frac{v}{2\,(\Delta f)} \tag{17}$$

If the scale is calibrated in thickness instead of frequency (based on $t_1 = v/2f_1$), successive **thickness-scale readings** can be used, as follows:

$$t = \frac{t_b \times t_a}{t_b - t_a} \tag{18}$$

where t_a and t_b are scale readings for successive thickness indications, $t_b > t_a$.

Alternative Arrangements. Modifications of the technique have been developed which display the impedance characteristic of the specimen,[27, 59] one application being for the inspection of adhesive-bonded aircraft components.

Calibration Problems

NEED FOR CALIBRATION. Interpretation of indications obtained from metallurgical discontinuities by various ultrasonic inspection methods is discussed in several subsequent sections. Determination of their seriousness is usually outside the scope of nondestructive testing. To permit such an evaluation, however, appropriate **calibration techniques** and **reference standards** are necessary. This is particularly true in the application of **pulse-reflection instrument** types because of the large number of variables possible.

BASIC CONSIDERATIONS. There is no equivalent of the X-ray penetrameter in ultrasonic testing. In most ultrasonic testing, only an **indirect calibration procedure** is practical. This usually involves comparison with **indications from reference blocks** containing drilled test holes, or in a limited number of cases, from reference surfaces within the specimen. Neither method, however, provides a direct calibration of system response to flaws which may be located anywhere within the specimen cross-section. Except for certain types of curved specimens, the signals obtained from the front face **(interface reflection)** or back surface **(first back reflection)** are usually of far too great amplitude for use as a reference during testing at high sensitivity for small defects. The use of small reflecting surfaces placed at some point in the beam path, but external to the sample in the manner of X-ray penetrameters, has only limited advantages and is usually impractical except for certain conditions in immersion testing. At the present time, therefore, calibration of instruments is done principally with sets of special reference blocks intended for specific applications.[30, 61, 62]

Several investigations of calibration factors have been undertaken to provide correlation factors for interrelating various parameters. An interesting and useful result has been a proposal to use small steel spheres of ⅛ to 1 in. diam. as a **basic sensitivity reference** for immersed testing and to check secondary standards such as test blocks.

The **required accuracy of calibration** can vary greatly with the application. In some cases only a crude check on instrument performance is necessary; in others, only reference settings, so that results can be duplicated later. When acceptance of material is based on rigid **ultrasonic test specifications,** considerable attention must be given to calibration techniques. Fabrication of duplicate sets of reference blocks required for such applications can prove to be a serious problem.

MAJOR PARAMETERS. The components of an ultrasonic-testing system and their principal variables are shown in Fig. 32. Some of the characteristics

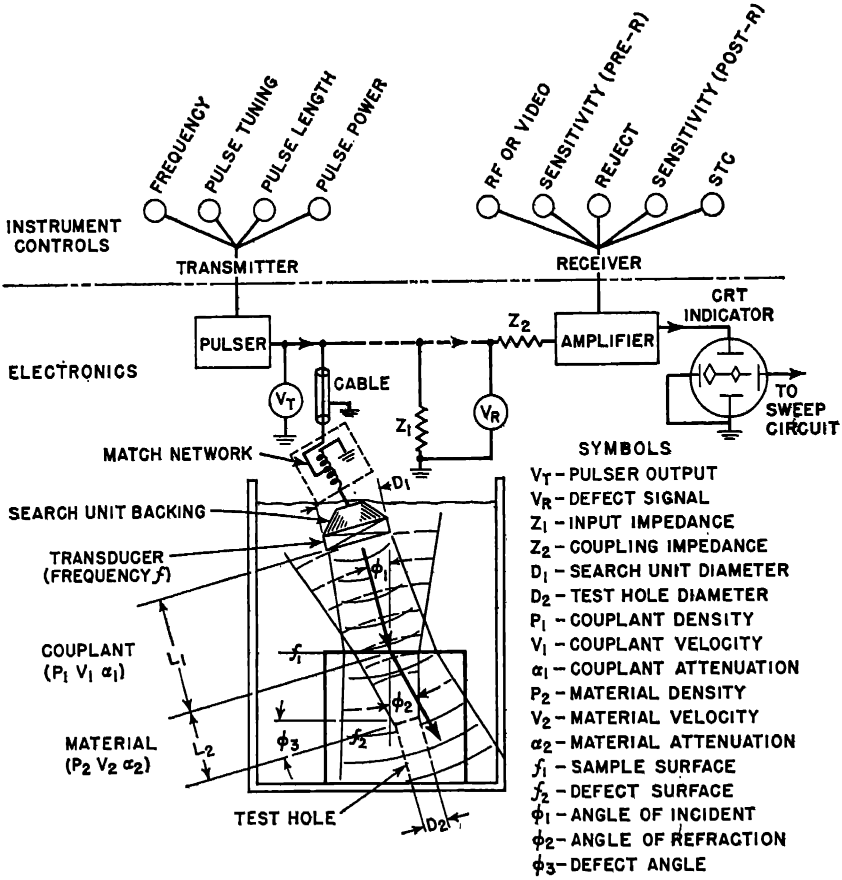

Fig. 32. Parameters affecting signals in ultrasonic pulse-reflection technique.

of such a system can be anticipated from fundamental principles of ultrasonic testing. Others may be related primarily to: the specific components used in the instrument or search units; wave shape; amplifier recovery time; and transducer field patterns (see section on Ultrasonic Transducers).

Operator-controlled Parameters. The major parameters controlled by the operator relate to:

1. Equipment selection
   a. Instrument type.
   b. Search unit-type and size.
2. Equipment operation
   a. Technique.
      (1) Coupling method.
      (2) Scanning sequence.
      (3) Peaking procedure.
   b. Control settings.
      (1) Frequency.
      (2) Pulse length.
      (3) Linearity.
      (4) Distance/time-varied gain (TVG) or sensitivity-time gain (STG).

Parameters Controlled by Inspection Problems. Those parameters determined by the specific inspection problem involve:

1. Specimen properties
   a. Velocity.
   b. Impedance.
   c. Geometry.
   d. Surface.
   e. Attenuation.
   f. Noise level.
2. Flaw conditions
   a. Depth.
   b. Size.
   c. Shape.
   d. Impedance.
   e. Orientation.

EVALUATION OF PARAMETERS. Numerous investigations have been undertaken to isolate and evaluate one or more of the many factors involved in calibration. Early work at the Aluminum Company Laboratories, relating to distance-amplitude factors and to the fabrication of reference blocks, is noteworthy.[63] Projects under U.S. Air Force sponsorship have yielded considerable data applicable to many inspection problems.[30, 61]

Several typical examples from work sponsored by the Air Materiel Command, U. S. Air Force, illustrate these results. Fig. 33 describes the several **types of test blocks** used during the project. Fig. 34 presents **normalized amplitude-distance data** (semi-log plot) in aluminum for several standard contact search units and test frequencies on the Type A-1 test blocks of Fig. 33. Fig. 35 represents the **beam profile** for one of these curves, i.e., the relative amplitudes obtained as the search unit traverses a flaw at different depths.

Fig. 36 shows amplitude-distance data (log-log plot) for several **test hole diameters.** Fig. 37 shows amplitude-distance data (log-log plot) for several different **test hole shapes** as shown in Fig. 33.

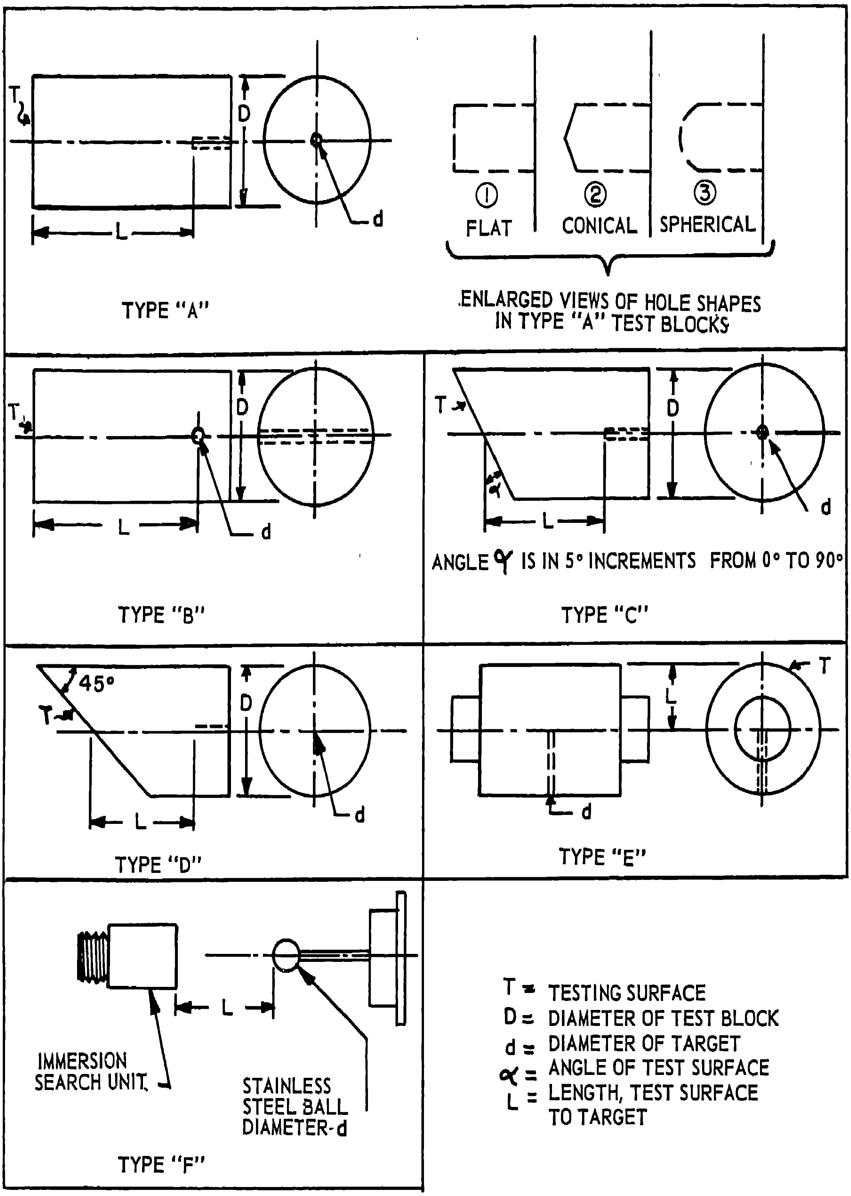
T
D
L
d
TYPE "A"
① FLAT
② CONICAL
③ SPHERICAL
ENLARGED VIEWS OF HOLE SHAPES IN TYPE "A" TEST BLOCKS
T
D
L
d
TYPE "B"
T
D
α
L
d
ANGLE α IS IN 5° INCREMENTS FROM 0° TO 90°
TYPE "C"
45°
T
D
L
d
TYPE "D"
T
L
d
TYPE "E"
L
IMMERSION SEARCH UNIT
STAINLESS STEEL BALL DIAMETER-d
TYPE "F"
T = TESTING SURFACE
D = DIAMETER OF TEST BLOCK
d = DIAMETER OF TARGET
α = ANGLE OF TEST SURFACE
L = LENGTH, TEST SURFACE TO TARGET

Fig. 33. Basic types of test blocks used for calibration.

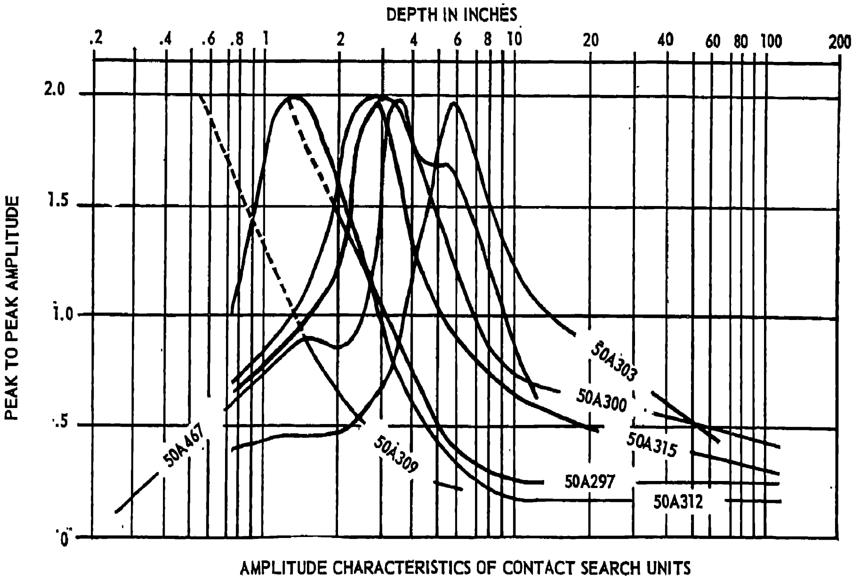

Fig. 34. Amplitude-distance data for standard contact search units.

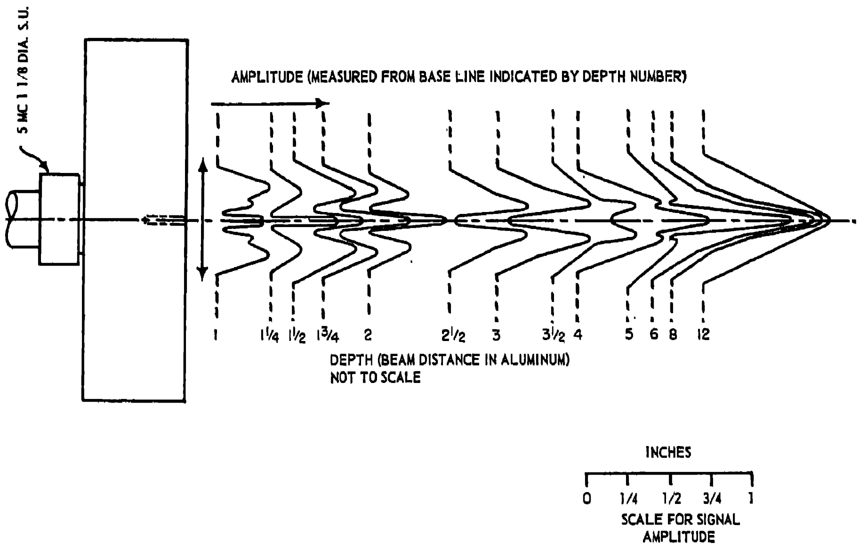
5 MC 1 1/8 DIA. S.U.
AMPLITUDE (MEASURED FROM BASE LINE INDICATED BY DEPTH NUMBER)
1
1¼
1½
1¾
2
2½
3
3½
4
5
6
8
12
DEPTH (BEAM DISTANCE IN ALUMINUM)
NOT TO SCALE
INCHES
0
1/4
1/2
3/4
1
SCALE FOR SIGNAL AMPLITUDE

Fig. 35. Beam profile variation with distance. 5 Mc., 1⅛-in. diam. contact search unit.

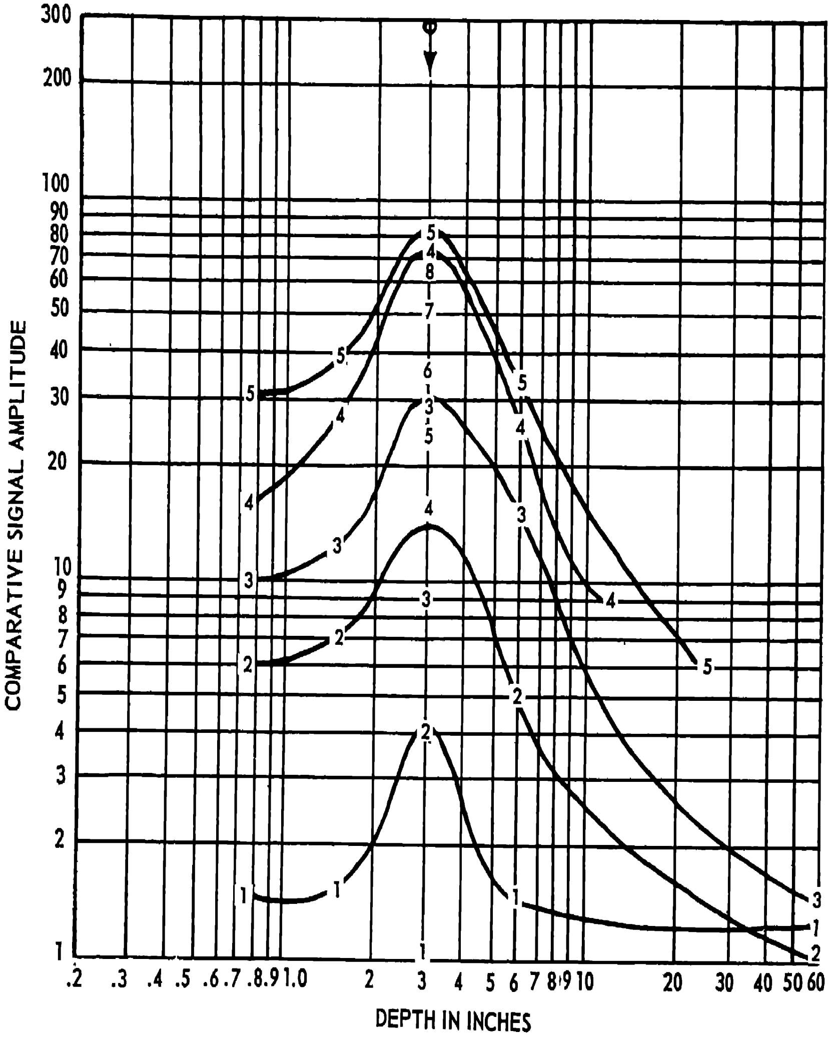

Fig. 36. Comparative amplitude-distance data, contact test, 5 Mc., ¾-in. diam. search unit data for 1/32-, 2/32-, 3/32-, 4/32-, and 5/32-in. diam. test holes.

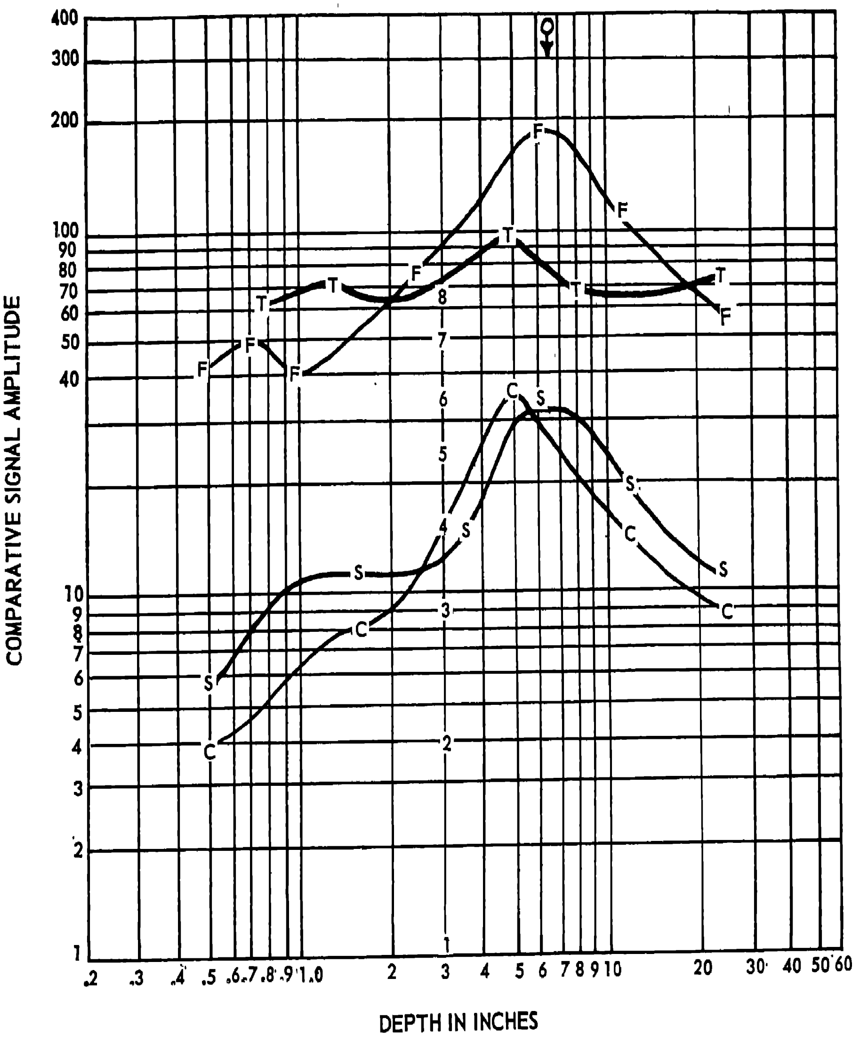

Fig. 37. Comparative amplitude-distance data, contact tests, 5 Mc., 1⅛-in. diam. search unit, for various hole shapes. (Flat-bottom, F; cylindrical, T; conical, C; spherical, S.)

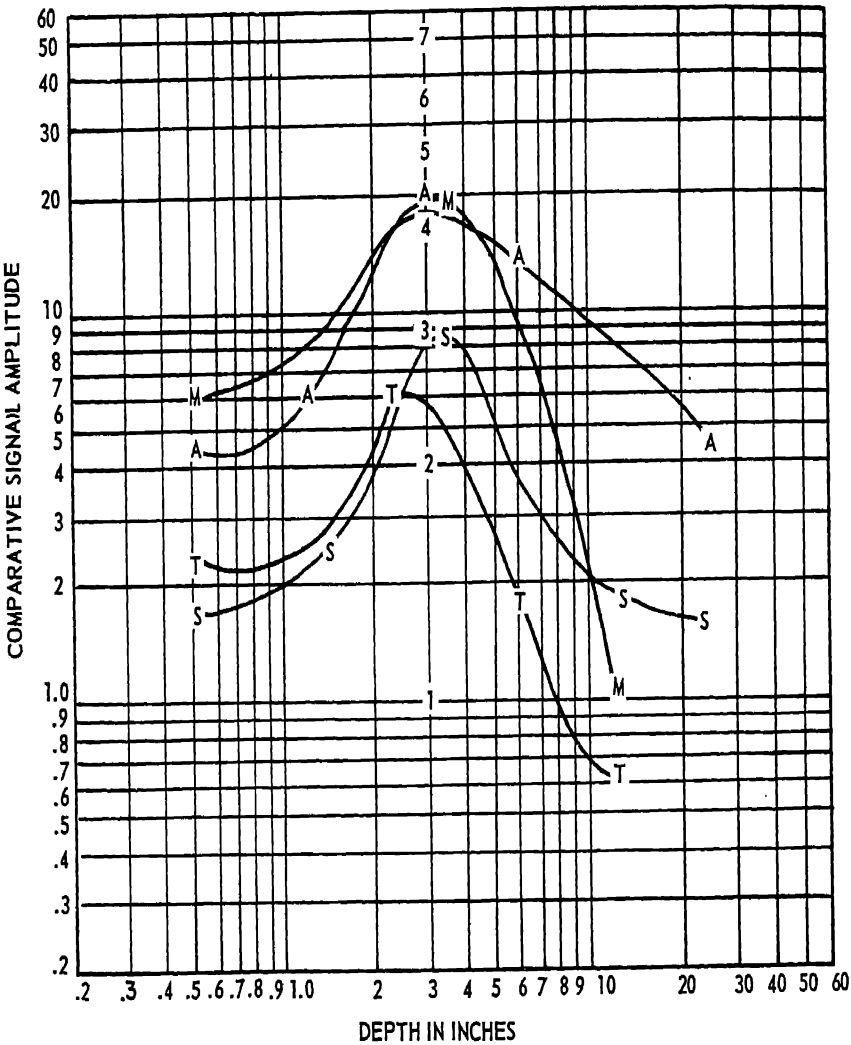

Fig. 38. Comparative amplitude-distance data; immersed tests for four materials. Magnesium, M; aluminum, A; titanium, T; steel, S.

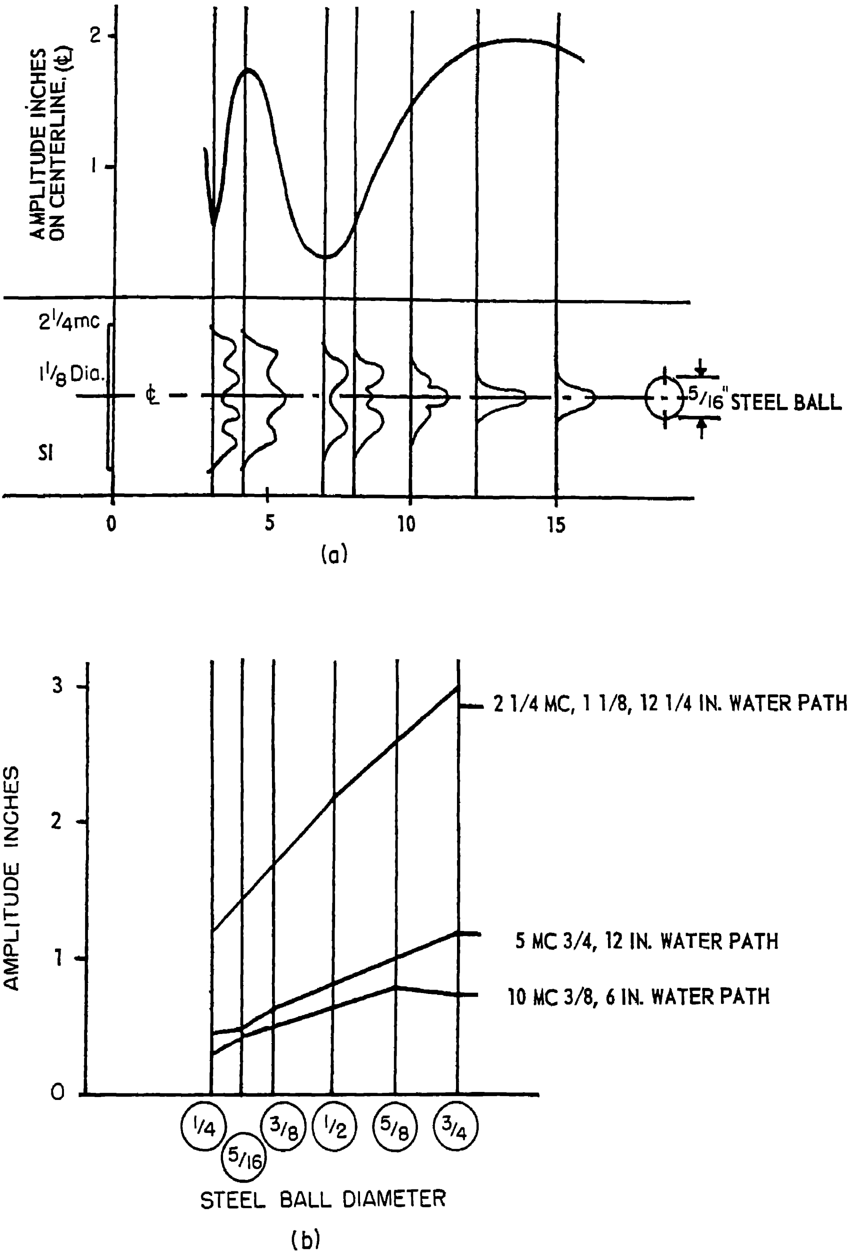

Fig. 39. Reflections from immersed steel spheres.

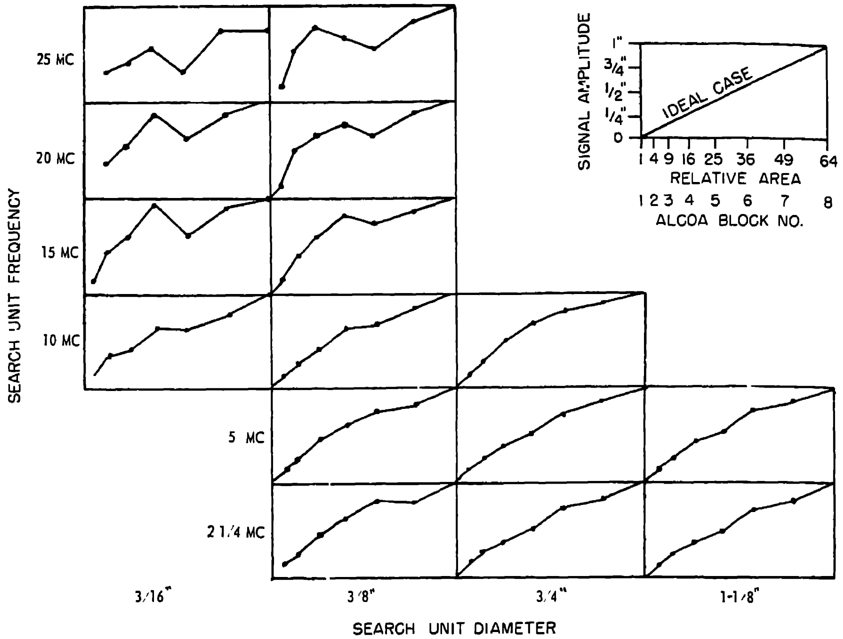

Fig. 40. Amplitude versus area calibration data. Immersion test on Alcoa reference blocks, Series A.

Fig. 38 shows amplitude-distance data (log-log plot) for several **typical aircraft materials.** Fig. 39 shows the amplitude of a calibrating signal obtained from an **immersed steel sphere.** Fig. 39(a) gives the amplitude-distance relationship and Fig. 39(b) gives amplitude-ball-diameter data for several frequencies at the close field limit. Fig. 40 presents amplitude-area data (linear plot) for one set of **Type A-1 blocks** at several test frequencies. Fig. 41 gives the calculated ratios between various reflection amplitudes for **various materials** immersed in water. Test conditions are shown in Fig. 42.

Item	Case 1 (Water Backed)			Case 2 (Air Backed)		
Reflection ratio	$\frac{B}{A}$	$\frac{C}{A}$	$\frac{C}{B}$	$\frac{B}{A}$	$\frac{C}{A}$	$\frac{C}{B}$
Formula	$\sqrt{R}$	$(1-R)\sqrt{R}$	$(1-R)$	$\sqrt{R}$	$(1-R)$	$\frac{(1-R)}{\sqrt{R}}$
Material	Signal Amplitude Ratio			Signal Amplitude Ratio		
Steel	.94	.11	.12	.94	.12	.13
Titanium	.90	.17	.19	.90	.19	.21
Aluminum	.85	.24	.28	.85	28	.33
Magnesium	.74	.33	.45	.74	.45	.61

$$R = \left(\frac{Z_2 - Z_1}{Z_2 + Z_1}\right)^2$$

Fig. 41. Calculated signal-amplitude ratios in immersed testing of various metals.

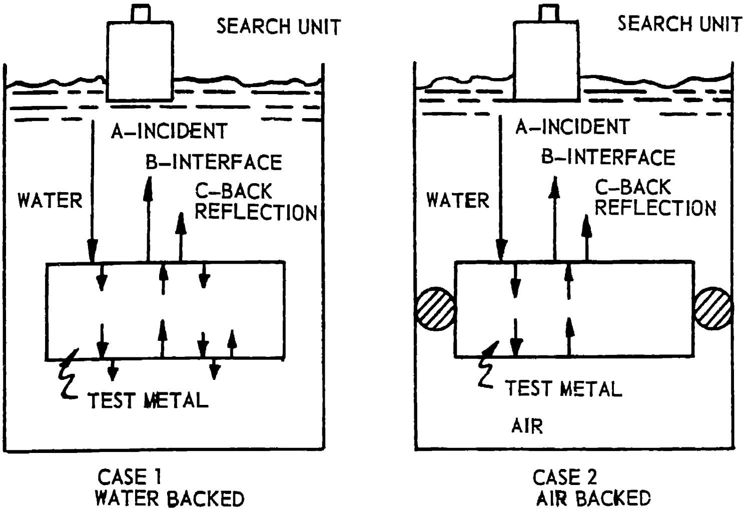

Fig. 42. Test conditions for Fig. 41.

Ultrasonic Test Features

TESTING APPLICABILITY. The features of ultrasonic techniques with respect to their applicability to nondestructive testing can be evaluated in terms of their advantages, capabilities, and limitations.

ADVANTAGES. Since only low-amplitude, inaudible sonic waves are utilized, the specimen is not damaged by the test.

Mechanical Testing. Ultrasonic waves are mechanical vibrations, and therefore ultrasonic inspection is especially suited to detection of elastic discontinuities and measurement of physical properties such as flaws, porosity, structure, and elastic constants. Optical, magnetic, chemical, and other properties are not ordinarily indicated. In order of detectibility, the discontinuities usually indicated are geometrical, gross flaws, minute defects, and finally structure.

Instantaneous Indication. Instrumentation is basically electronic, with indications being obtained almost instantaneously. This characteristic permits rapid scanning of parts, with automatic positioning, plotting, and alarming.

Volume Scanning. The ultrasonic beam almost instantaneously searches a complete volume of material extending from the front to the back surface of the specimen. Each incremental scan of volume requires only a fraction of a second. With a 1-in. square search unit and a pulse repetition rate of 60 c.p.s., a steel roll 10 ft. long could be tested at the rate of a quarter-ton per second. Since the instrument response time is negligible, practical inspection speeds are determined by such factors as the scanning mechanism, handling equipment, human reaction time, and pulse repetition rate.

Versatility. The ultrasonic method permits inspection of a wide range of samples as to size, geometry, area of flaw, and other requirements. Basically it detects internal, hidden defects which sometimes may be deep below the surfaces. Search units are available to generate waves of several types, including longitudinal, shear, and surface. Applications range from thickness measurements of thin steel plate to internal inspection of 100-ton turbine rotors.

Safety and Convenience. There is no hazard to the operator or to nearby personnel. Access to only one surface is necessary in most cases.

Wide Applicability. Most nonporous, resilient materials used for structural purposes (such as steel, aluminum, titanium, magnesium, and ceramics) can be penetrated. Even large cross-sections several feet thick can be tested successfully for minute flaws.

Sensitivity and Directivity. The use of a high frequency, well-defined beam of sound permits detection and location of the smallest flaws of structural importance. Disc-like defects or cracks of almost zero thickness are readily detected. Depth can be indicated to within a small fraction of an inch, even in thick specimens. The beams used have searchlight directivity, being confined to cones of low divergence by their short wavelengths. Angle-beam techniques permit direction of the beam toward any area of the object.

Portability. Some equipment can be used in shop, laboratory, warehouse, or field, thus permitting in-place inspection and requiring only moderate power from the a.-c. line or a small generator.

Ease of Operation. Operator training can be simple and brief for many specific applications where the problem is clear-cut and the technique is established. (Yet the method remains versatile and has flexibility for the solution of new and more advanced problems. Most operators soon find the technique interesting and challenging.)

High Development. Several years of development have resulted in the availability of several basic instruments, many application techniques, considerable knowledge, and a wide assortment of accessories, search units, fixtures, and other aids.

Wide Acceptability. Ultrasonic inspection techniques are widely accepted throughout industry. Ultrasonic tests are used for quality control and materials inspection in the major heavy industries, including electrical manufacturing, production of steel, aluminum, and titanium, in the fabrication of airframes, and in jet engine manufacture. Ultrasonic testing for preventive maintenance is used for in-place inspection to prevent failure of rolling stock axles, press columns, earth-moving gear, mill rolls, mining equipment, and other machines and components. Various technical societies and standards committees have recognized the necessity for ultrasonic inspection and are preparing test procedures, acceptance standards, and other essential data.

CAPABILITIES. A variety of classifications could be utilized to tabulate the principal applications. The division outlined here is intended to suggest rather than to present details.

Established Applications. Equipment now in everyday use is mainly concerned with (1) flaw detection and (2) thickness measurement. Examples of flaw detection, listed according to end use, are:

1. Mill components: rolls, shafts, drives, and press columns.
2. Power equipment: turbine forgings, generator rotors, and pressure piping.
3. Jet engine parts: turbine blanks and compressor rotors.
4. Airframe components: forging stock and frame sections.
5. Machinery materials: die blocks, tool steels, and drill pipe.

6. Rolling stock: axles, wheels, and crankpins.
7. Track maintenance: rail joint areas.
8. Nuclear reactors: clad fuel elements and heat exchanger tubing.

The **flaws to be detected** may be voids, cracks, inclusions, segregations, laminations, bursts, flakes, or other types. They may be inherent in the raw material, result from fabrication and heat treatment, or occur in service from fatigue, corrosion, and other causes. Testing may be performed manually or automatically, by immersion or by contact, depending upon the conditions.

Thickness measurements, the second general application, are made principally on aircraft propellers, wing sections, armor plate, steel castings, submarine hulls, and other structural components. Numerous special instruments available are applicable for thickness ranges of from ¹⁄₆₄ in. to several feet.

Applications Proved Feasible. Instrumentation already developed can be applied to many different problems, provided special techniques are worked out. Among such applications are:

1. Rate of growth of fatigue cracks.
2. Detection of bore-hole eccentricity.
3. Measurement of elastic moduli.
4. Study of press fits.
5. Investigation of corrosion rates.
6. Control of weld quality.
7. Metallurgical research relating to structure.
8. Inspection of grinding wheels, ceramics, and concrete.

Potential Applications. Investigations indicate the possibility of applying ultrasonic techniques to a variety of **unsolved problems** such as:

1. Metallurgical analysis and control of case depth and hardness, precipitation of alloy constituents, and grain refinement.
2. Detection of incipient metal fracture.
3. Theoretical crystallography and metallurgy.
4. Mechanical properties of liquids and plastics.

LIMITATIONS. Conditions may exist which prevent the application of ultrasonics to specific inspection problems. Usually these difficulties are related to one or more of these limiting factors:

1. Defect detectibility.
2. Coupling and scanning problems.
3. Economics of inspection.

Defect Detectibility. Detectibility is related to sensitivity, resolution, and noise discrimination. Briefly, **sensitivity** refers to the ability of the instrument to detect the minute amount of sound energy reflected from a discontinuity. **Resolution** measures the ability to separate indications occurring close together from two nearby points in an object. **Noise discrimination** is the capacity for indicating desired signals from defects in the presence of simultaneous, unwanted signals of either electrical or acoustical nature.

These factors of detectibility are not necessarily independent, so it is difficult to state the practical limits quantitatively. However, testing may be marginal or unsatisfactory if the specimen is extremely thin, geometrically complicated, or has exceedingly coarse grain structure.

Ordinarily the **size or type of flaw** is not an actual limit in practical use. For example, in the case of fatigue cracks in axles near press-fitted wheels, the smallest and shallowest crack which can be detected is limited less by the instrumentation or material than by the acoustic "noise" generated by the press fits. Similarly, testing of threaded parts for shallow root cracks may not be feasible.

Coupling and Scanning. Problems of coupling and scanning occur to some extent in every application. A liquid or paste couplant which "wets" the surface must normally be used between the search unit and specimen. (Certain soft solids can occasionally be used as couplants.) Total immersion of the piece sometimes can be used advantageously. **Extremely rough surfaces** may preclude any test by preventing effective sound coupling. Scanning of rough, complicated, or small parts may be difficult or impossible for practical testing.

Economics. The economic factors of ultrasonic testing are evaluated more readily with an understanding of the basic features of the technique. Economic factors vary in importance. For instance, safety aspects, customer requirements, or other factors may be the predominant considerations.

CRITERIA FOR SUCCESSFUL INSPECTION. An appraisal of some specific industrial applications in which ultrasonic inspection has been particularly successful indicates certain keys to success with the technique. Among factors common to its successful use are:

1. Clear definition of test problems.
2. Good supervision of operators.
3. Adequate reference specimens.
4. Practical test specifications.
5. Realistic acceptance standards.
6. Detailed test records.
7. Frequent inspection where required.

These considerations actually are common to the success of all types of nondestructive test methods. Since testing and inspection represent considerable investment in equipment and manpower and possible delays in production, careful attention to these factors of success is always warranted. Where safe usage of the product is contingent upon careful testing, rigorous adherence to these rules is essential.

References

1. Muhlhauser, O. "Verfahren zur Zustandsbestimmung von Werkstoffen, Besonders zur Ermittlung von Fehlern darin (Method of Determining the State of Work Materials, Particularly for the Investigations of Flaws in Them)." German Patent No. 569, 598 (1931).
2. Trost, A. "Nachweis von Werkstofftrennungen in Blechen mit Ultraschall (Detection of Material Separation in Metal Sheets by Ultrasonics)," *Z. Ver. deut. Ing.*, 87 (1943): 352.
3. Pohlman, R. "Ueber die Moeglichkeit einer akustischen Abbildung in Analogie zur Optischen (On the Possibility of an Acoustic Image in Analogy to an Optical One)," *Z. Physik,* 113 (1939): 697.
4. Sokoloff, S. "Zur Frage der Fortpflanzung Ultraakustischer Schwingungen in Verschiedenen Koerpern (On the Problem of Transmission of Ultrasonic Vibrations in Various Materials)," *Elek. Nachr.-Tech.*, 6 (1929): 454.
5. Van Valkenburg, H. E., F. H. Hardie, and R. C. Goodman. "Acoustic Image Inspection," *Final Rept., U.S. Navy, BuAer,* Contract No. NOa(s)8868 (1950).
6. Firestone, F. A. "Flaw Detecting Device and Measuring Instrument." U.S. Patent No. 2, 280, 226 (Apr. 21, 1942).

7. Firestone, F. A. "The Supersonic Reflectoscope for Interior Inspection." *Metal Progr.*, 48 (1945): 505.
8. Desch, C. H., W. J. Dawson, and D. O. Sproule. "Detection of Cracks in Steel by Means of Supersonic Waves," *Engineer,* 181 (1946): 467.
9. "Ultrasonic Testing of Gas Turbine Disks," *Metal Progr.*, 57 (1950): 468.
10. Firestone, F. A., and J. R. Frederick. "A Theoretical and Experimental Study of the Quartz Crystal as Applied to the Supersonic Reflectoscope." *Sperry Products Rept.* TR-004, Univ. Michigan, Dept. Phys. and Eng., Research Project M-530 (1945).
11. ———. "Refinements in Supersonic Reflectoscopy. Polarized Sound." *J. Acoust. Soc. Am.*, 18 (1946): 200.
12. Firestone, F. A. "Tricks With the Supersonic Reflectoscope," *Nondestructive Testing,* 7, No. 2 (1948): 5.
13. Firestone, F. A., and D. S. Ling, Jr. "Reflection and Refraction of Supersonic Waves—The Raybender," *Sperry Products Rept.* TR-001, Univ. Michigan, Dept. Phys. and Eng., Research Project M-530 (1945).
14. Firestone, F. A. (To Sperry Products, Inc.) "Supersonic Inspection for Flaws Lying Near the Surface of a Part," U.S. Patent No. 2, 467, 301 (Apr. 12, 1949).
15. ———. (To United Aircraft Corp.) "Resonance Inspection Method." U.S. Patent No. Re. 23,090 (Mar. 15, 1949).
16. Worlton, D. C. "Ultrasonic Testing with Lamb Waves." *Nondestructive Testing,* 15, No. 4 (1957): 218.
17. Erwin, W. S. "Supersonic Measurement," *Steel,* 116, No. 10 (1945): 131, 188.
18. Erwin, W. S., and G. M. Rassweiler. "The Automatic Sonigage," *Iron Age,* 160, No. 4 (1947): 48.
19. Erdman, D. C. "Design and Application of Supersonic Flaw Detectors," *Elec. Eng.*, 67 (1948): 181.
20. ———. "Ultrasonic Flaw Detector," U.S. Patent No. 2, 593, 865 (Apr. 22, 1952).
21. "Ultrasonic Flaw Detector," *Bull. Glass Developments, Ltd.,* Sudbourne Road, Brixton Hill S.W. 2, England (1951).
22. Erdman, D. C. "Weld Inspection Tool," *Final Rept., U.S. Navy, BuShips,* Contract No. NOBS-50564 (1951).
23. Reid, J. M., and J. J. Wild. "Ultrasonic Ranging for Cancer Diagnosis," *Electronics,* 25, No. 7 (1952): 136.
24. Howry, D. H. "Techniques Used in Ultrasonic Visualization of Soft Tissue Structures of the Body," *IRE Conv. Record* 1955, Pt. 9: 75.
25. Pringle, F. E., Jr. "SIMAC—Sonic Inspection. Measurement, and Control." *Nondestructive Testing,* 14, No. 3 (1956): 22.
26. Smack, J. C. "Immersed Ultrasonic Inspection with Automatic Scanning and Recording of Warning Signal," *Nondestructive Testing,* 12, No. 3 (1954): 29.
27. Hueter, T. F., and R. H. Bolt. *Sonics.* New York: John Wiley & Sons, Inc., 1955.
28. Mason, W. P. *Electromechanical Transducers and Wave Filters.* 2d ed. New York: D. Van Nostrand Co., Inc., 1948.
29. ———. *Piezoelectric Crystals and Their Applications to Ultrasonics.* New York: D. Van Nostrand Co., Inc., 1950.
30. Van Valkenburg, H. E., R. A. Wilson, and W. R. Olha. "Ultrasonic Inspection Equipment Program," *U.S. Air Force, Air Materiel Command, Final Rept.* TR-065, Contract AF 33(600)-29879 (1956).
31. Carlin, B. (To Sperry Products, Inc.) "Supersonic Testing." U.S. Patent No. 2, 527, 986 (Oct. 31, 1950).
32. Cook, E. G., and H. E. Van Valkenburg. "Surface Waves at Ultrasonic Frequencies," *ASTM Bull.,* No. 198 (1954): TP 127.
33. Moriarty, C. D. "Ultrasonic Flaw Detection in Pipes by Means of Shear Waves," *Trans. Am. Soc. Mech. Engrs.,* 73 (1951): 225.
34. Webb, R. H. (To Sperry Products, Inc.) "Variable Angle Ultrasonic Transducer." U.S. Patent No. 2, 602, 102 (July 1. 1952).

35. BERGMANN, L. *Der Ultraschall und seine Anwendung in Wissenschaft und Technik* (Ultrasonics and Their Applications in Science and Industry). Zurich: S. Hiral Verlag, 1954.
36. KINSLER, L. E., and A. R. FREY. *Fundamentals of Acoustics*. New York: John Wiley & Sons, Inc., 1950.
37. COCHRAN, D., and R. W. SAMSEL, "Ultrasonics," *Gen. Elec. Rev.*, 47, No. 8 (1944): 39.
38. GIACOMINI, A., and A. BERTINI. "Perfezionamento del metodo per accertare l'omogeneita dei solidi mediante ultrasuoni (Improvement of the Method of Testing the Homogeneity of Solids by Ultrasonic Waves)," *Ricerca sci.*, 10 (1939): 921.
39. KOLSKY, H. *Stress Waves in Solids*. London: Oxford University Press, 1953.
40. SCHOCH, A. "Schallreflexior, Schallbrechung und Schallbeugung (Sound Reflection, Transmission, and Refraction)," *Ergeb. exak. Naturw.*, 23 (1950): 127.
41. ARENBERG, D. L. "Ultrasonic Solid Delay Lines," *J. Acoust. Soc. Am.*, 20 (1948): 1.
42. McGAUGHEY, W. C. "Angle Beam Transmission Through Solid Interfaces," *Sperry Products, Inc., Eng. Rept.* 1050-8 (1953).
43. FIRESTONE, F. A. "Acoustics," Dwight E. Gray, ed., *American Institute of Physics Handbook,* Sect. 3. New York: McGraw-Hill Book Co., Inc., 1957.
44. RODERICK, R. L., and R. TRUELL. "The Measurement of Ultrasonic Attenuation in Solids by the Pulse Technique and Some Results in Steel," *J. Appl. Phys.*, 23 (1952): 267.
45. GROSSMAN, N. "New Methods Determine Grain Size Ultrasonically," *Iron Age*. 172, No. 27 (1953): 72.
46. TRUELL, R. "Ultrasonic Attenuation Measurements for Study of the Engineering Properties of Materials," *Mech. Eng*, 77 (1955): 585.
47. KRUSE, F. "Zur Werkstuckpruefung mittels Ultraschalls (Materials Testing with Ultrasonics)," *Akust. Z.*, 4 (1939): 153.
48. BECK, W. N. "An Ultrasonic Scanner and Recording System," *Nondestructive Testing,* 15, No. 1 (1957): 42.
49. McGONNAGLE, W. J., J. H. MONAWECK, and W. G. MARBURGER. "Methods of Bond Testing," *Nondestructive Testing,* 13, No. 2 (1955): 17.
50. WELLER, E. F., JR. "ABC's of Ultrasonic Inspection," *SAE Trans.*, 63 (1955): 177.
51. MORRIS, W. E., R. B. STAMBAUGH, and S. D. GEHMANN. "Ultrasonic Method of Tire Inspection," *Rev. Sci. Instr.*, 23 (1952): 729.
52. BUCHANAN, R. W., and C. H. HASTINGS. "Ultrasonic Flaw Plotting Equipment. A New Concept for Industrial Inspection," *Nondestructive Testing,* 13, No. 5 (1955): 17.
53. BENDZ, W. I. "Discussion—Describes Equipment for Making Permanent Acoustic Test Records," *SAE Trans.*, 63 (1955): 188.
54. KRAUTKRAMER, J., H. KRAUTKRAMER, and O. RUDIGER. "Ein Ueberschallgeraet zur zerstoerungsfreien Werkstoffpruefung (Ultrasonic Apparatus for Nondestructive Testing)," *Arch. Eisenhuettenw.*, 20 (1949): 355.
55. ERDMAN, D. C. "Ultrasonic Testing," *Nondestructive Testing,* 8, No. 2 (1949): 28.
56. VAN VALKENBURG, H. E., and E. A. HENRY. "Reflectoscope Equipment for Automatic Inspection of Gun Tube Forgings," *U.S. Army, Ordnance Corps, Watervliet Arsenal, Final Rept.* TR-060, Contract No. DA.30-144-ORD-4400, (1955).
57. BRANSON, N. G. "Portable Ultrasonic Thickness Gage," *Electronics,* 21, No. 1 (1948): 88.
58. COOK, E. G., and H. E. VAN VALKENBURG. "Thickness Measurement by Ultrasonic Resonance," *J. Acoust. Soc. Am.*, 27 (1955): 564.
59. ARNOLD, J. S. "An Ultrasonic Technique for Nondestructive Evaluation of Metal-to-Metal Adhesive Bonds," *Am. Soc. Testing Materials, Spec. Tech. Publ.*, 213 (1957): 79; *WADC* (Wright Air Development Center) *Status Repts.,* Contract No. AF 33 (616)-2035.

60. Fine, M. E. "Dynamic Methods for Determining the Elastic Constants and Their Temperature Variations in Metals," *Am. Soc. Testing Materials, Spec. Tech. Publ.*, 129 (1952): 43.

61. Guinn, H. D., R. D. McKown, J. C. Folz, and W. C. Hitt. "Research and Development Leading to the Establishment of Ultrasonic Test Standards for Aircraft Materials," *WADC* (Wright Air Development Center) *Rept.*, 57-268, Contract AF-33 (616)-3363 (1957).

62. Morgan, J. B. "Some Factors of Importance in Ultrasonic Testing," *Nondestructive Testing*, 12, No. 3 (1954): 13.

63. Cline, C. W., and J. B. Morgan. "Standardization in Ultrasonic Testing," *Nondestructive Testing*, 13, No. 4 (1955): 23.

64. "Metal Engineering Design," *ASME Handbook*. New York: Am. Soc. Mech. Engrs., 1953. P. 241.

65. Metz, Frank A. Jr., and Walther M. A. Andersen. "Improved Ultrasonic Delay Lines," *Electronics*, 22, No. 7 (1949): 96–100.

SECTION 44

ULTRASONIC TRANSDUCERS

CONTENTS

Transducer Materials

PAGE
Ultrasonic tests 1
Transducer types 1
  Piezoelectric phenomena 1
  Modes of vibration 2
    Basic deformations of piezoelectric plates (*f.* 1) 3
  Quartz transducers 2
  Barium titanate transducers 2
  Lithium sulfate transducers 3
  Characteristics of crystalline transducers .. 4
    Characteristics of common piezoelectric materials (*f.* 2) 4

Transducer Construction

Design considerations 4
  Definitions 4
  Electrodes 5
  Backing members 5
  Frontal members 6
  Shear modes 6
  Transmission systems 6
Focused transducers 6
  Usable range 6
  Effect of surface roughness 6
  Metal noise 7
  Design of acoustical lenses 7
  Focal lengths of lenses 7
    Focus effect in metal, demonstrating effect of second lens, created by the part with immersed inspection (*f.* 3) 8
  Resolving power 8
  Lenses for contour correction 9
    Transducer lenses for contour correction (*f.* 4) 9
    Improvement shown by contour-corrected transducer lens (*f.* 5) 10
  Useful thickness range 10
PAGE
  Curved crystals 10
  Advantages of focused transducers 11
Paint-brush transducers 11
  Uniform sensitivity requirements 11
    Amplitude response across 5-Mc., 5-in. paint-brush transducer (*f.* 6) 11
  Design considerations 12

The Near, or Fresnel, Field

Wave front characteristics 12
Central-axis maximum and minimum intensity points 13
    Graphic representation of near field (*f.* 7) 12
  Near-field effects in water 14
    Near-field measurements in water (*f.* 8) 14
    Crystal beam plots (⅝-in. diam., round transducers (*f.* 9) 15
  Near-field effect in metal; with water path 16
    Near-field measurements in aluminum with water path (*f.* 10) 16
    Near-field measurements with immersion test instrument and test blocks (*f.* 11) . 17
  Ultrasonic interpretation under near-field conditions 16
  Fresnel near-field effects with 3/64-in. diam. hole indications 17
    Fresnel zone effects (*f.* 12) 18
Side-lobe phenomena 19

Transducer Factors

Dynamic range 19
Transducer band width 19
  Pulse frequency spectrum 20
    Frequency spectrum of a pulse (*f.* 13) ... 20
  Typical equipment band widths 21
  Pulse system modifications 21
References 21

SECTION 44

ULTRASONIC TRANSDUCERS

Transducer Materials

ULTRASONIC TESTS. The technique of testing metal parts by ultrasonic methods has become a very valuable industrial tool. With ultrasonic inspection it is possible to find flaws in metal parts which cannot be detected by other nondestructive means and also to determine the actual **flaw geometry, size, and position.** The need for quality in various materials is increasing, and new applications are being developed for ultrasonic inspection. Under these conditions the necessity for accurate understanding of the factors influencing flaw indications has attained prime importance.

Some metallic materials and parts (such as certain stainless steels) do not lend themselves to accurate ultrasonic nondestructive testing with existing techniques. Correlation between flaw dimension and flaw indication can be difficult under some circumstances. Errors in flaw evaluation result from many correctible causes. In some cases these errors have resulted in overlooking defects of significant size in critically stressed parts. In other cases material has been needlessly rejected because of **erroneous interpretation** of ultrasonic test indications. The desired reliability of ultrasonic testing can be obtained only through comprehensive studies of the acoustical and electrical problems involved. Various organizations are actively engaged in such evaluation programs, the results of which can be summarized only briefly in this handbook. The objectives of these studies are to evaluate and classify **uncontrolled ultrasonic variables** so that ultrasonic testing methods can be improved and general quality-control standards evolved for industrial use. Thus greater reliability can be achieved by ultrasonic nondestructive testing methods in the future.

TRANSDUCER TYPES. A transducer is any device which transforms energy from one form to another. Ultrasonic transducers transform high-frequency electric energy into high-frequency mechanical energy, and only two types are in common usage in the ultrasonic range. Up to 100,000 c.p.s. (100 kc.) transducers often consist of **magnetostrictive elements.** Above that range they are usually **piezoelectric elements.** However, piezoelectric transducers for the 30- to 100-kc. range may find wider future use.

Magnetostrictive transducers make use of the expansion and contraction of magnetic materials under the influence of varying magnetic fields. Transducers of this type are widely used in **sonar and underwater signaling.**

Piezoelectric Phenomena. Piezoelectric transducers make use of the expansion and contraction of certain crystalline and ceramic materials under the influence of varying electrical fields. This phenomenon is reversible, since a mechanical strain input will create an electrical output signal. The efficiency of conversion differs between transmission and reception. In the field of ultrasonic nondestructive testing, piezoelectric transducers are used almost exclusively. Until recently, **quartz and Rochelle salt crystals** were the only efficient piezoelectric materials available for ultrasonic transducers. Since World War II, several **synthetic crystalline and ceramic materials** have been developed. Some of the more promising materials are lithium sulfate monohydride, ammonium dihydrogen phosphate crystals, barium titanate, potassium zirconium titanate, and lead metaniobate ceramics. Detailed information on piezoelectric phenomena is readily available in the published works of such authors as Cady,[1] Mason,[2] and Hueter and Bolt.[3] A few basic properties of piezoelectric plates presently used in nondestructive testing are described subsequently.

Modes of Vibration. Piezoelectric plates exhibit at least four modes of vibration, based on the plate's material and its orientation with respect to the crystallographic axis. **Basic deformations** or modes of vibration of piezoelectric plates are shown in Fig. 1. Of these deformations, the one most widely used in ultrasonic nondestructive testing is the **thickness-expansion mode** shown in Fig. 1(c). Generally, any plate will exhibit a combination of two or more modes of vibration, although these are usually of greatly different magnitudes.

Quartz Transducers. The three most common piezoelectric materials used in the manufacture of high-frequency ultrasonic transducers are quartz, barium titanate, and lithium sulfate. Of these materials, quartz is the most widely used at present. Some **advantages of quartz** for this application are its: (1) mechanical and electrical stability, (2) insolubility, (3) ability to operate at very high temperatures, and (4) resistance to aging. Some of the **disadvantages of quartz** are: (1) It suffers from mode conversion, i.e., interaction between various modes of vibration (see Fig. 1). When quartz is used as a thickness expander, some energy will also be generated in thickness-shear, face-shear, and transverse expansion modes. In the newer methods of testing, such as stress-wave analysis,[4] **mode conversion** will result in spurious signals following the main pulse. Mode conversion also is the cause of some reverberation noise following the front-surface signal in pulse echo testing. (2) It is the least efficient generator of **acoustic energy** of any of the common crystalline materials.

Barium Titanate Transducers. Barium titanate ceramic plates are insoluble, chemically inert, and are not affected by temperatures up to 100° C. Barium titanate is one of the most efficient of all the ultrasonic generator crystals. It is widely used in applications such as ultrasonic cleaning, where large amounts of acoustic power are required. Barium titanate has a **tendency to age** during the first few months of operation, although recent developments of this ceramic have modified this characteristic. It suffers from **mode conversion** in an even more serious manner than quartz, for during compression of the crystal a marked sidewise expansion takes place in all transverse directions. Barium titanate transducers will therefore usually ring simultaneously at two different frequencies, thus adding an enormous amount of interference to the pulse echo signal. Barium titanate also has a very high **mechanical impedance** and does not couple its mechanical energy to water as well as quartz or lithium sulfate. In addition it is a very poor receiver of ultrasonic waves. When a given stress is applied across the crystal, a lower voltage is produced than with lithium sulfate or quartz crystals. The high **dielectric constant** of barium titanate results in a transducer of large internal capacitance which requires a low-impedance driver not normally used in commercial ultrasonic test instruments in the United States. This transducer material has found extensive use in England and in Europe. (See section

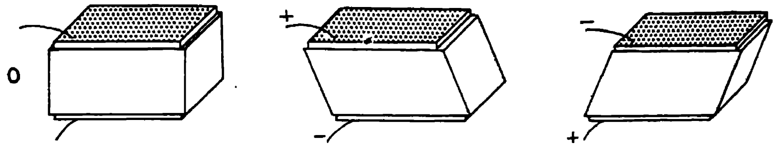

(A) THICKNESS SHEAR

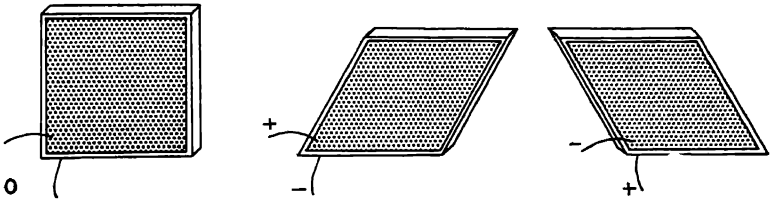

(B) FACE SHEAR

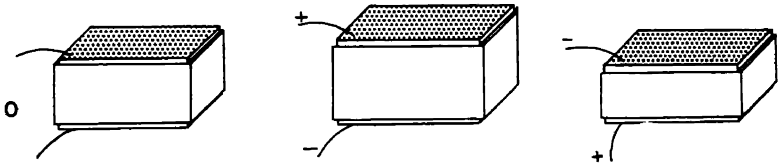

(C) THICKNESS EXPANSION

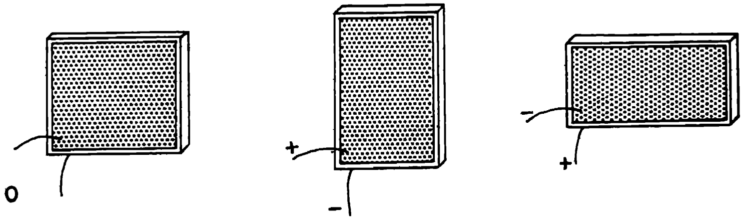

(D) TRANSVERSE EXPANSION

Fig. 1. Basic deformations of piezoelectric plates.

on Double-Transducer Ultrasonic Tests.) The high transducer capacitance restricts the use of barium titanate to frequencies below about 10 Mc.

Lithium Sulfate Transducers. Lithium sulfate monohydride crystals are intermediate between barium titanate and quartz in efficiency as sound transmitters. However, lithium sulfate is among the most efficient of all known receivers of ultrasonic energy. As compared with quartz crystals, the over-all voltage performance ratio (transmit and receive) is approximately 28 times greater than that of quartz. The electrical impedance of lithium sulfate is only slightly lower than that of quartz, making it easy to drive with standard ultrasonic instruments. Its mechanical impedance is lower than that of either quartz or barium titanate, which allows a better acoustic-energy transmission between the crystal and water. Little or no **aging** has been experienced with lithium sulfate, and it has one of the lowest **mode conversions** of any of the standard piezoelectric materials. Lithium sulfate is highly **soluble in water** and must be completely protected at all times by some type of plastic or metallic case. Since this crystal decomposes at 110° C., operation at high temperatures is impossible.

Characteristics of Crystalline Transducers. Fig. 2 lists some of the more important properties of the three crystals. In comparing the properties listed in Fig. 2, it can be seen that barium titanate is an efficient transmitter but requires a **low-impedance driver** because of its high dielectric constant. Quartz is the most rugged transducer element and operates at extremely high temperatures. Lithium sulfate is an efficient transducer for **echo-ranging applications** but is fragile and soluble in water.

Characteristic	Lithium Sulfate	Quartz	Barium Titanate Ceramic B
Crystallographic cut	0°, Y	0°, X	
Basic plate action	TE	TE	TE
Dielectric constant	10.3	4.5	1200
Density, gram/cm.^{3}	2.055	2.65	5.50
Acoustic impedance, gram/cm.^{2}-sec. $\times 10^{-5}$	11.2	15.2	31.5
Frequency constant, (Mc.) (mm.)	2.730	2.870	2.840
Electromechanical coefficient of coupling, meter/volt $\times 10^{-12}$	16	2.0	140
Mechano-electrical coefficient of coupling, volt-meters/newton $\times 10^{-3}$	175	50.0	13.0
Maximum safe operating temperatures in deg. C.	75	550	100

Fig. 2. Characteristics of common piezoelectric materials.

Transducer Construction

DESIGN CONSIDERATIONS. The design of a transducer for application in ultrasonic nondestructive testing requires a compromise among several conflicting factors and varies with each application. The basic considerations in design are: (1) selection of a piezoelectric element (discussed under Transducer Types in this section); (2) electrode type and configuration; (3) backing material and its characteristics; and (4) frontal member, such as a lens if required.

Definitions. Five terms are needed for the description of transducer operation. They are: Q, band width, sensitivity, acoustical impedance, and resolving power.

Q and band width are defined by

$$Q = \frac{f_o}{f_2 - f_1} \tag{1}$$

where f_o = central frequency of the element.

f_1 = frequency below f_c at which the amplitude of sound falls to 0.7 of the amplitude at f_o.

f_2 = frequency above f_c at which the amplitude of sound falls to 0.7 of the amplitude at f_o.

$f_2 - f_1$ = band width of the transducer.

Unmounted transducer elements can have Q's exceeding 20,000. Transducers for use in ultrasonic nondestructive testing usually have Q's in the range of one to ten.

Sensitivity is the ability of transducers to detect echoes from small defects. It is proportional to the product of the efficiencies of the transducer (1) as a transmitter and (2) as a receiver.

Acoustic impedance is the product of the density of the element and the velocity of sound within the element (assuming a loss-free element, which is approximately true in most cases).

Resolving power is the ability of transducers to separate the echoes from two targets which are close together in depth. An example would be the front-surface echo and the signal from a small discontinuity located just under the surface. The **limit of transducer resolving power** is the time required for it to stop vibrating or "ringing" after having been excited by a large voltage pulse. The higher the Q of the transducer, the longer it will ring. Long bursts of sound energy from a transducer which rings will cause a wide front-surface echo. The amplitude of the front-surface echo is many times greater than the desired echo from a small discontinuity and will mask the discontinuity echo. Therefore it is desirable to reduce the Q of a transducer for use in ultrasonic nondestructive testing applications.

The **product of sensitivity and band width** will remain roughly a constant, so that as band width of a transducer is increased, its sensitivity will decrease, or vice versa.

Electrodes. The purpose of using electrodes is to provide a means for applying a voltage gradient across the crystal element. This **voltage gradient** usually takes the form of a large (100- to 2000-volt) pulse lasting for less than 10 μsec. This voltage gradient causes acoustic energy to be developed in the crystal. The voltage gradient can be as high as 200,000 volts per inch, so that **adequate insulation** must be provided. Gold and silver electrodes are usually vapor-deposited on quartz plates. Barium titanate ceramic plates have **vapor-deposited electrodes** or fired-on, conducting-paint electrodes. Electrodes are difficult to deposit upon lithium sulfate, so that they are often made of **thin metallic foils** cemented to the crystals. In most applications, the front and rear electrodes are identical; in special cases, however, shaped electrodes are used, or the front electrode is eliminated for contact testing, for the part serves as the electrode. (See section on Ultrasonic Test Principles.)

Backing Members. The backing member supporting the crystal has a great influence upon the performance of the transducer. Variations in the construction or material of the backing member can make a transducer ideal for one application and useless for another.

The **impedance of the backing member** is a factor controlling transducer band width. The backing member places a load on the piezoelectric element and damps the ringing. The maximum damping occurs when the impedance of the backing member is equal to the impedance of the element.

To satisfy the sensitivity requirements of commercial instruments, quartz transducers have a **mismatch** of about 5 to 1 between the crystal and its backing member. This results in a Q of about 6. Lithium sulfate transducers, because of their higher sensitivity, have a mismatch of about 1.1 to 1 and a Q very close to 1. The two transducers are comparable in most properties, but lithium sulfate transducers have better resolving power and sensitivity.

Another important property which the backing member must have is the **ability to attenuate sonic energy.** Sound energy is transmitted from the piezoelectric element in both forward and backward directions. Energy transmitted in the backward direction must be attenuated and prevented from returning to the element as unwanted signals. For this reason backing members for pulse echo transducers are often made of **fibrous plastics** or **metal powders** combined with various plastic materials. Attenuation can be controlled by the grain size of the powder and impedance by the proportions of metal powder and plastic.

Frontal Members. A frontal member can be added to the transducer to protect the piezoelectric element from environmental conditions or to act as a lens to shape the sound beam. Frontal members should absorb little sound, and their **impedances** usually are intermediate between that of the element and the material with which the transducer is in contact.

Shear Modes. Contact or immersion inspection techniques require the same transducer construction. This also applies to shear-mode or longitudinal-mode transducers. Shear-mode energy is usually developed from piezoelectric elements operating in the longitudinal mode, by producing an **angular incidence** of the sonic energy upon the face of the test part. This produces a partial or total conversion of the longitudinal wave into a shear wave.

Transmission Systems. Systems using separate transmitting and receiving transducers are not widely used in ultrasonic nondestructive testing in the United States because of the difficulty in aligning the transducers. **Two-transducer systems** are frequently employed in Europe and Great Britain (see section on Double-Transducer Ultrasonic Tests). When such a system can be used, barium titanate transmitters and a lithium sulfate receiver will increase the sensitivity of the system several fold, providing the driver is designed to match the low electrical impedance of the barium titanate transducer. This is due to the high electrical-to-mechanical coupling coefficient of barium titanate and the equally high mechanical-to-electrical conversion of lithium sulfate; an over-all voltage gain can sometimes be achieved under special conditions (instead of the usual 1000 to 1 loss experienced with quartz-to-quartz transducers).

FOCUSED TRANSDUCERS. Sound can be focused by lenses in a manner similar to light. **Acoustical lenses** can improve testing reliability and usually are an integral part of the transducer assembly, to reduce and control certain energy losses. In most applications, the lens concentrates the energy into a long, narrow, cigar-shaped beam. This concentration of energy increases **beam intensity.** The use of a focused transducer is much like that of a magnifying glass; in both cases a smaller area is "viewed," but details in this area appear larger.

Usable Range. The most desirable portion of a sound beam starts at the point of maximum sound intensity and extends for a considerable distance beyond this maximum point. Focusing the sound beam moves the maximum-intensity point toward the transducer and shortens the usable range beyond. Special **sharp-focused units** have been made with a usable inspection range of less than 0.25 in., but these transducers could resolve a 0.016-in. diam. flat-bottomed hole located 0.05 in. beneath the surface of a steel block. These units are especially useful for the inspection of thin material and the determination of bonding qualities of laminar sandwich-type materials.

Effect of Surface Roughness. The sonic effects of surface roughness and "metal noise" can be reduced by concentrating the energy into a smaller beam.

The **side-lobe energy** produced by a flat transducer is normally reflected away by a smooth surface. When the surface is rough, some of the side-lobe energy returns to the transducer and widens the front-surface pulse, causing loss of resolving power. The use of a focusing lens on a transducer will reduce the side-lobe energy and the sonic effects of surface roughness.

Metal Noise. Metal noise is the random echo reflection from numerous small discontinuities distributed irregularly throughout areas of the part. Some of the **causes** of this condition are: grain boundaries, gas porosity, and segregations. Rolling, forging, and extrusion usually diminish this reflection. The larger the sound-beam area, the greater the number of small discontinuities illuminated by the sound. Several of these echoes returning at the same time can add and cause an ultrasonic flaw-type indication of rejectible amplitude. Focused beams reduce apparent noise in the metal by reducing the volume of metal inspected, while still allowing echoes from true defects to rise above the remaining noise level.

Design of Acoustical Lenses. Acoustical lenses are designed in a manner similar to that used for light lenses. The **index of refraction** is the ratio of the velocity of sound in the first medium to the velocity of sound in the second medium. A plane-convex lens has a **focal length** of

$$f = r\left(\frac{n}{n-1}\right) \tag{2}$$

where r = radius of curvature of lens.
f = focal length of lens.
n = index of refraction = the ratio of the velocities of sound in the lens to those in water or other acoustic media.

Lenses for immersed ultrasonic inspection generally use water as a couplant between transducer and part. Lenses can be made of many **materials,** such as Lucite, polystyrene, epoxy resins, aluminum, or magnesium. The important **properties of acoustical lens materials** for immersion inspection are:

1. A large index of refraction in water.
2. An impedance close to that of water or the crystal.
3. Very little attenuation of sound.
4. Ease of fabrication.

The lens should be as thin as possible, to reduce internal reverberation of sound energy.

Focal Lengths of Lenses. The focal length of a lens in water has very little relationship to its **focal depth in metal,** and moving the transducer back and forth in water produces very little change in the focal depth in a metal (usually less than one-quarter of the water change). The reasons for this phenomenon are shown in Fig. 3. It is due to large **velocity differentials** between water and metal. The velocity differential or **refractive index** causes sound to bend at a sharp angle when entering the part at any abnormal angle. Thus the metal surface forms a second sound lens which is much more powerful than the acoustical lens on the transducer. This effect pulls the focal spot very close to the metal surface, as compared to the focal length of a transducer in water. This second lens also makes the transducer act as a very directional and distance-sensitive receiver, sharpens the beam, and increases sensitivity for objects in the focal zone. **Large increases in sensitivity** are produced by these complex actions. This makes it possible to locate minute discontinuities and to study areas which produce very low-amplitude echoes, such as the bond juncture between stainless steel and electro-formed copper.

Resolving Power. Focused transducers also allow the highest possible resolving power to be achieved with standard ultrasonic equipment: i.e., 3/64-in. flaws can be seen which lie only 0.050 in. beneath the metal surface. This is because the front surface of the metal part is not in the focal zone, while the concentration of transmission and reception energy makes the echo amplitude from the 3/64-in. diam. test hole very large. This is the best simple way of changing the enormous (10,000:1) amplitude relationship between the front-surface echo and a flaw echo, using standard immersion equipment. This improvement in resolving power may be achieved to a lesser degree, without decreasing the horizontal width of the beam, by using a cylindrical lens. With this construction, a beam 3 in. wide can provide clear resolution of discontinuities from about 0.075 in. below the surface to a depth of ½ in. Such a transducer, at 10 Mc. and with standard ultrasonic equipment, has been produced for inspection of thin airframe aluminum extrusions.

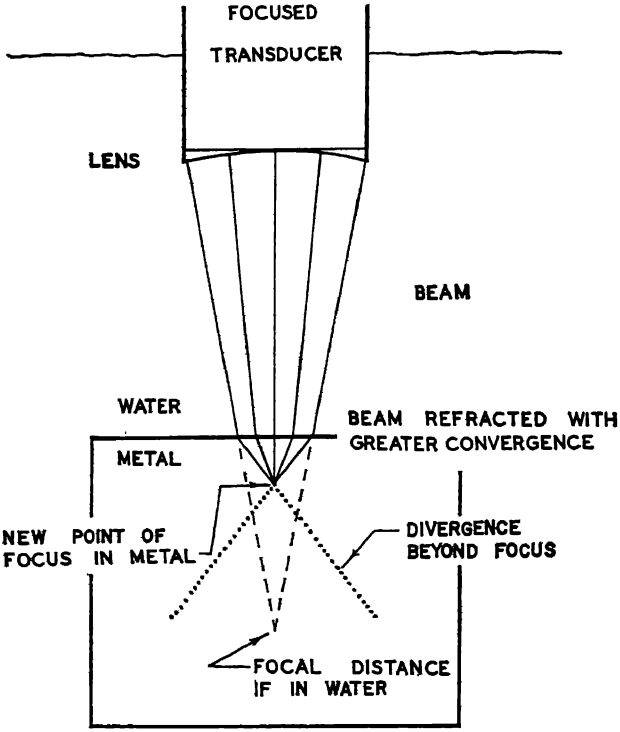
FOCUSED
TRANSDUCER
LENS
BEAM
WATER
METAL
BEAM REFRACTED WITH GREATER CONVERGENCE
NEW POINT OF FOCUS IN METAL
DIVERGENCE BEYOND FOCUS
FOCAL DISTANCE IF IN WATER

Automation Instruments, Inc.

Fig. 3. Focus effect in metal, demonstrating effect of second lens, created by the part with immersed inspection.

Computation and construction of focused ultrasonic transducers is complex, as is the basis for the theoretical and experimental results. Some of the basic mathematical theory has been developed by O'Neil.[5] Since focused units are usually designed for a particular application, it is far better to explain in detail the intended application to the manufacturer and rely on his recommendations, rather than try to specify a given focal length or other test parameters.

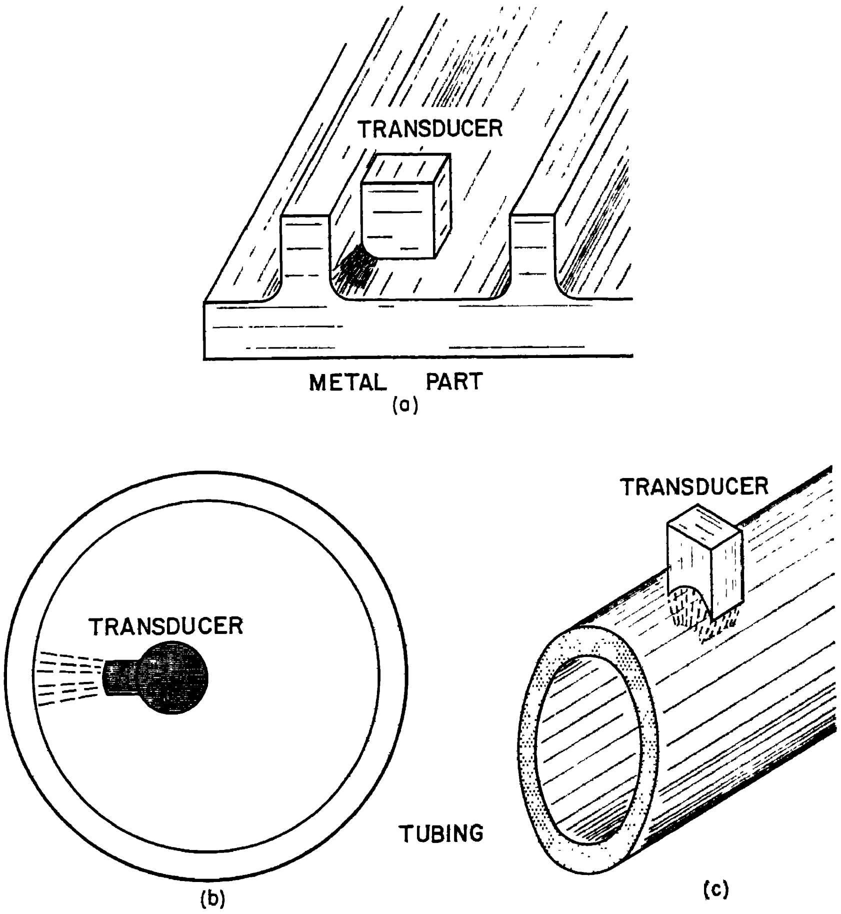

Automation Instruments, Inc.

Fig. 4. Transducer lenses for contour correction. (a) Transducer for inspecting radius of reinforcing member in a wing spar. (b) Transducer for inspecting cylinder from the inside. (c) Transducer for inspecting cylinder from the outside.

Lenses for Contour Correction. Acoustical lenses of many shapes are used for contour correction. Fig. 4 shows three types of lenses used for this purpose.

The three transducers shown in Fig. 4 are designed on the premise that sound must enter the part normal to the surface. Fig. 5 compares flat- and contoured-lens transducers applied to tubing inspection. The **wide front-surface echo,** caused by the changing water-path length across the width of the sound beam from the flat transducer, is completely eliminated by the cylindrically focused transducer. The resolving power of the system has been greatly improved by using a transducer designed to fit the application.

Useful Thickness Range. Focused transducers can be used to inspect material from 0.010 to 2 in. thick. In thinner materials, **resonance** or **anti-resonance techniques** are usually employed. These are based on changes in the duration of ringing of the echo or multiples of the back-surface echo. Beyond about 2 in. of metal, focusing offers little improvement.

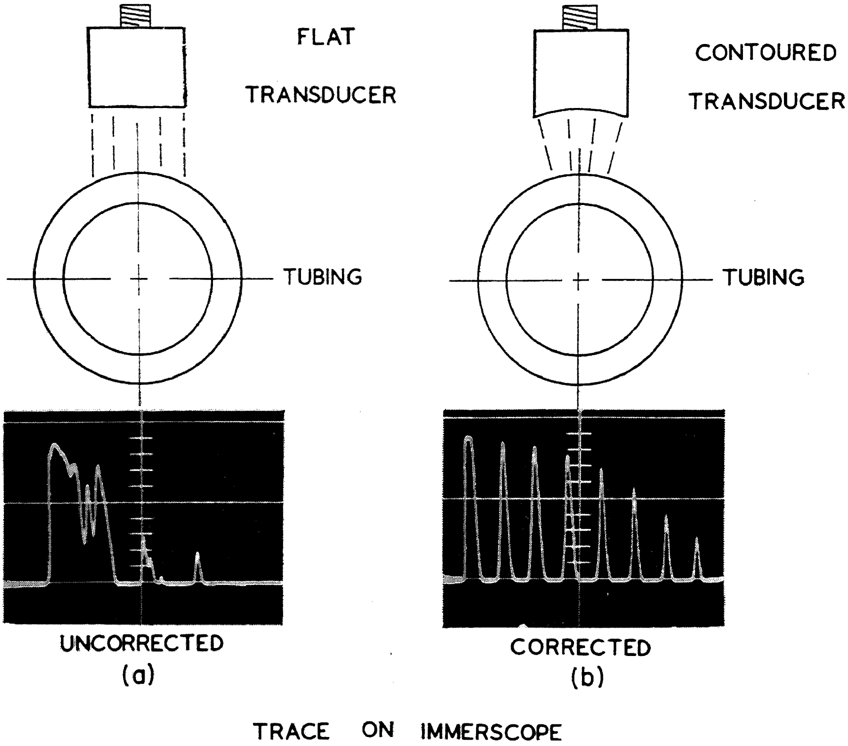

Automation Instruments, Inc.

Fig. 5. Improvement shown by contour-corrected transducer lens. (a) The confused front-surface echo caused by varying water path between transducer and part. (b) The elimination of this confusion, resulting from the use of a correctly contoured transducer.

Curved Crystals. A concentration or focusing of acoustic energy can be achieved by other methods. Quartz crystals are ground to cylindrical or spherical shapes for special purposes. Barium titanate can be formed into curved shapes before it is polarized. Small piezoelectric elements can be mounted on a curved backing member to achieve the same result. Focusing of this type is usually used for concentrating large amounts of energy for agitation of liquids or ultrasonic cleaning. Other methods of focusing are known.

Advantages of Focused Transducers. The advantages of using focused transducers in nondestructive testing are:

1. Increased sensitivity to small discontinuities.
2. Increased resolving power.
3. Reduction in effects of surface roughness.
4. Reduction in effects of contour.
5. Reduction of metal noise.

PAINT-BRUSH TRANSDUCERS. Large plate inspection with $\frac{3}{4}$-in. diam. transducers is a long and tedious process. To facilitate rapid inspection of such large plates, it is necessary to use transducers having a beam pattern capable of sweeping a wide swath, in the manner of a paint brush. Paint-brush transducers are usually constructed of a mosaic or series of matched crystal elements because long, thin crystal elements are not commercially available.

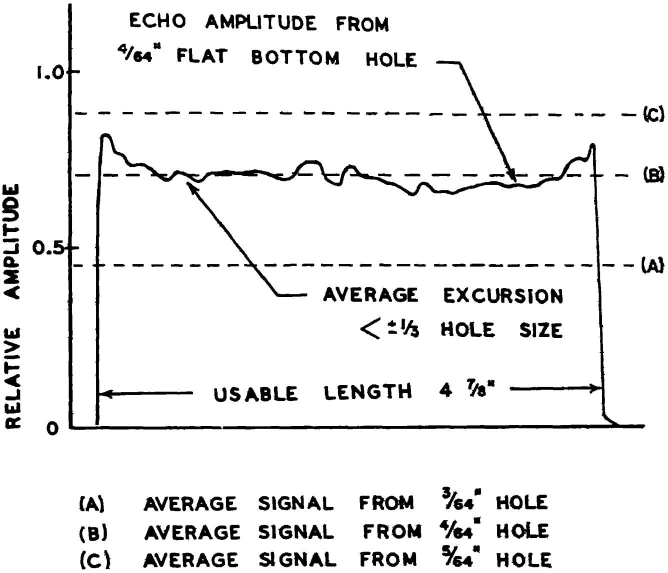

Automation Instruments, Inc.

Fig. 6. Amplitude response across 5-Mc., 5-in. paint-brush transducer.

Uniform Sensitivity Requirements. The primary requirement of a paint-brush transducer is that the intensity of the beam pattern not vary greatly over the entire length of the transducer. Many parameters can be specified, however. One of the most reproducible is based on the Alcoa series of standard ultrasonic test blocks, in which a variation greater than one hole size across the entire face of the brush is excessive. Fig. 6 shows the amplitude variation across the face of a 5-in. lithium sulfate, 5-Mc. transducer. *A* is the amplitude of a $\frac{3}{64}$-in. defect, *B* the amplitude of a $\frac{4}{64}$-in. defect, *C* the amplitude of a $\frac{5}{64}$-in. defect. In the past the control of this amplitude variation has been very difficult because of amplitude variations produced by **Fresnel, or near-field, zone effects.** Recently, methods of suppressing these effects have been developed so that the desired amplitude can be maintained over the transducer length.

At best, the paint-brush transducer is designed to be a gross inspection device. Its primary function is to reduce inspection time and still to give full area inspection. **Standard transducers** are usually employed in conjunction with the paint-brush type to pinpoint the location and size of a discontinuity after its discovery by the paint brush.

Design Considerations. In the design of a **paint-brush transducer,** the frequency, width, and length of transducer, the surface roughness and surface contour of the part, and the internal metal noise are all important factors to be considered. The frequency should be chosen to provide optimum inspection of parts, and the transducer should not be less than four wavelengths wide. The length of the transducer should be chosen with consideration of surface roughness, contour of the part, and internal metal noise. The use of a **cylindrical lens** will also depend upon the foregoing conditions. For the inspection of aluminum plate, it appears that 5 in. is about the limiting length for paint-brush transducers. At more than this length, metal noise becomes great enough to mask important information. However, this length can probably be increased for 2- and 5-Mc. operation if the width is optimized or a cylindrical lens is used.

The Near, or Fresnel, Field

WAVE FRONT CHARACTERISTICS. The effects of the **near field** part of a sound beam are often neglected or misunderstood. However, sound fields generally can be analyzed by methods used in the analysis of light beams, especially by **Huygens' principle.** This states that energy is radiated from a point source in all directions. The wave front is spherical in shape, and its **intensity** or **energy per unit area** decreases as the square of the distance from the source. If two point sources of sound energy are placed next to each other, the wave front will be

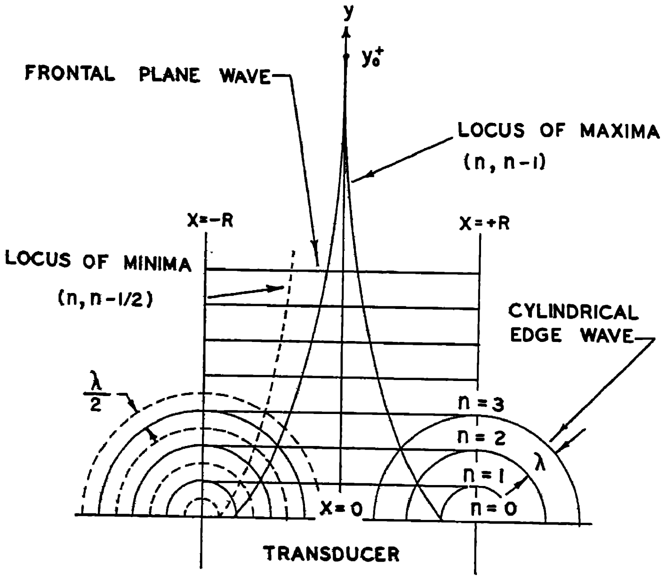

Fig. 7. Graphic representation of near field.

a combination of the two spherical wave fronts, and the combined wave front will no longer be spherical.

CENTRAL-AXIS MAXIMUM AND MINIMUM INTENSITY POINTS. A plane-piston radiator can be considered a large group of point sources close to each other. Fig. 7 shows a graphic construction of the **sound field** directly in front of a plane-piston radiator. The parallel lines represent the combination of Huygens' wavelets into a plane-wave front across the face of the piston. The circular lines represent the wavelets from the edges of the piston. Solid lines represent pressure maxima, and dashed lines, the pressure minima. The points where two maxima intersect are points of high intensity, and where maxima and minima intersect, low-intensity points occur.

If the piston radiator is approached from infinity with a point detector along the central axis of the radiator, the signal will gradually increase up to the point where the plane wave is intersected by the cylindrical waves from the edges. This will be the point of **first central-axis maximum.** This is the intersection of the pressure maximum from the edges of the piston and the maximum from the center which started 1 cycle later. The next central-axis maximum is caused by the intersection of the maximum from the edges and the maximum from the center, which started 2 cycles later. When the driver is an idealized plane piston, the position of these **points of maxima and minima on the central axis** can be predicted. If:

$Y+$ = a maximum,
$Y-$ = a minimum,
$Y+_0$ = the first maximum when approached from infinity,
$Y+_1$ = the second maximum when approached from infinity,
$Y-_1$ = the first minimum when approached from infinity,
$Y-_2$ = the second minimum when approached from infinity,
$Y+_n$ = the nth maximum when approached from infinity,
$Y-_n$ = the nth minimum when approached from infinity,
D = the distance across a piston,
R = the radius of a circular piston,
γ = the wavelength of sound in the medium in front of the piston,
m = a maximum point, and
n = a minimum or null point,

then for a square piston the **central-axis maxima** are located at distances $Y+_m$ from the piston, given by

$$Y+_m = \frac{D^2 - (2m\lambda)^2}{8m\lambda} \qquad (m = 0, 1, 2, \cdots) \tag{3}$$

The **central-axis minima** are located at distances $Y-_n$ from the piston, given by

$$Y-_n = \frac{D^2 - (n\lambda)^2}{4n\lambda} \qquad (n = 1, 2, 3, \cdots) \tag{4}$$

For a circular piston, the equations are

$$Y+_m = \frac{4R^2 - \lambda^2(2m+1)^2}{4\lambda(2m+1)} \qquad (m = 0, 1, 2, \cdots) \tag{5}$$

$$Y-_n = \frac{R^2 - \lambda^2 n^2}{2n\lambda} \qquad (n = 1, 2, 3, \cdots) \tag{6}$$

where R is the radius of the piston.

If the piston is driven with a **continuous wave,** the maxima are all equal, and the minima are all zero on the central axis. In the **pulse system** the output wave is a damped sinusoid; each succeeding maximum after $Y +_0$ will decrease, and each succeeding minimum after $Y-_1$ will increase. If the point detector is moved parallel to the piston through the central axis of the piston at $Y+_0$, the signal amplitude will increase, go through a maximum, and then decrease. If this is done at $Y-_1$, the signal will go through two maxima with a minimum on the central axis. At $Y+_1$ there will be three peaks; and at $Y-_2$, four peaks. Although the transducers used in ultrasonic nondestructive testing only approximate the action of a plane-piston radiator, the results of these calculations are close enough to be usable.

Near-Field Effects in Water. Crystal beam plots have been made, using quartz transducers, in an attempt to evaluate the near-field phenomena. Fig. 8 lists results calculated by Eqs. (3) and (4), with water as the medium, for several popular transducer sizes. The Y distances are in water. Particular attention has been called to the points $Y+_0$ (first maximum), and $Y-_1$ (first minimum) because these are points which determine the extent of the near field. The entire region between the transducer and some place between these two points is a **zone of confusion.** The characteristics of an echo from a reflector in this region are very difficult to compute. Fig. 9(a) illustrates the results obtained with a 5-Mc., ⅝-in. diam. quartz transducer and a small reflector in water. **Beam plots** were made every inch from the transducer up to 12 in. Point $Y+_0$ appears to be between 8 and 9 in., and $Y-_1$ between 4 and 5 in. These values correspond with those shown in Fig. 8. Note that the amplitudes of the peaks decrease as the target approaches the transducer. This is the result of the exponentially decaying sound wave from the transducer under pulse operation.

Frequency (Mc.)	⅜-in. diam.		¾-in. diam.		⅝-in. diam.	
	$Y-_1$ (in.)	$Y+_0$ (in.)	$Y-_1$ (in.)	$Y+_0$ (in.)	$Y-_1$ (in.)	$Y+_0$ (in.)
2.25	0.68	1.4	2.8	5.5	1.8	3.8
5	1.53	3.1	6.2	12.3	4.2	8.5
10	2.08	6.2	12.3	24.6	8.5	17.1
15	4.6	9.2	18.5	36.9	12.8	25.6
20	7.7	15.2	30.8	61.6	21.3	42.7

Automation Instruments, Inc.

Fig. 8. Near-field measurements in water.

If the **cross-section of the near field** were made very near the transducer, and areas of maximum intensity were painted white and minimum intensity painted black, the result would be very similar to a target. The bull's-eye would be either white or black, with alternate annular rings surrounding it. As this cross-section is moved along the axis away from the transducer, the rings will decrease in number and converge on the axis with the bull's-eye turning alternately black and white until the region of primary intensity is reached. In this region, the bull's-eye will become white and remain white for a longer distance than the previous white zones along the axis. A cross-section beyond this region will show additional diverging rings outside the ever-enlarging bull's-eye, but with a marked decrease in intensity from the previous rings. These are the **side lobes** of the transducer in the far field.

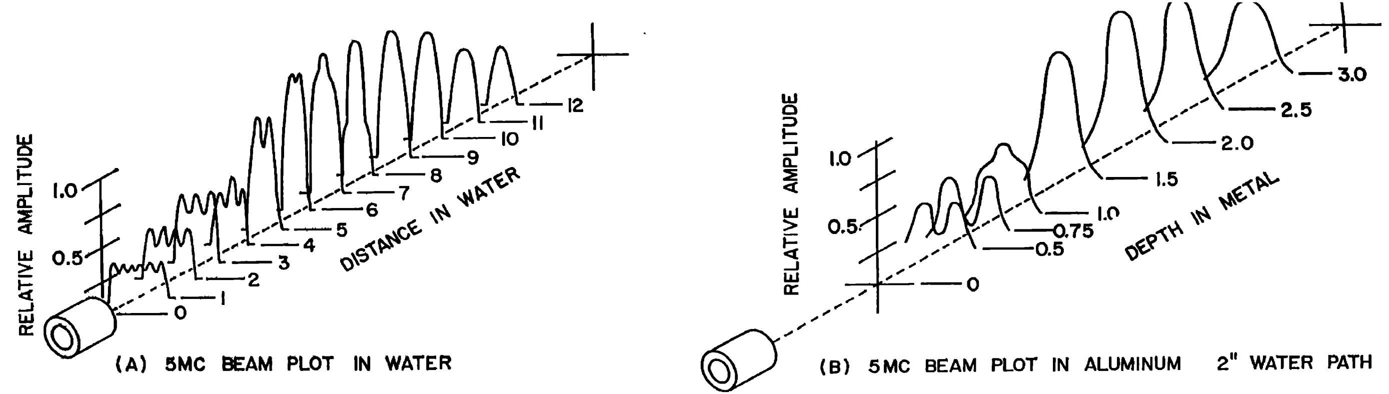

(A) 5MC BEAM PLOT IN WATER

(B) 5MC BEAM PLOT IN ALUMINUM 2" WATER PATH

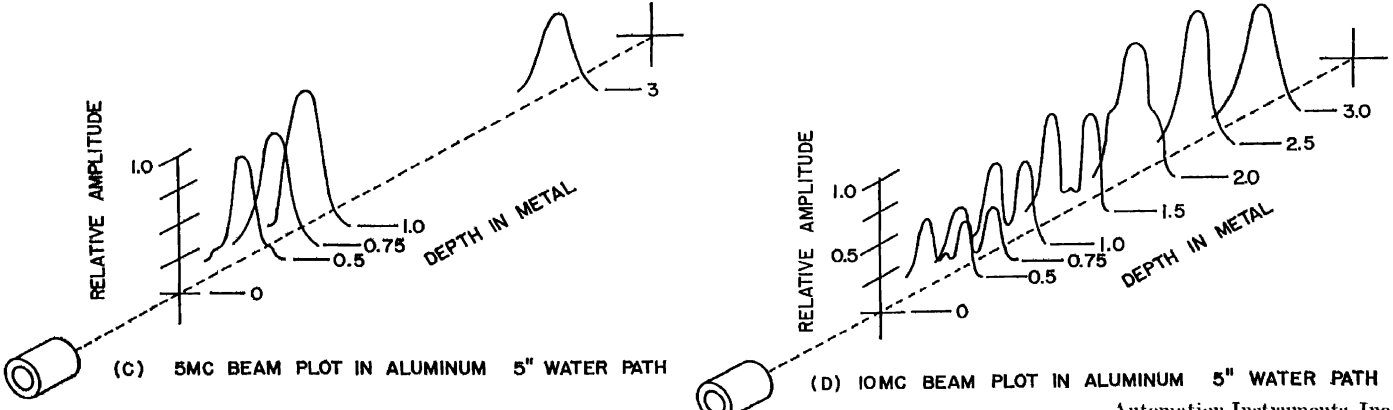

(C) 5MC BEAM PLOT IN ALUMINUM 5" WATER PATH

(D) 10MC BEAM PLOT IN ALUMINUM 5" WATER PATH

Automation Instruments, Inc.

Fig. 9. Crystal beam plots (⅝-in. diam., round transducers). Distances in water and depths in metal are in inches.

The near field comprises **discrete annular rings of energy** which are converging upon the axis at the region of primary intensity. From this standpoint the usual flat transducer can be considered to be a focused radiator with its principal focus situated at the last central-axis maximum. If a material in which the sound velocity increases is placed in the near field (flat surface), the region of primary intensity will move toward the transducer and will shorten in extent. This is caused by the refraction of energy (from the edges of the transducer) which is not normal to the surface of the new material. This pulling in of the "focus" is identical to that shown in Fig. 3.

Near-Field Effect in Metal; with Water Path. Points $Y+_0$ and $Y-_1$ will move closer to the transducer if the medium in front of the transducer is metal. The results in Fig. 10 have been computed by combining the effects of a water-metal path. Figs. 9(b), 9(c), and 9(d) show the results of measurements made at several water-path lengths and with No. 3 Alcoa B blocks.

5-Mc., ⅝-in. Quartz

Water Path (in.)	Aluminum Depth (in.)	
	$Y+_0$	$Y-_1$
1	1.9	0.8
1.5	1.8	0.7
2.0	1.6	0.6
3.0	1.4	0.3
4.0	1.1	0.1
5.0	0.9	0.0*
6.0	0.6	0.0*

* $Y-_1$ prior to aluminum front surfaces.

Automation Instruments, Inc.

Fig. 10. Near-field measurements in aluminum with water path.

There is a very little near field present in the metal with a 5-in. water path, using the 5-Mc., ⅝-in. diam. transducer, and none with a ⅜-in., 5-Mc. crystal at a 3-in. water path. However, the near field extends over 2 in. in the metal, using a 10-Mc. transducer with a 5-in. water path, as shown in Fig. 9(d).

Fig. 11(a) shows the variation in amplitude, produced at various **gain settings** of an immersion ultrasonic test instrument, as a function of hole diameters in the standard Alcoa A series of test blocks. Fig. 11(b) shows **calibration curves** made with ¾-in. diam. quartz transducers at various frequencies on a set of Alcoa B series blocks. The gain setting was comparable to that used in obtaining the second curve in Fig. 11(a) at 5 Mc. These curves are averages for several transducers and are typical for most transducers of this type. The echo amplitude decreases as the hole approaches the front surface of the part. This lack of sensitivity to defects near the front surface of the part must be considered when evaluating flaw indications.

Ultrasonic Interpretation Under Near-Field Conditions. The examination of near-field phenomena illustrates their importance in ultrasonic nondestructive testing interpretations. When comparing test objects to standard test blocks, a single defect can appear to be multiple defects, or the echo amplitude can vary more than a standard hole size from the true defect size if the frequency, water-

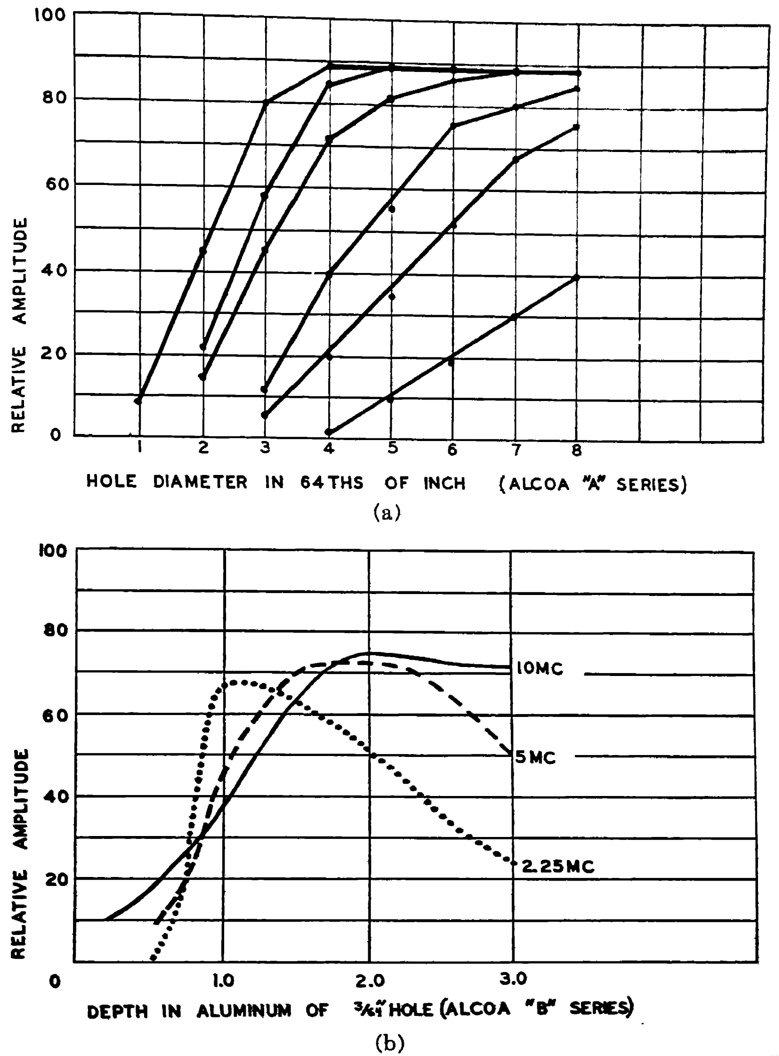

Automation Instruments, Inc.

Fig. 11. Near-field measurements with immersion test instrument and test blocks. (a) Echo amplitude as a function of hole sizes, at different gain settings. (b) Echo amplitude as a function of flaw depth in metal.

path length, and flaw depth are not identical. Since it is not always possible to operate beyond the near field, and since quality-control specifications with complete near-field explanations would be unwieldy, the solution to better ultrasonic inspection lies in **training of the operator.**

Fresnel Near-Field Effects with 3/64-In. Diam. Hole Indications. Fig. 12 serves to illustrate the nature of the problem and its solution. A 1/2-in., 5-Mc. transducer is illustrated in the upper portion of Fig. 12(a). Below the trans-

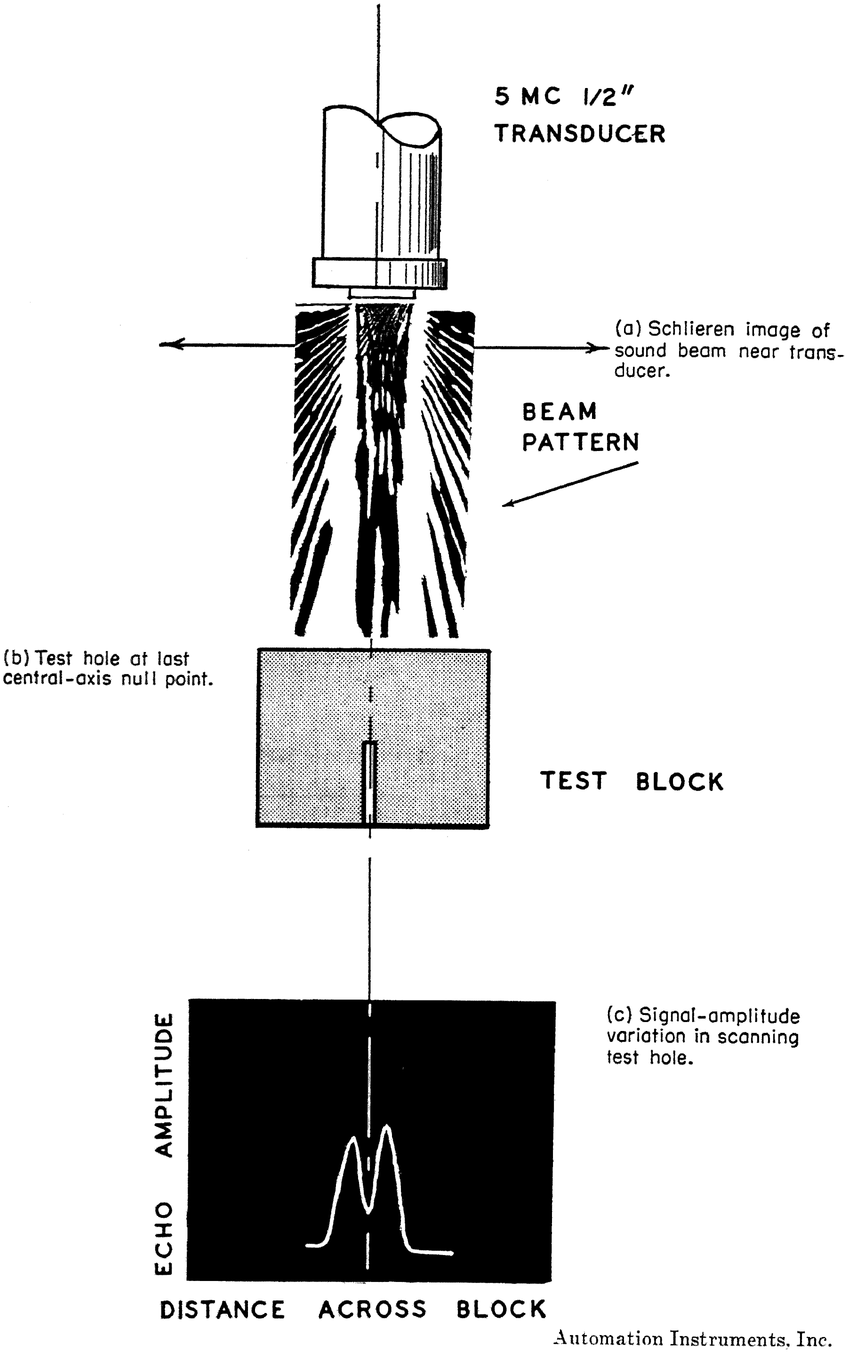
5 MC 1/2″ TRANSDUCER
(a) Schlieren image of sound beam near transducer.
BEAM PATTERN
(b) Test hole at last central-axis null point.
TEST BLOCK
(c) Signal-amplitude variation in scanning test hole.
ECHO AMPLITUDE
DISTANCE ACROSS BLOCK

Automation Instruments, Inc.

Fig. 12. Fresnel zone effects.

ducer is an actual photograph of the near field produced. (Methods for the direct optical visualization of continuous-wave sound systems are well known [6] and are usually modified schlieren-apparatus techniques.) The dark streaks are zones of increased sound intensity. The light areas are sonic minima. It is interesting to note the **side lobes** radiating at angles from the direction of the principal sound beam. Fig. 12(b) is a diagram of a test hole at approximately the position of the last central-axis null (Y_{-1} point). The amplitude variation produced by scanning this 3/64-in. test hole is shown in Fig. 12(c). It is apparent that noncritical operators could easily misinterpret a 3/64-in. flaw at this depth to be two 3/64-in. flaws separated by less than 1 in., and could needlessly reject a part according to some test specifications. If the operator scans across the **equivalent test-block hole,** as well as the part, to establish his position in the near field, such an error could not occur.

If the **inspector** has proper knowledge of near-field phenomena, he can correlate transducer beam patterns with the usual echo amplitude. This simple check, along with proper choice of water and metal paths, can result in accurate, usable information from the near field. Where confusion still exists, a **change of frequency** will usually clarify the interpretation.

New methods of transducer construction now under development show promise of eliminating near-field effects by

1. Shading the crystal electrodes.
2. Shaping the backing member to reduce the sound transmitted from the edge of the transducer.
3. Changing the crystal geometry.

SIDE-LOBE PHENOMENA. The influence of the side lobes of sonic energy has been indicated in previous sections. In Fig. 12 it can easily be seen that if the part has a **rough surface,** these side lobes will be reflected from the part to the transducer later than the main sound pulse from the front surface. This can drag out the front surface indication so that there may be a marked loss in resolving power. The worst type of roughness is a **regular machined finish.** These blinding phenomena from side-lobe reflections can be reduced by placing a gum-rubber **collimating tube** around the crystal to absorb this side energy, or by a random **grinding of the surface** of the test object to reduce any regular stepwise reflector. The effect of surface roughness will be considered more completely in a subsequent section (see section on Ultrasonic Fields). The side lobes are also largely a **crystal-edge effect** and can be reduced by the same methods used to suppress the near-field effects.

Transducer Factors

DYNAMIC RANGE. The ratio of power between the front-surface echo from an aluminum test block and the echo from a 1/64-in. diam. test hole within the block is approximately 80 db. This corresponds to a **voltage ratio** of 10,000:1. If these two echoes could be displayed upon the screen in a linear relationship and if the flaw echo were 6 in. high, then the front-surface echo would be almost a mile high. This is the dynamic range which the equipment, transducers, and instruments must be able to handle in the field of ultrasonic nondestructive testing.

TRANSDUCER BAND WIDTH. The conception of transducer band width is important, and it can readily be shown that a **highly damped crystal** (either of standard quartz construction or of special types) does not radiate a single frequency under pulse operation. Thus the statement "2.25- or 5.0-Mc. testing" means only that the **central frequency of the crystal pulse** is at this frequency. If the crystal is highly damped, as is the case of the lithium sulfate type, a band width of 100 percent or more will exist. Thus a 10.0-Mc. lithium sulfate crystal shows a very active response to frequencies extending above and below the central frequency for approximately 12 Mc. (from 3.5 to 15.5 Mc.). This extreme band width is very necessary if high **resolving power** is to be obtained, and resolving power can be accurately defined only in terms of the band width.

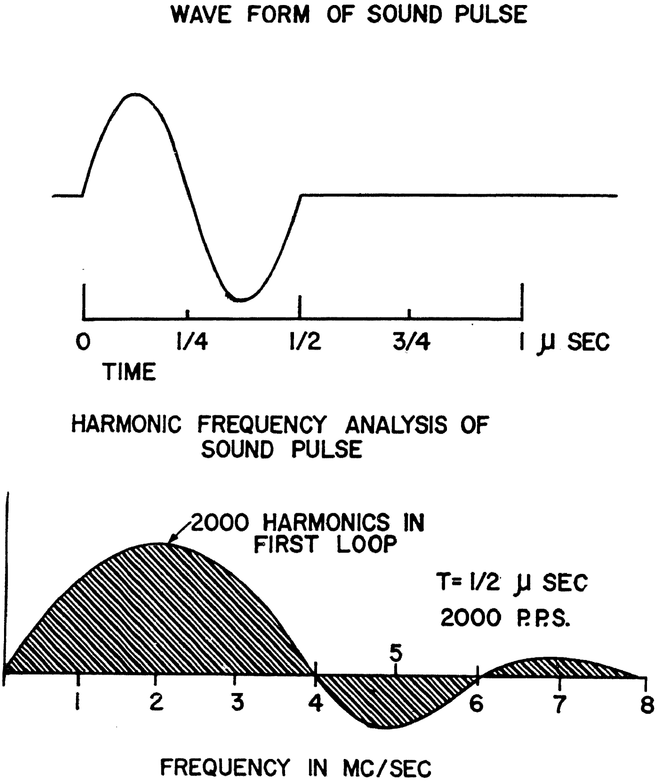
WAVE FORM OF SOUND PULSE

HARMONIC FREQUENCY ANALYSIS OF SOUND PULSE

Fig. 13. Frequency spectrum of a pulse.

Pulse Frequency Spectrum. Fig. 13 is a graph of the frequency spectrum actually required to produce a single cycle of sound. The period length of the pulse is such that it corresponds to the operation of a 2.0-Mc. lithium sulfate transducer. Interestingly, if any portion of the wide pulse spectrum is lost, there will be a comparable **loss in resolving power.** This condition often occurs, due to **acoustical absorption or scattering** which causes a selective loss of the high-frequency components of the spectrum. Under such conditions the sound pulse spreads out, developing a low-frequency ringing "tail" even though only a single-cycle sound wave is transmitted. One interesting feature of such differential absorption is that in any highly absorbing material, resolving power is lost with **depth of inspection.** The inspection is actually being done at a lower frequency deep in the part.

Typical Equipment Band Widths. Current commercial ultrasonic testing systems do not have the extremely wide band width described above. They do have the band-width sensitivity compromise required to reproduce faithfully the pulses generated by existing transducers and to detect very small discontinuities within metal parts. The band width typically obtained is from 3 to 6 Mc. for all center frequencies above 2 Mc. This wide band width and extreme dynamic range demonstrate the excellence of the equipment in use and indicate some of the problems to be overcome in efforts to improve this equipment.

Pulse System Modifications. At least two methods are known which do not depend upon highly damped (low Q) transducers for generating short ultrasonic pulses. They depend upon (1) the **double-pulse generator** and (2) the **phase-demodulation method** described by Howry.[7] Both methods will produce extremely short sonic pulses but are complex and critical in adjustment. The **frequency-modulated system** of ultrasonic flaw detection also offers a potential high resolving power.[8]

References

1. Cady, W. G. *Piezoelectricity.* New York: McGraw-Hill Book Co., Inc., 1946.
2. Mason, W. P. *Piezoelectric Crystals and Their Application to Ultrasonics.* New York: D. Van Nostrand Co., Inc., 1950.
3. Hueter, T. F., and R. H. Bolt. *Sonics.* New York: John Wiley & Sons, Inc., 1955.
4. Van Valkenburg, H. E. N., and R. A. Wilson. "Ultrasonic Inspection Program," *Interim Eng. Repts. I and II,* U.S. Air Force, Air Materiel Command, Contract No. AF33 (600)-29879:H (1957).
5. O'Neil, H. T. "Theory of Focusing Radiators," *J. Acoust. Soc. Am.,* 21 (1949): 516.
6. Willard, G. W. "Focusing Ultrasonic Radiators," *J. Acoust. Soc. Am.,* 21 (1949): 360.
7. Howry, D. H. "Techniques Used in Ultrasonic Visualization of Soft Tissue Structures of the Body," *IRE Conv. Record,* 1955, No. 9: 75.
8. Erdman, D. C. "Ultrasonic Flaw Detector," U.S. Patent No. 2,593,865 (Apr. 22, 1952).

SECTION 45

ULTRASONIC FIELDS

CONTENTS

PAGE

Transmission, Reflection, and Attenuation

- Significant material properties 1
  - Energy transfer at interfaces 1
- Acoustical impedance effects 1
  - Effects of changes in test material 1
  - Corrections for material differences 2
    - Usable energy returned in immersion testing as a function of impedance ratio (*f.* 1) 2
- Acoustical attenuation 3
  - Attenuation measurements 3
    - Amplitude decrement of multiple back-surface echoes as a function of impedance ratio (*f.* 2) 4
  - Selection of test blocks 5
  - Compensation with sensitivity-time control 5
  - Selection of test frequency 6
  - Contact attenuation measurements 6

Effects of Velocity of Sound

- Significance of sound velocity 6
- Sound-wave mechanisms 6
  - Sound-wave velocity 7
    - Ratio of longitudinal velocity to shear velocity of sound as a function of Poisson's ratio (*f.* 3) 8
  - Sound-velocity measurement techniques ... 7
- Angle of sound refraction and types of sound waves 9
    - Relationship for the sound beam at angular incidence to the metal surface (*f.* 4) 9
  - Calculation of refraction angles 10
  - Refractometer 10
    - Experimental results with sound at angular incidence (*f.* 5) 11
  - Modification of beam shape 10
  - Angulation of sound beams 10
  - Rayleigh, or surface, waves 11
  - Surface flaw detection 12
- Lamb waves 12
  - Characteristics of lamb waves 12
  - Generation of lamb waves 12
  - Lamb wave test systems 13

PAGE

Influence of Part Contour

- Effects of surface curvature 13
  - Near-field distribution 13
  - Blocks for contour study 13
  - Parts with concave surfaces 13
    - Reaction of plane waves with contoured parts (*f.* 6) .... 14 & 15
  - Parts with convex surfaces 14
- Surface roughness effects 15
  - Loss of echo amplitude 16
  - Experimental evidence 16
  - Resolving power 17
  - Corrections for surface roughness 17
  - Equipment for measuring surface roughness 17

Influence of Discontinuity Properties

- Factors influencing discontinuity indications . 18
- Standard ultrasonic test blocks 18
- Beam characteristics of the reflector 18
  - Reflections from small discontinuities 20
    - Radiation patterns (*f.* 7) 19
    - Diameter to wavelength ratio for standard hole sizes in aluminum and stainless steel (*f.* 8) 19
  - Reflected-beam radiation patterns 20
  - Nonmetallic inclusions, gas porosity, and cracks 21
  - Special "short-burst" polarity test method 21
  - Thickness of discontinuity 22

Geometry of Discontinuities

- Angle and surface roughness of discontinuity 22
    - Echo loss from adversely oriented discontinuities (*f.* 9) 23
- Contour of discontinuities 24
  - Techniques for determining geometry of discontinuities 24
  - Measurement of diameter or length of discontinuities 24
- Multiple-frequency inspection 26
    - Multiple-frequency inspection (*f.* 10) 25
- Guide to interpretation 26
- References 27

SECTION 45

ULTRASONIC FIELDS

Transmission, Reflection, and Attenuation

SIGNIFICANT MATERIAL PROPERTIES. To test materials ultrasonically with the highest degree of reliability, it is necessary to know the influence of the common variables of the test material. Those parameters which should be known accurately by the ultrasonic test engineer are:

1. Acoustical impedance of the test material.
2. Acoustical attenuation in the test material.
3. Velocity of sound propagation in the test material and relevant refractive indices.
4. Surface contour of test part.
5. Surface roughness of test part.

One method of evaluating the sonic effect of material properties and geometry is to drill **flat-bottomed test holes** or other suitable targets at graduated depths in one of the test parts and to use it as a standard. When testing production parts with or without such a reference specimen, it is imperative that the operator be familiar with the influence of material variables. Fortunately, the more important of these variables can be accurately measured by the inspector prior to testing. The influence of variables upon the echo amplitude will therefore be described in some detail.

Energy Transfer at Interfaces. When sound passes through a smooth surface and is perpendicular, or normal, to the surface, the principal factors which affect energy transfer and the resultant flaw-indication amplitude are:

1. Acoustical impedance.
2. Acoustical attenuation.
3. The ultrasonic beam distribution.
4. The distance of the transducer from the part inspected.

ACOUSTICAL IMPEDANCE EFFECTS. Specific acoustical impedance is one of the simplest variables to evaluate. It is the product of the **density** and the **velocity of sound** within the material. The **impedance ratio** of the materials establishes the proportion of power transmitted into one material from another material of different impedance. In immersed testing, the second material is usually water. In contact testing, it is the transducer material or an intermediate solid such as Plexiglas, with a suitable couplant.

Effects of Changes in Test Material. When sound travels from one material into another, some of the sound is reflected at the interface. The amount transmitted into the second material is a function of the ratio of the impedance Z_2 of the second material to the impedance of Z_1 of the first material. Impedance ratios of either whole numbers ($Z_2/Z_1 = 10$) or their reciprocal fractions $\left(Z_2/Z_1 = \frac{1}{10}\right)$ yield equivalent mismatch. The sound transmitted through the surface barrier decreases as the **impedance ratio** increases. There is another loss of energy at the surface when the sound again passes out through the interface.

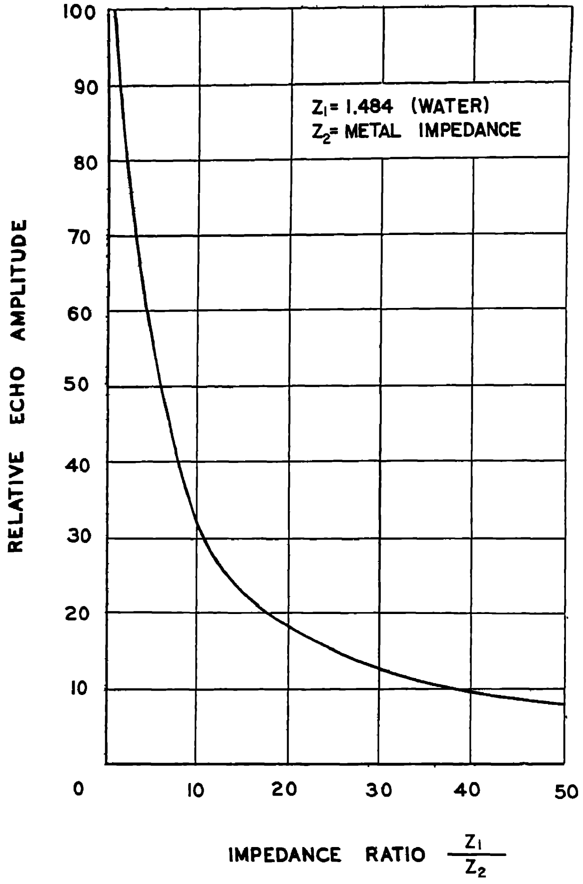

Automation Instruments, Inc.

Fig. 1. Usable energy returned in immersion testing as a function of impedance ratio.

Fig. 1 shows this two-way loss in amplitude as a function of the impedance ratio of a material with respect to water. It applies to the case of a 100 percent reflector within the second material, with no beam dispersion.

Corrections for Material Differences. The impedance ratio with respect to water is about 30 for steel and about 12 for aluminum. The proportion of sound which enters metal from water is about 0.117 (see Fig. 1) of the incident energy for steel and about 0.267 for aluminum. Therefore, if identical test holes are put into two parts, one of aluminum and the other of steel, the amplitude of the echo from the steel part will be about $0.117/0.267 = 0.44$ of the echo amplitude from the aluminum part, if all other acoustical factors are the same.

Test blocks of aluminum can be used for the evaluation of echoes from some other materials with closely similar sound velocities when this **correction for different impedance ratios** is used. However, possible beam spread and wavelength changes must also be considered. The nominal acoustical properties of density, velocity of sound, and impedance for several common materials are given in the table here.

Material	Density (gram/cm.^{3})	Velocity (cm./sec.) × 10^5	Impedance (gram/cm.^{2}-sec.) × 10^5
Stainless steel (303)	7.85	5.37	42.1
Aluminum	2.81	6.36	17.9
Brass	8.40	4.29	36.0
Copper	8.90	4.66	41.5
Water	1.0	1.49	1.49

These nominal values are subject to variation as a result of heat treatment, deformation (hot or cold), oxidation or other chemical changes, and other processes. Some materials are more subject to variability than others, as a result of different degrees of **crystallographic anisotropy.** (Additional data on acoustical properties of materials are given in the section on Ultrasonic Test Principles.)

ACOUSTICAL ATTENUATION. It is simplest to lump all the **losses of acoustical power** (those not due to sound-beam geometry) under the general term of "acoustical attenuation." The actual phenomena involved may be subclassified into numerous headings; for example:

1. Scattering.
2. Diffusion.
3. Viscous-damping losses.
4. Relaxation losses.

Truell,[1] Mason,[2] Grossman,[3] and Worlton [4] are among those who have studied many of these phenomena and have found interesting associations between acoustical losses and material properties such as:

1. Grain size.
2. Yield strength.
3. Crystalline damage.
4. Fatigue damage.
5. Impact strength.
6. Hardness.

Attenuation Measurements. Attenuation measurements can be made by placing a **frequency-compensated attenuator** in the input line to the receiver of the flaw detection equipment. After adjusting the transducer perpendicular to the surface of the test material, an attenuation of about 30 to 40 db. is set into the attenuator. The gain adjustment is set so that some multiple of the rear-surface echo from the part is of 50 percent of an arbitrary maximum amplitude. The attenuation is then reduced until the following multiple is of 50 percent amplitude. The change in attenuation required to bring two adjacent multiples of the rear-surface echo to the same amplitude is the **energy loss between the two multiples.**

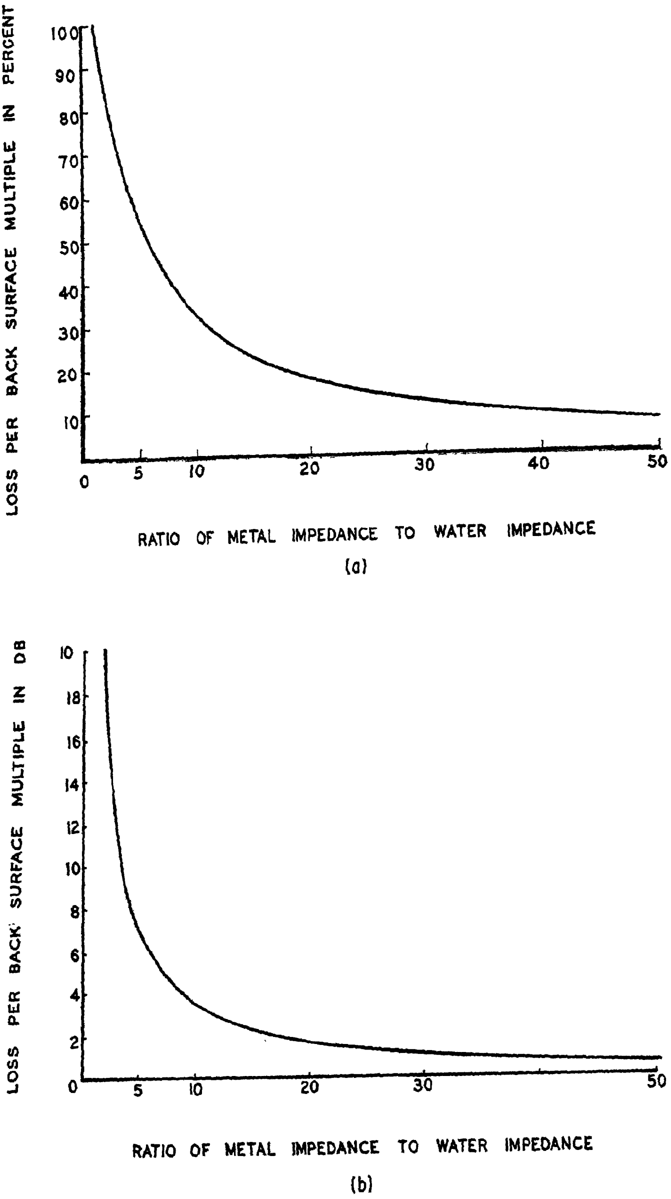

Automation Instruments, Inc.

Fig. 2. Amplitude decrement of multiple back-surface echoes as a function of impedance ratio. (a) Loss in percentage. (b) Loss in decibels.

This loss includes the interface loss and the attenuation loss. Fig. 2 shows the energy loss between adjacent multiples of the rear-surface echo, due to the **water-metal interfaces** when the part is surrounded by water, as a function of the impedance ratio of the part with respect to water. Since this curve is calculated for the front and rear surface transmission-reflection losses only, any measured increase of energy loss must be due to either beam geometry or attenuation.

In one test, a 2 in. thick sample of a stainless steel had a measured energy difference of 6 db. between the second and third multiple echoes of the rear surface. The difference in energy between multiples (from Fig. 2) for stainless steel (whose impedance ratio with respect to water is about 30) should be about 1.2 db. Therefore the energy loss due to attenuation in this sample was 4.8 db. The **round-trip coefficient of attenuation** was 2.4 db. per inch.

Selection of Test Blocks. Attenuation losses can be large, and wide variations can occur from place to place in a part. An ultrasonic inspector can generally detect variations in attenuation within a part which has parallel front and rear surfaces. Variation in the multiple-echo pattern is also an indication that the transducer is no longer normal to the front surface of the part.

For example, two samples of 304 **stainless steel** were compared ultrasonically. One sample was from 2-in. diam. **bar stock** and the other was a section from a **lightly forged part** about ½ in. thick. At a frequency of 10 Mc. several multiples of the back-surface echo from the 2 in. long sample of bar stock were present. Metal noise from within the forging obscured the back-surface echo from the forging.

At a 5-Mc. test frequency, the number of back-surface multiple echoes from the bar stock increased considerably over those observed at 10 Mc. This indicated that attenuation within the sample had decreased as a result of the **reduction in frequency.** With the forging, however, only the rear-surface echo and its first and second multiples were present at 5 Mc., indicating that metal noise and attenuation were reduced by lowering the test frequency. The attenuation remained so high that only very large area discontinuities could be detected at 5 Mc. The rear-surface echo would probably have disappeared with a forging thickness of about 3 in.

Test blocks should generally be similar to the test part in the following respects:

1. Alloy content.
2. Heat treatment.
3. Degree of hot or cold working due to forging, rolling, or extruding.

Each of these variables has an effect upon the attenuation of sound within a part. However, practical experience indicates that wrought aluminum alloys can be compared with a single set of aluminum test blocks with adequate accuracy. Test blocks made from **extruded bar stock** can lead to large errors in the evaluation of the defect area when echoes from holes in these blocks are compared with those from a **cast part.** In the case of many alloys, large variations in attenuation for a given heat treatment can be caused by variations in composition, within the commercially acceptable limits for chemical analysis.

Compensation with Sensitivity-Time Control. The sensitivity-time control (STC) or the time-varied gain (TVG) adjustments provided with many flaw detection instruments can be very helpful to the inspector when parts exhibit attenuation. These controls permit the sensitivity of the instrument to be adjusted so that it increases with **metal depth.** When the sensitivity increase due to the control is adjusted so that it just matches the loss due to attenuation, discontinuities of equal area but at different depths within the metal will return echoes of approximately equal amplitude.

There are two **methods for adjustment** of the sensitivity-time control. The first method utilizes a set of step-type test blocks made from material as nearly identical to the part as possible. The sensitivity-time control is adjusted so that **echoes from various depths** within the test blocks have equal amplitudes. The second method is to adjust the sensitivity-time control so that multiple echoes from the back surface of the part decrease in accordance with the theoretical curve of Fig. 2.

Selection of Test Frequency. Ultrasonic attenuation losses usually increase with increasing frequency, in most of the materials tested ultrasonically. With some materials this increase is gradual, while with some other materials, the increase is rapid. Attenuation losses can usually be reduced by lowering the test frequency.

Scattering of sound, frequently indicated by numerous echoes from small, randomly oriented discontinuities within the part, can cause large attenuation to sound. These discontinuities are usually caused by gas porosity, grain boundaries, subgrain structure, and similar **structural discontinuities.** Several discontinuities at very nearly the same depth in the part can return echoes which will add to an echo of considerable amplitude. This effect can be reduced by decreasing the cross-sectional area of the sound beam by collimation or by using small-diameter or focused transducers. The use of the shortest possible pulse also minimizes exaggerated echoes due to phase addition.

Contact Attenuation Measurements. In contact testing, a special crystal transducer should be used to measure the attenuation coefficient. This crystal should not have a damping member and should be "wrung" as carefully as possible onto a polished area of the metal. The front-rear multiple echoes which are outside the near field can then be used to measure attenuation directly, since there is substantially no radiation loss from the surface. The cross-section of the test specimen should considerably exceed the crystal area, since side-wall echoes can affect multiple-echo amplitudes.

Effects of Velocity of Sound

SIGNIFICANCE OF SOUND VELOCITY. Accurate knowledge of the velocity of sound in a part is important. In combination with material density, it

1. Establishes the impedance of the part.
2. Establishes the angle of refraction which the sound will take in the part if the sound beam does not enter normal to the surface.
3. Makes it possible to establish definitely whether a given discontinuity is in a critical area in the part or will be removed during subsequent machining.

SOUND-WAVE MECHANISMS. Sound travels by small elastic displacements of a medium. Many types of waves are possible, and their modes of vibration and analyses are well known. In nondestructive testing, the two most frequently used waves are the longitudinal, or L mode, and the shear, or S mode. **Longitudinal waves** are defined as those simple compression-rarefaction waves in which the particle displacement is in the direction in which the wave is traveling. This is the only significant sound wave that will travel through liquids. In **shear or transverse waves,** the particle displacement is at right angles to the direction of propagation of the wave. These waves are polarized, and a second transducer (used as a receiver on the far side of a part) usually shows a maximum response when it is rotated so that the direction of the sound vibration is identical to the vibrational axis of the transducer (see section on Ultrasonic Transducers). In forged or rolled metal parts with partially oriented crystalline structures, the velocity of shear waves will be slightly different, depending upon whether the direction of particle displacement is parallel or transverse to the **direction of the flow lines.** This difference in velocity can often amount to 3 to 5 percent. It is influenced by the type of preferred orientation, the type and degree of recrystallization, the degree of working a part has experienced, and the direction of its flow lines. The velocity of shear waves is generally considered to be approximately 3.1×10^5 cm. per second in aluminum and 3.2×10^5 cm. per second in steel.

Sound-Wave Velocity. The velocity with which sound travels in a medium depends upon the elastic constants of the medium. The velocity of the **longitudinal sound wave** is

$$(V_L)^2 = \frac{\lambda' + 2\mu}{\rho} = \frac{K_c + \frac{4\mu}{3}}{\rho} \tag{1}$$

where V_L = velocity of propagation of the longitudinal sound wave.
λ' = Lame's constant.
μ = shear modulus.
ρ = density.
K_c = modulus of volume elasticity.
V_T = velocity of propagation of the shear wave.

In solids $K_c = \lambda' + (2\mu/3)$, and in liquids, where $\mu = 0$, $K_c = \lambda'$. The velocity of the **shear wave** is

$$(V_T)^2 = \frac{\mu}{\rho} \tag{2}$$

The **ratio between longitudinal and shear velocities** is

$$\left(\frac{V_L}{V_T}\right)^2 = \frac{2(1-\sigma)}{1+2\sigma} \tag{3}$$

where σ is Poisson's ratio (see Fig. 3).

In the majority of crystalline materials, the elastic constants are a function of the **crystallographic direction.** The velocity of sound within these materials is anisotropic. The acoustical impedance of these materials also varies with the sound velocity. When the crystals are randomly oriented, the measured values of velocity and impedance are average values. They may vary widely from place to place within a part as a result of this random distribution. The random orientation of impedance discontinuities resulting from randomly oriented crystalline structure is probably the cause for much of the **metal noise** associated with many of the steel alloys which have large crystalline structures. By measuring the longitudinal and shear wave velocities, the **elastic constants** of metal can be approximated without special apparatus or special sample preparation.

Sound-Velocity Measurement Techniques. Accurate measurement of L and S velocities is best done by indirect measurement, since oscilloscopes do not have perfectly linear time bases (horizontal sweep). One technique involves placing a known thickness of the metal of unknown sound velocity in distilled water at room temperature. Using **immersion techniques,** the transducer is backed away from the part until a large number of front-rear multiple echoes can be seen ahead of the second water-multiple echo. R.F. presentation and technique may aid precision. Then the distance from the transducer to the metal is carefully ad-

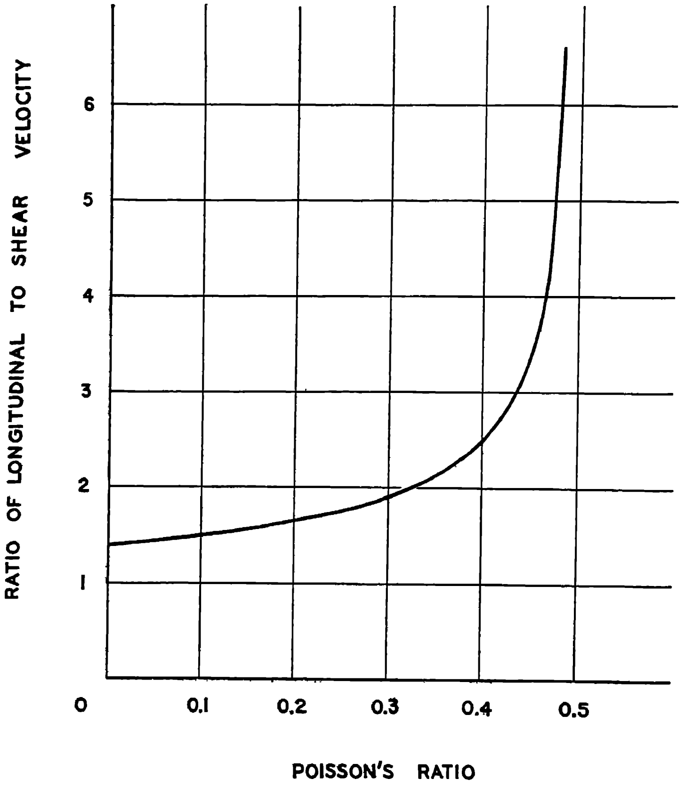

Fig. 3. Ratio of longitudinal velocity to shear velocity of sound as a function of Poisson's ratio.

justed so that the water-multiple coincides exactly with a metal-multiple echo. The distance from the transducer surface to the part is then measured. Now, since the velocity of sound in distilled water is 1.49 × 10^5 cm. per second at room temperature (25° C.), and the water distance, metal thickness, and number of metal-reflection multiples are known, we have

$$V_m = \frac{NBV_w}{A} \tag{4}$$

where V_m = velocity of the wave in metal, cm./sec.
V_w = velocity of L wave in water, cm./sec.
A = thickness of the metal part, cm.
B = water distance from transducer to the metal part, cm.
N = number of rear-surface multiples.

If distilled water is not available, the velocity of any liquid can be computed from the velocity of sound in a 2014F aluminum "Alcoa ultrasonic test block," which has a velocity of 6.36 × 10^5 cm. per second at room temperature. Then the velocity measurement of the unknown is made as before, using the correct velocity for the immersion liquid.

The **shear velocity** can be measured by a similar technique. A two-crystal system is used and includes one immersion L-wave type of crystal and one S-mode crystal. The two crystals are connected in parallel into the instrument. The shear-mode transducer is coupled to the metal part with viscous fluid. The immersion transducer is then aimed at a flat reflector in a liquid of known velocity. Its distance is adjusted and measured as before. Since the signals from both transducers will be seen simultaneously on the oscilloscope, and the position of the water multiple is adjustable, Eq. (4) will now give the shear-wave velocity.

When the wave velocity is known, this technique can also be used to measure the thickness of a part with very high accuracy, or to measure the depth of a flaw in the metal. **Reproducible accuracy** of about $\frac{1}{64}$ in. in several inches has been achieved. The accuracy of this method is essentially dependent only on the purity and temperature of the water and the accuracy of the measurement of the distance from transducer to reflector. It is not dependent upon the linearity of the sweep in the flaw detection equipment.

ANGLE OF SOUND REFRACTION AND TYPES OF SOUND WAVES. When sound travels from a liquid into a solid, the impedance change at the liquid-metal interface results in reflection of a large portion of the incident energy. Only a small portion of the sound is transmitted into the metal. When the incident energy is directed at an angle other than normal to the surface of the metal, the transmitted sound divides into both longitudinal and shear modes (see Fig. 4). Each of these waves travels in a different direction and at differing

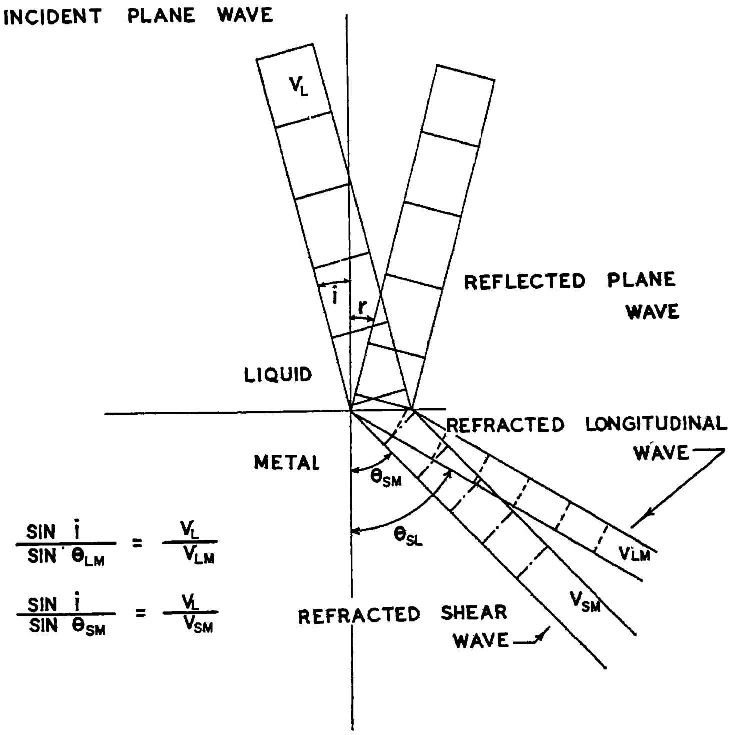
INCIDENT PLANE WAVE
V_L
i
r
REFLECTED PLANE WAVE
LIQUID
METAL
REFRACTED LONGITUDINAL WAVE
θ_{SM}
θ_{SL}
V_{LM}
V_{SM}
REFRACTED SHEAR WAVE
$\frac{\sin i}{\sin \theta_{LM}} = \frac{V_L}{V_{LM}}$
$\frac{\sin i}{\sin \theta_{SM}} = \frac{V_L}{V_{SM}}$

Fig. 4. Relationship for the sound beam at angular incidence to the metal surface

velocities. At an interface between two solids (for example, bonded metals), both reflected and refracted longitudinal and shear waves occur.

Calculation of Refraction Angles. The angle of refraction within the metal can be calculated for both longitudinal and shear waves by **Snell's law,** i.e.,

$$\frac{\sin \phi_i}{\sin \phi_L} = \frac{V_w}{V_{Lm}} \tag{5}$$

and

$$\frac{\sin \phi_i}{\sin \phi_S} = \frac{V_w}{V_{Sm}} \tag{6}$$

where ϕ_i = angle of incidence.
V_w = velocity of sound in water.
ϕ_L = angle of refraction for L waves.
V_{Lm} = longitudinal velocity of sound in metal.
ϕ_S = angle of refraction for S waves.
V_{Sm} = shear velocity of sound in metal.

(See section on Ultrasonic Immersion Tests.)

Refractometer. A semi-circular test block of 17ST aluminum alloy about 2 in. thick, with facets every 10 deg., was used to determine experimentally the relative amplitude of the returning echo as a function of the angle of refraction of *L* and *S* waves generated within the block when sound energy entered the block from a water-coupling path. This device is the **ultrasonic equivalent of the optical refractometer.** The results of this experiment are shown in Fig. 5. Fig. 5(a) shows the angle of incidence experimentally required to obtain a **desired angle of refraction** inside a part, for both the *L* and *S* waves, when sound travels from water into aluminum. [No saturation was observed, despite the "plateau" in the *L*-mode curve in Fig. 5(b).]

Modification of Beam Shape. Sound radiated from a circular crystal propagates with a tendency toward a cylindrically shaped intensity pattern, with some degree of beam spread. However, if this cylinder of energy strikes the part at an angle and is refracted, the cylinder is narrowed in the refracted direction (see Fig. 4). The beam becomes elliptical in cross-section, and the beam geometry and area are completely changed. This, in effect, tends to concentrate the energy of the sound into a narrow, intense beam. The echo indications received from small defects may appear slightly higher than if the beam had been at a normal incident angle. However, reflection losses are greater at an angle and can diminish echo amplitudes; hence they tend to counteract beam-concentration effects.

Angulation of Sound Beams. Very slight angulations of the incident sound beam produce relatively enormous **angles of refraction** in metal. The **critical angle for the *L* wave** is reached at an angulation of 13.5 deg. in aluminum or 14.5 deg. in steel. In this case the *L* mode is now traveling parallel to the surface of the part and is a totally reflected wave, with no *L*-wave energy being refracted into the part.

Fig. 5(b) also indicates that with the *L* mode, discontinuities lying at angles from 0 to 57 deg. should be found in aluminum. To detect discontinuities which lie at still greater angles to the surface of the part (up to 90 deg.), the *S* mode should be used to take advantage of the mode efficiency. The use of the *S* mode at **high refracted angles** may be valuable for the inspection of weldments, radial fatigue cracks, or forging bursts.

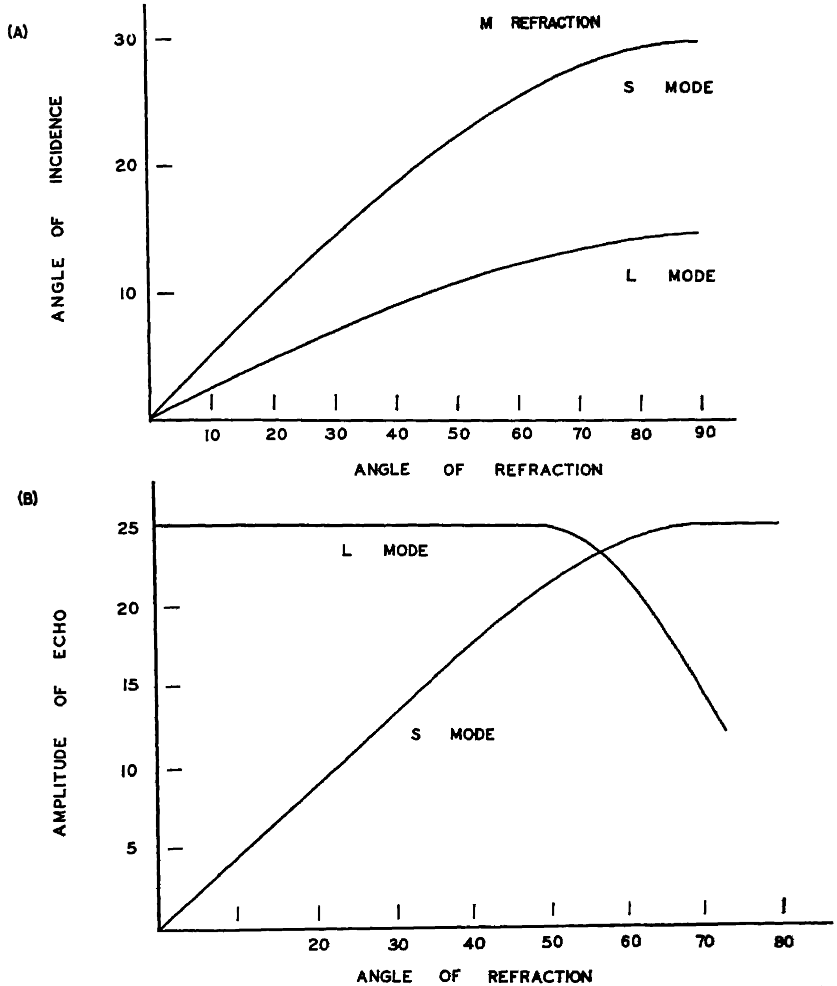

Automation Instruments, Inc.

Fig. 5. Experimental results with sound at angular incidence. Measurements made at 2.25 and 5 Mc.

Rayleigh, or Surface, Waves. When the incident angle reaches about 30 deg. in aluminum, the *S* wave is at the critical angle and is traveling parallel to the surface of the part. At this angle a third wave form is developed. This is known as the Rayleigh, or surface, wave and travels only on the surface of the part. The **particle motion** of the wave is elliptical, with its greatest amplitude perpendicular to the surface. In its motion and actions, it resembles a surface wave on water. This wave can be damped out by an object such as a finger or water touching the metal surface; thus it cannot be utilized in immersion techniques. For contact work, both the *S* and Rayleigh waves are usually generated by placing a **plastic wedge** on the front of an *L*-mode crystal. The wedge is of such an angle that the reflected sound is beyond the critical angle for the L mode, so only "shear" waves enter the part. By increasing the wedge angle to the critical angle for the S mode, surface waves are generated.

Surface Flaw Detection. It has been shown by Firestone[5] that the Rayleigh waves may be used to find **minute surface cracks** and flaws lying just beneath the surface. The velocity of Rayleigh waves will change with the surface condition of the part. Tension in the surface along the line of propagation tends to increase, and compression in the surface to decrease, the velocity of the Rayleigh waves. Surface-wave velocity and attenuation measurements may possibly also be found useful for measuring other surface conditions.

LAMB WAVES. Lamb waves were discovered theoretically by Lamb, who reported them in a paper to the Royal Society of London in 1916.[6] His work followed Pochammer's analysis of propagation in bars, which is generally analogous. Additional historical details and analyses are given by Kolsky.[7] Firestone and Ling succeeded in generating these waves in thin plates in 1946.[8] Worlton reported the use of these waves for testing thin-walled tubing and for detecting laminar defects which lie very close to the surface of a part, in 1957.[9] These waves have also been applied to the testing of sandwich-type material for quality of bond between the laminations.

Characteristics of Lamb Waves. There are two types of Lamb waves, **symmetrical** and **asymmetrical.** Each of these types can exist in an infinite series of **modes**; first, second, third, etc. The **velocity** at which these waves travel depends upon the thickness of the plate, the material of the plate, the frequency of the sound wave, and its mode and type. The velocity of sound for the longitudinal, shear, and surface waves depends only upon the material of the part. Firestone and Ling have calculated the **phase velocity of Lamb waves** as a function of frequency, plate thickness, and material.[8]

Generation of Lamb Waves. If the angle of incidence of a sound beam is adjusted so that the phase velocity of the incident longitudinal wave is equal to the phase velocity of a particular type and mode of a Lamb wave in a plate, the Lamb wave can be generated in the plate. The **phase velocity of the incident longitudinal wave** is given by the expression

$$V_p = \frac{V_L}{\sin \phi}$$

where V_p = the phase velocity of the incident L wave.
V_L = the group velocity of the incident L wave.
ϕ = the angle of incidence of the incident L wave.

To illustrate, for a plate of aluminum 0.030 in. thick and an ultrasonic frequency of 5 Mc., the **phase velocities of the first symmetrical and asymmetrical modes** are approximately 2.79×10^5 and 2.67×10^5 cm. per second, respectively. The angle of incidence required to generate these waves is about 32 deg. for the first symmetrical mode and 34 deg. for the first asymmetrical mode when the coupling path is water. The phase velocities of the various modes of the two types of sound waves depend upon the frequency of the sound and the thickness of the plate. The values given are for a frequency-thickness product of about 1.5×10^5 cycle-inches per second. These values are approximately constant for the first modes of the symmetrical and asymmetrical types for frequency-thickness products from 1.5×10^5 to 4.5×10^5 cycle-inches per second.

Lamb Wave Test Systems. Systems utilizing Lamb waves for nondestructive testing can use either a single transducer or separate transducers for transmission and reception. When a single transducer is used, an echo will be reflected from a discontinuity which interrupts the wave. In **two-transducer systems,** the receiving transducer can be set at the calculated angle to receive energy from the wave in the plate. This energy will tend to disappear when a discontinuity interrupts the wave, since there will be a considerable loss due to mode changing and reflection. The receiving transducer can also be set at such an angle as not to receive energy from the wave in the plate. When the wave is interrupted by a discontinuity, energy is reflected in many directions because of the mode conversion. Other Lamb modes and *L* and *S* modes are generated at the discontinuity. A receiving transducer set at an angle other than that suitable for receiving the radiated Lamb wave will respond to the energy in the other modes reflected from the discontinuity.

Systems of both types have been used successfully to detect **laminar-type defects very close to the surface** of a part, defects in thin-walled tubing, and the degree of bonding in laminated parts and honeycomb structures.

Influence of Part Contour

EFFECTS OF SURFACE CURVATURE. When a sound beam travels from a liquid into a metal through a contoured surface, the sound beam inside the metal will be convergent if the surface is concave and will be divergent if the surface is convex. This effect is further complicated by the near-field distribution of available transducers.

Near-Field Distribution. A cross-section of the sound beam from a circular transducer prior to the point $Y+_0$ contains alternate **annular rings of maximum and minimum energy.** (See The Fresnel, or Near, Field in the section on Ultrasonic Transducers for explanation of $Y+$ maxima.) These annular rings of energy decrease in number as the distance between the transducer and the plane of the cross-section increases. The surface of the test part is usually placed prior to the point $Y+_0$ when:

1. The water path is less than 6 in.
2. The transducer is 0.75 in. in diameter.
3. The frequency is 2.25 Mc. or above.

The surface of the metal part intercepts discrete annular rings of energy. When the surface is contoured, consideration of the sound energy and the angle of refraction inside the metal will help explain the measured results.

Blocks for Contour Study. Six sets of **step blocks** were made from stainless steel Type 303 extruded bar stock. Flat-bottomed holes of 5/64-in. diam. were drilled to depths of ⅛, ¼, ½, ¾, 1, 1½, 2, 3, and 4 in. from the front surface. These blocks were tested ultrasonically to ensure uniform echo amplitude from the test holes. The maximum variation in echo amplitude from the holes of comparable depths was ±10 percent.

The surfaces of these blocks were then contoured in sets. Three sets had concave spherical surfaces with radii of curvature of 30, 14, and 6 in. Three sets were made with convex spherical surfaces with radii of curvature of 30, 18, and 6 in.

Parts with Concave Surfaces. The results of measurements made on the concave blocks are shown in Fig. 6(a). The curve for the 6-in. radius of curvature rises above the curve for the flat block by an amount approximately equal to that caused by increasing the diameter of the test hole from 5/64 to 10/64 in. in a flat-surfaced block of the same material. The curve for the 14-in. radius of curvature shows an increase over the curve for the flat-surfaced blocks approximately equal to that caused by increasing the diameter of the test hole from 5/64 to 7/64 in. The curve for the 30-in. radius of curvature shows very little increase over that of the flat-surfaced blocks.

The point $Y+_0$ has been moved closer to the surface of the block, and the region has been shortened and narrowed to cause the increase in amplitude. All the energy incident upon the surface of the block has been refracted toward the test hole and is usable for ultrasonic testing.

Parts with Convex Surfaces. The results of measurements made on the convex blocks are shown in Fig. 6(b). The curve for the 20-in. radius of curvature shows a remarkable decrease from that of the flat-surfaced blocks. The **decrease in echo amplitude** caused by the change in curvature from 30 to 6 in. is less than that caused by the change from the flat blocks to the 30-in. radius of curvature.

Sound energy near the edges of a flat transducer is refracted at a larger angle than the sound energy near the center of the sound beam because of the increased angle of incidence upon convex surfaces. Energy contained in the **annular maxima rings** around the central axis of a circular transducer is refracted, so that it combines with the energy along the central axis of the transducer when the test-object surface is either flat or concave. When the surface is convex, the

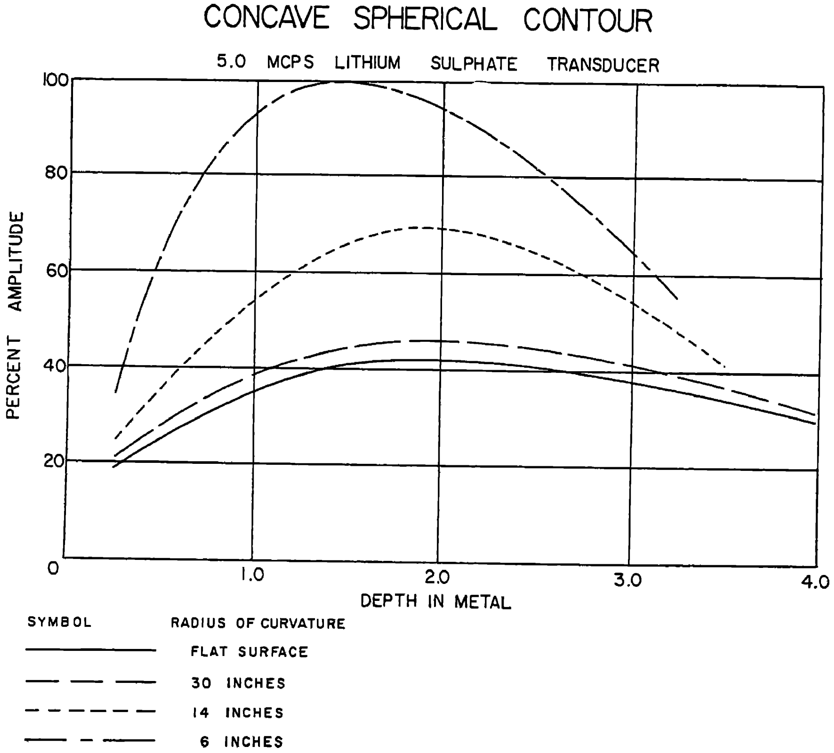

(a)

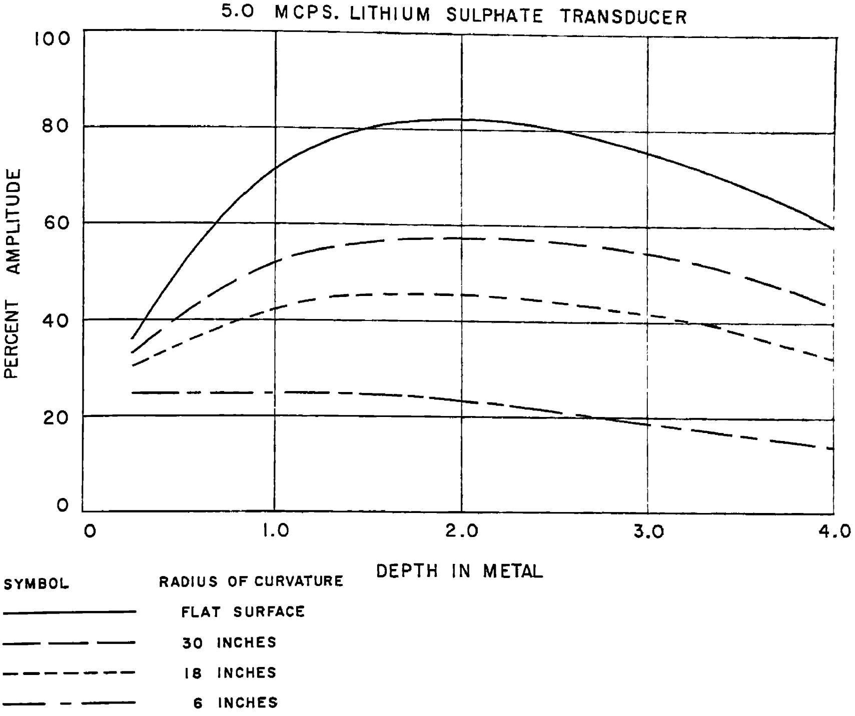

(b) Automation Instruments, Inc.

Fig. 6. Reaction of plane waves with contoured parts. (a) Amplitude of echo indication from flat-bottomed $\frac{5}{64}$-in. diam. holes at varying depths in spherically concave contoured parts. (b) Amplitude of echo indication from flat-bottomed $\frac{5}{64}$-in. diam. holes at varying depths in spherically convex contoured parts.

energy contained in the annular rings is refracted away, so that it no longer combines with the energy along the central axis of the transducer. If the index of refraction between the metal and water were low or the radius of curvature were large, there would be: (1) a gradual lengthening of the distance to Y_{+0} and the region of maximum intensity associated with Y_{+0}, and (2) a decrease in intensity throughout this region. With metals whose index of refraction approximates four, a spherical convex radius of curvature as large as 30 in. will require **contour correction** for echo amplitude, if comparison of echo amplitude is made against flat-surfaced test standards.

SURFACE ROUGHNESS EFFECTS. Rough surfaces can cause several undesirable effects which are noticeable when parts are tested ultrasonically, including:

1. A loss of echo amplitude from discontinuities within the part.
2. An increase in the width of the front-surface echo and consequent loss of resolving power.
3. Distortion of the directivity characteristic.
4. Spurious generation of surface waves.

Loss of Echo Amplitude. The decrease in echo amplitude from discontinuities within the part is a function of: (1) the average peak-to-valley roughness, (2) the index of refraction of the part, and (3) the frequency of sound. There is a short distance at the surface of the part where sound is traveling through liquid and metal simultaneously. The sound which travels through the liquid lags the sound which travels through metal because sound velocity in water is lower than in metal. The sound recombines inside the metal part so as to accommodate the **difference in travel time.** When this difference in travel time is equal to one-half the period of the sound wave, a pressure wave combines with a rarefaction wave, and the resultant energy is nearly zero inside the metal. The average peak-to-valley roughness which will cause this destructive interference is called the **critical roughness** and is given by the following expression:

$$R_c = \frac{\lambda_2 V_1}{2(V_2 - V_1)} = \frac{\lambda_1 V_2}{2(V_2 - V_1)} \tag{7}$$

where R_c = critical roughness.
λ_1 = wavelength of sound in liquid.
λ_2 = wavelength of sound in metal.
V_1 = velocity of sound in liquid.
V_2 = velocity of sound in metal.

There is a similar effect for roughness values of $2R_c$, $3R_c$, etc. These values could be called the first, second, etc., **multiples of the critical roughness value.**

This analysis assumes a continuous sound wave and a step-type surface with a profile similar to a square wave. In actual practice the sound wave is exponentially damped, and the surface roughness varies widely in profile. However, some of the effects of this idealized case should be noticed, especially with the surface-roughness profiles found on rough-machined parts.

Experimental Evidence. Rough surfaces were machined on a series of stainless steel blocks after they were ultrasonically inspected to ensure uniformity of echoes from their 5/64-in. diam. holes. These surfaces were machined on a shaper with a right-angle tool. It was positioned so that the roughness profile consisted of a series of alternate 45-deg. slopes. The peak-to-valley distance was controlled by the step-over on the shaper, in steps of 0.0025 in. Peak-to-valley distances from 0.0012 through 0.0088 in. were obtained by this process.

These blocks were then inspected ultrasonically at 2.25, 5, and 10 Mc. The **critical roughness values** (for both the calculated and measured values) for these Type 303 stainless steel blocks were as given in the accompanying table.

Frequency	R_c Calc. (in.)	R_c Meas. (in.)	$2R_c$ Meas. (in.)	40% Loss (in.)
2.25	0.018	none	none	0.009
5.0	0.008	0.0062	none	0.004
10.0	0.004	0.0038	0.0063	0.003

The dip in echo amplitude apparently occurred at a roughness value slightly less than the calculated value. However, there were not enough points on the roughness curve to determine the extent of this apparent error.

The dip corresponding to $2R_c$ obtained with a 10-Mc. quartz transducer was not obtained with a 10-Mc. lithium sulfate transducer. This result is attributed to the longer "ring-down" of the quartz unit. A reduction of echo amplitude of

40 percent is approximately equal to the difference between the reduction of echo amplitude between a 5/64- and a 4/64-in. diam. test hole. The roughness values resulting in this reduction of echo amplitude are also given in the table here. These results were obtained from surfaces which were carefully machined to ensure a uniform profile throughout the surface of the part. However, surface profiles generated by rough-machining processes such as lathes, fly-cutters, and coarse surface grinders are similar in appearance to these profiles and should cause similar effects.

Resolving Power. Another effect noticed when inspecting rough-surfaced parts is the **widening of the front-surface echo** and consequent loss in resolving power. The surfaces used in this experiment did not display this effect to a large extent. However, this effect has been very noticeable with some surface profiles. This effect is probably caused by a combination of:

1. Mode conversion (shear and surface wave) resulting from angular incidence of the sound wave at the surface of the part.
2. The difference in travel time through the peak-to-valley distance in water.
3. Reflection of the side-lobe energy from reflecting surfaces which are not present on smooth surfaces.

Rough-machined parts have in some instances returned echoes which appeared between the front- and rear-surface echoes with sufficient amplitude to cause rejection of the parts. These echoes appeared intermittently throughout the part, and for this reason the part was examined more closely. A section containing these echoes was resurfaced with a hand grinder, using a fine-grit paper. When this section was again examined ultrasonically, these echoes were not present in the resurfaced area but were still present in the areas with the original surface finish. This effect can be very serious when the parts are thin and the resolving power of the system represents almost one-half the thickness of the part.

Corrections for Surface Roughness. The cost of refinishing rough-machined parts is extremely high and is seldom allowable in production quantities. The most obvious method of reducing the effect of surface roughness is to reduce the inspection frequency. When this cannot be done, due to sensitivity or resolving-power requirements, the part may be lightly coated with grease or dipped or sprayed with a **thin coat of plastic or lacquer** which has a velocity of sound intermediate between that of water and the part. This will reduce the effect of surface roughness by reducing the velocity difference through the profile of the surface.

Equipment for Measuring Surface Roughness. Stylus-type instruments used for measuring surface roughness are usually calibrated for measuring either the center-line average or r.m.s. average value of the surface roughness of a part. They are usually designed so that the measurement is made over a very short distance along the profile of the surface. Usually this distance is between 0.03 and 0.1 in. For ultrasonic evaluations this measurement should be averaged over a profile at least as long as the beam diameter because **surface waviness** can be as important to acoustical effects as very short undulations of the surface. The r.m.s. average is approximately 10 percent larger than the center-line average. The average peak-to-valley roughness varies from about 3.5 to 4.5 times as large as the center-line average for the usual machined surface. This value was 4.0 for the profile on the blocks used in the experiment (see section on Ultrasonic Immersion Tests).

Influence of Discontinuity Properties

FACTORS INFLUENCING DISCONTINUITY INDICATIONS. It is common practice in industrial ultrasonic testing to relate echoes from subsurface discontinuities within a metal part to those from **standard test blocks** having flat-bottomed holes of varying depths and diameters. These test blocks serve also to calibrate the sensitivity of the instrument. Immersion ultrasonic methods for evaluating the size, shape, position, orientation, and impedance of discontinuities yield fairly accurate information. However, different material discontinuities and test conditions can cause similar ultrasonic phenomena. Only experience in relating the ultrasonic indications to the probable type of discontinuity can resolve the difficulty. Impedance of the material, surface roughness, surface contour, attenuation, and angle of incidence must all be considered when attempting to evaluate the size and location of an unknown discontinuity by its echo amplitude. The simplest method is to compare the defect with a test block of similar alloy, shape, and back reflections.

STANDARD ULTRASONIC TEST BLOCKS. The accepted testing standard throughout most industries in the United States has been based on flat-bottomed circular holes with machined surfaces and an air interface. Changes in contour, surface finish, impedance, area, or inclination of the test hole will tend to change the apparent echo amplitude. Since such a test hole has ideal geometry and surface condition, all **material discontinuities** whose echo height equals that received from the test hole will tend to be larger in dimension than the ideal test hole. The flaw can never be smaller than the equivalent test hole if the part and test block are comparable with respect to impedance, surface finish, and attenuation. This phenomenon can be readily demonstrated by machining a round-bottomed hole instead of a flat-bottomed hole into a test block.^{9} The resultant echo amplitude will be one-tenth (or less) of that from the flat-bottomed standard, even though both holes present equivalent cross-sectional diameter, equal impedance, and equal surface finish to the sound beam.

Since there has been confusion about the size of discontinuities studied only with relation to "amplitude of indication from a comparable flat-bottomed test hole," an attempt will be made to show when such correlation does and does not exist. Some suggestions will also be made which should aid in more accurate evaluation of discontinuity size when using standard commercial equipment.

BEAM CHARACTERISTICS OF THE REFLECTOR. One of the parameters to be considered in the application of ultrasonic testing is the relationship between the area of a reflector, or discontinuity, and the amplitude of the echo returned from it. The **echo amplitude** is a function of the area of the reflector and the response of the transducer. The reflector must be considered as a new sound source radiating energy proportional to the energy incident upon it. As long as the area of the reflector is less than the cross-sectional area of the sound beam and its dimensions are larger than two or three wavelengths, the energy reflected by it will be proportional to its area.

Piezoelectric transducers respond to a mechanical disturbance so that the electric power output is proportional to the mechanical power input as long as the mechanical disturbance has the same intensity over the entire front surface of the transducer. If the intensity of the mechanical disturbance is not uniform over the surface of the transducer, the electric power output is proportional to the average value of the mechanical power input over the surface of the transducer.

A transducer with a surface area of 10 cm.^{2} will yield the same electric power output for a mechanical input of 1 dyne per cm.^{2} over its entire surface as it will for a mechanical disturbance of 10 dynes per square centimeter over only 1 cm.^{2} of its surface.

The **energy returning from a reflector** is proportional to its area. The cross-sectional area of the reflected sound beam is also proportional to the area of the reflector. The electric power output of a transducer responding to the energy from a reflector will be proportional to the reflected energy and also to the area of the reflected sound beam as long as the reflected sound beam has a cross-sectional area less than that of the transducer. This condition holds for the energy reflected from the test holes used in the Alcoa Series A test block standards. A flaw detection instrument using piezoelectric transducers has an **over-all response** to the echo from a discontinuity with a cross-sectional area less than that of the sound beam, but larger than two or three wavelengths of sound, as follows:

1. The electric power output of the transducer is proportional to the square of the reflecting area of the discontinuity.
2. The amplitude of the output (peak voltage) is proportional to the reflecting area of the discontinuity.

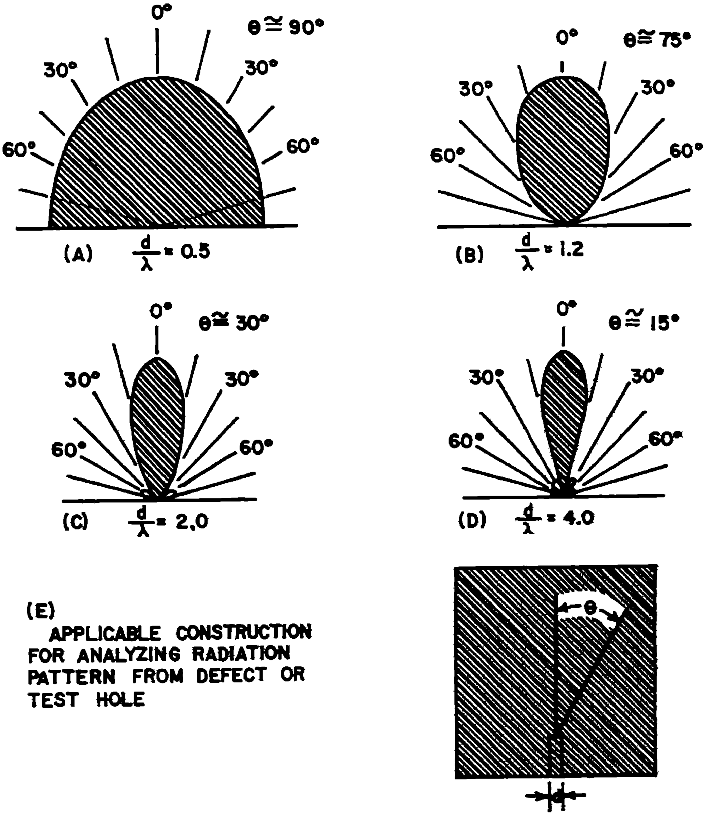
0°
θ ≅ 90°
30°
30°
60°
60°
(A) $\frac{d}{\lambda} = 0.5$
0°
θ ≅ 75°
30°
30°
60°
60°
(B) $\frac{d}{\lambda} = 1.2$
0°
θ ≅ 30°
30°
30°
60°
60°
(C) $\frac{d}{\lambda} = 2.0$
0°
θ ≅ 15°
30°
30°
60°
60°
(D) $\frac{d}{\lambda} = 4.0$
(E)
APPLICABLE CONSTRUCTION FOR ANALYZING RADIATION PATTERN FROM DEFECT OR TEST HOLE
θ
d

Automation Instruments, Inc.

Fig. 7. Radiation patterns.

Reflections from Small Discontinuities. A common method of explaining the transmission-reflection process is to assume that the **incident sound beam** enters the part (reflection from the front surface is neglected to avoid confusion) and progresses until it strikes a discontinuity in the test material. Upon striking the discontinuity, the segment of sound energy from the defect area is reflected back toward the source, like light from a plane mirror. This does not give an explanation or analysis of energy reflected from flat reflectors, however. A small reflector must be considered as a **new emitting source of energy** with its own directional properties, near field, and other characteristics. The **radiation patterns** from flat reflectors with various ratios of diameter to wavelength are shown in Fig. 7. In these patterns, the peak amplitude at an angle of zero degree is taken as unity. The relative amplitudes at other angles indicate the energy patterns on a radial decibel scale. Fig. 8 shows ratios of wavelength to diameter, in $\frac{1}{64}$-in. steps, for aluminum and stainless steel.

(a) *Aluminum*

Freq. (Mc.)	Alcoa hole-size numbers							
	1	2	3	4	5	6	7	8
2.25	0.140	0.282	0.423	0.563	0.704	0.845	0.986	1.126
5	0.312	0.626	0.938	1.25	1.56	1.88	2.19	2.50
10	0.624	1.25	1.88	2.50	3.12	3.75	4.38	5.00
15	0.936	1.87	2.81	3.75	4.68	5.64	6.57	7.50
25	1.56	3.13	4.69	6.25	7.80	9.40	11.0	12.5

(b) *Stainless steel*

Freq. (Mc.)	Alcoa hole-size numbers							
	1	2	3	4	5	6	7	8
2.25	0.150	0.301	0.451	0.601	0.751	0.902	1.05	1.20
5	0.333	0.669	1.00	1.34	1.67	2.00	2.34	2.67
10	0.667	1.34	2.00	2.67	3.34	4.00	4.68	5.34
15	1.000	2.01	3.00	4.02	5.01	6.00	7.02	8.01
25	1.66	3.34	5.00	6.70	8.35	10.0	11.7	13.4

Automation Instruments, Inc.

Fig. 8. Diameter-to-wavelength ratio for standard hole sizes in aluminum and stainless steel. Alcoa hole-size numbers are diameters in $\frac{1}{64}$ in.

Reflected-Beam Radiation Patterns. To predict accurately the useful portion of energy returned to the receiver by a small reflector, it is necessary to consider both the amount of transmitted energy intercepted and the radiation pattern of the reflector. These radiation patterns are analogous to those associated with high-frequency antennas. Fig. 7 shows these patterns from several **flat, circular reflectors.** The diameters of these reflectors are expressed as a function of wavelength. In Fig. 7 the maximum reflected intensity is assumed equal in each case. The importance of directivity is evident, since small diameter changes vary the radiation pattern.

Directional effects are important in ultrasonic testing. For example, consider the smallest and largest reflectors in Fig. 7 to be located in the same sound field. The echo from the small reflector could at best be only 1/64 as powerful as the echo from the large one, since it intercepts only that portion of the beam. Of this reduced return, an even smaller portion will reach the receiving transducer, since the reflected energy is scattered in a hemispherical pattern as contrasted with a specularly reflected return beam of the large reflector. Thus, as **reflector diameter** becomes small with respect to wavelength, the limiting size of discernible defect is reached. Obviously, if a higher frequency were used, the same discontinuity would have a greater ratio of diameter to wavelength, and its echo would appear greater in amplitude. The radiation patterns shown in Fig. 7 are approximately those of the holes in the Alcoa A series blocks, Nos. 1, 2, 4, and 8, at a frequency of 5 Mc.

Nonmetallic Inclusions, Gas Porosity, and Cracks. Slag, fire brick, oxide inclusions and intermetallic segregates usually have impedances nearer to that of the surrounding material than to that of air. By comparison, the **impedance mismatch for the flat-bottomed hole test standard** can be considered for practical purposes to be nearly unlimited. Thus, even if such discontinuities are flat and smooth, they are usually much larger than the test hole producing comparable amplitudes of indications.

Special "Short-Burst" Polarity Test Method. Some ultrasonic test instruments display the echo as it actually appears to the crystal, a cyclic vibration which builds up to a maximum and then decays exponentially to zero. This is called an **R.F. presentation.** Other test instruments rectify the echo and display only the envelope of the echo as it appears to the transducer. This is called a **video presentation.** If the R.F. presentation is available, one additional bit of information can be obtained. The technique, however, requires special test equipment. Special "short-burst" transmitters and broad-band receivers such as wide-band high-frequency test oscilloscopes are needed. Standard immersion ultrasonic test instruments cannot give easily interpretable indications for this test.

If the impedance of the discontinuity is higher than that of the surrounding material, the direction or polarity of the **first half-cycle of the echo** or an equivalent characteristic portion of the test signal will be the same as that of the first half-cycle echo from the front surface of the part in immersion inspection. However, if the discontinuity impedance is lower than that of the surrounding material, the polarity of the echo will be opposite to that seen at the front surface.

Mismatch is a function of the ratio $(Z_1 - Z_2)/(Z_1 + Z_2)$. **Discontinuities which are not bonded,** or are surrounded by a microscopic crack filled with gas, usually show this reversed polarity with respect to the front-surface echo. Often, when polarity is reversed, the discontinuity will be a crack, fissure, gas porosity, or similar discontinuity. If the **polarity of the signal** is the same as that of the front-surface echo, the discontinuity is probably composed of material with higher impedance than the surrounding material. Since gas voids have a nearly infinite impedance ratio mismatch $(Z_{\text{metal}}/Z_{\text{gas}})$ with respect to solid objects, they show closer correlation of flaw diameter to comparable test-hole diameter than would be obtained if the impedance polarity were reversed. Thus, when a discontinuity indication has the same polarity as the front-surface echo, the discontinuity will be many times larger in area than the equivalent flat-bottomed hole standard against which calibration is made and will be composed of a solid, dense material.

Thickness of Discontinuity. The thickness of a discontinuity also exerts an effect on its apparent impedance. In general, when a discontinuity is thin with respect to a wavelength, it is a poor reflector. When the discontinuity is a one-quarter wavelength thick, its reflection is at a maximum and the same as if it were infinitely thick. At a one-half wavelength thickness, the reflector again is a poor sound reflector. The same is true for other even and odd quarter-wavelengths. In general, the shorter the pulse (the wider its frequency spectrum), the less troublesome this phenomenon will be.

Geometry of Discontinuities

ANGLE AND SURFACE ROUGHNESS OF DISCONTINUITY. Reflections from flat or regular discontinuities normal to the beam axis have been considered. This condition is valid for most rolled plate, since rolling tends to reduce gas discontinuities to flat discs or other shapes parallel to the surface. (This does not necessarily apply to refractory types of inclusions.)

If the reflector or discontinuity is at an angle to the sound beam, the sound is reflected away from the transducer. Fig. 9 shows the effect on the echo amplitude of a large reflector, as the **angle of incidence changes.** Fig. 9(a) demonstrates the effect on echo amplitude that can be expected from a large, smooth reflector examined at different angles. Fig. 9(b) demonstrates the reflection of sound from a large, smooth reflector. Fig. 9(c) demonstrates the reflection of sound from a large, rough reflector viewed from an angle. It can be seen from Fig. 9(a) that a flat reflector in a metal part lying at an angle of 2½ deg. with respect to the front surface would return an echo approximately one-tenth the amplitude it would have had if it had been perpendicular to the sound beam. If this angle were increased to 12 deg., its amplitude would have been reduced to at least one-thousandth of the normal incidence values, and it would not have been detected. If, however, the discontinuity is less than two wavelengths in diameter, it would return small echoes nearly independently of the angle of the reflector (see Fig. 7).

Rough reflectors scatter sound and return some energy in all directions. But the amplitude in the frontal direction is lower than that with the comparable flat reflector. A reflector can be considered smooth if the peak-to-valley roughness of its surface is less than one-eighth of a wavelength for the frequency used. If the peak-to-valley distance is larger than this, the rough surface will scatter and distort the phase of the incident sound energy. As the small projecting points increase to one-half wavelength, they will reflect sound energy in all directions, as shown for a small flat reflector in Fig. 7(a). Still greater degrees of roughness produce multiple, planar reflecting surfaces, some of which reflect sound back to the receiver, as shown in Fig. 9(c). Notice that roughness can be considered only in terms of frequency. Thus a defect which is "rough" at one frequency is "smooth" at another.

If **high-frequency tests** produce an echo amplitude equivalent to that from a 3⁄64-in. flat-bottomed hole, the same rough discontinuity commonly gives a considerably higher echo amplitude at a lower frequency (if the discontinuity is of sufficient cross-sectional area). This phenomenon has long been recognized in the field of geoseismic testing for oil deposits. In such prospecting, filters are often introduced so that the low-frequency energy is utilized to reduce the effect of roughness of the basic rock structure. Prior knowledge of the types of discontinuity and flaw-surface roughness (obtained, for example, by fracturing test parts) assists the nondestructive test engineer to establish an approximate optimum frequency for testing. The computed degree of roughness which can occur

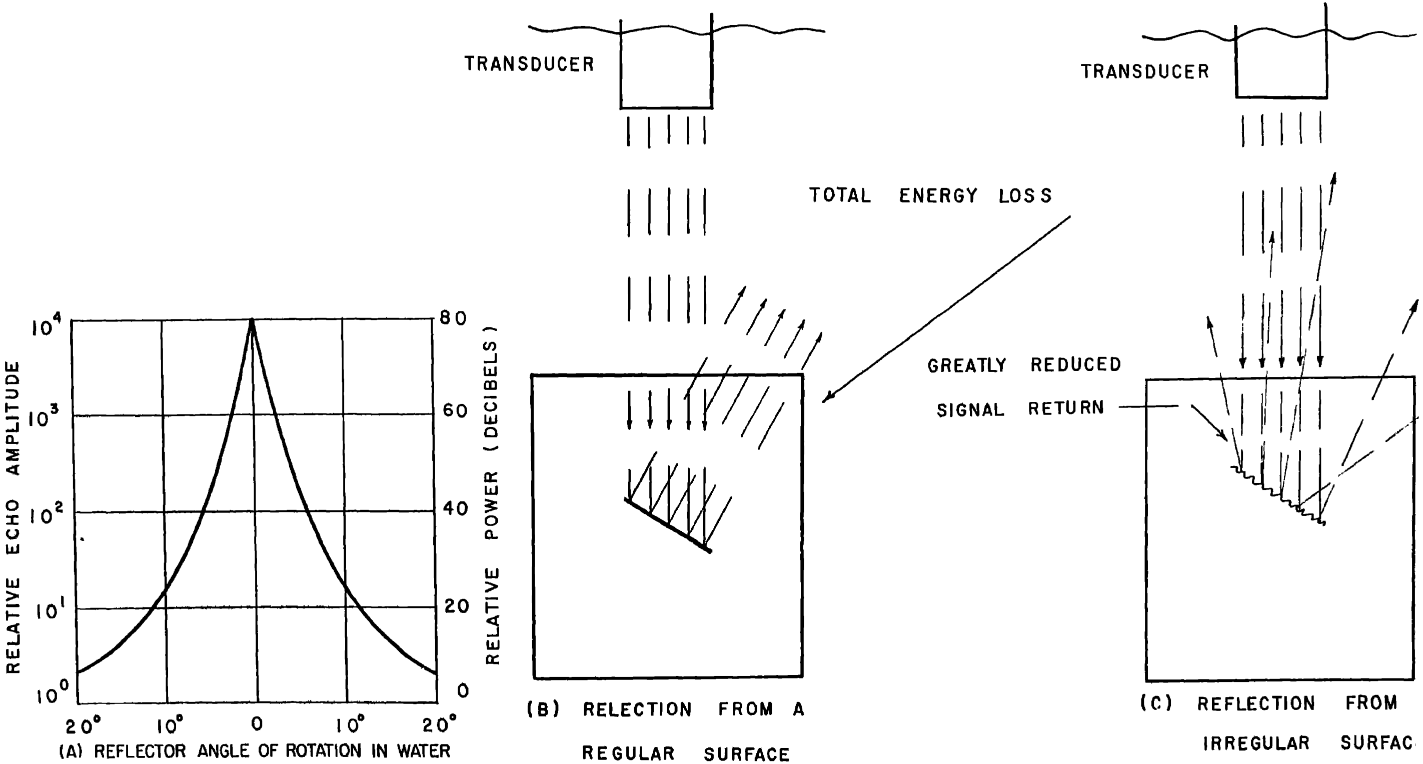
RELATIVE ECHO AMPLITUDE
10⁴
10³
10²
10¹
10⁰
RELATIVE POWER (DECIBELS)
80
60
40
20
0
20°
10°
0
10°
20°
(A) REFLECTOR ANGLE OF ROTATION IN WATER
TRANSDUCER
TOTAL ENERGY LOSS
(B) RELECTION FROM A REGULAR SURFACE
TRANSDUCER
GREATLY REDUCED SIGNAL RETURN
(C) REFLECTION FROM IRREGULAR SURFAC

Automation Instruments.

Fig. 9. Echo loss from adversely oriented discontinuities. (a) Reflector angle of rotation in water. (b) Reflection from a regular surface. (c) Reflection from an irregular surface.

in peak-to-valley fashion without having a pronounced effect on the reflected echo amplitude, as compared with that from a polished smooth reflector, has been given earlier in this section under Corrections for Material Differences.

CONTOUR OF DISCONTINUITIES. The case of flat reflectors, both normal and at angular incidence to the sound beam, with smooth or rough surfaces, has been considered. For discontinuity geometries other than flat, the echo amplitude is almost invariably decreased below that observed for a flat defect. With a **spherical defect,** the energy reflected from its surface will travel from it in a nearly full 360-deg. spherical pattern. The amplitude of the discontinuity indication, as seen from the front surface, will be much lower than that of a flat-bottomed-hole reflector of equal radius. If the spherical reflector has **rough surfaces,** the reflection pattern will be substantially the same as that from the smooth spherical defect. However, its amplitude will appear still lower, since **phase cancellation effects** decrease the apparent power of the returning energy.

Although a concave defect would presumably return more energy to the crystal than a flat defect, this is very seldom the case. Most **concave reflectors** will be of such short focal length that the reflected sound will pass through a focal point and diverge long before it returns to the crystal. Small-diameter concave reflectors (one-half to two wavelengths) behave substantially like flat reflectors.

Techniques for Determining Geometry of Discontinuities. To determine whether a given discontinuity is contoured or flat, the echo amplitude returned from it can be observed as it is **inspected at various angles.** Thus, if the inspector angulates to a 10-deg. incident angle on an aluminum part, he will be inspecting the discontinuity with the internal sound beam at a 45-deg. angle with respect to the part surface. Therefore, if a discontinuity exhibits an echo amplitude which is significant when seen from different angles and from different directions, the discontinuity is probably contoured. (The rate of amplitude decrease with angle should be compared on the equivalent test block to establish this condition.) A change of a few degrees in the incident angle will achieve nearly a 10 to 1 change in amplitude from a flat-bottomed test-hole standard if the ratio of diameter to wavelength is 2 or larger. The only other possibility is that the surface of the discontinuity is very rough, so that the energy is being reflected in all directions. This, again, must mean that the discontinuity is considerably larger than the equivalent flat-bottomed test-hole standard. This possibility could be partially analyzed by reinspecting at a low frequency. When a fairly large change in incidence angle (6 deg. or more) still permits easy visualization of the discontinuity, it is usually quite large in comparison with the diameter of the hole in the test-block standard.

Measurement of Diameter or Length of Discontinuities. Care must be used when measuring the diameter or length of a discontinuity. Measuring the length of horizontal scan for which the discontinuity-echo indication persists may prove misleading because of the inherent **amplitude variations in the near-field sound pattern** (see section on Ultrasonic Transducers). Best results are obtained by making this measurement only in the far field. For example, one could use a $\frac{3}{8}$-in., 5-Mc. transducer with a reasonable water path.

An operator can use a scanning technique to measure the apparent beam width (from the one-tenth amplitude point through the peak to the one-tenth amplitude point) both on the discontinuity and the test block with comparable echo amplitude. Then, by subtracting the width of the test-block measurement from the discontinuity measurement, an estimate of the diameter or length of the discontinuity is obtained. The known width of the hole in the test block can be

Characteristics of Discontinuity	Type of Ultrasonic Observation				
	Low-Frequency Test Amplitude	High-Frequency Test Amplitude	Angle Test, Low Frequency	Angle Test, High Frequency	Echo Polarity versus Surface Echoes
Flat, smooth, size comparable to test hole.	No change	No change	No change	No change	Opposite
Flat, smooth, size large with respect to test hole, impedance higher than metal.	No change or increase (depends on hole size of test block)	No change	Decrease	No change	Same
Flat, rough, size larger than test hole.	Increase	Decrease	Decrease	Increase	Either
Contoured, smooth, diameter larger than test hole.	No change	No change	Increase	Increase	Either
Contoured, rough, diameter larger than test hole.	Increase	Decrease	Increase	Increase	Either
Cluster of small discrete reflectors over a flat area, larger than diameter of test hole.	Decrease	Increase	Decrease	No change	Either
Cluster of small discrete reflectors over a contoured or rough area distribution.	Decrease	Increase	Increase	Increase	Either

Automation Instruments, Inc.

Fig. 10. Multiple-frequency inspection. Indications from preliminary work.

added if significant. An alternative method is to leave the transducer in one place and progressively shield the discontinuity (at the surface of the part) with a thin wooden board until the amplitude falls to one-tenth. This point is marked. Then the operation is repeated from the opposite direction. By marking and measuring the width on both the part and test block, the width is computed as before. The latter method is probably the more reliable. The most accurate measurements can be made by using a focused transducer with the first method, and plotting the defect area by a C scan. In contoured parts or discontinuities, the problem is obviously more complicated and requires special equipment (see section on Ultrasonic Immersion Tests).

MULTIPLE-FREQUENCY INSPECTION. The concept of evaluating a single discontinuity by testing it at two or more frequencies has been more widely referred to in the literature in Europe than in America. Additional information is obtained by testing a discontinuity and comparing it with the equivalent flat-bottomed hole standards at several frequencies. For example, detecting cracks and inclusions of foreign materials in a metallic test object may be important in a specific problem, whereas small, relatively discrete areas of fine gas porosity or inhomogeneous structure may be neglected. In such a case it may be possible to some extent to separate these two situations by testing at two different frequencies. The amplitude of reflection is greatly dependent upon the relationship of discontinuity diameter to frequency; and gas cavities are usually small with respect to a wavelength. Consequently it is often possible to obtain a marked **suppression of fine porosity or structure indications** by testing at a lower frequency or to obtain an increased amplitude of indication at a higher frequency. Conversely, a discontinuity which is relatively rough with respect to a wavelength at a given frequency may give a larger indication at a lower frequency. Application of similar methods may lead to further conclusions concerning the probable nature of a given discontinuity indicated in ultrasonic testing. More extensive evaluation may be based upon knowledge of the angle through which the discontinuity can be seen, the relative amplitude at two or more frequencies, and the phase polarity. Such detailed investigations can be costly and are not widely used in industry.

The preliminary observations obtained in this work are shown in Fig. 10 for various types of flaws. The results are, however, qualitative indications of the possibilities of this method of analysis.

GUIDE TO INTERPRETATION. The following rules of thumb may prove helpful to workers in the field:

1. An estimate of the depth of a discontinuity in metal is made by a measurement of the position of the flaw indication between the front and rear surface echoes, or its position may be accurately identified as described in the preceding text.
2. If the discontinuity is large, the transducer can be moved parallel to the surface of the part and an estimate obtained of its dimensions.
3. If the discontinuity lies at an angle, the transducer can be tilted until the echo amplitude becomes maximum. A simple calculation using Snell's law gives the angle at which it lies.
4. If the discontinuity echo remains relatively constant as the angle of incidence is changed, the reflector must be very small, rough, or curved.
5. If the discontinuity echo decreases rapidly with varying angle of incidence, the reflector must be relatively large and flat.
6. If the discontinuity-echo amplitude increases at lower frequencies, the discontinuity is rough.
7. If the discontinuity-echo amplitude decreases at lower frequencies, it probably contains many small discrete reflectors.

Impedance variations between discontinuities, such as inclusions, cracks, blow holes, and segregations are difficult to evaluate ultrasonically. The history of the type of discontinuity found in a particular part must be known. In cases where knowledge of the type of discontinuity and its echo characteristics has been accumulated over a period of time, close correlation between ultrasonic information and the type and size of discontinuity may be feasible.

Utilization of basic acoustical principles in the selection of operating procedures, test blocks, transducers, and equipment, along with the proper training of operators, can result in a further increase in the reliability of ultrasonic nondestructive testing.

References

1. CHICK, B., and R. TRUELL. *An Improved Ultrasonic Attenuation Measurement Unit with Applications to the Study of the Mechanical Properties of Solids.* The Metals Research Laboratory, Brown University.
2. MASON, W. P. *Piezoelectric Crystals and Their Application to Ultrasonics.* New York: D. Van Nostrand Co., Inc., 1950.
3. GROSSMAN, N. "New Methods Determine Grain Size Ultrasonically," *Iron Age,* 172, No. 27 (1953): 72.
4. WORLTON, D. C. "Nondestructive Grain Size Measurements with Ultrasonic Nondestructive Testing," *Nondestructive Testing,* 13, No. 6 (1955): 24.
5. FIRESTONE, F. A., and J. R. FREDERICK. "Refinements in Supersonic Reflectoscopy. Polarized Sound," *J. Acoust. Soc. Am.,* 18 (1946): 200.
6. LAMB, H. "On Waves in an Elastic Plate," *Proc. Roy. Soc.* (London), 93A (1917): 114.
7. KOLSKY, H. *Stress Waves in Solids.* Oxford: Clarendon Press, 1953.
8. FIRESTONE, F. A., and S. LING, JR. (To Sperry Products, Inc.) "Methods and Means of Generating and Utilizing Vibrations of Waves in Plates," U.S. Patent No. 2,536,128 (Jan. 2, 1951).
9. WORLTON, D. C. "Ultrasonic Testing with Lamb Waves," *Nondestructive Testing,* 15, No. 4 (1957): 218.
10. BUCHANAN, R. W., and C. H. HASTINGS. "Ultrasonic Flaw-Plotting Equipment—A New Concept for Industrial Inspection," *Nondestructive Testing,* 13, No. 5 (1955): 17.

SECTION 46

ULTRASONIC IMMERSION TESTS

CONTENTS

PAGE

Nature of Tests

Principle of method 1
Equipment considerations 1
    Hand-operated carriage and tank equipment for general parts inspection by immersion ultrasonic testing (*f.* 1) 2
Advantages and limitations 1
Automatic-scanning equipment 2
    Automatic equipment for immersion ultrasonic inspection in tank (*f.* 2) 3
Presentation of test indications 3
  A-scan presentation 3
    Presentation of ultrasonic test signals by A scan (*f.* 3) 4
  B-scan presentation 3
    Presentation of ultrasonic test signals by B scan (*f.* 4) 4
  C-scan presentation 4
    C-scan presentation of ultrasonic test signals from poor bond (*f.* 5) 5

Test Equipment and Techniques

Instrumentation 5
    "Immerscope" ultrasonic test instrument (*f.* 6) 5
  Transducers and search tubes 7
    Ultrasonic flaw detection crystals and search tubes (*f.* 7) 6
  Hand-scanning units 7
    Hand-scanning equipment for use with immersed crystals (*f.* 8) 6
Automatic-scanning equipment 7
    Unit for automatic scanning and recording of immersion ultrasonic test signals (*f.* 9) 7
  Advantages of automatic scanning 8
  Long tank units 8
  Turntable units 8
    Motor-driven turntable for immersion ultrasonic inspection of cylindrically shaped parts (*f.* 10) 9
Use of high-frequency waves 8
  Loss of near-surface resolution 9
Limitations in beam penetration 9
  Evaluating beam penetration 9
  Use of test blocks 10
  Control of water distance 10
  Adjusting marker circuit 10

PAGE

Effect of Test Materials

Composition of material 10
Structure of material 11
Surface finish and radius 11
    Ultrasonic test blocks used to determine surface shape and finish effect in relation to flaw-signal response (*f.* 11) 11
  Surface roughness 12
  Surface contour 12
  Angle of surface 12
Effect of heat treatment 12

Ultrasonic Test Blocks

Slotted-block technique for stringer-type flaw evaluation 12
    Slotted blocks used to determine length of discontinuities in ultrasonic testing (*f.* 12) 13
  Stringer length technique 12
  Stringer width technique 14
  System characteristics 14
  Slotted-block characteristics 14
Construction of standard test blocks 14
    Ultrasonic test blocks used to determine flaw sizes (*f.* 13) 15
  Test-hole depths 14
Use of standard blocks 14
  Estimating flaw area 15
Standard block response characteristics 15
  Test condition 15
    Comparison curves obtained by using various crystals and frequencies in immersion ultrasonic testing (*f.* 14) 16
  Results of tests 16

Industrial Inspection Procedures

Typical specifications 17
  Sensitivity adjustment 17
  Scanning procedure for flat surfaces 17
Checking flaw indications 17
  Identification of sources of A-scan indications 18
    Analysis of A-scan signals in angle-scan immersion ultrasonic testing (*f.* 15) 18
  Determining flaw position 18
Off-center scanning of cylindrical parts 19
  Scanning procedure for cylindrical surfaces 19

CONTENTS (*Continued*)

PAGE

Flaw evaluation with "cylindricator" 19
  "Cylindricator" used to determine sound path in off-center scanning of cylindrically shaped parts (*f.* 16) 20
 Measurement technique 19
 Setting up "cylindricator" 19
 Reading "cylindricator" 21

Typical Industrial Applications

Inspection of cylindrical forging 21
  Ultrasonic inspection of a typical aircraft part (*f.* 17) 21
 Parting line region 21
 Bosses or protrusions 22
  Etched section of aluminum alloy forging, showing "unhealed porosity" (*f.* 18) 22
  Fractured aluminum forging, showing (light) areas of "unhealed porosity" (*f.* 19) 23
Inspection of tubular or round bar stock 22
  Fixture used in immersion ultrasonic inspection of tubular and round bar stock (*f.* 20) 24
Inspection of flat or rectangular stock 22
Inspection of turbine parts 23
  Immersion ultrasonic inspection of shaft area of turbine part (position 1) (*f.* 21) 25
 Typical flaws 23
  Defects found in the shaft area of a turbine part by immersion ultrasonic inspection (*f.* 22) 25
Inspection of large, cast, cylindrical parts 23
Typical specifications for inspection 23
References 27

SECTION 46

ULTRASONIC IMMERSION TESTS

Nature of Tests

PRINCIPLE OF METHOD. Immersion ultrasonic tests utilize high-frequency mechanical vibrations to probe test objects. These vibrations are coupled to test objects by immersing the **crystal** (which provides the searching and receiving signals) and the **test object** in water or other suitable **liquid couplant.** Immersed ultrasonic inspection may, in a limited way, utilize the basic electronic equipment employed in contact pulse-reflection ultrasonic testing.

EQUIPMENT CONSIDERATIONS. Since the speed of sound is approximately four times slower in water than in metallic materials, a corresponding amount of usable viewing area of the conventional cathode-ray screen is lost through the extension of the base-line trace between the outgoing signal from the crystal and the reflection from the nearest surface of the part. Nearly all immersion ultrasonic units now employ **delayed-sweep circuits** to correct for water to crystal distance. Consequently the electronic system of contact equipment is modified by the addition of sweep-delay circuits to position and expand or to contract the scanning trace on the picture tube.

Since the crystal is not held manually in contact with the part being tested (as in contact scanning), it is necessary to provide a support for the crystal. Generally the crystal is mounted on the end of a **scanning tube.** The scanning tube is attached to a manipulator or fixture, which permits controlled movement of the tube in any direction and positions the scanning tube and crystal above the part. This provides a flexible method of projecting sound to and through submerged parts in any direction desired by the operator. To utilize this method to its fullest advantage, the manipulator is attached to a carriage with provisions for moving the assembly along the top of the **scanning tank.** The scanner can also be positioned crosswise of the tank with a screw thread and crank or by other methods. The whole assembly resembles a typical overhead crane installation. Fig. 1 shows such an installation designed for manual operation. It is especially adaptable to inspection of hand and die forgings, plate and bar stock, and other parts that fit in the tank.

ADVANTAGES AND LIMITATIONS. In evaluating the feasibility of **immersion testing,** these points should be considered first:

1. Is it possible to immerse the part in water during inspection?
2. Is it desirable to make a complete inspection of the part or piece of material?
3. Is near-surface flaw evaluation desirable?

Obviously, if an inspection that would require costly disassembly were to be made of a piece of machinery, an immersion test would be ill-advised if a contact test would be adequate. If the material or parts fall in the category of test objects that can easily be immersed, such as pipe, tubing, castings, weldments, forgings, extrusions, bar plate, ingots, and bloom, then immersion testing may have many advantages. **Forgings of irregular shape** can be given a practically complete inspection, including fillet areas. This type of part cannot be completely inspected by the contact method by any practical means. The greatest advantage of immersion testing (namely, speed of inspection) is most evident in the inspection of **symmetrically shaped parts.**

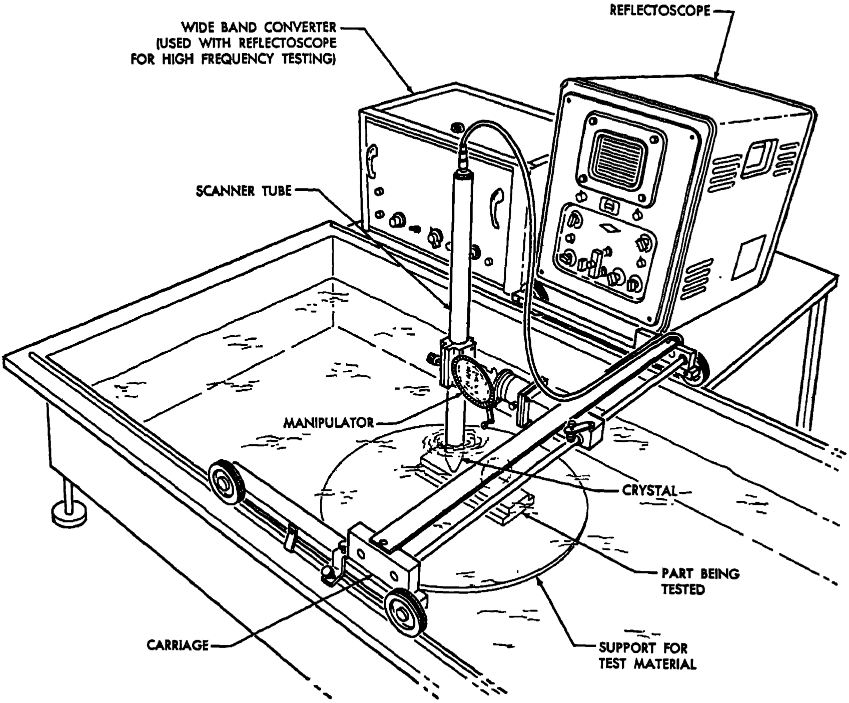
REFLECTOSCOPE
WIDE BAND CONVERTER (USED WITH REFLECTOSCOPE FOR HIGH FREQUENCY TESTING)
SCANNER TUBE
MANIPULATOR
CRYSTAL
PART BEING TESTED
SUPPORT FOR TEST MATERIAL
CARRIAGE

Fig. 1. Hand-operated carriage and tank equipment for general parts inspection by immersion ultrasonic testing.

In addition to the automation of scanning, another advantage of immersion testing is the **elimination of machining** sometimes required for contact testing. In immersion testing, "as-forged" surfaces do not present any particular problems, nor do normal machined surfaces. Another advantage of immersion testing is that **high test frequencies** can be used. The limit in contact testing is about 10 Mc. per second because quartz crystals ground for use at 10 Mc. and higher frequencies are very thin and fragile. Normal wear on such thin contact crystals shortens their useful life.

AUTOMATIC-SCANNING EQUIPMENT. If a means of motorizing the carriage is now added to a unit such as that shown in Fig. 1, the scan can be operated very smoothly at **speeds** up to 2 f.p.s. The development of **high-speed** recording devices may permit this speed to be increased in the future. If this motorized carriage is provided with a means of crystal indexing or automatic transverse positioning at the end of each stroke, a complete coverage of the material being inspected may be achieved without the continuous attention of the operator. Such a **motorized unit** is shown in Fig. 2. The immersion tank of this unit is 12 ft. wide, 45 ft. long, and 24 in. deep. The operation is automatic, and scanning speeds range up to 2 f.p.s. **Crystal indexing distance** and **speeds** can be selected by the operator. Remote control of the manipulator allows for maintaining **crystal and material surface parallelism** and for evaluating flaws anywhere on the material being tested. At the completion of the last scan over the material, the carriage automatically returns to its starting position. To do this same inspection by manual contact testing would require many hours of tedious work and would not produce completely satisfactory results.

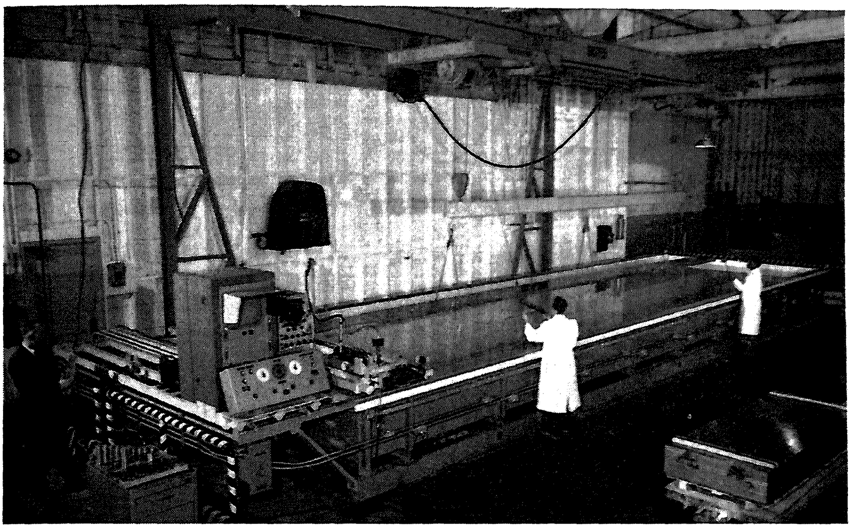

Douglas Aircraft Co.

Fig. 2. Automatic equipment for immersion ultrasonic inspection in tank.

PRESENTATION OF TEST INDICATIONS. The visible signals displayed with automatic ultrasonic equipment may be presented in several ways. The A and B scans (radar terminology) are generally used to display the signals from the material under test on the screen of a **cathode-ray oscilloscope.**

A-Scan Presentation. The A-scan signals in Fig. 3, reading from left to right, are:

1. The reflected signal from the top surface of the material being tested.
2. A reflection from a discontinuity within the material.
3. The reflection from the back surface of the part.
4. A spurious small signal.
5. A repetition of the first signal.

The horizontal line is the **time-base line.**

B-Scan Presentation. Fig. 4 illustrates a B-scan ultrasonic presentation of a **cross-sectional view** through a $\frac{5}{8}$-in. thick aluminum plate. The top line represents the top face of the material; the bottom line, the back face. Between these two are signals from flaws in the material under test. These flaws prevent the

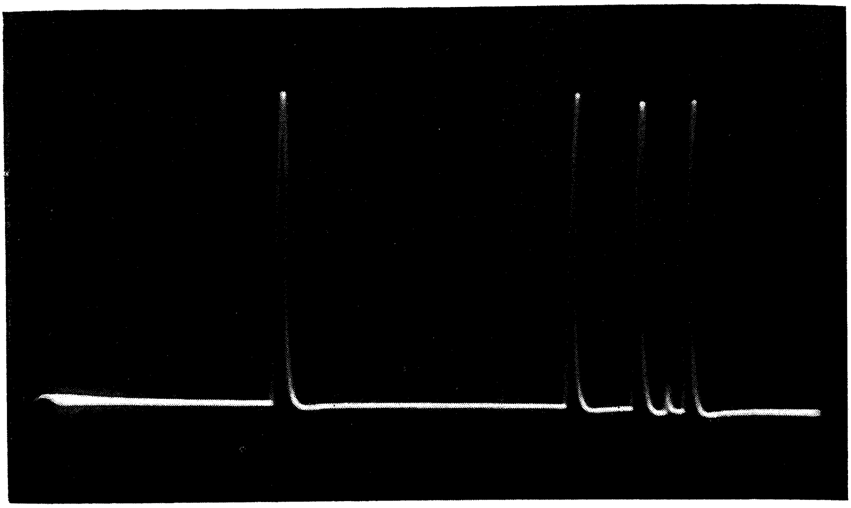

Electrocircuits, Inc.

Fig. 3. Presentation of ultrasonic test signals by A scan.

sound from reaching the bottom surface of the plate and so create a shadow on the bottom trace. B-scan presentations may be expanded or contracted to make the size of the presentation larger or smaller than the actual area being scanned. This permits **flaw amplification** and **faster scanning.** When long-persistence screen cathode-ray tubes are used in this application, images remain on the tube for several seconds. This lessens the possibility that the inspector may miss a flaw signal. After a flaw echo is found on the B scan, it is evaluated by reference to the A-scan presentation.

C-Scan Presentation. The C-scan recording of an area of lack of bond in a cemented joint is illustrated in Fig. 5. The C scan on a cathode-ray tube only shows a **plan view of the defective areas** without reference to flaw position between top and bottom surfaces.

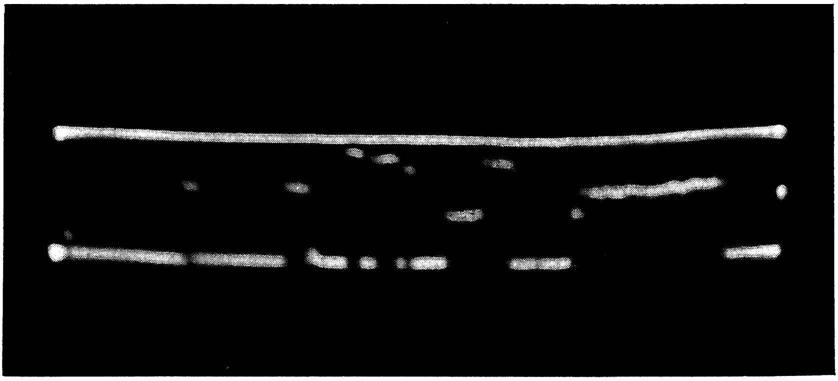

Electrocircuits, Inc.

Fig. 4. Presentation of ultrasonic test signals by B scan.

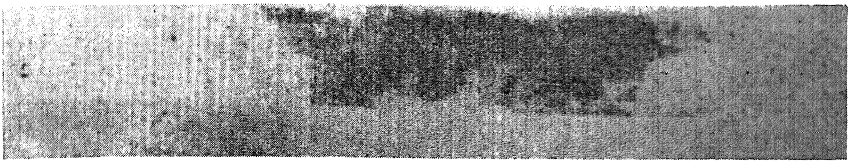

Electrocircuits, Inc.

Fig. 5. C-scan presentation of ultrasonic test signals from poor bond.

Test Equipment and Techniques

INSTRUMENTATION. Ultrasonic test instruments, with a selection of 2.25-, 5-, 10-, 15-, and 25-Mc. **frequencies,** were designed primarily for the inspection of aircraft material and parts by the immersion method (Fig. 6). Such units incorporate a **flaw-warning system,** inch markers to indicate the thickness

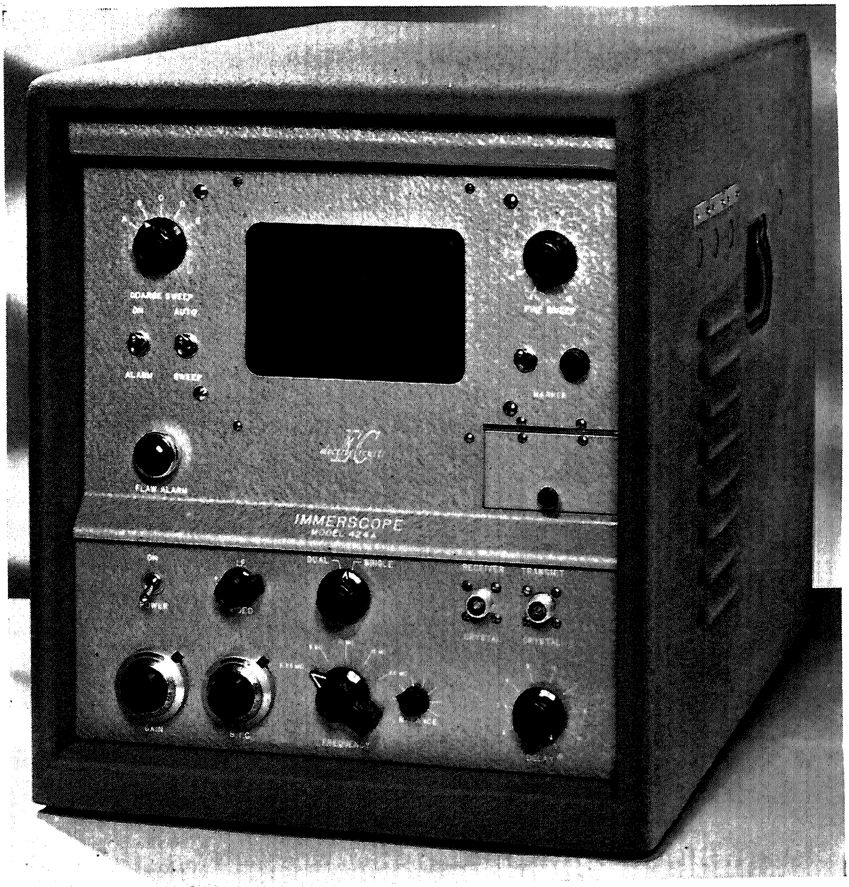

Electrocircuits, Inc.

Fig. 6. "Immerscope" ultrasonic test instrument.

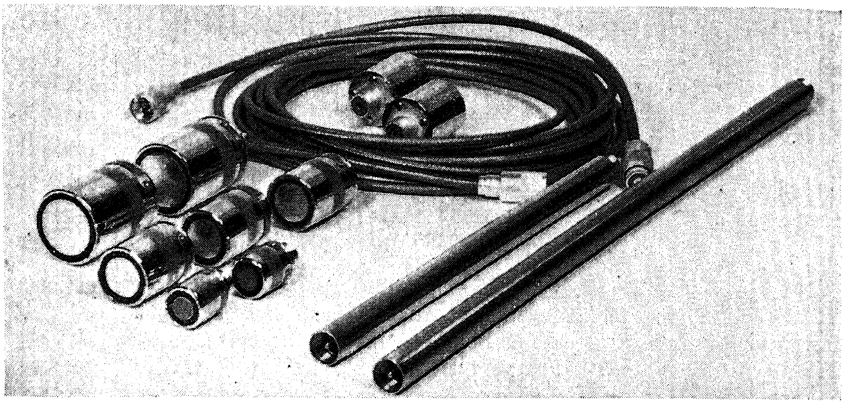

Fig. 7. Ultrasonic flaw detection crystals and search tubes.

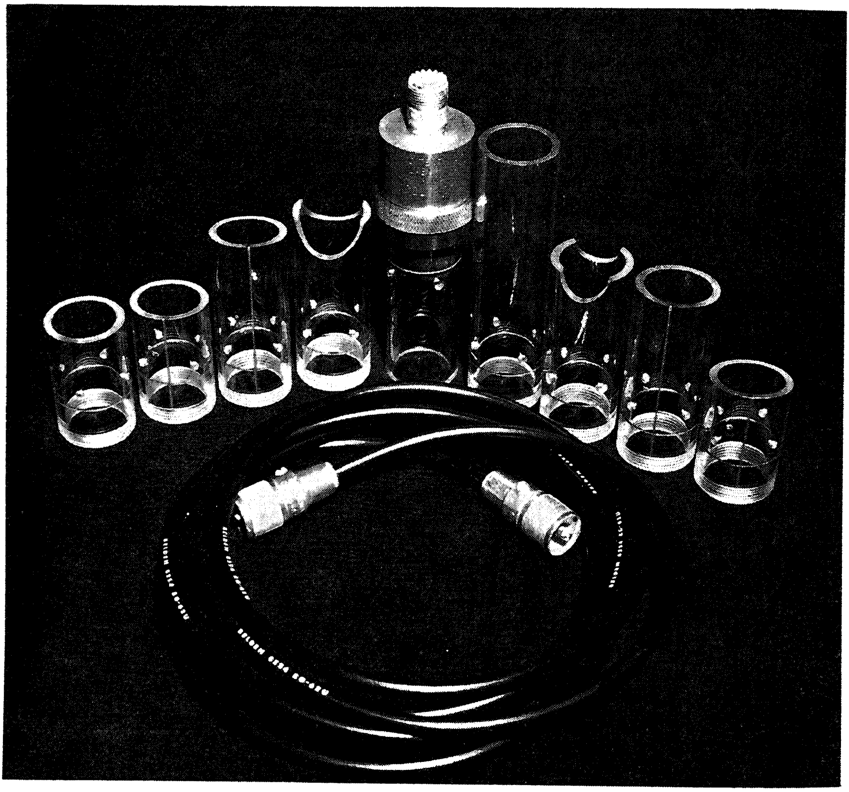

Ultrasonic Testing and Research Laboratory

Fig. 8. Hand-scanning equipment for use with immersed crystals.

of parts being tested, and provisions for recording equipment. The basic instrument presents the A-scan video (detected) signal, showing reflection-signal amplitude (vertically) as a function of time (horizontally).

Transducers and Search Tubes. Typical immersion crystals and search tubes are shown in Fig. 7. The smaller crystals are generally used for flaw evaluation and the larger ones for broad initial scanning. The crystals in general use include X-cut quartz, lithium sulfate, and barium titanate.

Hand-scanning Units. A hand scanner provides greater flexibility for the inspection of forgings and small parts (Fig. 8). Generally, parts are scanned by this technique at a high sensitivity setting. Any questionable areas are marked for a final evaluation with the conventional manipulator set-up. The Plexiglas tube extension which encloses the crystal maintains parallelism by contacting the part while following its contour.

Curved surfaces can be scanned by cutting the Plexiglas extension to fit the surface contour. Longer extensions are used for thicker sections, to maintain a correct water-to-parts interface dimension and to keep the second water-reflection (multiple) indication to the right of that of the first back reflection. **Angle-cut extensions** provide a means for projecting the sound into the test objects at any desired angle.

AUTOMATIC-SCANNING EQUIPMENT. In automatic scanning of a profile, it is essential to maintain parallelism between the crystal face and the profile of the test part. Fig 9 shows a complete unit designed to inspect a symmetrically shaped engine forging. A **punched tape** is made up to match the con-

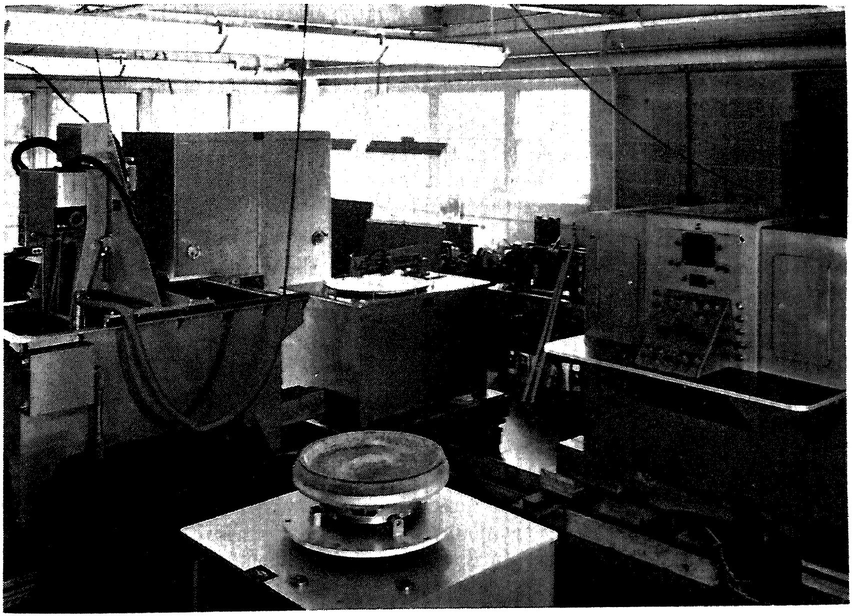

Sperry Products Inc.

Fig. 9. Unit for automatic scanning and recording of immersion ultrasonic test signals.

figuration of the part and is placed in a tape reader, which is similar in operation to a player piano. Before being placed in the ultrasonic scanning tank, the part is first placed on a **set-up table** and positioned both radially and axially. Then the part and set-up table are placed in the tank, and the machine is started. While the part and set-up are being rotated on a turntable, the holes in the tape actuate the scanning mechanism so that the submerged searching-unit crystal follows the contour of the test part. As sound waves penetrate the part, a **recorder** traces a line on a paper disc. When flaws are detected, deviations from the circular trace show their approximate size and locations. The flaw signals also appear on the oscilloscope screen in the monitor console. The sensitivity of the unit can be adjusted to overlook echoes from flaws of any predetermined size.

Advantages of Automatic Scanning. The advantages of automatic immersion ultrasonic testing are:

1. In the past, it was necessary to procure forgings that were oversized so that they could be "square cut" to provide flat and parallel surfaces for manual contact ultrasonic tests. Immersion units eliminate the need for flat and parallel surfaces. Consequently a smaller forging can be used. This reduces the investment in forgings, since they can be procured closer to final configuration.
2. Less inspection time is required.
3. Inspector decision is eliminated. Machines can be adjusted to sort automatically to predetermined standards.
4. Better control of quality is provided, since:
   a. The machine automatically searches the entire area of the test object, ensuring complete examination.
   b. Immersion testing makes it possible to search areas not accessible to manual contact testing.

Long Tank Units. Electrically driven, automatic units similar to the one shown in Fig. 2 are used for the inspection of long sections. Such units are particularly useful for inspection of extruded and rolled sections as well as of long blooms.

Turntable Units. Cylindrically shaped parts may be inspected conveniently by using a **motor-driven table** (Fig. 10). As the part is rotated, the scanner is positioned over the center of the part and travels toward its outer rim. The hand scanner may be used to project the sound through the sides of the pieces, or a **right-angle adapter** may be used in preference to the hand scanner.

USE OF HIGH-FREQUENCY WAVES. Higher test frequencies offer advantages in immersion ultrasonic testing. Low frequency or longer wavelengths permit ultrasonic penetration to greater depth in the material, but this deeper penetration may cause the loss of near-surface resolution and small flaw detection. To compensate for the loss of near-surface resolution, the part should be scanned from both surfaces. For example: A quartz crystal of 2.25-Mc. frequency range may not reveal flaws closer than 1 in. to the near-surface of the part. At 5 Mc. this **blind area** may be reduced to ½ in.; 15 Mc. may show flaws ⅛ in. from the surface; and at 25 Mc. this blind area is reduced to approximately ¹⁄₁₀ in. With short-duration pulses used at these high frequencies, **small discontinuities** with surfaces paralleling the face of the material are clearly defined if they are not too distant from the material face. In deciding which frequency to use, it must be remembered that the lower frequencies may reveal **unfavorably oriented flaws** that could be missed at the higher frequencies. Since the immersion method does not require the crystal to contact the material being tested, there is no **crystal wear** such as that occurring in contact testing, and hence the high-frequency technique becomes most useful.

Loss of Near-Surface Resolution. The loss of sensitivity to near-surface flaws is very important when the part will not receive sufficient machining to remove surface layers.

Various effects have been suggested to explain the **blind area** near the surface of the test material.[1] These include: (1) the near-field zone effect, and (2) the theory that the crystal (which alternately acts as a transmitter and a receiver) does not have enough time to stop ringing in this short interval. Consequently the received signal is partially blocked by the remaining vibrations of the original or transmitted pulse.

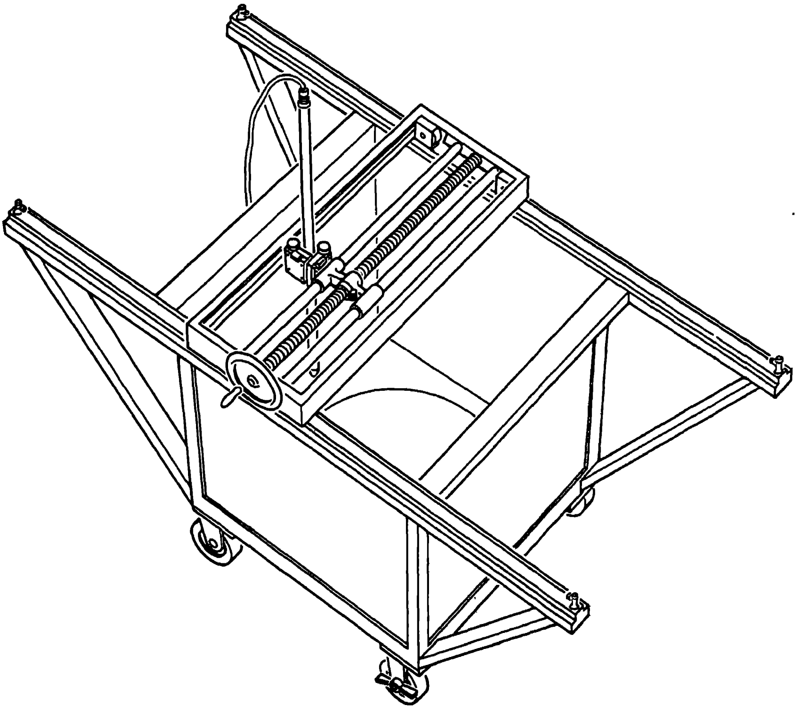

Aetna Engineering

Fig. 10. Motor-driven turntable for immersion ultrasonic inspection of cylindrically shaped parts.

LIMITATIONS IN BEAM PENETRATION. Unfortunately some materials cannot be tested at high frequencies. In such a case, one must sacrifice some of the near-surface inspection area in order to penetrate the material satisfactorily. This blind area can be inspected by turning the part over and **reinspecting from the opposite side,** if the geometry of the part makes this possible.

Evaluating Beam Penetration.[1] To determine the ability of the ultrasonic beam to penetrate the material at the selected frequency, one can select a piece of material having parallel front and back surfaces and count the total **number of back echoes** received from the part. If there is no back echo, it is necessary to use a lower frequency. A single back echo may indicate poor transmission, while several back echoes may represent a combination of frequency and gain setting very adaptable to the material under test.

Use of Test Blocks. To test a piece of rectangular hand-forged aluminum, a high-frequency crystal should be chosen to provide good back-signal resolution. A test block with its test-hole face about ½ in. below the block face should be selected to give an initial sensitivity of at least a full-amplitude signal from the test hole. Another test block should then be chosen, in which the distance from the front surface to the test hole is equal to the thickest section of the part being tested. This block should also give at least one full-amplitude signal from the hole. If this test-hole signal is greater than the signal from the block with the ½-in. dimension, the setting is left unchanged. If it is less, the sensitivity is increased to give at least one full-amplitude signal. When the proper signals are received from both blocks, this setting assures the operator that he will be able to "see" flaws, both in the near-zone and in the thickest area of the material, equal to the size of the flat-bottom test hole in the test block selected. (This technique applies to the "Immerscope" and may not be adaptable to other equipment.)

Control of Water Distance.[1] The water distance (between the crystal and the test block) should be equal within ¼ in. for both settings. This distance should be enough to keep the **second water reflection** to the right of the first back reflection. This second signal, and multiples of it, can be seen by moving the scanning tube up and down and watching the set of signals that starts to overlap the working signals. The normal loss of test-hole signal height is caused by the **attenuation of sound** going through the longer-length test blocks. This effect is common to all ultrasonic reflection testing. The use of test blocks permits compensation for variations in crystals, alloys, equipment, and equipment nonlinearity. Some equipment provides a **time sensitivity or swept-gain control** which automatically compensates for attenuation loss due to increasing thicknesses of material (for any one type of material). Test blocks should be used to adjust this control.

Adjusting Marker Circuit. If the ultrasonic equipment being used has a 1-in. marker circuit set for aluminum, the same test blocks can be used for adjusting these markers to correct for the **velocity-of-sound differences** in various materials. For example, when using a 10-Mc. quartz crystal and a piece of 4130N steel of 6-in. thickness, the markers would be adjusted to indicate 6 in. Then, if a 6-in. piece of aluminum is checked at this setting with no further adjustment, its thickness would be indicated as approximately 5½ in. The difference between the two indications represents the difference in time it takes for sound to travel through aluminum as compared with steel. Since sound travels slower in steel, the transit time increases and the distance between the face and back A-scan signals becomes greater.

Effect of Test Materials

COMPOSITION OF MATERIAL.[1] While the speed of sound varies somewhat in various metals and alloys, most metals and alloys are good conductors of ultrasound. **Wrought and forged aluminum** are relatively good conductors of sound at the test frequencies generally used. Carbon, molybdenum, and vanadium **steels** require slightly more energy but nevertheless are readily inspected with present equipment. Most alloys of **titanium** are ultrasonically similar to steel and can be inspected at the same frequencies. Some **stainless steel alloys** offer more resistance to sound, but present equipment can be used very successfully in the lower frequency ranges of 1 to 5 Mc. **Magnesium** in extruded, forged, or wrought form is readily inspected at the higher frequencies.

STRUCTURE OF MATERIAL. Generally, irregularly shaped parts **cast** from aluminum and magnesium are not adaptable to ultrasonic inspection except at low frequencies where gross defects, such as **gas pockets or large inclusions,** can be revealed. Variables which limit the use of higher frequencies include heavy gas porosity, grain size or orientation, and segregation. **Large cast ingots** of aluminum and titanium can be inspected over a frequency range from ½ to 10 Mc. by both contact and immersion methods. It is usually preferable to inspect typical nonferrous aircraft castings by radiography, fluoroscopy, or liquid-penetrant tests.

SURFACE FINISH AND RADIUS.[1] Normal rolling, extruding, and forging shapes and finishes do not materially affect the signal response or cause difficulty in evaluating flaw sizes. (See section on Ultrasonic Fields for detailed analysis of effects of surface roughness.) Fig. 11 shows test blocks made to evaluate these effects. The tests were made by first recording the signal response from test blocks with normal surface finishes, each having a flat-bottom test hole ¾ in. deep.

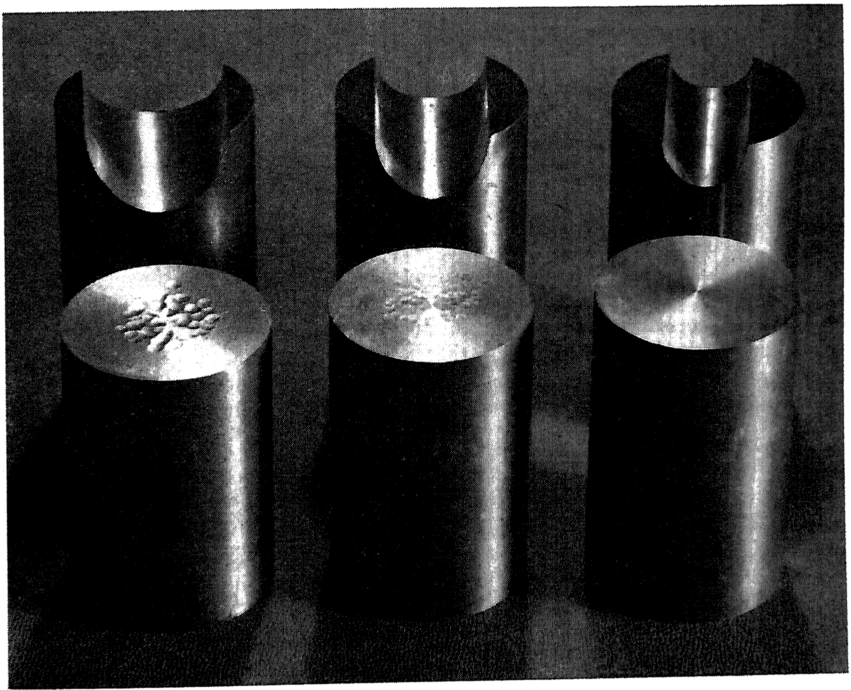

Ultrasonic Testing and Research Laboratory

Fig. 11. Ultrasonic test blocks used to determine surface shape and finish effect in relation to flaw-signal response.

Surface Roughness.[1] After these values were recorded, three test blocks were reworked as follows:

1. One block face was sandblasted; a retest did not indicate any loss of signal response.
2. The second block was lightly peened, and a loss of about 20 percent of the original signal response was noted.
3. The third block was heavily peened, and the signal response dropped to about 25 percent of its original height.

Surface Contour.[1] Three additional blocks had cylindrical grooves cut into their front surfaces, as shown in Fig. 11. The smallest radius reduced the signal response from the test hole to about 80 percent of its original height before the cylindrical cut. The second one reduced the signal height to about 45 percent. The third reduced the sound height to about 25 percent. With both peened and radius-cut blocks, the **loss of signal response** may be a consequence of refraction of the sound at the surface of the block.

Angle of Surface.[1] Tests of smooth-finished blocks with front surfaces at angles from the horizontal indicated no appreciable loss of energy when manipulation of the crystal was used to correct for the angle. **Angle-cut blocks** with angularity greater than 8 deg. caused increasingly greater loss of signal response.

EFFECT OF HEAT TREATMENT.[1] Some test work has been done to determine the effect of heat treatment on the signal response from flaws. Several 7075 SF aluminum alloy forgings which contained defects in the **"as-forged" condition** were carefully evaluated ultrasonically by recording the flaw signal height obtained from singular or individual types of defects. When these forgings were then **heat treated** to the T4 condition, the flaw signals increased in height. Similar forgings in the same (as-forged) condition were machined into symmetrical shapes to provide parallel face and back surfaces. The flaw signals were recorded; subsequent heat treatment (from T4 to T6) again gave a slight additional increase in the flaw signal height.

This would indicate that, for more **accurate flaw evaluation,** the forgings should be ultrasonically tested in the heat-treated condition. Since machining may be difficult, due to distortion from residual stress in the T4 or T6 condition, it may be necessary to heat-treat forgings, omit the quenching operation, and allow them to air-cool. It appears that taking the forgings up to solution temperature and air cooling has approximately the same effect (increased signal magnitude) as solution heat-treating followed by quenching to T4 condition.

Ultrasonic Test Blocks

SLOTTED-BLOCK TECHNIQUE FOR STRINGER-TYPE FLAW EVALUATION. When a discontinuity is found which appears to have appreciable length (up to 1 in.), and it is desirable to know how long it is, the test blocks illustrated in Fig. 12 are used.

Stringer Length Technique. The following technique is applicable for determining stringer length:

1. While the search crystal is over the major discontinuity area, increase signal amplitude, and at this high sensitivity setting, measure the distance that the crystal travels in scanning the flaw length.

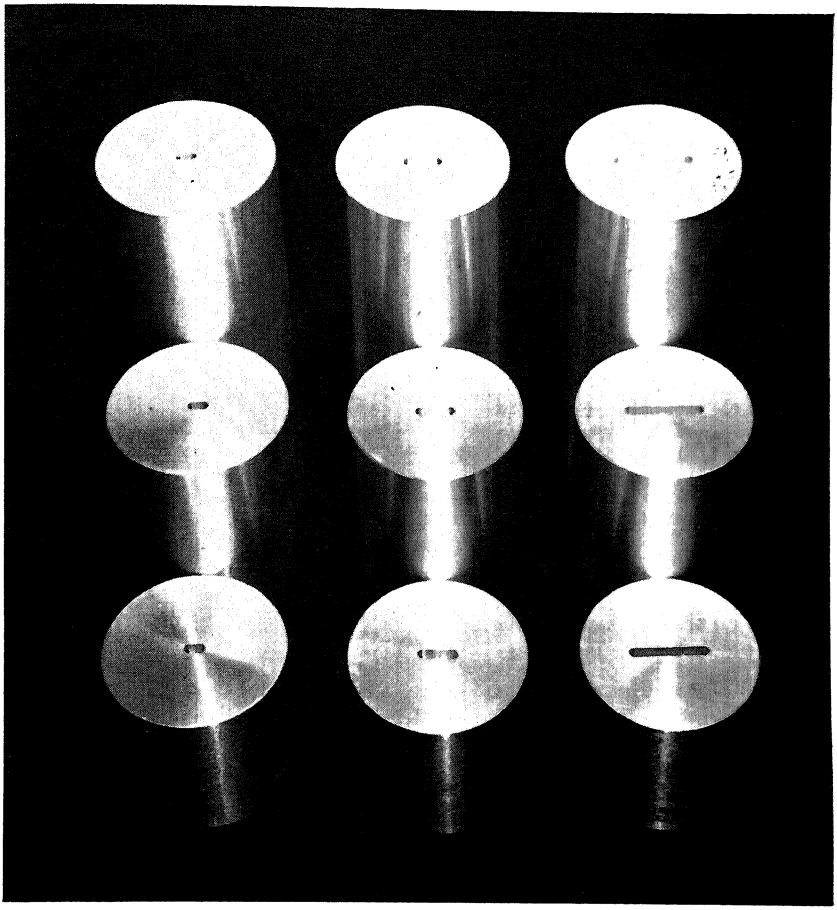

Ultrasonic Testing and Research Laboratory

Fig. 12. Slotted blocks used to determine length of discontinuities in ultrasonic testing.

2. To make this measurement, proceed as follows:
   a. Approach one end of the discontinuity with the crystal moving parallel to the front surface of the part and centered over the major area of discontinuity. As soon as the signal from the flaw reaches a height of approximately ¼ in., stop the carriage and note the carriage index position with a mark on the tank carriage track.
   b. Continue moving the crystal carriage over the discontinuity (the signal will increase in amplitude). As the end of the discontinuity is approached, the signal will decrease in amplitude.
   c. When the signal diminishes to ¼-in. amplitude, stop the carriage and again mark the tank track position to coincide with the reference mark on the carriage.
   d. Measure the distance between the two marks on the track. This is the distance the carriage moved while the defect signal was maintained on the cathode-ray tube.

3. Select a slotted test block of a similar alloy, whose length (from top surface to the slot) is equal to the approximate distance from the surface of the test piece to the flaw. Place this test block below the crystal so that (a) its slot-end is down and (b) long dimension of the slot parallels the direction in which the carriage will travel when moving the search crystal over the simulated flaw.
4. Adjust the vertical distance of the crystal to provide the same water distance as was used in measuring the flaw length. Do not make any changes in the instrument setting used to measure the length of the actual flaw. Use the same technique as that used to measure the flaw, and compare the travel distance for the two tests to determine flaw length. If the slot in the test block shows a longer carriage-travel distance than the flaw, select a test block with a shorter slot and repeat the test.

Stringer Width Technique. The same technique is used to measure the width of discontinuities. In this case **slotted blocks** are selected with slots cut across the center of the block. Each slot is ½ in. deep. The widths are cut to correspond to stringer-type flaw widths, varying in width from 1/64 to ½ in. The purpose of the technique is to measure the distance the carriage travels in crossing this slot and to compare this distance with the distance the carriage travels in crossing an actual stringer-type flaw. These blocks are made in various lengths.

System Characteristics. This system compensates for any combination of crystal sizes, frequencies, and gain-setting variables if the stringer and machined block are tested under the same conditions. Since signal response is a function of crystal size, frequency, and sensitivity, the use of test blocks of these types provides a practical method of determining the length and width of stringer-type flaws in production testing.

Slotted-Block Characteristics. Block lengths varying by 1-in. increments (measured from bottom of slot to face of block) should provide adequate accuracy for normal testing for stringer-type defects from ½ to 7 in. below the surface of the test material. These test blocks are made in sets of seven, all of equal length but with slot widths of 1/64, 1/32, 1/16, ⅛, 3/16, ¼, ⅜, and ½ in. An eighth block is a standard flat-bottomed reference block used for the initial sensitivity setting.

CONSTRUCTION OF STANDARD TEST BLOCKS.[1] The standard test blocks illustrated in Fig. 13 are made from carefully machined, ultrasonically inspected, rolled, 4130 normalized bar stock with 5/64-in. diam., flat-bottomed test holes. Similar test blocks can be produced in various metallic materials, in square or round shapes, and with flat-bottomed test holes of various diameters. Each flat-bottomed test hole is drilled ¾ in. deep in the bottom center of the test block. Extreme care must be taken in the preparation of test blocks. Stock is carefully selected to meet predetermined standards covering attenuation factors, grain size, and heat-treat condition. Ultrasonic equipment must be monitored and controlled.

Test-Hole Depths. The first test-hole face is 1/16 in. from the front surface or block face; the second, ⅛ in.; and subsequent hole depths increase in ⅛-in. increments up to 1 in. The next block is 1¼ in., and thereafter each subsequent block length increases in ½-in. increments up to 5¾ in.

USE OF STANDARD BLOCKS. Test blocks serve as a reference or a means of comparison to evaluate the size of small flaws in material. Blocks of different lengths are used as a means of adjusting test instrument sensitivity to indicate a simulated flaw (flat-bottomed test hole) at a prescribed height on the A-scan presentation.

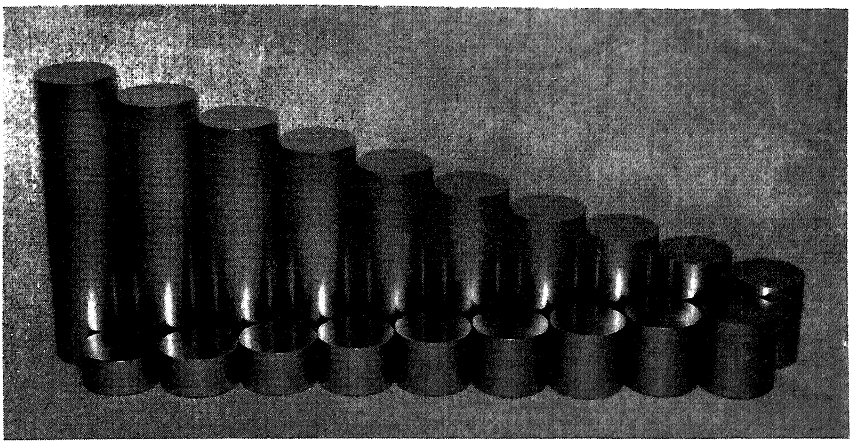

Ultrasonic Testing and Research Laboratory

Fig. 13. Ultrasonic test blocks used to determine flaw sizes.

Estimating Flaw Area. Suppose that a flaw is found at a depth of 4 in. and reflects a flaw-signal height of 1 in. on the screen of the cathode-ray oscilloscope. If the specification requires rejection of any part with a flaw having a cross-sectional area greater than a 5/64-in. diam. hole, the following procedure would be used:

1. Select a test block of similar alloy of rolled or forged stock with a 5/64-in. diam., flat-bottom hole approximately 4 in. from the block face.
2. Adjust the signal response from this test block (by sensitivity control) to display an arbitrary indication height of 1 or 2 in. (the choice of signal height is immaterial).
3. This signal height is then compared with the height of the signal from the flaw in the part. If the flaw-signal height at this setting is greater than that received from the test block, the cross-sectional area of the flaw will usually be greater than the acceptance standard. If it is less, the test object may be acceptable under the specification.
4. The same procedure can be repeated, using reference blocks with smaller-diameter test holes to determine the actual size of the flaw.

Test blocks may be used with any combinations of crystals and frequencies. However, the same combinations must be used for comparing defect size in the part being tested with the hole size in the test blocks.

STANDARD BLOCK RESPONSE CHARACTERISTICS.[1] The response curve obtained from a set of test blocks may vary with distance, frequency, crystal size, sensitivity level, ultrasonic instrument, and type of crystal in use.

Test Condition. Fig. 14 shows comparative response curves obtained by test under the following conditions:

1. A set of 19 blocks of 4130N steel with 5/64-in. test holes was used for all curves.
2. The ultrasonic test instrument was energized through a "Sola" constant-voltage regulator with harmonic suppressor.
3. Video-type presentation was used.

DATE 1-6-56

ULTRASONIC TEST CURVE

TEST ENG. KBA

CRYSTAL SIZE NOTED IMMERSED X CONTACT ____

FREQUENCY NOTED CRYSTAL TYPE NOTED TEST BLOCK HOLE DIA. 5/64"

CRYSTAL TO BAR FACE DISTANCE 1 1/2 APPROXIMATE

REFERENCE SETTING: VISIBLE SIGNAL FROM 1ST & LAST BLOCK

MATERIAL USED FOR MAKING TEST BARS: 4130 N

REFLECTOSCOPE ____ WIDE BAND CONVERTER ____ IMMERSCOPE X

3/4" 5MC LITHIUM SULFATE - - -
3/8" 10MC QUARTZ ——
3/8" 5MC QUARTZ ·······
3/4" 5MC QUARTZ ••••••
3/4" 10MC QUARTZ ——

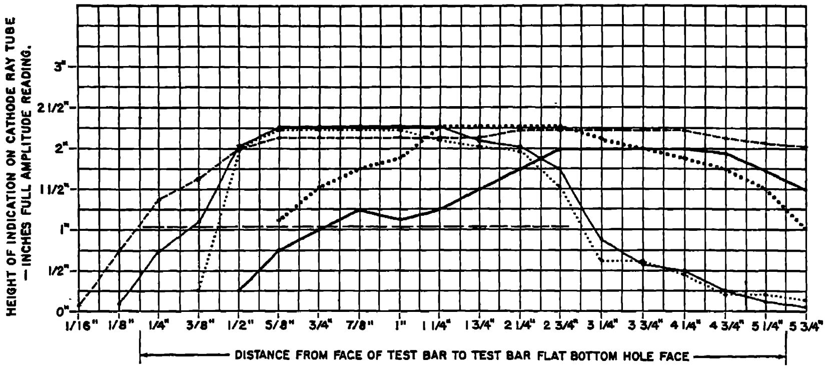

Ultrasonic Testing and Research Laboratory

Fig. 14. Comparison curves obtained by using various crystals and frequencies in immersion ultrasonic testing.

4. The initial amplifier gain setting for each curve was made by increasing the gain to the point where a readable signal could be obtained from the hole in the shortest block. Considerable gain is needed to obtain a signal from this short block, due to the near-zone effect (or jamming) of the received signal.

Results of Tests. From the tests, it was concluded that:

1. The flat area of the curves at the 2¼-in. height indicates saturation on the instrument amplifier.
2. The curves indicate that, at the frequencies and gain settings used, the near-zone lies between 1/16 in. and ⅝ in. (face-to-flaw distance) for the ⅜-in. diam. quartz crystals and the ¾-in. diam. lithium sulfate crystal.
3. The ¾-in., 10-Mc. quartz crystal response is affected by the near-zone between ½ in. and 2¾ in. The jamming of this crystal makes it blind in the 1/16-in. to ½-in. zone.
4. The ¾-in., 5-Mc. crystal is blind to ⅝ in. below the surface, and its near-zone extends to 1¼ in. depth.
5. At 10 Mc., the ⅜-in. quartz crystal "could see" as close as ⅛ in. from the surface, and its near-zone extended only to a ⅝-in. depth.
6. Excellent results are obtained from the ¾-in. lithium sulfate crystal. This obviously eliminates many of the difficulties found with other crystals used with this equipment. Next in performance to the lithium sulfate crystal is the ⅜-in. quartz crystal used at 10 or 15 Mc. It is excellent for near-surface evaluation, but response falls off rapidly in material over 2¾ in. thick.
7. All the ¾-in. diam. crystals operating either at 5- or 10-Mc. frequency can see much farther than ⅜-in. crystals. Their signal strengths do not start to drop off by any appreciable amount up to 5¾ in. of depth. Note the slight loss of signal strength in the lithium sulfate.

8. Operators should be aware of the limitations of ultrasonic equipment and crystals, and should select a combination best suited to the problem.

The curves of Fig. 14 were obtained under laboratory conditions. For practical testing, it would be advisable to use the next longer block for minimum near-surface readings.

Equipment manufacturers have designed electric circuitry within the instruments to provide automatic compensation for variations in response from flaws at various distances from the surface. This system is generally called S.T.C., or **sensitivity-time control.** To use this system, it is advisable to adjust the test unit to a set of test blocks of a material similar to the material being tested. For **flaws in the near-zone,** it is best not to depend on this method. It is a very practical method where the majority of work is done on one type of material and where the near-zone flaws are not too important.

Industrial Inspection Procedures

TYPICAL SPECIFICATIONS. Generally the sensitivity and flaw-evaluation scanning level are noted in the test specification. A typical specification for use in immersion testing may read as follows:

> For initial scanning, the sensitivity level will be such as to produce one full-amplitude signal from a test block of similar alloy having a flat-bottomed test-hole distance of ⅜ in. from the surface of the test block. A second check on another like test block whose distance to the test hole will be equal to the thickness of the part should produce equal or greater signal response from the flat-bottomed test hole.

If the specification does not state the setting, the preceding minimum requirements should be used. The specification may then say that "all flaws found at this setting having a signal height greater than ½ of full amplitude will be marked for final evaluation." The specification may next require that "for final evaluation, a ⅜-in. diam. or collimated crystal will be used (for pinpointing the flaw), and any indication greater than the signal received from a test block with a 3/64-in. or 5/64-in. diam. test hole at an approximately equal distance from the surface will be cause for review."

Sensitivity Adjustment. For this final evaluation it may be necessary to reduce the sensitivity to produce a test-block signal approximately 1 in. or more in height. This will provide a **working range** above and below the 1-in. indication for comparison with the test block. As part of the final evaluation it may be necessary to manipulate the crystal to effect **parallelism** between the crystal and flaw faces, to obtain maximum signal height.

Scanning Procedure for Flat Surfaces. If the test part is symmetrical, one may start at one edge and sweep its length while watching the A-scan picture tube for defect indications. At the end of this sweep, the search tube may be moved transversely for a distance equal to three-fourths of the width or diameter of the crystal, and another sweep may be made. This should be repeated until the total surface is scanned.

CHECKING FLAW INDICATIONS. If a flaw is found, it may be advisable to check it from both faces and through the side of the material if possible. If manipulation of the search tube is required, it must be remembered that the **actual refracted angle,** at which the sound is traveling through the part to intersect the flaw, will be of the order of four times the manipulated or incidence angle of the search tube (see section on Ultrasonic Fields).

Identification of Sources of A-Scan Indications. From left to right in the A-scan indication of Fig. 15, the first signal (1) is from the crystal-water interface, the second signal (2) from the water-to-material interface, and the third signal (3) from any flaw present in the piece being tested. The last signal (4) on the right is the echo from the back face of the part. Repetitions of these same signal groups (5) may appear still farther to the right of the back-surface echo (4).

Determining Flaw Position. Assuming that the flaw is 3 in. below the front surface of the part and that a 5-deg. manipulation angle is used, the flaw can be estimated as being approximately 3 in. below the surface at an angle of nearly 20 deg. from the point where the sound strikes the face of the material. This

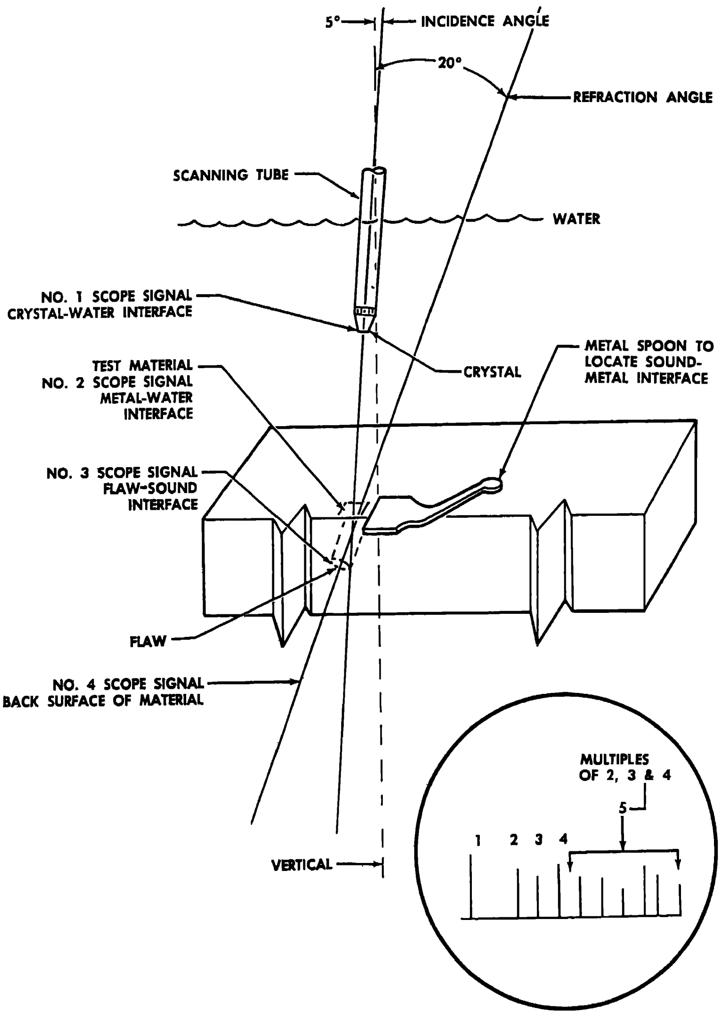
5°
INCIDENCE ANGLE
20°
REFRACTION ANGLE
SCANNING TUBE
WATER
NO. 1 SCOPE SIGNAL CRYSTAL-WATER INTERFACE
CRYSTAL
TEST MATERIAL NO. 2 SCOPE SIGNAL METAL-WATER INTERFACE
METAL SPOON TO LOCATE SOUND-METAL INTERFACE
NO. 3 SCOPE SIGNAL FLAW-SOUND INTERFACE
FLAW
NO. 4 SCOPE SIGNAL BACK SURFACE OF MATERIAL
VERTICAL
MULTIPLES OF 2, 3 & 4
5
1 2 3 4

Fig. 15. Analysis of A-scan signals in angle-scan immersion ultrasonic testing.

angle of refraction varies with materials of differing **acoustical velocities.** To determine where the sound is striking the material, one can place a straight-edged piece of metal **(metal spoon)** on the surface of the test object and move it toward the area where the sound is entering the test object. As soon as the leading edge of the metal plate enters this area, a signal will appear on the oscilloscope. This point is marked on the part. The same check is repeated from the other three sides of the beam, as illustrated in Fig. 15. It should be remembered, however, that only if the search tube is perpendicular to the surface of the test object will the flaw lie directly beneath the marked area. Otherwise an allowance must be made for the refraction of the sound beam.

OFF-CENTER SCANNING OF CYLINDRICAL PARTS. To obtain a complete inspection of round bar, tubing, and curved sections of die forgings, it is necessary to use a number of "off-center" scans. In these operations the search tube is positioned parallel to the vertical diameter of the section but is displaced to one side of the center of the test object. When the crystal is in an off-center position, the surface under test is at an angle other than normal to the path of the incident sound. Under these conditions, **ultrasonic refraction** occurs. The sound is transmitted through a chord of the cylinder and at a different angle from that which would be transmitted if the crystal had been directed vertically through the diameter.

Scanning Procedure for Cylindrical Surfaces. Successive scans should be made, starting from the center point where the refracted angle is zero, and indexing in one direction until a point is reached where the refracted angle is 90 deg. This technique ensures that **radial discontinuities** will be intersected normally or at right angles to the flaw face, so as to reflect the sound in the proper direction for detection.

FLAW EVALUATION WITH "CYLINDRICATOR." Flaw evaluation is facilitated by use of the "cylindricator" of Fig. 16. This calculator provides a means by which the sound path can be plotted when any of the intermediate stages of the preceding inspection method exist. It is intended that the "cylindricator" graphically simulate the actual test conditions and thus aid the operator in precisely locating any discontinuity.

Measurement Technique. The procedure for flaw location is as follows:

1. The crystal tube is positioned perpendicularly to the nearest tangent point of the part being tested (center line).
2. The sensitivity of the instrument is reduced, and the lateral crystal position is adjusted until a peaking effect of either the front or back signal is noted.
3. This position is marked on the crystal carriage. This should be the center point.
4. The sensitivity is now increased, and the crystal is indexed, without changing the angle of crystal tube. until the defect signal appears.
5. The peaking point of the defect signal is found in the manner described earlier, or by rotating the part until the highest signal magnitude is attained.
6. The position of the crystal carriage is marked at this point also.
7. The distance between these two marked points is referred to as the "horizontal distance from center line."

Setting Up "Cylindricator." The "cylindricator" is adjusted to indicate flaw location as follows:

1. The point is located on the calculator face where the horizontal distance from center line *A* intersects the arc *B*, designated in inches of diameter (see Fig. 16).

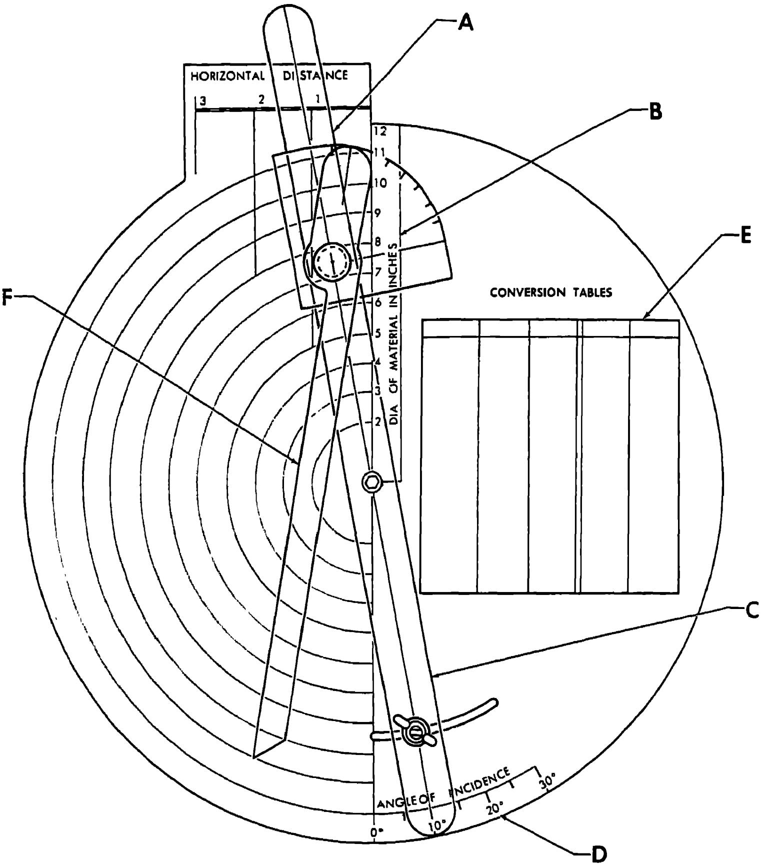

CONVERSION TABLES

ALUMINUM

Incident Angle	Longitudinal	Transverse
1°	4°10′	2°4′
2°	8°22′	4°8′
3°	12°36′	6°13′
4°	16°55′	8°18′
5°	21°19′	10°23′
6°	25°51′	12°29′
7°	30°32′	14°36′
8°	35°29′	16°44′
9°	40°46′	18°52′
10°	46°24′	21°3′
11°	52°43′	23°14′
12°	60°7′	25°28′
13°	69°44′	27°43′
13°52′	90°	
14°		30°2′
14°40′		

STEEL

Longitudinal	Transverse
3°57′	2°7′
7°56′	4°14′
11°56′	6°22′
15°59′	8°30′
20°8′	10°38′
24°33′	12°48′
28°46′	14°58′
33°21′	17°9′
38°10′	19°21′
43°18′	21°35′
48°54′	23°51′
55°12′	26°8′
62°41′	28°29′
72°50′	30°50′
90°	

Ultrasonic Testing and Research Laboratory

Fig. 16. "Cylindricator" used to determine sound path in off-center scanning of cylindrically shaped parts.

2. The angle indicator *C* is adjusted so that it also intersects the point *AB*.
3. The angle indicator is locked with the thumbscrew, and the angle of incidence is read from the scale at *D*.
4. The corresponding refracted angle is found in table *E*.
5. The refracted angle is set on protractor *F*.
6. Protractor *F* is positioned so that the pivot point is superposed over the point intersected by *A*, *B*, and *C*.

Reading "Cylindricator." The "cylindricator" is now set up to simulate test conditions. The intersection of *ABC* represents the **point where sound enters the part,** and the indicator on the protractor *F* denotes the **direction or path of sound.** For a numerical value of the **refracted angle** in relation to the original vertical center line, subtract the incident angle from the refracted angle. The distance from the point *ABC* to the defect can be determined by comparison with a standard reference block or by oscilloscope marker system.

Typical Industrial Applications

INSPECTION OF CYLINDRICAL FORGING. An inspection set-up for a typical **landing-gear forging** of aluminum alloy is shown in Fig. 17. The raw forgings have centers drilled at both ends to provide the means of mounting them in the fixture.

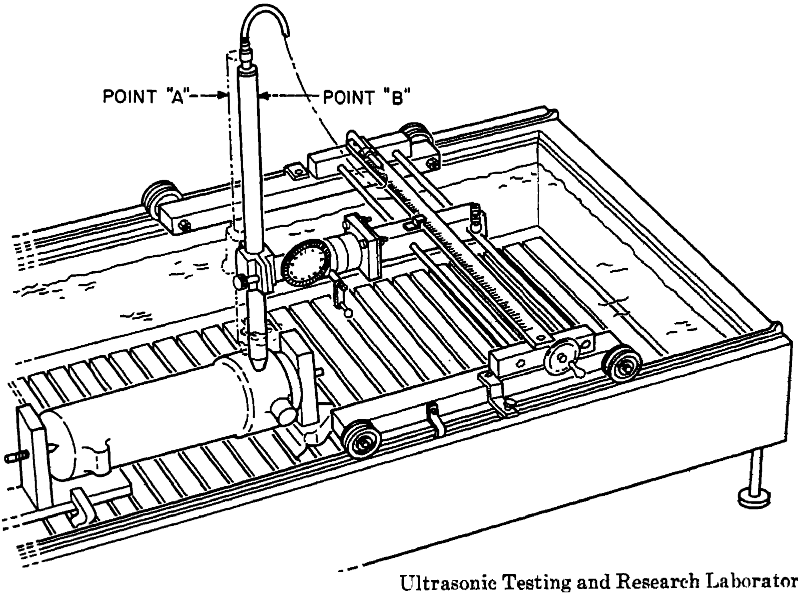

Ultrasonic Testing and Research Laboratory

Fig. 17. Ultrasonic inspection of a typical aircraft part.

Parting Line Region. The cylindrically shaped areas are scanned first with the crystal centered over the part at position *A* while it is rotated by hand. A second scan is made with the crystal moved to point *B*. This provides a shear-wave sound path adaptable to picking up **cracks** at or near the forging parting line.

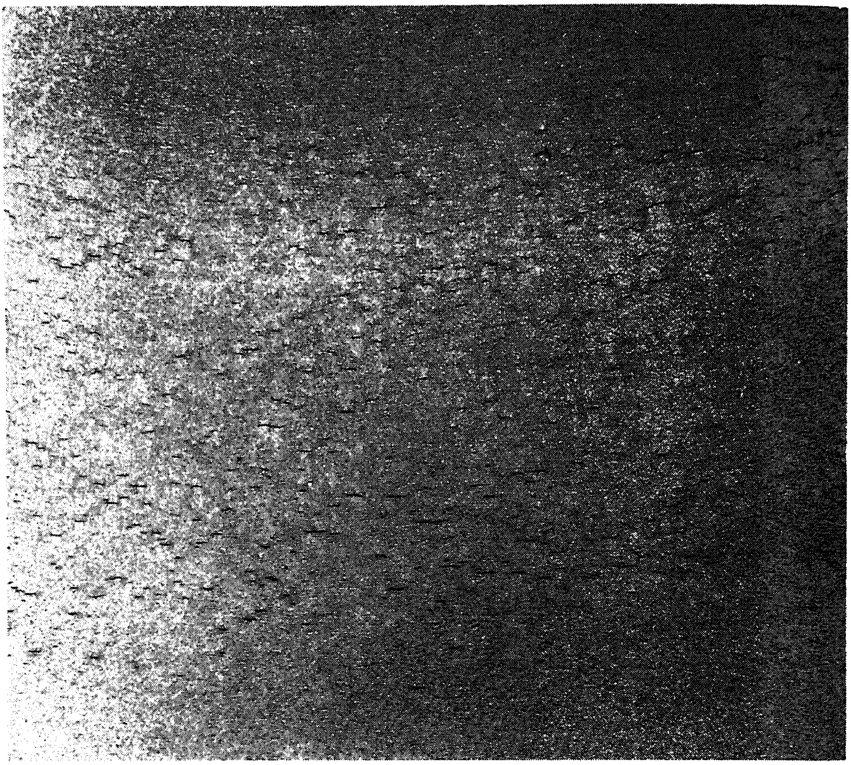

Fig. 18. Etched section of aluminum alloy forging, showing "unhealed porosity."

Bosses or Protrusions. The bosses or protrusions on the part are inspected by using a hand scanner such as those shown in Fig. 8. If defects are found, they are generally **internal cracks** or **unhealed porosity.** Fig. 18 shows an etched section of the forging with an unhealed porosity pattern. Fig. 19 shows these defects in a plan view. The specimen has been fractured to reveal the light areas of discontinuities.

INSPECTION OF TUBULAR OR ROUND BAR STOCK. Fig. 20 illustrates a unit designed primarily to inspect round and tubular stock. The bars to be inspected are placed on the rolls, with the crystals centered over the bars. Two bars may be inspected simultaneously. The **bar rotation and carriage travel speeds** are selected so that the carriage travels three-fourths of the selected crystal width for each revolution of the bar. This **overlap** is necessary to assure 100 percent coverage of the part being tested. If a defect is found in the bar, the operator determines the defective bar by a selector switch, and then, for flaw evaluation, disengages the motor-driven carriage and roll mechanism for hand motion of the carriage and bar.

INSPECTION OF FLAT OR RECTANGULAR STOCK. Flat stock, square, and rectangular materials are inspected with the same unit by removing the rotating mechanism and substituting a supporting fixture for the material. For this operation, an electrically driven carriage may be used.

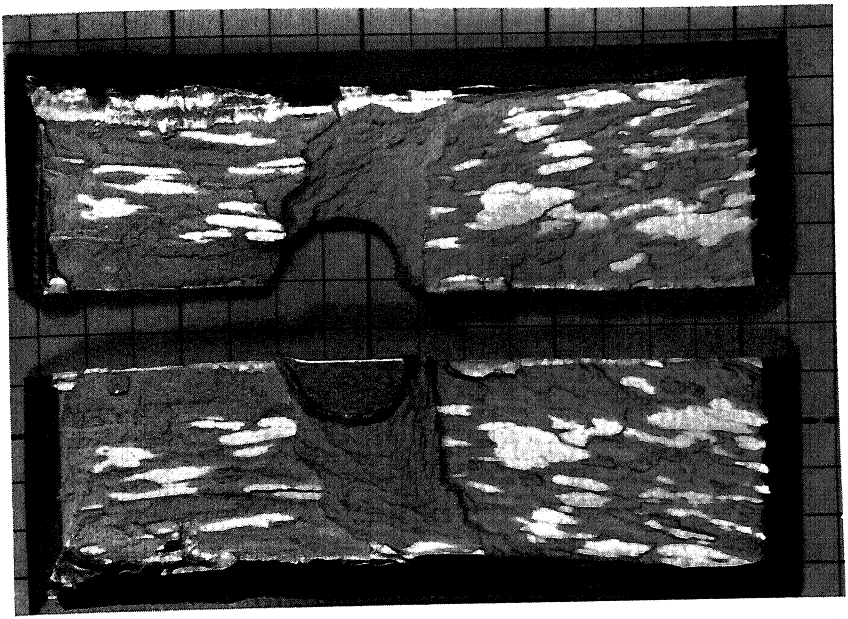

Fig. 19. Fractured aluminum forging, showing (light) areas of "unhealed porosity."

INSPECTION OF TURBINE PARTS. One of the more difficult parts to be inspected by immersed ultrasonics is shown in Fig. 21. The fixture holding the part allows for four **scanning positions.** Position 1 (shown in Fig. 21) is used to inspect the shaft area; position 2, for the face area; position 3, for the hub area; and position 4, for scanning between the fins. In this last position, the crystal position remains fixed. The part being tested is moved by a lever system which sweeps an arc so that the sound enters the curved surface normal to the face of the material. This allows sound to parallel the **forging flow line** where defects usually are found.

Typical Flaws. Fig. 22 shows typical flaws found in the shaft area by this technique. Defects have been found in other areas by using the four-position scan technique.

INSPECTION OF LARGE, CAST, CYLINDRICAL PARTS. Immersion ultrasonic methods of inspection are also adaptable for the inspection of large, cast cylindrical ingots. For example, a 3000-lb., cast titanium ingot may be tested. The ingot is rotated and scanned by projecting the sound through the part. The right angle adapter is used on the tube to project the sound through the side of the casting. This is an excellent method of determining the location of **gas holes and cracks.**

TYPICAL SPECIFICATIONS FOR INSPECTION. The following is a typical aircraft company **specification outline** patterned after the Society for Nondestructive Testing Airframe Committee's recommended specification for ultrasonic inspection of die forgings.

1. **Instrumentation.** The ultrasonic equipment used shall be capable of performing the inspection as governed by this standard, which is applicable to die forgings only.

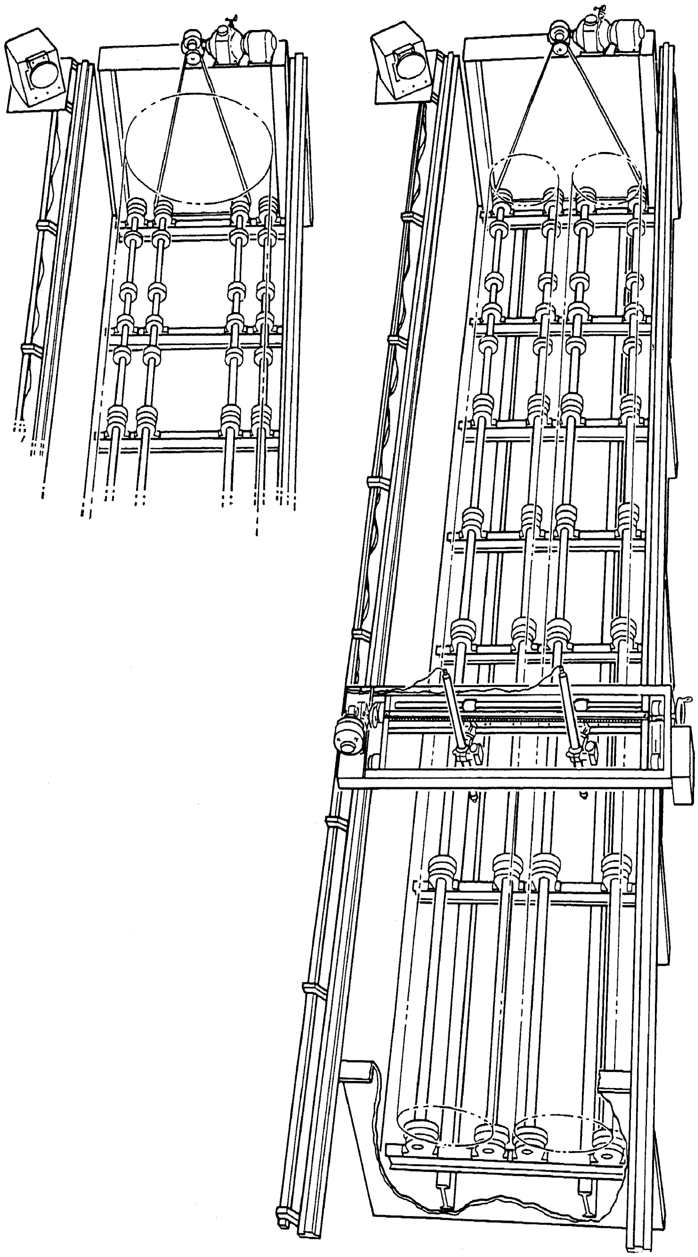

Ultrasonic Testing and Research Laboratory

Fig. 20. Fixture used in immersion ultrasonic inspection of tubular and round bar stock.

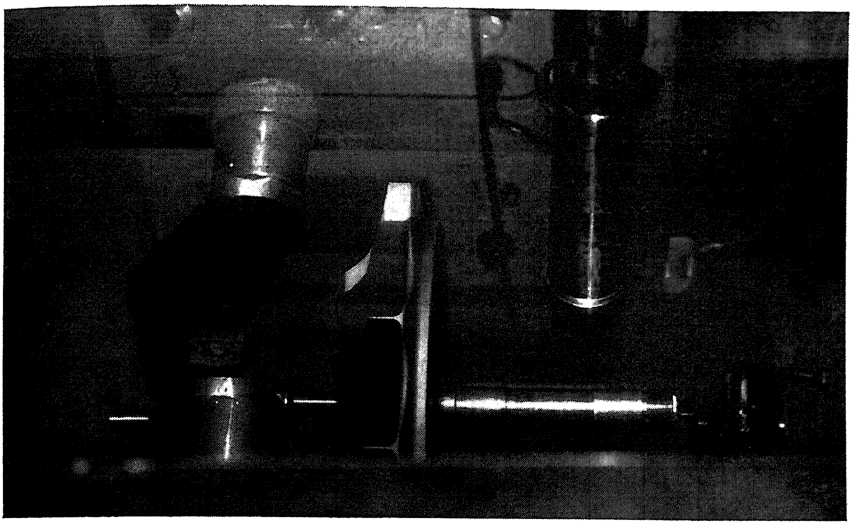

Ultrasonic Testing and Research Laboratory

Fig. 21. Immersion ultrasonic inspection of shaft area of turbine part (position 1).

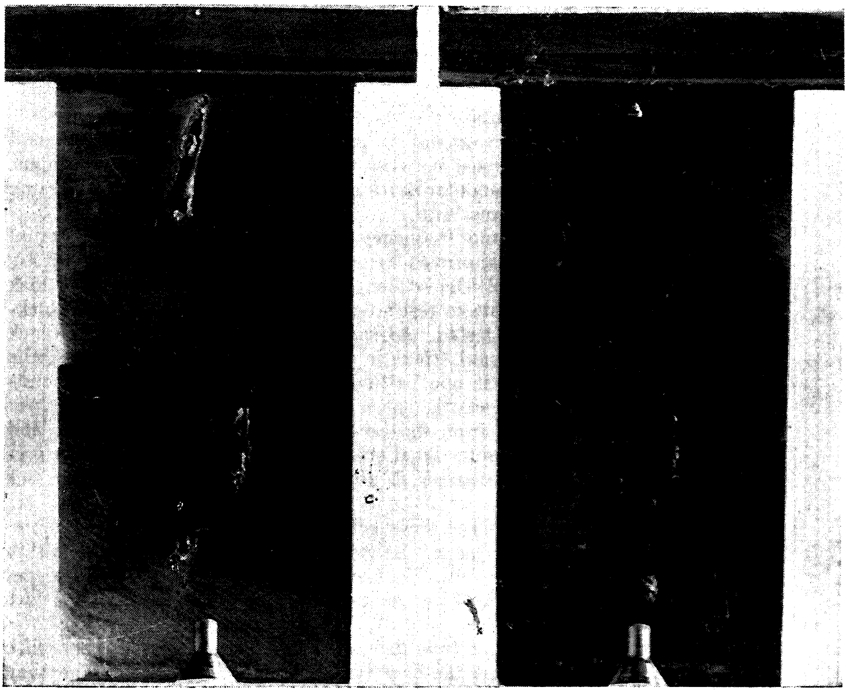

Ultrasonic Testing and Research Laboratory

Fig. 22. Defects found in the shaft area of a turbine part by immersion ultrasonic inspection.

2. **Inspection Technique.** Inspection shall be conducted by the immersion method or its equivalent. Scanning shall be performed either perpendicular to the inspection surface or by angular manipulation to obtain maximum response for individual discontinuities.
3. **Classification Requirements.** The ultrasonic inspection standards may be defined by zoning die forgings on the engineering drawings into three classifications as determined by the direction and amount of stress to be applied to the forging in service and as related to the limits of acceptance as described in Section 4 [of this specification]. If the drawing is not zoned, all areas will be considered Class A.
4. **Acceptance Limits.**
   a. **Class A Areas.**
      (1) No discontinuity indications in excess of 5/64-in. diameter flat-bottomed hole at the estimated discontinuity depth shall be acceptable.
      (2) Multiple indications in excess of a 3/64-in. diameter flat-bottomed hole shall not have their indicated centers closer than 1 in.
   b. **Class B Areas.**
      (1) No discontinuity indications in excess of an 8/64-in. diameter flat-bottomed hole at the estimated discontinuity depth shall be acceptable.
      (2) Discontinuity indications in excess of a 5/64-in. diameter flat-bottomed hole at the estimated discontinuity depth shall not have their indicated centers closer than 1 in.
   c. **Class C Areas.** No discontinuity indications in excess of an 8/64-in. diameter flat-bottomed hole at the estimated discontinuity depth shall be acceptable.
   d. Discontinuity indications in excess of the above acceptance limits shall be allowed if it is established that they will be removed by machining operations.
   e. These acceptance limits are applicable to die forgings which have been heat treated.
5. **Standardization of Instruments.**
   a. Water-travel distance from crystal to part shall be such that the second front reflection shall not appear between the first front and back reflections. The water travel for both standardization and inspection shall be the same distance within plus or minus 1/2 in.
   b. Select a suitable crystal and frequency for optimum results. For initial scanning settings, use an approved type (test blocks to be approved by customer's Quality Control Department) 3/64-in. diameter test-hole block with a distance from flat-bottom test hole to block face nearest to the thickness of the material being tested. Adjust instrument settings on this block to produce a minimum signal strength of one full-height signal from the test-block hole plus at least one half-height second signal from the test-block hole. At this same setting, check a 3/64-in. diameter test-hole block with a distance of 1/2 in. from flat-bottom test hole to block face, and observe whether the minimum signal strength has been maintained, as previously described in this paragraph. If not, increase sensitivity to obtain this minimum signal strength.
   c. For evaluation of singular type flaws, select an approved type 5/64-in. diameter test-hole block within 1/16 in. of the flaw depth up to 1 in., and within 1/4 in. for flaw depths above 1 in. Reduce sensitivity setting to give a signal from the test block equal to 75 percent of the height of the material face reflection.
   d. Re-scan the marked singular type flaw and determine by comparison with proper manipulation whether the flaw signal height is larger or smaller than the 5/64 in. test-hole signal height. If the flaw signal is less than indicated from the 5/64 in. test hole, reset sensitivity to give a signal from the 3/64 in. test hole equal to 75 percent of the height of the material-face reflection, and compare this with the flaw signal.

6. **Recommended Procedure for Ultrasonic Inspection.**
   a. **Frequency.** Those frequencies which provide the best resolution of discontinuities in the inspected parts shall be used.
   b. **Crystal Size.** The following crystal sizes are recommended for final quantitative measurements: ⅜-in. diameter for 5 to 25 Mc. in quartz, or ¾-in. diameter collimated in lithium sulfate.
7. **General Notes.** A typical set of test blocks consists of the following distances from test-hole face to block face: 1/16 in., ⅛ in., ¼ in., ⅜ in., ½ in., ⅝ in., ¾ in., ⅞ in., 1 in., 1¼ in., 1¾ in., 2¼ in., 2¾ in., 3¼ in., 3¾ in., 4¼ in., 4¾ in., 5¼ in., 5¾ in. All test blocks have a standard hole depth of ¾ in. To comply with this specification, it is necessary to have test blocks with 3/64 in., 5/64 in., and 8/64 in. diameter test holes in the alloys being tested.
8. **Acceptance Standard Changes or Alternate Procedure of Method and/or Technique.** This acceptance standard shall be altered as better instrumentation and general knowledge of the art of manufacture and ultrasonic inspection progresses.

References

1. GUINN, A. D., R. D. MCKOWN, J. C. FOLZ, and W. C. HITT. "Research and Development Leading to the Establishment of Ultrasonic Test Standards for Aircraft Materials," (WADC) Tech. Rept. 57-268, (1957). [ASTIA Document No. AD 142034, Air Research and Development Command, Materials Laboratory Contract AF33(616)-3363, Project No. 7360, (October, 1957). Offices of Technical Services, U.S. Department of Commerce, Washington, D.C.]

SECTION 47

ULTRASONIC IMMERSION TEST INDICATIONS

CONTENTS

PAGE

Airframe Components

Basic techniques 1
- Small defects 1
- Large defects 1
- Loss of back reflection 1

Interpretation of indications from test blocks 3
- A-scan indications from Alcoa Series A test blocks with flat-bottom test holes of 1/64 to 8/64-in. diam. (*f.* 1) 2
- B-scan presentation from Alcoa Series A test blocks (*f.* 2) 3

Interpretation of indications from typical discontinuities 3
- Small defects 4
  - A small wafer-thin defect revealed by fracturing (*f.* 3) 4
- Large defects 5
  - Ultrasonic indication of defect in an aluminum alloy die forging (*f.* 4) 5
- Three-dimensional defects 6
  - Three-dimensional discontinuity (*f.* 5) 6

Loss of back reflection 7
- A-scan indications from porous plate (*f.* 6) 8
- Photomicrograph of aluminum alloy plate containing porosity (*f.* 7) 9

Metallurgical factors 9
- Plate 9
  - Defect oriented in the short transverse direction in 2½ in. thick 7075-T6 aluminum alloy rolled plate (*f.* 8) 10
- Extrusions 9
  - Defect in aluminum alloy extrusion (*f.* 9) 11
- Die forgings 10

Indications Requiring Special Consideration

False indications 11
- Contoured surfaces 11
- Edge effects 12
- Surface conditions 12

Orientation and location of defects 12
- Defects oriented at an angle to surface 13
  - Variation of indication height with defect angle for 5/64-in. flat-bottom holes, using 5- and 25-Mc. crystals (*f.* 10) 13

Grain size effects 14
- Effect of grain size on ultrasonic indications from 4340 steel (*f.* 11) 14

Shear wave techniques 15
- Laminar discontinuity in 0.188-in. aluminum alloy sheet (*f.* 12) 15

Jet Engine Rotors

Test techniques 16

Inspection equipment 16
- Automatically operated equipment for the ultrasonic inspection of compressor rotor wheels in subassemblies (*f.* 13) 16
- Manual inspection equipment 17
- Semi-automatic equipment 17
- Fully automatic recording equipment 18
  - Control console of automatically operated equipment for the ultrasonic inspection of turbine rotor wheels (*f.* 14) 17

Interpretation of indications from rotor wheels 18
- Ultrasonic inspection of aluminum compressor rotor wheel, beam position 1 (*f.* 15) 18
- Crack indications 18
  - Ultrasonic inspection of aluminum compressor rotor wheel, beam position 2 (*f.* 16) 19
- Indications of weld cracks 19
  - Ultrasonic inspection of welded turbine rotor (*f.* 17) 20
- Indications of metallic inclusions 20
- Forging defects 20
  - Photomicrograph of sharp discontinuity in a turbine wheel, caused during forging operation (*f.* 18) 21
- Indications of segregates 20
  - Photomicrograph of a segregate in a forged turbine wheel (*f.* 19) 22
- Indications of forging bursts 21
  - Ultrasonic inspection of rim of stainless steel rotor wheel with forging bursts, *FB* (*f.* 20) 23
  - Photograph of B-scan presentation of a contour-forged turbine wheel rim containing forging bursts (*f.* 21) 24
- Indications of small inclusions 23

Spurious indications from surface conditions 23
- Indications from surface contour blending 24
  - False indication from surface contour blending (*f.* 22) 25
- Indications from heat-treating scale 25
  - False indications from heat-treating scale (*f.* 23) 26

Proving interpretation validity 26

CONTENTS (*Continued*)

PAGE

Pipe and Tubing

Principles of test 26
  Mode of beam propagation 26
    Propagation of sound in tube wall (*f.* 24) 27
  Test development 27
  Advantages of immersion scanning 27
  Scope of application 28
  Limitations in defect detection 28
Test equipment 28
  Impedance matching 29
  Selection of transducer 29
  Presentation of indications 29
  Characteristics of B-scan images 29
    Comparison of A-, B-, and C-scan techniques (*f.* 25) 30
    Block diagram of ultrasonic inspection of pipe and tubing (*f.* 26) 31
Scanning equipment 29
  Speed of scanning 30
  Couplant or immersion medium 31
Testing techniques and procedures 31
  Positioning of transducer 32
  Angles of incidence 32
  Control of sensitivity to defects 32
  Beam collimation 32
  Gated flaw alarm 32
    Alarm gate setting (*f.* 27) 33
Interpretation of test indications 34
  Nonrelevant indications 34
  Sources of nonrelevant indications 34
  Crack indications 34
    CX 900 Inconel tubing, 0.229 × 0.025 in., with crack approximately 0.011 in. deep (*f.* 28) 35
    Hastelloy "B" tubing, 0.0250 × 0.049 in., with crack approximately 0.027 in. deep (*f.* 29) 36
    Crack approximately 0.0015 in. deep in 3/16 × 0.025-in. Inconel tubing (*f.* 30) .. 37
    Seam in ¾-in., Schedule 40 pipe (*f.* 31) 38
    B-scan indication from seam in Fig. 31 (*f.* 32) 38
Quality and specifications 39
  Specified characteristics 39
Special applications 39
References 39

SECTION 47

ULTRASONIC IMMERSION TEST INDICATIONS

Airframe Components

BASIC TECHNIQUES. Interpretation of ultrasonic indications and evaluation of defects encountered in airframe components are generally accomplished with the pulse-echo technique and the A-scan presentation, even though the B- and C-scan presentations may be used for detecting defects. Basically the **information available** from the A-scan presentation is:

1. Amplitude of reflection from a discontinuity.
2. Loss of back reflection.
3. Range or distance of discontinuity from the surface of the part.

(See A-Scan Presentation in the section on Ultrasonic Test Principles for detailed description of A-scan presentations.)

Small Defects. In general, individual defects which are small compared with the crystal size are evaluated by comparing the amplitude of the indication (echo or reflection) from the defect with the amplitude of the indication from a standard hole in a test block (see section on Ultrasonic Immersion Tests). Extensive experience in the airframe industry has shown this technique of evaluating small defects to be reliable and reproducible. When employing test blocks to evaluate small defects, the **estimated defect size** is generally smaller than the actual defect size. The surface of a part and the surface of a defect in a part are usually not so flat and smooth as the surface of a test block and the flat-bottom hole in the test block (see section on Ultrasonic Fields).

Large Defects. Individual defects which are large compared with crystal size are also detected by an indication or pip occurring between the reflections from the front and back surfaces. Since the area of the discontinuity is larger than the crystal, the defect size cannot be determined by comparing it with a test block indication; therefore the signal amplitude does not have a quantitative meaning. However, the **extent of the defect** can be determined by the distance the **crystal or scanning head** may be moved along the surface of the material while still maintaining an indication of the defect (see section on Ultrasonic Immersion Tests).

Loss of Back Reflection. A loss or absence of back reflection is simply evidence that the transmitted sound is being absorbed, refracted, or reflected so that energy is not returned to the crystal. Several types of metallurgical conditions may cause a loss of back reflection, as will be discussed later. Measurement of loss of back reflection does not result in a quantitative evaluation to the extent possible with a small defect indication. With the gain settings normally used in the inspection of airframe parts, at least several back reflections are obtainable in sound material. Loss of back reflection may be determined by noting the ratio of **number of back reflections** in a known sound material of

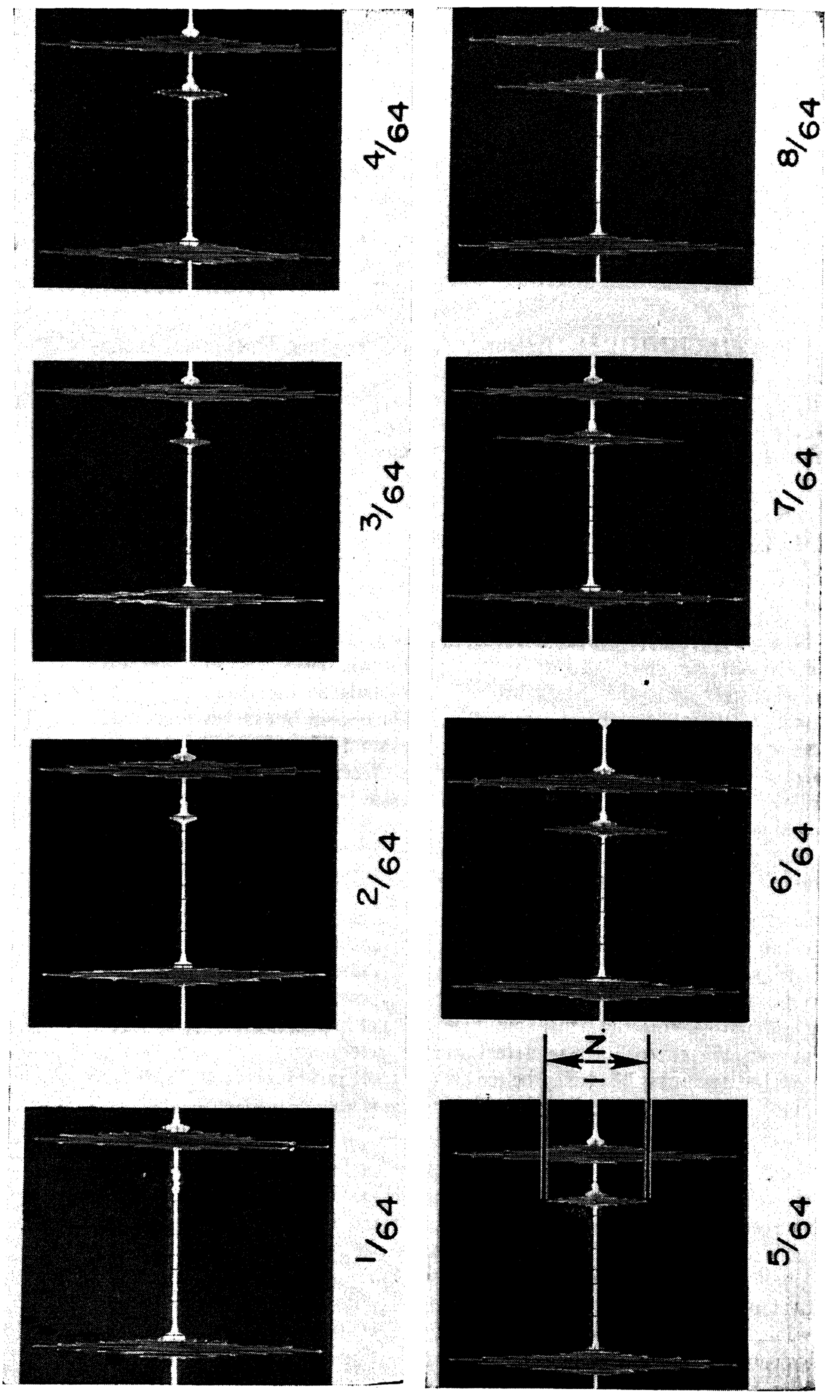

SNT Airframe Industry Committee

Fig. 1. A-scan indications from Alcoa Series A test blocks with flat-bottom test holes of $\frac{1}{64}$ to $\frac{8}{64}$-in. diam.

equivalent thickness to the number of back reflections in the material under consideration. A second method of evaluating loss of back reflection is to reduce the gain setting so as to give slightly less than a saturated (maximum amplitude) signal from the first back reflection in known sound material. The amplitude of this signal is then compared with the amplitude of the signal from the back reflection in the material being inspected.

INTERPRETATION OF INDICATIONS FROM TEST BLOCKS. If the general defect size is less than the crystal size, the defect size is related to the amplitude of the indications on the **A-scan display.** Fig. 1 illustrates ultrasonic indications from a set of **Alcoa Series A test blocks** (flaw-to-surface distance 3¼ in. and hole sizes 1/64 to 8/64 in. in increments of 1/64 in.). The same instrument gain setting was used for all test blocks. Fig. 1 shows that the 1/64-in. hole is hardly discernible, the 5/64-in. hole gives an indication 1 in. high, and the 8/64-in. defect gives an indication approximately 1⅝ in. high.

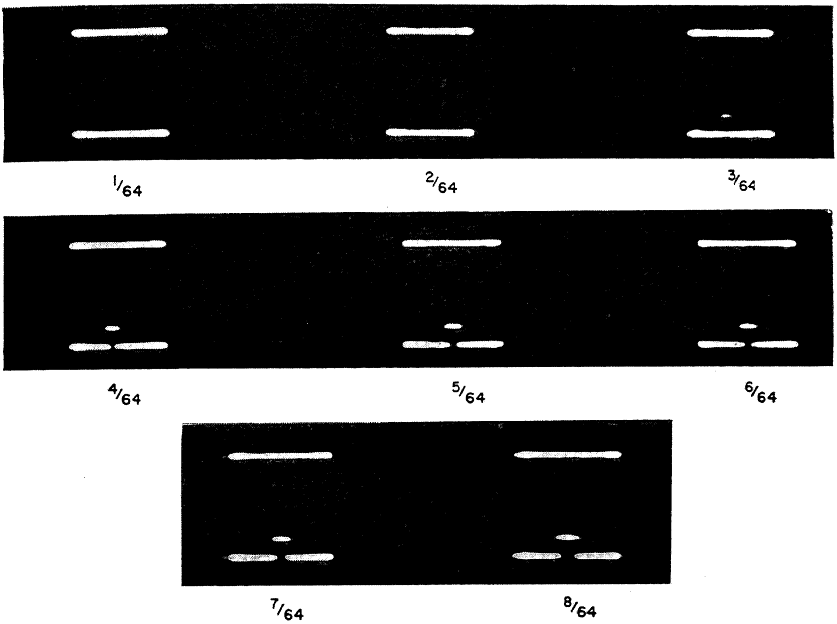

SNT Airframe Industry Committee

Fig. 2. B-scan presentation from Alcoa Series A test blocks.

The **relationship between defect size and indication height** is not the same for all instruments of the same type or all types of instruments. However, Fig. 1 illustrates qualitatively the relationship which exists between hole size and amplitude of indication. Fig. 2 shows a **B-scan presentation** for all eight of the Alcoa Series A test blocks. Gain setting was constant for all eight test blocks.

INTERPRETATION OF INDICATIONS FROM TYPICAL DISCONTINUITIES. Aside from conventional test blocks, probably the simplest type of defect to detect is one which

1. Is small compared with the face area of the crystal.
2. Has relatively smooth surfaces.

3. Has essentially only two dimensions but is several wavelengths in width.
4. Has its major dimensions parallel to the surface of the part so the ultrasonic beam intersects its major dimension with normal incidence.

Small Defects. Small defects form a significant portion of the defects encountered in ultrasonic inspection of airframe components, particularly in **wrought aluminum products.** Foreign material or porosity in the cast ingot are rolled, forged, or extruded into **wafer-thin defects** during the fabrication process. The fabrication process tends to orient the maximum dimensions of the defect parallel to the surface of the part. Such a defect and its ultrasonic indication are shown in Fig. 3. In the **oscillogram,** the first pip is the echo or reflection from the top

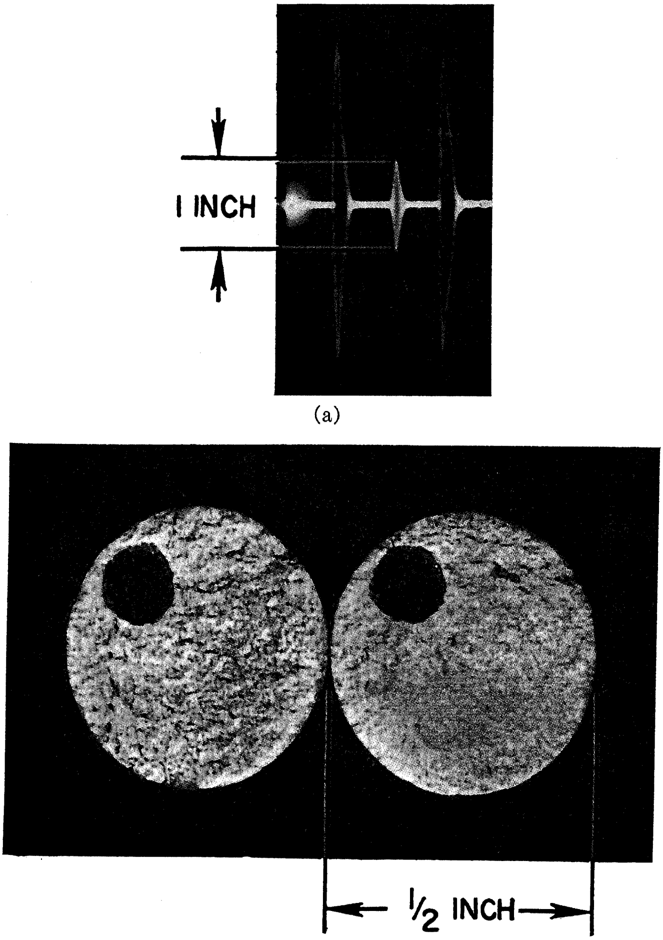

(a)

(b) SNT Airframe Industry Committee

Fig. 3. A small wafer-thin defect revealed by fracturing. (a) Defect indication obtained with a gain setting which would give a 1-in. indication height from a 5/64-in. Ultrasonic Testing and Research Laboratory test block. (b) Section through discontinuity.

or front surface, the second is the echo from the defect, and the third is the reflection from the back or bottom surface of the test material. The instrument gain was set to give a 1-in. pip from an Ultrasonic Testing and Research Laboratory No. 5 (5/64 in.) test block. The indication shown in Fig. 3 was also approximately 1 in. high.

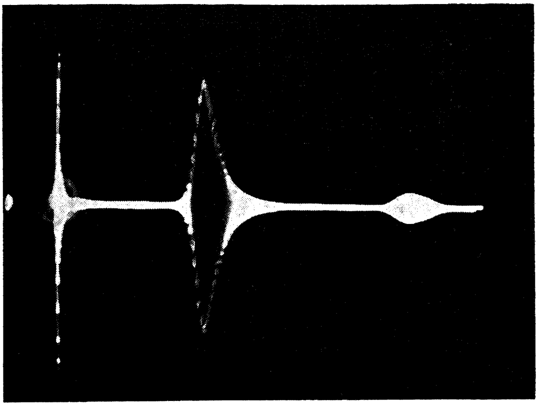

(a)

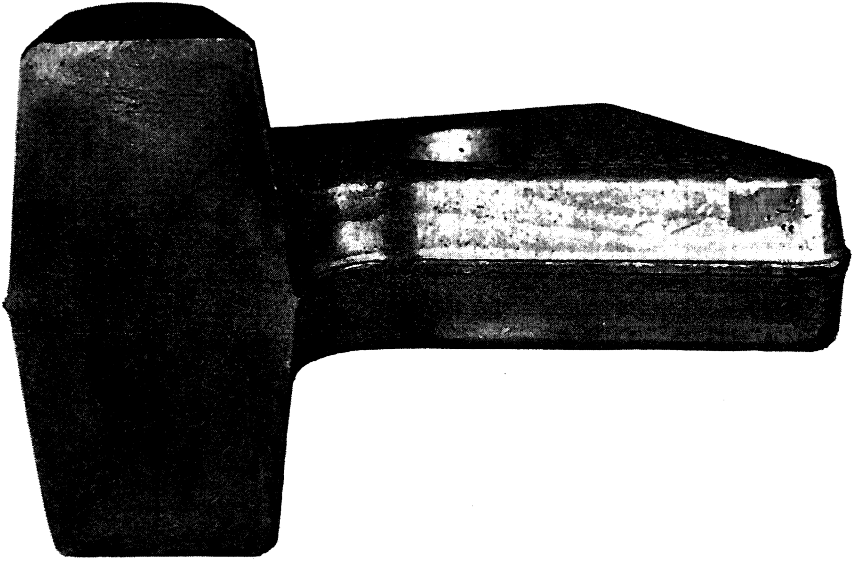

(b) SNT Airframe Industry Committee

Fig. 4. Ultrasonic indication of defect in an aluminum alloy die forging. (a) A-scan indication. (b) Cross-section through defect.

Large Defects. Defects which are large compared with the crystal size are generally easy to detect if their surfaces are reasonably smooth and parallel to the surface being inspected. A large defect in a **die forging** is illustrated in Fig. 4. When using normal gain settings, the defect indication saturates the display instrument, and the amplitude of the indication has little quantitative meaning. The loss of back reflection is typical, since the defect reflects nearly all the ultrasonic energy. The dimensions of the defect can be determined from the distance the crystal or scanning head can be moved while still maintaining an indication of the defect. (See section on Ultrasonic Immersion Tests.)

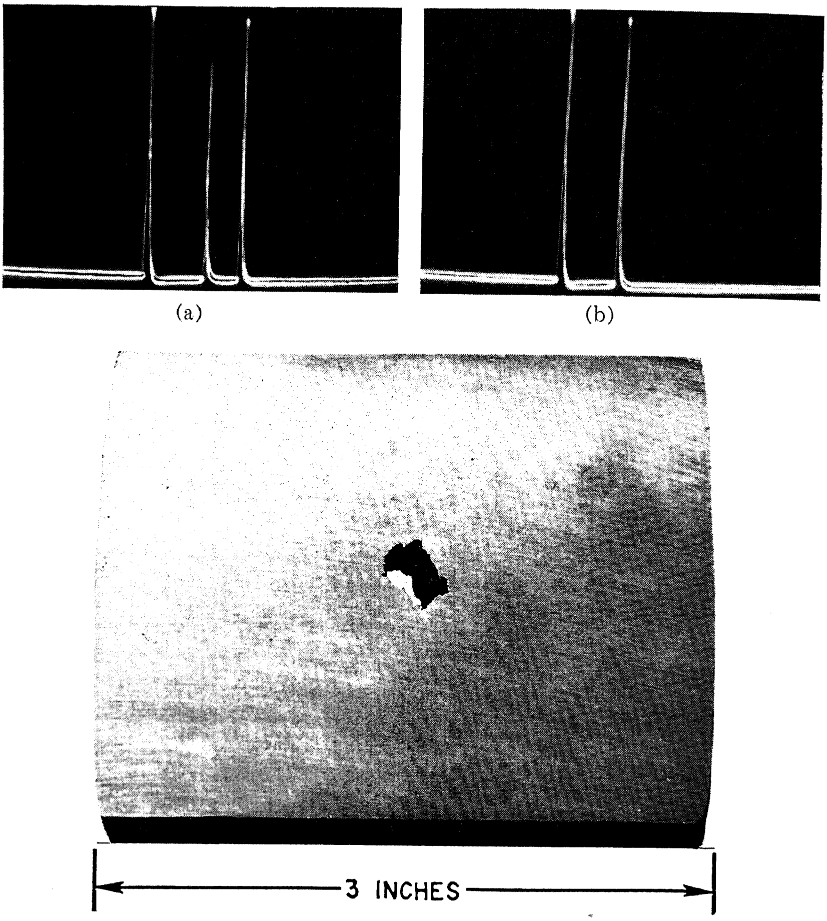

(a) (b)

(c) SNT Airframe Industry Committee

Fig. 5. Three-dimensional discontinuity. (a) A-scan indication from $\frac{5}{64}$-in. test block. (b) A-scan indication from defect shown in (c), using same gain setting as in (a). (c) Defect detected in $2\frac{1}{4} \times 3$ in. rolled steel bar.

Three-dimensional Defects. Discontinuities in wrought materials, i.e., materials which have been forged, rolled, or extruded, frequently are essentially only two dimensional. However, occasionally a three-dimensional defect will be encountered. Fig. 5 shows a section from $2\frac{1}{4} \times 3$-in. **rolled steel bar.** The oscillogram of Fig. 5(a) is the indication from a $\frac{5}{64}$-in. flat-bottom hole whose flaw-to-surface distance is equal to that of the defect. The oscillogram shown in Fig. 5(b) is from the defective material. The first indication is from the front face, the second is from the defect. Note that the indication from the defect saturates the display instrument. No reflection is obtained from the back (bottom) surface, since sound is not transmitted through the defect.

Inspection from one surface does not indicate whether the defect is a hole or void, such as is shown in Fig. 5(c), or whether it is a thin, laminar defect with only two major dimensions. However, this can be ascertained by **inspection from two opposite surfaces.** Inspection from the top surface of the material shown in Fig. 5(c) indicated that the defect was approximately 40 percent of the part thickness below the top surface. When the part was inspected from the opposite surface (bottom, as shown in Fig. 5), the results indicated the defect was approximately 40 percent of the part thickness from this surface. Thus inspection from the two opposite surfaces indicated that the defect had a thickness of the order of 20 percent of the part thickness. Of course two defects, each approximately 40 percent of the part thickness below each surface, would have given similar results. However, the likelihood of such an occurrence is considerably more remote than that of a single defect of the type shown in Fig. 5. The possibility of two defects was eliminated in this instance, since the part was inspected from all four sides and the results indicated that the defect had thickness in both planes.

LOSS OF BACK REFLECTION. Loss of back reflection is an important consideration in ultrasonic flaw detection. Care must be exercised when interpreting or measuring loss of back reflection to be certain that **geometric considerations** such as roughness and taper are not causing loss of back reflection. If the test material is relatively smooth and the front and back surfaces are nearly parallel, interpretation or measurement of loss of back reflection is relatively simple. Of course the large defect or even a small defect will cause a loss of back reflection, since some of the sound which would normally be reflected from the back surface is reflected from the defect. However, measurement of loss of back reflection is most valuable when it occurs in the absence of significant individual defects.

Among the **causes of a reduction or loss of back reflection,** in the absence of an indication of an individual defect, are:

1. Defects with rough surface or defects oriented at a severe angle to the surface.
2. Large grain size.
3. A number of very small defects such as porosity.
4. Fine precipitate particles.

The first two items are discussed subsequently. Fig. 6 illustrates ultrasonic indications from a 3 in. thick **aluminum plate.** The oscillogram of Fig. 6(a) is from a sound piece of 3-in. aluminum plate [Fig. 6(b)], with the instrument gain set to give a 1-in. pip from a No. 5 Alcoa test block. The oscillogram of Fig. 6(c) is from a **porous aluminum plate** of the same material and thickness, shown in Fig. 6(d). The oscillogram from the sound plate shows five visible back reflections, and the porous plate shows four visible reflections. The oscillogram of Fig. 6(c) shows no evidence of defects between the front and back reflection. Fig. 6(e) shows an oscillogram from the same area as the oscillogram of Fig. 6(c) but obtained by using a higher gain setting. Also, the sweep or time scale in Fig. 6(e) has been expanded as compared with the oscillogram shown in Fig. 6(c). The tall pips on the left and right of this oscillogram are reflections from the front and back surfaces of the material, respectively.

At a high gain setting (to give a 1-in. pip from a No. 2 Alcoa Series A test block), there is **hash** or a number of indications between the front and back re-

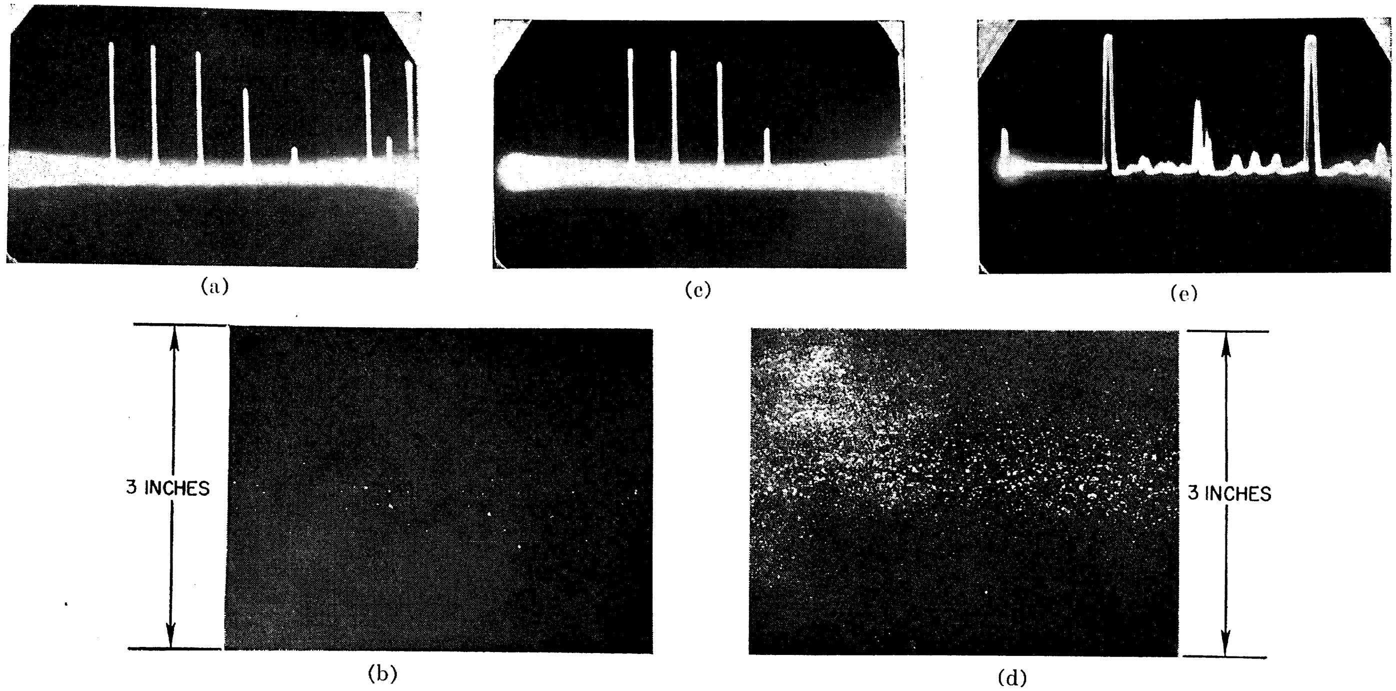

SNT Airframe Industry Committee

Fig. 6. A-scan indications from porous plate. (a) Back reflections from sound 3-in. aluminum alloy plate. (b) Cross-section of sound 3-in. aluminum alloy plate. (c) Back reflections from porous aluminum alloy plate. Gain setting same as shown in (a). (d) Cross-section of 3-in. aluminum alloy plate containing porosity. (e) Indication from 3-in. aluminum alloy plate showing porosity, but using higher gain setting than shown in (a) and (c).

flections. Figs. 6(c) and (e) are characteristic of material exhibiting **excessive small porosity,** or **coarse grain,** i.e., a loss of back reflection occurs at low gain settings, but an indication of defects between the front and back reflections does not necessarily occur. However, at the higher gain setting, "hash" or "grass" is generally evident in indications from porous material. Such patterns are not evident in sound material. The photomicrograph of Fig. 7 reveals the size of this porosity in the 3-in. plate.

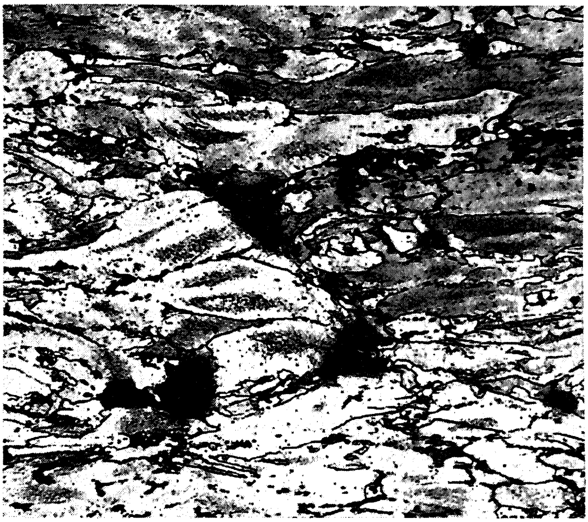

SNT Airframe Industry Committee

Fig. 7. Photomicrograph of aluminum alloy plate containing porosity. 100X.

METALLURGICAL FACTORS. Consideration of the metallurgical and fabrication history of material is extremely valuable in interpretation of ultrasonic indications. In general, **defects in wrought products** tend to be oriented in the direction of grain flow. The maximum dimension of the defect is in the direction of maximum metal flow during fabrication. Obviously this generalization is not true for defects which result from processes subsequent to forging, extrusion, or rolling operations.

Plate. Grain direction (the direction along which the metal flowed during working) is relatively simple to determine in plate. Defects in plate are generally parallel to the surface of the plate and elongated in the direction which received the maximum amount of rolling. The preceding generalization is not always true, however, as can be seen in Fig. 8.

Extrusions. Defects in extrusions are nearly always elongated in the direction of extrusion (i.e., along the long axis of the extrusion). In the case of plate and extrusions, it is very important to note any **recurring indications of defects** when scanning parallel to the direction of grain flow. When inspecting an extrusion or plate, a defect indication of apparently minor importance which recurs as the part is traversed can be extremely important. Such a situation is illustrated in the cross-section of an extrusion shown in Fig. 9. Ultrasonic inspection from the surface marked (a) indicated numerous defects equivalent to an indication from 5/64-in. flat-bottom hole along a 4-ft. length of the extrusion, but a continu-

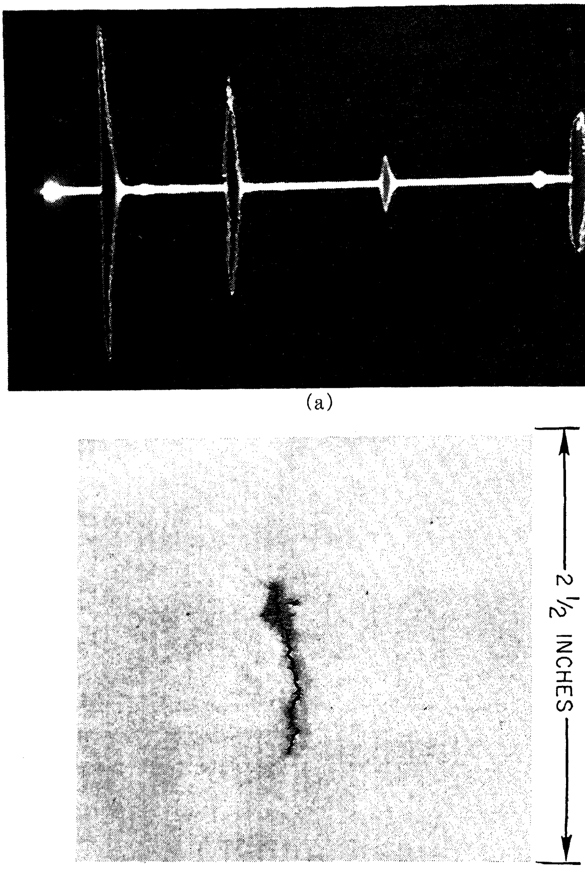

(a)

(b)

SNT Airframe Industry Committee

Fig. 8. Defect oriented in the short transverse direction in $2\frac{1}{2}$ in. thick 7075-T6 aluminum alloy rolled plate. (a) A-scan indication. (b) Section through defect.

ous defect was not evident. There was an attendant loss of back reflection with the individual indications or defects. The major clue to the fact that the defect was large and continuous was the consideration that the defects were approximately the same distance below the surface and in a line coinciding with the direction of grain flow. The type of defect shown in Fig. 9 is not unusual in extrusion; however, this type of defect is generally visible on the butt end of the extrusion. In this particular instance the defect extended approximately 4 ft. along the length of the extrusion, but it was not evident on either end of the extrusion, even after the ends were severely caustic-etched.

Die Forgings. The grain flow in die forgings is frequently complex. Defects in die forgings are not necessarily oriented parallel to the surface or elongated in the long dimension of the part. In addition to the generally complex geometry of die forgings, these factors make detection and interpretation of defects difficult. In some instances where large, complex-shaped die forgings are being inspected,

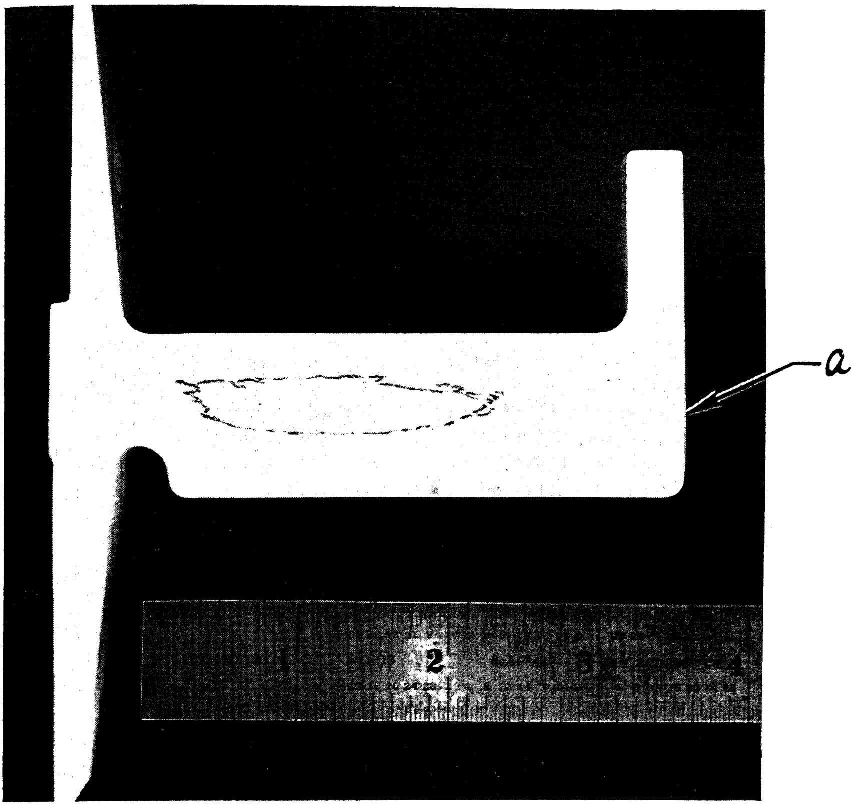

SNT Airframe Industry Committee

Fig. 9. Defect in aluminum alloy extrusion.

it is desirable to section a sample forging so as to determine **grain flow** in various sections of the part and thereby determine the most likely orientation of defects.

Indications Requiring Special Consideration

FALSE INDICATIONS. Several commonly encountered conditions may result in false indications on the cathode-ray tube.

Contoured Surfaces. Reflections from fillets and concave surfaces may result in indications between the front and back reflections which can be confused by the operator with indications from defects. These spurious indications result from sound that is reflected back to the crystal at a time which is equivalent to the length of time necessary for the sound to travel from a defect at some given distance below the surface. Although it is not always possible to distinguish clearly between defects and **false indications from curved surfaces,** there are several methods to check in attempting to discern the difference.

1. Frequently, if a false indication results from a contoured surface, the amplitude of the indication will be related to the amplitude of the reflection from the front surface. In this case the amplitude of the front surface echo will diminish as the false indication increases, or vice versa.

2. A false indication will tend to be consistent as the search unit is moved along the contoured surface, whereas a reflection from a defect will tend to be strong in localized areas.
3. If false indications result from reflections around the contoured surface, it is sometimes possible to distinguish them by interrupting the sound beam between the crystal and the surface of the part with a foreign object such as a piece of sheet metal. If the indication is reflecting from a curved surface, shielding a portion of the curved area may eliminate the irrelevant indication and yet allow the major portion of the sound beam to enter the part.
4. Irrelevant indications from contoured surfaces are more likely to result in a broad-based indication, as contrasted to a sharp spike or pip for an indication from most defects.

Edge Effects. It has been observed that irrelevant indications may be obtained near the edges of rectangular shapes. This type of indication can result when the crystal is perhaps ½ in. from the edge of the part. Apparently these irrelevant indications result from **reflections from the edge of the part,** even though the sound entered the top and was not refracted by the corner. One distinguishing characteristic of this type of irrelevant indication is its **consistency.** The apparent defect indication may exist at a distance equivalent to one-quarter to one-half the part thickness below the surface, but it is consistent with respect to location and nature of the indications. As the search unit travels parallel to the edge of the part, the indication will remain relatively uniform in appearance and amplitude. In contrast to this, an indication from a defect would generally show variation in amplitude due to roughness of the surface of the defect. Also, defects which would give a continuous indication over several inches of search-unit travel would generally be of sufficient size to give a significant reduction in back reflections.

Surface Conditions. Occasionally, inspection of parts with smooth, shiny surfaces will result in false indications. This type of indication has been observed, for example, in 2 in. thick aluminum plate which was machined to a smooth finish. The spurious indication existed at approximately one-third the part thickness below the surface and, again, was unusually consistent; i.e., as the search unit was moved across the material, the indication remained relatively uniform in shape and magnitude. Apparently this type of indication results from some kind of **surface wave** generated on the extremely smooth surface, possibly reflecting from a nearby edge. Such false indications can be eliminated by disturbing the entry surface slightly by **coating the surface** with wax crayon or a very thin film of petroleum jelly. In this instance, as well as the cases mentioned earlier, one of the distinguishing characteristics of the false indication is its consistency. Therefore it is a good rule to be suspicious of all indications which are unusually consistent in amplitude and appearance when the search unit is passing over the test material.

ORIENTATION AND LOCATION OF DEFECTS. Defects very near the surface being inspected cannot always be detected while scanning normal to the surface because of the **near-zone effect** and **equipment recovery time** (see section on Ultrasonic Fields). However, indications of defects are sometimes evident at a distance just slightly less than that at which a definite individual pip is evident. An interference of the front reflection occurs in this instance. The reflected sound wave from the defect near the surface interferes with sound reflected from the front surface, but the ultrasonic equipment is unable to resolve or separate the energy into two distinct signals.

A slight variation in the appearance of the front reflection is not necessarily an indication of a defect near the surface, since a variation in the flatness or roughness of the surface will also produce a variation or fluctuation of the indication from the front surface. **Roughness** or variation in flatness which will cause fluctuation in the indication of the front surface can usually be detected by touch. Therefore, when fluctuation of the front reflection cannot be attributed to surface condition, the possibility of a defect near the surface should be investigated by inspection of the part from the opposite surface. Also, defects near the surface may cause a loss of back-surface reflection. Alternatively, double-transducer techniques can often permit improved detection of near-surface defects (see section on Double-Transducer Ultrasonic Tests).

Defects Oriented at an Angle to Surface. Defects oriented at an angle to the front surface may be difficult to detect and evaluate if care is not exercised. Generally it is desirable to scan initially at a comparatively high gain setting, to detect defects which are oriented at an angle to the surface being inspected. It has been shown that, using a gain setting giving a 2-in. pip from a 5/64-in. flat-bottom hole at normal incidence, a 5/64-in. diam. flat-bottom hole oriented at 25 deg. to the front surface is not discernible on the A-scan instrument if the crystal is parallel to the front surface.[1]

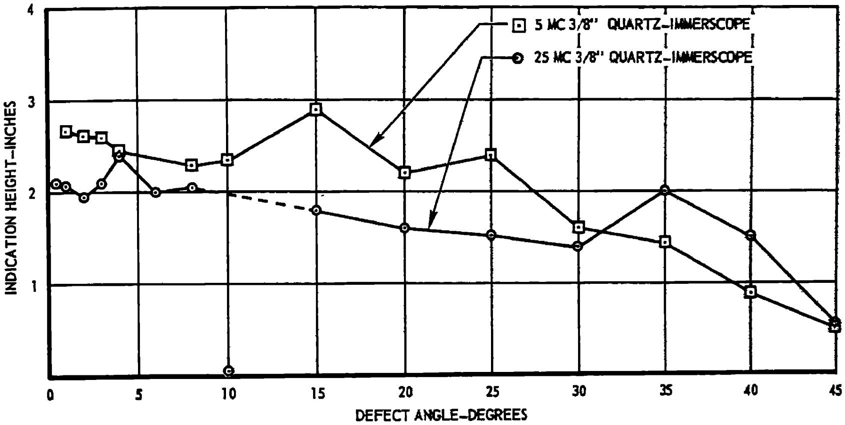

Fig. 10. Variation of indication height with defect angle for 5/64-in. flat-bottom holes, using 5- and 25-Mc. crystals. The crystal was oriented to give maximum indication height in each instance. Angle of defect is with respect to the front surface of test object.

Ultrasound obeys Snell's law in a fashion similar to light. Therefore it is necessary to **manipulate the crystal** when evaluating defects oriented at an angle to the surface so that the sound beam will strike the plane of the defect at right angles. Even though manipulation is accomplished, defects oriented at angles to the surface will result in an indication of magnitude slightly lower than an indication from a defect parallel to the surface. However, this difference is not so great as may be expected. Fig. 10 shows **indication height as a function of angle** between the defect plane and the front surface. In this instance the defects were 5/64-in. flat-bottom holes, the instrument gain setting was constant for all tests, and the crystal was manipulated to obtain maximum indication height.

In some instances, not only is the general plane of the defect oriented at an angle to the surface, but the **surface of the defect** may also be irregular, as in Fig. 9. The amplitude of the indication may not indicate a large defect because most of the sound may not be reflected to the crystal. Defects of this type are generally large compared with the crystal size, and evidence of the indication may persist as the crystal is moved over the test material.

Occasionally, defects which are large compared with the crystal have a relatively smooth, flat surface but lie at an angle to the surface. **Bursts in large forgings** fit this category and tend to lie at 45 deg. to the surface. Defects of this nature present a nearly continuous indication, but the indication moves along the base line of the display instrument as the crystal is moved because of the change in distance that the sound must travel.

GRAIN SIZE EFFECTS. In ultrasonic inspection of some 4340 chrome-molybdenum steel at 5-Mc. frequency, an unusual amount of hash or high noise

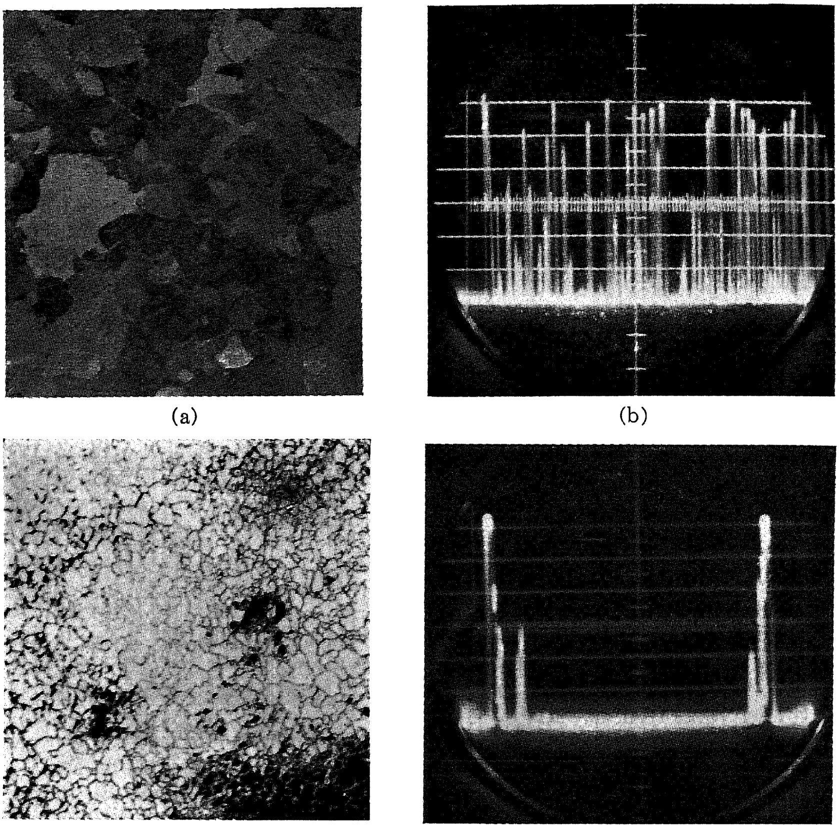

(a)

(b)

(c)

(d)

SNT Airframe Industry Committee

Fig. 11. Effect of grain size on ultrasonic indications from 4340 steel. Both oscillograms were obtained by using the same gain settings. (a) Large-grain material. (b) A-scan indication from large-grain steel. (c) Fine-grain material. (d) A-scan indication from fine-grain steel.

level was detected.[2] A study of this material showed very large grain size comparable with ASTM grain size standards 1 to 4 [Fig. 11(a)]. The large grains found in the "as-received" condition resulted from (1) high temperature during hot working and (2) subsequent improper annealing.

Ultrasonic inspection was performed on a similar sample which was again heat treated to attain grain refinement. The sample showed an absence of the hash on the reference line, indicating that after **proper heat treatment,** a finer grain size was obtained [Fig. 11(c)]. Ultrasonic inspection showed an absence of hash, and microscopic examination revealed a refined grain size of ASTM standards 6 to 8.

In a test program performed on **forged Inconel X parts,** a frequency of 5 Mc. was used. One inspected forging produced seven back reflections, while another part showed none with the same gain setting, crystal, and test frequency. Microscopic examination was made of these and other forgings to determine if any internal discontinuities were responsible for the ultrasonic pattern obtained, and also to compare the grain size of these forgings. No internal discontinuities were found that would affect the ultrasonic signal. Grain size determinations showed unusually large grains in the forgings in which ultrasound produced no back reflections. Further investigations revealed that **prolonged or improper forging temperature** caused the abnormally large grain size.

SHEAR WAVE TECHNIQUES. Angle-beam (longitudinal or shear wave) and surface-wave inspections have been used for various airframe materials. Techniques exist for employing surface-wave inspection and correlating ultrasonic

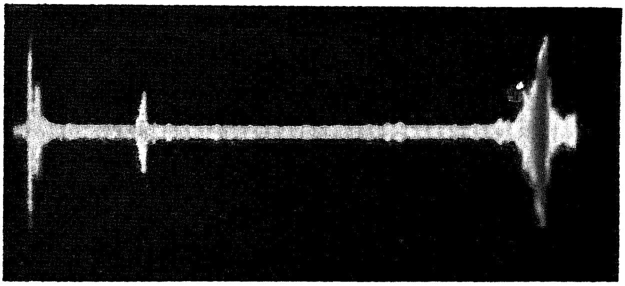

(a)

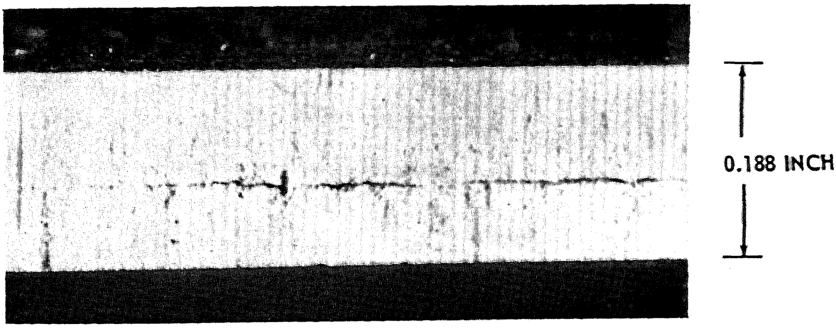

(b) SNT Airframe Industry Committee

Fig. 12. **Laminar discontinuity in 0.188-in. aluminum alloy sheet.** (a) Oscillogram obtained with shear-wave technique. (b) Cross-section of sheet showing oxide inclusions.

indications with defects.[3] Angle-beam inspection was employed to inspect 0.188-in. 7075-T6 **aluminum alloy rolled sheet,** using ultrasonic contact inspection.[4] Fig. 12(a) shows an indication from a discontinuity detected in 0.188-in. aluminum alloy sheets approximately 4 ft. wide with a 50-deg. angle shear-wave crystal. The crystal was near the edge, and the ultrasonic beam was directed across the 4-ft. width of the sheet. The signal indication on the extreme left is the initial pulse, and the signal on the extreme right is the indication or reflection from the opposite edge of the sheet. The discontinuity appears at a distance of one-fourth the length of the oscilloscope signal, which means that the discontinuity was approximately 1 ft. from the crystal in the sheet. Fig. 12(b) shows the defect **(oxide inclusions)** which caused the ultrasonic indication.

Jet Engine Rotors

TEST TECHNIQUES. Two different techniques are generally used for the detection of flaws in parts by the pulse-echo type of ultrasonic inspection. These are usually referred to as the "contact" and "immersion" techniques. **Immersion testing** is more commonly used for ultrasonic inspection of jet engine rotors, although **contact testing** is also widely used. This is due principally to the fact that thinner sections and more varying contours are encountered in rotors than in larger equipment such as steam turbines. In the aircraft-engine field, large quantities of parts are inspected, and the immersion ultrasonic techniques are easily adapted to automatic methods of inspection.

INSPECTION EQUIPMENT. Fig. 13 illustrates automatic ultrasonic inspection equipment designed to inspect peripheral areas of **aluminum compressor**

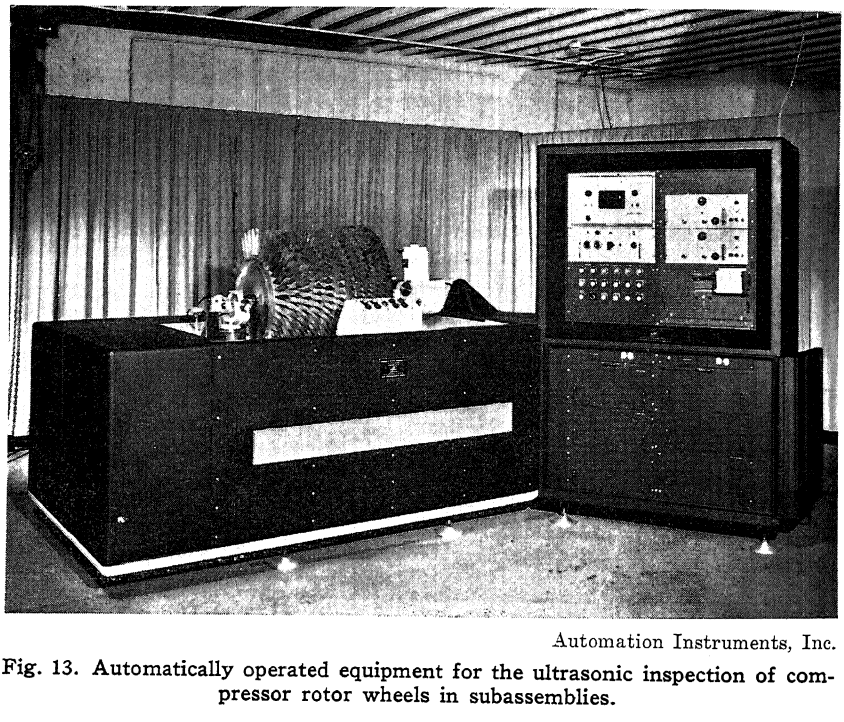

Automation Instruments, Inc.

Fig. 13. Automatically operated equipment for the ultrasonic inspection of compressor rotor wheels in subassemblies.

wheels assembled in a compressor rotor subassembly. These areas cannot be inspected reliably by any other method without a costly and lengthy dismantling job.

Manual Inspection Equipment. Manual ultrasonic inspection equipment can be set up to inspect rotor subassemblies. This equipment can be used to secure the statistical data necessary to determine if automatic equipment is required to inspect assemblies already in service. In one case an automatic installation was decided upon because each unit could be inspected in about one-twentieth of the time required for manual inspection. Statistical data collected by this manually operated equipment proved to be very accurate. The percentage of parts containing defects coincided exactly with those detected by the fully automatically operated equipment.

Semi-automatic Equipment. A typical ultrasonic installation is used for immersion testing of **turbine rotor wheels** with semi-manually operated equipment. A- and B-scan presentation screens are used with the ultrasonic generator, scanning means, and turbine-wheel rotating equipment.

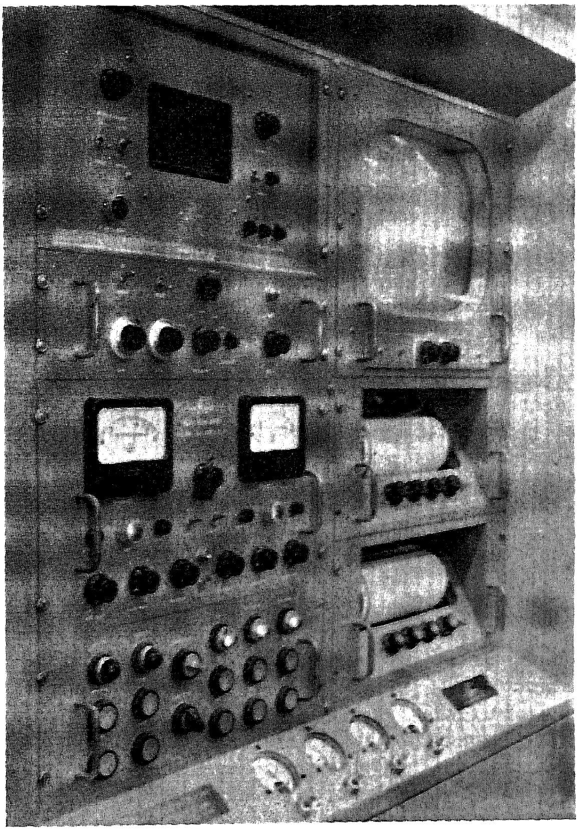

Automation Instruments, Inc.

Fig. 14. Control console of automatically operated equipment for the ultrasonic inspection of turbine rotor wheels.

Fully Automatic Recording Equipment. Fig. 14 illustrates the control console of an automatic ultrasonic installation for the inspection of turbine rotor wheels and rings. In these units all scanning and rotating operations are automatic, and indications from defects and back-surface reflections are recorded.

INTERPRETATION OF INDICATIONS FROM ROTOR WHEELS. Fig. 15(a) illustrates the area inspected ultrasonically in an aluminum compressor rotor wheel. The ultrasonic beam from the quartz crystal (*QC*) is directed into the surface on the periphery at an angle θ of 5 deg. to the normal (*N*). According to Snell's law, the angle of the refracted beam θ_1 will be about four times greater than θ, or about 20 deg. to the normal. A diagram of the A-scan at this point is shown in Fig. 15(b). The **main bang** (*MB*), or pulse emitted by the crystal, is shown at the left, and the reflection from the **front surface** (*FS*) is shown next. As the crystal moves in an axial direction, the refracted beam (position 1) is just cutting across the corner of the rabbit groove and producing a small indication (*CRG*). The reflection from some **rear surface** (*RS*) is shown at the far right.

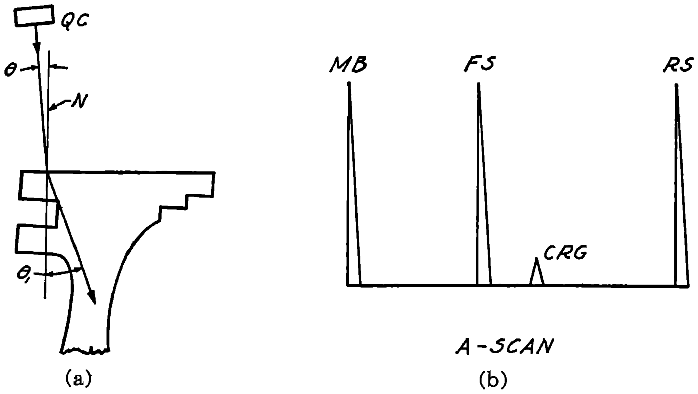

(a) (b)

Fig. 15. Ultrasonic inspection of aluminum compressor rotor wheel, beam position 1. (a) Beam position 1 at corner of rabbit groove. (b) A-scan indication from position 1, showing indications from front surface, *FS*, and corner of rabbit groove, *CRG*.

Crack Indications. In Fig. 16(a), the crystal (*QC*) has been moved farther to the right in an axial direction, and the sound beam (position 2) is reflected from a defect or crack. This produces an indication (*C*) on the A scan [Fig. 16(b)]. The indication (*CRG*) has disappeared because the ultrasonic beam no longer strikes the corner of the groove. Since the ultrasonic pulse requires about 8 μsec. to make a round trip through 1 in. of aluminum, the **time interval** between the indication from the front surface and that from the crack is 2 μsec. At the position shown in Fig. 16, the crack starts at about ¼ in. below the surface.

As the crystal is again moved axially, the refracted ultrasonic beam is reflected from the face of the crack at a depth of about ⅛ in. below the surface. The crack indication (*C*) moves toward the front-surface indication (*FS*), and the time interval between the two indications becomes about 1 μsec. As the crystal moves, the **crack indication** seems to walk or move toward the front-surface indication. This indicates that the crack is not parallel to the surface but instead is approaching the surface, since the angle of incidence of the sound beam has not changed with the change in axial position of the crystal.

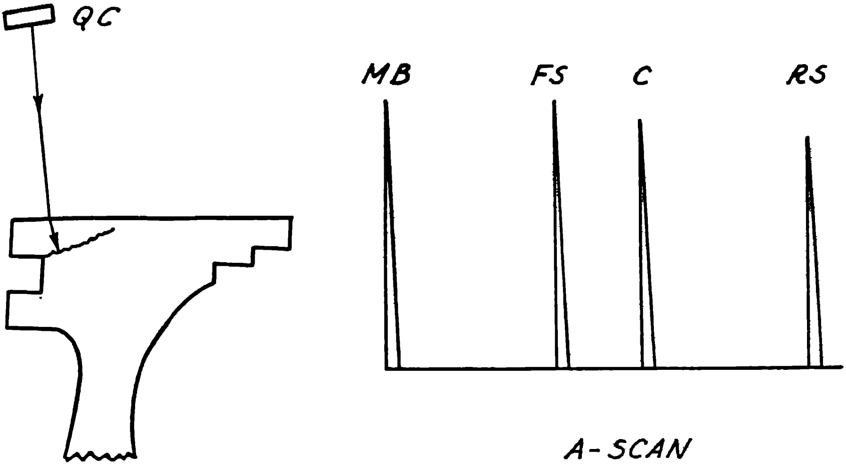

(a) (b)

Fig. 16. Ultrasonic inspection of aluminum compressor rotor wheel, beam position 2. (a) Beam position 2 missing rabbit groove and striking cracklike defect. (b) A-scan indication from position 2, showing crack reflection, *C*.

Indications of Weld Cracks. A cross-section of a welded turbine rotor is shown in Fig. 17. In this wheel a rim of **forged stainless steel** is welded to a hub of **forged ferritic material.** Despite the most advanced welding techniques, cracks develop occasionally in the rim side in the heat-affected zone, and these occur with sufficient frequency to require 100 percent inspection. These defects lie in a plane parallel to the face of the wheel and extend in a radial direction. It is necessary to use ultrasonic inspection to detect them, since they are oriented in the wrong direction for detection by radiography. Fig. 17(a) shows the direction of the path of the ultrasound and the position of the defect in the cross-section of a portion of the wheel. During inspection, the wheel is rotated on a table immersed in water. The A-scan presentation is shown in Fig. 17(b) for the condition in which the crystal is beamed over a solid metal path. Both the A- and B-scan presentations are shown [in Fig. 17(c) and (d)] when the crystal is over an area containing a crack. The defect is of such extent, in this case, as to cause a reflection of high amplitude and complete loss of the rear-surface reflection [see Fig. 17(d)]. The distance between the front-surface reflection *FS* and the reflection from the crack *C* indicates how deep it is below the surface. Care must be exercised when angulating the sound beam close to the interior **interface of weld and rim material** because the beam can be reflected off these faces and can cause false indications. Because of the cast nature of the weld material, the sound beam is rapidly attenuated. Consequently this area is not always effectively inspected by this method. Since most weld defects such as lack of fusion, slag inclusions, and cracks are more easily detected by radiography, **X-ray inspection** is used for the inspection of the weld area.

Indications of Metallic Inclusions. Metallic inclusions in the same plane as the cracks give indications very similar to cracks located in the heat-affected zone. They also are cause for rejection. They are found most frequently in the rim and farther away from the weld area.

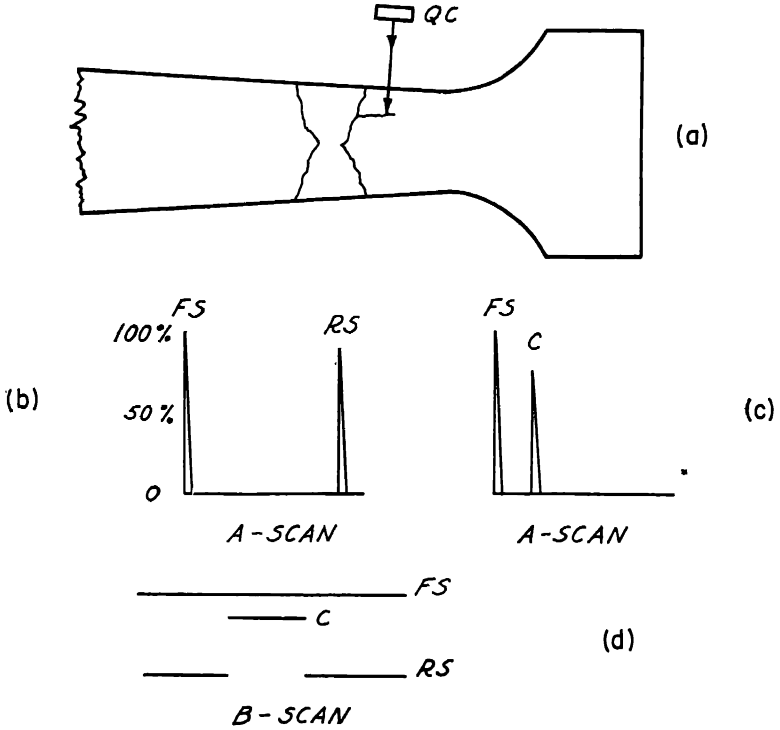

Fig. 17. Ultrasonic inspection of welded turbine rotor. (a) Beam position for detection of crack in heat-affected zone of weld. (b) A-scan indication over sound metal, showing no reflections between front surface, *FS*, and rear surface, *RS*. (c) A-scan indication over crack, showing crack indication, *C*, and loss of rear-surface reflection. (d) B-scan indication over crack region, showing lateral extent and depth of crack, *C*, and interrupted rear-surface indications, *RS*.

Forging Defects. Ultrasonic inspection is also used for **solid forged turbine-rotor wheels** of certain stainless steel alloys fabricated without welding. It is used chiefly to detect sharp, cracklike discontinuities resulting from the forging process (Fig. 18).

Indications of Segregates. Forgings may also contain segregates which reflect ultrasonic beams (Fig. 19). These indications cannot be distinguished from those caused by cracks. Metallurgists have determined that the mechanical properties of materials containing these segregates meet normal service requirements for room-temperature tensile and elevated-temperature stress-rupture properties. These segregates can cause indications with amplitudes of 15 to 90 percent of front-surface reflection [Fig. 17(c)]. The more highly concentrated ones cause the higher-amplitude indications. These pips can appear between the front- and rear-surface indications or between the first and second multiples of the rear-surface reflection.

Discontinuities in this stainless steel occur in either a loose or tightly bound condition. Fortunately these discontinuities do not occur too frequently. Although they do not adversely affect the mechanical properties, they cannot be accepted because, if they should occur in a critical area like the serrations of the rotor wheel, they might propagate and cause catastrophic failure.

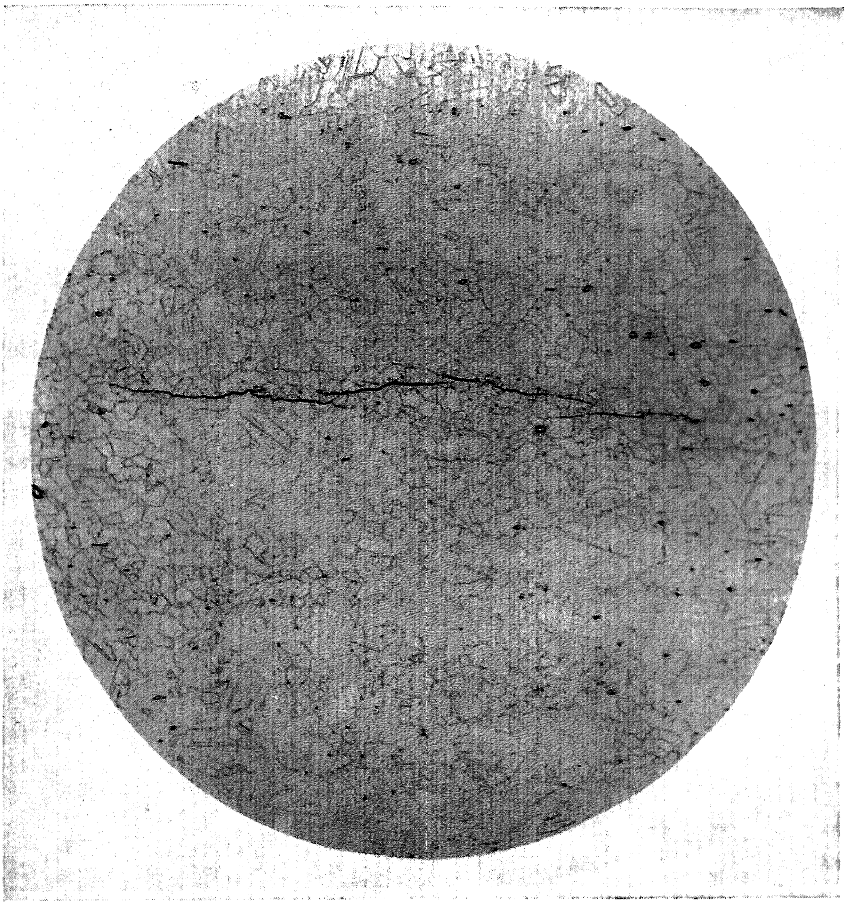

General Electric Co.

Fig. 18. Photomicrograph of sharp discontinuity in a turbine wheel, caused during forging operation.

Figs. 18 and 19 show photomicrographs of a typical sharp **cracklike discontinuity** and a **segregate type of inclusion,** respectively.

Indications of Forging Bursts. Fig. 20 illustrates the cross-section of a **stainless steel rim of a turbine wheel** containing forging bursts *FB*. These are irregularly shaped cavities caused by rupture of the material during forging.

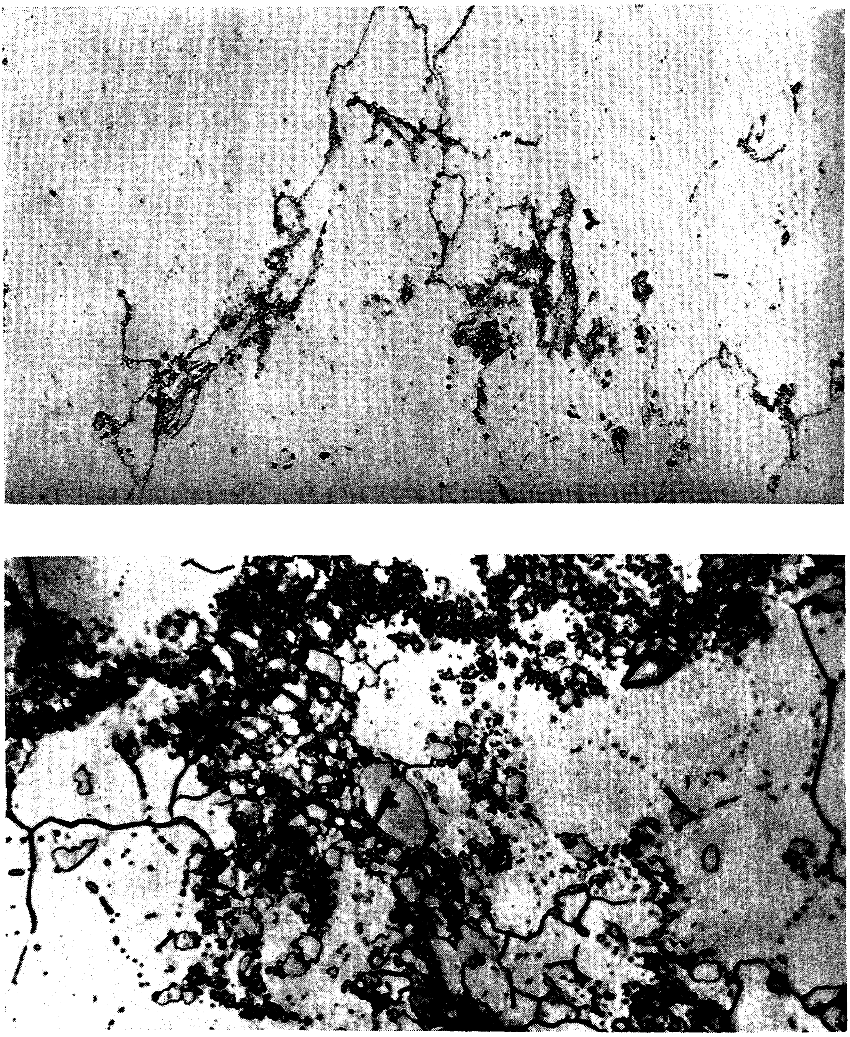

General Electric Co.

Fig. 19. Photomicrograph of a segregate in a forged turbine wheel.

Forging bursts are rejectable and are likely to be clustered in groups and produce many A-scan indications of varying degrees of amplitude. The reflections from inclusions will be of varying amplitude also but are more likely to be widely scattered. By comparison the indication from a crack will be continuous for as much as one-fourth the circumference of the rim, with complete loss of reflection from the rear surface.

Fig. 21 shows a B-scan presentation of a complete **contour-forged rim** with reflections from the O.D. and I.D. surfaces and from the familiar clustered group of indications from forging bursts.

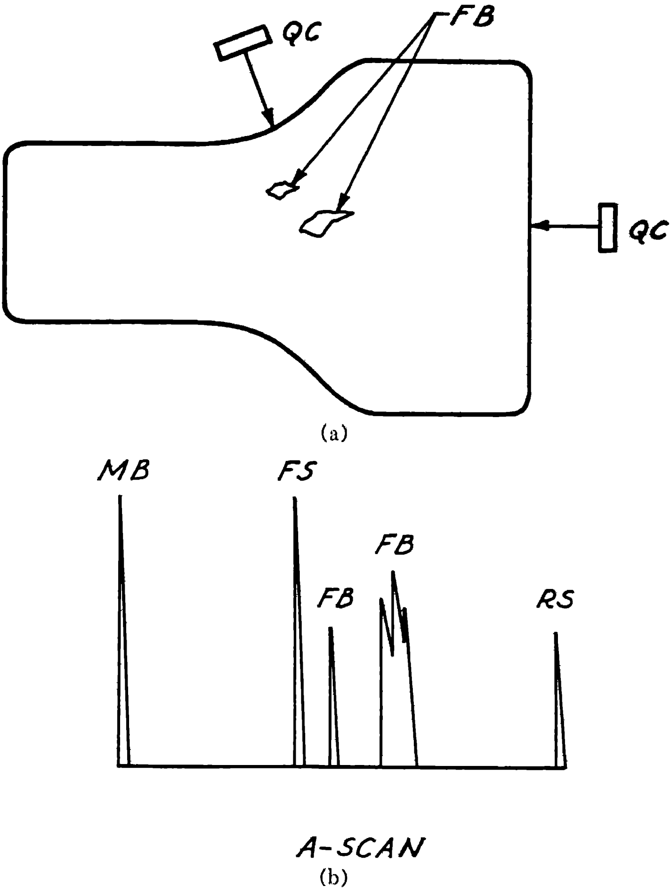

Fig. 20. Ultrasonic inspection of rim of stainless steel rotor wheel with forging bursts, *FB*. (a) Beam position on fillet area to detect forging bursts. (b) A-scan indications showing reflections from forging bursts, *FB*, between front-surface, *FS*, and rear-surface, *RS*, indications.

Indications of Small Inclusions. These rotor wheel rims are also inspected by ultrasonics for **nonmetallic inclusions** too small to be detected by radiography. These inclusions do not seriously affect the mechanical properties of the material as do cracks and forging bursts. They are randomly located, and if they are exposed on a **machined surface** like a serration used for the insertion of a bucket, a costly rejection is the result. The rim acceptance standard does not permit any ultrasonic indications between front- and rear-surface reflections.

SPURIOUS INDICATIONS FROM SURFACE CONDITIONS. A word of caution is necessary to warn the user of ultrasonics of the danger of obtaining false indications and mistaking them for indications from defects. The safest way to avoid these dangers when using ultrasonics is to have the surface prepared so that there is no possibility of sound-wave scattering. A common practice is to require that the surface of test objects have at least a 63 μin. r.m.s. **finish.**

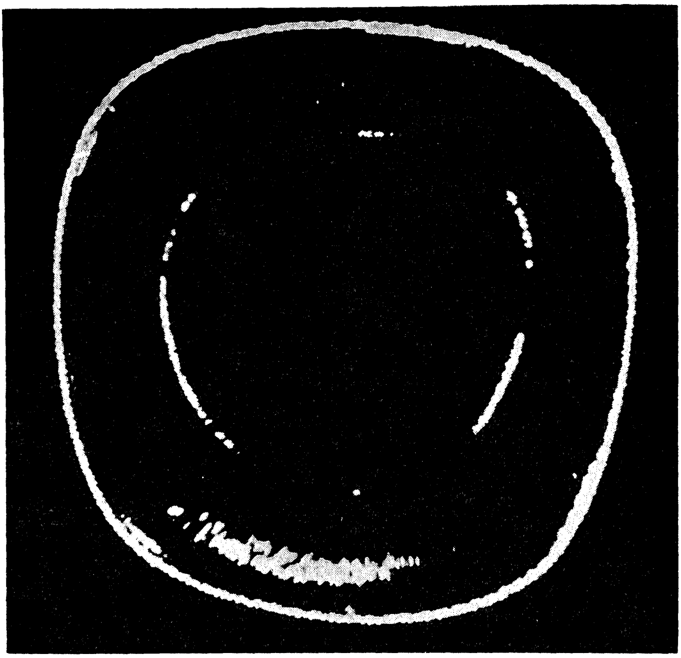

The Ladish Co.

Fig. 21. Photograph of B-scan presentation of a contour-forged turbine wheel rim containing forging bursts.

Indications from Surface Contour Blending. Surface treatment such as blending or grinding can produce misleading results. Fig. 22 shows a schematic drawing of a cross-section of a turbine rotor where a slight depression has been made in the otherwise smooth surface by a blending operation. The depression in this case has been exaggerated to illustrate the actual condition more clearly. However, in actual cases these depressions may be so slight that they cannot be seen under water, and their presence can be verified only by touch. Yet, under certain conditions, they can produce a false indication, *FI*, as depicted in the A-scan in Fig. 22(b). If the sound waves enter the surface at the edge of the blended area, they can divide or scatter in such a manner that part of the beam will travel across the surface of the blend, reflect from the opposite edge, and appear as an indication. Since sound travels much slower in water than in metals, the amplitudes and position of false indications with respect to front- and back-surface reflections will depend largely on the size, depth, and contour of the blended area and the path length in the metallic part.

A desirable practice is to machine the "as-forged" rotor wheel to a 63 μin. r.m.s. finish, with opposite faces parallel wherever possible, so that the effects of varying shape and contour can be minimized. This is more necessary when inspecting materials that may contain inclusions, such as **carbide bands,** whose reflections can be confused with those from serious defects. In these cases the forging vendor, who also ultrasonically inspects the wheels, is paid to prepare the part by machining. Enough stock is provided in the forging and after **machining prior to ultrasonic testing** so that the finish-machined contours and tolerances can be maintained. This procedure is more expensive but pays for itself in greater reliability of ultrasonic inspection of critical parts. After preliminary machining and ultrasonic inspection, the wheels are heat-treated before shipment from the forging vendor's plant.

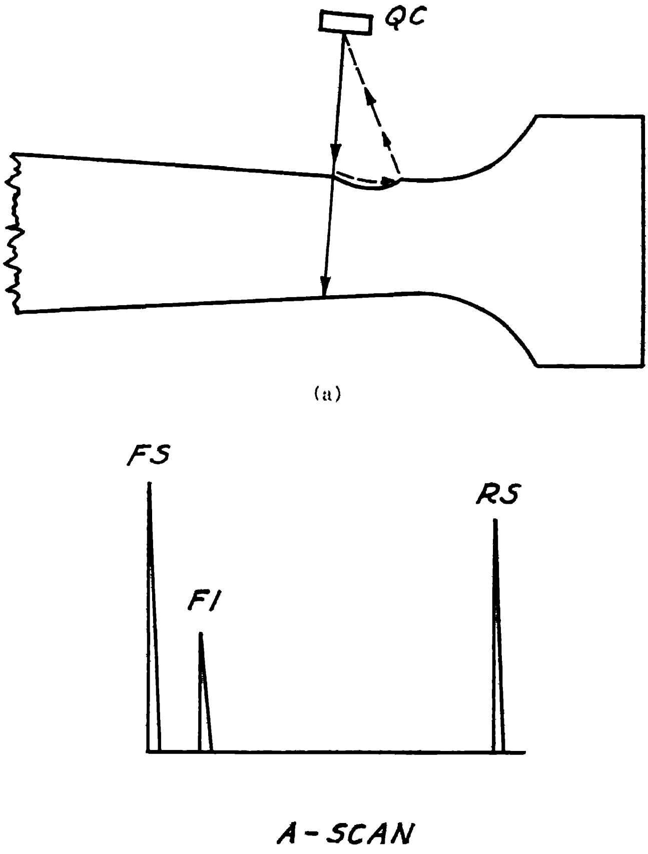

(a)

(b)

Fig. 22. False indication from surface contour blending. (a) Path of beam producing false indication (dotted). (b) A-scan indications showing false indication, *FI*, between front-surface, *FS*, and rear-surface, *RS*, indications.

Indications from Heat-treating Scale. Heat treating can produce a thin, imperceptible scale or film on the surface of the wheels, which may produce confusing indications. Fig. 23(a) shows a schematic drawing of cross-section of a machined turbine-rotor wheel as obtained from a forging vendor. The crystal *QC* is directed onto the surface of the rotor in an area containing a thin scale. The size of this scale has been exaggerated to illustrate the condition more clearly. The indications from this surface condition are depicted on the A-scan sketch of Fig. 23(b) and are generally characterized by having a greater width at the base than those from smooth reflecting surfaces. A slight surface etching will remove

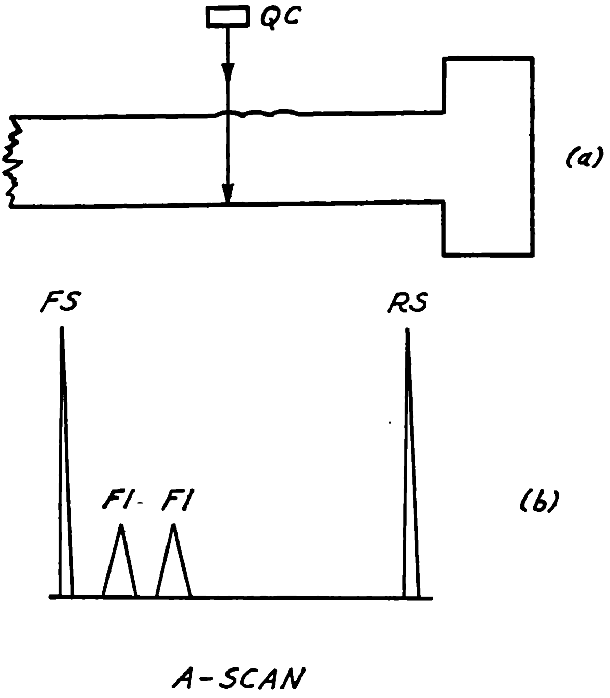

Fig. 23. **False indications from heat-treating scale.** (a) Path of beam entering scaled surface. (b) A-scan indications showing false indications, *FI*, between front-surface, *FS*, and rear-surface, *RS*, reflections.

the cause of these reflections. They are a nuisance because they may hide or be confused with an indication from an actual defect.

PROVING INTERPRETATION VALIDITY. To obtain maximum reliability with ultrasonic inspection, it is necessary, when working with newly designed parts or new materials, to inspect large numbers of parts and perform many metallurgical examinations before a reliable correlation can be obtained between the indications and their causes.

Pipe and Tubing

PRINCIPLES OF TEST. When an ultrasonic beam impinges upon a surface at an incident angle other than normal, the penetrating longitudinal sound wave will be refracted according to Snell's law. This phenomenon is utilized in the immersion ultrasonic inspection of tubular shapes, since the angles of the sound beam incident on the pipe or tubing surface are adjusted to range from approximately 10 to 30 deg. Thus the refraction sends the beam around the tubular annulus.

Mode of Beam Propagation. The sound is propagated around a pipe wall in a **saw-tooth or zigzag pattern,** and the mode of propagation is generally considered to be either shear or longitudinal vibration. The saw-tooth pattern is fairly sharp, and a defect can be detected only when its position coincides with one of the nodes. Observations seem to indicate that the sound is propagated around the thin wall of the small-diameter tubing as a severely retarded and **distorted longitudinal wave.** As the boundaries of the material through which the longitudinal wave is being propagated approach each other, they offer increased interference, and the **longitudinal velocity** is appreciably reduced. With progressively thinner tubular walls, the reflection nodes become less sharp.

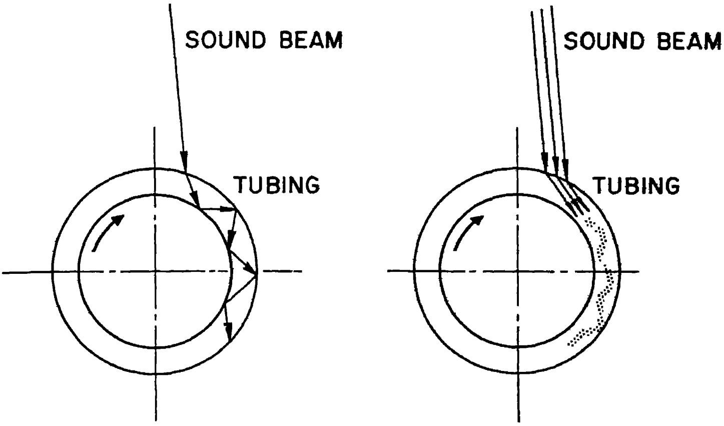

Fig. 24. Propagation of sound in tube wall.

When the wall is very thin, the sound floods around the very narrow metal annulus or wall. The two concepts of the travel pattern are depicted in Fig. 24. Observations in inspection of thin-wall tubing seem to indicate that the sound wave phenomenon may be explained by comparison with the formation of **Lamb waves.** (See section on Ultrasonic Fields for description of Lamb wave phenomena.)

Test Development. Inspection of pipe and tubing by the contact method, with a shear wave propagated around the circumference of the pipe, has been made on pipe sizes down to 1¾-in.[5] In tests on 0.080-in. O.D. tubing, a shear wave was propagated axially through the tube wall.[6]

Advantages of Immersion Scanning. Immersion scanning has several inherent advantages for the inspection of pipe and tubing, as follows:

1. The method allows the use of a highly damped piezoelectric transducer having one of the highest electromechanical couplings and short pulse length.
2. No special transducer adapters or shoes are required when changing the size or shape of the test object.
3. Simple continuous adjustment of the incident angle of the sound beam is permitted.
4. The coupling liquid is continuously available.
5. Since intimate contact is not required, limitations on inspection speed due to contact difficulties are eliminated.
6. The immersion technique is not influenced so greatly by loss of ultrasonic coupling due to ovalness, surface conditions, or dimensional variations as is the contact method.
7. Total immersion in a water bath aids in suppression of surface waves which inordinately increase signals from minor outside-surface discontinuities.

8. The water column provides a delay line that allows the very strong initial signal to pass through the amplifier before the weaker inspection signals return to the instrument. This point is particularly advantageous when inspecting small tube sizes.
9. The water column readily permits collimation or masking of the sound beam, blocking out a portion of the top surface of the pipe or tube. Thus the defect signal is compared with the smaller signal from the front surface of the test object rather than with the very strong signal transmitted to the crystal.

Scope of Application. The immersion technique has been used successfully for the critical inspection of **small-diameter tubing** down to $\frac{3}{16}$-in. O.D. by 0.025-in. wall and $\frac{1}{4}$-in. O.D. by 0.017-in. wall, and up to **pipe sizes** with outside diameters of 11-in. and over. In general this method is designed to detect longitudinal discontinuities, i.e., flaws having an orientation along the tubular axis. Typical examples of **longitudinal discontinuities** are cracks, laps, seams, folds, incomplete weld penetration, severe intergranular corrosion, scratches, gouges, laminations, etc. The apparent size of the discontinuity will be a function (1) of the reflecting area as determined by the cross-sectional size of the discontinuity and its orientation relative to the sound beam, and (2) of other changes in acoustic impedance related to the presence of the discontinuity. Obviously, the more nearly perpendicular the flaw is to the sound beam, the larger will be the reflected signal. It is difficult to differentiate between short, deep discontinuities and long, shallow defects having equal reflecting areas.

Limitations in Defect Detection. A cracklike defect returns the maximum signal only if the plane of the longitudinal defect contains a radius of the tubular shape. If this condition does not obtain, the defect is detectible when the sound beam is propagated around the tube in one direction, but the same defect may not be detectible if the sound is propagated in the other direction. For this reason all tubular objects should receive a **double inspection** to increase the confidence in the detection of nonradial defects.

Defects which offer very little **reflecting interface** are difficult to detect by this method. These include rounded grooves or gouges, pickling pits, small dimensional variations, small amounts of foreign metal pick-up, intergranular corrosion, pinholes (at normal inspection speeds), and internal metallurgical changes such as small variations in grain size. Experience shows that this ultrasonic technique should be utilized only for the detection of longitudinal-type defects.

TEST EQUIPMENT. Since the sizes of interest generally range from small-diameter, thin-wall tubing up to large-diameter, heavy-wall pipe, the **design criteria** include instrument characteristics compatible with the thin section of small tubing and mechanical designs flexible enough for adaptation to pipe sizes. Inspection rate is important, and therefore additional investment should be made in instrumentation to ensure the detection of defect signals at high inspection speeds. The basic instrumentation should have a very short pulse length to provide the necessary resolution for small-diameter tubing. A pulse-repetition rate adjustable from about 300 to 1000 c.p.s. is necessary to provide adequate circumferential coverage when inspecting pipe or tubing which is being rotated at 250 r.p.m. or faster. Also essential in an **adequate basic instrument** are circuits to provide for:

1. A gated alarm system.
2. Attenuation correction.
3. The necessary synchronization signals to provide for the use of a B-scan attachment.

Impedance Matching. The use of impedance-matching circuits at the transducer end of the coaxial cable reduces the effect of cable length and gives an increase in signal strength without an increase of background noise. In an immersion test instrument, the transducer is the signal generator, and a **matching network** consisting of a series inductance with a parallel resistance, tuned to the test frequency, gives the necessary impedance match for the received signal. The resulting increase in signal strength allows a reduction of amplifier gain and noise level, and hence the ability to detect small signals is enhanced.

Selection of Transducer. For inspection in which even the smallest discontinuity is important, the proper selection of the transducer becomes essential. Use of a **highly damped lithium-sulfate transducer** will provide a very short, sharp, initial pulse and will greatly enhance the available sensitivity and resolution.

Presentation of Indications. For the fast inspection rates which are normally required, it is necessary to use the B scan as auxiliary data-processing equipment. The **conventional A-scan presentation,** generally an integral part of ultrasonic flaw-detection instruments, exhibits instantaneous signal intensity as a function of the time of travel, or distance traveled by the sound. Since, for the inspection of pipe and tubing, the sound is channeled around the circumference in the wall of the rotating pipe or tubing, the signal from a defect travels across the A-scan oscilloscope. With high rotational speed, it is difficult to detect these rapidly moving defect signals and impossible to evaluate their magnitude.

Characteristics of B-Scan Images. The B-scan instrument samples the A-scan pattern 300 to 1000 times per second and presents this information on the vertical sweep of the B-scan oscilloscope. The horizontal sweep of the oscilloscope is driven by some positional signal supplied from the mechanical-scanning equipment. This method of presentation is analogous to a stroboscope and is nearly independent of scanning speed. For instance, in plate inspection the B scan would present an instantaneous cross-section of the plate. Fig. 25 compares the principal types of data presentation from a **laminate-like defect.**

If, when scanning tubing and pipe, a rotational signal is used to actuate the horizontal sweep, any defect moving with the pipe wall produces a signal which moves across the screen; also, this moving defect changes its distance from the transducer, and this distance variation is presented on the vertical sweep. The defect signal is a combination of these two sweeps and appears as an inclined line on the face of the B-scan screen. The length and brilliance of this inclined line are indicative of the depth and size of the defect. A **long-persistence phosphor** is used on the B-scan presentation tube because of its brilliance and memory. Thus a defect which may flash on the screen for approximately 0.05 sec. or less may be retained as an image for as long as 1 sec. Therefore the likelihood of detection of this defect signal by the operator is increased considerably; at the same time, operator strain and fatigue are reduced. A block diagram of this method of ultrasonic inspection appears in Fig. 26.

SCANNING EQUIPMENT. Mechanical equipment for the inspection of tubing must hold the tubing straight as it is rotated around its axis, keep the transducer in proper alignment at all times, and translate the transducer along the length of the tube at such a rate that the entire surface of the test object is covered by the sound beam with an overlapping helical scan.

When inspecting the **larger diameters and heavier wall** found in pipe, it has not seemed practical to hold the pipe straight while rotating it. Therefore, a

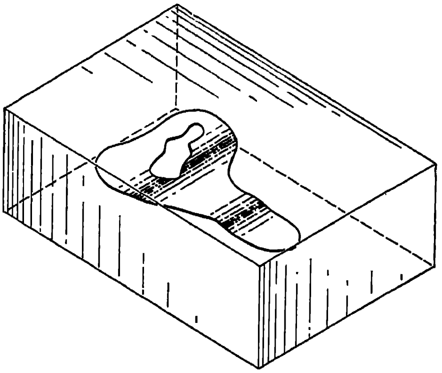

(a) LAMINATION IN PLATE

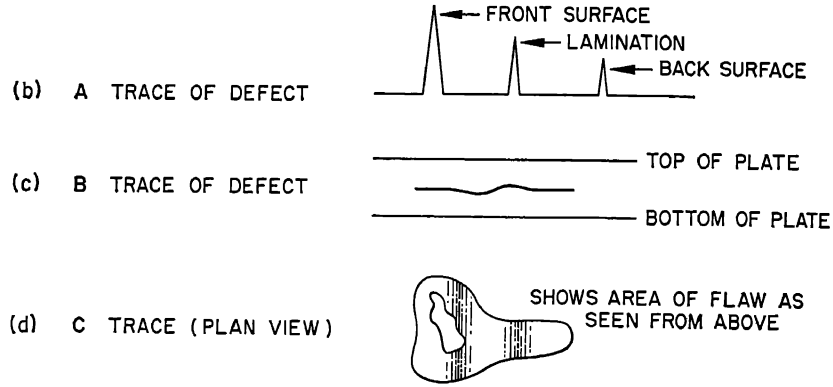

THE ENTIRE SURFACE OF THE PLATE MUST BE SCANNED TO PRODUCE THE PLAN VIEW

Fig. 25. Comparison of A-, B-, and C-scan techniques.

hand-held jig may best be used to enable the transducer to remain in proper alignment with the pipe, regardless of the movement of the pipe as it is rotated around its axis.

Speed of Scanning. Thin-wall, small-diameter tubing, if held in proper alignment, can be rotated and successfully inspected at rotational speeds of 250 to 300 r.p.m. and greater. Linear translation of the transducer relative to the rotation is dependent upon the degree of inspection desired. For **less critical inspection,** a larger transducer may be used, and less overlap between successive rotations will allow linear inspection speeds in the order of 20 feet per minute (f.p.m.). For **very critical inspection,** the smaller transducer and increased overlap per rotation will drop the inspection rate to 5 f.p.m. or less. Pipe can normally be rotated at speeds up to about 120 r.p.m. For normal inspection standards, inspection speeds may be as fast as 10 f.p.m., since large transducers and a mini-

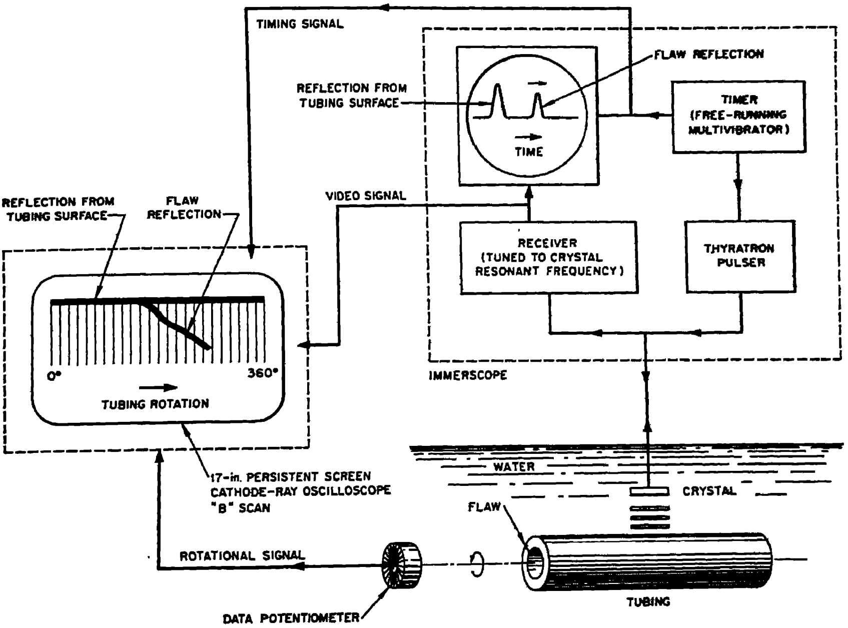
TIMING SIGNAL
REFLECTION FROM TUBING SURFACE
FLAW REFLECTION
TIME
TIMER (FREE-RUNNING MULTIVIBRATOR)
VIDEO SIGNAL
RECEIVER (TUNED TO CRYSTAL RESONANT FREQUENCY)
THYRATRON PULSER
REFLECTION FROM TUBING SURFACE
FLAW REFLECTION
0°
360°
TUBING ROTATION
IMMERSCOPE
17-in. PERSISTENT SCREEN CATHODE-RAY OSCILLOSCOPE "B" SCAN
WATER
CRYSTAL
FLAW
ROTATIONAL SIGNAL
TUBING
DATA POTENTIOMETER

Oak Ridge Nat'l. Lab.

Fig. 26. Block diagram of ultrasonic inspection of pipe and tubing.

mum of overlap on the helical scan may be permissible. For more critical inspection, reduction in the transducer size and increase in the overlap of the helical scan may reduce the inspection rate to 5 f.p.m.

Couplant or Immersion Medium. Tap water is normally used as the couplant in the immersion tanks. Small amounts of rust inhibitor and wetting agent are added to the bath. The wetting agent prevents the formation of small air bubbles which could cling to the test object and produce confusing echoes.

TESTING TECHNIQUES AND PROCEDURES. The proper interpretation and evaluation of the presented defect signals are essential to any nondestructive test or inspection. A common method for the estimation of defect size is the use of a **reference standard.** This reference standard should be a sample length of the same size of material as that being inspected. It should have a similar mechanical and thermal history, since a nondestructive estimation of defect size can best be made by a comparison with a known defect in the same material. The common defect in pipe and tube is a longitudinal crack, and therefore the simplest and most readily reproducible defect simulation is a very narrow longitudinal notch, equal in depth and length to that of a rejectible defect. These **longitudinal notches** should be machined on both the inner and outer surfaces of the object and on the same circumference. At best, this is only a Go—No Go gage used to determine whether the defect appears to be larger or smaller than the reference notch and also to give proof of the detection of inside diameter defects. It is not easy to prepare such a reference standard for small-diameter tubing because of the difficulty of working on the inner surfaces of bores with diameters as small as 0.135-in. For this reason a **naturally occurring**

defect can be used as a reference standard for small-diameter tubing. Comparisons with previous inspection and metallographic examinations indicate the approximate defect size of the reference standard.

Positioning of Transducer. For the inspection of tubular shapes, the transducer is aligned so that the sound beam produces a range of incident angles optimum for the particular ratio of wall thickness to diameter and for the velocity of sound propagation peculiar to the test material.

Angles of Incidence. A range of from 10 to 30 deg. is typical, with the lower third of this angular range demonstrating preferential sensitivity to inside diameter defects and the upper two-thirds having a preferential sensitivity to outside-diameter defects. There are several reasons for limiting the range of incident angles. **Small angles of incidence,** particularly those less than 10 deg., set up strong reverberations across the tube wall which mask defect indications. Unwanted **Rayleigh (or surface) waves** which inordinately emphasize shallow outside diameter defects are minimized by eliminating angles of 27 deg. and larger (for steel). (See the section on Ultrasonic Fields for a description of Rayleigh, or surface, waves.)

Control of Sensitivity to Defects. To interpret both inside and outside diameter defects on the same basis, a compromise must be made between the angular ranges which are sensitive to both. This is achieved by careful adjustment of the **range of angles** to be used within the limits dictated by the other two considerations mentioned in the preceding paragraph. This adjustment is best accomplished by use of the reference standard. The transducer should be positioned to "see" both inside and outside diameter notches with comparable signal strength when the reference defect signals are the same distance from the front-surface signal. This adjustment does not give the maximum signal from either defect, but it does present defects in their relative size regardless of their location in the tube or pipe wall. The **defects located on the inner surface** are the most difficult to detect, and therefore it is considered necessary to "prove" the technique used on the reference defects located on the inner surface.

Beam Collimation. In cases where the diameter of the tubing being inspected is smaller than the diameter of the transducer, a collimator is used to confine the sound beam to the proper range of angles. Also, when a noncollimated round transducer is properly aligned, only a short chord of the transducer is utilized. Thus the **effective width of the transducer** is not the crystal diameter but rather a short chord of the transducer, which is then the limiting factor in the linear translation of the transducer per revolution if full coverage is to be maintained. If proper collimation is used, the effective width then approaches the transducer diameter, and the linear translation is limited only by the beam diameter. When dealing with larger pipe sizes, collimation may not be necessary, since the radius of the pipe is large compared with that of the transducer, and hence a natural collimation is effected. An attempt has been made, with partial success, to use square or rectangular crystals in order to eliminate the need for collimation on smaller diameters. But even for these transducers the proper collimation is essential for best sensitivity.

Gated Flaw Alarm. The reference standard is used as an aid in the initial alignment of the transducer relative to the test pieces. At the same time, necessary instrument adjustments are made to assure adequate identification of discontinuities with reflecting interfaces equivalent to the notches in the reference standard. As an aid to qualitative interpretation, a gated flaw alarm can be used to advantage. If this circuit is adjusted properly with regard to time and sensitivity, only relevant signals will actuate the alarm. Fig. 27 illustrates the **proper use of a gate circuit**; the recessed portion of the horizontal sweep on the A-scan and the double-ended arrow (*B-B*) on the B-scan represent the position (in time) of the gate. The short, diagonal signals on the B-scan pattern do not extend into the gated region and may be ignored because they are indicative only of scratches or other insignificant discontinuities. The two diagonal signals which do extend into the gate have sufficient strength to actuate the alarm and are

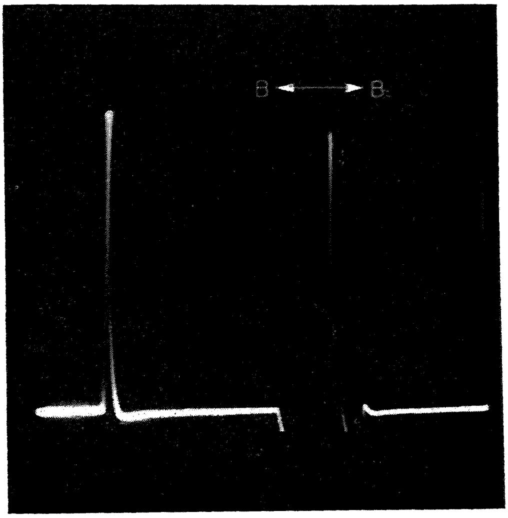

(a)

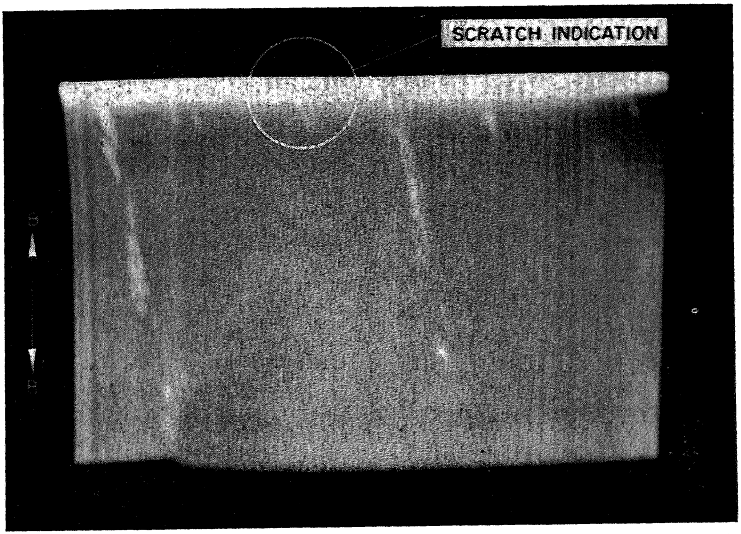

(b) Oak Ridge Nat'l. Lab.

Fig. 27. Alarm gate setting. (a) A-scan indication. (b) B-scan indication.

causes for rejection. The proper use of **attenuation correction,** which increases the amplification as a function of the distance from the front-surface signal, can be very important in amplifying relevant indications above spurious or nonrelevant signals.

INTERPRETATION OF TEST INDICATIONS. Any evaluation of defect size as a function of the reflected ultrasonic signal is simply a comparison with a known defect in similar material. **Inconsistencies** may arise in this evaluation if the detected discontinuity is not favorably oriented or is a nonradial defect. However, some idea of **relative defect depth** can be obtained by the magnitude of angular rotation through which the tubular specimen may turn and still present a detectible signal from the discontinuity. In general, shallow flaws will be detectible through less than 60 deg. of rotation, while the signals from deeper defects may be detected for 90 deg. or more. Some area of confusion may arise when inspecting very small tubing in which rejectible defects may have depths nearly equal to those of surface scratches.

Nonrelevant Indications. As in many inspection methods, spurious signals tend to make interpretation difficult; however, many of these signals can be ignored because of the testing characteristics of the specific technique. Since the object is rotating while being inspected, any defect will of necessity be moving with the same rotational speed as the pipe or tube and will be either increasing or decreasing the distance or time from the transducer. Therefore any signal which does not exhibit this **characteristic time change** may be ignored.

Sources of Nonrelevant Indications. General causes for spurious signals, particularly on small-diameter tubing, are the presence of **dirt, grease, or air bubbles** on the inside or outside of the tube. If these adhere to the tubular surface, they move with the piece and represent an acoustical mismatch leading to sonic reflection. In most instances these can be removed by wiping the tube. The inside of the tube should be purged to assure that the bore is completely filled with either water or air, an air-water interface being the undesirable factor.

In general, nonrelevant signals may be reflected from **smaller scratches and discontinuities** which are not serious enough (according to inspection specifications) to constitute rejectible defects. Severe **dimensional variations in pipe,** such as ovalness, eccentricity, outside diameter flats or inside diameter gouges, may produce characteristic ultrasonic indications which may or may not be relevant, depending upon the specification.

Crack Indications. Fig. 28 illustrates the typical B-scan pattern from an outside diameter crack which is about 0.011 in. deep in a 0.230-in. O.D. × 0.025-in. wall **Inconel tube.** This crack was relatively short but still presented a readily detectible signal. Typical of the larger defects detected by ultrasonics is the crack shown in Fig. 29 along with the B-scan pattern obtained from this crack: a 0.027-in. deep crack, in a 0.250 × 0.049-in. wall **Hastelloy tubing.** This crack extended through approximately 55 percent of the tube wall and was longer than the effective sound beam width. The large B-scan indication is evident through over 270 deg. of rotation. Among the smaller detectible defects which have been confirmed metallographically is the 0.0015 in. deep by 1/16-in. long crack on the inside diameter of a 3/16 × 0.025-in. wall Inconel tube, as illustrated by Fig. 30. The B-scan indication may be identified readily but is much smaller and less brilliant than previous indications. Fig. 31 shows a seam-type defect detected with ultrasound on the inside diameter of 3/4-in., Schedule 40 pipe. Fig. 32 is a typical B-scan pattern obtained from such a defect.

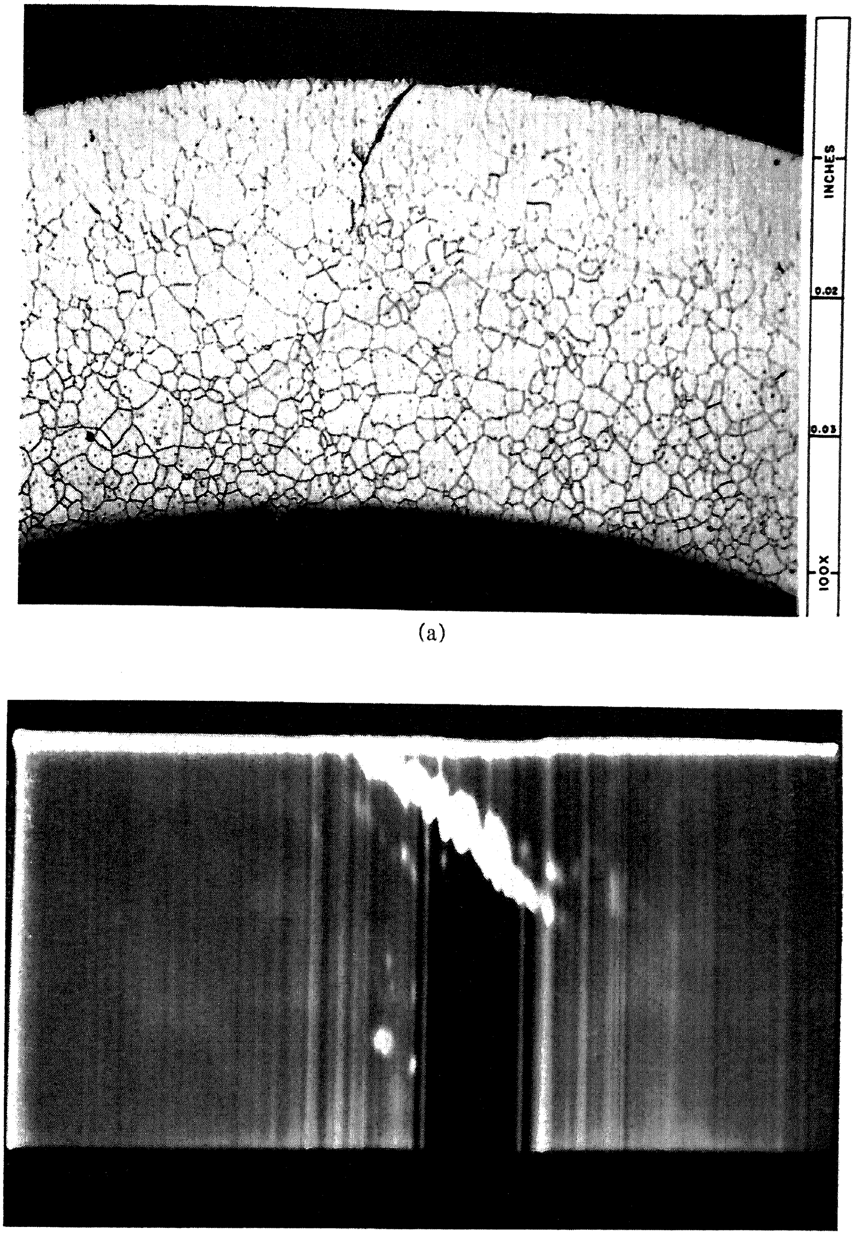

(a)

(b)

Oak Ridge Nat'l. Lab.

Fig. 28. CX 900 Inconel tubing, 0.229 × 0.025 in., with crack approximately 0.011 in. deep. (a) Cross-section of crack in tubing. (b) B-scan indication of crack.

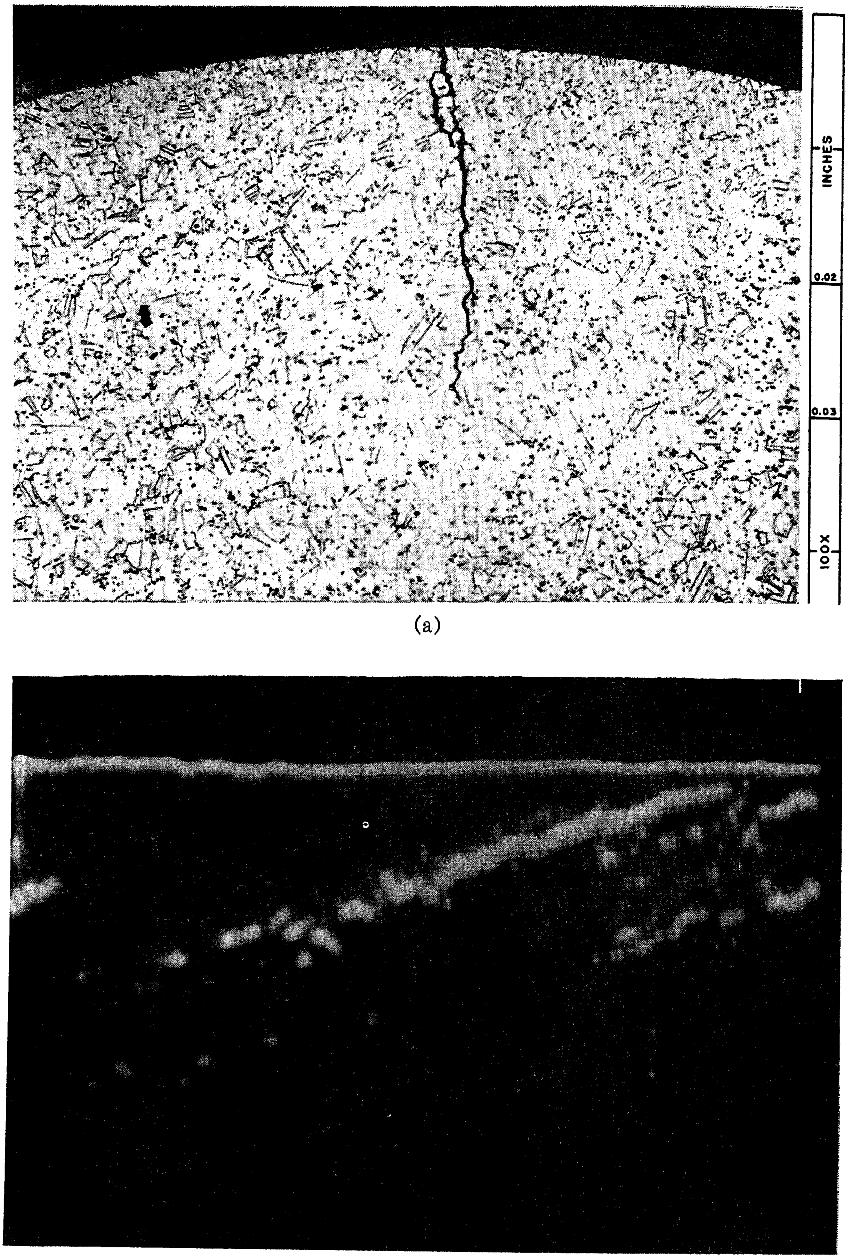

Oak Ridge Nat'l. Lab.

Fig 29. Hastelloy "B" tubing, 0.0250 × 0.049 in., with crack approximately 0.027 in. deep. (a) Cross-section of crack in tubing. (b) B-scan indication of crack.

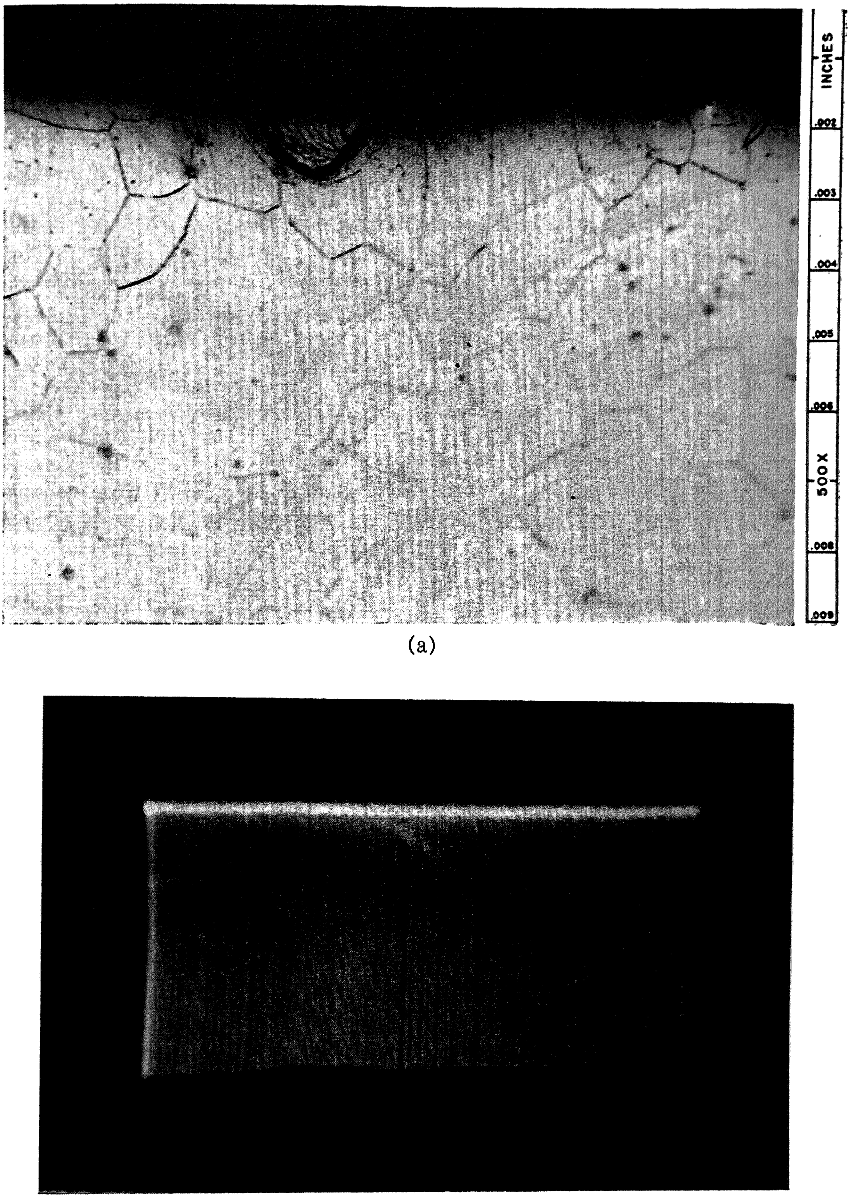

Oak Ridge Nat'l. Lab.

Fig. 30. Crack approximately 0.0015 in. deep in 3/16 × 0.025-in. Inconel tubing. (a) Cross-section of crack in tubing. (b) B-scan indication of crack.

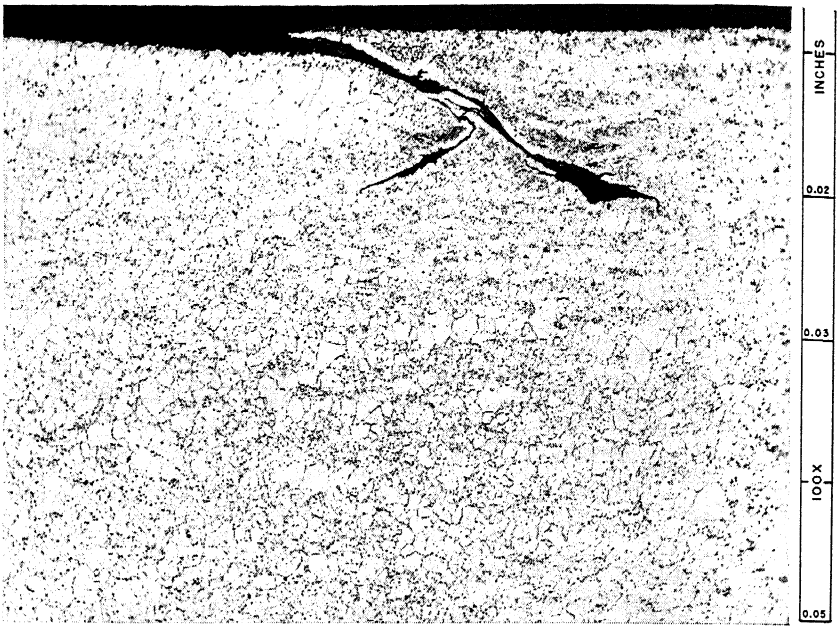

Oak Ridge Nat'l. Lab.

Fig 31. Seam in ¾-in., Schedule 40 pipe.

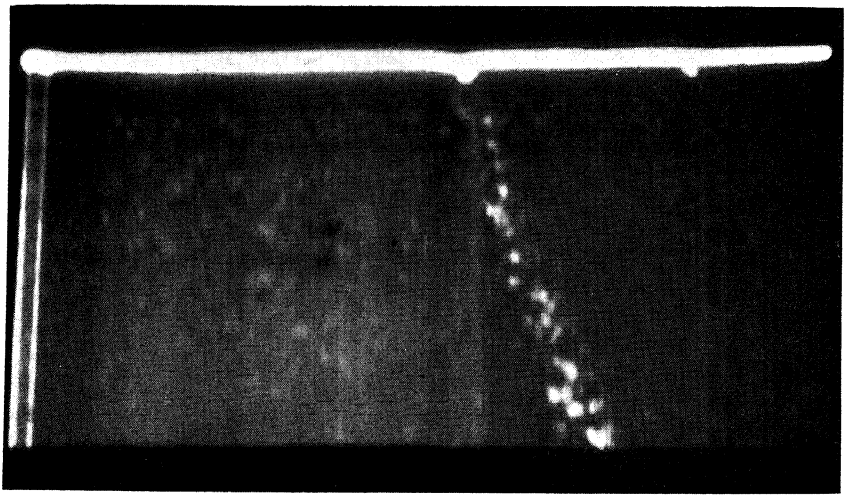

Oak Ridge Nat'l. Lab.

Fig. 32. B-scan indication from seam in Fig. 31.

QUALITY AND SPECIFICATIONS. Certainly the quality requirements for pipe or tubing would be dependent upon **service requirements,** taking into account such things as the corrosive environments, thermal gradients or stresses, mechanical loading, and cyclic fluctuations in any of these variables. From these considerations it may be possible to determine the **limits of acceptable discontinuities** for the particular application. In many instances, this quality may be readily obtainable as stock items from fabricators. If the quality desired is higher than that normally expected from the vendors, two approaches may be followed. One is the negotiation of a purchase specification to the quality desired; this may involve a premium price for the product. The other is the purchase of mill-run stock and use of an incoming inspection to separate the material of the required high quality from the down-graded, lower quality pipe or tubing. In many instances the latter procedure may be the better, although the most satisfactory approach may depend upon the quantity and quality of material needed.

Specified Characteristics. Typical quality specifications should include statements concerning outside and inside diameter surface finishes, minimum lengths, dimensional tolerances, the acceptability of certain fabrication methods such as pickling techniques, sand blasting, heat treatments, polishing or grinding techniques, in-plant inspection procedures, acceptable sizes of typical discontinuities, etc. Only through such detailed specifications can the purchaser be assured that the item will fulfill his particular need.

SPECIAL APPLICATIONS. These techniques have been applied successfully to seamless tubing, welded and redrawn tubing, welded pipe, and welded and rolled or swaged pipe. In general, **welds** which have been worked or reduced approximately 25 percent will not offer sufficient mismatch for an echo at the weld interface. If there has been little or no work subsequent to the welding, a small reflection can occur at this interface, but the resulting echo amplitude will not be comparable with that of a rejectible defect under normal standards. In some instances there will be a physical **misalignment** of the parent metal faces at the weld joint, due to variations in thickness of the initial metal strip. The ultrasonic technique offers an excellent gaging tool for measuring the degree of misalignment for the entire length of the pipe.

References

1. Kleint, R. E. "Relationship Between Defect Orientation and Ultrasonic Indications," *Nondestructive Testing,* 15, No. 1 (1957): 30.
2. *Metallurgical Investigation of a Sample of 4340 Steel,* Boeing Airplane Co., Rept., No. 330 (1955).
3. Binczewski, G. J. "Standardization and Application of Ultrasonic Surface-Wave Inspection," *Nondestructive Testing,* 15, No. 1 (1957): 36.
4. Soffa, L. L., and R. Hannum. *Ultrasonic Testing of 0.188 Gauge 7075-T6 Sheet by Shear Wave (Angle Beam) Inspection Method,* Northrop Aircraft, Inc., Rept. No. NA 1-55-242 (1955).
5. Moriarity, C. D. "Ultrasonic Flaw Detection in Pipes by Means of Shear Wave," *Trans. Am. Soc. Mech. Engrs.,* 73 (1951): 225.
6. Pardus, A. J. "Ultrasonic Testing Used for Small-Diameter Tubing," *Iron Age,* 171, No. 5 (1953): 110.
7. Oliver, R. B., R. W. McClung, and J. K. White. "Immersed Ultrasonic Inspection of Pipe and Tubing," *Nondestructive Testing,* 15, No. 3 (1957): 140.

SECTION 48

ULTRASONIC CONTACT TESTS

CONTENTS

PAGE

Transducers and Couplants

- Principle of test 1
- Transmission and reflection techniques 1
- Test frequencies 1
  - Selection of test frequencies 2
  - General guide 2
  - Influence of grain size 2
- Transducers and search units 2
  - Selection of search units 2
- Couplants 3
  - Selection of couplants 4

Test Instrumentation

- Requirements of test conditions 4
  - Surface finish 4
  - Metallurgical structure 4
  - Location, contour, and extent of areas to be tested 4
  - Type of defect 4
  - Method of calibration or interpretation of defect indications 5
  - Manual or automatic tests 5
  - Desired scanning speed 5
- Available forms of instrumentation 5
  - A-scan units 5
  - B-scan units 5
  - C-scan units 5
  - Meter indications 5
  - Gating and marking systems 5
  - Repetitive semi-automatic testing 6
    - Ultrasonic contact tests for cracks in journal area of freight car axles (*f.* 1) 6
  - Automatic-programming units 7
- Selection of instrumentation 7

Test Techniques

- Test advantages 8
- Test limitations 8
- Angle of test 8
  - Determining wedge angles 8
- Through-transmission systems 9
- Selection of test technique 9

Applications of Tests

- Castings 10
    - Ultrasonic contact testing for center condition of 24-in. ingots (*f.* 2) 10
- Forgings 11
    - Ultrasonic contact testing of a flanged steel forging for forging bursts, inclusions, and cracking (*f.* 3) 11
- Rolled sheet and plate 11
- Extrusions 12
- Weldments 12
  - Butt and tee welds 12
  - Rough beads and backing rings 12
  - Beam penetration 12
  - Double-transducer tests 13

Field Inspection Techniques

- Measurement of reflections 13
    - Index window used in recording signal amplitudes in contact testing (*f.* 4) 13
- Use of reference plate 15
    - Ultrasonic reference plate (*f.* 5) 14
  - Checking operating efficiency of instrument and accessories 15
  - Instrument calibration 15
    - Ultrasonic contact CRT indication from reference plate, with signal from reference hole set to index 5 on index window (*f.* 6) 15
    - Path of shear wave from angle search unit, showing node locations (*f.* 7) 16
- Linearity of instruments 16
- Selection of correct frequency for quality of material 16
- Inspection of weldments 16
    - Ultrasonic indications from weld at 2.25 Mc. (*f.* 8) 17
  - Indications of fusion zones 16
  - Typical weldment shear-wave indications 17
    - Contact ultrasonic indications from welds in 4½-in. thick steel (*f.* 9) 17
    - Ultrasonic indications of welding defects (*f.* 10) 18
    - Inadequate penetration at root of weld in ½-in. plate (*f.* 11) 18
    - Indications from welds with (a) incomplete and (b) excess penetration at the root (*f.* 12) 19
    - Excessive penetration or "run-through" of weld in ½-in. plate (*f.* 13) 19
  - Longitudinal-wave examination of weldments 18
    - Heavy steel casting containing a faulty weld repair (*f.* 14) 20
    - Ultrasonic indications from steel casting of Fig. 14 (*f.* 15) 20
- Interruption of shear waves 20

CONTENTS (*Continued*)

PAGE

Irrelevant Ultrasonic Indications

Significance of irrelevant indications 21
Causes of irrelevant indications 21
Electrical interference 21
Noise effects 21
Strong moving signals in a horizontal plane 21
Reverberations in test materials 21
Disturbances caused by the probe 22
Coupling-block disturbances 22
Sound path and reflection indications from disturbances within ultrasonic coupling block (*f.* 16) 22
Loose crystals in the probe 22
Crystal vibration decay patterns, showing (left) signals from a good crystal, and (right) prolonged ringing from a loose or defective crystal search unit (*f.* 17) . 23
Surface disturbances 23
Surface waves between transmitting and receiving probes 23
Sound path and ultrasonic indications resulting from travel of surface waves between sending and receiving crystals (*f.* 18) 23
Surface-wave reflections 24
Surface-wave reflection path (top) and indications (bottom) where waves reflect from corner of test specimen (*f.* 19) ... 24
Surface crack indications 25
Path of surface waves (top) and ultrasonic indications (bottom), showing reflection from a surface crack (*f.* 20) 25
Surface roughness effects 25
Disturbances caused by refraction 25

PAGE
Refraction of spreading sound beam in long specimens produces refraction of reflected beam, introducing spurious reflections from longer paths of refracted portions of beam (*f.* 21) 26
Transmitter pulse and bottom echo, followed by additional echoes t_1, t_2, t_3, etc., from refracted waves traveling longer paths (see Fig. 21) (*f.* 22) 26
Influence of longitudinal defects (right) removes signals from refracted beam paths in good materials (left) (*f.* 23) .. 27
Disturbances caused by form of the specimen 27
Fillets and corners 27
Example of sound paths leading to disturbing echoes from fillets and corners in test specimen (*f.* 24) 28
Example of sound path in part with internal bore, leading to spurious reflection signals (*f.* 25) 28
Cylindrical parts 28
Sound paths leading to spurious additional echoes in the examination of cylindrical specimens (*f.* 26) 29
Evaluating shape disturbances 29
Disturbances caused by structure of test materials 29
Loss of back reflection 29
Echoes following initial pulse 30
Disturbing echoes resulting from coarse-structured test specimens (*f.* 27) 30
Local changes in structure 30
Accidental disturbances 30
Couplant flow indications 31
Limitations in eliminating disturbing echoes . 31

SECTION 48

ULTRASONIC CONTACT TESTS

Transducers and Couplants

PRINCIPLE OF TEST. The theory of ultrasonic contact testing with pulsed techniques has been detailed (see section on Ultrasonic Test Principles). A **vibrating element,** such as quartz excited by a pulsed, oscillating voltage, is placed on material having elastic properties. The resulting **ultrasonic beam** passes into the material, provided that it is adequately coupled to the vibration source. The **coupling medium** is important and may be almost any liquid which will wet the surfaces and stay between the crystal and test material during the test. Couplants must be used in the uneven spaces to provide intimate coupling with the transducer.

TRANSMISSION AND REFLECTION TECHNIQUES. Two basic techniques are used for pulsed contact testing:

1. Through-transmission uses separate transducers for transmitter and receiver.
2. The reflection technique uses either one transducer as both transmitter and receiver or separate transducers for each function (see section on Double-Transducer Ultrasonic Tests).

The more widely used method is the reflection technique. It furnishes specific data as to relative size and distance of discontinuities from the test surface. The single transducer sends out a narrow beam of vibrations which may be directed like the beam of a searchlight. Separate transmitters and receivers must be properly oriented even when used side by side.

TEST FREQUENCIES. To cover the wide range of applications for which pulsed contact testing is applicable, test frequencies range from 25 kc. to 10 Mc. The ranges of test frequencies generally used for various applications are given in the table here.

Frequency Range	Test Applications
25–100 kc.	Concrete, wood poles, rock, and other coarse-structured materials.
200 kc.–1 Mc.	Castings: gray iron, nodular iron, and relatively coarse-structured materials, such as copper and stainless steels.
400 kc.–5 Mc.	Castings: steel, aluminum, brass, and other materials with refined grain size.
200 kc.–2.25 Mc. ..	Plastics and plastic-like materials, such as solid rocket propellants and powder grains.
1–5 Mc.	Rolled products: metallic sheet, plate, bars, and billets.
2.25–10 Mc.	Drawn and extruded products: bars, tubes, and shapes (ferrous and nonferrous).
1–10 Mc.	Forgings: ferrous and nonferrous.
2.25–10 Mc.	Glass and ceramics.
1–2.25 Mc.	Welds: ferrous and nonferrous.
1–10 Mc.	Maintenance inspection, especially for fatigue cracks.

Selection of Test Frequencies. When setting up an ultrasonic test program, one of the first considerations is the choice of test frequency. It is usually desirable to test at the lowest frequency that will locate specified minimum sizes and types of discontinuity consistently. Because of variations in the structure of materials, it is impossible to select the optimum frequency intelligently without experience or some experimental testing.

General Guide. In general, small-grained steels are inspected at 2.25 and 5 Mc. when the test is for **forging bursts, flaking, pipe,** and discontinuities of smaller magnitude. A 10-Mc. frequency is usually selected to locate small or **microscopic inclusions and segregations.** Large **medium-carbon steel castings** are generally inspected at 1 to 5 Mc., penetrating 10 ft. or more. **Small forgings** are inspected at 5 to 10 Mc.; **large forgings** at 2.25 to 5 Mc. for distances up to 100 ft. **High-carbon steel** may require a lower frequency, such as 500 kc., to penetrate any distance over a few feet, depending upon material heat treatment. This is also true of **cast iron,** in which the flakelike graphite structure causes scattering of the beam and lack of penetration, even at the low frequencies.

Influence of Grain Size. In most metals, the greater the grain refinement resulting from forging, rolling, or heat treating, the more homogeneous the structure and the higher the test frequency that may be used. Many **brass alloy castings** containing a small grain structure, due to controlled cooling or heat treatment, may be tested at 2.25 Mc., whereas other castings of similar alloy may be difficult to test even at 500 kc. because of their extremely large grain structure. Ultrasonic testing can respond to **differences in grain structure,** and test results may be compared with samples containing a known size of grain structure. Similar test variations exist with cast stainless steels, cast and worked aluminum, magnesium, titanium, and other metals. As in most nondestructive testing, when in doubt, results should be compared with samples of known material structure.

TRANSDUCERS AND SEARCH UNITS. The transducer is usually a piezoelectric material mounted in a suitable holder. The complete assembly is referred to as a search unit. The construction of a **contact-type search unit** should be sufficiently rugged to withstand severe handling and rubbing in contact with rough surfaces. **Quartz** is used extensively for contact testing, since it will not absorb couplant materials and can be used in direct contact. Other materials such as **barium titanate** or **lithium sulfate** require a sealed protective face, using quartz, hard metals, or other wear-resistant materials as the facing. Contact search units should be considered expendable because wear will eventually change the transducer characteristics.

Uniformity and reproducibility of test results can be achieved only if the search units of a given size and type maintain uniform characteristics for a reasonable time. Reproducible tests, as with standard blocks, should be used to check the uniformity of search units from time to time. The type of backing material, the construction, and the cementing material all contribute to the operating life of a search unit.

Selection of Search Units. The most desirable search unit for a given application is usually determined by experience. However, a few rules can be applied to narrow the selection for initial trials:

1. Maximum beam coverage and minimum number of scanning passes can be attained by using a search unit with large single crystals or a mosaic of crystals. The **crystal diameter** is limited only by the testing-surface flatness, which controls the crystal surface area that makes intimate contact at any given location.

The difficulty of defining a specific discontinuity in a large beam (as compared with that of a small beam) is also important. The **minimum size of discontinuity** that is to be detected, therefore, and the need to locate its position exactly, may limit the size of beam even though the sensitivity of the large-diameter crystal to small defects may be equal to that of a smaller one.

2. Breakage and chipping is often more of a problem with large-diameter search units (as compared with smaller units). This is especially true of the 5- and 10-Mc. crystals, which are quite thin.
3. Rough or painted surfaces can usually be tested with a plated and face-protected search unit which does not require a contact pin. This is also true when testing plastics, glass, and other **nonconducting materials** which do not provide a conducting metal surface to complete the electric circuit with the face of the transducer. With a contact-pin type of search unit, uniform testing results require reasonably clean and uniform surfaces to provide uniform electrical contact with the test material during testing.
4. A large-diameter search unit is usually indicated for **testing through greater distances.** For example, for testing through 10 to 30 ft. of steel casting, a 2- or 3-in. diam. 500-kc. search unit may be required. For the same distance in a steel forging, a 1- or 1½-in. diam., 1- or 2.25-Mc. search unit would be indicated.
5. Search units as small as ⅛-in. diam. have been used. However, ⅜- or ½-in. diam. are most often used for **close-to-surface testing** (for total test depths under 6 to 12 in.) at frequencies of 2.25, 5, or 10 Mc.
6. Available contact surface also limits the size of the search unit. Overhanging the edge of a test piece with the search unit is not usually detrimental to the test, but a search unit small enough to fit on the test surface is more often considered desirable.
7. Beam spread is often desirable to pick up **randomly oriented discontinuities** more readily. On the other hand, some applications require the straightest possible beam to minimize reflections from sides, shoulders, and other surfaces of the test piece. Also, a straight beam with little if any spread is useful in tracing out the **edges of a large discontinuity** such as a crack or in pinpointing a small discontinuity.

   At any frequency, the larger the crystal is, the straighter the beam; the smaller the crystal, the greater the **beam spread.** Also, at higher frequencies, there is less beam spread for the same diameter of search unit than at lower frequencies. The foregoing applies more or less to all types of search units for generating any of the three different modes of vibration.
8. A search unit of good mechanical and electrical construction should be selected so that it will retain its desirable characteristics for a reasonable length of time. A **poorly constructed or insensitive search unit** can make the best equipment inadequate.
9. Sensitivity of a search unit should be tested by actual evaluation of signal amplitude, shape of pulse indication, flare (pulse distortion), and beam spread on a block of material containing known discontinuities. These discontinuities may be either natural, machined slots, or flat-bottomed holes. **Industrial standards** have been established which are based on the reflections from flat-bottomed holes in standard reference blocks. The Airframe Committee of the Society for Nondestructive Testing (SNT), Committee E-7 of The American Society for Testing Materials (ASTM), and the Aircraft Industries Association (AIA) have standardized on specific **ultrasonic reference blocks.**

COUPLANTS. A contact test cannot be successful without a suitable couplant between the search unit and material. The couplant may be almost any material, liquid, semi-liquid, or paste, which:

1. Wets both the surface of the test material and the face of the search unit, excluding air between them.

2. Is easily applied.
3. Does not run off the surface too fast.
4. Is homogeneous and free from bubbles or solid particles which would reflect and scatter the beam.
5. Is not corrosive or toxic.
6. Has an acoustic impedance approaching that of the test material. (This is an ideal rather than a restrictive requirement.)

Selection of Couplants. The following examples illustrate how a suitable couplant may be selected:

1. Water is suitable but should have a wetting agent added. It is often too low in viscosity to stay on the test surface long enough to complete the test.
2. Various grades of oil are used more frequently because they stay on the test surface longer. Oils containing wetting agents, as do many commercial oils, are desirable.
3. Heavier oils and greases are used on hot or vertical surfaces and to fill surface irregularities on very rough surfaces, because they stay in place.
4. One part of glycerine in two parts of water with a wetting agent is often used because it adheres more effectively to surfaces and is an excellent couplant.

For most contact testing, the **film of couplant** should be thin. For consistent and uniform test results, its thickness should not vary appreciably. **Temperature variations in couplants** also influence crystal performance. This usually is due to variations in the temperature of the test piece or of the atmosphere.

Test Instrumentation

REQUIREMENTS OF TEST CONDITIONS. A wide range of ultrasonic testing equipment is available. Before an intelligent selection can be made for any given application or group of applications, it is necessary to analyze the problem carefully. Factors and conditions that affect an ultrasonic test and the selection of test instrumentation are covered in the subsequent paragraphs.

Surface Finish. Selection of frequency, couplant, and search units often depends upon surface finish. Rough surfaces require lower test frequencies and more viscous couplants than do smooth finishes. Search units are selected for best contact with test surface. **Curved surfaces** often require smaller search units than would normally be applied to flat surfaces. However, on **rough or corrosion-pitted surfaces,** large transducers may give higher test sensitivities, if effectively coupled.

Metallurgical Structure. Forged or cast, coarse or fine grain structures, and general uniformity of structure are significant. Lower frequencies are required for testing **coarse structures** than are needed for fine structures.

Location, Contour, and Extent of Areas To Be Tested. Large-area search units, either single-crystal or mosaics, can be used for faster inspection of **large flat surfaces.** Small-diameter search units are required to inspect through ridges, narrow shoulders, and other **restricted surfaces.** For curved surfaces, a flat search unit can be selected for best line contact. Alternatively, a mating, curved crystal face will provide maximum contact surface.

Type of Defect. Defect size, orientation, distribution, and distance from test surface are important. High frequencies are required to locate the smallest defects and for testing near the surface. Defect orientation not parallel to the test surface may also indicate the need for **angle testing.** Testing for defects at a distance of 10 ft. from the surface generally requires search units larger than those for testing closer to the surface (such as at 10 in.).

Method of Calibration or Interpretation of Defect Indications. Samples of material containing typical defects should be available. Alternatively, sample blocks with **simulated defects** (drilled holes or slots) may be used for comparison of reflected indications from known areas with unknown defect indications. Also, preliminary ultrasonic tests should be followed, if possible, by **destructive investigation** of parts to correlate defects with indications and to determine required test standards.

Manual or Automatic Tests. Manual testing is indicated on small lots, miscellaneous shapes, and nonuniform contours. For repetitive tests on large quantities of identical pieces of uniform shape and surface, or of continuous strip material, an automatic test should be considered. Poor surface conditions may hinder a satisfactory automatic test.

Desired Scanning Speed. The speed of scanning is determined by whether signaling, recording, or automatic marking for defect location is required. **Visual recognition of defect indications** is usually practical only at slow speeds or with manual scanning. Signaling with lights, bells, or other alarms can be used at higher scanning speeds to alert the operator. The **pulse-repetition rate** limits the test pulses, per inch per second of scanning, and should be calculated to determine the practical scanning speeds. Permanent records of the location and amplitude of defects may also be obtained. The test piece may be marked automatically for defect location if equipment with the required electronic circuits is provided.

AVAILABLE FORMS OF INSTRUMENTATION. Numerous variations of suitable electronic circuits are designed to provide ultrasonic contact testing.

A-Scan Units. A cathode-ray tube (CRT) with a medium-persistence screen and A-scan presentation has been used extensively both in the United States and abroad. Selection of the best instrument may be confused by references to various presentations of the A scan and to circuits such as RF (radio frequency), video, and FM (frequency-modulated).

B-Scan Units. If test conditions indicate the desirability of an automatic surface-contact test, other methods of presentation should be considered. A cathode-ray tube B scan, which shows a cross-section of the material during passage over one scanning line, provides the operator with an accumulation of data visible at one quick glance. Although it shows the **relative depth** of the reflecting area from the surface, it does not provide the amplitude information needed to evaluate defect area; these data are usually obtained from an A-scan.

C-Scan Units. If a continuous record is required, the monitor circuits can be fed into various types of recorders of standard and special design. These may provide a C scan or map of the location of discontinuities and amplitude of signal which indicate the **relative area** of the defect.

Meter Indications. Meter presentation of at least some of the data is also possible. For example, a voltmeter can be used to indicate amplitude of indication, a very useful addition for "peaking up" over a discontinuity.

Gating and Marking Systems. Included with some instruments, or available as additional attachments, are electronic circuits which provide adjustable time delays or gating circuits so that signals from a given depth of material can be applied to the **automatic location of defects.** With adjustable discriminator levels, the defect signal can be limited to any amplitude over a desired level. During continuous testing of pipe or strip, material can be marked automatically for location of defects. The output from the monitor may be used for aural or visual signaling.

Repetitive Semi-automatic Testing. If parts to be tested are uniform in size and shape and the ultrasonic test can be defined within specific limits, instrumentation is available for semi-automatic manual tests. An example of a test of this type is the testing of standard freight car axles for cracks in the journal area which may result from overheating of journal areas from hot boxes. Single-crystal search units are adequate for testing from each end of the axle, but these units take too much time and require extra careful manipulation to be sure that the entire surface area of the journal is tested.

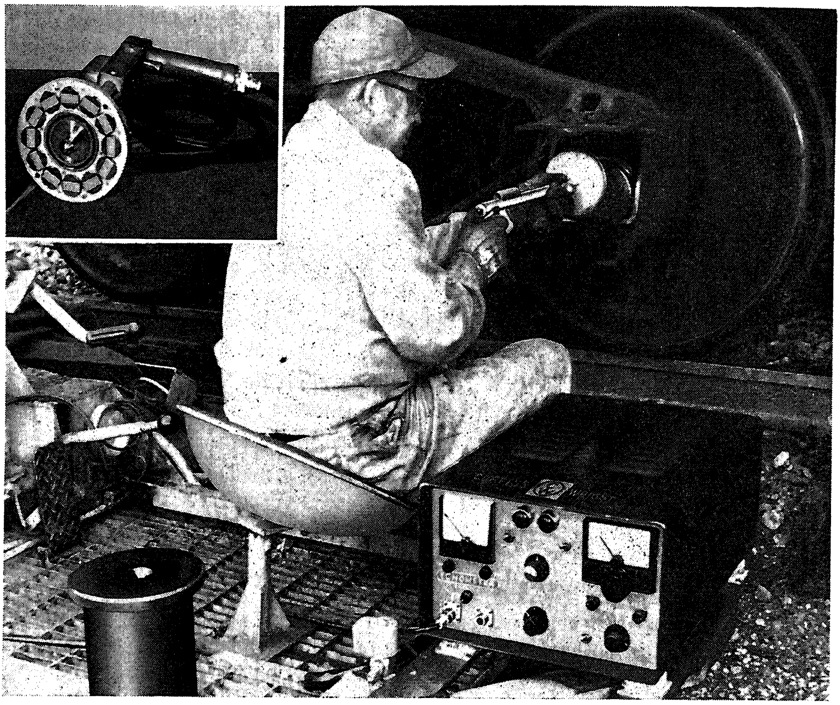

Curtiss-Wright Corp.

Fig. 1. Ultrasonic contact tests for cracks in journal area of freight car axles.

A special **multiple-transducer assembly** with a single-frequency, pulse-type, gated test instrument provides a "one shot" test, as shown in Fig. 1. The operator dips the transducer in a shallow pail of oil to provide a couplant for the end of the axle. Insertion of the spring-mounted and tapered centering pin into the center hole of the axle exactly locates the ring of transducers on the end of the axle. A trigger action in the pistol grip energizes an electromagnet which pulls the transducers against the end of the axle with a uniform pressure, independent of any manipulation by the operator. All twelve of the transducers are pulsed simultaneously at a test frequency of 2.25 Mc. These transducers also act as receivers, waiting between pulses to receive any reflection from cracks in the journal areas. An **adjustable electronic gating circuit** limits the test to the critical area, 3 to 13 in. from the end of the axle. The adjustable automatic-signaling amplitude level provides adjustment to a minimum standard of reflected signal from a standard dummy-axle journal with a shallow groove cut in the surface. Any crack deeper than this groove will signal its presence by the turning on of a red light, a loud buzzer, or an external signal such as a loud horn. The relative level of signal amplitude is indicated by the panel meter. No cathode-ray tube is necessary, thereby eliminating the need for operator interpretation once the proper set-up has been made on the test journal.

Insertion of the multiple-transducer probe in the journal box and completion of the test require only a few seconds per journal. Over 300 journals can be easily tested per hour by the operator as he rides on a small gasoline-motor-propelled car between the tracks in the freight yard. Cracked journals may be found as often as once in 400 freight cars, or at a rate of 1 to 3200 journals. A regular schedule for testing will eliminate costly freight accidents due to broken axles which do not usually fail until the crack has progressed through more than 50 percent of the cross-section.

Such equipment can also be used for other factory or field tests where rapid automatic or manual techniques are required for repetitive testing of duplicate parts.

Automatic-programming Units. Instrumentation is also available for completely automatic, programmed testing of uniformly shaped pieces. Many of the **programming systems** now applied to various machine tools can also be applied on specific test problems, with the available monitor attachments, to set up a programmed contact test. Such a system provides uniform and automatic ultrasonic inspection and removes human variables present in manual tests.

SELECTION OF INSTRUMENTATION. Careful consideration should be given to the following characteristics and performance requirements of an ultrasonic testing instrument when making a selection for a specific contact-testing application.

1. What test frequencies are required and available?
2. Will there be satisfactory resolution of indications
   a. At the required minimum distance under the test surface?
   b. For the required minimum area of discontinuity?
   c. Of a small indication close to a large indication?
3. Is a wide range of linearity required between indications from small and large discontinuities, or is the largest possible indication from the smallest detectible indication preferred?
4. What will be the lowest possible ambient illumination level in the testing area for maximum convenient viewing of the cathode-ray tube (CRT) by the operator? Indoor? Outdoor? What intensity of indication is provided on the CRT screen? Is a high pulse-repetition rate, or a variable repetition rate with a desirable maximum high rate, provided for maximum brightness? Is the minimum rate too high for testing through the maximum length of test specimen?
5. Do the pulse circuit and associated components provide sufficient power to penetrate the required distance in the material to be tested? Will the signal be highly attenuated or scattered by a coarse structure?

6. Is the gain in the receiver amplifier sufficient to produce indications of satisfactory amplitudes from the required minimum-detectible discontinuity?
7. Is there a calibrated scale or are there electronic markers for measuring the distance of the defect indication from the test-surface indication? Is the calibration adjustable to compensate for variations in velocity of at least 3 to 1, to measure distance in a wide variety of materials?
8. Will two search-unit operations be required? Does the instrument provide for an easy change-over from one search unit to two?

Answers to these questions should provide a basis for selection of suitable ultrasonic testing equipment for a specific application or group of applications requiring manual contact testing.

Test Techniques

TEST ADVANTAGES. Ultrasonic contact testing has the advantage of **flexibility of location,** since it usually offers the opportunity to take the test instrument to the material or equipment to be inspected. Also, contact testing requires only a minimum of test instrumentation and accessories. Where tests are to be made on large pieces, contact testing is usually the obvious solution.

TEST LIMITATIONS. The greatest disadvantage of contact testing is the difficulty of maintaining **uniform acoustical coupling** or contact on some surfaces. This erratic coupling contributes to loss of sensitivity and nonuniformity of results. Machined, rolled, or reasonably smooth surfaces are desirable. Use of couplant leaves oil or grease on test objects, and this coating may have to be removed later. Contact testing has a greater **dead time** near the front surface of test objects than that found in immersion testing. It is confined to lower test frequencies in practice. **Contact crystal angulation** cannot be varied continuously, as can be done in immersion testing.

ANGLE OF TEST. Pulsed ultrasonic vibrations can be introduced into materials at various angles from the surface by direct contact of a suitable search unit and couplant. By varying the angle of incidence of the beam, four different **modes of vibration** can be established:

1. Longitudinal (compressional).
2. Transverse (shear).
3. Surface (Rayleigh) waves.
4. In thin sheets, Lamb waves.

Typical search units and their construction are shown in the section on Ultrasonic Test Principles.

Determining Wedge Angles. For angle search units, a formula for calculating the wedge angle, resultant inspection angle, and mode of conversion in different materials is given in the section on Ultrasonic Test Principles, with a table giving some angles and mode conversion for typical materials. Reference to this table of **conversion angles** indicates that at certain angles of incidence, both longitudinal and shear waves can be generated simultaneously and can be directed at different angles. Because of the differences in sound velocity, the indication from each of these **modes** can be identified if the distances from the reflecting surfaces are known. With equal transmission distances, the longitudinal wave with the higher velocity will return to the search unit sooner than the transverse wave. However, considerable confusion may result if the reflecting surface in the path of the longitudinal beam is close to twice the distance of the reflecting surface in the path of the transverse beam. In this case the reflected indications will nearly coincide. For this reason it is advisable to choose an angle at which only one mode will appear most prominently.

For example, if inspection is to be performed in steel at a refracted angle in the material of 0 to 35 deg. from normal (90 to 55 deg. from the surface), **plastic-wedge angles** of 15 deg. or less should be used to provide a primarily **longitudinal test beam.** If the angle of the test beam in the steel is required to be in the range of 35 to 89 deg. from the normal (55 to 11 deg. from the surface), a **transverse mode** is indicated. This requires use of plastic-wedge angles in the range from 28 to 56 deg. When a **surface-wave** test on steel is required, a plastic-wedge angle of about 64 deg. is required. The angles for other materials will vary with their sound velocities as compared with that of steel. If the sound velocity in the test material is greater than the sound velocity in steel, the test angle in the material will be greater (angle from the surface will be less) than the angle in steel when using the same plastic-wedge angle. If the velocity is less than the velocity in steel, then the test angle will be less (angle from the test surface will be greater) than in steel when using the same plastic-wedge angle.

THROUGH-TRANSMISSION SYSTEMS. Although most contact ultrasonic testing can be best performed by using pulsed testing with one search unit, there are applications that may be tested by using through-transmission techniques with two search units. In general, through-transmission techniques are more adaptable to immersion testing than to contact testing. Inhomogeneities and discontinuities in some materials and some types of laminations, or lack of bond, can be located by using through-transmission, provided there is some uniformity of shape. Beams normal to the surface or angle beams may be used, provided the transmitting and receiving search units are kept in the same relative position to each other. In this way differences in the energy transmitted through the piece under test are due to differences in the homogeneity of the material, rather than to changes in beam coverage or to differences in attenuation due to changes in thickness of material.

SELECTION OF TEST TECHNIQUE. An ultrasonic testing technique can use a beam (1) normal to the surface, (2) at an angle to the surface, (3) along the surface, or (4) through the material from one side to the other. When should any one be selected? Reliable data concerning the basic testing problem are required before a testing technique can be selected. Availability of the following data will facilitate the **determination of proper test procedures:**

1. What are the nature, size, orientation, distribution, and number of discontinuities expected in the test materials? If little of this information is available, trial tests and destructive investigations (cross-sectioning and etching) will be necessary to obtain data. Obviously the orientation of the reflecting area of discontinuities will affect selection of a normal or angle beam. Random orientation may require more than one scan. If normally defective material contains a relatively uniform distribution of a large number of discontinuities, a much less than complete test coverage and less careful test are required than if the test objective is to locate only a few discontinuities having random distribution.
2. Shape, dimensions, and most critical areas of the test piece should be designated so that available areas for contact scanning can be determined and type of search unit and technique specified.
3. Surface conditions should be known, for example: as-forged, as-cast, fine- or rough-machined; smooth or rough; flat or wavy. Surface roughness determines the selection of heavy or light couplant and test frequency for search units.

4. Internal structure may be coarse- or fine-grained, homogeneous, uniformly worked by rolling or forging, or heat-treated. Structure affects attenuation and scattering of the ultrasonic vibrations and therefore the selection of test frequency.

Applications of Tests

CASTINGS. The lower range of testing frequencies is generally applied to castings. It is not yet practical to test many **coarse-grained castings** ultrasonically because of the extreme scattering resulting from **reflections at the grain boundaries.** Such castings include some alloys of brass, stainless steel, titanium, and cast iron. Brass alloys cast under conditions that control the grain growth can be tested at 1 and 2.25 Mc. because of the small, uniform grain structure. Most **steel castings** are easily tested ultrasonically until the structural characteristics begin to approach those of cast iron. Such objects as cast-steel pressure cylinders, back-up rolls, and ingots up to 50 in. in diameter and 15 ft. or longer have been inspected at frequencies of 400 kc., 1 Mc., and 2.25 Mc. (Fig. 2).

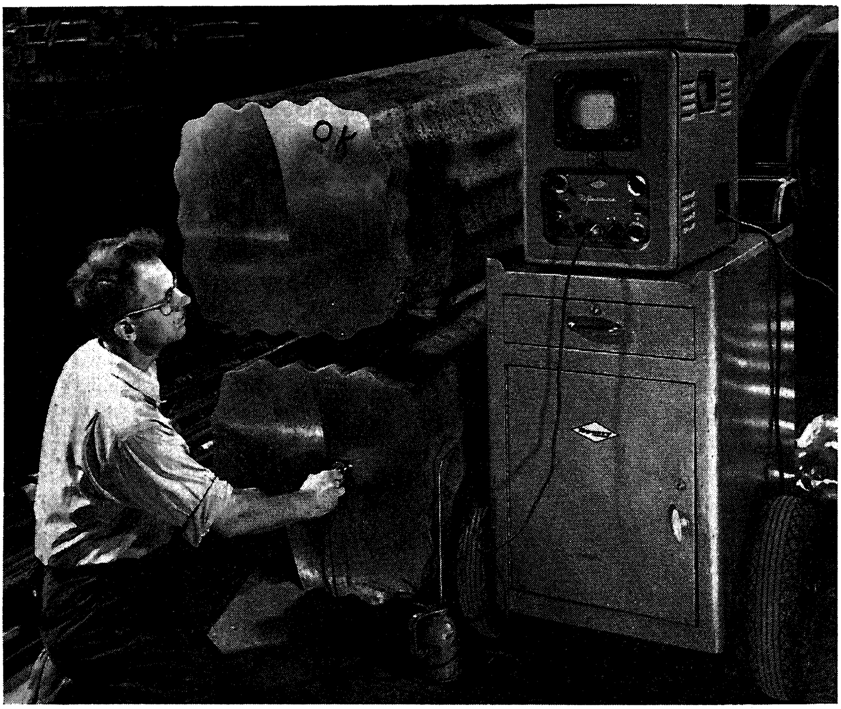

Sperry Products, Inc.

Fig. 2. Ultrasonic contact testing for center condition of 24-in. ingots.

Generally, **die castings** (because of their intricate shapes and small size) are difficult to test except in specific areas. Where size permits, 2.25- or 5-Mc. test frequencies are usually satisfactory.

Cast lead can be tested at 1 Mc. if it contains, for example, 6 percent antimony. But **pure lead** is a relatively poor transmitter of ultrasonic vibrations, and even low frequencies are attenuated within a few inches.

FORGINGS. Most forgings of a uniform size and shape are good objects for ultrasonic testing (Fig. 3). This applies to brass alloys, carbon steel, stainless steel, aluminum, magnesium, titanium, nickel alloys, and other less common metals. An ultrasonic test can determine whether the forging has been uniformly worked. For example, it is difficult to test through the centers of some wheel-shaped stainless steel forgings when some of the large grain structure has not been broken up in the center. **Large forgings** for generator rotors, 60 in. in diameter and up to 20 ft. long, are regularly tested at 1 and 2.25 Mc. for flaking or thermal cracks and forging bursts. Most testing of forgings is accomplished at 1, 2.25, or 5 Mc. with a beam normal both to the surface and to the direction of maximum working. In forged parts, **discontinuities** may be flattened out parallel to the test surface and thus present the best orientation for reflecting the ultrasonic beam.

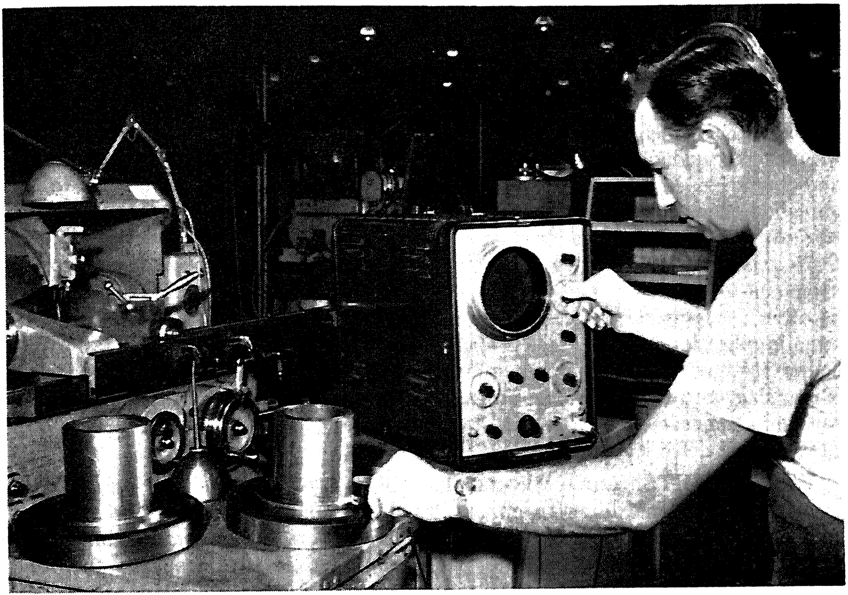

Curtiss-Wright Corp.

Fig. 3. Ultrasonic contact testing of a flanged steel forging for forging bursts, inclusions, and cracking.

ROLLED SHEET AND PLATE. Rolled materials are tested ultrasonically with a beam normal to the surface or with an angle beam. Depending on the test frequency, a beam normal to the surface cannot be used on sheet which is too thin to permit the first reflection from the other side to clear the initial pulse. A reduction in the multiple-reflection pattern will usually indicate presence of discontinuities. **Laminations** are easily located, but scanning a large plate manually is time consuming.

An **angle test,** longitudinal or shear, can be made from one edge of a plate. Most discontinuities, such as rough laminations, slag, laps, and flaking, can be located by projecting the beam across the plate to the opposite edge. One pass along one edge will then cover the entire plate for widths of 10 ft. or more for steel, brass, and aluminum. Difficulty may be encountered if laminations are smooth and parallel to the sheet surface. Brass tube sheets are regularly tested by this technique. For **thin sheet** and **moving strip**, shallow angles frequently have provided a better test. These angle tests are usually made at 1 Mc. and often at 2.25 Mc.

Another mode of vibration can be generated in thin sheet or plate with some advantageous results. **Lamb waves** can be generated in thin sheet; for example, in steel less than 0.100 in. thick. Use is made of a plastic-wedge type of angle-search unit with a higher angle than required for generating surface waves. Since there are many **modes** of Lamb waves with different propagation velocities, techniques and interpretation are not so simple as with longitudinal, shear, and surface waves. However, limitations on the use of shear waves in thin sheet material may make it necessary to use Lamb waves.

EXTRUSIONS. Discontinuities, if present in steel, aluminum, and other extrusions, usually extend lengthwise in the piece because of the elongation in the direction of extension. Inspection normal to the surface and perpendicular to the direction of extruding will usually locate most discontinuities. Even though they are elongated, there have been applications where **chromium segregation** in 7075 aluminum alloy has been located by sending a beam through the extrusion from end to end. The usual test frequencies are 2.25 and 5 Mc. However, 10 Mc. is often used for thinner sections and more refined discontinuities. In an unusual application, minute steel particles from the extrusion die were located just under the surface of aluminum extrusions by use of a 2.25-Mc. surface wave. **Pipe, slag, and other discontinuities** in the extrusion billet can also be located with an ultrasonic contact test before heating and extruding. This saves the cost of extruding defective material.

WELDMENTS. Automatic, manual, and flash or pressure butt-fusion welds are tested ultrasonically with either straight or angle-beam techniques. Fillet welds or welds which do not require complete penetration are more difficult to test because normal discontinuities (unwelded surfaces) adjacent to the weld confuse interpretation of indications reflected from defects.

Butt and Tee Welds. Tee welds of heavy plate may be tested with a straight beam through the top of the tee or with an angle beam from one side of the bottom of the tee. Other butt welds in sheet, plate, or pipe, in most metallic materials, can be tested with an angle beam of 45 deg. in the material. Some investigators have found that a 60-deg. angle (30 deg. from the surface) gives improved results. The object is to send the ultrasonic beam through the weld. Shear-wave transducers giving refracted incident angles from 41 to 45 deg. in the material will generally be satisfactory.

Rough Beads and Backing Rings. Reflection indications from the weld area will represent discontinuities if both top and bottom surfaces of the weld are fairly smooth. A rough bead may reflect parts of the beam but can be identified by a capable operator. Reflections from the **weld bead** are often identified by finger damping with oil. A **back-up plate** or ring will produce reflections so that evaluation becomes more complex. Careful placing of the search unit and an analysis of the beam path and part geometry will facilitate identification of the area from which the ultrasonic vibrations are reflected.

Beam Penetration. Carbon steel welds are usually adaptable to ultrasonic inspection, but **stainless alloys** which develop grain growth and large grains in the weld or heat-affected zone may be difficult to test because the large grains reflect and scatter the vibrations. Care should be taken to see that scattered indications from **micro-cracking** are not confused with scattering from grain borders. Penetration through a weld can be determined by placing a wedge of material on the surface of the plate at the opposite side of the weld. If it is on a node point of the angle beam, it will reflect some of the beam if coupled to the surface with a couplant. Holes drilled through the weld in a welded test plate can also be used to evaluate specific flaws in the weld.

Double-Transducer Tests. Combinations of two angle-search units, using the reflection method at various angles to the weld, and through-transmission have been used successfully on some weld applications. Coupling a **variable-angle search unit** to the surface with a column or stream of water has also been demonstrated as a practicable technique (see section on Double-Transducer Ultrasonic Tests).

Often the ultrasonic test of a weld reveals defects, such as serious cracking, which are not detectible by other means. Of prime importance is testing experience adequate to interpret ultrasonic indications correctly. With such experience, butt welds in storage and pressure vessels, pipelines, and other weld applications have been advantageously tested with ultrasonics.

Field Inspection Techniques

MEASUREMENT OF REFLECTIONS. Rough approximations of the heights of reflections during all types of ultrasonic examinations (longitudinal,

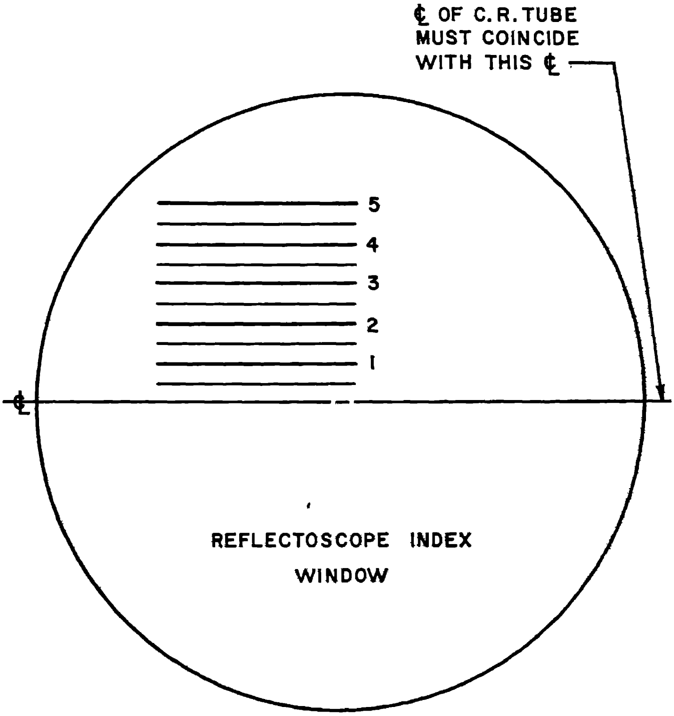

℄ OF C.R.TUBE MUST COINCIDE WITH THIS ℄
5
4
3
2
1
℄
REFLECTOSCOPE INDEX WINDOW

Union Carbide Chemicals Co.

Fig. 4. Index window used in recording signal amplitudes in contact testing.

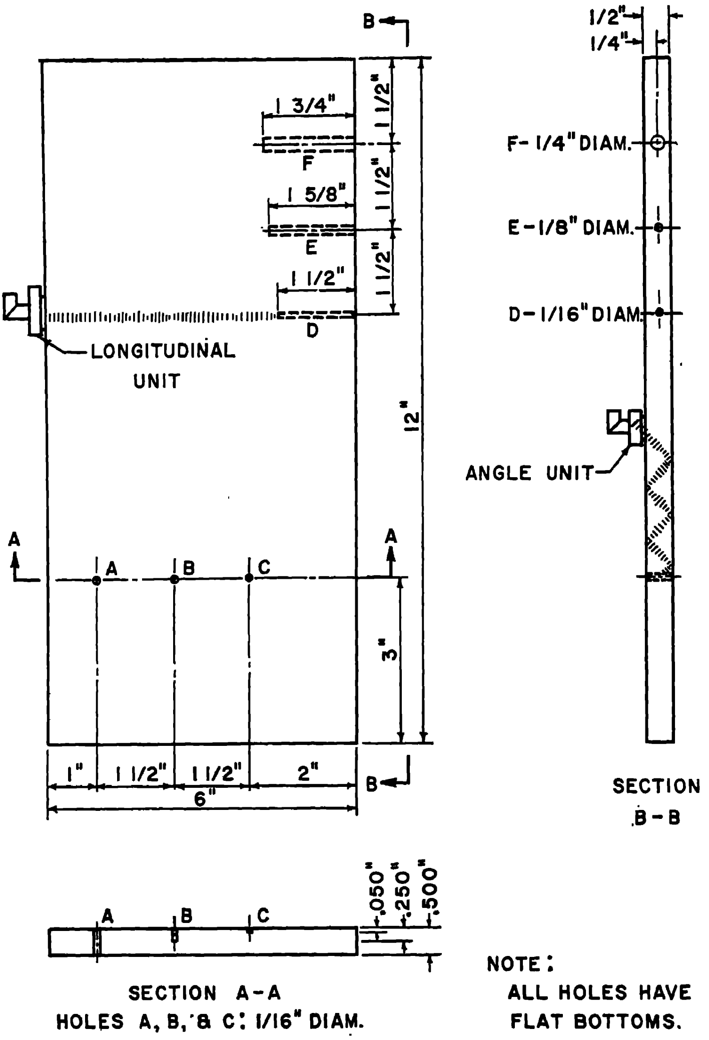

Union Carbide Chemicals Co.

Fig. 5. Ultrasonic reference plate.

shear, and surface waves) are entirely unsatisfactory. A simple method to be used for plotting, recording, and reporting weldment indications, and all "end" reflections, noise levels, and other signals is by an "index" system. The **index method** utilizes a transparent index window having permanent graduations, which is inserted in front of the cathode-ray tube (CRT). All reflections are bisected if the CRT center line is in correct vertical adjustment. It is therefore necessary to observe only the upper half of each reflection in an RF type of presentation. In video presentation the over-all height of reflection is used in the same manner.

The heavy numbered lines on the index window are equally spaced in 20 percent increments; the upper line, termed "index 5," equals a 100 percent reflection. The lighter lines are also equally spaced and are one-half values. A typical **index window** is shown in Fig. 4.

USE OF REFERENCE PLATE. The evaluation of reflections from flaws is comparative. The most practical way to appraise such reflections appears to be to estimate the approximate area which reflects the vibrations. A reference plate (Fig. 5) provides known measured areas with which the reflections can be compared. It also enables the operator to use three **reproducible levels of sensitivity,** usually adequate for evaluation of most weldments, forgings, steel castings, and rolled plates. Familiarity with these various levels of sensitivity also enables the operator to approximate the magnitude of flaws.

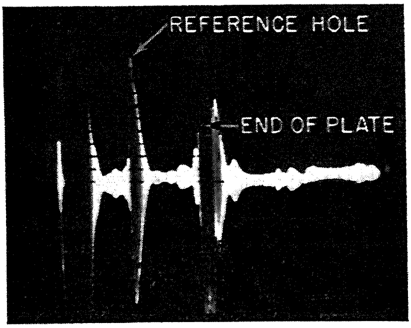

Union Carbide Chemicals Co.

Fig. 6. Ultrasonic contact CRT indication from reference plate, with signal from reference hole set to index 5 on index window.

The reference plate of Fig. 5 contains three vertically drilled 1/16-in. diam. holes *A*, *B*, and *C*, whose flat-bottom surfaces are at depths of 0.050, 0.250, and 0.500 in., respectively; and three horizontally drilled holes of 1/16-in., 1/8-in., and 1/4-in. diam. marked *D*, *E*, and *F*. All these holes are flat-bottomed. Holes *A*, *B*, and *C* are used for **shear waves,** while holes *D*, *E*, and *F* are used for **longitudinal waves.**

Checking Operating Efficiency of Instrument and Accessories. The reference plate also enables the operator to determine if all the equipment is responding satisfactorily. Instruction charts, obtainable from the instrument manufacturer, give details for instrument performance in accordance with the American Society of Mechanical Engineers Code and ASME Standard Procedures.

Instrument Calibration. The 1/16-in. diam. vertical holes *A*, *B*, and *C* are used when setting the instrument for shear-wave examinations. A suitable size of hole is selected and the search-unit beam is directed toward this hole. The reflection of the oscilloscope is adjusted to index 5 (see Fig. 6). The distance between its reflection and the initial pulse should be noted, or marked, so that future comparison of a reflection will be made at an equal **sound path distance** or on the same **node** (see Fig. 7). Otherwise the defect will appear larger when the reflecting area and searching unit are closer together and may appear smaller if their separation is increased. It should always be remembered that the entire cross-section of the hole does not reflect the ultrasonic beam. Only a small portion of the cylindrical surface, which is parallel to the axis of the node, reflects directly (with some beaming). The instrument is now adjusted so that the reflection from one of the holes in the reference plate is equal in height to the top heavy index line marked "5."

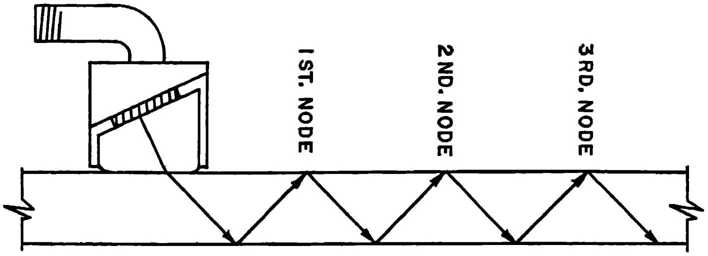

Fig. 7. Path of shear wave from angle search unit, showing node locations.

LINEARITY OF INSTRUMENTS. The index window and the reference plate were designed solely for use with instruments having a reasonably linear response. With such instruments the magnitude of flaws or interfaces can be evaluated with respect to a reference or known area. The instruments for such work should be capable of giving indications whose over-all heights vary in proportion to variations in the size of the areas reflecting the ultrasound. Such response can be expected only within the designed limits of the instrument and within the viewing area of the cathode-ray tube (CRT), equal distances being maintained between the transducer and interface.

SELECTION OF CORRECT FREQUENCY FOR QUALITY OF MATERIAL. A frequency of 2.25 Mc. generally gives a clearer pattern and a narrower initial pulse. It will also detect smaller flaws. A lower frequency of 1 Mc. is sometimes used purposely to ignore very small flaws. At other times a lower frequency is necessary to achieve the desired penetration because of the physical characteristics of the materials. Conversely, 5.0-Mc. frequency is occasionally used for fine grain and thin plate or sheets.

INSPECTION OF WELDMENTS. The higher frequency is usually tried first. It must be able to penetrate adequately through the weldment and into the parent metal beyond the weldment. Fig. 8(a) shows unsatisfactory ultrasonic penetration at 2.25 Mc. The weldment can be seen, but the indication does not reveal the weld conditions. There are no small reflections from the plate to indicate that the sound has penetrated the entire weldment and into the more distant plate or base metal.

Indications of Fusion Zones. Fusion zones on both sides of the deposited weld metal are clearly apparent in the 2.25-Mc. indications of Fig. 8(b). These are typical of the indications resulting from the **differences in acoustical impedances** of the rolled base metal and the deposited cast metal. Ultrasonic **penetration into the base metal** beyond the weldment is indicated by the small reflections from the structure of the more distant base metal.

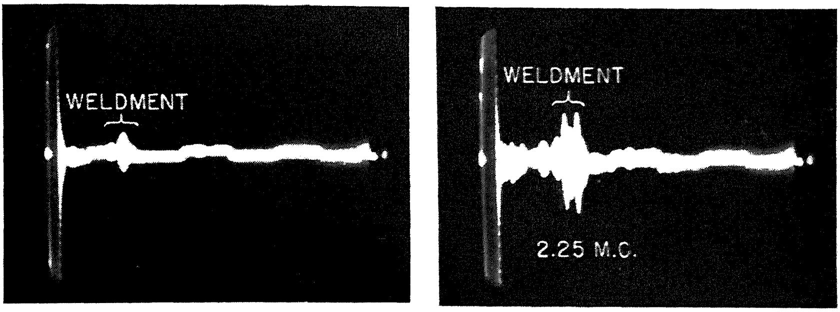

(a) (b)

Union Carbide Chemicals Co.

Fig. 8. Ultrasonic indications from weld at 2.25 Mc. (a) Unsatisfactory ultrasonic penetration which fails to reveal weld condition. (b) Satisfactory ultrasonic penetration of weld. Fusion zones on both sides of deposited weld metal and structure of more distant base metal are indicated.

Typical Weldment Shear-Wave Indications. Fig. 9(a) shows indications from a good weldment in 4½ in. thick steel. This thickness is ample to spread out the weld indications and makes it easy to see both **fusion lines** and the center. Electrodes of different compositions, used in the initial and later passes, gave this unusual center reflection. Fig. 9(b) illustrates indications from a **small isolated flaw** in the center of the 4½ in. thick weldment.

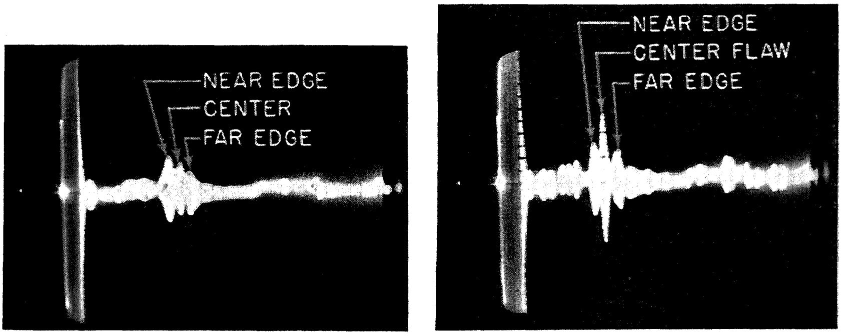

(a) (b)

Union Carbide Chemicals Co.

Fig. 9. Contact ultrasonic indications from welds in 4½-in thick steel. (a) Indication from a good weld. (b) Indication from small flaw in center of weld.

Fig. 10(a) shows indications of faults such as **porosity or small slag inclusions** which do not give distinct reflections such as those obtained from cracks or lack of fusion. The latter would appear similar to the reflection from the hole in Fig. 6, while reflections from porosity and small inclusions are not clearly defined. As some fade out with any transducer movement, others appear. Each isolated reflection will have no continuity parallel to the weld bead and will be lost when the transducer is moved parallel to the weldment. Fig. 10(b) shows an indication of a poorly fused weld repair in a casting.

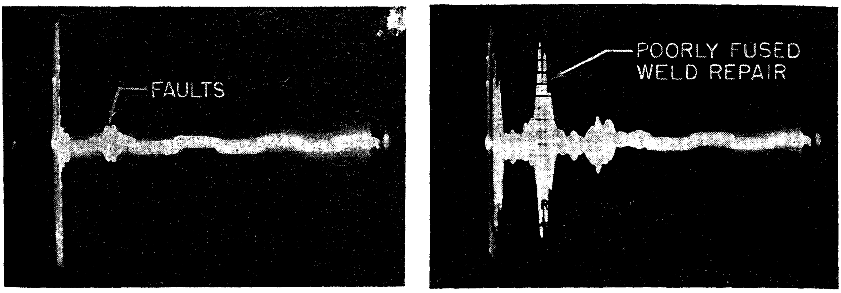

(a) (b)

Union Carbide Chemicals Co.

Fig. 10. Ultrasonic indications of welding defects. (a) Indications of small weld faults such as porosity or slag inclusions. (b) Indication of poorly fused weld repair in casting.

Fig. 11 illustrates **inadequate penetration** of the initial or root pass of a single-V weld in a ½-in. steel plate. Fig. 12(a) is the 1-Mc. oscillogram, which shows clear reflections from the unwelded root area. Fig. 13 illustrates **excessive welding penetration,** "run-through" or "icicles," on the root pass in a single-vee groove weld in ½-in. steel plate. Excessive welding penetration does not generally confuse the interpretation if 41 to 45 degree shear waves are used, as shown in Fig. 12(b).

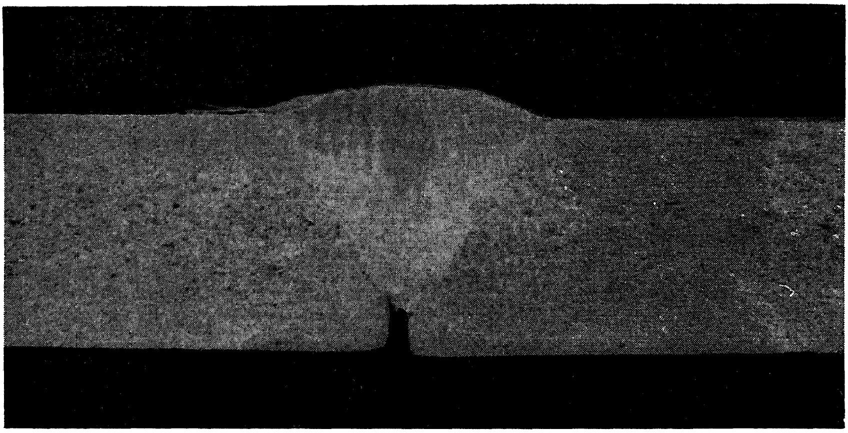

Union Carbide Chemicals Co.

Fig. 11. Inadequate penetration at root of weld in ½-in. plate.

Longitudinal-Wave Examination of Weldments. Longitudinal waves are less frequently used for examination of weldments. They are, however, used to examine steel castings for miscellaneous casting flaws and to determine whether welding repairs are sound. Longitudinal waves can sometimes be used to examine flange-to-shell or flange-to-pipe weldments, using the flange as a contact surface.

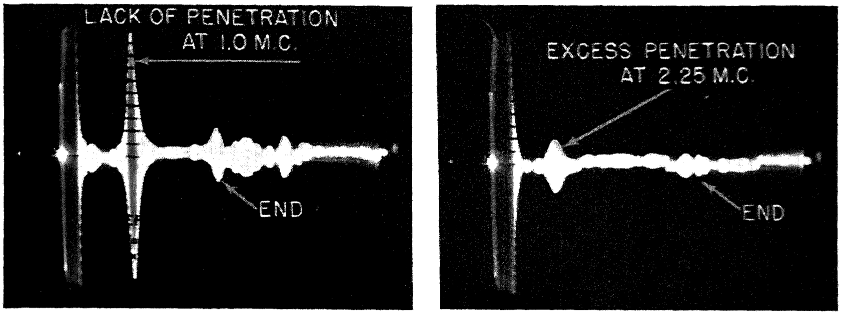

(a) (b)

Union Carbide Chemicals Co.

Fig. 12. (a) 1.0-Mc. indications from weld with incomplete penetration at the root (Fig. 11). (b) 2.25-Mc. indication of weld with excess penetration at the root (Fig. 13).

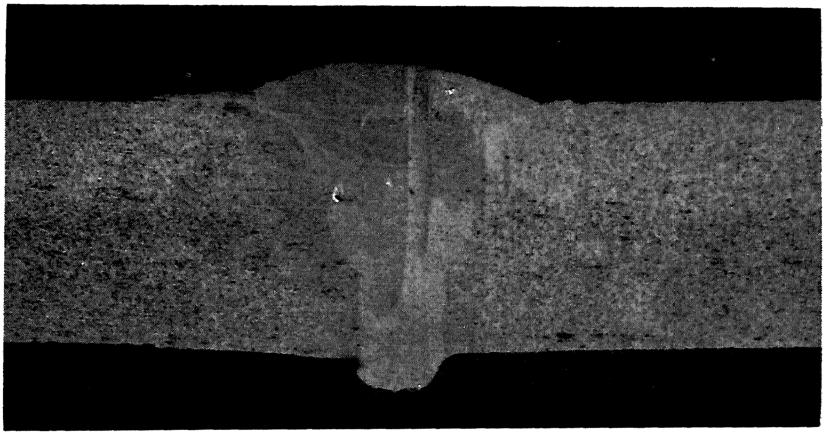

Union Carbide Chemicals Co.

Fig. 13. Excessive penetration or "run-through" of weld in ½-in. plate.

A heavy steel casting containing a **faulty weld repair** is shown in Fig. 14. Both machined ends were scanned with a longitudinal-beam transducer which sent the incident waves into the casting parallel to its main axis. The ultrasonic examination indicated **poor fusion** of the filler metal and the base metal. This condition is evident in the oscillogram of Fig. 10(b) where there is also a complete loss of the end reflection. A **hole or crack** was indicated beneath the weld repair, as evidenced by the reflection marked "Defect *A*" in the oscillogram of Fig. 15(a). In this case the transducer was in contact with the machined end where the faults are outlined. Both interpretations were correct. Satisfactory ultrasonic penetration of a good portion of the cylinder, showing small reflections from the metal structure and a large end reflection, using 2.25 Mc., is illustrated in Fig. 15(b).

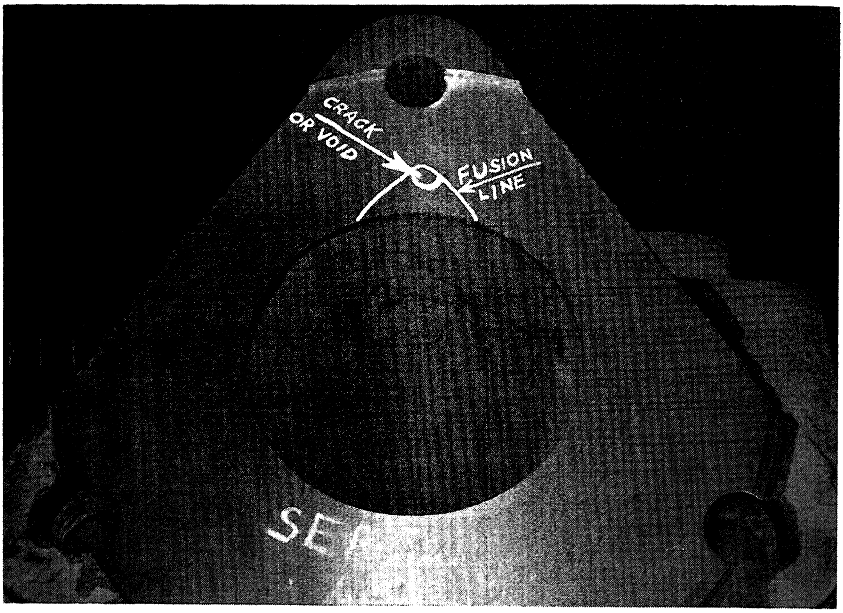

Union Carbide Chemicals Co.

Fig. 14. Heavy steel casting containing a faulty weld repair.

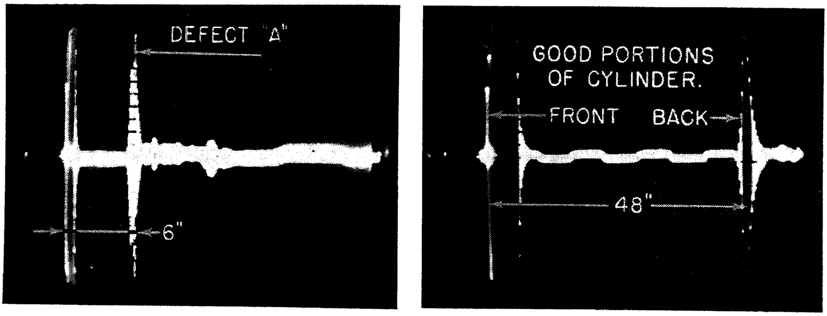

(a) (b)

Union Carbide Chemicals Co.

Fig. 15. Ultrasonic indications from steel casting of Fig. 14. (a) Indication of hole or crack beneath weld repair in casting. (b) Indication showing good penetration of cylinder (at 2.25 Mc.) of casting in Fig. 14.

INTERRUPTION OF SHEAR WAVES. The center of the diverging shear-wave beam reflects to the transducer. The center is termed a "node" each time it is deflected by either surface, as illustrated in Fig. 7. Rubbing the material, by hand or with an oiled brush, away from or toward the transducer along the sound path will interfere with reflections of sound at the nodes. Reflections on the oscilloscope will be damped at the point of interference so that the point of contact is readily apparent. Such interference is used to determine accurately the locations of reflections. This procedure is colloquially termed **feeling the location of reflections** or "finger damping."

Irrelevant Ultrasonic Indications

SIGNIFICANCE OF IRRELEVANT INDICATIONS. In practice the images on the cathode-ray tube ultrasonic test instruments are not always so simple as suggested by sketches that illustrate fundamental principles. **Interpretation difficulties** can arise because of differences between various ultrasonic test methods. In one case the appearance of an echo indication and in another case the disappearance of an echo indication on the screen may be reason for rejecting the part under examination. Some echoes are of no interest because they are produced by secondary effects. The experienced interpreter will recognize these additional **irrelevant echoes** and ignore them. To recognize whether or not an echo is of importance requires practical experience.

CAUSES OF IRRELEVANT INDICATIONS. In general, however, echoes caused by secondary influences, of no immediate interest for the examination, can be classified in seven groups. Except for the first and second groups, the following interfering effects are inherent to the ultrasonic test method:

1. Electrical interference.
2. Interference from the probes.
3. Interference from the surface of the material examined.
4. Interference caused by diffraction.
5. Interference caused by the shape of the piece being examined.
6. Interference caused by material structure.
7. Accidental interference.

ELECTRICAL INTERFERENCE. False indications arising from electrical sources can manifest themselves in the ways discussed in subsequent paragraphs.

Noise Effects. Noise can be recognized as a vertical broadening of the horizontal time-base line in A-scan indications. It can be caused by a poor **electrical contact** with the specimen when using a crystal which is silver-plated on one side only. It can also be caused by a bad contact in the coaxial lead. These conditions can be overcome in most cases by cleaning the various plugs and sockets. Noise effects can also be caused by **defective amplifier tubes.**

Strong Moving Signals in a Horizontal Plane. These can be caused by the main electric **power supply**; for example, by power lines to which electric furnaces or welding sets are connected. They can also be caused by defects in the ultrasonic test equipment; for example, by a **defective thyratron** (a gas-filled tube used in the transmitting and the time-base circuits). All these phenomena can be recognized immediately because they are irregular and not synchronized with the time-base.

Reverberations in Test Materials. Disturbance echoes can occur when materials with a very low attenuation are examined. In these materials the initial pulse has not been completely absorbed before the next pulse is sent out. These signals, which can interfere with interpretation, can be regular and synchronized with the time-base. To reduce the disturbances they create, the operator can reduce the amplification or the transmitter energy. The disturbances caused by electrical conditions should be identified and corrected because they interfere with a good interpretation of the screen image.

DISTURBANCES CAUSED BY THE PROBE. Search-unit disturbances occur only with the single-transducer method (transceiver).

Coupling-Block Disturbances. Reflections can be received from any standoff, prism, or coupling block (see Fig. 16). These indications appear immediately behind the transmitting pulse. They remain in the screen image when the probe is lifted off the test material.

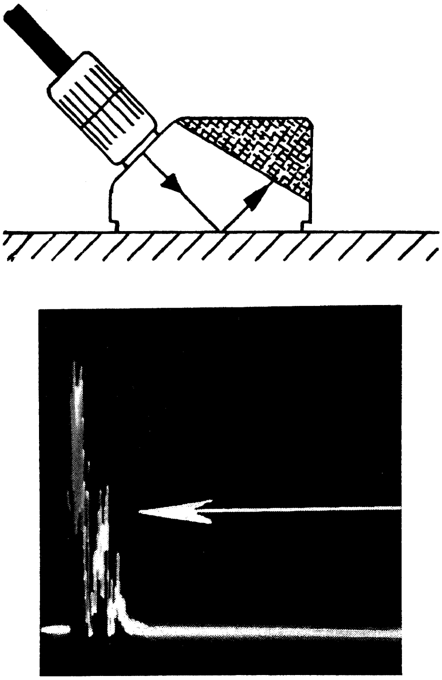

Röntgen Technische Dienst

Fig. 16. Sound path and reflection indications from disturbances within ultrasonic coupling block. Arrow indicates reflections from various sound paths inside the coupling block.

Loose Crystals in the Probe. Loose crystals can have a prolonged vibration or ringing which causes the transmitting pulse to become too long (see Fig. 17). Most manufacturers of ultrasonic test equipment will give tolerances for the **decay time of the transmitting pulse,** depending upon the frequencies and the dimensions of the crystals. To check such a probe, one should place the bare crystal on a piece of metal gauze. In **checking the duration of the initial pulse** of the crystal, one should prevent the absorption of vibrations by contact oils which occurs when placing the probe on the specimen under examination. It is seldom possible fully to overcome disturbances caused by a standoff or similar attachment to the probe. These possible disturbances ought to be studied in designing the shape of the probe and in the use of soft boundaries. Loose crystals should be repaired before further use.

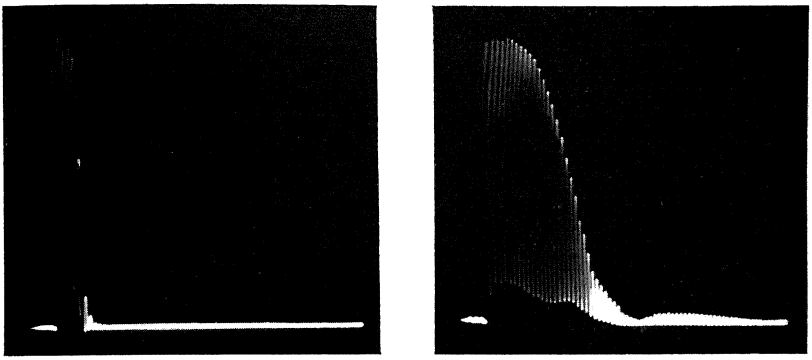

Good

Too long

Röntgen Technische Dienst

Fig. 17. Crystal vibration decay patterns, showing (left) signals from a good crystal, and (right) prolonged ringing from a loose or defective crystal search unit.

SURFACE DISTURBANCES. Surface disturbances can be of two kinds, as is seen when studying the appearance of additional echoes on the screen. Difficulties with coupling will not be considered under this heading.

Surface Waves Between Transmitting and Receiving Probes. When using separate probes, the sound pulse can be transmitted to the receiver along

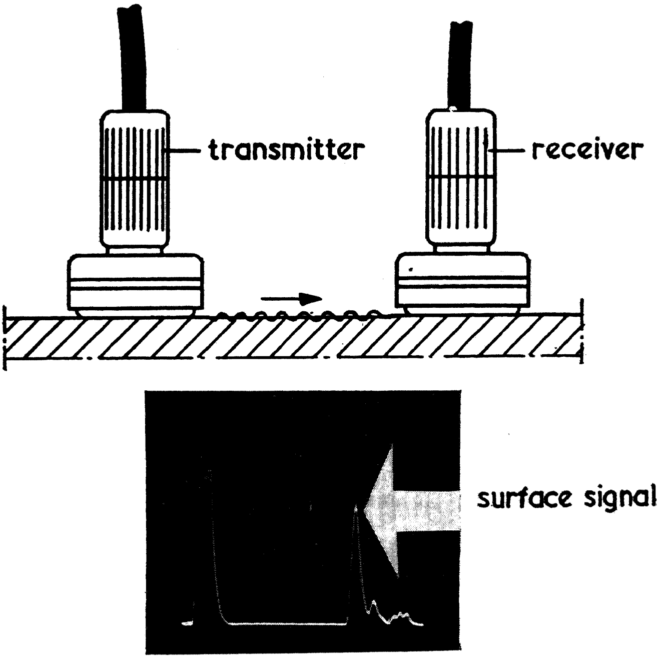

Röntgen Technische Dienst

Fig. 18. Sound path and ultrasonic indications resulting from travel of surface waves between sending and receiving crystals.

the surface of the specimen. This phenomenon can be recognized easily; by enlarging the distance between the probes, the disturbance echoes will move away from the transmitting pulse (see Fig. 18). This phenomenon needs to be watched, especially when examining **curved surfaces** such as axles or rotors. It can be reduced by using rubberized nylon or other **plastic sheet materials** between the probes and the test object.

Surface-Wave Reflections. Reflected surface waves can also cause additional disturbances which can be misleading. This situation can be explained and recognized, provided one is aware of it (see Fig. 19). The surface waves are transmitted from the transmitting crystal and propagate in all directions from the probe. They can be reflected at the **edges of the specimen,** and the reflected surface waves will produce an echo on the screen. This echo has usually a very sharp shape. Varying the position of the probe changes the distance from the probe to the edge of the specimen and modifies the travel path length. The echo of the surface waves will move over the screen simultaneously with the movement of the probe.

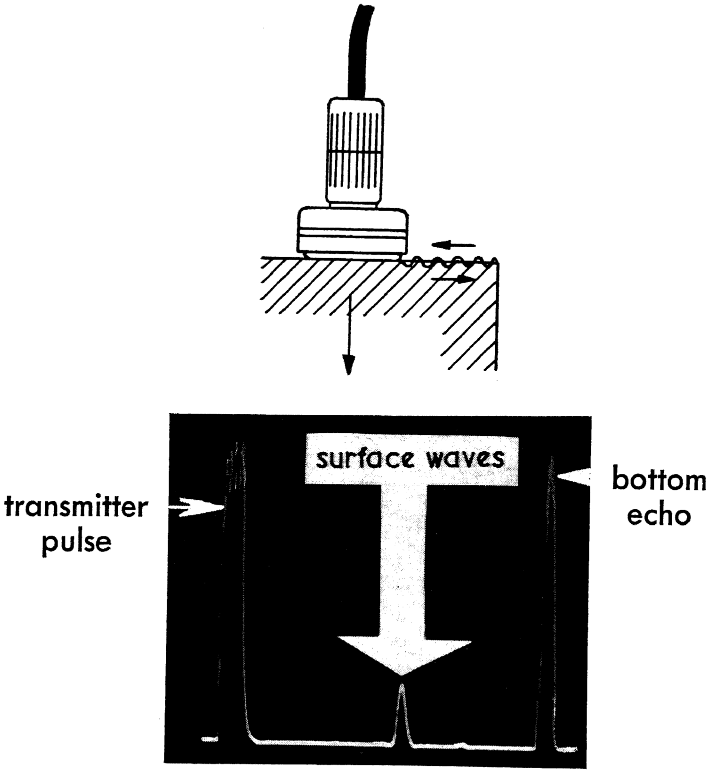

Röntgen Technische Dienst

Fig. 19. Surface-wave reflection path (top) and indications (bottom) where waves reflect from corner of test specimen. Left arrow indicates transmitter pulse; right arrow, bottom echo from vertically transmitted signal.

Surface Crack Indications. This phenomenon permits detection of surface cracks and should not always be regarded as a disturbance (see Fig. 20). This possibility should be a warning that, in detecting reflections of surface waves, one should see whether the reflection is really caused by the edges of the specimen. One can test by pressing a finger on the surface to damp the surface wave. In making sure where the reflection of the surface waves originates, one can move the probe until the reflection of the surface waves coincides with the echo of the transmitting pulse. With the probe in this position, the reflector (for example, a crack) is directly beneath the probe.

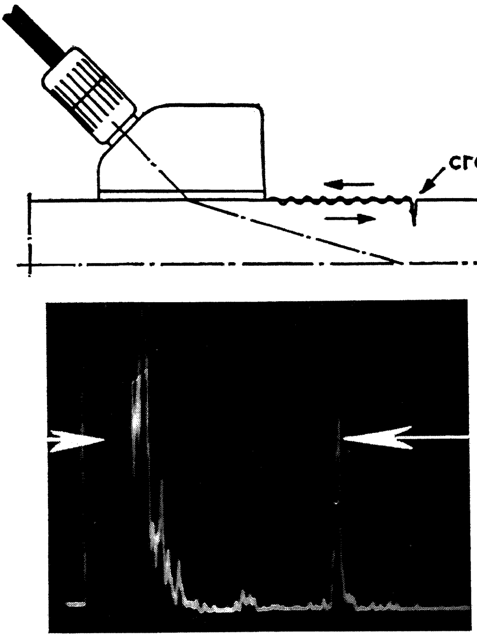

Röntgen Technische Dienst

Fig. 20. Path of surface waves (top) and ultrasonic indications (bottom), showing reflection from a surface crack. Left arrow indicates transmitter pulse; right arrow, surface-wave echo from crack.

Surface Roughness Effects. The preparation of the specimen surface can also be of importance with respect to **machined or planed surfaces** when the distance between the surface grooves or machining marks corresponds with the wavelength of the surface wave. Under these circumstances one can reduce the effect by placing both transmitting and receiving probes on a line parallel to the surface grooves.

DISTURBANCES CAUSED BY REFRACTION. Various refraction effects can occur during ultrasonic examination of a specimen which one would not expect when thinking in terms of a narrow, line-shaped sound beam. When an ultrasonic beam meets a reflecting surface, refraction can occur when the beam is not at right angles to the reflecting surface. When refraction takes place, **additional transverse waves** can, under certain circumstances, cause additional echoes on the screen. For example, the situation when examining long rods is illustrated in Fig. 21. It is obvious that the refracted waves will travel a longer distance and produce an echo on the screen behind the echo of the first reflection.

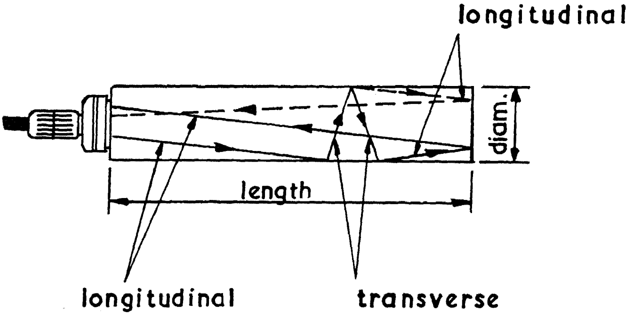

Röntgen Technische Dienst

Fig. 21. Refraction of spreading sound beam in long specimens produces refraction of reflected beam, introducing spurious reflections from longer paths of refracted portions of beam.

These additional echoes will occur at regular intervals. When examining simple rods, this phenomenon will not be misleading because the additional echoes appear after the first echo from the bottom of the specimen, and in addition they appear at regular intervals. This phenomenon can also have some advantages. Assume

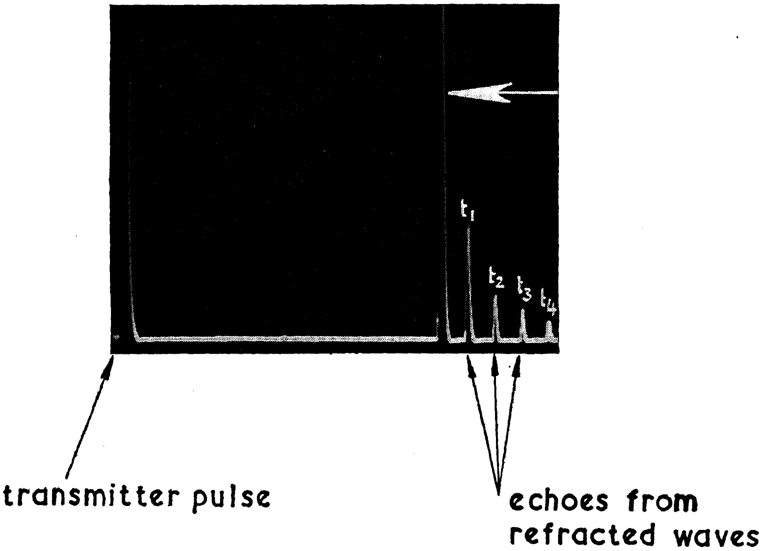

Röntgen Technische Dienst

Fig. 22. Transmitter pulse and bottom echo, followed by additional echoes t_1, t_2, t_3, etc., from refracted waves traveling longer paths (see Fig. 21). Top arrow indicates bottom echo.

that **small defects** present are oriented parallel to the longitudinal axis of the rod. These defects will probably not give rise to reflections of the main beam, which travels along the longitudinal axis of the rod. They will, however, absorb the transverse waves.

In a sound bar the bottom echo occurs with one or more additional echoes behind it at regular intervals (see Fig. 22). In a bar with longitudinal defects the bottom echo occurs normally, but there may be no additional echoes behind the bottom echo (see Fig. 23).

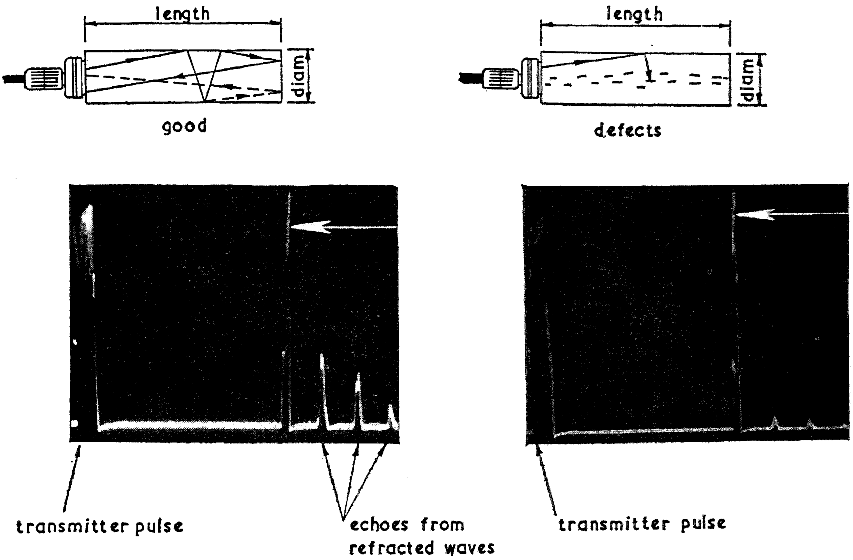

Röntgen Technische Dienst

Fig. 23. Influence of longitudinal defects (right) removes signals from refracted beam paths in good materials (left). Top arrows of oscilloscope trace indicate bottom echoes.

DISTURBANCES CAUSED BY FORM OF THE SPECIMEN. The disturbances caused by reflection and refraction can cause great difficulties in interpretation when examining **complicated structures** such as an axle with key holes or flanged parts. It is therefore of the highest importance to study the drawings of specimens which one has to examine in situ. Besides a close study of the drawing and a theoretical approach to the problem, the following methods can aid in analysis:

1. Examination from two opposite sides of the specimen, if possible.
2. Duplicate measurements at symmetrical points. In this way one can determine whether the findings are general for the whole specimen. With defects as described above, the same indications should result when measuring from various symmetrical probe locations.

Fillets and Corners. Other disturbances can be caused by fillets and corners, as indicated in Fig. 24. This possibility should be kept in mind when examining castings because it may give the impression that a defect is present. The same

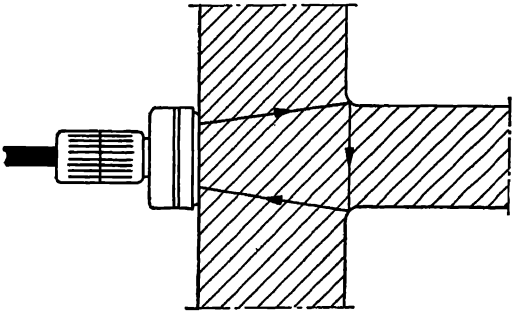

Röntgen Technische Dienst

Fig. 24. Example of sound paths leading to disturbing echoes from fillets and corners in test specimen.

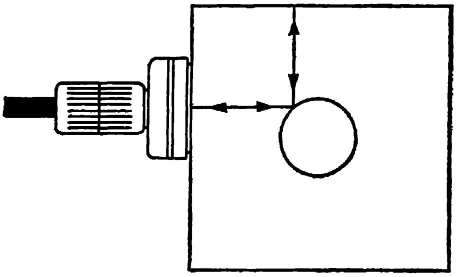

Röntgen Technische Dienst

Fig. 25. Example of sound path in part with internal bore, leading to spurious reflection signals.

applies to **rectangular specimens with internal bores** (Fig. 25). In general these cases do not cause much difficulty.

Cylindrical Parts. In addition to the disturbances mentioned before, additional echoes can occur on cylindrical specimens after the first bottom echo, as shown in Fig. 26. This is especially true in the case where the probe is not made especially for the curved surface. The **beam spread** of the sound wave depends upon the size of the transmitting area. When a flat probe is placed on a curved surface, the contact area is nearly linear. This means that the beam spread is practically 180 deg. The additional echoes will occur after the first bottom echo. These echoes will occur sooner and more frequently, the smoother the surface of the cylinder. On a rough surface of a casting, for example, the echoes will not often be noticed. The explanation is that the rough surface scatters the sound.

These reflections need not be misleading when examining cylindrically shaped specimens because they will re-occur in the same way along the entire cylindrical surface. When in an exceptional case they result from a defect which exists over the full length of the specimen, such reflections will not correspond with a normal reception of the bottom echo. Above all, reflections from real defects can always be recognized by a changing screen image when moving the probe.

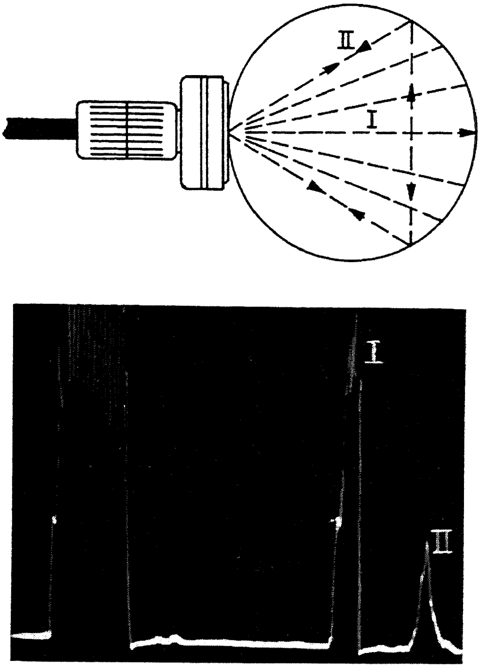

Röntgen Technische Dienst

Fig. 26. Sound paths leading to spurious additional echoes in the examination of cylindrical specimens.

Evaluating Shape Disturbances. All possible disturbing echoes due to the shape of the specimen cannot be described. To distinguish the various echoes:

1. Mark the echoes found. From material and technical considerations it will soon become clear whether the reflections can come from possible defects or not.
2. Study symmetrical considerations.
3. Where possible, examine from more than one surface, if necessary by using angle probes.
4. Make accurate measurements of the location, with the aid of an interferometer, by using calibration blocks or other accurate means.

DISTURBANCES CAUSED BY STRUCTURE OF TEST MATERIALS. The structure of the material has an important influence on its acoustical properties. With fine-structured steel (for example, a forging of high alloy steel) very low **damping** may be observed. Castings of large dimensions, especially when they have not been heat treated, show a coarse structure and have large damping effects. The direction of the sound beam, with respect to the direction of oriented crystal structure, also plays an important part. This phenomenon can be found even after extensive rolling.

Loss of Back Reflection. Often sufficient sound transmission cannot be obtained even with the strongest signal and maximum amplification. For this reason it may not be possible to get a bottom echo, and the sensitivity for finding defects may be nil. This condition, however, is not misleading because no additional echoes will occur. Improvement of transmission can be obtained by using a lower frequency.

Echoes Following Initial Pulse. Disturbing echoes can sometimes be noticed when examining a coarse structure, these echoes occurring close behind the initial pulse. Such indications can cover a large part of the screen (Fig. 27). This is another reason for the use of lower frequencies when examining **coarse structures.** It is not difficult to recognize these disturbing echoes because of their great irregularity. When moving the probe a little, it may be extremely difficult, however, to discover flaw echoes between these structural echoes. In some cases this may even be impossible. There is little that can be done except lowering the frequency and changing the direction of the sound beam by using angle probes, for example. It is advisable to examine **coarse-structured materials after heat treatment** whenever possible. This improves the acoustical characteristics to a great extent. The same applies when examining bronze and other alloys, as well as steel. **Aluminum ingots,** however, even with coarse structure, often have reasonably good sound transmission except when they contain impurities or other defects.

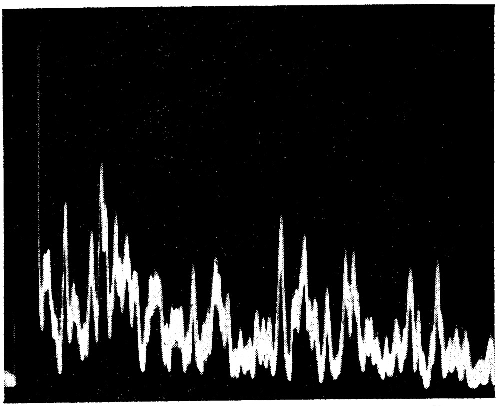

Röntgen Technische Dienst

Fig. 27. Disturbing echoes resulting from coarse-structured test specimens.

Local Changes in Structure. Only under exceptional circumstances can one find reflections from changes in structure except, for example, when one of the structures is very coarse. When this coarse structure is examined separately, the scattering phenomenon will be observed. This will occur, however, only when the **area of the transition zone** is relatively large. It is still an open question whether this is an advantage or a disadvantage because sudden changes in structure can also indicate sudden changes in mechanical properties.

ACCIDENTAL DISTURBANCES. With all these possibilities for getting disturbing echoes, the neophyte may be very sceptical of employing ultrasonics and may doubt whether he will ever be able to carry out a proper interpretation. In practice, it is not so complicated as may appear from the foregoing discussion. The most important objective is to recognize **flaw echoes.** One of the most essentially recognizable characteristics of the flaw echo is its stable position with a fixed probe position. With **accidental echoes,** for example, as described subsequently, this is not the case.

Couplant Flow Indications. The observer can differentiate one form of accidental echo because it slowly alters its position or amplitude. A simple explanation for this is that the coupling liquid moves along the surface of the specimen. This effect is seldom noticed. In most cases the cause for the special echo is discovered by measuring the location of its source. This effect may be noticed when using angle probes, especially when working with high sensitivity. This possibility for disturbances needs to be considered in this particular case.

LIMITATIONS IN ELIMINATING DISTURBING ECHOES. All disturbance echoes, except those coming from the equipment, are inherent in the **ultrasonic test method** itself. This means that special improvements in the equipment will not overcome the difficulties. It may be that the use of the **maximum possible frequency** will reduce some of the disturbances described previously. However, the choice of frequency is also influenced by many other limiting factors (see section on Ultrasonic Test Principles).

Since all disturbance reflections are indicated on the cathode-ray tube, their presence makes interpretation of the image more difficult. Even when using an **indicating meter** with the through-transmission ultrasonic test method instead of a cathode-ray tube indicator, the disturbing echoes are all registered. In this case they cannot be differentiated from the defect echoes, and quite often the presence of the disturbing echoes is not even suspected. This accentuates the need to standardize all test conditions when utilizing the through-transmission method and a pointer-type indicating instrument.

SECTION 49

DOUBLE-TRANSDUCER ULTRASONIC TESTS

CONTENTS

PAGE

Characteristics of Two-Transducer Systems

- Separate transmitter and receiver elements .. 1
- Equipment design considerations 1
- Design trends 1
- Gap-scanning techniques 3
- Classification of search units 3
- Combined transmit-receive search units 3
    - Principles of combined-type search unit (*f.* 1) 2
  - Test indications 3
    - Typical indications with combined probe (*f.* 2) 4
  - Test sensitivity 3
  - Advantages of coupling blocks 5
    - Explanation of combined and separate TR oscillograms (*f.* 3) 5
  - Depth sensitivity 5
    - Variation of sensitivity along axis of combined TR search unit (*f.* 4) 6
  - Beam diameter 5
  - Paint-brush transducers 6
  - Limitations 6
    - Two limitations of separate TR search units (*f.* 5) 7
  - Surface roughness effects 6
  - Angle-beam search units 8
    - Combined TR weld-testing search unit and typical oscillograms (*f.* 6) 8
    - Typical energy distribution for combined TR search unit of transverse-wave type (*f.* 7) 9
  - Vertically stacked, angle-beam search units 9
    - Combined TR search unit design for testing welded pipe (*f.* 8) 9
- Separate transmit-receive search units 9
  - Search units for laminar flaw detection 10
    - Separate TR search unit design and characteristics (*f.* 9) 10
  - Selection of wedge material 11
  - Depth sensitivity 11
  - Transverse-wave search units 11
    - Use of double search-unit arrangement to examine weld area selectively (*f.* 10) .. 12
- Transducer damping 11
- Acoustical coupling 12

Applications of Two-Transducer Systems

- Fine-grained test materials 12
    - Results of tests with combined TR search units on forged rotor disc (*f.* 11) 13
- Coarse-grained materials 13
    - Use of angle-wedge, separate TR search units to improve clarity on coarse-grained Nimonic alloy (*f.* 12) 14
- Materials with inclusions 14
- Contoured materials 14
- Large steel ingots 14
    - Separate TR search-unit technique for 10-ton octagonal ingots (*f.* 13) 15
- Flash-butt welds 16
    - Double search-unit test of a flash-butt weld (*f.* 14) 16
- Hydrogen flaking in cylindrical forgings 16
    - Double search unit test of roller bearing (*f.* 15) 17
- Transmission testing of attenuating materials 17
- Use of double-transducer units for automatic testing 18
  - Limitations of contact testing 18
  - Limitations of immersion testing 18
  - Gap testing 19
  - Full immersion testing 19
  - Use of flaw gating systems 19
- Safety devices in automatic testing 19
  - Automatic gain control 19
  - System fault warning 20
  - Double-transducer fault-warning systems .. 20
    - Double-transducer monitoring system for weld testing (*f.* 16) 20
- Test selection 21
- References 21

SECTION 49

DOUBLE-TRANSDUCER ULTRASONIC TESTS

Characteristics of Two-Transducer Systems

SEPARATE TRANSMITTER AND RECEIVER ELEMENTS. British experience in ultrasonic flaw detection dates back to 1942, when Sproule developed a practical pulse-echo instrument on behalf of the Hairline Crack Sub-Committee of the Iron and Steel Institute.[1] This equipment employed two transducers, one of which transmitted the ultrasonic pulses, the other serving as the detector. In this particular respect the equipment was essentially different from that devised by Firestone during the same period.[2]

The general lines along which ultrasonic testing has been subsequently developed are common to the United States and Europe and are discussed in other sections. However, the use of **acoustically and electrically separated transmitter and receiver elements** in search-unit design has remained as a feature which is more or less peculiar to British practice. Progressive development work has resulted in a series of search units possessing characteristics which are valuable both for manual and automatic testing purposes. A survey of this work supplements the information provided by American authorities.

EQUIPMENT DESIGN CONSIDERATIONS. This discussion is confined mainly to the design, characteristics, selection, and use of search units having separate transmitter and receiver elements. It includes a critical analysis of their performance as compared with that of single-transducer contact and immersion search units. In providing examples of application, some reference will be made to British automatic-testing equipment, which incorporates a number of unique features such as **automatic gain control** and **system fault-warning alarm devices.** Such devices provide safeguards needed for high-speed production testing. They are employed effectively with both single- and double-transducer search units. For **weld testing,** to take one specific example, two-transducer search-unit systems provide more reliable facilities for monitoring acoustic coupling efficiency and attenuation changes than those obtained with a single search unit.

DESIGN TRENDS. The practical development of immersion testing techniques by Erdman and Hitt[3] was a major development which has strongly influenced equipment design in the United States. Since the major field of interest has been the inspection of **wrought aluminum,** which is reasonably isotropic elastically, test frequencies of 10 Mc. or higher are most commonly used. This not only permits relatively large indications to be obtained from small flaws of the order of 1/64-in diam. but also minimizes the "dead zone" associated with the front-surface echo.

Much of the progress in ultrasonic flaw detection in Britain, on the other hand, has been stimulated by the combined needs of a number of different engineering groups. Although inspection of wrought aluminum has assumed considerable importance, the establishment of ultrasonic testing techniques for steel, nickel alloys, and titanium alloys has had equal priority. Since these are relatively **anisotropic materials,** and are not necessarily fine-grained, it is customary to employ test frequencies not exceeding 5 Mc. Consequently, difficulties arising from scatter of the ultrasonic energy, due to microstructural sources, are avoided.

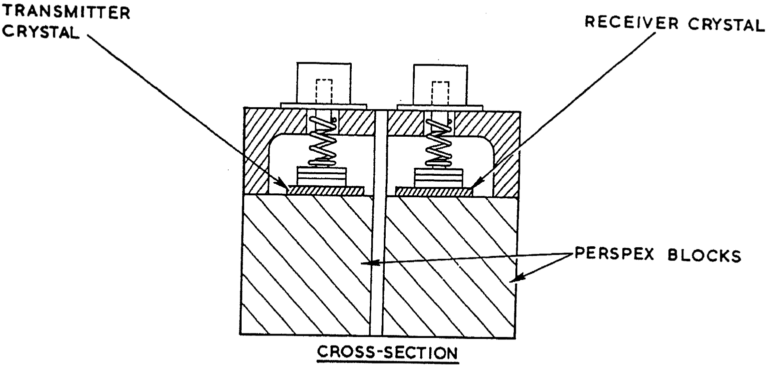

(a)

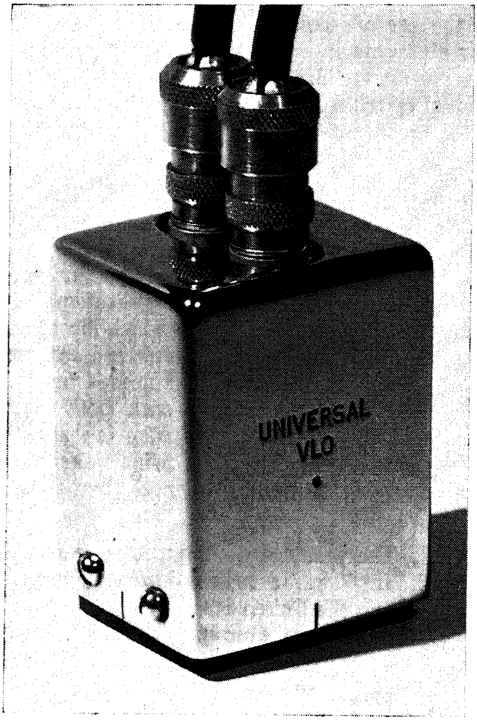

(b) Kelvin & Hughes, Ltd.

Fig. 1. Principles of combined-type search unit. (a) Crystal and Perspex block arrangement. (b) Universal VLO probe.

At these lower frequencies, the ability of a single-transducer search unit to detect **flaws near the top surface** is impaired, and this is one of the conditions under which a double-transducer search unit can provide improved results. Again, with coarse-grained cast-steel ingots, difficulties due to **excessive ultrasonic scatter** can often be overcome by arranging different transmission and echo paths using two separate search units.

GAP-SCANNING TECHIQUES. Another important point which has influenced development is the unsuitability of immersion testing for **very large components** such as heavy steel plates and rotor forgings. As an alternative, a "gap-scanning" technique, where a water-filled gap of several thousandths of an inch is maintained under the search unit, has been devised.[4] To preserve reasonable performance at short range, the use of a double-transducer search unit is preferred for this type of work.

CLASSIFICATION OF SEARCH UNITS. It is convenient to classify transmit-receive (TR) search-unit systems into three general groups:

1. Common TR search units where a single transducer is employed with common connections to the transmitter and receiver amplifier units.
2. Combined TR search units, where two transducers are mounted in a single head, connected separately to transmitter and receiver amplifier units, and insulated acoustically from each other.
3. Separate TR search units where two heads are employed, one transmitting and the other detecting the ultrasonic pulses, with separate electrical connections to the transmitter and receiver amplifier units.

COMBINED TRANSMIT-RECEIVE SEARCH UNITS. The general design of a combined TR search unit for contact testing is shown in Fig. 1. The transmitting and detecting sections of the unit are very similar, each comprising a **backed barium titanate transducer element** which is coupled to the test material through a block of Plexiglas (British name, Perspex) and the usual film of oil. The two sections are acoustically insulated from each other by a thin layer of cork.

Test Indications. Fig. 2 shows typical results obtained with a search unit of this type, using test blocks with flat-bottomed drill holes of 3/64-in. diam. Fig. 2(a) shows the cathode-ray tube pattern for this target at a range of 11½ in. in a 12 in. long aluminum alloy extrusion of 2½-in. hexagonal section. Fig. 2(b) shows the echo from this target at a range of 1/10 in. in a 1 in. long specimen of the same section and material. To demonstrate long-range characteristics, Fig. 2(c) shows the result for the same target at a range of 9 ft. 10½ in. in a 10-ft. length of the same section. In all cases the test frequency is 2.5 Mc.

Test Sensitivity. The three illustrations of Fig. 2 serve to emphasize the sensitivity of the combined TR arrangement at a variety of ranges. There is no **large pulse corresponding to the top surface of the test material,** as in the patterns obtained when working with common TR search units. This is the most important point of difference between the two techniques. A common TR search unit cannot detect flaw signals until its function as a transmitter is complete; this characteristic gives rise to an appreciable **dead zone** at the top surface of the specimen. A combined TR search unit can detect flaw signals before the transmission is complete, if so required, because there is no direct electrical or acoustical linkage between the transmitter and the receiver amplifier. An associated advantage is that **amplifier paralysis,** due to the large electric pulse required for transmission, is avoided.

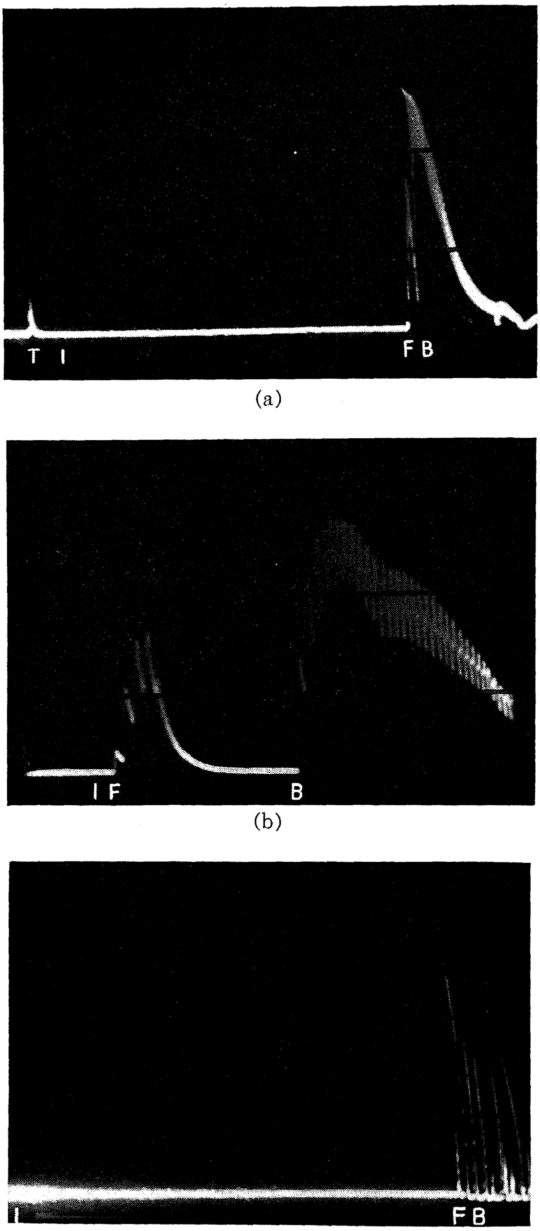

(a)

(b)

(c)

Kelvin & Hughes, Ltd.

Fig. 2. Typical indications with combined probe. (a) Target at 11½ in. from surface. (b) Target at 1⁄10 in. from surface. (c) Target at 9 ft. 10½ in. from surface. All targets 3⁄64-in. flat-bottomed drill holes. *T*, transmission mark; *I*, interface position; *F*, flaw echo; *B*, boundary echo.

Advantages of Coupling Blocks. The interposing of Plexiglas blocks between transducers and the test object has been found experimentally to assist tremendously in **reducing the transmission of Rayleigh waves** across the surface of the specimen from the transmitter to the receiver section of the probe. Since the ultrasonic pulse passes through these two blocks of Plexiglas during the transmission and reflection process, a **delay** of 60 μsec. or so is incurred (Fig. 3).

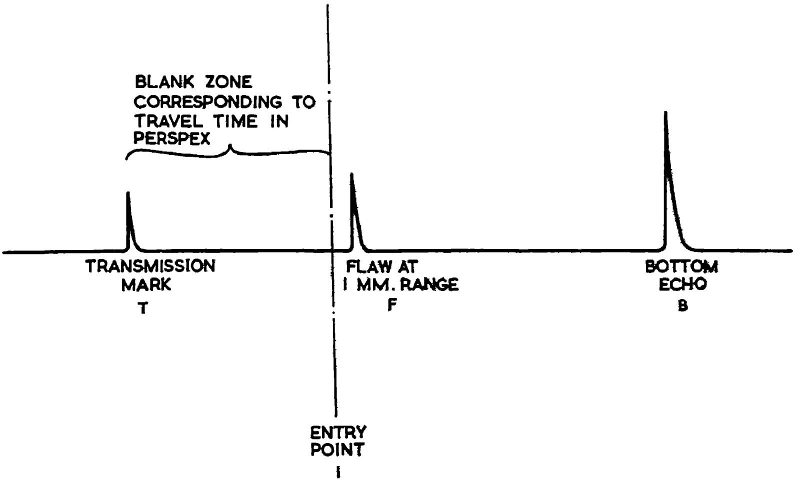

Fig. 3. Explanation of combined and separate TR oscillograms.

For this reason the echo from a flaw very near the top surface of the test material is not associated with a **transmission-initiation signal,** which may be introduced, if so desired, into the receiver amplifier to establish a convenient zero marker. This transmission signal can be seen in Fig. 2(a), where the delay in the Plexiglas blocks is negligible compared with the total length of the specimen. For automatic flaw-detection purposes, this delay is invaluable, as will be explained later.

Depth Sensitivity. In Fig. 4 the variation of sensitivity with depth is shown quantitatively for a 2.5-Mc. search unit of the type described before, using a 3⁄64-in. flat-bottomed drill hole as a target. The sensitivity rises to a maximum at about 2 in., then falls away fairly gradually. Taking the signal level at 2 in. as a reference position, the signal level for a range of ¼ in. is 9 decibels (db.) lower. At a range of 1⁄10 in., it is 16 db. lower. Generally speaking, this variation is of the same nature as that observed with a common TR search unit. However, the combined TR search unit does not exhibit such a large difference between maximum and minimum values. Of course a similar curve taken with a common TR search unit operating at the same frequency would not be extended to small depths because of the limitations imposed by the act of transmission and by amplifier blocking.

Beam Diameter. It may be thought that the use of two separate transducers would lead to a comparatively wide ultrasonic beam. However, by using a pair of transducers, each 20 × 10 mm., the **active diameter of the beam** at a depth of 1¾ in. is only about ½ in. This compares favorably with the beam spread of

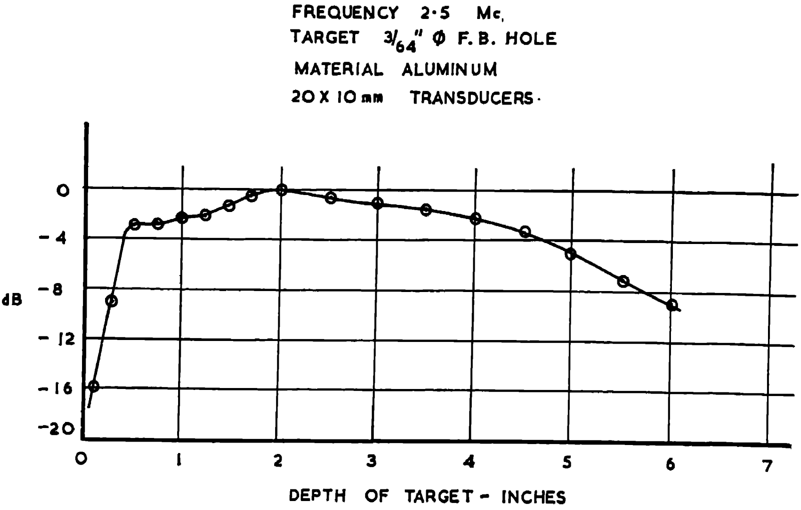

Fig. 4. Variation of sensitivity along axis of combined TR search unit.

a single-transducer search unit of similar size. Again, a frequency of 2.5 Mc. was employed in these tests.

Paint-Brush Transducers. These search units can also be designed in wider versions. Energy distribution measurements over a width of 140 mm., using **twin barium titanate mosaic transducers** built up from 20 × 10-mm. elements, show a variation of less than 6 db.

Limitations. At this point certain limitations of combined search units can be usefully discussed. Although, as demonstrated in Fig. 2(b), a small flaw at a depth of only 1/10 in. is readily detectible, they cannot usually be employed on **section thicknesses** of less than 1/4 in. This limitation arises as a result of a simple geometrical effect known as the **slant-range** condition. Consider Fig. 5(a) where transmitter and receiver point transducers, separated by a distance $2a$, are applied to a specimen of thickness t. The path length followed by the ultrasonic pulse I can be regarded as linearly related to the thickness t when a is small by comparison. For decreasing values of thickness, however, the curve approaches a horizontal value of a.

The distance along the cathode-ray-tube trace is the **range,** proportional to I. To differentiate between a flaw echo and a bottom echo, the latter must be on the rising part of the curve. In modern combined search units, the value of a is very small, and curve II is typical in such a case. A bottom echo from the back wall of a plate 1/4 in. thick is just on the linear part of the curve, but thicknesses of less than this prove difficult from the point of view of range differentiation. Fortunately, at thicknesses of less than 1/4 in., other methods of approach are available; for example, Lamb-wave techniques.[5]

Surface Roughness Effects. Another difficulty which occasionally occurs is known as the **diffraction-grating effect.** This may arise when the surface of the test material has machining or other **marks of a regular nature,** due perhaps to milling or turning. When ultrasonic energy is incident upon such a surface, strong diffraction of energy occurs, and energy passes directly from

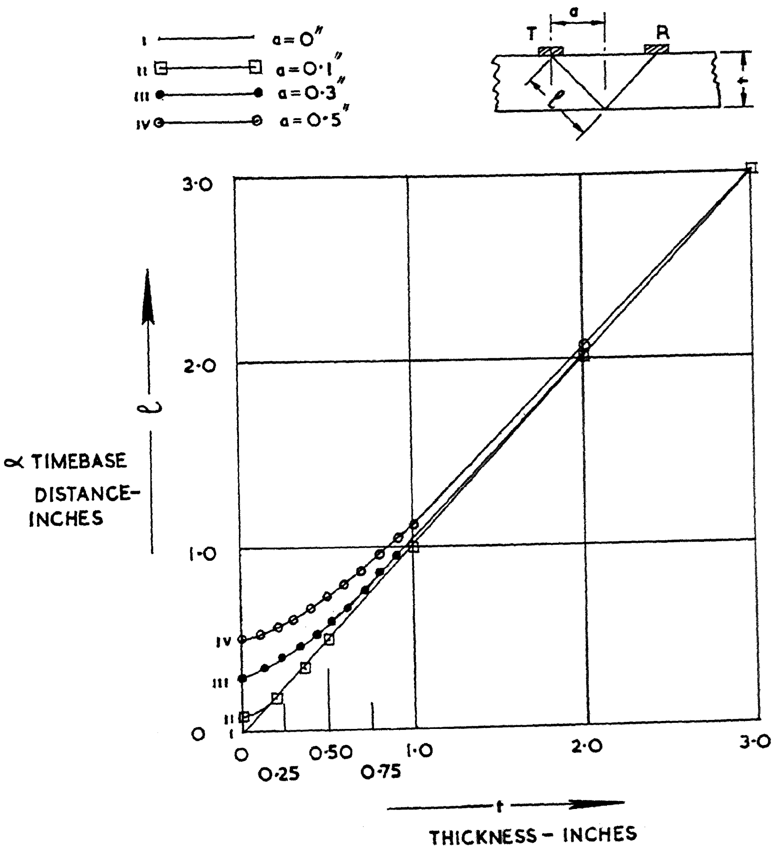

(a)

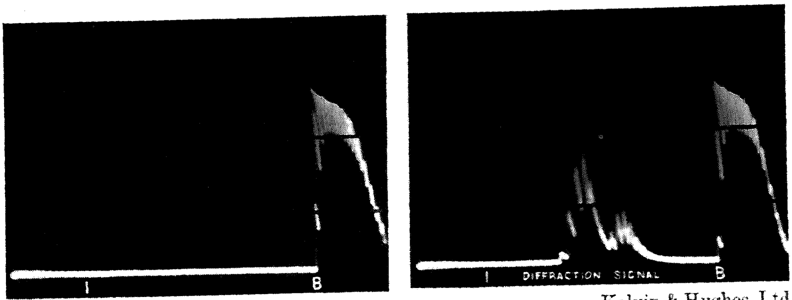

(b)

Kelvin & Hughes, Ltd.

Fig. 5. Two limitations of separate TR search units. (a) Slant-range effect upon range differentiation. (b) Diffraction grating effect on milled surface of 2-in. titanium block: (left) transducer separation across corrugations; (right) transducer separation along corrugations.

transmitter to receiver sections of the search unit. The condition is worst when the spacing between surface corrugations corresponds to an **integral number of half-wavelengths** (see the section on Ultrasonic Fields). In practice, it may be possible to avoid diffraction by placing the length direction of the probe at right angles to the corrugations; typical **cathode-ray-tube patterns** are shown in Fig. 5(b).

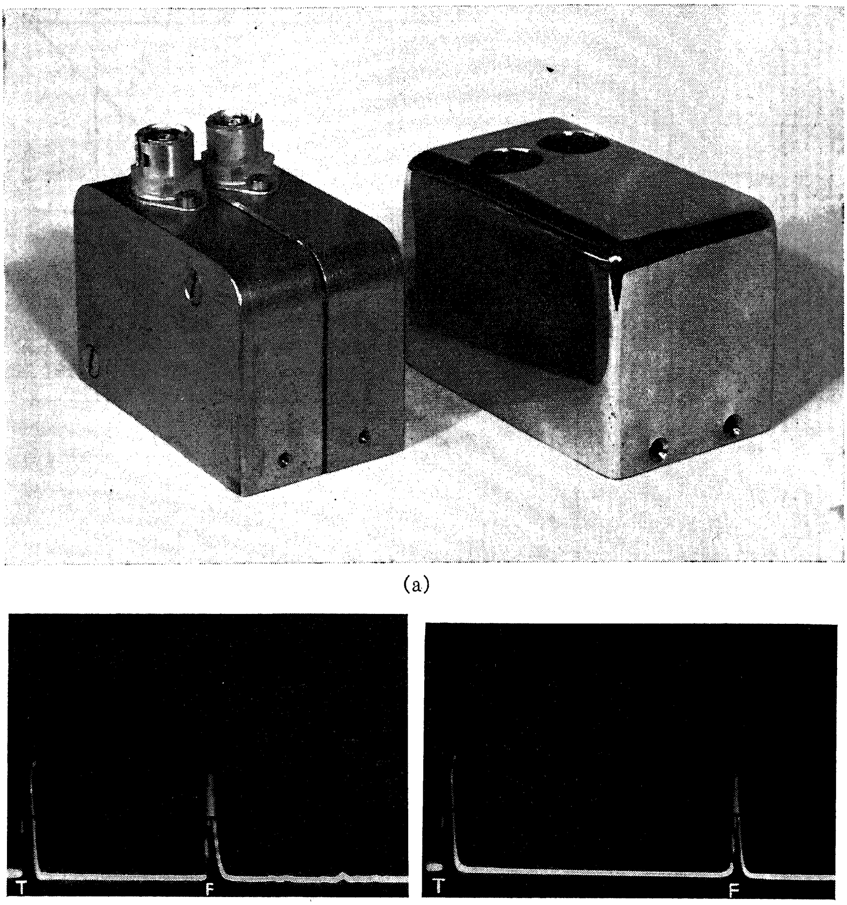

(a)

(b) (c)

Kelvin & Hughes, Ltd.

Fig. 6. Combined TR weld-testing search unit and typical oscillograms. (a) Sectional construction of combined TR weld-testing search unit. (b) Indication from small crack in weld (1-in. plate). Probe axis 1 in. from weld center (70-deg. angle of refraction), 2.5-Mc. frequency. (c) Indication from small crack in weld (1-in. plate). Probe axis 3 in. from weld center (70-deg. angle of refraction), 2.5-Mc. frequency.

Angle-Beam Search Units. A similar general arrangement of transducer elements is also employed for testing at angles of refraction other than zero. Both longitudinal- and transverse-wave-type units have been designed. A typical **weld-testing search unit** is shown in Fig. 6(a). This unit clearly detects normal welding faults such as lack of penetration, cracking, and slag inclusions. Again, a useful characteristic is freedom from **probe hash,** so that the search unit can be positioned very close to the weld if required. Figs. 6(b) and (c) show two typical oscillograms with explanatory captions, while Fig. 7 shows a typical **energy-distribution characteristic.**

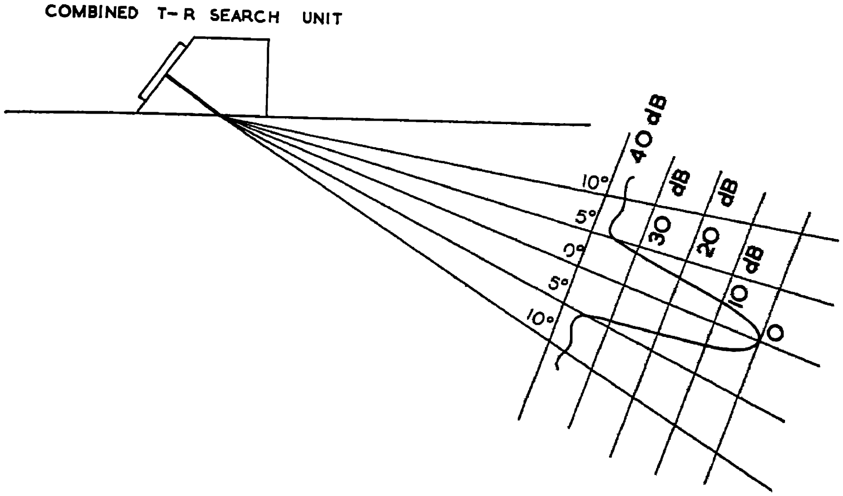

Fig. 7. Typical energy distribution for combined TR search unit of transverse-wave type.

Vertically Stacked, Angle-Beam Search Units. One point of interest regarding the design of combined TR search units for the **testing of circumferential welds** in pipes of less than about 12-in. O.D. is that the line of separation of the transmitter and receiver sections has to be positioned across the longitudinal axis of the pipe. In this case the arrangement of the two sections is "above and below" rather than "side by side" (Fig. 8).

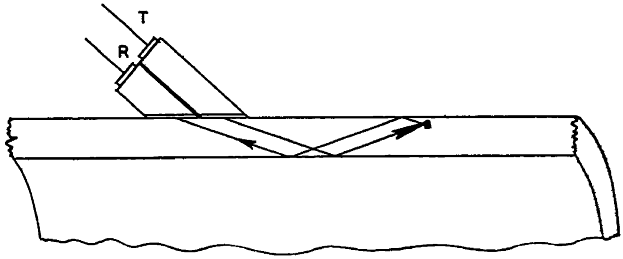

Fig. 8. Combined TR search unit design for testing welded pipe.

SEPARATE TRANSMIT-RECEIVE SEARCH UNITS. Consider next the design and characteristics of separate TR search units. These are almost always used in pairs, with two units of identical design. A **mechanical link** is commonly employed to clamp the two search units together. Where the fronts of the two heads are close together, a cork layer is inserted to prevent the couplant from building up in the space between them.

Search Units for Laminar Flaw Detection. It has been found experimentally that a general arrangement as shown in Fig. 9(a) is very effective for many testing purposes when flaws have a reflecting surface substantially parallel to the surfaces of the component being tested. The **angles of refraction** can be selected to suit the application; in practice, the angles are standardized at 0, 5, 10, 20, and 30 deg. A chart showing the **depth of maximum sensitivity** for each angle, along with the minimum and maximum range, is shown in Fig. 9(c).

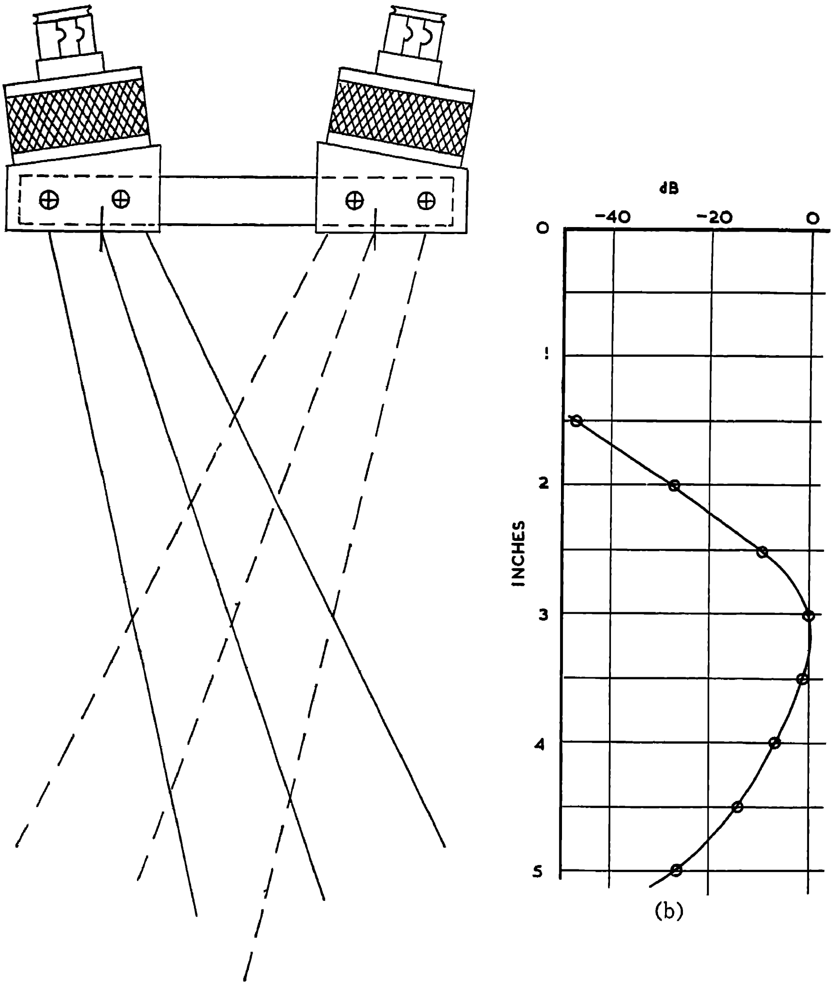

(a)

(b)

Fig. 9. Separate TR search unit design and characteristics. (a) Search unit arrangement. (b) Depth of maximum sensitivity for probe angles.

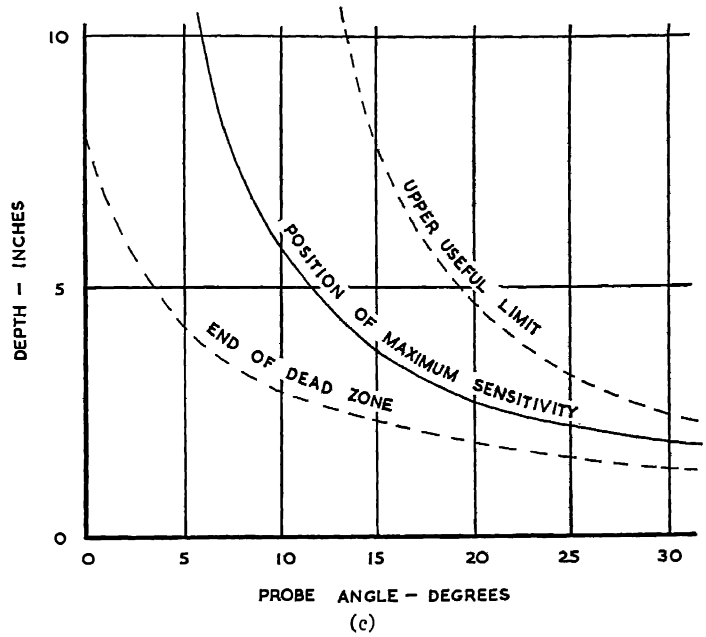

Fig. 9. (Continued.) (c) General form of depth-sensitivity characteristic.

Selection of Wedge Material. Experience shows that Plexiglas wedges provide a satisfactory balance between the need for good sensitivity and the need to avoid **internal multiple reflection** of the ultrasonic pulses. Steel and aluminum wedges are not very satisfactory in this latter respect and yield comparatively poor results, due to the generation and detection of Rayleigh waves.

Depth Sensitivity. The depth-sensitivity characteristic of this search unit arrangement can be adjusted by (1) using different angles of refraction and (2) using different probe separations. The general form of the characteristic is shown in Fig. 9(c). It reaches a maximum at one specific depth. It exhibits a well-defined **low-sensitivity zone** near the top surface and a diminution of sensitivity beyond the maximum, both of which can be controlled by the adjustments mentioned here. Controlling the variation of sensitivity in this way has proved valuable when testing materials which tend to exhibit **troublesome scatter** of ultrasonic energy. Variable-angle search units have also been designed.

Transverse-Wave Search Units. Similar principles can also be applied to advantage in the case of transverse-wave search units. The response of these units is at a maximum in a selected area of the specimen, as indicated in Fig. 10, which represents a welding application. By using this technique, **echoes from insignificant sources** can be avoided. Such spurious echoes can arise from inclusions in the parent metal and from surface imperfections of unmachined plates.

TRANSDUCER DAMPING. To achieve the desired sensitivity-depth characteristics, there is no necessity to use heavily damped transducers. However, it is normal practice to do so, since resolution of echoes from flaws which are situated closely together is desirable. Modern search units of this type are based

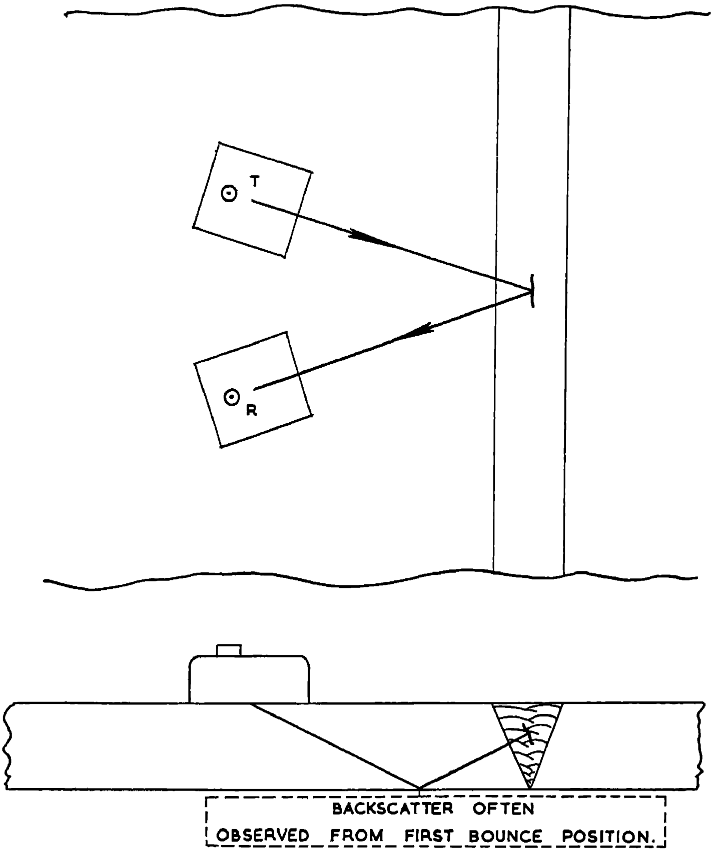

Fig. 10. Use of double search-unit arrangement to examine weld area selectively.

upon barium titanate **transducers backed with a loaded epoxy resin** of high acoustical impedance.

ACOUSTICAL COUPLING. Barium titanate is preferred to quartz and lithium sulfate for most double-transducer search units, mainly because of its high **electromechanical coupling coefficient.** Since the acoustical and electrical matching of the transmitter and receiver elements can be arranged independently, the low mechanical-electrical coupling coefficient does not pose a serious problem. The **capacitance of the transducer** is usually very high, relative to the capacitance of feeder cables, and the length of feeder cable is not so critical as in the case of quartz. **Mode interaction,** leading to low-frequency generation, is not too troublesome in double-transducer search units, although care has to be paid to the phenomenon in the design of transducers and matching transformers.

Applications of Two-Transducer Systems

FINE-GRAINED TEST MATERIALS. In general, when the structure of the materials to be tested is uniform and fine-grained, the use of a **combined TR arrangement** is satisfactory and gives maximum possible cross-sectional coverage. A typical test result upon a forged rotor disc is shown in Fig. 11. The **frequency** employed depends upon a number of factors: surface roughness, size of the flaws to be detected, and the general level of ultrasonic scatter, which is usually set primarily by the grain size. Scatter associated with grain size depends upon the degree of **elastic anisotropy** exhibited by the metal and is substantially greater for steel than for light alloys, to cite one example.

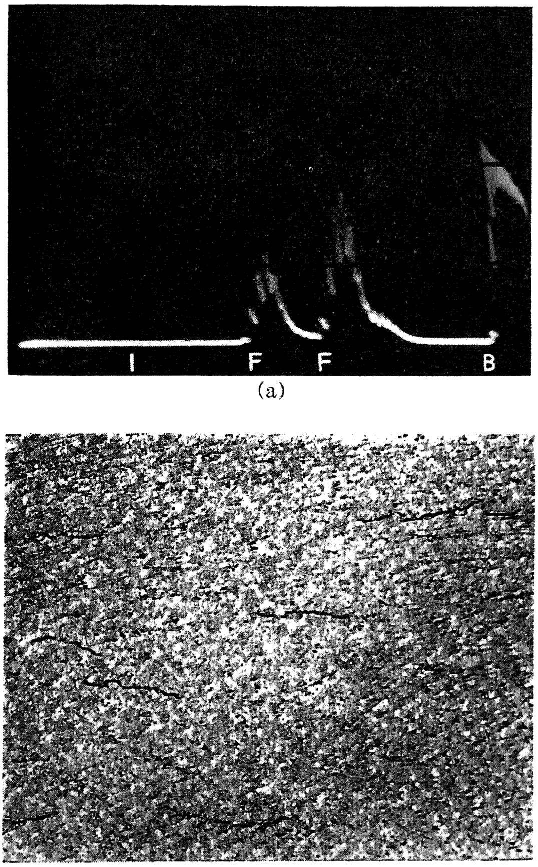

(a)

(b) Kelvin & Hughes, Ltd.

Fig. 11. Results of tests with combined TR search units on forged rotor disc. (a) Result on 2-in. thick rotor disc. (b) Typical cracks in rotor disc (6×).

COARSE-GRAINED MATERIALS. When the structure is such that it produces considerable scatter, due to a general or a local coarsening of the grain size, improved results are very often obtained by the use of **double-wedge search units** of suitable angle. While this gives a poorer minimum range, often making it necessary to inspect from both surfaces of the test material, there is generally a considerable improvement in the **clarity of the flaw indications** obtained. As a result the speed at which testing is carried out can often be increased, offsetting the disadvantage of a **double scan.** Fig. 12 provides an example of the degree of improvement which can be achieved in practice. The **intensity of scatter** is at a maximum when observations are made along the axis followed by the incident ultrasonic beam. By transmitting and receiving at different angles, the amount of scatter is considerably reduced without affecting the reflection from a flat target.

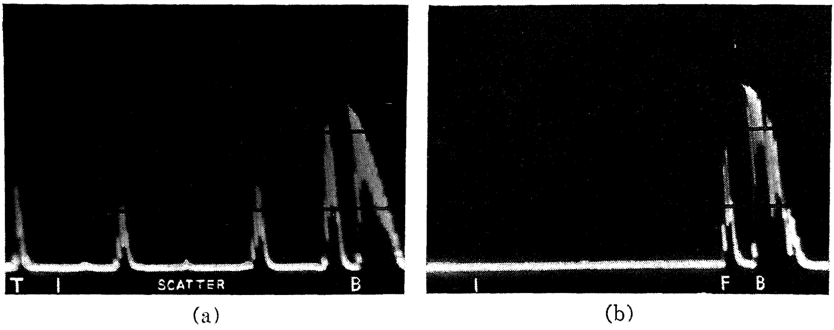

(a) (b)

Kelvin & Hughes, Ltd.

Fig. 12. Use of angle-wedge, separate TR search units to improve clarity on coarse-grained Nimonic alloy. (a) Vertical probe, combined TR (frequency 1.5 Mc.). (b) Five-degree refraction Perspex wedges, separate TR (frequency 1.5 Mc.).

MATERIALS WITH INCLUSIONS. Double-wedge techniques can also be used to considerable advantage upon metals containing a large number of inclusions; for example, high-sulfur, free-cutting steel. In such materials it is usually desirable to detect only **major defects** such as primary piping on the axis. High attenuation of ultrasonic energy requires the use of considerable amplification, so that **signals due to scatter** in the first inch of the test material tend to be exaggerated. Indications due to this scatter can be eliminated by using a steeply rising and falling sensitivity-depth characteristic with the maximum at the section axis. This makes the task of an operator easier.

CONTOURED MATERIALS. Combined and separate TR systems also work well upon **small-diameter sections,** even though only line contact is possible. Search units can be shaped to fit regularly curved surfaces without difficulty or high cost. This involves only the shaping of Plexiglas, which is a relatively simple and inexpensive operation.

Angle search units for weld testing and similar applications are selected with angles determined by the geometry of the test object in the same way as determined for a single-transducer search unit. Rankin offers some guidance in the methods of selection and application in weld testing.[6]

LARGE STEEL INGOTS. In Fig. 13 an example is given where it was found essential to use **completely separated search units.** Attempts to carry out tests with single-transducer and coupled double-transducer search units in large steel ingots are more often than not abortive, due to extremely heavy scatter associated with the columnar crystal region of the ingot. To establish the extent of **axial defects** such as primary piping or shrinkage cavities, it is possible to arrange the probes as shown in Fig. 13 to obtain clear-cut echoes from flaws in

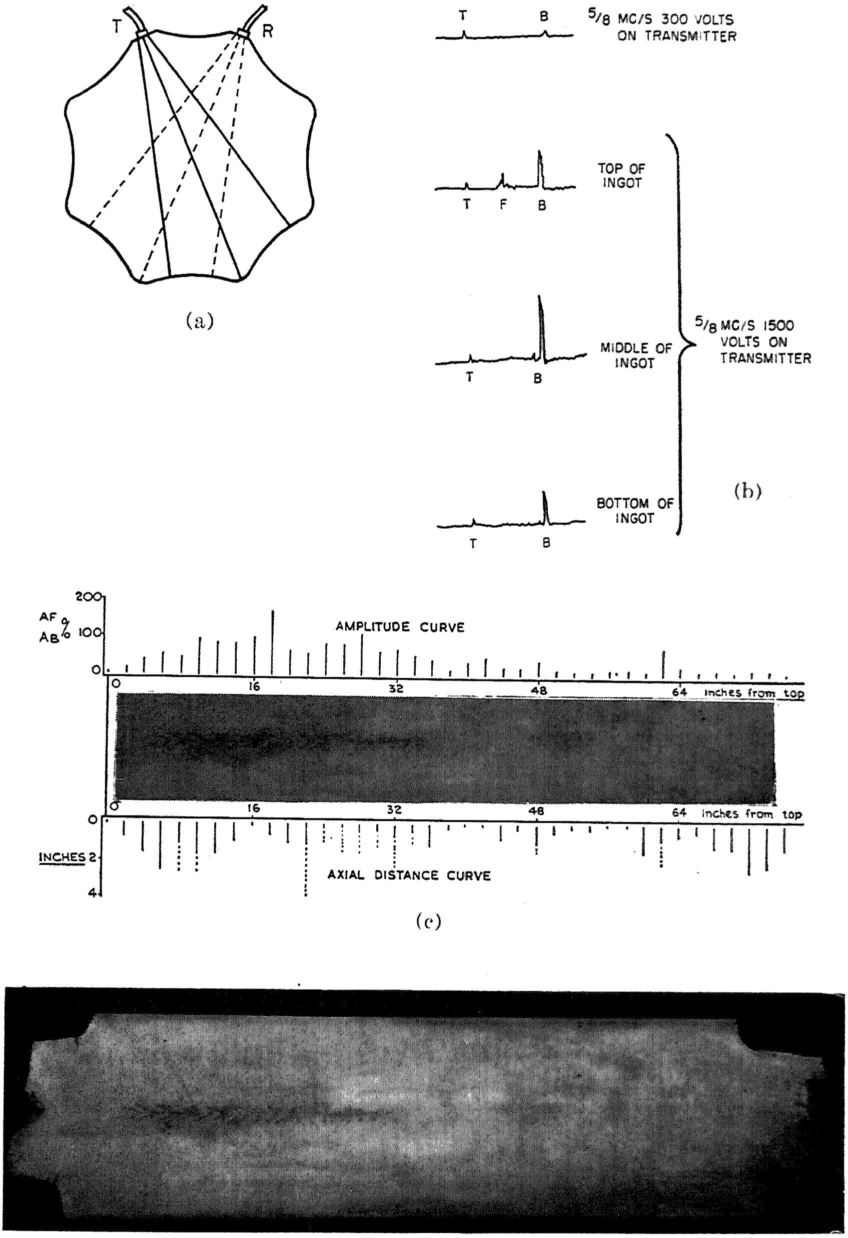

(a)

(b)

(c)

(d)

Kelvin & Hughes, Ltd.

Fig. 13. Separate TR search-unit technique for 10-ton octagonal ingots. (a) Adjacent corner arrangement of TR transducers. (b) A-scan signals from top, middle, and bottom of ingot. (c) Flaw amplitude and position plots. (d) Complete section through ingot.

the axial region. With this arrangement the centrally situated equi-axised structure does not produce scatter of the same order of magnitude. Because there is a considerable separation of the transmitter and receiver elements, **scatter from the transmitted beam** passing through the columnar region does not arrive at the receiver probe.

FLASH-BUTT WELDS. In some applications the geometry of the test material sometimes makes essential the use of a double-probe arrangement. One particularly important case is the testing of flash-butt welds where the **flaws** are very smooth and flat and lie at right angles to the accessible surfaces of the material (Fig. 14). The use of a search unit from only one side of the work cannot be considered satisfactory for the detection of defects away from the surfaces of the material excepting when the section thickness is small. Under these conditions it is usually possible to employ a **separate TR system,** as shown in Fig. 14, so that the specular reflection from the flaw reaches the receiving probe directly.

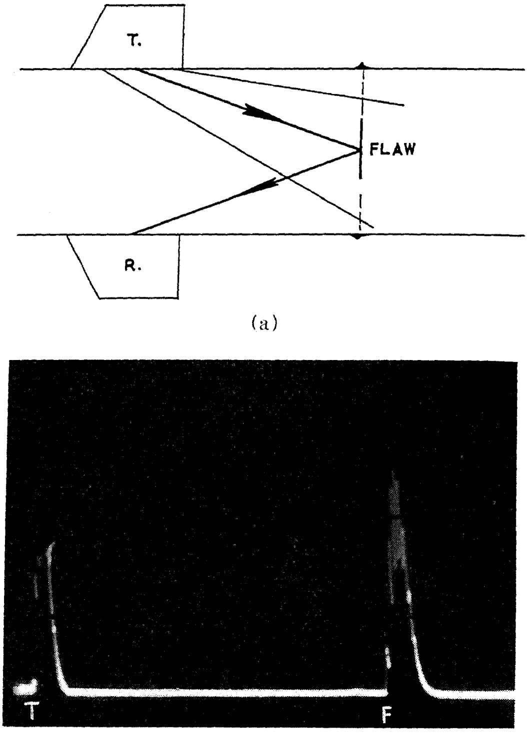

(b) Kelvin & Hughes, Ltd.

Fig. 14. Double search-unit test of a flash-butt weld. (a) Path of sound beam. (b) A-scan recording.

HYDROGEN FLAKING IN CYLINDRICAL FORGINGS. Another more unusual application is the detection of small hydrogen flakes in **gas-carburized roller-bearing forgings** of a shape shown in Fig. 15. Here the flaws are small and the **flaw echo due to diffraction** can be detected even though the crack orientation is far from being ideal. To permit extremely high amplifier sensitivity to be employed without the **difficulties of wedge reverberation**, and to place the flaws in a region at which the sensitivity of detection local to the known flaw site is high, a double search-unit system is extremely useful.

TRANSMISSION TESTING OF ATTENUATING MATERIALS. Finally, of course, some reference should be made to the long established methods of transmission testing, in which separate TR search units are employed. Such methods are still of considerable value, particularly on the **more opaque materials.** Pulse-testing units can be used effectively for transmission testing and have considerable advantages when compared with continuous-wave instruments, since difficulties due to reverberation are avoided by the use of pulse-timing techniques.

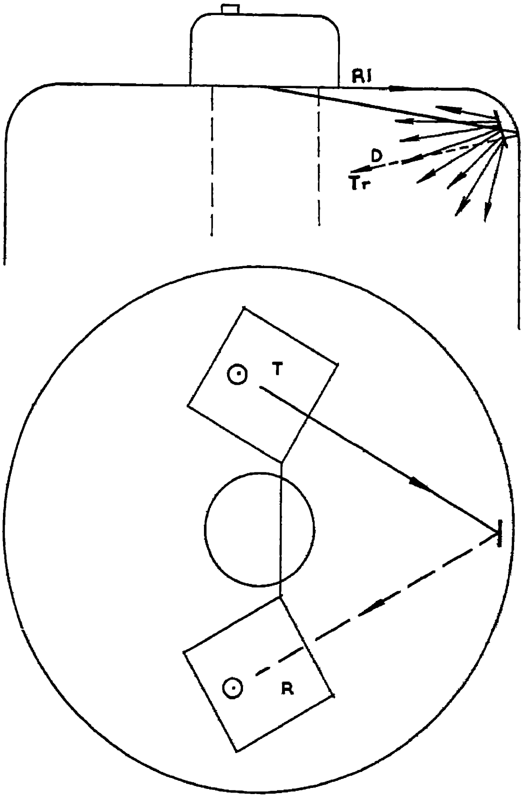

RL—Path of Rayleigh waves.
D—Diffracted energy due to crack.
Tr—Path of transverse waves.
T = Transmitter.
R = Receiver.

(a)

Fig. 15. Double search unit test of roller bearing. (a) Path of sound beam.

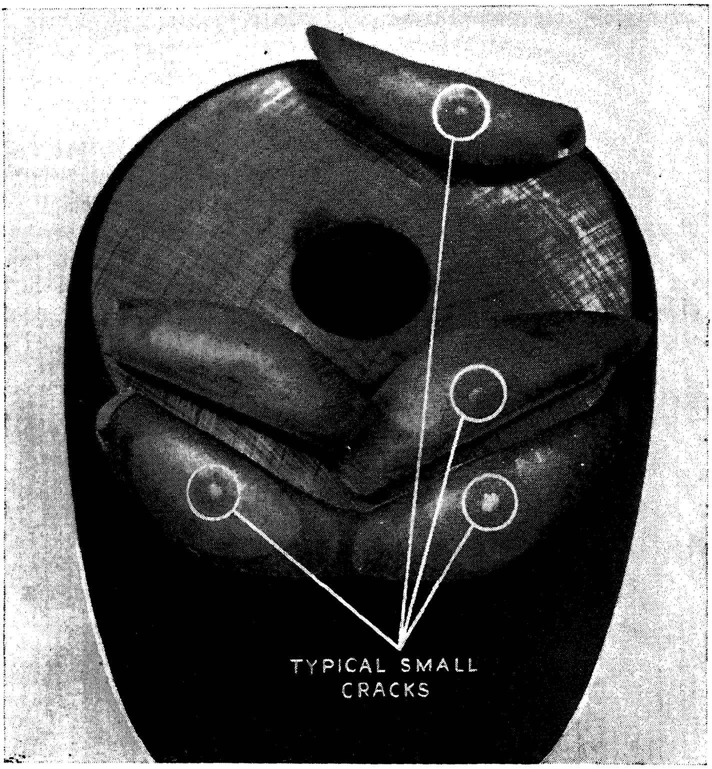

(b) Kelvin & Hughes, Ltd.

Fig. 15. (Continued.) (b) Small cracks found by ultrasonic tests.

USE OF DOUBLE-TRANSDUCER UNITS FOR AUTOMATIC TESTING. Two-transducer systems offer advantages and overcome certain limitations of single-transducer systems in automatic testing.

Limitations of Contact Testing. When there is a need to carry out tests at high speed and to secure reliable data, certain difficulties arise in the use of contact testing techniques. **Acoustical coupling through films of oil** and similar media is known to be variable, and in addition the ultrasonic component of **frictional noise** produces undesirable transient signals which create considerable difficulty in the receiver amplifier circuits.

Limitations of Immersion Testing. Immersion-testing techniques have provided one excellent method of overcoming such difficulties. However, there are many test objects which cannot be tested in this way without extensive mechanization. The **problem of the "dead zone"** associated with common TR practice is a limiting factor. The extent of this "dead zone" can be reduced by careful attention to the pulse-length characteristics. No serious difficulty arises when a very high frequency can be employed. However, when testing ferrous materials or other alloys such as nickel, titanium, and copper-base alloys, **scatter** obtained at frequencies above 5 Mc. may be considerable. Indeed there are many materials upon which frequencies of 1.5 Mc. or less must be used.

Double-transducer techniques can be adapted to overcome the **difficulties associated with the front-surface echo,** which is an inherent feature of immersion testing with a single-transducer search unit.

Gap Testing. One approach which has proved extremely popular is "gap" testing, which uses a double-transducer search unit and dolly. The technique is extremely simple in principle. Instead of making pressure contact between the transducer and the test material through an oil film, a gap of a few thousandths of an inch is left between the base of the search unit and the surface of the test object. A **continuous flow of water** or other suitable liquid is passed through this gap. Apart from a necessity to increase the sensitivity slightly, there is no difference in procedure or result from the ordinary contact-testing case. However, the **constancy of coupling efficiency** is very much improved. For example, the maintenance of good coupling is possible with **scanning speeds** of as much as 450 f.p.m. on rolled and extruded stock. Since search units of (up to) at least 6-in. width are available, fast production-testing rates can be achieved. Gaps of as much as ½ in. can be used, provided that an acoustically insulating sheet is introduced to separate the paths of the transmitted and received beams in the water.

Full Immersion Testing. The same general principles, using combined or separate TR transducer arrangements, can be adapted for full immersion testing. In this case the Plexiglas is replaced by water. Under these conditions, at a test frequency of 2.5 Mc., a ³⁄₆₄-in. diam. flat defect can be readily detected when situated at a distance of less than ¹⁄₁₀ in. from the upper boundary of the test material.

Use of Flaw Gating Systems. It is particularly advantageous to use a system which avoids a front-surface echo by incorporating an automatic test equipment with **electronic gating circuits.** To provide a voltage which operates visual and audible alarms, it is normal practice when using common TR immersion techniques to initiate the "flaw gate" immediately after the tail of the front-surface echo. The pulse length thus determines the "dead zone" in which echoes from small flaws will remain undetected. However, if the front-surface echo is avoided by the use of a double-transducer system, the **opening of the gate** can be set at a position prior to the entry of the ultrasonic pulse into the specimen. Thus any signals above the detectible level will be detected within ¹⁄₁₀ in. from the top surface.

SAFETY DEVICES IN AUTOMATIC TESTING. It is important that automatic ultrasonic-testing units should be provided with safety devices which give an assurance that the test has been carried out according to the procedure prescribed in the testing specification. When a test is being carried out at a **high rate of scanning,** the use of ordinary A-scan presentation tends to be difficult, since the flaw echoes are transient. As convenient ways of overcoming the difficulties, B- and C-scan presentation techniques are valuable. Alternatively, a suitable mechanical recording system can be used, with the advantage that the indications recorded are permanent. Even with such precautions it is still possible for the sensitivity during a particular portion of the test to be reduced, due perhaps to surface condition. During such intervals, defects of significant dimensions may remain undetected. The equipment should be designed to sense such a condition and to correct it.

Automatic Gain Control. To remove the possibility of undetected defects, a form of automatic gain control (AGC) has been described by Brown, Rankin, and Haslett,[7] and Rankin.[4] As well as gating flaw signals, an additional gated amplifier selects a **suitable monitor signal,** such as the bottom echo, and feeds this as a voltage amplitude to a comparator unit. This unit compares the monitor signal with a **standard reference voltage.** When the monitor signal drops in amplitude for any reason, a bias voltage is applied to the main receiver amplifier. This adjusts the monitor signal to the standard amplitude selected for the test. The **correction** is made over a large dynamic range, often as much as 40 db.

System Fault Warning. Should a condition arise which cannot be controlled satisfactorily, a system **fault-warning device** operates. Thus, putting the properties of this system into their broadest terms, either a test is carried out under the desired sensitivity conditions, or immediate indication is given to the operator that something is amiss. In fully automatic scanning units, the **scanning motor drives** are stopped automatically when a system fault occurs.

Double-Transducer Fault-warning Systems. Although this equipment works with any of the conventional types of search units, it is particularly useful with double-transducer arrangements. Here, very satisfactory monitoring techniques can be derived in many cases where **no bottom echo** is available, or where the measurement of the bottom-echo amplitude is in itself of importance.

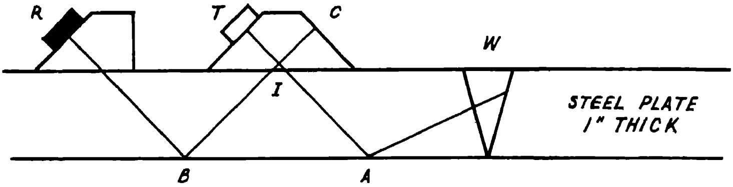

Fig. 16. Double-transducer monitoring system for weld testing.

A **weld-testing application** is diagrammed in Fig. 16. A pulse is transmitted from the transducer at *T* and this travels through the Plexiglas wedge. It is refracted into the steel as transverse waves and travels forward to the weld where part of it is reflected from a flaw. Traveling in the reverse direction, it follows the same path but then travels still farther to the receiver search unit *R*.

Due to the mismatch at the interface at *I*, a good deal of energy is reflected within the transmitter wedge and is returned from *C* back to the interface. It passes across the interface, transforming to transverse waves. These proceed directly to the receiver probe, following the same path as the flaw-echo energy. This signal provides a very useful monitor signal, since it passes through the same interfaces as the test signal, is produced by the same transducers, and suffers the same attenuation (at least approximately) as the test beam. Using "gap" scanning in particular, the amount of **energy reflected within the probe** at *I* is substantially constant. As long as the surface of the test material is randomly rough, the transformation to transverse waves is of the same order of efficiency in both the forward and backward directions.

Measurement of the variation of the **bottom boundary signal** in contact testing, without and with automatic sensitivity control, shows marked improvement with use of AGC. Variations of the order of 30 db. can often be reduced to perhaps 1 or 2 db. with AGC.

TEST SELECTION. Ultrasonic-testing techniques involving the use of double transducers or two separate units can often be used to considerable advantage. By careful attention to probe design, the units can be made suitable for single-handed manual testing as well as for automatic testing.

Single- and double-transducer techniques are in many ways complementary to each other, and it is suggested that careful examination of all possibilities should be made before deciding which approach should be used.

References

1. Desch, C. H., D. O. Sproule, and W. J. Dawson. "The Detection of Cracks in Steel by Means of Supersonic Waves." *J. Iron Steel Inst.* (London), 153 (1946): 319P.
2. Firestone, F. A. "The Supersonic Reflectoscope for Interior Inspection." *Metal Progr.*, 48 (1945): 505.
3. Compte rendu général des travaux de la conférence internationale sur les méthodes non destructives pour l'étude et le contrôle des matériaux (Proceedings of the International Conference on Nondestructive Methods for Materials Study and Control), 1st, Brussels, 1955: 312.
4. Rankin, A. C. "Application of Ultrasonic Flaw Detection in the Steel Industry." Publ. No. IND611. London: Kelvin and Hughes (Industrial) Ltd. 1955.
5. Wilson, R. "Recent Developments in the Ultrasonic Inspection of Thin Metallic Sheet or Plate," *Sheet Metal Inds.*, 30, No. 310 (1953): 146.
6. Rankin, A. C. "Practical Butt Weld Inspection." *Welding* (London), 18 (1950): 243.
7. Brown, T. G., A. C. Rankin, and R. W. G. Haslett. "Automatic Scanning and Recording." U.K. Patent Application No. 5146/55 (Provisional).

SECTION 50

ULTRASONIC RESONANCE TESTS

CONTENTS

PAGE

Characteristics of Method

- Principle of test ... 1
    - Conditions of ultrasonic resonance in a metal plate (*f.* 1) ... 2
  - Fundamental resonant frequency ... 1
  - Plate thickness ... 1
    - Fundamental resonant frequencies of typical materials (*f.* 2) ... 4
  - Harmonic frequency interval ... 3
- Test development ... 3
- Thickness measurements ... 4
  - Materials ... 4
  - Thickness range ... 5
  - Accuracy ... 5
  - Shape of part ... 5
  - Coupling ... 5
  - Temperature ... 5
  - Detection of discontinuities ... 5

Test Equipment

- Equipment components ... 6
  - Basic circuit ... 6
    - Basic circuit for a thickness gage operating on the ultrasonic-resonance principle (*f.* 3) ... 6
    - Resonance indications in a 0.125-in. thick aluminum plate (*f.* 4) ... 7
  - Frequency characteristics ... 7
  - Transducer characteristics ... 7
    - Relative sensitivity of a 9.0-Mc. transducer, as a function of frequency (*f.* 5) ... 8
- Types of instrumentation ... 8
  - Capacitance-modulated cathode-ray tube indication ... 8
  - Inductance-modulated cathode-ray tube indication ... 8
    - Schematic block diagram of inductance-modulated ultrasonic resonance instrument with cathode-ray tube presentation (*f.* 6) ... 9
  - Stroboscopic presentation ... 10
  - Meter and headphone indicators ... 10
  - Automatic indicators and recorders ... 10

Operating Techniques

- Selection of frequency ... 11
- Instrument calibration with frequency scales ... 11
- Calibration of instruments with direct-reading thickness scales ... 11

PAGE

- Recorders ... 12
- Constants ... 12
- Operation at harmonic frequencies ... 12
    - Relationships between frequency, thickness, and harmonic numbers for aluminum (*f.* 7) ... 13
  - Instruments with frequency scales ... 14
  - Instruments with thickness scales, fundamental frequency only ... 14
  - Instruments with thickness scales for harmonics ... 14
    - Transparent thickness scale for harmonics, used over face of cathode-ray oscilloscope of ultrasonic resonance instrument (*f.* 8) ... 15
- Coupling media ... 14
- Transducers and mountings ... 14
  - Frequency ... 15
  - Material ... 15
  - Shape ... 16
  - Area ... 16
  - Mountings ... 16
    - Ultrasonic transducer construction for resonance and contact testing (*f.* 9) ... 17
  - Thickness ... 16
- Surface preparation ... 16
- Shape of part ... 18
- Spurious thickness resonances ... 18
- Accuracy ... 18

Typical Applications

- Industrial thickness gaging ... 19
- Hollow parts ... 19
  - Extrusions ... 19
    - Ultrasonic-resonance thickness gaging of walls of hollow propeller blades (*f.* 10) ... 20
  - Drawn tubes ... 19
  - Tube bends ... 19
  - Bored shafts ... 20
  - Castings ... 20
  - Miscellaneous machining operations ... 20
- Sheet and plate ... 20
  - Flat sheet ... 20
  - Stretch-formed, spun, and forged parts ... 21
  - Skin-milled plate ... 21
  - Chemically milled sheet ... 21
  - Plating ... 21
- Detection of discontinuities ... 21
    - Typical discontinuities detected by ultrasonic resonance testing (*f.* 11) ... 22
  - Discontinuities in homogeneous structures ... 22

CONTENTS (*Continued*)

PAGE

- Laminar discontinuities detected by ultrasonic resonance testing (*f.* 12) 23
- Lack of bond in cladding 22
- Weldments 23
- Damping materials 23

Detection of structural differences 23
- Velocity measurements 24
- Attenuation measurements 24
  - Relative transmission of ultrasonic energy through gray and nodular iron, as a function of frequency (*f.* 13) 24
  - Ultrasonic-resonance response characteristics and corresponding microstructures of gray and nodular iron; at 5 to 10 Mc. (*f.* 14) 25

Maintenance Inspection

Primary uses 25
Thickness gaging 25
- Selection of test points 26

Safety inspection 26
- Boiler tubes 26
- Heat-exchanger tubes 26
- Gas cylinders 27
- Storage tanks 27
- Ship structures 27
- Pulp digesters 27
- Aircraft propellers 27

Corrosion-rate determination 27
Detection of laminar flaws 28
- Hydrogen blistering 28
- Hot taps in pipelines 28
- Rail testing 28
  - Ultrasonic inspection of rail ends (*f.* 15).. 29

Tests of Corrosion Wall Thinning

Corrosion losses 29
Development of nondestructive tests 29
Advantages of ultrasonic tests 30
Limitations of ultrasonic tests 30

PAGE

Test equipment 31
- Resonance-type instruments 31
- Manually operated instruments with headphone or meter indication 31
  - Resonance frequencies obtained with various surface conditions (*f.* 16) 32
- Effect of corrosion product accumulations .. 32
  - Effect of back-up materials on ultrasonic waves (*f.* 17) 33
- Slide-rule thickness calculations 33
  - Slide rule for converting measured frequencies to thickness indications (*f.* 18) 34
- Cathode-ray-tube resonance instruments .. 34
- Pulse equipment with cathode-ray tube indication 35

Corrosion Test Techniques and Procedures

Gasoline plants and refineries 35
Storage tanks 35
- Test procedures 36
- Personnel positioning 36
- Selection of frequency ranges 36

Pipelines 36
Boiler tubes 37
Oil-tank ships and other marine applications 37
  - Cathode-ray-tube ultrasonic instrument used in tanker survey (*f.* 19) 38
- Corrosion control areas 37
- Test procedures 38
  - Characteristics of ultrasonic thickness measurements (*f.* 20) 39

Pulp digesters 39
- Relocation of test points 41

Test records 41
  - Bulkhead thickness measurement (*f.* 21) 40

Evaluation of data 42
  - Corrosion rate on Type T-2 tanker (*f.* 22) 41

Guide to proper application of corrosion tests 42
References 42

ULTRASONIC RESONANCE TESTS

Characteristics of Method

PRINCIPLE OF TEST. The ultrasonic resonance method utilizes continuous, compressional, ultrasonic waves transmitted into plate material from one surface. The frequency (and therefore the wavelength) of these waves is varied manually or automatically until a wave is twice reflected and leaves the first material surface in phase with another incoming wave. Standing waves are then set up within the plate, causing it to resonate or vibrate at a larger amplitude. If the thickness is one-half of the wavelength, the plate will resonate. Resonance is indicated by its loading effect upon an ultrasonic transducer intimately coupled with the test specimen. (See sections on Ultrasonic Test Principles and Ultrasonic Transducers for descriptions of transducers.)

Fig. 1(a) shows the lowest frequency, or fundamental frequency, of resonance for the plate. Similar conditions occur at multiples or harmonics of this fundamental frequency. Figs. 1(b), 1(c), and 1(d) show the second, third, and fourth harmonic frequencies, corresponding to two, three, and four times the fundamental frequency. In each case a **standing wave** is set up and the plate resonates.

Fundamental Resonant Frequency. The fundamental resonant frequency in the thickness direction of a plate is

$$F = \frac{V}{\lambda} = \frac{V}{2T} = \frac{K}{T} \qquad (1)$$

where F = fundamental frequency, Mc.
V = sound velocity, million in./sec.
T = thickness, in.
K = constant, million in./sec.
λ = wavelength of sound, in.

Since sound velocities in most solids range between 90,000 and 350,000 in. per sec., it is convenient to express frequency in megacycles per second (Mc.) and the constants in millions of inches per second. (See section on Ultrasonic Test Principles for velocities of sound in various materials.)

Plate Thickness. The thickness T of a plate can therefore be measured from one side by determining the fundamental resonant frequencies F from

$$T = \frac{K}{F} \qquad (2)$$

Since frequency and thickness are inversely proportional, an increase in thickness produces a decrease in fundamental frequency. The relationship between funda-

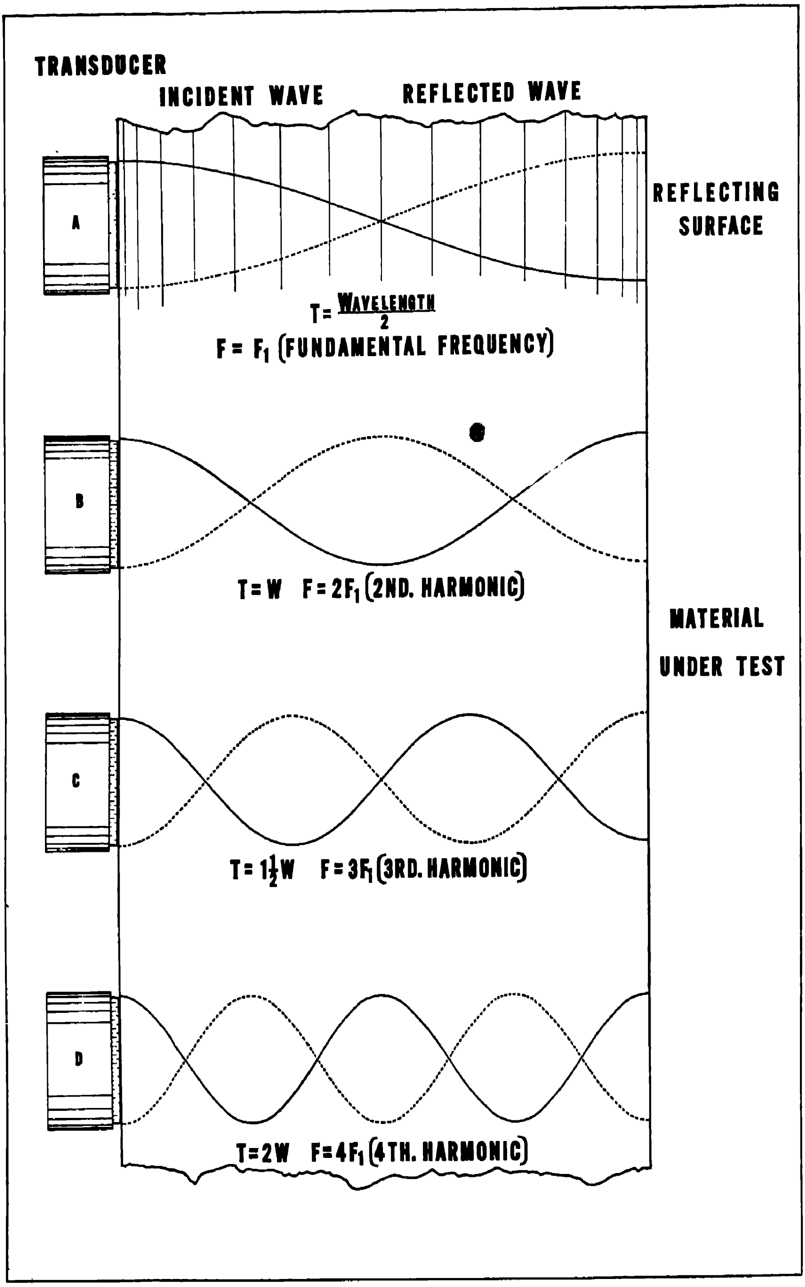
TRANSDUCER
INCIDENT WAVE
REFLECTED WAVE
REFLECTING SURFACE
A
T= WAVELENGTH/2
F = F1 (FUNDAMENTAL FREQUENCY)
B
T=W F=2F1 (2ND. HARMONIC)
MATERIAL UNDER TEST
C
T= 1½W F=3F1 (3RD. HARMONIC)
D
T=2W F=4F1 (4TH. HARMONIC)

Fig. 1. Conditions of ultrasonic resonance in a metal plate.

mental frequency and thickness for typical materials is shown in Fig. 2. Constants K for various materials are:

Material	Constant K, million in./sec.
Aluminum	0.121–0.131
Aluminum oxide	0.188–0.193
Brass	0.086–0.092
Copper	0.092–0.093
Cast iron	0.087–0.110
Cast steel	0.110–0.116
Glass	0.115–0.134
Lead	0.047–0.049
Magnesium	0.114–0.116
Monel	0.106–0.108
Nickel	0.113–0.115
Petroleum	0.026 (approx.)
Polyethylene	0.036
Phenolic laminate (paper base)	0.052
Quartz	0.114
Stainless steel	0.112–0.114
Steel	0.115–0.118
Teflon	0.0245–0.0335
Titanium	0.121–0.126
Uranium	0.066–0.070
Water, fresh	0.028 (approx.)
Water, sea	0.030 (approx.)
Zirconium	0.093–0.102

Harmonic Frequency Interval. The frequency interval between any two adjoining harmonic frequencies equals the fundamental frequency. The difference between any two adjoining resonant frequencies can therefore be substituted for F in Eq. 2, and the thickness can then be computed from harmonic frequencies as

$$T = \frac{K}{3F - 2F} = \frac{K}{nF - (n-1)F} \tag{3}$$

where nF and $(n-1)F$ are any two adjoining harmonics.

It is not necessary to know the harmonic number n in order to measure the thickness.

TEST DEVELOPMENT. The measurement of resonant frequency was used in interferometers for measuring the sound velocity of liquids and gases.[1] The need for accurate methods of measuring thickness of large or complex structures from one side became acute during World War II. Practical equipment using relatively simple basic circuits was designed at the General Motors Research Laboratory in Detroit, Michigan.[2, 3, 4] Limited numbers of instruments were built by General Motors during World War II under the trademark "Sonigage." These were used primarily for testing hollow steel propeller blades. The design of portable, battery-operated equipment led to the acceptance of the method for field corrosion surveys and for the detection of discontinuities in rails.[5] Continuous development work by several manufacturers has resulted in a broad range of instruments for **thickness testing** from one side and for the **detection of laminar discontinuities** or lack of bond.

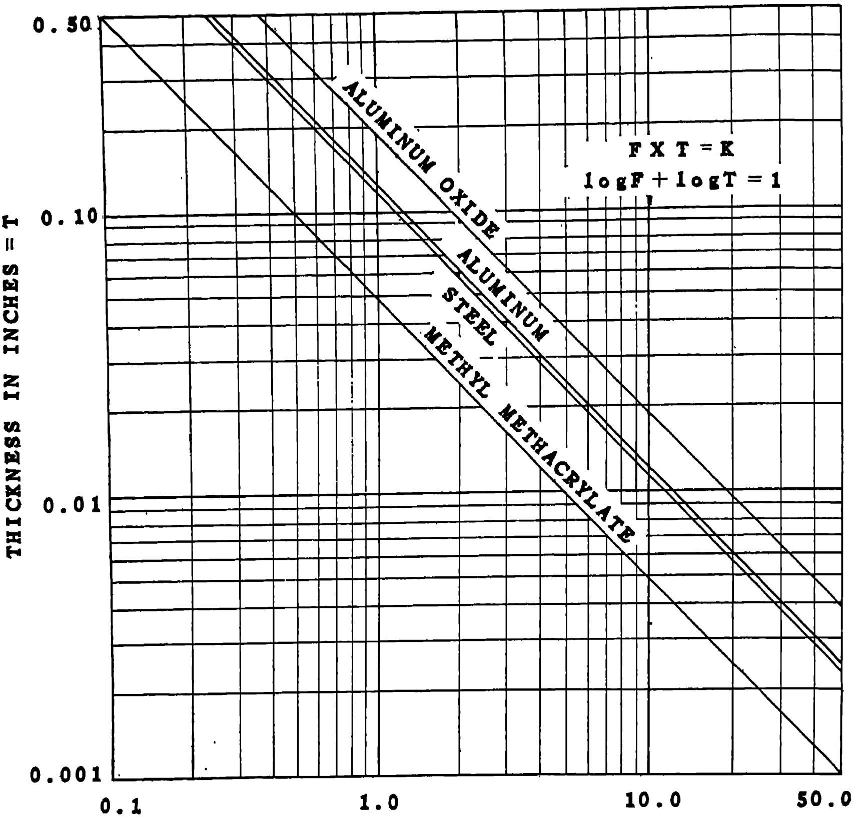

Branson Instruments, Inc.

Fig. 2. Fundamental resonant frequencies of typical materials.

THICKNESS MEASUREMENTS. Ultrasonic resonance tests are used extensively for thickness measurements on parts where access to both sides for conventional gaging is difficult or impossible. The **applications** fall into three broad classifications:

1. Gaging during manufacture.
2. Corrosion inspection.
3. Detection of discontinuities.

Typical parts gaged with ultrasonic resonance equipment include extruded, drawn, or bored tubes; hollow castings; rolled, stretch-formed, or milled sheet and plate; hollow forgings; and parts machined by grinding, turning, spinning, and milling. The use of resonance gaging in lieu of drilling of pressure vessels, piping, boiler tubes, ship hulls, and bulkheads is accepted by marine and insurance underwriters.

Materials. Most metals, glass, ceramics, rigid plastics, and similar materials can be tested with ultrasonic resonance equipment, using frequencies of the order of 250 kc. to 25 Mc. Some cast metals with relatively large grain size may be difficult to test. Wood, concrete, soft rubber, and similar materials require the use of low ultrasonic frequencies of the order of 20 to 200 kc.

Thickness Range. The maximum frequency which can be used for the test will determine the minimum thickness, as indicated by Eq. 2. At 25 Mc., ultrasonic resonance equipment will measure to 0.005 in. of steel and aluminum and to 0.004 in. of copper or brass. Some materials do not transmit sound waves at high ultrasonic frequencies, so that their minimum measurable thickness is higher. The maximum thickness which can be measured depends on the frequency used and the design of the test instrument. It normally ranges from 3 to 12 in.

Accuracy. The accuracy of ultrasonic resonance measurements is not appreciably affected by common variables such as ambient temperature, shape of part, magnetic properties, small differences in alloy or heat treatment, deposits on the reflecting surface, or proximity to an edge or fillet. Accuracy is limited by the resolution of the instrument, slight variations in the value of K, variations in contact between transducer and part, and calibration of the instrument. Ultrasonic resonance thickness measurements are normally within 0.1 to 3.0 percent of actual thickness.

Shape of Part. Sharp and strong resonance indications are obtained when the transmitting and reflecting surfaces are parallel. **Tapers** of 1 to 2 deg. can be tolerated, but they reduce signal amplitude. No resonance indications will be obtained on severely tapered sections or on corroded sections where thickness variation exceeds about one-half wavelength. Concentric-wall cylindrically and spherically **curved sections** can be tested, and measurements have been obtained on tubing down to 3⁄16-in. outside diameter.

Coupling. Compressional waves are transmitted from the transducer through a thin coupling layer into the test material. While the transducer and part can be immersed, the transducer must always be relatively close to the surface of the test object. It is not practical to couple the energy through a long liquid column, since the instruments would detect and indicate resonant frequencies for the liquid column.

Temperature. High temperature limitations are imposed by the transducer mountings. Conventional transducer mountings are limited to maximum temperatures of 200° F. to 500° F., depending upon the materials used for the adhesive and support. Special mountings have been designed for operation up to 700° F.

Detection of Discontinuities. Discontinuities are generally detectible if their cross-sectional area, projected to the test surface, is at least one-quarter to one-half of the transducer area. Discontinuities can be detected regardless of their location in the part. The test is limited to parts with relatively favorable geometry. Either the total thickness or the section down to the discontinuities must be capable of producing a strong resonance signal in the instrument. If the discontinuity is close to the transmitting surface, but the distance is within the thickness range of the instrument, it will appear as a thickness change. If the distance to the discontinuity is less than the minimum thickness, it will be indicated by a disappearance of the resonance signals. Discontinuities close to the reflecting surface will be indicated by a change in thickness indications. There are therefore no **blind areas** close to either surface. A tightly shut lamination will partially transmit and partially reflect the ultrasonic energy. As frequency is increased and wavelength decreased, more energy is reflected and less is transmitted. The **sensitivity of the test** will therefore be increased as the test frequency is raised. Discontinuities will be indicated on the instrument as a change in thickness or by the appearance or disappearance of the resonance indications.

Test Equipment

EQUIPMENT COMPONENTS. The test equipment consists of the following three major components:

1. Power supply and oscillator, to convert direct current or 50- or 60-c.p.s. a.-c. line inputs to continuous high-frequency electric energy.
2. Detection, amplification, and indicating circuits.
3. A transducer, to convert high-frequency **electric** energy to high-frequency **mechanical** energy.

Basic Circuit. The simplest form of resonance-test instrument is shown in Fig. 3. The **self-excited oscillator** circuit has provisions for changing the frequency by adjusting a variable capacitor or a variable inductor. The transducer is connected to the plate or anode of the oscillator tube. If the oscillator is tuned to a resonant frequency of the metal, it will vibrate at a larger amplitude. This increases the loading of the transducer and produces an increase in plate current which can be indicated on a meter.

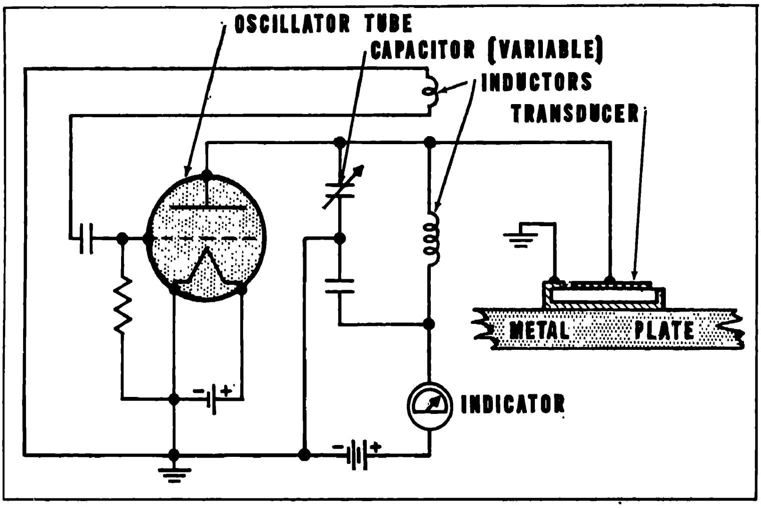

Branson Instruments, Inc.

Fig. 3. Basic circuit for a thickness gage operating on the ultrasonic resonance principle.

The variation of plate current with frequency can be obtained with simple equipment of this type. The fundamental frequency for a 0.125-in. aluminum plate, as given by Fig. 4, is 1.0 Mc. The plate resonates at 1 Mc. and at multiples of 1 Mc., such as 2, 3, 4, 5 Mc. The plate current increases at these frequencies.

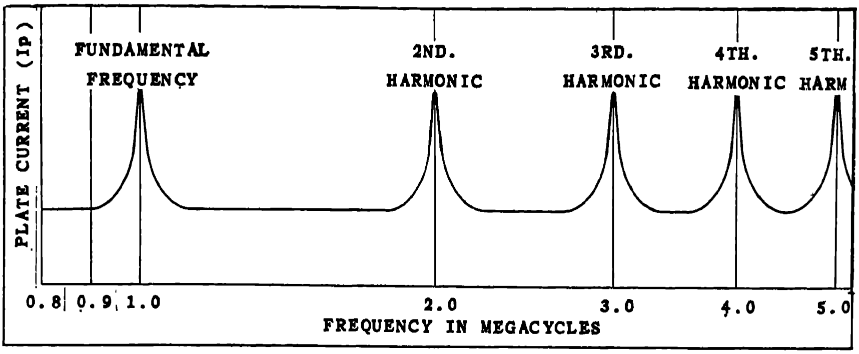

Fig. 4. Resonance indications in a 0.125-in. thick aluminum plate.

Frequency Characteristics. Commercial instruments usually contain one or more stages of amplification of the plate current. Maximum frequency on a single range is usually two or three times the minimum frequency. Some instruments contain provisions for using several overlapping frequency ranges by changing transducers, some oscillator components, and the indicating scale. Sensitivity is usually highest at the high-frequency end of each range. It decreases gradually as the frequency is lowered.

The **resonant frequency** of the oscillator is determined by the capacitance and inductance of the oscillator, frequency-modulating circuits, coaxial cable, and transducer according to

$$F = \frac{1}{2\pi\sqrt{LC}} \tag{4}$$

where F = frequency, c.p.s.
L = inductance, henries.
C = capacitance, farads.

At high frequencies, above 5 Mc., the coaxial cable will normally have to be very short to reduce its capacitance. Frequencies above 10 Mc. can be obtained only by keeping the capacitance of the oscillator and modulating circuit very low.

A wide choice of presentations can be used to indicate resonant frequencies. Commercial equipment is available with cathode-ray tube presentations, headphones, loudspeakers, panel meters, stroboscopic presentations, visual alarms, and recorders.

Transducer Characteristics. Piezoelectric transducers such as **X-cut quartz** or **polarized ceramics** are generally used for ultrasonic resonance testing. Wide varieties of transducer types and mountings have been designed to meet the requirements of specific test applications. The **resonant frequency** of the transducer is normally 10 to 20 percent higher than the maximum frequency of the tuning range. For example, a 9-Mc. transducer is normally used with a 4- to 8-Mc. tuning range. The transducer is most sensitive at its natural frequency. This **sensitivity** decreases as the frequency decreases, as shown by Fig. 5. If the resonant frequency of the transducer is within the tuning range, a strong resonance indication for this frequency will be seen on the indicating instrument. This transducer resonance indication will confuse the indications of resonance in the material being tested.

In addition to the strong fundamental resonance determined by the thickness of the transducer, complex vibrational modes will cause the transducer to have weak resonances at lower frequencies. These transducer resonances produce **false indications** on the instrument at high gain settings. Damping one surface of the transducer by cementing it to a plastic support reduces this effect. Further **damping of the transducer resonance** occurs when the transducer contacts the part to be tested. Transducer resonances can be observed by electrically grounding the transducer, without placing it in contact with the work, and by increasing the gain of the instrument.

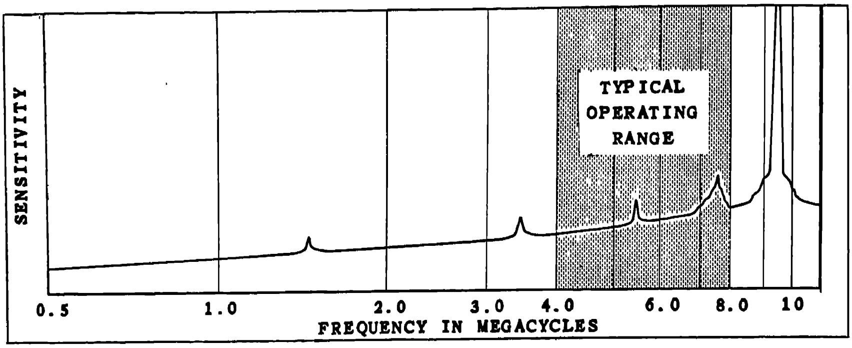

Fig. 5. Relative sensitivity of a 9.0-Mc. transducer, as a function of frequency.

TYPES OF INSTRUMENTATION. Various forms of instruments which use the ultrasonic method for thickness gaging and flaw detection are commercially available. These instruments differ primarily in the method and width of frequency modulation and in the type of presentation.

Capacitance-modulated Cathode-Ray Tube Indication. In some instruments the oscillator circuit contains a motor-driven capacitor whose rotor is connected into the circuit through brushes or wipers. The rotation of the capacitor is synchronized with the horizontal sweep of the trace across the cathode-ray tube. Each cycle of capacitance change of the motor-driven capacitor produces a corresponding frequency change. The horizontal axis of the cathode-ray tube therefore represents a frequency range. If this frequency range contains resonant frequencies, the trace line will be deflected vertically. **Calibrated, transparent plastic scales,** placed in front of the cathode-ray tube, enable the operator to read deflection lines directly in terms of thickness.

The instruments normally operate between 0.25 and 10 Mc. on four or five bands. The total **thickness range** of a series of direct-reading scales is approximately 0.010 to 0.500 in. of steel. Thicker sections can be measured by calculating from harmonics; for example,

$$T = \frac{T_n \times T_{n-1}}{T_n - T_{n-1}} \qquad (5)$$

where T_n and T_{n-1} are two adjoining readings on the thickness scale. A two-to-one frequency and thickness range is normally covered on a single scale. Typical direct-reading thickness ranges are 0.025 to 0.050 in. and 0.040 to 0.080 in.

Inductance-modulated Cathode-Ray Tube Indication. An electrically variable inductor can be used instead of the motor-driven capacitor as part of the oscillator circuit. The control current on the variable inductor can be adjusted to change the tuning range. Narrow tuning ranges such as 1.1 to 1 are used for high accuracy over a limited thickness range. Wide tuning ranges and the use of scales calibrated for multiple harmonic lines make it possible to cover a very wide thickness range on a single thickness scale. A typical narrow-scale range is 0.41 to 0.45 in.; typical wide-scale ranges are 0.010 to 0.070 in. and 0.400 to 0.925 in.

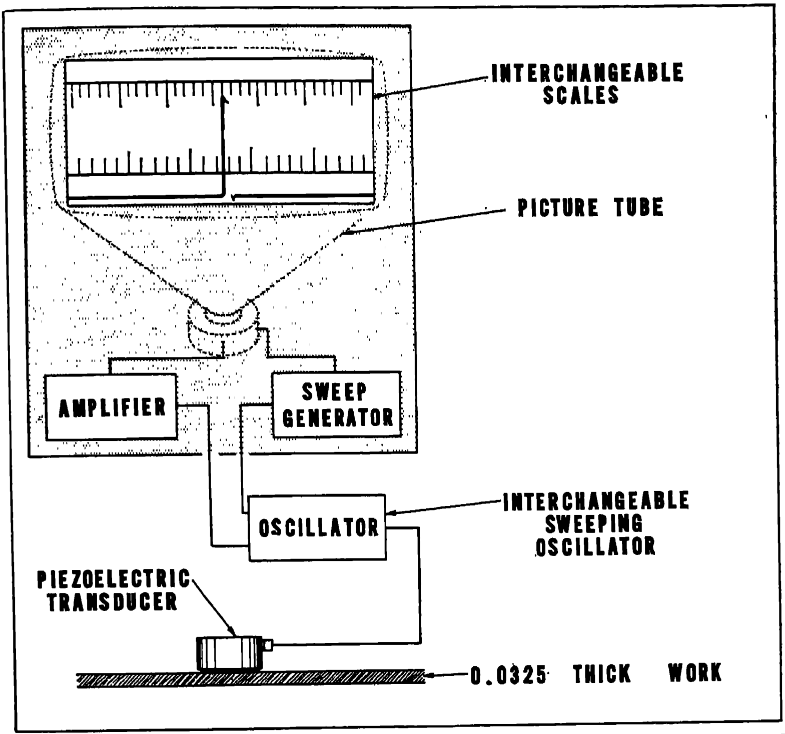

Branson Instruments, Inc.

Fig. 6. Schematic block diagram of inductance-modulated ultrasonic resonance instrument with cathode-ray tube presentation.

Inductance-modulated instruments have relatively low oscillator capacitance. They can therefore be operated at frequencies up to 30 Mc. per sec., corresponding to a minimum measurable thickness of 0.004 in. of steel or aluminum. The use of harmonic scales makes it possible to read thickness directly up to 3.0 in. Fig. 6 shows a schematic diagram of a typical cathode-ray-tube instrument with inductance modulation. Coaxial cable length from the transducer to the oscillator is usually limited, ranging from 2 ft. at high frequencies to 25 ft. at low frequencies. If the oscillator is removed from the test instrument, long extension cables can be inserted between these components. The circuit of the test instrument is similar to that of a television set and contains sweep generators, amplifiers, and similar circuitry.

Stroboscopic Presentation. One type of equipment utilizes a capacitance-modulated, motor-driven, sweep oscillator arrangement in conjunction with a modified slide rule of the harmonic-matching type. A small neon lamp is made to flash at the instant that the sweep capacitor sweeps the oscillator through the fundamental frequency or any harmonic frequency. This neon lamp is affixed to a disk which rotates with the sweep capacitor, and it is viewed through an arc-shaped window over which the special **slide rule** is mounted. Due to the stroboscopic effect of the rotating disk, a steady **light pattern** results which is characteristic of the thickness of the material being measured. The slide rule is then rotated until the marks on its harmonic scale match up with the light pattern. Then an index on the rule will indicate the thickness of the material. The sweep motor and circuitry are battery-operated, thus producing an easily readable portable instrument for thickness measurement.

Meter and Headphone Indicators. Battery-operated instruments, designed primarily for field work, usually use meters or headphones as the indicator instead of a cathode-ray tube. Typical battery-operated instruments are available with wide or narrow modulation ranges.

The **narrow-modulation type of instrument** is manually tuned and frequency-modulated over a very narrow range, such as 0.5 to 2.0 percent of the base frequency. If this modulation range contains a resonant frequency for the metal, an **audible tone** is produced in a headset or loudspeaker. Resonance is simultaneously indicated by increased deflection of a panel meter. The instrument scale is calibrated in frequencies, such as 1 to 3 Mc. If only one resonance signal is obtained, it is converted to thickness by the use of Eq. 2. If several resonance indications are obtained, two adjoining indications can be converted to thickness by using Eq. 3. A frequency range of 1 to 3 Mc. corresponds to a thickness range of 0.040 to 6.0 in. of steel. Frequency-thickness conversion is made on a **circular slide rule** attached to the instrument or on a **conversion table.**

Discontinuities in thick plates are detected instantaneously with a battery-operated instrument using **wide modulation.** An 8-in. thick steel plate, for example, will have a fundamental frequency of 0.0145 Mc. If the modulation width is 0.1 Mc., each sweep will produce seven resonance signals. Modulating at 100 sweeps per second will produce an audible 700-c.p.s. signal in a headset. A decrease in thickness, due to a **laminar discontinuity,** will produce a proportional decrease in the frequency or the pitch of the audible signal.

Automatic Indicators and Recorders. Gating circuits can be added to cathode-ray-tube instruments to determine whether there is a resonance signal within pre-set limits. The location and width of the gate can be adjusted to coincide with the allowable thickness range of the material. **Gating limits** are marked on the screen by brightening the base line or by small vertical edge lines. A strong signal within these limits will trip a relay, which in turn actuates audible alarms, marking devices, or automatic sorting attachments. **Multiple gating circuits** can be used, since they do not interfere with each other. This makes it possible to sort material into a number of groups according to thickness.

Several **methods of recording resonant frequencies** and thickness are theoretically possible. These include (1) recording the distance from the beginning of the sweep to the first resonance signal, (2) **panoramic recording** of all resonant frequencies, and (3) recording the distance from one edge of a gate to the resonant frequency. A gating circuit designed for recording produces an output voltage proportional to the distance of the resonance signal from one edge of the gate.

Since this voltage is a function of thickness, it can be used to actuate a recording pen which produces a record of thickness on a **potentiometer-type recorder.** Very small thickness changes can be detected by a recording system of this type. The recording paper is calibrated by recording the frequency from tuned circuits.

Operating Techniques

SELECTION OF FREQUENCY. Frequency and wavelength are inversely proportional, as indicated by Eq. 1. In aluminum, for example, the wavelength at 25 Mc. will be 0.010 in.; at 0.5 Mc., it will be 0.5 in. Long waves penetrate through relatively coarse materials, whereas short waves are reflected more easily by small discontinuities. Short waves are transmitted into the part in a straight beam, with a relatively small angle of divergence from the axis of the beam. This angle of divergence, θ, is also a function of the radius r of the transducer, since

$$\sin\theta = \frac{0.61\lambda}{r} \tag{6}$$

Many tests can be performed satisfactorily at high or low ultrasonic frequencies. However, optimum results can be attained by selecting the best frequency range. **Recommended ranges** for various applications are given in the table here.

Application	Low, 0.5–3 Mc.	Intermediate, 3–10 Mc.	High, 10–25 Mc.
Gaging thick materials	X		
Gaging thin materials	..	X	X
Maximum thickness range on one scale	X		
Maximum accuracy	..	..	X
Gaging of small-diameter tubes	..	X	X
Gaging of tapered or corroded materials	X		
Gaging of coarse structures	X		
Detection of gross discontinuities	X	X	X
Detection of tight laminations and small discontinuities	..	..	X
Detection of liquid level or bonding to a damping material	X		

INSTRUMENT CALIBRATION WITH FREQUENCY SCALES. The calibration of the frequency scale is checked with a **frequency standard, tuned circuit,** or **thickness standard** which resonates at known frequencies within the tuning range. Resonant frequencies obtained on unknown specimens are converted to thickness by using Eq. 2 or Eq. 3 and the constants K listed previously. If the instrument readings are consistently high or low, or if a constant is not available, a set of frequency readings should be obtained on a section of known thickness. The constant will then be obtained by multiplying the fundamental frequency or frequency interval (in megacycles) by the thickness (in inches).

CALIBRATION OF INSTRUMENTS WITH DIRECT-READING THICKNESS SCALES. Resonance instruments with direct-reading thickness scales are analogous to comparator-type thickness gages and will give accurate results only after they have been calibrated with test blocks of known thickness and alloy. Two or more **test blocks,** within the range of the scale, can be used to check the calibration. The length and the width of the test block should be at least twice, and preferably five times, the thickness. In the case of thick test blocks, it is desirable to cut slots or notches into the edges to avoid wave interference from side reflections. Polishing of the surfaces is unnecessary; a finish of the order of 50 to 250 μin. r.m.s. is satisfactory. Gage blocks with a slight taper are suitable for checking the calibration of the scale over its entire length. If very high accuracy is desired, the calibration on test blocks should be followed by a final adjustment on a section of the part to be tested. This compensates for slight errors caused by differences in geometry, alloy, surface finish, and temperature.

A convenient and accurate method of calibration involves the use of **tuned circuits** which produce sharp resonance lines on the scale. A section of the part to be tested is used as a primary calibration standard, and the instrument is aligned accurately on this section. Two or more tuned circuits are then loosely coupled to the oscillator, and the position of the resulting resonance line is marked on the scale with arrows. Subsequent calibration checks will then require only the insertion of the tuned circuit and the adjustment of the controls until the resonance lines correspond to the arrows.

Two **matched transducers** and coaxial cables can be connected to the test instrument through a switch. One transducer, placed over a calibration block, produces resonance lines at specific locations. The other transducer measures the unknown thickness.

RECORDERS. Recording paper can be calibrated by switching periodically from the test part to tuned circuits. The signal from one tuned circuit will produce a straight line on the recording paper, representing a frequency or thickness. Two tuned circuits may be recorded to correspond, for example, to the high and low **acceptance limits** for the parts. Lines produced by the tuned circuits are connected by straight lines. These lines establish the high and low limits for the part.

CONSTANTS. The resonant frequency for a known thickness can be calculated by using Eq. 1 and K constants listed previously. Actual resonant frequencies measured with the instrument will deviate somewhat from the theoretical values.[6] Factors which appear to influence this **deviation** include:

1. Material under test.
2. Shape of part.
3. Surface finish of part.
4. Couplant.
5. Type of transducer facing.
6. Ratio of transducer frequency to test frequency.
7. Operating frequency.

Resonant frequencies close to theoretical values are generally obtained by using loose coupling, by operating at high frequencies and high harmonics, and by working close to the transducer resonant frequency. The effect of deviations is further minimized by using properly calibrated scales and the same operating conditions for instrument calibration and measurement of the unknown thickness.

OPERATION AT HARMONIC FREQUENCIES. Operation at harmonic frequencies extends the thickness range of the instruments considerably. It frequently results in higher accuracy than operation at the fundamental frequency. The spacing between harmonics should correspond closely to calculated values. It can be used to check the accuracy of the test and to distinguish thick-

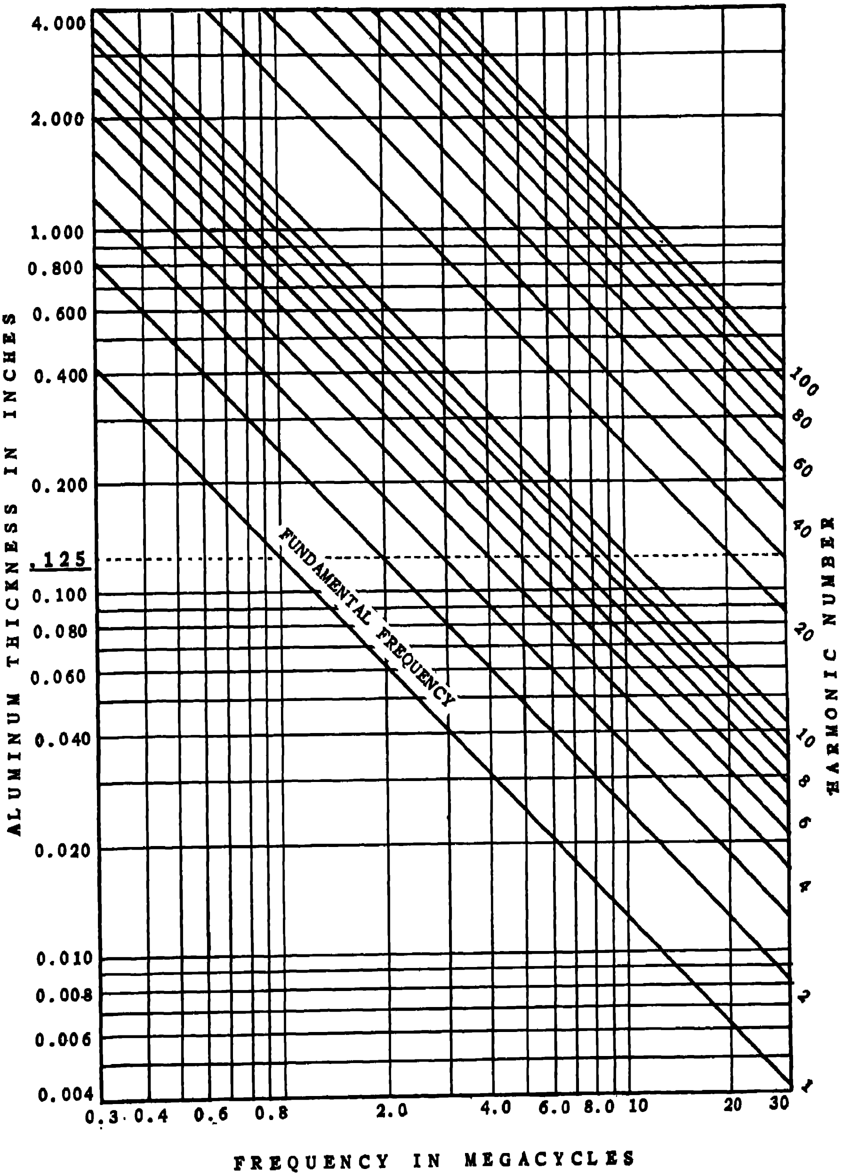

Branson Instruments, Inc.

Fig. 7. Relationships between frequency, thickness, and harmonic numbers for aluminum.

ness-resonance indications from spurious signals. Detailed instructions for interpretation of harmonic indications are furnished by instrument manufacturers.

The relationships between **frequency, thickness, and harmonic number for aluminum** are shown in Fig. 7. The horizontal lines, representing thickness, cross the diagonal lines at the resonant frequencies. A 0.125-in. aluminum plate will resonate at approximately 1.0, 2.0, 3.0 Mc., etc.

Instruments with Frequency Scales. The standard operating technique is based on the use of harmonics. Very high harmonics can be used by averaging the frequency intervals between a large number of these harmonics. On low harmonics the accuracy of the measurement can be increased by determining the harmonic number.[7] Conversion from frequency to thickness and determination of harmonic number are facilitated by using special circular slide rules.

Instruments with Thickness Scales, Fundamental Frequency Only. Thickness measurements can be computed from harmonic frequencies by using Eq. 5. More accurate results are obtained by determining the harmonic number and by dividing the apparent thickness by the harmonic number. Special **slide rule calculators** with scales calibrated for fundamental frequencies have been developed to aid the operator when using harmonics. Thus a slide rule can be used for determining the fundamental thickness by matching harmonic thicknesses obtained from a cathode-ray-tube instrument with the orders of harmonics imprinted on the inner dial of the slide rule. (See Fig. 18.)

Thickness can also be measured with harmonics by using a **tapered test block** and switch. One transducer is applied to the unknown thickness; the other is applied to a tapered block. Two sets of harmonic lines are produced on the face of the cathode-ray tube. The transducer is moved along the tapered block until the two sets of readings coincide. The thickness is then read from the tapered block.

Instruments with Thickness Scales for Harmonics. Fig. 8 shows a typical **harmonic scale,** covering a range of 0.090 to 0.180 in. and utilizing the second, third, and fourth harmonics. The left resonance line is read as 0.100 or 0.133 in. The right resonance line is read as 0.100 or 0.148 in. The correct thickness is 0.100 in., since it lines up on both scale lines. The left resonance indication is the third harmonic; the right indication is the second harmonic.

COUPLING MEDIA. Various oils, greases, or other liquids can be used as coupling fluids for excluding the air between transducer and the test object and for transmitting the ultrasonic waves. Coupling fluids affect the sensitivity and accuracy of the instrument considerably, and the selection of the most suitable fluid frequently makes it easier to obtain reliable readings. When **maximum sensitivity** is required, a coupling medium whose acoustic impedance, ρV, is comparable to that of the material under test would be most satisfactory. However, few coupling liquids approximate this ideal. On new materials with relatively **smooth surfaces,** it is best to use light coupling of very light oils or water. When thickness resonances are difficult to obtain (due to surface contours, **surface roughness,** or tapered or rough reflecting surfaces), glycerine with a wetting agent is generally most satisfactory. Accuracy is increased by keeping uniform the transducer pressure or the thickness of the coupling fluid.

TRANSDUCERS AND MOUNTINGS. The performance of the equipment can frequently be substantially improved by selecting a transducer of the proper frequency, type, and mounting.

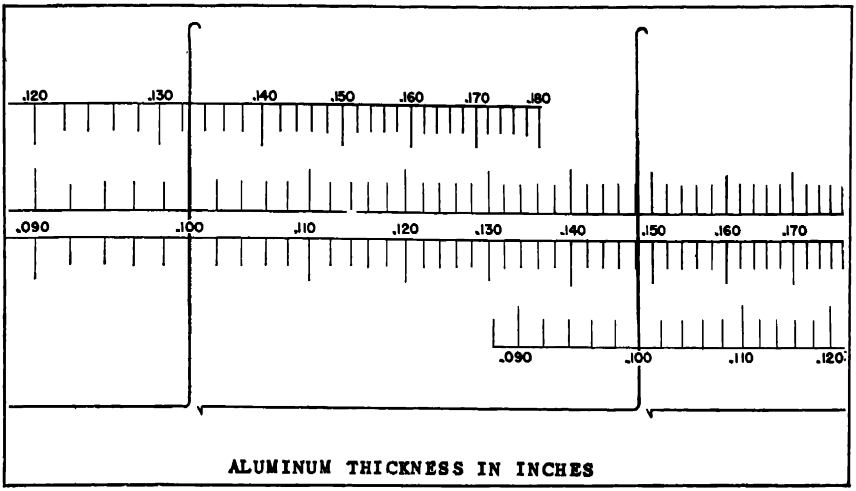

Branson Instruments, Inc.

Fig. 8. Transparent thickness scale for harmonics, used over face of cathode-ray oscilloscope of ultrasonic resonance instrument.

Frequency. The frequency of the transducer is normally 10 to 20 percent higher than the maximum frequency of the tuning range. Transducers which fall within the tuning range can be used when the oscillator is operated over a very narrow frequency range. Transducers can also be operated at odd multiples of their fundamental frequencies. **Sandwich-type transducers** with low fundamental frequencies can usually be operated at high frequencies, i.e., within limited frequency bands.

Material. X-cut **quartz discs** are used most frequently as the transducer material. The oscillators of test instruments are usually designed for quartz. The activity of quartz is not appreciably affected by temperature variations; it can be operated up to approximately 1000° F. Since quartz is relatively dense and strong, it can be lapped very thin. This makes it possible to design quartz transducers for use at frequencies of 25 Mc. or higher. Quartz transducers can be used without wear plates because of their abrasion resistance.

Polarized **barium-titanate** ceramic has been used instead of quartz, especially on applications requiring high sensitivity. The piezoelectric constant of barium titanate is 82 times that of quartz; for the same applied voltage, the motion of the face will therefore be 82 times greater. The dielectric constant of barium titanate is 200 to 350 times greater than quartz. The electrical capacitance of the barium-titanate transducer is therefore much higher. This makes it necessary to modify the oscillator circuit or to design special barium-titanate transducers for use with oscillators intended for quartz. Barium titanate is generally limited to operation below 200° F. The use of wear plates is recommended so that excessive abrasion of the barium titanate will be avoided. Barium-titanate transducers are generally limited to frequencies below 10 Mc.

While various **other piezoelectric materials,** such as rochelle salt, lithium sulfate, and tourmaline, could be used as transducers, they do not appear to have any particular advantages. Several new ceramic materials are being developed and are proving to be useful for ultrasonic resonance testing.

Shape. Flat transducers are satisfactory for testing flat surfaces as well as cylindrical or spherical convex surfaces. The use of concave curved transducers will generally improve sensitivity and signal sharpness on small curvatures (below about 6-in. diam. at 2 Mc.), especially at low ultrasonic-test frequencies. Convex, cylindrical, curved transducers are recommended for tests from the inside of tubes less than 12-in. inside diameter.

Area. Transducers are round, square, or rectangular, with active areas ranging from 1/16 to 2 sq. in. Relatively large transducers are usually required at low ultrasonic frequencies. Transducer areas for low ultrasonic frequencies can often be reduced by using ceramics instead of quartz.

Mountings. Some typical transducer **supports** are illustrated in Fig. 9. Fig. 9(a) shows a simple quartz plate cemented along its edge to a plastic support. A metal foil is placed in contact with the back of the plate and connected to the R.-F. oscillator through a contact spring. The ground connection is made through the metal holder in contact with the test material. This design has high sensitivity but cannot be used at very high frequencies because the unsupported quartz plate would be too weak. Variations in the thickness of the coupling film will affect the electrical capacitance of the transducer and cause an error in the thickness measurement.

This source of error is eliminated in the **grounded transducers** shown in Fig. 9(b). The face of the transducer is plated; a soldered connection is made from this face to the holder. The transducer is rigidly cemented along its entire area to a plastic support. For applications where the abrasion of the face is severe, the plating can be protected with an **abrasion-resistant wear plate** [Fig. 9(c)]. Typical wear-plate materials are aluminum, stainless steel, quartz, abrasion-resistant plastics, and ceramics.

The transducer and support are usually mounted in a holder designed for convenience in testing. Rigid mounting to the holder, and spring mountings, are used most frequently. **Transducers without holders** can be used for testing in narrow recesses or for working close to protruding fillets or shoulders. Various special mountings have been designed for specific applications. **Swivel-mounted transducers** are very useful for hand scanning of tubular parts, rails, and large flat sheet. This mounting maintains the transducer face in contact with the part despite tilting of the holder. **Spring-mounted, cylindrical, convex transducers** are frequently used for scanning tubing or pipe from the inside. A split holder, separated by springs, maintains the transducer in proper alignment inside the tube. This type of mounting is also useful for testing cylinder bores.

Cementing the transducer to a support usually limits its **maximum operating temperature** to a range of 200° F. to 500° F. Transducers suitable for operation up to approximately 700° F. can be made by supporting them from shoulders machined into the quartz blank.

Thickness. The thickness of the quartz or barium-titanate blanks for any frequency can be calculated from Eq. 2, using the K constants given earlier. Silver plating, plastic coating, or attachment of wear plates reduces the resonant frequency of the transducer. The actual thickness of quartz or barium titanate must be reduced proportionately when wear plates are used.

SURFACE PREPARATION. Proper surface preparation of the test material is very important in many testing applications. The accessible test surface does not need to be electrically clean, and small pits, thin well-adhering paint, scale, or oxide need not be removed. However, since the amount of mechanical

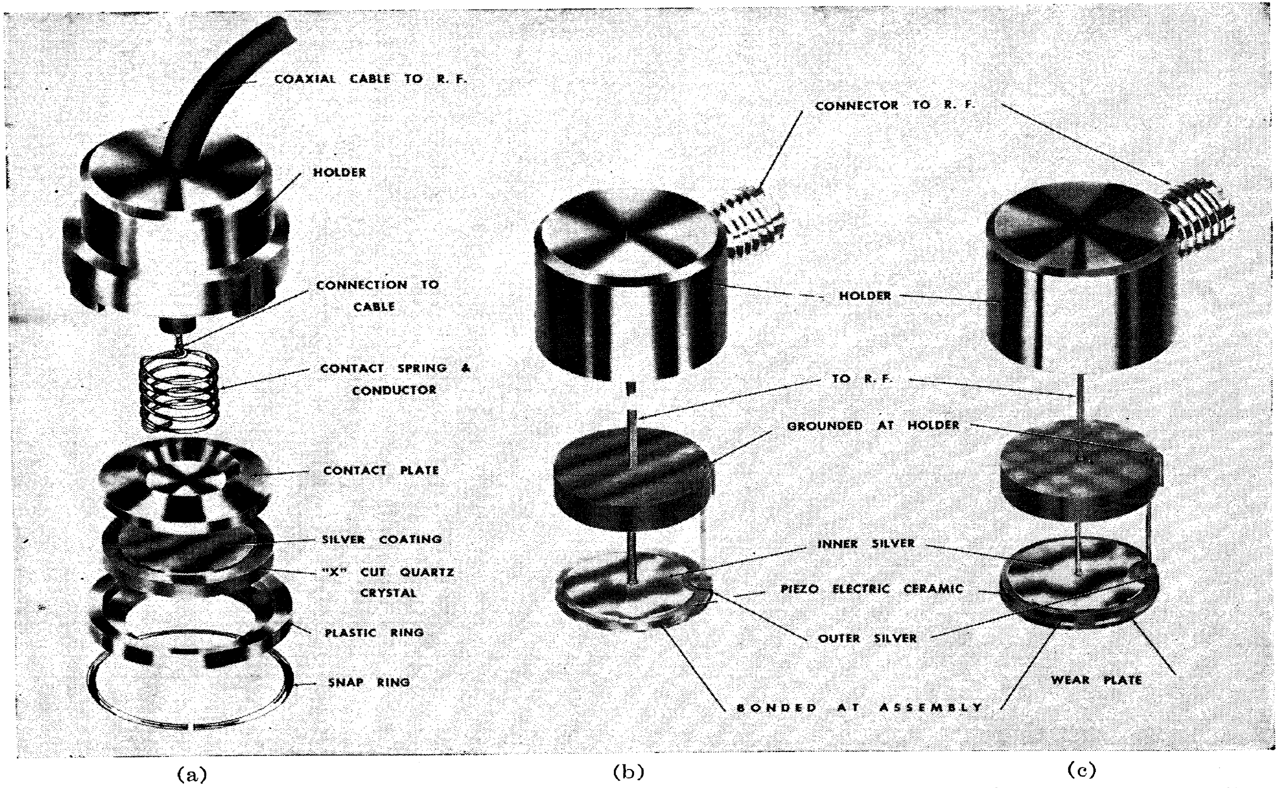

Branson Instruments, Inc.

Fig. 9. Ultrasonic transducer construction for resonance and contact testing. (a) Ungrounded, edge-damped transducer. (b) Grounded, damped transducer. (c) Transducer with wear plate.

energy transmitted does depend on the surface condition, it is usually necessary to remove **loose paint, thick or loose scale, or severe surface irregularities.**

The extent of surface preparation depends most significantly on the condition of the **inaccessible surface.** If it is seriously pitted and scaled, the resonance signals will be very weak. It is then necessary to prepare the accessible surface quite thoroughly. When the inaccessible surface is smooth, it is usually not necessary to prepare the accessible surface except for removal of high spots in the paint or when there is a severely corroded surface.

The best **power tool for surface preparation** on rough surfaces is a portable disc sander. This tool is better than a grinder, since it leaves a mechanically flat surface. Where thick, hard scale is present, it is desirable to remove it with a chipping hammer or a **power chipper.** It is usually best to clean an area considerably larger than the transducer, approximately 4 to 6 in. square. This permits the instrument operator to determine local variations in metal thickness. When local pitting is severe, it is often possible to obtain measurements by moving the transducer slightly away from the point where it was first applied to the work.

It is not necessary or desirable to prepare a polished surface. **Polished surfaces** frequently cause overcoupling and result in a shifting of the resonance frequencies.

SHAPE OF PART. One question frequently asked is, "What does the instrument measure?" The instrument will measure the **major thickness component** beneath the transducer. Proximity to the edge of a plate will not affect the readings. A **small isolated pit** will not be usually detected. In the case of taper or wavy pitting, the instrument will read the average thickness of the material under the transducer. In the case of **pipe-bend erosion,** most of the metal is at the minimum thickness; the instrument will therefore read minimum. If taper is very severe, the indications will disappear and there will be no reading.

SPURIOUS THICKNESS RESONANCES. In addition to the thickness-resonant frequencies based on compressional waves, the instruments will occasionally display resonance indications caused by **other vibrational modes.** These are usually weaker than the thickness resonances, have somewhat different characteristics, and do not fit into the harmonic resonance pattern. Resonance indications may also be produced by reflections from the sides of the part and by energy traveling around a tubular part.

ACCURACY. The accuracy of ultrasonic-resonance thickness measurements is limited by the design of specific test instruments and by inherent limitations of the method. The instrument must be capable of detecting and displaying a small frequency change caused by a thickness change. Under ideal conditions, where it is possible to use a scale covering a limited frequency range, a change of approximately 2 kc. can be detected. This represents 0.5 percent at a testing frequency of 10 Mc. On wide-range scales a thickness change of the order of 0.01 percent to 2 percent is normally detected.

Variations in the mechanical properties of the material will affect the sound velocity; high accuracy can therefore not be expected if the mechanical properties vary, as they do in many cast materials. Uniform **coupling** between the transducer and the work is essential for high-precision tests. Very light coupling through a thin film of water or very light oil and the use of mechanical spacers to control the thickness of the coupling film are usually most effective. Errors due to **instrument drift** and variations in transducer capacitance can be eliminated by frequent calibration or by display of a secondary resonance signal produced by a tuned circuit or a calibrating transducer.

Typical Applications

INDUSTRIAL THICKNESS GAGING. Applications of resonance thickness testing for receiving inspection, production tests during fabrication, and final inspection are quite similar. It is always desirable to apply the test as early as possible in the manufacturing process, to avoid the expense of subsequent fabrication of unsatisfactory material and excessive handling of scrap.

The shape of manufactured parts is becoming increasingly complex, and tolerances are becoming tighter. Conventional gaging, using micrometers, is frequently too slow. In the case of complex structures, **mechanical gaging** may be awkward, exceedingly difficult, or impossible. Ultrasonic gaging, requiring access to only one surface of the part, frequently makes it possible to test materials during manufacture without interruption of the process or removal from the machine tool.

HOLLOW PARTS. In thickness testing of hollow structures, the transducer can be applied to either the inside or the outside of the part.

Extrusions. Extruded parts can be tested a few minutes after the extrusion process is completed. Round tubes can be inspected on a spiral pattern by moving the transducer longitudinally while rotating the tube. Rejection of off-gage sections of the extrusion facilitates subsequent fabrication operations, improves scheduling, and makes it possible to correct the extrusion process promptly. Ferrous and nonferrous tubes and irregular shapes can be checked. Fig. 10 illustrates ultrasonic gaging of hollow aluminum propeller blades. Ultrasonic gages are used for measuring the **wall thickness** of hollow aluminum extrusions at several stages of blade manufacture:

1. As received from the aluminum fabricator.
2. After machining on tracer-controlled planers.
3. During the final machining for balancing.
4. For final inspection.

Ultrasonic gaging can also be applied to the measurement of the thickness of **lead sheath** extruded over a core of wire and insulating material. The core does not affect the accuracy of measurements. Since extrusion speeds are slow, the cable can be checked continuously as it emerges from the cooling tank. Variations in lead thickness around the circumference of the cable are detected promptly. Adjustments in the lead press can be made while the cable is still within tolerance limits.

Drawn Tubes. Inspection techniques for drawn tube are similar to those used for testing of extrusions. Some "hashy" resonance indications, due to energy traveling around the tube, may be observed. This effect can be reduced by using high frequencies or by using **cylindrical, curved transducers.** Gating circuits for automatic acceptance and rejection and recording attachments can be used.

Tube Bends. Metal thinning on the outside of a tube can be measured accurately by testing before and after bending. Since most tubes will have some thickness variation, it is desirable to take a band of readings around the circumference of the tube prior to bending. This makes it possible to place the originally thick side of the tube on the outside before bending the tube.

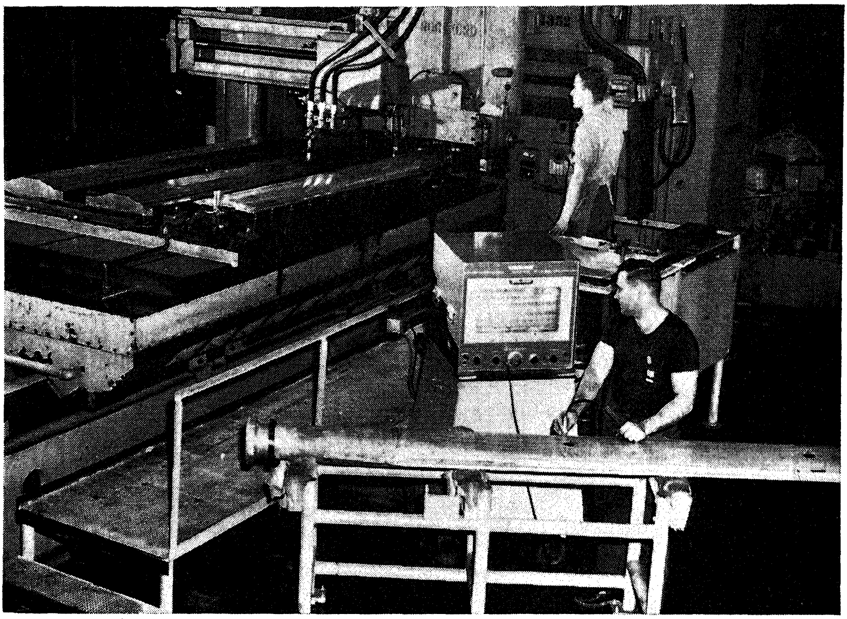

Hamilton Standard Division, United Aircraft Corp.

Fig. 10. Ultrasonic-resonance thickness gaging of walls of hollow propeller blades.

Bored Shafts. Thickness of a heavy-walled shaft can be checked during and after the boring operation. The shaft is rotated slowly, with the transducer placed on the outside. If the wall thickness is uniform, the resonance lines will be stationary. Variations in wall thickness can be read directly from the scale in inches or as a percentage change. Horizontal **rubber-covered shafts** can be checked from the inside by pulling a weighted transducer through the bore while the shaft is rotated slowly.

Castings. Centrifugally cast pipes, iron pipes, cast-iron cylinder blocks, magnesium and aluminum aircraft components, and similar parts can be checked for wall-thickness variations. Low ultrasonic **test frequencies** should be used on gray-iron castings. High frequencies can be used on cast steel, nodular iron, and high-quality aluminum or magnesium castings. Since the sound velocity in some types of castings may vary considerably, it is desirable to determine the constant on a number of samples (see Eq. 7).

Miscellaneous Machining Operations. Metal loss due to grinding, lathe turning, spinning, and other machining operations can be determined by ultrasonic gaging. Precision machining of large parts is facilitated by making ultrasonic thickness measurements prior to the final cut, without removal of the part from the machine tool.

SHEET AND PLATE. Ultrasonic-resonance thickness tests are widely used on platelike materials.

Flat Sheet. Thin sheets used in aircraft manufacture are frequently held to **close tolerances.** This makes it necessary to obtain a substantial number of thickness measurements over the entire sheet. Ultrasonic gaging can be used for receiving inspection or for inspecting warehouse stock. The top sheet in a stack can be tested without removing it from the stack. **Semi-automatic scanning arrangements** can be used to locate the minimum thickness on a sheet. A transducer can be mounted in a solenoid-operated spring fixture attached to a mechanical scanner. Ultrasonic gaging with mechanical scanners is faster and more accurate than mechanical gaging with deep-throat calipers.

Stretch-formed, Spun, and Forged Parts. Reduction in thickness due to various forming operations can be measured accurately. Flat transducers are usually satisfactory for thickness measurement from the outside of large-diameter, compound curvatures.

Skin-milled Plate. Skin-milled, jet-aircraft wing sections can be gaged while they are held on a vacuum chuck. In the case of simple contouring operations, the transducer can be mounted behind the milling cutter for gaging immediately after machining. The cutting oil used for machining is satisfactory as a couplant.

Chemically Milled Sheet. Chemically milled sheet can be gaged from the etched side immediately after removal from the etching tank. The **masking compound** on the other surface will not interfere with the accuracy of the measurement. Transducers can also be attached to the masked side for thickness measurement during chemical-milling operations. A number of transducers can be attached to one part at various locations, and the instrument can be switched from one to another automatically or manually. **Automatic gating circuits** can be used to remove the part from the etching tank when it has reached the desired minimum thickness.

Plating. Ultrasonic resonance equipment will usually measure the total thickness of base material plus plating. If the instrument has a scale calibrated for the base material, it will read the thickness of the base material plus the equivalent thickness of plating. If the sound velocities or constants of the two materials are similar, the instrument will measure total thickness. If the sound velocity of the plating differs appreciably, the equivalent thickness will be the base thickness plus the actual thickness of the plating multiplied by the constant for the base metal, divided by the constant for the plating. For example, if 0.050-in. steel with 0.040-in. copper plating is measured, the instrument will indicate 0.102 in. on a steel scale. This could have been calculated as follows:

$$T_{\text{total}} = T_{\text{base}} + \left(\frac{T_{\text{plating}} \times K_{\text{base}}}{K_{\text{plating}}}\right) \tag{7}$$

$$= 0.050\text{ in.} + \left(\frac{0.040\text{ in.} \times 0.116}{0.089}\right) = 0.102\text{ in.}$$

Plating thickness can be measured if the thickness of the base material is uniform or if the base material thickness can be measured prior to plating. Scales can be calibrated to read plating thickness directly if the base material thickness is uniform. If there is a substantial difference between the **acoustical impedance** of the base material and plating, the instrument will display separate resonance patterns for the base material thickness and the plating thickness. Interpretation of this multiple resonance pattern is usually impractical.

DETECTION OF DISCONTINUITIES. Discontinuities in the material under test can be detected with ultrasonic resonance instruments by observing changes in the strength or location of the resonance indications.[8] While the

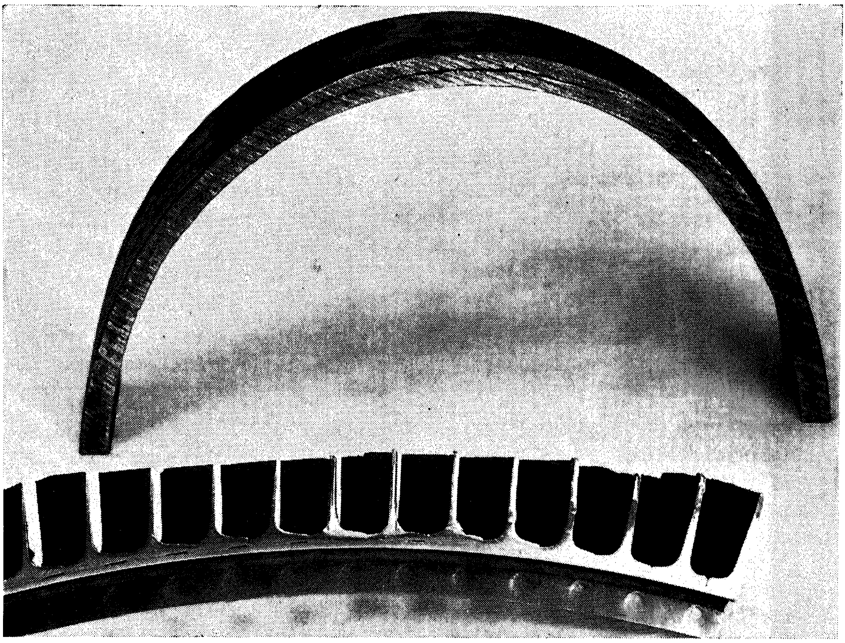

Branson Instruments, Inc.

Fig. 11. Typical discontinuities detected by ultrasonic resonance testing.

behavior of the equipment can generally be predicted, it is usually desirable to conduct preliminary tests on sections with known discontinuities. Discontinuities detected by ultrasonic resonance testing are shown in Fig. 11.

Discontinuities in Homogeneous Structures. Resonance indications obtained on a plate with various discontinuities are shown in Fig. 12. The instrument can be set up to measure the thickness directly. It is frequently more convenient to set it up so that three or four resonance lines will be shown for the full thickness. Discontinuities will then be indicated by a sudden shifting of the indications or by disappearance of all or some of the indications. It is relatively easy to locate the **edge of a discontinuity.** If the transducer is partly over the discontinuity and partly over sound metal, both resonance patterns will appear, as shown in point B in Fig. 12.

Lack of Bond in Cladding. Lack of bond between clad metals or metals which have been rolled together is similar to a laminar discontinuity. In the case of **two-layer materials,** the ratio of the reflected to refracted wave energy is

$$R = \left[\frac{\rho_1 V_1 - \rho_2 V_2}{\rho_1 V_1 + \rho_2 V_2}\right]^2 \qquad (8)$$

where ρ = material density.
V = velocity of sound.
Subscript 1 = first material.
Subscript 2 = second material.

Weak, spongy bonds will usually transmit quite well at 5 Mc. and are therefore not detected at low frequencies. They can be detected quite readily

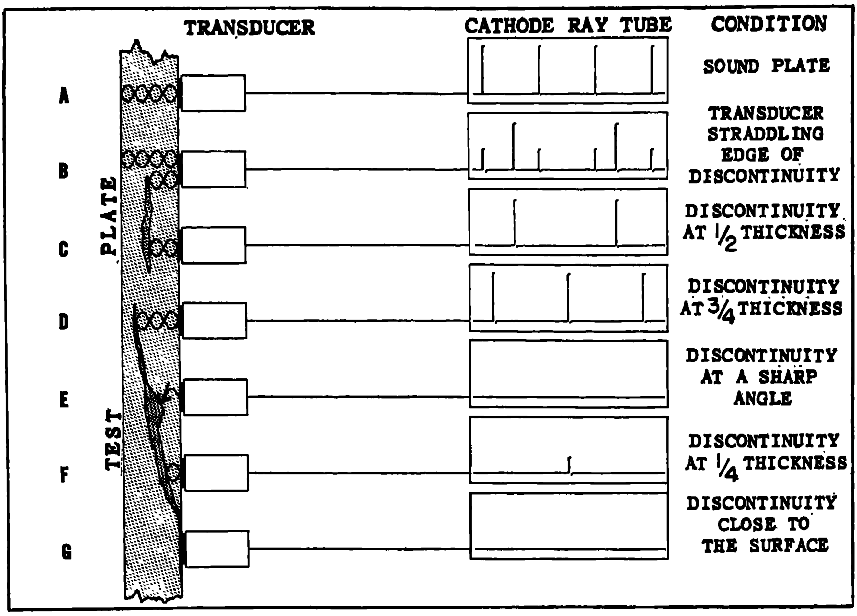
TRANSDUCER
CATHODE RAY TUBE
CONDITION
A
B
C
D
E
F
G
TEST PLATE
SOUND PLATE
TRANSDUCER STRADDLING EDGE OF DISCONTINUITY
DISCONTINUITY AT 1/2 THICKNESS
DISCONTINUITY AT 3/4 THICKNESS
DISCONTINUITY AT A SHARP ANGLE
DISCONTINUITY AT 1/4 THICKNESS
DISCONTINUITY CLOSE TO THE SURFACE

Fig. 12. Laminar discontinuities detected by ultrasonic resonance testing.

at approximately 12 to 15 Mc. Clad metals consisting of steel and stainless steel, steel and nickel, steel and aluminum, and even steel and copper will act as a single piece. The inspection of **lead-clad equipment** is fairly complex. The instrument will actually indicate two separate sets of resonance indications—one for the steel, the other for the lead. The test is normally made from the steel side, since the surface on the lead side is usually quite rough. If there is good bond, there will be weak indications for steel and very weak indications for lead. If there is no bond, there will be very strong indications for steel and no indications for lead.

Weldments. Resonance instruments can be used on welded or brazed assemblies with favorable geometry. If two flat sheets are bonded together by welding or brazing, the test will be similar to the detection of a laminar discontinuity (points *A* and *C*, Fig. 12). It is also possible to test assemblies where a flat sheet is bonded to a wedge-shaped piece. If there is good bonding, the instrument will give no signal at low sensitivity settings. Lack of bond will be indicated by a strong resonance signal for the first layer.

Damping Materials. Bonding between a good transmitter (such as metal) and a poor transmitter (such as rubber or certain plastics) can be determined by **testing from the metal side.** If there is a good bond, the second layer will absorb a considerable proportion of the energy and scatter it. The resonance signal for the metal layer will therefore be reduced in amplitude, or "damped." If there is no bond, a strong indication for the metal thickness will be obtained. Relatively low ultrasonic frequencies should be used for this test.

DETECTION OF STRUCTURAL DIFFERENCES. Differences in internal structure of a material can be detected in some specialized cases by measuring differences in sound velocity or in the ability of the material to transmit ultrasonic energy at various frequencies.

Velocity Measurements. Sound velocity in a material is a function of its density and its elastic constants. In the case of a plate, the velocity is given by

$$V = \left[\frac{E}{\rho}\left(\frac{1-\sigma}{(1+\sigma)(1-2\sigma)}\right)\right]^{1/2} \tag{9}$$

where V = velocity of longitudinal waves, cm./sec.
E = Young's modulus, dynes per sq. cm.
ρ = density, grams/cc.
σ = Poisson's ratio.

If the thickness of the part is known, the instruments will measure the sound velocity by

$$\text{Velocity} = 2\ (\text{fundamental frequency}) \times (\text{thickness}) \tag{10}$$

While this method does not result in absolute sound-velocity values of high accuracy, it is quite satisfactory for detecting **differences in sound velocity** between various structures. When sections of uniform thickness are tested, the instrument scales can be calibrated to read sound velocity directly.

Attenuation Measurements. Transmission of ultrasonic energy is influenced by grain size, shape of grain boundary, size and shape of inclusions, and similar factors. There appears to be a definite relationship between the size of the interfaces and the wavelength. Relatively **coarse-structured materials** will transmit at low frequencies but not at high frequencies.

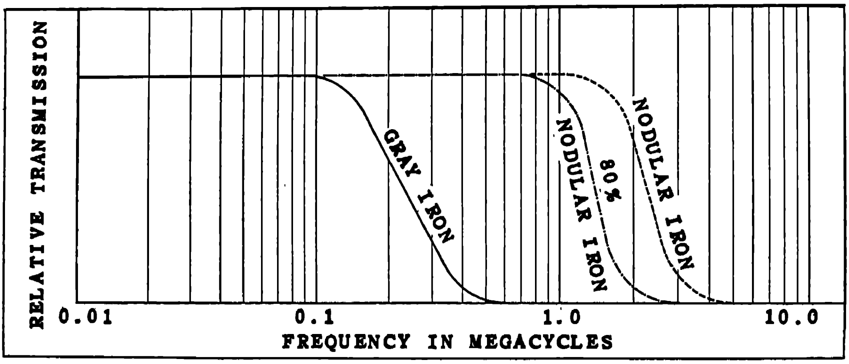

Branson Instruments, Inc.

Fig. 13. Relative transmission of ultrasonic energy through gray and nodular iron, as a function of frequency.

All solids will transmit at very low frequencies. As the frequency is increased for a given material, there will be a region where transmission decreases quite suddenly. In the case of concrete, wood, and similar materials, this **transition region** is well below 500 kc. Most plastics, cast iron, low-quality cast aluminum, and similar coarse-structured materials pass through this transition between 0.5 and 10 Mc. (see Fig. 13).

This phenomenon can be used to distinguish between **gray iron and nodular iron.** Gray iron contains graphite in the form of flakes. Nodular iron contains graphite in the form of spheres. Gray iron shows considerable loss of sensitivity at 2 Mc. and practically no transmission above 5 Mc. Nodular iron will transmit quite well at 10 Mc. Intermediate grades, such as 50 percent spheroidal graphite, will show gradual loss of transmission between 5 and 10 Mc.

These materials can be separated by examining, between 5 and 10 Mc., the resonance pattern on a relatively thick specimen (see Fig. 14). Nodular iron has good resonance lines across the entire band. If the gain setting is reduced, the resonance line will disappear first at the low-frequency side (6 Mc.) because the instruments and transducers are inherently less sensitive at the low-frequency side of the range. Gray iron will produce no resonance line. Some intermediate grades of cast iron with 40 to 70 percent spheroidal graphite will produce strong resonance lines at 6 Mc. and very weak lines or no lines at 10 Mc. Care must be taken to avoid **other variables** which could influence this test. These include variations in heat treatment, in surface finish, and in parallelism between the two surfaces. Sound velocity, as well as absorption, changes with the coarseness and quantity of graphite.

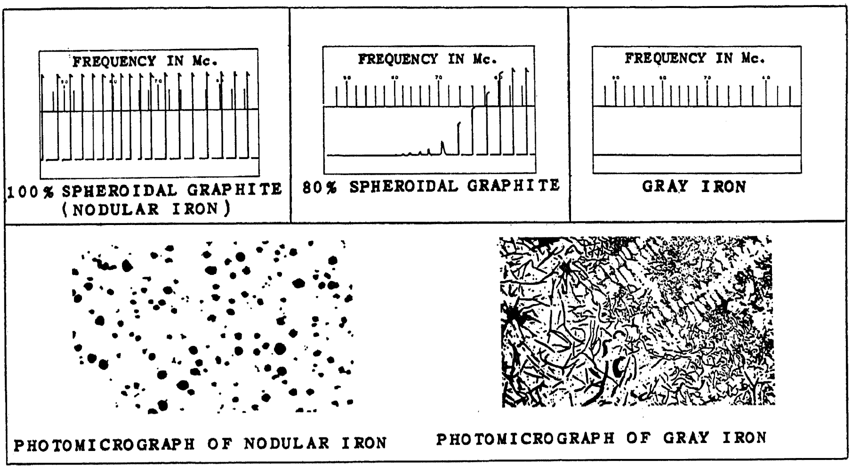
FREQUENCY IN Mc.
FREQUENCY IN Mc.
FREQUENCY IN Mc.
100% SPHEROIDAL GRAPHITE (NODULAR IRON)
80% SPHEROIDAL GRAPHITE
GRAY IRON
PHOTOMICROGRAPH OF NODULAR IRON
PHOTOMICROGRAPH OF GRAY IRON

Branson Instruments, Inc.

Fig. 14. Ultrasonic-resonance response characteristics and corresponding microstructures of gray and nodular iron; at 5 to 10 Mc.

Maintenance Inspection

PRIMARY USES. Ultrasonic equipment is widely used for nondestructive thickness gaging of in-service equipment subject to corrosion and erosion, and for the detection of laminar discontinuities. Inherent accuracy, small size, and battery operation have made ultrasonic resonance equipment particularly suitable for field inspection.

THICKNESS GAGING. The traditional method of gaging the thickness of equipment subject to corrosion has consisted of drilling test holes in suspected locations, measuring with a micrometer, and closing the test hole by welding or by insertion of a threaded plug. This method not only was costly but also required emptying the vessel or pipe and removing corrosion products from the inside. **Drilling and plugging** is gradually being eliminated in many industries by the substitution of ultrasonic resonance gaging. The method is inherently accurate, being independent of various process variables; it has therefore been accepted, in lieu of drilling test holes, by pressure-vessel insurance companies, state boards, and marine classifying societies. The **number of readings** which can be obtained in one day depends on the ease of access to the test location, condition of the test surface, and test equipment used. It normally ranges from 50 to 2000 readings per day. The direct-labor cost of nondestructive testing is usually a fraction of the cost of drilling and plugging.

Selection of Test Points. The number and location of the test points should be selected on the basis of past corrosion experience. Whenever possible, the vessel should be checked from the corroded surface, so that the nondestructive test can be combined with visual inspection. **Severely corroded surfaces** must be prepared by removing at least one-half of the "peaks." Measurements should always be taken in areas of local turbulence, such as the outside of the tube bends and close to an inlet or outlet in a tank.

In case of a cylindrical vessel, a horizontal and vertical **belt of readings** should be taken at fairly close intervals. Analysis of these readings will frequently locate the levels of maximum corrosion. Additional readings should then be taken at these levels.

Ultrasonic thickness gaging may be used to aid in determining the safety of equipment or in measuring corrosion rates. Since the techniques are somewhat different, these two applications are described here and under Tests of Corrosion Wall Thinning in this section.

SAFETY INSPECTION. Safety inspections with ultrasonic resonance equipment can frequently be carried on while production equipment is in operation, since **liquids on the inside** will not affect the accuracy of the measurements. The use of ultrasonic equipment during shut-down increases reliability by permitting a large number of measurements. Inspection time is frequently reduced substantially, resulting in less loss of production. Applications in the chemical-processing, oil-refining, and pulp-manufacturing industries, and in marine and airline transportation, as well as in public utilities and other industries are quite similar; a few typical examples will be described to illustrate various inspection techniques.

Boiler Tubes. Power-plant boiler tubes have failed in service because of corrosion and erosion from the outside and inside or because of deep grooving. In a large majority of cases the attack takes place along the fire side of the tube. The recent trend toward higher pressures and higher temperatures appears to have accelerated this type of attack.

Despite the high speed of ultrasonic testing, it is not practical to inspect every inch of every tube. **Locations for ultrasonic testing** are usually selected on the basis of past operating experience. Surfaces are prepared by sandblasting, chipping, or filing. Measurements are then taken on an inside tangential plane at intervals such as 3 in. or 1 ft. Tube bends and areas close to the weld usually receive special attention.

Heat-Exchanger Tubes. Straight heat-exchanger tubes can be checked from the inside in cases where access to the outside is not practical. The surface must be carefully cleaned; chemical cleaning or turbining is frequently used. **Convex curved transducers** mounted in spring fixtures can then be moved through the inside of the tube. If the transducer is attached to a rigid handle, it can be rotated for a spiral inspection pattern. As an alternative the transducer can be pulled straight through the tube four or eight times in succession.

Gas Cylinders. Wall thickness of gas cylinders can be checked rapidly by mounting the cylinder on motor-driven rolls. Manual movement of the transducer along the axis of the cylinder will then generate a spiral inspection pattern and ensure complete inspection. The cylinder can therefore be completely inspected in approximately 5 min.

Storage Tanks. Storage tanks can be checked while they are filled with liquid, by working from the outside. When large numbers of tanks have to be inspected, it may be desirable to use special scaffolding or cranes to speed the movement of the operator. A more thorough inspection can usually be conducted from the inside. The heavy grease which frequently covers oil storage tanks usually does not have to be removed.

Ship Structures. **Hull thickness** on submarines, destroyers, and cargo vessels, and **bulkhead thickness** on oil tankers, must be checked periodically to satisfy the requirements of the regulatory societies. Ship owners normally prefer nondestructive tests, and ultrasonic gaging therefore is gradually replacing drilling. Some measurements can be obtained before the ship moves into drydock. Bottom hulls can be checked from the inside. If one of the tanks contains ballast or cargo, measurements on the bulkhead can be obtained from the surrounding tanks.

Pulp Digesters. Ultrasonic resonance gaging has been accepted as the standard method for periodic inspection of pulp-digester wall thickness. Property damage and loss of production in the explosion of one digester exceeded the cost of inspecting 700 digesters at six-month intervals for five years. Digesters are normally checked from the inside. Readings are taken at eight points around the circumference at 2-ft. vertical intervals. Additional measurements are taken in areas showing visual signs of accelerated corrosion.

Aircraft Propellers. Aircraft propellers are frequently nicked by stones and pitted by corrosion. Grinding and sanding subsequently reduce the thickness. In the case of hollow propellers there is very little corrosion allowance, and careful thickness control is required in order to avoid failures. Periodic ultrasonic gaging is therefore specified for hollow propellers.

Rubber and plastic bonded to the inside of the propeller will cause a slight error in readings taken at the fundamental frequency. This is avoided by using higher frequencies and obtaining readings from the higher harmonics.

CORROSION-RATE DETERMINATION. Comparison of a safety-inspection thickness measurement with the originally specified wall thickness will provide a very approximate "historical" corrosion rate. This corrosion rate can be quite erroneous because the manufactured wall thickness may vary considerably from the drawing specification, due to manufacturing tolerances or the substitution of heavier plate. Moreover, the corrosion rate may have changed because of variations in the operating conditions.

More reliable data can be obtained from present corrosion-rate determinations, based on two sequential sets of nondestructive thickness measurements. The use of present corrosion rates makes it possible to predict equipment life and to stock replacement parts. The corrosion resistance of various materials in a new process can be evaluated before additional units are installed. The effect of process variations on the corrosion rate can be measured. The effectiveness of various corrosion-protective systems such as coating and cathodic protection can be evaluated accurately.

Measurements taken for the determination of corrosion rate require higher testing accuracy and more care in the location of test points. A complete thickness survey must be made on **new equipment** before it is installed in the process. Whenever possible the test location should be marked accurately so that subsequent surveys will be made at the same points. In the case of **insulated equipment,** subsequent inspections can be facilitated by installing removable plugs of insulation. If the surveys are made from the corroding surface, it may be difficult to re-locate the test points. Points can sometimes be located by referring them to prominent reference points such as weld lines or inlets.

In the case of pulp digesters, eight studs can be welded inside the digester, at 45 deg. apart, close to the top. During inspection, chains are hung from these studs, with washers spaced at 2-ft. intervals. The transducer is then inserted inside the washer to ensure proper positioning.

DETECTION OF LAMINAR FLAWS. Resonance tests are particularly useful in detection of laminar discontinuities.

Hydrogen Blistering. Chemical and refining equipment is occasionally subjected to hydrogen-blistering attack, caused by the migration of atomic hydrogen into laminations. Large blisters can be detected visually, through bulging of the metal or blistering of the paint. A more thorough inspection can be carried on by ultrasonic resonance testing. Measurements are usually taken at 3- or 6-in. centers; laminations are indicated by a sudden increase in the spacing between resonance indications.

Hot Taps in Pipelines. Side connections must occasionally be made in gas pipelines which are in operation. The area where the connection is made must be free from lamination. This area is checked ultrasonically, therefore, to confirm that the metal is sound. Similar techniques are used on ship hulls and other structures prior to the attachment of stiffeners.

Rail Testing. Discontinuities occasionally develop near the end of railroad rails in the **area covered by the joint bar.** The complexity of the section makes it impractical to use electric current test methods. The joint bar hides the rail from visual inspection. The former method of removing the joint bar for visual inspection has now been superseded by the use of ultrasonic resonance or pulse testing.[9]

The most common discontinuities in the rail end are **head and web separations,** which start in the fillet section at the end of the rail and work back. **Bolt-hole cracks,** which normally radiate diagonally from the bolt hole, also cause discontinuities. The method of detecting these discontinuities is shown schematically in Fig. 15.

Resonance instruments produce an **audible signal** which is proportional in frequency to the distance from the transducer to the first reflecting surface. At *A* the sound waves are reflected by the base of the rail, and a high-pitched tone is received in the headphone. The bolt hole, shown at *B*, results in a characteristic lower pitch. A head and web separation will produce a very low-pitched signal. At a diagonal bolt-hole crack, the energy will be scattered and no audible signal will be obtained. Since the ear is very sensitive to changes in

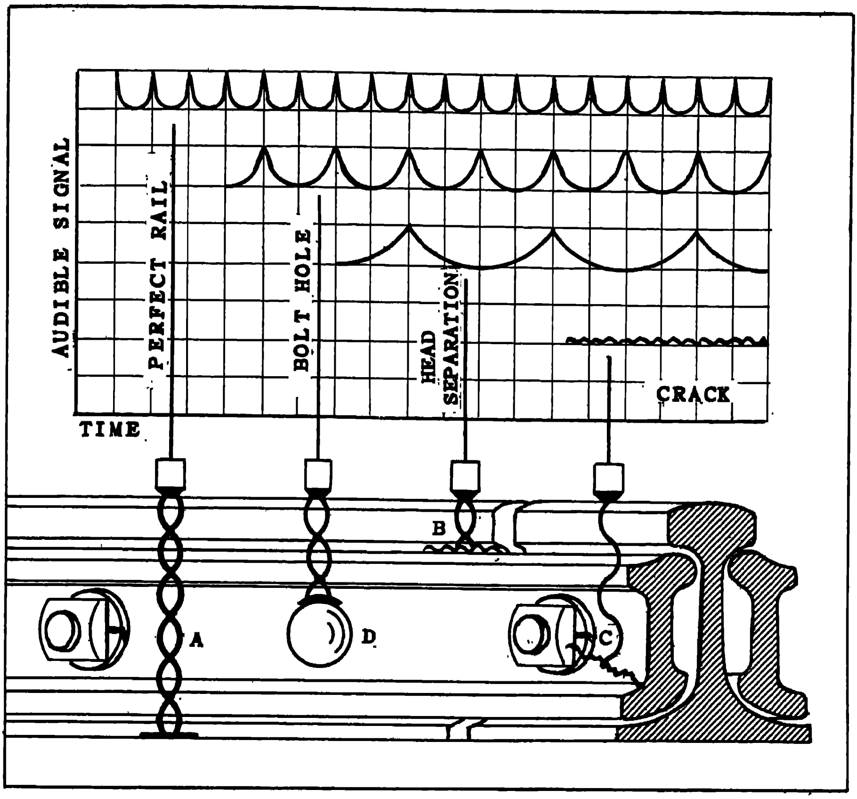

Fig. 15. Ultrasonic inspection of rail ends.

pitch, the operator can scan the rail rapidly and detect discontinuities. A skilled operator can test approximately 1000 rail ends per day. Service failures due to rail-end discontinuities have been virtually eliminated since ultrasonic testing was adopted by the railroads.

Tests of Corrosion Wall Thinning

CORROSION LOSSES. The cost of corrosion in the United States has been estimated to be at least several billion dollars per year, not including increased costs attributable to hazards to personnel and property. Corrosion problems are particularly serious in processing and transportation activities such as oil refining, chemical manufacturing, power production, and in the marine industry. To reduce these costs and hazards, corrosion rates should be carefully observed, allowances made for corrosion loss, preventive measures taken if possible, and rigid requirements established, particularly in industries where public safety is involved.

DEVELOPMENT OF NONDESTRUCTIVE TESTS. The need for a reliable, rapid, and inexpensive method of measuring corrosion loss and for evaluating corrosion-control systems led to the development of nondestructive thickness-measurement instruments capable of measuring thickness from one surface. In various industries these instruments are gradually replacing the older method of cutting and plugging test holes. The rate depends upon industrial progressiveness and capabilities in training of test personnel. Cost for each measurement has been reduced to 10 to 20 percent of that of the older method, and in addition large savings result from reducing or eliminating shut-down time, drydock charges for a ship, or periods of "outage." Regulatory bodies such as insurance underwriters, the American Bureau of Shipping, and the United States Coast Guard accept these nondestructive measurements as valid, provided the accuracy of the instruments and the capability of personnel using them are demonstrated to the agent concerned.

Development of nondestructive thickness-measurement instruments began during World War II, and various methods have been used and evaluated since then. The methods include those based on gamma- or X-ray absorption, electric current conduction, or magnetic flux as a function of thickness. Also used are ultrasonic methods utilizing the resonance or reflection techniques. The ultrasonic and gamma-ray methods have been proven most practical for corrosion measurement and are now in general use.

ADVANTAGES OF ULTRASONIC TESTS. Ultrasonic equipment is now widely used for measurement of corroded materials. Its primary advantages are:

1. Simplicity (particularly the resonance-type instruments).
2. Portability.
3. A thickness range much greater than other methods.
4. Safety.
5. An accuracy range of 1/10 of 1 percent to 1 percent, depending upon the instrument and proficiency of the operator.

In addition, ultrasonic tests provide information such as presence of scale and permit qualitative analysis of opposite surfaces. **Accuracy of metal-thickness measurement** is not appreciably affected by corrosion products on the opposite surface or by other conditions usually encountered, such as oil, gasoline, or sea water in contact with the opposite surface. The accuracy of gamma-ray equipment is seriously affected by these conditions unless quantity of scale and correction factors are known.

LIMITATIONS OF ULTRASONIC TESTS. Disadvantages of the ultrasonic test for corrosion work are the relatively high degree of proficiency required of the operator, the fact that a firm acoustical contact must be established between the transducer and the test material, and the fact that maximum thickness variation in the part cannot exceed about 0.125 in. under the transducer area. It will not measure **depth of isolated pits** having an area less than about 1/4-in. diam., but it will indicate their presence. In many corrosion applications, pitting is relatively uniform in areas comparable in size to the transducer (produces a wavy surface), and therefore an average between maximum and minimum thickness under the transducer can be obtained. This average is desirable, both from the standpoint of structural requirements and measurement of corrosion loss. The accuracy of the test is comparable to the loss-of-weight method of measuring corrosion rates on test coupons.

Ultrasonic thickness measurement of **new materials** in the manufacturing plant or in the field is relatively simple when compared to measurement of materials having corroded surfaces and corrosion deposits. Basically, materials with uniform thickness and a smooth reflecting surface provide a strong, sharp reflection or signal that is easily detected. **Corroded reflection surfaces** produce a band of signals covering the many thicknesses between maximum and minimum. When the damping effects of corrosion products are added, it is obvious that the operator must be thoroughly familiar with the characteristics of the method and with his equipment.

TEST EQUIPMENT. Corrosion surveys in the field are often made under extremely variable **operating conditions,** ambient temperatures, and humidity. Readings may be required at relatively **inaccessible locations,** such as the top of a fractionating tower, the side of a ship, or the sides or top of storage tanks. Consequently instruments must be portable, simple, and not affected by wide variations in temperature or humidity. They should be relatively waterproof, since they are usually used in exposed locations. In many cases, particularly in the oil fields, a.-c. power is not available and **battery operation** is necessary.

Resonance-Type Instruments. Ultrasonic resonance instruments are usually best adapted to corrosion measurement. These can be either **direct reading** with thickness presentation on a cathode-ray tube, or small, portable, manually tuned equipment operating from dry-cell batteries and providing **meter or headphone indication.** These instruments measure thickness from one side by transmitting compression waves into the test material. The waves travel through the wall, reflect at the opposite side, and return to the transducer. Since the velocity of the wave is a constant in any specific material, thickness is proportional to the elapsed-time interval between projection of a wave and its return to the transducer. Resonance-type instruments measure this time interval by mechanically or electronically adjusting transducer driving frequencies so that travel time is equal to a period of one cycle or multiples thereof. At these points wave interference occurs, loading on the transducer is increased, and a resonance signal is obtained (see Figs. 1 and 2).

Manually Operated Instruments with Headphone or Meter Indication. Portable, manually operated instruments are simple and are used for field work, especially when readings must be obtained in scattered locations throughout a plant or ship. They are extremely rugged and are often used under extreme conditions of temperature and humidity. They do not read thickness directly, but the operator manually adjusts frequencies and records resonant frequencies or multiples thereof.

Fig. 16 illustrates types of **signals** obtained with resonance equipment under various surface conditions. Two harmonics, or multiples of the fundamental frequency, are shown. Smooth materials provide sharp, strong indications, whereas corroded materials produce a wide band of frequencies covering an infinite number of thicknesses between maximum and minimum. This condition is normally encountered in corrosion measurements. The signal is relatively weak and must not be confused with spurious responses from variations in the plate-current frequency curve under high gain conditions.

The center of the resonance band from corroded materials is an approximate average of the thickness variation under the transducer. This average is used to determine **average corrosion loss.** Although thickness may vary as much as 0.10 in., an average corrosion loss of the order of 0.005 to 0.010 in. can be measured if the variation is uniform. The **maximum measurable variation in thickness** of corroded surfaces is reached when the resonance bands increase in width to a point where they blend together, i.e., when the resonance frequency of the

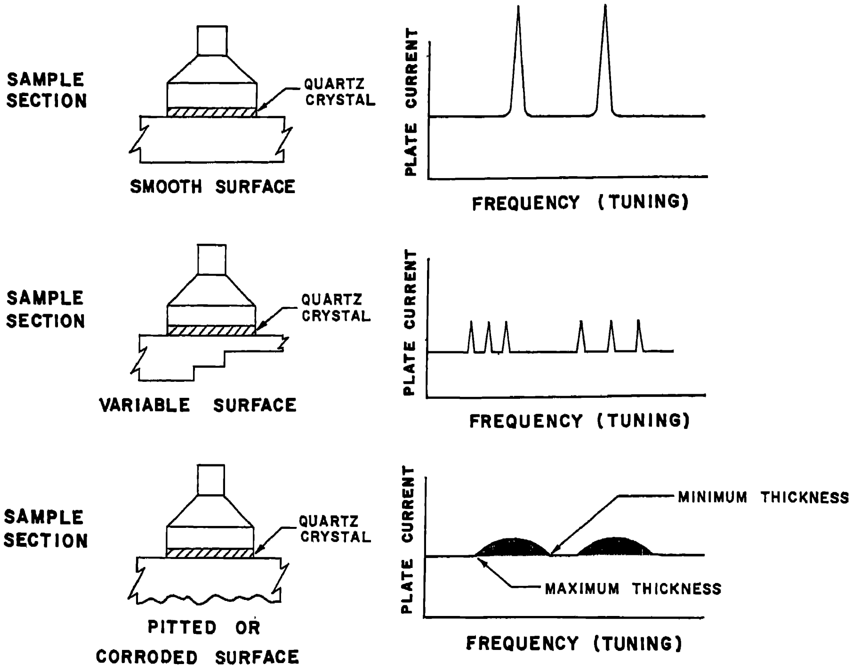

f_n = frequency at the nth harmonic

$f_{(n-1)}$ = frequency of the $(n-1)$th harmonic

$$\text{Thickness (steel)} = \frac{0.116}{f_n - f_{(n-1)}}$$

Fig. 16. Resonance frequencies obtained with various surface conditions.

smallest thickness component equals the second-harmonic resonance frequency of the heaviest component, or integral multiples thereof. At this point no thickness measurement can be obtained, and the operator should note that the thickness variation under the transducer exceeds about 0.125 in. (in steel). This condition is not usually encountered. However, in a few cases, corroded materials have been removed from service on this basis alone. Maximum measurable thickness variation is also affected by the frequency at which resonances are obtained. The short wavelengths of the higher frequencies are comparable in size to the irregularities of the corroded surface, and the reflected wave is effectively dispersed rather than returned to the transducer. Frequencies above 3 Mc. are usually not practical for corrosion work and preferably should not exceed 2.0 Mc.

Effect of Corrosion Product Accumulations. Fig. 17 illustrates the effect of corrosion products on the surface opposite the transducer. The strength of the signal is greatly reduced by accumulations on the back surface. Accuracy is not appreciably affected if a reflection can be obtained from the interface between test material and corrosion products. As shown in Fig. 17, the **ratio of reflected energy to refracted energy at the interface** is a function of sound velocities and density.[10] If the ratio is high, the signal will be strong, whereas a low ratio will produce only a weak signal. Usual corrosion products or deposits may reduce signal strength 75 to 95 percent as compared with that of a steel-air interface.

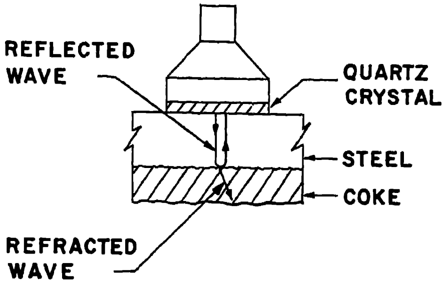

$$R_E = \left[\frac{\rho_1 V_1 - \rho_2 V_2}{\rho_1 V_1 + \rho_2 V_2}\right]^2$$

ρ_1 = density of steel
V_1 = sound velocity in steel
ρ_2 = density of steel
V_2 = sound velocity in steel
R_E = density of coke

$$V_L = \sqrt{\frac{E}{\rho}\frac{(1-\sigma)}{(1+\sigma)(1-2\sigma)}}$$

V_L = longitudinal wave velocity in cm./sec.
E = Young's modulus of elasticity
ρ = density in gm./cm.^{3}
σ = Poisson's ratio.

Fig. 17. Effect of back-up materials on ultrasonic waves.

Test frequency is also a factor. Lower frequencies tend to penetrate a dense, closely adherent scale more readily than a higher frequency. In general, test frequencies above 1 Mc. should be used.

Slide-Rule Thickness Calculations. A slide-rule method of converting frequency to thickness has been developed for precision work and is recommended for all corrosion measurement unless signals are extremely good and an accuracy of 3 percent is sufficient. A standard 10-in. slide rule can be used to verify authenticity of the frequency signals, average them, and calculate thickness. A special rule has been developed for this purpose and is shown in Fig. 18. The difference between any two adjacent harmonic frequencies is approximately equal to the fundamental frequency, or basic time interval. Therefore each resonance signal must be an integral multiple of this fundamental frequency. **Authenticity of signals** can be checked on the slide rule by multiplying the difference frequency by successive harmonic numbers, observing whether or not the product coincides with resonance points obtained.

If a **standard slide rule** is to be used, set the index of the C-scale on the average frequency difference between harmonics on the D-scale. Harmonic numbers on the C-scale should then coincide, or nearly so, with numbers on the D-scale representing the frequency obtained. For example, resonance frequencies of 1.80, 1.50, and 1.20 Mc. are obtained in a steel measurement test with a 1- to 2-Mc. instrument. The difference frequency is 0.30 Mc., and the right index of the C-scale is set at 0.30 on the D-scale. It is obvious that the sixth harmonic coincides with 1.80 Mc., the fifth with 1.50 Mc., and the fourth with 1.20 Mc. Proper harmonic numbers will always be whole numbers in the proper frequency range; in this example, 1.0 to 2.0 on the D-scale. Thickness is then read by setting the slide indicator at 0.116 on the D-scale and reading thickness on the C-scale (simple substitution in the equation shown in Fig. 16). If there are slight discrepancies, as is usually the case, the slide should be adjusted for the best average. This adjustment provides a 3 to 4 percent gain in accuracy, giving an **over-all accuracy** within 1 percent or better. If harmonic numbers do not coincide with the resonance points obtained, or nearly so, the reading is questionable and should be discarded.

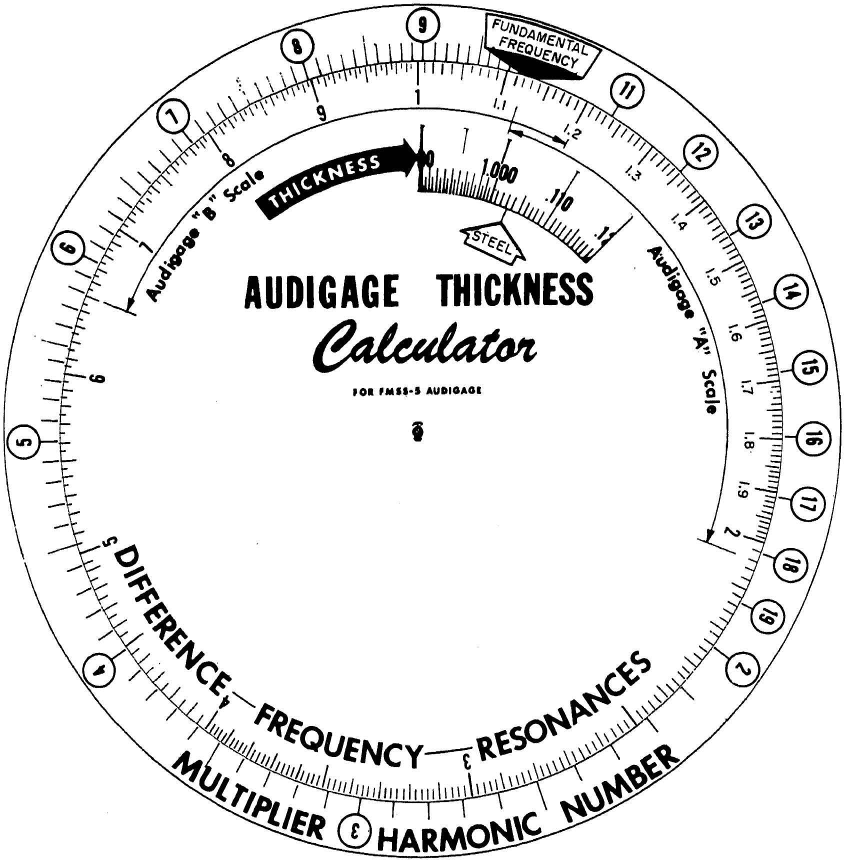

Engineering Test Services, Inc.

Fig. 18. Slide rule for converting measured frequencies to thickness indications.

Cathode-Ray-Tube Resonance Instruments. Resonance-type equipment using a cathode-ray tube presentation is usually calibrated directly in thickness. The plate-current frequency curve shown in Fig. 16 is presented directly on the cathode-ray tube. However, in the case of the broad band from corroded materials, only the center is amplified and presented on the cathode-ray tube. The **measurable thickness range** is limited by the number of harmonics that can be presented at one time, usually not more than five. This type of equipment is best adapted for corrosion applications where numerous readings are required in a relatively small area; for example, storage tanks and boiler tubes. It is larger and more cumbersome than the manually tuned equipment but has the advantage of direct reading and much greater speed in obtaining data. Slide-rule checks are unnecessary, since harmonics must occur at the proper thickness. Extension cables up to several hundred feet in length are normally used between the instrument and transducer for corrosion surveys. Thus a large number of readings can be obtained from one instrument location. Accuracy of measurement is well within 1 percent for typical corrosion work. It greatly exceeds this value on new material.

Pulse Equipment with Cathode-Ray Tube Indication. Pulse-reflection ultrasonic equipment, presently available in the United States, is inherently large and cumbersome for corrosion measurements in the field, since considerably more electronic circuitry is required than for resonance equipment. Extension cables more than 15 ft. in length are not practical. (However, with recently developed barium-titanate transducers, cable lengths up to 60 feet have been used.) Such equipment does not have wide application in corrosion measurement for these reasons and because the pulse width from the transmitter limits minimum measurable thickness to ⅜ in. or more. This thickness range is frequently encountered in corrosion work. **Single-transducer, pulse-type equipment** is best adapted for measuring thick material (2 in. and above) and is usually used for these applications. With dual-transducer systems developed abroad, thickness measurements are practiced down to ⅛-in. (see section on Ultrasonic Contact Tests).

A **multiple reflection method of thickness measurement** with pulse-type equipment will improve accuracy to about ±3 percent in the lower thickness ranges. Usually five back reflections per inch are used, and thus error is divided by five. A suitable scale of plastic or heavy paper tape is made and placed across the tube face. The instrument is adjusted for four or five reflections per inch (obtained by placing the transducer on a 1-in. test block identical to the material tested), and each reflection is marked on the scale. Four reflections are used for readings in fractions, and five for decimals. The scale is then removed and divided into suitable subdivisions such as twentieths of an inch. When the transducer is applied to the test material, thickness will be read at the position of the fifth back reflection.

Scales and appropriate number of back reflections can be varied to fit the application. The instrument should be thoroughly warm before the scales are made, and the sweep-length control should be checked frequently for drift or accidental movement.

Corrosion Test Techniques and Procedures

GASOLINE PLANTS AND REFINERIES. A typical gasoline-plant survey normally consists of about 600 to 700 scattered thickness readings. These readings are taken at various critical locations in the plant system, including such places as piping bends, accumulators, pressure vessels, and stills. When such a survey is conducted by a competent operator, the survey can be completed in about five to six days. **Total cost,** based on 1958 commercial test rates, is of the order of $0.50 to $1.50 per reading, depending upon accessibility, spacing of test spots, and other factors. Each test location should be carefully marked for later tests. Most surveys are made with the small, headphone-type equipment.

STORAGE TANKS. A corrosion survey on large oil-storage tanks may require 100 to 1000 readings per tank, depending upon conditions and degree of corrosion. Surveys can be made with either headphone or cathode-ray tube resonance-type equipment. **Cathode-ray tube equipment** is preferable if a 100-ft. or longer extension cable is available, since readings are concentrated in one area and all can be obtained from one instrument location.

Test Procedures. Metal-thickness measurements are made on the walls and roofs of tanks containing gasoline, diesel fuel, or kerosene. If the small portable equipment is used, a total of about 175 thickness readings can be obtained per day at a **cost** of about $0.75 per reading. All readings are normally taken in a regular pattern from the outside surfaces of the tanks. Three to ten readings are taken on each plate, and more if corrosion loss is indicated. In one example, measurements taken on each plate were 6 in. above the bottom edge, at the center, and 6 in. below the top edge. All **test points** were located on vertical lines down the north, east, south, and west sides of the tank, making a total of 72 thickness measurements on the walls of tanks with six rings. In addition, 20 readings were taken on each tank roof. Locations were carefully designated by measurements from convenient seams, so that future readings could be taken in identical locations. Whenever signals indicated that the surface opposite the transducer was corroded or pitted, such information was recorded.

Personnel Positioning. A **bo'sun's chair or portable scaffolding** can be used to move the test engineer up the sides of each tank. A block and tackle is attached to the top of the tank, and the bo'sun's chair is secured to the lower end so that the inspector, together with his equipment, can be raised or lowered by an assistant on the ground. If the paint on the tank is smooth and has good ultrasonic properties, accurate readings can be obtained without removing paint. (Paint thickness will also be measured when between transducer and test material.)

Detailed surveys utilizing cathode-ray tube instruments and extension cables have been made under favorable conditions at the rate of about 1000 readings per day. In these tests the operator and equipment are stationed at a central point, and an assistant with the transducer moves up and down the sides of the tank on either a bo'sun's chair or portable scaffolding.

Selection of Frequency Ranges. An added advantage of this cathode-ray equipment is the fact that frequency ranges are easily interchangeable. Further, any one oscillator can be changed slightly to provide the most advantageous test. A recent example of this advantage occurred during an extensive survey of ten, 100,000-barrel, oil-storage tanks. Many badly corroded plates had an average thickness of about 0.150 in. This thickness is difficult to measure with the headphone-type equipment, since the fundamental frequency occurs at about 0.77 Mc., the second harmonic at 1.54 Mc., and the third at 2.31 Mc. The 0.77-Mc. frequency is in an extremely insensitive area and the third is beyond the upper frequency range of the instrument. Therefore only one signal and no check point could be obtained. Comparable conditions exist in the standard 0.75 to 1.5-Mc. range of the cathode-ray type instrument. In this survey the 2.0- to 4.0-Mc. oscillator did not provide satisfactory results because of the effect of corroded surfaces on the high frequency. Therefore a special frequency range of 1.2 to 2.4 Mc., together with the proper scale, was devised for the cathode-ray tube equipment, and then the second and third harmonics thus obtained provided excellent results.

PIPELINES. Other surveys are made on pipelines by taking readings at bell holes and at exposed locations such as **river crossings.** In one particular case, detailed thickness surveys were made at several exposed pipeline river crossings without removing the line from service. The pipe had been exposed to the elements over a number of years and external corrosion was evident. Since the surface to which the transducer was to be applied was pitted, it was necessary to smooth it with a disc sander.

BOILER TUBES. Boiler-tube surveys have been made with both the manually tuned and cathode-ray types of resonance equipment. Cathode-ray instruments are preferable if large numbers of readings are desired, since boiler tubes are concentrated in one location and all are of the same approximate thickness. In this type of work, tubes in the critical area are checked in a vertical line at intervals such as 2 to 4 ft. Access to the tube walls is by bosun's chair or scaffolding. In a few cases internal pitting and corrosion were found to exceed the thickness-variation limits of the equipment, and the tube was declared inadequate on this basis alone.

Curved transducers cut to fit the outside diameter of the tube are used when test frequencies are 2.0 Mc. and below. If test frequency is over 2.0 Mc., small, flat, high-sensitivity transducers are usually satisfactory. If the tubes are not badly pitted internally, the higher frequencies provide excellent results.

OIL-TANK SHIPS AND OTHER MARINE APPLICATIONS. An average corrosion survey on the standard, Type T-2, oil-tank ship requires approximately 550 thickness readings on **hull and bulkhead plates.** Readings are also obtained on various structural members of the ship. A hull-and-bulkhead-plate survey includes one reading on each plate in the bulkheads dividing the ship into various cargo tanks, approximately 100 thickness readings on strategic shell plates (usually in the forward, central and after sections of the ship), and about 100 thickness readings on deck plates. Most of this work has been done with portable equipment. **Working conditions** are far from ideal, and access to measurement areas is usually difficult. Fig. 19 illustrates a tanker survey using cathode-ray tube equipment. An extension cable, 125 ft. in length, is connected between the instrument shown in Fig. 19 and the transducer. Communication between instrument and transducer operators is maintained with telephones.

On Type T-2 tankers, nine plates are welded together to form the vertical bulkheads. The distance from the top plate immediately below the deck to the plate at the bottom of the bulkhead is about 40 ft. It is therefore necessary to provide a means of access to the upper plates. To expedite taking measurements and to eliminate scaffolding, various techniques have been developed for obtaining thickness readings rapidly.

A **basket and hoist system** has been developed specifically for this work. In this method a hole is drilled in the top deck adjacent to two bulkheads, the cable from the hoist is lowered through the hole, and a basket is attached at the bottom of the cargo tank. The test engineer is then moved up this bulkhead, taking readings on each plate. Test locations are identified by a weld bead or similar marking or by careful measurement of their distances from the edge of the plate.

Corrosion Control Areas. It is often desirable to know the **corrosion rate on each side of a bulkhead,** particularly on bulkheads separating protected and nonprotected tanks, tanks protected with different methods of corrosion control, and ballast and nonballast tanks. In such cases a method of complete protection from corrosion for the measurement area on one side of the plate is necessary for accurate evaluation of the rate on the opposite side. Various methods have

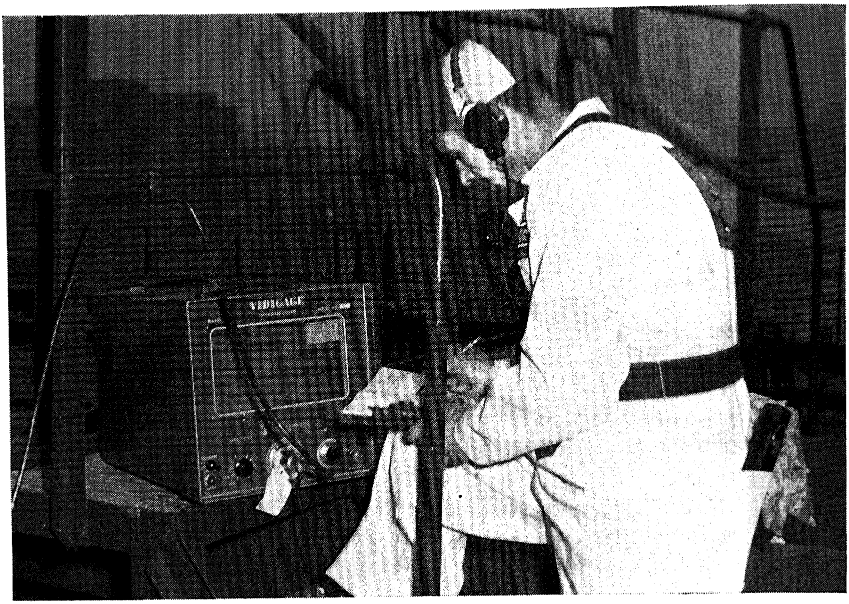

Engineering Test Services, Inc.

Fig. 19. Cathode-ray-tube ultrasonic instrument used in tanker survey.

been developed, one of which uses a **Mylar film patch,** 0.001 in. thick and 6 in. in diameter. The film has a self-adhering back and is imprinted on the face with the exact test locations. It is applied by grinding the bulkhead surface smooth, cleaning with a solvent such as ethylmethyl ketone, and pressing the patch firmly in place.

The Mylar film appears to be an economical and practical method of **protecting the measurement area** on one side of the bulkhead. The first installations were made in 1954. Records indicate that about 95 percent of the film patches remain in place throughout each year. Approximately 15 percent of this number become damaged and are replaced as a precautionary measure. In most cases readings are taken through the film on subsequent years, thus greatly reducing survey costs because the **cost of cleaning the test location,** usually at least 50 percent of the survey cost, is eliminated. If readings are taken through the film, a correction factor of 0.002 in. must be applied.

Other methods of protecting test locations include various forms of neoprene pads. In several installations "hold-down" studs have been welded about 6 in. apart on either side of the test location. Then a neoprene pad has been placed over the clean metal surface, covered by a piece of wood, and clamped in place by means of the "hold-down" studs. This method is very effective in protecting the test location, but it is more expensive per measurement. Since readings cannot be taken through the wood and neoprene, the pads must be removed and replaced each time a test is made.

Test Procedures. In a typical test, four basket units are used and are employed first by laborers in the **cleaning of the test locations.** Since bulkheads are usually pitted and covered by scale on both sides, one side must be smoothed with a disc sander. About one-half of the peaks should be removed to

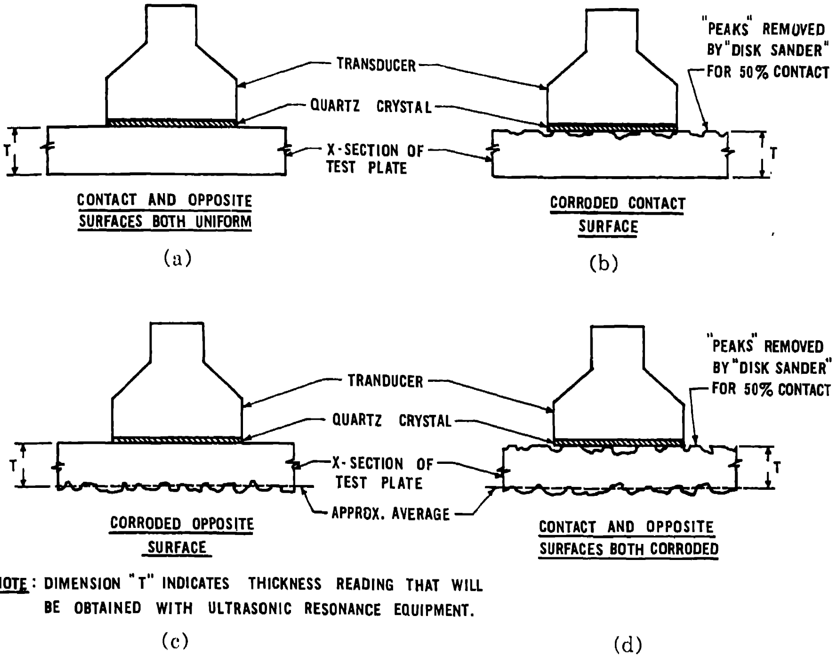
TRANSDUCER
QUARTZ CRYSTAL
X-SECTION OF TEST PLATE
T
"PEAKS" REMOVED BY "DISK SANDER" FOR 50% CONTACT
CONTACT AND OPPOSITE SURFACES BOTH UNIFORM
(a)
CORRODED CONTACT SURFACE
(b)
TRANDUCER
QUARTZ CRYSTAL
X-SECTION OF TEST PLATE
APPROX. AVERAGE
"PEAKS" REMOVED BY "DISK SANDER" FOR 50% CONTACT
CORRODED OPPOSITE SURFACE
CONTACT AND OPPOSITE SURFACES BOTH CORRODED
NOTE: DIMENSION "T" INDICATES THICKNESS READING THAT WILL BE OBTAINED WITH ULTRASONIC RESONANCE EQUIPMENT.
(c)
(d)

Fig. 20. Characteristics of ultrasonic thickness measurements.

provide a 50 percent flat area for the transducer. **Typical surface conditions** are shown in Fig. 20. Transducers 1⅜ in. in diameter are usually used, and the cleaned area is at least 6 in. in diameter.

After the locations are cleaned, the test engineers consecutively measure all bulkhead plates in each tank. An assistant records the resonance readings on the data sheets Approximately 550 readings can be obtained in about five man-days. About one day is required for checking the readings and calculating the thicknesses by slide-rule conversion.

When the baskets and hoists are not available, an adjustable scaffolding is sometimes used. Two sets of rope blocks are attached to beams immediately below the deck, a plank is attached, and the operator is raised or lowered along the bulkhead. Hull plates of the ship are tested in various ways. **Bottom plates** below the waterline usually are measured from the inside of the ship's cargo tanks. Access to **side plates** above the waterline is obtained in various ways, often by boat or barge alongside, by a hoist or scaffolding on the outside, or from inside the cargo tanks.

PULP DIGESTERS. Pulp digesters are often subject to corrosion or erosion attack and are checked periodically with resonance-type instruments. Wall-thickness measurements are usually taken from the inside during a shut-down period, after which the corrosion rate is plotted.

Since the digesters are usually at least 25 ft. in height, some means of **access to the inside surface** must be provided. The digester may be filled with wood chips at various levels, or some form of scaffolding may be used. A very satis-

TYPICAL T-2 TANKER

Fwd. Trans. Bhd. No. 3. Tanks Frame No. 58.

Transverse Bulkhead Plate	Thickness of Construction, inches	Port			Center			Stbd.		
		Resonant Frequency, Mc.	Thickness, in.	Per-cent Wastage	Resonant Frequency, Mc.	Thickness, in.	Per-cent Wastage	Resonant Frequency, Mc.	Thickness, in.	Per-cent Wastage
Top panel plate	0.461	1.70–1.36 *G*	0.342	25.8	2.00–1.67–1.34 *G*	0.347	24.7	1.73–1.38 *M*	0.336	27.1
1st plate	0.461	1.94–1.61–1.29*M*	0.359	22.1	1.88–1.57–1.26 *G*	0.370	19.7	1.98–1.65–1.33 *M*	0.352	23.6
2d plate	0.380	1.73–1.29 *P*	0.268	29.5	1.80–1.36 *G*	0.258	32.1	1.90–1.42 *P*	0.246	35.3
3d plate	0.420	1.68–1.35 *P*	0.345	17.8	1.93–1.61–1.29 *P*	0.360	14.3	1.79–1.37 *P*	0.324	22.8
4th plate	0.440	1.73–1.38 *P*	0.336	23.6	1.96–1.64–1.32 *M*	0.354	19.5	1.79–1.43 *P*	0.329	25.2
5th plate	0.461	1.93–1.60 *P*	0.362	21.4	1.82–1.52 *P*	0.382	17.1	1.92–1.60–1.29 *P*	0.363	21.2
6th plate	0.500	1.93–1.67–1.39 *P*	0.420	16.0	1.85–1.59–1.33 *P*	0.438	12.4	1.77–1.47 *P*	0.394	21.2
7th plate	0.520	1.78–1.53–1.27 *M*	0.456	12.3	1.92–1.68–1.44 *G*	0.483	7.1	1.99–1.75–1.50 *P*	0.465	10.6
Bottom panel plate	0.540	1.72–1.46–1.22 *M*	0.475	12.0	1.94–1.72–1.47 *G*	0.477	11.7	1.97–1.73–1.48 *P*	0.470	13.0

Engineering Test Services, Inc.

Note: *G*, good reading, slight pitting; *M*, medium pitting up to 0.060 in.; *P*, pitting to 0.120 in.

Fig. 21. Bulkhead thickness measurement.

factory type of scaffolding consists of a **collapsible "umbrella" type of steel or aluminum platform.** The platform is folded like an umbrella, and lowered through a small outlet at the top. It is then expanded and raised or lowered to the desired level.

Relocation of Test Points. Various methods of relocation have evolved. Test locations may be spaced at 2-ft. intervals along vertical lines, spaced evenly around the inside surface, and about 2 ft. apart (or at closer intervals if desired). They can be located by measuring from a convenient point or by some form of guide. One unique method consists of using a **chain with large washers** spaced at the desired intervals. The chain is suspended from the top of the digester and the transducer located by fitting into each washer.

TEST RECORDS. Standard-data work forms should be devised for recording thickness data and resonance readings. Resonances are required for slide-rule conversion and are vital for future reference. Fig. 21 shows a **typical form for recording tanker data** obtained with the manually tuned instrument. Resonance readings are recorded in the field. Thickness is calculated and inserted in the proper column as soon as possible thereafter. Signals are classified as to strength and quality, as shown in Fig. 21. The notation *G* indicates a good signal with slight pitting; *M* indicates medium pitting of the order of 0.060 in. or less; and *P* indicates a broad, weak signal with pitting of 0.060 to about 0.120 in. under the transducer area. Complete records of resonant frequencies and signal quality will be invaluable for correlating or comparing with data taken in later years and should be filed for future reference. The fact that this information can be obtained by the manually tuned frequency-reading instrument is a definite advantage in using it.

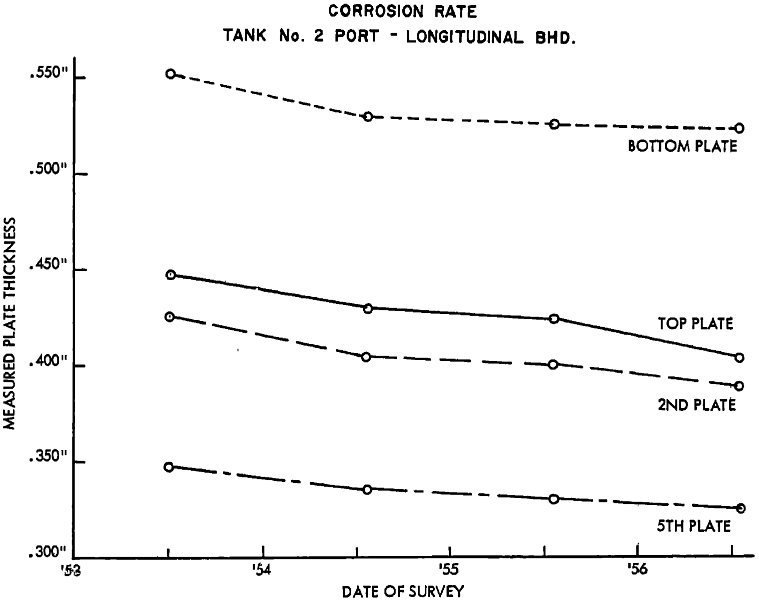

Engineering Test Services, Inc.

Fig. 22. Corrosion rate on Type T-2 tanker. No. 2 port longitudinal bulkhead determined by Audigage measurements.

EVALUATION OF DATA. An example of evaluations of thickness data is shown in Fig. 22. It is a typical graphical presentation of corrosion rate in an oil-tank ship. In this case a corrosion control system was installed in 1954, and thickness readings were taken at the same locations to evaluate the system each succeeding year. Each point represents one test location on the bulkhead. These readings were obtained with a manually tuned, ultrasonic resonance instrument on plates with a thickness variation of about 0.060 in. under the transducer. Thicknesses were calculated by the slide-rule method. Surface conditions were similar to those shown in Fig. 20(d).

GUIDE TO PROPER APPLICATION OF CORROSION TESTS. For corrosion tests to be most effective, the following points should be observed:

1. Nondestructive test methods should be used where drilling test holes is impractical or expensive, or will accelerate corrosion in repair areas. Under conditions where interior scale cannot be removed easily, ultrasonic tests are generally more accurate than micrometer measurement.
2. Ultrasonic resonance instruments should be used in preference to gamma-radiation type of equipment when the extent of internal scale or the absorption factor of the contents of the vessel is unknown.
3. In addition to thickness measurement, ultrasonic resonance equipment provides information as to degree of pitting (or corrosion) and presence of scale on the opposite, and usually unseen, surface of the test material.
4. Corrosion evaluation by ultrasonic methods should be undertaken only by competent and trained personnel who have a thorough understanding of the various factors involved.

References

1. Hubbard, J. C. "The Acoustic Resonator Interferometer: I. The Acoustic System and its Equivalent Electric Network," *Phys. Rev.*, [2] 38 (1931): 1011.
2. Erwin, W. S. (To General Motors Corp.) "Supersonic Measuring Means." U.S. Patent No. 2,431,233 (Nov. 18, 1947).
3. Rassweiler, G. M., and W. S. Erwin. (To General Motors Corp.) "Automatic Sonic Measuring Means." U.S. Patent No. 2,431,234 (Nov. 18, 1947).
4. Erwin, W. S., and G. M. Rassweiler. "The Automatic Sonigage," *Iron Age,* 160, No. 4 (1947): 48.
5. Branson, N. G. "Portable Ultrasonic Thickness Gage," *Electronics,* 21, No. 1 (1948): 88.
6. Cook, E. G., and H. E. Van Valkenburg. "Thickness Measurement by Ultrasonic Resonance," *J. Acoust. Soc. Am.*, 27 (1955): 564.
7. Evans, D. J. "Corrosion Evaluation of Ship Bulkhead and Hull Plating by Audigage Thickness Measurements," *Corrosion,* 11 (1955): 109t.
8. Baumeister, G. B. "Production Testing of Bonded Materials with Ultrasonics," *ASTM Bull.*, 204 (1955): 50.
9. Bloch, P. K. "Testing of Railroad Rails by the Ultrasonic Resonance Method," *Nondestructive Testing,* 10, No. 3 (Winter, 1951–1952): 16.
10. Hastings, Carlton H., and S. W. Carter. "Inspection, Processing, and Manufacturing Control of Metals by Ultrasonic Methods," *Am. Soc. Testing Materials, Spec. Tech. Publ.*, No. 101 (1951).

SECTION 51

NATURAL FREQUENCY VIBRATION TESTS

CONTENTS

PAGE

Characteristics of Resonance

- Principle of test 1
- Resonance 1
- Factors governing natural frequency 1
- Modes of vibration 1
  - Flexural mode 2
    - Fundamental flexural mode of vibration of a rectangular bar (*f.* 1) 2
  - Longitudinal mode 2
    - Fundamental longitudinal mode of vibration of a rectangular bar (*f.* 2) 2
  - Torsional mode 2
    - Fundamental torsional mode of vibration of a rectangular bar (*f.* 3) 2
  - Overtones or harmonics 2
    - Three-nodal (harmonic) flexural mode of vibration of a rectangular bar (*f.* 4) .. 3
  - Diametrical mode 3
    - Fundamental diameter mode of vibration of a thin circular disc (*f.* 5) 3
  - Radial mode 3
    - Fundamental radial mode of vibration of a thin circular disc (*f.* 6) 3
  - Annular mode 4
    - Fundamental flexural mode of vibration of a thin circular disc (*f.* 7) 4
  - Complex modes 4
- Frequency equations 4
  - Rectangular bar 4
  - Square bar 4
  - Circular plate 5
  - Circular plate with axial hole 5
  - Complex shapes 6
  - Measurable characteristics 6
  - Use of overtones 6

Equipment and Techniques

- Test equipment 6
  - Body supports 6
  - Excitation 7
  - Advantages of continuous excitation 7
  - Vibration detectors 7
- Test techniques 7
- Electrical connections 9
  - Block circuit diagram of Sonic Comparator (*f.* 8) 7
- Frequency scanning 9
- Interpreting indications 9
  - Sonic Comparator (*f.* 9) 8

PAGE

Industrial Applications

- Testing abrasive wheels 9
  - Correlation of impact and resonant frequency tests 10
    - Correlation of resonant frequencies with impact penetration tests of vitrified-bond abrasive wheels (*f.* 10) 10
  - Correcting frequency for dimensions 11
  - Variations in radial dimensions 11
  - Variations in thickness 11
  - Effects of composition 11
    - Correlation of resonant frequency with percentage of bonding material in vitrified-bond aluminum oxide grinding wheels (*f.* 11) 12
  - Modulus of rupture 12
- Flaw detection 12
  - Cracks in abrasive-honing sticks 12
    - Orientations of flaw simulated by saw cut (dotted line) with respect to directions of vibration (arrows) in tests of abrasive-honing sticks (*f.* 12) 13
    - Relation of depth of flaw (simulated by saw cut) to resonant frequencies in abrasive-honing stick (*f.* 13) 13
    - Relation of flaw depth (simulated by saw cut) to ratio of overtone to fundamental frequency in abrasive-honing sticks (orientation *A* of Fig. 12) (*f.* 14) 13
  - Radial cracks in grinding wheels 14
    - Possible locations of a radial flaw with respect to vibration nodes (dotted lines) in a grinding wheel (*f.* 15) 14
    - Relation of radial flaw depth (simulated by saw cut) to resonant frequency in grinding wheels (*f.* 16) 14
- References 15

SECTION 51

NATURAL FREQUENCY VIBRATION TESTS

Characteristics of Resonance

PRINCIPLE OF TEST. Ultrasonic resonance testing methods discussed in preceding sections use a beam of high-frequency vibrational energy transmitted into the test object (see section on Ultrasonic Resonance Tests). In addition a resonance vibration technique exists in which the test body itself is caused to vibrate as a whole in one of its natural frequency modes. Many physical characteristics of the body may be determined from the characteristics of the induced vibration. In most practical applications, the **natural frequencies** lie largely within the audible range, from a few to about 20,000 cycles per second (c.p.s.). For this reason resonance vibration testing often is called **sonic testing.** There is no theoretical reason why the principles may not be extended to higher frequencies, and tests have been made in the megacycle range.

RESONANCE. When a periodic disturbing force with a small displacement is applied to a body, the amplitude of vibration of the body approximates that of the disturbing force. As the frequency of the disturbing force approaches a natural frequency of vibration of the body, the **amplitude of vibration** increases, and when the two frequencies become equal, the vibration of the body reaches an indefinitely large amplitude, except as limited by **system losses.** This condition is known as **resonance.**

FACTORS GOVERNING NATURAL FREQUENCY. The natural frequency of mechanical vibration of a body is controlled by a number of factors which may be generalized in the expression:

$$\text{Frequency} = (\text{shape factor}) \times (\text{physical-constants factor}) \tag{1}$$

Shape factor includes the geometrical design of the body and the dimensional factors of length, width, and thickness. The **physical-constants factor** includes the modulus of elasticity, density, and Poisson's ratio for the test material.

It is axiomatic that two bodies, identical in every respect, will manifest identical natural frequencies of vibration. Eq. 1 indicates that if the shape factor of a number of bodies is held constant, the natural frequency of vibration of each of the bodies will be a discrete measure of the physical-constants factor. On the other hand, if the effect of the shape factor on frequency can be determined, compensation for differences in shape or size may be applied. Fortunately the influence of shape factor already has been studied by many investigators, although only for relatively simple geometric shapes.

MODES OF VIBRATION. Every object has many natural frequencies of vibration. The manner in which the object vibrates is known as the mode of vibration.

Flexural Mode. A simple, unsupported **rectangular bar** may vibrate in the bending or flexural mode, as shown in Fig. 1. In this mode there are two vibrational **nodes,** or planes of essentially zero amplitude of vibration, located approximately 0.22 times the over-all length from each end. The **antinodes,** or areas of maximum vibration, occur in the center and at each end of the bar.

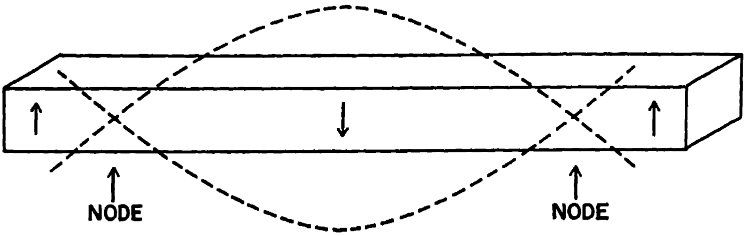

Fig. 1. Fundamental flexural mode of vibration of a rectangular bar.

Longitudinal Mode. The bar may also vibrate in the compression-tension or longitudinal mode, as diagrammed in Fig. 2, with a single nodal plane at its geometric center.

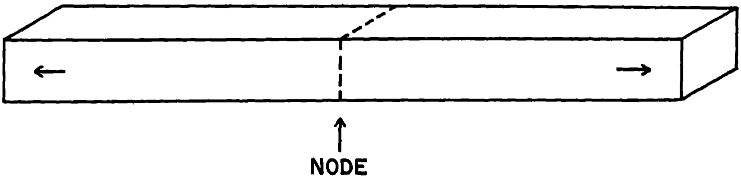

Fig. 2. Fundamental longitudinal mode of vibration of a rectangular bar.

Torsional Mode. The bar may vibrate in the twisting or torsional mode, as shown in Fig. 3, with a single nodal plane at its center.

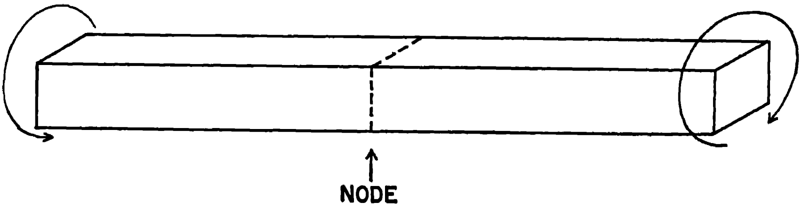

Fig. 3. Fundamental torsional mode of vibration of a rectangular bar.

Overtones or Harmonics. Only the fundamental flexural, longitudinal, and torsional modes have been discussed. In addition, each of these simple (gravest) modes exhibits higher-order **overtone natural frequencies** of vibration. For example, the first overtone of the flexural mode of vibration for an unsupported rectangular bar is shown in Fig. 4 and may be described as the **three-nodal flexural mode.** The frequency of this three-nodal flexural mode is approximately 2.7 times that of the two-nodal flexural mode pictured in Fig. 1. All three basic modes described have progressively higher overtones with a proportionally increasing number of nodes and antinodes of vibration. A body may be supported or clamped at its nodes without disturbing its natural vibration frequency or damping characteristics.

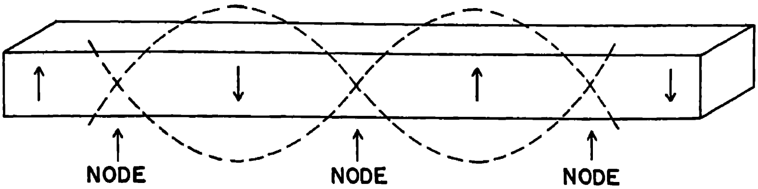

Fig. 4. Three-nodal (harmonic) flexural mode of vibration of a rectangular bar.

Diametrical Mode. A thin unsupported circular plate (disc) may vibrate in **flexure** in the gravest diametrical mode, shown in Fig. 5, with two nodal diameters crossing at right angles.

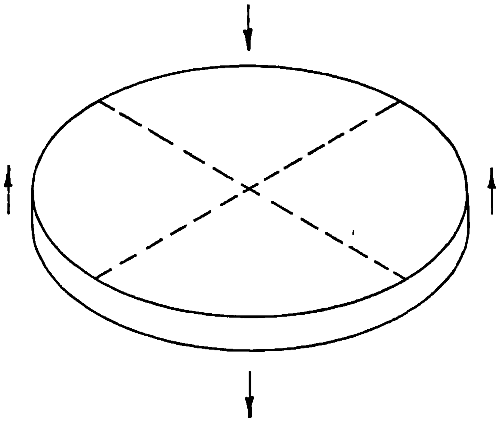

Fig. 5. Fundamental diameter mode of vibration of a thin circular disc.

Radial Mode. The same plate may vibrate in **compression tension** in the gravest radial mode, shown in Fig. 6, with a single node at its center and vibration in phase around its periphery.

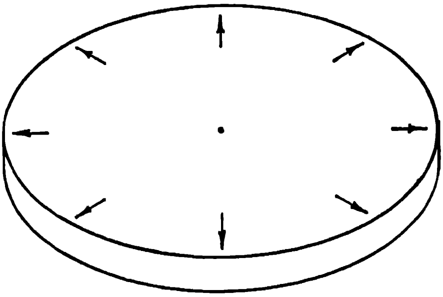

Fig. 6. Fundamental radial mode of vibration of a thin circular disc.

Annular Mode. In addition, circular plates may vibrate in flexure in the gravest annular mode, shown in Fig. 7, with a single annular node. For each of these modes, higher-order overtones and combinations of modes exist.[1]

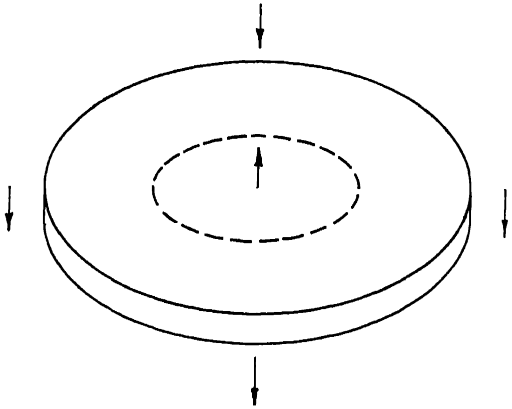

Fig. 7. Fundamental flexural mode of vibration of a thin circular disc.

Complex Modes. It may be expected that the complexity of modes and overtones would complicate the resonance vibration test. In general this is not the case because of the relatively large difference in the natural frequencies of each mode, together with the difficulty in exciting the **higher-order overtones.** Usually the lowest natural frequency of vibration is the most convenient to employ for a test.

FREQUENCY EQUATIONS. For simple geometric shapes the references to be cited are adequate for establishing the equations for the frequency of vibration of the bodies to be tested or compared. Three specific cases will be discussed to indicate the method used: the rectangular bar, the circular plate, and the circular plate with an axial hole.

Rectangular Bar. For a rectangular bar, the general expression is[2]

$$f = \frac{k^2}{2\pi l^2}\sqrt{\frac{EIg}{A\rho}} \tag{2}$$

where f = frequency, c.p.s.
k = constant, depending upon mode of vibration.
l = length, in.
E = Young's modulus, p.s.i.
I = moment of inertia, $bh^3/12$.
g = acceleration due to gravity, in./sec.^{2}.
A = area of cross-section, square in.
ρ = density, lb./cu. in.
b = width normal to direction of flexure, in.
h = depth in direction of flexure, in.

Square Bar. For a square bar in which the depth (thickness) and width are equal, the equation takes the form of

$$f = \frac{k^2 h}{2\pi l^2}\sqrt{\frac{Eg}{12\rho}} \tag{3}$$

or collecting the constants and using for k a value of 4.73 for the fundamental flexural mode of an unsupported bar,

$$f = \frac{20.3h}{l^2}\sqrt{\frac{E}{\rho}} \tag{4}$$

To compare the **moduli of elasticity** of a number of similar square bars, the equation is rewritten as

$$E = \frac{0.00242f^2l^4\rho}{h^2} \tag{5}$$

Circular Plate. For the circular plate,[3] the general form of the expression is

$$f = \frac{k}{2\pi r^2}\sqrt{\frac{gD}{\rho h}} \tag{6}$$

where f = frequency, c.p.s.
g = acceleration due to gravity, in./sec.^{2}.
$D = Eh^3/12\ (1 - \sigma^2)$ modulus of flexural rigidity, lb.-in.
E = modulus of elasticity, p.s.i.
r = radius, in.
h = depth, in.
k = constant, depending upon mode of vibration.
ρ = density, lb./cu. in.
σ = Poisson's ratio.

Solving for the **equation for frequency,** using a value for k of 5.25 for the two-nodal diameter mode, gives

$$f = \frac{4.74h}{r^2}\sqrt{\frac{E}{\rho(1 - \sigma^2)}} \tag{7}$$

To compare the **modulus of elasticity** of a number of similar circular plates, the equation is rewritten as

$$E = \frac{0.0445f^2r^4\rho(1 - \sigma^2)}{h^2} \tag{8}$$

Circular Plate with Axial Hole. A special case is the circular plate with an axial hole, such as an abrasive wheel. A **correction factor** has been developed for the two-nodal diameter mode, which involves the hole radius and the plate radius, as

$$\left[1 - \left(\frac{R}{r}\right)^2\right] \tag{9}$$

where R = hole radius, in.
r = plate radius, in.

When this factor is applied to the **frequency equation for the two-nodal diameter mode** of the plate, the revised expression, including all dimensions, takes the form of

$$f = \frac{4.74h\ (r^2 - R^2)}{r^4}\sqrt{\frac{E}{\rho(1 - \sigma^2)}} \tag{10}$$

The correction has been checked empirically and is accurate for thin plates within approximately 1 percent for ratios of plate radius to hole radius exceeding 3:1 or 4:1. As the hole radius approaches the plate radius, the body begins to take the form of a ring. Its frequency characteristics are best studied by investigating references to flexural, radial, and torsional vibrations of circular rings.[4]

Further, the validity of this correction has not been established for diameter-to-thickness ratios below 6:1 or 7:1.

Complex Shapes. Cases may occur in which the geometry of the articles to be compared by resonance vibration testing is more complex. If frequency equations cannot be developed, one solution is to change the dimensions of a typical article progressively and to measure the resulting change in frequency. Such techniques can be used to evaluate the influence of shape factor and permit correction to be applied for small dimensional differences.

A second solution is to produce a **dummy article** of simple geometric shape from the same materials and by the same processing techniques used for the complex articles. Measurements on the dummy article permit evaluation of the physical characteristics of the articles in question.

Measurable Characteristics. The frequency equations include the effects of all dimensions and physical properties. When the equation is available, it is possible to evaluate one unknown factor (where all other factors are known) by the rapid measurement of the natural frequency of vibration. Theoretically, and in many practical applications, the resonance vibration test is adaptable to the measurement or detection of:

1. Length
2. Width.
3. Thickness.
4. Diameter.
5. Modulus of elasticity.
6. Density.
7. Poisson's ratio.
8. Modulus of rupture.
9. Flaws.
10. Damping capacity.
11. Shear modulus.
12. Temperature dependence of items 5, 7, 8, 10, and 11.
13. Metallurgical factors.

By comparing natural frequencies of vibration for modes of vibration which produce shear, flexure, and compression tension, it should be possible to study **compression-tension, shear, and bulk moduli** as well as **Poisson's ratio** through their direct mathematical relationships.[5] It will be shown later how **flaws** and other **inhomogeneities** can be detected by resonance vibration testing.

Use of Overtones. It is of practical interest to note that as long as the mode and overtone of vibration are held constant, any overtone may be employed to evaluate the **relative physical constants factor.** As shown in Eqs. 2 and 6, the constant k is determined only by the mode of vibration. It is conceivable that the dimensions of a body could be so large as to throw the lowest natural frequency of vibration below the range of available frequency-determining instruments. It is possible in such cases to employ higher-order overtones and the resulting higher frequencies.

Equipment and Techniques

TEST EQUIPMENT. Selection of test equipment involves consideration of test body supports, means of exciting vibrations, and detection of resonance vibrations.

Body Supports. The body under test should be supported for the preferred mode of vibration with supports located at the **nodes of vibration** for the mode and overtone employed. For example, referring to Fig. 1 for the fundamental flexural mode of a bar of length l, two supports can be placed under the bar at a distance $0.22l$ from each end. Referring to Fig. 5 for the fundamental diametrical mode of a circular plate, four supports can be placed under the plate along the nodal diameters. Alternatively a single support or clamp can be arranged at the center of the plate at the intersection of the two nodal diameters.

In selecting means for supporting or clamping other shapes, it is important that support be provided only at the nodes of vibration, to prevent **damping the vibrations** under study.

Excitation. Two methods for exciting the natural period of vibration are available: (1) shock excitation or (2) continuous excitation. For shock excitation a **manual or mechanized striker** device can be employed. For continuous excitation, an **electromechanical vibration exciter** is used in conjunction with a variable-frequency generator covering the frequency range of interest.

Advantages of Continuous Excitation. Continuous excitation has several advantages for resonance vibration testing of materials. It permits:

1. Detection of the natural frequency of vibration in bodies having high damping characteristics.
2. Examination of the mode of vibration with sand patterns, or with sound or vibration pick-ups.
3. Excitation of a single natural frequency at one time so that the fundamental frequency is not masked by other modes or overtones.
4. Less critical attention to the damping introduced by the supports.

Vibration Detectors. Of the several methods available for detecting natural frequency or resonance vibrations, the **microphone** and **vibration pick-ups** have found the widest general use. The microphone, which employs air coupling to the vibrating body, need not be repositioned each time an article is placed on the testing supports, nor does it load the specimen under test. On the other hand it is sensitive to **ambient noise.** The vibration pick-up, which employs mechanical coupling to the vibrating body and is not so sensitive to ambient noise, is influenced by **floor vibrations** transmitted to the body through its supports. The most suitable vibration detector is best determined by considering the limitations inherent in a particular testing process. It is a simple matter to shift from one type of detector to the other for different conditions.

TEST TECHNIQUES. References 6 to 22 (end of section) give several methods for **measuring the natural frequency** of vibration of solid objects as

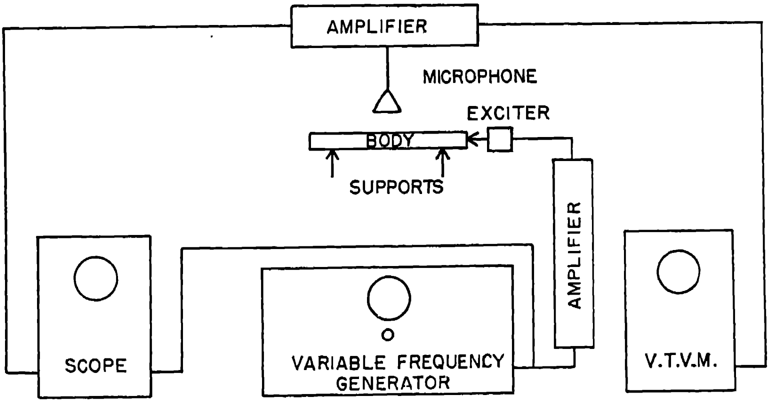

Saturn Electronics Co.

Fig. 8. Block circuit diagram of Sonic Comparator.

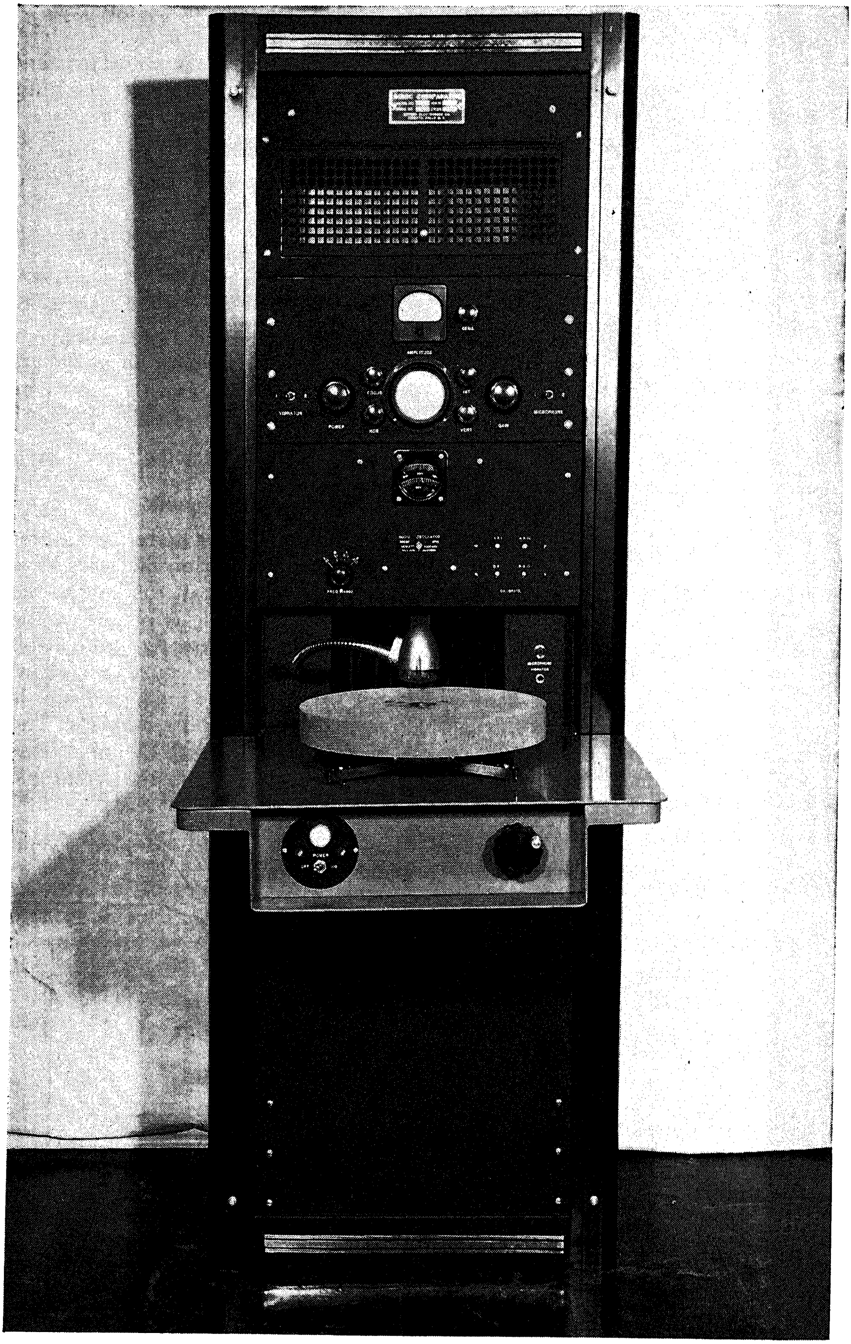

Saturn Electronics Co.

Fig. 9. Sonic Comparator.

well as various applications of these methods. For illustrative purposes one instrument, the **Sonic Comparator** (Saturn Electronics Company, Niagara Falls, New York), integrates the elements necessary to make such measurements.[6] In this apparatus the test body is supported at the nodes of a preferred mode of vibration. The stylus of an electromagnetic vibration exciter is positioned in contact with the test object near an antinode of vibration.

Electrical Connections. The exciter is driven through a power amplifier by a calibrated variable-frequency generator, which is connected to the horizontal deflection plates of a **cathode-ray oscilloscope.** A microphone is positioned near an antinode of vibration of the body and connected through an amplifier to the vertical deflection plates of the oscilloscope. An auxiliary jack and switch facilitate the connection of a vibration pick-up. A second connection from the microphone amplifier is made to a front-panel **vacuum-tube voltmeter** to indicate relative amplitudes of vibration. The diagrammatic circuit is shown in Fig. 8.

Frequency Scanning. When the frequency of the preferred mode of vibration is unknown, yet within the range of the generator, the **frequency spectrum** is scanned from the lowest toward the highest frequency with the variable-frequency generator. As the spectrum is scanned, the normally horizontal trace on the oscilloscope periodically forms various **Lissajous patterns** of four, three, or two loops lying along a horizontal line. This effect occurs because the output of the electromechanical driving system contains **harmonics** of the generator frequency in sufficient amplitude to excite the body at its natural frequency. This effect is helpful. For example, when a three-loop trace is observed, the generator can be set to three times its indicated frequency to produce resonance between the driving mechanism and the test body. Because of resonance phenomena and the resulting vibrational amplitude amplification, little **driving energy** is required by materials with low damping factors.

Interpreting Indications. The increase in vibrational amplitude at resonance actuates the vibration detector and amplifier, causing the normally straight, horizontal **oscilloscope trace** to take the form of a canted straight line, ellipse, or circle, depending upon phase relationships. This same signal actuates a vacuum-tube voltmeter which indicates the relative amplitude of vibration.

In **production testing,** the frequency of the body is known within relatively narrow limits, and it is necessary to scan only between these limits. This reduces the time required for frequency determination to a bare minimum. Depending upon size, as many as 250 to 300 pieces per hour can be tested with the Sonic Comparator shown in Fig. 9.

Industrial Applications

TESTING ABRASIVE WHEELS. The application of resonance vibration or sonic tests to the manufacture of abrasive articles will illustrate principles for evaluating other potential uses. An important characteristic of bonded abrasive products is **grade or hardness,** which measures the tenacity with which the individual abrasive particles are bonded together, and hence determines the action of the grinding wheel. One method for estimating grade employs a **chisel-shaped tool** pressed manually into the grinding wheel by a skilled operator. The operator grades the wheel within broad limits by the "feel." A second method, known as the **impact method,** involves a mechanism for repeatedly dropping a hardened tool upon the wheel surface and measuring the depth of tool penetration after a fixed number of drops. Alternatively a **pointed oscillating tool** can be forced into the abrasive wheel by a known pressure, and the depth of tool penetration can be measured after a fixed number of oscillations. These tests are not intended to compare different types of abrasive products containing different abrasives, bonds, or abrasive grain sizes. Rather, they are applied to supposedly identical abrasive products to determine the difference between them. While relatively time-consuming, the mechanized tests correlate well with actual grinding data.

Correlation of Impact and Resonant Frequency Tests. When several vitrified-bond abrasive wheels are arranged in order of increasing hardness, as determined by the impact penetration test, the **natural period of vibration** of the wheels shows an orderly increasing frequency. Plotting the natural frequency of the two-nodal diameter mode of vibration against the impact penetration results in essentially linear relationships, as typified by Fig. 10. Graphs of this type indicate that an excellent correlation exists between the two methods, at least for abrasive **grit size numbers** of the order of 36 and finer. (For data on abrasive grit size numbers, see "Simplified Practice Recommendations," Bull. No. 118–50, U.S. Department of Commerce, National Bureau of Standards.) For **larger grit sizes,** of the order of 20 and coarser, a poorer correlation is obtained, presumably because the accuracy of the impact test is impaired when the abrasive grit size approaches the dimensions of the point of the impact tool. In such experiments it has been observed that the greater the number of impact holes which are averaged in securing the impact penetration, the greater the tendency for all points to fall into a smooth curve. This can be expected because the sonic test averages the entire wheel grade, whereas the impact test gives the grade at the point immediately under the tip of the impact tool. Thus, for each type and size of abrasive wheel, **high and low frequency limits** can be estab-

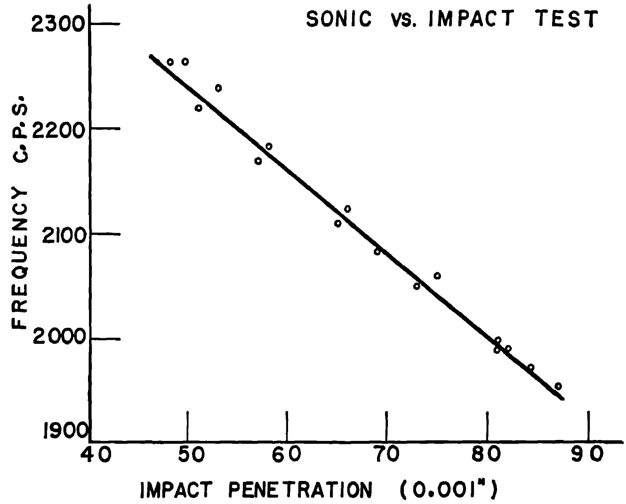

Fig. 10. Correlation of resonant frequencies with impact penetration tests of vitrified-bond abrasive wheels.

lished. Wheels within the limits are passed, and those beyond the limits are rejected.[7]

The success of the sonic test for bonded abrasive products is due to the fact that the quality or measured characteristic varies with the physical-constants factor in Eq. 1 and hence with the natural frequency of vibration. This relationship, or a variation of it, probably exists for many other articles of manufacture.

Correcting Frequency for Dimensions. Because the natural frequency varies with dimensions as well as physical properties, it is necessary to consider the effect of dimensions on the results of the test.[8] In practice, wheels manufactured by certain processes are sufficiently similar in dimensions to permit sonic testing for grade before edging and facing. Thus **off-grade wheels** can be rejected prior to expensive finishing operations. Other manufacturing techniques may produce wheels with less dimensional uniformity. In these instances sonic testing can be employed after the **edging and facing operation.** Grading methods based on surface penetration or attrition generally are limited to application only after facing because of adverse effects of surface skins and irregularities.

Variations in Radial Dimensions. In sonic testing of most abrasive wheels, two factors combine to minimize the users' concern with the influence of radial dimensions on the natural frequency. Since the wheels are formed in a mold of fixed diameter with an arbor pin of fixed diameter, variations in these dimensions are not large. Secondly, by definition, a circular plate has a small thickness dimension in relation to its radial dimension. As indicated by Eq. 7, variations of several thousandths of an inch in a radial dimension of 3 to 4 in. or more do not produce a large change in frequency.

Variations in Thickness. On the other hand, variations of several thousandths of an inch in a thickness of less than one-quarter of an inch are of greater significance. With certain types of **unfinished thin wheels,** where thickness variations are large and close limits on grade accuracy are required, the thickness can be measured and the frequency corrected by substitution in Eq. 11; i.e.,

$$F = \frac{fh_n}{h_m} \tag{11}$$

where F = corrected frequency.
h_n = nominal thickness.
f = measured frequency.
h_m = measured thickness.

For a series of wheels, each nominally ½ in. thick, variations from nominal thickness occur in manufacture. The corrected frequency is the natural resonant frequency which would be observed if the wheel were actually ½ in. thick. Whether **correction** need be applied is governed by (1) the grading accuracy required, (2) the accuracy of the facing equipment, or (3) the dimensional uniformity produced by the particular manufacturing process.

Effects of Composition. The effect of innumerable combinations of abrasive grain and bond is beyond the scope of this discussion. However, for illustrative purposes, the variations in frequency with two different bonds and three bond percentages are shown in Fig. 11. The data have been taken from a series of 8 × ½ × 1½-in., 80-grit, vitrified-bond aluminum oxide wheels. They illustrate the manner in which frequency increases with increasing bond percentage. Similar curves characterize silicon carbide abrasive wheels as well as different bond and grain aggregations.

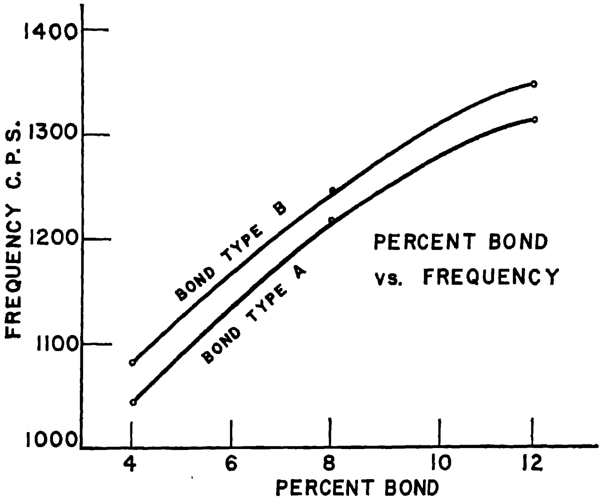

Fig. 11. Correlation of resonant frequency with percentage of bonding material in vitrified-bond aluminum oxide grinding wheels.

Modulus of Rupture. The sonic test is finding increasing use for the nondestructive comparison of rupture moduli of resin-bonded abrasive products. Investigators have established that a correlation exists between natural frequency of vibration and modulus of rupture.[9, 10] In practice, the **ultimate bursting speed** of supposedly identical resin-bonded abrasive wheels varies with the natural frequency of vibration. A typical correlation between rotational bursting speeds and resonant frequencies for a series of resin-bonded, 18 × 2 × 7-in. abrasive wheels is given in the table here.

Resonant Frequency, c.p.s.	Breaking Speed, r.p.m.
670	3500
680	3550
692	3600
700	3650

FLAW DETECTION. Resonance vibration testing can be used to detect many types of flaws in bodies of different shapes, depending upon the skill with which the testing procedure is conceived and applied. Several examples pertaining to abrasive articles are discussed to illustrate typical applications.

Cracks in Abrasive-honing Sticks. An abrasive-honing stick, which may take the form of a square bar with dimensions 5/16 × 5/16 × 8¼-in., can be arranged for the fundamental flexural mode of vibration as in Fig. 1. In this example the flaw is simulated by a lateral saw cut at the center of the bar. The flaw can be oriented in two directions with respect to the direction of vibration, as shown in Fig. 12, which shows end views of the same bar in two positions.

The **method for detecting the flaw** consists of measuring the resonant frequencies of the fundamental mode after placing the bar in each of the *A* and *B* orientations. Fig. 13 has been prepared from actual measurements of a simulated and progressively deepened flaw. The **difference in frequency** between orientations *A* and *B* progressively increases with the depth of the flaw. If the flaw is nearer one end of the bar, the frequency difference will be reduced.

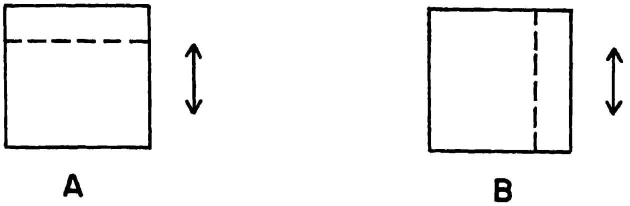

Fig. 12. Orientations of flaw simulated by saw cut (dotted line) with respect to directions of vibration (arrows) in tests of abrasive-honing sticks.

In working with **flexural vibrations of flawless bars** of apparently square cross-section, sometimes two resonant frequencies lying close together are detected. This phenomenon occurs because the bar is not exactly square. Most methods of exciting vibration in a particular direction produce components of motion in other directions. In this case one resonant frequency results from vibration in the thickness direction and the other from vibration in the width direction.

Depth of Flaw, in.	Frequency in c.p.s. with Orientation*		Frequency Difference
	A	*B*	
0	1552	1552	0
¹⁄₁₆	1533	1541	8
⅛	1469	1533	64
³⁄₁₆	1400	1513	113
¼	1327	1507	180

* Orientations *A* and *B* are shown in Fig. 12.

Fig. 13. Relation of depth of flaw (simulated by saw cut) to resonant frequencies in abrasive-honing stick.

A second method for detecting the flaw consists of measuring the ratio of the frequency of overtone modes to that of the fundamental mode. In the honing stick, the frequency f_2 of the first overtone flexural mode is compared with the

Depth of Flaw, in.	Frequency, c.p.s.		
	f_1	f_2	f_2/f_1
0	1552	4260	2.74
¹⁄₁₆	1533	4259	2.78
⅛	1469	4258	2.90
³⁄₁₆	1400	4257	3.04
¼	1327	4256	3.21

Fig. 14. Relation of flaw depth (simulated by saw cut) to ratio of overtone to fundamental frequency in abrasive-honing sticks (orientation *A* of Fig. 12).

frequency f_1 of the fundamental flexural mode. The data given in Fig. 14 result when using orientation *A* of Fig. 12. In this case the frequency ratio increases progressively with the depth of the flaw.

Radial Cracks in Grinding Wheels. A type of flaw encountered in certain abrasive wheels consists of radial cracks extending from the arbor hole toward the periphery. The effects on natural frequency produced by such flaws can be demonstrated with an 8¼-in. diam. by ½ in. thick by 1½-in. bore vitrified-bond wheel. The fundamental flexural mode of vibration for a disc is used. A progressively deepened radial saw cut serves as the **simulated flaw,** extending from the arbor hole toward the periphery. When the wheel is placed in contact with the vibration exciter, the two nodal diameters are established with angular orientations of plus and minus 45 deg. from the exciter. Thus the angular position of the nodal radii within the wheel is determined by the position of the wheel with respect to the exciter.

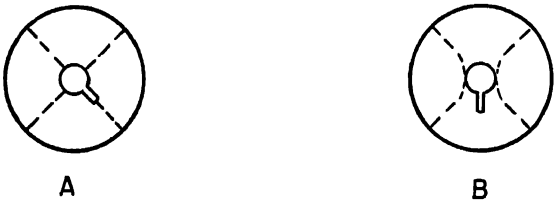

Fig. 15. Possible locations of a radial flaw with respect to vibration nodes (dotted lines) in a grinding wheel.

Of the many possible **orientations of the flaw** with respect to a nodal radius, the flaw may lie on the center of a node or of an antinode, as illustrated by *A* and *B* in Fig. 15. Fig. 16 was prepared by measuring the frequency for the two orientations when progressively lengthening the simulated flaw. A practical test for radial cracks consists of orienting the wheel in several different positions some 10 or 20 deg. apart and scanning the adjacent frequency spectrum for a second resonant frequency.

These procedures indicate how the sonic test for flaw detection extends the scope and utility of resonance vibration techniques.

Depth of Flaw, in.	Frequency, c.p.s.		Frequency Difference
	Flaw at Node	Flaw at Antinode	
0	1243	1243	0
¼	1242	1239	3
½	1238	1233	5
¾	1236	1226	10
1	1232	1215	17

Fig. 16. Relation of radial flaw depth (simulated by saw cut) to resonant frequency in grinding wheels.

References

1. Waller, M. D. "'Vibrations of Free Circular Plates. Part 1: Normal Modes," *Proc. Phys. Soc.* (London), 50, No. 1 (1938): 70.
2. Timoshenko, S. *Vibration Problems in Engineering.* New York: D. Van Nostrand Co., Inc., 1928. P. 199.
3. ———. *Vibration Problems in Engineering.* New York: D. Van Nostrand Co., Inc., 1928. P. 312.
4. ———. *Vibration Problems in Engineering.* New York: D. Van Nostrand Co., Inc., 1928. P. 292.
5. Marks, L. S. (ed.). *Mechanical Engineering Handbook.* 4th ed. New York: McGraw-Hill Book Co., Inc., 1941. P. 444.
6. Rowe, R. G. (To The Carborundum Co.) "Vibration Apparatus for Testing Articles," U.S. Patent No. 2, 486, 984 (Nov. 1, 1949).
7. ———. "Sonic Tests Grade Abrasive Wheels," *Steel,* 126, No. 26 (1950): 74, 84.
8. ———. "Testing Abrasive Wheels with the Sonic Comparator," *Nondestructive Testing,* 10, No. 2 (1951): 29.
9. Prigge, R. E. "Correlation of Modulus of Rupture and Modulus of Elasticity." B.S. Thesis, New York State College of Ceramics (May, 1951).
10. Williams, R. M. "Sonic Apparatus for Measuring Modulus of Elasticity of Resin Bonded Abrasives." M.S. Thesis, New York State College of Ceramics (May, 1951).
11. Grime, G. "Determination of Young's Modulus for Building Materials by a Vibration Method," *Phil. Mag.* [7] 20 (1935): 304.
12. Grime, G., and J. E. Eaton. "Determination of Young's Modulus by Flexural Vibrations," *Phil. Mag.* [7] 23 (1937): 96.
13. Powers, T. C. "Measuring Young's Modulus of Elasticity by Means of Sonic Vibrations," *Am. Soc. Testing Materials, Proc.,* 38, Pt. II (1938): 460.
14. Obert, L. "Sonic Method of Determining Modulus of Elasticity of Building Materials under Pressure," *Am. Soc. Testing Materials, Proc.,* 39 (1939): 987.
15. Hornibrook, F. B. "Discussion on Sonic Method for Modulus of Elasticity," *Am. Soc. Testing Materials, Proc.,* 39 (1939): 996.
16. Forgue, S. V., and G. A. Loomis. "Modulus of Elasticity of Dinnerware Bodies by a Sonic-Vibration Method," *Bull. Am. Ceram. Soc.,* 20, No. 12 (1941): 425.
17. Pickett, G. "Equations for Computing Elastic Constants from Flexural and Torsional Resonant Frequencies of Vibration of Prisms and Cylinders," *Am. Soc. Testing Materials, Proc.,* 45, Pt. II (1945): 846.
18. Colonna-Ceccaldi, J. "L'essai au son des meules céramiques (Sound Tests of Ceramic Grindstones)," *Mécanique,* 30 (1946): 253.
19. Baab, K. A., and H. M. Kramer. "Sonic Method for Determining Young's Modulus of Elasticity," *J. Am. Ceram. Soc.,* 31 (1948): 318.
20. Decker, A. R. "Note Regarding the Sonic Determination of Modulus of Elasticity Using Round-Section Bars," *J. Am. Ceram. Soc.,* 33 (1950): 192.
21. Dorn, J. E., and T. E. Teitz. "The Modulus of Elasticity—A Review of Metallurgical Factors," *Metal Progr.,* 58, No. 1 (1950): 81.
22. Andrews, C. W. "Effect of Temperature on the Modulus of Elasticity," *Metal Progr.,* 58, No. 1 (1950): 85; "Dynamic Modulus," *Metal Progr.,* 58, No. 1 (1950): 96.

SECTION 52

BRITTLE-COATING TESTS

CONTENTS

PAGE

Brittle-Coating Materials

- Principle of test ... 1
  - Calibration ... 1
    - Brittle-coating calibration apparatus (*f.* 1) 2
  - Brittle coatings ... 1
  - Operating range ... 1
  - Applications ... 2
    - Dye-etched brittle-coating crack patterns on a Catalin disc which has been rotated at various speeds (*f.* 2) ... 3
- Characteristics of resin-type brittle coatings 3
  - Effects of temperature and humidity ... 4
  - Response to strain ... 4
  - Use of several different coatings ... 4
- Selection of resin-type coatings ... 5
  - Coating selection chart ... 5
    - Resin-type, brittle-coating selection chart (*f.* 3) ... 5
  - Selecting coatings for high-threshold strain 6
- Characteristics of ceramic-type brittle coatings ... 7
  - Coefficient of thermal expansion ... 7
  - Calibration ... 7
- Selection of ceramic-type brittle coatings ... 8
    - Ceramic-coating selection chart (*f.* 4) ... 8
  - Safety precautions ... 8

Test Techniques

- Preparation of test specimens for resin-type coatings ... 9
  - Applying aluminum undercoat ... 9
  - Applying resin coatings ... 9
  - Temperature during resin-coating application 9
  - Drying of resin coatings ... 9
- Calibration of resin coatings ... 10
  - Tension-strain calibration procedure ... 10
  - Compression-strain calibration procedure .. 10
  - Calibrating resin coatings for high-threshold strain ... 10
  - Computing stress from strain ... 10
  - Creep correction ... 11
    - Creep correction chart (*f.* 5) ... 12
- Detecting cracks in resin coatings ... 11

PAGE

  - Visual inspection ... 13
    - Cracks in brittle coating as seen visually with proper illumination (*f.* 6) ... 13
  - Dye-etching technique ... 14
    - Dye-etched crack patterns (*f.* 7) ... 14
  - Electrified-particle technique ... 15
    - Electrified-particle indication of cracks in a brittle coating (*f.* 8) ... 15
- Preparation of test specimens for ceramic-type coatings ... 16
  - Preparing coating materials ... 16
  - Applying ceramic coatings ... 16
  - Firing of ceramic coatings ... 17
  - Detecting cracks in ceramic coatings ... 17

Applications of Brittle-Coating Tests

- Basic considerations ... 18
- Jigs and testing apparatus ... 18
  - Static tests ... 18
  - Dynamic tests ... 18
  - Control of temperature ... 19
- Measuring strain under static loading ... 19
    - Marking of various values of threshold strain (*f.* 9) ... 20
  - Tension strains ... 19
  - Compression strains ... 19
- Measuring strain under dynamic loading ... 21
  - Outdoor tests ... 21
- Typical brittle-coating tests ... 21
  - Measuring tension strains: continuous-load-ing technique ... 22
  - Measuring tension strains: return to zero-load technique ... 23
  - Measuring compression strains ... 23
- Sensitization and measuring small strains ... 23
- Measuring residual stress ... 24
    - Residual tension and compression stresses revealed by drilling small holes into specimen surface (*f.* 10) ... 24
- Indicating gross strain by flaking of coating 25
- Correction for direct pressure effect in hydraulic loading ... 26
- Photographing crack patterns ... 26
- Bibliography ... 27

SECTION 52

BRITTLE-COATING TESTS

Brittle-Coating Materials

PRINCIPLE OF TEST. A brittle coating is defined as one which will fracture in response to strain in the structure beneath it. To be useful, a brittle coating should indicate the **direction and magnitude of strain** within the elastic limit of the base material. Brittle coatings provide a graphic picture of the distribution, direction, location, sequence, and magnitude of tensile strains. The coatings fracture at a predetermined value, and cracks occur normal to the **principal tension strain.** The strain values at which the coatings fracture are determined by a method of calibration.

Calibration. Brittle coatings are calibrated by coating the part and a **calibration test bar.** The bar is deflected a fixed amount in a **cantilever-beam test fixture** shown in Fig. 1(a). By placing the test bar in a **strain scale,** as shown in Fig. 1(b), the least amount of strain required to fracture the coating is determined. The first crack appearing on the coated test part occurs at the same strain as those on the calibration bar.

Brittle Coatings. The brittle coatings in use are of two types. **Resin-type brittle coatings** are most widely used in the moderate temperature range (50° F. to 110° F.). **Ceramic-type brittle coatings** are used where temperatures may reach 700° F., for operation in water and oil, or for prolonged out-of-doors testing. The resin coatings permit higher accuracy of strain measurement, where they can be used, but the ceramic coatings can give a qualitative **stress pattern** under severe test conditions for which resin coatings are not suitable.

Operating Range. Under normal conditions of use, the range in which resin-type brittle coatings begin to fracture is from about 500 to 3000 μin. per in. strain. In steel these values correspond to stresses from 15,000 to about 90,000 p.s.i. With careful handling, resin-type brittle coatings yield quantitative results accurate to about ±10 percent.

Ceramic-type coatings for use on various steels are most useful in types designed for the medium and lower range of **coefficient of thermal expansion.** In types designed for higher ranges of expansion coefficients, they have more limited usefulness, due to poorer strain sensitivity. Depending upon the type of steel on which the coating is used, strain sensitivity ranges from about 400 to 1200, 1800, or higher μin. per in. strain. The greatest sensitivity attainable is about 2000 μin. per in., for at this point the ceramic coatings are about to craze. With presently available coatings this **crazing** generally occurs only for metals with a thermal coefficient of expansion of about 7.2×10^{-6} in. per inch per degree Fahrenheit, or less.

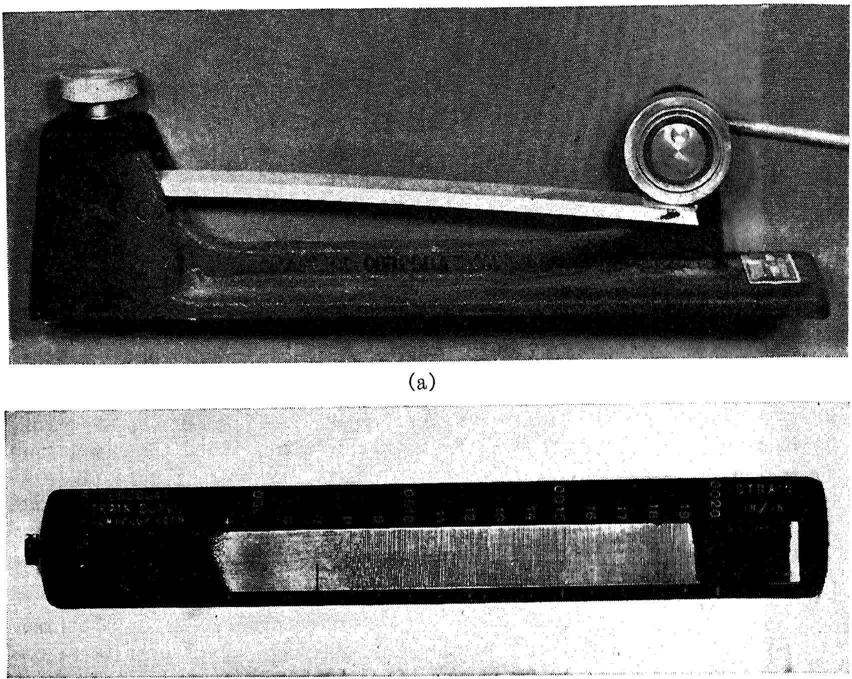

(a)

(b)

Magnaflux Corporation

Fig. 1. Brittle-coating calibration apparatus. (a) Cantilever-beam test fixture. (b) Test bar in strain scale.

Applications. Brittle coatings can show general stress distribution over the surface of complex structures, as shown in Fig. 2. A preliminary brittle-coating test can indicate points and directions to which **wire-resistance strain gages** can be applied to obtain more accurate quantitative values of maximum stress (see section on Resistance Strain-Gage Tests). Accurate, localized **stress-analysis data** obtained by brittle-coating tests are of primary importance in designs utilizing:

1. Ductile materials operating under repeated loading conditions.
2. Brittle materials under any type of load.

Correlation between possible failure and high local stress is excellent under these conditions. Ductile materials under static load show little correlation between localized stresses and failure. Designers of such structures are best aided by analyses showing the broader patterns of stress distribution.

Residual stresses induced in structures by heat treatment or assembly operations can be measured in the final product by a technique involving the drilling of small holes to a shallow depth through a very brittle coating. When locked-up stresses are induced by a process not involving appreciable temperature or time, they can be measured by having a coating on the part during the application of the load. **Thermal stresses** imposed by differences of temperature of the order of several hundred degrees are the only major source of stress that cannot be directly measured. Indirect methods can be applied to some problems, however. For simple problems **mechanical loading** can be imposed at room temperature

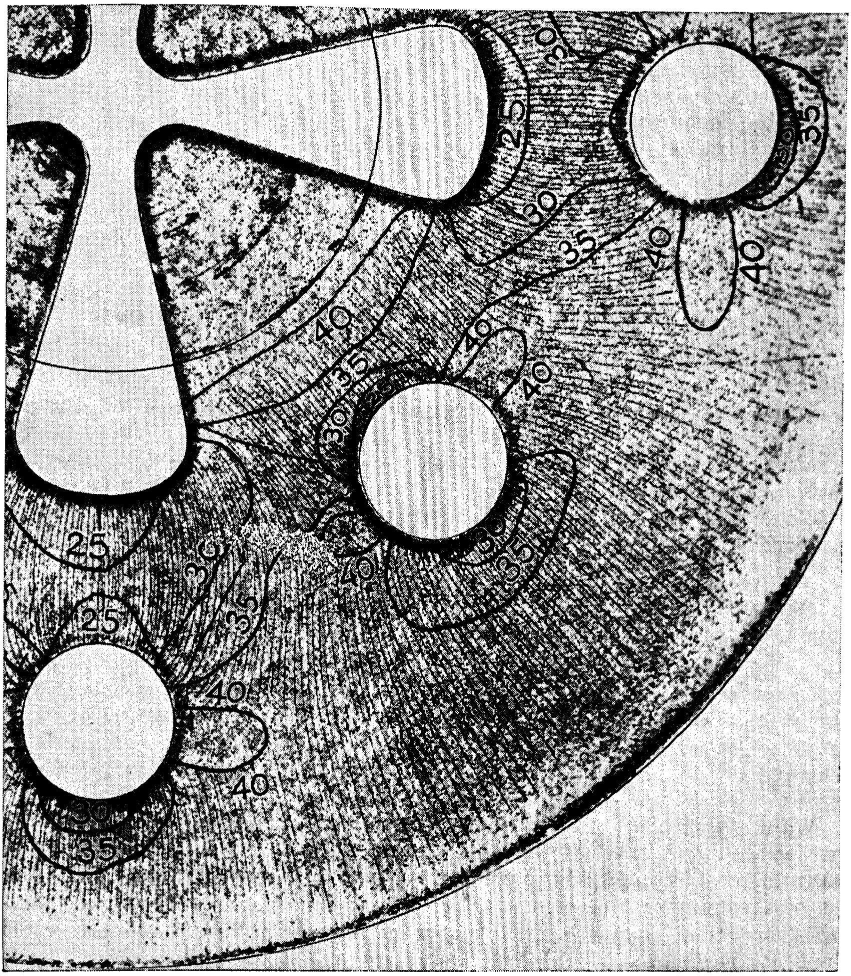

Armour Research Foundation

Fig. 2. Dye-etched brittle-coating crack patterns on a Catalin disc which has been rotated at various speeds.

to simulate thermal loading under operation. If the structure yields under load at high temperature, it may be possible to cool the structure to room temperature and measure the distribution of residual stress, thus giving some clue to the stress imposed during operation.

Although brittle coatings are sensitive to temperature changes, they can be used out-of-doors to obtain important operating stresses.

CHARACTERISTICS OF RESIN-TYPE BRITTLE COATINGS. It has long been recognized that a brittle coating on stressed metal parts furnishes an excellent means of detecting overloaded regions. Since the days of wrought-iron bridges, the cracking of brittle oxide scale on hot-rolled and annealed steel has been used to indicate local yielding. Attempts to use varnish, lacquer, or molten resins which would crack at values of strain within the elastic range have been described as early as 1932. In 1937, a more complete study of brittle lacquer behavior was started. Extensive work resulted in the removal of several limitations encountered earlier. In 1938, coatings were marketed in the form of **air-drying lacquers** (Magnaflux Corporation "Stresscoat") which are sprayed on a test part and used after a period of drying.

Effects of Temperature and Humidity. The brittleness of strain-indicating coatings is affected by temperature and humidity during drying and testing. To overcome these effects, it is necessary to select and calibrate the proper coating for every test. Coatings are selected for the conditions prevailing at the time and place where testing will be done. For outdoor work the local weather bureau can be consulted. Indoors, the prevailing temperature and humidity can be measured with a **sling psychrometer.** This will aid in predicting actual test conditions.

Response to Strain. Brittle coatings fracture at right angles to the principal tension strains. As load is increased on a structure, areas which are most highly strained in tension will be the first to form patterns. These areas of maximum tension stress almost always correlate with location of fatigue failure in service.

Brittle coating tests can provide **quantitative results** when certain conditions are fulfilled. These are:

1. The material of the structure must remain in its elastic range.
2. The distribution of loading must not change.

When these two conditions are fulfilled, the assumption that all local strains vary directly in proportion with the load will be valid. Then the strain measured at one load value can be extrapolated to other values of load. Under some conditions it may be necessary to cause **localized yielding** to obtain patterns on other areas of the structure. If the areas which have yielded have not appreciably changed the shape of the structure or distribution of load, the results will be valid.

When a preliminary analysis indicates that stress is not proportional to load, greater accuracy can be obtained by using coatings with the ability to crack at or near the rated load. A preliminary test run helps to establish approximate values of local strains. Additional quantitative accuracy can be obtained by using wire-resistance strain gages at the points and directions of maximum stress indicated by brittle coatings.

Use of Several Different Coatings. Quantitative data can be obtained by using various coatings during the same test. This technique may be used for **static** work as well as **dynamic.** However, it is particularly useful in tests which operate at one load. For example, coatings with **strain thresholds** of 600, 800, 1000, and 1200 μin. per in. can be applied to the four blades of a fan. **Calibration bars** are also prepared for each of the coatings. The fan is loaded, stopped, and examined for crack patterns. The blade with 600-μin. per in. coating may have several areas of pattern on it, whereas none will appear on the blade with the 1200-μin. per in. coating. Therefore the strains are between 600 and 1200 μin. per in. An examination of the patterns on the other blades will give a better approximation of the strain present.

The study of stresses in **symmetrical structures** can also be done with several coatings of different thresholds. By bracketing the strain patterns, good quantitative results can be obtained. If several similar parts are available for test, each may be coated with a different threshold strain and tested at the same time.

SELECTION OF RESIN-TYPE COATINGS. Resin-type brittle coatings are selected on the basis of:

1. Test-operating temperature and humidity.
2. Desired threshold strain values at which cracking first appears.

Coating Selection Chart. The resin-type brittle coating selection chart shown in Fig. 3 is used to select coatings as follows: project **wet-** and **dry-bulb tem-**

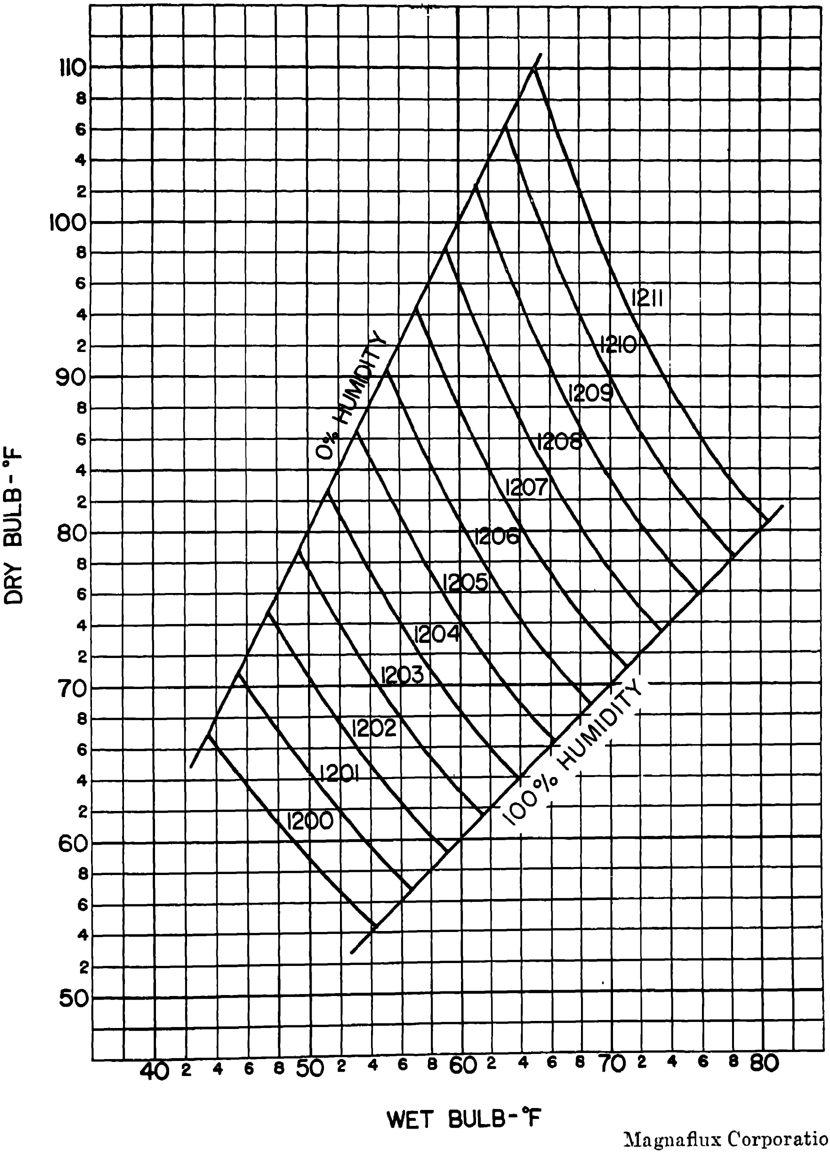

Magnaflux Corporation

Fig. 3. Resin-type, brittle-coating selection chart.

perature readings to their intersection on the coating selection chart. The **coating number** which lies in the valley between two curves where the intersection occurs is the best one for average use. This coating will give a threshold strain value of approximately 800-μin. per in. strain. This value is the least amount of strain required to crack the coating.

If lower threshold values of strains are desired, higher number strain-indicating coatings should be used. Conversely, lower number strain-indicating coatings will have higher threshold values of strain. The variation in strain sensitivity is approximately 100-μin. per in. strain per coating number at the strain threshold value of 800 μin. per in. At lower threshold values the variation in sensitivity is greater, and at higher threshold values, less per coating number. An example of the **strain-threshold relationship** between coatings follows:

At wet- and dry-bulb readings of 60° F. and 75° F., respectively, the coating selection chart indicates that coating 1205 will start a crack pattern formation in the vicinity of 800-μin. per in. strain. Under the same circumstances, other coatings will react approximately as shown in the table here.

Coating Number	Variation from Chart Selection	Threshold Strain, μin./in.	Remarks
1201	−4	1140	Patterns apt to close upon release of load.
1202	−3	1060	
1203	−2	980	
1204	−1	900	Best coatings for normal use.
1205	0	800	
1206	+1	700	
1207	+2	580	Craze or nonpreferential cracking likely to develop.
1208	+3	440	

Selecting Coatings for High-Threshold Strain. The data in the accompanying table are used to select the proper coating for measuring high-threshold values of strain.

Threshold Sensitivity, μin./in.	**Coating Number Below Chart Selection (Fig. 3)**
1500	15
2000	20
2800	30
3500	40

These data are used in the following manner: If it is assumed that a threshold strain of 2500 μin. per in. is desired at testing conditions of 75° F. dry bulb, 66° F. wet bulb, the coating selection chart (Fig. 3) shows that 1206 is the normal coating to use. The table indicates that a coating 25 numbers lower should be used. This is 1180. Surface preparation and the spraying of undercoatings should be performed normally.

Loading must be done rapidly, since **creep** is greatly accelerated with softer coatings. Because cracks which occur in coatings of high-threshold strain will close upon removal of load, it is necessary that the invisible cracks be detected with **electrified particles** (see section on Electrified-Particle Tests) or with a **dye etchant.**

CHARACTERISTICS OF CERAMIC-TYPE BRITTLE COATINGS. The development of ceramic-base brittle-coating materials has extended the useful operating range of brittle coatings by providing means for studying operating stresses under **severe operating conditions** without reference to humidity conditions. These coatings permit the study of stress, design, and loading problems under the following conditions:

1. Service at elevated temperatures up to 700° F.
2. Operation where cyclic thermal stressing is important in loading parts, as in furnaces where alternating cycles of heating and cooling may have caused failures.
3. Dynamic or static test conditions even though water, oil, or other mild liquids are present (strong acids or bases are not recommended).
4. Dynamic tests at high rotational speeds where abrasion of air or dust would damage the softer resin-type coatings.
5. Slow-loading tests where loads increase to maximum peak loads over a period of several hours.
6. Out-of-door tests for indefinite lengths of time.

The ceramic-coating materials are sprayed onto a part, air-dried, and then fired at about 1000° F. The **fired coatings** are glasslike and brittle. Their operation is similar to that of resin-type coatings in that the coatings fracture at predetermined amounts of strain and at right angles to the direction of the principal strain.

Coefficient of Thermal Expansion. Ceramic brittle coatings are designed to match the mean linear thermal-expansion coefficient of the metallic material being tested, throughout the test-temperature range. The **strain sensitivity** varies in accordance with the mean coefficient of expansion of the coatings selected. For example, if a coating is selected with a coefficient of expansion greater than that of the base material, less strain will be needed to crack the coating because cooling from firing temperature induces a **residual tensile stress** in the coating. This results from the greater contraction of the coating just below the firing temperature. Conversely a coating with a smaller coefficient of expansion than the base material will crack only at higher strains because of an induced **residual compressive stress** in the coating. Thus coating selection must be based on the coefficient of thermal expansion of the base material to be tested.

Calibration. It is recommended that the strain sensitivity of a ceramic brittle coating on a particular base material be determined by **calibration test** because accurate determination of the thermal-expansion coefficient of metallic materials is often difficult. Measuring equipment for the coefficient of expansion is elaborate and expensive and results are affected by such factors as:

1. The method of measurement.
2. The size of the test specimen.
3. The thermal history of the test specimen.
4. The composition of the test specimen.
5. The temperature range of the measurement.

As a consequence, even the published data vary considerably.

Calibration of ceramic brittle coatings is most easily done by the use of calibration bars, calibrating-test fixture, and strain scale as shown in Fig. 1. For ceramic coatings, however, the **calibration bar** must be made of the same metallic material as the part to be tested. The calibration bars are 1 × ¼ × 12 in. in size, with the 0.250-in. dimension being held closely. In general, however, calibration can be obtained from any known strain distribution; for example, from tension bar specimens.

SELECTION OF CERAMIC-TYPE BRITTLE COATINGS. The ceramic coating selection chart (Fig. 4) is intended as an approximate guide for selecting a coating and not for accurately determining the strain sensitivity. Strain sensitivity should always be determined by calibration. In 1958 six **ceramic coatings** were available for:

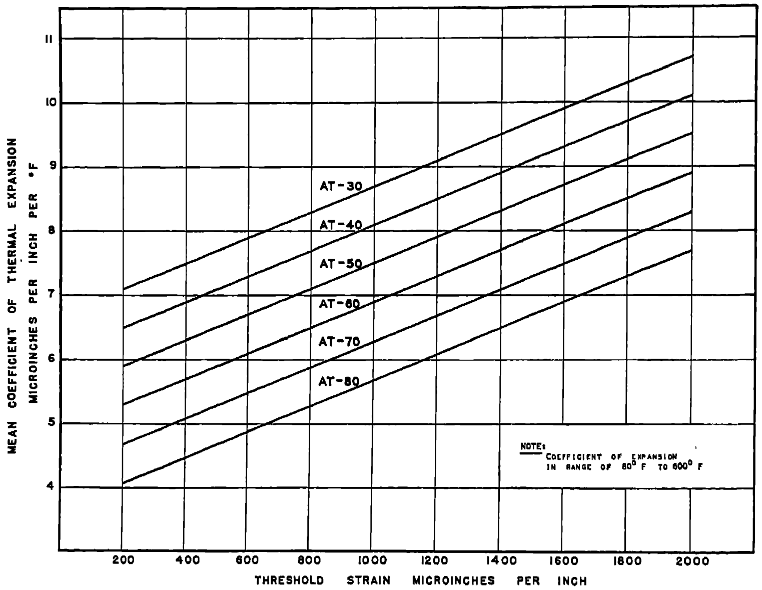

Magnaflux Corporation

Fig. 4. Ceramic-coating selection chart.

1. Carbon steels.
2. Straight chromium steels.
3. Chromium-nickel stainless steels.

These coatings are most useful in the medium and lower range of coefficient of expansion (see Fig. 4) but have limited usefulness, due to poorer strain sensitivity in the higher range of expansion coefficients. For example, on 1090 carbon steel (medium range), the strain sensitivity range is from about 400 to about 1800 μin. per in. On 410 stainless steel (lower range), it is from 400 to about 1200 μin. per in. Conversely, in higher ranges of coefficient expansion, strain sensitivities may range only above 1800 μin. per in.

Safety Precautions. The solvent used in ceramic coatings is flammable, and the ceramic material has a high content of **hazardous inorganic chemicals,** especially lead. The following safety precautions are to be taken:

1. Keep cans away from heat and open flame.
2. Avoid vapor and dust inhalation by use of a respirator or a spray booth.
3. Use with adequate ventilation.
4. Cleanse hands thoroughly before smoking or eating.

Test Techniques

PREPARATION OF TEST SPECIMENS FOR RESIN-TYPE COATINGS. Brittle coatings have been used successfully on all types of metals and metal surfaces, glass, wood, and plastics. All **loose scale, grease, and oil** must be removed. Any surface coating which may be affected by the various thinners used in coating materials should also be removed. Ordinarily, most hard, dry, **paint films** are unaffected by such materials and can be left intact. Smoothing of the surface can be performed by a rotating wire brush or sand blasting. Vapor degreasing generally is the best way to remove oil or grease. It is good practice to smooth the surface of small, critical areas such as fillets or other hard-to-view areas. A little extra trouble taken at this time will increase the visibility of initial strain patterns.

Applying Aluminum Undercoat. Aluminum-pigmented lacquer provides a uniform background on all types of parts regardless of their surface finish, i.e., whether dull or polished. This uniformity also makes it easier to judge the thickness of the strain-indicating coating during spraying. Frequently, scratches and disfigurations which might resemble strain patterns are minimized.

Applying Resin Coatings. For most applications the resin-type strain-indicating coating as received is of the correct consistency for **spraying.** The advantage of spraying is that it is the easiest way to obtain coatings of uniform thickness. In addition, multitudes of small **bubbles** are introduced into the coating. These bubbles increase the regularity and dependability of the formation of strain patterns.

The **air supply** should be free from oil and excessive moisture. Oil vapors or droplets are particularly undesirable because they destroy the brittleness of the coatings.

Temperature During Resin-Coating Application. It is best to spray resin coatings at temperatures equal to, or higher than, those expected during the testing period. In humid weather, moisture will condense into the sprayed coating, reducing brittleness and producing a discoloration which may cause difficulty in detecting subsequent crack patterns. Heating parts to approximately 125° F. before spraying overcomes this problem. When it is necessary to spray at temperatures below those used for testing, the parts should be warmed before spraying and rewarmed when necessary during the operation. Parts should be moved to warmer drying areas immediately after spraying.

Drying of Resin Coatings. Resin coatings are dried at a temperature somewhat higher than the temperature for which the coating was selected. When testing indoors at a temperature of 75° F., it is good practice to dry the coating at a **temperature** from 80° F. to 100° F. All coatings should be dried at temperatures of 70° F. or higher. The best **drying period** is about 18 hr.

A typical procedure for indoor testing is to coat the test piece in the afternoon and test the next morning. This **drying cycle** keeps the effect of varying coating thicknesses upon threshold sensitivity to a minimum. Drying time of about 6 hr. can be employed, but extreme care must be taken to keep the thickness of the coating very uniform at some value between 0.003 and 0.005 in. When **accelerated drying** is desired, the following data are used for quick drying times: 4 hr. at 100° F., 2 hr. at 120° F., or 1 hr. at 140° F. Parts are allowed to remain at room temperature for 30 min. before introducing additional heat. After drying, one or more hours before testing are allowed for the structure to come to temperature equilibrium with the atmosphere. Heavy structures require more time than light ones.

CALIBRATION OF RESIN COATINGS. The commercially available calibration bars are satisfactory for use regardless of the material in the structure, since strain rather than stress is being measured. Bars should be coated, dried, and tested along with the structure. It is possible to use other calibration bodies, providing the stress distribution is known. The **accuracy of calibration** is primarily dependent upon maintaining the calibration bars at the same conditions of temperature and humidity as the structure. Whenever possible the bars should be directly in or on the test part. On heavy structures it is advisable to place the dried calibration bars with coating side down and to cover them with cloth or paper to eliminate the effects of temporary drafts. The complete calibration operation should be performed as quickly as possible to minimize temperature differences on the calibration bars while they are away from the structure.

Tension-Strain Calibration Procedure. The calibration technique for measuring tension strains is:

1. Scrape coating off 1 in. of each end of a calibration bar.
2. Place bar, coating side up, in the calibrator. Adjust knurled knob at rear until bar just touches cam in front.
3. Deflect cam fully in 1 sec. Mark lowest strain pattern toward cam.
4. Remove load, and put calibration bar in strain scale (Fig. 1). Lowest pattern marked is the threshold strain value.

Compression-Strain Calibration Procedure. The calibration technique for measuring compression strains is more complex. The coatings can be made to respond to compressive strains in two ways:

1. Coat calibration bar and place in calibrator upside down. Depress cam and allow bar to dry in loaded condition. Release of cam will permit patterns to form on bar in a manner similar to those occurring in the normal tension-calibration technique.
2. Coat and dry bar in normal fashion. Place in calibrator upside down and depress cam. The coating is now under compression and should remain so for a predetermined period of time, as discussed later. At the end of this period of time, release of cam will produce patterns in a manner similar to those formed under tension-calibration techniques.

When either of these techniques is used, remove the bar from the calibrator, place in the strain scale, and mark the lowest pattern.

Calibrating Resin Coatings for High-Threshold Strain. Modified calibration techniques are used with resin coatings of high-threshold strain. It is essential to load the calibration bars in the same time cycle as the structure. Calibration at higher threshold values can be made as follows: Place the calibration bar in the calibrator in a normal fashion, with the cam up. Place an **additional calibration bar** between the bottom of the cam and the calibration bar under test. Load in a normal fashion. The additional deflection provided by the inserted calibration bar requires a correction factor in order to obtain the true strain. Multiply all values obtained on strain scale by 1.43. If higher strain calibration is required, add a second calibration bar. The multiplication factor in this case is 1.86.

Computing Stress from Strain. Apparent stress is computed by multiplying strain by the simple tension modulus of elasticity of the material used in the structure, regardless of the type of loading. For example, if the first crack in a coated steel structure occurred at 600 μin. per in., the apparent stress would be $(600 \times 10^{-6}) \times (30 \times 10^{6}) = 18{,}000$ p.s.i.

Representative values of the **tension modulus of elasticity** for several common engineering materials are:

Steel	30,000,000 p.s.i.
Gray cast iron	15,000,000
Alloy cast iron	20,000,000
Malleable iron	25,000,000
Brass and bronze	15,000,000
Monel	25,000,000
Aluminum, Dural	10,000,000
Magnesium	6,000,000
Bakelite	600,000
Celluloid	400,000
Wood	500,000 to 2,000,000

Creep Correction. Resin brittle coatings are normally considered to be very brittle materials which fracture readily. Under the influence of time and load, however, the coatings tend to creep and relieve the stress within the coating induced by the original load on the base structure. Therefore, creep is a factor which must be taken into consideration on all tests.

There are two ways in which a creep correction can be applied. The first method is to load the calibration bar in the same length of time as taken to load the structure. In this way the coating on both calibration bar and test part are in the same condition, and the strain threshold value will be reasonably accurate.

In the second method the calibration bar can be loaded in 1 sec., and the correct value for its strain threshold can be obtained from the creep correction chart (Fig. 5) for the length of time taken to apply each increment of load to the structure. Corrected stress is given in μin. per in.

When **control of loading** is too awkward to allow release of load between increments, it is necessary to add load and correct for creep of the coating. Load must be added at a constant rate. This need not be a continuous increase of load but may be a series of equal increments added at equal intervals of time. The calibration bar should be loaded in 1 sec. and the corrected strain threshold obtained from the creep correction chart. The actual value of strain present in the structure is derived by locating the total length of time since the start of the test (along the abscissa of Fig. 5). The **threshold strain value** for the calibration bar is interpolated in the family of curves, and the **actual strain value** appears as the ordinate of the intersection.

Creep of coatings must always be taken into consideration. There are few conditions possible where creep can be ignored, with the possible exception of **impact loads.** If the creep-correction chart technique is not used, it is essential to deflect the calibration bar in the same length of time taken to apply the load to the test part.

DETECTING CRACKS IN RESIN COATINGS. The successful usage of resin-type brittle coatings hinges upon the detection of **crack patterns** occurring in the coating during actual tests. Usually the whole test depends upon locating the first crack. If it is missed, inaccuracies may result and repetition of the test may be required. Often the reason for performing a stress analysis is that a part has failed in service, and it is desired to locate some of the contributing stresses. Thus the operator will know approximately where to look. After

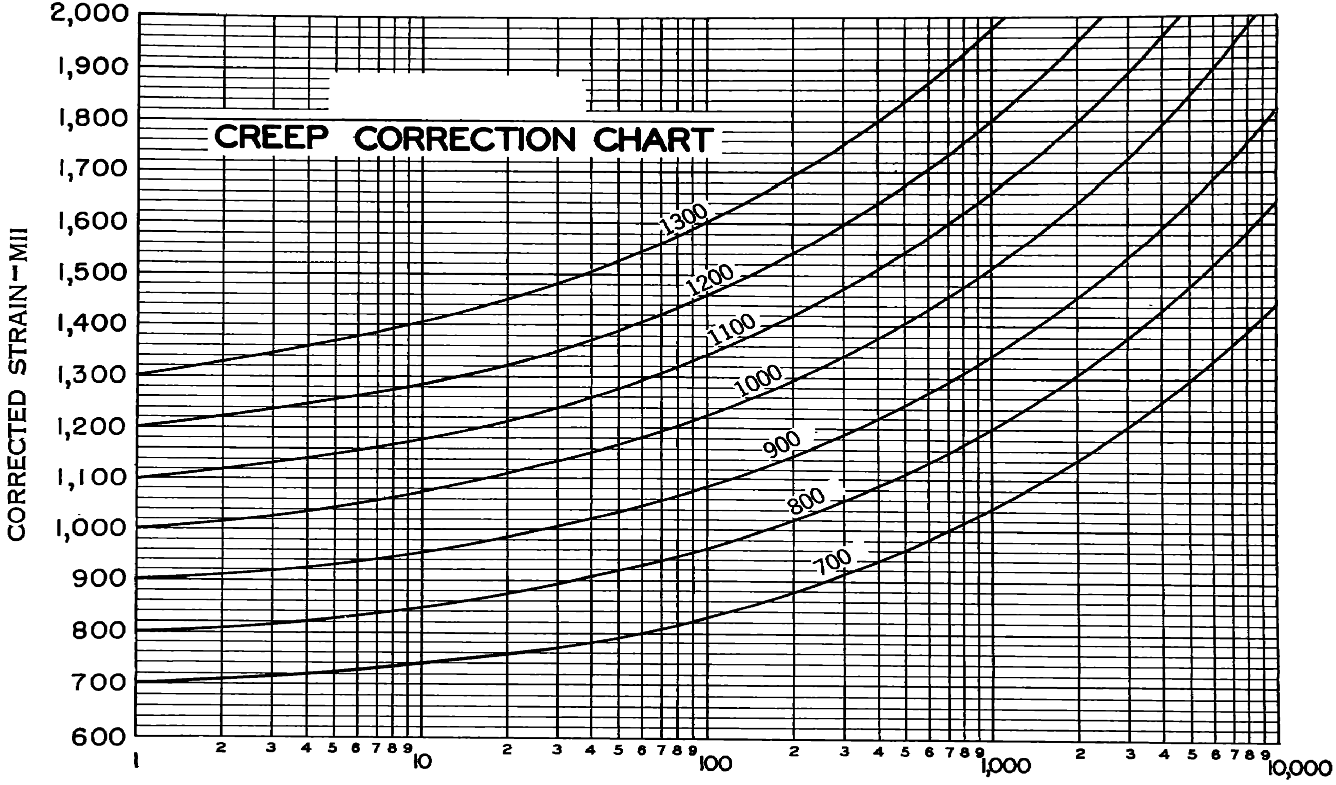

Magnaflux Corporation

Fig. 5. Creep correction chart.

experience has been gained in working with brittle coatings, one becomes more successful in locating crack patterns.

Visual Inspection. The average coatings will crack and stay open. The cracks can be detected by directing light perpendicular to the direction of the crack; they appear as shown in Fig. 6. The light should come from a point approximately tangent to the surface under examination. Obviously on complex shapes it is not always possible to meet these **light conditions.** However, experience will teach the observer how much deviation may be tolerated.

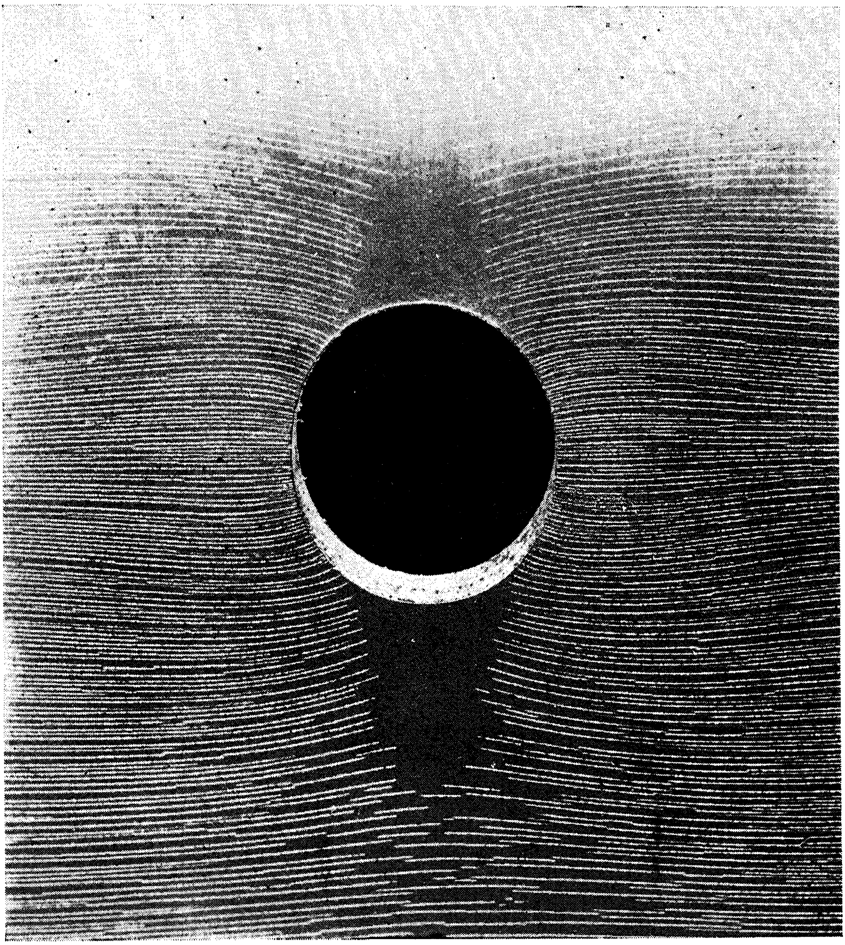

Magnaflux Corporation

Fig. 6. Cracks in brittle coating as seen visually with proper illumination.

When light from a small, focused source is flashed on the coating, cracks will tend to light up or shine. Light enters the crack and reflects from the internal faces. A highly reflective coating on the surface of the test piece helps illuminate the cracks. When cracks in coatings are closed very tightly, they will not reflect light. This situation occurs with high-threshold strains when load is removed. Under these circumstances cracks are impossible to detect with the human eye aided by lighting of any kind. The cracks must then be located by some other technique.

Dye-etching Technique. Dye etchant is a fluid containing a dye which can selectively etch cracks in resin-type brittle coatings and leave a visible residue of dye within the cracks, as shown in Fig. 7. This material has the ability to etch

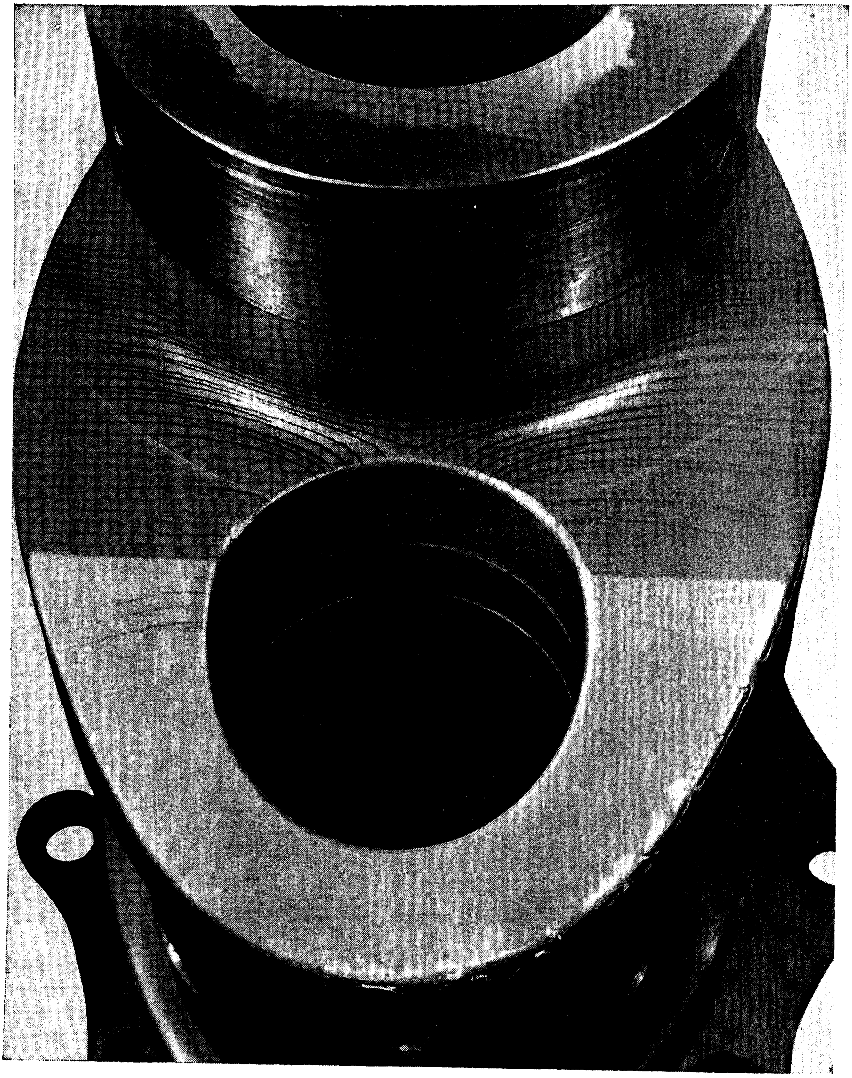

Magnaflux Corporation

Fig. 7. Dye-etched crack patterns.

cracks which are completely invisible to the human eye. The main disadvantage of dye etchant is that once it is applied to a coating, the coating cannot be re-used for test purposes.

Dye etchant is used in the following manner: First, a coat of room-temperature dye etchant is brushed on the test piece. After a short interval of time, the material is wiped off with a soft, clean cloth. It is fairly easy to detect the **limit of the dye-etching process** when the general surface of the coating begins to take on a red coloration. It is useless to continue dye etching beyond this point. A commercially available **etchant emulsifier** will help in the removal of dye etchant. In addition it stops the action of the etchant. The emulsifier can be applied by brush, cloth, or dipping.

Best results will be obtained from the dye-etching process when it is carried out at the temperature of the original test. For example: A structure which is tested outdoors at 40° F. should be dye-etched outdoors at the same temperature.

Dye etching of **compression strain patterns** should be postponed for at least 2 hr. after a test, since the etchant sensitizes the coating and induces pattern formation in otherwise blank areas. After several hours, the coating will relax, and no extraneous patterns will appear upon using dye etchant.

Electrified-Particle Technique. The electrified-particle inspection method is used to overcome the disadvantages of visual and dye-etching techniques for detecting crack patterns in brittle coatings. This technique has one great advantage. It does not injure the brittle coating. For this reason it is possible

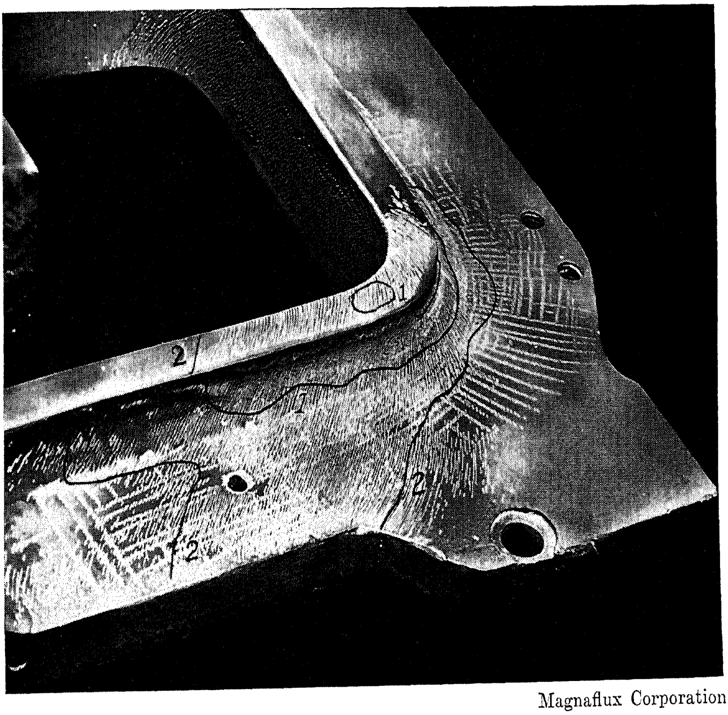

Magnaflux Corporation

Fig. 8. Electrified-particle indication of cracks in a brittle coating.

to run **repeated tests.** This is a decided advantage when impact loads with high-threshold values of strain are being studied. In the past, when studying impact loads, it was necessary to use dye etchant to locate the invisible crack patterns. If crack patterns were not found during the loading, the etching process destroyed the coating and necessitated repetition of the test. With electrified particles the impact-load cycle can be performed, and if no patterns appear, the part may be repeatedly retested at higher loads until patterns appear.

The general **procedure for using the electrified-particle method** on resin coatings is:

1. A special water-based penetrant, which is a mild electrolyte, is applied to the test piece. If the cracks are open, the penetrant will enter.
2. The surface of the part is dried with a soft cloth.
3. Powder is then blown from a special gun which electrifies the powder (see section on Electrified-Particle Tests). The particles blown onto the surface of the coating are charged positively. The positive particles attract negative ions contained within the penetrant in the crack. Thus the top of the crack will tend to be negative.
4. Positively charged powder particles will gather at the top of the crack and form a highly visible crack indication, as shown in Fig. 8.

Cracks in coatings of high-threshold strain close so tightly upon removal of load that even penetrant will not enter crack patterns. Therefore penetrant should be applied to the coating prior to the test and kept moist until the load cycle is completed. After loading, the part can be wiped off and charged powder applied to the coating. If no patterns appear, the part may be again penetrated, reloaded, and powder applied.

PREPARATION OF TEST SPECIMENS FOR CERAMIC-TYPE COATINGS. A properly prepared surface is essential to the successful operation of ceramic brittle coatings. The surface must be free of oil, grease, rust, and scale. It should be velvety smooth (not polished). The best method of **surface preparation** is by blasting with sand, steel grit, silicon carbide, alumina, or vapor blast. The size of grit and amount of air pressure depend upon the surface condition of the metal. Soft surfaces require lower pressures and a fine grit. For hard surfaces, higher pressures and large grit are more suitable. Grit size and air pressure are not critical, so that a grit size range from 16 to 100 mesh and air pressures from 40 to 100 p.s.i. are usable. An example of a satisfactory combination is a grit size of 24 to 36 mesh with 50 p.s.i. of air pressure. This will produce a clean surface which is also roughened to a velvety finish and ready to be coated.

Preparing Coating Materials. Ceramic-coating materials settle out after standing. They are a mixture of finely milled ceramic particles which must be thoroughly mixed and held in suspension before being used. **Mixing and suspension** are easily attained by first stirring the coating material in the container and then shaking the container vigorously. The coatings have the proper consistency for spraying as supplied and have a specific gravity of about 1.9. When desirable, consistency can be adjusted by adding thinner in very small amounts.

Applying Ceramic Coatings. The best method for applying ceramic brittle coatings is by **spraying.** The recommended technique and equipment are similar to those used with resin coatings, and the same type of gravity-feed, high-quality air brush is recommended. The purpose of the spraying technique is to apply coatings of a definite and uniform thickness. The most important **factors affecting spraying technique** are:

1. Air pressure.
2. Fluid control.
3. Distance of spray gun from test surface.
4. Gun movement.

The gun must be moved in a decisive manner and also at a uniform distance from the part. This distance will vary, depending upon the object being sprayed, but is usually about 4 to 5 in. The **air pressure** to be used is influenced considerably by the size and shape of the part. Small parts and complex sections require about 5 to 10 p.s.i., whereas larger parts require 15 to 20 p.s.i. because a greater output is needed. Since low pressures are used, the **gravity-feed spray gun** is recommended. It allows free flow of coating at low pressures. The fluid flow adjustment is determined by the air pressure. It should be set to produce a wet spray with enough fluid to "wet out" the coating. This will produce a smooth and glossy fired coating. The **applied coating** should be about 0.003 to 0.005 in. thick. It is recommended that small areas be sprayed to this thickness before spraying adjacent areas. Rewetting a dried coating tends to produce blisters which will result in a poorly fired coating. Because the coating tends to settle even in the spray gun, it is necessary to agitate the gun periodically during spraying.

Firing of Ceramic Coatings. The sprayed and dried coating consists of finely divided particles which must be fused into a smooth, glassy coating. Either an electric furnace or a muffle-type gas furnace can be used for firing. However, it must provide an **oxidizing atmosphere** of air or an oxidizing flame. Firing is a matter of time and temperature. The **firing temperature range** is from 950° F. to 1100° F., with the optimum at about 1000° F. The **firing time** depends upon the size of the parts, their thickness, and the capacity of the furnace. The essential point is that the parts are "up to heat" and are held at the firing temperature for 4 or 5 min. A properly fired coating is best determined by observing it at intervals during firing, looking for the coating to become smooth and glassy and slightly yellow in color. An overfired coating looks rough and very yellow by comparison.

When test parts have sections with **large variations in thickness,** uneven heating will occur, and the coating on thin sections may be overfired. The following **firing schedule** will reduce this tendency on such parts:

1. Heat the part to about 850° F.
2. When the part is uniformly heated, increase the temperature to 1000° F. and complete firing.

This method tends to reduce the time during which the thin sections are at firing temperature. When fired to a glossy, smooth coat, the parts are removed from the furnace and air-cooled to room temperature. They are then ready for testing.

Detecting Cracks in Ceramic Coatings. Crack patterns occurring in ceramic coatings cannot be seen directly and must be detected by the use of the **electrified-particle technique.** When the charged powder is applied by means of a special gun, it builds up over the cracks to make them readily visible. The method is similar to the use of electrified particles on resin coatings, with the exception that penetrant need not be introduced into cracks to obtain patterns.

Applications of Brittle-Coating Tests

BASIC CONSIDERATIONS. Engineering structures are designed to transmit loads. The basis of design always assumes that loads must be carried and must flow through a structure. Consideration of these factors assists the designer in deciding upon the shape and selection of materials. The primary role of stress analysis is to check a design for the distribution of forces carried. In many cases several alternative designs are available, and the best or least expensive must be selected. To aid in this study, **loads which simulate service conditions** often are applied to the structure, and strains are measured at critical areas. It is frequently desirable to make at least one test of a structure under actual service conditions. Mechanical, optical, or electrical strain gages down to approximately 1/16-in. gage length may be used but cannot easily be applied to fillets, curved surfaces, or inaccessible regions. They are also inadequate because of the number of separate measurements that must be made at different points and in different directions to be reasonably certain that critical strains are located. The perfect strain gage may be thought of as one which simultaneously gives an infinite number of readings of infinitesimal gage length over the entire surface of a structure. Brittle coatings under proper control approximate this ideal. While not so precise as strain gages, they furnish an over-all survey with sufficient accuracy for most engineering purposes.

JIGS AND TESTING APPARATUS. Successful application of brittle-coating tests depends upon the ingenuity and thoughtfulness expended upon the jigs and apparatus used to apply the loads. Generally, the simpler the loading device, the easier the test.

Static Tests. Static loading rigs should always simulate the worst dynamic loading which the test part is expected to receive in actual service. Control of loading should be positive and allow for quick placement and removal of loads. Facilities should be arranged to measure the loads within an accuracy of ± 5 percent.

Care should be taken to assure a uniform distribution of load on the structure throughout the test. Tension or compression loads can be applied through some form of flexible-joint arrangement which will minimize the introduction of unwanted bending moments. **Flexible cables, chain links,** or a **universal joint** provide freedom in both directions so that concentric application of the load is achieved. Where loads are transmitted through joints such as a piston pin in the eye of a connecting rod, the load distribution may change considerably at higher loads as one structure wraps itself around the other and receives different support. Under these circumstances sufficient clearance should be allowed to prevent wrapping contact under the loads being investigated.

Simple, **manually loaded rigs** can be constructed, using standard scale weights, although frequently it is convenient to pour sand or water into an ordinary pail. Loads can be added quickly and decisively with inexpensive hydraulic jacks and pumps.

Dynamic Tests. Dynamic tests invariably call for operating the equipment in the field under operating or service conditions. This introduces several new problems not generally encountered with static work. The first problem involves the changing of temperature during the loading cycle. Sometimes a temperature rise is unavoidable. However, if it does occur, it should be kept to a minimum, since heat will tend to close the crack patterns which were formed prior to the rise in temperature. Heat may be avoided during loading cycles by remembering that only one cycle of maximum load is needed to produce all the patterns. In the event that crack patterns close, they can be detected by the use of dye etchant or penetrants and electrified particles.

Control of Temperature. Sometimes the effects of an excessive temperature rise can be combated by sprinkling water over the test part and calibration bars. It is also possible to place the part in a water bath. Brittle coatings need no protection from water. Specific resin coatings should be selected along the 100 percent humidity line (Fig. 3) for the temperature of the water which will be used in the test. Resin coatings should be air-dried at temperatures higher than the water temperature.

Care is required in applying the water to make sure that the coatings on the parts do not craze. Tests should not be started until the structures have reached temperature equilibrium. The water temperature should be kept reasonably stable throughout the test. After loads have been applied, the resin-coated structures are dried with soft cloths and dye-etched immediately. This use of water submersion is an excellent way to obtain uniform threshold strains for long periods of time regardless of air temperatures.

MEASURING STRAIN UNDER STATIC LOADING. As brittle-coating crack patterns form on a structure, the position and direction in which they occur should be recorded along with the threshold strain value of the coating, as shown in Fig. 9. The amount of load placed on the structure and the time taken to reach that load are recorded. Frequently it is desirable to mark the pattern directly on the test structure with a marking pencil, ball-point pen, or scriber.

Tension Strains. Strain patterns which have just formed give the most accurate quantitative results. Some initial patterns are difficult to locate, and when in doubt, dubious patterns are circled and their growth observed with increased load. To be sure that patterns are observed in their initial stages of formation, it is best to limit each additional **increment of load** to 25 percent or less of the preceding total load. The general **procedure for measuring tension strains** is as follows:

1. Apply load to a predetermined value, hold while checking for patterns, and remove load.
2. Allow the test structure to rest for at least twice the total length of time of the preceding loading cycle. This permits the coating to relax.
3. Load and unload to higher increments of load in a similar fashion until full analysis has been completed.
4. Load calibration bars in the same length of time taken to reach each load on the structure, or load the bar in 1 sec. and obtain the correct value for its strain threshold from the creep correction chart (Fig. 5).

Sometimes it is difficult to control loading and allow release of load between increments. It may be necessary to add load continually and **correct for creep** of the coating by means of the creep correction chart. Under these conditions, add load at a constant rate. This need not be a continuous increase of load but may be a series of equal increments added at equal intervals of time. Total length of time from the start of the test is the correct time value to use.

Compression Strains. A complete stress analysis involves both tension and compression strains. After tension tests are completed, compression strains can be obtained by maintaining the full load on the part. Under load, the coating creeps and tends to relax. When the load is removed, the released compression strains react on the coating, producing cracks just as though they were tension strains.

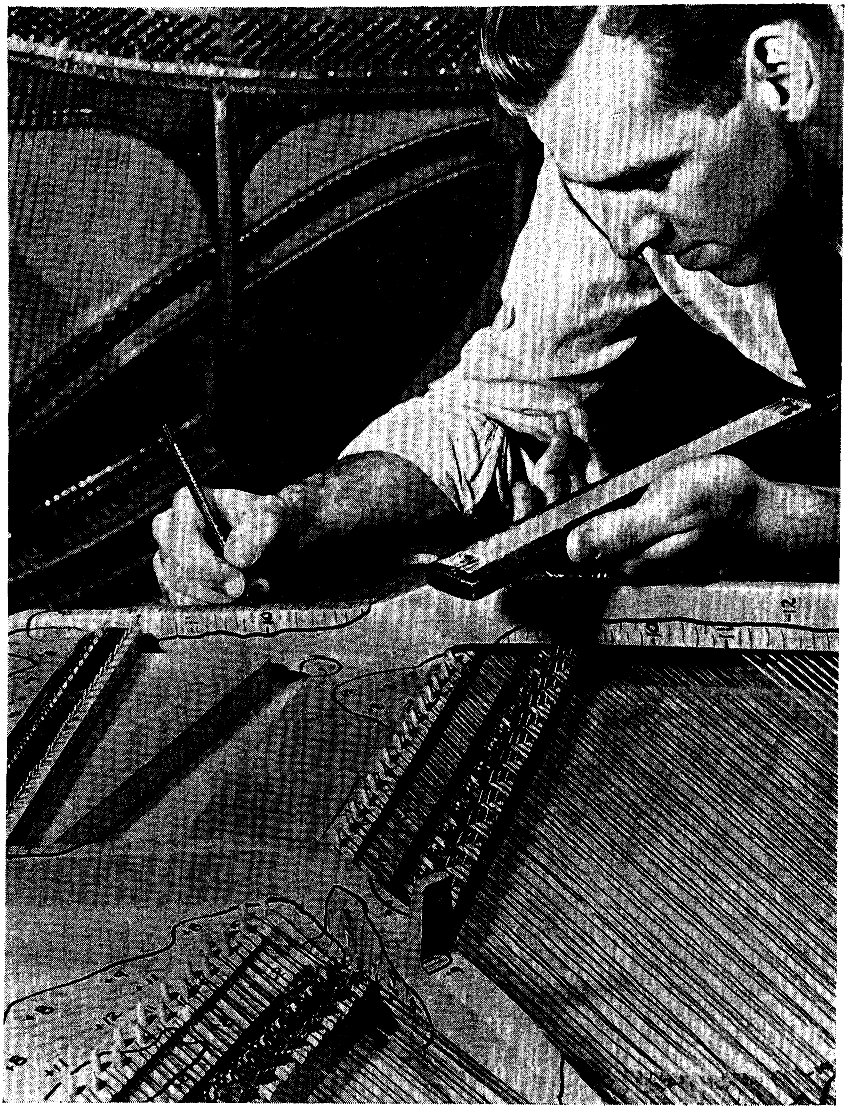

Aluminum Co. of America

Fig. 9. Marking of various values of threshold strain.

The **calibration bar** must be treated with the same hold and release time as the test part. Be sure to invert the calibration bar in the calibrator to place the coating in compression.

An **alternate method** of obtaining compression-strain results is to dry the coating while the test part is under load. The part can be coated while under load, or sprayed and then loaded. Be sure to treat calibration bars in the same manner as the test part.

A typical compression test is operated in essentially the same manner as a tension test. In this case the **load increments** are removed instead of being added, as was the case with tension tests. In other words, the load which is removed is the actual load being applied to the coating.

Creep is a factor in compression tests just as it is in tension tests. Coatings must be returned to their initial state and allowed to rest in the normal fashion described earlier. Crack patterns are located after removing increments of load because cracks seldom remain open after load is reapplied.

MEASURING STRAIN UNDER DYNAMIC LOADING. It is frequently desirable to test a part in actual service to substantiate laboratory findings. On other occasions, information regarding load factors and components is very meager, and it is inadvisable to resort to laboratory tests with assumed loads. In the final analysis the design efficiency and life expectancy depend upon the conditions under which the part is expected to operate. Strain-gage readings undoubtedly will be required eventually. On parts of complex shape, however, brittle coatings usually are quite convenient to use.

Outdoor Tests. Satisfactory results can be obtained outdoors with brittle coatings under a wide variety of temperature conditions. Tests should be run at the desired temperature as the outdoor temperatures swing through their daily cycle.

Outdoor temperatures usually reach a minimum value at about 7:00 A.M. Maximum temperatures occur at about 3:00 P.M. and start to drop slowly at 5:00 P.M. The difference between minimum and maximum temperatures ordinarily is of the order of 20° F. The weather bureau can usually give a reasonable prediction of the temperature to be expected during the test. If the temperatures are off more than expected, and threshold strains are not satisfactory, it is often possible to wait until the conditions reach a favorable point and then run the test.

An excellent **summer operating procedure** is to coat the parts in the morning and allow them to dry all afternoon. Protect the parts from direct sunlight during drying and testing. Start testing operations after the temperature has started to drop. Test calibration bars from time to time. When the threshold strain reaches an appropriate value, begin the test.

Another procedure which can be used is to coat the parts in the afternoon with a coating selected for the temperatures expected the next morning. Dry the parts and calibration bars indoors at a temperature of 70° F., or more, overnight. On the next morning, an hour or two prior to the expected test, take a calibration bar outdoors. After bar has reached temperature equilibrium, note whether it crazes. If it does not craze, note the threshold strain and bring the test part outdoors. After the structure has been brought outdoors, wait for it to reach temperature equilibrium. In this case the threshold value of strain is rising continuously as the temperature rises during the morning.

If the structures are constructed of thin sheet metal, cover with cloth or paper to reduce their cooling rate. **Sudden cooling** of the structure may craze the coating. In all cases avoid subjecting parts to drafts or strong winds. When proper conditions are reached, remove coverings and begin the test.

TYPICAL BRITTLE-COATING TESTS. A typical test procedure illustrates the methodical manner in which a stress analysis should be performed to obtain optimum results. Many test schedules do not permit the collection of extensive data. However, where possible, a methodical listing of the pertinent bits of information may assist in the analysis of results. A typical test is described, utilizing three techniques:

1. An object is loaded in tension where the load is continuously applied. This requires the use of the creep correction chart (Fig. 5).
2. Tension strain is measured under tension loadings where the load is returned to zero after each loading.
3. Compression strains are measured.

The sample selected for this idealized test is a simple steel crane hook mounted in a testing machine with flexible wire cables. The hook is conservatively rated at 2000-lb. capacity so that the loading schedule is started at half of the rated load. This immediately suggests that each increment of load will be 25 percent of the preceding total load. A watch with a sweep hand is used to determine the time taken to go from initial load to the actual load. The total amount of time taken during the load cycle is also recorded.

The steel crane hook and numerous calibration bars are coated and dried overnight at a temperature slightly above the predicted test temperatures. Prior to the test, the parts are allowed to come to equilibrium with the room temperature at the test location. The calibration bars are kept close to the hook throughout the test.

As the crack patterns appear on the piece, their contours are marked for future photographing. The **value of stress** is clearly marked on the piece itself with arrows pointing to the **contour markings.**

The modulus of elasticity for steel is assumed to be 30,000,000 p.s.i. Local strains are assumed to be proportional to load. **Computations** are made as follows:

$$\text{Strain in } \mu\text{in./in.} \times \frac{2000\text{ lb.}}{\text{test load}} = \text{strain in } \mu\text{in./in. at 2000-lb. load.}$$

Typical calculation:

$$(800)\,\frac{2000}{1250} = 1280\ \mu\text{in./in.}$$

Strain in μin./in. × modulus of elasticity = apparent stress in p.s.i. at 2000-lb. load.

Typical calculation:

$$(1280 \times 10^{-6})\,(30 \times 10^{6}) = 38{,}400\text{ p.s.i.}$$

Measuring Tension Strains: Continuous-loading Technique. The calibration bar is loaded in 1 sec. Strains are corrected with creep correction chart (Fig. 5). The strain threshold is assumed to be 800 μin. per in.

Time to Load, sec.	Time to Inspect, sec.	Total Time, sec.	Test Load, lb.	Pattern Location, by Area	Creep Corrected Strain, μin./in.	Strains of 2000-lb. Load, μin./in.	Apparent Stress at 2000 lb., p.s.i.
60	10	70	1000	None	–	–	–
120	10	130	1250	None	–	–	–
180	10	190	1560	A	1010	1300	39,000
240	10	250	1950	A grows	1040	1070	32,100
300	10	310	2440	A grows	1060	870	26,100
360	10	370	3050	A grows B added	1080	710	21,300
420	10	430	3810	A grows B grows	1100	580	17,400
480	10	490	4760	A grows B grows	1110	470	14,100

Measuring Tension Strains: Return to Zero-Load Technique. The calibration bar is loaded in 45 sec. The time of loading in all cases is 45 sec. The threshold strain is assumed to be 800 μin. per in.

Test Load, lb.	Pattern Location, by Area	Strain at 2000 lb., μin./in.	Apparent Stress at 2000 lb., p.s.i.
1000	None	–	–
0	. .		
1250	A	1280	38,400
0	. .		
1560	A grows	1030	30,900
0	. .		
1950	No additional patterns	–	–
0	. .		
2440	A grows B added	655	19,700
0	. .		
3050	A grows B grows	525	15,700

Measuring Compression Strains. Load removal is assumed to be ¼ sec. The hook and calibration bar are held at initial load for 2 hr. The threshold strain is assumed to be 1000 μin. per in.; initial load is 4000 lb.

Initial Load, lb.	Load Removed, lb.	Remaining Load, lb.	Pattern Location, by Area	Strain at 2000-lb. Load, μin./in.	Apparent Stress at 2000-lb. Load, p.s.i.
4000					
4000	2000	2000	None	–	–
4000	. . .	4000			
4000	2500	1500	C	800	24,000
4000	. . .	4000			
4000	3125	875	C grows D added	640	19,200
4000	. . .	4000			
4000	4000	0	C grows D grows	500	15,000

SENSITIZATION AND MEASURING SMALL STRAINS. It is often useful to obtain a qualitative picture of stress distribution of very small strains. When brittle-coating patterns are not obtained on areas of interest, the **direction of principal strain** can be determined by sensitizing the coating while the structure is under load.

The simplest means of sensitization is by **chilling the coating** with ice water, cold air, or snow from a carbon dioxide fire extinguisher. **Dye etchant** will also sensitize the coatings. These techniques can lower the threshold strain level to a minimum of 50 μin. per in.

Rough quantitative data sometimes can be obtained by the use of dye etchant. A completely etched coating will have its threshold strain reduced by 600 μin. per in. The degree of sensitization depends upon the threshold strain and the time intervening between application of load and the sensitizing material.

Successful sensitization techniques depend upon practice. Better definition of stress patterns is obtained by less severe cooling. For example, it is better to apply the **cooling carbon dioxide cloud** from a distance and work toward the part rather than blast the piece at close range. **Ice water** applied by cloth or spray is better than placing ice in direct contact with the part.

MEASURING RESIDUAL STRESS. Brittle coatings are useful for the measurement of residual stresses whenever these stresses are of an appreciable amount. Stresses induced by processing or assembly in most types of materials can be measured with brittle coatings by using a technique involving the **drilling of small holes.** This method permits the measurement of stresses only at the point where a hole is drilled. The removal of material from a stressed part causes the surrounding area to indicate strain.

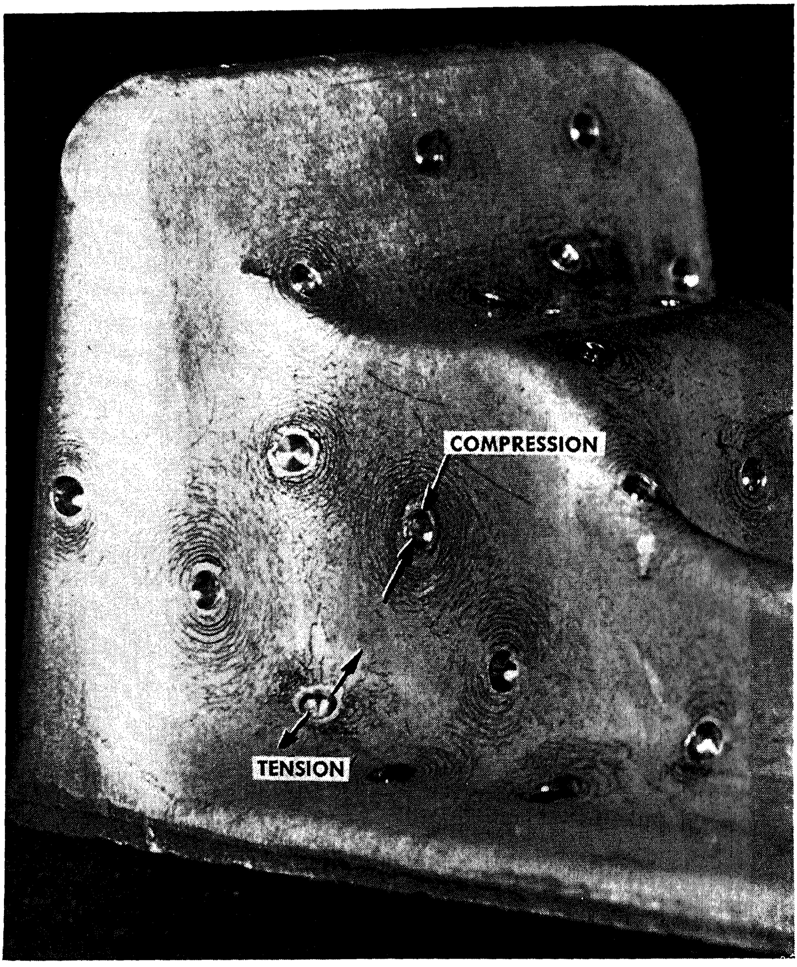

Magnaflux Corporation

Fig. 10. Residual tension and compression stresses revealed by drilling small holes into specimen surface.

The strains produced by drilling small holes are comparatively small, and results can be obtained only by sensitizing the coatings with dye etchant. The steps used in this technique are as follows:

1. Apply a coating which will have a threshold strain value of 200 to 600 μin. per in.
2. Drill a hole to a depth equal to the drill diameter. A tungsten-carbide-tipped, ⅛-in. diam. drill is a good average size to use on steel. Drills as small as 1/32-in. diam. can be used. Larger sizes will produce larger patterns.
3. Apply dye etchant to the area surrounding the hole immediately after drilling. Keep wet for 5 min. or longer; remove and examine patterns to see if they are fully etched. Repeat the process if necessary.
4. Residual tension produces **radiating star patterns,** whereas residual compression is indicated by a **circular pattern** surrounding the hole, as illustrated in Fig. 10. The boundary between the pattern and the surrounding craze is not distinct.

The amount of strain can be estimated by measuring the size of the pattern extending from the edge of the hole to the boundary of the surrounding craze in terms of drill-hole diameters. Allow 700 μin. per hole diameter. For example, if a pattern extends ¼ in. away from the edge of a ⅛-in. hole in steel, residual strain present at the hole is 1400 μin. per in. This is approximately 42,000 p.s.i. of residual stress in the steel.

Generally there seems to be no practical advantage in drilling deeper than the **depth** equal to 1 diam. The section of material lying next to the surface and within the first one-quarter diameter of the hole in depth appears to contribute about half the reaction to the pattern. The remaining layers at greater depths contribute lessening amounts to the residual reaction.

INDICATING GROSS STRAIN BY FLAKING OF COATING. Brittle coatings flake off during yielding. Flaking is a direct function of the **compression strain** present, and the most sensitive resin coating will begin flaking at 1 percent compression strain. A tension strain of 2 percent will also cause flaking because Poisson's ratio is 0.5 at yield. Torsion or shear loading will cause flaking at 1 percent strain. **Bi-axial stress** occurring on the surface of a sphere loaded hydrostatically will not cause flaking because a compression component is not present on the surface.

The most sensitive **flaking coating** is four numbers above the optimum for elastic strain measurement as indicated on the resin coating selection chart (Fig. 3). These coatings should be applied moderately thin (0.002 to 0.004 in.). Sensitive flaking coatings craze so completely during drying that they cannot be used to indicate elastic strain. Evaluation of yielding threshold strain with coating numbers is approxmately 3000 μin. per in. per coating number. **Typical flaking sensitivities** are given in the table here.

Resin Coating Number	Flaking Sensitivity Compression-Strain Component, μin./in.
1203	24,000
1204	21,000
1205	18,000
1206	15,000
1207	12,000
1208	10,000
1209	12,000
1210	15,000

The resin coating selection chart (Fig. 3) indicates that No. 1204 coating is optimum for elastic pattern formation.

CORRECTION FOR DIRECT PRESSURE EFFECT IN HYDRAULIC LOADING. Direct fluid pressure on a coated surface has a sensitization effect. Approximately 1500-p.s.i.g. direct pressure will start indiscriminate tension patterns on coated surfaces. The pressure effect can be calibrated by taking a **test coupon** similar to that of the structure and testing it and the calibration bars inside the structure.

Typical tests are very similar to other static loads except that water must be removed from the interior of the test object after each increment of load is applied and removed. The part is examined for patterns, and calibration bars are tested in the usual manner. As the pressure loads increase and eventually reach 1500 p.s.i.g., indiscriminate patterns will begin forming on the test coupon. The **true value of strain** can be computed from the following formula:

$$S = S_1 \left(\frac{P_s - P_1}{P_s} \right)$$

where P_1 = pressure at which strain patterns on structure are first observed.
P_s = pressure at which patterns began forming on test coupon.
S = the true value of strain.
S_1 = observed strain.

If it is not possible to reach 1500 p.s.i.g. during the test and to observe the direct pressure effect on the coated test coupon, a satisfactory approximation may be made by assuming P_s to be 1600 p.s.i.g.

PHOTOGRAPHING CRACK PATTERNS. Photographs for most report work can be easily made by taking pictures of **heavily crayoned contours** of the stress patterns with a few lines added to show the direction of the pattern within the contours. The contours may be marked with the values of stress they represent and data written on the part itself. The data can include the **value of working load** for which stresses are expressed. Thus all results will be contained in one photograph. If several similar structures are available with different sensitivities of coatings on each, it makes a particularly valuable display to line them up in order of threshold strain, each with contours marked and amount of stress indicated by each contour. Standard **photographic equipment** may be used. If the part has been dye-etched, much of the red coloration will disappear when panchromatic film is used. A **light-red filter** will aid in the removal of the characteristic reddish background. The absence of red background is particularly desirable when ink or crayon markings are recorded at the same time.

If it is necessary to take pictures of the patterns themselves, it is best to use large-size films on commercial studio equipment. Here the image size is approximately equal to object size. Invariably, it will be desirable to dye-etch the crack patterns before photographing them. With this type of equipment, process orthochromatic or panchromatic film with a blue filter will give the best contrast.

When it is desirable to photograph the patterns themselves before dye etching, the **light** must be perpendicular and tangent to the crack patterns. Great care will be required in arranging the light and camera. Bright lights invariably will heat up the specimen, and occasionally the original crack patterns will close up.

If electrified particles have been used to indicate the crack patterns, it is suggested that **edge lighting** be used rather than direct frontal illumination. These indications have appreciable height, so that when a tangential light source is used, the indications themselves still cause shadows and give very striking results. Direct frontal photographs of such indications on strain-indicating coatings are useful, but the background powder frequently tends to reduce the contrast between indications and background.

Bibliography

ALMEN, J. O. "Fatigue Weakness of Surfaces," *Prod. Eng.*, 21, No. 11 (1950): 118.

ANDERSON, R. G. "Factors Involved in Improving Aircraft Engine Piston Design," *Proc. Soc. Exptl. Stress Anal.*, 1, No. 1 (1943): 61.

———. "Improving Engine Parts by Direct Measurement of Strain," *SAE Journal*, 54 (1946): 466, 501.

BEAN, W. T., JR. "Simplification of Light Metal Casting Design and Its Effect Upon Serviceability," *Trans. Am. Foundrymen's Assoc.*, 55 (1947): 430.

CLENSHAW, W. J. "The Measurement of Strain in Components of Complicated Form by Brittle Lacquer Coatings," *Inst. Mech. Engrs., Proc.* (London), 152 (1945): 221.

DEFOREST, A. V. "A New Method of Measuring Strain Distribution Brittle Coatings," *Instruments*, 12 (1939): 113.

DEFOREST, A. V., and G. ELLIS. "Brittle Lacquers as an Aid to Stress Analysis," *J. Aero. Sci.*, 7 (1940): 205.

DEFOREST, A. V., G. ELLIS, and F. B. STERN, JR. "Brittle Coatings for Quantitative Strain Measurements," *Trans. ASME*, 64 (1942): 184.

DEFOREST, A. V., and F. B. STERN, JR. "Stresscoat and Wire Strain Gage Indications of Residual Stresses," *Proc. Soc. Exptl. Stress Anal.*, 2, No. 1 (1944): 161.

DURELLI, A. J. "Experimental Determination of Isostatic Lines," *Trans. ASME*, 64 (1942): A-155.

DURELLI, A. J., and S. OKUBO. "Crack Density Studies in Stresscoat," *Proc. Soc. Exptl. Stress Anal.*, 11, No. 2 (1954): 153.

———. "Heat Treated Brittle Coating Increases Sensitivity," *Prod. Eng.*, 22, No. 12 (1951): 144.

DURELLI, A. J., and E. A. PHILLIPS. "Criteria for Selecting Experimental Stress Analysis Methods," *Prod. Eng.*, 26, No. 1 (1955): 182.

DURELLI, A. J., and C. H. TSAO. "Use of Brittle Coating Data in Stress Analysis," *Proc. Soc. Exptl. Stress Anal.*, 11, No. 1 (1953): 181.

DURELLI, A. J., and T. N. DEWOLF. "Law of Failure of Stresscoat," *Proc. Soc. Exptl. Stress Anal.*, 6, No. 2 (1948): 68.

EISENHARDT, G. H., and W. L. WALSH. "Stress Analysis of a Pipe Wrench," *Proc. Soc. Exptl. Stress Anal.*, 10, No. 1 (1952): 227.

ELLIS, G. "Practical Strain Analysis by Use of Brittle Coatings," *Proc. Soc. Exptl. Stress Anal.*, 1, No. 1 (1943): 46.

———. "Stress Determination by Brittle Coatings," *Mech. Eng.*, 69 (1947): 567.

ELLIS, G., and F. B. STERN, JR. "Dynamic Stress Analysis with Brittle Coatings," *Proc. Soc. Exptl. Stress Anal.*, 3, No 1 (1945): 102.

EVANS, F. G., and H. R. LISSNER. "Stresscoat Deformation Studies of the Femur Under Static Vertical Loading," *Anat. Record*, 100 (1948): 159.

EVANS, F. G., H. E. PEDERSEN, and H. R. LISSNER. "The Role of Tensile Stress in the Mechanism of Femoral Fractures," *J. Bone and Joint Surg.*, 33A (1951): 485.

GADD, C. W. "Residual Stress Indications in Brittle Lacquer," *Proc. Soc. Exptl. Stress Anal.*, 4, No. 1 (1946): 74.

GURDJIAN, E. S., and H. R. LISSNER. "Deformation of the Skull in Head Injury," *Surg., Gynecol. Obstet.*, 81 (1943): 679.

HARTMAN, J. B., and R. E. BENNER. "Stress Analysis in Design," *Machine Design*, 26, No. 3 (1954): 135; No. 4 (1954): 186; No. 6 (1954): 144; No. 7 (1954): 139.

HETÉNYI, M. "Brittle Models and Brittle Coatings," *Handbook of Experimental Stress Analysis*. New York: John Wiley & Sons, Inc., 1950. P. 636.

HETÉNYI, M., and W. E. YOUNG. "Applications of the Brittle Lacquer Method in the Stress Analysis of Machine Parts," *Proc. Soc. Exptl. Stress Anal.*, 1, No. 2 (1943): 116.

HETÉNYI, M., and W. E. YOUNG. "How Brittle Lacquer Strain Analysis Aids Design," *Machine Design,* 16 (1944): 147, 268.

LEHR, D., and E. LEHR. "Das Dehnungslinienverfahren (The Method of the Stress Lines)," *Z. Ver. deut. Ing.,* 76 (1932): 973.

MOULD, R. E. "The Behavior of Glass Bottles Under Impact," *J. Am. Ceram. Soc.,* 35 (1952): 230.

NEUBER, H. "Der ebene Stromlinienspannungszustand mit lastfreiem Rand (The Planar Streamlined State of Tension with Load-Free Margin)," *Ing.-Arch.,* 6 (1935): 325.

NEW, J. C. "An Example of Efficient Design Through Strain Measurements," *Proc. Soc. Exptl. Stress Anal.,* 6, No. 2 (1948): 111.

POLZIN, M. H. "The Experimental Determination of Strains in Aircraft Landing Wheels and Brakes," *SAE Journal,* 55, No. 6 (1947): 26, 32.

———. "Performance Evaluation of a Magnesium Alloy Truck Wheel," *Proc. Soc. Exptl. Stress Anal.,* 11, No. 1 (1953): 65.

PORTEVIN, A., and M. CYMBOLISTE. "Procédé d'étude de la distribution des efforts élastiques dans les pièces métalliques (Method for the Study of Stress Distribution in Metallic Pieces)," *Rev. met.,* 31 (1934): 147.

SCHMITTNER, W. G. "Determination of Centrifugal Stresses in a Turbosupercharger Impeller by Means of Stresscoat," *Proc. Soc. Exptl. Stress Anal.,* 10, No. 2 (1952): 9.

STAATS, H. N., and BARANOWSKI, S. J. "Calibrated Porcelain Enamel Coatings," *Bull. Am. Ceram. Soc.,* 35 (1952): 232.

STOKEY, W. F. "Elastic and Creep Properties of Stresscoat," *Proc. Soc. Exptl. Stress Anal.,* 10, No. 1 (1952): 179.

TOKARCIK, A. G., and M. H. POLZIN. "Quantitative Evaluation of Residual Stresses by the Stresscoat Drilling Technique." *Proc. Soc. Exptl. Stress Anal.,* 9, No. 2 (1951): 195.

SECTION 53

PHOTOELASTIC-COATING TESTS

CONTENTS

PAGE

Basic Principles

- Principle of test ... 1
- Test development ... 1
- Photoelastic-coating technique definitions ... 2
  - Double refraction, or bi-refringence ... 2
    - Splitting of unpolarized light into two perpendicular plane-polarized rays by a bi-refringent material (*f.* 1) ... 2
    - Optical principles of photoelastic measurements (*f.* 2) ... 2
    - Vector resolution of light rays in stressed photoelastic models or in photoelastic plastic, and in analyzer (*f.* 3) ... 3
    - Path of light through a crossed-plane reflection polariscope (*f.* 4) ... 4
  - Isochromatic lines ... 4
    - Color-stress conversion table (*f.* 5) ... 5
  - Isoclinic lines ... 6
  - Circular polarization ... 6
  - Compensators ... 6

Mathematical Theory

- Identification of symbols ... 6
- Normal incidence analysis ... 7
- Oblique incidence analysis ... 8
  - Vector relationships for analysis of oblique incidence and principal strains (*f.* 6) ... 9

Test Techniques and Materials

- General test procedure ... 11
- Photoelastic coatings ... 11
  - Photoelastic plastic sheets ... 12
  - Photoelastic liquid plastics ... 12
  - Photoelastic contoured sheets ... 12
  - Selection of plastic ... 13
    - Photoelastic plastic coating selection chart (*f.* 7) ... 13
- Calibration of the plastic ... 13
  - Curve showing strain versus polariscope reading (*f.* 8) ... 14
- Preparation of the part to be analyzed ... 14
  - Coating of the surface with plastic ... 15
- Measurement of the value of principal strains 15
- Measurement of the direction of principal strains ... 16

PAGE

Instrumentation

- Classification of instruments ... 16
  - Meter selection chart (*f.* 9) ... 17
- Polarizing quarter-wave viewer for static tests 16
  - Photoelastic-coating patterns in a stressed aluminum plate with drilled holes, as seen with the polarizing quarter-wave viewer (*f.* 10) ... 18
  - Arrangements of the polarizer *P* and quarter-wave plate *Q* (*f.* 11) ... 19
  - Applications ... 19
- Large-field instrument for static tests ... 19
  - Large-field instrument for static tests (*f.* 12) ... 20
  - Light paths through a large field meter (*f.* 13) ... 21
  - Applications ... 21
- Large-field meter for dynamic tests ... 21
- Small-field instrument for static tests ... 23
  - Small-field meter (crossed-plane polariscope) with photocell attachment (*f.* 14) 22
  - Diagram of the light path through a small-field crossed-plane polariscope (*f.* 15) ... 23
  - Use of compensator ... 23
- Small-field electronic meter for static and dynamic tests ... 24
  - Applications ... 24
- The oblique-incidence meter ... 24
  - Oblique-incidence meter (*f.* 16) ... 25
  - Applications ... 24
- Selection of measuring instrument ... 24

Industrial Applications

- Classification of application areas ... 25
- Sheet pile design ... 26
  - Photoelastic-coating analysis in sheet pile design (*f.* 17) ... 28
- Stress analysis of guided-missile tail section 26
  - Photoelastic-coating tests of guided-missile fuselage and tail surfaces under static loading (*f.* 18) ... 30
  - Meters ... 27
  - Loading and stress patterns ... 27
  - Analysis ... 27
  - Results of test ... 27
- Spot-welded assembly ... 27
  - Photoelastic-coating tests of stress distributions in spot-welded joint in 0.125-in. stainless steel (*f.* 19) ... 32

CONTENTS (*Continued*)

PAGE
Welded bridge assemblies 27
  Arc-welded structural steel assembly used in bridges (*f.* 20) 33
Transducer applications 34
  Photoelastic-coating torquemeter (*f.* 21) 34
Telemetering 35
Survey of service life of structures and machines 35
Alignment and calibration of testing machines 35
Visual education 36

PAGE

Advantages and Disadvantages

Advantages 36
Limitations 36
  Curve showing *K* factor versus temperature (*f.* 22) 37
  Curve showing corrections for *K* factor in case of specimens subjected to bending by a known load (*f.* 23) 38
References 38
Bibliography 39

SECTION 53

PHOTOELASTIC-COATING TESTS

Basic Principles

PRINCIPLE OF TEST. Photoelastic-coating tests are an experimental **stress-analysis technique.** The actual structure to be stress-analyzed is coated with a special transparent plastic, and when a load is applied, strains are transmitted to the plastic coating, which then becomes bi-refringent. This change, or **bi-refringence,** is directly proportional to the intensity of strain. A reflective surface is provided on the structure or on the inner face of the plastic bonded to it. Bi-refringence can be observed and measured with polarized light in a specially designed instrument called a **reflection polariscope.** When the plastic coating is examined in the field of polarized light from the instrument, black and colored fringe patterns are seen. These reveal the complete geography of mechanical strains in the actual structure.

From the preceding description it can be seen that this technique differs basically from conventional methods based on photoelastic models. In the photoelastic-coating method, the stress analyst bonds a transparent plastic to the test object itself and then determines the stresses in the coated part under the actual loading system. Conventional photoelastic model techniques involve making a transparent **plastic model** and determining stresses in this model under a simulated load.

The photoelastic-coating test, being essentially a surface-strain technique, differs from the strain-gage technique in that strains are quantitatively determined not only at areas where strain gages are located but also in a continuous manner at every point of the surface coated with the photoelastic plastic.

TEST DEVELOPMENT. The principle of the photoelastic-coating method is credited to Mesnager (France, 1930),[1] who was unable to obtain practical results because he used glass as a bi-refringent layer. Subsequent attempts were made by Mabboux[2] in France and Oppel[3] in Germany in 1932 and 1937. The plastics used at that time did not have sufficient adhesion to metals and were not sufficiently sensitive and stable in time for practical use. In March, 1953, Jessop in England reported research on this subject by the British Aeronautics Laboratory. In July, 1954, Mylonas and Drucker[4] of the United States presented a paper in Brussels at the convention of IUTAM on research conducted at Brown University. The technique cited could be applied only to flat parts. In 1953 the first practical results in both **elastic** and **plastic ranges of deformation** applicable to any size and shape of part (flat or curved) were achieved in industrial applications in France.[5, 6, 7, 8, 9] The accuracy of the results, stability in time, and facility of application have caused this technique to be widely applied in European industry. The method has been applied recently in various industries in the United States.

PHOTOELASTIC-COATING TECHNIQUE DEFINITIONS. The theory of photoelastic-coating tests involves basic principles of optics and of stress analysis. Basic optical phenomena are described in the section on Vision and Optics. Details on photoelastic fundamentals are given in References 10, 11, and 12.

Double Refraction, or Bi-refringence. Certain transparent materials such as crystals of calcite and mica demonstrate the phenomenon of double refraction, or bi-refringence. They divide an incident ray of light into two beams, R_1 and R_2, which travel with different speeds through the material (Fig. 1). This means that one beam will be retarded in relationship to the other while traveling through the plastic. This relative retardation, δ, divided by the thickness of the crystal or plastic, is called bi-refringence (δ/t). In addition the two beams transmitted through the **doubly refractive materials** are polarized at right angles to each other, as shown in Figs. 1 and 2. The **direction of polarization** corresponds to the direction of principal strains in the bi-refringent material. Fig. 1 shows how an unpolarized beam is split in two when traversing the bi-refringent

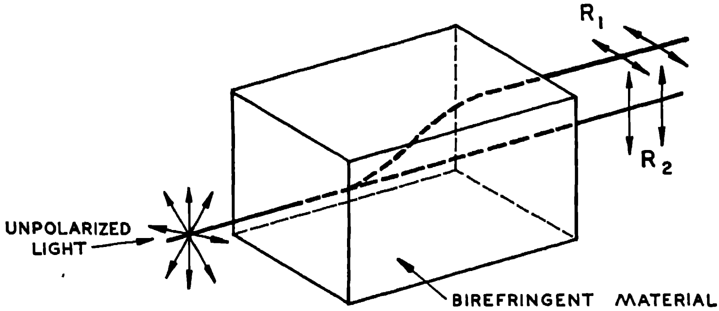

Fig. 1. Splitting of unpolarized light into two perpendicular plane-polarized rays by a bi-refringent material.

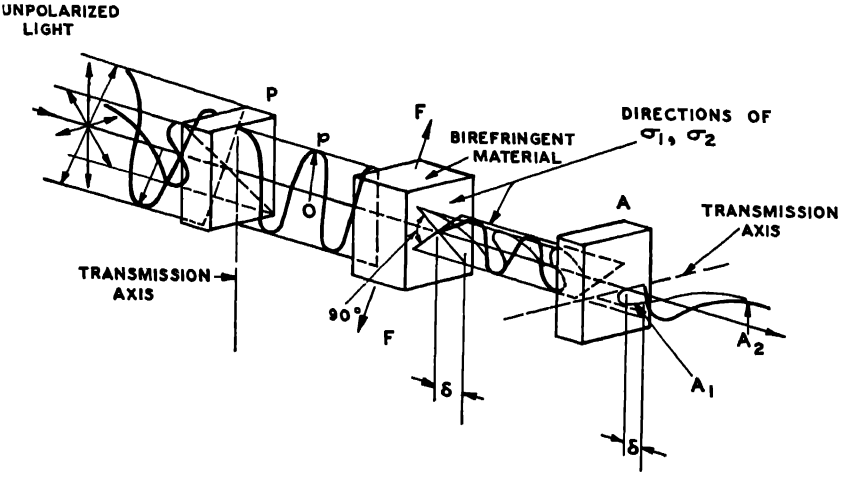

Fig. 2. Optical principles of photoelastic measurements.

material. Fig. 2 shows how these two beams are analyzed by a **polarizing analyzer.**

As shown in Fig. 2, the unpolarized light becomes plane-polarized after passage through the polarizer *P*. The incident plane-polarized vibration *Op* is divided into two component vibrations in the directions of the principal stresses, σ_1 and σ_2, by the bi-refringent material under load *F*. The light emerging from the plastic is called **elliptically polarized light.** The relative retardation of these components is δ. Only the components A_1 and A_2 parallel to the transmission axis of the analyzer pass through the analyzer. Their relative retardation is also δ.

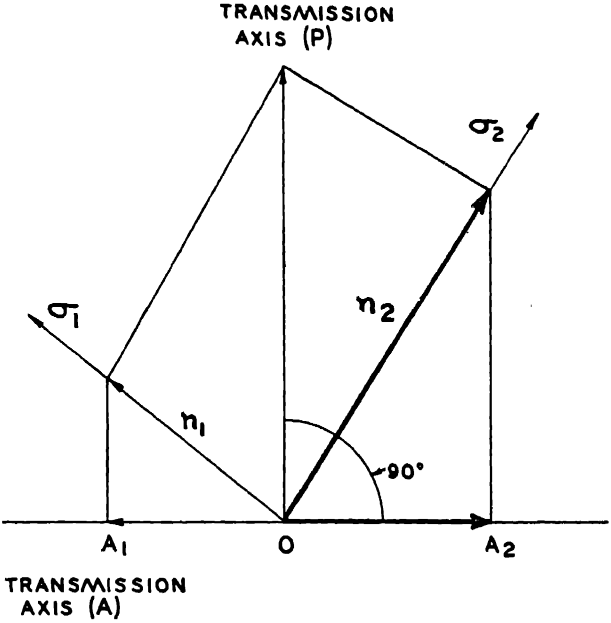

Fig. 3. Vector resolution of light rays in stressed photoelastic models or in photoelastic plastic, and in analyzer.

Fig. 3 shows the vector resolution of *OP* into two vectors, n_1 and n_2, along σ_1 and σ_2 in the stressed model of Fig. 2 or the photoelastic coating of Fig. 4. Figure 3 also shows the resolution of n_1 and n_2 into A_1 and A_2, respectively, in the analyzer.

The path of light through one of the reflection polariscopes used in the photoelastic-coating technique is shown in Fig. 4. Here *P* and *A* are the polarizer and the analyzer, respectively. *G* is a half-mirror. The layer *PC* is the photoelastic coating.

In **photoelastic stress analysis,** polarized light is used to reveal the presence of strains in special transparent materials such as the photoelastic coatings. These substances are not normally doubly refractive but become so when strained. Two sets of **fringes** are visible in the coating when looking at it through a polariscope:

1. **Isochromatic** fringes related to the magnitude of the principal strains.
2. **Isoclinic** fringes related to the directions of the principal strains.

Isochromatic Lines. When the two plane-polarized rays transmitted by the plastic coating are retarded in relationship to each other, colored lines appear. These are known as **isochromatic lines,** or lines of equal color. By using **monochromatic light** (light possessing one color), each point where $\delta = n\lambda$ ($n = 0, 1, 2 \cdots$) will appear in black, the polarizer and analyzer of the polariscope being crossed. Here λ is the wavelength of the monochromatic light used. When two colors of light are used (for example, light composed of blue and red radiations), each point where $\delta = \lambda_{\text{red}}, 2\lambda_{\text{red}}, 3\lambda_{\text{red}}$, etc., will appear in blue because of extinction of the λ_{reds}. Conversely each point where $\delta = \lambda_{\text{blue}}, 2\lambda_{\text{blue}}, 3\lambda_{\text{blue}}$, etc., will appear in red because of the extinction of the λ_{blues}. Other points will appear as a mixing of these two colors. If light with a great number of different colors is used (white light, for example), different **color fringes** appear in the field and correspond to $\delta = n\lambda_1$, $\delta = n\lambda_2, \cdots$, where $\lambda_c \cdots$ is the wavelength (or color) which was extinguished by the polarizing analyzer. The **tint of passage,** which is a sharp dividing line between the reds and the blues or greens, is very often chosen as a characteristic color. The δ corresponding to this tint of passage of first order ($n = 1$) is 2.27×10^{-5} in. The values of δ corresponding to different colors appearing in the field of observation are given in terms of strains in Fig. 5.

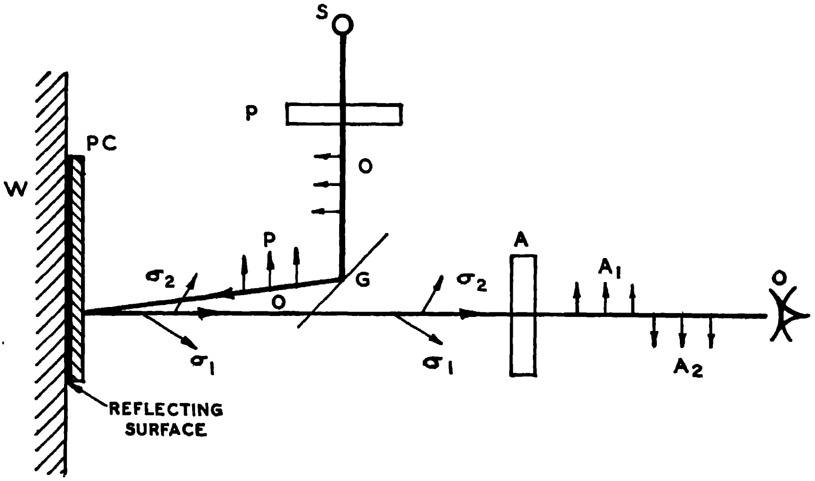

Fig. 4. Path of light through a crossed-plane reflection polariscope.

The **quantitative law of photoelasticity** is: "The intensity of the principal strain difference $\varepsilon_1 - \varepsilon_2$ is directly proportional to the value of δ/t, δ being the relative retardation of polarized light going normal to the plastic, and t being the thickness of the plastic coating." If the axes of the polarizers of the meter are crossed, $\delta = n\lambda$; if they are parallel, $\delta = (n + 1)(\lambda/2)$, λ being expressed in the same units as the thickness of the plastic and $n = 0, 1, 2 \cdots$.

The human eye differs in its sensitivity to different colors. For precise measurements it is necessary to refer to a fringe, usually the sharp line between red and blue, called a "tint of passage." At each point of this fringe the **average sensitivity in strain determination** corresponds to 10 μin. per in. (using the most sensitive plastic, Type S, in 0.120-in. thickness). Outside this fringe, the

Color		Strain[1] (μin./in.), $\varepsilon_1 - \varepsilon_2$	Stress,[2] p.s.i.		Relative Retardation, .00001 mm., δ
in Crossed System	in Parallel System		Steel,[3] $\sigma_1 - \sigma_2$	Aluminum,[3] $\sigma_1 - \sigma_2$	
Black	White	0	0	0	0
Gray	Yellowish-white	170	3,900	1,300	10
White	Light red	430	9,900	3,300	26
Very pale yellow	Dark red-brown	460	10,600	3,500	27.5
—	Tint of passage n'_1	473	10,800	3,600	28.7
Light yellow	Indigo	500	11,500	3,800	30
Brown-yellow	Gray-blue	720	16,600	5,500	43
Reddish-orange	Bluish-green	840	19,400	6,500	50.5
Red	Pale green	900	20,800	6,900	54
Tint of passage n_1	—	945	21,700	7,200	57.5
Indigo	Gold-yellow	980	22,600	7,500	59
Blue	Orange	1100	25,400	8,500	66
Green	Red	1250	28,800	9,600	75
—	Tint of passage n'_2	1418	32,600	10.900	86.2
Greenish-yellow	Violet —	1450	33,500	11.200	87
Pure yellow	Indigo	1520	35,100	11,700	91
Orange	Greenish-blue	1670	38,600	12,800	100
Dark red	Green	1830	42,300	14,100	110
Tint of passage n_2		1890	43.400	14,400	115
Indigo	Gray-yellow	1910	44,000	14,700	116
Green	Brown-red	2200	51,300	17,100	133
—	Tint of passage n'_3	2363	54,200	18,100	143.7
Greenish-yellow	Grayish-indigo	2380	55.000	18,300	145
Carmine red	Green	2550	58,900	19,600	153
Tint of passage n_3	—	2835	65,000	21,700	172
Green	Pale pink	2900	67,000	22,300	174

NOTES:

1. Principal strain difference: $\varepsilon_1 - \varepsilon_2$.
2. Principal stress difference: $\sigma_1 - \sigma_2$.
3. For steel and aluminum: $\mu = 0.3$, $E = 30 \times 10^6$ and 10×10^6 p.s.i., respectively.

$$\varepsilon_1 - \varepsilon_2 = \sigma_1 - \sigma_2 \frac{(1 + \mu)}{E}$$

4. This chart is valid for thickness of plastic, $t = 0.120$ in. and $K = 0.1$ (plastics Type S or A). If the thickness t of the plastic used in the test is different from 0.120 in., the values of stresses and strains have to be multiplied by a factor 0.120 in./X, where X is the thickness of the plastic used.

5. If the constant K of the plastic used in the test is different from 0.1, the values of stresses and strains have to be multiplied by a factor $0.1/K$.

Fig. 5. Color-stress conversion table.

sensitivity can drop to 150 μin. per in. **Compensators** will, however, give the same sensitivity of 10 μin. per in. at each point under study.

A **uniform strain distribution** (in a tensile specimen with rectangular cross-section, for example) produces a uniform color. For each variation in intensity of the strain, the color will be different. A **nonuniform strain distribution** yields variously colored striations which on analysis (under normal incidence and oblique incidence)[5, 12, 13] indicate the magnitude and sign of the principal strains.

Isoclinic Lines. When the plane of incidence of the polarized light coincides with the direction of one of the principal stresses, the light passes unimpeded through the plastic. If the analyzer is at right angles to the polarizer (crossed polarizers), no light is visible at that point. An extinction line of such points is known as an **isoclinic.** At every point of an isoclinic, the directions of principal strains are constant and the same as the directions of the crossed polarizer-analyzer system in the polariscope. With the aid of isoclinics it is possible to plot **isostatics, or stress trajectories.** Isostatics are lines tangent to either the σ_1 or σ_2 principal stress at every point.

Circular Polarization. In some investigations, isochromatic lines can be examined more easily when the black isoclinic lines are removed. This can be done satisfactorily by placing a **quarter-wave retardation plate** between each polarizer and the coated part. The light emerging from a combination of polarizer and quarter-wave plates with their optical axis at 45 deg. is known as "circularly polarized light." A quarter-wave plate is a permanently bi-refringent material in which the relative retardation δ is equal to $\lambda/4$.

Compensators. Compensators are used if the number of isochromatics (tints of passage) is insufficient for an accurate whole-field stress determination or if the stresses are to be determined at a point outside a fringe. These compensators are devices which artificially produce a tint-of-passage fringe at any given point of the bi-refringent plastic. The underlying principle of better known compensators involves:

1. Adding or subtracting a "known bi-refringence" (usually by means of a calibrated quartz wedge) to the "unknown bi-refringence" so as to produce a tint of passage at the point under consideration; or
2. Transforming, by means of a quarter-wave plate, the elliptically polarized light emerging from the plastic into plane-polarized light and then quenching the latter by means of the analyzer.[10, 11, 12]

Mathematical Theory

IDENTIFICATION OF SYMBOLS. The functional relationships given here prove useful in stress analysis by the photoelastic-coating technique. In the following equations:

t = thickness of the plastic.
E = modulus of elasticity.
μ = Poisson's ratio.
K = strain optical constant.
C = stress optical constant. (Photoelastic-coating tests are concerned only with the strain optical constant K.)
n_1 and n_2 = principal indices of refraction of the bi-refringent plastic.
σ_1 and σ_2 = principal surface stresses.
σ'_1 and σ'_2 = "secondary" principal stresses (maximum and minimum stresses in a nonprincipal plane).

ε_1 and ε_2 = principal surface strains.
p = plastic symbol
w = work-piece symbol.
δ_n = relative retardation measured when polarized light is traversing the plastic under normal incidence.
δ_{o1} and δ_{o2} = relative retardations measured when polarized light is traversing the plastic under oblique incidence.
θ_{o1} and θ_{o2} = angles of incidence of the beam of light

NORMAL INCIDENCE ANALYSIS. The difference of principal strains or maximum shear strains is determined in normal incidence analysis. In any material which exhibits artificial or temporary bi-refringence when stressed, relative retardation δ is related to principal stress-difference by **Newmann's equation:**

$$\delta_n = (n_1 - n_2)2t = C(\sigma_1 - \sigma_2)_p 2t$$

or

$$\frac{\delta_n}{2tC} = (\sigma_1 - \sigma_2)_p \tag{1}$$

The formula calls for $2t$ because light is reflected from the surface of the work piece, passing through the plastic twice.

Since only surface stresses are considered here, the stress σ_3 normal to the surface is equal to zero, and **Hooke's general expressions for strains** become

$$\varepsilon_1 = \frac{\sigma_1}{E} - \frac{\sigma_2}{E}\mu$$

$$\varepsilon_2 = \frac{\sigma_2}{E} - \frac{\sigma_1}{E}\mu$$

Therefore

$$\sigma_1 - \sigma_2 = (\varepsilon_1 - \varepsilon_2)\frac{E}{1 + \mu}$$

and

$$(\sigma_1 - \sigma_2)_w = \frac{(\varepsilon_1 - \varepsilon_2)_w E_w}{(1 + \mu_w)} \tag{2}$$

$$(\sigma_1 - \sigma_2)_p = \frac{(\varepsilon_1 - \varepsilon_2)_p E_p}{(1 + \mu_p)}$$

Combining Eq. 2 with Eq. 1,

$$\frac{\delta_n}{2tC} = \frac{(\varepsilon_1 - \varepsilon_2)_p E_p}{(1 + \mu_p)} \tag{3}$$

Since the plastic follows exactly the deformations of the work piece,

$$(\varepsilon_1 - \varepsilon_2)_p = (\varepsilon_1 - \varepsilon_2)_w$$

so that

$$\begin{aligned}(\sigma_1 - \sigma_2)_w &= \frac{(\varepsilon_1 - \varepsilon_2)_p E_w}{(1 + \mu_w)} \\ &= \left(\frac{\delta_n}{2tC}\right)\frac{E_w(1 + \mu_p)}{E_p(1 + \mu_w)} \\ &= \left(\frac{\delta_n}{2t}\right)\frac{E_w}{K(1 + \mu_w)} \qquad (4)\end{aligned}$$

and

$$\varepsilon_1 - \varepsilon_2 = \frac{\delta_n}{2tK} \tag{5}$$

where

$$K = \frac{CE_p}{1 + \mu_p} \tag{6}$$

Inspection of Eq. 4 shows that the **principal stress-difference** in the structure can be found by measuring under normal incidence the bi-refringence $\delta_n/2t$ of the plastic, provided the three factors, E_w, μ_w, and K are already known. Since the relative maximum shear stress $(\tau_{\max.})_w$ is equal to $\frac{1}{2}(\sigma_1 - \sigma_2)_w$, and the relative maximum shear strain is equal to $(\varepsilon_1 - \varepsilon_2)$, the measurement of $\delta/2t$ will give these values of maximum shear directly.

The principal stress normal to a free boundary is always zero. Therefore the measurement of $\delta/2t$ under normal incidence along free edges gives directly the **principal stress tangential to the free boundary,** i.e.,

$$\sigma_1 = \frac{\delta[E/(1+\mu)]}{2tK}$$

$$\sigma_2 = 0$$

and

$$\varepsilon_1 = \frac{\delta}{2tK(1+\mu)}$$

$$\varepsilon_2 = -\mu\varepsilon_1$$

To determine the separate values of principal stresses outside a free boundary, it is possible either to use graphical integration (see Frocht's treatment, Photoelasticity,[11] for example) or to make an additional measurement of $\delta/2t$ with polarized light traversing the plastic under oblique incidence, as described subsequently.

OBLIQUE INCIDENCE ANALYSIS. The separate values of principal strains are determined in oblique incidence analysis. Let *1*, *2*, and *3* be the directions of principal stresses [Fig. 6(a)]. The plane of the plastic coincides with plane *1–2*, and the principal stress σ_3 perpendicular to this plane is zero in surface problems. Analysis of a plane-polarized light wave parallel to plane *1–2* (ray of light in direction *3*) provides the principal stress-difference $(\sigma_1 - \sigma_2)$. When the system of axes, *1*, *2*, *3* is rotated through an angle θ_{O1} around axis *1*, *3* moves to *3′* and *2* moves to *2′*. Now the light ray travels along direction *3′*, and analysis of the plane-polarized wave parallel to plane *1–2′* provides the difference $(\sigma_1 - \sigma'_2)$ between the principal stress σ_1 and the "secondary" principal stress σ'_2 (the wave front of the vibration cuts the ellipsoid of indices in a "secondary" ellipse, which contains only one principal axis). A similar rotation about axis *2* determines $(\sigma'_1 - \sigma_2)$.

The relationship between $(\sigma'_1 - \sigma_2)$, $(\sigma_1 - \sigma'_2)$ and angles θ_{o1}, θ_{o2}, and principal stresses σ_1 and σ_2 may be derived from Fig. 6(b), Mohr's stress circles.

$$(\sigma_1 - \sigma'_2)_p = (\sigma_1 - \sigma_2 \cos^2 \theta_{o1})_p = \frac{\delta_{O1}}{2(t/\cos\theta)C} \qquad (7a)$$

$$(\sigma_2 - \sigma'_1)_p = (\sigma_2 - \sigma_1 \cos^2 \theta_{o2})_p = \frac{\delta_{O2}}{2(t/\cos\theta)C} \qquad (7b)$$

Here δ_{O1} and δ_{O2} are the relative retardations corresponding to the rotations about axes *1* and *2* (analysis in planes *1–2′* and *1′–2*), and θ_{O1} and θ_{O2} are the angles that correspond to these rotations. The thickness of the plastic through which light passes is now $2t/\cos\theta$. If $\theta_{O1} = \theta_{O2}$, then

$$(\sigma_1)_p = \frac{\delta_{o1} + \delta_{o2}\cos^2\theta}{1 - \cos^4\theta}\left[\frac{1}{2(t/\cos\theta)C}\right]$$

$$(\sigma_2)_p = \frac{\delta_{o2} + \delta_{o1}\cos^2\theta}{1 - \cos^4\theta}\left[\frac{1}{2(t/\cos\theta)C}\right]$$

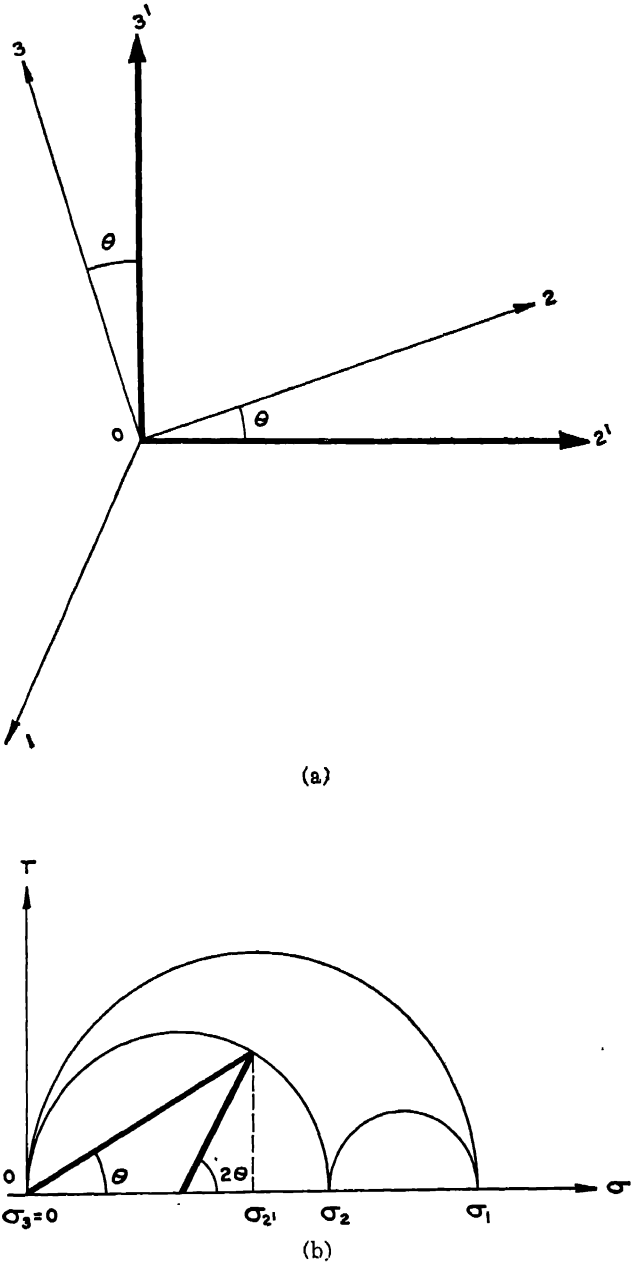

Fig. 6. Vector relationships for analysis of oblique incidence and principal strains. (a) Rotation θ of axis of principal stresses. (b) Mohr's stress circles.

and if $\theta_{O1} = \theta_{O2} = 45$ deg.,

$$(\sigma_1)_p = \frac{\sqrt{2}}{3tC}\left(\delta_{o1} + \frac{\delta_{o2}}{2}\right) \qquad (8)$$

$$(\sigma_2)_p = \frac{\sqrt{2}}{3tC}\left(\delta_{o2} + \frac{\delta_{o1}}{2}\right)$$

When one measurement is taken under oblique incidence (Eq. 7a) and the other measurement under normal incidence (Eq. 1),

$$(\sigma_1)_p = \left(\delta_n + \frac{\sqrt{2}}{2}\delta_{o2}\right)\frac{1}{tC} \qquad (9)$$

$$(\sigma_2)_p = \left(\frac{\delta_n}{2} + \frac{\sqrt{2}}{2}\delta_{o2}\right)\frac{1}{tC}$$

It is sufficient to measure δ_{o1} and δ_{o2}, or δ_{o1} and δ_{normal}, or δ_{o2} and δ_{normal} in order to obtain separate values for $(\sigma_1)_p$ and $(\sigma_2)_p$, both in magnitude and sign, from which values of the principal stresses in the part, $(\sigma_1)_w$ and $(\sigma_2)_w$, may be derived.

1. With two oblique readings,

$$(\sigma_1)_w = \left(\frac{\sqrt{2}}{3}\right)\frac{E_w}{kt(1+\mu)}\left(\delta_{o1} + \frac{\delta_{o2}}{2}\right) \qquad (10)$$

$$(\sigma_2)_w = \left(\frac{\sqrt{2}}{3}\right)\frac{E_w}{kt(1+\mu)}\left(\delta_{o2} + \frac{\delta_{o1}}{2}\right)$$

2. With one normal reading and δ_{o1},

$$\sigma_1 = \frac{E_w}{tk(1+\mu)}\left(\frac{\sqrt{2}}{2}\delta_{o1} - \frac{\delta_n}{2}\right) \qquad (11)$$

$$\sigma_2 = \frac{E_w}{tk(1+\mu)}\left(\frac{\sqrt{2}}{2}\delta_{o1} - \delta_n\right)$$

3. With one normal reading and δ_{o2},

$$\sigma_1 = \frac{E_w}{tk(1+\mu)}\left(\frac{\sqrt{2}}{2}\delta_{o2} + \delta_n\right) \qquad (12)$$

$$\sigma_2 = \frac{E_w}{tk(1+\mu)}\left(\frac{\sqrt{2}}{2}\delta_{o2} + \frac{\delta_n}{2}\right)$$

where δ_{o1} and δ_{o2} are the relative retardations (or color) measured under oblique incidence and δ_n is measured under normal incidence. For simplification of formulas, it is assumed that $\mu_p = \mu_w$.

Note that under oblique incidence the reflection from the work piece will give a relative retardation that depends on the nature of the surface as well as the angle of incidence. In order to eliminate this source of error from calculations, two sets of measurements should be taken in different planes of incidence, $O1$ and $O2$: one set, δ'_{o1} and δ'_{o2} under load, and another under no load, δ''_{o1} and δ''_{o2}. Then the true relative retardations are, respectively,

$$\delta_{o1} = \delta'_{o1} - \delta''_{o1}$$

and

$$\delta_{o2} = \delta'_{o2} - \delta''_{o2}$$

Test Techniques and Materials

GENERAL TEST PROCEDURE. In general, to stress-analyze a part with the photoelastic-coating technique, the following steps are recommended:

1. Choose the proper plastic.
2. Clean the part and make it reflective by polishing or by spraying with aluminum paint.
3. Apply the photoelastic plastic.
4. Apply the loads to the part to be stress-analyzed.
5. Use the appropriate polariscope instrumentation for the observation of the over-all distribution of the strains. These will appear as color fringes. Areas where color fringes are concentrated correspond to areas with stress concentrations. Generally these are the areas to be investigated.
6. After deciding which areas have to be investigated quantitatively, use large-field or small-field instruments for measurement of the magnitude of the difference of the principal strains and of the directions of the principal strains. If separate values of principal strains are required, use the oblique-incidence instrument in conjunction with the large-field or small-field instruments.
7. If point-by-point measurements are required, trace the points to be measured with a scriber on top of the plastic. Focus the eye at a given point through the instrument and make the measurement. If the over-all distribution of strains is required, trace the isochromatics (as seen through the large-field instrument) with a grease crayon directly on the plastic that covers the area on the part. The same method applies to the isoclinics. Transfer these drawings to a transparent paper and note the value of the strain on each isochromatic. From the isoclinic drawings, if required, trace the two families of the isostatics.
8. If liquid plastic has been used, measure the thickness of the coating; if sheets have been used, the thickness is constant and known.
9. If a dynamic test is required, use the large-field dynamic instrument or the dynamic-electronic instrument, depending upon the nature of the investigation, i.e., over-all strain distribution or point-by-point measurements.
10. Whenever possible, use still photography or motion pictures in each case for recording the position of the fringes and their displacement during the loading. Identify each fringe on the photograph by its order and mark the value of strain on it.
11. After recording measurements under load, unload the part and observe if some colors or fringes remain. If these are present, it means that the part has been permanently deformed. Then, if necessary, take measurements of residual strains.
12. Apply formulas of Eqs. 4 and/or 10, 11, or 12 for conversion of bi-refringence values into stresses.

The detailed procedure for each of the preceding steps is given in subsequent portions of this section.

PHOTOELASTIC COATINGS. The application of the theory of photoelasticity to real parts imposes the condition that the photoelastic coating be strongly bonded to the part to be stress-analyzed. This coating may consist of a **liquid plastic** (applied by brushing or dipping) or of **plastic sheets** bonded to the part with a special cement. The coating must have the following **characteristics:**

1. It must be highly sensitive from the point of view of photoelasticity, i.e., have a strain-optical effect as high as possible.
2. It should adhere to any kind of material and any shape and size of part.
3. The optical effect (bi-refringence) of the coating should be strictly proportional to the principal strains, regardless of the amplitude of the strain (elastic or

plastic deformation) or the time of maintaining the loading and speed of the loading (dynamic tests).

4. It should be transparent.
5. It should not have parasitic bi-refringence before the part is loaded.
6. It should be stable with time.
7. It should be easily machinable.
8. It should be insensitive to ambient conditions. (This is very important for outdoor tests under any humidity conditions, in water, oil, etc.)
9. It should be usable at different temperatures.

Photoelastic Plastic Sheets. Commercially available plastic sheets are either clear or metallized on one face. They are held to thickness tolerances of approximately 0.002 in. They have uniform strain-optical properties. They are free from internal stresses and therefore free from parasitic bi-refringence. The coefficient *K*, which relates the mechanical effect (strain) to the optical effect (bi-refringence or color), is the same at every point of the surface of any given sheet. Both **clear or metallized sheets** are manufactured as flat sheets or in contoured shapes, provided there is no very sharp radius of curvature.

Flat or contoured sheets are bonded with a special adhesive to the structure to be stress-analyzed. This is applied like any ordinary cement and dries in about 24 hr. at room temperatures.

The two available types of sheets differ in maximum elongation characteristics and strain-optical constant *K*. For the **low-strain sheet**, the limit of linear strain-optical response $\varepsilon_{\text{max.}}$ is 2.5 percent, and the constant *K* is about 0.1 at room temperatures. When used on mechanical parts operating above 250° F., this plastic can be stretched 30 percent, but the strain-optical constant *K* drops to 0.03. Variations of *K* with temperature outside the range of —44° F. to 85° F. (where *K* is practically constant) can be plotted easily with a calibration device (see Fig. 22).

In **high-strain sheets,** $\varepsilon_{\text{max.}}$ **at room temperature** is equal to 30 percent, and *K* is about 0.02. This type is used for stress-analysis of rubber and, in general, for studies of very deformable materials.

Photoelastic Liquid Plastics. Two types of liquid plastic are available. These differ in maximum elongation characteristics and strain-optical constant *K*. They are applied to the part by brushing or dipping and are hardened by heating.

The low-strain type of liquid plastic, when used for tests at room temperatures, has a limit of linear strain-optical response $\varepsilon_{\text{max.}}$ of about 3 percent. The constant *K* is approximately 0.1. It is similar to the first type of sheet material.

Another high-strain type of liquid plastic, also used for tests at room temperature, has a limit of strain-optical response $\varepsilon_{\text{max.}}$ of approximately 30 to 50 percent, and *K* is approximately 0.02. It is similar to the high-strain type of sheet material.

Photoelastic Contoured Sheets. When photoelastic plastic is to be applied to a relatively large contoured surface, it is best to form contoured sheets from liquid plastic. The plastic is mixed with hardener and poured to the desired thickness into a level mold. The plastic is then polymerized at 50° C. for 45 min. approximately, after which time the sheets can be removed from the form, shaped over the part, and bonded directly to the part under investigation. This method produces a sheet of uniform thickness with no residual bi-refringence. Contoured sheets can be made from either low-strain or high-strain types of liquid plastic, depending on the maximum elongation required for the test.

Selection of Plastic. Selection of the proper plastic is governed by the shape of the test object, the nature of the work surface, and the strength of the work piece. The estimated maximum strain to which the work piece will be subjected during the test is also an important consideration.

The **shape of the work piece** will determine whether the photoelastic plastic should be in sheet or liquid form. Sheets should be used whenever possible because their thickness is constant and they can be bonded to the surface at room temperature. Liquid should be used for analysis of small parts and of structures having closely spaced rivets, fillets, or recesses with very small radii, and whenever it is impossible to cement a prefabricated strip to the structure. It is also recommended for studies of the behavior of sheet metal during drawing or laminating, for studies of the rupture of mild steels, and for problems involving extreme plastic deformations.

The **nature of the work-piece** surface, whether reflective or nonreflective, will determine whether the plastic should be transparent (standard sheets or liquid), or metallized (mirror sheets). The **strength of the work piece** will determine the thickness of the plastic. The greater the plastic thickness, the greater the over-all sensitivity of measurements, but too great a thickness may increase the strength of the work piece and corrections of measurements will be required. (The modulus of elasticity of the low-strain plastic is approximately 450,000 p.s.i.; of high-strain plastic, approximately 40,000 p.s.i.)

The **estimated maximum strain** to which the work piece will be subjected during the test will determine, by comparison with the $\varepsilon_{\text{max.}}$ listed in column 4 of Fig. 7, what type of plastic should satisfy this test condition.

(1) Plastic Coating		(2) Type	(3) Thickness t, in.	(4) Limit of Linear Strain-optical Response, %	(5) Strain-optical Constant K
Sheets	Standard Mirror	S S_m	0.048, 0.072, or 0.120	2.5	0.1
	Standard Mirror	M M_m	0.048, 0.072, or 0.120	30	0.02
Liquid		A	From 0.001 to 0.120	3	0.1
		G	From 0.001 to 0.120	30–50	0.02

Tatnall Measuring Systems Co.

Fig. 7. Photoelastic plastic coating selection chart.

CALIBRATION OF THE PLASTIC. It is possible to apply a known strain to a test specimen coated with the plastic to be calibrated. Relative retardation resulting from this strain is then measured. Application of the formula of Eq. 5,

$$\varepsilon_1 - \varepsilon_2 = \frac{\delta_n}{2tK}$$

permits verification of the value of K and the determination of variations in K which may occur as a result of wide temperature changes during test. The simplest **test devices** are a cantilever beam, a tensile specimen, or a pure bending specimen made of a material with known mechanical characteristics.

It is also possible to calibrate in one over-all operation the plastic and the instrument used. A piece of plastic taken from the same sheet used for the part under test is bonded to a tensile specimen, for example. The instrument used for the test is focused on the plastic, and measurements are taken for different known strains applied to the tensile specimen. A curve of strain versus polariscope reading is plotted (the curve should always be a straight line, since there is linearity between ε and δ) (see Fig. 8).

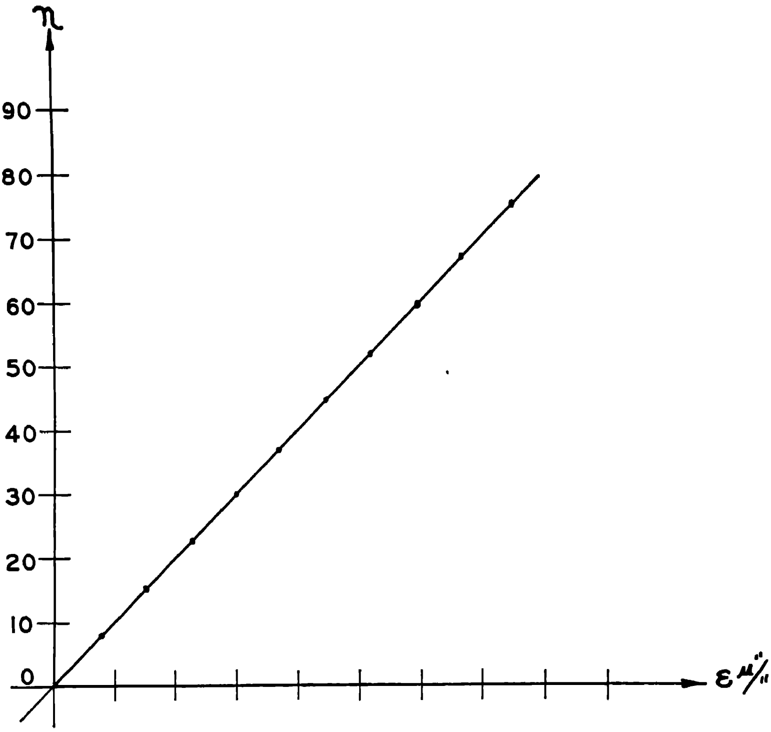

η = value of reading on the polariscope

ε = applied known strain

Fig. 8. Curve showing strain versus polariscope reading.

From this calibration it is seen that one division of the polariscope reading corresponds to *X* microinches per inch of strain. The polariscope reading can now be expressed directly in terms of strain, since the thickness of the plastic and the wavelength of light are the same on the test piece and on the calibration device. The polariscope reading on the part should then be multiplied by *X* microinches per inch.

PREPARATION OF THE PART TO BE ANALYZED. The test-object surface must be reflective, and it should be thoroughly cleaned in order to ensure proper adhesion of the plastic. **Degreasing the surface** is done with trichlorethylene or acetone. The surface to be stress-studied may, of course, already be reflective. If not, it should be made **reflective** by:

1. Polishing. The degree of polishing is not too critical; the finish obtained with emery paper or even by rough grinding is sufficient.
2. Spraying with an aluminum undercoat, or by coating (after proper degreasing, as mentioned here) with a photoelastic mirror-sheet. This is recommended especially when a high degree of accuracy is desired in measurements for such nonreflective surfaces as concrete and wood.
3. By bonding the plastic sheets to the test-object surface with an aluminum-filled cement.

Coating of the Surface with Plastic. Photoelastic sheets or liquid can be applied to steel, aluminum, copper, light alloys, high-temperature-resisting alloys, concrete, plaster, ceramics, some plastic materials, rubber, glass, wood, rocks, and other materials. Flat or contoured standard or mirror-sheets are bonded to the structure with a special adhesive which is applied like any ordinary cement and which dries in about 24 hr. at room temperature. When using liquid, the work piece is coated with a first layer of plastic and then heated to from 150° F. to 230° F., depending upon the facilities available, such as infrared, oven or gas range. As soon as the plastic hardens (it takes only a few minutes), a new layer is applied and the process is repeated until a suitable thickness is reached (generally between 0.001 and 0.060 in.). Any irregularities in the coating can be removed by filing, scraping, or other methods. A coating of uniform thickness is not mandatory, for only the coating thickness at the point of measurement is required, and this can be measured readily.

MEASUREMENT OF THE VALUE OF PRINCIPAL STRAINS. The value of principal strains is measured by isochromatic lines (or by bi-refringence). Bi-refringence, $\delta/2t$, is obtained by separate measurements of t and δ. Thickness t of plastic sheets is given within 0.002 in. by the manufacturer. The thickness of the liquid coating can be measured readily with any of the thickness gages available on the market or with one of the small-field meters described subsequently. Two vernier readings are taken: one after focusing the instrument on the surface of the structure, and the other after focusing on the surface of the plastic coating (previously identified by means of a small pencil mark). The difference between the two readings provides the thickness of the plastic coating within an accuracy of a few percent.

Measurement of δ (isochromatics or colors) under normal incidence determines the principal stress difference $(\sigma_1 - \sigma_2)_w$, and under oblique incidence, the separate values of the principal stresses σ_1 and σ_2 (see Mathematical Theory in this section).

Four basic methods are used with a circular polariscope system to **measure bi-refringence** (color) in the plastic and hence strain in the parts. In the order of their increasing sensitivity, these are:

1. Identify the color observed and look up its corresponding strain value in the color-stress conversion chart (Fig. 5) or match the color on the part with the color of a calibration device coated with the same plastic as the part.
2. Find a black line, and from this line count the number of successive "tint-of-passage" fringes. (By tint of passage is meant a sharp line between red and blue.) This method permits strain determinations at any point located on such a fringe, as follows: The black fringe corresponds to zero principal strain difference, and its order n is zero. The first tint of passage (fringe order $n = 1$) corresponds to a strain $(\varepsilon_1 - \varepsilon_2)$ whose value in microinches per inch is known,

for it depends solely on the type and thickness of the photoelastic plastic used. For example: the first fringe will correspond to approximately 945 μin. per in. ($\varepsilon_1 - \varepsilon_2$), using low-strain plastic sheet in 0.120-in. thickness. The second tint ($n = 2$) corresponds to $2(\varepsilon_1 - \varepsilon_2)$; the nth fringe to $n(\varepsilon_1 - \varepsilon_2)$, etc. In case the thickness or the type of plastic used is different from the plastic mentioned here, use the corrections indicated in the color-stress conversion chart (Fig. 5).

3. Use an "optical compensator" calibrated in terms of strains. This method permits very accurate strain determinations at any point—whether located on a fringe or not. Strain sensitivity is ±10 μin./in. for a plastic sheet of 0.120-in. thickness.
4. Convert colors into photoelectric currents and measure these by means of highly sensitive electronic meters (described later).

MEASUREMENT OF THE DIRECTION OF PRINCIPAL STRAINS. The directions of the principal strains are determined by the isoclinics or black fringes visible with a plane-crossed polariscope system. At each point of these fringes, the directions of the principal strains are constant and are the same as the directions of the transmission axis of the polariscope. When the transmission axes are known, the directions of the principal strains can be identified. Photoelastic-coating analysis meters permit the measurement of these directions, either point-by-point or in a continuous manner over the entire field. The accuracy of measurement of these directions is ±2 deg. for visual methods and ±0.3 deg. when using photoelectric instruments. The determination of the directions of principal stresses does not depend on the thickness of the plastic.

Instrumentation

CLASSIFICATION OF INSTRUMENTS. Various instruments which have been developed for photoelastic-coating analysis include:

1. The polarizing quarter-wave viewer for static tests.
2. The large-field instrument for static tests.
3. The large-field instrument for dynamic tests.
4. The small-field instrument for static tests.
5. The small-field electronic meter for static and dynamic tests.
6. The oblique-incidence instrument.

Fig. 9 lists the various instruments available, with their sensitivities and ranges of measurements.

POLARIZING QUARTER-WAVE VIEWER FOR STATIC TESTS. The simplest instrument consists of a polarizing plate P and a quarter-wave plate Q which has its optical axis set at 45 deg. to the principal plane or transmission axis of the polarizer. It is placed against the plastic-coated structure and exposed to a light source (Fig. 10b).

When the polarizing plate P is between the quarter-wave plate and the structure, the unit behaves like a parallel-plane polariscope with a light field, as shown in Fig. 11(a). The polarizer also serves as an analyzer. Every point at which directions of stresses are 45 deg. to the transmission axis of the polarizer will appear in pure color (isochromatic fringes) and will correspond to the condition: $\delta = (n + 1)(\lambda/2)$, where $n = 0, 1, 2 \cdots$. All other points will be "washed out" or completely colorless if the directions of stresses coincide with those of the polarizer axis (designated on the instrument). The approximate directions of the principal stresses may therefore be estimated.

Designation	Strain Sensitivity * Minimum Measurable Strain, μin./in.	Maximum Measurable Strain, μin./in.	Meter Constant, D^x microinch *	To Be Used for
1. Polarizing quarter-wave viewer	100	30,000 or 500,000 †	1.2	Observations of stress distributions and rough estimations of $(\varepsilon_1 - \varepsilon_2)$.
2. Large-field static meter (portable)	20	30,000 or 500,000 †	0.24	Observations of stress distributions and measurements of $(\varepsilon_1 - \varepsilon_2)$ on large surfaces in static tests.
3. Large-field dynamic meter	20	30,000 or 500,000 †	0.24	Observations of stress distributions and measurements of $(\varepsilon_1 - \varepsilon_2)$ on small or large surfaces; in dynamic tests; stroboscope. photography (white, or monochromatic, light); films (color, or black and white).
4. Small-field static meter	10	30,000 or 500,000 †	0.12	Point-by-point measurements of $(\varepsilon_1 - \varepsilon_2)$ in static tests; determination of t.
5. Small-field static and dynamic electronic meter	0.1	±500 *	0.0012	Point-by-point measurements of $(\varepsilon_1 - \varepsilon_2)$, generally in dynamic tests; determination of t.
6. Oblique-incidence meter	10	3,000 *	0.12	Point-by-point measurements of the value of each principal stress; in static tests.

Tatnall Measuring Systems Co.

* For $K = 0.1$ and $t = 0.120$ in.
If K is different, multiply the numbers by $0.1/K$.
If t is different, multiply the numbers by 0.120 in. per t inch.
† Depending upon plastic used.

Fig. 9. Meter selection chart.

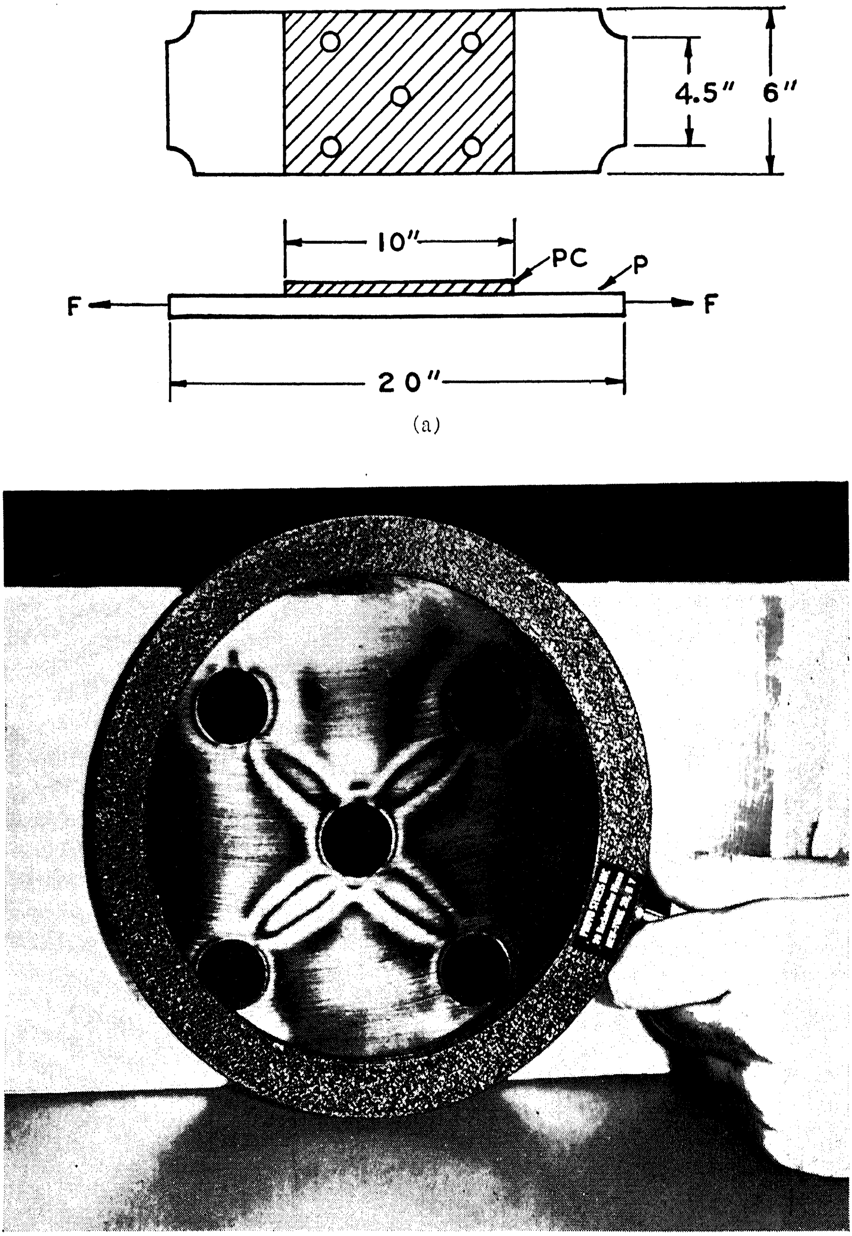

(a)

(b) Tatnall Measuring Systems Co.

Fig. 10. Photoelastic-coating patterns in a stressed aluminum plate with drilled holes, as seen with the polarizing quarter-wave viewer. (a) Tensile test specimen with drilled holes. (b) Stress patterns revealed with polarizing quarter-wave viewer.

Values of $(\varepsilon_1 - \varepsilon_2)$ may be determined along half-order fringes corresponding to relative retardations of multiples of half-wavelengths. Each fringe is the locus of points of constant difference of principal stresses.

If the quarter-wave plate Q is placed between the work piece and polarizer P, plane-polarized light transmitted by polarizer P is circularly polarized when passing through the quarter-wave plate, as shown in Fig. 11(b). After it has passed through the plastic coating, has been reflected from the surface of the work piece, and has passed a second time through the plastic, this circularly polarized light is again plane-polarized upon passing a second time through the quarter-wave plate Q. Now, however, its plane of polarization is 90 deg. to that of the incident plane of vibration. The system behaves like a **crossed-circular polariscope.** Fringes will appear, irrespective of the orientation of the polarizer and quarter-plate combination, and will correspond to a relative retardation: $\delta = n\lambda$.

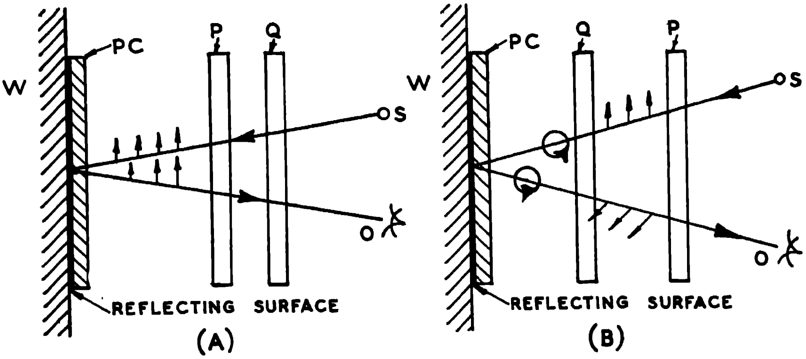

Fig. 11. Arrangements of the polarizer P and quarter-wave plate Q. (a) In a plane-parallel polariscope. (b) In a circular-crossed polariscope.

Applications. This instrument permits determination of the approximate direction of principal stresses and of the magnitude $(\sigma_1 - \sigma_2)$ of the principal stress difference along the half-order fringes (δ corresponding to $\lambda/2$, $3\lambda/2$, $5\lambda/2$) and along the integral fringes (δ corresponding to 0, λ, 2λ, 3λ). It is also possible to determine approximate magnitude of stresses by means of the tints observed. These tints correspond to Newton's colors for which the value of strains can be found in Fig. 5. This polarizer quarter-wave plate viewer is used only for approximate analyses. Its average accuracy is ±10 deg. for directions of principal stresses and ±100 μin. for magnitudes of strains (using low-strain plastic in 0.120-in. thickness).

LARGE-FIELD INSTRUMENT FOR STATIC TESTS. The portable large-field instrument (Fig. 12) consists of an illuminator equipped with an adjustable optical system and a polarizer P and analyzer A lying in the same plane. Polarizer P is placed in front of the illuminator, and the observer looks at the work piece through analyzer A. The rotation of both polarizer P and analyzer A about its axis can be independent or synchronized with that of the other. In addition, the instrument includes two quarter-wave plates, Q_1 and Q_2, which can be placed in front of P and A, respectively, or swung out of position.

Two sets of fringes are seen through this analyzer, a set of colored fringes (under white light) called **isochromatics** and a set of black fringes called

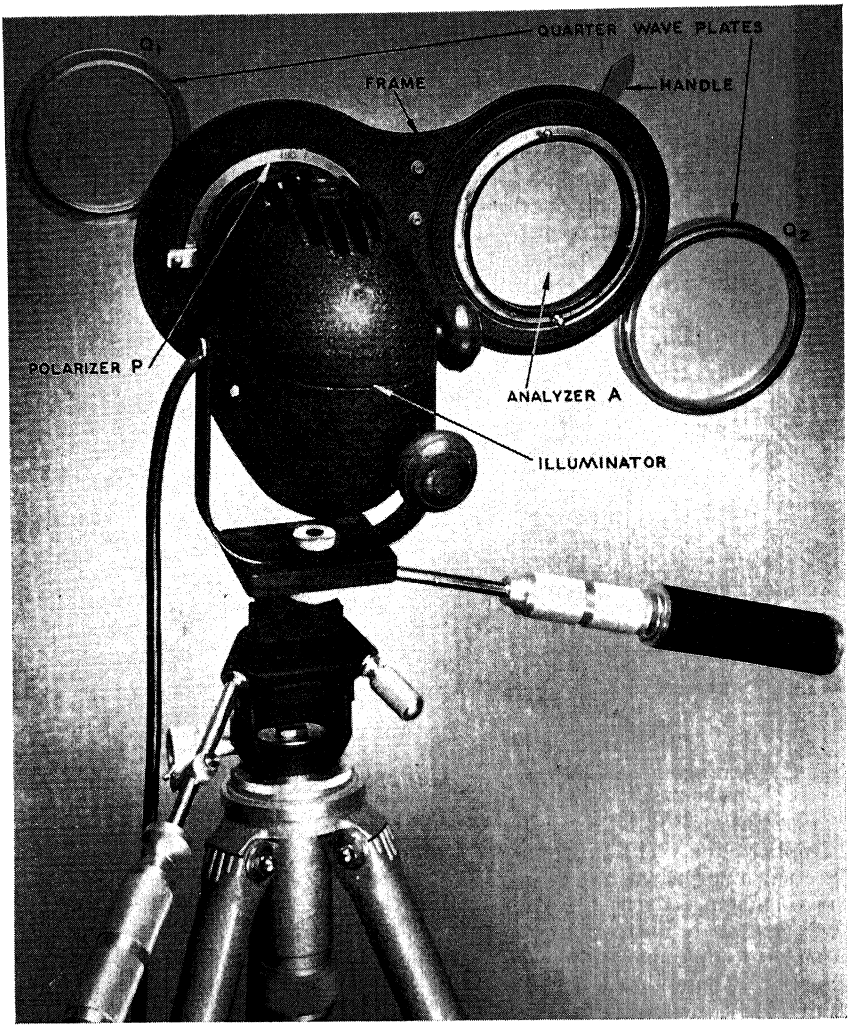

Tatnall Measuring Systems Co.

Fig. 12. Large-field instrument for static tests.

isoclinics. The isochromatics give the magnitudes of differences between principal stresses. The isoclinics give the directions of principal stresses. These lines can also be plotted directly on the surface of the plastic. One isoclinic corresponds to each angular position of *P* and *A* when they are at 90 deg. to each other. Therefore, if *P* and *A* are rotated through a 90-deg. angle, all the isoclinics will be observed successively. The isostatics or stress trajectories can be plotted with the aid of these isoclinics.

Schematic diagrams showing the operational principle of the two different arrangements of this system are shown in Fig. 13. Note that Fig. 13(a) is valid for any position of *A* relative to *P* and not only for 90 deg., as implied by the designation "crossed-plane polariscope."

Applications. The large-field unit is a universal instrument permitting both qualitative and quantitative stress analysis. **Qualitative analysis** permits determination of the location of the stress concentrations by observation of the whole field of stress patterns. This highlights the dangerous areas in which fringes are close to one another, hence indicating where stress gradients are high. **Quantitative analysis** permits determination of the magnitude of principal stress difference ($\sigma_1 - \sigma_2$) (isochromatics), and the directions of principal stresses σ_1 and σ_2 (isoclinics).

Isochromatics can be obtained with either of the two arrangements shown in Fig. 13. In Fig. 13(b), however, isoclinics are no longer present in the field of observation, and study of the isochromatics is facilitated. Let β be the angle between the transmission axes of P and A. Then if $\beta = 90$ deg., the polarizers are crossed. The fringes observed are integral fringes corresponding to $\delta = n\lambda$. If $\beta = 0$, the polarizers are parallel. The fringes observed in this case are half-order fringes corresponding to $\delta = (n + 1)\ (\lambda/2)$.

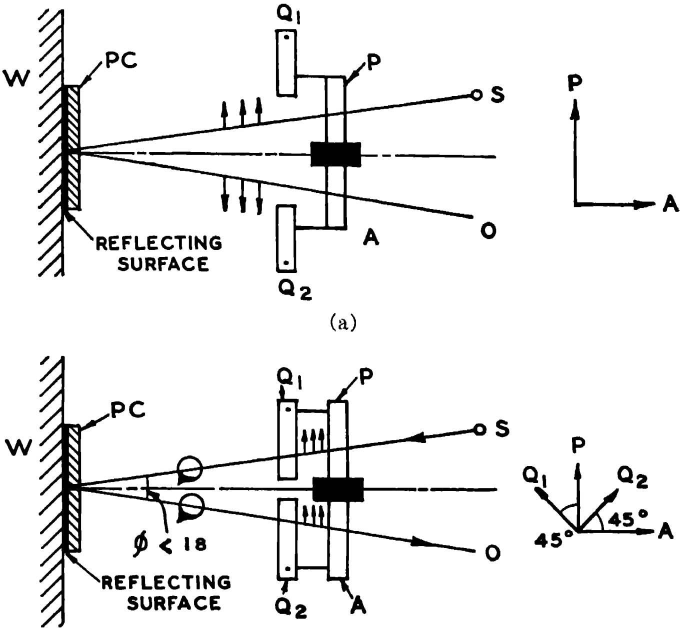

(a)

(b)

Tatnall Measuring Systems Co.

Fig. 13. Light paths through a large field meter. (a) As a crossed-plane polariscope. (b) As a circular-crossed polariscope.

Suppose that A is rotated relative to P (goniometric compensation) under circularly polarized light [see Fig. 13(b)] until the angle α it makes with P is $0° < \alpha < 90°$. The fringes are then fractional-order fringes corresponding to $\delta = n\lambda + \alpha\lambda/180$. Isoclinics are obtained only under plane-polarized light with $\beta = 90°$.

LARGE-FIELD METER FOR DYNAMIC TESTS. The arrangement of polarizers P and A and quarter-wave plates Q_1 and Q_2 in the dynamic large-field instrument is similar to that of the static large-field meter previously described. However, the field of light in the dynamic meter and its field of observation are much greater. This type can be fitted with a **stroboscope** for observation and measurement of alternating loads. A floodlight and a **high-speed camera** provide recordings, in black-and-white or color, of the stress patterns caused by dynamic loading. A special telescope, which can be mounted on the instrument or used independently so that an observer can analyze **stress concentrations on small surfaces** from some distance, is supplied with the instrument.

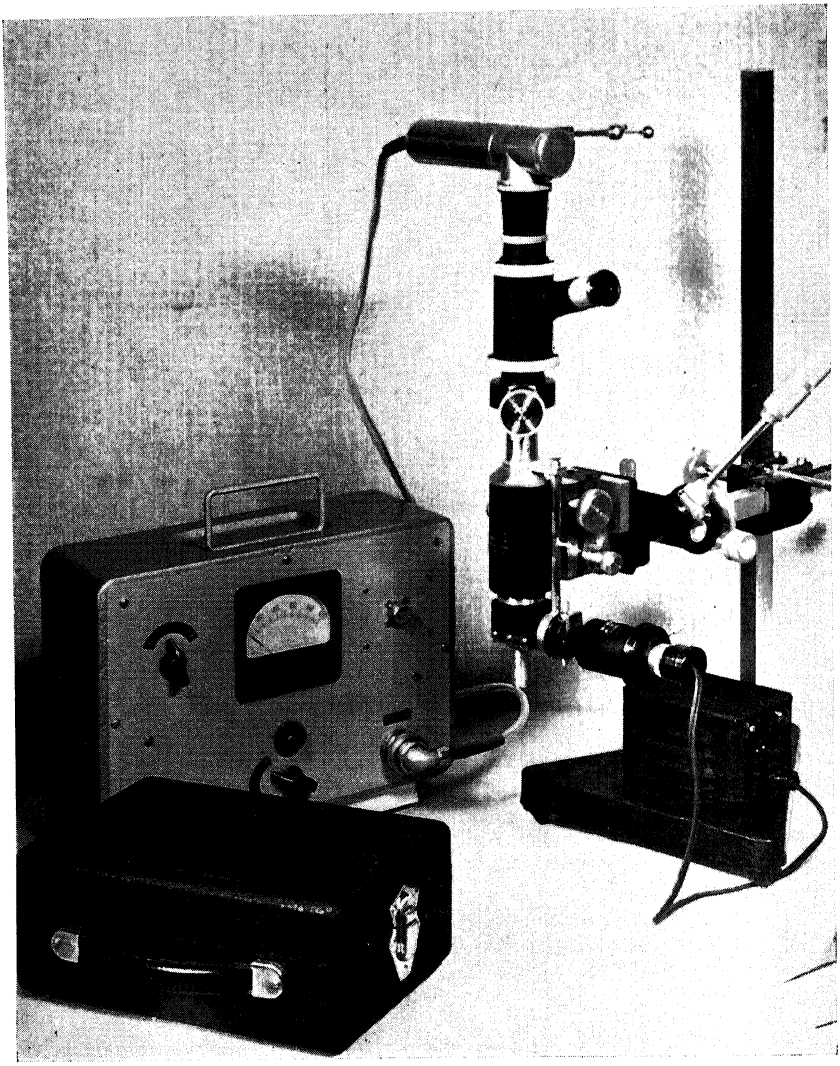

Tatnall Measuring Systems Co.

Fig. 14. Small-field meter (crossed-plane polariscope) with photocell attachment.

For recording isochromatics on black-and-white photographs, a **monochromatic light source** should be used. When the order of isochromatic fringes exceeds a certain number (generally four), the monochromatic light source becomes indispensable in compensating for the loss in definition inherent in high-order fringes when observed with white light.

SMALL-FIELD INSTRUMENT FOR STATIC TESTS. The small-field instrument (Fig. 14) is used on small parts or for point-by-point measurements. It is adapted with a Babinet Compensator (a combination of quartz wedges) or with a photoelectric cell. As shown in Fig. 15, the light beam coming from source *S* passes through polarizer *P* which plane-polarizes the light in the *OP* direction (small arrows). After reflection from the glass plate *G*, the light rays pass through the plastic coating *V* and are reflected from the surface of the metal or of the work piece made reflective, *M*, and pass again through the plastic layer. **Artificial bi-refringence,** caused by strain, resolves the plane-polarized vibration *OP* into two vibrations, *1* and *2*, at right angles to each other. These correspond to the directions of principal stresses and are characterized by the principal indices of refraction n_1 and n_2, of Fresnel's ellipsoid of indices, caused by the deformation. The velocity of propagation of light is different in these two directions; therefore, the two waves will have a relative retardation. After traversing glass plate *G*, the two waves pass through a compensator *C* and an analyzer *A* before reaching the eye of the observer or a photoelectric cell *O*. Compensator *C* makes it possible to measure the relative retardation δ.

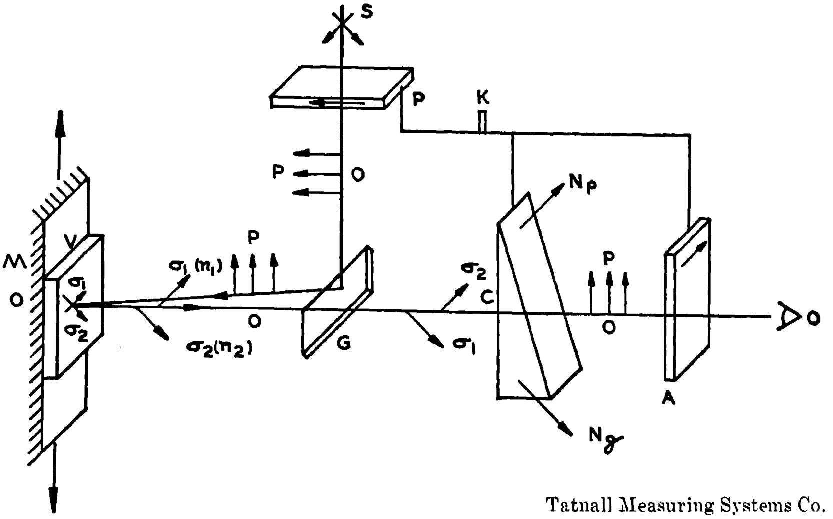

Tatnall Measuring Systems Co.

Fig. 15. Diagram of the light path through a small-field crossed-plane polariscope.

Use of Compensator. Selection of the compensator to be used is governed by the desired sensitivity, $\varepsilon_{\mathrm{min.}}$, or minimum strain to be determined. If $\varepsilon_{\mathrm{min.}} = 10$ μin. per in. (for $K = 0.1$ and $t = 0.120$ in.), a compensator of the Babinet type should be used.

To determine δ with this type of compensator, the elliptically polarized light emerging from the plastic must be reconverted into plane-polarized light. In other words the phase shift between the two vibrations n_1 and n_2 must be zero.

This is done by means of a wedge of quartz (Babinet Compensator) whose relative retardation, $(N_1 - N_2)\ t_{\text{quartz}}$ is known at every point. N_1 and N_2 are the principal indices of refraction of the quartz wedge. Its thickness t varies according to the position of the wedge in relation to the ray of light. If the quartz wedge is adjusted to shut off the light, relative retardation in the plastic $\delta_{pc} = (n_1 - n_2)\ 2t_{\text{plastic}}$ is then equal to the relative retardation in that particular section of the calibrated compensator.

SMALL-FIELD ELECTRONIC METER FOR STATIC AND DYNAMIC TESTS. When $\varepsilon_{\text{min.}} = 0.1$ μin. per in. (for $K = 0.1$ and $t = 0.120$ in.), a photoelectric cell and amplifier are required. This adapter permits observations and measurements with a compensator to be made concurrently with photometric measurements. Variation in intensity of photoelectric current resulting from a variation of the bi-refringence is measured:

1. In static tests by means of a null method using a milliammeter and a compensator, or a deviation method using the meter alone.
2. In dynamic tests by means of an oscilloscope.

Applications. This instrument is generally used in conjunction with measuring instruments based on the use of the plastic as a strain gage. It is used in torquemeters, dynamometers, pressure pick-ups, and similar devices. It performs like a transducer. It may be used for measurements where the bi-refringence δ/t is very small and may be employed also for dynamic tests. It may be used for determination of the directions of σ_1 and σ_2. At any given point of the surface, the intensity of light transmitted by the plastic is usually not zero. The field is not dark. By rotating the crossed polarizers P and A as a unit, about the optical axis of the instrument by means of lever K, a position can be found for which the field is dark (an isoclinic is crossing the point under study and the photocell output will indicate a minimum). For such a position the directions of the axes of the polarizers, which are known, coincide with the directions of the principal stresses at the point under study.

THE OBLIQUE-INCIDENCE METER. The oblique-incidence instrument is used for point-by-point determination of the value of each principal stress. Fig. 16(a) is a schematic diagram and Fig. 16(b) is a photograph of this instrument. The light beam coming from source S passes through polarizer P, through a prism K whose index of refraction is the same as that of the plastic so that the beam passes through it without any refraction, and through plastic coating PC. It is then reflected from the surface of the work piece W, passes again through plastic PC, prism K, a system comprising a compensator C (generally Babinet) and an analyzer A, and finally it enters the eye of the observer.

Applications. The measurement of δ under oblique incidence makes possible the determination of the value of each principal stress σ_1 and σ_2 (see Mathematical Theory in this section). This instrument can be used only for measurements on flat parts or on parts that have a large radius of curvature.

SELECTION OF MEASURING INSTRUMENT. Selection of the proper instrument, from the point of view of sensitivity of measurements, is governed by the plastic thickness t, strain-optical constant K, and the minimum strain $\varepsilon_{\text{min.}}$ to be measured. Any instrument whose constant D_x satisfies the relation $D_x \leqq D$, where $D = \varepsilon_{\text{min.}} tK$ microinches, can be used for the analysis under consideration. For other considerations concerning the choice of instruments, see the preceding descriptions and Fig. 9.

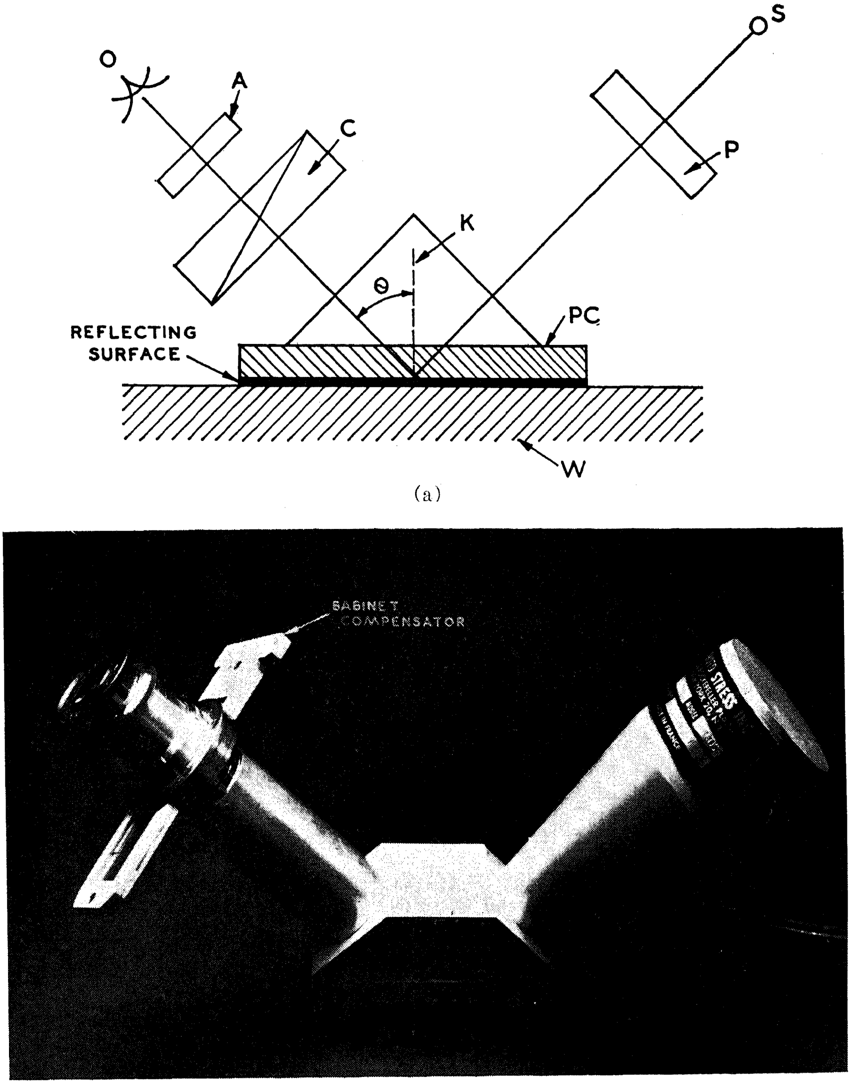

(b) Tatnall Measuring Systems Co.

Fig. 16. Oblique-incidence meter. (a) Schematic diagram. (b) Instrument showing compensator.

Industrial Applications

CLASSIFICATION OF APPLICATION AREAS. The photoelastic coating technique is applicable to many problems including:

1. Determination of elastic and/or plastic strain distribution in structures or parts subjected to static or dynamic loads.

2. Determination of the best design from a stress-analysis point of view.
3. Instantaneous location of stress concentrations and determination of stress-concentration factors.
4. Survey of safety of structures.
5. Measurements of residual stresses.
6. Determination of the true yield point of materials.
7. Measurements on heterogeneous materials (concrete, reinforced concrete, wood, etc.).
8. Investigation of propagation of plastic deformations.
9. Determination of the stress concentration factor in very small areas such as corrosion spots, for example.
10. Study of stress concentrations due to very small cracks.
11. Strain measurements on the crystalline-grain scale.
12. Strain measurements around rivets and welds.

Some examples and photographs of typical applications are given in subsequent sections.

SHEET PILE DESIGN. The problem in this case was to determine the strain distribution in elastic and plastic ranges of deformation and the yield point of a sheet pile: (1) to compare the merits of its design with those of another sheet pile, and (2) to determine the maximum service load in the elastoplastic range of deformation.

The steel test specimen was coated with standard low-strain plastic sheet, 0.120 in. thick, placed in a testing machine, and subjected to load increases up to point of rupture. Visual and photographic observations were made of the isochromatics (see Fig. 17) with the large-field dynamic instrument. Monochromatic light was used to increase the contrast of isochromatics in black-and-white photography. A point-by-point determination of the stresses was established with the aid of the small-field instrument (Fig. 14).

Fig. 17(a) shows the sheet pile under tension load in a testing machine, under observation with the small-field meter. In these tests the pile was loaded in tension by means of two interlocking sheet sections which simulated the actual working conditions of the assembly. Fig. 17(b) is a graph of the tangential strains for the free boundaries of the sheet pile, based on data derived from the study of the isochromatics. The magnitude of tangential strain at a point is plotted on the normal to the boundary at each point. Fig. 17(c) shows the isochromatics as they appeared through the large-field meter. Fringes are identified as *1*, *2*, *3*, etc. (fringe orders). Fringe *1* corresponds to a strain of 900 μin. per in. Fringe *2* corresponds to twice this strain level or to $2 \times 900 = 1800$ μin. per in., and fringe *3* to 2700 μin. per in., etc. Fig. 17(d) shows the actual test piece after rupture under a load of approximately 7700 lb. A complete fracture has occurred at point *A*. Incipient fractures are visible at points *B*, *C*, and *D*. These fractures correspond to the points of maximum stress and were predicted as potential points of failure by analysis of the isochromatics of Fig. 17(c).

STRESS ANALYSIS OF GUIDED-MISSILE TAIL SECTION. It was desired to make a stress analysis of the tail section of a guided missile for various loading systems corresponding to elastic and elastoplastic deformations (Fig. 18). (Photographs and data released by special permission of the French Ministry of National Defense, Permit No. D.M. 24 677 S.T.-D.E.F.A.-N.A.D. The study was made under the supervision of M. Berthier.) Sixteen flat or contoured low-strain plastic sheets, 0.080 in. thick, representing a total area of 32 sq. ft., were bonded to the surface of the missile, which was standing upright and rigidly secured to a steel frame.

Meters. Instrumentation employed included:

1. The large-field static meter, for whole-field observations and measurements of bi-refringence by direct plotting of the isochromatics.
2. The large-field dynamic meter for photographic recordings of the whole-field or the most highly stressed areas.
3. The small-field meter for point-by-point measurements in stress concentration areas.

Loading and Stress Patterns. Static loads were applied by means of horizontal hydraulic jacks mounted on the frame supporting the missile, located and dimensioned to simulate aerodynamic loads [Fig. 18(a)]. Fig. 18(b) provides an over-all view of the stress distribution in the fuselage and the tail surfaces, as revealed through the large-field meter. Four stress-concentration areas (*a*, *b*, *c*, and *d*) are seen along the inboard section and around the Phillips recessed screws that fasten the skin to the ribs. The most highly stressed area, *d*, is near the rib. A close view of this most highly stressed area around the fourth rib appears in Fig. 18(c), which shows the isochromatics plotted directly on the surface of the photoelastic plastic. Fig. 18(d) is a plot of the isochromatic lines appearing in the plastic for a load of 257 p.s.i. in the hydraulic loading system. The line of probable buckling corresponds to the highest stress gradient. Further loading produced a wrinkle along this line, as forecast.

Analysis. When using the large-field meter, bi-refringence was measured by counting the number of fringes (the fringe order). For each loading system, the integral fringes ($n = 0, 1, 2,$ etc.) were observed through the large-field meter and plotted (with a grease crayon) directly on the surface of the plastic [Fig. 18(c)].

When using the small-field meter, bi-refringence was measured by means of a Babinet Compensator. Sensitivity of the measurements was 10 μin. per in. for the magnitude of the principal strains.

Results of Test. Some immediate findings of the foregoing analysis were:

1. The ribs near the inboard section should be reinforced. (Data obtained during the test made the reinforcement factor readily available.)
2. A change in number of ribs and their inclination should be investigated.
3. Outboard areas should be lightened, since they revealed few if any stresses.

SPOT-WELDED ASSEMBLY. Tests were made to determine the best disposition of the spot welds (in terms of number, spacing, and number of rows) consistent with a rational distribution of the stresses in a spot-welded assembly. Two ⅛-in., stainless steel plates, 4 in. wide and approximately 10 in. long, were spot-welded, coated (by brushing) with a thin layer of low-strain liquid plastic, and loaded in tension in a testing machine. The fringe patterns were observed, measured, and photographed in monochromatic light ($\lambda = 5460$ Å) with the aid of a large-field dynamic meter (see Fig. 19). From these stress distributions it can be observed that the first row of spot welds constitutes a real barrier to the progression of the deformations.

WELDED BRIDGE ASSEMBLIES. Photoelastic-coating techniques were applied in the analysis of stresses in an assembly of two 16-in. I-beams welded crosswise, simulating a portion of a welded bridge structure. One beam was loaded at both ends by means of hydraulic jacks, while the ends of the other beam were held stationary between two jaws. One part of the assembly was analyzed with wire-resistance strain gages; the other symmetrical part was analyzed with the aid of the large-field instrument and the oblique-incidence

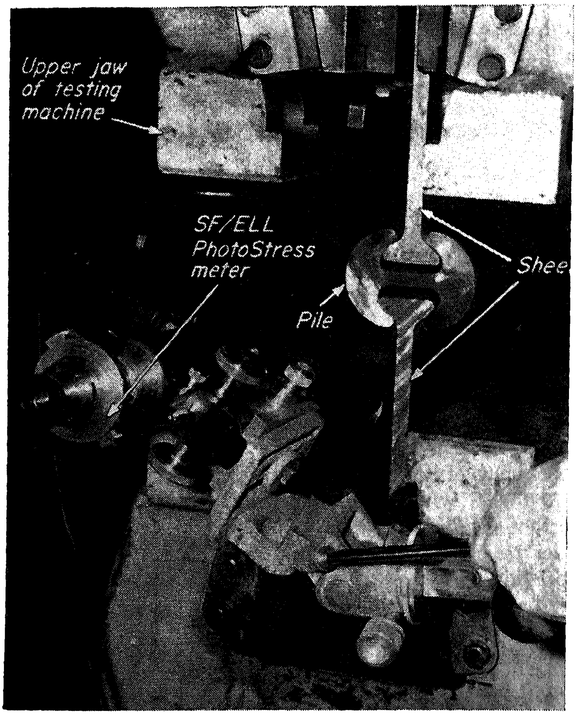

(a)

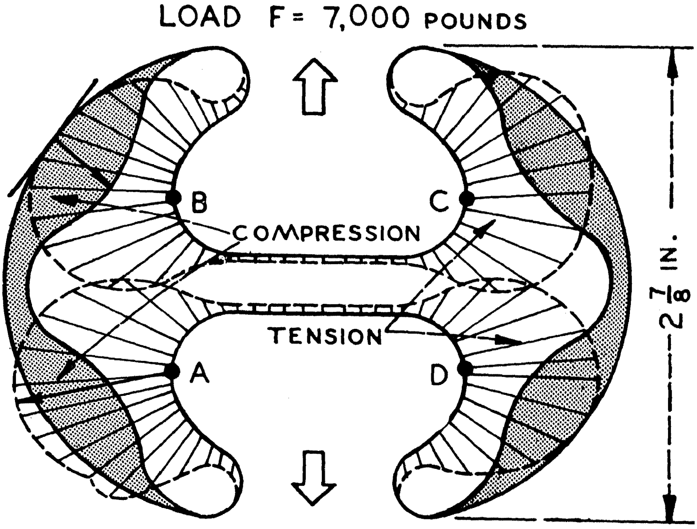

(b)

Lorraine-Esceult, Inc., France

Fig. 17. Photoelastic-coating analysis in sheet pile design. (a) Sheet pile under tension load. (b) Tangential strains in sheet pile.

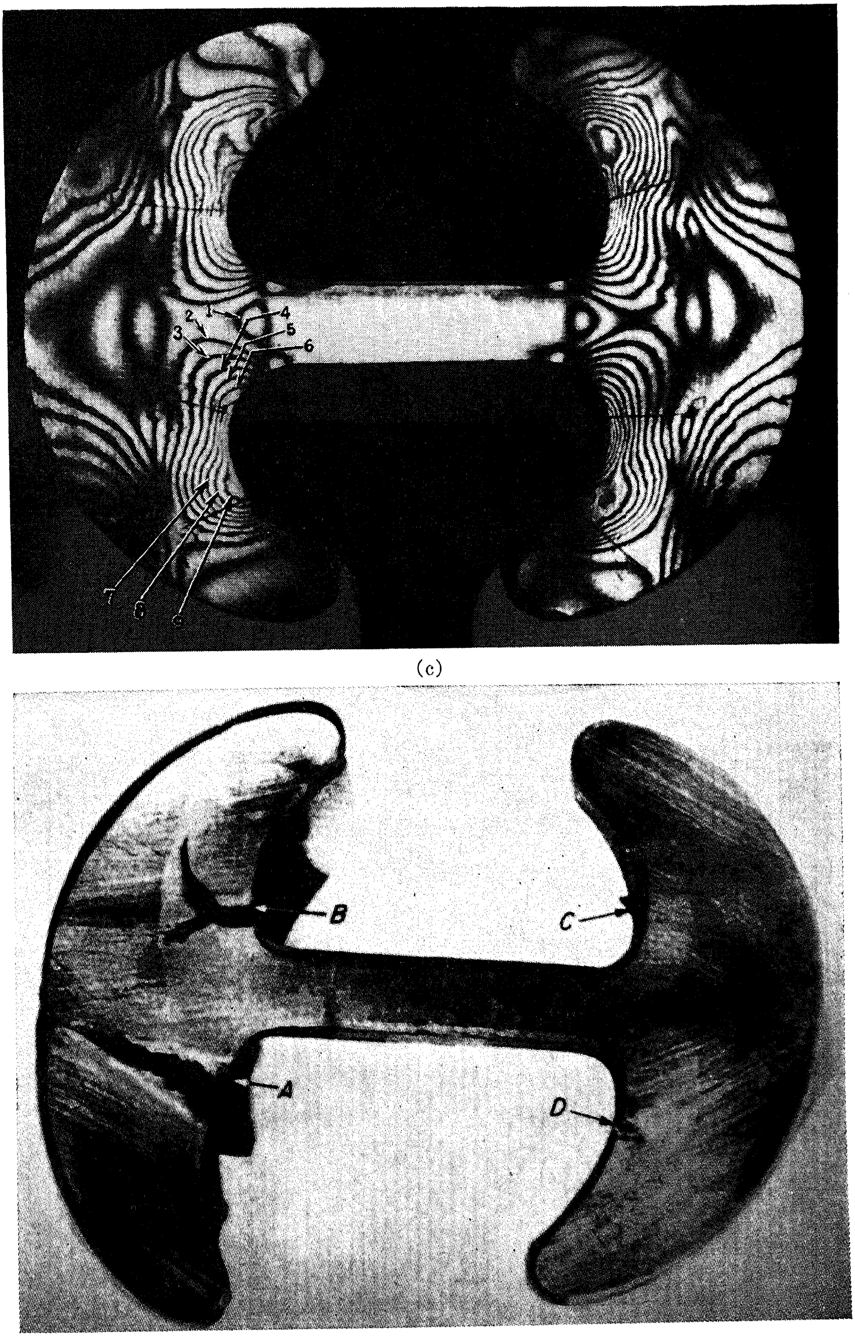

Fig. 17. (Continued.) (c) Isochromatic patterns shown through large-field meter. (d) Test piece after rupture.

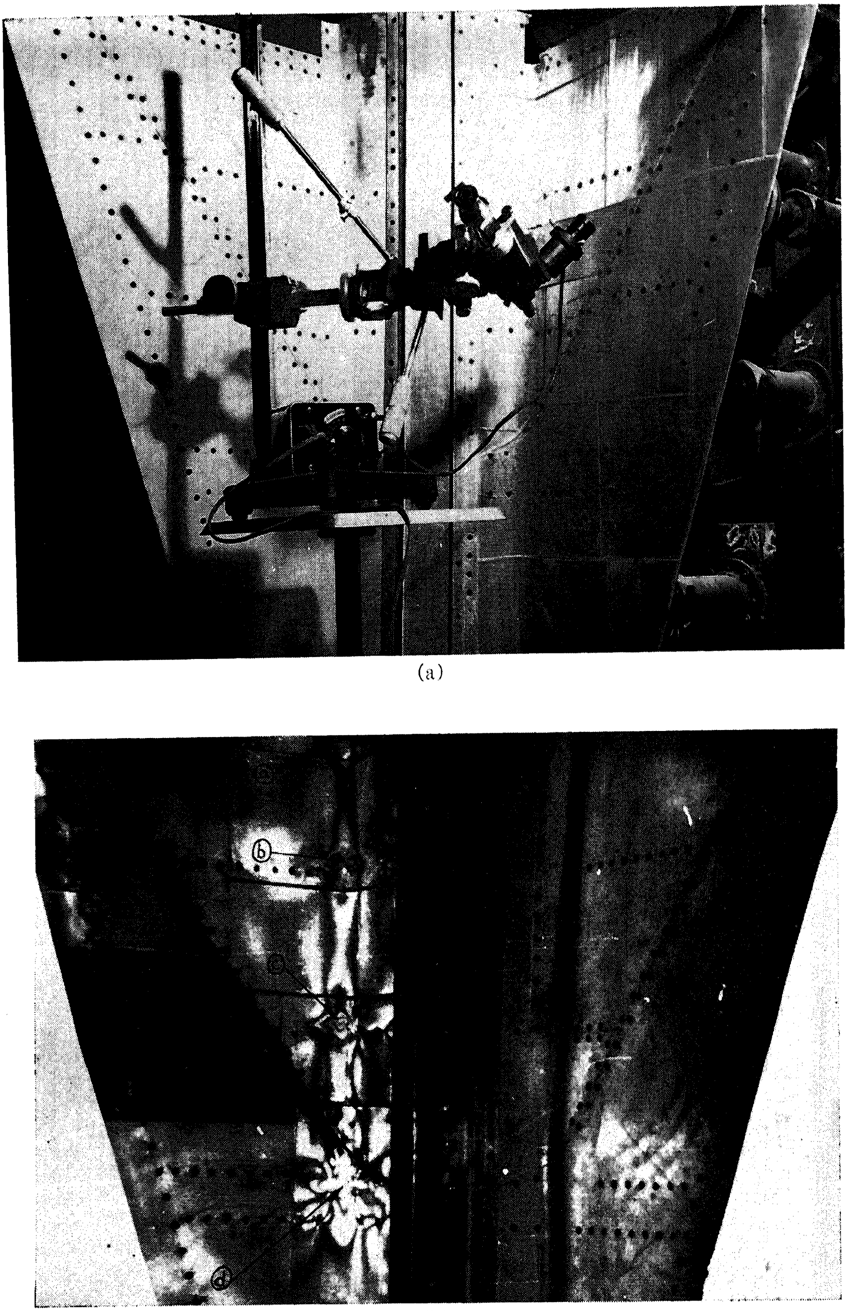

(a)

(b)

Fig. 18. Photoelastic-coating tests of guided-missile fuselage and tail surfaces under static loading. (a) Tail section, small-field meter, and hydraulic-jack loading system for static tests of missile. (b) Stress distribution in fuselage and tail sections,

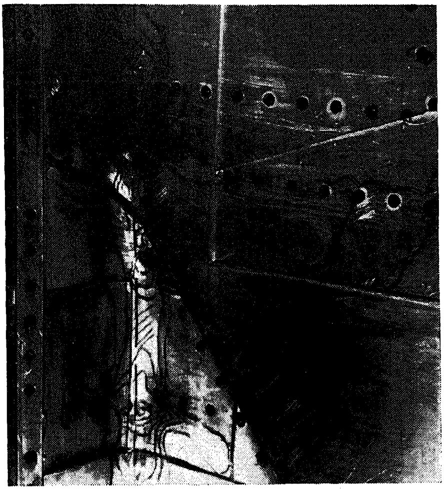

(c)

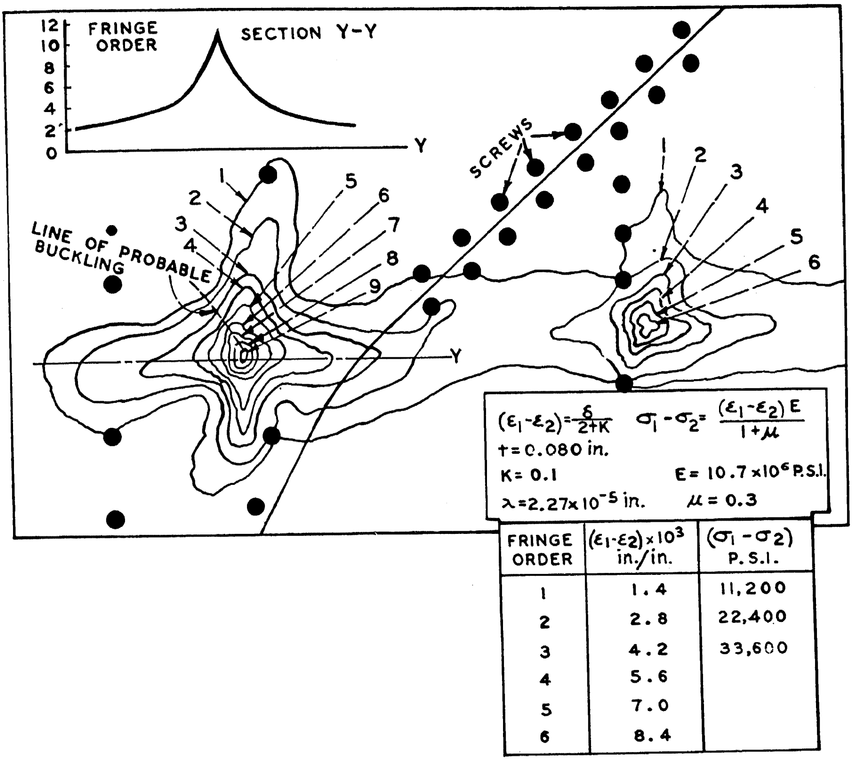

$(\varepsilon_1-\varepsilon_2)=\frac{\delta}{2+K}$ $\sigma_1-\sigma_2=\frac{(\varepsilon_1-\varepsilon_2)E}{1+\mu}$

$t=0.080$ in.

$K=0.1$ $E=10.7\times10^6$ P.S.I.

$\lambda=2.27\times10^{-5}$ in. $\mu=0.3$

FRINGE ORDER	$(\varepsilon_1-\varepsilon_2)\times10^3$ in./in.	$(\sigma_1-\sigma_2)$ P.S.I.
1	1.4	11,200
2	2.8	22,400
3	4.2	33,600
4	5.6	
5	7.0	
6	8.4	

(d)

DEFA, France

as seen through large-field meter. (c) Isochromatics plotted directly over photoelastic plastic in most highly stressed areas. (d) Plot of isochromatic lines appearing in plastic for a load of 257 p.s.i. in hydraulic loading system.

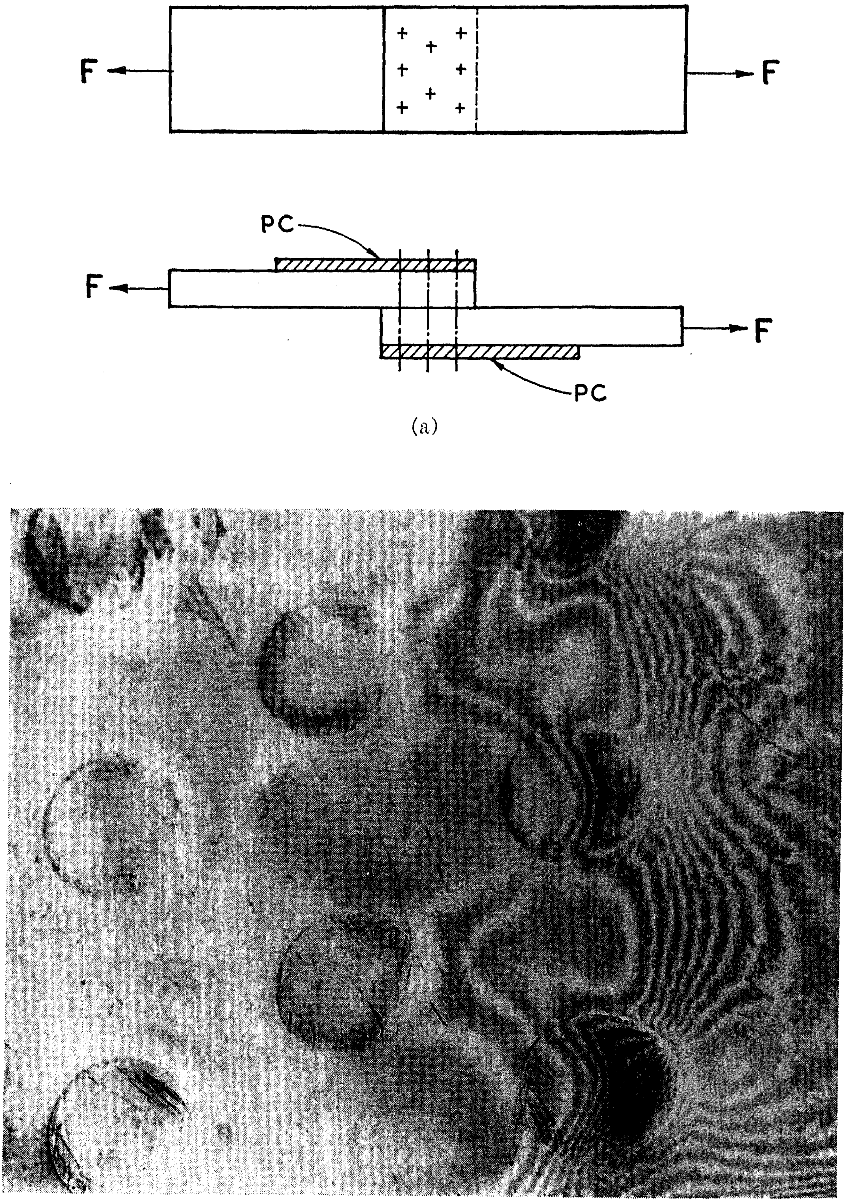

(a)

(b)

Fig. 19. Photoelastic-coating tests of stress distributions in spot-welded joint in 0.125-in. stainless steel. (a) Arrangement of welds in spot-welded assembly of two stainless steel plates in tension. (b) Isochromatics indicating distribution of stresses and their concentration around the spot welds.

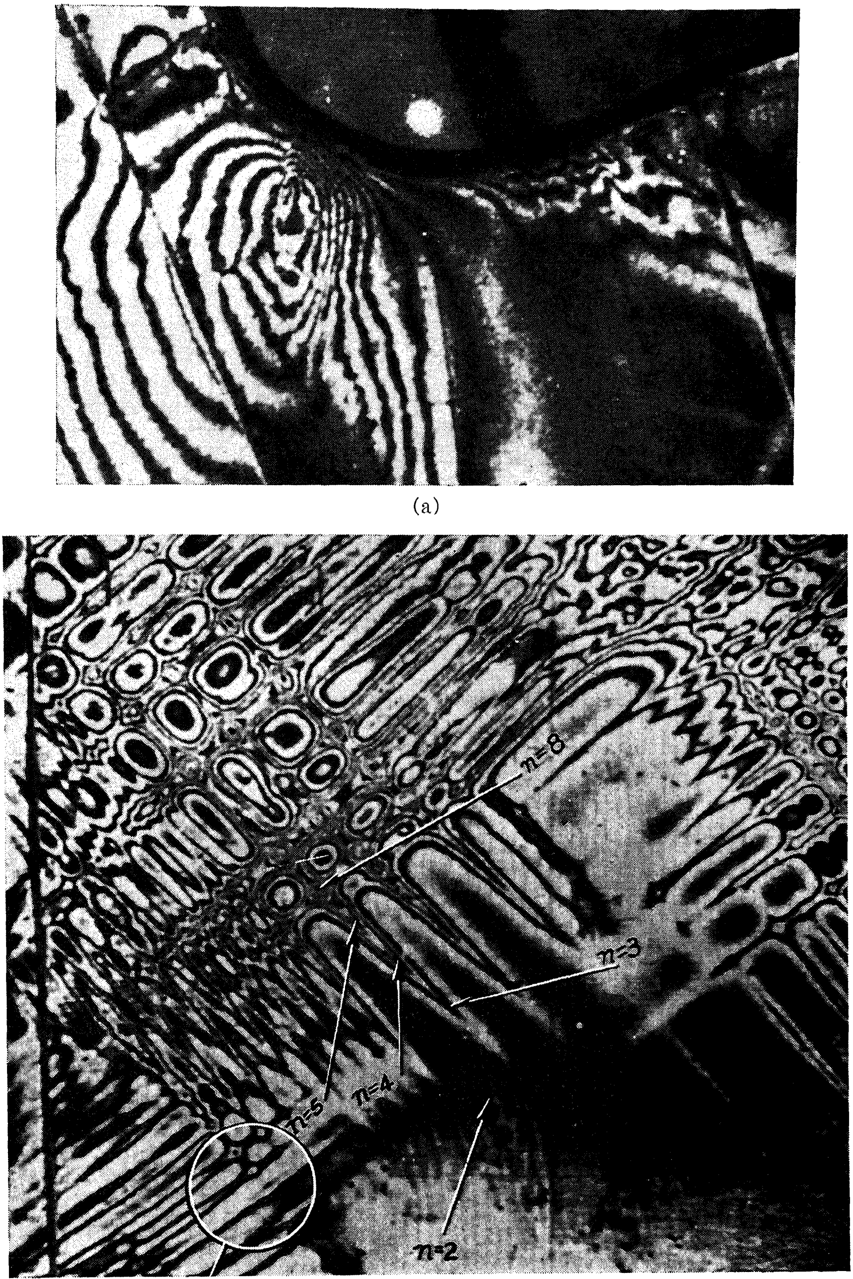

(a)

(b)

CECM, Belgium

Fig. 20. Arc-welded structural steel assembly used in bridges. (a) Isochromatic fringes showing a critical area in the structure. (b) Plastic deformations near a welded area. Circled area corresponds to a rosette strain gage. Fringe *2* corresponds to 2000 μin./in.

meter. Fig. 20 shows a critical area of the structure, with isochromatics photographed in monochromatic sodium-vapor light. These isochromatics [Fig. 20(b)] correspond to plastic deformations and were identified (after removing the plastic) with the slip lines (Leuder's lines). The strain concentrations due to these slip lines were very localized and high in magnitude. (These tests were conducted under the supervision of M. Hebrant in the laboratory of the Association d'Industriels Belges, in Brussels, in collaboration with the Centre d'Étude de la Construction Métallique of the same city.)

TRANSDUCER APPLICATIONS. The photoelastic-coating method, like any strain measurement technique, can be used as a transducer technique. Devices such as load cells, weighing systems, torquemeters, and pressure cells can be built by using a photoelastic plastic bonded to the mechanical part that transmits the effect to be measured. The deformations of the part are transmitted to the plastic which then shows variations of colors (bi-refringence) when white polarized light is used for observation. These variations of colors can be picked up by a photocell and converted into variations of electric current. The electric current produced in this way can be then sent to any recorder or oscilloscope. The strain sensitivity can be as high as one-hundredth of a microinch per inch. These types of transducers can be very useful in all cases where mechanical contact between the sensitive part and the recording instrument is prohibited. This is especially important for torquemeters on high-speed shafts, where it is very difficult to build slip rings that collect the current from the sensing device so that it can be sent to the recorder.

A specific example of a photoelastic coating used as a transducer is the torquemeter sensing element shown in Fig. 21. The system is a servo-operated, null-balance system consisting of two polarizing channels aligned perpendicularly

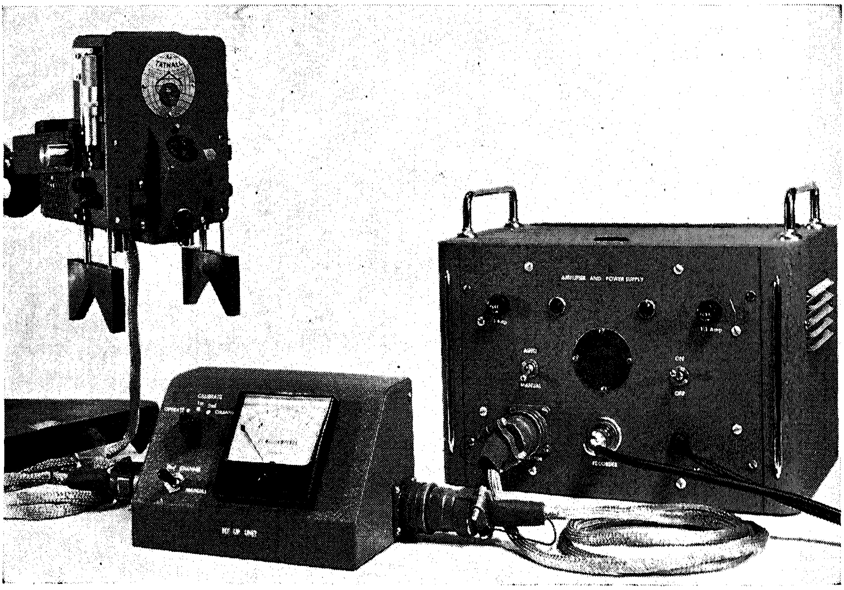

Tatnall Measuring Systems Co.

Fig. 21. Photoelastic-coating torquemeter.

to the shaft. One half of the length of a cylinder of photoelastic plastic is bonded to the shaft without cutting the shaft and without attaching slip rings. (Note: The vees shown in Fig. 21 are then brought in contact with the shaft to align the instrument, after which they are removed from contact with the shaft.) The other half of the cylinder remains unbonded. One channel scans the bonded plastic, the other channel scans the unbonded dummy plastic, canceling out the effects of temperature and external light, photocell sensitivity, and power-supply stability. The read-out is taken directly in digits and in millivolts into any recorder. The accuracy is better than ±0.5 percent of full scale, with long-term stability of 0.2 percent of full scale, and 1.5 μin. per in. strain accuracy. The same system can be used with pressure cells, load cells, and extensometers.

TELEMETERING. Television can be used in connection with the photoelastic-coating technique. A **television camera** can be placed behind the large-field instrument and measurements or observations made on the screen of the receiver. In this case the signal can be transmitted by cable or by radio.

In each case, if observation can be made, measurements are possible. This depends only on the power of the polarized light used for lighting the part under study and the magnification power of the instrument through which optical measurements are made. It is possible in this case to investigate what is happening several miles away from the technician. Telemetering techniques find application for stress measurements in dams, bridges, airplanes in flight, atomic structures subject to nuclear radiations and dangerous for close investigation, and similar applications.

SURVEY OF SERVICE LIFE OF STRUCTURES AND MACHINES. Vital parts can be coated with the plastic and then mounted in a structure. Stresses due to the mounting and to external loading of the structure in operation can be observed through the large-field instrument. A survey continuing over a period of time can be made easily by inspecting the plastic through a suitable instrument. If some fringes other than those due to mounting appear in the plastic after a given time of operation of the structure or machine, it can be said with certainty that some changes have occurred in the structure (often yielding). These may require the replacement or reinforcing of the damaged parts. A very good example of this application would be an airplane coated with plastic and subjected to survey after each landing. Where yielding occurred, fringes should be visible.

ALIGNMENT AND CALIBRATION OF TESTING MACHINES. It is of very great importance to be sure that a testing machine is correctly transmitting the load applied to a specimen under study. The photoelastic-coating technique can be used easily for control of correct loading. In the case of a tensile test specimen, the bi-refringence phenomenon in the specimen coated with photoelastic plastic will appear as a uniform color if the specimen is subjected to pure tension. If parasitic bending is present, a color gradient (or color striations) will be seen. If parasitic torque is present, the isoclinic lines will show that the directions of principal strains do not coincide with the direction of the load. In general, a symmetrical specimen loaded in a symmetrical way should exhibit a symmetrical strain pattern and therefore a symmetrical fringe pattern.

Knowing the K factor of the photoelastic plastic, it is also possible to calibrate a testing machine. In case of dynamic calibration of a fatigue testing machine, a strobe light should be used in connection with the dynamic optical meter.

VISUAL EDUCATION. The possibility of collective observation of the stress pattern directly on the structure makes the photoelastic-coating technique of great potential value from the educational point of view. In this way engineers, designers, and other technicians can evaluate their designs, principally by seeing where the stress concentrations are located. Students can learn, by direct observation of the part they are studying, how stresses are distributed in different specimens.

Advantages and Disadvantages

ADVANTAGES. The photoelastic-coating technique offers the following advantages in stress analysis:

1. It is the equivalent of an infinite number of strain gages with virtually zero-gage length, distributed uniformly and continuously over the entire surface of the actual structure or part to be stress-analyzed.
2. It can be applied to any structural material (metals, concrete, wood, glass, rubber, etc.).
3. It permits the direct observation of the over-all strain distribution.
4. It permits the recording of the strain phenomena on the photoelastic plastic bonded to the structure. Photographs may be made of the strain patterns.
5. It permits both static and dynamic measurements.
6. It establishes the value of the difference ($\varepsilon_1 - \varepsilon_2$) in principal strains, and hence the maximum shear stress (analysis under normal incidence).
7. It permits determination of magnitude and sign of the two principal strains, ε_1 and ε_2 (analysis under oblique incidence).
8. It gives the directions of principal strains within approximately ±2 deg. Isostatics or stress trajectories can be plotted.
9. It permits measurements of very small strains varying from 10 to 0.1 μin. per in. (depending upon the meter used), and of large elongations up to 3 or 50 percent (depending upon the photoelastic plastic used).
10. It permits measurements of residual strains.
11. It makes possible measurements on surfaces ranging in size from a crystalline grain to any large surface.
12. It permits measurements in areas with any stress gradient.
13. It provides a means of following the life-history of the stresses in any component part, assembly, or entire structure, from the moment it is coated with plastic.
14. It makes possible the determination of the localized yield point of materials or structures with a high degree of accuracy.
15. It permits measurements over extended periods of time.
16. It permits measurements under any atmospheric conditions.
17. It permits measurements in transparent liquids (water, oil, etc.).
18. It makes possible observation and measurements of strains from a distance.
19. It permits telemetering (using television).
20. It permits electrical readings (using photocells to convert color variations into electric signals).
21. It permits automatic measurements (combination of photocells and servomechanisms).
22. It permits measurements in plant, field, and laboratory.

LIMITATIONS. The photoelastic-coating technique is subject to the following limitations:

1. Stresses cannot be measured in areas of an assembly which are inaccessible to light. Residual strains, however, can be measured if a previously coated component part, stressed beyond the elastic limit, becomes accessible to light after dismantling.

2. The strain-optical constant K (relating the mechanical effect, strain, to the optical effect, i.e., bi-refringence or color) varies for temperatures outside the range of −44° F. to +85° F. Corrections of K can be made for such temperatures (see Fig. 22).

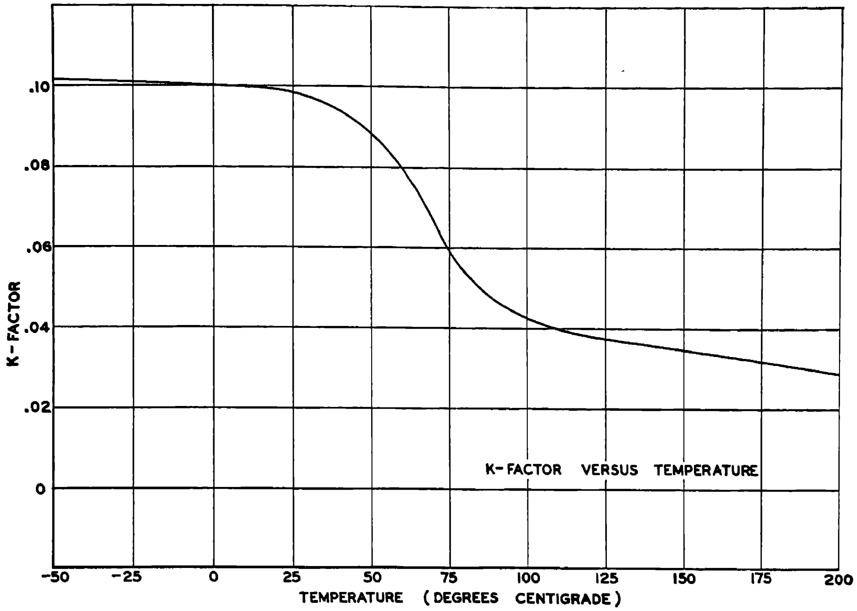

Fig. 22. Curve showing *K* factor versus temperature. Curve obtained experimentally by Riegner, Tatnall Measuring Systems Co.

3. An exceptionally wide temperature variation during a test may result in a parasitic bi-refringence caused by the difference in expansion between the work piece and the plastic. In this case it is necessary to take a measurement of the bi-refringence before and after loading so as to cancel the bi-refringence present under no load.

4. The maximum temperature which can be applied during a test is approximately 500° F.; however, measurements should be made only during 30 min. after application of this temperature. For long-term measurements the maximum temperature is approximately 300° F.

5. Thickness effect of the plastic. The following errors can be made if the thickness of plastic is comparable to the thickness of the part under study:

   a. Error due to the fact that the photoelastic-coating indication corresponds to a measurement which is not made on the surface of the part but somewhere inside the plastic if the part is subjected to bending in a plane perpendicular to the surface of the plastic (see Fig. 23).

   b. Error due to the reinforcement of the part by coating it with a plastic (modulus of elasticity of the photoelastic plastic = 450,000 p.s.i. or 40,000 p.s.i. approximately, depending upon plastic used).

These errors can be corrected by means of the curves represented in Fig. 23. Because of errors due to the thickness of the plastic, there may be a tendency to use only thin sheets of plastic; however, the thinner the plastic, the less sensitive it is to strain (see Eq. 5, for example). Therefore, relatively thick sheets of plastic can be used, but corrections should be made for the effects

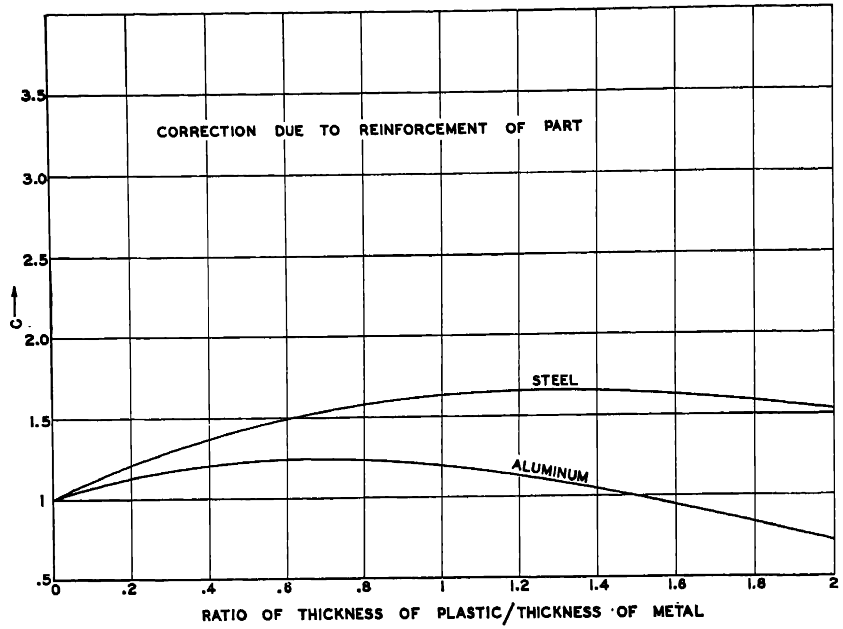

Fig. 23. Curve showing corrections for *K* factor in case of specimens subjected to bending by a known load. *C* factor by which *K* (strain-optical coefficient of plastic) should be multiplied. Modulus of elasticity of plastic: 450,000 p.s.i. Curve experimentally and analytically computed by Riegner, Tatnall Measuring Systems Co.

enumerated here. However, the error due to reinforcement can generally be neglected in the case of a bi-dimensional stress field.

There are other minor limitations which are now under investigation, such as: (1) the influence of centrifugal force on the photoelastic plastic, (2) effect of thickness of plastic on points of very high stress concentrations (for instance, at a microscopic flaw in the part under test), and (3) the effect of integrating through the thickness of plastic for oblique measurements (gage length for oblique measurements is not zero, due to the angle of measurement).

References

1. Mesnager, M. "Sur la détermination optique des tensions intervenues dans les solides à trois dimensions (On the Optical Determination of Interposed Stresses in Three-Dimensional Solids)," *Compt. rend.*, 190 (1930): 1249.
2. Mabboux, G. *Applications de la photoélasticité dans les ouvrages en béton* (Applications of Photoelasticity in Concrete Structures). Delmar-Chapon-Gounouihou, 1933.
3. Oppel, G. "Das Polarisationsoptische Schichtverfahren zur Messung der Oberflaechenspannung am beanspruchten Bauteil ohne Modell (Method for the Measurement of Surface Tension of Real Solids by Bi-refringent Layer, without Model)," *VDI Zeitschrift*, 81 (1937): 803.
4. D'Agostino, J., D. C. Drucker, C. K. Liu, and C. Mylonas. "Epoxy Adhesives and Casting Resins as Photoelastic Plastics," *Proc. Soc. Exptl. Stress Anal.*, 12, No. 2 (1955): 123.

5. Zandman, F. "Analyse de contraintes par vernis photoélastiques (Stress Analysis by Photoelastic Varnish)," *Group. avance. méthodes anal. contraintes,* 2, No. 6 (1955): 1.
6. ———. "Mesures photoélastiques des déformations élastiques et plastiques et des fragmentations cristallines dans les métaux (Photoelastic Measurements of Elastic Deformations and Crystalline Fragmentations in Metals)," *Rev. mét.,* 53 (1956): 638.
7. ———. "Analyse des contraintes par vernis photoélastiques (Stress Analysis by Photoelastic Varnish)." *Acier-Stahl-Steel,* 21 (1956): 356.
8. Zandman, F., and M. R. Wood. "Photostress, A New Technique for Photoelastic Stress Analysis for Observing and Measuring Surface Strains on Actual Structures and Parts." *Prod. Eng.,* 27 (1956): 167.
9. Dantu, P. "Étude des contraintes dans les milieux hétérogènés. Application au béton (Study of Strains in Heterogeneous Media. Applications in Concrete)," *Ann. lab. central ponts et chaussées* (Paris), Publ. No. 57-6.
10. Coker, E. G., and L. N. G. Filon. *A Treatise on Photoelasticity.* London: Cambridge University Press, 1957.
11. Frocht, M. M. *Photoelasticity.* New York: John Wiley & Sons, Inc., 1948.
12. Hetényi, H. *Handbook of Experimental Stress Analysis.* New York: John Wiley & Sons, Inc., 1950.
13. Zandman, F. "Emploi de la platine théodolite dans la photoélasticimétrie tridimensionnelle (Use of a Tilting Stage in Three-Dimensional Photoelasticity)," *Group. avance. méthodes anal. contraintes* (1953).

Bibliography

Baes, D. *Résistance des matériaux et éléments de la théorie de l'élasticité et de la plasticité des corps solides* (Strength of materials and theoretical principles of elasticity and plasticity of solids), Vols. I & II. Brussels: Lamertin, 1930–1934.

Foeppl, L. and H. Neuber. *Festigkeitslehre mittels Spannungsoptik* (Strength of Materials by Means of Photoelasticity). Munich: Oldenbourg Verlag, 1935.

Kammerer, A. *Recherches sur la photoélasticimétrie* (Research on Photoelasticity). Paris: Hermann & Co., 1944.

Le Boiteux, H., and R. Boussart. *Élasticité et photoélasticimétrie* (Elasticity and Photoelasticity). Paris: Hermann & Co., 1940.

Pirard, A. *La Photoélasticité* (Photoelasticity). Paris: Dunod, 1947.

SECTION 54

RESISTANCE STRAIN-GAGE TESTS

CONTENTS

PAGE

Nature of Resistance Strain-Gage Tests

- Strain measurement 1
- Development of strain-measuring devices 1
  - Auxiliary stress-analysis tools 2
- Development of electric resistance strain gages 2
- Resistance strain-gage applications and limitations 2
  - Stress analysis by strain measurement 3
  - Measurement of quantities other than strain 3
- Influence of mechanical properties of base material 3
  - Modulus of elasticity 4
  - Poisson ratio 4
  - Linearity of the stress-strain curve 4
  - Hysteresis of the stress-strain curve 4
  - Temperature coefficient of linear expansion 4
  - Other properties 5
  - Selection of base materials for transducers 5

Strain-Gage Construction and Installation

- Gage materials and construction 5
  - Grid configurations 5
    - Grid configurations for wire resistance strain gages (*f.* 1) 6
    - Configurations of foil gages (*f.* 2) 7
  - Gage wire materials 6
    - Some normal properties of strain-gage materials (*f.* 3) 8
  - Gage resistance 6
  - Gage bonding 10
  - Gage-backing materials 10
  - Special gage designs 10
  - Gage length of the gage 11
  - Gage factors 11
- Gage mounting 12
  - Resin adhesives 12
  - Cellulosic adhesives 12
  - Criteria for curing 13
  - Response to strain rate 13
  - Thickness of layer of cement beneath the gage 13

Strain-Gage Circuits

- Development of instrumentation 13
  - Maximum circuit sensitivity 13
- The potentiometric circuit 14
  - Potentiometric strain-gage circuit (*f.* 4) 14
  - Advantages and disadvantages of circuit .. 15
- The Wheatstone bridge 16
  - Wheatstone-bridge strain-gage circuit (*f.* 5) 16
  - Balanced Wheatstone bridge with incremental strain-induced current output fed into a load resistance R_L (*f.* 6) 17
  - Thévenin equivalent circuit of balanced Wheatstone bridge and load of Fig. 6 (*f.* 7) 17
- Properties of the bridge circuit 18
  - Temperature compensation 18
  - Increasing the bridge sensitivity 18
  - Measuring sums and differences of strains .. 18
  - Unequal bridge arms 18
  - Finite load resistances 19
- Varying the sensitivity of strain gages and circuits 19
  - Planned desensitization 19
  - Parasitic desensitization 19
- Desensitization methods 19
  - Some common strain-gage sensitivity-control methods (*f.* 8) 20
  - Single gage desensitization 19
  - Two-gage desensitization 20
  - Four-gage desensitization 20
- Applications of complete bridge desensitization 20
- Balancing strain-gage bridges 21
  - Some bridge-balancing networks (*f.* 9) .. 21

Operational Characteristics

- Effects of temperature 22
  - Zero-strain temperature-resistance effects .. 22
  - Compensated gages 22
  - Deterioration at elevated temperatures 23
  - Effect of temperature on strain sensitivity 23
  - Magnitude of temperature variation 23
  - Length of time temperature is applied 23
  - Number of temperature cycles applied 24
  - Degree of cure of cement 24
- Effects of moisture 24
  - Gage-to-ground resistance check 24
  - Water immersion of gages 25
  - Electrolytic corrosion 25
  - Waterproofing of gages 25
- Effects of strain 25
  - Number of strain cycles 26
  - Rate of application of strain 27
  - Frequency of strain variation 27
  - Length of time strain is applied 27

CONTENTS (*Continued*)

PAGE
Effects of stress field 28
  Effect of transverse sensitivity 28
  Correction for transverse sensitivity 28
  Determination of Poisson ratio 29
  The stress gage 29
  Measurement of principal stress 29
    Circuit for conversion of T-strain-gage rosette into two equivalent stress-gage circuits (*f.* 10) 30
  Effect of hydrostatic pressure 30
  Effect of gage stiffness and rigidity 30
Electrical effects 30
  Thermoelectric potentials 31
  Maximum gage current 31
  Lead wires used from the gages 31
  Measuring lead resistance 32
  Leads to high-temperature gages 32
  Shielding of lead wires 32
  Switches or slip-rings in the gage circuit .. 32

Strain-Gage Tests on Large Structures

Industrial applications 33
  Design improvements 33
  Off-shore drilling barges 33
Test equipment 33
  Standard strain gages 34
  Special strain gages 34
  Rosette gages 34
  Instrumentation 35
Installation of gages 35
  Preparing the surface 35
  Cleaning 36
  Cementing 36
  Drying 36
Installation of lead wires 36
  Anchoring lead wires 36
  Capacitance balancing 37
Testing gages 37
Moisture proofing 37
Strain measurements 38
  Residual stresses 38
  Temperature effects 38
  Accuracy 40
  Test records 41
    Typical strain-gage work sheet (*f.* 11) .. 39
    Strain computed from readings in Fig. 11 (*f.* 12) 40
Evaluation of data 41
    Stresses calculated from strain readings in Fig. 12 (p.s.i.) (*f.* 13) 41
Guide to proper application 42
Bibliography 42

SECTION 54

RESISTANCE STRAIN-GAGE TESTS

Nature of Resistance Strain-Gage Tests

STRAIN MEASUREMENT. The criterion of failure of a material, machine, or structure is usually expressed in terms of the **stress**, or force per unit area, which must exist in the material before failure will occur. The concept of stress, being somewhat artificial in nature, has always had as its main disadvantage the fact that stress itself is not a quantity which can be measured directly. The unit elongation or strain of a material under stress, however, can be measured. **Strain** is used almost universally, in conjunction with the elastic and plastic constants of the material, to arrive at experimental values of stress. In the simplest case, i.e., uniaxial stress, the stress and the strain in the material are directly related by the **modulus of elasticity** of the material within its elastic range. Other states of stress present more complicated relationships among the material constants, stress, and strain.

As modern designs become more complex, it is more difficult to predict their behavior theoretically, and the experimental verification of design criteria becomes extremely important. The **experimental verification** and measurement of stresses and strains is a vital portion of modern technology in all fields of engineering endeavor.

DEVELOPMENT OF STRAIN-MEASURING DEVICES. Strain measurement is of prime importance in the experimental analysis of materials, structures, and machines. The very definition of "strain" as a unit or percentage change in length creates the impression that its measurement is no more complex than measurement of changes in length. Indeed, for many years, calipers and a ruler were standard strain-measuring instruments. These were succeeded, in later years, by mechanical lever systems, gear trains, and optical, acoustical, and pneumatic systems. Typical examples of some of these **extensometers** are the Berry, Huggenberger, Whittemore, and Tuckerman units. The most accurate strain-measuring devices, frequently used as standards, are optical in nature and include both interferometric means and optical lever-arm techniques.

Subsequent developments occurred in the electrical fields, where capacitance, inductance, reluctance, and resistance were made the bases of numerous extensometer instruments. Today, by far the most popular strain-measuring device is the **electric resistance strain gage,** both in its bonded and unbonded forms. The remainder of this section is devoted to resistance strain gages, although it should be remembered that it is only one of a large family of instruments designed to measure strain. [Portions of the material in this section have been adapted from Strain Gage Readings (P. K. Stein, ed.) and from Strain Gage Techniques (W. M. Murray and P. K. Stein).]

Auxiliary Stress-Analysis Tools. Several other methods of stress analysis have been proven extremely helpful in conjunction with the resistance gage technique of measuring strains at individual points over the surface of a structure. The **brittle-coating technique** (see the section on Brittle-Coating Tests) enables the experimenter to obtain an excellent qualitative presentation of the stress distribution, both in magnitude and direction, over the entire surface of two- or three-dimensional specimens. The entire test part is sprayed with a brittle coating designed to crack at known values of mechanical strain in the material beneath the coating. The cracks indicate both magnitude and direction of strain. This permits intelligent **selection of the locations and directions of individual strain gages** for more accurate analysis.

The **photoelastic model technique,** another stress-analysis tool, requires that geometric scale models of the prototype be made from special plastic materials which exhibit the property of stress-dependent optical bi-refringence (see the section on Vision and Optics). The stress distribution throughout the interior of models can frequently be determined in this manner. Recently **photoelastic coatings** have been developed (see the section on Photoelastic Coating Tests). These coatings can be cemented or sprayed onto the surface of two- or three-dimensional parts to determine strain distributions. Other stress-analysis tools fall into the large category of **analogies** such as electrical, electrical field, fluid flow, membrane, and arithmetical.

DEVELOPMENT OF ELECTRIC RESISTANCE STRAIN GAGES. The principle of the resistance strain gage was discovered by William Thompson, later Lord Kelvin, and presented to the Royal Society in 1856. In his researches on "The Electrodynamic Qualities of Metals," he discovered that metallic wires, when subjected to mechanical strain, will change in electrical resistance, and that this change is not always predictable by considering only the geometric changes in shape of a wire under stress. There is a basic **strain-dependence of the electrical resistivity** of individual materials. Subsequent investigators found that different materials exhibited different resistance-strain characteristics, varying even as to the sign of the effect. Carlson was the first to utilize this phenomenon to measure strain. In the late 1920's he wound fine wires between binding posts anchored in different locations on concrete dam structures and measured the strains within the concrete by measuring the changes in electrical resistance of the wire windings.

The concept of the **bonded resistance strain gage** was born in the late 1930's, almost simultaneously at the California Institute of Technology by Simmons and Clark and at the Massachusetts Institute of Technology by Ruge, DeForest, and Walsh. The idea of bonding a length of fine wire directly to the part to be tested, with the cement acting as an electrical insulator, made possible the wide applications of resistance strain gages. Today the **unbonded strain gage** is utilized mainly in the measurement of quantities other than strain, such as acceleration, force, or pressure. The bonded gage is used to measure these quantities as well as strain. Strain gages and strain-gage-based transducers have become indispensable tools in stress analysis, instrumentation, and process control.

RESISTANCE STRAIN-GAGE APPLICATIONS AND LIMITATIONS. Resistance strain gages have been used to measure strains as low as fractions of a millionth of an inch per inch, as well as strains up to 23 percent on rubber and plastics. They have withstood **environments** from liquid helium to 2000° F. combustion exhaust gases. They have operated submerged in seawater on ships' hulls for periods in excess of a year and a half, and have been used in hydrostatic environments at pressures above 50,000 p.s.i. Resistance strain gages can faithfully follow strains from zero frequency (d.c.) to over 50,000 c.p.s., and upper **frequency** limits have not yet been determined. They have been mounted to withstand 600,000-g. loading on rotating machinery, and signals have been obtained from them at close to 100,000 r.p.m. rotational speeds. When used to measure quantities other than strains, such as load, pressure, and torque, they have exhibited **accuracies** better than one-tenth of 1 percent for periods of 20 years.

Resistance strain gages have been used on almost all metals, on concrete, cement, brick, bones (live and dead), wood, rubber, and plastics. They have even been woven into fabrics. They have been used in and on operating gas turbines, reciprocating engines, airplanes, submarine hulls, cranes, earth-moving equipment, and automobiles, and wherever a stress problem required their use.

Load cells operating on the strain-gage principle are used in process and control industries for chemical batching, automatic mixing. continuous conveyor-belt weighing, and totalizing. They have been applied to servo and control systems of all types, and have proved to be reliable components of such systems. The two major fields of utilization of resistance strain gages are differentiated mainly by the widely different accuracies achievable in each case.

Stress Analysis by Strain Measurement. When used for stress analysis, the strain gage is used either singly, in pairs, or in rosette configurations. The gage is mounted at the location where strain is to be measured, and the resistance change of the gage is correlated with the stress produced within the structure. It is not usual, and actually is extremely difficult, to calibrate an individual gage and then to use the same gage to measure strains. Instead, strain gages are calibrated by the manufacturer on a statistical basis. The **gage factors** are usually given to plus or minus 1 percent tolerance on each package of gages. Thus, for stress-analysis purposes, strain gages are not expected to exhibit accuracies better than 1 percent. Furthermore, instrument errors and differences in the mounting technique used by different operators can contribute another probable 1 or 2 percent of error. It is optimistic to expect better than 2 to 3 percent **over-all accuracies** on stress-analysis tests with strain gages.

Measurement of Quantities Other than Strain. Strain gages are frequently attached to specimens designed to act as transducers. For example, a column may be used to transduce a force applied to the column into a strain in the column material. A strain gage attached to the column then acts as another transducer, changing this strain into an equivalent resistance variation in the gage. The over-all instrument is then a load-measuring instrument and no longer a strain-measuring device. These composite structures are frequently called **strain-gage-based transducers** (or just strain-gage transducers). They are widely used in the measurement of force, torque, pressure, acceleration, surface finish, speed, displacement, straightness, dimensions, blood-pressure, and many other variables. Since such transducers can be calibrated individually prior to use, a magnitude of accuracy not attainable with individual commercial strain gages can be achieved. Commercial instruments utilizing such transducers exhibit accuracies from 1 percent to better than 0.05 percent, depending on the application. **Linearity** and **hysteresis figures** are usually well within these values and can be obtained from most transducer manufacturers.

INFLUENCE OF MECHANICAL PROPERTIES OF BASE MATERIAL. In strain measurement the mechanical properties of the material to which the gage is attached do not affect basic gage behavior markedly. The mechanical properties will, however:

1. Govern the effect of the transverse sensitivity of the gage.
2. Affect gage readings if the modulus of the material is comparable to that of the gage, or if the thermal conductivity is so low as to lead to gage overheating.

When a strain-gage-based transducer is constructed to measure quantities other than strain, the characteristics of the base material determine the behavior of the transducer. Here the entire system is subjected to calibration for output, as a function of applied torque, pressure, acceleration, force, or other parameter. Of the large number of properties of the base material which will affect transducer performance, those mentioned in subsequent paragraphs will be discussed briefly.

Modulus of Elasticity. The applied force usually creates a stress distribution within the base material of the transducer. This results in a strain distribution beneath the gage, to which the gage reacts by means of a resistance change. A low modulus of elasticity will result in higher strains than a high modulus. What is more critical, however, is that the modulus remain constant with time and **temperature.** The modulus of elasticity of most materials decreases with increasing temperature. Thus, for the same stress in the base material (load on the transducer), the strain gages will experience higher strains at higher temperatures. The sensitivity of the transducer thus usually increases with increasing temperature. This is offset to some degree by the decrease of the gage factor with increasing temperature.

Electrical methods of compensating for the modulus-temperature effect will be discussed later. In steels the change in modulus of elasticity with change in temperature is usually a decrease of the order of 2 percent per 100° F.

Poisson Ratio. The Poisson ratio of a material is frequently used to increase the sensitivity of a strain-gage-based transducer. The Poisson ratio of the base material must therefore remain constant with temperature; otherwise the relative contributions of the various gages in the system will vary, thus affecting the sensitivity of the device.

Linearity of the Stress-Strain Curve. A linear relationship between the physical quantity applied and the output of a transducer is most desirable. The linearity of a transducer depends not only on its geometrical shape but also on the stress-strain characteristics of the material. There are some stainless steels and aluminum alloys which possess highly **nonlinear stress-strain curves,** even in regions normally considered below the yield point.

Hysteresis of the Stress-Strain Curve. The effects of hysteresis within the stress-strain curve of the base material are twofold:

1. After a stress cycle the final value of strain for a state of zero stress is different from the original zero-stress strain value; i.e., a zero shift has occurred, which is not permissible in a good transducer.
2. The value of strain for a given stress is dependent on whether the stress is approached from a lower or higher value.

Hysteresis in transducers can be an inherent property of the base material or of the geometric design of the device.

Temperature Coefficient of Linear Expansion. The thermal expansion coefficient should be chosen so that no appreciable temperature-induced **zero**

shift occurs when a particular strain gage is mounted on the material. This minimum zero shift can usually be obtained only over a limited temperature range. It is important, however, that the thermal expansion coefficient be repeatable from one temperature cycle to the next. These precautions are needed even though the effects of temperature variations can be eliminated in electrical circuits where two or more gages have identical temperatures.

Other Properties. The effects of properties such as yield point, ultimate strength, thermal conductivity, homogeneity and isotropy, endurance limit, ability to withstand moisture absorption, and absence of metallurgical phase changes in the working range of the transducer are reasonably obvious and need not be discussed.

Selection of Base Materials for Transducers. In view of these requirements, the following materials have been found to be satisfactory base materials for strain-gage-based transducers:

1. High-grade tool steels (4140 series), heat treated.
2. 24S–T or 75S–T aluminum.
3. The 400 series of stainless steels.
4. Beryllium-copper.

Strain-Gage Construction and Installation

GAGE MATERIALS AND CONSTRUCTION. From 1 to 6 in. of wire are required to produce a normal gage. Wires from 0.001 to 0.0005-in **diam.** are used most commonly. Foils from 0.001 to 0.00012 in. thick are used for etched-foil gages. The wires are wound into some geometrical shape or grid so that the over-all length of the gage is between 1/32 and 6 in., the "gage length" of the gage. The winding is sandwiched between two thin sheets of a **carrier material,** which may be a paper, paper impregnated with resin, or a plastic. **Lead wires** are attached to the fine, strain-sensitive filament by soldering or welding. The resulting miniature postage-stamp size of sandwich is a strain gage ready to be cemented to any location where strain is to be measured. Occasionally, and especially for high-temperature applications, either foil or wire gages are made without backing or with a strip-off backing.

Grid Configurations. Murray and Stein (Strain Gage Techniques) show various gage grid configurations in Fig. 1. Some **foil gages** are illustrated in Fig. 2. In addition, there are special gage types such as wire spirals and V-form stress gages.

In general the **flat grid gage** is superior to the wrap-around (or bobbin) type of gage in gage factor, stability, creep, hysteresis, conformability, and current-carrying capacity. **Wrap-around gages** may show negligible or even zero transverse effects. **Foil gages** exhibit less transverse sensitivity than flat grid gages. Foil gages are produced by acid-etching of the foil rather than by the winding procedure used for wire. Foil gages are proving themselves superior to flat grid gages in all the aspects mentioned here. Foil gages are made down to 1/64-in. gage length, whereas both flat grid and bobbin-type wire gages are available only in gage lengths to 1/32 in.

Other special grid configurations are embodied in the **T-gage** and **rosette gage configurations,** which may contain two, three, or four separate strain-sensitive windings so that strains may be measured in different directions at essentially a single point. This procedure permits the determination of the complete state of stress in two dimensions.

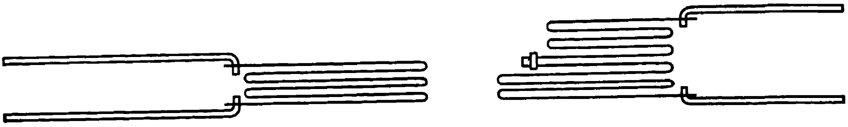

(a) Flat Grid

(b) Temperature Compensated (Dual Element)

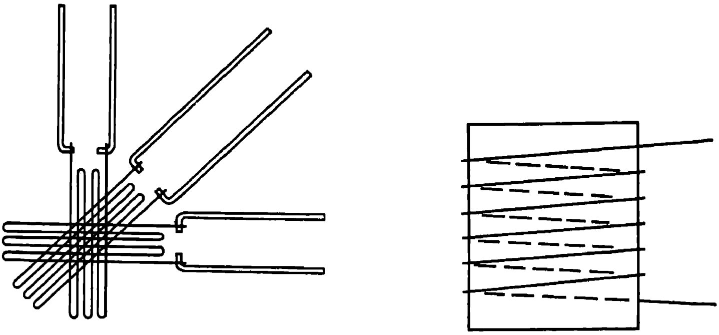

(c) Rosette

(d) Wrap Around or Bobbin Type

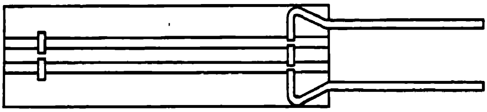

(e) G-H Tepic Gage

Fig. 1. Grid configurations for wire resistance strain gages. (a) Flat grid. (b) Temperature-compensated grid, dual element. (c) Rosette grid. (d) Wrap-around or bobbin type of grid. (e) G-H tepic gage.

Gage Wire Materials. Materials most frequently used for strain gages will fall into four main categories:

1. Copper-nickel alloys.
2. Nickel-chrome alloys.
3. Modified nickel-chrome alloys.
4. Nickel-iron alloy.

Fig. 3 presents average characteristics for each group, taken from the literature.

Gage Resistance. Resistances of about 100 ohms or higher are required of strain gages to accommodate the usual magnitudes of strain encountered when using wires or foils of commonly available strain sensitivities and when using instrumentation presently available. Lower resistances would result in extremely small strain-induced resistance changes, and extraneous sources of error would loom extremely large. **Commercially available gages** are made with resistances

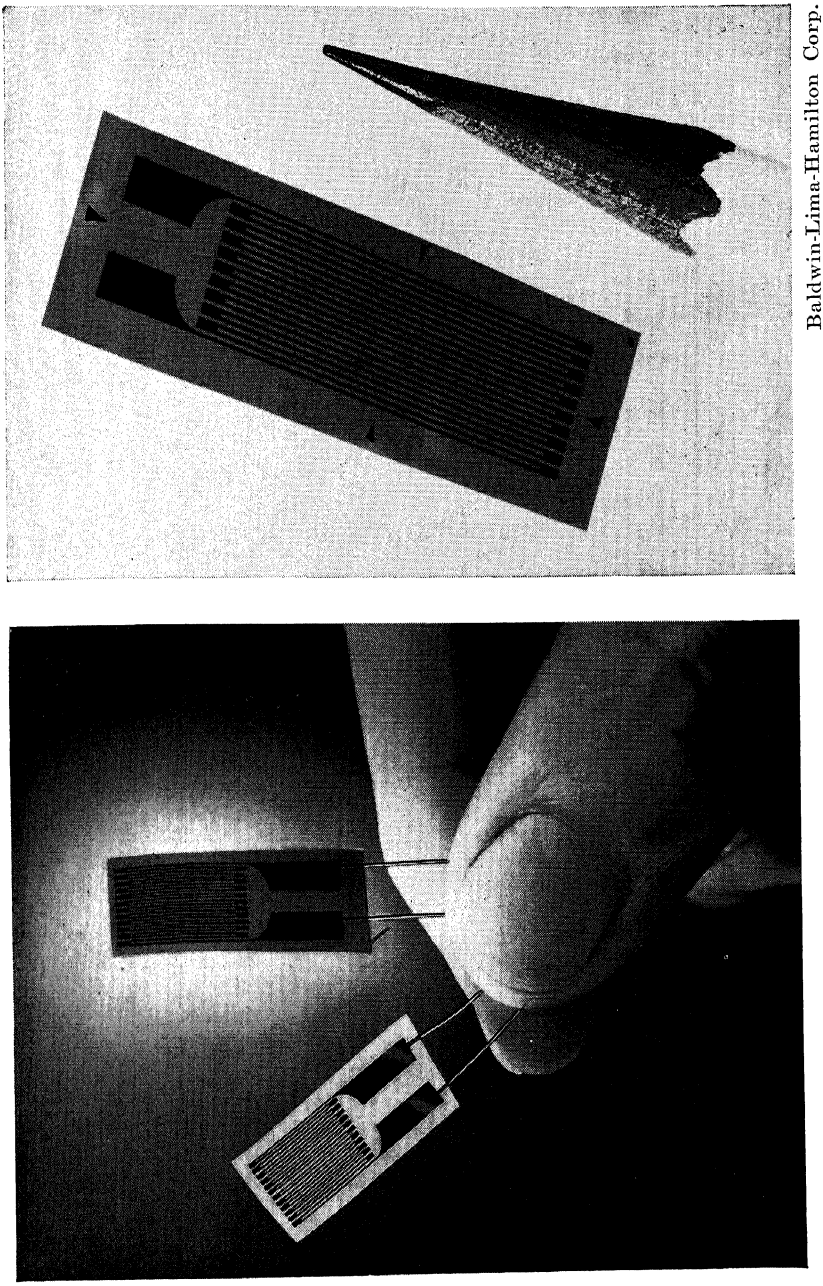

Baldwin-Lima-Hamilton Corp.

Fig. 2. Configurations of foil gages.

Composition	Copper-Nickel; 43–45% Ni; rem. is Cu	Medium Nickel-Chrome; 73–75% Ni, 20% Cr, Al, Fe	Nickel-Chrome; 80% Ni, 20% Cr	Nickel-Iron; 36% Ni, 8% Cr, ½% Mo; rem. is Fe
Resistivity at 68% F.:				
micro-ohm-cm.	49	134	110	
ohms/circ. mil-ft.	294	800	660	528
Resistance-temperature coefficient, 20°–100° C., micro-ohms/ohm/° C.	+20	+20	125	
Specific heat, gram-cal.	0.094	0.104	0.107	
Thermal conductivity, 100° C., watts/cm./° C.	0.212	0.130	0.132	
Melting point, °F.	2210	2550	2550	
Linear expansion coefficient, 20°–100° C., μin./in./° C.	14.9	13.5	15–17	4
Tensile strength, 20° C., p.s.i.	60,000–135,000	130.000–180,000	100,000–200,000	170.000
Young's modulus, p.s.i.	23.3×10^6		28×10^6	26×10^6
Specific gravity	8.9	8.1	8.3	8.1

Density, lb./in.^{3}	0.322	0.293	0.304	0.292
Thermal e.m.f. against Cu, 0°–100° C., μvolts/° C.	43	3 approx.	5 approx.	13 approx.
Tensile strength, 1-mil wire, lb.	0.062			
Yield strength, 1-mil wire, lb.	0.051			
Magnetic attraction	None	None	None	Yes
Strain sensitivity	2.05–2.15	2.2–2.6	2.4–2.6	3.6
Thermal coefficient of modulus of elasticity, per °F.	...	...	...	-20×10^{-6} to 15×10^{-6}
Approximate linear limit for strain-gage use, strain	20%	½ to 1%	½%	¾%
Approximate temperature limit for strain-gage use, °F.	600, static	900, static strain	1800, dynamic strain	250, dynamic strain
Approximate equivalent indicated strain for gage on steel, μin./in./°F. at 80° F.	1.3	1–2	20	133

Fig. 3. Some normal properties of strain-gage materials.

between approximately 60 and 10,000 ohms. The 120- and 350-ohm gages are accepted as a kind of standard in the United States.

Gage Bonding. The surface area of a 1-in. length of gage wire is more than 4000 times the cross-sectional area of the wire. Consequently the **shear strength of the cement** attaching the wire to the carrier material and to the structure need be only a small fraction of the stress in the wire. Such bonding will force the wire to follow faithfully the dimensional changes of the test specimen as mechanical strains occur. The cement transmits these strains by the mechanism of shear, and the wire resists deformation by direct tension or compression. The strength of cements generally used with strain gages is sufficient to force the wires or foils to follow tensile strains beyond their own yield point, while allowing them to return to the initial wire or foil dimensions under zero-strain conditions. **Compressive strains** are accommodated, and the wire is prevented from buckling by the same phenomenon.

The **cements** generally used with strain gages fall into three categories:

1. Thermoplastic (cellulose nitrate, cellulose acetate or De Khotinsky).
2. Thermosetting (phenolformaldehyde, epoxy, or combinations of these two).
3. Ceramic.

The approximate **temperature limitations** of these three types of adhesive have given rise to the definitions of the boundaries between "room," "elevated," and "high" temperature. **Cellulose cements** may be used to about 130° F., which is still regarded as "room temperature." **Phenolic and epoxy adhesives** perform up to a range of 500° F. to 600° F., the point where Constantan also ceases to perform well as a strain-sensitive material. The "elevated temperature" boundary may be taken as 600° F. **Ceramic cements** presently have been used to 1800° F. and are expected to solve the strain-gage-adhesion problem for temperatures above 600° F.

Gage-backing Materials. Carriers usually used with strain gages are:

1. Paper impregnated with cellulose nitrate (known as paper gages).
2. Paper impregnated with phenolformaldehyde resin (bakelite gages).
3. Sprayed epoxy or phenolformaldehyde backing for foil gages.
4. Sprayed elastomer backing which can be stripped from foil gages.
5. No backing; the strain-sensitive grid (wire or foil) is free.
6. Metal backing; weldable gages.

Special Gage Designs. Several special strain gages have been designed to circumvent some of the difficulties associated with the ordinary bonded and unbonded resistance strain gages, although they sacrifice some of the advantages of these types. One of these special gage types is a **weldable gage** for which a filament of strain-sensitive wire is chemically milled in its center portion to about 0.001-in. diam., the over-all length of the milled portion being somewhat less than an inch in most cases. With a ceramic acting as insulator, this filament is then swaged into a stainless steel or Inconel outer sheath which is equipped with a small flange which can be welded to the test surface. About 50 welds per inch are satisfactory and the strain-sensitive filament, by virtue of being swaged into its sheath, follows strains in the test specimen faithfully.

Another special gage type is the **woven-wire strain gage** wherein a strain-sensitive filament forms part of the weave of a ribbon (the width of the ribbon is the gage length of the gage). The strain-sensitive filament lies flat, with glass fibers weaving in and out. A length of ribbon is cut (this length then becomes the gage width), leads are welded onto the ends of the gage, and the entire assembly is mounted on the test specimen.

Gage Length of the Gage. The choice of gage length of a gage (defined as the active length of strain-sensitive filament) is a compromise between different factors. The length of the gage must be commensurate with the **strain gradient** beneath the gage, since the gage will approximately average the strain beneath its gage length, thus possibly hiding peak strains. Gage lengths larger than the radius of the fillet into which the gage is to be placed, for example, are not recommended. On the other hand, the larger the gage, the less it is subject to **creep.** With larger gage lengths, **hysteresis effects** are reduced. For use on nonhomogeneous materials such as concrete, the gage length must bear a certain limiting relationship to the maximum aggregate size in order to avoid large, localized errors.

Gage Factors. The **strain sensitivity** of a straight, unbonded filament of material can be expressed as:

$$\text{Strain sensitivity factor} = \frac{\text{percentage resistance change in the wire}}{\text{percentage strain which created this resistance change}} \tag{1}$$

or

$$K = \frac{\Delta R/R}{\Delta L/L} \tag{2}$$

Here, K = **strain sensitivity** if

$\frac{\Delta R}{R}$ = strain-induced unit change in resistance of a straight, unbonded wire subject to a strain $\Delta L/L$

The winding of the filament into a grid form, the sandwiching of the grid between carrier layers, and the subsequent mounting of this assembly on a test specimen result in a relationship between the strain in the test specimen beneath the gage and the resistance change in the strain-sensitive filament, which is no longer equal to the strain sensitivity of the wire itself. The ratio of unit resistance change divided by strain for the assembly is called the "gage factor," and is smaller than the intrinsic strain sensitivity of a straight, unbonded wire of the same material as the gage. In Eq. 2:

K = manufacturer's gage factor

if $\frac{\Delta R}{R}$ = strain-induced unit change of resistance at the terminals of a completed gage tested under standard calibration conditions.

$\frac{\Delta L}{L}$ = strain in the specimen, to which the gage is attached, beneath the gage.

K = effective gage factor

if $\frac{\Delta R}{R}$ = strain-induced change of resistance indicated at the output of the entire strain-measuring system.

$\frac{\Delta L}{L}$ = strain in the specimen, to which the gage is mounted, beneath the gage.

The gage factor is determined on a statistical basis by the gage manufacturer for each batch of gages. This procedure is especially important, since the properties listed in Fig. 3 vary from melt to melt of the same material, from batch to batch of the same melt, and even along the same spool of wire. Each package of gages is usually marked with the gage factor, the gage resistance (with tolerance figures on each), and the lot number of the wire from which the gage is made. In any one experiment, therefore, gages of the **same lot number** should be used whenever practical.

GAGE MOUNTING. The exact method by which the specimen surface is cleaned, the gage attached, and the adhesive cured are of prime importance to the quality of the bond developed between the strain gage and the test specimen. The nature of bonding requires exact conformity with established procedure in order to duplicate successful results. No **variation in routine** can be tolerated unless a complete evaluation can be made of the effects of the variation. There are many variables, and none can be changed without affecting the over-all result; thus no amount of care is too great if it assures good installation of the gage and proper bonding to the test specimen.

A strain gage, of course, must be mounted properly over its entire length, without **air-bubbles, rough spots,** or **inclusions** beneath the gage. Unless the user is an adhesives expert, the cements must be cured or fired strictly according to instructions without even the slightest modifications until these have been proven to give superior results. Meticulous attention to detail is essential in obtaining a satisfactory strain-gage installation.

Resin Adhesives. Phenolic adhesives or thermosetting resins require application of pressure as well as temperature for curing because water vapor is liberated during the curing process. If **pressure** is not applied, the vapor is trapped in the adhesive layer, forming friable, porous bonds which are completely unsatisfactory for strain-gage use. Pads placed over the gage to allow application of pressure, therefore, should not be much larger than the gage area (otherwise the vapors cannot escape), nor should heat be suddenly applied during curing if **vapor blisters** in the adhesive are to be avoided.

Epoxy resins (also thermosetting) do not liberate any vapors during cure, and thus do not require any pressure higher than contact pressure for curing. The bond strength formed, however, is frequently critically dependent on the amount of **activator** used with the adhesive and on the **curing time-temperature cycle** used. Because of exothermic reactions, epoxies are mixed in small batches; thus a drop more or less of activator can amount to a sizable percentage of activator used. Some of the newer high-temperature adhesives contain both epoxy and phenolic resins, and some of these cements have been known to be serviceable to temperatures of 700° F. to 800° F.

At **elevated temperatures,** the oxidation of the adhesive manifests itself in loss of weight and strength in the cement. This phenomenon, however, is time-dependent. Some information has been obtained with strain gages when using these adhesives at high temperatures in short-term tests or by covering the gage installation with a material which prevents access of air to the phenolic and/or epoxy adhesive.

Both epoxy and phenolic resins contain **fillers** which govern properties of the adhesive such as its thermal expansion coefficient, modulus of elasticity, resistance to radiation, and creep characteristics. Each type of adhesive is compounded for a specific purpose, and it is extremely unwise to modify the composition of an adhesive without thoroughly testing the resulting resin.

Cellulosic Adhesives. Cellulose nitrate or cellulose acetate adhesives are **thermoplastic cements** and therefore are essentially restricted to room temperature operation. They lose up to 85 percent of their initial weight, due to solvent evaporation during drying. Thus the pads placed over the gages should not be much larger than the gage area in order to permit **vapor egress.** Application of a hot-air blast materially hastens drying of the cement; radiant heat alone is insufficient. Due to the process of adhesive penetration of the gage matrix and the subsequent curing, gages will change in resistance during drying.

Criteria for Curing. Completion-of-cure criteria have variously been taken as the time necessary for the gage resistance to stabilize, for maximum gage-factor achievement, or for minimum hysteresis. Some of the best results with cellulose nitrate cements are obtained where the cure criterion is the development of a minimum of 10,000 megohms **resistance between the strain gage and the specimen** to which the gage is attached.

Response to Strain Rate. Since the reaction of polymeric materials to mechanical stress or strain is visco-elastic, the properties of the various adhesives used with strain gages will depend on the rate of application of strain, i.e., on the frequency of the applied strain. Various properties will assume maxima and minima in different regions of the frequency spectrum, depending on the **resonant frequencies of the adhesive** in terms of its bonding forces.

Thickness of Layer of Cement Beneath the Gage. In stress fields where bending is present beneath the gage location, the layer of cement serves to increase the distance between the strain-sensitive filament and the **neutral axis** of the specimen as compared with the distance between the neutral axis and the specimen surface. Thus strains are observed at a larger radius from the neutral axis than that at which they occur; this leads to error. In thin-skin construction such as air foils, and in situations where the neutral axis may be extremely close to the specimen surface, such as in turbine blades, errors of 50 percent are not uncommon in strain readings. Adhesive-layer thickness for common gage installations is about 0.003 in., depending on the gage type, adhesive, and operator technique. With many adhesives, a rather severe reduction of shear strength of a glued joint occurs with **increasing glue-line thickness.** This effect is more severe for phenolic adhesives than for epoxy ones. In general it is good practice to try to obtain the thinnest possible thickness of adhesive between the gage and the test specimen.

Strain-Gage Circuits

DEVELOPMENT OF INSTRUMENTATION. The "Differential Resistance Measurer" introduced to the Royal Society by Mr. Wheatstone early in 1843, which has become known as the Wheatstone bridge, is the circuit most commonly used for static strain-gage instrumentation. It permits signals from individual strain gages to be read individually, or to be combined and added to, subtracted from, multiplied with, or divided by one another, thus offering limitless computer and control possibilities. Some immediate applications of these computer principles are electrical temperature compensation, the torquemeter, and the shear meter.

The **potentiometric circuit, ballast,** or **series circuit,** as it is also known, is the most commonly used arrangement for dynamic strain studies.

Maximum Circuit Sensitivity. An important item to note immediately is that the maximum output from any given strain gage, in any of the circuits generally used with strain gages under open-circuit output conditions, is a function of only three gage properties. The maximum circuit sensitivity in microvolts open-circuit·output per microinch per inch of strain beneath the gage is equal to the product of (1) gage factor, (2) gage resistance, and (3) current, in amperes, passing through the gage. It is also known that the **equal-arm bridge** produces only one-half of this output, i.e., exhibits a circuit efficiency of 50 percent.

The foregoing results are abstracted from the analyses discussed in subsequent paragraphs because of their importance and because they enable an experimenter to plan his entire **instrumentation system** even before the first strain gage is mounted.

THE POTENTIOMETRIC CIRCUIT. A potentiometric circuit is shown in Fig. 4. R_g is a strain gage, and R_b may be either a strain gage or a fixed resistor. This network is fed from a d.-c. voltage supply (a dry cell, for example) of voltage V, resulting in a current of I amperes passing through the gage. If the ratio

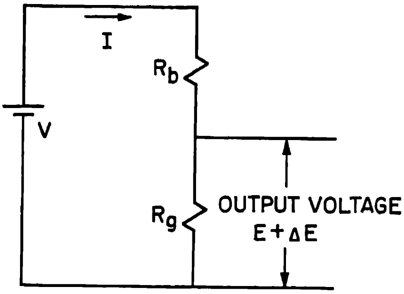

Fig. 4. Potentiometric strain-gage circuit.

$$a = \frac{R_b}{R_g}$$

the output from this circuit consists of a steady voltage E, i.e.,

$$E = V\left(\frac{1}{1+a}\right) \tag{3}$$

and a strain-induced incremental voltage ΔE, i.e.,

$$\Delta E = V\left[\frac{a}{(1+a)^2}\right]\left(\frac{\Delta R_g}{R_g} - \frac{\Delta R_b}{R_b}\right)(1-n) \tag{4}$$

Here n is the term incorporating second-order nonlinearity quantities:

$$\frac{1}{n} = 1 + \frac{a+1}{(\Delta R_g/R_g) + a(\Delta R_b/R_b)} \tag{5}$$

The nonlinearity of the circuit can become appreciable, although it is negligible for many applications. Eq. 4 can be rewritten in terms of the current I through the gages as

$$\Delta E = IR_g\left(\frac{\Delta R_g}{R_g} - \frac{\Delta R_b}{R_b}\right)\frac{a}{1+a} \tag{6}$$

For a given current rating of a gage I, the circuit output is higher for higher values of a (hence higher values of V), and in the limit approaches

$$\Delta E_{\max} = IR_g\left(\frac{\Delta R_g}{R_g} - \frac{\Delta R_b}{R_b}\right) \tag{7}$$

but since

$$\frac{\Delta R}{R} = \varepsilon K \tag{8}$$

this limit is

$$\Delta E_{\max} = IR_g\,(\varepsilon_g - \varepsilon_b)K \tag{9}$$

Here ε is strain, K is gage factor, and subscripts g and b refer to gages of resistance R_g and R_b. If R_b is a fixed resistor, then $\Delta R_b/R_b$ is zero. If R_b is a strain gage similar to R_g but subjected to strains of the same magnitude and opposite in sign to those experienced by R_g, the nonlinearity term vanishes, since

$$\frac{\Delta R_b}{R_b} = -\frac{\Delta R_g}{R_g} \tag{10}$$

The sensitivity for the combination of both gages becomes equal to the maximum sensitivity attainable with a single gage. Such cases exist on opposite sides of beams in pure bending, for example.

Furthermore, if R_b is a gage from the same package as R_g, mounted by the same operator at the same time on a piece of the same material as gage R_g, and if the piece of material to which R_b is attached is not strained mechanically but maintained at the same temperature as R_g, then R_b is a **temperature-compensating "dummy" gage.** Any temperature-induced resistance changes experienced by both gages will be equal and thus will cancel each other (see Eq. 6). Strain-induced resistance changes, acting only on R_g, will appear as voltage variations at the circuit output. This method of eliminating temperature-induced resistance fluctuations is known as **electrical temperature compensation** by means of a dummy gage. It is to be noted that the use of such a dummy gage automatically restricts the **circuit sensitivity** to 50 percent of its maximum value.

The placing of several gages in series to form R_g will not increase the circuit output unless the supply voltage V is increased proportionately, thus maintaining the same current I for multiple gages as existed for a single gage.

It has been noted that the circuit output consists of both a steady component E, which is independent of the strain in the gage, and of a strain-dependent incremental output voltage ΔE. The relative magnitudes of these voltages differ by factors of about 10^3 to 10^5, depending on the strain levels involved. Thus it is not feasible to measure the composite voltage $(E + \Delta E)$. It is necessary to eliminate E either by inserting a **bucking voltage** of value E (a process which has not been successfully used as yet) or by eliminating the d.-c. component E by means of a **resistance-capacitance filter.**

Not only does such a filter eliminate the voltage E, but it also eliminates or attenuates all voltages between zero and f_0 contained in ΔE, where f_0 is the **cut-off frequency of the filter.** Thus the potentiometric circuit is not applicable to static strain measurements and will produce satisfactory results only for strains whose frequency lies well above the value of f_0 for the filter used.

For this reason temperature compensation is seldom used in the potentiometric circuit. Unless temperature fluctuations occur at a rate higher than f_0, their effect will not be transmitted through the filter, and hence their presence will not be noted on the read-out instrument. Thus it is usually possible to obtain up to 95 percent of the maximum available gage output by using values for R_b higher than ten times the value for R_g.

Advantages and Disadvantages of Circuit. Significant performance characteristics of potentiometer circuits include:

1. The circuit, as used for a single gage, is not temperature-compensated as such in the sense that temperature-induced resistance changes in the gage will produce an output from the circuit just as much as strain-induced resistance changes.
2. It is possible to temperature-compensate a potentiometric circuit, with a loss of 50 percent of the maximum sensitivity, if a dummy gage is used.

3. The circuit responds to sums and differences of strains in different gages (see Eq. 6) and hence may be employed as a multiple-gage computing circuit.
4. It has been shown that the circuit must be followed by a device which can eliminate the steady component of d.-c. voltage present in the output. This elimination is usually accomplished by means of a frequency-sensitive element which follows the strain-gage circuit (a filter). Thus neither strain nor temperature-induced strains of frequencies below the cut-off point of the filter will be present in the output.
5. It is possible to run a common ground lead connecting one side of the supply voltage, one end of the gage, and the ground terminal of the successive instrumentation, thus eliminating one of the prime sources of electrical pick-up present in a bridge circuit. Since pick-up is most annoying in dynamic work, the potentiometric circuit is superior to a bridge circuit for dynamic strain measurements made with d.-c. supplies.
6. The incremental, strain-induced output voltage is directly proportional to the supply voltage V and will therefore reflect any changes in this voltage.

THE WHEATSTONE BRIDGE. Insofar as strain-gage application is concerned, the bridge circuit shown in Fig. 5 can be considered as nothing more than two potentiometric circuits (R_1, R_2) and (R_3, R_4) connected to the same supply voltage. It is thus possible for the steady d.-c. output from one potentiometric circuit to cancel exactly that of the other, independently of the supply voltage V.

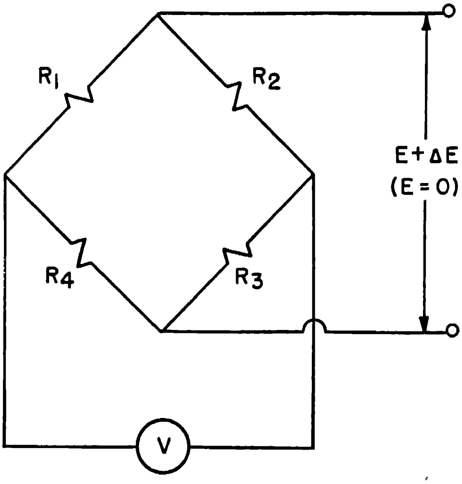

Fig. 5. Wheatstone-bridge strain-gage circuit.

Such cancellation of outputs is known as a **balanced bridge.** Normally the bridge will exhibit a steady, d.-c. output, not related to strain, and a strain-induced, incremental output. The steady output is

$$E = V\left[\frac{(R_2R_4) - (R_1R_3)}{(R_1 + R_2)(R_3 + R_4)}\right] \tag{11}$$

and the strain-induced, incremental output is

$$\Delta E = V\frac{a}{(1 + a)^2}\left[\frac{\Delta R_1}{R_1} - \frac{\Delta R_2}{R_2} + \frac{\Delta R_3}{R_3} - \frac{\Delta R_4}{R_4}\right](1 - n) \tag{12}$$

provided that E is zero. The ratio a is defined as

$$a = \frac{R_2}{R_1} = \frac{R_3}{R_4} \tag{13}$$

The term containing the nonlinearity factors is approximately equal to

$$\frac{1}{n} = 1 + \frac{a+1}{(\Delta R_1/R_1) + (\Delta R_2/R_2) + (\Delta R_3/R_3) + (\Delta R_4/R_4)} \tag{14}$$

and Eq. 9 for maximum bridge output becomes

$$\Delta E = IR_1K(\varepsilon_1 - \varepsilon_2 + \varepsilon_3 - \varepsilon_4) \tag{15}$$

The preceding relationships are given for open-circuit conditions at the bridge output. Subscripts 1, 2, 3, and 4 refer to the bridge arms in Fig. 5. Whenever a resistance is fixed and not strain-sensitive, the value for $\Delta R/R$ is, of course, zero. For a single active gage, therefore, Eq. 12 can be rewritten (neglecting nonlinearities) as

$$\frac{\Delta E}{\varepsilon_1} = IR_1K\left(\frac{a}{1+a}\right) \tag{16}$$

For conditions other than open circuit where a load-resistance R_L exists at the bridge output as shown in Fig. 6, the **Thévénin equivalent circuit** (i.e., the simplified circuit exhibiting identical electrical behavior) can be drawn as shown in Fig. 7. If

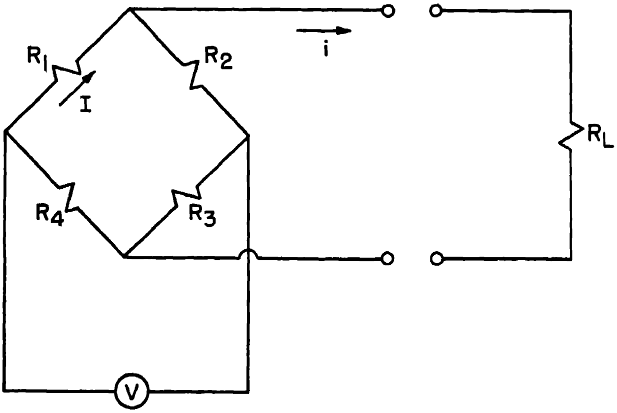

Fig. 6. Balanced Wheatstone bridge with incremental strain-induced current output fed into a load resistance R_L.

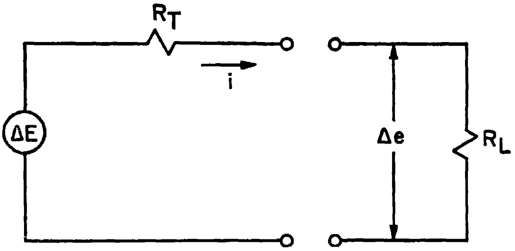

Fig. 7. Thévénin equivalent circuit of balanced Wheatstone bridge and load of Fig. 6.

$$R_T = \frac{R_1R_2}{R_1 + R_2} + \frac{R_3R_4}{R_3 + R_4} \tag{17}$$

then

$$\Delta E = V\left(\frac{a}{(1+a)^2}\right)\left(\frac{\Delta R_1}{R_1} - \frac{\Delta R_2}{R_2} + \frac{\Delta R_3}{R_3} - \frac{\Delta R_4}{R_4}\right) \tag{18}$$

and

$$i = \frac{\Delta E}{R_T + R_L} \tag{19}$$

$$\Delta e = \Delta E \frac{R_L}{R_T + R_L} \tag{20}$$

so that either voltage or current sensitivities may be computed.

PROPERTIES OF THE BRIDGE CIRCUIT. Several properties of the bridge circuit have far-reaching consequences insofar as strain-gage techniques are concerned. Some of the more important ones will be mentioned here.

Temperature Compensation. As in the potentiometric circuit, it can be shown that as long as two adjacent arms of the bridge are made up of strain gages of the same type, which are bonded to the same material and maintained at the same temperature, the bridge will be insensitive to temperature-induced resistance changes acting simultaneously on these two gages. If only one of the bridge arms contains active gages, the other arm is known as a **temperature-compensating dummy arm.** If both arms contain active gages, one is said to temperature-compensate the other. An **active gage** is a gage subjected to mechanical strains.

Thus bridge arms 1 and 4 may be at temperature T_1, and arms 2 and 3 may be at temperature T_2; the bridge output will be independent of variations in temperatures T_1 and T_2 (in theory). In practice, it is always necessary to check whether or not such compensation actually exists, since subtle experimental conditions which may escape the casual observer can completely destroy the compensating effect of two gages supposedly at identical temperatures at each instant of time during the test.

Increasing the Bridge Sensitivity. Two gages mounted side by side and subjected to the same strains may be placed in opposite arms of a bridge (such as 1 and 3), thus producing twice the bridge output available from a single gage, as may be seen from Eq. 12. The bridge can be completed with fixed resistors or temperature-compensating dummy gages, as required. It is to be noted that this method is the only one in which bridge sensitivity is increased without affecting the type of strain condition to which the circuit will respond. (Of course it is possible to place the two gages in series with each other in one bridge arm and to use twice the supply voltage V used for a single gage.)

Measuring Sums and Differences of Strains. Since the strain signals from the gages in arms 1, 2, 3, and 4 of the bridge add to and subtract from each other, as shown in Eqs. 12 and 15, the proper placement of gages in appropriate bridge arms can result in an elementary adding and subtracting computer.

Unequal Bridge Arms. The bridge circuit is frequently used with all arms of the bridge initially equal in resistance, in which case the ratio a is unity and the circuit presents only one-half of its maximum output. By choosing high values for a, it is possible to obtain an output from a two-active-gage bridge that is equal to that obtained from a four-active-gage, equal-arm bridge. The choice of bridge arm, however, is important. Two gages located, for example, in arms 1 and 4 of the bridge will permit the use of high values of a for R_2 and R_3. This permits a high **circuit efficiency** [as the ratio $a/(1+a)$ appearing in Eq. 16 is often called] through selection of fixed resistors of the order of ten times the gage resistance. If these same gages had been located in arms 2 and 1 of the bridge, the ratio a would automatically be unity, no matter what the values of R_3 and R_4, resulting in a 50 percent efficient circuit.

Finite Load Resistances. Bridge circuit sensitivities under open-circuit conditions at the bridge output are frequently expressed in terms of the bridge voltage output per bridge voltage input per unit strain in one of the arms of the bridge. For finite load resistances (no longer representing open-circuit conditions), Eqs. 18, 19, and 20 can be used to compute either the voltage across the load resistance or the current through it.

VARYING THE SENSITIVITY OF STRAIN GAGES AND CIRCUITS. Variations in the sensitivity of strain gages, or the circuits of which they form a part, almost invariably take the form of decreasing the "rated" sensitivity of the gage as expressed by the manufacturer's gage factor. Such a desensitization may be planned or may be parasitic.

Planned Desensitization. Deliberate sensitivity control is desirable when:

1. It is desired to obtain the sum or difference of a strain at one location and a fractional part of the strain at another location. The problem of measuring the bending moment directly at remote locations demonstrates this approach.
2. The range of accommodation of a measuring instrument is insufficient to accommodate certain strain magnitudes encountered (for example, in post-yield studies) but where appropriate gage desensitization will permit use of that instrument.
3. An instrument exhibits a limited linear-input region but the strain magnitudes exceed that limit, and desensitization circuits can be profitably used.
4. A preplanned variation in circuit sensitivity will result in some other desired phenomenon. The variation of modulus of elasticity of the structural material of a transducer with temperature, for instance, seriously affects the calibration sensitivity of the device. By varying the circuit sensitivity with temperature in a preplanned manner, the two temperature-induced phenomena can be made to cancel each other.
5. A single instrument, calibrated in certain units, is to be used with strain gages or transducers of varying sensitivities, and approximate desensitization of the gages or transducers can result in common applicability of the instrument scale.
6. Certain combinations of different percentages of various strain-gage readings, which are together desensitized by a common amount, will result in a desired reading.

Parasitic Desensitization. Unplanned desensitization, of course, also plagues the experimenter in the form of lead resistances and other problems already discussed.

DESENSITIZATION METHODS. Fig. 8 shows three methods of gage sensitivity control in which n is the **desensitization factor** defined by

$$\text{Indicated strain} = n \text{ (true strain)}$$

Single Gage Desensitization. The approach of Fig. 8(a) changes the sensitivity of only one gage on a bridge for bridge-balance purposes, by means of a series and shunt resistance while maintaining the original gage resistance across the composite network. Special precautions are necessary to maintain temperature compensation. This method of sensitivity control will function for either null-balance or unbalance bridge measurement.

Two-Gage Desensitization. A practical extension with slight modification of the single gage approach, as shown in Fig. 8(b), results in the maintenance of temperature compensation while varying the sensitivity of either gage pair connected across the bridge voltage supply. It is to be noted that the gage pairs across the output terminals of the bridge are not susceptible to this type of sensitivity control. This method will work for either null-balance or unbalance measuring bridge arrangements.

	CIRCUIT	RELATIONSHIPS	APPLICATION AND COMMENTS
(a) SINGLE GAGE OR BRIDGE ARM	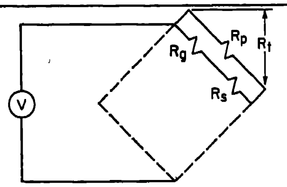	$\frac{R_s}{R_g}=\frac{1-\sqrt{n}}{\sqrt{n}}$ $\frac{R_p}{R_g}=\frac{1}{1-\sqrt{n}}$	1. For Null-Balance or Unbalance Measurement Applications. 2. Assuming $R_g = R_t$, $\frac{\Delta R_t}{R_t} = n\,\frac{\Delta R_g}{R_g}$ 3. Temperature compensation may be maintained through proper choice of material for R_s and R_p.
(b) TWO ADJACENT BRIDGE ARMS	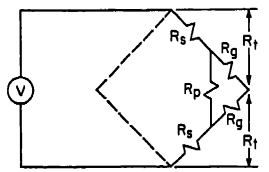	$\frac{R_s}{R_g}=1-n$ $\frac{R_p}{R_g}=\frac{2n}{1-n}$	1. For Null-Balance or Unbalance Measurement Applications. 2. Assuming $R_g = R_t$, $\frac{\Delta R_t}{R_t} = n\,\frac{\Delta R_g}{R_g}$ 3. Temperature compensation maintained. 4. Measuring instrument input impedance must be high.
(c) ENTIRE BRIDGE	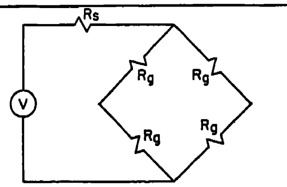	$\frac{R_s}{R_g}=\frac{1-n}{n}$	1. For Unbalance Measurement Applications. 2. Temperature Compensation maintained.

Fig. 8. Some common strain-gage sensitivity-control methods.

Four-Gage Desensitization. All four bridge arms are desensitized by a common amount (without, however, affecting the calibration sensitivity of the measuring instrument) in the circuit of Fig. 8(c). Temperature compensation is maintained if it existed prior to desensitization, and the method is applicable to any instrument in which the unbalance of the strain-gage bridge is measured. This method will not perform on a true null-balance system. It is to be noted, however, that instruments like the Baldwin strain indicator series are **reference-bridge null-balance systems** and therefore compare the measuring bridge output with a reference bridge within the instrument. This method of desensitization will function for instruments of that type.

APPLICATIONS OF COMPLETE BRIDGE DESENSITIZATION.

The resistor R_s shown in the circuit for "entire bridge" desensitization in Fig. 8(c), can be used for the following purposes:

1. Gage factor dial to maintain constant output from the bridge in terms of voltage per strain in a gage.

2. Modulus-temperature compensation: A resistor whose resistance increases with increasing temperature can, if properly designed, function to maintain the sensitivity of a transducer constant even though the modulus of elasticity of the transducer material decreases with increasing temperature.
3. Division: If the resistance R_s is a function of variable B, whereas the resistance of the strain gages in the bridge are a function of variable A, proper selection of R_s can result in a bridge output which is directly proportional to A/B.

BALANCING STRAIN-GAGE BRIDGES. Two types of measurement can be made with a Wheatstone bridge:

1. Unbalance measurement in which the strain-induced unbalance voltage at the bridge output is measured or recorded.
2. Null-balance measurement in which the strain-induced unbalance of the bridge is nullified by an artificially introduced resistance variation in the bridge network. The amount of variation necessary to bring the bridge back into balance after it has been subjected to a strain-induced unbalance is a measure of the strain.

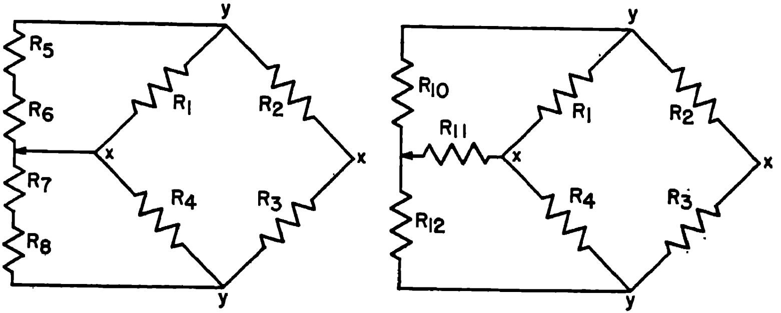

(a) Parallel Balancing Network "A" (b) Parallel Balancing Network "B"

Networks which may be used on a closed Bridge.

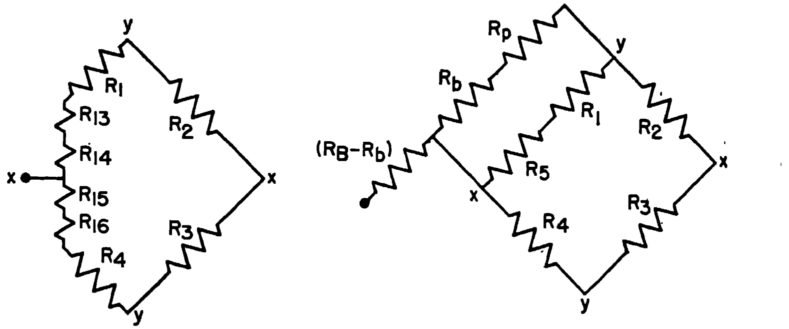

(c) Series Balancing Network (d) Single-Arm Balancing Network

Networks which form an integral part of the Bridge.

Fig. 9. Some bridge-balancing networks. (a) Parallel balancing network *A*. (b) Parallel balancing network *B*. (c) Series balancing network. (d) Single-arm balancing network. (a) and (b) networks can be used on a closed bridge. (c) and (d) networks form an integral part of the bridge.

Balancing networks, therefore, may serve one of two purposes: (1) to bring an initially unbalanced bridge either to zero output or to some reference output for subsequent use as an **unbalance-measuring system,** or (2) to serve as the **strain read-out system.**

Fig. 9 (a and b) shows two types of **parallel balancing networks** which act across two bridge arms and which may be connected to a "closed" bridge without breaking into individual bridge arms. Fig. 9(c) shows a **series balancing network** wherein the balancing network is placed entirely in series with two bridge arms. A balancing network composed of both series and parallel resistors, but acting only across one bridge arm, is shown in Fig. 9(d). Parallel balancing networks are the most popular in the United States because they can be connected to closed bridges.

Balancing networks always create some **error** in the readings of the gages to which they are connected. In many instances, these errors are small.

Operational Characteristics

EFFECTS OF TEMPERATURE. Numerous variables must be considered when a gage is to be attached to a test specimen and measurements are to be made. Environmental and operational conditions have a bearing on the selection of the gage, the instruments, and the bonding cements, and on the interpretation of the resulting data. For example, operating temperature has several disturbing effects.

Zero-Strain Temperature-Resistance Effects. Even though the mechanical strain were zero, the resistance of a mounted strain gage would vary with temperature as a composite result of:

1. The differential thermal expansion of the strain-gage material and the test specimen.
2. The resistance-temperature coefficient of the strain-gage material.
3. The gage factor.
4. The cement properties.

The exact prediction of this phenomenon is difficult. The **resistance-temperature coefficient of strain-sensitive materials** depends upon the strain level and upon the amount and kind of heat treating, cold working, and annealing. Even minor changes in alloy composition, cold working, and other conditions can profoundly influence the temperature behavior of strain gages made of the same alloy. One of the largest manufacturers of strain gages in the United States assigns **lot numbers** to the various melts and batches of wire used for strain-gage materials. Two gages, even though of the same type, size, and manufacturer, may not exhibit the same temperature characteristics unless the same lot number of wire or foil has been used in their manufacture.

Compensated Gages. Various attempts have been made to eliminate changes of resistance with temperature for completed gage installations. In one series, gages consist of two lengths of strain-sensitive material selected to match the **thermal expansion coefficient** of most common structural materials. This permits almost complete cancellation of various effects which would tend to produce resistance changes under fluctuating temperatures. A recent development for foil gages includes an **adjustable resistance in foil form** between the gage tabs which is mounted simultaneously with the strain gage. This resistance is then used in a bridge arm adjacent to that containing the strain gage and is adjusted to compensate for temperature-induced resistance changes of the strain-gage installation. Various other methods of temperature compensation are based on **thermocouples, or thermistors,** as parts of the strain-gage circuit. Gages incorporating thermocouples as parts of their construction are made in the United States. It must be noted that all methods devised so far to eliminate temperature-induced resistance changes of gage installations will function only over limited temperature ranges and with certain specific base materials.

Deterioration at Elevated Temperatures. At elevated temperatures, **selective oxidation** of certain constituents may occur in the strain-gage material. This simultaneously changes both the wire composition and its cross-section, and thus its resistance. The measuring instrument cannot separate temperature-created resistance changes in the gage from those resulting from strain. Consequently interpretation of data becomes impossible if temperature fluctuations occur during the experiment, unless some means exists for eliminating the effect of, or accounting for, such variations. Recent efforts have included attempts to devise an alloy in which the change in resistance of the wire, due to selective oxidation of one of its constituents, is counterbalanced by the change in resistance due to variation in cross-section of the wire during oxidation. Since the oxidation process also depends on the type of adhesive used with the gage, this approach has proven to be difficult, although encouraging results have been reported.

Effect of Temperature on Strain Sensitivity. The strain sensitivity of a wire or foil is temperature-dependent to some extent. There are almost no data existing on the variation of strain sensitivity with temperature, although such variations appear to be small. The **variation of gage factor with temperature,** however, has received considerable investigation, the conflicting results of which are often traceable to the choice of adhesives. Not only is the sensitivity-temperature variation of a strain gage dependent on the gage type, gage length, and adhesive but also on the curing cycle for the adhesive.

Magnitude of Temperature Variation. Many strain-gage materials undergo **metallurgical phase changes,** intergranular corrosion, oxidation, or other phenomena rendering them useless as strain-sensitive materials at high temperatures. These changes usually occur at fairly well-defined temperatures, but they are also time-dependent. Many of the **plastic resin adhesives** soften at elevated temperatures, whereas **ceramic cements** often exhibit inversion points.

Some gage manufacturers in the United States use solder to join the fine, strain-sensitive filament to the heavier lead wire protruding from the gage. Many English gages are welded so that **solder difficulties** are not encountered. The solder exhibits resistance-temperature characteristics of its own and has a softening and melting point at temperatures well below those at which the wire deteriorates. Although cases are on record where dynamic data have been obtained at temperatures at which the internal soldered joint in the gage must have melted, it is not desirable to operate at temperatures over 400° F. with gages that have internal solder joints.

Other limits on temperature excursion are posed by self-temperature-compensated strain gages, many of which are compensated only for a certain temperature region and which may behave in an unpredictable manner outside that region. The maximum temperature reached during a test is therefore an important variable in the selection of gage material, carriers, adhesives, lead wires, and solders.

Length of Time Temperature Is Applied. Creep at elevated temperature is also a property of the adhesive, although other time-temperature-dependent phenomena appear above 600° F. Most **phenolic and epoxy adhesives** slowly decompose at these temperatures. The rate of decomposition depends on the adhesive and its fabrication. Intergranular corrosion, depending both on time and temperature, makes **copper-nickel alloys** undesirable as strain-sensitive elements above 600° F. Still another strain-gage material undergoes time-dependent changes at about 900° F. At higher temperatures of perhaps 1200° F., strain-gage alloys may tend to oxidize. This changes their resistance because of changes in cross-sectional area and the changing resistivity due to the alteration of composition (oxidation is preferential). **Ceramic adhesives** exhibit inversion points within the 1200° F. temperature range, frequently leading to questionable data obtained with strain gages.

Number of Temperature Cycles Applied. Zero shift and hysteresis will be evidenced when a gage is first cycled from room temperature to some operating temperature (above or below room temperature) and then back to its original temperature. Prior to the taking of test data, a gage installation should be subjected to several cycles throughout the range of expected temperature variations during test. If a gage installation has been permitted to remain at room temperature and humidity conditions for long periods of time, it may have absorbed sufficient moisture to require additional temperature cycling before use.

Degree of Cure of Cement. The zero shift and hysteresis in temperature cycling is strongly influenced by the degree of cure of the cement. **Phenolic cements** shrink markedly during cure, thus inducing compressive stresses in the gage matrix. If the cement is not completely cured initially, the cure will continue when the gage installation is heated. Usually, the higher the temperature, the faster the continuation of the cure. Upwards of 200 hr. at operating temperature are often required to cure a phenolic installation. **Cellulose nitrate** exhibits similar characteristics, requiring 12 to 24 hr. at 140° F. to complete the cure. **Epoxy adhesives** do not shrink nearly so much as phenolics, since no solvents are eliminated. However, time at temperature, even under no mechanical strain, will affect the zero shift of a gage installation using epoxies on a smaller scale, unless the adhesive cure is complete.

EFFECTS OF MOISTURE. The strain gage, being an electrical device, is sensitive to humidity. The effect of humidity on the wire or foil gage is due to the **absorption of moisture** by the matrix and layer of adhesive. Most organic materials undergo changes in their mechanical or electrical properties to a greater or lesser extent with changes in humidity. Moisture can affect gages in several ways:

1. Moisture absorption by the matrix and adhesive can cause a reduction in resistance to ground.
2. The presence of moisture can cause electrolysis when a current is passed through the gage, and consequently can lead to corrosion of the gage filament.
3. The mechanical strength of the bond may be reduced by the absorption of moisture.

Gage-to-Ground Resistance Check. For room-temperature applications with plastic resins, the resistance between the gage filament and the test specimen to which it is attached (the so-called gage-to-ground resistance) serves as a handy criterion of the moisture content of the gage installation. Resistances of less than 50 megohms are not considered satisfactory for testing, whereas resistances of 10,000 megohms are considered standard for long-term strain measurements where creep is an important factor. With plastic resins the fact that current leaks through the adhesive layer is not so important as the cause which permits this leak. However, at elevated temperatures and with **ceramic cements,** the leakage itself becomes serious, since many ceramics actually become fairly good conductors at elevated temperatures (900° F. to 1200° F.).

Water Immersion of Gages. A gage can be immersed in water for long periods of time without showing any marked change of resistance, as long as no current is passed through it. In one test, gage factor and zero-strain resistance before and after the **weathering** were measured after the weathered gages had dried out in the laboratory. No calibration factor changed by more than 1 percent, and zero shifts ranged from none for the control gages through 5 to 7 μin. per in. for weathered and waterproofed gages, to 65 to 134 μin. per in. for weathered and unwaterproofed gages. The adhesive used was cellulose nitrate cement.

Electrolytic Corrosion. As soon as current is passed through a wet strain gage, however, resistance increases because of **electrolysis,** leading eventually to complete failure. While this increase in resistance is taking place, **bubbles** may be seen rising from some part of the gage winding. If, after such treatment, the gage is examined under a microscope, corroded patches can be observed on the gage wire. It is therefore clear that the increase in resistance is due to electrolytic corrosion of the gage wire.

Waterproofing of Gages. Numerous methods of waterproofing have been set forth in the literature. In general, **petroleum jelly** does a satisfactory job unless water flows past the gage and tends to remove the jelly or unless temperatures rise sufficiently to melt it. A **microcrystalline wax** also performs well. For long-term underwater operation with the possibility of applied pressure and high-velocity flow over the gage location, **epoxy compounds** have been used successfully, together with the artifice of embedding a layer of foil over the gage but under the waterproofing compound so that any leakage cannot take place directly through the compound. Suffice it to say that gage installations on the submerged portion of ships have continuously operated in excess of 18 months on test runs under severe conditions.

EFFECTS OF STRAIN. The relationship between mechanical strain and resistance change in a material is not necessarily linear and hysteresis-free. Most materials possess **nonlinear characteristics** above some minimum strain value. One copper-nickel alloy has been shown to be linear in resistance-strain characteristic up to 21 percent. Commercial gages are available which will surpass 12 percent strains. It can be shown that the strain sensitivity of materials in their plastic range is numerically equal to 2. Thus any material for which the strain sensitivity in the elastic state is other than 2 will show a break point in the resistance-strain curve when yielding is reached. Certain copper-nickel alloys which exhibit strain sensitivities close to 2 in the elastic range therefore exhibit constant strain sensitivity throughout their elastic and plastic range, making **high-strain-level gages** possible.

The adhesive and the carrier on which the strain-sensitive filament is wound also dictate the maximum strain which can be applied to a gage installation before nonlinearity occurs. **Cellulose nitrate cements,** for example, have been known to operate with paper gages up to 0.5 percent strains. Commercial post-yield gages operate up to above 12 percent strains. At −320° F., for gages on aluminum, **filled epoxies** subjected to elevated temperature post-cure are satisfactory strain-gage adhesives up to 1.2 percent; without post-cure, only up to

0.7 percent. **Phenolic resin** is useful to about 0.6 percent, and cellulose nitrates to about 0.5 percent.

Number of Strain Cycles. A strain gage, once attached to a test specimen, will exhibit considerable hysteresis and zero shift during the first few strain cycles. This phenomenon is attributed to the **relief of the residual stresses** remaining in the bond, which has been cured at temperatures and pressures other than ambient and which therefore contains a complex and large field of residual stress. The **amount of zero shift and hysteresis** depends on:

1. The degree of cure of the bond.
2. The gage length of the gage.
3. The number of strain cycles applied.
4. The direction of the preceding strain cycle.

A gage which has been strained in tension but never in compression will, for example, exhibit a larger zero shift on its first compressive strain cycle than it would if it had not been strained in tension first.

Since **epoxy adhesives** do not require pressure for bonding, well-cured gage installations with these resins have been known to exhibit no hysteresis or zero shift even after the first strain cycle. If a gage installation does not exhibit negligible zero shift after the first ten load cycles, the installation should be discarded.

Another problem related to the number of cycles to which a gage has been subjected is the aspect of the fatigue life of a strain gage. The **fatigue life of strain gages** is a function of various elements. For example:

1. Isoelastic wire exhibits about 62 times the endurance limit of a strain-sensitive grid made of copper-nickel alloy.
2. The average life of gages with the wrap-around construction is about twice that of the flat-grid type.
3. The "dual lead" construction available in some commercial gages increases fatigue life of gages at least 33 times.
4. Bakelite gages last longer, by a factor of 30 on the average, than comparable paper gages.

Cases have been reported where gage failure actually occurred in the bakelite bond between the gage and the specimen. In most of these cases, however, the joint between the fine, strain-sensitive wire and the heavier lead-out wire was responsible for **premature gage failure** due to fatigue. There is a lack of data on strain-gage performance at various strain levels up to large numbers of cycles. A **special gage construction** which brings the joint between the gage wire and the lead wire into a direction of low strain (making an angle with the major gage axis) has given no failures up to five million cycles of 1480 μin. per in. strain, and gages subjected to 600 μin. per in. alternating strain performed up to about ten million cycles.

Foil gages nearing failure in fatigue will often increase their resistance as a function of the number of strain cycles to which they have been exposed. Thus **large, unaccounted-for zero shifts** give warning of impending gage failure. Unfortunately the gage sensitivity may also increase during this near-failure period; thus care must be used when using foil gages in fatigue-producing environments. Wire gages, on the other hand, fail rather suddenly, although at a lower fatigue life.

When **large dynamic strains** are to be measured for large numbers of cycles (surpassing the capabilities of a strain gage in terms of fatigue life), it is common practice to mount a second strain gage at a lower-strain location near the first gage and to obtain an effective strain-ratio between the two gages during the lifetime of the first gage. The second gage, lasting longer than the first because it is exposed to lower strain levels, can then be used to obtain fairly good approximations of the high-level strains after the first gage has failed.

Rate of Application of Strain. Some gage materials are magnetic and thus susceptible to **magnetostrictive effects** which depend on the rate of change of strain rather than on actual strain magnitude. Since this effect is self-generating, one method of detecting its presence is to disconnect the supply voltage to the strain-gage circuit and to replace it with a **short circuit.** Any signals then observed at the circuit output during test are due either to the magnetostrictive effect or pick-up (magnetic or electrical).

Various opinions on the effect have been put forward. The magnetostrictive effect is important in impact studies, where the choice of the wrong gage can result in a signal composed both of strains and of rate of change of strain. **Spurious outputs** up to 3 m.v. from certain gages are attributed to this magnetostrictive effect.

The effect of rate of change of strain on the adhesive has not been treated to any great extent in the literature, although it is known that stress and strain are not necessarily in phase, giving rise to complex moduli of elasticity and definite frequency patterns of behavior for various adhesive properties.

Frequency of Strain Variation. The strain-sensitive filament of a strain gage will follow dynamic strain variations faithfully up to one of two limits. In one, the cement acts as a **damper** and attenuates strain signals above some minimum frequency. No information about this effect seems to be available. The other limit arises when the gage length of the gage becomes an appreciable percentage of the **wavelength of the vibration.** In the limit, an entire wavelength of even high-amplitude strains completely beneath a single gage length will register as zero strain on the gage (theoretically). The frequency figure determined by this criterion depends on the material, the temperature, the gage length, and the definition of "appreciable" insofar as an appreciable effect sets in.

When the wavelength of the strain vibration to be measured becomes less than about 20 times the gage length, some errors in reading are to be expected. For a ⅜-in. gage length, the **allowable wavelength** is then ⅜ × (20/12) = 0.625 ft. For steel in which the velocity of sound at room temperature is 16,800 f.p.s., the allowable frequency is roughly 16,800/0.625 = 27,000 c.p.s., approximately. It is to be noted that gages will respond to much higher frequencies, but just what the gage output signal really means, once such a limit is surpassed, is a moot point.

Length of Time Strain Is Applied. The behavior of a plastic material under load can be subdivided into two effects. The stress will tend to keep extending the material after the load has been applied (the **sliding of molecular chains,** one with respect to the other, and the breaking of bonds between chains are time-dependent phenomena). The other effect is the **continuance of the cure** of the material, frequently resulting in shrinkage stresses. Thus, depending on the magnitude of the applied load and the degree of cure, the plastic may exhibit creep in the same direction as the applied load or in the opposite direction.

These phenomena explain the violent discrepancies found in the literature on the subject of **strain-gage creep.** As the adhesive creeps according to the composite effects of load and of additional curing, the strain-sensitive wires embedded in the adhesive are subjected to strains dictated by the adhesive behavior.

Creep values as low as 0.1 to 0.6 μin. per in. per day have occurred as long as 25 days after test for paper-backed gages mounted with cellulose nitrate adhesive. It is known that:

1. Short gages creep more than long gages.
2. Wrap-around gages creep more than flat-grid gages.
3. Creep is accelerated at elevated temperatures.
4. Creep rate is roughly proportional to applied strain.

In terms of the stress distribution in the gage filament and in the adhesive, these phenomena are to be expected.

Since the pull in the gages is put in mainly from the ends of the gage loops, **close trimming** of a gage will result in increased creep; furthermore, foil gages (offering, as they do, considerable latitude of loop-end tab design) have been shown to creep less than wire gages.

EFFECTS OF STRESS FIELD. A strain gage, like most other types of transducers, exhibits major and minor **axes of sensitivity.** Gage factors as given by the gage manufacturer are usually determined with respect to the major axis, i.e., parallel to the wires in a flat-grid gage, and in a specified stress field. Thus gages made by one United States manufacturer are calibrated in a pure tensile field on a material with a Poisson ratio of 0.285.

Effect of Transverse Sensitivity. Almost all gages, therefore, will experience resistance changes which are functions both of the strain along the major and minor gage axes. It can be shown that the general expression for the **unit resistance change in a strain gage** may take the following form:

$$\frac{\Delta R}{R} = \frac{S_t}{1+K}(\varepsilon_x + K\varepsilon_y) \tag{21}$$

where ΔR = strain-induced resistance change in a gage of original resistance R.

ε = strain, with subscript x referring to the major gage axis and subscript y to the minor gage axis (perpendicular to the x-direction).

S_t = strain sensitivity of a straight, unbonded portion of the strain-sensitive filament in the gage.

K = transverse sensitivity coefficient.

The general expression for K is given by

$$K = \frac{\left(\dfrac{\Delta R/R}{\varepsilon_y}\right)_{\varepsilon_x=0}}{\left(\dfrac{\Delta R/R}{\varepsilon_x}\right)_{\varepsilon_y=0}} \tag{22}$$

For **flat-grid gages with semi-circular loops** at the ends, a theoretical analysis can be made to determine K as a function of the grid geometry; thus

$$K = \frac{\pi y/4}{x + (\pi y/4)} \tag{23}$$

Here y = the spacing between the parallel strands of the flat grid gage (equal to the diameter of the end loops).

x = the total length of straight wire associated with one loop (i.e., the total length of straight wire in the gage divided by the number of loops).

Correction for Transverse Sensitivity. For the cases where the gage factor S_m of a gage and the Poisson ratio μ_m of the material, on which the manufacturer calibrates his gages, are known, the unit resistance change of the gage in any other stress field can be computed. Let

$$a = \frac{\varepsilon_y}{\varepsilon_x} \tag{24}$$

for the stress field in which the gage is located and at the point of gage location. Then, if a given $\Delta R/R$ of the gage is measured, the strain ε_x is given by

$$\varepsilon_x = \frac{\Delta R/R}{S_m}\left(\frac{1-\mu_m K}{1+aK}\right) \tag{25}$$

This relationship indicates that the correction factor

$$\phi = \frac{1-\mu_m K}{1+aK} \tag{26}$$

must be used to account for the **transverse sensitivity** of a strain gage. In general this correction factor is negligible, not surpassing 3 percent in most cases. The correction factor will be largest in those cases where strains are usually small.

Determination of Poisson Ratio. One instance where serious errors can be made if the transverse effect of a gage is neglected is in the determination of the Poisson ratio of a material when using strain gages. Assume that the approximate value of the Poisson ratio is known to be 0.3. For the gage located along the major axis of the test specimen, $a_x = -0.3$; for the gage located along the minor axis of the test specimen, $a_y = -(1/0.3) = -3.33$. Assuming that the gages are of the type where $\mu_m = 0.285$ and $K = 0.035$, the **correction factor for the axial gage** will be

$$\phi = \frac{1-\mu_m K}{1+a_x K} = \frac{1-(0.285 \times 0.035)}{1-(0.3 \times 0.035)} \cong 1 \tag{27}$$

For the **transverse gage perpendicular to the axial gage,** the correction factor is

$$\phi = \frac{1-\mu_m K}{1+a_y K} = \frac{1-(0.285 \times 0.035)}{1-(3.33 \times 0.035)} = 1.12 \tag{28}$$

It is thus seen that the determination of Poisson's ratio for the material, by taking simply the ratios of two strain-gage readings, would have been in error by 12 percent had the transverse sensitivity of the gages been neglected.

The Stress Gage. The stress gage is an example of a special grid configuration which utilizes both the properties of the material on which the gage is to be mounted and those of the flat-grid gage. If the transverse sensitivity coefficient K of the gage is made equal to the Poisson ratio of the base material, μ, the unit resistance change in the gage will be proportional to the stress along the major gage axis, independently of the stresses or strains existing at right angles to this axis. Grid configurations can be designed for which the transverse sensitivity coefficient can be made to equal any given value, and in particular made to equal the Poisson ratio of a material to which the gage is to be attached. Such gages have been made commercially.

Measurement of Principal Stress. If it is desired to measure a principal stress, conditions of symmetry about the principal stress axis will permit the use of a single ordinary strain gage inclined at the proper angle θ to the principal stress axis. It is also possible to utilize two gages mounted at right angles to each other in a special circuit, as shown in Fig. 10, to obtain electrical signals proportional to the normal stresses along the two gage axes.

Effect of Hydrostatic Pressure. The gage factor of strain gage is a pressure-dependent quantity, although it would be more correct to say that there also exists a **pressure coefficient of resistivity** for wires and foils. This coefficient is small and negligible until pressures exceed 10,000 p.s.i. The literature is not in agreement as to the magnitude of the effect. In general it appears that foil gages are less pressure-sensitive than wire gages, varying between ½ and 3½ μin. per in. per 1000 p.s.i. Wire gages are reported as varying between 2 and 8 μin. per in. per 1000 p.s.i. for flat-grid paper gages and for bakelite gages. Wrap-around paper gages seem to show 160 to 300 μin. per in. per 1000-p.s.i. pressure sensitivity. These results are for copper-nickel gages. Other materials possess different sensitivities.

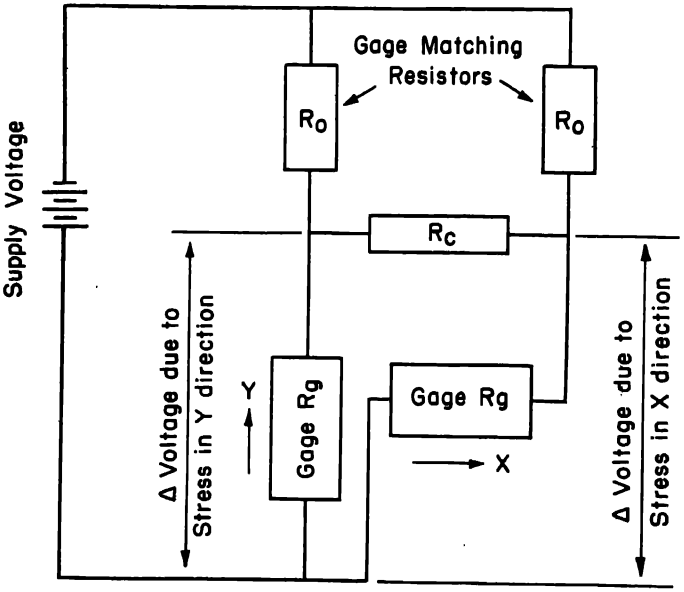
Gage Matching Resistors
R_o
R_o
Supply Voltage
R_c
Δ Voltage due to Stress in Y direction
Y
Gage Rg
Gage Rg
X
Δ Voltage due to Stress in X direction

Fig. 10. Circuit for conversion of T-strain-gage rosette into two equivalent stress-gage circuits.

Effect of Gage Stiffness and Rigidity. When conventional strain gages are bonded to the surface of materials which have a very low modulus of elasticity, the **local stiffening effect of the gage** may be of great importance. Not only is the recorded strain less than the value of strain which would exist if the gage were not present, but the distribution of strain in the materials is also altered. These effects are usually negligible in metals, even in the thinner structural items. It is estimated that the **force exerted by a gage** is about 6½ lb. when strained to ½ percent. With two paper gages, one on each side of a strip of material, this effect can be shown to be about 1 percent on strain readings in an aluminum strip 1/16 in. thick by ⅜ in. wide, 22 percent for a plastic of the same size, and up to 555 percent for 1 × ⅜-in. rubber of 1000-p.s.i. modulus of elasticity.

ELECTRICAL EFFECTS. The **permissible current** in a gage has an upper and a lower limit. The upper limit is attained when the self-heating of the gage reaches proportions where the gage factor decreases or the gage burns out.

The lower limit is governed by the **noise level** in the strain-gage circuit, since it is naturally desired that the strain-induced electric output from the circuit be larger than the quantities (such as thermocouple voltages) which are not related to strain. Another lower limit on the gage current is the **sensitivity of the measuring instrument.**

Thermoelectric Potentials. Thermoelectric potentials are generated when two junctions between unlike materials are exposed to different temperatures. These parasitic signals manifest themselves only when d.-c. instrumentation is used. **Carrier-frequency a.-c. systems** are not subject to the effects of thermocouple potentials. One simple means of estimating the effect of thermoelectric potentials in a d.-c. circuit is to disconnect the supply battery from the circuit and to short-circuit the terminals to which it was connected. Any signals emanating from the circuit must then be due to thermoelectric potentials (provided that magnetostrictive and slip-ring potentials are absent). The zero setting of the instrumentation may then be adjusted to account for these stray voltages. If such an adjustment is made periodically, d.-c. instrumentation may be used with surety. It will also be remembered that thermoelectric potentials can be so designed as to offset the resistance-temperature characteristics of the strain gages. Gages of this type are fabricated with **built-in thermocouples.**

Maximum Gage Current. The upper limit on current magnitude flowing through the gage is determined by the heat-dissipating ability of the gage and of the material to which the gage is attached. The heat-dissipating ability of the gage depends on the gage material, the filament spacing, etc. A bobbin-type gage will reach the same temperature as a flat-grid gage of comparable size, even though it carries only one-fifth of the current that the flat-grid gage carries. Likewise, high-resistivity wire cannot carry as high a current as low-resistivity wire.

Foil gages are better able to dissipate heat to the structure to which they are attached, and gage currents up to 0.5 amp. have been used. Normal **wire gages** are restricted to 10 to 20 ma. for long-term studies and 30 to 50 ma. for short-term experiments where high output from the gage circuit is necessary. These current ratings must be dropped drastically for work on materials such as plastics, which do not carry heat away from the gage location. It is also dangerous to use a **single dummy gage,** through which current passes continuously, with a large number of active gages which are energized only periodically. The effect of continuous heating of the dummy gage is particularly severe if the dummy gage is mounted on a piece of material which is small compared with the thermal mass to which the active gages are attached, or if it is mounted on a poor heat conductor such as a plastic.

Lead Wires Used from the Gages. The type of lead wire used to join the gage to the remainder of the electric circuit has a profound influence on the readings obtained from the gage. Primarily the resistance of the wire in series with the gage and the variation of this resistance with temperature are critical. **Resistances in series with the gage** decrease the effective gage factor by the approximate ratio of the series resistance to the gage resistance. Changes in lead-wire resistance due to temperature cannot be separated by the measuring instrument from strain-induced resistance changes in the gage; therefore spurious readings result. There is considerable advantage in locating series resistances, such as lead resistance, in series with a closed bridge rather than with a single gage. This same analysis will hold for switching and slip-ring resistances.

For **direct-current instrumentation,** lead wires may be chosen so as to eliminate thermocouple effects or chosen so as to create definite thermocouple effects to counterbalance other temperature-dependent phenomena. For applications where self-temperature-compensated strain gages are used, a three-wire circuit must be used to eliminate errors introduced by **lead-wire resistance variations due to temperature,** which can be of the order of 10 μin. per in. per °F. per ohm of conductor (for copper wire).

Measuring Lead Resistance. If it is found desirable to measure the lead resistance in order to make corrections for temperature effects, the following scheme can be used: Connect two lead wires which pass through identical temperature environments to one gage terminal. At the measuring instrument. periodic measurements of the resistance variations of this loop of wire will yield the desired results. A regular strain indicator can be adapted to read directly the lead resistance and its variation with temperature. This method may be used when lead wires other than copper are used (i.e., wires with much higher resistivity) and where temperature effects are appreciable even for closed bridges.

Leads to High-Temperature Gages. Because of the difficulty of welding to copper wires or foil, it is frequently necessary to bring noncopper lead wires or foils from the gages to some point at which the temperature permits joining these to copper wires by means of some type of solder. Thus **Constantan ribbon** may be used from Constantan high-temperature foil gages, even though it is known that the gage sensitivity will be decreased and that resistance-temperature effects in the lead wires may be annoying. Frequently **special cabling,** designed to withstand the temperatures and abrasion environments encountered, must be made to order for high-temperature gage or transducer applications. It is good practice to build one or two sets of **thermocouple wires** into such special cabling in order to monitor gage temperatures.

Shielding of Lead Wires. Lead wires should be twisted to avoid magnetic pick-up, and should be shielded to avoid electrical noise. Leads should not be allowed to be stressed (as by swinging freely from great heights, such as cranes), or the **stress-induced resistance change** in the lead wires will superimpose its effect on that in the strain gage.

In a.-c. systems, where the supply to the strain-gage bridge and the bridge output are carried in a single four-conductor shielded cable, and where long lengths of such cable are used (say over 20 ft.), the **rotation of the wires** within the sheath must be correct. It will be found that bridge balance for amplitude as well as for phase can be achieved only when a certain pair of the four wires is used to excite the bridge (or to carry the output). It is frequently simplest to determine the proper arrangement experimentally. Even with high-temperature strain gages, harness and lead-wire problems are becoming as critical as the strain gage itself.

Switches or Slip-Rings in the Gage Circuit. Both switches and slip-rings offer a constant resistance to the passage of current through them and constitute a variable resistance superimposed on the constant one. The **variable resistance** may be a function of the age of the switch, the manner in which it makes contact each time it is thrown, the speed of the slip-rings, the brush pressure, slip-ring wear, etc. It is preferable to locate switches and slip-rings in series with a completed bridge rather than in series with a single gage. That this arrangement is not always possible or economical goes without saying, and good results have been reported with strain gages up to 90,000-r.p.m. rotational speed.

Commonly, a **coin-silver slip-ring,** rotating with the test specimen, makes contact with a **silver-graphite brush** which is held against the ring either by means of mechanical springs or by air pressure. This provides electrical continuity for signals to pass to and from strain gages on the rotating member. In addition to the slip-ring, **noncontacting inductive means** have been used to transfer signals from rotating members. **Mercury slip-rings** have been used successfully even for shaft-to-shaft coupling.

Strain-Gage Tests on Large Structures

INDUSTRIAL APPLICATIONS. Experimental stress analysis on large structures by means of strain measurements with bonded-wire resistance strain gages can be described as one form of nondestructive testing. However, it is often not included in this category, primarily because of the different fields of interest and activity between the stress analyst and the engineer engaged in nondestructive detection of discontinuities in structural or other materials. The stress analyst is usually concerned with design of structures and strength of materials, whereas the nondestructive test engineer is normally interested in locating hidden discontinuities in the material or in some form of nondestructive measurement such as thickness measurement from one side. Separate technical societies have evolved for each field, and there is relatively little exchange of information between these two groups.

Design Improvements. Many significant improvements since 1940 in the design of bridges, ships, airframes and aircraft engines, automobiles, and similar machines were aided by use of bonded-wire resistance strain gages. Their application has largely eliminated former methods, has simplified structures, and has enabled design engineers to make large **savings in weight and in material cost.** Large industrial organizations have engineering specialists in this field who use strain gages as an essential tool in the design and development of their products. Hundreds of engineers in this category have developed techniques and instrumentation for solving their particular strain-measurement problems, and have found the application of the wire-resistance strain gage almost unlimited. Complicated instrumentation for measuring and recording both static and dynamic loads has been developed, particularly in the aircraft industry.

Off-Shore Drilling Barges. Smaller organizations and those engaged in activities other than manufacturing have not utilized strain gages so extensively because of limited engineering manpower or lack of knowledge of the applications, techniques, and possibilities of this equipment. For example, the technique is valuable to engineers concerned with the design of large structures, such as **oil-well drilling equipment** and off-shore drilling barges. As oil wells become deeper, and the new off-shore drilling techniques and equipment are developed, the factors of weight, equipment reliability, and safety become vital, particularly in the off-shore drilling programs. Drilling barges offer stress problems never before encountered and therefore require every design tool available in order to serve the unusual dual function of a floating barge with a heavy superstructure mounted high above pontoons (up to 100 ft.) and a solid drilling platform resting on the ocean bottom.

TEST EQUIPMENT. Strain measurements with bonded-wire resistance strain gages are based on the fact that electrical resistance of a wire varies with the tension (or compression) to which it is subjected. This basic principle has been known since about 1856, a result of Lord Kelvin's experiments. It was later confirmed by Bridgeman in 1923, but little use was made of it until after 1930. In 1938 Simmons and Ruge, working independently, applied the principle by using a fine wire bonded directly to the structure under test. The present application, popularity, and knowledge of today's strain gage is largely a result of Tatnall's activity in this field for the past 15 years.

Standard Strain Gages. Strain gages consist of about a 5-in length of Constantan or isoelastic wire 0.001 in. in diameter, looped in the form of a grid, and cemented to a thin paper base about the size of a postage stamp. The relationship between change in gage resistance and change in gage length is defined as **gage factor** and is marked on each package of gages. Gage factor can be defined as follows:

$$\text{G.F.} = \frac{\Delta R/R}{\Delta L/L} \tag{29}$$

where G.F. = gage factor.
R = initial resistance of gage.
L = initial length of gage.
ΔR = change in resistance of gage.
ΔL = change in length of gage.

Here gage factor is known, R is known, and ΔR can be measured; therefore the total strain ΔL, or unit strain $\Delta L/L$, can be found. The ΔR measurement can be made with a simple Wheatstone bridge circuit and galvanometer. However, commercially available instrumentation for strain measurement is much more satisfactory and is recommended for field work. Gage factor is set on the proper dial, and strain is read directly in millionths of an inch per inch of length (hereinafter referred to as microinches per inch, μin./in.). Unit stresses up to the proportional limit can then be calculated from Hooke's law as

$$E = \frac{\text{stress}}{\text{strain}} \tag{30}$$

if Young's modulus of elasticity, E, is known.

Special Strain Gages. There are numerous sizes, types, and classifications of bonded-wire strain gages, each designed for its specific application, whether it be high temperatures (up to 1500° F., with special wire alloys and techniques), extremely small size (1/16-in. gage length), or various other special problems. Gages are available on standard paper backing, bakelite backing, or on a special thin paper base that permits rapid evaporation of the solvent. Recently, etched-foil gages have been developed. This type offers the advantages of proximity to the surface and large cross-sections at the ends to minimize the effect of transverse strains.

For the testing of structures, **thin paper-base gages** are recommended. These gages do not require clamping during the drying period and are particularly easy to install. Such ease of installation is essential for outdoor testing on large structures.

Rosette Gages. If the direction of stress is not known, a rosette gage should be used in order to determine direction and magnitude of maximum and minimum principal stress. Rosette gages consist of three strain elements placed at 0-, 45- and 90-deg. angles (rectangular rosettes), or three strain elements arranged in the form of a delta (delta rosettes). Equations for calculating **maximum and minimum stresses** and angles, when using rectangular rosettes, are

$$S_{\text{max.}} = \frac{E}{2}\left\{\frac{\varepsilon_L + \varepsilon_T}{1-\mu} + \frac{1}{1+\mu}\sqrt{(\varepsilon_L - \varepsilon_T)^2 + [2\varepsilon_{45^\circ} - (\varepsilon_L + \epsilon_T)]^2}\right\} \tag{31}$$

$$S_{\text{min.}} = \frac{E}{2}\left\{\frac{\varepsilon_L + \varepsilon_T}{1-\mu} - \frac{1}{1+\mu}\sqrt{(\varepsilon_L - \varepsilon_T)^2 + [2\varepsilon_{45^\circ} - (\varepsilon_L + \epsilon_T)]^2}\right\} \tag{32}$$

$$\phi = \frac{1}{2}\tan^{-1}\left[\frac{2\varepsilon_{45^\circ} - (\varepsilon_L + \epsilon_T)}{\varepsilon_L - \varepsilon_T}\right] \tag{33}$$

where $S_{\text{max.}}$ = magnitude of maximum principal stress.
$S_{\text{min.}}$ = magnitude of minimum principal stress.
ε_L = strain readings on longitudinal gage (parallel to longitudinal axis of test cylinder).
ε_T = strain readings on transverse gages (right angles to longitudinal axis of test cylinder).
ε_{45° = strain readings on gage whose axis is 45 deg. to longitudinal axis.
μ = Poisson's ratio.
E = Young's modulus of elasticity.
ϕ = direction of maximum principal stress, measured counterclockwise from ε_L gage. Plus sign indicates counterclockwise; minus sign indicates clockwise.

A rosette strain gage can be oriented in any manner, and by suitable calculations the angle and amplitude of maximum and minimum stresses can be determined. The theory involved is described in the literature (see Bibliography at the end of this section).

Instrumentation. Complicated instrumentation systems, including multi-channel oscillographs and oscilloscopes for dynamic measurements, and multi-channel recording systems, are available. However, in most cases, tests on large structures are made under **static load conditions** and only relatively simple instrumentation is required. Multi-channel switching units (40 or 60 channels) and a suitable static-strain indicator reading directly in microinches per inch are satisfactory unless stress data involving impact loads, effect of wave motion, or similar phenomena are desired.

INSTALLATION OF GAGES. If accurate and dependable results are to be obtained, gages must be carefully installed and insulated, and lead-wires must be firmly soldered. Careful consideration should be given to location of the various gages, and the installation must be planned for the maximum possible data that can be obtained within practical installation limits. If stresses are known to be uni-axial and their direction is also known, single-element gages can be installed along this axis. If stresses are uni-axial but **bending** is possible, as in a pipe-support column, two gages should be installed, one on each side of the pipe in the bending plane. When **bi-axial stresses** are expected, three-element rosette gages should be installed. Preliminary strain-sensitive coating tests can be used to determine stress concentration points and direction of maximum stress (see section on Brittle-Coating Tests). Gages can then be installed at these locations. Brittle-coating tests may be impractical on large outdoor structures, particularly when there are appreciable variations of temperature and humidity or rainfall during the drying and test period. In these cases, photoelastic-coating tests may be applicable. (See section on Photoelastic-Coating Tests.)

Preparing the Surface. The surface to which the gage is applied must be smooth and even but not highly polished. All **loose scale and rust** must be removed from metal surfaces. If the surface is pitted or uneven, **grinding** may be necessary. A power-driven disc sander is preferred. If the surface is very smooth or polished (which is not likely in structural testing), it is desirable to roughen it with 180-grit emery paper. If sand-blasting equipment is available, a light **sand blast** will provide an excellent surface.

Cleaning. After the surface is prepared, it must be absolutely clean before the gage is cemented into place. An area at least 3 in. in diameter should be thoroughly cleaned with a clean cotton swab dipped in **clean solvent** such as acetone or carbon tetrachloride. The surface should be scrubbed with successive cotton swabs, at least four or five per location. The final swab should show absolutely no trace of color or dirt. Extreme cleanliness is essential if the cement bond is to be satisfactory.

Cementing. Recommended cementing technique for the thin paper-base gages is as follows:

First, a thin **precoat of cement** should be applied and allowed to dry 10 to 15 min. The dry coat should not be over 0.001 in. in thickness and almost invisible to the unaided eye. (A precoat is absolutely necessary only on smooth surfaces such as polished steel or aluminum.) A liberal coat of **strain-gage cement** or Duco household cement should be applied over the precoat; the gage is immediately placed in the proper position and held in place for 30 to 40 sec. The gage will then lie in place without further pressure. It should not be rubbed or moved the first few seconds after it is put into place, since wires can be damaged easily while the paper is in the softened condition. The back of the gage should be clean and free from finger marks before it is applied.

Drying. Gages should be dry and ready for use within 5 or 6 hr. under normal conditions. If the humidity is high or the temperature low, drying will be much slower, and **application of heat** by a hot-air "hair dryer" or by infrared lamps is recommended. The **drying temperature** should not exceed 180° F. to 190° F., and heat should be applied gradually. If the drying gages are to be exposed to possible rain or high overnight humidity, they should be protected with a small canvas "tent" or similar cover.

If standard gages are used rather than the thin, paper-base gages recommended, it will be necessary to apply a 1-lb. weight or **clamping force** for approximately 1 hr. About 24 hr. will be necessary for drying these gages.

INSTALLATION OF LEAD WIRES. Strain-gage installations on large outdoor structures may require lead-wire lengths of perhaps 50 ft. or more between the gages and a central instrument and switch-unit location. In such cases, lead resistance is an appreciable percentage of gage resistance R shown in Eq. 29. Therefore the **gage factor** will be reduced below the stated value by the percentage amount equal to total lead resistance (to and from gage) divided by the specified gage resistance. The corrected value should be used for the instrument gage-factor dial. In general, size 14, 18, or 20 **solid copper conductor wires** are recommended. Stranded wire should not be used unless all strands are soldered securely, since a loose strand will introduce a small resistance change that will be indicated as a change in gage resistance due to strain. If clearance or other factors prohibit large lead wires near the gage, a short section of size 22 or 24 Teflon wire can be used between the gage and a convenient anchorage point.

Anchoring Lead Wires. A means of anchoring heavy leads in a position near the strain gage is essential if the installation is to be even semi-permanent. Small

rods or clamps may be welded to the structure about 3 in. from gage leads. Wires can be anchored at this point, leaving a short **pig-tail** for connection to the gage. Lead wires from each gage location should then be cabled together and run to the test station location. A common practice is to connect one side of each gage to a **common wire.** In this way, only one long lead from each gage is necessary, plus one common wire from all gages. All lead wires should be labeled with the gage number. Small adhesive tape numbers, available in most electrical or radio-supply houses, provide a very convenient means of designation.

Capacitance Balancing. Most commercial strain indicators use a.-c. bridge excitation for reliability and "ruggedness." If leads are over 50 ft. in length and the distances to active and compensating gages are not equal, the capacitance effect of the leads may be so great that **sensitivity** is greatly reduced or, in extreme cases, that the bridge cannot be balanced at all. (In a typical strain indicator, a reduction of sensitivity is indicated when a few degrees rotation of the balance dial does not result in a comparable strain reading on the balance meter.) When this occurs, the **capacitance effect** should be neutralized by placing capacitance in parallel with one of the bridge arms until phase balance is obtained. The proper bridge arm and capacitance value are best obtained by trial and error, using a capacitor decade box of perhaps 0 to 5000 μμf. or a continuously variable capacitor.

TESTING GAGES. All gages should be tested for leakage resistance to ground, proper resistance, and open circuits before the lead wires are attached. Since the gages operate on low voltage and thus need very little insulation, they should never be tested with an insulation tester that has an output of more than 22 volts. A vacuum-tube voltmeter that can measure ohmic resistance up to 1000 megohms is recommended.

Drying of the cement will be indicated by an increase in **leakage resistance** between the gage leads and the metal underneath. When completely dry, leakage resistance to ground should be on the order of 1000 megohms. If leakage is less than 50 megohms, the gage is unreliable, and unless the leakage is due to moisture that can be removed by heating, the gage should be replaced or eliminated.

Gage resistance should be within about 1 percent of the value designated on the package. If resistance exceeds this percentage, or if the gage has an open circuit, it has been damaged and should be replaced.

After resistance tests are complete, lead wires are attached and soldered securely. Gages can then be tested for **air pockets** or **imperfect bond** by connecting to a sensitive strain indicator, balancing the bridge, and gently pressing (about 1 lb.) the gage at various points with a finger or the eraser of a lead pencil. If the bond is satisfactory, the pressure will result in a few microinches-per-inch change which will disappear when pressure is removed. If the indicator becomes "jittery" or does not return to zero, the gage is probably imperfectly bonded or damaged and should be eliminated or replaced.

MOISTURE PROOFING. After the preceding tests have been completed, each gage should be moisture-proofed, unless strain measurements will be confined to a few hours on a bright, sunny day. **Rain or high humidity** can easily lower leakage resistance between leads (or to ground) to perhaps 0.1 megohm or less. This will result in serious errors if the gage is not waterproofed. For example, a change in leakage from 1000 megohms to 0.1 megohm would be indicated as a compressive strain of approximately 580 μin. (about 17,400 p.s.i. in steel) when using a 120-ohm gage with a 2.04 gage factor. In addition to changing resistance, moisture affects the dimensions of the bonding medium, which in turn results in apparent strains in the gage filament.

The simplest moisture-proofing consists of coating the gage and adjacent lead wires with **grease, petroleum jelly,** or one of the **silicone protective compounds.** This technique is excellent for rapid application and convenience, but it is definitely temporary, since the coating can easily be rubbed off. Some **microcrystalline wax coatings** are excellent for installations that are subject to rain or high humidity, but these cannot withstand mechanical damage or temperatures over 150° F. These should be melted in a ladle or other container (melting point 170° F.) and painted over the gage and lead wires. For best adhesion the gage and surrounding structure should be heated to about 150° F. The wax should cover an area extending at least several inches beyond the gage. Solder connections to the lead wires should also be coated, pushed down into the surrounding wax, and the complete assembly given a final coat.

Neoprene coating or synthetic rubber compounds are excellent for permanent installations that will be subject to mechanical abrasion or long periods of immersion. Directions for applying these coatings are supplied by the manufacturer or are available in the literature.

STRAIN MEASUREMENTS. After gages have been tested, waterproofed, and instruments checked, actual strain readings can be made. The method of loading, load intervals, and best time for the tests must be established, and suitable **data sheets** should be prepared. In some cases it may be preferable to conduct **tests at night,** since temperatures will normally be relatively constant. A complete set of **zero readings,** i.e., balance points between each measuring gage and the temperature-compensating gage under no-load conditions, should be taken immediately before actual load tests. If at all possible, load should be removed midway or at the end of the load cycle, and zero readings should be repeated again. Measured strains under the various load conditions will be the difference between load measurements and zero load. If readings return to the original no-load values (within a few microinches), the strain gages and instrumentation are all operating satisfactorily.

Of course, if there is **yielding in the structure,** readings cannot be expected to return to zero. All gage readings should be carefully observed during the load increments, and approximate calculations should be made to determine the stresses present. If values are approaching the yield point, load should be immediately removed, zero repeated, and a decision made as to future action. For example, if stresses are being measured in a steel drilling-barge structure where the yield point is 35,000 p.s.i., and Young's modulus is 30×10^6 p.s.i., loading should be discontinued when strain measurements approach 1000 μin. per in. ($30 \times 10^6 \times 1000 \times 10^{-6} = 30{,}000$ p.s.i.).

Residual Stresses. It should be emphasized that all strain readings obtained are the differences between the so-called no-load conditions and the various test loads. The gages do not measure residual or other stresses that may be present in the structure at the time they are cemented in place, unless such stresses can be removed. If **prestressing** is suspected, its magnitude can be determined by removing a **trepan plug** containing a gage and by measuring the change in strain readings from those obtained in the installed position on the structure.

Temperature Effects. If there is a definite change in zero readings at the end of the test, and such change cannot be attributed to yielding of the structure, moisture, gage slippage, or instrumentation difficulties, it is apparent that the

STRAIN-GAGE READINGS
(in μin. per in.)

TEST NO. ____

Instrument: Baldwin SR-4 Type L
Date: February 9, ____

Switch Position No.	Lead No.	Gage No.	Gage Factor	Time 3:00 P.M. Zero Load Rng.-Slctr.-Dial	Test Load in Thousands of Pounds: Time 3:15 P.M. 650 Rng.-Slctr.-Dial	Time 3:30 P.M. 800 Rng.-Slctr.-Dial	Time 3:45 P.M. 900 Rng.-Slctr.-Dial	Time 4:00 P.M. Zero Check Rng.-Slctr.-Dial
1	1 L	1 Rosette	2.03	0–12–1010	0–12–1165	0–12–1200	0–12–1230	0–12–1015
2	2 T	1 Rosette	2.03	0–10–0045	0–10–0195	0–10–0230	0–10–0260	0–10–0045
3	3–45°	1 Rosette	2.03	0–10–0820	0–10–0960	0–10–0995	0–10–1020	0–10–0820
4	4 L	2 Rosette	2.03	0–10–1310	0–10–0695	0–10–0585	0–10–0500	0–10–1340
5	5 T	2 Rosette	2.03	0–12–0625	0–12–0360	0–12–0315	0–12–0285	0–12–0650
6	6–45°	2 Rosette	2.03	0–10–0405	0– 8–1965	0– 8–1885	0– 8–1830	0–10–0425
7	7 L	3 Rosette	2.03	0–10–0370	0–10–0240	0–10–0220	0–10–0200	0–10–0375
8	8 T	3 Rosette	2.03	0–10–0165	0–10–0005	0– 8–1975	0– 8–1950	0–10–0160
9	9–45°	3 Rosette	2.03	0–10–0235	0–10–0090	0–10–0060	0–10–0045	0–10–0235
10	10	4 Linear	1.97	0– 5–0590	0– 5–0340	0– 5–0290	0– 5–0260	0– 5–0580
11	11 L	5 Rosette	2.03	0– 2–1210	0– 2–1525	0– 2–1585	0– 2–1615	0– 2–1195
12	12 T	5 Rosette	2.03	0– 4–0435	0– 4–0685	0– 4–0735	0– 4–0760	0– 4–0435
13	13–45°	5 Rosette	2.03	0– 4–0380	0– 4–0625	0– 4–0675	0– 4–0695	0– 4–0375
14	14 T	6 Rosette	1.97	0– 0–0570	0– 0–0480	0– 0–0465	0– 0–0460	0– 0–0570
15	15 L	6 Rosette	1.97	0– 3–1185	0– 3–1090	0– 3–1070	0– 3–1060	0– 3–1185
16	16–45°	6 Rosette	1.97	0– 1–0790	0– 1–0645	0– 1–0610	0– 1–0595	0– 1–0800
17	17 L	7 Rosette	1.99	0– 6–1100	0– 6–1120	0– 6–1120	0– 6–1120	0– 6–1095
18	18 T	7 Rosette	1.99	0– 6–1120	0– 6–0925	0– 6–0880	0– 6–0845	0– 6–1110
19	19–45°	7 Rosette	1.99	0– 7–1185	0– 7–1095	0– 7–1070	0– 7–1055	0– 7–1170
20	20	8 Linear	1.99	0– 9–0535	0–10–0345	0–10–0445	0–10–0480	0– 9–0535
21	21	9 Linear	1.97	0– 7–0825	0– 7–0970	0– 7–1000	0– 7–1050	0– 7–0835
22	22	10 Linear	1.92	0–10–1390	0–10–1520	0–10–1550	0–10–1565	0–10–1400
23	23	11 Linear	1.92	0–10–0535	0–10–0555	0–10–0560	0–10–0575	0–10–0530

Engineering Test Services, Inc.

Fig. 11. Typical strain-gage work sheet.

TEST LOAD
(In thousands of pounds)

Gage No.	650	800	900
1 Rosette	+155	+190	+220
1 Rosette	+150	+185	+215
1 Rosette	+140	+175	+200
2 Rosette	−615	−725	−810
2 Rosette	−265	−310	−340
2 Rosette	−440	−520	−575
3 Rosette	−130	−150	−170
3 Rosette	−160	−190	−215
3 Rosette	−145	−175	−190
4 Linear	−250	−300	−330
5 Rosette	+315	+375	+405
5 Rosette	+250	+300	+325
5 Rosette	+245	+295	+315
6 Rosette	− 90	−105	−110
6 Rosette	− 95	−115	−125
6 Rosette	−145	−180	−195
7 Rosette	+ 20	+ 20	+ 20
7 Rosette	−195	−240	−275
7 Rosette	− 90	−115	−130
8 Linear	+810	+910	+945
9 Linear	+145	+175	+225
10 Linear	+130	+160	+175
11 Linear	+ 20	+ 25	+ 40

Note: Zero at 3:00 P.M. used for calculation of these strains. (+) indicates tension; (−) indicates compression. Strains calculated by adding range-switch reading (thousands constant) attached to instrument, selector switch (thousands), and dial readings, as follows:

	Zero	650,000 lb.
Range	00,000	00,000
Selector	12,000	12,000
Dial	1,010	1,165
Total	13,010	13,165

Strain reading = gage reading − zero reading = 13,165 − 13,010 = +155 μin.

Engineering Test Services, Inc.

Fig. 12. Strain computed from readings in Fig. 11 (μin. per in.).

change is a result of temperature differences between the measuring and temperature-compensating gages. This is a frequent occurrence when daylight tests are made on large outdoor structures, since portions of the structure and its gages may be exposed to bright sun at various times of the day, whereas others are in shaded areas. In this case approximate **temperature corrections** can be made by prorating the total change for each load interval.

Accuracy. Provided that instrumentation is operating satisfactorily, over-all accuracy is determined by:

1. The manufacturer's stated accuracy of the gage itself.
2. Changes in leakage resistance.

3. Proper temperature compensation.
4. Errors in instrument reading.
5. A satisfactory cement bond.

If the installation is made carefully, **accuracy obtained under field conditions** of the outdoor testing is usually within the range of ±4 to 10 percent. Since some of the errors possible are fixed values (temperature changes, errors in exact balance of the bridge, etc.), the percentage accuracy will vary from a relatively high value at low loads, to a small value at high loads. For example, if total fixed error is about ±20 μin. and gage accuracy is ±2 percent, over-all accuracy at 300-μin. strain (about 9000 p.s.i. in steel) will be about ±8.7 percent. If strain is 1000 μin., however, accuracy will be ±4 percent under the same conditions.

Test Records. Data forms such as are shown in Fig. 11 are recommended for strain-indicator work sheets. Strain computations are made as shown in Fig. 12. If the loading cycle is to extend over several hours, it is important that time be recorded as well as any other unusual condition.

EVALUATION OF DATA. In cases where the stress is uni-axial, its direction is known, and the gage is oriented along its axis, computation of stresses is quite simple, as shown for gages 8 to 11 in Fig. 13. If rosettes are used, stresses and direction are calculated from the rosette equations, Eqs. 31, 32, and 33. If more than a few calculations are involved, use of an **electronic computer** is recommended. **Graphical solutions** may be used, as described in the literature. Stress values shown in Fig. 13 were obtained with an electronic computer.

Evaluation of measured stresses and of design changes are beyond the scope of this discussion and are left to stress analysts or structure specialists. As an exam-

TEST LOAD

(In thousands of pounds)

Gage No.	650		800		900	
	p.s.i.	angle	p.s.i.	angle	p.s.i.	angle
1 Rosette	6,437	−45.0°	7,887	−45.0°	9.241	−45.0°
2 Rosette	−23,331	−12.0°	−27,264	− 7.0°	−30,261	− 9.0°
3 Rosette	− 6,230	0°	− 7,395	−92°	− 8,369	−41.0°
4 Linear	− 6,960	...	− 8,410	...	− 9,280	
5 Rosette	13,267	−22.5°	15,712	−22.5°	17,011	−23.9°
6 Rosette	− 5,227	43.8°	− 6,345	43.2°	− 6,826	42.5°
7 Rosette	− 5,659	14.9°	− 7,091	6.0°	− 8,202	10.0°
8 Linear	23,490	...	26,390	...	27,405	
9 Linear	3,915	...	4,785	...	5.220	
10 Linear	3,480	...	4,350	...	4,785	
11 Linear	725	...	870	...	1,305	

Notes: (+) indicates max. tension (or counterclockwise angle from ε_L gage). (−) indicates max. compression (or clockwise angle from ε_L gage).

Engineering Test Services, Inc.

Fig. 13. Stresses calculated from strain readings in Fig. 12 (p.s.i.). Stresses on standard gages were calculated from Eq. 30, with Young's modulus assumed to be 29×10^6 p.s.i. Rosette gage stresses were calculated from Eqs. 31, 32, and 33.

ple of design changes, the 30,000-p.s.i. compressive stress shown on gage No. 2, Fig. 13, was reduced by removing metal in a heavy lug mounted on the side of a drilling-barge support column. Load on the original lug resulted in excessive bending stresses at the location of gage No. 2 on the column wall.

GUIDE TO PROPER APPLICATION. Nondestructive stress-analysis tests are recommended whenever stresses are important or dangerous to personnel safety and cannot be calculated, as was the case for the drilling-barge structure. In many cases use of this method eliminates large amounts of unnecessary weight and provides a structure in which all parts carry an equal share of the load. Savings in weight result in dollar savings both for the manufacturer and the consumer. Of course simplified manufacturing processes can also be an important factor.

Bibliography

"Characteristics and Applications of Resistance Strain Gages," *U.S. Natl. Bur. Standards, Circ.*, No. 528 (1954).

DEAN, MILLS, III. "Techniques for Protecting and Waterproofing Resistance Wire Strain Gages," *Navy Dept. Rept.*, No. 797 (March, 1956).

DOBIE, W. B., and P. C. G. ISAAC. *Electric Resistance Strain Gauges.* London: English Universities Press. New York: The Macmillan Company, 1948.

FINK, K., and C. ROHRBACH. *Handbuch der Spannungs- und Dehnungsmessung* (Handbook of Stress and Strain Measurement). Duesseldorf: V.D.I. Verlag, 1958.

HETÉNYI, M. (ed.). *Handbook of Experimental Stress Analysis.* New York: John Wiley & Sons, Inc., 1950.

"How to Apply SR-4 Strain Gages," *Baldwin-Lima-Hamilton Bull.*, 279B.

INSTITUTE OF PHYSICS, LONDON. *The Measurement of Stress and Strain in Solids.* London: Cambridge University Press, 1948.

LEE, G. H. *An Introduction to Experimental Stress Analysis.* New York: John Wiley & Sons, Inc., 1950.

MURRAY, W. M., and P. K. STEIN. *Strain Gage Techniques.* Cambridge, Mass., 1959.

PERRY, C. C., W. T. BEAN, JR., G. ELLIS, R. M. GRAY, C. W. LAWTON, and E. O. STITZ. *Manual on Experimental Stress Analysis Techniques* (Preliminary). Cambridge, Mass.: Soc. Exptl. Stress Analysis, 1956.

PERRY, C. C., and H. R. LISSNER. *The Strain Gage Primer.* New York: McGraw-Hill Book Co., Inc., 1955.

Proc. Soc. Exptl. Stress Anal. Vol 1, No. 1 to date (Vol. 10, No. 2 contains complete cumulative index to Vols. 1–10).

ROBERTS, H. C. *Mechanical Measurements by Electrical Methods.* Pittsburgh: Instruments Publishing Co., 1946.

STEIN, P. K. (ed.). *Strain Gage Readings.* Vol. I, No. 1 to date. Phoenix, Arizona.

INDEX

(Boldface numbers, followed by a dot, refer to sections; lightface numbers following are the pages of the section. Sections 1–27 are in Vol. I; sections 28–54 are in Vol. II.)

A

- **Abrasive Articles** (See also "Emery Paper," "Grinding Wheels," "Hones")
  - defect detection in, by sonic testing, 51·12
  - honing sticks, crack detection in, 51·12–13
  - rupture moduli of, sonic testing for, 51·12
  - sonic and other testing of, 51·9–14
- **Absorbed Substances,** effect on filtered-particle testing, 9·5
- **Absorbents,** masking with liquid, in radiography, 20·22
- **Absorption** (See also "Attenuation")
  - of beta, gamma, and X rays, 18·4
  - of beta rays in thickness gaging, 18·18
  - of gamma and X rays by specimens, 20·13–15
    - mass coefficients for, 18·31
  - of gamma rays in radiography, 15·24
  - of neutrons, calculation of, 15·9
  - of radiation, absorber thickness and, 15·7
    - coefficients of, in thickness gaging, 18·17–18
    - in fluoroscopy, 19·4
  - of ultrasonic waves, energy losses in, 43·25
    - resolving-power loss from, 44·20
  - of water by strain-gage adhesives and its effects, 54·24–25
  - of X rays, 19·19 (See also "Filtration")
    - by aluminum and magnesium, 19·19
    - curves of, in radiography, 15·25
    - by glass and liquid barrier substances, 19·14, 19·15
  - of X rays and half-value layers for, 19·15
  - of X rays (high-energy), 23·1
- **Absorption Edges,** *K* and *L*, curves for uranium, 13·19
- **Acceleration,** measurement with unbonded strain gages, 54·2–3
- **Accessibility,** limitations in nondestructive testing, 1·20
- **Accidents,** prevention of, nondestructive testing in, 1·2
- **Accuracy** (See also "Sensitivity")
  - of eddy-current testing of conductivity and diameter, 42·1
  - specifying of, in nondestructive testing, 1·19
  - of strain gages, in measurement of quantities other than strain, 54·3
    - in stress analysis, 54·3
    - in testing of large structures outdoors, 54·40–41
    - using transducers, 54·3
- **Acetic Acid,** in X-ray film processing as stop bath and safety precautions in dilution of, 21·7
- **Acids**
  - effect on penetrants in liquid-penetrant testing, 6·6
- **Acids** (*Continued*)
  - etching with, as supplement to magnetic-particle testing, 32·25
- **Acoustic Attenuation**
  - in ultrasonic testing by contact, 45·6
    - and its measurement, 45·3–6
    - of stainless steel, 45·5
- **Acoustic Impedance**
  - change at liquid-solid interfaces, 45·9–10
  - of crystalline materials in relation to crystallographic direction and sound velocity, 45·7
  - definition and formula, 43·12
  - discontinuity-thickness effect on, 45·22
  - of metals (common) and water, 45·3
  - metal-water ratio *vs.* energy loss per back-surface multiple, 45·4
  - mismatch for flat-bottomed holes in ultrasonic testing, 45·21
  - of piezoelectric materials, 44·4
  - in ultrasonic testing, 45·27
    - definition, effects, and ratio, 45·1–3
  - of ultrasonic transducers, 44·5–6
  - for ultrasonic-wave transmission in metals and nonmetals, 43·8
    - ratio for, 43·13
- **Acoustic Lenses** (See "Lenses")
- **Acoustic Properties**
  - of metals and nonmetals, 43·8
  - of ultrasonic-test search units, 43·5
- **Acrylic Resins,** acoustic and ultrasonic properties of, 43·8
- **Actinide Elements,** atomic orbital make-up and properties of, 13·6
- **Activators**
  - in luminescent compounds, effect on fluorescence color, 16·14
  - in phosphors (crystal), impurities as, 16·10
- **Activity**
  - of beta-ray sources for thickness gaging, 18·19
  - specific
    - of Cesium-137, 15·22
    - of Cobalt-60, 15·14
    - of Iridium-192, 15·17
    - from neutron irradiation, calculation of, 15·10
    - of radioisotopes, definition of, 15·5
  - of X-ray-film developer solutions, decrease during standing and use, 21·6
  - of X-ray-film fixation solutions and their replenishment, 21·8
- **Activity Constants,** of ultrasonic-wave transducer elements, 43·4
- **Adhesives** (See also "Cement")
  - in aircraft joints, radiographic inspection problems from, 3·30
  - epoxy-resin, strain gages low in hysteresis and zero shift using, 54·26

Adhesives (*Continued*)
strain-gage, creep, decomposition, and inversion at elevated temperatures, 54·23–24
creep of, 54·27–28
epoxy and phenolic, 54·10
moisture absorption by, and its effects, 54·24–25
resinous, 54·12–13
softening at elevated temperatures, 54·23
response to strain rate, and resonant frequency in relation to, 54·13
Afterglow, of fluoroscopic screens, 16·15
Aging
of barium titanate transducers, 44·2
of steel (Thomas), eddy-current Magnatest Q experiments on, 42·60
Agitation, in X-ray-film development, 21·5
Air
absorption coefficients (mass), their absorption components and photon energies for γ and X rays, 18·39
acoustic and ultrasonic properties of, 43·8
bubbles or pockets, avoidance in liquid-penetrant application, 6·14
for electrified-particle testing, pressure-regulated supply of, 28·9
mass absorption coefficients of, for radiation, 18·2
pressure for blasting and spraying of specimens for ceramic-type brittle coatings, 52·16–17
ultrasonic-wave attenuation *vs.* frequency in, 43·26
Aircraft
borescopic inspection in manufacture of, 11·13
defects (small) in parts of, detection by ultrasonic immersion inspection, 47·4
design (fail-safe) of, 3·29
engines, magnetic-particle testing of cylinders of, 31·12
exhaust stacks of, maintenance testing of, 3·34
fatigue cracks in, detection of, 3·27
foils, strain-gage tests of, effect of cement thickness on, 54·13
inspection of, radiographic, 3·30
for structural integrity, 3·27–29
inspection of parts of, borescopic, 11·13
by shear-wave techniques, 47·15
magnetic-particle testing of parts of, electric current for, 30·13
equipment for, 31·9
maintenance testing of, 3·26
cost savings and personnel requirements, 3·36
materials for, ultrasonic-wave amplitude-distance curves for, 43·44, 43·46
propellers, ultrasonic resonance testing of, 50·27
service life of, survey by photoelastic-coating tests, 53·35
sonic and ultrasonic testing of parts of, 5·24
stress measurement (photoelastic) in flight, telemetering of, 53·35
structures (honeycomb) for, fluoroscopy of, 24·28–29
ultrasonic immersion tests of parts of, 47·1
wing spars, ultrasonic transducer for inspecting, 44·9
Air Pollution, testing instruments for, 3·25
Airy Disc, formation in diffraction of light, 10·26
Alcohol, mixtures with nitric acid as etching fluid for metallography, 32·29
Alcohols, as suspending media for filtered-particle tests, 9·7
Alkali Metal Halides, ultrasonic energy losses in, 43·25
Alloys
coercive force in analysis of, 34·5
eddy-current separation of similar, harmonics in, 42·34
eddy-current testing by electrical conductivities of, and sorting by, 42·15
eddy-current testing of, for carbon content, statistical distribution, 41·13
electrical conductivity changes related to composition and structure in, 37·6
significance of hysteresis loop in, 46·1
tabular summary of, 36·4–8
eddy-current testing of rods of mixed, with Magnatest FM-100, 42·11
electric-current (direct) nondestructive testing of, surface preparation for, 35·3
identification and sorting of, tribo-electricity in, 5·22
liquid-penetrant testing of high-temperature, penetration time in, 6·8, 6·10
phase changes in, ultrasonic-energy losses from, 43·25
radiographic equivalence factors for, 20·14
segregation in, electrical conductivity as indicator of, in eddy-current tests, 42·1
microradiography of, 20·42
sorting of, for composition and hardness, by ellipse eddy-current methods, 40·28
with eddy-current, suppression of undesired signals in, 40·40
eddy-current apparatus for, 40·2–3
by electrical conductivity in eddy-current tests, 42·1
with Magnatest Q eddy-current instrument, 42·33, 42·42
with magnetic apparatus, transparent paper masks in, 2·28
spread bands of, as standard for nondestructive testing, 2·28
ultrasonic testing of, "noise" caused by discontinuities during, 44·7
potential applications of, 43·49
X-ray analysis of, 17·14
X-ray fluorescence spectroscopy in analysis of, 17·27
Alpha Particles (See "Alpha Rays")
Alpha Rays
emission and kinetic energy of, 15·3
emission in U-238 series, 15·1
ionization (specific) of, 16·1
in nondestructive testing, 5·19
Alternating Current (See "Electric Current")
Aluminum
absorption coefficients (mass) for γ and X rays and photon energies of, 18·33, 27·9
absorption components of mass absorption coefficients of, for γ and X rays, 18·40
acoustic and ultrasonic properties of, 43·8
acoustic impedance, density and sound velocity in, 45·3
attenuation coefficients of, for γ rays and X rays, 27·9
castings, ASTM reference radiographs for, 24·3
shrink porosity in, 24·9
ultrasonic contact testing of, grain structure effect on, 48·2
castings and wire, composition control by eddy-current testing, 42·14–15
coatings on nickel and nickel coatings on aluminum, fluorescent radiation in determination of thickness, 24·36–37

Aluminum (*Continued*)
- coating with, of photoelastic-test specimens before application of plastic coatings, **53·15**
- eddy-current testing of, compensation for expansion coefficient in, **40·12**
  - effective permeability calculations for, **36·20**
  - separation of effects of conductivity and diameter of rods in, **37·1–2**
  - similarity law in, for cylinders, **37·11**
- effect on electrical conductivity of copper, **42·12**
- elasticity tension modulus of, **52·11**
- electrical conductivity of, **42·16**
- extrusions, focused transducer for inspection of, **44·8**
- fluorography of, penetrameter sensitivity in, **19·44**
- fluoroscopy of, glass *vs.* beryllium windows in, **19·17**
- fluoroscopy with image-amplifier tubes, sensitivity in, **19·39**
  - instrument characteristics for, **19·48**
  - with Lumicon, penetrameter sensitivity in, **19·40**
  - penetrameter sensitivity in, **19·23–24**
- foil, complex transmission coefficient *T* in eddy-current testing of, **39·14**
  - thickness measurement of, **18·4**
- fundamental ultrasonic resonant frequency of, **50·4**
- gamma-ray shielding equivalent of, **26·10**
- lacquer containing, use as undercoat for resinous brittle coatings, **52·9**
- liquid-penetrant testing of, penetration time in, **6·8**, **6·10**
- mass absorption coefficients of, for radiation, **18·2**
- photoelastic-coating test color fringes in, for various strains and stresses, **53·5**
- plates, defects in welds in, radiographs of, **24·13**
  - with drilled holes, photoelastic-coating patterns in, **53·18**
  - fundamental ultrasonic resonance frequency for, **50·7**
  - ultrasonic inspection with paint-brush transducers, **44·12**
  - xeroradiograph of holes in, **22·10**
- radiography of
  - carbon tetrachloride as masking agent in, **20·22**
  - density calculations for, **23·9**
  - equivalence factors for, **20·14**
  - exposure-thickness curves for, **15·27**
  - lead-foil screens in, **20·27**
  - with Thulium-170, **15·22**
- relations between ultrasonic frequency, thickness, and harmonic number of, **50·14**
- strain gages on, strain limits with various adhesives, **54·25–26**
- strain-gage tests on strips of, effect of rigidity of gage on, **54·30**
- thickness measurement range with Sr-90 beta gages, **18·16**
- ultrasonic contact testing of forgings, **48·11**
  - of ingots, structural disturbances in, **48·30**
- ultrasonic energy losses in single crystals of, **43·25**
- ultrasonic energy ratio between front surface and test hole in block of, **44·19**
- ultrasonic reflection coefficients at interfaces with other materials, **43·13**

Aluminum (*Continued*)
- ultrasonic testing of, acoustic impedance ratio with respect to water for, **45·2**
  - frequencies for contact, **48·1**
  - immersion, **46·10**
  - *K* value in resonance, **50·3**
  - test blocks for, **45·5**
- ultrasonic testing of compressor and turbine rotor wheels of, **47·16–18**
- ultrasonic testing of wrought, **47·4**, **49·1**
- ultrasonic waves in, amplitude as function of flaw depth and hole diameter for different gain settings, **44·17**
  - amplitude-distance curves for, **43·44**
  - amplitude in relation to depth for contact search units, **43·39**
  - amplitude variation with depth, **44·15**
  - angle of incidence *vs.* angle of refraction, **45·10–11**
  - critical angle of longitudinal, **45·10**
  - Fresnel-zone effects in, with water path, **44·15–17**
  - length of, in relation to hole diameter, **45·20**
  - phase velocities in Lamb type, **45·12**
  - profile variation with depth in, **43·41**
  - reflection amplitudes for water-immersed, **43·46**
  - train length in, for various frequencies, **43·31**
- welds in, dye-penetrant penetration time for, **6·14**
- as xeroradiographic-plate base material, **22·4**
- xeroradiography of, charts for, **22·9–10**
- X-ray absorption and transmission by, **19·19**
- X-ray diffraction photograph of, **17·5**
- X-ray transmission curves (constant-percentage) for, **19·22**

Aluminum Alloys
- acoustic and ultrasonic properties of, **43·8**
- blocks of, in liquid-penetrant-uniformity control, **7·26–27**
- castings of, detectible defect size in fluoroscopy of, **24·24**
  - radiographs of gas holes and gas porosity in, **24·4**
- chromium segregation in, determination by ultrasonic contact testing, **48·12**
- copper-, microradiograph of, **20·42**
  - ultrasonic energy losses from internal oxidation in single crystals of, **43·25**
- copper-magnesium-, diameter variations of rods of, indications of Magnatest FW-300 eddy-current instrument, **42·2**
  - eddy-current density and field strength in rods of, as function of radial position, **37·9**
  - effect of segregation on electrical conductivity of cast, **42·15**
  - electrical conductivity and hardness *vs.* quenching temperature of, **42·19**
  - hardness of pressed parts of, and its distribution with Multitest and Statimat eddy-current instruments, **41·16–17**
- defects in plates of, ultrasonic immersion indications of, **47·9–10**
- eddy-current testing of, equipment for, **40·2–3**
- electrical conductivity of cast and wrought, **42·17**
- forgings, inspection by ultrasonic immersion tests, **46·21**
- hardness of, eddy-current test of electrical conductivity as indication of, **42·1**, **42·18**
- honeycomb structures of, fluoroscopy of, **24·29**

Aluminum Alloys (*Continued*)
- radiography of, equivalence factors for, **20·14**
  - with Thulium-170, exposure-thickness curves for, **15·27**
- silver-, ultrasonic energy losses in single crystals of, **43·25**
- soft-spot detection in, by eddy-current conductivity measurement, **42·3**
- sorting of parts of, for hardness with Multitest eddy-current instruments, **41·2**
- for strain-gage-based transducers, **54·5**
- stress-strain curves (nonlinear) of, **54·4**
- test blocks as ultrasonic refractometers, **45·10**
- ultrasonic inspection of sheet, **47·16**
- ultrasonic-wave attenuation *vs.* frequency in, **43·26**

Aluminum Oxide
- abrasive wheels, sonic testing of, correlation of sonic resonant frequency with percentage of bonding material in, **51·12**
- constant *K* value in ultrasonic resonance tests, **50·3**
- fundamental ultrasonic resonant frequency of, **50·4**
- X-ray powder diffraction of α-type, **17·8**

Ammeters, surge crest, for measuring lightning currents, **33·17**

Ammonium Dihydrogen Phosphate, as ultrasonic-wave transducer material, **44·2**

Ammonium Persulfate, etching with, as supplement to magnetic-particle testing, **32·26**

Amorphous Materials, X-ray diffraction analysis of, **17·16**

Amperage (See "Electric Current")

Amplifiers
- for electric-current railroad-rail testing, **35·16**
- for fluoroscopic images, **19·37**
- image, solid-state, **11·21**
- for ionization chambers, **16·5**
- noise effects from tubes of, in ultrasonic contact testing, irrelevant indications from, **48·21**
- recorders using, for magnetic-field meters, **33·11**
- for signals in nondestructive testing, elimination of drift of, **4·9**
- for ultrasonic-test A-scan systems, **43·32**

Amplitude
- of ultrasonic echoes
  - effects of discontinuities or reflectors on, **45·18**
  - loss from test-object surface roughness, **45·16**
  - from parts with various curvatures, **45·13–15**
  - from rough and smooth spherical reflectors, **45·24**
- of ultrasonic waves, **43·18–21**
  - in aluminum
    - angle of refraction in relation to, **45·11**
    - depth in relation to, for contact search units, **43·39**
  - in aluminum and water, variation with depth, **44·15**
  - in aluminum as function of flaw depth and hole diameter, **44·17**
  - area compared with, for Alcoa reference block Series A, **43·46**
  - A-scan presentation of, **43·29**
  - distance in relation to
    - for common aircraft materials, **43·44, 43·46**
    - for various test-hole diameters and shapes, **43·39, 43·43**
  - impedance ratio in relation to, **45·2**

Amplitude (*Continued*)
- of ultrasonic waves (*Continued*)
  - losses from adversely oriented discontinuities, **45·23**
  - in Lucite and steel, **43·21, 43·23**
  - near-field sound pattern of, in measurement of discontinuities, **45·24**
  - reflected from common metals immersed in water, **43·46**
  - reflected from flat reflectors at various angles, **45·20**
  - of refracted shear type, **43·21**
  - in scanning test hole, Fresnel zone effect on, **44·18**
  - variation across lithium sulfate transducer, **44·11–12**

Angles, measurement, with optical projectors, **12·3**

Anisotropic Media, in optical tests using polarized light, **10·18–19**

Anisotropy
- causes of, **10·19**
- crystallographic, effects on acoustic impedance, density, and sound velocity in common metals, **45·3**
- of crystal structure, elastic constants, and sound velocity, **45·7**
- effect on apparent impedance plane in eddy-current testing of spheres, **39·11**
- X-ray analysis of, **17·18–20**

Annealing
- of steel (ball-bearing), effect of, on Magnatest Q eddy-current spread bands, **42·58**
- of steel (carbon), effect on Magnatest Q eddy-current wave forms, **42·52–53**
- of steel (cold-drawn carbon), effect on coercive force, internal stresses, and eddy-current hysteresis loops, **42·25**
- stress-relief, effects on Magnatest Q eddy-current spread bands of alloy steel wire, **42·50**

Annihilation Quanta, production in beta-ray thickness gaging, **18·18**

Annular Mode, of sonic vibration of thin circular discs, **51·4**

Anodes
- X-ray-tube, **14·27, 14·34**
  - hooded, to prevent random radiation, **14·34**
  - rotating, **14·4**
  - thermal load limits and cooling of, **14·33**

Anodization
- chromic acid, defect detection by, **8·6**
- effect on liquid-penetrant indication of defects, **8·6**

Anthracene, in beta-ray detection, **18·22**

Antimony
- attenuation coefficients of, for γ rays and X rays, **27·30**
- effect of, on electrical conductivity of copper, **42·12**

Antinodes, of sonic vibration of rectangular bars, **51·2**

Antiproton, as elementary particle, **13·4**

Antiresonance, in ultrasonic testing of thin materials, **44·10**

Apparatus (See "Equipment")

Apparent Permeability (See "Apparent" under "Permeability")

Archives
- X-ray films for, special processing procedures for, **21·9**
  - tests for fixer removal for, **21·11**

Arc Lamps, carbons for, eddy-current sorting by thickness ot copper plating on, 41·2
Argentometer, for eddy-current testing, 36·7
Argon
  absorption coefficients (mass) for γ and X rays and photon energies of, 18·34, 27·11
  attenuation coefficients of, for γ rays and X rays, 27·11
Argument
  of basic function for eddy-current behavior in thin-walled tubes, 38·1–2
  of hyperbolic functions for determination of limit frequency in eddy-current testing of spheres, 39·1
Armed Forces, specifications, role of nondestructive testing laboratory in meeting, 2·4
Arsenic, effect on electrical conductivity of copper, 42·12
Art Objects, radiography (low-voltage) of, to determine authenticity, 24·40
Asbestos
  thickness measurement range with Sr-90 beta gages, 18·16
  X-ray diffraction photograph of fibers of chrysotile, 17·5
A-Scan
  equipment and methods for presentation of ultrasonic test data, 43·29–33
  ultrasonic immersion, indications from, 47·1
  ultrasonic indications from aluminum-alloy plate, 47·8
    identification of sources of, 46·18
    from test blocks, 47·3
  ultrasonic test signals by, 46·3, 47·29
  units, for ultrasonic contact testing, 48·5
Assemblies
  failure probability of, 1·2
  fluoroscopic inspection of enclosed, 24·19
  inspection by high-brightness fluoroscopy, 19·42
  inspection of, fluoroscopy in, 19·48
  internal, inspection with Thulium-170, 15·22
Assembly of Parts, optical projection control in, 12·21
Astatic Magnetometer Probe, for determination of sample magnetization and arrangement of, 33·2
Atmospheres, oxidizing, for firing of brittle-type ceramic coatings, 52·17
Atomic Nuclei, half-life and mean life of, 13·12
Atomic Structure, concepts of, 13·6
Atoms (See also "Elements")
  core or nucleus of, 13·4
  orbital electrons as determinant of chemical properties of, 13·4
  radioactive (See "Radioisotopes")
Attenuation
  acoustic (See also "Acoustic Attenuation")
  broad- and narrow-beam, in radiography, 15·35
  of gamma rays in radiography, 15·24
  of radiation in thickness gaging, 18·17
  in ultrasonic contact testing, 45·6
  of ultrasonic waves, 43·22–23, 45·1–6
    by backing members, 44·6
    in immersion testing, 46·10
    measurement of, 50·24
    in plastic sheets, measurement of, 43·15
    in solids, data, sources, and relationships, 43·25–26
Attenuation Coefficients
  of elements for X rays and gamma rays, 27·1
Attenuation Coefficients (*Continued*)
  photoelectric, of atoms in general and of uranium, 13·19–20
  of radiation absorption, 13·18
Austenite
  in steel, determination by eddy-current testing, 2·25
    by magnetic saturation flux density, 34·4
Automatic Gain Control, in ultrasonic testing, 49·19
Automation
  of combined nondestructive tests, 41·19
  of crack testing of steel rods with Magnatest D eddy-current instrument, 41·10
  of eddy-current testing, 2·32–33, 41·1–19
    with Magnatest Q eddy-current instrument, 41·7–8
    of small-diameter tubing, problems in, 38·37
    in statistical quality control, 41·12
  effect on involuntary visual inspection, 5·12
  of Magnatest Q eddy-current tests, 41·5
  of magnetic-particle test equipment, with photoelectric scanner, 31·14
  in nondestructive testing, cost in relation to, 1·15
  of production, nondestructive testing in relation to, 2·27
  in simultaneous defect testing and eddy-current sorting of mixed alloy steel parts, apparatus for, 42·68
  sorting for cracks, automatic eddy-current apparatus for, 41·1
  in ultrasonic inspection of jet-engine forgings, 43·35
Automobiles
  borescopic inspection in manufacture of, 11·14
  parts, effect of tensile strength on Magnatest Q eddy-current wave forms and slit value, 42·52
    hardness control of tempered parts of, by coercive-force tests, 34·7
    semi-automatic magnetic-particle-testing equipment for, 31·10, 31·12–13
    sorting by tensile strength with Magnatest Q eddy-current instrument, 42·54–55
  steering spindles of, magnetic-particle-testing unit for, 31·12
Avalanches, in radiation measurement with proportional counters, 16·5
Aviation (See "Aircraft")
Axles (See also "Shafts")
  railroad-car, ultrasonic contact testing of, 48·7
  ultrasonic testing of, variable-angle units for, 43·7

B

Babbitt Metal, electrical conductivity of, 42·16
Babinet Compensator (See "Compensators")
Backing Material, for strain gages, 54·5, 54·10
Backing Rings, pipe welds made with, radiography of, 25·15
Backings, for ultrasonic transducer crystals, 44·5
Back-Scattering (See "Reflection")
Back-Scatter Systems, for X-ray thickness gaging, 18·9
Bacon, inspection (fluoroscopic) of, 19·36
Bakelite
  elasticity tension modulus of, 52·11
  strain gages, fatigue life of, 54·26
  ultrasonic reflection coefficients at interfaces with other materials, 43·13
Balances, in gravitational-field detection, 5·11

Baldwin Strain Indicators, 54·20

Ball Bearings (See "Bearings, Ball")

Balls (See also "Spheres")
- for bearings, sorting with Magnatest Q eddy-current methods, 42·58
- golf, fluoroscopic inspection of, 24·19
- sorting for cracks, automatic eddy-current apparatus for, 41·1

Balsa, gamma-ray shielding equivalent of, 26·10

Bands, Spread (Magnatest Q Eddy-Current Instrument)
- of ball-bearing rings, effect of annealing and hardening temperatures on, 42·58
- of drop-forged steel parts of various tensile strengths, 42·57
- of hot-rolled steel billets, 42·39
- of spring steel rolled billets, 42·41–42
- of steel, in annealed, cold-drawn and tempered conditions, 42·52
  - frequency effect on, 42·44
  - at high field strength and high and low frequencies, 42·48–49
  - with optimum screen utilization, 42·43–44
  - tensile-strength effect on, 42·53, 42·55
- of steel (alloy) wire, effect of stress relief by annealing on, 42·50
  - straightened by hammering, frequency effect on, 42·49–50
- of steel rods, 42·33
  - harmonics in, 42·37
- of steel wire, frequency effect on, 42·46
- of valve stems (case-hardened), 42·58

Band Width
- of ultrasonic test equipment (commercial), 44·21
- of ultrasonic transducers, 44·4, 44·19

Barges, for oil-well drilling off-shore, strain-gage tests in design of, 54·33

Barium
- absorption coefficients (mass) for γ and X rays and photon energies of, 18·37, 27·33
- attenuation coefficients of, for γ rays and X rays, 27·33

Barium-137, radiation-dosage-output of, 26·6

Barium Clay, masking with, for scattering prevention in radiography, 20·22

Barium Concrete, radiation-shielding equivalent of, 26·9

Barium Lead Sulfate, in X-ray intensifying screens, 16·16

Barium Oxide, glasses containing, protection coefficient for X rays, 19·13

Barium Platinocyanide, fluorescent screens, peak kilovoltage of, 19·11

Barium Titanate
- ceramic plates with vapor-deposited electrodes, 44·5
- crystals for ultrasonic immersion testing, 46·7
- transducers for ultrasonic waves, 44·2–4
- as ultrasonic transducer element, 43·4–5, 49·3, 49·6, 49·12
- for ultrasonic transducers, 50·15
- as ultrasonic-wave transducer material, 44·2, 48·2

Bars
- cracks (cooling) in rolled, magnetic-particle indications of, 32·7
- cracks in, filing as supplement to magnetic-particle testing, 32·21
- seams (surface) in rolled, magnetic-particle indications of, 32·6
- sonic vibration (flexural) of, which are not exactly square, 51·13

Bars (*Continued*)
- sonic vibration frequency equations for rectangular and square, 51·4
- sonic vibration modes of rectangular, 51·2
- stainless steel, ultrasonic attenuation in, 45·5
- test for gas porosity evaluation in castings, 24·8
- ultrasonic contact testing of, frequencies for, 48·1
- ultrasonic immersion inspection of round, apparatus for, 46·22, 46·24
- ultrasonic immersion testing of, 46·22
- ultrasonic-wave propagation velocity in, 43·9

Bases, for fluorescent X-ray intensifying screens, 16·16

Baskets, for handling small parts in liquid-penetrant testing, 7·5

Baths
- for magnetic-particle testing, and their checking, 30·15–18
- stop, in X-ray-film processing to arrest development, 21·6–7

Batteries
- solar (See "Solar Batteries")
- storage, for magnetization for magnetic-particle testing, 30·8

Beams, ultrasonic (See "Ultrasonic Waves")

Bearings
- races of, checking demagnetization of, after magnetic-particle testing, 30·28
- stresses in, fringe patterns in, 10·19

Bearings, Ball
- crack testing and sorting of, automatic eddy-current instruments for, 41·14
- hardness testing with Magnatest Q eddy-current instrument, 42·58
- rings of, sorting with Magnatest Q eddy-current methods, 42·58
- sorting by coercive-force tests, 34·7
- steel for, hardness values and their distribution as shown by Magnatest Q and Statimat eddy-current instruments, 41·15

Bearings, Roller
- hardness testing with Magnatest Q eddy-current instrument, 42·58
- ultrasonic testing with double search unit, 49·18

Bending
- of aluminum and steel under known load, corrections of strain-optical constant in photoelastic-coating tests during, 53·38
- measurement of moment of, at remote locations with strain gages, desensitization in, 54·19

Beryllium
- absorption coefficients (mass) for γ and X rays and photon energies of, 18·32, 27·3
- acoustic and ultrasonic properties of, 43·8
- attenuation coefficients of, for γ rays and X rays, 27·3
- windows
  - X-ray absorption by, compared with glass, 19·17
  - in X-ray tubes for trapping electrons, 14·34

Beryllium Alloys, copper-, for strain-gage-based transducers, 54·5

Bessel Functions, argument A of, in calculation of effective permeability in eddy-current tests, 36·13

Beta Rays (See also "Electrons")
- absorption, range and source selection for thickness gaging, 18·18
- absorption of, 18·4
- detection by scintillation counting, 18·22

Beta Rays (*Continued*)
  in determination of thickness of coatings and paper, **18·4**
  discovery of, **13·1**
  emission of, and its Fermi distribution, **15·3**
    in U-238 series, **15·1**
  ionization chambers for detection of, **18·20**
  ionization (specific) of, **16·1**
  in nondestructive testing, **4·11**
  penetration by, **26·8**
  reflection thickness gaging, **18·12**
  sources of, **5·16**, **18·1**
    selection for thickness gages, **18·18**
  thickness gages using energy and half-life of sources for, **18·17**
  in thickness gaging, **5·19**, **18·1**
  thickness ranges measured with Sr-90 transmission-type gages using, **18·16**
Betatrons
  diagram of, **14·18**
  radiography with, **23·4**
    geometrical enlargement in, **20·10**
    of steel, exposure chart for, **23·11–12**
    of steel sections, **14·11**
  X-ray tube, **14·11**
Billets
  sorting of steel, with Magnatest Q eddy-current instrument, **42·35**
  ultrasonic contact testing of, frequencies for, **48·1**
Binders, for fluoroscopic screens, **16·14**
Biological Methods, in detection of poisonous gases, **5·4**
Biology, microradiography in, **20·41**
Bi-Refringence
  artificial, in photoelastic-coating tests with small-field meter, **53·23**
  in control of photoelastic-coating-test loading, **53·35**
  measurement in photoelastic-coating tests, **53·15**
    with Babinet Compensator and large-field meters in photoelastic-coating tests, **53·27**
  in photoelastic-coating tests, **53·1**
  principles of, and use in photoelastic-coating tests, **53·3**
  strain, in stress analysis, **10·19**
Bismuth, absorption coefficients (mass) for γ and X rays and photon energies of, **18·38**
Black Light (See also "Light, Ultraviolet")
  effect on human eye, **9·12**
  for filtered-particle tests, **9·11**
  filters for, for penetrant testing, **7·13**
  for fluorescent magnetic-particle testing, **30·19**
  illumination level for penetrant testing, **7·15**
  in liquid-penetrant testing, **7·2**, **7·11**
  meters for, **7·13**
  in nondestructive testing, **5·8**
  physiological effects of, **7·17**
  scanning with, in automatic magnetic-particle inspection of welded tubing, **31·14**
  sources of, **7·12**
Black Lights
  fixtures for, for penetrant testing, **7·13**
  life of, and its extension, **7·16**
  for liquid-penetrant inspection booths, **7·7**, **7·10**
  maintenance of, **7·15**
Blades, Turbine (See "blades" under "Turbines")
Blasting
  of metal surfaces before strain-gage application, **54·36**
Blasting (*Continued*)
  of specimens for ceramic-type brittle-coating tests, **52·16**
Blasting Cartridges, location of unexploded, by magnetic means, **34·22**
Blending, liquid-density control with radioisotopes in, **18·30**
Blistering, hydrogen, of chemical equipment, detection by ultrasonic-resonance method, **50·28**
Blisters, formation in X-ray-film emulsions from developer containing sodium carbonate, and their prevention, **21·7**
Blocking, in radiography to minimize scattering, **23·9**
Blocking Media, in radiography with fluorescent intensifying screens, **20·29**
Blocks, Reference (See "Test Blocks")
Blood-Pressure, strain-gage-based transducers in measurement of, **54·3**
Blowholes
  in cast-steel flanges, magnetic-particle indications of, **32·9**
  in welds, causes and radiography of, **25·3**
Blueing, of metal parts by heating, fracturing after, as supplement to magnetic-particle testing, **32·23**
Blueprints, in X-ray-image interpretation, **24·6**
Boilers
  thickness measurements of, with Hall generator, **34·17**
  tubes (See "Tubes")
Bolts
  cracks (quench) in, magnetic-particle indications of, **32·12–13**
  magnetic-particle testing of, semi-automatic equipment for, **31·10**
Bombs, detection of buried unexploded, by magnetic means, **34·23**
Bonding
  of plastic sheets to materials for photoelastic-coating tests, **53·15**
  of strain gages, **54·12–13**
    cements for, **54·10**
Bonds
  in cladding, detection of weak spongy, **50·22**
    lack of, detection of, **50·22**
  metal-to-plastic, ultrasonic resonance testing of, **50·23**
  thermal tests for, **5·24**
Bones, strain-gage tests on living and dead, **54·3**
Booths, for radiography (high-voltage), **23·15**
Borescopes, **11·12** (See also "Cystoscopes," "Gastroscopes," "Telescopes")
  for aircraft-engine-cylinder inspection, **3·32**
  construction, specifications, types, and uses of, **11·17–24**
  flexible, **11·15**
  optical systems of, **11·16**
  for testing of hollow tubes and small cavities, **10·10**
Boron, absorption coefficients (mass) for γ and X rays and photon energies of, **18·32**
Bottles (See "glass" under "Containers")
Boxboard (See "Fiberboard")
Bragg Equation, **17·4**, **17·13**
Brass
  acoustic and ultrasonic properties of Naval, **43·8**
  acoustic impedance, density, and sound velocity in, **45·3**
  crack propagation in plates of, **35·11**

Brass (*Continued*)
- elasticity tension modulus of, **52·11**
- electrical conductivity of, **42·16**
- gamma-ray shielding, equivalent of, **26·10**
- penetration time for, in liquid-penetrant testing, **6·8**, **6·10**
- radiographic equivalence factors for, **20·14**
- thickness measurement range with Sr-90 beta gages, **18·16**
- tubes, eddy-current testing of, magnetic-field-strength effects in, **38·16–17**
- ultrasonic contact testing of, frequencies for, **48·1**
- ultrasonic contact testing of
  - castings of, **48·2**
  - forgings of, **48·11**
- ultrasonic reflection coefficients at interfaces with other materials, **43·13**
- ultrasonic resonance testing of, constant K value in, **50·3**
- X-ray absorption by, **20·14**
- X-ray diffraction, photograph of, **17·5**

Brazed Parts
- of honeycomb structures, fluoroscopy of, **24·29**
- liquid-penetrant testing of, penetration time for, **6·14**
- penetration times for, in liquid-penetrant testing, **6·8**, **6·10**
- rejection of cracked, basis for, **8·13**
- of stainless steel, radiograph of defects in, **24·13**

Break-Even Point, in nondestructive testing, **1·14**

Bremsstrahlung (See "Continuous" under "X rays")

Bricks
- inspection of plastic porous, **24·38**
- radiation-shielding equivalent of, **26·9**
- strain-gage tests on, **54·3**

Bridges
- sonic testing of, **5·24**
- stress measurement (photoelastic-coating) of, telemetering of, **53·35**
- welded, photoelastic-coating tests of, **53·27**, **53·34**

Bridges (electric circuits)
- eddy-current-test, balancing of, **40·6**
- in eddy-current testing, **42·29–61**
- Wheatstone, for strain gages, **54·16–17**

Brightness or Brilliance
- of fluoroscopic and photofluorographic screens, **19·9–13**
- of fluoroscopic images, for aluminum and magnesium sheet, **19·19**
  - increasing of, by image amplifiers, **19·37**
- of fluoroscopic screens, **16·15**
- in fluoroscopy, amplification by the Lumicon in, **19·40**
  - electric-current frequency and apparent, **19·24**
  - level of, **19·23**, **19·33**
  - minimum discernible difference of, **19·27–28**
  - visual factors in relation to, **19·24**
  - X-ray-tube output in relation to, **19·17**
- of liquid penetrants (used), measurement of, **7·24**

Brine Tests, for failure detection in coatings, **29·11**

Brittle Coatings
- ceramic, material selection for, **52·8**
  - for nondestructive testing, **52·7**
  - preparation, application, and firing of, **52·16–17**

Brittle Coatings (*Continued*)
- ceramic (*Continued*)
  - safety precautions in handling materials and solvents for, **52·8**
  - specimen preparation for, **52·16**
- ceramic and resin type compared, **52·1**
- flaking of, as indicator of gross strain, **52·25**
- fracture and pattern formation under strain, **52·4**
- resin-type, **52·5**, **53·3**
  - calibration of, and bars for, **52·10–11**
  - crack detection in, **52·11–16**
  - drying of, **52·9**
  - selection of, **52·5–6**
  - spraying of, and air supply for, **52·9**
- selection for high threshold strain, **52·6**
- strain gages compared with, in design of structures, **52·18**
- stress-distribution indication with, on complex structures, **52·2**, **52·3**
- in stress (residual) measurement, **52·24**
- use of several, during same test, **52·4**

Brittle-Coating Tests
- applications of, **52·17–27**
- crack-pattern photography in, **52·26**
- creep correction in resin-type, **52·11–12**
- with electrified-particle testing for locating stress-indicating cracks, **29·20**
- loading in, apparatus for, **52·18**
  - correlation for direct-pressure effect in, **52·26**
- materials for, **52·1–8**
- nondestructive, **52·1–27**
- resin-type, specimen preparation for, **52·9**
- of steel crane hook as typical example, **52·21**
- as strain-gage test supplement, **54·2**, **54·35**
- strain measurement in, under dynamic and static loading, **52·19**
- strain thresholds in, **52·6**
- temperature control in, **52·19**
- temperature factors in outdoor, **52·21**

Bromine, absorption coefficients (mass) for γ and X rays and photon energies of, **18·36**

Bronze
- acoustic and ultrasonic properties of phosphor, **43·8**
- cast tin, radiographs of hot tears and shrinkage in, **24·15**
- composition of, control by eddy-current methods, **42·13**
- elasticity tension modulus of, **52·11**
- electrical conductivity of, **42·16**
- penetration time for, in liquid-penetrant testing, **6·8**, **6·10**
- structural disturbances in ultrasonic contact testing of, **48·30**

Brownian Movement, 13·2

Brush Carriages, for railroad-rail-test detector cars, **35·13-15**

B-Scan
- equipment and methods for presentation of ultrasonic test data, **43·33–34**
- frequency, probe-coil eddy-current for Inconel tubing, **38·38**
- indications from ultrasonic test blocks by, **47·3**
- photographs from probe-coil eddy-current testing of tubing, **38·37**
- ultrasonic test signals by, **46·3**, **47·29**

Bubbles
- in brittle coatings (sprayed), benefits of, **52·9**
- in liquid-penetrant application, and their prevention, **6·14**

Bubbles (*Continued*)
  in X-ray-film processing and their prevention, 21·21
Buildings (See "Structures")
Build-Up Factors, for radiography, 15·36
Bulkheads, corrosion rate measurement of, by ultrasonic resonance testing, 50·37–38, 50·40
Bunsen-Roscoe Reciprocity Law, and its failure, 16·23 (See also "Reciprocity Law")
Bursting Speed, of abrasive wheels (resin-bonded), variation with sonic resonant frequency, 51·12
Bursts, forging, magnetic-particle indications of, 32·9
Bushings, chain, case-hardening depths of, Magnatest Q bands for, 41·17

C

Cable Boxes, detection of buried, by magnetic means, 34·23
Cables
  magnetization with, of large parts for magnetic-particle testing, 30·6
    of localized areas in magnetic-particle tests, 30·6
    for magnetic-particle testing, 30·14
    portable equipment for, in magnetic-particle tests, 31·2–3
  for strain gages for high temperatures, 54·32
Cadmium
  attenuation coefficients of, for γ rays and X rays, 27·28
  effect on electrical conductivity of copper, 42·12–13
Cadmium Selenide (CdSe)
  crystals, fabrication of photoconductive, 16·12
  as photoconductor, 16·8
  semi-conductors in X-ray thickness gaging, 18·7
  X-irradiated, photocurrent, sensitivity and time constant of, 16·11
Cadmium Sulfide (CdS)
  crystals, fabrication of photoconductive, 16·12
  in gamma-ray detection, 18·21
  as photoconductor, 16·8
  semi-conductors in X-ray thickness gaging, 18·7
  X-irradiated, photocurrent, sensitivity and time constant of, 16·11
Cadmium Tungstate, fluorescent screens, peak kilovoltage of, 19·11
Cadmium Zinc Sulfide (See "Zinc Cadmium Sulfide")
Calcium
  absorption coefficients (mass) for γ and X rays, and photon energies of, 18·34, 27·12
  attenuation coefficients of, for γ rays and X rays, 27·12
Calcium Carbonate
  in electrified-particle testing, 28·2, 28·4
    advantages of, 28·8
Calcium Tungstate
  fluorescent intensifying screens in radiography, 23·8
  fluorescent screens, peak kilovoltage response of, 19·11
  in X-ray-intensifying screens, 16·16
Calibration
  automatic device for, in watch-spring sorting apparatus, 41·2

Calibration (*Continued*)
  bars for brittle coating tests, 52·4
    treatment in compression-strain measurements, 52·20
  in brittle-coating testing for pressure effects, 52·26
  in brittle-coating tests, and apparatus for, 52·1, 52·2
  of brittle resin coatings and bars for, 52·10–11
  of ceramic brittle-coating strain sensitivity, and bars for, 52·7
  in crack-depth and wall-thickness measurements by direct-current method, 35·1
  curves for electric-current testing of flat plates, 35·4–5
    for long and short perpendicular surface cracks in electric current testing, 35·7
  department for, at Institut Dr. Foerster, 2·27
  of eddy-current-test-instrument sensitivity, 37·30
  of fluoroscopes, 19·36
  of instrument for determination of conductivity-thickness product of metallic sheets, 39·17
  of instruments for ultrasonic contact testing, 48·15
  of linear time-base eddy-current instruments, 40·30
  of Magnatest Q eddy-current instruments, 42·33
    for sorting of steel parts, 42·54
  of Multitest eddy-current-test instruments, 40·21
  of photoelastic-coating-test machines, 53·35
  of plastic materials and instruments for photoelastic-coating tests, 53·13–14
  in ultrasonic testing, 43·37–47
    for ultrasonic testing of aluminum blocks with quartz transducers, 44·16
Camera Obscura, 10·5
Cameras
  close-focusing, for recording optical projector screen images, 12·37
  fluorographic, 19·44
  gamma, for radiography with Cobalt-60 and Iridium-192, 25·18
  high-speed, in photoelastic-coating tests, 53·22
  television, for closed-circuit systems, 19·45, 11·36–38
  X-ray, for study of powdered samples, 17·4–5
  X-ray diffraction, 17·5
Camshaft, true magnetic field strength at surface of magnetized, 33·17
Canal Rays, source of, 13·2
Candy, fluoroscopic inspection of, 24·19
Capacitance (See "Electric Capacitance")
Carbide-Tipped Tools, penetration time for, in liquid-penetrant testing, 6·8, 6·10, 6·14
Carbon
  absorption coefficients (mass) for γ and X rays and photon energies of, 18·32, 27·4
  attenuation coefficients of, for γ rays and X rays, 27·4
  hysteresis-loop effects, 42·26, 42·28
  in iron, determination from magnetic permeability, 42·1
  in iron rods, effect in eddy-current linear time-base tests, 40·35
  in steel, automatic statistical quality control indicator for, 41·13
    determination by point-pole method, 34·11
    eddy-current apparatus for determination of, 40·2–3

Carbon-14, energy and half-life of, as beta-ray source, 18·17

Carbon Dixode, solid
  chilling of brittle coatings with, for measurement of small strains, 52·23
  chilling of metal parts with, before fracturing as supplement to magnetic-particle testing, 32·24

Carbons, arc-lamp, eddy-current sorting by thickness of copper plating on, 41·2

Carbon Tetrachloride
  as masking agent for aluminum in radiography, 20·22
  ultrasonic-wave attenuation *vs.* frequency in, 43·26

Carborundum Cloth, in belt sanding as supplement to magnetic-particle testing, 32·25

Carburization, effects on hysteresis loops of carbon steel, 42·26, 42·28

Cardboard (See "Fiberboard")

Care (See "Maintenance")

Carrier Material (See "Backing Material")

Cars, Railroad (See "Railroad Cars")

Cascade Principle, in phototubes (multiplier), 11·31

Cascade Process, in X-ray-film washing, 21·9

Cascades, in radiation measurement with proportional counters, 16·5

Case Depth (See "Depth of Case")

Casting Process, for metals, motion-picture fluorography with image intensifier in study of, 19·45

Castings
  aluminum, electrical conductivity in eddy-current control of composition of, 42·14–15
    shrink porosity in, 24·9
    ultrasonic test blocks from, *vs.* forgings, 45·5
  aluminum and magnesium, ASTM reference radiographs for, 24·3
  aluminum-copper-magnesium, segregation effect on electrical conductivity of, 42·14
  borescopic inspection of, 11·14
  chipping at defects in, as supplement to magnetic-particle testing, 32·22
  cold shuts in highly stressed, 8·19
  copper, composition control by eddy-current test of electrical conductivity, 42·12
  cracked, evaluation of, 8·13
    radiograph of, 24·13
  cracks in, causes and repair of, 24·12
  cracks (thermal) in, magnetic-particle indications of, 32·9
  defects in, detection by ultrasonic reflection, 5·25
    fluoroscopic indications of, 24·27, 24·28
    liquid-penetrant indication of, 8·6
    radiographic interpretation of, 24·4
  die, ultrasonic contact testing of, 48·10
  drilling (core) or trepanning of, as supplement to magnetic-particle testing, 32·24
  dye-penetrant penetration time for, 6·14
  etching of cross-sections of, as supplement to magnetic-particle testing, 32·26
  fatigue cracks in light alloy, liquid-penetrant indication of, 8·17
  flame gouging of defective, before welding, 32·22
  fluoroscopy of, 24·19
  fluoroscopy of light-alloy, detectible defect size in, 24·24

Castings (*Continued*)
  gas holes in, detection by liquid penetrants, 8·3
    effect on strength, 24·7
  illumination of, for optical projectors, 12·13
  impregnation of porous, 24·8
  iron core-wire in nonferrous, location by magnetic means, 34·22
  magnetic-particle testing of, medium- and heavy-duty equipment for, 31·4–10
  mechanical testing of, to supplement radiography, 24·7
  penetration time for, in liquid-penetrant testing, 6·8, 6·10
  porosity (gas) in, magnetic-particle indications of, 32·9
  quality (dual) requirements in X-ray inspection, 24·1
  radiography of, 14·40
    filling cavities with shot for, 20·22
    with high-voltage X rays, 23·14
  radiography of cylindrical, apparatus for, 24·39
  repair of defective, by welding, 32·22
  sorting of tempered, by coercive-force tests, 34·8
  steel, faulty weld repair in, ultrasonic-contact test of, 48·20
    ultrasonic contact indications from, 48·20
    ultrasonic contact testing of, 48·10
  strength of, effect of gas porosity on, 24·8
  ultrasonic contact testing of, 48·10
    frequencies for, 48·1, 48·2
  ultrasonic gaging of, 50·20
  xeroradiographic image of defective, 22·2
  X-ray inspection of, machining considerations in interpretation, 24·7

Cast Iron
  carbon determination in, by coercive force and magnetic point-pole indications, 34·13
  ultrasonic-contact test frequency for, 48·2

Cast Nonferrous Metals, thickness measurements by magnetic-field tests, 34·16

Catalysts, X-ray diffraction analysis of, 17·16

Cathode-Ray Oscilloscope
  in Sonic Comparator circuit, 51·7, 51·9
  in ultrasonic immersion testing, 46·3

Cathode-Ray Tube Indication, capacitance and inductance modulated, in ultrasonic resonance testing, 50·8

Cathode-Ray-Tube Resonance Instruments, for thickness measurement, 50·34

Cathode-Ray Tubes
  ellipse method eddy-current apparatus and tests using, 40·23–29
  field-of-view adjustment on screen of, in Multitest instrument, 40·21
  screens of, eddy-current-test elliptical patterns on, 37·33
  vector-point apparatus and tests using, 40·20

Cathodes, X-ray-tube, 14·26, 14·35

Cavities
  concentric, detection by eddy-current testing, 38·20
  detection of, by eddy-current testing, 36·3
    by penetrating radiation, 5·12
  filling with shot in radiography, 20·22
  shrinkage, in castings, causes and X-ray interpretation of, 24·9, 24·11
    detectible size in fluoroscopy of, 24·24
    fluoroscopic indications of, 24·28

Cells, liquid-barrier, for X rays, 19·14

Celluloid, elasticity tension modulus of, 52·11

- **Cellulose Acetate,** adhesives for strain gages from, 54·10, 54·12
- **Cellulose Nitrate**
  - adhesives for strain gages and their curing, 54·12–13
  - adhesives from, for strain gages, 54·10
    - effect of degree of cure on hysteresis and zero shift of strain gages, 54·24
    - in strain gages, strain limits of, 54·25–26
    - strain gages bonded with, creep of, 54·28
- **Cement** (See also "Adhesives")
  - strain-gage, as damper of strain signals above minimum frequency, 54·27
    - effect of degree of cure of, on hysteresis and zero shift, 54·24
    - leakage resistance as indicator of drying of, 54·37
    - strain limits of, 54·25–26
  - for strain gages, 54·10
    - ceramic, inversion points of, 54·23–24
  - thickness of, beneath strain gages, 54·18
- **Cementing,** of strain gages (thin paper-base), 54·36
- **Central-Axis Maxima and Minima** (See "Fresnel Zone," "Ultrasonic Waves")
- **Ceramic Materials**
  - electrified-particle testing of, atmospheric water vapor effects in, 28·10
  - liquid penetrant, testing of, 29·8
  - magnetic properties of, crystal orientation and, 17·19
  - polycrystalline, as ultrasonic-wave transducers, 43·4
  - for ultrasonic-wave transducers, 44·2
- **Ceramics**
  - for brittle coatings, selection of, 52·8
  - brittle coatings of ceramic type, comparison with resin coatings, 52·1
    - for nondestructive testing, 52·7
    - preparation, application, and firing of, 52·16–17
    - specimen preparation for, 52·16
  - cements for strain gages at high temperatures, 54·10
    - inversion points, 54·23–24
  - dye-penetrant penetration time for, 6·14
  - fatigue cracks in, liquid-penetrant penetration time for detection of, 6·19
  - porosity in, detection with liquid penetrants, 8·22
  - testing of, with electrified or filtered particles, 5·5
  - testing of unfired, by filtered-particle methods, 5·3
  - tubes, wall-thickness determination with X rays, 24·36
  - ultrasonic contact testing of, frequencies for, 48·1
  - ultrasonic inspection of, 43·49
- **Cerium**
  - absorption coefficients (mass) for γ and X rays and photon energies of, 18·37
  - glass containing, for X-ray barriers, 19·13
- **Cerium-144**
  - energy and half-life of, as beta-ray and gamma-ray source, 18·17
  - radiation-dosage output of, 26·6
- **Cesium,** attenuation coefficients of, for γ rays and X rays, 27·32
- **Cesium-134**
  - energy and half-life of, as gamma-ray source, 18·17
  - radiation-dosage output of, 26·6
- **Cesium-137**
  - disintegration scheme of, 15·14
  - energy and half-life of, as beta-ray and gamma-ray source, 18·17
  - from fission of Uranium-235, 15·9
  - radiation dosage output of, 26·6
  - as radiographic source, 15·22
    - characteristics of, 15·13
  - in radiography, 2·17
    - equivalent voltage of, 25·17
  - radiography with, exposure-thickness curves for, 15·27
    - sharpness in, 15·35
  - reduction-factors for gamma rays from, 26·12–13
    - by lead, 26·11
  - steel radiography with, build-up curve for, 15·36
- **Cesium Chloride (Cs^{137}Cl)**
  - gamma-ray and neutron absorption of, 15·11
  - as radiographic source, 15·22
- **Chains,** bushings for, case-hardening depths of, Magnatest Q bands for, 41·17
- **Characteristic Function**
  - eddy-current test curves for, on complex impedance and complex voltage planes, 37·2
  - in eddy-current testing, 36·17, 36·18, 36·19
    - of cylindrical objects, 37·1–2
    - in reactance magnitude tests, 40·8
    - variation with frequency, on complex impedance and voltage plane, 37·2
- **Charged Particles,** absorption of, 13·24
- **Charts**
  - in optical projection systems, 12·17–20
  - for optical projectors, 12·17
    - making of, 12·20
    - materials for, 12·20
    - overlay, 12·19
    - radius, 12·17–18
    - reference, 12·17
    - replacement, 12·18–19
    - screen, 12·17–18, 12·27
    - screw thread, 12·18
    - tool-room, 12·18
  - transparent paper, for recording Magnatest Q eddy-current test results, 42·32
- **Chemical Equipment,** hydrogen blistering of, inspection by ultrasonic resonance testing, 50·28
- **Chemical Industry**
  - borescopic inspection in, 11·14
  - liquid-density control with radioisotopes in, 18·30
- **Chemically Induced Artifacts,** in electrified-particle testing, 29·7
- **Chemical Reactions**
  - in nondestructive testing, 4·11, 5·17
  - X-ray diffraction analysis in following, 17·14
- **Chemicals,** effect on X-ray film, precautions against, 20·41
- **Chilling** (See "Cooling")
- **Chipping**
  - cracks or seams as supplement to magnetic-particle testing, 32·22
  - to remove defects and determine their extent, 32·22
- **Chisels,** in trepanning as supplement to magnetic-particle testing, 32·24
- **Chlorine,** absorption coefficients (mass) for γ and X rays and photon energies, 18·34
- **Chromates**
  - effect on liquid-penetrant indication of defects, 8·6

Chromates (*Continued*)
- effect on penetrants in liquid-penetrant testing, 6·6

Chromium
- absorption coefficients (mass) for γ and X rays and photon energies of, 18·35, 27·15
- attenuation coefficients of, for γ rays and X rays, 27·15
- effect on electrical conductivity of aluminum, 42·14
- electrical conductivity of, 42·16

Chromium Alloys, nickel-, wire for strain gages, 54·6, 54·8–9

Cigarettes, density of, radiation in control of, 18·29

Cineradiography (See "motion-picture" under "Radiography")

Circle Diagram, for electric current in resonant circuit eddy-current testing, 40·43

Circuits, Electric (See "Electric Circuits")

Clad Metals
- lack of bond in, detection by ultrasonic test methods, 50·22
- ultrasonic resonance testing of, 50·23

Clamps, for specimens in sonic testing, 51·7

Clayware
- chasing out defects in, 9·17
- contaminants in, 9·16
- cracks produced by glaze application to, 9·16
- defect detection in, 9·9
- defects in unfired, 9·16
- determination of water contained in, 9·15
- filtered-particle testing of, 9·2
- prewetting of, in filtered-particle tests, 9·15

Cleaners, in liquid-penetrant test systems, maintenance of, 7·31

Cleaning
- of lead-foil screens for radiography, 20·28
- of metals after acid etching, 32·28
- of parts, effect of residual magnetism on, in magnetic-particle testing, 30·20
  - for liquid-penetrant testing, 6·13
  - for visible dye penetrants in field tests, 6·18
- of specimens
  - for ceramic-type brittle coatings, 52·16
  - for resin-type brittle coatings, 52·9
- of surfaces before application of photoelastic coatings, 53·15
  - for examination with magnifying glass as supplement to magnetic-particle testing, 32·20
  - for strain-gage application, 54·36
- vapor degreasing in liquid-penetrant inspection, 7·34
- of xeroradiographic plates, 22·15
- of X-ray-intensifying screens, 16·17

Cleanliness
- necessity for, in liquid-penetrant testing, 7·30
- in X-ray-film processing, 21·2

Clearing Time, in X-ray-film fixation, 21·7

Coal, suspensions of, radioisotopes in control of density of, 18·30

Coating
- with metals by vacuum deposition, eddy-current control of film-resistance during, 39·19
- with photoelastic liquids or sheets for photoelastic-coating tests, 53·15
- of photoelastic-test specimens with aluminum before application of plastic coatings, 53·15

Coating Number, in brittle-coating tests, 52·6

Coatings
- asphalt, indication of distribution of blended materials in, by electrified-particle testing, 26·6
- brine test for failures in, 29·13
  - limitation of, 29·13
- brittle, for nondestructive testing (See "Brittle Coatings")
- copper, on arc-lamp carbons, eddy-current sorting by thickness of, 41·2
- crack indication in metal-backed, by electrified-particle testing, 29·5
- eddy-current testing of, 39·12
- effect on electron emission and nondestructive tests using, 5·22
- effect on magnetic-particle testing, 30·8
- electrified-particle testing of, 28·4, 29·11, 29·13
- for fluorescent X-ray-intensifying screens, 16·16
- for fluoroscopic screens, 16·14
- glass, stress cracks in, 29·14
- insulating, on nonferrous metals, eddy-current testing of, 36·8
- on iron or steel, eddy-current thickness determination of, 36·7
- metallic, determination of thickness with X rays, 24·36
- on paper, radiation in control of, 18·29
- for parts to decrease surface-roughness effects in ultrasonic testing, 45·17
- photoelastic (See "Photoelastic Coatings")
- pinhole breakdown of, in electrified-particle testing, and its prevention, 29·5
- removal and addition of, in nondestructive-testing laboratories, 2·10
- spalled, eddy-current testing of, 36·7
- for strain-gage waterproofing, 54·38
- temperature-indicating, 5·24
- Tesla coil test for failures in, 29·13
- testing by phase microscopy, 10·18
- thickness control in metallizing of condenser paper, eddy-current apparatus for, 41·4
- thickness gaging of, 10·16–17, 18·27
  - with beta rays and X rays, 18·4
  - electromagnetic induction tests for, 5·20
  - fluorescent radiation in, 24·36
- thickness of nonferromagnetic, determination by magnetic field tests, 34·17
- for walls of X-ray-film-processing areas, 21·13

Cobalt
- attenuation coefficients of, for γ rays and X rays, 27·18
- effect on electrical conductivity of copper, 42·12
- properties of, 15·14

Cobalt-60
- disintegration scheme of, 15·14
- energy and half-life of, as gamma-ray source, 18·17
- gamma ray and neutron absorption by, 15·11
- gamma rays from
  - penetrating ability of, 15·5
  - photographic-film shielding against, 20·39
  - in radiography of steel, fluorescent-screen intensification factor in, 20·28
- radiation dosage output of, 26·6
- as radiographic source, characteristics of, 15·13
- in radiography, 2·17, 15·14
  - equivalent voltage of, 25·17
  - of pipelines, 3·14–15, 25·17

Cobalt-60 (*Continued*)
  radiography with, build-up curve for steel, **15·36**
    exposure-thickness curve for steel, **15·26**
    sharpness in, **15·35**
  reduction factor for gamma rays from, **26·12–13**
    by lead, **26·11**
  shielding of, **15·14**
Cobalt Alloys, Magnatest Q eddy-current test indications of, **42·33**
Coercive Force
  definition of, **34·2**
  in demagnetization of ferromagnetic substances after magnetic-particle tests, **30·21**
  equipment for measuring, **34·3**
  of ferromagnetic materials in eddy-current testing, **42·21**
  hardness in relation to, in magnetic-particle testing, **30·22**
  measurement of, **34·1**
    advantages of, **34·1**
    compensation for earth's field in, **34·3**
    at high temperatures, **34·4**
    probe-coil method for, range of applications in, **34·3**
  residual field relationship with, **34·9**
  residual magnetization as a measure of, **34·5**
  of steel, effects of annealing on, **42·25**
Coercive Force Meter, 34·2
Coercive Force Tests
  automatic sorting of production parts by, **34·5–7**
  on automotive parts, **34·7**
  on ball bearings, **34·7**
  carbon determination in cast iron by, **34·14**
  deep-drawing ability determination by, **34·10**
  on diesel motor parts, **34·7**
  on electrical relay parts, **34·9**
  mechanical properties determined by, **34·5**
  metallurgical properties determined by, **34·5**
  sorting by
    applications of, **34·7**
    of sheets, **34·10**
  on tempered cast parts, **34·8**
  tungsten carbide quality evaluation by, **34·4**
  on wrist pins, **34·7**
Coherent Scattering, in radiation absorption, **13·21**
Coils
  alternating-current, in demagnetization, after magnetic-particle tests, **30·23**
  arrangements of
    for eddy-current feed-through testing of cylinders, **37·15–18**
    for eddy-current testing of spheres and short parts, **39·3–4**
  automatic tilting or moving, in eddy-current testing, **41·8**
  demagnetizing, field-strength problems with, after magnetic-particle testing, **30·28**
  differential, for eddy-current testing of sound *vs.* defective cylinders, **37·22**
  distance between primary and secondary, in eddy-current testing of metallic sheets, determination of, **39·17**
  eddy-current, effect of length in sphere testing, **39·4**
  eddy-current test, and their circuits, **40·1–3**
  eddy-current test feed-through, **40·1**
    complex voltage and impedance planes for, **37·15**
    crack testing with, and ellipse method indications, **42·6**

Coils (*Continued*)
  eddy-current test feed-through (*Continued*)
    in measurement of electrical conductivity, **42·3**
  eddy-current test forked, **40·1**
    sensitivity diagram for, **39·15**
    for testing of sheet materials, **39·12**
  for eddy-current testing
    arrangement and impedance characteristics of, **36·1–2**
    normalized characteristics of, **36·20**
    tabular summary of shapes of, **36·4–9**
  electric impedance of single, in eddy-current testing, **36·19**
  geometry in eddy-current testing of sheet materials, **39·14**
  impedance plane for, around nonferromagnetic metal tubes in eddy-current testing, **38·24**
  inside test, **40·1**
  internal, in eddy-current testing of tubes, **38·15–18**
  of Magnatest Q eddy-current instrument, complex voltage plane of, **42·42**
  microprobe, for eddy-current detection of cracks inside holes, **40·47**
  primary and secondary, in eddy-current testing, **36·10**
  probe and yoke, use with Magnatest Q eddy-current testing, **42·59**
  probe eddy-current test, **40·1**
    crack detection in finished electrical contacts with Defectometer having, **42·10**
    in eddy-current testing, **42·10–12**
  searching, reactions in electric current rail testing, **35·12**
  secondary, in eddy-current testing, containing objects of smaller diameter than the coil, **36·17**
    voltage signals from, in eddy-current crack testing of ferromagnetic cylinders, **40·36**
  surface-probe, for eddy-current testing of tubes and holder assembly for, **38·35–39**
  systems for eddy-current testing of small-diameter tubing, **38·25–26**
  Tesla, for detection of failures in coatings, **29·13**
    for detection of high-voltage breakdown, **3·35**
  test
    for eddy-current ellipse-test instruments, and holders and inserts for, **40·28**
    for Magnatest FS-300 or Q instruments, **40·38**
  spacing of, to tube in eddy-current testing with probe coils, control of, **38·35–36**
Cold-Drawing, of steel (carbon), effect on Magnatest Q eddy-current wave forms, **42·52–53**
Cold Shuts
  in castings and molded plastic articles, X-ray detection and evaluation of, **24·12**
  detection of penetration time for
    in die castings, **6·19**
    with dye penetrants, **6·14**
    in liquid-penetrant testing, **6·8**, **6·10**
  evaluation of parts showing, basis for, **8·12**, **8·19**
  fluoroscopy in light-alloy castings, dimensional factors in, **24·24**
  liquid-penetrant indications of, **8·2**
Cold-Working, of metals, stresses from, eddy-current test permeability changes from, determination of conductivity changes independently of, **37·6**

- **Collimating Tubes,** in ultrasonic testing to decrease surface roughness effects, 44·19
- **Collimation,** of radiation for safety in gaging, 18·24
- **Color** (See also "Spectrum")
  - evaluation of, in visual inspection, 10·3–4
  - of fluoroscopic and photofluorographic screens, 19·9
  - of fluoroscopic screens, effect on visual response, 19·13
  - of fringes in photoelastic coating tests, 53·4–5
  - of paste for magnetic-particle testing, 30·15
  - vision, 10·2
- **Color Blindness**
  - effect on filtered-particle tests, 9·13
  - effects of, in visual inspection methods, 5·9
- **Colored Media,** in filtered-particle tests, 9·10
- **Colorimetry,** 10·5
  - phototubes in, 11·34
- **Color-Spray Devices,** for marking of defective rods in Magnatest D eddy-current crack testing, 41·10
- **Columbium,** electrical conductivity of, 42·16
- **Combustion,** hazards of liquid penetrants, 7·18
- **Communications,** in industrialized *vs.* remote areas in relation to work of nondestructive-testing organizations, 2·19
- **Compacting,** of tungsten rods and wire, Magnatest FW-200 eddy-current indications and microsections showing defects from, 42·7–8
- **Comparator Bridges** [See "Bridges (electric-circuits)"]
- **Comparators, Surface** (See "Surface Comparators")
- **Comparison,** measurement by, optical comparators in, 12·2
- **Compasses**
  - effect of residual magnetism on, 30·20
  - in magnetic-leakage-field indication, in magnetic-particle testing, 30·27
- **Compensation Systems,** for X-ray thickness gaging, 18·8
- **Compensators**
  - Babinet, in bi-refringence measurement, in photoelastic-coating tests, 53·27
  - complex
    - in linear time-base eddy-current instrument, 40·30
    - in Sigmaflux eddy-current instrument, 40·26
  - in Multitest eddy-current-test apparatus, 40·20
  - in photoelastic-coating testing, 53·6
    - with small-field instruments, 53·23–24
- **Complex Effective Permeability Plane** (See "Complex Permeability Plane")
- **Complex Impedance Plane** (See also "Complex Permeability Plane," "Complex Voltage Plane")
  - analysis of slit values in eddy-current linear time-base tests, 40·32
  - for coils around nonferromagnetic metal tubes in eddy-current testing, 38·23
  - for Cyclograph in eddy-current testing, 40·18
  - displays of Multitest eddy-current apparatus, 40·22
  - in eddy-current linear time-base tests of ferromagnetic cylinders, 40·34
  - in eddy-current testing, 36·20
    - analysis of ellipse patterns in, 40·24
    - basic form of, for nonferromagnetic cylinders for various fill factors, 37·2
    - of ferromagnetic cylinders with various relative permeabilities, 37·4
- **Complex Impedance Plane** (*Continued*)
  - in eddy-current testing (*Continued*)
    - of nonferromagnetic spheres, 39·8–10
    - of spheres, 39·4
  - in feedback-controlled impedance testing, 40·17–19
  - for feed-through coils for eddy-current testing, 37·15
  - for nonferromagnetic tubes of various wall thicknesses, 38·9, 38·11
  - response characteristics in eddy-current testing, 40·2–4
  - showing variation of lift-off direction with conductivity and crack directions in eddy-current testing, 40·44
  - test-coil characteristics plotted on, 36·1
  - for thin-walled nonferrous tubes in eddy-current testing, 38·1
- **Complex Permeability Plane** (See also "Complex Impedance Plane," "Complex Voltage Plane")
  - in eddy-current testing, 36·17–19, 36·20
    - basic form, for test objects smaller than secondary coil, 36·18
    - basic forms of, for cylinders, 36·14, 36·18
    - frequency ratio *vs.* effective permeability in, 36·13
    - for nonferromagnetic tubes of various thicknesses, 38·9, 38·11
    - for solid conducting cylinders, 36·14
    - use with various fill factors, 36·17
- **Complex Plane of Secondary Voltage,** in eddy-current testing, 36·20
- **Complex Plane of Transmission Coefficient *T*,** as function of frequency ratio in eddy-current testing of sheet materials, 93·14
- **Complex Voltage Plane** (See also "Complex Impedance Plane," "Complex Permeability Plane")
  - in eddy-current linear time-base tests, 40·32–33
  - in eddy-current testing, basic form of, for various fill factors for nonferromagnetic cylinders, 37·2
    - for comparison specimen test for crack detection, 37·29
    - for ferromagnetic cylinders with various relative permeabilities, 37·5
    - of Magnatest Q coils, 42·42
    - of nonferromagnetic spheres, 39·8–10
    - of spheres, 39·4
    - of thin-walled nonferrous tubes, 38·1
  - for feed-through coils for eddy-current testing, 37·15
- **Composition**
  - of alloys
    - eddy-current apparatus for sorting by, 40·2–3
    - eddy-current testing in classification by, 36·4–8
    - electrical conductivity changes related to, in eddy-current testing, 37·6
  - compensation for variations in, in thickness measurement of metallic sheets and foils with *RC* oscillator, 39·18
- **Compression**
  - -strain in brittle-coating tests, calibration for, 52·10
  - strains, measurement for steel crane hook in brittle-coating testing, 52·23
    - measurement in brittle-coating tests, 52·19
  - -tension sonic vibration radial mode of thin circular discs, 51·3

Compression Failures, in porcelain enamel, 29·9
Compressors
  blades, crack detector for light alloy, 40·47
  gas-turbine, magnetic-particle-testing apparatus for blades of, 31·10–11
  ultrasonic inspection equipment for rotor wheels of, 47·16–18
Compton Effect, 13·20
Compton Process, in X-ray (high-energy) absorption and scattering, 23·1
Compton Scattering
  in radiation absorption, 13·20
  radiation absorption in relation to, 18·2
  in uranium, 13·21
Computers, electronic, in stress calculation from strain-gage readings, 54·41
Concavity, at weld root, causes and radiography of, 25·11
Concrete
  loading of ore trestle of, strain-gage testing of, 3·25
  photoelastic-coating testing of, undercoating for, 53·15
  radiation-shielding equivalent of, 26·9–10
  reduction factors for gamma radiation by, 26·13
  as shielding material for radiation, aggregates and, 26·14
  siliceous, radiation-shielding equivalent of, 26·9
  strain gages for, length in relation to maximum aggregate size in, 54·11
  strains in structures of, measurement with resistance strain gages, 54·2
  ultrasonic contact testing of, frequencies for, 48·1
  ultrasonic inspection of, 43·49
Concrete Block, radiation-shielding equivalent of, 26·9
Conductivity, Electric
  determination of, of test object in eddy-current testing, 37·4
  in selenium electrodeposits, crystal orientation and, 17·19
Conductivity, Thermal, of alloys for strain gages, 54·8
Conductors, eccentricity of, in insulating covering, determination by magnetic field tests, 34·18
Conferences, technical, of Institut Dr. Foerster, 2·30
Coning, of X-ray beams in radiography, 23·8
Constantan
  electrical conductivity of, 42·16
  ribbon as lead-in to Constantan high-temperature foil strain gages, 54·32
Consultation, by central nondestructive-testing organization, 2·15
Consumer Goods, fluoroscopic inspection of, 24·18
Containers
  Aerosol, for liquid-penetrant test materials, 7·2
  borescopic inspection of, 11·15
  for cesium chloride radiographic sources, 15·22
  corrosion wall thinning of, detection of, 5·24
  fluoroscopy to check filling of, 24·19
  glass
   electrified-particle testing of, 29·11
   phototubes in detection of dirty, 11·34
   rim defects in, 29·11
  glass-lined
   craze pattern in, 29·13
Containers (*Continued*)
  glass-lined (*Continued*)
   electrified-particle testing of, 29·14
   effect of chemical residues on, 29·15
   pinholes in, 29·15
   cracks through, 29·15
   wavy cracks in, 29·14
  pressure, leak detection in, by liquid penetrants, 8·2
  pressurized spray, detection of leaks in, 5·5
  shipping and storage, for radiation sources, 26·15
  tank-type, for X-ray-film processing, 21·15–16
  for X-ray-film processing solutions, 21·2
Contaminants
  detection of defects containing, in liquid-penetrant testing, 6·9
  fluorescent, from oil from air nozzles, in liquid-penetrant tests, 6·17
Contour
  correction for, in ultrasonic testing, lenses for, 44·9–10
  of discontinuities, effects in ultrasonic testing, 45·24
  effects in ultrasonic testing, step blocks for study of, 45·13
  internal, duplication by tracer fixtures, 12·24
  of parts, effect in ultrasonic testing, 45·13–15
Contrast
  brightness, in fluoroscopy, 19·4
  of fluoroscopic images, 24·22
  in fluoroscopy, perceptible defect size in relation to, 19·28, 19·31, 19·32
  in fluoroscopy and X-ray inspection, 19·1
  local, sensitivity in xeroradiography, 22·9
  radiographic, 15·32, 15·35, 20·34–35
   calculation of, 15·36
   excessive or inadequate, causes and correction of, 21·19
   film and subject, 20·16–17
   lead-foil screens in increasing, 20·26
  of radiographic film, relation to density-exposure curve, 16·20
  X ray, in relation to thickness of half-value layer, 19·15
Contrast Ratio, of penetrants (dye and fluorescent), 7·20
Contrast Sensitivity (See "Sensitivity")
Conveyors
  belt, Magnatest Q eddy-current instruments with, 41·8
  in engine (aircraft) cylinder magnetic-particle testing, 31·12
  in liquid-penetrant testing, 7·8
  in magnetic-particle-testing set-ups, 31·10
Coolant, Liquid, for X-ray tubes, 14·3
Cooling
  of anodes of X-ray tubes, 14·33
  with Dry Ice before fracturing as suplement to magnetic-particle testing, 32·24
  of parts during sectioning with cut-off wheels, 32·24
  rapid, of brittle coatings to sensitize them for measurement of small strains, 52·23–24
   effect on brittle-coating tests outdoors, 52·21
  of X-ray generators, 14·38
  of X-ray tubes, 14·21, 14·22, 14·37
Cooling Apparatus, for liquid-penetrant testing, 7·7, 7·10
Copper
  absorption coefficients (mass) for γ and X rays and photon energies of, 18·35, 27·20
  acoustic and ultrasonic properties of, 43·8

Copper (*Continued*)
- acoustic impedance, density, and sound velocity in, **45·3**
- attenuation coefficients of, for γ rays and X rays, **27·20**
- composition control by eddy-current test of electrical conductivity, **42·12**
- constant K value in ultrasonic resonance tests, **50·3**
- eddy-current testing of, effective permeability calculations for, **36·20**
- effect on electrical conductivity of aluminum, **42·14**
- electrical conductivity of, **42·16**
- mass absorption coefficients of, for radiation, **18·2**
- melting of, oxygen-content control by eddy-current testing during, **42·13**
- plating on arc-lamp carbons, eddy-current sorting by thickness of, **41·2**
- radiographic equivalence factors for, **20·14**
- rods, effective permeability and induced secondary voltage of, calculation for eddy-current testing, **36·13**
- segregation in Al-Cu-Mg castings, effect on electrical conductivity, **42·15**
- shot, masking and filling cavities with, in radiography, **20·22**
- strain-gage lead wire of, **54·36**
- thickness measurement range with Sr-90 beta gages, **18·16**
- tubes, eddy-current testing of, magnetic field strength effects in, **38·16–17**
- ultrasonic contact testing of, frequencies for, **48·1**
- ultrasonic reflection coefficients at interfaces with other materials, **43·13**

Copper Alloys
- aluminum-, ultrasonic energy losses from internal oxidation of single crystals of, **43·25**
- aluminum-magnesium-
  - diameter variations of rods of, indications of Magnaflux FW-300 eddy-current instrument, **42·2**
  - eddy-current density and field strength in rods of, as function of radial position, **37·9**
  - electrical conductivity and hardness *vs.* quenching temperature of, **42·19**
  - hardness of pressed parts of, and its distribution with Multitest and Statimat eddy-current instruments, **41·16–17**
  - hardness *vs.* electrical conductivity of, **42·18**
  - segregation effect on electrical conductivity of cast, **42·15**
- beryllium-, for strain-gage-based transducers, **54·5**
- nickel-
  - effect of hydrostatic pressure on resistance of strain gages of, **54·30**
  - resistance-strain characteristics of, for strain gages, **54·25**
  - wire for strain gages, **54·6**, **54·8–9**

Cores
- effects in eddy-current testing of cylinders and tubes, **38·21**
- shifting of, in casting process, X-ray detection and evaluation of, **24·11**

Cornelius Eddy-Current Instrument, response characteristics of, **40·20**

Correlation Degree, in testing, **4·3**

Corrosion
- annual cost of losses by, **50·29**

Corrosion (*Continued*)
- detection
  - in pipes, portable thickness gage for, **18·30**
  - in tubes by eddy-current methods, **42·3**
  - of tube thinning from internal, by eddy-current testing, **38·17**
- determination of rate of, by ultrasonic resonance gaging, **50·26–27**
- eddy-current measurement of external and intergranular, frequency calculation for, **40·14**
- inspection
  - of gasoline plants and refineries, **50·35**
  - of storage tanks for oil, **50·35**
  - by ultrasonic test methods, **50·4**, **50·42**
- intergranular
  - of copper-nickel alloys in strain gages at high temperatures, **54·24**
  - inside small-diameter tubing, eddy-current indications of, **38·30**
- measurement of
  - limitations of ultrasonic test method for, **50·30**
  - of pulp digester, **50·39**
  - by ultrasonic resonance method, **50·30**
  - rate of, by Audigage, **50·41**
- prevention of, in liquid-penetrant systems, **7·30**
- product accumulation effect on ultrasonic resonance tests, **50·32**
- resonance, ultrasonic resonance equipment for studies of, **50·31**
- of steel plates, direct-current measurement of thinning of, **35·9**
- of strain gages (wet), effect on electric resistance, **54·25**
- stress
  - liquid-penetrant indications of cracks from, **8·18**
  - of tubes, internal test coils in eddy-current detection of, **38·15**
- ultrasonic study of, **43·49**
- wall thinning from
  - detection in pipes and tanks, **5·24**
  - determination by ultrasonic resonance tests, **50·29–35**

Costs (See also "Economics")
- of failures of parts, rise in, **1·6**
- of nondestructive testing, **1·10**
  - evaluation of, **1·12**
- saving in manufacturing, nondestructive testing in, **1·3**
- of standards which are arbitrary or inadequate, **1·22**

Counters
- fission, in neutron detection, **16·2**
- Geiger-Muller, **16·6**
  - in radiation detection in thickness gaging, **18·20**
  - in radiation monitoring, **26·5**
- Geiger-Muller and proportional, in thickness gaging, **18·7**
- in Magnatest Q eddy-current instrument, **41·8**
- proportional, for radiation, **16·5–6**
- scintillation, in radiation detection, **18·21**
- for X-ray analysis, **17·10**

Couplants (See "Coupling Media")

Coupling
- of source to test object in matter-and-energy tests, **5·15**
- ultrasonic-energy losses from, **43·25**
- in ultrasonic testing, problems in, **43·50**

Coupling Blocks, Plexiglas, in ultrasonic testing, **49·5**

Coupling Coefficients, electromechanical and mechanoelectrical, for common piezoelectric materials, **44·4**
Coupling Media
  temperature variations in, **48·4**
  in ultrasonic contact tests, **48·1**, **48·3**
    flow indications in, **48·31**
    selection of, **48·4**
  for ultrasonic resonance tests, **50·14**
Coupon Tests, comparison with nondestructive tests, **4·1**
Cracking, radial, in porcelain enamel, **29·11**
Cracks (See also "Discontinuities," "Seams")
  in abrasive-honing sticks, sonic detection of, **51·12–13**
  absorption by, in filtered-particle test of porous material, **9·3**
  acoustic impedance effects in ultrasonic testing for, **45·21**
  automatic statistical quality control indicator for, **41·13**
  in ball bearings, automatic eddy-current instruments for sorting by, **41·14**
  calibration curves and depth indications for, in electric-current testing, **35·7–9**
  in castings and welds, causes and repair of, **24·12**
  chipping at surface, as supplement to magnetic-particle testing, **32·22**
  cooling, in rolled bars, magnetic-particle indications of, **32·7**
  depth
    analysis of Magnatest Q screen patterns and impedance-plane characteristics for, **40·35**
    eddy-current linear time-base indications for, **40·32–33**
    eddy-current testing of, with Defectometer, **40·47**
    effect on frequency in eddy-current testing of nonferromagnetic cylinders, **40·11–15**
    equipment for direct-current measurement of, **35·2**
    indication with Sedac eddy-current-test apparatus, **40·18**
    measurement of, **3·21**
      by direct-current methods, **35·1**, **35·10**
      by eddy-current testing, **37·27–31**, **38·12**, **38·14**
      by Hall generators, in magnetic field tests, **34·20**
    in nonferromagnetic cylinders, calculation in eddy-current testing, **37·31**
    self-comparison eddy-current tests with Magnatest D instrument, **40·35**
  detection of
    in aircraft structures by radiography, **3·31**
    charts for selection of methods for, **1·29**
    by coil or longitudinal magnetization in magnetic-particle tests, **30·7**
    in cylinders by eddy-current testing, **37·4**
    by deep etching as supplement to magnetic-particle testing, **32·25**
    by eddy-current differential or self-comparison arrangements, **37·18**
    by eddy-current ellipse testing, **40·28**
    by eddy-current testing, **36·3**
      by comparison with crack-free specimens, **37·28**
      with compensation for undesired effects, **40·45**
      frequency selection for, **40·11**
      similarity law in, **37·11**
Cracks (*Continued*)
  detection of (*Continued*)
    by eddy-current testing (*Continued*)
      in spheres, **39·10**
      tabular summary of, **36·4**, **36·6–7**
    by electric-current tests, **5·20**
    in ferromagnetic materials, **5·13**
    by filtered-particle tests, **9·8**
    fluoroscopic, alignment and width factors in, and limitations of, **24·24**
    grinding and heat treat, by liquid-penetrant tests, penetration time for, **6·19**
    in grinding wheels and railroad car wheels, **5·24**
    independently of diameter variations in eddy-current testing of cylinders, **37·38–39**
    by liquid-penetrant testing, **5·4**
      black-light illumination level for, **7·15**
    liquid penetration time for, **6·8**, **6·10**
      for dye penetrants, **6·14**
      in nonferrous cylinders, **37·18–27**
    at parting line in aluminum alloy forgings, **46·22**
    in thin-walled tubes, eddy-current test frequency selection for, **38·7**
    in tungsten wire by eddy-current methods, **40·6**
  detection of fatigue
    alternating-current magnetization for, in magnetic-particle tests, **30·8**
  detection of surface and subsurface, in nonferromagnetic cylinders, frequency selection for, eddy-current tests for, **37·23**
  detector for
    magnetic-particle, **31·4**
    radiofrequency, **40·14**
  development in railroad rails, electric current indications of, **35·20**
  directions in eddy-current testing, impedance plane showing variations of conductivity and lift-off directions with, **40·44**
  eddy-current detection and measurement of, apparatus for, **40·2–3**
  eddy-current testing with feed-through coils and ellipse method indications, **42·6**
  edge, propagation studies by direct-current methods, **35·11**
  effective permeability variation from, calculation of, **37·15**
  effects of
    in cathode-ray-tube eddy-current ellipse tests, separation from diameter effects, **40·24–26**
    in eddy-current testing, separation from diameter effects, **37·33**
    in eddy-current testing of nonferrous cylinders, **37·32**
    in eddy-current testing with Cyclograph, **40·19**
    separation from stress effects in Magnatest D eddy-current testing, **42·61**
  etching or plating from residual stresses, **32·12**
    and their prevention, **32·26–27**
  evaluation of, in glass-to-metal seals, **29·17**
  fatigue
    of aircraft structures, **3·27**
    in aluminum pistons and light-alloy castings, **8·17**
    causes, prevention, and magnetic-particle indication of, **32·12**
    detection by ultrasonic reflection, **5·25**
    detection in aircraft maintenance, **3·34**

Cracks (*Continued*)
  fatigue (*Continued*)
    detection of, penetration time for, in liquid-penetrant testing, 6·8, 6·10
    evaluation of parts showing, 8·15
    fracturing at, as supplement to magnetic-particle testing, 32·23
    ultrasonic investigation of rate of growth of, 43·49
    ultrasonic shear waves in inspection of, 45·10
  in ferromagnetic cylinders, eddy-current detection of, 37·25
    frequency selection for eddy-current detection of, 37·26
  filing at, as supplement to magnetic-particle testing, 32·21
  in fired clayware, 9·17
  formation
    in clayware from glaze application, 9·16
    in porcelain enamels, 29·9
  in glass-to-metal seals, 29·15
  grinding, magnetic-particle indications of, 32·11
  grinding and fatigue, post-emulsification penetrants in detection of, 8·5
  growth in glass and porcelain enamels, 29·7
  heat-treating or quenching, magnetic-particle indications of, 32·11
  in holes (drilled), apparatus for eddy-current detection of, 40·47
  incipient, ultrasonic detection of, 43·49
  in Inconel tubing, eddy-current signals from, with encircling and probe coils, 38·38
  indications of
    in aluminum compressor rotor wheels, 47·18
    in magnetic-particle tests, 33·14
    in ultrasonic immersion testing, 47·34
  in iron rods, effects in eddy-current linear time-base tests, 40·35
  in large structural clay bodies, identification of, 9·18
  liquid-penetrant indications of, 8·2
  in magnetized bars and rings, effects in magnetic-particle testing, 30·3
  metallography of, as supplement to magnetic-particle testing, 32·28
  in molybdenum and tungsten wire and rod, microsections and Magnatest FW-200 eddy-current indications of, 42·7, 42·9
  netlike, in electrical contacts, detection with Defectometer eddy-current instrument with probe coil, 42·10
  in nonferromagnetic tubes, eddy-current data on, 38·12–15
  overheating effect on, during sectioning with cut-off wheels, 32·24
  in parts (hollow and solid), circular magnetization in detection of, in magnetic-particle tests, 30·5
  patterns
    in brittle-coating tests, photography of, 52·26
    detection
      in brittle coatings by electrified-particle method, 52·15–16
      in ceramic-type brittle coatings, 52·17
      in resin-type brittle coatings, 52·11-16
    dye-etched, in resin-type brittle coatings, 52·14
  through pinholes in coatings, 29·15
  in pipeline welds, definition and sensitivity in radiography of, 25·22

Cracks (*Continued*)
  radial, in abrasive wheels, sonic detection of, 51·14
  rejection of parts showing, basis for, 8·12
  in rods (metallic), eddy-current testing for, automatic handling apparatus for, 41·2
  sawing across, as supplement to magnetic-particle testing, 32·24
  sensitivity (maximum) to, in eddy-current testing of tubes, 38·17
  shrinkage, in welds, magnetic-particle indications of, 32·10
  signals (secondary-coil-voltage) from, in eddy-current testing of ferromagnetic cylinders, 40·36
    normalized components of, 37·20
  size of, indication by electrified-particle tests, 29·3
  sorting (automatic) for, with Multitest eddy-current instruments, 41·1
  in spherical objects, combined automatic tester and sorter for dimensions and, 41·19
  standard sample for, for electrified-particle testing, 28·11
  in steel parts, Magnatest D eddy-current testing of, 42·61–69
  in steel rods, automation of eddy-current testing of, 41·10
    comparative indications with Magnatest D eddy-current instrument and macro- and microsections, 42·62–69
    Magnatest D eddy-current instrument multiexposure picture of, 42·63
  stress, in glass coating, 29·14
  stress-corrosion, liquid-penetrant indications of, 8·18
  surface, eddy-current-test response to, in relation to frequency ratio, 37·10
    in cylinders, detection by eddy-current testing, 37·5
    examination with magnifying glass after magnetic-particle testing, 32·4
    indications in magnetic-particle tests, 32·1
    indications in ultrasonic contact testing, 48·25
    optical projection of, 12·14
    Rayleigh waves in detection of, 45·12
  testing by tangential magnetic-field gradient probe, 33·2
  thermal, in castings, magnetic-particle indications of, 32·9
  in tubes (thin-walled), effects of inside and outside, in eddy-current testing, 38·7
  types of, in glass-to-metal seals, 29·17
  ultrasonic detection of, multiple-frequency inspection in, 45·26
  in unfired clayware, 9·16
  in valve heads, liquid-penetrant indications of, 8·17–18
  wavy, on cast iron sanitary wave and glass-lined vessels, 29·14
  in welds, causes and radiography of, 25·7
  in wire, detection with Ziljstra eddy-current instrument, 40·19
  X-ray detection and evaluation of, and its limitations, 24·12
Crane Hooks, stresses in, fringe patterns of, 10·19
Cranes, strain-gage tests of, 54·3
Crankshafts
  cracks (grinding) in, magnetic-particle indications of, 32·14

Crankshafts (*Continued*)
  determination of case depth on, by magnetic point-pole tests, **34·13**
  eddy-current Magnatest Q testing of journals of, **42·55**
  fatigue cracks in, magnetic-particle indications of, **32·15**
  magnetic-field strength at surface of, in magnetic-particle tests, **33·15**
  of ships, ultrasonic pulse-reflection test of, **3·20**
Craters, liquid-penetrant indication of, in welds, **8·3**
Crazing, of brittle coatings on metals, expansion coefficient in relation to, **52·1**
Creep
  correction for
    in measurement of strains in brittle-coating testing, **52·19**
    in resin-type brittle-coating tests, **52·11–12**
  effect on strain gages, length in relation to, **54·11**
  minimizing effects of, in brittle-coating testing, **52·6**
  of strain-gage adhesives, **54·27–28**
    at high temperatures, **54·23**
Cross-Sections, pair, photoelectric, and scattering, for the elements for γ and X rays, **27·1–41**
Cross-Talk, effects in ultrasonic testing, **43·28**
Crystalline Solids, identification by X-ray diffraction, **17·10-12**
Crystallography, ultrasonic test, potential applications in, **43·49**
Crystals
  atomic structure determination by magnification of, **10·33**
  curved, in ultrasonic testing, **44·10**
  luminescent, in radiation detection, **18·21**
  as photoconductors, **16·8–11**
  preferred orientation of, **17·18**
  single, ultrasonic energy losses in, **43·25**
    X-ray analysis in determination of orientation of, **17·20**
  size in fluoroscopic screens, unsharpness and, **19·31**
  thickness in special ultrasonic test units, **43·7**
  transducer, **43·4–5**
    for ultrasonic contact testing, **45·6**
  for ultrasonic immersion testing equipment, **46·7**
Crystal Structure
  anisotropy of, effect on elastic constants and sound velocity, **45·7**
  factors insensitive and sensitive to, in eddy-current testing of ferromagnetic materials, **42·21**
C-Scan
  equipment and methods for presentation of ultrasonic test data, **43·34**
  ultrasonic test signals by, **46·4**
  units, for ultrasonic contact testing, **48·5**
Curie, definition of, **13·13, 15·5**
Curie Point, demagnetization by heating above, after magnetic-particle tests, **30·22**
Curing
  of plastic strain-gage materials, shrinkage stresses and negative creep from, **54·27**
  of strain-gage adhesives and cements, **54·13**
Curvature (See "Contour")
Curves, limit, for eddy-current testing large objects, **2·28**
Customers
  contacts with, value in quality-control programs, **1·18**
  inspection by, in independent laboratories, **2·11**
  satisfaction of, role of nondestructive testing in, **1·3**
Cutting Tools, Rejection
  of cracked, basis for, **8·14**
  for lack of bond of cutting insert with support, **8·13**
Cyclic Loading Failures, in porcelain enamel, **29·9**
Cyclograph Eddy-Current Instrument, response characteristics of, **40·18**
Cylinders
  apparent impedance for short, in eddy-current testing, **39·8**
  crack depth
    in metallic, self-comparison eddy-current testing of, **40·36**
    in nonferromagnetic, calculation in eddy-current testing, **37·31**
  crack detection in nonferrous, independently of diameter variations, **37·39**
  cracks in ferromagnetic, eddy-current detection of, **37·25**
  crack testing of, with feed-through coils, and eddy-current ellipse-method indications, **42·6**
  diameter and electrical conductivity of, measurement by eddy-current methods and tolerances for, **37·36**
  diameter effects in eddy-current testing, suppression of, **37·21**
  distribution of eddy-current and field strength in, model for verification of calculated, **37·12**
  eddy-current and magnetic-field strength distribution in, **37·6–10**
  eddy-current testing of, **37·1–39**
    mercury-model tests of effects of discontinuities in, **37·13**
  eddy-current testing of metallic, frequency selection for, **40·11**
  eddy-current testing of solid, tabular summary of, **36·4, 36·7, 36·9**
  eddy-current testing of solid nonferrous, **37·18–39**
    instrument for, **37·32**
  effective permeability in eddy-current testing of, **36·12**
  effective permeability of solid, in eddy-current testing, **38·9**
  ferromagnetic, complex voltage plane of test coil containing, in eddy-current linear time-base tests, **40·33**
    crack-depth analysis in eddy-current testing, **40·35**
    eddy-current testing of, separation of effects of electrical conductivity, diameter, and magnetic permeability in, **37·4**
    reactance testing of, diameter variations corresponding to 5% crack depth in, **40·14**
  gas, ultrasonic resonance testing of, **50·27**
  nonferromagnetic
    calculation of frequency ratios for temperature compensation in eddy-current testing of, **40·13**
    effects of conductivity and diameter on secondary-coil voltages in, **37·35**
    frequency-ratio determination in, **37·27**
    frequency variation with
      conductivity in, **40·8**

Cylinders (*Continued*)
  nonferromagnetic (*Continued*)
    frequency variation with (*Continued*)
      cracks in, 40·11
      diameter in, 40·10
    permeability quotient for, as function of frequency ratio, in eddy-current tests, 37·37
    separation of effects of conductivity and diameter in, 37·1–2
    sensitivity diagrams for conductivity and diameter effects in, 37·35
  off-center scanning of, in ultrasonic immersion testing, 46·19
  radiography of, apparatus for, 24·39
  shape permeability for eddy-current testing of short, 39·6, 39·8
  solid, complex permeability plane for, 36·14
  ultrasonic inspection of, from inside and outside, transducers for, 44·9
Cylindrical Parts, disturbances in ultrasonic contact testing caused by, 48·28
Cylindricator
  for determination of sound path in off-center scanning of cylindrical parts, 46·21
    scanning of cylindrically shaped parts, 46·19
  setting up, 46·19
Cystoscopes, 11·15

D

Damping, of ultrasonic-transducer crystals, effect on band width, 44·19
Dams
  concrete, strain measurement in, with resistance strain gages, 54·2
  stress measurement in, telemetering of photoelastic coating, 53·35
Darkness, adaptation to
  for filtered-particle test with fluorescent media, 9·13
  for fluorescent-penetrant inspection, 7·11
  in fluoroscopy with red and white light, 19·25
  in testing with fluorescent magnetic particles, 30·20
Darkrooms, mobile, for radiographic-film processing, 25·21, 25·23
Data Sheets, for strain-gage tests, 54·38–41
Dead Time, of Geiger-Muller counters, 16·7
Decarburization
  edge, of alloy steel wire, effect on Magnatest Q eddy-current instrument spread bands, 42·52
  measurement of, by eddy-current methods, 36·4
Decay, competitive, in U-238 series, 15·1
Decimal Equivalents, numerical digits *vs.*, in optical projection system, 12·6
Decomposition, of strain-gage adhesives at high temperatures, 54·24
Deep-Drawing Ability, measurement by coercive force, 34·10
Defectometer
  in eddy-current crack testing, lift-off effect suppression with, 40·47
  eddy-current indications of porosity with, in light-metal blocks, 40·46
  with probe coil in eddy-current crack detection in finished electrical contacts, 42·10
Defects (See also "Discontinuities")
  in abrasive-honing sticks, orientation with respect to direction of vibration in sonic testing, 51·13
  area of, estimation by ultrasonic immersion testing, 46·15
  automatic location of, in ultrasonic contact testing, 48·6

Defects (*Continued*)
  in ball bearings, automatic eddy-current instruments for sorting for, 41·15
  depth, relation to resonant frequencies in sonic testing of abrasive-honing sticks, 51·13
    ultrasonic measurement of, 45·9
  depth and orientation in relation to sonic vibration frequencies and nodes in sonic testing of abrasive wheels, 51·14
  depth localization of, by stereoradiography, 20·46–47
  detectibility in ultrasonic testing with B-scan systems, 43·33
  detection of
    in abrasive articles by sonic testing, 51·12–14
    charts for selection of methods for, 1·29
    in cylinders by eddy-current testing, 37·8
    by eddy-current testing, tabular summary of, 36·4–7
    in flash-butt welds, 49·16
    instrumentation for ultrasonic, 50·8
    in thin-walled stainless-steel tubes, eddy-current apparatus for, 40·14
  detection of shallow, 6·12, 6·17
  detection of small, by post-emulsification fluorescent liquid-penetrant process, 6·9
  detection of subsurface, by electrified-particle tests, 29·4
  detection of surface, by liquid penetrants, 6·1, 8·1
  in electric conductors carrying current, effect on surrounding magnetic field, 35·12
  evaluation of, with cylindricator, 46·19
    by ultrasonic immersion tests, 46·12
  extrusions having, basis for rejection of, 8·20
  fluoroscopy of, detectible size of, 24·24
  identification of, in fluoroscopy, 19·36
  indication of, by ultrasonic immersion tests, 46·17
  laminar, detection by ultrasonic inspection, 49·10
    detection by ultrasonic resonance testing, 50·28
    Lamb waves in detection of, 45·12–13
  length and width of, measurement by stringer technique, 46·12
  location of position of, by ultrasonic immersion testing, 46·18
  minimum discernibility curves for, in fluoroscopy, 19·5
  minimum observable, in fluoroscopy, 19·3, 19·27, 19·28, 19·29, 19·31
  in molybdenum and tungsten rods and wire, indications with Magnatest FW-200 eddy-current instrument, 42·6–10
  nature of, radiographic standards and, 19·46
  orientation and location of, in ultrasonic immersion testing, 47·12
  oriented at an angle to surface, 47·13
  in parts (semi-finished), quality number in statistical testing for, 41·18
  percentage in nondestructive testing, cost in relation to, 1·15
  probe-coil eddy-current B-scan indications of, for tubing, 38·37
  in radiographs, causes and correction of, 21·18–22
  in railroad rails
    classification of, 35·20
    and electric current test indications of, 35·20
    marking of, 35·21
    searching-coil reactions in electric current testing of, 35·12
  removal of, chipping and grinding in, 32·22

Defects (*Continued*)
  removal of surface, in nondestructive-testing laboratories, **2·10**
  sensitivity to, in eddy-current testing of small-diameter tubing, **38·29**
  size, orientation, and distribution in relation to ultrasonic contact test equipment selection, **48·5**
  size of, indication developing time and persistence in relation to, in liquid-penetrant testing, **8·4**
  spherical, ultrasonic indications of, **45·24**
  in steel parts, automatic unit for simultaneous eddy-current detection of, and sorting by composition, **42·68**
  surface
    magnetic-particle-test indications of, **32·1**
    Rayleigh waves in detection of, **45·12**
  tubing internal and external, effect on eddy-current gaging of diameter and wall thickness, **38·33, 38·35**
  types detectible by ultrasonic methods, **43·49**
  ultrasonic depth indication of, distance or time scale markers for, **43·30**
  ultrasonic detection of, **43·47**
    British practice of, **49·1**
    by loss-of-back-reflection method, **43·24**
    by through-transmission method, **43·27**
  ultrasonic immersion indications of, **47·1**
  ultrasonic pulse-time detector for, **43·28**
  ultrasonic test indications of, factors affecting, **45·1**
  in welds, ultrasonic contact indications for, **48·17, 48·18**
  in welds in pipelines, sources of, **25·25–26**
  in xeroradiographic plates, **22·16**
Definition (Image)
  of fluoroscopic images, **24·22**
  in fluoroscopy and X-ray inspection, **19·1**
  improvement in fluoroscopy by X-ray projection magnification, **19·1**
  radiographic, **20·34–35**
    in pipeline-weld inspection, **25·22**
  in radiography with fluorescent intensifying screens, **20·28**
  in X-ray (high-energy) inspection, **23·4**
  of X-ray images, causes and correction of poor, **21·19**
  in X-ray inspection by closed-circuit television, **19·41**
Deformation
  inhomogeneous, effects on Magnatest Q eddy-current testing, **42·43**
  irreversible, in tensile testing of steel, Magnatest Q eddy-current indications of, **42·60**
  lattice, X rays in study of, **17·14**
Degreasing (See "Cleaning")
Demagnetization
  automatic apparatus for, in mechanized magnetic-particle-testing set ups, **31·10**
  by free poles, in magnetic-field and magnetic-particle tests, **33·15**
  hardness in relation to, after magnetic-particle testing, **30·22**
  heavy-duty a.-c. half-wave magnetization unit with automatic apparatus for, in magnetic-particle tests, **31·6**
  intensity of, from free poles, in magnetized test objects, **33·15**
  after magnetic-particle testing, **30·20–25**
    equipment for, **31·15**
    limitations with circularly magnetized parts and testing of, **30·27–28**
Demagnetization (*Continued*)
  magnetization apparatus with automatic devices for, for magnetic-particle testing, **31·9**
Demagnetization Factor, 34·9
  calculation of, **33·16**
  definition of, **33·16**
  for eddy-current testing of short cylinders, **39·6**
  in eddy-current testing of spheres, **39·4**
Demagnetizers, alternating-current coil, for magnetic-particle testing, **30·24**
Dense Materials, radiography with high-voltage X rays, **23·15**
Densitometers
  for measuring blackness of exposed photographic plate or film, **10·5**
  micro-
    for dual—pinhole fine—structure test, **10·30**
    for evaluation of line patterns obtained from Schlieren methods, **10·22**
    in X-ray measurements, **24·35**
  for photographic film, **20·32**
Density
  of cigarettes, liquids, and suspensions, radiation in control of, **18·29**
  control and measurement of, **5·13**
  effect on natural frequency of sonic vibration of bodies, **51·1**
  measurement by sonic resonance vibration tests, **51·6**
  of piezoelectric materials, **44·4**
  of strain-gage alloys, **54·8–9**
Density (Photo)
  curves *vs.* exposure in radiography, **16·19**
  definition of, **16·19**
  of radiographic film, exposure to gamma or X rays in relation to, **16·22**
  of radiographic images
    causes and correction of excessive or inadequate, **21·18–19**
    factors controlling, **20·3**
Dentures, porcelain, electrified-particle testing of, **29·17**
Deoxidation (See "removal" under "Oxygen")
Depth (See "Dimensions")
  of penetration in eddy-current testing (See "Penetration Depth")
Depth of Case
  automatic statistical quality control indicator for, **41·13**
  of chain bushings, Magnatest Q bands for, **41·17**
  determination
    by coercive force, **34·5**
    by eddy-current testing, **2·25, 36·4**
    by magnetic point-pole tests, **34·13**
  Magnatest Q eddy-current testing of, **42·58**
  ultrasonic control of, **43·49**
Dermatitis
  from liquid penetrants and its prevention, **7·19**
  from suspension media for filtered-particle tests, **9·13**
Desensitization
  factor in strain-gage sensitivity control, **54·19**
  single-, two-, and four-gage strain-gage, **54·19–20**
  of strain gages (See "Sensitivity," "Strain Gages")
  of strain gages and circuits, parasitic and planned, **54·19–21**
  of Wheatstone-bridge strain-gage circuits, applications of complete, **54·20–21**
Design
  evaluation by photoelastic-coating tests, **53·36**

Design (*Continued*)
- of machinery and structures, strain gages in, **54·32**
- of products, role of nondestructive testing in, **1·3**
- of structures, stress analysis in, brittle coatings *vs.* strain gages for, **52·18**

Designer, as information source in nondestructive testing, **1·19**

Destructive Testing
- definition, **4·1**
- comparison with nondestructive, **4·4**
- magnetic-particle-test supplemented by means of, **32·22–30**
- as supplement in nondestructive test program, **1·19**

Detector Response, in radiation transmission thickness measurement, **18·5**

Detectors
- in motion-of-matter tests, **5·2**
- phase-sensitive, in eddy-current testing of small-diameter tubing, **38·28**
- point or volume, for penetrating radiation, **5·10**
- for transmission-of-energy tests, **5·9**
- for X-ray thickness gages, **18·7**

Detector Sensitivity, limitations in, effect on test feasibility, **4·9**

Detector Unit Carriage, for electric current railroad-rail testing, **35·16**

Detergency, of liquid penetrants, **7·19**

Deterioration, of strain gages at elevated temperatures by selective oxidation and its compensation, **54·23**

Developers, Liquid-Penetrant
- action of, in liquid-penetrant testing, **6·2**
- application of
  - in field tests with visible-dye penetrants, **6·19**
  - in liquid-penetrant testing, **6·4**
  - in post-emulsification-penetrant process, **6·15**
- dry
  - application in liquid-penetrant field tests, **6·17**
  - application in using liquid-penetrant testing, **6·9**
- handling, precautions in, **7·35**
- for liquid-penetrant testing, maintenance of dry, solvent, and wet types, **7·31**
- in liquid-penetrant testing and their control and maintenance, **7·28–29**
- removal from parts in penetrant testing, **7·29**
- selection of, for liquid-penetrant testing, **8·5**
- temperature limitations of, in liquid-penetrant testing, **7·34**
- types of, for liquid-penetrant testing, **6·2**
- for water-emulsifiable fluorescent penetrants, **6·12**
- wet
  - application in liquid-penetrant testing, **6·7**
  - for fluorescent-penetrant testing, field application of, **6·17**
  - in liquid-penetrant testing, and their control and maintenance, **7·29**

Developing Apparatus, for liquid-penetrant testing, **7·4, 7·7, 7·10**

Developing Powder, for xeroradiography, **22·1**

Developing Time, in post-emulsification dye-penetrant process, **6·15**

Development
- of electrostatic images in xeroradiography, **22·1**
- over- and under-, of X-ray film, causes and correction of, **21·18–19**

Development (*Continued*)
- of xeroradiographic images and powders for, **22·13**
- of X-ray film
  - and its arresting, **21·4–5**
  - stains and streaks associated with, **21·21**

Devitrification, detection in silica glass by X-ray diffraction, **17·16**

Diameter (See also "Dimensions")
- compensation for, in sorting for composition or conductivity with Multitest eddy-current instrument, **40·22**
- of cylinders
  - in eddy-current testing, effects of, **37·1–6**
  - measurement by eddy-current methods, and tolerances for, **37·38**
  - suppression of effects of, in eddy-current testing, **37·21**
- of discontinuities, ultrasonic measurement of, **45·24**
- disc (thin circular) sonic vibration mode along, **51·3**
- eddy-current measurement of
  - accuracy and sensitivity of, **42·1**
  - independently of conductivity, with σ-D eddy-current instrument, **40·40**
- effect on frequency in eddy-current testing of nonferromagnetic cylinders, **40·10**
- effects
  - in cathode-ray-tube eddy-current ellipse tests, separation from crack effects, **40·24**
  - on complex voltage plane for Magnatest Q eddy-current test coil, **42·47**
  - in crack-depth analysis of Magnatest Q screen patterns and impedance-plane characteristics, **40·34–35**
  - in eddy-current linear time-base tests on ferromagnetic cylinders, **40·32**
  - in eddy-current testing, separation from crack effects, **37·38**
  - in eddy-current testing of cylinders, frequency selection for separation from conductivity effects, **37·2–3**
  - in eddy-current testing of ferromagnetic cylinders, separation from effects of conductivity and magnetic permeability, **37·4–6**
  - in eddy-current testing of nonferromagnetic cylinders, sensitivity diagrams for, **37·34**
  - in eddy-current testing of nonferrous cylinders, instrument for determination of, **37·32**
  - in eddy-current testing with Cyclograph, **40·19**
  - on effective permeability quotient for eddy-current tests of nonferromagnetic cylinders as function of frequency ratio, **37·35**
  - on secondary-coil voltages in eddy-current testing of nonferromagnetic cylinders, **37·35**
  - separation of, from conductivity and permeability effects in Magnatest Q eddy-current sorting, **42·39**
- of holes in aluminum blocks, ultrasonic-wave amplitude in relation to, **44·17**
- of holes (test), ultrasonic wave amplitude-distance curves for various, **43·39**
- inside, of tubes (thick-walled nonferrous), effect of variations of, in eddy-current testing, **38·8–11**
- measurement by eddy-current testing, tabular summary of, **36·4**
- of molybdenum and tungsten wire, eddy-current testing of, **42·3**

Diameter (*Continued*)
  of nonferromagnetic cylinders, effect in eddy-current testing and separation from effects of conductivity, **37·1–2**
  permeability direction in Magnatest Q eddy-current testing, angle with conductivity direction as function of frequency ratio, **42·42**
  ratio in eddy-current testing of solid cylinders and tubes, **38·19**
  of rods, tubes and wire, determination by eddy-current ellipse methods, **40·28**
  of rods of Al-Cu-Mg alloy, indications of Magnatest FW-300 eddy-current instrument, **42·2–3**
  sensitivity (maximum) to, in eddy-current testing of nonferromagnetic cylinders, **40·12**
  of spheres
    effects in eddy-current testing, **39·4**
    in relation to test coils, effects in eddy-current testing, **39·4**
  tube inside, effect in eddy-current testing with internal coils, **38·15**
  of tubes (nonferromagnetic), effect on eddy-current-test normalized apparent impedance planes, **38·3–5**
  of tubes (small), eddy-current gaging of, **38·31**
  of tubes (thin-walled), effective permeability variation with, in eddy-current testing, **38·6**
  variations
    corresponding to 5% crack depth in reactance testing of nonferromagnetic cylinders, **40·14**
    in cylindrical specimens, comparison specimens in evaluation of, in eddy-current testing, **37·30**
    in ferromagnetic cylinders, suppression of effects of, in eddy-current testing, **37·25**
    indications on Sigmaflux eddy-current instruments, **40·26**
  wavelength (ultrasonic) ratio for standard hole sizes in aluminum and stainless steel, **45·20**
Diamonds
  in gamma-ray detection, **18·21**
  X-ray diffraction patterns of, **17·11**
Diaphragming, of X-ray beams in radiography, **23.8**
Diaphragms, in scattering prevention in radiography, **20·22**
Die Castings
  cold shuts and porosity in, liquid-penetrant penetration time for detection of, **6·19**
  cold shuts in, evaluation of parts showing, **8·20**
  dye-penetrant penetration time for, **6·14**
Die Forgings, defects in
  detection by ultrasonic inspection, **47·5**
  ultrasonic immersion indications of, **47·10**
Dielectric Constant
  of barium titanate, effects in transducer use, **44·2–4**
  of piezoelectric materials, **44·4**
Dielectric Heating, in nondestructive testing, **5·17**
Dielectrics, testing of, displacement currents in, **5·21**
Diesel Motor Parts, sorting by coercive-force tests, **34·7**
Diesel Motors, injection-nozzle hole for, hardness measurement by magnetic point-pole tests, **34·14**
Difference-Coil Method, for eddy-current testing of metal rods, automatic handling apparatus for, **41·3**
Differential Absorption
  in filtered-particle testing, **9·4**, **9·14**
    effect of porosity of test object on, **9·4**
Diffraction
  of electrons, patterns of, **5·15**
  ultrasonic-energy losses from, **43·25**
  of ultrasonic waves, **43·21**
Diffraction-Grating Effect, in ultrasonics, **49·6**
Diffraction Methods, in optical testing, **10·26–33**
Diffraction Rings, formation of light, **10·26**
Diffusion, measurement in alloys and metals by eddy-current methods, **36·4**
Dilution, liquid-density control with radioisotopes in, **18·30**
Dimensional Testing, of workpiece, **12·1**
Dimensions
  of discontinuities
    in cylinders, effects in mercury-model tests, **37·14**
    ultrasonic measurement of, **45·24**
  effect
    on natural frequency of sonic vibration of bodies, **51·1**
    of variations in, suppression in eddy-current feedback-controlled impedance testing, **40·20**
    on vibration frequency in sonic testing, **51·11**
  limitations in nondestructive testing, **1·20**
  measurement of
    eddy-current apparatus for, **40·2–3**
    by eddy-current testing, **36·3**
      without contact, **42·2**
      tabular summary of, **36·4–8**
    by sonic resonance vibration test, **51·6**
    strain-gage-based transducers in, **54·3**
  of spherical objects, combined automatic tester and sorter for cracks and, **41·19**
  of tubes (small-diameter)
    distinguishing variations in, from those resulting from discontinuities in eddy-current testing, **38·26**
    effects in eddy-current testing, **38·24**
  variations, compensation for, in sorting for composition or conductivity with Multitest eddy-current instrument, **40·22**
  of wire, eddy-current measurement of, suppression of undesired signals in, **40·40**
Dip-and-Drain Apparatus, for liquid-penetrant testing, **7·3**, **7·6**
Direct Current (See "Electric Current")
Directional Effects, in ultrasonic testing, **45·21**
Directivity, in ultrasonic testing, **43·48**
Dirt, effect on magnetic-particle testing, **30·1**
Discontinuities (See also "Defects")
  contour of, effects in ultrasonic testing, **45·24**
  detection by eddy-current testing, **36·3**
    similarity law in, **37·11**
  detection by ultrasonic resonance tests, **50·2**, **50·5**
  in eddy-current testing of tubes, **38·1**
  effects in ultrasonic testing, **45·18–22**
    geometry of, **45·22–27**
  geometry of, ultrasonic determination of, **45·24**
  metallography of, as supplement to magnetic-particle testing, **32·28**
  nonbonded, in ultrasonic testing, reversed polarity from, **45·21**
  probing of, as supplement to magnetic-particle testing, **32·21–22**
  radiation patterns and reflections from small, in ultrasonic testing, **45·20**
  rejection of parts showing laminar, **8·19**

- **Discontinuities** (*Continued*)
  - sawing across, as supplement to magnetic-particle testing, **32·24**
  - sensitivity to, in eddy-current testing of small-diameter tubing, **38·29, 38·31**
  - short, in steel rods, Magnatest D eddy-current wave forms and macro- and microsections of, **42·68**
  - simulation with models, for eddy-current testing, **37·13–15**
  - subsurface
    - magnetic-particle-test indications of, and comparison of wet and dry methods, **32·3**
    - microscopic examination of magnetic-particle patterns from, **32·20**
    - in welds, magnetic-particle indications of, **32·10**
  - surface
    - alternating-current magnetization for magnetic-particle detection of, **30·8**
    - magnetic-particle-test indications of, **32·1**
  - thickness of, effects in ultrasonic testing, **45·22**
  - in tubes (small-diameter)
    - distinguishing effects of, from effects of dimensional variations in eddy-current testing, **38·26**
    - effects of, in eddy-current testing, **38·24**
  - ultrasonic echo
    - amplitudes from, **45·18**
    - losses from adversely oriented, **45·23**
    - losses from, **45·16**
  - ultrasonic immersion indications of, **47·3**
  - ultrasonic multiple-frequency inspection of, **45·25–26**
  - ultrasonic testing of, interpretation guide for, **45·26–27**
  - ultrasonic-wave scattering by, in testing, and its compensation, **45·6**
  - in welds, radiographic interpretation of, **25·2–15**
- **Discs**
  - sonic vibration frequency equations for, **51·5**
  - sonic vibration modes of, **51·3, 51·4**
- **Disintegration,** of radioactive atoms, **15·2–4**
- **Dislocations,** ultrasonic-energy losses from, **43·25**
- **Displacement**
  - of particles in ultrasonic beams, **43·12**
  - strain-gage-based transducers in measurement of, **54·3**
- **Distortion**
  - of forgings for rotors, proof tests for, **5·24**
  - of gamma- and X-ray images, **20·6–7**
  - of honeycomb structures, fluoroscopy of, **24·29**
  - of stainless steel brazed honeycomb, radiograph of, **24·15**
- **Doors,** opening of, phototubes in, **11·34**
- **Dosimeters,** pocket, for radiation monitoring of personnel, **26·4**
- **Double Exposures,** in stereoradiography, **20·47**
- **Double-Pole Tests,** on magnetized parts in interfering fields, **34·14**
- **Double-Pulse Generator,** for ultrasonic testing, **44·21**
- **Double Refraction** (See "Bi-Refringence")
- **Double Spectrometer,** monochromatic X rays from, **13·10**
- **Double-Transducer Ultrasonic Fault-Warning Systems, 49·20**
- **Double Transducer Ultrasonic Tests, 49·1–21**
  - application of, **49·12**
  - gap-scanning techniques in, **49·3**
- **Draining Apparatus,** for liquid-penetrant testing, **7·9**
- **Drain Marks,** avoidance and identification of, in filtered-particle tests, **9·18**
- **Drift Velocity,** of gases for ionization chambers, **16·2**
- **Drilling**
  - core, as supplement to magnetic-particle testing, **32·24**
  - of oil wells off-shore, strain-gage tests in design of barges for, **54·33**
- **Drills**
  - core, to supplement magnetic-particle testing, **32·24**
  - eddy-current testing of, automatic tilting or moving coils in, **41·8**
  - hardness of tips of
    - automatic sorting by, with Multitest eddy-current instruments, **41·1**
    - Multitest eddy-current instrument in testing of, **40·23**
  - twist, etching cracks in, **32·27**
- **Dross,** in castings
  - fluoroscopic indications of, **24·27**
  - gas holes containing, fluoroscopy of, **24·24**
  - gas holes from, **24·5**
- **Dry Ice** (See "solid" under "Carbon Dioxide")
- **Drying**
  - of brittle resin coatings, **52·9**
  - of developer in liquid-penetrant testing by post-emulsification process, **6·13**
  - in liquid-penetrant testing, temperature limits of, **7·34**
  - of parts
    - in liquid-penetrant field tests, **6·17**
    - in post-emulsification dye-penetrant process, **6·15**
  - of strain-gage cement, leakage resistance as indicator of, **54·37**
  - of strain gages after cementing, **54·36**
  - of surfaces for electrified-particle testing, **28·11**
  - of wet developers, in liquid-penetrant testing, **6·8**
  - of X-ray film, streaks associated with, **21·21**
- **Drying Apparatus**
  - for liquid-penetrant testing, **7·4, 7·7, 7·10**
  - for X-ray films, **21·9, 21·10, 21·16**
- **Dual Image System,** for comparison by optical projectors of two workpiece outlines, **12·35–37**
- **Dual—Pinhole Fine—Structure Test**
  - applications of, **10·30**
  - for minute local inhomogeneities, **10·29**
- **Duplicating,** with optical projectors of workpiece sections, **12·22**
- **Durometer,** instrument for eddy-current testing, **36·4**
- **Dust,** X-ray analysis of industrial, **17·20**
- **Duty Cycle,** for X-ray generators, **14·47**
- **Dye Etchants** (See also "Liquid-Penetrant Testing")
  - brittle-coating sensitization with, for measurement of small strains, **52·23**
  - in crack detection in resin-type brittle coatings, **52·14–15**
  - in detection of invisible cracks in brittle-coating testing, **52·6**
  - in stress (residual) measurement with brittle coatings, **52·25**
- **Dye-Penetrant Process,** for liquid-penetrant testing, **6·13**
  - water-washable, **6·16**

Dye Penetrants
contrast ratios of, 7·20
use with portable equipment, 7·1
Dyes
liquid penetrants using, 6·1
penetrant classification and, 6·2
penetrants containing, field tests with, 6·18
Dynamic Electromagnetic-Field Energy, in nondestructive testing, 4·10
Dynamic Electromagnetic Fields, in nondestructive testing, 5·5
Dynamic Range, of transducers for ultrasonic waves, 44·19
Dynamometers, small-field electronic meters used in, with photoelastic coatings, 53·24

E

Earth-Moving Equipment, strain-gage tests of, 54·3
Eberhardt Fine Thread Test, 10·28–29
Eccentricity
measurement of, by magnetic-field tests, 34·19
of tubes, definition and formula for, 38·1
of tube walls, probe-coil eddy-current indications of, 38·37
Echoes
accidental, in ultrasonic contact testing, 48·31
amplitude in ultrasonic testing
of aluminum, angle of refraction in relation to, 45·11
reflector effects on, 45·18
disturbance, in ultrasonic contact testing, irrelevant indications from, 48·21
flaw, in ultrasonic contact testing, 48·30
front-surface, widening of, and its effects on ultrasonic testing of rough-surfaced parts, 45·17
front-surface and hole, ratio in ultrasonic testing of aluminum block, 44·19
losses from adversely oriented discontinuities in ultrasonic testing, 45·23
ultrasonic (See also "Ultrasonic Waves")
amplitude loss from test object surface roughness, 45·16
contraction of front-surface, by contour-corrected transducer lens, 44·9
radio-frequency and video presentation of, 45·21
Echo Ranging, lithium sulfate as transducer for, 44·4
Economics (See also "Costs")
of destructive *vs.* nondestructive tests, 4·7
of nondestructive testing, 1·2, 1·9
Eddy Currents
control of magnitude of, 37·10
correction for effects of, in hysteresis-loop patterns, 42·24
density, penetration depth of, as function of frequency ratio, 37·9
distribution
in cylinders, 37·6–10
model for verification of calculations, 37·12
in spheres, 39·11
induction
by alternating-current magnetic field, 36·1
in test objects and magnetic-field generation thereby, 36·11
reaction field in sheet materials, 39·14
Eddy-Current Testing
in aircraft maintenance, 3·35
applications (special) of, 42·69
automation of, 41·1–19
Eddy-Current Testing (*Continued*)
basic equations for, 36·15
with cathode-ray tubes
by ellipse methods, 40·23–29
by vector-point methods, 40·20–23
characteristic function in
on complex impedance and voltage plane, 37·2
of cylindrical objects, 37·1–2
comparator-bridge, 42·29–61
complex planes for data from, 36·20
for conductivity and diameter, accuracy and sensitivity of, 42·1
of copper rods, calculations for, 36·13
of cylinders, 37·1–39
coil arrangements for feed-through, 37·15–18
crack detection in, independently of diameter variations, 37·38–39
differential or self-comparison arrangements for, 37·18
similarity law in, 37·10–11
solid nonferrous, 37·18–39
direct and indirect measuring instruments in, 2·31
effective permeability in, and its determination, 36·9–21
electrical-conductivity measurements in, 42·10–21
equipment, and its classification, 40·1–48
for ellipse method, 37·31
for feedback-control, response characteristics of specific, 40·18
sensitivity calibration of, 37·30
equipment characteristics in, 36·3
experimental verification of calculations in, 37·11–12
feedback-controlled impedance method, 40·15–20
equipment for, 40·15
in film-resistance control during vacuum-deposition of metals, 39·19
of foils and sheets, 39·12–19
of heat-exchanger tubes using probes, 3·23
hysteresis-loop, 42·21–29
impedance-magnitude, 40·5, 40·7
limitations of, 40·7
in impurity-particle detection in nonmetallic substances, 39·1
indication or patterns in, 42·1–69
presentation methods for, 40·2–4
at Institut Dr. Foerster, 2·23
linear time base, 40·29–38
with Magnatest Q in materials research, 42·60
mathematical analysis and models in, 36·8
in metallic-particle detection in nonmetallic objects, 39·10
in metallurgy, 2·25
Multitest instrument in, 40·26
nondestructive, 5·6, 5·20
of nonferromagnetic cylinders, instrument sensitivity graphs for, 37·35
in oil refineries, 3·12
principles of, 36·1–21
problems (typical) solved by, tabular summary of, 36·9
quality control (statistical) in, automation of, 41·12–19
reactance magnitude tests, and limitations of, 40·7–15
research (fundamental) in, and problems solved by, 2·24–25
research on new uses of, at Institut Dr. Foerster, 2·27

Eddy-Current Testing (*Continued*)
- screen patterns in, analysis of, **37·33**
- separation of variable parameters in, **37·6**
- of sheet materials by fork-coil method, sensitivity diagram for, **39·15–16**
- Sigmaflux instrument in, **40·26**
- of spheres, **39·1–11**
  - for cracks, **39·10**
- of steels with Magnatest Q eddy-current instrument, optimum utilization of screen area in, **42·39**
- suppression of undesired effects in, **40·38**
- time requirements of, **36·3**
- tolerance limits in, for conductivity and diameter, **37·38**
- trends in, **2·32–33**
- of tubes, **38·1–39**
  - with internal test coils, **38·15–18**
  - small-diameter, problems in automation of, **38·37**
  - surface probe-coil system for, **38·35–39**

Edge Effects
- corrections for, in electric-current testing of plates, **35·5**
- in crack-depth and wall-thickness measurement by direct-current method, **35·1**
- false indications from, in ultrasonic immersion testing, **47·12**

Education (See also "Training Programs")
- for safety in use of radiation, **18·26**
- visual, photoelastic-coating technique in, **53·36**

Effective Permeability
- calculation in eddy-current testing
  - of ellipsoids, short cylinders, and spheres, **39·7**
  - of tubes, **38·3**
- changes caused by cracks of various depths in ferromagnetic substances, as function of frequency ratio, **37·27**
- complex plane of (See "Complex Permeability Plane")
- components of, in eddy-current testing, **36·13**
  - as function of frequency ratio, **37·4**
- cylinder diameter in relation to, in eddy-current testing, **37·6**
- determination of, **36·10**
- of eddy-current test coils for thin-walled nonferrous tubes, **38·1**
- in eddy-current testing, **36·9–21**
  - calculation of effects of discontinuities on, **37·15**
  - of nonferromagnetic cylinders, **37·23–26**
  - of thin-walled tubes, variation with conductivity, diameter, wall thickness, etc., **38·6**
- as function
  - of crack depth and frequency ratio in eddy-current testing of nonferromagnetic cylinders, **37·30**
  - of frequency ratio for crack depth in relation to diameter of nonferrous cylinders, **37·39**
  - of frequency ratio in eddy-current testing, **36·13–14**, **37·36**, **38·2**
- imaginary and real components of, **36·14**, **39·7**
  - for spheres in eddy-current testing, **39·3**
- $\mu_{\text{eff.}}$/absolute, for nonferromagnetic cylinders as function of frequency ratio, **37·36**
- as multiple of limit frequency, **36·13**
- of nonferrous tubes (thick-walled) in eddy-current testing, **38·8–9**
- in reactance magnitude tests, **40·8**
- sample calculation for, **36·13**
- of solid conducting cylinders, **36·14**, **36·18**
- of solid cylinders in eddy-current testing, **38·9**

Effective Permeability (*Continued*)
- of spheres in eddy-current testing, **39·3**
- of test objects smaller than secondary coil, in eddy-current testing, **36·18**

Elastic Properties
- of bars (square), equation for, **51·5**
- constants
  - approximation from longitudinal and shear sound-wave velocities, **45·7**
  - formulas and relation to ultrasonic-wave velocities in isotropic solids, **43·10**
  - as function of crystallographic direction, **45·7**
- effect
  - on natural frequency of sonic vibration of bodies, **51·1**
  - in strain-gage tests, **54·4**
- measurement
  - by sonic resonance vibration tests, **51·6**
  - by ultrasonic waves, **43·12**, **43·47**, **43·49**
- of plates (circular), equation for, **51·5**
- of steel, variation with temperature, **54·4**
- of strain-gage-alloy wire and its temperature coefficient, **54·8–9**
- strain-gage compensation for variation in temperature, bridge desensitization in, **54·21**
- stress and strain in relation to, **54·1**
- tension modulus of, for common engineering materials, **52·11**

Electrical Steel Laminations, hysteresis loss of, sorting by, **34·10**

Electric Apparatus
- for eddy-current testing at Institut Dr. Foerster, **2·25**
- for liquid-penetrant systems, maintenance of, **7·30**
- motion of, motion-picture fluorography in study of internal, **19·45**
- testing with electrical fields, **5·13**

Electric Capacitance
- internal, of barium titanate and its effects in transducer use, **44·2**
- of strain-gage lead wires, balancing of, **54·37**
- of ultrasonic transducers, **49·12**
- of ultrasonic-wave transducer elements, **43·4**

Electric Capacitance Tests, in nondestructive testing, **5·21**

Electric Capacitive Layer, charging of, in xeroradiography, **22·1**

Electric Charge Carriers, moving across solid boundaries, uses in nondestructive testing, **5·22**

Electric Charges, static, effect on radiographs and its prevention, **20·39**

Electric Circuits
- basic oscillator, for feedback-controlled impedance eddy-current testing, **40·15–18**
- bridges (See "Bridges")
- components for ultrasonic testing with A-scan presentation, **43·32–33**
- for conductivity-thickness product determination for metallic sheets, **39·17**
- for conversion of T-strain-gage rosette into two equivalent stress-gage circuits, **54·30**
- of eddy-current ellipse-method test instrument, **37·31**, **40·24**
- of eddy-current probe system for inspection of tubing, **38·35**
- of eddy-current test coils and their impedance-plane response characteristics, **40·1–4**
- of electrometers (vacuum-tube direct-current), **18·23**
- of impedance-magnitude eddy-current-test apparatus, **40·5–6**

- **Electric Circuits** (*Continued*)
  - of Magnatest Q linear time-base eddy-current instrument, 40·29
  - for magnetic field-difference measurement, 33·6
  - of magnetic-field meters, 33·9
  - of Multitest instrument, 40·20
  - for phototubes (multiplier), 11·33
  - printed
    - fluoroscopy of, 24·30
    - optical projection inspection of, 12·14
  - for resistance measurement per unit square for thin metallic foil, 39·19
  - resonant
    - circle diagram for current in, in eddy-current testing, 40·43
    - impedance-variation eddy-current test using, 40·42–45
  - shorted, in detection of magnetostrictive effects in strain gages, 54·27
  - for simulation of effects of discontinuities with mercury models in eddy-current testing, 37·13
  - of Sonic Comparator, 51·7, 51·9
  - for Sperry railroad-rail testing system, 35·15
  - strain-gage, 52·13–22
    - planned and parasitic variation of, 54·19–21
    - potentiometric, 54·14–16
    - sensitivity, calculation of maximum, 54·13–14
    - for sensitivity control, 54·20
    - testing for open, 54·37
  - for ultrasonic-resonance thickness testing, 50·6
  - Villard rectifying, for X-ray generators, 14·23–25, 23·41
  - Wheatstone bridge, for strain-gage balancing, 54·21–22
  - for X-ray generators, 14·4, 14·20
- **Electric Condensers**
  - foils for, film-resistance control during manufacture of, by vacuum deposition, 39·19
  - paper for, eddy-current apparatus for control of metallizing of, 41·4
- **Electric Conductivity**
  - of alloys, and eddy-current separation thereby, 42·16
  - of aluminum, effect of metallic additives on, 42·14
  - of aluminum-Cu-Mg castings, segregation effect on, 42·15
  - of aluminum-Cu-Mg sheets, hardness and quenching temperature in relation to, 42·19
  - of copper blocks and rings, control by eddy-current testing, 42·13
  - of copper castings and wire, composition control by eddy-current tests of, 42·12
  - of copper melts, variation during deoxidation, 42·13
  - of cylinders
    - effects on eddy-current testing, 37·1–6
    - measurement by eddy-current testing and tolerances for, 37·36
  - of cylinders (ferromagnetic) in eddy-current linear time-base tests, 40·32
  - direction in Magnatest Q eddy-current testing, angle with diameter-permeability direction, as function of frequency ratio, 42·48
  - eddy-current methods measuring, 42·10–21
  - in eddy-current testing
    - comparison specimens in evaluation of variation of, 37·30
    - of nonferromagnetic cylinders, sensitivity diagrams for variation of, 37·34
  - effective permeability variation with, in eddy-current testing of thin-walled tubes, 38·6
- **Electric Conductivity** (*Continued*)
  - effects
    - on complex voltage plane for Magnatest Q eddy-current test coil, 42·47
    - in crack-depth analysis of Magnatest Q screen patterns and impedance-plane characteristics, 40·34–35
    - in eddy-current testing, 36·3
      - with Cyclograph, 40·19
      - of cylinders, frequency selection for separation from diameter effects, 37·2–3
      - of ferromagnetic cylinders, separation from effects of diameter and magnetic permeability, 37·4–6
      - of nonferrous cylinders, instrument for determination of, 37·32
      - of nonferrous metals, 42·1
      - of sheet materials, 39·16
      - of spheres, 39·4
    - on effective permeability quotient for eddy-current tests of nonferromagnetic cylinders as function of frequency ratio, 37·35
    - on frequency in eddy-current testing of nonferromagnetic cylinders, 40·8
    - on secondary-coil voltages in eddy-current testing of nonferromagnetic cylinders, 37·35
    - separation from diameter and permeability effects in Magnatest Q eddy-current sorting, 42·39
    - separation from permeability effects in Magnatest Q eddy-current testing, effect of frequency ratio on, 42·44
  - impedance plane showing variation of lift-off and crack directions with, 40·44
  - of iron rods in eddy-current linear time-base tests, 40·35
  - measurement of
    - accuracy and sensitivity of eddy-current, 42·1
    - eddy-current apparatus for, 40·2–3
    - by eddy-current testing, tabular summary of, 36·4–6
    - in eddy-current testing
      - of cylinders, 37·34
      - of spheres, 39·10
    - with feed-through coils in eddy-current testing, 42·3
    - of foils and sheets by eddy-current methods, 39·12
    - independently of diameter with σ-D eddy-current instrument, 40·40
    - of nonferromagnetic cylinders, 37·27
  - of nonferromagnetic substances, effect in eddy-current testing and separation from effects of diameter, 37·1–2
  - sensitivity (maximum) to, in eddy-current testing
    - of nonferromagnetic cylinders, 40·12
    - of tubes, 38·17
  - sorting for variations in, with Multitest eddy-current instrument, 40·22
  - thickness, product of metallic sheets, determination of, 39·16–17
  - of tubes, effect in eddy-current testing with internal coils, 38·15
  - of tubes (nonferromagnetic) in eddy-current testing, 38·9–10
  - of tubes (small-diameter), effects in eddy-current testing, 38·24
- **Electric Conductors**
  - eddy-current testing of flat, similarity law for, 39·14

Electric Conductors (*Continued*)
- magnetic field surrounding current-carrying, effect of cross-section changes and defects on, 35·12
- metallic-sheet eddy-current determination of conductivity-thickness product of, 39·16
- semi-conductors (See "Semi-Conductors")

Electric Contacts
- cracks (netlike) in, detection with Defectometer eddy-current instrument with probe coil, 42·10
- motion of cam-operated, high-speed photography in study of, 3·26
- tungsten, effects of wavy fiber texture on, 42·6

Electric Current (See also "Photocurrent")
- alternating, in demagnetization, after magnetic-particle tests, 30·23
- alternating circular-field and yoke, demagnetization with, after magnetic-particle tests, 30·25
- amplifiers for (See "Amplifiers")
- circle diagram of, in resonant-circuit eddy-current tests, 40·43
- for crack-depth and wall-thickness measurement with direct current, 35·9–10
- direct
  - crack-depth and wall-thickness determination by conduction of, 35·1
  - demagnetization with reversing, after magnetic-particle tests, 30·25
  - lead wires for strain gages using, 54·32
- displacement, in nondestructive testing, 5·21
- eddy-current-test, frequency ratio (See "Frequency Ratio")
- frequencies (harmonic)
  - for ferromagnetic materials, and their analysis by eddy-current linear time base tests, 40·29
  - in Magnatest Q eddy-current separation of similar alloys, 42·34
  - suppression of undesired, in eddy-current testing of ferromagnetic materials, 40·41–42
- frequency
  - of alternating-current field of test coils in eddy-current testing, 36·3
  - for case-depth measurement with Magnatest Q eddy-current instrument, 42·59
  - (characteristic) in eddy-current testing of nonferromagnetic tubes, 38·23
  - for eddy-current crack detection
    - in ferromagnetic cylinders, 37·27
    - in nonferromagnetic cylinders, 37·23–26
  - for eddy-current linear time base tests, 40·30, 40·37
  - for eddy-current testing, 40·11
    - of cylindrical objects, 37·1
    - of nonferromagnetic tubes, 38·9, 38·17
    - of tubing diameter and wall thickness, 38·31, 38·33
    - with Sedac, 40·19
  - effect on eddy-current shielding tests, 38·21
  - effect on Magnatest Q eddy-current sorting of steel wire, 42·46
  - effect on Magnatest Q eddy-current spread bands
    - of alloy and carbon steels, 42·40
    - of alloy steel wire straightened by hammering, 42·49–50
    - of annealed alloy-steel wire, 42·51
    - of steels at high field strength, 42·48

Electric Current (*Continued*)
- frequency (*Continued*)
  - of encircling and probe coils in eddy-current testing of Inconel tubing, 38·38
  - in fluoroscopy, apparent brightness and inspection rate in relation to, 19·24
  - and harmonics, selection in eddy-current testing with Magnatest Q instrument, 41·6
  - for Magnatest Q eddy-current sorting, 42·31
  - and phase position, selection for Magnatest Q eddy-current sorting of alloys, 42·33
  - for separation of conductivity and diameter effects in eddy-current testing, 37·2–3
  - variation
    - with conductivity in eddy-current testing of nonferromagnetic cylinders, 40·8
    - with cracks in eddy-current testing of nonferromagnetic cylinders, 40·11
    - with diameter, in eddy-current testing of nonferromagnetic cylinders, 40·10
- frequency (limit) (See "Limit Frequency")
- frequency (oscillation) in eddy-current testing, 40·7–15
- input and output, for magnetization equipment for magnetic-particle testing, 31·4–10
- from ionization chambers, measurement of, 16·4
- leakage through glass-to-metal seals, 29·16
- for magnetic-particle testing, selection of type, 30·8, 31·1
- for magnetization
  - with flexible cable, for magnetic-particle testing, 30·14
  - for magnetic-particle testing, selection of type, 31·1
- magnetization caused by, 30·21
- for magnetization (circular), for magnetic-particle testing, 30·13–14
- for magnetization (longitudinal), for magnetic-particle testing, 30·13
- magnetization with, for magnetic-particle testing, 30·4–7
- pulse size *vs.* applied voltage in radiation detection, 16·2–5
- rectifiers (See "Rectifiers")
- sources for nondestructive testing, 5·16, 35·2
- in strain gages, limits of, 54·30–31
- in Wheatstone bridge circuits, calculation of, 54·19
- from X-ray machine (60-cycle self-rectified), modulated component of, 16·11
- in X-ray tubes
  - control of, 18·8
  - radiation intensity in relation to, 20·3

Electric-Current Testing
- applications of, 5·20
- of crack depth, 35·10
  - and wall-thickness, 35·1–2
- for crack detection, 35·4
- indications in, interpretation of, 35·4
- nondestructive, 4·11, 35·1–21
- preparation of parts for, 35·3
- of railroad rails, 35·11–21
  - equipment for, 35·13–20
  - personnel for, 35·20
- recording test results in, at Institut Dr. Foerster, 2·28
- for wall thickness, 9·10, 35·3

Electric Fields
- detection of, 5·11
- of eddy-current test coils, frequency of, 36·3
- sources of, 5·8
- tests using, 5·13

Electric Impedance
- apparent
  - calculating initial points of curves of, in eddy-current testing of spheres, etc., **39·7**
  - of coils in eddy-current testing of spheres, effect of relative magnetic permeability on, **39·6**
  - diagram for short circular coil containing a sphere, **39·5**, **39·7**
  - in eddy-current testing
    - of nonferromagnetic cylinders, diameter effects on, **37·23–26**
    - of short cylinders, variation caused by inexact positioning, **39·6**
    - of thin-walled tubes, **38·1**, **38·7**
  - imaginary and real components of,
    - calculation of, **39·7**
    - for thin-walled tubes, **38·3**
  - inside thin- and thick-walled nonferromagnetic tubes in eddy-current testing, **38·17**
  - plane for spheres with cracks in eddy-current testing, **39·11**
  - plane showing effects of cracks in nonferromagnetic tubes for different wall thicknesses and frequency ratios, **38·13–14**
  - for short cylinders or parts or ellipsoids, **39·8**
- characteristic function in calculation of, for eddy-current testing of cylindrical objects, **37·1**
- complex plane of (See "Complex Impedance Plane")
- of eddy-current test coils, **36·1**, **36·3**
- in eddy-current testing, **42·2**
- eddy-current tests using, **40·5**
  - and equipment for, **40·1–7**, **40·15–20**
- eddy-current tests using resonant-circuit variation of, **40·42–45**
- as function of frequency ratio in eddy-current testing of nonmagnetic cylinders, **37·34–35**
- of lithium sulfate crystals for ultrasonic-wave transducers, **44·3**
- matching in ultrasonic immersion test equipment, **47·29**
- normalized, of eddy-current-test coils, **36·20**
- normalized components of, in eddy-current testing of spheres and short parts, **39·3–4**
- real and imaginary components of
  - of circular coil with nonferromagnetic sphere, **39·9**
  - for various fill factors, **37·3**
- of single coil in eddy-current testing, **36·19**
- variations from cracks in nonferrous cylinders in eddy-current testing, **37·18–22**

Electric Inductance
- normalized, of eddy-current test coils, **36·20**
- self
  - of cylindrical coils with and without test objects, in eddy-current testing, **36·19**
  - of test coil in reactance magnitude tests, **40·8**
- in strain-gage signal transfer from rotating members, **54·33**

Electric Insulation (See "Insulation, Electric")

Electric Interference, irrelevant indications from, in ultrasonic contact testing, **48·21**

Electricity
- radiation conversion into, **18·19**
- static (See "Electric Charges")
- xeroradiographic-plate damage by excessive voltages, **22·5**

Electric Potential (See "Electromotive Force," "Potential, Electric," "Voltage")

Electric Power
- generators
  - distortion testing of forgings for rotors of, **5·24**
  - for electric-current testing of railroad rails, **35·13**
  - ultrasonic contact testing of rotors of, **48·11**
  - ultrasonic testing of rotor shafts of, **2·17**
- plants
  - borescopic inspection in, **11·14**
  - maintenance testing in, **3·7**
  - nondestructive testing in, **3·3**
- supplies for electric-current testing of railroad rails, **35·16**

Electric Properties
- detected by nondestructive tests, **4·13**
- of ultrasonic-test search units, types to be considered, **43·5**
- of xeroradiographic plates, **22·3·4**

Electric Reactance, eddy-current tests using, and their limitations, **40·7–15**

Electric Relays, sorting of parts of, by coercive-force tests, **34·8**

Electric Resistance
- of condenser paper in control of metallizing, **41·4**
- control during vacuum deposition of metals by eddy-current methods, **39·19**
- of eddy-current test coils, *vs.* inductive reactance, **36·1–2**
- eddy-current test-coil voltage drop due to, **36·20**
- eddy-current test instruments for measuring, as component of impedance changes, **38·28**
- of foils (thin metallic), differential arrangement for measurement of, **39·19**
- homogeneous and isotropic, in crack-depth and wall-thickness determination, **35·1**
- measurement of, per unit square, and definition, **39·18**
- normalized, of eddy-current test coils, **36·20**
- of strain-gage-alloy wire and its temperature coefficient, **54·8**
- between strain gage and specimen as criterion of completion of curing of cement, **54·13**
- in strain-gage circuits of slip-rings and switches, **54·32**
- of strain-gage lead wires
  - and its effects, **54·31–32**, **54·36**
  - measurement of, **54·32**
- in strain gages, **54·6**, **54·10**
  - effect of electrolytic corrosion on, **54·25**
  - effect of high humidity or rain on leakage of, **54·36–37**
  - equations for variations of, **54·28–29**
  - pressure effect on, **54·30**
  - testing of, **54·37**
  - variation with temperature at zero strain, **54·22**
- strain-gage testing for leakage to ground, as indicator of cement drying, **54·37**
- strain-gage tests using, **54·1–42**
- strain-gage to ground, as indicator of moisture content, **54·24–25**
- strain in relation to, **54·2**
- -strain relations of strain gages, **54·25–28**
- -temperature coefficient of strain-sensitive materials, **54·22**
- of Wheatstone bridge circuits at finite load, **54·19**
- of xeroradiographic plates and time constants of, **22·4**

Electric Resistors
  adjustable foil, for strain-gage temperature compensation, 54·22–23
  with strain gages, effects and location of, 54·31
Electric Shocks, prevention of, in electrified-particle testing, 28·9
Electric Switches, in strain-gage circuits and their resistance, 54·32–33
Electrified-Particle Testing, 5·13
  advantages and limitations of, 28·1
  air supply for, 28·9
  applications of, 28·2, 29·17
  with brittle-coating testing for locating stress-indication cracks, 29·21
  of ceramics and glass, 5·5
  coating pinhole breakdown by, 29·5
  on coatings, 29·13
    and nonconducting materials, 28·4
  in crack detection in brittle coatings, 52·6, 52·15, 52·17
  development of, 28·1
  electrical charging effects in, 28·10
  of enamel (porcelain), 28·2, 29·4
  equipment and materials for, 28·8
  of glass containers, 29·11
  of glass-to-metal seals, 28·8
  humidity effects on, 28·10
  indications in, 29·1
    blinking, 29·4
    false, 29·7
    fugitive, 28·11
    loss of, 28·11
    negative, 29·5
  with liquid penetrant, 28·4
  liquid penetrant (heated) use in, 28·10
  mechanism of, 28·2
  on nonconducting materials, 28·6, 28·7, 29·1
    metal-backed, 28·4, 28·6
  nondestructive, 4·10
  powder blotting in, 29·6
  powder-gun for, and its operation, 28·8–9
  standard crack sample for, 28·11
Electrochemical Tests, nondestructive, 5·17, 5·19, 5·23
Electrodeposition, in nondestructive testing, 5·19
Electrodeposits, X-ray diffraction of, 17·19 (See also "Electroplates")
Electrodes
  arrangement
    for direct-current crack-depth and wall-thickness measurement, 35·9–10
    for electric-current testing of flat plates, 35·4
    for direct-current crack-depth and wall-thickness measurement and their spacing, 35·2–3
  four-point, in crack detection and wall-thickness measurement by direct-current conduction, 35·1
  K′ values for equally spaced, near edge of semi-infinite plate, 35·6
  square array of, in wall-thickness measurement by direct-current methods, 35·10
  for ultrasonic transducers, 44·5
  welding (See "electrodes" under "Welding")
Electromagnetic Fields
  audio-frequency, in nondestructive testing, 4·10
  high-frequency, in nondestructive testing, 4·11
  low-frequency, in nondestructive testing, 4·10
  in nondestructive testing, 5·5
  sources of, 5·8
Electromagnetic Frequency Spectrum, 5·6
Electromagnetic-Induction Testing (See "Eddy-Current Testing")
Electromagnetic Radiation, 13·8–12
Electromagnetic Waves, radio-frequency, in nondestructive testing, 4·11
Electromechanical Coupling Coefficient, of ultrasonic transducers, 49·12
Electrometers
  drift in ionization chambers, minimizing of, 18·7
  quartz-fiber, in radiation measurement, 16·4
  for radiation detection, 18·23
Electromotive Force (See also "Potential, electric," "Voltage")
  induced by coils moving through magnetic fields, 35·12
  thermal, at contacting electrodes in direct-current testing, 35·2
Electron Accelerators, linear
  radiographic characteristics of, 23·4
  X-ray exposure chart for steel radiography with, 23·13
Electron Beams, in nondestructive testing, 4·11
Electron Diffraction, sensitivity as probing media, 5·14
Electronic Apparatus
  fluoroscopic inspection of, 24·19
  testing with electrical fields, 5·18
Electronic Computers, for plotting densitometer curves, 10·5
Electronic Image Conversion Apparatus, 10·4
Electronic Radiation Sources, 14·1–48
  application requirements, 14·1
  X-ray generation by, 14·1
Electronics Industry, X-ray inspection in, establishing acceptance levels for, 24·2
Electron Microscopes, 11·38–40
  resolving power of, 10·31
Electron Microscopy, 11·40
  beams of neutral atoms and molecules and shadow casting in, 5·18
Electrons (See also "Beta Rays")
  atmospheric, effect on charged xeroradiographic plates, 22·6
  Bremsstrahlung production by high-energy, 13·27
  capture by nucleus in radioactive disintegration, 15·3
  charge of, 13·1
  charge-to-mass ratio of, 13·1
  diffraction patterns of, 5·15
  as elementary particles, 13·1–2
  emission
    in nondestructive testing, 4·12
    from solids near coatings, effect on nondestructive testing, 5·22
  emission (secondary) of, multiplier-phototube action and, 11·31
  in etching (cathodic), 5·19
  mass stopping power for, 13·27
  multiplication in scintillation counting, 18·22
  properties of, 13·2
  sources of, 5·16
  traps in crystal phosphors, 16·10
Electron Tubes (See also "Image-Converter Tubes," "Phototubes," "Television Tubes")
  beam-deflection, in automation of Magnatest Q eddy-current instrument, 41·5
  inspection of, thulium-170 in, 15·22

- **Electron Tubes** (*Continued*)
  - memory, in ultrasonic-test C-scan systems, **43·34**
  - movable-electrode, in detection of motion of solid probes, **5·2**
  - radiographs of, **24·17**
  - X-ray inspection of, establishing acceptance levels for, **24·2**
- **Electrophoresis,** analysis and separation by, **5·20**
- **Electroplates,** thickness control of, **18·27** (See also "Electrodeposits")
- **Electroplating,** in nondestructive testing, **5·19**
- **Electrostatic Images,** formation of latent, and powder-cloud development in xeroradiography, **22·1**
- **Electrostrictive Motors,** for vibration testing, **5·17**
- **Elements** (See also "Atoms")
  - attenuation coefficients of, for γ and X rays, **27·1–41**
  - definition of, **13·4**
  - gamma- and X-ray absorption by, mass coefficients for, **18·31–40, 27·1–41**
  - periodic table of, **13·6–7**
  - trilinear plot of, and their isotopes, **13·5**
- **Ellipses,** on cathode-ray-tube screens in eddy-current testing, **37·33**
- **Ellipse Tests,** applications of eddy-current, **40·28–29**
  - eddy-current cathode-ray tube, **40·23–29**
  - for eddy-current crack indication in cylinders, **42·3**
- **Ellipsoids,** eddy-current testing of
  - prolate, apparent impedance curves and effective permeability in eddy-current testing of, **39·8**
  - tabular summary of, **36·6**
- **Emery Paper**
  - in belt sanding as supplement to magnetic-particle testing, **32·25**
  - in cleaning of surfaces for examination with magnifiers as supplement to magnetic-particle testing, **32·20**
- **Emulsification Time,** in liquid-penetrant testing
  - in post-emulsification process, **6·11**
  - shallow defects and, **6·17**
- **Emulsifiers**
  - in liquid-penetrant removal, **6·2**
  - in liquid-penetrant testing, **6·9–11**
    - field application of, **6·17**
    - maintenance of, **7·32**
    - in post-emulsification dye-penetrant process, **6·15**
  - water determination in, for liquid-penetrant testing, **7·32**
- **Emulsions, Photographic** (See "Photographic Emulsions")
- **Enamel, Porcelain** (See "Porcelain Enamels")
- **Enameling,** thickness control in, **18·27**
- **Energy**
  - of beta- and gamma-ray sources, **18·17**
  - converters for, photovoltaic cells as, **11·34**
  - of gamma rays, **15·3, 15·5**
  - kinetic, of α-ray emission, **15·3**
  - luminous (See "Light, Visible," "Luminous-Energy Tests")
  - of phosphors (crystal), band model of, **16·9**
  - photon, of absorption of γ and X rays by elements, **18·32–40**
  - of radiation, effect on spectral sensitivity of film, **16·23**
    - film graininess in relation to, **16·22**
- **Energy** (*Continued*)
  - scintillation counters as spectrometers for, **18·22**
  - in sonic testing of materials with low damping factors, **51·9**
  - transmission of, as probing media, **4·10**
  - ultrasonic (See "Ultrasonic Waves")
  - from X-ray generators, maxima and wave forms of, **23·4**
- **Energy Fields,** characteristics of, **5·9**
- **Energy Transmission Tests, 5·5–14**
  - applications of, **5·12–13**
  - detectors for, **5·9–11**
  - probing media for, **5·5–9**
- **Engineering,** optical projectors in, **12·21–22**
- **Engineering Departments,** liaison with, in quality-control programs, **1·18**
- **Engines**
  - aircraft, magnetic-particle testing of cylinders of, **31·12**
  - automobile, rebuilding of, cost savings from use of nondestructive testing in, **1·9**
  - borescopic inspection of, **11·13–14**
  - diesel, magnetic-particle-test indication of seam in wrist pin of, **32·2**
  - jet, automatic ultrasonic testing of forgings for, **43·35**
    - turbine blades of, radiography of, **23·15**
    - ultrasonic immersion testing of parts of, **5·25**
    - ultrasonic inspection of rotors for, **47·16**
  - strain-gage tests on reciprocating, **54·3**
- **Engravings,** optical projection inspection of, **12·14**
- **Entrances,** to X-ray-film-processing areas, **21·14**
- **Epoxy Resins**
  - adhesives for strain gages, decomposition at elevated temperatures, **54·24**
    - strain gages low in hysteresis and zero shift using, **54·26**
    - strain limits for strain gages on aluminum with, **54·25–26**
  - as scale models for photoelastic stress analysis, **12·31**
  - in strain-gage mounting, **54·12**
  - in strain-gage waterproofing, **54·25**
  - for ultrasonic-transducer damping, **49·12**
- **Equalization,** in X-radiography to minimize scattering, **23·9**
- **Equipment** (See specific test methods)
  - for filtered-particle tests, **9·11**
  - layout in nondestructive-testing laboratories, **2·5**
  - for magnetic-particle testing, **31·1–15**
  - for nondestructive testing, comparison of reliability and transportation requirements in industrialized and remote areas, **2·21**
    - mobile, **2·20**
  - for ultrasonic contact testing, **48·4**
  - for ultrasonic immersion tests, **46·1**
    - automatic-scanning, **46·2**
    - of pipes and tubing, **47·28**
  - for xeroradiography, **22·4**
- **Erosion,** detection in pipes, portable thickness gage for, **18·30**
- **Errors,** proportional and zero shift, in X-ray transmission thickness measurement, **18·7**
- **Etalon,** interferometer for testing transparent media, **10·13**

- **Etching**
  - acid or deep, and reagents for, **32·27–28**
  - cathodic, by electron beams, **5·19**
  - crack formation during or after, from residual stresses, **32·12**
  - defects in printed circuits, fluoroscopy of, **24·30**
  - of discontinuities as supplement to magnetic-particle testing, **32·25–29**
  - macro- and micro-, **32·25**
  - metallographic, reagents for, **32·29**
  - surface preparation for, **32·26**
- **Ethics,** in nondestructive-testing laboratory management, **2·5**
- **Ethyl Alcohol** (See "Alcohol")
- **Europe,** nondestructive-testing development in, and central cooperative institutes for, **2·13**
- **Europium-152-154,** radiation output dosage of, **26·6**
- **Excitation,** continuous and shock, in sonic testing, **51·7**
- **Expansion, Thermal**
  - of ceramic-type brittle coatings, **52·7**
  - coefficient of linear, choice to minimize zero shift in strain-gage tests, **54·4–5**
  - compensation for, in eddy-current testing of nonferromagnetic cylinders, **40·12**
  - of metals, effect on brittle-coating test suitability, **52·1**
  - of strain-gage alloys, **54·8**
  - strain gages compensated for, **54·22–23**
- **Explosions**
  - hazards of liquid penetrants, **7·18**
  - precautions against, in electrified-particle testing, **29·6**
- **Exposure**
  - calculation, for radiographic film, **20·32**
    - in radiography, **20·10**
    - in radiography with radioisotopes, **15·28**
  - -density curves of radiographic films, **16·19**
  - estimation in X-radiography, **23·9**
  - factors in radiograph interpretation, **25·1**
  - to gamma rays, formula for, **20·5**
  - over- and under-, of X-ray film, causes and correction of, **21·18–19**
  - of personnel to radiation, control of, **26·6**
  - in radiography, **15·24–30, 20·1–2**
    - factors affecting, **20·15–16**
  - speed of, with various radiation energies and absorbers and in xeroradiography, **22·8**
  - -thickness factors in gamma radiography of metals, **15·26**
  - of xeroradiographic charged plates, **22·7–12**
  - in X-radiography of steel, charts for, **23·9**
  - to X-rays, formula for, **20·4**
  - in X-ray-film development, **21·4**
  - in X-ray (high-energy) radiography, **23·7**
- **Extensometers**
  - photoelastic coatings in, **53·35**
  - for strain measurement, early developments in, **54·1**
- **Extrusion,** of alloys and metals, effect on ultrasonic-test "noise," **44·7**
- **Extrusions**
  - aluminum, focused transducer for inspection of, **44·8**
    - ultrasonic test blocks from, *vs.* castings, **45·5**
  - aluminum-alloy, ultrasonic immersion indications of defects in, **47·9**
  - defects in, liquid-penetrant evaluation of, **8·20**
  - hardness control in heat treatment of, with Magnatest FW-300 eddy-current instrument, **42·19–20**
- **Extrusions** (*Continued*)
  - thickness measurements of, by ultrasonic resonance method, **50·19**
  - ultrasonic contact testing for discontinuities in, **48·12**
- **Eye**
  - darkness adaptation of, for fluorescent-penetrant inspection, **7·11**
  - in inspection by visual methods, **5·9**
  - light receptors in, **10·2**
  - refractive power of the cornea and lens of, **10·1**
  - visual functions of, **10·1**
- **Eyeball Fluorescence**
  - from black light, **9·12**
  - in liquid-penetrant testing, **7·12, 7·17**

F

- **Fabrication,** defect detection in, by nondestructive tests, **4·7**
- **Fabrics** (See also "Textiles")
  - rubber-coated, radioisotope gaging of, **18·12**
  - strain-gage tests on, **54·3**
- **Facsimile,** in ultrasonic-test C-scan systems, **43·34**
- **Fading Resistance,** of liquid penetrants, determination of, **7·24**
- **Failure**
  - of parts and equipment, rising costs of, **1·6**
  - probability of, for assemblies and components, **1·2**
  - of strain gages, causes of premature, **54·26**
- **Fatigue**
  - cracks (See "Cracks")
  - crescents, **32·14**
  - of inspectors in filtered-particle tests, **9·13**
  - in machinery (modern) with increased speeds, **1·5**
  - of xeroradiographic plates, **22·5**
- **Fatigue Strength,** of strain gages, **54·26**
- **Fault-Warning Systems,** in ultrasonic testing, **49·20**
- **Feedback-Controlled Impedance Tests** (See "Electric Impedance")
- **Feedback Factor,** in eddy-current impedance testing, **40·16**
- **Fermi Distribution,** of beta-ray emission, **15·3**
- **Ferrite,** determination of, in steel
  - by eddy-current testing, **2·25**
  - by magnetic-saturation flux density, **34·4**
- **Ferrograph,** hysteresis-loop screen pictures on, **42·23–26**
- **Ferromagnetic Substances**
  - crack detection and measurement in, with Defectometer eddy-current instrument, **40·45**
  - cracks in cylinders of, eddy-current detection of, **37·25**
  - cylinders
    - complex voltage plane of test coil containing, in eddy-current linear time-base tests, **40·33**
    - crack-depth analysis in eddy-current testing of, **40·35**
  - demagnetization of, after magnetic-particle tests, **30·20–25**
  - eddy-current testing of, calculation of magnetic permeability and secondary-voltage components of, **36·16**
    - with hysteresis loop, **42·1, 42·21**
    - with linear-time-base, **40·29**
    - magnetic permeability limitations of, **38·20**
    - secondary voltage in, with air space between coil and specimen, **36·19**

Ferromagnetic Substances (*Continued*)
  eddy-current testing of (*Continued*)
    with Sedac, frequency for prevention of "lift-off" effect in, **40·19**
    suppression of undesired harmonics in, **40·41**
  eddy-current testing of cylinders of, separation of effects of electrical conductivity, diameter, magnetic permeability in, **37·4–6**
  eddy-current testing of nonferrous plating on, **36·6–7**
  eddy-current testing of thin-walled tubes of, **38·6**
  impurity particles of, detection in nonmetallic substances, **39·1**
  magnetic-field testing of, **5·13**
  magnetic-particle inspection of, **30·1**
  magnetization curve of, **33·3**
Ferromagnetism, definition of, **30·2**
Ferrous Material, detection in foods, **34·22**
Fiberboard
  filler-stock control in manufacture of, radiation gaging in, **18·29**
  foil-covered, for surface imprints, **12·30**
Fibers
  microscopy (phase-contrast) of, **10·18**
  X-ray analysis of, **17·20**
Fieldistor, 5·11
Field of View, of telescopic systems, **11·17**
Field Size, in optical projectors, for combinations of screen sizes and magnifications, **12·9**
Field Tests, 3·1–36 (See also "Maintenance Tests")
  equipment for, **3·2**
  personnel requirements for, **3·2**
  in power plants, **3·3**
  radioisotope positioners in, **3·3**
  requirements for, **3·1**
Filing, as supplement to magnetic-particle testing, **31·24, 32·21**
Fillets and Corners, disturbances in ultrasonic contact testing caused by, **48·27**
Fill Factor
  for air space between coil and specimen, **36·17**
  crack effects in relation to, **37·28**
  for cylindrical objects, **37·1**
  determination for spherical objects, **39·11**
  effects at constant frequency, **37·4**
    in testing of spheres, **39·4**
  frequency variation with, for nonferromagnetic cylinders as function of conductivity, **40·9**
    for nonferromagnetic cylinders as function of cracks, **40·11**
    for nonferromagnetic cylinders as function of diameter, **40·10**
  for heavy-walled nonferrous tube with test coil inside, **38·18**
  for nonferromagnetic cylinders, complex impedance and voltage planes for, **37·3**
  for nonferromagnetic tubes, diameter effects in relation to, **38·10**
  for tubes, effective permeability in relation to, **38·19**
Film Badge Meters, for radiation monitoring of personnel, **26·4**
Films (See "Coatings")
Films, X Ray (See "X-Ray Film")
Filtered Particles
  motion of, detection of, **5·3**
  in testing of ceramics, **5·5**
Filtered-Particle Tests, 9·1–16
  absorbed substance effect on, **9·5**
  black light for, **9·11**
  characteristics of media for, **9·5**
  of clayware, **9·2**

Filtered-Particle Tests (*Continued*)
  drain marks in, **9·18**
  equipment for, **9·11–12**
  fluorescent media in, **9·8, 9·10**
  inspection media for, **9·1**
  interpretation of, **9·16**
  irrelevant indications in, **9·18**
  materials for, **9·7–10**
  nonfluorescent media in, **9·10**
  particle size in, **9·8**
  principles of, **9·3**
  suspending media for, **9·7**
    health and safety precautions in use of, **9·13**
  water effect on, **9·14**
Filtering, of signals in electric-current railroad-rail testing, **35·16**
Filters
  for black light
    for liquid-penetrant testing, **7·13**
    for magnetic testing with fluorescent particles, **30·19**
  interference, uses of, **10·16**
  lead-sheet, X-ray beam filtration with, **23·8**
  for photography
    of crack patterns in brittle-coating testing, **52·26**
    of fluorescent magnetic-particle test indications, **32·19**
  for photometers for penetrant-brilliance determination, **7·21**
  in radiography for absorbing scattered radiation, **20·22–23**
  for X-ray (high-energy) radiography, **23·7–8**
  for X-ray (monochromatic) production, **13·10**
Filters, Electrical, resistance-capacitance, in potentiometric-circuit strain-gage tests, **54·15**
Filtration, inherent, of X-ray tube parts, **19·17**
Finger Damping, to locate reflections in ultrasonic testing, **48·21**
Fingerprints, replicas of, for optical projection, **12·29**
Fire Hazards, from suspending media for filtered-particle tests, **9·13**
Firing, of ceramic-type brittle coatings, **52·17**
Fission, Nuclear (See "Nuclear Fission")
Fissures (See "Cracks")
Fixation
  of xeroradiographic images transferred to paper, **22·13**
  of X-ray films
    after development, **21·7**
    stains and streaks associated with, **21·21**
Fixation Solutions
  for X-ray film
    activity decrease and replenishment, **21·8**
    removal when water supply is limited, hypo clearing agent in, **21·9**
    test for completeness of removal, **21·11**
    white-scum formation in, and its prevention, **21·22**
Flakes, in forgings, magnetic-particle indications of, **32·9**
Flaking
  of brittle coatings during yielding, as indication of compression strain, **52·25**
  hydrogen, detection in cylindrical forgings, **49·16**
  of steels, ultrasonic contact test frequencies for detection of, **48·2**
Flame Gouging, in casting-defect removal before welding, **32·22**
Flanges, leak detection in, by liquid penetrants, **8·2**

Flash Point, of liquid penetrants, limitations and measurement of, **7·18**
Flatness, inspection for, of thrust washers for power-recovery turbine units, **3·34**
Flat Stock (See "Sheet Materials")
Flaw Gating Systems, for double-transducer ultrasonic testing with combined transmit-receive search units, **49·19**
Flaws (See "Cracks," "Defects," "Discontinuities," etc.)
Flexure, mode of sonic vibration of rectangular bars, **51·2**
Floors, of X-ray-film-processing areas, coverings for, **21·14**
Flow Lines
  direction in metal parts, effect on ultrasonic shear-wave velocity in, **45·7**
  in metals, detection by etching, **32·25**
Flow Meters, liquid, with magnetic turbine wheel, **34·23**
Fluctuation, in fluoroscopy, **19·25–26, 19·28**
Fluorescence (See also "Light, Fluorescent")
  brilliance of, measurement of, **7·21**
  of eyeball in liquid-penetrant testing, **7·12**
  K radiation in microradiography, **20·43**
  in magnetic-particle inspection of welded tubes, **31·14**
  measurement of, laboratory set-up for, **24·38**
  random, effect on photography of fluorescent magnetic-particle test indications, **32·19**
  in scintillation counting, efficiency of, **18·22**
  scintillators, radiation-detection devices using, **18·21**
  in thickness measurement of coatings, **24·36**
  ultraviolet-radiation detection by, **10·5**
  X-ray thickness gages using, **18·10**
  in X-ray thickness gaging, **18·6**
Fluorescent Particles
  in filtered-particle inspection, **9·1, 9·8**
  magnetic, photography of test indications of, **32·18**
Fluorescent-Penetrant Inspection, darkness adaptation of eyes for, **7·11**
Fluorescent Penetrants (See "fluorescent" under "Liquid Penetrants")
Fluorescent Screens, 16·13–17, 19·8–13
  binders for, **16·14**
  care and maintenance of, **16·15**
  coatings for, **16·14**
  color of emission from, **16·14**
  color *vs.* visual response, **19·13**
  dimensional factors of, **19·33**
  intensifying
    coatings for, **16·16**
    construction and materials for, **16·16**
    graininess in radiography with, **20·36**
    graininess of X-ray film image, correction of, **21·20**
    in high-energy X-ray radiography, **23·8**
    maintenance of, **16·7**
    properties of, **16·16**
    in radiography, **20·28**
    radiography with, failure of Bunsen-Roscoe reciprocity law in, **16·23**
    radiography with, mottle in, **16·22**
    in xeroradiography, **22·8**
    for X rays, **16·16**
  in isotope radiography, **15·30**
    grainy images from, **15·33**
  unsharpness of, **19·11**
Fluorescent Substances
  in liquid-penetrant testing, **6·6**
  in magnetic-particle testing, **30·18–20**
Fluorine, absorption coefficients (mass) for γ and X rays and photon energies of, **18·33**
Fluorographs, characteristics of, **19·48**
Fluorography
  in inspection, **19·44**
  motion-picture, uses of, **19·45**
Fluoroscopes
  amplifying, **11·36**
  calibration of, **19·36**
  in inspection, characteristics of, **19·48**
Fluoroscopic Screens (See "Fluorescent Screens")
Fluoroscopy
  of aircraft honeycomb structures, **24·28**
  applications of, **19·48, 24·18**
  blurred-contour perception in, **19·27**
  brightness in, amplification of, **19·37, 19·40**
    level for, **19·23, 19·33**
  of castings, defect indications in, **24·27**
  and comparison of fluoroscopes with X-ray image devices, **19·1–49**
  contrast sensitivity in, **19·4**
  conventional, **19·42**
  defect identification in, **19·36**
  defect size detectible in, **24·24**
  electronic, **19·37–41**
  focal spot size in, **14·42**
  geometry, magnification and screen size in, **19·33**
  high-brightness and definition, **19·42**
  images in
    characteristics of, **24·20**
    contrast in, **24·22**
    definition in, **24·22**
    enlargement in, **14·42**
    interpretation of, **24·18**
  in inspection, survey of, **19·36**
  inspection quality index *vs.* penetrameter sensitivity in, **19·47**
  limitations of, **19·47**
    and depth *vs.* width sensitivity in, **19·27**
  magnification in, **19·6, 19·33**
  optical systems (auxiliary) in, **19·27**
  penetrameter for use in, **24·25**
  personnel requirements for, **19·36, 24·23**
  photography in, **19·44**
  of printed electric circuits, **24·30**
  quality levels in, evaluation system for, **24·31**
  radiography compared to, with respect to linear absorption coefficients, **19·19**
  red *vs.* white light in, **19·35**
  reports and report forms, **24·31, 24·35**
  safety precautions in, **14·42, 24·23**
  sample-handling apparatus and methods in, **19·35**
  samples with known defects for comparison in, **24·27**
  scanning rate and frequency in, **19·25**
  sensitivity, comparison with radiographic sensitivity, **19·6**
  sensitivity (penetrameter) in, of aluminum, **19·23, 19·24**
  statistical control in and of, **19·37**
  television (closed-circuit) in, **19·39**
  television-screen adaptation to, **14·43**
  unsharpness of screen in, **19·30–31**
  viewing-surface limitations in, **19·1**
  viewing systems for, **19·42–45**
    remote, **24·20**
  visual limitations in, **19·24–27**
  X-ray detection in, **5·10**
  X-ray source for continuous, **14·42**
  X-ray tube kilovoltage range for industrial, **19·18**

Fluoroscopy (*Continued*)
- X-ray tubes for, **19·15**

Flux Density (See "Magnetic Field")

Focal Length
- of lenses (acoustical) in metals and water, **44·7**
- of lenses (acoustical plane-convex), **44·7**
- of lenses as function of magnification, in optical projectors, **12·6**

Focal Spot
- measurement of, of X-ray targets, **14·32**
- minimum defect discernibility and, in fluoroscopy, **19·5**
- reduction of, in rotating-anode X-ray tubes, **14·32**
- size of
  - fluoroscopic magnification and sensitivity in relation to, **19·18**
  - fluoroscopic sensitivity in relation to, **19·38**
  - in fluoroscopy, **14·42**
- of X-ray tubes, **14·29**
  - line-focus, **14·30**
- of X-ray tube targets, **14·4**

Focus
- depth of, of lens, **12·32**
  - of telescopic systems, **11·17**
- measurement by, on optical projection screen, **12·31–32**

Foerster Instrument, ellipse method, wiring diagram for, **40·24**

Foerster Isometer, for thickness measurement of insulating layers, **36·9, 40·47**

Foerster Probes, arrangements for magnetic field testing, **33·1**

Fogging
- of photographic film, development time in relation to, **16·21**
- of radiographic images from scattering, **20·17**
- of xeroradiographic plates and its prevention, **22·8**
- of X-ray films, causes and correction of, **21·20**
  - during development and its prevention, **21·4**

Foil
- aluminum, complex transmission coefficient T in eddy-current testing of, **39·14**
- condenser, film-resistance control during vacuum deposition of metals in manufacture of, **39·19**
- eddy-current testing of, **39·12–19**
- electrodes of metallic, on ultrasonic transducers, **44·5**
- resistance of metallic, differential arrangement for measurement of, **39·19**
- strain gages of, **54·5, 54·7**
  - effect of hydrostatic pressure on electric resistance of, **54·30**
  - heat-dissipating ability and maximum electric current compared with wire gages, **54·31**
  - resistance increase near fatigue failure, **54·26**
- strain sensitivity of, effect of temperature on, **54·23**
- thickness measurement of
  - eddy-current-test meter for, with automatic feedback control of rolls, **41·3**
  - with radiation, **18·3**
  - with *RC* oscillator, **39·18**

Food
- ferrous material detection in, **34·22**
- fluoroscopic inspection of, **19·36, 24·19**
- impurity-particle detection in, by eddy-current methods, **39·1**

Food Industry, liquid-density control with radioisotopes in, **18·30**

Force, measurement with unbonded strain gages, **54·2–3**

Forging
- of alloys and metals, effect on ultrasonic-test "noise," **44·7**
- effect on liquid-penetrant indication of defects, **8·5**
- flow lines from, detection by etching, **32·25**

Forgings
- aluminum-alloy cylindrical, ultrasonic immersion testing of, **46·21**
- borescopic inspection of, **11·14**
- bursts
  - ultrasonic immersion indications of, **47·21**
  - ultrasonic contact test frequencies for detection of, **48·2**
  - ultrasonic shear waves in inspection of, **45·10**
- bursts and flakes in, magnetic-particle indications of, **32·9**
- chipping at defects in, as supplement to magnetic-particle testing, **32·22**
- cracks
  - direct-current detection and measurement of, **35·10**
  - evaluation of, **8·14**
- cracks (fatigue) and laps in, liquid-penetrant penetration time for detection of, **6·19**
- distortion of rotor, tests for, **5·24**
- drilling (core) or trepanning of, as supplement to magnetic-particle testing, **32·24**
- dye-penetrant penetration time for, **6·14**
- eddy-current testing of, automatic tilting or moving coils in, **41·8**
- flaking in cylindrical, from hydrogen, detection of, **49·16**
- grain structure (unrefined) in, ultrasonic detection of, **43·24**
- grinding of, to remove defects, **32·22**
- laps
  - emulsifying time in liquid-penetrant detection of, **6·12**
  - evaluation of parts showing, **8·20**
  - grinding as supplement to magnetic-particle indications of, **32·22**
  - liquid-penetrant indications of, **8·2**
  - liquid-penetrant penetration time for detection of, **6·8, 6·10, 6·14, 6·19**
  - magnetic-particle indications of, **32·7–9**
- liquid-penetrant testing of, penetration times in, **6·8, 6·10**
- magnetic-particle testing of
  - medium- and heavy-duty equipment for, **31·4–10**
  - multi-purpose semi-automatic equipment for, **31·12–13**
- porosity detection in aircraft, by immersion ultrasonic testing, **5·25**
- radiography with high-voltage X rays, **23·14**
- repair by welding, **32·22**
- sorting of heat-treated, Magnatest Q eddy-current curves and bands for, **41·5**
- stainless steel, ultrasonic attenuation in, **45·5**
- tensile strength of, Magnatest Q eddy-current instrument for determination of, **2·28**
  - Magnatest Q eddy-current sorting by, **42·54–55, 42·57**
- thickness testing of, by ultrasonic resonance tests, **50·21**
- ultrasonic contact testing of, **48·11**
  - frequencies for, **48·1**
- ultrasonic contact testing of steel, structural disturbances in, **48·29**
- ultrasonic immersion indications of defects in, **47·14, 47·20**

Forgings (*Continued*)
- ultrasonic immersion testing of, 46·2
- ultrasonic immersion testing of die, specifications for, 46·23
- ultrasonic inspection (automatic) of jet-engine, 43·35
- ultrasonic reflection in defect detection in, 5·25
- ultrasonic shear-wave velocity in, effect of flow-line direction on, 45·7
- ultrasonic testing (double-transducer) of rotor, 49·3
- ultrasonic-wave frequencies for testing of, 48·2

Fovea Centralis, in eye as maximum visual acuity spot, 10·2

Fractures (See also "Cracks")
- progressive, development from fatigue cracks, 32·14
- in sheet piles, photoelastic-coating pattern showing, 53·26, 53·28–29

Fracturing
- of brittle coatings under strain, 52·4
- as magnetic-particle test supplement, 32·23

Freon, leaks in refrigeration systems, detection of, 5·4

Freon-12, as insulator for resonance-transformer type X-ray generators, 14·14

Frequency
- electric-current (See "Electric Current," "Frequency Ratio," "Limit Frequency")
- of electromagnetic waves, selection for probing media, 5·6
- sonic (See "Sound Waves")
- of strain variation (See "Strain")
- ultrasonic (See "Ultrasonic Waves")
- vibration (See "Vibration")

Frequency-Modulated System, for ultrasonic testing, 44·21

Frequency Ratio
- advantages of low, in Magnatest Q eddy-current sorting of alloys, 42·42
- angle between conductivity direction and diameter-permeability direction as a function of, in eddy-current testing, 42·48
- calculation of, for eddy-current testing of spheres, 39·3
  - for temperature compensation in eddy-current testing of nonferromagnetic cylinders, 40·13
- crack effects for various, in eddy-current testing of nonferromagnetic tubes, 38·13–14
- determination in eddy-current testing of cylinders, 37·27, 37·34
- eddy-current density and field strength as function of radial position for various, 37·9
- in eddy-current testing, of aluminum foil, 39·14
  - effective permeability as function of, 36·13, 36·14, 37·4
  - effective permeability as function of, of thin-walled nonmagnetic tube, 38·2
  - effective permeability changes caused by cracks as a function of, 37·23, 37·27
  - effective-permeability-component calculation from, for thin-walled nonferrous tubes, 38·3
  - effective permeability quotient as function of, for crack depth in relation to diameter of nonferrous cylinders, 37·39
  - as function of effective permeability of nonferromagnetic cylinders, 37·36
  - as function of electric impedance of nonmagnetic cylinders, 37·34–36
  - as a function of sphere diameter, 39·4

Frequency Ratio (*Continued*)
- in eddy-current testing (*Continued*)
  - for maximum sensitivity in testing of thick-walled tubes, 38·12
  - of nonferromagnetic cylinders, 37·20–22
  - of nonferromagnetic cylinders, crack depth and magnetic permeability in relation to, 37·30
  - of nonferromagnetic cylinders, effective permeability quotient as function of, 37·37
  - penetration depth as function of, 37·9, 37·10
  - penetration depth for different instrument sensitivities in eddy-current testing, 38·19
  - selection for crack detection in thin-walled tubes, 38·7
- permeability effects at high, in Magnatest Q eddy-current testing, 42·42
- selection
  - for maximum sensitivity in eddy-current testing of tubes, 38·17
  - of sheet materials, 39·13–14
  - of sheet materials, complex plane of transmission coefficient T as function of, 39·14
  - of sheet materials, equations for, 39·18
  - of thick-walled nonferromagnetic tubes, 38·17
  - of thin-walled tubes, determination of, 38·7

Fresnel Zone (Ultrasonic)
- in aluminum as function of flaw depth and hole size at different gain settings, 44·17
- central-axis maximum and minimum intensity points in, 44·12
- effects on hole indications in ultrasonic testing, 44·17–18
  - in water, in ultrasonic testing, 44·14
- pattern, amplitude variations in effects on ultrasonic measurement of discontinuities, 45·24
- in ultrasonic testing, 44·12–19
  - distribution of, 45·13
  - graphic representation of, 44·12
  - of metals with water path, 44·15–17
  - with paint-brush transducers, 44·11
- ultrasonic-test interpretation under conditions of, 44·16

Friction, effect of residual magnetism on, 30·20

Frilling, of X-ray-film emulsions and its prevention, 21·22

Fringes
- color, in photoelastic-coating tests with polarizing quarter-wave viewer, 53·16, 53·19 (See also "Isochromatic Lines")
- isochromatic and isoclinic
  - in large-field instrument for photoelastic-coating tests, 53·19, 53·21
  - in photoelastic coating stress analysis, 53·3–5
- patterns, of stresses in crane hooks and bearings, 10·19

Frontal Members, for ultrasonic transducers, 44·6

Fruit, citrus, fluoroscopic inspection of, 19·36, 24·19

Fumes, from acid etching of metals, protection against, 32·28

Fundamental Ultrasonic Resonance Frequency, in ultrasonic testing
- causes of deviations from, 50·12
- equation for, 50·1
- plate-thickness measurements from, 50·1

Furnaces
- flames of, phototubes in control of, 11·34
  - television in observation of, 11·37
- photography inside, during operation, 11·25

- **Fusion, Incomplete Weld**
  - causes and radiography of, 25·9
  - magnetic-particle indications, 32·10

G

- **Gages, Pneumatic Orifice,** in detection of motion of solid probes, 5·2
- **Gages, Strain** (See "Strain Gages")
- **Gages, Thickness** (See "Thickness Gages")
- **Gaging**
  - of machining operations by ultrasonic-resonance method, 50·20
  - mechanical, 5·4
  - of parts, ultrasonic resonance testing in, 50·4
  - of tube diameter and thickness by eddy current methods, 38·31
  - by ultrasonic-resonance method, 50·19
- **Gain Settings,** in ultrasonic testing, amplitude variations with, for aluminum blocks with different flaw depths and hole diameters, 44·16
- **Galvanizing,** thickness control in, 18·27
- **Galvanoelectric Tests,** in nondestructive testing, 5·20
- **Gamma Rays** (See also "Radiography")
  - absorption, attenuation, and scattering in radiography, 15·24
  - absorption (mass) coefficients for, 18·31–40
  - absorption of, 18·4
    - by alloys and metals, equivalence factors for, 20·14
    - by specimens, 20·15
    - by typical radioactive sources, 15·11
  - attenuation coefficients of elements for, 27·1
  - detection by scintillation counting, 18·22
  - detectors in thickness gaging, 18·12
  - effect on photographic-film density, 16·22
  - emission of, 13·9
    - in radioactive disintegration, 15·3
    - from radioisotopes and formula for exposure to, 20·5
  - energy of, 15·5
    - from Cobalt-60, 15·14
    - radiation intensity compared with, 15·6
  - ionization by, 16·1
  - ionization chambers for detection of, 18·20
  - from Iridium-192, 15·17
  - narrow-beam conditions, reduction factors for, 26·10
  - from neutron-irradiated sphere, calculation of, 15·10
  - in nondestructive testing, 4·11
  - photoelectric absorption of, solid detectors in, 18·21
  - photographic-film shielding against, in storage, 20·39–40
  - radiography with
    - film exposure in, 20·1
    - fluorescent-screen intensification factor in, 20·28
    - industrial, 20·1
    - scattering in, and its control, 20·17
    - sources for, calculation of, 15·9
  - from radium and radon, 15·8
  - shadow formation by, geometry of, 20·5–7
  - shielding from, broad-beam, 26·11
    - equivalents for, 26·10
  - sources of, 5·8, 13·16, 18·1
  - thickness gages using, energy and half-life of sources for, 18·17
  - in thickness measurement, 18·1
- **Gap Testing,** ultrasonic, with double-transducer search units, 49·19
- **Gas, Natural** (See "Natural Gas")
- **Gases**
  - detection of poisonous, by biological methods, 5·4
  - electronegative, effect on radiation measurement with proportional counters, 16·6
  - inclusions containing (See also "Gas Holes")
    - at weld root, and their radiography, 25·6
    - in welds, causes and radiography of, 25·3
  - for ionization chambers, 16·2
  - leakage detection of, 5·3
  - porosity from, in castings, magnetic-particle indications of, 32·9
  - as probing media in nondestructive tests, 4·10
  - radioactive (See "Radioactive Substances")
- **Gas Holes** (See also "inclusions" under "Gases")
  - aligned, as propagating discontinuity in castings, 24·7
  - in castings, effect on strength, 24·7
  - detection in aluminum and magnesium castings by ultrasonic immersion tests, 46·11
    - liquid-penetrant indication of, 8·3
    - radiographic interpretation and distinction from gas porosity, 24·4
  - fluoroscopy of
    - in castings, 24·27
    - detectible size in, 24·24
  - parts having, standards for evaluation of, 8·21
- **Gas Multiplication,** in radiation measurement with proportional counters, 16·5
- **Gasoline Plants,** corrosion testing in, 50·35
- **Gas Porosity** (See "Porosity")
- **Gastroscopes,** 11·15
- **Gates, Electronic,** in ultrasonic-test systems, 43·34–35
- **Gating and Marking Systems,** for defect location in ultrasonic contact testing, 48·5
- **Gaussian Curve**
  - of dimensions of spherical objects, obtained with combined automatic crack tester and sorter, 41·19
  - with Statimat instrument and evaluation of its deviations in statistical quality control, 41·18
- **Geiger-Muller Counters** (See "Geiger-Muller" under "Counters")
- **Gelatin,** hardening by fixation solution after development of X-ray film, 21·7
- **Gems,** radiography (low-voltage) of, 24·40
- **Generators**
  - electric-power (See "generators" under "Electric Power")
  - X ray (See "X-Ray Generators")
- **Geodesy,** survey markers in, location by magnetic means, 34·23
- **Geometric Properties,** detected by nondestructive testing, 4·12
- **Geometry**
  - of discontinuities
    - determination by ultrasonic testing methods, 45·24
    - effects in ultrasonic testing, 45·22–27
  - effect on amplitude in ultrasonic testing by through-transmission method, 43·28
    - on natural frequency of sonic vibration of bodies, 51·1
  - fluoroscopic, 19·33
  - of gamma- and X-ray shadow formation, 20·5–7
  - limitations from, in nondestructive testing, 1·20–21

Geometry (*Continued*)
  of radiographic definition, factors affecting, 20·34
  of radiographic unsharpness, 20·7–10
  ultrasonic-energy losses from, 43·25
Geophysics, longitudinal magnetic field probe in, 33·1
Germanium
  absorption coefficients (mass) for γ and X rays and photon energies of, 18·35, 27·22
  attenuation coefficients of, for γ and X rays, 27·22
  in gamma-ray detection, 18·21
  ultrasonic energy losses in, 43·25
Getters, for X-ray tubes, 14·35
G-H Tepic Strain Gage, 54·6
Glare, avoidance by use of polarized light in optical tests, 10·3
Glass
  acoustic and ultrasonic properties of plate and Pyrex, 43·8
  borosilicate, for X-ray tubes, 14·34
  as chart material in optical projectors, 12·20
  cleaning for resin-type brittle coatings, 52·9
  coatings on, interferometric measurement of thickness of, 10·14
  constant *K* value in ultrasonic resonance tests, 50·3
  crack growth in, 29·7
  discoloration of X-ray-absorbing, by high-energy radiation, 19·14
  electrified-particle testing of, 5·5, 28·6, 29·1
    for subsurface defects, 29·3
  failure mechanism of, 29·7
  impurities in, optical projection of, 12·22
  light transmission by lead and standard, 19·14
  liquid-penetrant testing of, 8·19
  microscopy (phase) in testing of, 10·18
  nondestructive testing of, 10·10
  optical, testing by refractometers, 10·10–11
  penetration time for, in liquid-penetrant testing, 6·8, 6·10
  thickness measurement range with Sr-90 beta gages, 18·16
  ultrasonic contact testing of, frequencies for, 48·1
  ultrasonic reflection coefficients at interfaces with other materials, 43·13
  ultrasonic-wave attenuation *vs.* frequency in, 43·26
  X-ray absorption by windows of, compared with beryllium, 19·17
  for X-ray barrier windows, 19·13
Glass Articles, taper in, optical projection of, 12·22
Glass-to-Metal Seals (See "Seals, Glass-to-Metal")
Glycols, as suspending media for filtered particle tests, 9·7
Gold
  absorption coefficients (mass) for γ and X rays and photon energies of, 18·38, 27·38
  attenuation coefficients of, for γ and X rays, 27·38
  electrical conductivity of, 42·16
Goniometer, for X-ray fluorescent analysis, 17·25
Gouging (See "Flame Gouging")
Graetz Circuit, for full-wave rectification in X-ray generators, 14·23
Grain Boundaries, in alloys and metals
  detection by etching, 32·25
  ultrasonic-test "noise" from, 44·7
Grain Flow (See "Flow Lines")
Graininess
  of photographic silver deposits, 16·21
  in radiography, 15·32, 20·34, 20·36
  of X-ray film used with fluorescent intensifying screens and its correction, 21·20
    with fluorescent intensifying screens, 20·28
Grain Orientation, effect on apparent impedance plane in eddy-current testing of spheres, 39·11
Grain Structure, of metals (See "Microstructure")
Granite, radiation-shielding equivalent of, 26·9
Graphs, in stress calculation from strain-gage readings, 54·41
Grating, for microscope conversion to schlieren methods, 10·20–21
Gravitational Fields
  detectors of, 5·11
  in nondestructive testing, 4·10, 5·5
  sources of, 5·9
  tests using, 5·13
Grease
  coatings for moistureproofing of strain gages and their application, 54·38
  as coupling medium in ultrasonic contact tests, 48·4
  effect on magnetic-particle testing, 30·1
  removal from parts for liquid-penetrant testing, 6·6, 6·13
Grenz Rays, in nondestructive testing, 4·11 (See also "X Rays")
Grid Configurations, strain-gage, 54·5–6
Grinding
  chips or dust from, phase microscopy of, 10·18
  cracks from, evaluation of parts with, 8·14
    magnetic-particle indications of, 32·11–12
  of metal surfaces before strain-gage application, 54·36
  to remove defects and determine their extent, 32·22
  as supplement to magnetic-particle testing and apparatus for, 32·22
  surface, in ultrasonic testing to decrease side-lobe effects, 44·19
  of welds, radiography of marks from imperfect, 25·14
Grinding Wheels
  bursting speed (ultimate) of resin-bonded, variation with sonic resonant frequency, 51·12
  sectioning with, as supplement to magnetic-particle testing, 32·24
  sonic testing of, 51·9–12
    crack detection in, 5·24, 51·14
    vibration frequency in, 51·11–12
  ultrasonic testing of, 43·49
Grit, for blasting of specimens for ceramic-type brittle-coating testing, 52·16
Guided Missiles, photoelastic-coating tests of fuselage and tail of, 53·26–27, 53·30–31
Guns
  borescopes for inspection of small arms, 10·10
  borescopic inspection of, 11·14
  ultrasonic inspection of tubes of, pre-set program for, 43·35

H

Halation, in fluorescent-penetrant testing, 7·20
Half-Life
  of beta- and gamma-ray sources, 18·17
  formula for, for radioactive nuclei, 13·12
  of radioisotopes, definition of, 15·1, 15·5

Half-Value Layer
  definition of, **26·9**
  of materials for radiographic shielding, **26·9**
  of radiation absorbers, **15·7**
  in radiography, **13·30**
    of steel with high-voltage generators, **23·5**
  of X rays, calculation of, **23·9**
  in X-ray fluoroscopy, **19·15**
Hall Effect, in magnetic-field detection, **5·10**
Hall Generators
  applications of, **33·14**
  crack-depth measurements by magnetic field tests with, **34·20**
  magnetic-field meters, **33·11–12**
  in magnetic-field testing, **33·1**
  probes of, design of, **33·12**
    materials for, **33·11**
    semiconductor combinations for, **33·12**
  for sheet-metal automatic thickness sorting, **34·17**
  thickness measurements by magnetic field tests with, **34·17**
Halogens, detection of vapor of, **5·4**
Hammering, fracturing by, as magnetic-particle test supplement, **32·23**
Hand Contactor, in electric current testing of railroad rails, **35·19**
H and D Curves, of photographic film, **20·32–34**
Handling (See also "Materials Handling")
  of acid etching reagents, precautions in, **32·28**
  of radioisotope radiographic sources, apparatus for, **15·22–24**
Hardening
  age (See "Aging")
  control of
    of semifinished parts quenched after extrusion, by eddy-current ellipse methods, **40·28**
    of steel (ball-bearing), effect on Magnatest Q eddy-current spread bands, **42·58**
Hardness
  of abrasive products, mechanical and sonic measurement of, **51·9**
  of alloys, electrical conductivity changes related to, in eddy-current testing, **37·6**
  of alloys and metals, eddy-current apparatus for sorting by, **40·2–3**
    ultrasonic control of, **43·49**
  of aluminum alloys, determination from electrical conductivity in eddy-current tests, **42·18**
  of aluminum and titanium alloys, electrical conductivity as indication of, **42·1**
  of aluminum-Cu-Mg alloy parts and its distribution, Multitest and Statimat patterns of, **41·16–17**
  coercive force, demagnetization, and retentivity in relation to, in magnetic-particle tests, **30·22**
  measurement of
    of ball and roller bearings with Magnatest Q eddy-current instrument, **42·58**
    by coercive force, **34·5**
    by conductivity with Magnatest FM-100, **42·12**
    of drill tips and sewing-machine needles, Multitest eddy-current instrument in, **40·23**
    by eddy-current testing, **2·25**
    by eddy-current testing, tabular summary of, **36·4–5, 36·7**
    by magnetic point-pole method, **34·13**
  measurement of Brinell, microscope for, **11·7**
  measurement of local, with magnetic field difference probe, **33·1**
Hardness (*Continued*)
  sorting by
    of age-hardenable light alloys by ellipse eddy-current methods, **40·28**
    automatic, with Multitest eddy-current instruments, **41·1–3**
    with Magnatest Q eddy-current instrument, **41·10**
    of steel parts, magnetic hysteresis loop in, **42·1**
  statistical quality control indicator (automatic) for, **41·13**
  of steel, magnetic hysteresis-loop effects, **42·27**
  of steel (ball-bearing) and its statistical distribution as shown by Magnatest Q and Statimat eddy-current instruments, **41·15**
Harmonics (See also "frequencies (harmonic)" under "Electric Current")
  modes, frequency ratio in sonic flaw detection, **51·13**
  of sonic vibration of rectangular bars, **51·2**
    use to evaluate relative physical constants factor, **51·6**
  in ultrasonic resonance testing, **50·12**
  ultrasonic resonance thickness measurements using, **50·3**
Hastelloy B Tubing, eddy-current signal trace of defective, **38·29**
Hastelloy Tubing, crack indication in, by ultrasonic immersion inspection, **47·34**
Haziness (See "Fogging")
Health, precautions in liquid-penetrant testing, **7·35**
Heat
  dissipation of, in X-ray generators, **14·45**
    in X-ray tubes, **14·3**
  sources in nondestructive testing, **5·17**
Heat Checks, parts having, evaluation of, **8·18**
Heat Exchangers, tubes, eddy-current testing of, **3·23**
  ultrasonic resonance testing of, **50·26**
Heat-Flow Tests, nondestructive, **5·23**
Heating
  over-, during sectioning with cut-off wheels, effects and prevention of, **32·24**
  of parts to fracture them after blueing, as supplement to magnetic-particle testing, **32·23**
Heating, Dielectric (See "Dielectric Heating")
Heating, Induction (See "Induction Heating")
Heating Unit, cast into aluminum casting, radiograph of, **24·18**
Heat Treatment (See also "Thermal History")
  of alloys and metals, control by eddy-current electrical conductivity, **42·19**
  of ball-bearing balls, rings, and rollers, Magnatest Q eddy-current sorting by, **42·58**
  cracks from, evaluation of parts with, **8·14**
  effect on liquid-penetrant indication of defects, **8·6**
    on ultrasonic immersion testing, **46·12**
  false indications from scale from, in ultrasonic immersion testing, **47·25**
  uniformity of, magnetic point-pole tests for, **34·11**
Helium
  absorption coefficients (mass) for γ and X rays and photon energies of, **18·32**
  in gas-leak detection, **5·3**
Helium Nuclei (See "Alpha Rays")
Hides, inspection (fluoroscopic) of, **19·36**
History
  of brittle-coating testing, **52·3**

History (*Continued*)
  of photoelastic-coating methods, **53·1**
  of radiation and particle physics, **13·1–4**
  of radioisotopes (artificial), **15·4**
  of strain-gage development, **54·1–2**, **54·13**
  of strain-gage theory and test development, **54·34**
  of ultrasonic testing, **43·3**
Holders, for X-ray film against specimens, **20·43**
Holes (See also "Gas Holes")
  cracks in drilled, eddy-current detector for, **40·2–3**, **40·47**
  diameter and shape, ultrasonic-wave amplitude-distance curves for various, **43·39**, **43·43**
  diameter in aluminum and stainless steel, ultrasonic wavelength in relation to, **45·20**
  diameter in aluminum blocks, ultrasonic-wave amplitude in relation to, **44·17**
  drilling of small, in measurement of residual stresses with brittle coatings, **52·24**
  eccentricity of bore, ultrasonic testing of, **43·49**
  ultrasonic indications of, Fresnel near-field effects on, **44·17–18**
Hollow Parts, thickness measurements of, by ultrasonic resonance method, **50·19**
Holograms, in electron microscopy, **10·31**
Hones, illumination of, for optical projectors, **12·13**
Honeycomb Structures
  brazed stainless steel, radiograph of defects in, **24·14**
  fluoroscopy of, **24·28**, **24·29**
  laminated (See "Laminated Products")'
Honing, effect on liquid-penetrant indications, **8·5**
Hooke's Equations, for strains in photoelastic-coating tests, **53·7**
Hooks, crane, brittle-coating testing of, as typical test, **52·22**
Horticulture, microradiography in, **20·41**
Hot Tears, in bronze (cast tin), radiographs of, **24·15**
Hue, color, characteristics of, **10·2–3**
Human Body, internal inspection of, cystoscopes and gastroscopes in, **11·15**
Humidity, effect on electrified-particle tests, **28·10** (See also "Water")
  on resin-type brittle-coating tests, **52·4–6**
  on strain-gage leakage resistance, **54·37–38**
  on strain gages, **54·24–25**
Huygen's Principle (Ultrasonics), definition of, **44·12**
Hydrochloric Acid, and mixtures with sulfuric acid in etching of metals, **32·27–28**
Hydrogen
  absorption coefficients (mass) for γ and X rays and photon energies of, **18·32**, **27·2**
  attenuation coefficients of, for γ and X rays, **27·2**
Hydrostatic Testing, of gas and water lines, **5·5**
Hydrostatic Pressure (See "hydrostatic" under "Pressure")
Hydraulic Systems
  borescopic inspection of, **11·14**
  in detection of motion of solid probes, **5·2**
Hypo
  clearing agent for, use in X-ray-film processing, **21·9**
  determination in X-ray-film emulsions, mercuric chloride test for, **21·12**
Hysteresis
  effect on strain gages, length in relation to, **54·11**
  of strain-gage-based transducer measurements, **54·3**
  of strain gages
    effect of number of strain cycles on, **54·26**
    prevention by temperature cycling and effect of degree of cure of cement on, **54·24**
  of stress-strain curves, effect on strain-gage tests, **54·4**
Hysteresis Loops
  for alternating and direct current, in magnetic field tests, **33·3**
  determination of static, **42·23**
  determination (precision) of, **42·21–23**
  in eddy-current testing, **42·21–29**
    of ferromagnetic alloys, **42·1**
  ferrograph screen wave forms of, **42·23**, **42·29**
  of nickel wire, tensile-stress effect on, **42·29**
  of steel (carbon), **42·29**
  wave forms, analysis of, **42·25–29**

I

Ice, acoustic and ultrasonic properties of, **43·8**
Identification, of parts in nondestructive-testing laboratories, **2·10**
Illumination (See also "Light, Visible")
  background
    in fluoroscopy, **24·22**
    for X-ray-film processing, **21·17**
  for brittle-coating crack-pattern photography, **52·26**
  combined shadow and surface, for optical projection systems, **12·16–17**
  for crack detection (visual) in brittle-coating inspection, **52·13**
  from incandescent lamps, response of CdS and CdSe to, **16·11**
  for liquid-penetrant testing, **7·11**, **8·9**
  for nondestructive testing, **4·11**, **5·8**
  shadow and surface, for optical projection systems, **12·11**
  surface, head-on system in optical projectors, **12·11–14**
    high-intensity, in optical projectors, **12·13–14**
    for optical projection systems, **12·11**
    selection for optical projectors, **12·12–13**
    sources for optical projectors, **12·11–12**
  for X-ray-film processing areas, **21·16**
Illuminators, for radiograph viewing, **21·17–18** (See also "Lamps")
Image-Converter Tubes, 11·35
  combinations with closed-circuit television and motion-picture fluorography, **19·45**
  for fluoroscopic inspection, **19·37–38**, **19·48**, **24·20**
Image-Orthicon Tubes
  for television pick-up, **11·36**
  in X-ray inspection by closed-circuit television, **19·39**
Images
  amplifiers, solid-state, **11·21**
  fluoroscopic, and their control, contrast, and definition, **24·20–22**
  formation of optical, **10·4**
  in optical projection systems, **12·17–20**
  oscilloscope (See "Oscillograms")
  radiographic (See "Radiographs")
  xeroradiographic (See "Xeroradiographs")

- **Imaginary Component**
  - of apparent impedance of test coil or secondary coil for thin-walled tubes, 38·3
  - of effective permeability, 36·14, 36·18
    - of spheres in eddy-current testing, 39·3
  - of impedance of circular coil with nonferromagnetic sphere, 39·9
  - of transmission coefficient *T* in eddy-current testing of sheet material, 39·14
  - of voltage of circular coil with nonferromagnetic sphere, 39·9
  - of voltage (secondary), calculation of, 36·15
- **Immerscope**
  - test block use with, in ultrasonic testing, 46·10
  - trace on, of tubing, showing effects of contour-corrected transducer lens, 44·10
  - in ultrasonic testing, 46·5
- **Immersion,** ultrasonic-test search units using, 43·7
- **Immersion Media,** for ultrasonic immersion inspection, 47·31
- **Impact Testing,** of abrasive products, and correlation with sonic resonant frequency tests, 51·9–10
- **Impedance, Acoustic** (See "Acoustic Impedance")
- **Impedance, Electric** (See "Electric Impedance")
- **Impedance, Mechanical**
  - of barium titanate transducers, 44·2
  - of lithium sulfate transducers, 44·3
- **Impregnation,** of paper, radiation in control of, 18·29
- **Impurities**
  - detection of ferromagnetic, by field difference probe, 33·1
  - detection of particles of, in nonmetallic substances, 39·1
  - metallic, detection of particulate, in eddy-current testing of nonmetallic objects, 39·10
- **Inclusions**
  - in castings, fluoroscopic indications of, 24·28
  - detection in aluminum and magnesium casting by ultrasonic immersion tests, 46·11
    - in metals, density factor in fluoroscopic, 24·24
    - by penetrating radiation, 5·12
    - in steel, ultrasonic contact test frequencies for, 48·2
  - gas (See "Porosity")
  - in hot-worked materials, magnetic-particle-test indications of, 32·4
  - metallic, detection in aircraft engine cams and bearing races, 3·34
  - nonmetallic, impedances in ultrasonic testing, 45·21
    - magnetic-particle-test indications of, 32·4–6
    - in steel rods, Magnatest D eddy-current wave forms and macro- and microsections showing, 42·63–64
  - nonplastic, magnetic-particle indications of, 32·6
  - slag weld, causes and radiography of, 25·4
    - magnetic-particle indications of, 32·10
  - tungsten, in welds, causes and radiography of, 25·9
  - ultrasonic detection of, multiple-frequency inspection in, 45·26
  - ultrasonic immersion indication of nonmetallic, 47·23
  - ultrasonic immersion indications of, 47·20
  - in welds, ultrasonic contact indications for, 48·17
- **Inclusions** (*Continued*)
  - X-ray indication of, in castings and plastic articles, 24·11
- **Inconel**
  - acoustic and ultrasonic properties of wrought, 43·8
  - tubing
    - crack indication in, by ultrasonic immersion inspection, 47·34
    - eddy-current signals from defective, with encircling and probe coils, 38·38
    - eddy-current testing of, resistive and reactive component signal traces *vs.* dimensional variations, 38·33
    - intergranular corrosion in, eddy-current indications of, 38·31–32
- **Inconel X,** ultrasonic inspection of forged, 47·15
- **Index of Refraction** (See "Refractive Index")
- **Indications** (See also "Signals")
  - eddy-current, 42·1–69
    - of cracks and other defects in steel rods with Magnatest D and macro- and microsections, 42·62–69
    - for impedance-magnitude method, 40·5
    - Magnatest Q, selection for sorting of alloys, 42·33
    - Multitest, 40·22
    - presentation methods for, 40·2–4
    - of tubing with probe coils, 38·37
  - electric-current test
    - interpretation of, 35·4–9
    - of railroad rails, 35·20
  - electrified-particle
    - blinking, on secondary surfaces, 29·6
    - false, 29·6
    - fugitive, 28·11
    - loss of, 28·11
    - loss of, of slightly conductive materials, 29·7
  - filtered-particle, 9·16
    - irrelevant, 9·18
  - liquid-penetrant
    - appearance of, 8·2
    - brilliance and extent of, discontinuity in relation to, 8·4
    - of cracks, cold sheets and forging laps, 8·2
    - developing time for, extent of defect in relation to, 8·4
    - diffuse, of porosity in castings, 8·3
    - evaluation of, 8·23
    - factors affecting, testing, 8·5
    - of forging laps and cracks, 8·2
    - of gas holes or pin holes in castings, 8·3
    - mechanism of formation of, 8·1
    - nonrelevant, 8·23
    - persistance of, size of defect in relation to, 8·6
    - of porous castings, 8·3
    - in post-emulsification process, 6·15
  - sharpness of
    - discontinuities in relation to, 8·3
    - standards for, 8·9
    - weak, 8·3
  - magnetic-particle
    - checking of, 32·3
    - classification of, 32·1
    - and their interpretation, 32·1–30
    - irrelevant, 32·14–17
    - of nonmetallic inclusions, 32·4–6
    - permanent records of, 32·18
  - nondestructive-test, suitability of, 4·9
  - sonic-test, interpretation of, 51·9
  - ultrasonic-contact irrelevant, 48·21

Indications (*Continued*)
- ultrasonic-immersion, **46·17**, **47·1–39**
  - false, **47·11**
  - interpretation of, **47·3**
  - from test blocks, **47·3**
- ultrasonic-test
  - factors affecting, **45·18**
  - from transmit-receive search units, **49·3**

Indicators (See also "Instruments")
- for ultrasonic resonance equipment, **50·10**
- visual, in Magnatest Q eddy-current instrument, **41·7–8**

Inductance, Electric (See "Electric Inductance")

Induction Heating
- magnetization by low-frequency, **30·21**
- in nondestructive testing, **5·17**

Inductive Reactance, of eddy-current test coils *vs.* electrical resistance, **36·1**, **36·3**

Industry
- nondestructive-test experience, dissemination in, by cooperative agreements, **2·28–30**
- nondestructive-test-method introduction to, by Institut Dr. Foerster, **2·30–31**
- nondestructive tests in modern, **1·1**

Inflammability Test, instruments for, **3·25**

Information
- exchange among national testing institutes in Europe, **2·17–22**
- sources for nondestructive testing, **1·19**

Infrared Light (See "Light, Infrared")

Ingots
- cracks and gas holes, detection of, **46·23**
- etching of cross-sections of, as supplement to magnetic-particle testing, **32·26**
- inspection by ultrasonic immersion tests, **46·23**

Inspection (See also "Nondestructive Testing" and specific methods of testing)
- combined methods with eddy-current testing, **2·34**
- by customers in independent laboratories, **2·11**
- direct surface, to supplement magnetic-particle testing, **32·19**
- field-test, **6·17**
- fluorescent-coated magnetic particles in, **30·19**
- fluorography in, **19·44**
- fluoroscopic, **19·36**, **19·42**
- of forgings, grinding as supplement to magnetic-particle testing in, **32·22**
- industrial, requirements for optical projectors and comparators, **12·1–3**
- of instruments at Institut Dr. Foerster, department for, **2·27**
- liquid-penetrant, **6·5**, **7·10**
  - apparatus for, **7·5**, **7·7**, **7·10**
  - field, **6·16**
  - selection of process for, **6·21**
  - with visible dyes in field tests, **6·20**
- magnetic-particle, mechanized equipment for, **31·10–15**
- with magnifiers as supplement to magnetic-particle testing, **32·19**
- outside of nondestructive-testing department, **1·17**
- optical projectors in, of incoming materials, **12·21**
- of pipeline welds, **25·16–28**
  - by radiography, percentage examination desirable, **25·26**
- previous methods of, effect on liquid-penetrant indication of defects, **8·6**
- production-line, management of, **1·17**

Inspection (*Continued*)
- of radiation safety procedures by outside personnel, **26·16**
- of raw materials, aims and management of, **1·16**
- of raw materials and semi-finished parts, economic value of, **1·12**
- re-, by post-emulsification fluorescent-penetrant process, **6·9**
- scrap reduction and production increase by, **1·14**
- standards and tolerances for dimensional, **1·10**
- standards for fluoroscopic and radiographic, penetrameter sensitivity in relation to, **19·47**
- ultrasonic
  - basic methods of, **43·1–3**
  - criteria for successful, **43·50**
- ultraviolet light in, **6·9**
- visual
  - for cracks in resin-type brittle coatings, **52·13**
  - involuntary, **5·12**
- X-ray
  - requirements for, **19·45**
  - of specific areas, **19·46**

Inspectors (See "Personnel")

Institut Dr. Foerster
- eddy-current-test problems solved by, tabular summary of, **36·9**
- nondestructive testing research and development laboratory, **2·23–34**

Institutes (See also "Laboratories")
- cooperative, for nondestructive testing, **2·13–23**
- national testing, of Europe, information exchange among, **2·17–19**

Instrumentation (See also "Instruments")
- strain-gage
  - development of, **54·13–14**
  - for large structures, **54·35**
- for ultrasonic contact tests, **48·4–5**, **48·7**
- for ultrasonic immersion testing, **46·5**
  - specifications for, **46·23**
- for ultrasonic resonance testing, **50·8**

Instruments (See also "Indicators," "Instrumentation," "Meters")
- department for production and special, at Institut Dr. Foerster, **2·26–27**
- eddy-current test
  - direct and indirect, **2·31–32**
  - for ellipse method, **37·31**
  - feedback-control, response characteristics of specific, **40·18**
  - for feedback-controlled impedance tests, **40·15**
  - for foil-thickness with automatic feedback control of rolls, **41·3**
  - sensitivity calibration of, **37·30**
  - sensitivity of, **37·35**
  - for small-diameter tubes, **38·27–28**
  - standard, **2·31**
  - tabular summary of, **36·4**
- magnetic thickness-measuring, **3·23**
- for photoelastic-coating-test calibration, **53·13**
- for photoelastic-coating tests, **53·16–24**
- quality control (automatic statistical), **41·12**
- for ultrasonic contact testing
  - calibration of, **48·15**
  - efficiency of, **48·15**
  - linearity of, **48·16**
- for ultrasonic immersion testing, standardization of, **46·26**
- for ultrasonic resonance thickness determination, **43·15**, **50·3**

Instruments (*Continued*)
  ultrasonic-test, **43·26–37**
Insulation, Electric
  for aircraft wiring, testing of, **3·35**
  coatings and base materials, eddy-current testing of, **36·8**
  in counter (proportional) design, **16·6**
  halogenated hydrocarbons as, for X-ray units, **14·14**
  resistance of, testing of, **5·13**
  testing of, **5·11, 5·21**
  thickness measurement of, eddy-current apparatus for, **40·2–3**
    with Foerster Isometer, **40·48**
  for ultrasonic testing, **44·5**
  ultrasonic test search units for, **43·5**
Intensification Factor, of radiographic film by fluorescent screens, **20·28**
Intensity, Radiation (See "intensity" under "Radiation" and specific types of radiation)
Interfaces
  metal-water, energy losses at, in ultrasonic testing, **45·5**
  sound refraction at liquid-solid, angle of, **45·9**
  steel-water, ultrasonic-beam intensities at various angles of incidence, **43·20–21**
  ultrasonic-wave effects at plane, **43·12–21**
  ultrasonic wave reflection at, **43·13**
  ultrasonic-wave refraction at, **43·15**
  ultrasonic wave transfer at, **45·1**
Interferences, in ultrasonic-wave transmission through thin plates, **43·15**
Interference Techniques, for thickness testing of thin coatings, **10·17**
Interferometers
  for sound velocity in liquids and gases, **50·3**
  for surface testing, **10·14–16**
    of accurate mechanical and optical units, **10·13**
  for transparent samples, **10·13**
Interferometry, microscopic, advantages and limitations of, **10·14**
Interlocks, protective, for X-ray rooms, **26·14**
Internal Conversion, of nuclei in radioactive disintegration, **15·3**
Interposers, for section measurement with optical projectors, **12·22–24**
Interpretation (See "Indications")
Inverse Square Law
  for radiation intensity, **15·6**
  in radiography, **20·10**
Inversion Method, for electric current in resonance circuit eddy-current testing, **40·43**
Iodine
  absorption coefficients (mass) for γ and X rays and photon energies for, **18·37, 27·31**
  attenuation coefficients of, for γ and X rays, **27·31**
Ionization
  of air, undercutting from, in xeroradiography, **22·11–12**
  by charged particles, **13·24**
  definitions applied to, **13·24**
  detectors for, **16·1**
  by electrons, **13·26**
  by gamma rays, **16·1**
  by heavy particles, **13·25**
  mechanism of, **16·1**
  by neutrons, **16·1**
  in nondestructive testing, **4·11**
  in radiation detection, **18·19**
  specific, **16·1**
  by X rays, amplification of, **16·8**
Ionization Chambers, 16·2–5
  for radiation detection in thickness gaging, **18·20**
  for radiation monitoring (personal), **16·4, 26·5**
  for X-ray thickness gages, **18·7**
Ionography, detection of penetrating radiation in, **5·10**
Ions, Electrolytic
  in nondestructive testing, **5·19**
  sources of, **5·16**
Ions, Gaseous
  atmospheric, effect on charged xeroradiographic plates, **22·6**
  beams in nondestructive testing, **4·11**
  sources of, **5·16**
Iridium, properties of, **15·17**
Iridium-192
  disintegration scheme of, **15·16**
  energy and half-life of, as gamma-ray source, **18·17**
  gamma-ray and neutron absorption of, **15·11**
  gamma rays from
    reduction factor for, by concrete, **26·13**
    reduction factor for, by lead, **26·11**
  photographic film shielding against, **20·39, 20·41**
  radiation dosage output of, **26·6**
  in radiography, **2·17, 15·17–19, 25·18**
    characteristics of, **15·13**
    equivalent voltage of, **25·17**
    exposure-thickness curves for, **15·27**
    sharpness with, **15·35**
    of steel, build-up curve for, **15·36**
    of welds in pipes, **25·20**
Iron
  absorption coefficients (mass) for γ and X rays and photon energies of, **18·35, 27·17**
  absorption components of mass absorption coefficients of, for γ and X rays, **18·40**
  attenuation coefficients of, for γ and X rays, **27·17**
  carbon determination in, from magnetic permeability, **42·1**
  detection of, magnetic field difference probe in, **33·1**
    in nonferrous scrap, by magnetic-field tests, **34·22**
  determination in nonmagnetic materials, by magnetic-field tests, **34·21**
  eddy-current linear time-base tests on rods of, **40·32–33, 40·35**
  eddy-current testing of, tabular summary of, **36·4**
  eddy-current testing of tubes of, depth penetration in, **38·21**
  effect on electrical conductivity of aluminum, **42·14**
  elasticity tension modulus of, **52·11**
  gamma-ray absorption and scattering in, effect of energy on, **15·25**
  gamma-ray attenuation by, reduction factors for, **26·12**
  gamma-ray shielding equivalent of, **26·10**
  mass absorption coefficients of, for radiation, **18·2**
  ultrasonic contact testing of, frequencies for, **48·1**
  ultrasonic-energy transmission through gray and nodular, **50·24–25**
  ultrasonic-resonance response and corresponding microstructures of gray and nodular, **50·25**

Iron (*Continued*)
  ultrasonic resonance testing of cast, constant-K value in, 50·3
  wire
    eddy-current testing of, similarity law in, 37·11
    magnetic-field-leakage indicator of, in magnetic-particle testing, 30·27
Iron Alloys
  nickel-, wire for strain gages, 54·6, 54·8–9
  silicon-, ultrasonic energy losses in, 43·25
Isobars, in trilinear plot of elements and isotopes, 13·5
Isochromatic Lines, 10·19 (See also "Fringes")
  from photoelastic-coating analysis of sheet pile, 53·26, 53·28–29
  in photoelastic-coating tests, 53·4
    for bridge assemblies (welded), 53·33–34
    examination with removal of isoclinic lines, 53·6
    of guided-missile fuselage and tail surfaces, 53·30–31
    in large-field instrument, 53·19, 53·21
    recording on black-and-white photographs, 53·23
    for stainless-steel spot-welded assembly, 53·32
Isoclinic Lines (See also "Fringes")
  in control of photoelastic-coating-test loading, 53·35
  in large-field instrument for photoelastic-coating tests, 53·19, 53·21
  in photoelastic-coating tests, and their removal, 53·6
Isodose Curves and Surfaces, for radiation safety, 18·24–25
Isomeric Transition (See "emission of" under "Gamma Rays")
Isometer (See "Foerster Isometer")
Isopachic Lines, in models under load, 10·19
Isostatics, in photoelastic-coating testing, 53·6
Isotones, in trilinear plot of elements and isotopes, 13·5
Isotope Exposure Holders, for radiography with Cobalt-60 and Iridium-192, 15·23–24
Isotopes, trilinear plot of, 13·5
Isotopes, Radioactive (See "Radioisotopes")
Isotopic Radiation (See "Radiation")
Isotropic Media, light transmission by, and effect of polarization on, 10·18–19

J

Jackscrews, inclusions (nonmetallic) in, magnetic-particle indications of, 32·4, 32·6
Jet Engines (See "jet" under "Engines")
Jigs, for brittle-coating-test loading, 52·18
Job Cards, in nondestructive testing laboratories, 2·9
Journals, of crankshafts and support levers, tensile testing with Magnatest Q eddy-current instrument, 42·54, 42·56–57

K

***K* Absorption Edge,** definition of, and curve for uranium, 13·19–20
***K* Capture** (See "capture" under "Electrons")
Kerosene, ultrasonic-wave attenuation *vs.* frequency in, 43·26
Kilovoltage (See "Voltage")
Kinetic Energy (See "kinetic" under "Energy")
Kits
  dye-penetrant, maintenance of, 7·32
  for liquid-penetrant testing, 7·1
Klasen's Equivalent Blur, in fluoroscopy or radiography, 19·2
Knott's Equations, for ultrasonic-wave energy, 43·18
***K* Radiation** (See "X Rays")
Krypton, absorption coefficients (mass) for γ and X rays and photon energies of, 18·36
Krypton-85
  energy and half-life of, as β-ray source, 18·17
  from fission of Uranium-235, 15·9

L

Laboratories, nondestructive-testing, 2·1–34 (See also "Institutes")
  control techniques in, 2·8
  cooperative, 2·13–23
  equipment and personnel for, 2·2
  floor plan of, 2·8
  flow of materials and data through, 2·6
  layout of, 2·5
  materials handling in, 2·2
  personnel for, 2·11
  research and development, 2·23–27
  of Roentgen Technische Dienst, 2·16
Lacquering
  to decrease test-object roughness effects in ultrasonic testing, 45·17
  for magnetic-particle-test-indication fixation, 32·18
Lacquers
  aluminum-containing, as undercoat for resinous brittle coatings, 52·9
  brittle coatings from air-drying, 52·4
Lamb Waves (See "Ultrasonic Waves")
Laminated Products
  eddy-current testing of, tabular summary of, 36·6
  electrical steel, sorting by hysteresis loss, 34·10
  honeycomb, sonic testing of, 5·24
  phenolic, constant K value in ultrasonic resonance tests, 50·3
  ultrasonic Lamb waves in testing of bonding of, 45·12–13
  ultrasonic testing of, with sharp-focused transducers, 44·6
Laminations
  detection in rolled plate or tubes, 5·25
  in metal plates and sheets, magnetic-particle indications of, 32·7
Lamps (See also "Black Lights," "Illuminators")
  filament (closely wrapped, single-coil), for shadow-projection systems, 12·5
  incandescent projection, for optical equipment, 12·5
  multicoil, for optical projectors with large screens, 12·5
  safe, arrangement in X-ray-film processing areas and allowable exposure to, 21·16
  signal, in Magnatest Q eddy-current instrument, 41·8
  vapor-discharge, for monochromatic light, 10·4
Laps, forging (See "Forgings")
Latent Image, in photography, 16·18
Lathes, turret, optical projection control of, 12·21
Latitude, in radiography (high-voltage), 23·4
Lattice Deformation, X rays in study of, 17·14

Layout, of nondestructive-testing laboratories, 2·5, 2·8

L/D Ratio (See "Length/Diameter Ratio")

Lead
- absorption coefficients (mass) for γ and X rays and photon energies of, 18·38, 27·39
- absorption components of mass absorption coefficients of, for γ and X rays, 18·40
- acoustic and ultrasonic properties of, 43·8
- attenuation coefficients of, for γ and X rays, 27·39
- effect on electrical conductivity of copper, 42·12–13
- electrical conductivity of, 42·16
- fluoroscopic barrier-window equivalence to, 19·13
- foil
  - coated with tin, deficiencies as screen material for radiography, 20·27
  - radiographic screens from, 16·24–25, 20·25
- gamma-ray attenuation by, reduction factors for, 26·11
- mass absorption coefficients of, for radiation, 18·2
- radiation-shielding equivalent of, 26·9–10
- as radiation shielding material, 26·14
- in radiography
  - equivalence factors for, 20·14
  - for reduction of scattering, 20·20–23, 20·25
- screens (See "Lead Screens")
- sheaths on wire, ultrasonic gaging of thickness of, 50·19
- sheets as backing in X radiography, 23·8
- radiography (X ray) of, density calculations for, 23·9
- ultrasonic contact testing of, 48·10
- ultrasonic reflection coefficients at interfaces with other materials, 43·13
- in ultrasonic resonance testing, constant *K* value in, 50·3
- X-ray absorption by, 20·14

Lead Acetate, mixtures with lead nitrate in radiographic masking, 20·22

Lead Alloys, antimony-, acoustic and ultrasonic properties of, 43·8

Lead Metaniobate, as ultrasonic-wave transducer material, 44·2

Lead Nitrate
- mixtures with lead acetate in radiographic masking, 20·22
- X-ray diffraction photograph of, 17·5

Lead Oxide
- glasses containing, protection coefficient for X rays, 19·13
- photoconductive, in X-ray pick-up tubes, 19·41

Lead Perchlorate, X-ray barrier cells containing, 19·14, 19·15

Lead Phosphate, glass containing, for X-ray barriers, 19·13

Leads, Electrical (See "Lead Wires")

Lead Screens, for radiography, 15·29, 20·25, 23·7
- care and selection of, 20·27
- for reduction of scattering, 20·20

Lead Silicate
- glass
  - for fluoroscopic inspection, discoloration by X rays, 19·14
  - for X-ray barriers, 19·13
- light transmission by cell containing, 19·14

Lead Sulfide, as photoconductor in X-ray amplification, 16·8

Lead Wires
- for electron tubes, microsections of defects in tungsten, 42·10
- through glass envelopes, crack detection in, 40·19
- strain-gage, 54·5
  - anchoring and installation of, 54·36–37
  - for high temperatures, 54·32
  - resistance measurement of, 54·32
  - resistance variation with temperature, compensation for, 54·32
  - shielding and stress avoidance of, 54·32
  - and their effects and shielding, 54·31–32

Leakage Radiation, control of, 26·13

Leaks
- detection of
  - of gas, 5·3
  - by liquid-penetrant testing, 5·5
  - in radiation sources, 26·5
  - in tanks, tubing, and welds by penetrant tests, 6·1
  - in tubing flanges, welds, etc., by liquid penetrants, 8·2
  - by visible-dye penetrants, 6·20
- liquid-penetrant testing for, standards for rejection in, 8·12

Leather, radiography (low-voltage) of, 24·40

Legal Requirements, for nondestructive-testing organizations in various countries, 2·22

Length (See "Dimensions")

Length/Diameter Ratio, in magnetization for magnetic-particle testing, 30·13–14

Lenses
- aberrations of, 10·6
- acoustic
  - for contour correction in ultrasonic testing, 44·9–10
  - design of, 44·7
  - for ultrasonic testing, 44·6–11
  - ultrasonic-test search units using, 43·7
- apertures of, for maximum illumination and depth of field in optical projectors, 12·7
- collimator, for optical projection equipment, 12·4–5
- curvature of, formula for, 10·7
- depth of focus of, used in optical projectors, 12·32
- electrified-particle testing of, 29·20
- field of, calculation for optical projectors, 12·16
- focal length of, as function of magnification, in optical projectors, 12·6
- focal plane range of, for optical projectors, 12·32
- formulas for calculation of optical, 10·7
- Fresnel, for optical projection equipment, 12·4
- image-carrying, for optical projectors, 12·6
- light loss by reflection from, 10·16
- for optical projection equipment, 12·4
- relay, in optical projectors, 12·6
- systems (optical), 10·5–7

Level, liquid control
- by magnetic means, 34·23
- with photoelectric refractometers, 10·11

Levers, support, of carbon steel, sorting for tensile strength with Magnatest Q eddy-current instrument, 42·56

Lever Systems, in detection of motion of solid probes, 5·2

Licensing, of radiation sources, 26·15

Lift-Off Effect
- in eddy-current indication of soft spots in sheets, 42·20

- **Lift-Off Effect** (*Continued*)
  - in eddy-current testing, circuit for suppression of, 40·42
  - prevention
    - in eddy-current feedback-controlled impedance testing, 40·20
    - in eddy-current testing with Sedac, 40·18
  - suppression with Defectometer eddy-current instrument, 40·47
- **Light, Fluorescent,** cadmium selenide and sulfide response to, 16·11
- **Light, Infrared**
  - conversion to visible images, tubes for, 11·35
  - in nondestructive testing, 4·11
- **Light, Polarized,** glare reduction by, 10·3
- **Light, Ultraviolet** (See also "Black Light")
  - conversion to visible images, tubes for, 11·35
  - detection by fluorescence, 10·5
  - liquid-penetrant fluorescence in, 6·2
  - in nondestructive testing, 4·11
  - phototubes for, 11·28
- **Light, Visible** (See also "Illumination")
  - from atoms (excited), source of, 10·12
  - behavior of, 10·12
  - brightness amplification by image converter tubes and solid-state amplifiers, 11·35
  - detection
    - and measurement of, phototubes in, 11·34
    - and recording of, 10·4
  - detectors for, in nondestructive testing, 5·9
  - diffraction of, 10·26
  - elliptically polarized, 53·3
  - level and spectral characteristics of, for liquid-penetrant inspection, 7·11
  - loss by reflection from lens, 10·16
  - monochromatic
    - for Eberhardt fine-thread test, 10·28
    - for dual-pinhole fine-structure test, 10·29
    - for nondestructive testing, 5·8
    - from vapor-discharge lamps, 10·4
  - paths
    - through crossed-plane reflection polariscope, 53·4
    - through large-field meter in photoelastic-coating tests, 53·21
    - in oblique-incidence photoelastic-coating meter, 53·24–25
    - through small-field crossed-plane polariscope, 53·23
  - polarization of, 10·18
    - by bi-refringent material, 53·2
  - polarized
    - for optical projectors, 12·30–31
    - optical tests with, 10·18
  - red *vs.* white in fluoroscopy, 19·35
  - resolution (vector) in stressed photoelastic models and in analyzer, 53·8
  - scattered, viewing xeroradiographic images with, 22·14
  - scattering of, 10·26
    - mechanism of, 10·26–27
    - for testing minute local inhomogeneities, 10·29
    - tests using, 10·27
  - sources
    - monochromatic, for recording isochromatics on black-and-white photographs, 53·23
    - for optical projection equipment, 12·4–5
    - for photometers for penetrant-brilliance determination, 7·22
  - stroboscopic, 10·4
- **Light, Visible** (*Continued*)
  - transmission of
    - by photographic film, density in relation to, 20·32
    - phototubes in measurement of, 11·34
    - by X-ray barrier glasses and liquids, 19·14
  - visual inspection using, in industry, 5·12
  - wave nature of, 10·12–19
- **Lighting** (See "Illumination")
- **Lights** (See "Lamps")
- **Light-Section Methods**
  - for measurement of refraction, optical thickness and flatness, 10·19–26
  - for surface testing, 10·19–20
- **Limestone,** radiation-shielding equivalent of, 26·9
- **Limit Frequency**
  - determination for eddy-current testing
    - of cylinders, 37·4
    - of spherical objects, 39·1
  - in eddy-current testing
    - of aluminum foil, 39·14
    - of cylindrical objects, 37·1
    - of primary field, 36·13
    - of sheet materials, 39·13, 39·18
    - of thick-walled nonferromagnetic tubes, 38·17
    - of thin-walled nonmagnetic tubes, 38·2
- **Linearity,** of strain-gage-based transducer measurements, 54·3
- **Linearizing,** of X-ray thickness gage output signals, 18·9
- **Linear Time Base Tests**
  - eddy-current, 40·29–38
  - with Magnatest Q eddy-current instrument, automation of, 41·5
- **Lines,** on X-ray film, and their prevention, 21·22
- **Liquid Penetrants** (See also "Dye Etchants")
  - application of, 6·2
    - in field tests, 6·16, 6·19
    - dye-type, 6·13
  - brightness and fading resistance of, determination of, 7·24
  - brilliance variation of, as shown by crack samples, 7·24
  - classes or types of, 6·2
  - concentration control of, 7·23
  - control of, aluminum-alloy blocks in, 7·26
  - in crack detection in brittle coatings by electrified-particle testing, 52·16
  - developers for, and their control and maintenance, 7·28
  - in electrified-particle testing, 28·3, 28·8
    - of nonconducting materials, 28·6
    - with heated, 28·10
  - emulsifier-containing, disadvantages of, 8·5
  - failure of, from water contamination, 7·33
  - fluorescent
    - contaminants in, and their detection, 7·33
    - contrast of, 7·20
    - development of, 6·1
    - evaluation of used, photometer for, 7·21
    - in field inspection, 6·16
    - maintenance of, 7·33
    - use with portable equipment, 7·1
    - water determination in, 7·33
  - handling of, precautions in, 7·35
  - hazards of, 7·18
  - motion of, detection of, 5·3
  - penetration time for dye-type, 6·14
  - post-emulsifiable, 6·9, 8·5
    - advantages of, 8·5

Liquid Penetrants (*Continued*)
  post-emulsifiable (*Continued*)
    in field tests, 6·17
    sensitivity of, 8·17
  removal from test specimen, 6·2, 6·4
    in post-emulsification dye-penetrant process, 6·15
  removal of visible-dye-type, in field tests, 6·19
  removal of water-washable, in field inspection, 6·17
  requirements for, 7·17–21
  sample preparation for determination of brilliance of, 7·23
  selection of, 8·5
  toxicity of, 7·19
  visible-dye
    advantages of, 6·18
    field tests with, 6·18
  in water-washable dye-penetrant process, 6·16
  water-washable fluorescent, 6·6
    applications of, 6·7
Liquid-Penetrant Testing, 6·1–15, 7·1–35
  in aircraft maintenance, 3·32–33
  applications of, 5·4
  basic principles and history of, 6·1
  basic processes in, 6·6
  in central cooperative institutes in Western Europe, 2·13
  of ceramic materials, 29·3
  cleaning of parts for, 6·13
  control specimens in, 7·26
  conveyorized automatic unit for, 7·8
  for cracks and leaks in oil refineries, 3·13
  for crankshafts and tailshafts of ships, 3·21
  defect indications in, effect of technique on, 8·7
  by dye process, parts preparation for, 6·13
  equipment for, 7·1–11
    high-volume units, 7·7
    maintenance of, 7·30
    portable, 7·1
    self-contained, 7·3–6
    stationary, 7·3–11
  illumination for, 7·11–17
    black light, 7·11–15
    white light, 7·11
  indications in, 8·1–24
    appearance of, 8·2–3
    evaluation of, 8·24
    irrelevant, 8·23
    persistence of, 8·4
  for leaks of valve assemblies, 3·23
  materials for, 7·17
  multiple-component stationary units for, 7·6–7
  parts preparation for, 6·6
  post-emulsification processes for, 6·9–12
    dye-penetrant, 6·15
    fluorescent-penetrant, 6·23
  precautions in, 7·34
  training (recognition) for, 8·23
  reinspection in, 7·34
  selection of process for, 6·21
  standards (acceptance) for, establishment of, 8·10–11
  temperature limitations of, 7·34
  visible-dye-penetrant process for, 6·23
  water-washable dye-penetrant process for, 6·16
  water-washable fluorescent penetrant process for, 6·6, 6·22
  water-washable visible-dye-penetrant process for, 6·23
Liquids
  dense, in minimizing X-ray scattering, 23·9
Liquids (*Continued*)
  density control of, radiation in, 18·29
  level
    control of, 10·11
    detection by radiation, 3·24
  mechanical properties of, ultrasonics in determination of, 43·49
  -metal interfaces, sound wave reflection and refraction at, 45·9
  as probing media, 4·10
  refractivity of, measurement of, 10·11
  ultrasonic-wave reflection time in, 43·31
Lissajous Patterns, in sonic-test frequency scanning, 51·9
Lithium, absorption coefficients (mass) for γ and X rays and photon energies of, 18·32
Lithium Sulfate
  crystals as ultrasonic-wave transducers, 43·4, 44·2–4, 50·15
    band width of, 44·20
    for contact testing, 48·2
    for immersion testing, 46·7
    mismatch, resolving power and sensitivity of, 44·5
  transducers (paint-brush), amplitude variation across, 44·11
Load, measurement with strain gages, accuracy of, 54·3
Load Cells, operating on strain-gage principle, applications of, 54·3
Loading
  for brittle-coating dynamic and static tests, apparatus for, 52·18–19
  control in resin-type brittle-coating testing, 52·11
  hydraulic, of brittle coatings, pressure effect in, 52·26
  of ore trestle (concrete), strain-gage testing of, 3·25
  in photoelastic-coating tests of guided missiles, 53·27
  of structures to simulate service conditions and measurement of strains in engineering design, 52·18
Loading Bench, for X-ray-film holders, 21·14
Logarithmic Scale, in density-exposure curves for radiographic film, 16·19
Longitudinal Magnetic Field Probe, for magnetic-field testing, 33·1
Loss-Sensing Tests, eddy-current, 40·15
Lucite
  models for photoelastic stress analysis, 12·31
  ultrasonic-wave amplitudes and angles in, 43·21, 43·23
  ultrasonic-wave attenuation *vs.* frequency in, 43·26
Lumicon, in fluoroscopy with closed-circuit television, 19·39
Luminescence, of fluoroscopic screens, decay of, 16·15
Luminescent Crystals (See "luminescent" under "Crystals")
Luminous Energy (See "Light, Visible")
Luminous-Energy Tests, nondestructive, 5·12, 10·1

M

McElroy-McNutt Technique, use of, 3·5
Machineability, of tempered cast parts, determination by coercive force, 34·8
Machine Processing, of X-ray film, and apparatus for, 21·2–3

- **Machinery**
  - design of, strain-gage tests in, **54·33**
  - increased complexity and demands on, growth of nondestructive testing in relation to, **1·4**, **1·5**
  - radiography of, in motion, **20·46**
  - service life of, photoelastic-coating tests in survey of, **53·35**
- **Machine Shops,** of Institut Dr. Foerster, **2·27**
- **Machining**
  - of castings, consideration in X-ray inspection, **24·7**
  - effect on side-lobe phenomena in ultrasonic testing, **44·19**
  - optical projection control over, **12·21**
  - residual magnetism effect on, **30·20**
  - rough, effect on liquid-penetrant indication of defects, **8·6**
  - ultrasonic gaging of, **50·20**
- **Macrosections,** of steel rods showing cracks and other defects, **42·64–67**
- **Magnaflux Eddy-Current Instruments,** FW-300, Al-Cu-Mg-rod diameter-variation indications of, **42·2**
- **Magnagage,** for plating thickness measurements, **3·35**
- **Magnatest Eddy-Current Instruments** (See also "Foerster Instrument")
  - D, **2·28**
    - in automatic crack testing of steel rods, **41·10**
    - in crack testing of various steel parts, **42·61–69**
    - indications of cracks and other defects in steel rods, in comparison with macro- and microsections, **42·62–69**
    - screen patterns of, analysis of, **42·63**
    - in self-comparison crack-depth tests, **40·35**
  - for eddy-current testing, summary of uses, **36·4–5**, **36·7**
  - FM-100
    - for eddy-current testing, **36·7**
    - in eddy-current testing, **42·10–21**
  - FM-100 and FW-300, suppression of undesired effects in use of, **40·46**
  - FS-300 or Q
    - adjustment and calibration of, **42·33**
    - in alloy sorting, **2·28**
    - automatic testing applications of, **41·8**
    - automation of, **2·33**
    - automation of eddy-current tests with, **41·5**
    - bands showing case depths of chain bushings, **41·17**
    - complex voltage plane of coils of, **42·42**
    - with conveyor belt, **41·8**
    - eddy-current testing with, selecting test conditions for, **41·6**
    - in materials research, **42·60**
    - patterns of, **42·29–61**
    - picture of ball-bearing steel test parts using, **41·15**
    - for quality control and sorting, automation of, **41·7**
    - screen patterns in crack-depth analysis of ferromagnetic cylinders, **40·35**
    - slit value of, as function of tensile strength of steel parts, **42·54**
    - sorting with, **42·31**
    - in tensile strength determination, **2·29**
    - test coils for, **40·38**
    - wiring diagram of, **40·29**
  - FW-200, tungsten-rod-defect indications with, **42·7**
- **Magnatest Eddy-Current Instruments** (*Continued*)
  - FW-300
    - circuit diagram for, **40·24**
    - for eddy-current testing, **36·4–5**, **37·31**, **40·26**
    - in measurement of electrical conductivity with feed-through coils, **42·3**
    - rectifiers (phase-controlled) in, **40·38**
- **Magnavisa,** optical projector for surface viewing at low magnifications, **12·12–13**
- **Magneprobe,** in aircraft maintenance, **3·34**
- **Magnesium**
  - absorption coefficients (mass) for γ and X rays and photon energies of, **18·33**, **27·8**
  - acoustic and ultrasonic properties of, **43·8**
  - attenuation coefficients of, for γ rays and X rays, **27·8**
  - castings, ASTM reference radiographs for, **24·3**
  - constant *K* value in ultrasonic resonance tests, **50·3**
  - effect on electrical conductivity of aluminum, **42·14**
  - elasticity tension modulus of, **52·11**
  - electrical conductivity of; **42·16**
  - fluoroscopy of, glass *vs.* beryllium windows in, **19·17**
  - forgings, ultrasonic contact testing of, **48·11**
  - penetration time for, in liquid penetrant testing, **6·8**, **6·10**
  - radiographic equivalence factors for, **20·14**
  - radiography of, exposure-thickness curves for, **15·27**
  - ultrasonic immersion testing of, **46·11**
  - ultrasonic-wave amplitude—distance curves for, **43·44**
  - ultrasonic-wave attenuation *vs.* frequency in, **43·26**
  - ultrasonic-wave reflection amplitudes for water-immersed, **43·46**
  - X-ray absorption and transmission by, **19·19**
- **Magnesium Alloys**
  - aluminum-, hardness *vs.* electrical conductivity of, **42·18**
  - aluminum-copper-
    - diameter variations of rods of, indications of Magnaflux FW-300 eddy-current instrument, **42·2**
    - eddy-current density and field strength in rods of, as function of radial position, **37·9**
    - electrical conductivity and hardness *vs.* quenching temperature of, **42·19**
    - hardness of and frequency distribution picture with Multitest and Statimat eddy-current instruments, **41·16–17**
    - segregation effect on electrical conductivity of cast, **42·15**
  - electrical conductivity of cast and wrought, **42·17**
  - radiography with Thulium-170, exposure-thickness curve for, **15·27**
  - shrinkage (micro-) in, X-ray interpretation of, **24·8**
  - soft-spot detection in, by eddy-current conductivity measurement, **42·3**
- **Magnetic-Analysis Eddy-Current Instruments,** Zuschlag, for crack testing, **41·11**
- **Magnetic Anisotropy,** in sheet materials, determination of, **34·9**
- **Magnetic Apparatus**
  - for detecting movement of nonferrous materials, **34·23**
  - for eddy-current testing at Institut Dr. Foerster, **2·25**

Magnetic Apparatus (*Continued*)
- for flow measurements, **34·23**
- for liquid-level control, **34·23**

Magnetic Field (See also "Magnetism")
- alternating-current, in eddy-current testing, **36·1**
- circular a.-c., in demagnetization after magnetic-particle tests, **30·25**
- circular and longitudinal residual, and their removal after magnetic-particle tests, **30·21**
- continuous, dry and wet methods in magnetic-particle testing, **30·12**
- around current-carrying conductors and effect of defects on, **35·11**
- around defective and sound railroad rails in Sperry system, **35·12**
- description of, **30·2**
- detection of, **5·10**
- difference, measurement of, **33·6**
- diminishing a.-c., in demagnetization after magnetic-particle tests, **30·22**
- direction of, in magnetic-particle testing, **30·8**
- of earth
  - cancellation by magnetic field meter, **33·10**
  - compensation for, **34·3**
  - magnetization from, **30·20**
  - minimizing effects of, in a.-c.-coil demagnetization after magnetic-particle tests, **30·25**
- eddy-current reaction, in sheet materials, **39·14**
- electromotive force induced by coil moving through, **35·12**
- equation for, in test objects, **33·15**
- generation and strength in eddy-current testing, **36·11**
- gradient measurements, **33·10**
  - accuracy of, **33·8**
- indicators for, in magnetic-particle testing, **30·26–27**
- leakage
  - detection of, by field meters, **33·10**
  - intensity of, measurement in magnetic-particle testing, **30·25–29**
- measurement
  - of d.-c., circuit for, **33·3**
  - of field recorder method in, **33·16**
  - of, on magnetized camshaft, **33·17**
  - of nonuniform, **33·10**
  - of strong, with Hall generators, **33·14**
  - of uniform, **33·10**
- measuring impulse, **33·17**
- in nondestructive testing, **30·1**
- orientation of, defect direction and, in magnetic-particle tests, **30·11**
- residual, in magnetic-particle testing, **30·11**
- sources of, **5·8**
- strength
  - for crack testing with Magnatest D eddy-current instrument, **42·61**
  - distribution
    - in cylinders, model for verification, **37·12**
    - in cylinders in eddy-current testing, **37·6–10**
    - in eddy-current testing of spheres, **39·11**
  - in eddy-current testing of brass, copper, and stainless steel tubes upon insertion between two coils, **38·16–17**
  - effect
    - on hysteresis loops of carbon steels, **42·30**
    - on Magnatest Q eddy-current sorting, **42·31**
    - on Magnatest Q eddy-current sorting of steels, **42·44**
  - in empty coil, in eddy-current testing, **36·11**

Magnetic Field (*Continued*).
- strength (*Continued*)
  - external, in eddy-current testing of tubes at various frequencies, **38·21**
  - high, limitations on use of, in eddy-current testing, **38·21**
  - of hysteresis-loop standard samples, apparatus for measurement of, **42·22**
  - measurement at surface of complicated parts, **33·15**
  - penetration depth of, as function of frequency ratio in eddy-current tests, **37·9**
  - phase displacement between, of outside and inside tube surfaces, in eddy-current crack evaluation, **38·14**
  - selection for Magnatest Q eddy-current sorting of alloys, **42·38**
  - selection in eddy-current testing with Magnatest Q instrument, **41.6**
  - steel (carbon) external relative magnetic permeability as function of, **38·20**
  - of steel (cold-drawn carbon), effect on magnetization with and without internal stresses, **42·25**
  - tangential, measurement with Hall generator, **33·12**
  - true tangential, determination of, **33·16**
  - use of low, in Magnatest Q eddy-current separation of two spring-steel alloys, **42·38**
- strength and direction of, effects in magnetic-particle testing, **30·12**
- tests using, **5·12**
- true field strength determination in, **33·16**
- true tangential field strength determination in, **33·16**

Magnetic-Field Meters, 33·6
- calibration of, **33·9**
- cancellation of earth's field with, **33·10**
- electric circuit of, **33·9**
- in leakage field exploration of steel surfaces, **33·10**
- pick-up probes for, **33·9**
- probe-type, **33·8–12**
- recording instruments for, **33·11**
- tape-probe measurements with, **33·10**
- tape test technique with, **33·11**
- for weak magnetic fields, **33·8**

Magnetic-Field Probes, 33·1–8

Magnetic-Field Testing
- advantages of, **34·1**
- apparatus (d.-c.) for, Institut Dr. Foerster development laboratory for, **2·26**
- apparatus for, **34·1–23**
- blasting cartridge location by, **34·22**
- detection of ferrous material in packaged foods by, **34·22**
- difference-field meter for, **33·6**
- field probe arrangements for, derivation of secondary-voltage wave forms for, **33·5**
- for industrial use, **33·1**
- at Institut Dr. Foerster, **2·23**
- instrument design for, **33·8**
- iron core wire location in nonferrous castings, **34·22**
- iron impurity determination in nonmagnetic materials by, **34·22**
- for iron in nonferrous scrap, **34·22**
- of large wall thickness, **34·16**
- for location of buried unexploded bombs, pipelines, and cable boxes, **34·23**
- for location of survey markers in geodesy, **34·23**

Magnetic-Field Testing (*Continued*)
- metallurgical applications of, 34·1
- multiple-point measurements of wall thickness, 34·16
- nondestructive, 33·1–17
- recording test results in, at Institut Dr. Foerster, 2·28
- secondary voltage in, 33·7
- for thickness
  - of automotive piston heads, 34·16
  - of cast nonferrous parts, 34·16
  - continuous operation, 34·17
  - of nonmagnetic walls, 34·15

Magnetic Flux Density (See "Magnetic Field")

Magnetic Focusing, of electron beam in X-ray tubes, 14·10

Magnetic Hysteresis (See also "Hysteresis Loops")
- in demagnetization after magnetic-particle testing, 30·21
- effects in eddy-current testing, 37·6

Magnetic Materials, nondestructive testing of metallic, chart for selection of methods for, 1·24, 1·25

Magnetic Particles
- for dry method of magnetic-particle testing and their application, 30·18
- in examination of cut sections, 32·24–26
- fluorescent, in turbine-blade testing, 3·12
- for nondestructive testing, 30·15
- reapplication at file cuts to recheck magnetic-particle-test indications, 32·21

Magnetic-Particle Testing
- for aircraft maintenance, 3·34
- of aircraft propeller hub, 2·16
- apparatus for, 2·7, 31·1–15
- in central cooperative institutes in Western Europe, 2·13
- in chemical and industrial plants, 3·23
- crack indications by, 33·14
- for crankshafts and tailshafts of ships, 3·21
- in defect detection, 1·29
- destructive tests supplemental to, 32·22–30
- effect on subsequent liquid-penetrant tests, 8·6
- of engine (aircraft) cylinders, semi-automatic apparatus for, 31·12
- fluorescent, black light for, 30·19
- with fluorescent particles, 30·18
- of gas-turbine compressor blades, semi-automatic equipment for, 31·10–11
- indications in, and their interpretation, 32·1–30
- indications in, permanent recording of, 32·18
- interpretation limitations in, 1·20
- magnetic field (surface) measurement in, 33·14
- magnetic paste for, 30·15
- materials for, 30·15–19, 31·2
- mobile wet-method units for, 31·10
- in nondestructive testing, 5·6
- nondestructive tests supplemental to, 32·19–22
- nonrelevant indications in, 32·14–17
- oil baths for, 30·15–16
- for oil refinery maintenance, 3·14
- portable units for, 3·35
- principles of, 30·1–29
- procedures for, 30·11
- semi-automatic equipment for, 31·10
- sensitivity range in, 1·8
- stationary equipment for, 31·8
- of steering spindles, automatic unit for, 31·12
- for turbine maintenance, 3·10
- wet fluorescent, apparatus for, 31·9

Magnetic Permeability
- of air space between coil and specimen in eddy-current testing, 36·17
- of cylindrical specimens, effect in eddy-current testing, 37·1–6
- in the determination of carbon in ferrous metals, 42·2
- -diameter direction in Magnatest Q eddy-current testing, angle with conductivity direction as function of frequency ratio, 42·42
- differential, of hysteresis loops, 42·30
- in eddy-current testing of tubes, depth penetration limitations from, 38·20
- effect in eddy-current testing, and its determination, 36·3
- effect on complex voltage plane for Magnatest Q coil in eddy-current testing, 42·47
- effects in crack-depth analysis of Magnatest Q wave forms and impedance-plane characteristics, 40·34–35
  - in eddy-current crack testing of steel rods, 41·10
  - in eddy-current testing of ferromagnetic cylinders, separation from effects of conductivity and diameter, 37·4–6
  - in eddy-current testing of sheet materials, 39·16
  - in eddy-current testing small-diameter of tubes, 38·24
  - in Magnatest Q eddy-current testing at high frequency ratios, 42·42
  - separation from conductivity and diameter effects in Magnatest Q eddy-current sorting, 42·39
- measurement of
  - advantages of, 34·1
  - by eddy-current testing, tabular summary of, 36·4–6
  - of foils and sheets by eddy-current methods, 39·12
- of parts which are mechanically deformed, effect on Magnatest Q eddy-current sorting, 42·31
- relative, effect in eddy-current testing of spheres, 39·4
  - effect on apparent test-coil impedance in eddy-current testing of spheres, 39·6
  - in evaluation of eddy-current crack tests on nonferromagnetic tubes, 38·15
  - of ferromagnetic cylinders in eddy-current linear time-base tests, 40·32
  - of nonferromagnetic materials, 36·16
  - in reactance magnitude eddy-current tests, 40·8
  - of steel (carbon), as function of external magnetic field strength, 38·20
  - of tubes, effect of, in eddy-current testing with internal coils, 38·15
- sensitivity (maximum) to, in eddy-current testing of tubes, 38·17
- of tubes, layer of maximum, in eddy-current testing, 38·21

Magnetic Point-Pole Tests
- double pole, 34·14
- magnetic-field, 34·9–14

Magnetic Poles, fugitive, in demagnetization after magnetic-particle testing, 30·28

Magnetic Properties
- of ceramic materials, crystal orientation and, 17·19
- detected by nondestructive tests, 4·13
- measurement of, 34·4
- of strain-gage alloys, 54·9

Magnetic Properties (*Continued*)
- variation in eddy-current testing of rods and tubes, from magnetic crane and straightening stresses, 2·31

Magnetic Saturation, of ferromagnetic materials in eddy-current testing, 42·21

Magnetic-Saturation Flux Density, as indication of residual austenite content and ferrite content of steel, 34·4

Magnetic Writing, magnetic-particle-test nonrelevant indications from, 32·17

Magnetism (See also "Magnetic Field")
- removal of (See "Demagnetization")
- residual
  - in checking of magnetic-particle-test indications, 32·4, 32·19
  - measurement with external probes, 34·6
  - as measure of coercive force, 34·5

Magnetization
- with cables and prods, portable equipment for, for magnetic-particle tests, 31·2–3
- with cables for magnetic-particle testing, electric-current for, 30·14
- circular
  - of electric conductors, hollow parts and solid parts, for magnetic-particle tests, 30·4
  - electric-current requirements for, for magnetic-particle testing, 30·13
  - in magnetic-particle testing, 30·3, 30·8
- coil
  - electric current requirements for, length/diameter ratio, for magnetic-particle tests, 30·13–14
  - for magnetic-particle testing, 30·10
- coil or longitudinal, in magnetic-particle testing, 30·6
- contact, nonrelevant magnetic-particle-test indications from, 32·17
- with electric current, for magnetic-particle tests, 30·4–7
- electric-current-type selection for, for magnetic-particle testing, 30·8, 31·1
- heavy-duty, a.-c., half-wave unit with automatic demagnetizer for, magnetic-particle testing, 31·6
- of hollow parts or tubes by using a central conductor, in magnetic-particle testing, 30·9
- of hysteresis-loop standard samples, apparatus for, 42·22
- longitudinal, for magnetic-particle testing, 30·3, 30·9
  - electric-current requirements for, 30·13
- for magnetic-particle testing, medium- and heavy-duty equipment for, 31·4
- medium-service a.-c. and half-wave unit for, 31·4–10
- methods selection for, for magnetic-particle testing, 30·7–11
- over-, in magnetic-particle testing, nonrelevant indications from, 32·14
- parallel, limitations in magnetic-particle testing, 30·9
- by passing current through entire part, for magnetic-particle testing, 30·9
- prod, of large parts for magnetic-particle testing, 30·9
- stationary equipment for, magnetic-particle testing, 31·7–10
- of steel (cold-drawn carbon), effect of annealing and magnetic-field strength on, 42·25
- swinging-field, for magnetic-particle testing, 30·11
- of test parts, causes of, 30·20

Magnetization (*Continued*)
- three-phase rectifier, a.-c. unit for, for magnetic-particle testing, 31·7
- yoke, for magnetic-particle testing, 30·10

Magnetization Curve, for ferromagnetic materials, 33·3

Magnetization Loops (See "Hysteresis Loops")

Magnetizing Field, direction in eddy-current crack testing of spheres, sensitivity in relation to, 39·10

Magnetostrictive Effects, in strain gages, strain-application rate effect on, and their detection, 54·27

Magnetostrictive Elements, for transducers for ultrasonic waves, 44·1

Magnetostrictive Materials, stresses (internal) in, hysteresis-loop effects, 42·28

Magnetostrictive Motors, for vibration testing, 5·17

Magnets
- bar, horseshoe, and ring, paths of magnetic fields in, 30·2–3
- magnetization caused by permanent, 30·21
- permanent, eddy-current-test curves for, 39·6

Magnification
- calculation of optimum, in fluoroscopy, 19·4
- change of, in optical projectors, 12·6–7
- extreme, wave-front reconstruction for, 10·30–33
- as factor in determination of surface waviness with optical projectors, 12·33
- of fluoroscopic images, 19·27, 19·33
  - focal-spot size and sensitivity in relation to, 19·18
- as function of lens design and projection distance, in optical projectors, 12·6
- limits, of microscopes, 10·8
- precision, in industrial testing, 12·1
- of telescopic systems, 11·17
- X-ray projection, for improvement of definition, 19·2

Magnifiers, 11·1 (See also "Microscopes")
- in checking magnetic-particle-test indications, 32·4
- illuminated, 11·4
- inspection glasses for supplementation of magnetic-particle testing, 32·20
- measuring, 11·4
- in surface inspection as supplement to magnetic-particle-testing, 32·19

Maintenance
- of fluoroscopic screens, 16·15
- of liquid penetrants, cracked aluminum-alloy blocks in, 7·28
- of liquid-penetrant test systems, 7·30
- nondestructive testing in, 1·17
- of X-ray intensifying screens, 16·17

Maintenance Tests
- of aircraft, 3·26
  - cost savings in, 3·36
- nondestructive tests in, 4·7
- in oil refineries, 3·12
- of parts in service, scheduling of, 1·23
- personnel characteristics for, 3·36
- of pipelines, 3·14
- of power plants, 3·7
- ultrasonic contact testing in, frequencies for, 48·1
- ultrasonic resonance tests in, 50·25–29

Management
- of nondestructive testing, 1·16
- of nondestructive-testing laboratories, 2·4

Management (*Continued*)
- of nondestructive testing organizations in industrialized *vs.* remote areas, **2·19**

Manganese
- attenuation coefficients of, for γ rays and X rays, **27·16**
- effect on electrical conductivity
  - of aluminum, **42·14**
  - of copper, **42·12**

Manipulators, for radioisotope radioactive sources, **15·23**

Manufacturing
- control of processes in, nondestructive testing in, **1·3**
- cost reduction in, role of nondestructive testing, **1·3**
- nondestructive-testing needs of, and role of independent laboratory in, **2·1–3**

Marble, radiation-shielding equivalent of, **26·9–10**

Marcasite, atomic structure of rhombic, **10·32–33**

Marker Circuit, adjustment, in ultrasonic immersion testing, **46·10**

Markers
- distance or time-scale, for flaw-depth indication in ultrasonic testing, **43·30**
- precision, in ultrasonic testing with A-scan presentation, **43·32**
- for ultrasonic-test A-scan systems, **43·33**

Marking
- of defective parts, Sigmaflux meter indications in, **40·27**
- of defective rods in Magnatest D eddy-current crack testing, **41·10**
- of strains (threshold) in brittle-coating tests, **52·19–20**

Marks
- crimp, pressure and static, on X-ray film, and their prevention, **21·21–22**
- paint, in recording of railroad-rail electric current test results, **35·19**

Masking, in radiography
- to avoid excessive contrast, **21·19**
- with metallic shot and lead mask, **20·20**
- for scattering prevention, **20·22**

Masks, transparent paper, in recording nondestructive-test data, **2·28**

Masonite, gamma-ray shielding equivalent of, **26·10**

Mass Absorption Coefficients, of elements for radiation, **18·2, 27·1–41**

Mass Spectrometers, in gas-leak detection, **5·3**

Mass Spectroscopy, uses of, **5·19**

Materials
- effect on acoustic impedance in ultrasonic testing, **45·1–2**
- effects in ultrasonic immersion testing, **46·10–12**
- flow through nondestructive-testing laboratory, **2·6**
- inspection of processed, scheduling of, **1·23**
- limitations in nondestructive testing, **1·21**
- modern demands for sound, nondestructive-testing growth and, **1·6**
- nondestructive testing of new, **1·5**
- research on, Magnatest Q eddy-current methods in, **42·60–61**
- for transducers for ultrasonic waves, **44·1–4**
- ultrasonic testing of, significant properties in, **45·1**

Materials Engineer, as information source in nondestructive testing, **1·19**

Materials Handling
- in automatic testing of metal rods, **41·2**
- in eddy-current testing of large parts, electronic-slit method in, **41·8**
- in liquid-penetrant testing of small parts, apparatus for, **7·5**
- in nondestructive testing, cost factors in relation to, **1·15**
- in nondestructive testing laboratories, **2·2, 2·12**

Mathematical Analysis, of eddy-current test problems, summary of problem types, **36·8**

Matter
- atomic nature of, **13·2**
- motion of, combined with energy transmission, in nondestructive testing, **4·11**
- motion of, tests, **4·8, 4·10, 5·1–5**

Matter-and-Energy Tests, **5·14–25**
- charged particle beams, **5·18–19**
- electric current, **5·20–23**
- electric current sources for, **5·16–17**
- heat sources for, **5·17, 5·23–24**
- high energy particles, **5·14**
- high energy particle sources for, **5·15–16**
- ions, **5·19–20**
- probing media for, **5·14–17**
- vibration, mechanical, **5·24–25**
- vibration sources for, **5·17**
- waves, **5·15**

Maxwell's Equations, in calculation of forked-coil theory in eddy-current testing of sheet materials, **39·13**

Mean Life, of isotopes, **13·12**

Mechanical Impedance (See "Impedance, Mechanical")

Mechanical Properties
- of base materials, effects in strain-gage tests, **54·3–5**
- detected by nondestructive testing, **4·12**
- determination by coercive force, **34·5**
- of ultrasonic-test search units, types to be considered, **43·5**

Mechanical Testing, of castings to supplement X-ray inspection, **24·7**

Mechanical Testing Apparatus, fracturing with, as supplement to magnetic-particle testing, **32·23**

Mechanical Treatment, of tubes (small-diameter), effects in eddy-current testing, **38·24** (See also "Working")

Mechanization, of liquid-penetrant testing, **7·7**

Medicine, radiography in, fluorescent-screen intensification factor in, **20·28**

Megger, for electrical insulation inspection, **3·35**

Melting, examination of, by reflecting objectives of optical systems, **10·9**

Melting Point, of strain-gage alloys, **54·8**

Memory Tubes (See "Electron Tubes")

Mercaptans, in natural gas-leak detection, **5·4**

Mercury
- absorption coefficients (mass) for γ and X rays and photon energies of, **18·38**
- acoustic and ultrasonic properties of, **43·8**
- detection of vapor of, **5·3**
- model experiments using
  - for eddy-current testing of cracks in nonferromagnetic tubes, **38·12**
  - for verification of distribution of eddy-current and field strength in cylinders, **37·11**
- models in simulation of effects of discontinuities in eddy-current testing, **37·13**
- slip rings in strain-gage circuits, **54·33**
- ultrasonic reflection coefficients at interfaces with other materials, **43·13**

Mercury Chloride ($HgCl_2$), test for hypo content of X-ray-film emulsions, **21·12**
Mercury Sulfide (HgS), as photoconductor, **16·8**
Mercury-Vapor Lamps
  for liquid-penetrant testing, **7·12**
  for magnetic testing with fluorescent magnetic particles, **30·19**
Mesons, as elementary particles, **13·4**
Metallizing, of condenser paper, eddy-current control of metal thickness in, **41·4**
Metallography
  of cracks and other defects in steel rods, compared with Magnatest D eddy-current patterns, **42·64–67**
  as magnetic-particle-test supplement, **32·28–29**
  microscopes for, **11·8**
Metallurgical History, effect on ultrasonic immersion indications, **47·9**
Metallurgical Properties, determination by coercive force, **34·5**
Metallurgical Structure, selection of ultrasonic contact test equipment in relation to, **48·4**
Metallurgy
  eddy-current testing in, **2·25**
  factors, study by sonic resonance vibration tests, **51·6**
  magnetic field tests in, **34·1**
  microscopes for, **11·8**
  phase changes in strain-gage materials at high temperatures, **54·23**
  research using ultrasonics, **43·49**
Metal Plate, ultrasonic contact testing of, frequencies for, **48·1**
Metals
  acoustic and ultrasonic properties of, **43·8**
  casting of, motion-picture fluorography of, **19·45**
  cleaning for resin-type brittle coatings, **52·9**
  coatings, determination of thickness with X rays, **24·36**
  coatings on, measurement of thickness of, by interferometers, **10·14**
  coating with, by vacuum deposition, eddy-current control of film resistance during, **39·19**
  defect depth in, ultrasonic measurement of, **45·9**
  detection in nonmetallic specimens by eddy-current testing, **39·10**
  direct-current nondestructive testing of, surface preparation for, **35·3**
  dye-penetrant penetration time for, **6·14**
  focal depth in, for ultrasonic waves, **44·7**
  foils (thin) of, differential arrangement for measurement of resistance of, **39·19**
  forged or rolled parts of, effect of structure on ultrasonic shear-wave velocity in, **45·7**
  forging and rolling of, etching in detection of flow lines from, **32·25**
  Fresnel-zone ultrasonic-wave effects in, with water path, **44·15–17**
  gas release from molten, casting porosity from, **24·8**
  identification and sorting of, triboelectricity in, **5·22**
  light (See also "Aluminum" and "Magnesium")
    porosity in, detection with eddy-current Defectometer, **40·47**
    radiography of, fluorescent screens for, **20·28**
    sorting of pressed parts of, by hardness with Multitest eddy-current instruments, **41·2**
  -liquid interfaces, sound-wave reflection and refraction at, **45·9**
Metals (*Continued*)
  machined, surface waviness of, **12·32–33**
  "noise" in ultrasonic testing and its causes and reduction, **44·7**
  nondestructive testing of heavy or magnetic, chart for selection of methods for, **1·24, 1·25**
  nondestructive testing of light or nonmagnetic, chart for selection of methods for, **1·26–27**
  nonferrous
    eddy-current testing of, tabular summary of, **36·4–5, 36·7**
    significance of electrical conductivity in eddy-current testing of, **42·1**
  polished, surface waviness of, **12·32–33**
  powdered, ultrasonic transducer backings containing fibrous plastics and, **44·6**
  radiographic equivalence factors for, **20·14**
  radiography of
    Cobalt-60 in, **15·14**
    exposure-thickness factors for, **15·26**
  segregation in, electrical conductivity as indication of, in eddy-current testing, **42·1**
  sheets (See also "Plates," "Sheet Materials")
    coils for eddy-current testing of, **40·38**
    eddy-current determination of conductivity-thickness product for, **39·16**
    thickness gaging in rolling of, **18·26**
    thickness measurement with *RC* oscillator, **39·18**
  surface preparation for strain gage application, **54·35–36**
  ultrasonic testing of, noise in, **45·7**
  ultrasonic-test potential, applications in, **43·49**
  ultrasonic-wave reflection time in, **43·31**
  ultrasonic-wave refraction in, effect of angulation of incident beam on, **45·10**
  -water interfaces in ultrasonic testing, energy losses at, **45·5**
Meter Indications
  of Sigmaflux eddy-current instruments, **40·26**
  in ultrasonic contact testing, **48·5**
  uncertainty in radiation-transmission thickness measurements, **18·5**
Meters (See also "Instruments" and specific named instruments)
  for black light, **7·14**
  large-field, for dynamic and static photoelastic-coating tests, **53·19–21**
  oblique-incidence, for photoelastic-coating tests, **53·24–25**
  for photoelastic-coating tests of guided missiles, **53·27**
  selection chart for photoelastic-coating tests, **53·17**
  small-field, for dynamic and static photoelastic-coating tests, **53·22–23**
  survey, for radiation measurement, **16·4**
Methacrylate Resins, as wedge materials for ultrasonic-beam direction, **43·5**
Methylene Chloride, as solvent in liquid-penetrant concentration control, **7·23**
Methyl Methacrylate, fundamental ultrasonic resonant frequency of, **50·4**
Microborescopes, **11·12, 11·22**
Microdensitometers (See "Densitometers")
Micrometers
  in detection of motion of solid probes, **5·2**
  vertical, measurement of focus with, **12·32**
Microphones, as vibration detectors in sonic testing, **51·7**
Microradiography (See "Radiography")

- **Microscopes, 11·1** (See also "Magnifiers")
  - binocular, for surface inspection as supplement to magnetic-particle testing, **32·20**
  - for Brinell hardness testing, **11·7**
  - compound *vs.* simple, **10·7**
  - electron (See "Electron Microscopes")
  - high-power, **11·7**
  - infrared, reflecting objectives in, **10·9**
  - interference, **11·10**
  - interferometer
    - double-focus system, **10·13–14**
    - double-refracting system, **10·13–14**
    - produced by Zeiss, West Germany, **10·15**
    - two-objective, **10·14**
  - laboratory, **11·7**
  - low-power, **11·5**
  - magnification limits of, **10·8**
  - medium-power, **11·5**
  - metallographic, **11·8**
  - metallurgical, **11·8, 32·29**
  - numerical aperture of objective lens of, **10·7**
  - phase-contrast, **11·10**
  - polarizing, **11·8**
  - resolving power of, **10·7**
    - equation for, **10·7**
  - schlieren-grating
    - adjustment of slit diaphragm of, **10·21**
    - optical principle of, **10·21**
  - shop, **11·6**
  - stereoscopic, **11·5**
  - ultraviolet, reflecting objectives in, **10·9**
  - wide-field, **11·5**
- **Microscopy**
  - electron (See "Electron Microscopy")
  - of metals (etched), and reagents for, **32·29**
  - of metals (nonetched) as supplement to magnetic-particle testing, **32·29**
  - phase
    - applications of, **10·18**
    - bright-contrast, **10·18**
    - dark-contrast, **10·18**
    - principle of operation in, **10·17**
    - theory of, **10·18**
  - in radiography (micro-), **20·41**
  - television in, **11·37**
  - two-wavelength, **10·31**
- **Microsections,** of steel rods showing cracks and other defects, **42·64–67**
- **Microshrinkage** (See "Shrinkage")
- **Microstructure**
  - effect on ultrasonic contact testing, **48·2**
  - of forgings, ultrasonic detection of unrefined, **43·24**
  - grain-size effects in ultrasonic immersion testing, **47·14**
  - of metals, microetching in determination of, **32·25**
  - of tungsten and molybdenum rods and wire showing defects, **42·10**
- **Milliamperage** (See "Electric Current")
- **Military** (See "Armed Forces")
- **Mirrors,** for optical projection equipment, **12·4, 12·7**
- **Mirror Viewing,** in fluoroscopy, **24·20**
- **Mismatch** (See also "Polarity, Reversed")
  - impedance for flat-bottomed holes in ultrasonic testing, **45·21**
  - between transducer crystals and their backing members, **44·5**
  - in ultrasonic testing, **45·21**
- **Mismatch Factor,** for ultrasonic-wave transmission, **43·13**
- **Misruns**
  - in castings, X-ray detection and evaluation of, **24·11**
  - fluoroscopy in light-alloy castings, **24·24**
- **Missiles, Guided** (See "Guided Missiles")
- **Mixers,** for X-ray-film processing solutions, **21·2**
- **Mixing**
  - automatic, load cells operating on strain-gage principle in, **54·3**
  - of ceramic brittle-coating materials, **52·16**
  - of sulfuric acid solutions, precautions in, **32·28**
- **Mixtures,** X-ray analysis of, **17·12**
- **Mode Conversion**
  - in ultrasonic testing
    - with barium titanate and quartz transducers, **44·2**
    - with lithium sulfate transducers, **44·4**
    - of rough-surfaced parts, **45·17**
  - of ultrasonic waves at plane interfaces, **43·15–18**
- **Models**
  - for determination of effects of discontinuities in eddy-current testing, **37·13–15**
  - in eddy-current detection of discontinuities, similarity law in, **37·11**
  - in eddy-current testing, summary of, **36·4, 36·9**
  - for experimental verification of distribution of eddy-current and field strength in cylinders, **37·12**
  - experiments on eddy-current testing of cracks in nonferromagnetic tubes, **38·12**
  - photoelastic (See "Photoelastic Models")
  - for sonic vibration-frequency testing of complex shapes, **51·6**
- **Modes**
  - of ultrasonic Lamb waves, **45·12**
  - of vibration of rectangular bars, **51·2**
- **Mohr's Stress Circles,** in analysis of oblique incidence and principal strains in photoelastic-coating testing, **53·8–9**
- **Moisture** (See "Water")
- **Molds,** gas release from, casting porosity from, **24·8**
- **Molecules,** large, light-scattering tests of, **10·27**
- **Molybdenum**
  - absorption coefficients (mass) for γ and X rays and photon energies of, **18·36**
  - acoustic and ultrasonic properties of, **43·8**
  - attenuation coefficients of, for γ rays and X rays, **27·26**
  - electrical conductivity of, **42·16**
  - rods and wire, defect indications with Magnatest FW-200 eddy-current instrument, **42·6–10**
  - wire
    - crack detection in, with Ziljstra eddy-current instrument, **40·19**
    - diameter variations of, eddy-current testing of, **42·3**
- **Monel**
  - acoustic and ultrasonic properties of wrought, **43·8**
  - constant *K* value in ultrasonic resonance tests, **50·3**
  - elasticity tension modulus of, **52·11**
- **Monitoring,** radiation
  - instruments for, **26·5**
  - management responsibility for, **26·16**
  - of personnel contamination, **26·3–4**
- **Monitors,** for ultrasonic-test gated systems, **43·35**

- **Montmorillonite,** X-ray diffraction photograph of, 17·5
- **Motion**
  - fluoroscopic inspection of, and of objects in motion, 24·22
  - measurement by, with optical projectors, 12·2–3
- **Motion-of-Matter Tests**
  - detectors in, 5·2
  - industrial applications of, 5·4
  - probing media for, 5·1
  - survey of, 5·1–5
- **Motion-Picture Photography,** borescopic uses of, 11·25
- **Motors,** copper rings of squirrel-cage induction, Magnatest FW-100 eddy-current instrument in control of conductivity of, 42·13
- **Mottling,** in radiography
  - and its control, 20·24
  - with fluorescent intensifying screens, 16·22
- **Mountings,** for transducers for ultrasonic resonance testing, 50·14, 50·16
- **Multitest Eddy-Current Instruments** (See also "FS-200" under "Magnatest Instruments")
  - automatic testing with, 41·1
  - for eddy-current testing, 36·4–5, 36·7, 40·20, 40·23
  - point picture of hardness of Al-Cu-Mg parts with Statimat picture, 41·17
  - rectifiers (phase-controlled) in, 40·38
- **Munitions,** filling with explosives, weight control in, 5·14
- **Mylar,** for protection of measurement areas of bulkheads in ultrasonic test methods, 50·38

N

- **Natural Frequency Vibration Tests** (See "Sonic Testing")
- **Natural Gas,** leaks of, detection of, 5·4
- **Near Field** (See "Fresnel Zone")
- **Near Ultraviolet Light** (See "Black Light")
- **Near-Zone Effect,** in ultrasonic immersion testing, 47·12
- **Needles**
  - automatic sorting of, 41·1
  - hardness of sewing-machine, Multitest eddy-current instrument in testing, 40·23
- **Negative Indications,** in electrified-particle testing, 29·5
- **Neodymium,** absorption coefficients (mass) for γ and X rays and photon energies of, 18·37
- **Neon,** absorption coefficients (mass) for γ and X rays and photon energies of, 18·33
- **Neon Lamps,** in ultrasonic-test-data presentation, 43·34
- **Neoprene**
  - coatings for moistureproofing of strain gages, 54·38
  - for protection of measurement areas of bulkheads in ultrasonic test methods, 50·38
  - ultrasonic-wave attenuation *vs.* frequency in, 43·26
- **Nephelometry,** definition of, 10·27
- **Netherlands, The,** nondestructive-testing development in, and central cooperative institutes for, 2·13
- **Networks, Electrical** (See "Electric Circuits")
- **Neutrino,** as elementary particle, 13·3
- **Neutron Flux Density,** control in nuclear reactors, 5·18
- **Neutron Radiography,** in nondestructive testing, 5·18
- **Neutrons**
  - absorption of
    - calculation of, 15·9
    - by typical radiographic sources, 15·11
  - capture probability of stable isotopes, 15·8
  - detection of, 16·2
  - as elementary particles, 13·3
  - generation and radioisotope production with, 15·4
  - ionization by, 16·1
  - in nondestructive testing, 4·11
  - in oil-well logging, 5·18
  - properties of, 13·3
  - slow, capture cross-section of Iridium-192, 15·17
  - sources of, 5·16
  - thermal, definition of, 15·8
- **Newmann's Equation,** in photoelastic stress analysis, 53·7
- **Nickel**
  - absorption coefficients (mass) for γ and X rays and photon energies, 18·35
  - acoustic and ultrasonic properties of, 43·8
  - attenuation coefficients of, for γ rays and X rays, 27·19
  - coatings on aluminum and aluminum coatings on nickel, fluorescent radiation in determination of thickness, 24·36, 24·37
  - constant *K* value in ultrasonic resonance tests, 50·3
  - effect on electrical conductivity of aluminum, 42·14
  - effect on electrical conductivity of copper, 42·12–13
  - ultrasonic energy losses in, 43·25
  - ultrasonic reflection coefficients at interfaces with other materials, 43·13
  - wire, effect of tensile stress on hysteresis loop of, 42·28
- **Nickel Alloys** (See also "Inconel," "Monel")
  - chromium-, copper-, and iron-, wire for strain gages, 54·6, 54·8–9
  - copper-
    - effect of hydrostatic pressure on resistance of strain gages of, 54·30
    - resistance-strain characteristics of, for strain gages, 54·25
  - forgings, ultrasonic contact testing of, 48·11
  - silver-, acoustic and ultrasonic properties of, 43·8
  - ultrasonic inspection of, 49·2
- **Nickel Silver,** electrical conductivity of, 42·16
- **Nimonic,** tubing, intergranular corrosion in, eddy-current indications of, 38·30
- **Nital,** as etching fluid for metallography, 32·29
- **Nitric Acid,** mixtures with alcohol, as etching fluid for metallography, 32·29
- **Nitrogen**
  - absorption coefficients (mass) for γ and X rays and photon energies of, 18·32
  - attenuation coefficients of, for γ rays and X rays, 27·5
  - segregation in Thomas steel during aging, effect on Magnatest Q eddy-current indications, 42·61
- **Noise**
  - in metals during ultrasonic testing and its reduction, 44·7
  - in ultrasonic contact testing, irrelevant indications from, 48·21
  - in ultrasonic testing of metals, 45·7
- **Noise Discrimination,** in ultrasonic testing, 43·49

Nonconductors, electrified-particle testing of, 28·4, 29·1

Nondestructive Testing (See also "Inspection")
  acceptance and growth of, 1·4, 1·7
    complexity of modern machinery in relation to, 1·4
    engineering demands for sounder materials in relation to, 1·6
    increased demand on machines in relation to, 1·5
    public demands for greater safety in relation to, 1·6
    rising costs of failure in relation to, 1·6
  accuracy and sensitivity in, specifying required, 1·19
  airline application of, 3·29
  application of, 4·3
  basic elements of, 4·8
  basic methods, survey of, 5·1
  charts for selection of methods, 1·23
  combined automatic tests in, 41·19
  cooperation in, among customer, service groups, etc., 2·22–23
  costs of, 1·14
  definition, 4·1
  design in, 1·18
  dissemination of industrial experience in, by cooperative agreements, 2·28–30
  economics of, 1·9
  European development of, 2·13
  functions of, 1·1
  information sources for, 1·19
  integrity of reports in, 2·14
  introduction to industry, 2·30–31
  laboratories for, 2·1–34
  limitations of, 4·1, 4·13
    interpretation of, 1·20
  limits of acceptability or rejectability, establishment of, 1·19
  magnetic-particle-test supplemental, 32·19–22
  management and application of, 1·1–2
  management of, 1·16
  mobile equipment for, 2·20
  photoelectric devices in, 10·4
  in plant departments, 1·17
  production-testing ratios in, 1·9
  punch-card system for sorting data from, 2·30
  quality-control indicator (automatic statistical) for, 41·12
  reasons for, 1·1
  reliability of, 4·3
  research (fundamental) in, for eddy-current tests, 2·24–25
  scheduling and specifying nature of tests in, 1·18
  scheduling of, for maximum economy and effectiveness, 1·22
  sorting (automatic) instrument for, 41·13
  standards for, 2·18
  test-evaluation department for, at Institut Dr. Foerster, 2·26
  ultrasonic, 43·1–50
  vision and optics in, 10·1–33

Nonferromagnetic Materials (See also "Nonferrous Materials")
  crack detection and measurement in, with eddy-current Defectometer, 40·45
  cylinders, reactance testing of diameter variations corresponding to 5% crack depth in, 40·14
  detection of impurity particles of, in nonmetallic substances, 39·1

Nonferromagnetic Materials (*Continued*)
  eddy-current testing of, complex impedance and voltage planes for, for various fill factors, 37·3
  eddy-current testing of cylinders of
    calculation of crack depth in, 37·31
    calculation of frequency ratios for temperature compensation in, 40·13
    crack detection in, 37·19–26
    effects of conductivity and diameter on secondary-coil voltages in, 37·35
    frequency-ratio determination in, 37·27
    frequency variation with conductivity in, 40·8
    frequency variation with cracks in, 40·11
    frequency variation with diameter in, 40·10
    sensitivity diagrams for conductivity and diameter effects in, 37·35
    separation of effects of conductivity and diameter in, 37·1–2
  eddy-current testing of spheres of
    coil impedance *vs.* effective permeability in, 39·6
    complex voltage and impedance planes for, 39·8–10
  eddy-current testing of thin- and thick-walled tubes of, 38·17
  eddy-current testing of thin-walled tubes of
    normalized apparent impedance planes for, 38·4–5
    variation of angle α with frequency ratio in, 38·7
  eddy-current testing of tubes of, 38·23–39
    complex permeability or impedance planes for, 38·9, 38·11
  effective permeability of, in eddy-current testing, 36·20
  effective permeability quotient of cylinders of, as function of frequency ratio, 37·37
  magnetic permeability (relative) of, in eddy-current testing, 36·16
  tubes, cracks in, eddy-current data on, 38·12–15
  voltage (secondary) in eddy-current testing with air space between coil and specimen, 36·17

Nonferrous Materials (See also "Nonferromagnetic Materials")
  crack detection in cylindrical objects of, by eddy-current testing, 37·18–25
  eddy-current testing of cylinders of, instrument for, 37·32
  eddy-current testing of thick-walled tubes of, 38·8–12
  effective permeability quotient in eddy-current tests of cylinders of, as function of frequency ratio, for crack depth in relation to diameter, 37·39
  movement of, detection by magnetic apparatus, 34·23
  tubes (thin-walled) of, eddy-current testing of, 38·1–6

Nonmagnetic Materials
  coatings of, thickness determination of, 24·38
  iron impurity determination in, by magnetic field tests, 34·21

Nonmetallic Materials
  acoustic and ultrasonic properties of common, 43·8
  metallic impurity detection in, by eddy-current testing, 39·1, 39·10

Normal Incidence Analysis, in photoelastic coating testing, 53·7

Normalized Apparent Impedance Plane
  for heavy-walled nonferrous tube with test coil inside tube, for various fill factors, **38·16**
  for thin-walled nonferromagnetic tubes with varying diameters and thicknesses, **38·4**
Nuclear Fission
  products of Uranium-235 for radiography, **15·9**
  in radioisotope production, **15·4**
Nuclear Reactors
  fluxes of, corrections for irradiation yield calculations, **15·13**
  neutron flux-density control in, **5·18**
Nucleic Acids, light-scattering tests on, **10·27**
Null-Balance Method, in radioisotope thickness gaging, **18·12**
Numerical Digits, decimal equivalents *vs.*, in optical projection system, **12·6**
Nuts (Edible), fluoroscopic inspection of, **24·19**
Nuts (Mechanical), forging lap in lock, magnetic-particle indication of, **32·8**
Nylon, absorption coefficients (mass) for γ and X rays and photon energies of, **18·39**

O

Objectives, Reflecting (See "Reflecting Objectives")
Oblique Incidence Analysis, in photoelastic-coating testing, **53·8–10**
Oil (See also "Petroleum")
  effect on magnetic-particle testing, **30·1**
  suspensoids for magnetic-particle testing, **30·15**
Oil-and-Whiting Method, in nondestructive testing, **5·4**
Oil Refineries
  liquid-penetrant testing in, for cracks and leaks, **3·13**
  maintenance testing in, **3·12**
  ultrasonic resonance tests for wall corrosion and scale accumulation in, **3·13**
Oil, Transformer (See "Transformer Oil")
Oils
  as coupling media in ultrasonic contact tests, **48·4**
  effect on liquid-penetrant testing, **6·6**
Oil Wells
  drilling barges for off-shore strain-gage tests in design of, **54·33**
  logging of, neutrons in, **5·18**
Opaque Materials, separate ultrasonic transmit-receive testing of, **49·17**
Operators (See "Personnel")
Optical Aids, in visual inspection, **5·9**
Optical Comparators, 12·1–37
  for comparison gaging, **12·2**
Optical Equipment, for horizontal projector with relay lens, **12·4**
Optical Inhomogeneities, occurrence of, as schlieren, **10·20**
Optical Interference, 10·12–19
  causes of, **10·12–13**
  principle of testing surfaces by, **10·14**
Optical Measuring Methods, basic, in industrial testing, **12·1**
Optical Projection System
  components of, **12·4**
  looped-back, **12·7**
  setting of image to screen reference point as source of error, **12·17**
Optical Projectors, 12·1–37
  advantages of, in industrial testing, **12·1**
  angular measurements by, **12·3**
Optical Projectors (*Continued*)
  capacity of, as function of screen size, viewable field size, and standard measuring travel, **12·8–9**
  image and screen chart comparisons in, **12·17**
  image-positioning accuracy in, **12·17**
  industrial uses of, **12·21–22**
  outline measurements by, **12·2–3**
  in photoelastic stress analysis, **12·30–31**
  special techniques for using, **12·22–37**
  surface illumination for, **12·11–12**
  translation measurements by, **12·3**
  versatility of, **12·21**
Optical Systems
  of borescopes and telescopes, **11·16**
  for X-ray film density measurement, **24·35**
Optical Tests
  in nondestructive testing, **10·1**
  with polarized light, **10·18**
Optics
  geometrical, **10·4–12**
    application of, **10·4–12**
  in nondestructive testing, **10·1–35**
    limitations in, **10·26**
Organization Chart, for inspection departments, **1·16**
Orientation, Preferred, in metals, effect on ultrasonic shear-wave velocity, **45·7**
Oscillations
  amplitude of, in eddy-current testing by controlled-feedback method, **40·16**
  self-excited, in eddy-current testing by controlled-feedback method, **40·16**
Oscillators
  calibrated *RC*, in determination of thickness of metallic sheets, **39·18**
  mechanical, for vibration testing, **5·17**
Oscillograms, in eddy-current linear time-base testing, **40·31**
Oscilloscope Traces
  hysteresis-loop, analysis of, **42·25–29**
  in sonic testing, **51·9**
Overheating (See "Heating")
Overlap, in welding (submerged-arc), causes and radiography of, **25·12**
Overtones (See "Harmonics")
Oxidation
  in aluminum-copper single crystals, ultrasonic energy losses from, **43·25**
  of strain-gage constituents at elevated temperatures and its compensation, **54·23**
Oxides, layers at weld interfaces, lack of fusion from, **25·9**
Oxygen
  absorption coefficients (mass) for γ and X rays and photon energies of, **18·33**
  attenuation coefficients of, for γ rays and X rays, **27·6**
  content in melting of copper, eddy-current control of, **42·13**
  detection of, **5·4**
  removal from copper, electrical conductivity variation during, **42·13**

P

Packaging, weight control in, **5·13**
Paint (See also "Coatings")
  impurity-particle detection in, by eddy-current methods, **39·1**
  removal from parts for liquid-penetrant testing, **6·13**
  for walls of X-ray-film processing areas, **21·12**

- **Paint Guns**, in recording of electric-current railroad-rail test results, 35·19
- **Painting**, effect on liquid-penetrant indication of defects, 8·6
- **Paintings**, radiography (low-voltage) of, to determine authenticity, 24·40
- **Pair Production**
  - in photon absorption, 13·22
  - in X-ray (high-energy) absorption, 23·1
- **Palladium**, absorption coefficients (mass) for γ and X rays and photon energies of, 18·36
- **Paper**
  - basis weight of, radioisotope back-scattering in determination of, 18·15
    - radioisotopes in control of, 18·29
  - for chart material in optical projectors, 12·20
  - coating and impregnation of, radiation control of, 18·29
  - for condensers, eddy-current apparatus for control of metallizing of, 41·4
  - lamination with polyethylene, radiation gages in control of, 18·28
  - phase microscopy of, 10·18
  - strain gages backed with, 54·34
    - creep of, 54·28
    - effect of hydrostatic pressure on resistance of, 54·30
  - strain gages of, strain limits with cellulose nitrate cements, 54·25
  - thickness measurement of, by β-ray reflection, 18·4
    - range with Sr-90 beta gages, 18·16
  - transparent, for recording eddy-current nondestructive-test results, 2·29
  - xeroradiographic-image transfer to, and fixation on, 22·13
- **Paper Work** (See "Records")
- **Parallax Method**, in stereoradiography, 20·47
- **Particles**
  - characteristics and sources of high-energy, 5·14
  - charged and uncharged, in nondestructive testing, 5·18
  - displacement, pressure and velocity in ultrasonic beams, 43·12
  - for filtered-particle test media, 9·8
  - metallic, inside small-diameter tubing, eddy-current indications of, 38·31
- **Parts**
  - automatic unit for simultaneous eddy-current defect detection and composition sorting of steel, 42·68
  - automobile, effect of tensile strength on Magnatest Q eddy-current instrument pattern and slit value, 42·52
    - magnetic-particle testing of, multipurpose semi-automatic equipment for, 31·12–13
    - sorting by tensile strength with Magnatest Q eddy-current instrument, 42·54–55
  - case depth of, Magnatest Q eddy-current testing of, 42·58
  - cavities in machined, measurement of depth of, 12·32
  - concave and convex, curvature effects in ultrasonic testing, 45·13–15
  - cracks in pressed, detection with Defectometer eddy-current instrument, 40·47
  - crack testing of steel, with Magnatest D eddy-current instrument, 42·61–69
  - defects in semi-finished, quality number in statistical testing for, 41·18
  - demagnetization of, after magnetic-particle testing, 30·20
- **Parts** (*Continued*)
  - demagnetization of small, after magnetic-particle tests, 30·28
  - diameter of semi-finished, eddy-current indications of, 42·3
  - drying of, in post-emulsification dye-penetrant process, 6·15
  - dye-penetrant testing of, preparation for, 6·13
  - eddy-current testing of, apparatus for, 40·2–3
    - by ellipse method, 40·28
    - with Multitest eddy-current instrument, 40·23
  - eddy-current testing of forged, automatic tilting or moving coils in, 41·8
  - eddy-current testing of short, 39·1
  - failure probability of, 1·2
  - handling apparatus for, in automatic eddy-current testing, 41·2
  - handling of large, in eddy-current testing, electronic-slit method in, 41·8
  - handling of small, in liquid-penetrant inspection, baskets for, 7·5
  - impedance (apparent) of short, in eddy-current testing, 39·8
  - inspection of, cost factors in, 1·15
  - location (precision) of internal, by radiography, 23·15
  - machine, reliability requirements of, 1·5
  - magnetic field strength and permeability variation of mechanically deformed, effect on Magnatest Q eddy-current sorting, 42·31
  - magnetic-particle testing of small, semi-automatic equipment for, 31·10
    - stationary equipment for, 31·7
  - magnetic-particle testing of threaded, with fluorescent particles, 30·18
  - magnetization (circular) of hollow and solid, for magnetic-particle tests, 30·5–6
  - marking or sorting defective, Sigmaflux eddy-current indications in, 40·27
  - reworking of, in nondestructive-testing laboratories, 2·10
  - semi-finished, limitations of reactance magnitude tests of, 40·14
  - shape of, nonrelevant magnetic-particle test indications from irregularities in, 32·15
  - soft spots in semi-finished, eddy-current testing in control of, 42·20
  - sorting of, automatic, with Magnatest Q eddy-current instrument, 41·10
    - by coercive force, 34·5
    - by hardness by electromagnetic induction method, 42·1
    - by magnetic point-pole method, 34·11
    - with Multitest eddy-current instruments, 40·2–3
  - sorting of hot-rolled semi-finished, with Magnatest Q eddy-current instrument, 42·35
  - tempering of hardened, to remove residual stresses before etching, 32·26
  - ultrasonic shear-wave velocity in, effect of structure on, 45·7
  - ultrasonic testing of, coatings to decrease surface roughness effects in, 45·17
  - working of, in nondestructive-testing laboratories, 2·10
- **Pastes**, for magnetic-particle testing, 30·15, 30·17–18
- **Patterns** (See "Oscilloscope Traces")
  - Magnatest D eddy-current screen, analysis of, 42·63

Patterns (*Continued*)
  Magnatest Q eddy-current instrument, **42·29–61**
    adjustment of, **42·35**
    photographic recording of, **42·32**
Peanuts, inspection (fluoroscopic) of, **19·36**
Penetrameters
  in fluorography and fluoroscopy, **19·47**
  for fluoroscopic dark-adaptation test and for evaluation of discontinuities, **24·26**
  placement of, **15·31**
  for radiographic evaluation, **20·36**
  in radiographic-sensitivity determination, **15·30**
  in xeroradiography, to establish techniques, **22·9**
    for image interpretation, **22·16**
Penetrameter Sensitivity (See "Sensitivity")
Penetrants (See "Liquid Penetrants")
Penetrating Power
  of filtered-particle test media, **9·5**
  of liquid penetrants, requirements for, **7·17**
  of X rays, **14·6**
Penetration
  depth, in eddy-current testing, of carbon-steel tubes, **38·22**
    curves and definition of, **37·9**
    of tubes, limitations of, **38·19–23**
  time, for liquid-dye penetrants, **6·14**
    for liquid penetrants, importance of, **6·3**
    for visible-dye penetrants in field tests, **6·19**
    for water-washable fluorescent penetrants, **6·7**
  in welding, causes and radiography of excessive, **25·12**
    causes and radiography of lack of, **25·5–7**
    magnetic-particle indications of incomplete, **32·10**
  by X rays (high-energy), **23·3**
Pens, recording, for electric-current railroad-rail testing, **35·17**
Penumbra
  image width of, **19·2** (See also "radiography" under "Unsharpness")
  in radiographic-image formation and nomogram for, **20·8–9**
Periodic Table, of the elements, **13·6–7**
Periscopes (See also "Telescopes")
  for visual inspection, **11·13**
  for wind-tunnel tests, **11·23**
Permeability (See also "Effective Permeability," "Magnetic Permeability")
  apparent, of short cylinders in eddy-current testing, **39·8**
Personnel
  for destructive *vs.* nondestructive testing, **4·6**
  for electric-current testing of railroad rails, **35·20**
  exposure to radiation, records of, **26·16–17**
  for fluoroscopy, **19·36**, **24·23**
  for nondestructive testing, **2·2**, **2·11**
    costs in relation to, **1·15**
    judgment and skill factors, **1·22**
    responsibilities in industrialized *vs.* remote areas, **2·21**
    role of inspectors, **1·7**
  for pipeline-weld radiography, **25·28**
Petroleum
  constant *K* value in ultrasonic resonance tests, **50·3**
  distillates as suspending media
    for filtered-particle test, **9·7**
    magnetic-particle testing, **30·15–16**
Petroleum Industry
  borescopic inspection in, **11·15**
  liquid-density control with radioisotopes in, **18·30**
Petroleum Jelly
  coatings for moistureproofing of strain gages and their application, **54·39**
  in strain-gage waterproofing, **54·25**
Petroleum Refineries, corrosion testing in, **50·35** (See also Oil Refineries)
Phase Cancellation Effects, on ultrasonic-echo amplitudes from spherical reflectors, **45·24**
Phase Changes, X-ray detection of, **17·13**
Phase-Contrast Techniques, for testing transparent material and surfaces, **10·17**
Phase-Demodulation System, for ultrasonic testing, **44·21**
Phase Displacement, of magnetic field strength in eddy-current testing, **36·11**
Phase Rotation, in cathode-ray-tube eddy-current ellipse tests, **40·23**
Phase Shifters (See "phase-controlled" under "Rectifiers")
Phase Velocity, of ultrasonic Lamb waves, **45·12**
Phenolic Resins (See "Plastic Materials," "Resins")
Phosphors
  energy band model of crystal, **16·9**
  luminescent, combined with multiplier phototubes in radiation measurement, **16·8**
  as radiation detectors in nondestructive testing, **5·10**
Phosphorus
  absorption coefficients (mass) for γ and X rays and photon energies of, **18·34**
  effect on electrical conductivity of bronze and copper and control of its content by eddy-current testing, **42·12**
Photocells or Photodiodes, 11·33
  in light detection, **5·10**
  selenium barrier-layer, **11·34**
Photochemical Process, in vision, **10·2**
Photoconductivity
  definition of, **18·21**
  mechanism of, **16·10**
Photoconductors, 11·33
  powdered, and large-area cells therefrom, **16·12**
  as radiation detectors, **18·21**
  in X-ray amplification, **16·8**
  X-ray sensitive, **22·1**
Photocurrent
  from irradiated CdS and CdSe, **16·11**
  modulation by pulsating X-ray source, **16·13**
Photodisintegration, in radiation absorption, **13·22**
Photoelastic Coatings
  for nondestructive testing, **53·11–13**
  plastic, measurement of thickness of, **53·15**
    thickness effects, **53·37–38**
Photoelastic-Coating Tests (See also "Photoelastic Testing")
  advantages and disadvantages of, **53·36–38**
  apparatus for, alignment and calibration of, **53·35**
  applications of, **53·25–36**
  of bridges (welded), **53·27**, **53·34**
  calibration of instruments and plastic coatings for, **53·13–14**
  in design evaluation and visual education, **53·36**
  of guided-missile fuselages and tails, **53·26–27**, **53·30–31**
  history of, **53·1**
  instruments for, **53·16–24**

Photoelastic-Coating Tests (*Continued*)
  instruments (small field) for dynamic and static, **53·22–23**
  isochromatic lines in, **53·4**
  large-field instruments for dynamic and static, **53·19–20, 53·23**
  materials and techniques for, **53·11**
  nondestructive, **53·1–38**
  oblique-incidence meters for, **53·24–25**
  patterns in aluminum plate seen with polarizing quarter-wave viewer, **53·18**
  plastic material for, effect of properties and shape of workpiece on selection of, **53·13**
  service life surveys with, of machines and structures, **53·35**
  as supplement to strain-gage tests, **54·2, 54·35**
  surface preparation for, **53·14**
  telemetering of, **53·35**
  theory (mathematical) of, **53·6–8, 53·10**
  transducer applications of, **53·34**
  of welded assemblies, **53·27, 53·33–34**
Photoelasticity, quantitative law of, **53·4**
Photoelastic Models
  photoelastic testing with, compared with photoelastic-coating tests, **53·1**
  resolution of light rays in, **53·3**
  as supplement to resistance strain-gage tests, **54·2**
Photoelastic Testing (See also "Photoelastic-Coating Tests")
  optical principles of, **53·2**
  with plastic models compared with photoelastic-coating tests, **53·1**
  stress analysis by, **53·3**
Photoelectric Apparatus
  in nondestructive testing, **10·4**
  as vision aid, **11·25–40**
Photoelectric Attenuation Coefficient, of atoms in general and of uranium, **13·19–20**
Photoelectric Effect, definition of, **13·18**
Photoelectric Emission, definition of, **11·25**
Photoelectric Imaging Devices, 11·35–38
Photoelectricity
  effect on radiation absorption, **18·2**
  emission efficiency in scintillation counting, **18·22**
  scanning with, in automatic magnetic-particle testing, **31·14**
Photoemitters, 11·26
  cathode, **11·26**
  as vision aids, **11·25–33**
Photographic Emulsions
  in microradiography, **20·41**
  nuclear track, examination by reflecting objectives of optical systems, **10·9**
Photographic Film (See also "X-Ray Film")
  for chart material in optical projectors, **12·20**
  densitometers for, **20·32**
  density, definition and relation to light transmittance, **20·31**
    light transmittance in relation to, **20·32**
  development of, **16·18**
    graininess in relation to degree of, **16·22**
  fogging in γ radiography, **15·24**
  graininess of, effect on radiographic sensitivity, **15·32**
  H and D (sensitometric) curves of, **20·32–34**
  in radiation detection and measurement, **16·8**
    spectral sensitivity of, **16·22**
  radiographic, exposures for, **15·28**
  reciprocity curve for, visible light, **16·24**
Photographs, X-ray powder, obtained with copper radiation, **17·5**
Photography (See also "Motion-Picture Photography")
  borescopic uses of, **11·25**
  of brittle-coating crack patterns, **52·26**
  density-exposure curves in, **16·19**
  enlargement of radiographs of small objects, **24·38**
  flash, for recording high-speed motion, **10·4**
  in fluorography and fluoroscopy, **19·44**
  of fluoroscopic images, **19·27**
  high-speed, for maintenance inspection, **3·26**
  image graininess in, **16·21**
  of images on optical projector screen for permanent record, **12·37**
  of Magnatest Q eddy-current screen patterns, **42·32**
  of magnetic-particle-test indications, **32·18**
  in nondestructive testing, **5·10**
  in photoelastic-coating dynamic tests, **53·22**
  time-lapse, applications of, **3·26**
  in ultrasonic-test-data presentation, **43·34**
  of xeroradiographic powder images, **22·13**
Photometers, Filter, for fluorescence-brilliance measurement of penetrants, **7·21**
Photomultipliers, phosphor, for X-ray thickness gages, **18·7**
Photons
  absorption coefficients of elements for, **27·1–41**
  absorption of, **13·17**
  Bremsstrahlung production by high-energy, **13·27**
  characteristics of, **13·8**
  energy of absorption of γ and X rays by elements, **18·32–40**
  mass stopping power of metals for, **13·25**
  pair production from, **13·22**
  scattering of, **13·20**
  X-ray, in fluoroscopy, **19·26**
Photoradiography (See "Radiography")
Photoresistances, selenium as, in X-ray amplification, **16·8**
Phototubes (See also "Television Tubes")
  gas-filled, **11·28**
  multiplier, **11·31–32**
    combined with luminescent phosphors in radiation measurement, **16·8**
  in nondestructive testing, **11·34**
  for photometers for liquid-penetrant fluorescent-brilliance determination, **7·22**
  vacuum, **11·28**
Photovoltaic Devices, 11·34
Physical Constants
  of elementary particles in nondestructive testing, **13·6**
  factor, effect on natural frequency of sonic vibration of bodies, **51·1**
Physical Examinations, for personnel exposed to radiation, **26·4**
Physics, radiation and particle, **13·1–31**
Physiological Effects, of black light, **7·17**
Physiological Factors, in fluoroscopy, **19·24**
Picket Bridge Imposers, for section measurement with optical projectors, **12·23–25**
Piezoelectric Elements, for transducers for ultrasonic waves, **44·1**
Piezoelectricity, 44·1–3
Piezoelectric Materials, characteristics of common, **44·4**
Piezoelectric Motors (See "Transducers")
Piezoelectric Transducers (See "Transducers")
Pine, gamma-ray shielding equivalent of yellow, **26·10**

Pinholes
- in coating on vessels, detection by electrified-particle tests, **29·15**
- in porcelain enamel, detection by electrified-particle tests, **29·4**

Pins, testing with Multitest eddy-current instrument, **40·23**

Pipelines
- borescopes for inspection of, **10·10**
- corrosion inspection by ultrasonic test methods, **50·36**
- detection of buried, by magnetic means, **34·23**
- hydrostatic testing of, **5·5**
- maintenance inspection of, **3·14**
  - with Cobalt-60, **25·17**
  - mobile film-processing equipment for, **25·23**
  - X-ray equipment for, **25·21–24**
- ultrasonic resonance testing of, **50·28**
- welds in, inspection and radiography of, **25·16–28**
  - quality control of, **25·25–28**
  - radiographers for, qualifications of, **25·28**
  - radiography of, definition and sensitivity in, **25·22**
  - radiography of, elliptical projection in, **25·21**
  - radiography of, percentage examination desirable, **25·26**
  - radiography of, source location and size in, **25·20**
  - radiography of, 3-exposure techniques in, **25·20–21**
  - radiography of, variation of percentage rejection during project, **25·26**

Pipes
- corrosion wall thinning of, detection of, **5·24**
- hot water, radiographic inspection in maintenance of, **3·17**
- misalignment of, measurement by ultrasonic immersion inspection, **47·39**
- quality and specifications for, **47·39**
- radiography of, apparatus for, **24·39**
- steam, radiographic inspection in maintenance of, **3·18**
- ultrasonic inspection of, angle-beam contact units for, **43·7**
  - applications of immersion-type, **47·39**
  - frequencies for, **48·2**
  - by immersion methods, **47·26**
- wall-thickness gaging of, and portable apparatus for, **18·30**
  - radiation in, **18·27**
- welds in, automatic magnetic-particle inspection of, **31·14**
  - with backing rings, radiographs of, **25·15**
  - concavity at root in, **25·11**
  - excessive penetration in, and its radiography, **25·12**
  - radiographs of cracks in inside reinforcement of, **25·9**
  - radiography with external source, **25·23**
  - radiography with internal source, **25·22**
- for X-ray-film processing apparatus, materials for, **21·16**

Piston Rods
- bands (spread) of, from Magnatest Q eddy-current testing, harmonics in wave forms of, **42·37**
- cracks in, detection with Defectometer eddy-current instrument, **40·47**

Pistons
- cracks in, detection with Defectometer eddy-current instrument, **40·47**

Pistons *(Continued)*
- fatigue cracks in aluminum, liquid-penetrant indications of, **8·17**

Pits, in surfaces, optical projection of, **12·14**

Plaster, radiation-shielding equivalent of, **26·9**

Plastic Deformation
- of steel during tensile tests, Magnatest Q eddy-current indications of, **42·60**
- near welds in bridge assemblies as indicated by photoelastic-coating tests, **53·33**

Plastic Film, measurement on metal rolls, radioisotope back-scattering in, **18·15**

Plastic Materials (See also "Resins")
- adhesives from phenolic, effect of degree of cure on hysteresis and zero shift of strain gages, **54·24**
  - for strain gages, decomposition at elevated temperatures, **54·24**
  - strain limits of strain gages with, **54·26**
- for chart material in optical projectors, **12·20**
- cleaning for resin-type brittle coatings, **52·9**
- coatings, to decrease test object surface roughness effects in ultrasonic testing, **45·17**
  - for photoelastic-coating tests, calibration of, **53·13–14**
  - on photoelastic-coating test specimens, measurement of thickness of, **53·15**
  - in photoelastic stress analysis, thickness effects of, **53·37–38**
- coatings (liquid) and sheets of, for photoelastic-coating tests, **53·11–12**
- coating with, for photoelastic-coating tests, **53·15**
- cold shuts in, X-ray detection and evaluation of, **24·12**
- cracks (fatigue) in, liquid-penetrant penetration time for detection of, **6·19**
- creep and shrinkage under load, **54·27–28**
- dye-penetrant penetration time for, **6·14**
- electrified-particle testing of, for distribution of blended materials, **29·6**
- inclusions in, X-ray detection and evaluation of, **24·11**
- light-scattering tests on synthetic, **10·27**
- liquid-penetrant testing of, **8·19**
- mechanical properties of, ultrasonics in determination of, **43·49**
- penetration time for, in liquid-penetrant testing, **6·8**, **6·10**
- phenolic, in strain-gage mounting, **54·12**
- phenolic laminates, constant *K* value in ultrasonic resonance tests, **50·3**
- for photoelastic-coating tests, **53·11**, **53·13**
- pressure printing on, for permanent outline records, **12·30**
- quality control of porous, by radiography, **24·38**
- radiography (low-voltage) of, **24·40**
- strain-gage tests on strips of, effect of rigidity of gage on, **54·30**
- thickness gaging in, **18·28**
- thickness measurement range with Sr-90 β gages, **18·16**
- ultrasonic contact testing of, frequencies for, **48·1**
- ultrasonic transducer backings from fibrous, **44·6**
- ultrasonic-wave attenuation and velocity in sheets of, measurement of, **43·15**
- ultrasonic-wave reflection time in, **43·31**

Plateau Range, of Geiger-Muller counters, **16·7**

Plated Articles, eddy-current testing of, tabular summary of, **36·4–5**

Plates (See also "Sheet Materials")
- aluminum, inspection with ultrasonic paintbrush transducers, 44·12
- brass, crack propagation in, 35·11
- circular (See "Discs")
- corrosion thinning of steel, direct-current measurement of, 35·9
- eddy-current testing of metallic, tabular summary of, 36·6
- laminations in, detection by ultrasonic resonance tests, 50·22
- laminations in metallic, magnetic-particle indications of, 32·7
- stainless-steel, photoelastic-coating tests for determination of optimum spot-weld distribution in, 53·27, 53·32
- thickness of, interpretation of electric-current-test indications of, 35·4–9
  - measurement from fundamental ultrasonic resonance frequency, 50·1
- ultrasonic testing of, search unit for, 43·5
- ultrasonic-wave transmission through thin, 43·14–15

Plating (See also "Electroplating")
- crack formation during or after, from residual stresses, 32·12
- eddy-current testing of nonferrous, on ferromagnetic materials, 36·6
- effect on liquid-penetrant indication of defects, 8·6
- thickness measurement of, of flat areas of irregular shape, magnetic-reluctance instrument for, 3·35
  - by ultrasonic resonance method, 50·21

Platinum
- absorption coefficients (mass) for γ and X rays and photon energies of, 18·38
- attenuation coefficients of, for γ and X rays, 27·37
- electrical conductivity of, 42·16

Plexiglas, as model for photoelastic stress analysis, 12·31

Plumbing Fixtures, for X-ray-film processing, 21·16

Plutonium, attenuation coefficients of, for γ and X rays, 27·41

Points in Space, determination of, by optical projectors, 12·34–35

Poisson's Ratio (See also "Elastic Properties")
- amplitude ratio between incident and reflected ultrasonic beams as function of angle for various, 43·18
- effect on natural frequency of sonic vibration of bodies, 51·1
  - on sensitivity of strain-gage-based transducers, 54·4
- formulas for, and ultrasonic-wave velocity in relation to, 43·10–11
- measurement of, by sonic resonance vibration tests, 51·6
  - in eddy-current tensile testing of metal rods, 42·3
  - with strain gages, correction for transverse effects in, 54·29
- sound-wave longitudinal-shear ratio as function of, 45·8

Polariscopes
- circular-crossed and crossed plane, light paths through large-field, 53·21
- circular-crossed and parallel-plane, arrangement of polarizer and quarter-wave plates in, 53·16, 53·19
- crossed-plane, with photocell attachment, 53·22

Polariscopes (*Continued*)
- light path through crossed-plane reflection, 53·4
- readings *vs.* strain in photoelastic-test-material calibration, 53·14
- reflection, in bi-refringence observation and measurement in photoelastic-coating tests, 53·1

Polarity, Reversed (See also "Mismatch")
- of ultrasonic-test signals, interpretation of, 45·21

Polarization
- circular, in photoelastic-coating testing using quarter-wave retardation plates, 53·6
- of light, 10·18
  - by bi-refringent material and analyzer for, 53·2–3
- in thickness testing of thin coatings, 10·17

Polarized Light (See "Light, Polarized")

Polarizers
- in circular-crossed and plane-parallel polariscopes, 53·16, 53·19
- for microscopes, 11·8
- for photoelastic-coating analysis, 53·16–24

Polarizing Quarter-Wave Viewer, for photoelastic-coating static tests, 53·16

Pole Pieces, ferromagnetic, in demagnetization of small parts having a small length/diameter ratio, after magnetic-particle tests, 30·28

Polishing
- before application of photoelastic coatings, 53·15
- of cut surfaces as supplement to magnetic-particle testing, 32·24
- effect on liquid-penetrant indication of defects, 8·6
- metallographic, 32·29

Polycrystalline Materials
- ultrasonic-energy losses in granular, 43·25

Polyethylene
- absorption coefficients (mass) for γ and X rays and photon energies of, 18·39
- constant K value in ultrasonic resonance tests, 50·3
- lamination with paper, radiation gages in control of, 18·28

Polymers (See "Plastic Materials," "Resins," "Rubber")

Polymorphic Substances, X-ray analysis of, 17·11

Polystyrene
- absorption coefficients (mass) for γ and X rays and photon energies of, 18·39
- for chart material in optical projectors, 12·20
- ultrasonic reflection coefficients at interfaces with other materials, 43·13
- ultrasonic-wave attenuation *vs.* frequency in, 43·26

Porcelain Enamels
- cracks and other failures in, mechanism and electrified-particle indication of, 29·7–11
- cracks in, electrified-particle indication of, 29·5
- electrified-particle tests for, 28·2
- stress concentration indication of, by electrified-particle testing, 29·8

Porosity
- in aluminum-alloy forgings, detection of unhealed, 46·22
- in ceramics, die castings and welds, liquid-penetration time for detection of, 6·19
- classification of, for filtered-particle test, 9·5

Porosity (*Continued*)
- detection of, by eddy-current methods, **36·6**
  - with dye-penetrants, penetration time for, **6·14**
  - in light-metal blocks with Defectometer eddy-current instrument, **40·47**
  - by liquid-penetrant testing, **6·1**
  - by liquid-penetrant testing, black-light illumination level for, **7·15**
  - by liquid-penetrant testing, penetration time in, **6·8**, **6·10**
  - by penetrating radiation, **5·12**
  - with visible dye penetrants in field test, **6·20**
  - by weighing, **5·13**
- effects in filtered-particle tests, **9·5**
- of forgings (aircraft), immersion ultrasonic detection of, **5·25**
- gas, in alloys and metals, ultrasonic-test "noise" from, **44·7**
  - in aluminum-alloy castings, **24·5**, **24·6**
  - in castings, **24·7**
  - in castings, distinguishing from gas holes, **24·6**
  - in castings, magnetic-particle indications of, **32·9**
  - in castings, test bars for evaluation of, **24·8**
  - impedance effects in ultrasonic testing, **45·21**
  - ultrasonic detection of, multiple-frequency inspection in, **45·26**
  - at weld roots and its radiography, **25·6**
  - in welds, causes and radiography of, **25·3**
- liquid-penetrant indications of, **8·3**, **8·21**
- shrink, in aluminum castings, **24·9**
  - in castings, X-ray interpretation of, **24·8**
- ultrasonic detection and measurement of, **43·47**
- in welds, magnetic-particle indications of, **32·10**

Porous Materials, filtered-particle testing of, **9·1**

Portability, of ultrasonic test equipment, **43·48**

Positional Intelligence, in eddy-current signal-display systems, **38·38**

Positioners, work, for optical projectors, **12·4**, **12·8**

Positioning, image, as source of error in optical projection, **12·17**

Positive-Ion Probes, in halogen-vapor detection, **5·4**

Positrons, **13·3**

Post-Emulsification Fluorescent Process (See also "Liquid-Penetrant Testing")
- for liquid-penetrant testing, advantages of, **6·9**
  - apparatus for, **7·5**, **7·7**

Potassium, absorption coefficients (mass) for γ and X rays and photon energies of, **18·34**

Potassium Iodide, X-ray barrier cells containing, **19·14**

Potassium Sodium Tartrate (See "Rochelle Salt")

Potassium Zirconium Titanate, as ultrasonic-wave transducer material, **44·2**

Potential, Electric (See also "Voltage")
- contact, in conversion of radiation into electrical energy, **18·19**
- measurement in direct-current nondestructive testing, **35·2**
- rise, in electric-current hand testing of railroad rails, **35·19**
- of strain-gage alloys *vs.* copper, **54·9**
- -thickness relation for electric-current testing of flat plates, **35·4**

Potential, Saturation (See "Saturation Potential")

Potentials, Thermoelectric, in strain-gage circuits and their compensation, **54·31**

Potentiometric Circuits (See "Electric Circuits")

Powder Blotting, in electrified-particle testing, **29·6**

Powder Gun, for electrified-particle testing, **28·8**

Powder Method, for X-ray diffraction study of powdered samples, and camera for, **17·5–7**

Powders, for xeroradiographic-plate development, **22·13**

Power Generators (See "generators" under "Electric Power")

Power Plants (See "Electric Power")

Precipitation, in alloys, ultrasonic control of, **43·49**

Press Fits, ultrasonic study of, **43·49**

Pressure
- effects in hydraulic loading of brittle coatings, **52·26**
  - in ultrasonic testing, **43·28**
- hydrostatic, effect in strain-gage tests, **54·30**
- measurement of, with photoelastic coatings, **53·34**
  - with photoelastic coatings, small-field electronic meters in, **53·24**
  - with strain gages, accuracy of, **54·3**
  - with unbonded strain gages, **54·2–3**
- of particles in ultrasonic beams, **43·12**
- in strain-gage mounting, **54·19**

Pressure Apparatus, for filtered-particle tests, **9·12**

Pressure Printing, on plastic materials for permanent outline records, **12·30**

Prestressing (See "residual" under "Stress")

Prewetting, in filtered particle tests of clayware, **9·2**, **9·15**

Printed Circuits (See "Electric Circuits")

Probes, **4·10**
- ball-pointed, **12·27**
- characteristics and limitations of, **4·8**, **4·9**
- coils for, operation in magnetic field tests, **33·2**
- combined matter and energy, **4·8**
- functions of, **4·12**
- for Hall generators and their arrangement, **33·12**
- magnetic-field, **33·1–8**
  - for magnetic tapes and recorder wires, **33·2**
  - tangential-gradient, **33·2**
  - tape, **33·10**
- for matter-and-energy tests, sensitivity range of, **5·14**
- motion of, sources of, **5·1**
- for motion-of-matter tests, **4·8**, **5·1**
- moving, in optical projection measurements by translation, **12·3**
- pick-up, for magnetic-field meters, **33·9**
- review of, **4·7**
- surface coil, for eddy-current testing of tubes, **38·35–39**
- for transmission-of-energy tests, **4·8**, **5·5**
  - sources of, **5·8**
- in ultrasonic contact testing, disturbances caused by irrelevant indications from, **48·22–23**

Probing, of discontinuities as supplement to magnetic-particle testing, **32·21**

Probing Media (See "Probes")

Probolog Method, for inspection of boiler tubes by eddy currents, **3·8**

Process Engineer, as information source in nondestructive testing, **1·19**

Prods
- in magnetic-particle testing of large objects, **30·7**
- magnetization with, circular, of localized areas in magnetic-particle testing, **30·6**
  - of large parts, for magnetic-particle testing, **30·9**
  - in magnetic-particle testing, portable equipment for, **31·2–3**

Production Departments, optical projector use by, **12·21**

Production Line, inspection on, management of, **1·17**

Production Rates, nondestructive testing development in relation to, **1·7**

Profits (See "Economics")

Programming, in automatic ultrasonic testing, **43·35**

Projectiles, radiography of, in motion, **20·46**

Projection
- horizontal and vertical, in optical projectors, **12·10**
- in microradiography, **20·41**
- of X-ray beams in radiography, **23·9**

Projection and Illumination Systems, in optical projectors, **12·10–14**

Promethium-147, energy and half-life of, as β-ray source, **18·17**

Proof Tests, definition of, **4·2**

Propellers
- magnetic-particle testing of airplane, **2·16**
- radiography of ships', **2·15**
- of ships, ultrasonic pulse-reflection testing of shafts of, **3·20**
- ultrasonic gaging of blades of, **50·19**

Protection Coefficient, of X-ray barrier windows, **19·13**

Protective Creams, for liquid-penetrant inspectors, **7·19**

Proteins
- analysis or separation by electrophoresis, **5·20**
- light-scattering tests on, **10·27**

Protons
- as elementary particle, **13·2**
- in nondestructive testing, **5·19**
- properties of, **13·3**

Pulp Digesters
- ultrasonic resonance testing of, **50·27**
  - for corrosion rate, **50·39**

Pulse Frequency Spectrum, of sound waves, **44·20**

Pulsers, for ultrasonic-test A-scan system, **43·32**

Pulses, ultrasonic (See "Ultrasonic Waves")

Punch-Card System, for sorting nondestructive test data, **2·30**

Punch-Press Die Sets, checking clearance between punches and die openings of, by pressure printing on plastic sheets, **12·30**

Purkinje Effect, 19·13

Q

Q, of ultrasonic transducers, **44·4**

Quality
- in fluoroscopy, numerical system for reporting, **24·31**
- level of, establishment of, **1·8, 1·9**
  - maintenance of, nondestructive testing in, **1·4**
- uniformity of, destructive *vs.* nondestructive tests in determination of, **4·7**

Quality Control
- customer contacts and liaison with other departments in, **1·18**
- department and engineers for, **1·8**
- eddy-current-test, automation with Magnatest Q instruments, **41·7–8**
  - tabular summary of, **36·4–5, 36·7**
- in nondestructive testing, **1·7**
- of pipeline welds, **25·25–28**
- of plastics (porous) by radiography, **24·38**
- requirements
  - for radiography, **24·4**
  - for X-ray inspection, **24·1–2**
- specifications, establishment of, **1·16**
- statistical, comparison with nondestructive tests, **4·2**
- statistical, in automatic eddy-current sorting, **2·34**
  - automation of, in eddy-current testing, **2·23, 41·12–19**
  - in coupon tests, **4·2**
  - in fluoroscopy, **19·37**
  - with Statimat instrument, Gaussian curve in, **41·18**
- ultrasonic, early applications of, **43·3**

Quality Number Q, in statistical testing for defects in semi-finished parts, **41·19**

Quantum Theory, Planck's equation for, **13·8**

Quarter-Wave Plates
- in circular-crossed and plane-parallel polariscopes, **53·16**
- retardation, in photoelastic-coating testing, **53·6**

Quartz
- acoustic and ultrasonic properties of fused and natural, **43·8**
- constant *K* value in ultrasonic resonance tests, **50·3**
- crystals, as transducers in ultrasonic contact testing, **48·2**
  - for ultrasonic immersion testing, **46·7**
  - for ultrasonic transducers, **43·4–5, 44·2, 44·4, 50·15**
  - ultrasonic-wave attenuation *vs.* frequency in, **43·26**
- ultrasonic reflection coefficients at interfaces with other materials, **43·13**
- ultrasonic transducer plates with gold and silver vapor-deposited electrodes, **44·5**
- X-ray powder photograph of, **17·5**

R

Rad., definition of, **26·2**

Radial Mode, of vibration of thin circular discs, **51·3**

Radiation (See also "Alpha Rays," "Beta Rays," "Gamma Rays," "Light," "X Rays," etc.)
- absorption, attenuation coefficients of compounds and mixtures in, **13·23**
  - attenuation coefficient (total) in, **13·18**
  - of charged particles by ionization, **13·24**
  - of charged particles by production of bremstrahlung, **13·24**
  - charged-particle scattering in, by collision with electrons in, **13·28**
  - charged-particle scattering by collision with nuclei in, **13·29**
  - coherent scattering in, **13·21**
  - Compton scattering in, **13·20**
  - in nondestructive testing, **13·17**
  - pair production from photons in, **13·22**
  - photodisintegration in, **13·23**

Radiation (*Continued*)
- absorption (*Continued*)
  - photoelectric attenuation coefficient of, **13·20**
  - photon energy in, **13·20**
  - in radiography, **20·13–14**
- absorption of monochromatic, in fluoroscopy, **19·4**
- back-scattered, in radiography, **20·19–20**
- characteristic, in coating-thickness determination, **18·4**
- conversion into electrical energy, **18·19**
- detection and recording of, **16·1–25**
- detection of, **18·19**
  - calibration and characteristics of equipment for, **26·5**
  - by fluorescent scintillators, **18·21**
  - by ionization chambers, **18·10**
  - by photoconductors, **16·13, 18·21**
  - by scintillation counters, **18·21**
- detectors (solid-state) for, **16·8**
- detector systems and sources, **18·22**
- electromagnetic, **16·1**
- exposure to, nature of and biological aspects of, **26·1**
  - permissible, **26·2**
- high-voltage short-wavelength, effect on fluorescent X-ray-intensifying screens, **16·16**
- intensity, calculation of, **15·10**
  - definition of, **15·5–6**
  - effect of absorption, distance, and scattering on, **15·6**
  - as function of gamma-ray energy, **15·6**
- intensity of transmitted, in radiography, **15·35**
- leakage control of, **26·13**
- meters (survey) for, **16·4**
- monitoring and surveying of, **26·3**
  - management responsibility for, **26·16**
  - for safety, **18·24**
- monitoring of, instruments for, **26·4**
  - ionization chambers for, **16·4**
- penetrating, detectors of, **5·10**
  - sources of, **5·8**
  - tests using, **5·12**
  - unusual uses of, **24·35**
- properties detected by, in nondestructive testing, **4·13**
- protection against, standards for, **26·3**
- protection against random, from X-ray tubes, **14·33**
- from radioisotopes, formula for, **20·5**
- safety precautions, in field and shop, **26·15**
  - in gaging, **18·23–26**
  - protective enclosures, **26·11**
- scattered, control of low-energy, in xeroradiography, **22·8**
  - undercutting in xeroradiography from, **22·10**
  - from X-ray generator, **14·38**
- scattering of, **26·10**
  - in radiography, and its control, **20·17–25**
- secondary, broad-beam attenuation of, **13·30**
  - build-up factor for, **13·30**
  - radiographic effects of, **13·29**
  - sources of, **13·29**
- shielding from, **26·8–14**
  - materials for, **26·14**
  - surveys in testing installations for, **26·14**
- sources of, handling of unshielded, **26·7**
  - for isotope and X-ray gaging, **18·1**
  - leak testing of sealed radioisotope, **26·5**
  - operation and licensing of, **26·15**
- sources of isotopic, **15·1–36**
  - X-ray and gamma-ray output of, **26·6**

Radiation (*Continued*)
- sources of penetrating, and protection against, **26·1**
- structures subject to nuclear, telemetering of photoelastic-coating stress-analysis data for, **53·35**
- for thickness gaging, properties of, **18·17**
- types of, **16·1**
- warning signs for, **26·15**
- from X-ray tubes, **20·3–5**

Radiation, Leakage (See "Leakage Radiation")

Radioactive Atoms (See "Radioisotopes")

Radioactive Substances
- as beta-ray sources, **5·16**
- gases, detection of, **5·4**
- natural, **15·7**
- testing of, television in, **11·37**

Radioactivity
- artificial, production by neutron capture and nuclear fission, **15·4**
- calculation of, **15·10–11**
- natural, **15·1**

Radiofrequency Crack Detector, 40·14

Radiographers (See "Personnel," "Radiography")

Radiographic Screens, 16·24–25, 20·25–29

Radiographs
- ASTM reference, for aluminum and magnesium castings, **24·3**
- defective, causes and correction of, **21·18–22**
- definition of, **20·1**
- penetrameter evaluation of, **20·36**
- reference, need for files of, **23·3**
  - of welds in steel plates, **2·19**
- viewing of, and apparatus for, **25·2**
  - illuminators for, **21·17**
- of welding-electrode spatter, **25·14**
- of welds (submerged-arc) with excessive reinforcement, **25·12**
  - with overlap, **25·12**
- of welds with arc-starting or spitting defects, **25·15**
  - with concavity at root, **25·11**
  - with cracks and their interpretation, **25·8**
  - with defects at electrode-change points, **25·14**
  - with excessive penetration, **25·13**
  - with gas holes and inclusions, **25·3**
  - with grinding marks, **25·14**
  - with inclusions (tungsten), **25·10**
  - with incompletely filled grooves, **25·11**
  - interpretation of, **25·1–2**
  - with lack of fusion, **25·9**
  - with lack of penetration, **25·6**
  - with lines and slag inclusions, **25·4–5**
  - with longitudinal grooves, **25·13**
  - in pipelines, interpretation of, **25·25**
  - in pipes, made with backing rings, **25·15**
  - with undercutting, and distinction from slag lines, **25·13**

Radiography (See also "Xeroradiography")
- absorption in, of γ and X rays, **20·13–15**
- acceptance quality level for, **24·2**
- of aircraft, **3·27, 3·29**
  - without disassembly, **3·31**
  - in manufacture and repair, **3·31**
- with beta-ray (pure) sources, **15·4**
- booths or cubicles for, **23·15**
- of buildings before pipeline installation, **3·22**
- build-up factors in, **15·36**
- of castings, **14·40**
- circumferential or panoramic, **23·6–7**
- contrast in, **15·35–36, 20·16–17, 20·34–35**

Radiography (*Continued*)
- of cylindrical objects, apparatus for, **24·39**
- definition in, **20·34, 23·4**
- density and half-value layer calculations for, **23·9**
- equipment for large-area, **23·15**
- exposure factors in, **20·15**
- exposure speeds in, with various sources and absorbers in comparison with xeroradiography, **22·8**
- exposure techniques in, **23·7**
- exposure time determination in, **20·10, 23·9–13**
- film holders (water-cooled) for, **3·5**
- films for, **20·1–47, 23·7**
  - density-exposure curves of, **16·19–22**
  - exposure formulas for isotope, **15·28**
- flash or high-speed, **20·46**
  - of rapidly moving objects, **14·20**
- with fluorescent intensifying screens, **20·28**
  - failure of Bunsen-Roscoe reciprocity law in, **16·23**
  - intensification factor in, **20·28**
  - mottle in, **16·22**
- fluorescent intensifying screens for, **23·8**
- fluoroscopy compared with, **19·1**
- gamma-ray sources for, calculation of, **15·9**
- geometrical enlargement in, **20·10**
- geometrical relations in, for best results, **20·7**
- half-value layer in, **13·30**
  - of steel, **23·5**
- high-speed flash, reciprocity curve for, **16·24**
- with high-voltage X rays, **23·1–16**
  - applications of, **23·14**
- hot, **3·3, 3·5–6**
  - in inspection of steam lines, **3·18**
  - of welds, **3·3**
- images in, factors controlling density in, **20·3**
  - graininess of, **16·21**
  - interpretation of, **24·1**
    - comparison with fluoroscopy, **24·18**
    - limitations in, **1·20**
- in industry, **20·1**
- inspection quality index *vs.* penetrameter sensitivity in, **19·47**
- in institutes (central cooperative) in Western Europe, **2·13**
- inverse square law in, **20·10**
- isotope, radiation used in, **15·3**
- latitude and sensitivity in, **23·3–4**
- lead screens and filters for, **23·7–8**
- lead screens in, **15·30, 20·25–28**
- limitations of, **19·47**
- low-voltage techniques and their uses, **24·40**
- micro-, **20·41–46**
  - projection, **20·44**
- in million-volt range, scattering in, and its prevention, **20·25**
- motion-picture, **19·45**
- panoramic, of steel weldments, **23·6**
- in petroleum refineries, **3·12**
- photo-, **20·45**
- photographic enlargement in, for small objects, **24·38**
- of pipelines, with cobalt-60 and iridium-192, **25·17**
  - radiation sources for, **3·14**
  - standards for, **25·17**
- of pipeline welds, **25·16–28**
  - definition and sensitivity in, **25·22**
  - qualifications of personnel for, **25·28**
  - source location and size in, **25·20**
  - three-exposure techniques in, **25·20–21**
- of pipes (hot-water), **3·17**

Radiography (*Continued*)
- of pipe welds, advantages of internal source, **25·22**
- of plastics (porous), **24·38**
- radiation sources in, handling of, **3·3**
- radioisotopes for, **15·13**
- reciprocity law in, and deviations therefrom, **20·13**
- reports and report forms for, **24·31, 24·35**
- safety precautions in, **3·31**
- safety regulations for, in Western Europe, **2·18**
- scattered-radiation control in, **23·8–9**
- scattering in, and its control, **20·17–25**
- secondary radiation effects in, **13·30**
- sensitivity in, **15·30–36, 20·34–36**
  - comparison with fluoroscopic sensitivity, **19·6**
  - range of, **1·8**
- of ships' propellers and boiler tubes, **2·14**
- of ship welds, **3·19–20**
- spot, **14·47**
- standards for, **15·31**
  - and their development, **2·18**
- of steel, cooperative research on, **2·19**
  - maximum X-ray voltages for various thicknesses of, **25·17**
  - unsharpness standards for, **2·18**
- stereo-, in depth localization of defects, **20·46–47**
- tank units for, **14·36**
- of thin metal specimens, mottling in, and its control, **20·24**
- of tubes (boiler), **3·8**
- unsharpness in, geometry of, **20·7–10**
- uses of electron autoradiography and, **5·18**
- of weld beads which are out-of-line, **25·14**
- of welds, **3·3, 14·40, 25·1–28**
  - in high-pressure steam lines, **3·3**
  - in pipelines, percentage examination desirable, **25·26**
  - in pipelines, variation of percentage rejection during project, **25·26**
  - in pipes, flanges, etc., **14·42**
  - in pipes using external X-ray source, **25·23**
- X-ray generator selection for, **14·40**

Radioisotopes (See also "Isotopes")
- artificial, **13·15, 15·4–36**
- containers for shipment of, **26·15**
- daughter products of, **13·13**
- disintegration of, **13·12–14, 15·2**
- disposal of waste, **26·16**
- gamma radiation from, reduction factors for, **26·10**
- half-life of, **13·12**
- handling in radiography, **3·19**
  - equipment for, **15·22–24**
- neutron-activated, **15·8**
- in nondestructive testing, **5·8**
  - cooperation among laboratories using, **2·17**
- positioners for, for field tests, **3·3**
- properties of, measurement of, **15·5–7**
  - for radiography, **15·13**
- radiation from, **13·12–17, 20·5**
- for radiography, voltage equivalents of, **25·17**
- radiography with, control of, **20·16**
- safety in use of, publications on, **25·18**
- sources of, **15·7**
  - for gaging, **18·16**
- specific activity of, **13·13**
  - formula for, **13·17**
- storage of, **26·16**
- thickness gaging with, **18·1–40**

Radium
- capsules for, leak testing of, **26·6**

Radium (*Continued*)
  formation from uranium, **15·7**
  gamma rays from, broad-beam shielding for attenuation in concrete, iron, and lead, **26·11–13**
  as isotope (naturally occurring), **13·14**
  photographic-film shielding against, **20·41**
  radiation dosage output of, **26·6**
  in radiography, equivalent voltage of, **25·17**
    of pipeline welds, **25·16**
    of steel, fluorescent-screen intensification factor in, **20·28**
  as radon source, **13·15**
  sources and source strengths of, **15·8**
Radon
  equilibrium with radium, **13·15**
  formation from radium, **15·7**
Railroad Cars
  axles, ultrasonic contact testing for cracks in, **48·6**
  for electric-current rail testing, **35·13–17**
  subway, strain-gage measurements of truck frames of, **3·25**
  tank, inspection of, **11·14**
  wheels, sonic testing of, **5·24**
Rails, Railroad
  defects in, classification of, **35·20**
    detection by electric-current tests, **5·20**
    marking of, **35·21**
  electric-current testing of, **35·11–21**
    equipment for, **35·13–20**
    interpretation of indications in, **35·20**
    magnetic-field effects in, **35·12**
    personnel for, **35·20**
  joint bars of, fractured at fatigue crack, **32·23**
  ultrasonic resonance testing of, **50·28–29**
Raman Effect, definition of, **10·27**
Raman Lines, for study of molecular energy states, **10·27**
Rare Earth Elements, atomic structure and chemical properties of, **13·6**
Raw Materials
  flow
    from plant through independent nondestructive-testing laboratory to manufacturer, **2·3**
    in plant with internal nondestructive-testing facilities, **2·2**
  inspection of, aims and management of, **1·16**
    scheduling of, **1·23**
Rayleigh Waves (See "Ultrasonic Waves")
Real Components
  of apparent impedance of test coil and secondary coil for thin-walled tubes, **38·3**
  of effective permeability, **36·14, 36·18**
    for spheres in eddy-current testing, **39·3**
  of impedance of circular coil with nonferromagnetic sphere, **39·9**
  of secondary voltages, calculation of, **36·15**
  of transmission coefficient T in eddy-current testing of sheet material, **39·14**
  of voltage of circular coil with nonferromagnetic sphere, **39·9**
Reciprocity Law (See also "Bunsen-Roscoe Reciprocity Law")
  in radiography and deviations therefrom, **20·13**
Recording
  apparatus for, calibration of, in ultrasonic resonance testing, **50·12**
    for magnetic-field meters, **33·11**
    ultrasonic resonance equipment with automatic, **50·10**
    in ultrasonic-test C-scan systems, **43·34**
    for X-ray film density measurement, **24·35**

Recording (*Continued*)
  of Magnatest Q eddy-current test results, **42·32**
  of signals in electric-current railroad rail testing, paint guns, pen units, and tape for, **35·16–17, 35·19**
Records
  of nondestructive-testing laboratories, **2·9**
  of personnel exposure to radiation, **26·16–17**
Recovery Time, of Geiger-Muller counters, **16·7**
Recrystallization, in metals, effect on ultrasonic shear-wave velocity, **45·7**
Rectifiers
  dry-plate, for magnetization for magnetic-particle testing, **30·8**
  Graetz full wave, **14·23**
  phase-controlled, in eddy-current cathode-ray-tube ellipse-test instruments, **40·24**
    in eddy-current testing, adjustment of, **37·34**
    in linear time-base eddy-current instruments, **40·30**
    in Multitest eddy-current-test instruments, **40·22**
    in Sigmaflux eddy-current instruments, **40·26**
    in suppression of undesired effects in eddy-current testing, **40·38–42**
  selenium, **14·25**
  Villard modified, for X-ray generators, **14·41**
  Villard voltage doubling, **14·24**
    modified, **14·25**
  for X-ray apparatus, **14·6**
Reference Blocks (See "Test Blocks")
Reference-Bridge Null-Balance Systems, for strain gages, **54·20**
Reference Wedges, in X-ray thickness gaging, **18·9**
Reflectance (See "Reflectivity")
Reflecting Objectives, for infrared and ultraviolet microscopes and their working distance, **10·8–9**
Reflection
  measurement of, in ultrasonic contact testing, **48·13–14**
  multi-path, effects in ultrasonic testing by through-transmission method, **43·28**
  in nondestructive tests, **5·15**
  in radiography, lead screens in prevention of, **20·27**
  radioisotope thickness gages using, **18·15**
  of sound waves at liquid-metal interfaces, **45·9**
  in thickness measurement, accuracy of, **18·6**
  of ultrasonic surface-waves in contact testing, irrelevant indications from, **48·24**
  of ultrasonic waves, **45·1–6**
    amplitudes for common metals immersed in water, **43·46**
    and its coefficient, **43·12**
    energy losses in, **43·25**
    from rough and smooth surfaces, **45·23**
    from small discontinuities, **45·20**
    test methods using, **43·1**
    time in liquids, metals, and plastics, **43·31**
Reflectivity
  of materials in photoelastic-coating tests, effect on type of plastic for, **53·13**
  measurement of, **10·12**
    phototubes in, **11·34**
Reflectors
  ultrasonic
    angle of rotation in water, relative echo amplitude and power in relation to, **45·23**
    echo amplitudes and energy from, **45·18–22**

Reflectors (*Continued*)
  ultrasonic (*Continued*)
    echo amplitudes from concave and spherical, 45·24
    radiation patterns for flat circular, for various diameters, 45·20
Reflectoscope, index window for ultrasonic contact tests, 48·13
Refraction
  of sound waves at liquid-solid interfaces, angle of, 45·9–10
  in ultrasonic contact testing, disturbances by, 48·25
  of ultrasonic waves, analyzer for, 43·20
    angle of, *vs.* angle of incidence and amplitude of echo, 45·11
    angles in metals, effects of angulation of incident beam on, 45·10
    at interfaces, 43·15–16
Refraction, Double (See "Bi-Refringence")
Refractive Index
  definition of ultrasonic, 44·7
  determination of, by schlieren methods, formula for, 10·24
Refractivity
  of cornea and lens of the eye, 10·1
  of liquids, measurement of, 10·11
Refractometers
  for gases and liquids, 10·10
  photoelectric, optical system of, 10·11
  in testing of optical components, 10·10
  for ultrasonic waves, aluminum-alloy blocks as, 45·10
Refrigeration Systems, leaks in, detection of, 5·4
Registration, of laboratories using ionizing radiations in Western Europe, 2·18
Regulations, for shipping radiation sources, 26·15
Reinforcement, excessive, in submerged-arc welding, causes and radiography of, 25·12
Reliability
  of components of modern machinery, requirements for, 1·5
  in nondestructive testing, 1·18, 2·4, 2·12
    establishment of, 1·21
  of products, establishing degree of, 1·7
    nondestructive tests in ensuring, 1·1
  of test determinations, 1·21
Rem., definition of, 26·2
Remote Handling Equipment, for radioisotopes, 15·23
Replicas
  in electron microscopy, 11·40
  plastic, for surface imprints, 12·29
  pressure-sensitive tape for, 12·30
Reports
  forms for fluoroscopy, radiography, and X-ray inspection, 24·31
  published, of Institut Dr. Foerster, 2·30
Research
  fundamental, in eddy-current nondestructive testing, 2·24–25
  groups, nondestructive-testing laboratory service to, 2·3
  laboratories for nondestructive testing, 2·23–27
  on materials, Magnatest Q eddy-current testing in, 42·60–61
  by nondestructive-testing laboratories in Europe, 2·16
  optical projectors in, 12·21
Residual Magnetization (See "Magnetization")
Resins (See also "Plastic Materials")
  adhesives from, for strain gages, 54·12–13
    softening at elevated temperatures, 54·23
  brittle coatings from, comparison with ceramic coatings, 52·1
    for nondestructive testing, 52·3–5
    specimen preparation for application of, 52·9
  cracks in, electrified-particle indications of, 29·5
Resistance, Electric (See "Electric Resistance")
Resistance Strain Gages (See "Strain Gages")
Resistance Strain-Gage Tests (See "Strain-Gage Tests")
Resistivity (See "Electric Resistance")
Resolving Power
  of magnifiers, definition of, 11·3
  of microscopes, 10·7
  in ultrasonic immersion testing, loss near surface, 46·8
  in ultrasonic testing, 43·49, 44·20
    band width in relation to, 44·20
    effects of test object surface roughness on, 45·17
    of search units, 43·5
    in systems using amplitude and transit-time indication, 43·31
  of ultrasonic transducers, 44·5, 44·8
  in X-ray fluoroscopy, determination of, 19·18
Resonance
  effects in ultrasonic testing by through-transmission method, 43·28
  frequencies (ultrasonic), 43·36–37
  in sonic and ultrasonic testing, 51·1
  in ultrasonic testing of thin materials, 44·10
  of ultrasonic waves, thickness measurement with, 43·15, 43·35–37
Resonant Circuits (See "Electric Circuits")
Resonant Frequency [See "frequency (resonant)" under "Ultrasonic Waves"]
Resonant Frequency Testing (See "Sonic Testing," "Ultrasonic Testing")
Response, of photoconductive cells, 11·33
Retentivity, magnetic, hardness in relation to, 30·22
Reticle, for checking workpiece section outlines, 12·27
Reticulation, of X-ray-film emulsions and its prevention, 21·8, 21·22
R.F. Presentation, of ultrasonic test indications, 45·21
Rhodopsin, chemical transformations in vision, 10·2
Right-Hand Rule, in magnetization (circular), 30·5
Rigidity, of strain gages, effect in tests on materials of low elasticity, 54·30
Rinsing
  in field inspection liquid-penetrant tests, 6·17
  in liquid-penetrant removal, 6·7, 6·12, 6·17
  of X-ray film to arrest development, 21·6–7
Rochelle Salt, crystals for ultrasonic transducers, 44·2, 50·15
Rock, ultrasonic contact testing of, frequencies for, 48·1
Rods
  alloy mixed, eddy-current testing with Magnatest FM-100, 42·11
  aluminum, eddy-current testing of, separation of effects of conductivity and diameter in, 37·1–2
  cracks in, detection with Defectometer eddy-current instrument, 40·47
  eddy-current-test apparatus for, 40·2–3

- **Rods** (*Continued*)
  - cracks in (*Continued*)
    - self-comparison eddy-current testing of depth of, **40·35**
  - crack testing and sorting of, by eddy-current methods, automatic handling apparatus for, **41·2**
  - diameter, aluminum-alloy, indications of Magnaflux FW-300 eddy-current instrument, **42·2**
  - eddy-current density and field strength in, as function of radial position, **37·9**
  - eddy-current linear time-base tests on iron, **40·32**
  - eddy-current testing of, by ellipse methods, **40·28**
    - interferences with, **2·31**
  - heat treatment of, hardness control in, with Magnatest FW-300 eddy-current instrument, **42·19**
  - magnetic field strength and permeability variation of mechanically deformed, effect on Magnatest Q eddy-current sorting, **42·31**
  - spring, automatic sorting by hardness, with Magnatest Q eddy-current instrument, **41·10**
  - statistical quality number in testing of, **41·18**
  - steel, with cracks and inhomogeneous stresses, Magnatest D eddy-current instrument multi-exposure pictures of, **42·63**
    - crack testing of, with Magnatest D eddy-current instruments, **41·10, 42·61–69**
    - Magnatest D eddy-current indications of cracks and other defects in, compared with macro- and microsections, **42·62–69**
    - Magnatest Q eddy-current spread bands of, **42·33**
    - Magnatest Q eddy-current test spread bands of harmonics in wave forms of, **42·37**
  - tensile strength of metallic, eddy-current testing of, **42·3**
  - tungsten, defects in, microsections and eddy-current indications of, **42·7–9**
  - ultrasonic-wave velocity in thin, **43·9–11**
- **Roentgen,** definitions of, **13·13, 15·5, 26·2**
- **Roller Bearings** (See "Bearings, Roller")
- **Rollers** (See also "Cylinders," "Rolls")
  - automatic sorting of, by hardness with Magnatest Q eddy-current instrument, **41·10**
  - for bearings, sorting with Magnatest Q eddy-current methods, **42·58**
  - testing with Multitest eddy-current instrument, **40·23**
- **Rolling**
  - of alloys and metals, effect on ultrasonic-test "noise," **44·7**
  - of metals, etching in detection of flow lines from, **32·25**
  - of metal sheets, thickness gaging in, **18·26**
- **Rolls** (See also "Rollers")
  - ultrasonic resonance test on built-up steel, **3·22**
- **Ronchi Ruling,** as Schlieren edge for microscope conversion, **10·20**
- **Rooms,** for X-ray-film processing, **21·12–17**
- **Rosette,** strain-gage configuration, **54·5–6**
- **Rotor Buckets** (See "blades" under "Turbines")
- **Rotors**
  - generator and turbine, distortion testing of forgings for, **5·24**
  - ultrasonic immersion testing of jet-engine, **47·16**
- **Roughness** (See also "finish" under "Surface")
  - critical, in ultrasonic testing, and values for stainless steel blocks, **45·16–17**
- **Roughness** (*Continued*)
  - measurement of, equipment for, **45·17**
  - of surfaces, optical projection of, **12·14**
- **Rubber**
  - coatings of synthetic, for moistureproofing of strain gages, **54·38**
  - photoelastic-coating testing of, high-strain plastic sheets for, **53·12**
  - strain-gage tests on strips of, effect of rigidity of gage on, **54·30**
  - thickness gaging in industry of, **18·27**
  - thickness measurement range with Sr-90 beta gages, **18·16**
- **Rubidium,** absorption coefficients (mass) for γ and X rays and photon energies of, **18·36**
- **Rupture**
  - modulus, of abrasive products, sonic testing in determination of, **51·12**
    - measurement by sonic resonance vibration tests, **51·6**
- **Rust**
  - removal from metals before strain-gage application, **54·35–36**
  - removal from parts for liquid-penetrant testing, **6·6, 6·13**
- **Ruthenium-106,** energy and half-life of, as β-ray source, **18·17**
- **Rutherford Scattering Formula,** in radiation absorption, **13·28**

S

- **Safelights** (See "Lamps")
- **Safety**
  - in acetic acid dilution, for short-stop baths for X-ray film processing, **21·7**
  - demands of public, role in development of nondestructive testing, **1·6**
  - department of, nondestructive testing in, **1·17**
  - devices in automatic ultrasonic testing, **49·19**
  - factors in modern construction, **2·23**
    - in modern machinery, nondestructive testing in relation to, **1·5**
  - in fluoroscopy, precautions for, **24·23**
  - in handling and mixing of acid etching solutions, **32·28**
  - in handling ceramic brittle-coating materials and solvents, **52·8**
  - inspection for, by ultrasonic resonance methods, **50·26**
  - in liquid-penetrant testing, **7·35**
  - from radiation, management responsibility for, **26·16**
  - in radiation use in gaging, **18·23**
  - in radiography, with radioisotopes, publications on, **25·18**
    - regulations in Western Europe, **2·18**
  - in sectioning with cut-off wheels, **32·24**
- **Sales Department,** liaison with, in quality-control programs, **1·18**
- **Salvage**
  - of clayware, using filtered-particle tests, **9·1, 9·9–10**
  - of defective parts by chipping and welding, **32·22**
- **Samples**
  - of defective parts for training for liquid-penetrant testing, **8·23**
  - for fluoroscopic comparison, having known defects, **24·27**
  - handling in fluoroscopy, **19·35**
  - holders for photometers for penetrant brilliance determination, **7·22**

Samples (*Continued*)
- preparation for destructive *vs.* nondestructive testing, 4·7
  - for determination of brilliance of liquid penetrants, 7·23
- prior processing of, liquid-penetrant testing in relation to, 8·5
- tube-ring, for precision determination of hysteresis loop, and apparatus for magnetizing, 42·22

Sand, illumination of, for magnified viewing, 12·13
Sanding, belt, as supplement to magnetic-particle testing, 32·25
Sandstone, radiation-shielding equivalent of, 26·9
Sanitary Ware, wavy cracks in cast iron, 29·14
Saturation Potential, of gases for ionization chambers, 16·2
Sawing, across cracks or discontinuities as supplement to magnetic-particle testing, 32·24
Saws, slotting, in trepanning as supplement to magnetic-particle testing, 32·24

Scale
- false indications from, in ultrasonic immersion testing, 47·25
- formation in pipes, portable wall-thickness gage for, 18·31
- removal
  - from metals before strain-gage application, 54·34–35
  - from parts for liquid-penetrant testing, 6·6, 6·13

Scalers, for amplifier output in radiation detection, 16·5
Scales (See "Balances")

Scanning
- problems in ultrasonic testing, 43·50
- speed, ultrasonic contact-test equipment selection in relation to, 48·5
  - in ultrasonic immersion inspection, 47·30
- volume, ultrasonic, 43·47

Scanning Equipment, for ultrasonic immersion inspection of pipe and tubing, 47·29

Scattering
- back (See "Reflection")
- of charged particles, 13·27
- Compton (See "Compton Scattering")
- effect on radiation intensity, 15·7
  - on X-ray film density variation and contrast sensitivity in radiography, 19·8
- of gamma rays in radiography, 15·24–25
- of radiation, 26·10
  - collimators for minimizing, in gaging, 18·24
  - overhead in X-ray rooms, 26·14
  - in radiography, and its control, 20·17–25
  - in radiography, lead-foil screens in control of, 20·26
  - in radiography, minimizing of, 23·9
  - in X-ray inspection, shape effect on, 19·46
- of ultrasonic waves by discontinuities and its compensation, 45·6
  - energy losses in, 43·25
  - resolving-power loss from, 44·20
- of X-rays, 19·19
  - by barrier windows, 19·13
  - in fluoroscopy, 19·15
  - of high-energy, 23·1

Schlieren
- advantages of optical tests using, 10·25–26
- analysis of, 10·22–24
- color, 10·25

Schlieren (*Continued*)
- definition of, 10·20
- equipment
  - for optical testing, 10·20–21
  - modified, 10·24–25
- formula
  - for dry mass of localized inhomogeneities and impurities within test samples, 10·24
  - for mass concentrations in solutions from, 10·24
  - for refractive index from, 10·24
- for measurement of refraction, optical thickness and flatness, 10·19–26
- microscope conversion for testing with, 10·20–21
- for optical glass testing, 10·10
- for optical testing, principles of, 10·20
- patterns, 10·22
  - dislocations and displacement of lines in, 10·22
  - microdensitometric line measurements of, 10·22
- of ultrasonic beam near transducer, 44·18

Scintillation Counters (See "scintillation" under "Counters")

Scrap Metal
- decreasing amount of, by preliminary inspection, and increasing production thereby, 1·14
- nonferrous, iron detection in, 34·22
- sorting by electrical conductivity eddy-current tests, 42·15

Scratches
- detection of, by liquid-penetrant testing, 6·9
- optical projection of, 12·14
- removal of surface, for metallography, 32·28–29

Screening Effect, of tubes in eddy-current testing, apparatus for measuring, 38·16
Screen Patterns, elliptical, in eddy-current testing, 37·33

Screens (See also "Fluorescent Screens," "Lead Screens")
- effect on image produced by penetrating radiation on X-ray film, 15·28
- frosted or ground-glass, advantages and disadvantages on optical projectors, 12·11
- intensifying, difficulties in application in xeroradiography, 22·8
- optical-projector, 12·4, 12·8
  - permanent record of images obtained on, 12·37
  - polarizing, 12·31
- photofluorographic, 16·14
  - brightness of, 19·9
  - size of, 12·8–9
- radiographic (See "Radiographic Screens")
- wire-mesh (See "Sieves")

Screws, eddy-current testing of, automatic tilting of moving coils in, 41·8
Scum, in fixation solutions for X-ray-film processing and its prevention, 21·22
Sealants (See "Adhesives")

Seals, Glass-to-Metal
- cracks in, 29·15
  - electrical leakage from, 29·16
  - evaluation of, 29·17
  - moisture effects on, 29·16
  - patterns of, 29·18
- electrified-particle testing of, 28·8
- inspection of, 29·15

Seams (See also "Cracks")
- depth indication with Sedac eddy-current-test apparatus, 40·18

Seams (*Continued*)
  detection of, penetration time for, for dye-penetrants, **6·14**
  in diesel-engine wrist pin and locomotive spring, magnetic-particle-test indications of, **32·1–2**
  eddy-current-test apparatus for detection of, **40·2–3**
  filing at, as supplement to magnetic-particle testing, **32·21**
  liquid-penetrant indications of, **8·2, 8·21**
  liquid-penetrant test penetration time for detection of, **6·19**
  surface
    chipping at, as supplement to magnetic-particle testing, **32·22**
    examination with magnifying glass after magnetic-particle testing, **32·4**
    in rolled bars, magnetic-particle indications of, **32·6**
Search Units
  for electric-current railroad-rail testing, **35·16**
  ultrasonic, Plexiglas coupling blocks in, **49·5, 49·11**
  for ultrasonic contact testing, **48·2**
    calculation of wedge angle in, **48·8**
  for ultrasonic double-transducer tests
    angle-beam, **49·8–9**
    combined transmit-receive, **49·2–9**
      applications of, **49·12–14**
      for automatic testing, **49·18**
      fault-warning systems in, **49·20**
      full immersion testing by, **49·19**
    separate transmit-receive, **49·1, 49·9–11**
      for contoured materials, **49·14**
      full immersion testing by, **49·19**
      for laminar flaw detection, **49·10**
      transmission testing of attenuating materials by, **49·17**
    transmit-receive, classification, of **49·3**
    transverse-wave, **49·11**
  for ultrasonic immersion testing, **46·7**
  for ultrasonic testing, **43·5–7**
    frequencies and sizes most commonly used, **43·7**
Secondary Coil Voltages (See "Voltage")
Sectioning, with cut-off wheels as supplement to magnetic-particle testing, **32·24**
Security, commercial and military, in nondestructive testing laboratories, **2·5**
Sedac Eddy-Current Instrument, response characteristics of, **40·18**
Segregation
  in alloys, microradiography of, **20·42**
  in alloys and metals, electrical conductivity curve as indication of, in eddy-current tests, **42·1**
    ultrasonic-test noise from, **44·7**
  in aluminum alloys, ultrasonic contact testing for, **48·12**
  in aluminum-copper-magnesium alloys, electrical conductivity variation from, **42·14**
  in castings, X-ray detection and evaluation of, **24·11**
  detection in steel, ultrasonic contact test frequencies for, **48·2**
  in metals, detection by deep etching as supplement to magnetic-particle testing, **32·25**
  of nitrogen during aging of Thomas steel, effect on Magnatest Q eddy-current indications, **42·61**
  in pistons, Defectometer indications of, in eddy-current tests, **40·47**
Segregation (*Continued*)
  in steel rods, Magnatest D eddy-current instrument wave form and macro- and microsections showing, **42·63**
  ultrasonic immersion indications of, in forged turbine wheels, **47·20**
Selenium
  absorption coefficients (mass) for γ and X rays and photon energies of, **18·35, 27·23**
  attenuation coefficients of, for γ and X rays, **27·23**
  as barrier-layer cell or photoresistance in X-ray amplificatiton, **16·8**
  barrier-layer cells of, **11·34**
  crystal orientation in electrodeposited, **17·19**
  layers on xeroradiographic plates
    mechanical damage and its prevention, **22·4**
    thickness of, **22·4**
  photoconductive, in X-ray pick-up tubes, **19·41**
  as photoconductor for xeroradiography, **22·1**
  rectifiers, for X-ray equipment, **14·25**
Selenium-75, energy and half-life of, as γ-ray source, **18·17**
Self-Inductance (See "Electric Inductance")
Semi-conductors
  analysis by nondestructive tests, **5·21**
  as charge-carrier sources, **5·16**
  in conversion of radiation into electrical energy, **18·20**
  detection systems using, for X-ray thickness gages, **18·7**
  for Hall generator probes, **33·12**
  photoconducting, **11·33**
Sensitivity
  of amplifiers in electric-current railroad rail testing, setting of, **35·17**
  of bi-refringence measurements with Babinet Compensator in photoelastic-coating tests, **53·27**
  of brittle coatings (resinous) to flaking as indicator of gross strain, **52·25**
  depth
    in eddy-current testing, **37·6**
    of ultrasonic transmit-receive search units, **49·5, 49·10**
  in eddy-current testing
    of conductivity and diameter, **40·12, 42·1**
    of flat sheets with fork-coil arrangement, **39·15–16**
    with Magnatest Q instrument, calibration of, **42·33**
    with Multitest instrument, **40·23**
    selection for Magnatest Q sorting of alloys, **42·33**
    of small-diameter tubing, **38·26, 38·29**
    of spheres for cracks, magnetizing-field direction in relation to, **39·10**
    of thick-walled tubes, and frequency-ratio calculation for maximum, **38·12**
    of thin-walled tubes, **38·6**
    of tubing for very small discontinuities, **38·31**
  of eddy-current-test instruments
    calibration of, **37·30**
    graphs of, **37·34**
    tube penetration depth in relation to, **38·19**
  eddy-current-test maximum
    to conductivity and diameter in eddy-current testing of nonferromagnetic cylinders, **40·12**
    in feedback-controlled impedance eddy-current testing, **40·18**

- **Sensitivity** (*Continued*)
  - eddy-current-test maximum (*Continued*)
    - of tubes for crack effects, conductivity and permeability, 38·17
  - of electrodes in square array for wall-thickness measurement, 35·11
  - of eye to colors in photoelastic-coating testing, and use of tint-of-passage for precise measurements, 53·4
  - of fluoroscopic-image amplifiers, 19·39
  - fluoroscopic *vs.* radiographic, 19·6
  - in fluoroscopy
    - contrast, 19·4
    - focal-spot size and magnification in relation to, 19·18
    - thickness variation of, 19·31, 19·34
  - in magnetic-particle testing, requirements for, 31·2
  - in nondestructive testing, 1·8
    - cost in relation to, 1·15
  - penetrameter
    - of aluminum in fluoroscopy, 19·23
    - in fluorography, 19·44
    - in fluoroscopy and radiography, inspection quality in relation to, 19·47
    - in fluoroscopy of aluminum with Lumicon, 19·40
    - in hot radiography, 3·6
    - in radiography, 20·37
      - definition of, 20·35
    - in X-ray inspection, 19·1
  - in photoelastic-coating tests, effect of coating thickness on, 53·13
  - of phototubes, gas-filled *vs.* vacuum, 11·28
  - radiographic, 15·30–36, 20·34–36
    - factors affecting, 15·32
    - in pipeline-weld inspection, 25·22
  - in radiography (high-voltage), 23·3
  - selection in nondestructive testing, 1·19
  - spectral, of photographic film, effect of radiation energy on, 16·22
  - strain
    - in brittle-coating tests, variation with threshold values, 52·6
    - of ceramic brittle coatings, 52·1
      - and their calibration, 52·7
      - on steel, 52·8
    - of foil or wire for strain gages, temperature effect on, 54·23
    - of materials in their plastic range, 54·25
    - of plastic sheets for photoelastic-coating testing, 53·16
    - of strain-gage-alloy wire, 54·9
    - of unbonded filaments, gage factor in relation to, 54·11
    - with various instruments in photoelastic-coating tests, 53·17
  - of strain-gage circuits
    - calculation of maximum, 54·13–14
    - effect of temperature compensation with "dummy" gage on, 54·15
  - of strain gages (See also "Desensitization")
    - axes of, 54·28
    - capacitance effect on, and its balancing, 54·37
    - and circuits, planned or parasitic variation of, 54·19–21
    - effect of mechanical properties on transverse, 54·4
    - of various configurations, 54·5
  - of strain-gage transducers, temperature effect on, 54·4
  - of thickness measurement by radiation transmission, 18·5
- **Sensitivity** (*Continued*)
  - -time control for depth in ultrasonic testing, 45·5
  - transverse, effects on strain gages and their correction, 54·28–29
  - in ultrasonic immersion testing
    - adjustment of, 46·17
    - control of, 47·32
  - of ultrasonic paint-brush transducers, requirements for, 44·11–12
  - in ultrasonic testing, 43·48–49
    - with A-scan presentation, 43·31
    - with transmit-receive search units, 49·3
  - of ultrasonic-test search units, 43·5
  - of ultrasonic transducers, 44·5
    - frequency in relation to, 50·7
  - of Wheatstone bridge circuits at finite load resistance, 54·19
  - in xeroradiography, local contrast and penetrameter, 22·9
  - in X-ray inspection
    - by closed-circuit television, 19·41
    - definitions of, 19·1
- **Sensitization,** in measurement of very small strains by brittle-coating method, 52·23
- **Sensitometric Curves,** of photographic film, 20·32–34
- **Service Conditions,** role in radiographic interpretation, 25·2
- **Service Damage or Failure**
  - mechanism of, destructive *vs.* nondestructive tests in determination of, 4·7
  - nondestructive tests in determination of cumulative, 4·7
- **Service Department,** liaison with, in quality-control programs, 1·18
- **Service Life,** of machines and structures, photoelastic-coating tests in survey of, 53·35
- **Servo Systems**
  - load cells operating on strain-gage principle in, 54·3
  - in radioisotope thickness gaging, 18·12
- **Shadow Casting,** in electron microscopy, 5·18, 11·40
- **Shadows,** formation by γ and X rays, geometry of, 20·5–7
- **Shafts** (See also "Axles"), ultrasonic gaging of bored, 50·20
- **Shape**
  - effect on natural frequency of sonic vibration of bodies, 51·1
  - limitations in nondestructive testing, 1·20
  - measurement by eddy-current testing, tabular summary of, 36·4–5
- **Shape Permeability,** effects in eddy-current testing of short parts, 39·4, 39·6
- **Sharpness**
  - of shadows, geometry of, 20·5
  - un- (See "Unsharpness")
- **Shear Modes,** in ultrasonic testing, 44·6
- **Shear Strength,** of cement for strain gages, 54·10
- **Shear Waves,** interruption of, in ultrasonic contact testing, 48·20
- **Sheaths,** lead, on wire, ultrasonic thickness gaging of, 50·19
- **Sheet Materials**
  - anisotropy of, magnetic field point-pole tests for, 34·9–10
  - classification and regrading of, isotopes and X rays in, 18·26
  - cracks in, frequency selection for eddy-current testing for, 40·12

Sheet Materials (*Continued*)
- defects and thickness of, capacitance tests in determination of, 5·22
- discontinuities in, detection by direct-current tests, 5·20
- eddy-current testing of, 39·12–19
  - for conductivity-thickness product, 39·16–17
  - metallic coils for, 40·38
  - reaction field in, 39·14
  - sensitivity diagram for, 39·15
  - tabular summary of, 36·6
- electrical conductivity of thin Al-Cu-Mg, hardness and quenching temperature in relation to, 42·19
- electrical steel laminated, sorting by hysteresis loss, 34·10
- grain orientation in steel, determination of, 34·9
- liquid-penetrant indications of cracked, 8·14
- magnetic-field polar diagram about a point pole for steel, 34·10
- magnetic-particle indications of laminations in metallic, 32·7
- piles of
  - photoelastic-coating analysis in design of, 53·28–29
  - strain distribution in, photoelastic coatings in determination of, 53·26
- plastic
  - clear or metallized, for photoelastic-coating tests, 53·11–12
  - measurement of ultrasonic-wave attenuation and velocity in, 43·15
- thickness of
  - automatic eddy-current apparatus for sorting by, 41·14
  - gaging of, 18·15
  - measurement from one side only, 5·20, 5·24
- thickness of metallic, measurement with *RC* oscillator, 39·18
- ultrasonic contact testing, frequencies for, 48·1
- ultrasonic contact testing of rolled, 48·11
- ultrasonic immersion testing of, 46·22
- ultrasonic-resonance gaging of chemically milled and skin milled, 50·21
- ultrasonic testing of, with sharp-focused transducers, 44·6
- ultrasonic-wave propagation in, 43·9
- X-ray analysis of rolled, 17·20

Shells, shotgun, fluoroscopic inspection of, 19·36

Shielding
- for Cobalt-60, 15·14
- in eddy-current testing at various frequencies and field strengths with and without cores, 38·21
- equivalents of various materials, 26·9
- for Iridium-192, 15·17, 15·19
- of lead wires for strain gages, 54·32
- by magnetic shunting as problem in demagnetization of assemblies or small parts, after magnetic-particle testing, 30·28
- materials for radiation, 26·14
- of radiation for safety in gaging, 18·23
- of radiation sources, 26·8
- for Thulium-170, 15·22
- wall thickness for radiation, 26·14
- of X-ray film against γ and X rays, 20·39
- of X-ray generators, 14·38

Shipment, of radiation sources, regulations for, 26·15

Ships
- bulkhead and hull-thickness of, measurement by ultrasonic resonance, 50·27

Ships (*Continued*)
- corrosion inspection of, by ultrasonic methods, 50·37
- corrosion rate of, measurement by Audigage, 50·41
- corrosion thinning of hull plates of, direct-current measurement of, 35·9
- degaussing of, longitudinal field probe for, 33·1
- nondestructive testing in maintenance of, 3·19
- plate thickness of, measurement by ultrasonic resonance methods, 3·20
- stern frames of, ultrasonic pulse-reflection testing of, 3·21
- ultrasonic resonance testing of structure of, 50·27

Shoes
- heels of, fluoroscopic inspection of, 24·19
- inspection (fluoroscopic) of, 19·36

Short-Burst Polarity Method, for ultrasonic testing, 45·21

Short Circuits (See "Electric Circuits")

Shot
- lead mask combined with, in reduction of scattering in radiography, 20·20
- masking and filling cavities with metallic, in radiography, 20·22
- metallic, in minimizing X-ray scattering, 23·9

Shot Blasting, effect on liquid-penetrant indication of defects, 8·5

Shrinkage
- in bronze (cast gun-metal), radiographs of, 24·15
- cavities and porosity from, X-ray interpretation of, 24·8
- cavities from
  - causes and X-ray interpretation of, 24·9, 24·11
  - detectible size in fluoroscopy of, 24·24
  - fluoroscopic indications of, 24·28
  - liquid-penetrant indications of, 8·22
- of cylinders, eddy-current testing of, mercury-model indications of, 37·14
- detection with visible dye penetrants, 6·20
- evaluation of parts showing, basis for, 8·22
- measurement by eddy-current methods, 36·5
- micro-, in magnesium-alloy castings, radiography of, 24·8, 24·9

Shrinkage Porosity (See "Porosity")

Side Lobes
- phenomena in ultrasonic testing, 44·19
- in ultrasonic scanning of test holes, 44·19
- of ultrasonic-wave transducers in far field, 44·14

Sieves, in resolution determination in fluoroscopy, 19·18

σ-D Instrument, for eddy-current testing to measure variations of conductivity and diameter independently, 40·40

Sigmaflux Eddy-Current Instruments (See "FW-300" under "Magnatest Eddy-Current Instruments")

Sigmatest Eddy-Current Instruments (See "FM-100" under "Magnatest Eddy-Current Instruments")

Signaling, underwater, magnetostrictive transducers in, 44·1

Signals
- amplification limitations of, effect on test feasibility, 4·9
- amplifiers for, elimination of drift of, 4·9

Signals (*Continued*)
- in eddy-current linear time-base tests, selection in slit analysis, 40·30
- in eddy-current testing
  - display systems for, 38·38–39
  - of small-diameter tubing, discrimination among, 38·26
  - suppression of undesired, 40·39
  - of tubes, feeding mechanism for prevention of spurious, 38·27
- horizontal sweep, in linear time-base eddy-current instruments, 40·30
- secondary-coil-voltage, in eddy-current crack testing of ferromagnetic cylinders, 40·36
- ultrasonic
  - A-scan presentation of amplitude of, 43·29
  - displays and gates for A-scan systems, 43·32–38

Silicon
- absorption coefficients (mass) for γ and X rays and photon energies of, 18·33, 27·10
- attenuation coefficients of, for γ and X rays, 27·10
- effect on electrical conductivity of
  - aluminum, 42·14
  - copper, 42·12–13
- ultrasonic energy losses in, 43·25
- X-ray diffraction patterns of, 17·11

Silicon Alloys
- aluminum-magnesium-, electrical conductivity *vs.* hardness of, 42·18
- iron-, ultrasonic energy losses in, 43·25

Silicones, coatings for moistureproofing of strain gages and their application, 54·38

Silver
- absorption coefficients (mass) for γ and X rays and photon energies of, 18·36, 27·27
- attenuation coefficients of, for γ and X rays, 27·27
- effect on electrical conductivity of
  - aluminum, 42·14
  - copper, 42·12
- electrical conductivity of, 42·16
- slip rings in strain-gage circuits, 54·33

Silver Alloys
- aluminum-, ultrasonic energy losses in single crystals of, 43·25
- nickel-, acoustic and ultrasonic properties of, 43·8

Silver-110, energy and half-life of, as gamma-ray source, 18·17

Silver Halides, in gamma-ray detection, 18·21

Silver Salts, removal of undeveloped, from X-ray-film emulsions during fixation, 21·7

Similarity Law
- in eddy-current testing
  - application to detection of discontinuities, 37·11
  - of cylinders, 37·10–11
  - of flat conductors, 39·14
  - with models, 36·8
  - of sheet materials, 39·13
- in experimental verification of eddy-current-test calculations, 37·11–12

Sink-and-Float Process, in sorting of plastic porous bricks by density, 24·38

Sintering, defects in tungsten rods and wire, eddy-current detection of, 42·10

Size (See "Dimensions")

Skin Effect, on magnetic field strength in eddy-current testing, 36·11

Sky Shine (See "of radiation overhead" under "Scattering")

Slag
- entrapment at root of welds, 25·6
- inclusions and lines in welds, causes and radiography of, 25·4–5
- inclusions in welds, magnetic-particle indications of, 32·10
- lines, distinction from undercutting in radiography, 25·14

Slide Rules
- for converting measured ultrasonic-resonance frequencies to thickness indications, 50·33
- for thickness measurements by ultrasonic resonance test methods, 50·33

Slip-Rings, in strain-gage circuits and their resistance, 54·32–33

Slit Analysis, in eddy-current linear time-base tests, 40·30

Slits, electronic, in Magnatest Q eddy-current instrument, 41·7

Smoke
- control of, phototubes in, 11·34
- light-scattering tests on industrial, 10·27

Snell's Law
- in sound-wave refraction-angle calculation, 45·10
- in ultrasonic immersion testing, 47·13
  - of pipe and tubing, 47·26
- for ultrasonic plane-wave propagation, 43·15

Soap Solutions, in gas-leak detection, 5·3

Sodium
- absorption coefficients (mass) for γ and X rays and photon energies of, 18·33, 27·7
- attenuation coefficients of, for γ and X rays, 27·7

Sodium Chloride, in gamma-ray detection, 18·21

Sodium Iodide, in scintillation counters, 18·22

Sodium Thiosulfate (See "Hypo")

Soft Spots
- detection in light alloys by eddy-current conductivity measurement, 42·3
- in parts (semi-finished), eddy-current testing in control of, 42·20
- in steel wire, effects in eddy-current Magnatest Q testing, 42·52

Soil, radiation shielding equivalent of, 26·9

Solar Batteries, 11·34

Solder
- lead-tin, electrical conductivity of, 42·16
- in strain gages, difficulties from, at high temperatures, 54·23

Solids
- isotropic, relation between elastic constants and ultrasonic velocities for, 43·10
- as probing media, 4·10
- radiation-detection devices using, 18·21
- ultrasonic energy losses in, 43·25
- ultrasonic-wave velocity in, 43·9–12

Solid Solutions
- interstitial, X-ray analysis of, 17·14
- X-ray analysis of, 17·12–14

Sonar, transducers (magnetostrictive) for, 44·1

Sonic Testing, 51·1–14
- of abrasive wheels, correlation with impact penetration tests, 51·10
- applications of, 5·24, 51·9–14
- comparator for measuring natural frequency of sonic vibration of solid objects, 51·7–9
- equipment and techniques, 51·6
- nondestructive, 51·1–14

Sonigage, for ultrasonic testing of hollow steel propeller blades, 50·3

- **Sorting**
  - of alloys
    - by composition and hardness by ellipse eddy-current methods, **40·28**
    - by eddy-current electrical conductivity, **42·1**
    - by eddy-current methods, suppression of undesired signals in, **40·40**
    - with Magnatest Q eddy-current instrument, **42·33–35**
    - and steel for composition and hardness by eddy-current tests, **40·2–3**
  - automatic
    - by coercive force, **34·5–6**
    - eddy-current, with Magnatest Q instruments, **41·7–8, 41·10**
    - eddy-current, with Multitest instruments, **41·1–2**
    - instrument for, in nondestructive testing, **41·13**
  - of automobile parts by tensile strength with Magnatest Q eddy-current instrument, **42·54–55**
  - of ball-bearing balls, rings, and rollers with Magnatest Q eddy-current instrument, **42·58**
  - of ball bearings for defects, automatic eddy-current instruments for, **41·15**
  - of defective parts, Sigmaflux eddy-current meter indications in, **40·27**
  - by electrical conductivity with Magnatest FM-100 eddy-current instrument, **42·11**
  - of forgings
    - Magnatest Q bands and curves for, in eddy-current tests, **41·5**
    - by tensile strength with Magnatest Q eddy-current instrument, **42·56**
  - gates in Magnatest Q eddy-current instrument, **41·8**
  - limits in eddy-current testing, **37·38**
    - with Magnatest Q instrument, **41·6–7**
  - with Magnatest Q eddy-current instrument, **42·31**
  - of materials with inhomogeneous stresses by hysteresis-loop methods, **42·25**
  - with Multitest eddy-current apparatus, **40·22**
  - of parts by hardness, **34·13**
  - phototubes in, **11·34**
  - of rods (metallic) by eddy-current methods, automatic handling apparatus for, **41·2**
  - of scrap metal by electrical conductivity and supplementary methods, in eddy-current testing, **42·15**
  - of spherical objects, combined automatic eddy-current apparatus for crack testing and, **41·19**
  - of steel (alloy) mixed lots with Magnatest Q eddy-current instrument, **42·35**
  - of steel billets with Magnatest Q eddy-current instrument, **42·35**
  - of steel parts by hardness, by magnetic method, **42·1**
  - of steel parts combined with defect detection, automatic unit for, **42·68**
  - thermoelectric, **5·23**
  - triboelectric, **5·22**
- **Sound** (See also "Sound Waves," "Ultrasonic Waves")
  - pulse frequency spectrum of, **44·20**
  - ratio between front-surface and test-lobe echoes in ultrasonic testing of aluminum block, **44·19**
  - refraction at liquid-solid interfaces, angle of, **45·9–10**

Sound (*Continued*)
  - velocity
    - in common metals and water, **45·3**
    - effects in ultrasonic testing, **45·6–13**
    - measurement in various materials, **50·24**
- **Sound Waves** (See also "Sound," "Ultrasonic Waves")
  - frequencies (natural) of, **51·1**
  - longitudinal, shear or transverse, **45·6**
  - mechanisms of travel of, **45·6**
  - in nondestructive testing, **4·12**
  - reflection and refraction at angular incidence to metal surfaces, **45·9**
  - types of, **45·9–12**
  - velocity of longitudinal and shear, measurement of ratio between them and its relation to Poisson's ratio, **45·7–9**
- **Space Charge,** in radiation measurement with proportional counters, **16·6**
- **Spark Plugs,** fluoroscopic inspection of, **19·36**
- **Specifications or Standards**
  - for alloys, colored spread bands as, **2·28**
  - in destructive *vs.* nondestructive testing, **4·6**
  - for hysteresis-loop determination, samples for, and apparatus for magnetizing, **42·22**
  - inspection, establishment of, **1·16**
  - for liquid-peentrant indications of defects, **8·9**
  - for manufacturing, establishment of, **1·11**
  - military, role of nondestructive-testing laboratories in meeting, **2·4**
  - for nondestructive testing, **2·22**
    - costs of arbitrary or inadequate, **1·22**
    - development of, **2·18**
  - for pipeline radiography, **25·17**
    - source location and size in, **25·20**
  - for radiography, **15·31**
  - in thickness gaging with radioisotopes, **18·12**
  - for ultrasonic immersion tests, **46·26**
  - for ultrasonic inspection of die forgings, **46·23**
  - for ultrasonic testing
    - flat-bottomed holes for, **45·1**
    - test blocks for, **45·18**
  - for ultrasonic-test search units, **43·7**
  - U. S. government, for penetrant inspection, **8·11**
  - for X-ray inspection, **24·2**
- **Specific Activity** (See "Activity")
- **Specific Gravity** (See "Density")
- **Specific Heat,** of strain-gage-alloy wire, **54·8**
- **Specimens** (See "Samples")
- **Spectral Characteristics**
  - of light for liquid-penetrant testing, **7·11**
  - of mercury-vapor lamps for fluorescent-penetrant testing, **7·13**
- **Spectral Limits,** of visibility, **10·3**
- **Spectrographic Tests,** optical arrangements for, **10·9**
- **Spectrographs,** ultraviolet, reflecting systems in, **10·9**
- **Spectrography, 10·5**
- **Spectrometers,** for energy, scintillation counters as, **18·22**
- **Spectrophotometry, 10·5**
  - phototubes in, **11·34**
- **Spectroscopy, Emission,** comparison with X-ray fluorescent spectroscopy, **17·26**
- **Spectroscopy, Mass** (See "Mass Spectroscopy")
- **Spectrum**
  - of barium lead sulfate and calcium tungstate under X-ray excitation, **16·16**
  - electromagnetic, **10·3**

Spectrum (*Continued*)
- of luminescent materials for fluorescent screens, **16·14**
- radiation, from $\mathrm{Tm}_2^{170}\ \mathrm{O}_3$, **15·20**
- of X rays, continuous, **15·4**
  - effect of current and voltage on, **20·3**

Speed, strain-gage-based transducers in measurement of, **54·3** (See also "Velocity")

Sperry System, for railroad-rail testing, **35·12–17**

Sphalerite, X-ray patterns of, **17·11**

Spheres
- automatic tester and sorter for cracks and dimensions in, **41·19**
- cracks in
  - apparent impedance plane for, **39·11**
  - eddy-current testing of, **39·1–11**
    - complex voltage or impedance planes in, **39·4**
    - demagnetization factor in, **39·6**
    - effects of conductivity, diameter, relative permeability, and test-coil length on, **39·4**
  - frequency selection for, **40·11**
  - nonferromagnetic, complex voltage and impedance planes for, **39·8–10**
  - normalized components of impedance and secondary coil voltage in, **39·3–4**
  - tabular summary of, **36·6**
- sorting (automatic) of, by harness with Magnatest eddy-current Q instrument, **40·23**
- steel, in checking ultrasonic-test reference blocks, **43·38**
- testing of, with Multitest instrument, **40·23**
  - ultrasonic-wave amplitude relations to diameter and distance for, **43·45–46**

Split Heads, horizontal and vertical, in railroad rails and their electric-current detection, **35·20**

Splitting
- detection in tungsten wire by eddy-current methods, **40·6**

Spitting, in welding, radiography of, **25·14**

Spots, on X-ray films
- and their prevention, **21·21–22**
- from water droplets and their prevention, **21·9**

Spot Tests, chemical, **5·19**

Spot Welds (See "Welds")

Spray Apparatus, for liquid-penetrant testing, **7·9**

Spray Guns
- for applying suspensions in filtered-particle tests, **9·12**
- for ceramic-type brittle-coating application, **52·17**
- for developer application in post-emulsification dye-penetrant process, **6·15**
- in filtered-particle tests for applying suspensions, **9·12**

Spraying
- of ceramic-type brittle coatings, **52·16**
- in liquid-penetrant removal, **6·7**
- of resin-type brittle coatings and air supply for, **52·9**

Spread Bands (See "Bands, Spread")

Springs
- crack depth in, magnetic-particle indication on sectioned, **32·25**
- locomotive, magnetic-particle-test indication of transverse quench crack and longitudinal seams in, **32·1**
- magnetic-particle testing of coil, fluorescent particles in, **30·18**

Springs (*Continued*)
- steels for, Magnatest Q eddy-current sorting of, with low field strengths, **42·38**
- watch
  - automatic eddy-current inspection apparatus for, **2·32**
  - automatic eddy-current sorting by thermoelastic coefficient, unit for, **41·2**
  - sorting by thermoelastic coefficient with Multitest eddy-current instrument, **40·23**

Spun Parts, thickness testing of, by ultrasonic resonance tests, **50·21**

Staining
- of X-ray film during processing, causes and prevention of yellow, **21·21**
- of X-ray images during fixation and its prevention, **21·8**

Stainless Steel
- acoustic and ultrasonic properties of, **43·8**
- acoustic impedance, density and sound velocity in, **45·3**
- bars and forgings, ultrasonic-wave attenuation in, **45·5**
- blocks for contour study in ultrasonic testing, **45·13**
- ceramic brittle coatings for testing of, **52·8**
- eddy-current sorting of austenitic, **42·15**
- eddy-current testing of, effective permeability calculations for, **36·20**
- honeycomb (brazed) of, radiograph of defects in, **24·13**
- honeycomb structures, fluoroscopy of, **24·29**
- penetration time for, in liquid penetrant testing, **6·8**, **6·10**
- photoelastic-coating tests for determination of optimum spot-weld distribution in plates of, **53·27**, **53·32**
- radiography of
  - equivalence factors for, **20·14**
  - with Thulium-170, exposure-thickness curve for, **15·27**
- spheres, coil impedance *vs.* effective permeability in eddy-current testing of, **39·6**
- for strain-gage-based transducers, **54·5**
- stress-strain curves (nonlinear) of, **54·4**
- test objects, critical roughness values for, in ultrasonic testing, **45·16**
- tubes
  - calculation of effective permeability and secondary-coil voltages in eddy-current testing of, **38·3**
  - defect detection in, eddy-current apparatus for, **40·14**
  - eddy-current-test apparatus for, **40·2–3**
  - eddy-current testing of, magnetic-field strength effects in, **38·16**
- ultrasonic contact testing of
  - cast, grain-size effect on, **48·2**
  - forgings of, **48·11**
- ultrasonic resonance testing of, constant *K* value in, **50·3**
- ultrasonic testing of, acoustic attenuation coefficient in, **45·5**
- ultrasonic wavelength in, in relation to hole diameter, **45·20**

Standards (See "Specifications or Standards")

Static Electricity (See "Electric Charges")

Static Screening, longitudinal magnetic field probes for evaluation of, **33·1**

Statiflux, electrified-particle apparatus and procedure, **28·1–12**

Statimat Instruments
- alloy separation by, **34·12**

Statimat Instruments (*Continued*)
- for automatic statistical quality control, 2·34, 34·8, 41·12
- hardness pattern shown with
  - of Al-Cu-Mg parts, accompanying Multitest point picture, 41·17
  - for ball-bearing steel, 41·15
- quality control (statistical) with, and Gaussian curve in, 41·18

Statistical Evaluation Instrument, in automatic watch-spring sorter, 41·2

Statistical Quality Control (See "Quality Control")

Steel
- acoustic and ultrasonic properties of, 43·8
- aging of Thomas, Magnatest Q eddy-current experiments on, 42·60
- for ball-bearing rings, effect of annealing and hardening temperatures on Magnatest Q eddy-current spread bands of, 42·58
- billets, sorting with Magnatest Q eddy-current instrument, 42·35
- blocks, coils for eddy-current testing of, 40·38
- brittle-coating materials for testing of, 52·1
- brittle coatings (ceramic) for testing carbon and chromium, 52·8
- carbon in, determination of statistical distribution of, by eddy-current testing, 41·13
- carburization of, effect on hysteresis loops, 42·26, 42·28
- carburized or induction-hardened layers in, determination by magnetic-field tests, 34·11
- chromium, Magnatest Q eddy-current spread bands of, in comparison with carbon steel, 42·38
- coatings of tin and zinc on
  - radioisotope gaging of, 18·15
  - X-ray fluorescence gaging of, 18·11
- corrosion thinning of plates of, direct-current measurement of, 35·9
- cracks in, Magnatest D eddy-current testing for, 42·61–69
- cracks (surface) in cylindrical objects of, detection by eddy-current testing, 37·5
- eddy-current testing of
  - with Magnatest Q eddy-current instrument, optimum utilization of screen area in, 42·39
  - tabular summary of, 36·4–5, 36·7
- elasticity modulus of, variation with temperature, 54·4
- elasticity tension modulus of, 52·11
- etching of, reagents for, 32·27, 32·29
- fluorography of, penetrameter sensitivity in, 19·44
- fluoroscopy of, instrument characteristics for, 19·48
- fracturing after chilling of, as supplement to magnetic-particle testing, 32·24
- hardness of, hysteresis-loop effects on, 42·27
- hardness of ball-bearing, and its statistical distribution, as shown by Magnatest Q and Statimat instruments, 41·15
- honeycomb structures of, fluoroscopy of, 24·29
- hysteresis loops and Magnatest Q eddy-current patterns of, 42·29–30
- hysteresis loops of, precision determination of, 42·22
- hysteresis loops of cold-drawn, before and after annealing, 42·24, 42·26–27
- laminated electrical sheet, sorting by hysteresis loss, 34·10

Steel (*Continued*)
- Magnatest Q eddy-current spread bands for, frequency effect on, 42·44
- Magnatest Q eddy-current spread bands for carbon and free-cutting, 42·33
- magnetic-particle indications of blowholes in cast flanges of, 32·9
- magnetic-particle testing of hard and soft, 30·11
- magnetic permeability (relative) of, as function of external field strength, 38·20
- manufacturing of, inspection, rejection, and salvage in, 1·11
- parts
  - automatic eddy-current unit for simultaneous defect detection and composition sorting of, 42·68
  - for automobiles, sorting by tensile strength with Magnatest Q eddy-current instrument, 42·54–55
- penetration by X rays, 16·13
- photoelastic-test color fringes in, for various strains and stresses, 53·5
- plastic flow during tensile testing, Magnatest Q eddy-current indications of, 42·60
- radiation-shielding equivalent of, 26·9
- radiography of
  - build-up curves for, 15·36
  - cooperative research on optimum techniques, 2·19
  - equivalence factors for, 20·14
  - exposure, intensity, thickness, and voltage in, 20·35
  - exposure-thickness factors for, 15·26
  - fluorescent-screen intensification factor in, 20·28
  - with high-energy X rays, exposure charts for, 23·9
  - Iridium-192 in, 15·17
  - lead-foil screens in, 20·26–27
  - maximum X-ray voltages for various thicknesses, 25·17
  - with Thulium-170, 15·22
  - unsharpness standards for, 2·18
- rods
  - automatic crack testing of, with Magnatest D eddy-current instrument, 41·10
  - with cracks and inhomogeneous stresses, Magnatest D eddy-current instrument multi-exposure pictures of, 42·63
  - cracks and other defects in, indications with Magnatest D eddy-current instrument and macro- and microsections, 42·62–69
  - spread bands of, from Magnatest Q eddy-current testing, harmonics in, 42·37
- rolls, ultrasonic resonance test on built-up, 3·23
- sheets (piles) of, photoelastic-coatings in determination of strain distribution in, 53·26
- shot, masking and filling cavities with, in radiography, 20·22
- sorting of, eddy-current equipment for, 40·2–3
- sorting (automatic) of parts of, with Magnatest Q eddy-current instrument, 41·10
- sorting of alloy, in mixed lots with Magnatest Q eddy-current instrument, 42·35
- sorting of annealed, drawn, and tempered carbon, with Magnatest Q eddy-current instrument, 42·52–53
- sorting of parts of
  - by coercive force, 34·7
  - by hardness by magnetic method, 42·1

Steel (*Continued*)
  sorting of parts of (*Continued*)
    with Multitest eddy-current instruments, 41·2
  spheres, ultrasonic-wave amplitude relations to diameter and distance for, 43·45–46
  spring, Magnatest Q eddy-current sorting of, with low field strengths, 42·38
  stainless (See "Stainless Steel")
  strain gage on, approximate equivalent indicated strain for, 54·9
  strain-gage testing of, allowable frequency of strain variation in, 54·27
  tensile strength of support levers of, Magnatest Q eddy-current sorting by, 42·56
  thickness measurement ranges
    for radiography with different high-voltage sources, 23·3
    with Strontium-90 β gages, 18·16
  tool, for strain-gage-based transducers, 54·5
  tubes, eddy-current testing of, depth penetration in, 38·21
  ultrasonic contact testing of
    castings of medium-carbon, frequency selection in, 48·2
    forgings of, 48·11
    frequencies for, 48·1
    small-grained, frequency selection in, 48·2
    surface-wave test in, 48·9
  ultrasonic double-transducer testing of, 49·2–3
  ultrasonic immersion testing of, 46·10
  ultrasonic longitudinal-wave critical angle in, 45·10
  ultrasonic reflection coefficients at interfaces with other materials, 43·13
  ultrasonic resonance testing of, constant *K* value in, 50·3
  ultrasonic test frequency for high-carbon, 48·2
  ultrasonic testing of
    acoustic impedance ratio with respect to water for, 45·2
    alloy, noise in, 45·7
    effect of grain size on indications in, 47·14
    fundamental resonant frequencies in, 50·4
    high-sulfur free-cutting, 49·14
    ingots of, with single-transducer and coupled double-transducer search units, 49·14
  ultrasonic-wave amplitude-distance curves for, 43·44
  ultrasonic-wave amplitudes and angles in, 43·21, 43·23
  ultrasonic-wave reflection amplitudes for water-immersed, 43·46
  -water interfaces, ultrasonic-beam intensities at various angles of incidence, 43·20–21
  welds
    dye-penetrant penetration times for, 6·14
    fluoroscopy with image-amplifier tube, 19·39
    radiography (panoramic) of, 23·6
  welds in plates of, reference radiographs of, 2·19
  wire
    edge decarburization of, effect on spread-band width in Magnatest Q eddy-current testing, 42·52
    Magnatest Q eddy-current sorting of, frequency effect on, 42·41
    Magnatest Q eddy-current spread bands of alloy, after stress-relief annealing, 42·51
    magnetic-leakage-field indicator of, 30·27
    straightening by hammering, effect on Magnatest Q eddy-current sorting, 42·47, 42·50
  xeroradiography of, charts for, 22·9

Steel (*Continued*)
  X-ray absorption by, 20·14
  X-ray inspection of
    by closed-circuit television, sensitivity in, 19·41
    kilovoltages *vs.* thicknesses in, 19·46
Steering Apparatus, for automobiles, magnetic-particle-testing apparatus for, 31·12–13
Step Blocks (See "Test Blocks")
Stereomicroscopes (See "Microscopes")
Stereoradiography (See "Radiography")
Stereoscopes, in radiography, 20·46
Stereoscopic Vision, in visual inspection, and effects of lack of, 5·9 (See also "Vision")
Stiffness (See "Rigidity")
Storage
  of radioisotopes, 26·16
  of xeroradiographic plates
    charged, 22·6
    effect of temperature on life during, 22·5
Storage Batteries (See "Batteries")
Storage Tanks
  corrosion tests of oil, 50·35
  ultrasonic resonance testing of, 50·27
  wall-thickness measurements by ultrasonic resonance tests, 50·36
Straightening
  of rods, Magnatest D eddy-current indications of stresses from, 42·61
  of steel wire by hammering, effect on Magnatest Q eddy-current sorting, 42·43, 42·47, 42·50
Straightness, measurement of, strain-gage-based transducers in, 54·8
Strain (See also "Stress")
  in aluminum and steel, photoelastic-coating-test color fringes in relation to, 53·5
  application rate to strain gages, magnetostrictive effects of, 54·27
  application time in strain-gage tests, creep in relation to, 54·27–28
  bi-refringence in stress analysis, 10·19
  brittle-coating calibration under compression and tension, 52·10
  brittle-coating response to, 52·4
  brittle-resin-coating calibration for high-threshold, 52·10
  calculation and formula for, from hydraulic loading of brittle coatings, 52·26
  calculation from strain-gage work sheet data, 54·40
  compression
    accommodation by strain-gage cements, 54·10
    dye etching of patterns of, in brittle-coating testing, 52·15
    indication of gross, by flaking of brittle coating, 52·25
    measurement for steel crane hook in brittle-coating testing, 52·23
  cycles of, effect on hysteresis and zero shift of strain gages, 54·26–27
  detection by X-ray analysis, 17·18
  distribution in sheet piles, photoelastic coatings in determination of, 53·26
  electric resistance in relation to, 54·2
  frequency of variation, limits of strain-gage following of, 54·27
  gage length in relation to gradient of, 54·11
  for gage on steel, approximate equivalent indicated, 54·9
  Hooke's general expressions for, in photoelastic-coating tests, 53·7
  maximum, during photoelastic-coating tests, plastic-coating selection on basis of, 53·13

Strain (*Continued*)
  measurement of (See also "Strain-Gage Tests")
    accuracies, environments, and ranges using resistance strain gages, 54·2–3
    brittle-coating tests for determination of direction and magnitude of, 52·1
    with ceramic *vs.* resin brittle coatings, 52·1
    in concrete dams with resistance strain gages, 54·2
    development of apparatus for, 54·1
    under dynamic and static loading in brittle-coating testing, 52·19, 52·21
    with photoelastic coatings, 53·36
    and relation to stress, 54·1
  measurement of actual and threshold, in brittle-coating testing, 52·11
  measurement of difference of principal or maximum shear, by normal incidence analysis, 53·7
  measurement of direction and value of principal, in photoelastic-coating tests, 53·15–16
  measurement of dynamic, for large numbers of cycles with two gages, 54·26–27
  measurement of principal, by oblique incidence analysis in photoelastic-coating testing, and vector relationships for, 53·8–10
  measurement of small, with brittle coatings, sensitization for, 52·23
  measurement of sums and differences of, with Wheatstone bridge circuit, 54·18
  minimum and maximum measurable, with various instruments in photoelastic-coating tests, 53·17
  polariscope readings *vs.*, in photoelastic-coating-test-material calibration, 53·14
  rate, response of strain-gage adhesives to, 54·13
  -resistance relations of strain gages, 54·25–28
  sensitivity
    of ceramic brittle coatings
      and their calibration, 52·7
      on steel, 52·8
    of foil or wire for resistance gages, temperature effect on, 54·23
    of materials in their plastic range, 54·25
    for plastic sheet for photoelastic-coating tests, 53·16
    of strain-gage-alloy wire, 54·9
    of unbonded filaments, gage factor in relation to, 54·11
  stress calculation from, 52·10
  -stress curves
    of aluminum alloys and stainless steel, 54·4
    hysteresis of, effect on strain-gage tests, 54·4
    linearity of, strain-gage transducer output in relation to, 54·4
  tangential, in sheet piles, shown by photoelastic-coating analysis, 53·26, 53·28–29
  tension, measurement by continuous-loading and zero-load techniques in brittle-coating testing, 52·22
  threshold
    in brittle-coating tests, 52·4, 52·6
    marking in brittle-coating testing, 52·19–20
Strain Gages
  adhesives for, creep of, 54·27–28
  air pockets and imperfect bonding of, testing for, 54·37
  applications and limitations of, 54·2–3
  backing or carrier materials for, 54·10
  bonded and unbonded, and their applications, 54·2
Strain Gages (*Continued*)
  bonding of, cements for, 54·10
  brittle coatings compared with, in design of structures, 52·18
  brittle-coating-test supplementation with, 52·4
  cementing of thin paper-base, 54·36
  circuit for conversion of T-strain-gage rosette into two equivalent stress-gage circuits, 54·30
  creep of, effect of close trimming on, 54·28
  construction, installation, and materials, 54·5–13
  copper-nickel-alloy, of high strain level, 54·25
  corrosion (electrolytic) of wet, and effect on electric resistance, 54·25
  in detection of motion of solid probes, 5·2
  deterioration at elevated temperatures by selective oxidation and its compensation, 54·23
  development of, 54·2
  direct-current, lead wires for, 54·32
  direction and location of, brittle-coating tests in selection of, 52·2, 54·2
  drying after cementing, 54·36
  "dummy," for temperature compensation in potentiometric circuits, 54·15
  electric circuits of, 54·13–22
    potentiometric, 54·14–16
    slip-rings and switches in, and their resistance, 54·32–33
    Wheatstone bridge, 54·16–19
      balancing of, 54·21–22
  electric resistance of, 54·6, 54·10
    between filament and specimen as moisture-content indication, 54·24–25
  factors
    equation for, 54·34
    and strain sensitivity of wire in relation to, 54·11
    variation with temperature, 54·23
  failure (premature) of, causes of, 54·26
  fatigue life of, 54·26
  foil, resistance increase near fatigue failure, 54·26
  foil and wire, heat-dissipating ability and maximum electric current of, 54·31
  heating and cooling of, prevention of hysteresis and zero shift by, 54·24
  for high temperatures, lead wires for, 54·32
  humidity effect on, 54·24–25
  hysteresis and zero shift of, effect of strain cycling on, 54·26–27
  installation of, 54·35–36
  instrumentation for systems for large structures, 54·35
  lead wires for
    capacitance balancing of, 54·37
    effects and shielding of, 54·31–32
    installation of, and resistance effects, 54·36–37
    measuring electrical resistance of, 54·32
    shielding and stress avoidance of, 54·32
  length of, 54·11
  linear and temperature limits of use of alloy wire, 54·9
  long-lived, 54·26
  magnetostrictive effects in, detection and effect of strain-application rate on, 54·27
  metallurgical and other changes of materials of, at high temperature, 54·23
  mounting of, 54·12–13
  operational characteristics of, 54·22–32
  resistance changes in, equations for, 54·28–29
  rigidity and stiffness of, effect in tests on materials of low elasticity, 54·30

Strain Gages (*Continued*)
- rosette, special and standard, **54·34–35**
- sensitivity of, planned and parasitic variation of, **54·19–21**
- sensitivity (transverse) effects on, and their correction, **54·28–29**
- strain-variation-measurement limits of, **54·27**
- stress-field effects on, **54·28–30**
- for stress tests during building modification, **3·25**
- surface preparation for application of, **54·35–36**
- temperature-compensated, **54·22–23**
- temperature effects on, **54·22–24**
- testing of, **54·37**
- transducers
  - materials for, **54·5**
  - for measurement of quantities other than strain, **54·3**
- water-immersion and weathering effects on, **54·25**
- weldable and woven-wire, **54·10–11**
- wire of, materials for, **54·6**

Strain-Gage Tests, 54·1–42
- applications of, **54·42**
- in barge design for off-shore oil-well drilling, **54·33**
- during building modification, of ore-trestle loading, and of subway-car truck frames, **3·25–26**
- cement-thickness effects in, **54·13**
- data sheets, tests at night, and zero readings for, **54·38**
- desensitization (parasitic and planned) in, **54·19–21**
- in design of machinery and structures, **54·33**
- effects of mechanical properties of base materials in, **54·3–5**
- electrical effects in, **54·30–33**
- equipment for, **54·33–34**
- hydrostatic-pressure effects in, **54·30**
- for Poisson ratio determination, correction for transverse effects in, **54·29**
- of steel, allowable frequency of strain variation in, **54·27**
- stress calculations from, **54·41**
- stress (residual) effects on, and determination in, **54·38**
- on structures (large), **54·33–42**
  - outdoors, accuracy of, **54·40–41**
  - recommendations concerning yielding in, **54·38**
  - temperature effects and their correction, **54·39–41**

Strain-Optical Constants
- in photoelastic-coating tests, temperature in relation to, **53·37**
- of plastic coatings on aluminum and steel under bending load, corrections of, **53·38**
- of plastic sheets for photoelastic-coating tests, **53·12–13**

Streaks, on X-ray films, causes and correction of, **21·21**

Strength
- of aluminum castings, effect of shrink porosity on, **24·9**
- of castings, effect of gas holes and porosity on, **24·7–8**
- of materials in photoelastic-coating tests, effect on type of plastic for, **53·13**

Stress (See also "Strain")
- in aluminum and steel, photoelastic-coating-test color fringes in relation to, **53·5**

Stress (*Continued*)
- analysis
  - applications of nondestructive, **54·42**
  - in conjunction with resistance strain gages, **54·2**
  - in engineering design, brittle coatings *vs.* strain gages in, **52·18**
  - experimental, in product design, **1·3**
  - of guided-missile tail section by photoelastic-coating tests, **53·26–27, 53·30–31**
  - of patterns caused by dynamic loading and on small surfaces from some distance in photoelastic-coating tests, **53·22**
  - photoelastic-coating, **53·3**
    - optical projectors for, **12·30–31**
  - photoelastic coatings in, **53·1, 53·36**
  - qualitative and quantitative, with large-field photoelastic-coating-test instrument, **53·21**
  - by resistance strain-gage measurements, **54·3**
  - strain bi-refringence in, **10·19**
  - of welded bridge assemblies by photoelastic-coating methods, **53·27, 53·33–34**
- analysis of biaxial and uniaxial, strain-gage types for, **54·35**
- apparent, in measurement of compression and tension strains in brittle-coating testing, **52·22–23**
- calculation
  - from strain, **52·10**
  - from strain-gage readings, **54·40–41**
- from cold-working, eddy-current test permeability changes from, determination of conductivity changes independently of, **37·6**
- corrosion (See "Corrosion")
- cracks (fatigue) from alternating, **32·12**
- cracks from, self-comparison eddy-current testing for, **40·36**
- data on
  - from brittle-coating tests, applications of, **52·2**
  - obtained in nondestructive-testing laboratories, **2·12**
- definition and determination from values, **54·1**
- design, role in radiograph interpretation, **25·2**
- difference, calculation of principal, in photoelastic-coating testing, **53·8**
- distribution or pattern
  - in aluminum plate with holes, revealed with polarizing quarter-wave viewer, **53·18**
  - with ceramic and resin brittle coatings, **52·1**
  - over complex structures, brittle-coating indication of, **52·2–3**
  - in guided-missile fuselage and tail surfaces indicated by photoelastic-coating tests, **53·26–27, 53·30–31**
  - in photoelastic-coating tests in engineering design and visual education, **53·36**
  - in radiographic interpretation, **24·3, 24·5**
  - in spot-welded assemblies, photoelastic-coating tests for, **53·27, 53·32**
- effects, separation from crack effects in Magnatest D eddy-current testing, **42·61**
- field of strain gages, effects of, **54·28–30**
- inclusions (nonmetallic) in areas of high, evaluation of magnetic-particle-test indications of, **32·4**
- inhomogeneous
  - effect in eddy-current crack testing of steel rods, **41·11**
  - effect in hysteresis-loop eddy-current testing, **42·25**
  - effect in Magnatest Q eddy-current testing, **42·43**

Stress (*Continued*)
- inhomogeneous (*Continued*)
  - effect in Magnatest Q eddy-current testing in relation to field strength, **42·44**
  - effect on initial magnetic permeability of ferromagnetic tubes, **38·21**
  - in steel rods, Magnatest D multi-exposure picture of, in eddy-current testing, **42·63**
  - in steel wire, effect on Magnatest Q eddy-current sorting, **42·46**
- in machinery (modern) with increased speeds, **1·5**
- in machines and structures, photoelastic-coatings in measurement of, for service-life surveys, **53·35**
- in magnetostrictive materials, hysteresis-loop effects, **42·28**
- maximum and minimum, with rosette strain gages, calculation of, **54·35**
- measurement of
  - gages for, related to strain gages, **54·29**
  - by photoelastic coatings, telemetering of, **53·35**
  - under severe operating conditions without humidity effects using ceramic-type brittle coatings, **52·7**
- in photoelastic-coating testing, tangential to free boundary, **53·8**
- principal
  - measurement in photoelastic-coating tests with large-field instrument, **53·20**
  - measurement with one or two strain gages, **54·29**
- relief by annealing, effect on Magnatest Q eddy-current spread bands of alloy steels, **42·50**
- residual
  - brittle coatings in measurement of, **52·2**, **52·24**
  - compressive and tensile, in ceramic brittle coatings induced by firing, **52·7**
  - cracks caused by, during or after etching or plating, **32·12**
  - detection and effects on strain-gage readings, **54·38**
  - etch cracking from, and its prevention, **32·26**
  - relief in strain gages by strain cycling, **54·26**
  - removal by tempering before etching, **32·26**
- in rods and tubes from straightening
  - interference with eddy-current testing, **2·31**
  - Magnatest D eddy-current testing of, **42·61**
- separation from conductivity effects in Magnatest Q eddy-current testing, **42·42**
- in steel (cold-drawn), effects on hysteresis-loop traces, **42·24**
- in steel rods, Magnatest D eddy-current patterns and macro- and microsections of, **42·63**
- in steel (structural), determination by magnetic point-pole method, **34·10**
- -strain curves
  - hysteresis of, effect on strain-gage tests, **54·4**
  - linearity of, strain-gage-transducer output in relation to, **54·4**
  - nonlinear, of aluminum alloys and stainless steel, **54·4**
- in strain-gage lead wires, avoidance of, **54·32**
- of symmetrical structures, study with several brittle coatings, **52·4**
- thermal, indirect measurement using brittle coatings and mechanical loading, **52·2**
- trajectories in photoelastic-coating testing, **53·6**
- ultrasonic, ranges in nondestructive testing, **43·1**

Stress (*Continued*)
- in unfired clayware, detection of locked-in, **9·16**, **9·18**

Stress and Motion Analysis, applications of, **3·25**

Stress Engineer, as information source in nondestructive testing, **1·19**

Stretch-Formed Parts, thickness testing of, by ultrasonic resonance tests, **50·21**

Stringers, magnetic-particle-test indications of, evaluation of, **32·4**

Stroboscopes
- in photoelastic-coating tests, **53·22**
- in ultrasonic resonance tests, **50·10**

Stroboscopic Effect, in recording of high-speed motion, **10·4**

Strontium, absorption coefficients (mass) for γ and X rays and photon energies of, **18·36**

Strontium-90
- energy and half-life of, as beta-ray source, **18·17**
- from fission of Uranium-235, **15·9**
- as radiographic source, **15·4**
- thickness gaging with, **18·15**

Structure
- of alloys
  - electrical-conductivity changes related to, in eddy-current testing, **37·6**
  - properties detected by nondestructive testing, **4·12**
- detection of differences in internal, by sound velocity, in ultrasonic-resonance tests, **50·23**
- inhomogeneous, multiple-frequency ultrasonic detection of, **45·26**

Structures
- buildings, modification of, strain-gage testing during, **3·25**
- concrete ore trestle, strain-gage testing of, **3·25**
- design of
  - strain-gage tests in, **54·33**
  - stress analysis in, brittle coatings *vs.* strain gages for, **52·18**
- service life of, photoelastic-coating tests in survey of, **53·35**
- strain-gage testing of, **54·33–42**
  - accuracy of, **54·40–41**
  - temperature effects and their compensation in, **54·39–41**
  - yielding during, recommendations concerning, **54·38**

Submarines, hulls of, strain-gage tests of, **54·3**

Sulfur, absorption coefficients (mass) for γ and X rays and photon energies of, **18·34**

Sulfur Hexafluoride, as insulator for resonance-transformer type of X-ray generators, **14·14**

Sulfuric Acid, mixtures with hydrochloric acid as etching reagents for metals, **32·28**

Suppliers, contacts with, value in quality-control programs, **1·18**

Supports, for specimens in sonic testing, **51·6**

Surface Comparators, for surface finish magnification, **11·2–3**

Surfaces
- angle and contour, effect on ultrasonic immersion testing, **46·12**
- contour blending, false indications from, in ultrasonic immersion testing, **47·24**
- curved
  - false indications from, in ultrasonic immersion testing, **47·11**
  - interference pattern of, **10·16**
- cut, examination as supplement to magnetic-particle testing, **32·24–26**

Surfaces (*Continued*)
  discontinuities on, testing by phase microscopy, **10·18**
  electrified-particle indications on secondary, **29·5**
  finish (See also "Roughness")
    corrections in ultrasonic testing, **45·17**
    determination of waviness with optical projectors, **12·32–33**
    effect on
      emulsification time in liquid-penetrant testing, **6·12**
      liquid-penetrant indications, **8·5**, **8·7**
      magnetic-particle testing, **30·8**
      selection of ultrasonic contact test equipment, **48·4**
      ultrasonic contact testing, **48·25**
      ultrasonic immersion indications, **46·12**, **47·13**
      ultrasonic testing, **45·15–17**, **45·22–24**
      ultrasonic testing and its reduction, **44·6**, **44·19**
    inspection (visual) as supplement to magnetic-particle testing, **32·19**
    inspection with magnifiers as supplement to magnetic-particle testing, **32·19**
    interferometry of, **10·14**
    optical inspection of, **12·1**, **12·14–17**
    optical projectors for simultaneous comparison of two areas of the same, **12·16**
    of spherical reflectors, effects on ultrasonic-echo amplitude, **45·24**
    strain-gage-based transducers in measurement of, **54·3**
    and waviness of, effects and measurement of, **45·17**
  imprints of, temporary or permanent, **12·29**
  imprints of machined, **12·29**
  indications (false) from polished, in ultrasonic immersion testing, **47·12**
  interference pattern of rough, **10·15**
  of metals, preparation for direct-current nondestructive testing, **35·3**
  photoelastic testing of rough, **10·16**
  preparation of, for strain-gage tests, **54·35–36**
    for ultrasonic resonance tests, **50·16**
  replicas of, as permanent records, **12·1**
  scanning of flat, in ultrasonic immersion testing, **46·17**
  testing of, by light-section method, **10·19–20**
  ultrasonic-test search units for rough, **43·5**
Suspension, of ceramic brittle-coating materials, **52·16**
Suspensions, density of, radioisotopes in control of, **18·30**
Swedging, of tungsten wire, wavy fiber texture from improper technique in, **42·6**
Sweep, electric circuits in ultrasonic-test A-scan systems, **43·32**
Symbols, mathematical, in photoelastic testing, **53·6**
Synchronizers, for ultrasonic-test A-scan system, **43·32**
Synchrotron, for generation of X rays, **14·19**

T

Table Movement, in evaluation of optical projector capacity, **12·9**
Tanks (See "Containers")
Tantalum
  absorption coefficients (mass) for γ and X rays and photon energies of, **18·38**, **27·35**
Tantalum (*Continued*)
  attenuation coefficients of, for γ and X rays, **27·35**
  electrical conductivity of, **42·16**
Tape
  pressure-sensitive, for temporary replicas of surface imprints, **12·30**
    transparent, in preservation of magnetic-particle-test indications, **32·18**
Tape Probes (See "Probes")
Tape Recording, multiple-channel, in electric-current railroad-rail testing, **35·16**
Target-Film Distances, in X-ray (high-energy) radiography, **23·7**
Technical Societies
  in nondestructive-testing programs, **1·18**
  relations with European nondestructive testing organizations, **2·17**
Teeth, electrified-particle testing of porcelain, **29·17**
Teflon
  constant *K* value in ultrasonic resonance tests, **50·3**
  strain-gage lead wire of, **54·36**
Telemetering, of photoelastic-coating data, **53·35**
Telescopes (See also "Borescopes," "Periscopes")
  optical systems of, **11·16**
  in photoelastic-coating tests, **53·22**
  reading, **11·24**
  for testing of hollow tubes, **10·10**
  for visual inspection, **11·12**
Television
  in automatic magnetic-particle testing, **31·14**
  cameras for closed-circuit, **19·45**
  in control, inspection and testing, **11·37**
  in fluoroscopy, **19·48**
  photoelastic-coating-test data transmission by, **53·35**
  use in combination with image-amplifier tubes, **19·45**
  in ultrasonic test-indication presentation, **45·21**
  in visual inspection, **5·9**
  in X-ray inspection, **19·39**
Television Tubes, pick-up, **11·36**
Tellurium, absorption coefficients (mass) for γ and X rays and photon energies of, **18·37**
Temperature
  of brittle-coating (resinous) application, **52·9**
  in brittle-coating testing outdoors, **52·21**
  compensation, for expansion in eddy-current testing of nonferromagnetic cylinders, frequency selection and calculation for, **40·12**
    for modulus of elasticity in strain-gage tests, bridge desensitization in, **54·21**
    in potentiometric circuits, **54·15**
    in strain gages for lead-wire resistance, **54·32**
    in thickness measurement of metallic sheets with *RC* oscillator, **39·18**
    of Wheatstone bridge strain-gage circuits, **54·18**
  control in brittle-coating testing, **52·19**
    in electric-current testing of flat plates, **35·7**
    in X-ray-film development, **21·4**
  effects, cancellation by desensitization in strain-gage tests, **54·19**
    on elasticity modulus and strain-gage readings, **54·4**
    on electrified-particle testing, **28·11**
    on liquid-penetrant tests, **8·7**
    on resin-type brittle-coating tests, **52·4–6**
    on strain gages, **54·22–24**
    in strain-gage testing of large structures and their correction, **54·39–41**

Temperature (*Continued*)
  effects (*Continued*)
    on strain sensitivity and strain-gage factor, 54·23
  limits for strain-gage use, 54·9
  measurement in nondestructive testing, 5·23
    with thermocouples in cables for high-temperature strain gages, 54·32
  -resistance coefficient of strain-sensitive materials, 54·22
  strain-gage (mounted) resistance variation with, at zero strain, 54·22
Tempering
  of parts (hardened) before etching to remove residual stresses and prevent cracking, 32·26
  of steel (carbon), effect on Magnatest Q eddy-current pattern, 42·52–53
Tenite, as model material for photoelastic stress analysis, 12·31
Tensile Strength
  measurement of, automatic statistical quality control in, 41·13
    by coercive force, 34·5
    by eddy-current methods, 2·25
      adjusting and establishing sorting limits in, 41·7
      tabular summary of, 36·4–5
    of forgings, Magnatest Q eddy-current instrument for, 2·29
    of metal rods, by eddy-current methods, 42·3
    of metal rods with σ-D eddy-current instrument, 40·40
  sorting by, of steel automobile parts with Magnatest Q eddy-current instrument, 42·54–55
    of steel, Magnatest Q eddy-current indications of plastic flow during, 42·60
    of steel (carbon) forgings with Magnatest Q eddy-current instrument, 42·56
  of steel parts, effect on Magnatest Q eddy-current wave forms and slit value, 42·52
  of strain-gage-alloy wire, 54·8–9
Tension
  -compression sonic vibration radial mode of thin circular discs, 51·3
  porcelain enamel failures from, 29·9
  strains, in brittle-coating tests, calibration for, 52·10
    measurement by continuous and zero-loading techniques, in brittle-coating testing, 52·22
    measurement in brittle-coating testing, 52·19
Terbium, absorption coefficients (mass) for γ and X rays and photon energies of, 18·38
Terra Cotta, electrified-particle testing of, 29·19
Tesla Coils (See "Coils")
Test Blocks
  aluminum-alloy, for ultrasonic immersion tests, 47·2–3
    for ultrasonic tests, 45·10
  for contour-effect studies in ultrasonic testing, 45·13
  for ultrasonic immersion testing, 46·10
    response characteristics of, 46·15–17
    slotted, for stringer-type flaw evaluation, 46·12–15
  for ultrasonic testing, 43·37, 43·39–40, 45·5, 45·18
  ultrasonic-wave amplitude *vs.* area calibration data for Alcoa Series A, 43·46
Test Holes, in ultrasonic testing as standards, 45·1
Tests, qualification, for radiographers for pipeline welds, 25·28
Tests, Field (See "Field Tests")
Tests, Maintenance (See "Maintenance Tests")
Textiles (See also "Fabrics")
  basis weight measurement range with Sr-90 beta gages, 18·16
  testing by phase microscopy, 10·18
Textile Spindle Tips, hardness sorting of, by magnetic-field point-pole tests, 34·14
T-Gage, strain-gage configuration, 54·5
Thallium, sodium iodide activation with, for scintillation counting, 18·22
Thallium-204, energy and half-life of, as β-ray source, 18·17
Thallium Oxide, gamma-ray and neutron absorption of, 15·11
Thallium Sulfide, as photoconductor in X-ray amplification, 16·8
Thermal Cross-Section, of isotopes, 15·9
Thermal History, of tubes (small-diameter), effect in eddy-current testing, 38·24
Thermal Neutrons (See "Neutrons")
Thermal Properties, detected by nondestructive tests, 4·13
Thermal Tests, nondestructive, 5·23
Thermistors, in strain-gage temperature compensation, 54·23
Thermocouples
  coupling to test objects and sources of error therein, 5·23
  location in ceramic materials with X-rays, 24·36
  in strain gages, to offset resistance-variations with temperature, 54·31
    for temperature compensation, 54·23
Thermoelastic Coefficient
  sorting by, of watch springs with Multitest eddy-current instrument, 40·23
    of watch springs, automatic eddy-current unit for, 41·2
  watch-spring eddy-current testing and sorting by measurement of, 2·32
Thermoelectricity
  in nondestructive testing, 5·22
    sources of, 5·16
  in sorting of materials, 5·23
Thermoelectric Potentials (See "Potentials, Thermoelectric")
Thermopiles, in conversion of radiation into electrical energy, 18·20
Thévénin Equivalent Circuit, of Wheatstone balanced bridge, 54·17–18
Thickness
  -conductivity product of metallic sheets, determination of, 39·16–17
  control in metallizing of condenser paper, eddy-current apparatus for, 41·4
  effects of cement beneath strain gages, 54·13
    on crack detection in lead-in wires with Ziljstra eddy-current instrument, 40·19
    of discontinuities in ultrasonic testing, 45·22
    on eddy-current testing of sheet materials, 39·16
    on firing of ceramic-type brittle coatings, 52·17
    on fluoroscopic sensitivity, 19·31, 19·34
    of nonferromagnetic tube walls in eddy-current testing, 38·23
    of nonferromagnetic tube walls on effective permeability or impedance in eddy-current testing, 38·9
    of nonferrous tube walls in eddy-current testing, normalized apparent impedance planes for, 38·3–5

Thickness (*Continued*)
- effects of cement beneath strain gages (*Continued*)
  - of tube walls
    - in eddy-current testing with internal coils, 38·15–17
    - on effective permeability in eddy-current testing, 38·6
    - on resistance-loss indications in eddy-current testing, 38·28
  - on vibration frequency in sonic testing, 51·11
- expanders in ultrasonic testing, transducer elements acting as, 43·4
- exposure factors in γ radiography of metals, 15·26
- of foil, eddy-current meter for, with automatic feedback control of rolls, 41·3
- of lead-foil screens for radiography, 16·24–25
- limitations in nondestructive testing, 1·20
- measurement of, applications of, 18·26
  - with beta rays, 5·19
  - of bulkheads by ultrasonic resonance methods, 50·39–40
  - capacitance tests in, 5·22
  - of ceramic wet extruded tubes with X rays, 24·36–38
  - charts for selection of methods for, 1·29
  - of coatings, sheets, and walls from one side only, 5·20
  - of coatings and walls with X rays, 24·36
  - of coatings with fluorescent radiation, 24·36
  - by eddy-current methods, 36·4
  - of extrusions by ultrasonic resonance method, 50·19
  - of ferromagnetic coatings and sheets, 5·13
  - of ferromagnetic metals, 33·2
  - by fluoroscopy, range of, 19·23
  - of foils and sheets by eddy-current testing, 39·12
  - gages for (See "Thickness Gages")
  - by Hall generators, 34·17
  - of hollow parts by ultrasonic resonance method, 50·19
  - of insulating layers, eddy-current apparatus for, 40·2–3
  - magnetic-field apparatus for continuous, 34·17
  - of metallic sheets with *RC* oscillator, 39·18
  - of nonmetallic layers, eddy-current instrument for, 40·47
  - from one side only, 5·24
  - of plastic coatings on photoelastic-coating test specimens, 53·15
  - of plates by electric-current methods, 35·4–9
  - of platings by ultrasonic resonance method, 50·21
  - by radiation absorption and reflection, accuracy of, 18·4–6
  - from sound-wave velocities, 45·9
  - of storage-tank walls by ultrasonic resonance methods, 50·36
  - of thin layers by optical methods, 10·16–17
  - of threads, 10·29
  - of tubes and tubular parts by eddy-current methods, 36·5
  - of tube (small-diameter) walls by eddy-current methods, 38·31
  - by ultrasonic methods
    - applications of, 43·49
    - with focused transducers, range of, 44·10
    - using resonance or transducer-loading effects, 43·35–37

Thickness (*Continued*)
- measurement of (*Continued*)
  - by ultrasonic resonance methods, 43·15, 50·4, 50·19
    - accuracy of, 50·5, 50·18, 50·30
    - frequency selection for, 50·11
    - harmonic frequencies in, 50·3, 50·14
    - instrumentation for, 50·7
    - instruments for, 50·3
    - range of, 50·5
    - shape effects on, 50·5
    - to study corrosion, 50·25–26
  - by ultrasonic-resonance multiple-reflection method, 50·35
  - of walls, direct current in, 5·20, 35·1–2, 35·9
  - of walls (curved) by electric-current methods, 35·7
  - of walls (nonmagnetic)
    - by magnetic-field methods, 34·15–16
    - ten-point magnetic-field device for, 34·16
  - of walls with square electrode array by direct-current methods, 35·10
- of plastic coatings
  - in photoelastic-coating testing, effect on sensitivity, 53·13
  - in photoelastic stress analysis, errors from, and their correction, 53·37–38
- potential relation for electric-current testing of flat plates, 35·4
- sorting by, of copper plating on arc-lamp carbons by eddy-current methods, 41·2
  - of sheet materials, automatic eddy-current instrument for, 41·14
- of steel, effects in X-radiography, 20·35
- of ultrasonic transducers, resonant frequency in relation to, 50·16

Thickness Gages
- magnetic-field-difference probe as, 33·1
- portable, for pipe walls, 18·30
- radioisotope, 18·12–16
- radioisotope and X-ray, 18·1
  - uses of, 18·26
- X-ray, 18·6
  - balanced-beam, 18·10
  - fluorescence, 18·10
  - indication systems for, 18·9
  - setting of, 18·10
  - substitution, 18·9

Thorium
- absorption coefficients (mass) for γ and X rays and photon energies of, 18·38
- radioactivity of, 15·7

Threads, thickness of, determination by optical methods, and apparatus for, 10·28–29

Thulium, attenuation coefficients of, for γ and X rays, 27·34

Thulium-170
- decay processes of, 15·18
- disintegration of, internal conversion in, 15·3
  - scheme for, 15·14
- energy and half-life of, as gamma-ray source, 18·17
- production in nuclear reactors, 15·21
- radiation-dosage output of, 26·6
- radiation from, intensification by lead screen, 15·29
- radiography with, 15·13, 15·17
  - exposure-thickness curves for, 15·27
  - sharpness in, 15·35

Thulium Oxide, as radiographic source, 15·17

Thyratrons, ultrasonic contact testing with defective, irrelevant indications in, 48·21

Tile
- for floor and walls of X-ray-film processing areas, 21·12, 21·14
- radiation shielding equivalent of, 26·9

Time, transit, in ultrasonic testing (See "Transit Time")

Time-Temperature System, in X-ray-film development, 21·4–5

Tin
- absorption coefficients (mass) for γ and X rays and photon energies of, 18·35, 27·29
- attenuation coefficients of, for γ and X rays, 27·29
- coatings on iron or steel, eddy-current determination of thickness of, 36·7
  - on iron or steel, thickness determination with X rays, 18·4
  - on steel
    - determination of thickness of, 18·4
    - fluorescence X-ray gaging of, 18·10
    - radioisotope gaging of, 18·15
- effect on electrical conductivity of copper, 42·12–13
- electrical conductivity of, 42·16

Tint-of-Passage
- of color fringes in photoelastic-coating testing, 53·4
- in photoelastic-coating testing for maximum eye sensitivity, 53·4

Tires
- inspection (fluoroscopic) of, 19·36
- thickness gaging in manufacture of, 18·28

Titanium
- absorption coefficients (mass) for γ and X rays and photon energies of, 18·34, 27·13
- attenuation coefficients of, for γ and X rays, 27·13
- effect on electrical conductivity of aluminum, 42·14
- electrical conductivity of, 42·16
- liquid-penetrant testing of, penetration time in, 6·8, 6·10
  - post-emulsification process for, 6·9
- radiography of, exposure-thickness curves for, 15·27
- ultrasonic contact testing of forgings of, 48·11
- ultrasonic immersion testing of, 46·11
- ultrasonic resonance testing of, constant *K* value in, 50·3
- ultrasonic-wave amplitude-distance curves for, 43·44
- ultrasonic-wave reflection amplitudes for water-immersed, 43·46

Titanium Alloys
- acoustic and ultrasonic properties of Ti-150A, 43·8
- hardness of, eddy-current test of electrical conductivity as indication of, 42·1
- hardness testing of, with Magnatest FW-300 eddy-current instrument, 42·21
- radiography with Thulium-170, exposure-thickness curve for, 15·27
- ultrasonic inspection of, 49·2

Tolerances (See also "Specifications or Standards")
- in eddy-current testing for conductivity and diameter, 37·38
- in inspection (dimensional), 1·10
- in nondestructive testing, 1·4, 1·20
  - in relation to costs, 1·15

Tools
- carbide-tipped, penetration time for, in liquid-penetrant testing, 6·8, 6·10

Tools (*Continued*)
- chisel-shaped and pointed oscillating, in testing of abrasive products, 51·9
- dye-penetrant penetration time for cutting, 6·14
- fatigue cracks in cutting, liquid-penetrant penetration time for detection of, 6·19
- marks from, detection of, 6·9
- optical projection of, 12·21
- wear of wire-drawing, eddy-current indication of, 42·3

Torque
- measurement with strain gages, accuracy of, 54·3

Torquemeters
- photoelastic coatings in, 53·34–35
- small-field electronic meters used in, with photoelastic coatings, 53·24

Torsion, mode of sonic vibration of rectangular bars, 51·2

Tourmaline, for ultrasonic transducers, 50·15

Toxicity, of liquid penetrants, 7·19

Tracer Fixtures, for section measurement by translation, 12·24–29

Tractor, conduit, for pipeline X-ray inspection, 25·21

Training Programs (See also "Education")
- for liquid-penetrant testing, 8·23
- for magnetic-particle-test interpretation, need for, 32·1
- of nondestructive-testing laboratories, 2·11

Transducers
- loading effects, ultrasonic thickness measurement with, 43·35–37
- mechanical, for detection of motion of solid probes, 5·2
- photoelastic-coating use as, 53·34
- strain-gage
  - effect of temperature on sensitivity of, 54·4
  - materials for, 54·5
- strain-gage applications as, 54·3
- for ultrasonic contact and resonance testing, 50·17
- for ultrasonic contact testing, 47·29, 48·1–2
- for ultrasonic immersion testing, 46·7
  - positioning of, 47·32
- for ultrasonic resonance testing, 50·7
  - area of, 50·16
  - coupling in, 50·5
  - grounded, 50·16
  - material for, 50·15
  - mountings for, 50·16
  - sandwich-type, 50·15
  - selection of, 50·14
  - sensitivity of, 50·7
  - shape of, 50·16
  - spring-mounted, cylindrical, convex, 50·16
  - swivel-mounted, 50·16
  - temperature limitations of, 50·16
- for ultrasonic testing, 5·17, 44·1–21
  - band width of, 44·19–21
  - barium titanate as element for, 49·3, 49·6, 49·12
  - beam diameter with double, 49·5
  - capacitance of, 49·12
  - characteristics of systems of double, 49·1
  - of cylinders, tubing, wing spars, etc., 44·9–10
  - damping of, 49·11
  - design of, 44·4
  - dynamic range of, 44·19
  - electromechanical and piezoelectric, 43·4
  - electromechanical coupling coefficient of, 49·12

- **Transducers** (*Continued*)
  - for ultrasonic testing (*Continued*)
    - elimination of near-field effects in, **44·19**
    - focused, **5·25, 44·6–11**
    - magnetostrictive and piezoelectric, **5·17**
    - materials for, **43·4**
    - paint-brush, **44·11–12, 49·6**
    - piezoelectric, response to mechanical disturbances, **45·18**
  - in weight measurement, **5·11**
- **Transformer Oil**
  - acoustic and ultrasonic properties of, **43·8**
  - ultrasonic reflection coefficients at interfaces with other materials, **43·13**
- **Transformers**
  - high-voltage, developments in, **14·5**
    - housing for, **14·5**
    - for X-ray generators, **14·4, 14·36**
  - linear differential, in detection of motion of solid probes, **5·2**
  - resonant, radiographic characteristics of X-ray generators with, **23·4**
- **Transistors,** failures in, radiography to determine causes of, **24·38**
- **Transition Region,** for transmission of ultrasonic waves, **50·24**
- **Transit Time,** of ultrasonic waves, measurement of, and test systems using, **43·28–35**
- **Translation,** section measurement by, with optical projectors, **12·3, 12·24**
- **Transmission**
  - of ultrasonic waves, **45·1–6**
    - coefficient of, **43·12**
    - through specimen, equipment and methods using, **43·27–28**
    - test methods using, **43·1**
    - through thin plates, **43·14–15**
  - of X rays by aluminum and magnesium, **19·19**
- **Transmission Coefficient *T***
  - in determination of conductivity-thickness product of metallic sheets, **39·17**
  - in testing of sheet materials, **39·13**
  - real and imaginary coefficient of, in eddy-current testing of sheet materials, **39·14**
- **Transmission of Energy Tests** (See "Energy Transmission Tests")
- **Transparent Materials**
  - microscopy (phase-contrast) of, **11·12**
  - optical interference and Schlieren effects for testing, **10·22**
- **Transuranic Elements,** X-ray analysis of, **17·20**
- **Trepanning,** as magnetic-particle-test supplement, **32·24**
- **Triangulation,** in stereoradiography, **20·47**
- **Triboelectric Effect, 28·4**
  - in electrified-particle tests, **28·2**
  - in identification and sorting, **5·22**
  - in nondestructive testing, **5·16**
- **Triboelectric Series,** definition of, **28·4**
- **Tropical Conditions,** X-ray-film processing for, **21·12**
- **Trucks,** parts, semi-automatic magnetic-particle testing equipment for, **31·10**
- **Tubes**
  - bends in, ultrasonic gaging of, **50·19**
  - boiler, corrosion inspection of, by ultrasonic test methods, **50·37**
    - thickness measurement of, by Hall generator, **34·17**
    - ultrasonic resonance testing of, **50·26**
    - ultrasonic testing of, **3·8**
  - ceramic, wall-thickness determination with X rays, **24·36**
- **Tubes** (*Continued*)
  - cracks in, as basis for rejection in liquid-penetrant testing, **8·14**
    - frequency selection for eddy-current testing for, **40·11**
  - cracks in nonferromagnetic, eddy-current data on, **38·12–15**
  - cracks in thin-walled, eddy-current testing of, **38·7**
  - eccentricity of, measurement of, by magnetic-field tests, **34·19–20**
    - probe-coil eddy-current indications of, **38·37**
  - eddy-current testing of, **38·1–39**
    - for corrosion inside, **42·3**
    - for diameter and wall thickness, **38·31**
    - by ellipse methods, **40·28**
    - equipment for, **40·2–3**
    - feeding mechanism for, **38·27**
    - interferences with, **2·31**
    - with internal test coil, **38·15–18**
    - with probe coils, control of coil spacing in, **38·36**
    - resistance-loss indications as function of wall thickness in, **38·28**
    - statistical quality number in, **41·18**
    - surface probe-coil system for, **38·35–39**
    - tabular summary of, **36·5**
  - eddy-current testing of carbon-steel, penetration depths in, **38·22**
  - eddy-current testing of nonferromagnetic, impedance plane for coils around, **38·24**
  - eddy-current testing of nonferrous, effect of outside diameter changes in, normalized apparent impedance plane for, **38·3–5**
  - eddy current testing of nonmagnetic, **3·12**
  - eddy-current testing of small-diameter, automation of, **38·37**
    - coil configurations for, **38·25–26**
    - instruments for, **38·27**
  - eddy-current testing of small-diameter nonferromagnetic, **38·23–39**
  - eddy-current testing of thick-walled, frequency ratio selection for, **38·12**
  - eddy-current testing of thick-walled nonferrous, **38·8–12**
    - complex permeability plane for inside diameter variation in, **38·8**
  - eddy-current testing of thin-walled, sensitivity of, **38·6**
  - eddy-current testing of thin-walled ferromagnetic, **38·6**
  - for guns, ultrasonic-inspection program for, **43·35**
  - heat-exchanger, eddy-current testing of, **3·23**
    - ultrasonic resonance testing of, **50·26**
  - heat treatment of, hardness control in, with Magnatest FW-300 eddy-current instrument, **42·20**
  - inspection (borescopic) of, **11·14**
  - inspection (visual) of hollow tubes, deep holes, long bores, etc., **10·10**
  - laminations in rolled, detection of, **5·25**
  - leak detection in, with liquid penetrants, **8·2**
  - magnetization using central conductor for magnetic-particle testing, **30·9**
  - radiography of boiler, **2·14**
  - stainless-steel, eddy-current apparatus for defect detection in, **40·14**
  - ultrasonic gaging of drawn, **50·19**
  - ultrasonic immersion inspection of, **47·26**
    - apparatus for, **46·22, 46·24**
    - application of, **47·39**
    - quality specifications for, **47·39**

Tubes (*Continued*)
- ultrasonic testing of, transducers for, **44·9–10**
- ultrasonic waves (Lamb) in testing of thin-walled, **45·12–13**
- welds in, automatic magnetic-particle testing of, **31·14**

Tungsten
- absorption coefficients (mass) for γ and X rays and photon energies of, **18·38, 27·36**
- acoustic and ultrasonic properties of, **43·8**
- attenuation coefficients of, for γ and X rays, **27·36**
- electrical conductivity of, **42·16**
- inclusions in welds, causes and radiography of, **25·9**
- rods and wire, defect indications with Magnatest FW-200 eddy-current instrument, **42·6–10**
- as target material for X-ray tubes, **14·3**
- wire, diameter variations of, eddy-current indication of, **42·3**
  - eddy-current test apparatus for, **40·2–3**
  - eddy-current testing with feed-through coils, **42·6**
  - splitting of, eddy-current test for, **40·6**
  - wavy fiber texture from swedging of, **42·3**
- wires (lead-in), crack detection in, with Ziljstra eddy-current instrument, **40·19**

Tungsten Alloy, gamma-ray shielding equivalent of, **26·10**

Tungsten Carbide
- coercive force of, quality and, **34·4**
- eddy-current-test curves for, **39·6**

Turbidity, determination by light scattering, **10·30**

Turbines
- blades, edge crack propagation in, during thermal cycling, **35·11**
  - fatigue cracks in, liquid-penetrant indications of, **8·15**
  - holes in, eddy-current detector for cracks in, **40·47**
  - magnetic-particle-testing apparatus for, **31·10–11**
  - radiography with high-voltage X rays, **23·15**
  - strain-gage tests of, effect of cement thickness on, **54·13**
- cracks in, inspection of, **3·12**
- magnetic-particle tests for maintenance of, **3·10**
- rotors of, distortion testing of forgings for, **5·24**
- strain-gage tests on gas, **54·3**
- testing of, during overhaul, **3·10**
- ultrasonic immersion inspection of parts of, **46·23**
- ultrasonic inspection of rotor wheels of, equipment for, **47·17–18**
- washers (thrust) of power-recovery, flatness inspection for, **3·34**

Turntables
- for ultrasonic immersion testing, **46·8**

Tyndall Effect, definition of, **10·27**

U

Ultrasonic Contact Testing, **48·1–31**
- advantages of, **48·8**
- applications for, **48·1**
- coupling medium for, **48·1**
- disturbances in, accidental, **48·30**
  - from coupling-block and probe, irrelevant indications from, **48·22**
  - from refraction, **48·25**
  - from specimen form, **48·27**
  - surface, irrelevant indications from, **48·23**
  - from test material, **48·29**
- double-transducer, **48·13, 49·1–21**
- electrical interference in, **48·21**
- frequencies for, **48·1**
- frequency selection for, **48·2, 48·16**
- instrumentation for, **48·4**
  - for automatic programming systems, **48·7**
- irrelevant indications in, **48·21**
- limitations of, **48·8, 49·18**
- reference plates in, **48·14–15**
  - for instrument calibration, **48·15–16**
- reflections in, measurement of, **48·13**
- of rods on extrusion and compacting presses, **3·23**
- scanning speeds in, **48·5**
- search units for, **48·2**
- of ship cast-steel stern frames, **3·21**
- of ship crankshafts and tailshafts, **3·20**
- through-transmission techniques in, **48·9**
- transmission and reflection techniques in, **48·1**
- wedge-angle determination for, **48·8**

Ultrasonic Energy (See "Ultrasonic Waves")

Ultrasonic Fields (See "Ultrasonic Waves")

Ultrasonic Immersion Indications
- of aluminum-alloy extrusion defects, **47·11**
- of aluminum compressor rotor wheels, **47·16, 47·18**
- comparison of A-, B-, and C-scan, **47·30**
- of cracks, in Hastelloy tubing, **47·36**
  - in Inconel tubing, **47·34**
- of defects, checking of, **46·17–19**
- of defects (large), **47·1, 47·5**
- of defects oriented at an angle to surface, **47·13**
- of defects (small), **47·1, 47·4**
- false indications from curved surfaces, **47·11**
  - from surface conditions, **47·12, 47·23**
  - from surface contour blending, **47·24**
- of forging defects, **47·10, 47·14**
- grain-size effects on, **47·15**
- of Inconel X forged parts, **47·15**
- interpretation of, **47·34**
- metallurgical factors in, **47·9**
- nonrelevant, **47·34**
- of pipe welds for measuring alignment, **47·39**
- reliability of, **47·26**
- surface roughness effects on, **47·13**
- of turbine rotors with forging defects, **47·20**
  - with heat-treating scale, **47·25**
  - with metallic inclusions, **47·20**
  - with nonmetallic inclusions, **47·23**
  - with weld cracks, **47·20**
- of turbine wheels (forged) showing segregation, **47·22**

Ultrasonic Immersion Testing, 5·25, **46·1–27, 47·31**
- A-, B-, and C-scan presentation in, **46·3, 46·5**
- acceptance limits for, **46·26**
- advantages and limitations of, **46·1**
- of airframe components, **47·1**
- of aluminum-alloy forgings, **46·21**
- angles of incidence in, **47·32**
- applications of, **46·21–23**
- A-scan signals in, **46·18**
- back-reflection loss in, **47·1**
- beam collimation in, **47·32**

Ultrasonic Immersion Testing (*Continued*)
- classification requirements for, 46·26
- of curved surfaces, 46·7
- curves for various crystals and test frequencies in, 46·15–17
- of cylindrical parts by off-center scanning, 46·19
- cylindricator in, 46·19
- for defect location, 46·18–19
- defect location and orientation in, 47·12
- equipment for, 46·5
  - automatic, 46·2, 46·7, 47·16, 47·18
  - manual, 46·1, 47·17
  - impedance matching in, 47·29
  - for pipe and tubing, 47·28
  - semi-automatic, 47·17
  - transducer selection for, 47·29
  - for tubing, 47·29
- of flat or rectangular stock, 46·22
- of forgings of irregular shape, 46·2
- full, with double-transducer search units, 49·19
- gated flaw alarm in, 47·32
- high-frequency waves in, 46·8
- immersion medium for, 47·31
- industrial inspection procedures in, 46·17–21
- of ingots (cast cylindrical), 46·23
- instrumentation for, 46·23
- instrument standardization for, 46·26
- of jet-engine rotors, 47·16
- limitations of, 49·18
- marker-circuit adjustment in, 46·10
- materials for, 46·2, 46·10
  - effect of heat treatment on, 46·12
  - structure of, 46·11
  - surface finish and radius of, 46·11
- of parts (symmetrical), 46·2
- of pipe and tubing, 47·26–28
- resolution in, loss of near-surface, 46·8
- scanning in, automatic, 46·8
  - of flat surfaces, 46·17
  - hand units for, 46·6
  - speed of, 47·30
- sensitivity in, adjustment of, 46·17
  - control of, 47·32
- shear-wave techniques in, 47·15
- specifications for, 46·17
  - of die forgings, 46·23
  - typical, 46·26–27
- standards (reference) in, 47·31
- of stringer-type-flaw length and width, evaluation by slotted block, 46·12–14
- test blocks in, 46·12, 46·14
- transducer positioning in, 47·32
- of tubular or round bar stock, 46·22
- of turbine parts, 46·23
- turntable units for, 46·8
- using different crystals and frequencies, 46·16–17
- water-distance control in, 46·10
- of welds in pipe, 47·39

Ultrasonic Pulse-Reflection Testing (See "Ultrasonic Contact Testing," "Ultrasonic Immersion Testing")

Ultrasonic Resonance Testing, 3·20, 50·1–42
- in aircraft maintenance, 3·32
- applications of, 50·19
- for corrosion measurement, 50·30
- discontinuity detection by, 50·21
- effect of corrosion product accumulations on, 50·32
- equipment for
  - with automatic indicators and recorders, 50·10

Ultrasonic Resonance Testing (*Continued*)
- equipment for (*Continued*)
  - calibration of
    - with direct-reading thickness scales, 50·11
    - with frequency scales, 50·11
  - with capacitance-modulated cathode-ray tube indication, 50·8
  - with cathode-ray tube presentation, 50·34
  - components of, 50·6
  - for corrosion surveys, 50·31
  - coupling media for, 50·14
  - frequency characteristics of, 50·7
  - with frequency scales, 50·14
  - for gaging of parts during manufacture, 50·4
  - with inductance-modulated cathode-ray tube indication, 50·9
  - with meter and headphone indicators, 50·10
  - pulse-reflection, for corrosion measurements, 50·35
  - recorders for, 50·12
  - with stroboscopic presentation, 50·10
  - with thickness scales, 50·14–15
  - transducer characteristics of, 50·7
  - transducer selection for, 50·15
- frequencies and signals obtained under various surface conditions, 50·32
- frequency selection for, 50·11
  - in corrosion testing of storage tanks, 50·36
- laminar-discontinuity detection by, 50·23
- in maintenance inspection, 50·25
- for marine applications, 50·37
- material suitable for, 50·4
- in measuring wall thickness, 50·26
- in petroleum refineries, 3·13
- principles of, 50·1–3
- safety inspections by, 50·26
- of ship-plate thickness, 3·20
- of steel roll (built-up) to locate end of journal hub, 3·22
- surface preparation for, 50·16, 50·18
- for thickness, basic circuit for, 50·6
  - of conveyor pipes, 3·23

Ultrasonic Testing
- acoustic impedance effects in, 45·1–3
- advantages, applications, and limitations of, 43·2, 43·47
- with amplitude and transit-time simultaneous indication, 43·28–35
- applications (present and potential) of, 43·48–49
- beam-shape modification in, and its compensation, 45·10
- calibration in, 43·37–47
  - curves for, of aluminum blocks, 44·16
- in central cooperative institutes of Western Europe, 2·13
- contour or curvature effects in, 45·13–15
- directional effects in, 45·21
- of discontinuities, interpretation guide for, 45·26–27
- discontinuity effects in, 45·18–22
- discontinuity-shape effects in, 45·22–27
- discontinuity-thickness effects in, 45·22
- disturbing influences in, 43·24
- double-transducer, 49·1–21
  - automatic gain control in equipment for, 49·19
  - safety devices in equipment for, 49·19
  - system fault warning in, equipment for, 49·20
  - typical band widths of equipment for, 44·21
- echo-amplitude loss in, from test object surface roughness, 45·16

Ultrasonic Testing (*Continued*)
- effects of cracks, gas porosity, and nonmetallic inclusions in, **45·21**
- equipment for, classification of, **43·26**
  - gated *vs.* modified pulse-time, **43·28**
- Fresnel zone effects in, **44·12**
- history of, **43·3**
- improvements (recent) in, **43·3**
- inspection, criteria for successful, **43·50**
- instrumentation and techniques, **43·26–37**
- interpretation under near-field conditions, **44·16**
- Lamb-wave systems for, **45·13**
- limitations of, **43·49–50**
- loss-of-back-reflection method in, **43·24**
- material properties (significant) in, **45·1**
- at multiple frequencies, **45·26**
- parameters and their evaluation, **43·38–47**
- of power-generator rotor shaft, **2·17**
- principles, **43·1–50**
- pulse-reflection system for, **43·29**
- pulse-system modifications for, **44·21**
- radiation patterns and reflection from small discontinuities in, **45·20**
- resolution loss in, from acoustical absorption and scattering, **44·20**
- search units for, **43·5–7**
- sensitivity-time control compensation in, **45·5**
- short-burst polarity method, **45·21**
- side-lobe phenomena in, **44·19**
- sound velocity effects in, **45·6–13**
- standards for, flat-bottomed holes as, **45·1**
- stress ranges in, **43·1**
- systems, **43·1–3**
- test blocks for, **2·19, 45·5, 45·18**
- for thickness measurement using transducer-loading effects, **43·35–37**
- through-transmission, **43·27–28**

Ultrasonic Vibrations (See "Ultrasonic Waves")

Ultrasonic Waves (See also "Sound," "Sound Waves")
- absorption and scattering of, loss of resolution in testing from, **44·20**
- acoustic properties in metals and nonmetals, **43·8**
- amplitudes and angle curves for Lucite and steel, **43·21, 43·23**
- amplitudes in aluminum and water, variation with depth, **44·15**
  - of beam or echo from discontinuities or reflectors, **45·18–22**
  - of echo indications from parts with various curvatures, **45·13–15**
- angle and straight, test units using, **43·5–6**
- angles of, effect on angle of refraction in metals, **45·10**
- angular and amplitude relationships of, **43·18–21**
- angular incidence of, **43·19**
- attenuation, reflection, and transmission of, **45·1–6**
- attenuation and velocity in plastic sheets, measurement of, **43·15**
- attenuation of, **43·22–23**
  - by backing members, **44·6**
  - frequency compared with, for common materials, **43·26**
- beam diameter in double-transducer testing, **49·5**
- beam-profile variation with depth in aluminum, **43·41**
- beam-sharpening in B-scan test systems, **43·33**
- beam spread of refracted shear, as function of receiver angle, **43·24**

Ultrasonic Waves (*Continued*)
- collimation of, in immersion testing of pipe and tubing, **47·32**
- in contact testing, types of, **48·8**
- in defect detection, **1·29**
- diffraction of, **43·21**
- effects at plane interfaces, **43·12–21**
- energy of, calculation of, **43·18**
  - discrete annular rings in near field, **44·16**
  - distribution for combined transmit-receive search units, **49·9**
  - losses in
    - reflection from rough and smooth surfaces, **45·23**
    - solids, **43·25**
    - transmission, **43·22**
    - ultrasonic testing between two multiples of rear-surface echo, **45·3–5**
  - from reflectors, **45·19**
  - returned in immersion testing as function of impedance ratio, **45·2**
  - transfer at interfaces, **45·1**
- fields, **45·1–27**
- frequency of, changes to clarify test interpretation, **44·19**
  - constants for common piezoelectric materials, **44·4**
  - in contact tests, **48·1**
  - effects in corrosion testing, **50·33**
  - effects in testing and uses of multiple frequencies, **45·25–26**
  - effects on acoustic attenuation in testing, **45·5**
  - ranges in nondestructive testing, **43·1**
  - selection for
    - contact testing, **48·16**
    - resonance testing, **50·11**
    - testing, **45·6**
  - in special test units, **43·7**
- frequency (resonant), of oscillator in test equipment, **50·7**
  - recording of, **50·10**
  - of transducers in test equipment, **50·7**
- front characteristics of, **44·12**
- generation of, and sources or transducers for, **43·4–8**
- high-frequency, in immersion testing, **46·8**
  - in nondestructive testing, **4·12**
- intensities, central-axis maximum and minimum, **44·12**
- Lamb, **45·12–13**
  - in contact tests, **48·8**
  - formation in ultrasonic immersion testing of pipes and tubing, **47·27**
  - modes of, **48·12**
- length of, formula and values for common materials, **43·9**
  - in relation to hole diameter in aluminum and stainless steel, **45·20**
- lenses for, focal depth in metals and water, **44·7**
- longitudinal and shear amplitude ratio of reflected-to-incident, **43·17**
- longitudinal, critical angle for, in aluminum and steel, **45·10**
- modification of beam shape by reflection and refraction, **45·10**
- penetration by, frequency in relation to, **46·9**
  - limitations in immersion testing, **46·9–10**
  - range of, **5·14**
  - in welds, **48·12**
- presentation of, equipment and methods for, **43·29–35**

- **Ultrasonic Waves** (*Continued*)
  - propagation of, **43·9–26**
    - angular relationships for, **43·15**
    - in pipes and tubing, **47·26**
    - in solids, velocity of, **43·9–12**
  - radiation patterns and reflection from small discontinuities, **45·20**
  - Rayleigh, Plexiglas blocks in search units to reduce transmission of, **49·5**
    - and their use in surface-flaw detection, **45·11–12**
  - reflected-beam radiation patterns for flat, circular reflectors, **45·20**
  - reflection and transmission of, and test methods using, **43·1**
  - reflection of, **43·12**, **43·14**
    - amplitudes for common metals immersed in water, **43·46**
    - coefficients for, at interfaces, **43·13**
    - time in liquids, metals, and plastics, **43·31**
  - refraction of, analyzer for, **43·20**
    - at interfaces, **43·15–16**
  - resonance of, in metal plates, **50·2**
    - in thickness measurement, **43·15**
  - shear, uses of, **45·10**
  - sources of, for nondestructive testing, **5·17**
  - standing, effects in ultrasonic testing by through-transmission method, **43·28**
  - tests using, **5·24**
  - transducers for, **44·1–21**
  - transmission of, frequency effect on, **50·24**
    - systems for, **44·6**
  - transverse, crystals generating, **43·4**
  - velocity of, elastic constants in relation to, **43·10**
    - formulas for, **43·10**
    - measurement of, **50·24**
    - Poisson's ratio in relation to, **43·12**
  - velocity ratio equations for, **43·10**
  - vibration modes in contact tests, **48·8**
- **Ultraviolet Light** (See "Light, Ultraviolet")
- **Undercutting**
  - definition of, in γ radiography, **15·24**
  - scattering in radiography, **20·19**
  - in welding, causes and radiography of, **25·13**
  - xeroradiographic, and its prevention, **22·10–12**
- **Unsharpness**, **19·2**
  - of fluoroscopic image-amplifier screens, **19·39**
  - of fluoroscopic images, theory of, **19·30–31**
  - of fluoroscopic screens, **19·11–12**
  - in fluoroscopy and X-ray inspection, **19·1**
  - in radiography, **15·32**
    - geometry of, **20·7–10**
    - inherent, γ-ray energy in relation to, **15·33**
    - nomogram for, **20·9**
    - standards for, **2·18**
    - total, **15·34**
  - of X-ray (high-energy) images, **23·4**
- **Upsetting**, defects, magnetic-particle indications of, **32·11**
- **Uranium**
  - absorption coefficients (mass) for γ and X rays and photon energies of, **18·38**, **27·40**
  - attenuation coefficients of, for γ and X rays, **27·40**
  - Compton scattering in, **13·21**
  - electrical conductivity of, **42·16**
  - gamma-ray shielding equivalent of, **26·10**
  - photoelectric attenuation coefficient of, curves of components of, as function of energy, **13·19**
  - radioactivity of, **15·7**
    - with high-voltage X rays, **23·15**
- **Uranium** (*Continued*)
  - ultrasonic resonance testing of, constant K value in, **50·3**
- **Uranium-238**, disintegration series of, **13·15**, **15·1**
- **Uranium Alloys**, radiography with high-voltage X rays, **23·15**

V

- **Vacuum Deposition**, of metals, eddy-current control of film resistance during, **39·19**
- **Vacuum Systems**, leaks in, detection of, **5·5**
- **Vacuum Tubes** (See "Electron Tubes")
- **Validity** (See "Reliability")
- **Valves**
  - cracks in heads of, liquid-penetrant indications for rejection of, **8·17**
  - Magnatest Q eddy-current spread bands of case-hardened, **42·59–60**
  - radiography of body castings of, with Cobalt-60, **25·17**
  - rockers, case depth of, eddy-current nondestructive-test curves for, **2·28**
- **Vanadium**
  - attenuation coefficients of, for γ and X rays, **27·14**
  - effect on electrical conductivity of aluminum, **42·14**
- **Van de Graff Generators**, radiographic characteristics of, **23·4**
- **Velocity** (See also "Speed")
  - of particles in ultrasonic beams, **43·12**
  - of ultrasonic waves
    - in plastic sheets, measurement of, **43·15**
    - in solids and their calculation, **43·9–12**
- **Velocity Ratio Equations**, for ultrasonic waves, **43·10**
- **Vibration**
  - analysis of, before installation of precision equipment, **3·24**
  - detectors for sonic testing, **51·7**
  - direction in sonic testing of abrasive-honing sticks, flaw orientation with respect to, **51·13**
  - frequencies
    - natural, **51·1**
    - in sonic testing of abrasive wheels, correction for dimensions, **51·11**
    - resonant
      - of resin-bonded abrasive wheels, correlation with bursting speed, **51·12**
      - in sonic testing of abrasive-honing sticks in relation to flaw depth, **51·13**
      - in sonic testing of abrasive wheels, correlation with impact penetration tests, **51·10**
      - in sonic testing of aluminum oxide abrasive wheels, correlation with percentage of bonding material, **51·12**
    - scanning by, in sonic testing, **51·9**
  - frequencies of sonic
    - of abrasive wheels with radial cracks in sonic testing, **51·14**
    - characteristics measurable by, **51·6**
    - of complex shapes, **51·6**
    - equations for circular plates and rectangular bars, **51·4–6**
    - flexural, of flawless bars which are not exactly square, **51·13**
  - longitudinal, in ultrasonic contact testing, **48·8**
  - modes of sonic, of objects, **51·1–4**
    - of piezoelectric plates, **44·2**
    - in ultrasonic contact testing, **48·8**
  - sonic (See also "Sound," "Sound Waves")

- **Vibration** (*Continued*)
  - sources for nondestructive testing, **5·17**
  - tests using, **5·24**
  - transverse, in ultrasonic contact testing, **48·8**
  - wavelength of, strain-gage limitations in relation to, **54·27**
- **Vibration, Ultrasonic** (See "Ultrasonic Waves")
- **Vibration Tests,** natural-frequency, **51·1–14** (See also "Sonic Testing," "Ultrasonic Testing")
- **Vibratory or Wave Motions,** in nondestructive testing, **4·12**
- **Vidicon Tubes**
  - for television pick-up, **11·36**
  - in X-ray inspection using closed-circuit television, **19·39, 19·40**
- **Villard Rectifying Circuits,** for X-ray generators, **14·23–25, 14·41**
- **Viscosity,** of liquid penetrants, requirements for, **7·18**
- **Visibility,** of liquid penetrants, requirements for, **7·17, 7·20**
- **Vision**
  - binocular, for distance judgment, **10·1–2**
  - clouding of, by black light, and its prevention, **30·19**
  - color, characteristics of, **10·2–3**
  - electronic aids to, **11·25–40**
  - in fluoroscopy
    - acuity and dark adaptation in, **19·25**
    - limitations of, **19·24–27**
    - penetrameter for testing of, **24·26**
  - as function of perception, image, focus, and brightness, **10·1**
  - light brightness as factor in, **10·3**
  - limitations in, in nondestructive testing, **10·26**
  - mechanism of, **10·2**
  - spectral limits of, **10·3**
  - stereoscopic, **10·2, 20·46**
- **Visual Education** (See "Education")
- **Visual Inspection**
  - electronic devices for, **11·25**
  - equipment for, **11·1**
  - nondestructive, **10·1–35**
  - observer differences in, **10·4**
- **Visual Purple,** transformations in retina in vision, **10·2**
- **Voids**
  - in steel rods, Magnatest D eddy-current waveforms and macro- and microsections showing, **42·64, 42·68**
  - in welds, causes and radiography of, **25·5**
- **Volatility,** of liquid penetrants, requirements for, **7·18**
- **Voltage** (See also "Potential, Electric")
  - for black lights for fluorescent-magnetic-particle testing, **30·19**
  - bucking, in potentiometric-circuit strain-gage tests, **54·15**
  - complex plane of (See "Complex Voltage Plane")
  - crack signal, normalized components of, in eddy-current testing, **37·20**
  - current pulse size *vs.*, in radiation detection instruments, **16·2–5**
  - distorted wave forms in eddy-current testing of ferromagnetic materials, **40·41**
  - drop in eddy-current-test coils caused by ohmic resistance and self-inductance, **36·19**
  - in eddy-current-test coils, normalized components of, **36·20**
  - eddy-current-test output, imaginary and real components of, for various fill factors, **37·3**
- **Voltage** (*Continued*)
  - empty coil, in eddy-current testing, **36·10**
  - equivalents of radioisotopes used in radiography, **25·17**
  - for fluoroscopic inspection, range of X ray, **19·18**
  - gradient in ultrasonic testing across crystal elements, **44·5**
  - in radiography, choice of, **20·16**
  - ratio corresponding to sound power ratio between front surface and hole in ultrasonic testing of aluminum block, **44·19**
  - real and imaginary components of, for circular coil with nonferromagnetic spheres, **39·9**
  - regulation in X-ray generators, **18·8**
  - secondary, appearance in non-uniform field, in magnetic-field tests, **33·7**
    - in eddy-current testing, calculation of, **36·15**
  - secondary, of magnetic-field probes, **33·4**
  - secondary-coil
    - in eddy-current testing, **36·10–12**
      - calculation of **36·11, 36·13, 36·15, 36·17**
      - of cylindrical objects, characteristic function in calculation of, **37·1**
      - of nonferromagnetic cylinders, effects of conductivity and diameter on, **37·35**
      - of thin-walled tubes, calculation of, **38·3**
      - of tubes, determination of, **38·20**
    - normalized components in eddy-current testing of spheres and short parts, **39·3–4**
      - signals from, in eddy-current crack testing of ferromagnetic cylinders, **40·36**
  - secondary components of, of ferromagnetic test objects, calculation of, **36·16**
  - second harmonic, of magnetic-field probes, **33·4**
  - signal, components in eddy-current testing of ferromagnetic cylinders, **37·25**
  - stabilization in counter design, **16·6**
  - test coil, differential, for sound and defective cylinders in eddy-current testing, **37·19**
  - threshold, of Geiger-Muller counters, **16·7**
  - in Wheatstone bridge circuits, calculation of, **54·19**
  - in xeroradiographic-plate charging, **22·6**
  - for xeroradiography, **22·9**
  - of X-ray sources for inspection, **19·46**
  - X-ray tube
    - effect on composition and intensity of beam, **20·4**
    - effect on intensity, **20·15**
    - effect on variation of sensitivity with thickness, **19·34**
    - film graininess in relation to, **20·36**
    - in fluoroscopy, **19·15–16**
    - limits of, **14·33**
    - relation of effective, to peak, **19·10–11**
    - for various steel thicknesses, **25·17**
- **Voltmeters**
  - for strain-gage testing, **54·37**
  - vacuum tube, in Sonic Comparator circuit, **51·7, 51·9**

W

- **Wall Effect,** in optical projection, **12·22–23**
- **Wall Thickness** (See "Thickness")
- **Walls**
  - corrosion of, ultrasonic measurement of thinning from, **50·29**
  - corrosion of steel, direct-current measurement of thinning from, **35·9**

Walls (*Continued*)
  of X-ray-film processing areas, coverings for, 21·12–13
Warning Signs, for radiation areas, 26·15
Washers, flatness inspection of thrust, by interference light-band readings, 3·34
Washing
  technique effect on liquid-penetrant indication of defects, 8·8
  of X-ray films, 21·8–9
Washing Apparatus, for liquid-penetrant testing, 7·4, 7·9
Wastes, radioactive, disposal of, 26·16
Watch Springs (See "Springs")
Water (See also "Humidity")
  absorbed by strain gages, gage-to-ground resistance as indicator of, 54·24
  absorption by strain-gage adhesives and its effects, 54·24–25
  absorption coefficients (mass), their absorption components and photon energies for γ and X rays, 18·39
  acoustic and ultrasonic properties of, 43·8
  acoustic impedance, density and sound velocity in, 45·3
  attenuation coefficient for radiation absorption, 13·23
  as barrier in filtered-particle testing, 9·4
  in ceramic unfired ware, effect on filtered-particle tests, 9·5
  as coupling medium in ultrasonic-contact test, 48·4
  determination in emulsifiers for liquid-penetrant testing, 7·32
    in fluorescent penetrants, 7·33
  effect on filtered-particle tests, 9·14
    on liquid-penetrant testing, 6·6
    on magnetic-particle testing, 30·1
    on strain-gage leakage resistance, 54·37–38
  films on test objects in electrified-particle testing, removal of, 28·10
  fresh and sea, constant *K* value in ultrasonic resonance tests, 50·3
  Fresnel-zone effects in, in ultrasonic testing, 44·14–16
  liquid-penetrant removal by, 6·7
  in liquid penetrants, failure from, 7·33
  magnetic-particle-testing pastes for suspension in, 30·18
  metal interfaces in ultrasonic testing, energy losses at, 45·5
  reflectivity measurement of, 10·12
  -steel interfaces, ultrasonic-beam intensities at various angles of incidence, 43·20–21
    on strain gages when immersed, 54·25
  as suspending medium for filtered-particle tests, 9·7
  ultrasonic reflection coefficients at interfaces with other materials, 43·13
  ultrasonic-wave amplitude in, variation with depth, 44·15
  ultrasonic-wave attenuation *vs.* frequency in, 43·26
Waterproofing, of strain gages, 54·25, 54·37–38
Wavelength
  ultrasonic, formula and values for common materials, 43·9
  of vibration (mechanical), strain-gage limits in relation to, 54·27
Waves, characteristics of, 5·15 (See also "Sound," "Sound Waves," "Ultrasonic Waves," "X Rays," etc.)
Waviness, of test-object surfaces, effects in ultrasonic testing, 45·17
Waxes
  microcrystalline, coatings for moistureproofing of strain gages and their application, 54·38
    in strain-gage waterproofing, 54·25
  temperature-indicating, 5·24
Wax-Line Interposers, for section measurement with optical projectors, 12·23–24
Wear, of wire-drawing tools, eddy-current indication of, 42·3
Wear Plates, abrasion-resistant, for ultrasonic transducers, 50·16
Weathering, effects on strain gages with and without waterproofing, 54·25
Wedges
  angles, determination for ultrasonic contact search units, 48·8–9
  materials
    for double-transducer ultrasonic testing, 49·11
    for ultrasonic testing, 43·5
  plastic, in generation of ultrasonic Rayleigh and shear waves, 45·11
  step, for establishment of xeroradiographic techniques, 22·9
    penetrameters using, 20·38
    xeroradiograph of aluminum, 22·10
  in X-ray-scattering prevention, 23·9
Weighing
  continuous, load cells operating on strain-gage principle in, 54·3
  photoelastic coatings in, 53·34
Weight
  control in packaging, 5·13
  measurement of, 5·11
Welding
  bridges assembled by, photoelastic-coating tests of, 53·27, 53·34
  butt, lack of penetration in, causes and radiography of, 25·5–7
  defects at electrode-change points, causes and radiography, 25·14
  downhand and overhead, causes and radiography of concavity in, 25·11
  effect of residual magnetism on arc of, 30·20
  electrodes, defects at change points of, radiography of, 25·14
    determination of eccentric position of metallic core in covered, by magnetic-field tests, 34·19
  electrode spatter in, radiography of, 25·14
  error trends in, correction of, 25·26
  examination of, by reflecting objectives of optical systems, 10·9
  magnetization caused by arc, 30·21
  overlap in submerged-arc, causes and radiography of, 25·12
  of pipes with backing rings, effect on radiographic interpretation, 25·15
  in repair of defective castings, forgings, and welds, 32·22
Welds
  in aluminum and steel, dye-penetrant penetration times for, 6·14
  in aluminum plate, radiographs of defects in, 24·13
  concavity at roots of, causes and radiography of, 25·11
  cracks (fatigue) and porosity in, penetration time for detection of, in liquid-penetrant testing, 6·19

Welds (*Continued*)
- cracks in, causes and radiography of, 25·7
  - causes and repair of, 24·12
  - liquid-penetrant indications of, 8·12–13
  - ultrasonic immersion indications of, 47·19
- defects in chipping at, as supplement to magnetic-particle testing, 32·22
  - magnetic-particle indications of, 32·10
  - ultrasonic contact indications of, 48·18
- discontinuities in butt, radiographic interpretation of, 25·2–15
- drilling (core) or trepanning of, as supplement to magnetic-particle testing, 32·24
- etching with ammonium persulfate as supplement to magnetic-particle testing, 32·26
- flash-butt, detection of flaws in, 49·16
  - double search-unit ultrasonic testing of, 49·16
- fluoroscopy of steel, with image-amplifier tube, 19·39
- fusion lack in, causes and radiography of, 25·9
- grinding marks on, radiography of, 25·14
- grooves (incompletely filled) in, causes and radiography of, 25·11
- grooves (longitudinal) in, radiography of, 25·13
- inclusions (gas) in, causes and radiography of, 25·3
- inclusions in, ultrasonic contact indications of, 48·17
- inclusions (tungsten) in, causes and radiography of, 25·9
- leak detection in, by liquid penetrants, 8·2
- liquid-penetrant indication of defects of, 8·6
- magnetic-particle testing of, for medium- and heavy-duty equipment, 31·4–10
- magnetic-particle testing, nonrelevant indications from boundaries of, 32·17
- marks in, from arc starting or spitting, causes and radiography of, 25·14
- out-of-line, causes and radiography of, 25·14
- penetration (excessive) at roots of, ultrasonic-contact tests of, 48·18
- penetration (excessive) in, causes and radiography of, 25·12
- penetration (inadequate) at roots of, ultrasonic-contact tests of, 48·18
- penetration times for, in liquid-penetrant testing, 6·8, 6·10
- pipeline, defects in, sources of, 25·25–26
  - inspection and radiography of, 25·16–28
  - quality control of, 25·26–28
  - radiographers for, qualification tests for, 25·28
  - radiography of, definition and sensitivity in, 25·22
    - elliptical projection in, 25·21
    - percentage examination desirable in, 25·26
    - source location and size in, 25·20
    - three-exposure techniques in, 25·20–21
  - variation in percentage rejection during project, 25·27
- in pipes, radiography with external X-ray source, 25·23
- in pipes or tubes, automatic magnetic-particle inspection of, 31·14
- quality requirements in X-ray inspection, 24·2
- radiography of, 3·3, 14·40
  - in high-pressure steam lines, 3·3
  - with high-voltage X rays, 23·14
  - panoramic, in steel, 23·6
  - in ships, 3·19
- radiography of circumferential, 14·42
- reference radiographs for, in steel plates, 2·19

Welds (*Continued*)
- reinforcement (excessive) in submerged-arc, causes and radiographs of, 25·12
- repair of defective, by welding, 32·22
- root defects in, causes and radiography of, 25·7
- slag inclusions and lines in, causes and radiography of, 25·4–5
- spot, photoelastic-coating tests in determination of best arrangement of, 53·27, 53·32
- tack, in prevention of lack of penetration, 25·5
- in tanks (storage), testing of, 3·12
- ultrasonic-contact longitudinal-wave examination of, 48·18
- ultrasonic contact testing of, 48·12, 48·16
  - butt, 48·12
  - carbon-steel, 48·12
  - flaw indications in, 48·17
  - frequencies for, 48·1
  - fusion-zone indications by, 48·16
  - indications in, 48·17
  - shear-wave indications for, 48·17
  - stainless alloy, 48·12
  - steel, indications for, 48·17
  - tee, 48·12
- ultrasonic immersion inspection of, 47·39
- ultrasonic inspection of circumferential, 49·9
- ultrasonic resonance testing of, 50·23
- ultrasonic testing of
  - double-transducer units in, 48·13, 49·1–2, 49·8, 49·20
  - for quality control, 43·49
  - shear waves in, 45·10
- underbead cracking in, detection of, 3·3
- undercutting in, radiography of, and distinction from slag lines, 25·13
- X-ray inspection of, 25·1–28

Wetting Ability, of liquid penetrants, requirements for, 7·18

Wetting Agents
- in developers for liquid-penetrant testing, 7·31
- in X-ray film washing to prevent spotting, 21·9

Wheatstone Bridges [See also "Bridges (electric circuit)"]
- history of, 54·13
- strain-gage, 54·16–19
  - balancing of, 54·21–22
  - desensitization (complete) of, 54·20–21
  - electric resistance of, at finite load resistances, 54·19
  - sensitivity of, increasing of, 54·18
  - temperature compensation of, 54·18
  - with unequal bridge arms, 54·18–19

Wheels, Abrasive or Grinding (See "Grinding Wheels")

Whiskey, inspection (fluoroscopic) of, 19·36

White Light (See "Light, Visual")

White Metal (See "Babbitt Metal")

Windows
- X-ray barrier, 19·13
- for X-ray tubes, beryllium *vs.* glass, 19·17

Wind Tunnels, periscope for use in, 11·23

Wings, aircraft, ultrasonic transducer for inspecting spars of, 44·9

Wire
- aluminum, eddy-current test of electrical conductivity in control of composition of, 42·14
- copper, eddy-current test of electrical conductivity in control of composition of, 42·12
- copper or Teflon, for strain-gage leads, 54·36

Wire (*Continued*)
- crack detection in, with Ziljstra eddy-current instrument, **40·19**
- decarburization (edge) of steel, effect on spread-band width in Magnatest Q eddy-current testing, **42·52**
- eddy-current measurement of dimensions of, suppression of undesired signals in, **40·40**
- eddy-current testing of, by ellipse methods, **40·28**
- eddy-current testing of iron, similarity law in, **37·11**
- incandescent, examination by reflecting objectives of optical systems, **10·9**
- isoelastic, endurance limit in strain gages, **54·26**
- lead sheaths on, ultrasonic gaging of thickness of, **50·19**
- Magnatest Q eddy-current sorting of steel, frequency effect on, **42·41**
- Magnatest Q eddy-current spread bands of alloy steel, effect of stress-relief annealing on, **42·50**
- molybdenum and tungsten, eddy-current testing of diameter of, **42·3**
  - eddy-current testing with Magnatest FW-200, **42·6–10**
- nickel, effect of tensile stress on hysteresis loop of, **42·28**
- statistical quality number in testing of, **41·19**
- steel, straightening by hammering, effect on Magnatest Q eddy-current sorting, **42·43**, **42·50**
- for strain gages, **54·5–6**, **54·8–9**
- strain gages of, effect of hydrostatic pressure on electric resistance of, **54·30**
  - heat dissipating ability and maximum electric current compared with foil gages, **54·31**
  - strain sensitivity of, effect of temperature on, **54·23**
- tungsten, eddy-current apparatus for testing, **40·2–3**
  - eddy-current test for splitting of, **40·6**
  - eddy-current testing with feed-through coils, **42·6**
  - wavy fiber texture from swedging of, **42·3**
- X-ray analysis of drawn, **17·20**

Wire-Crack Test Instrument, Foerster (See "FW-200" under "Magnatest Eddy-Current Instruments")

Wire Drawing, tools for, eddy-current indication of wear of, **42·3**

Wood
- cleaning for resin-type brittle coatings, **52·9**
- elasticity tension modulus of, **52·11**
- photoelastic-coating testing of, undercoating for, **53·15**
- radiography (low-voltage) of, **24·40**
- ultrasonic contact testing of, frequencies for, **48·1**

Working (See also "Mechanical Treatment")
- cold, nonrelevant magnetic-particle test indications from, **32·17**
- of metals, effect on ultrasonic shear-wave velocity, **45·7**

Working Distance, of reflecting objectives for visual inspection, **10·9**

Work Orders, in nondestructive-testing laboratories, **2·9**

Work Sheets (See "Data Sheets")

Wormholes, weld defect called, and its radiography, **25·3**

Wrist Pins, sorting by coercive-force tests, **34·7**

Wurtzite, X-ray patterns of, **17·11**

X

Xenon, absorption coefficients (mass) for γ and X rays and photon energies for, **18·37**

Xeroradiographs
- of defective casting, **22·2**
- development of, **22·13**
- interpretation of, **22·16**
- permanent, formation of, **22·1**
- photography of, **22·13**, **22·15**
- transfer to paper and fixation, **22·13**, **22·15**
- viewing of, and apparatus for, **22·13**

Xeroradiography, 22·1–16
- equipment and procedures, **22·4**
- intensifying screens in, **22·8**
- penetrameters in, **22·9**
- plates for
  - care and maintenance, **22·4**
  - cleaning of, **22·15**
  - defects in used, **22·16**
  - development of, and powders for, **22·13**
  - electrical characteristics of, **22·3**
  - exposure of charged, **22·7**
  - fatigue of, **22·5**
  - life of, **22·6**
  - powder image on, and re-use of, **22·2**
  - sensitizing of, and apparatus for, **22·6**
  - storage of charged, **22·6**
  - time constants of, **22·3**
- sensitivity in, **22·9**
- undercutting in, from scattered radiation, **22·10–12**
- voltage selection for, **22·9**
- X-ray detection in, **5·10**

X-Ray Beam Current, milliamperage-distance and -time relations in radiography, **20·12**

X-Ray Diffraction, 14·1, **17·1**
- applications and limitations of, **17·20–22**
- Avogadro number determination by, **13·2**
- crystallite-size determination by, **17·16**
- patterns, of α-aluminum oxide, **17·8**
  - of amorphous materials, **17·16**
  - apparatus for recording of, **17·7–8**
  - of barium titanate single crystallites, **17·18**
  - catalog for, **17·11**
  - of copper-nickel solid solution and mixture, **17·12**
  - crystallite-size effect on, **17·14**
  - of devitrification in silica glass, **17·18**
  - of Ferroxdure (barium magnetoplumbite), **17·19**
  - of silicon powder, **17·14**
- principles of, **17·6**
- in radiography, mottling from, and its control, **20·24**

X-Ray Diffraction Analysis, 17·1–22
- of alloys (binary and ternary), **17·14**
- amorphous constituents in, **17·21**
- comparison with X-ray fluorescence spectroscopy, **17·27**
- concentration effect in, **17·21–22**
- counter tubes for, **17·10**
- in determination of chemical reactions, **17·14**
  - of single-crystal orientation, **17·21**
- of dusts (industrial), **17·20**
- of electrodeposited metals, **17·19**
- of fibers, **17·20**
- limitations of, **17·21**
- of oriented materials, **17·18**, **17·21**
- pattern changes in, **17·12**
- phase changes in, **17·13**
- in phase-diagram determination, **17·13**

- **X-Ray Diffraction Analysis** (*Continued*)
  - of polymorphic substances, **17·11**
  - reference standards in, **17·21**
  - of rolled sheets, **17·20**
  - of solid solutions, **17·13–14**
  - statistical errors in, **17·21**
  - of strained materials, **17·18**
  - of transuranic elements, **17·20**
  - of wire, **17·20**
- **X-Ray Film** (See also "Photographic Film"), **20·29–41, 23·7**
  - characteristic curves of, **20·33**
  - classification of, **20·29**
  - contrast in, **20·17, 20·34–35**
  - density in relation to, **20·35**
  - density measurement of, **24·35**
  - density of images in, **21·19**
  - development of
    - agitation in, **21·5**
    - causes and corrections for over- and under-, **21·18–19**
    - degree of, effect on density-exposure curves, **16·20**
    - exposure time in, **21·4**
    - and its arresting, **21·2–6**
    - tanks for, **21·15–16**
    - temperature control in, **21·4**
  - drying apparatus for, **21·9, 21·16**
  - emulsions for, **16·18, 20·29**
  - exposure of, **20·1–2**
    - allowable, to safelights, **21·16**
  - film gradient *vs.* density of, **19·7**
  - fixation of, **21·7**
  - fogging of, prevention of, **21·4**
  - graininess of, **21·20**
  - handling of, **20·38**
  - holders for, **23·8**
    - lead-backed, **20·21**
    - for low voltages, **24·40**
  - and its processing, **16·18–23**
  - latent image on, **16·18**
  - for microradiography, processing and selection of, **20·43**
  - processing of, **21·1–22, 23·14**
    - apparatus and rooms for, **21·10–17**
    - containers for, **21·2**
    - illumination for, **21·16–17**
    - mobile equipment for, **25·23**
  - processing of archival, **21·9**
  - securing good contact with specimens, **20·43**
  - storage of, **20·39**
- **X-Ray-Film Developers,** activity decrease and replenishment, **21·6**
- **X-Ray Fluorescence Spectroscopy, 17·1, 17·22–27**
  - apparatus for, **17·25**
  - applications of, **17·27**
  - comparison of, with optical-emission spectroscopy, **17·26**
    - with X-ray diffraction analysis, **17·27**
  - development of, **17·22**
  - effect of crystal analyzer in, **17·25–26**
  - long and short wavelengths in, limitations of, **17·26**
  - principles of, **17·23, 17·25**
  - for trace-element analysis, **17·26**
- **X-Ray Generators, 18·8**
  - center-tap, grounded-tank type, **14·22**
  - circuit for rectified, **14·5–6**
  - components of, **14·2**
  - controls for, **14·2, 14·39, 14·44**
    - functions of, **14·6**
  - design limitations of, **14·39**
- **X-Ray Generators** (*Continued*)
  - development of, **14·12–36**
  - dosage output of, **26·7**
  - duty cycle in, **14·47**
  - electric circuits of, **14·20–21**
  - electrostatic-belt type, **14·16**
  - grounded-anode tank-type, **14·22**
  - grounded-cathode tank-type, **14·21**
  - high-voltage, **14·2, 14·12, 14·16, 23·5**
  - high-voltage transformers in, **14·4**
  - insulation for, halogenated hydrocarbons as, **14·14**
  - lead protective lining for, **14·38**
  - leakage radiation from, measurement of, **14·38**
  - linear-accelerator type, **14·17–18**
  - low-voltage, **14·12**
  - medium-voltage, **14·12**
  - million-volt, **14·12**
  - nondestructive-testing requirements for, **14·7**
  - operation of, **26·7**
    - safety in, **14·38**
  - performance requirements for, **14·41**
  - pulse-type, high-current, high-intensity, **14·20**
  - rectification systems in, **14·5**
  - resonance-transformer type, **14·13**
  - scattering (overhead) from, **26·14**
  - selection for radiography, **14·40**
  - with separated elements, **14·41**
  - synchrotron-type, **14·19**
  - tank type, **14·20, 14·36, 14·40, 14·44–45**
    - cooling and insulation of, **14·38**
    - geometry of beam of, **14·47**
    - heat dissipation in, **14·45**
    - insulation for, **14·37**
    - maximum voltage in, **14·45**
  - for thickness measurement, **18·2**
  - transformers for, **14·37**
  - tube housings in, **14·3**
  - two hundred fifty kv.p., **2·7**
  - two-million-volt, **14·16**
    - electrostatic-belt, **14·17**
- **X-Ray Powder Diffraction** (See "X-Ray Diffraction")
- **X Rays** (See also "Radiography")
  - absorption and scattering of, **19·19, 23·1**
    - by aluminum, **19·19**
  - absorption edge and critical excitation potential of elements for, **17·23**
  - absorption of, **18·4**
    - in air above xeroradiographic plates, undercutting from, **22·12**
    - by alloys and metals, equivalence factors for, **20·14**
    - critical wavelengths of, **13·11**
    - in fluoroscopy and half-value layers for, **19·15**
    - by glass and liquid barrier substances, **19·14, 19·15**
    - by pair production, **23·1**
    - by phosphors, mechanism of, **16·10–13**
    - in radiography, curves of, **15·25**
    - by specimens, **20·14**
  - absorption (mass) coefficients for, **18·31–40, 27·1–41**
  - alignment of central ray of, in thickness measurement, **24·36**
  - attenuation coefficients of elements for, **27·1–41**
  - barrier cells (liquid) for, **19·14**
  - barrier windows for, **19·13–15**
  - beams, geometry of, **14·47**
  - cadmium selenide and sulfide response to, **16·11**

X Rays (*Continued*)
- continuous
  - from charged particles, 13·24
  - energy loss due to production of, 13·29
  - energy loss of electrons from production of, 13·27
  - in lead, energy distribution of radiation emitted by electrons because of, 13·28
  - from radioactive disintegration, 15·3
  - sources for thickness gaging, 18·18
- from Thulium-170, 15·20
- detection of high-level, photoconductors in, 16·13
- detectors for, 5·10, 16·8
- dimensional measurement with, 24·35
- discovery of, 13·8
- dosage output by various sources of, 26·6
- effect on radiographic-film density, 16·22
- emission in electron capture by nuclei, 15·3
  - in internal conversion, 15·3
- energy transformation to, 13·9
- exposure to, in xeroradiography, 22·1
- film (See "X-Ray Film")
- filters for producing monochromatic, 13·10
- fluorescence, in spectroscopy, 17·23
- generation of, 13·9, 14·1, 14·27
  - heel effect in, 14·29
- generators for (See "X-Ray Generators")
- high-voltage, 23·1
- image devices using, and comparison with fluoroscopy, 19·1–49
- in industrial radiography, 20·1
- inspection with, image interpretation in, 24·1
  - requirements for, 19·45–46
  - sensitivity in, 19·1
  - using closed-circuit television, 19·39
- intensity and voltage of, fluorescent-screen brightness in relation to, 19·10
- intensity of, brightness in fluoroscopy in relation to, 19·15
  - effect of current and voltage on, 20·3–4
  - in radiography of steel, exposure, thickness, and voltage in relation to, 20·35
  - spatial distribution of, 23·1–3
- intensity of continuous, 15·4
- *K*-characteristic and *K*-fluorescence, for microradiography, 20·42
- monochromatic, in diffraction measurements, 17·5
  - production of, 13·9
- in nondestructive testing, 4·11
- penetrating power of, 14·6
- penetration by high-energy, 23·3
- photoconductors sensitive to, 22·1
- photocurrent modulation by pulsating, 16·13
- photographic-film protection against, in storage, 20·39–40
- photons in fluoroscopy, 19·26
- in pipeline radiography, equipment for, 25·21–25
- potential (kilovoltage) of, relation of effective to peak, 19·10–13
- projection magnification for definition improvement, 19·2
- properties of, 17·1
- scattering of, from crystalline substances, 17·3
  - from powdered samples, 17·5
  - in radiography, and its control, 20·17–25, 23·8
- screens (intensifying) for, 16·16
- shadow formation by, geometry of, 20·5–9
- sources of, 5·8

X Rays (*Continued*)
- spectrum of, 13·9, 17·1
  - continuous, 14·2
- steel penetration by, 16·13
- steel radiography with, exposure charts for, 23·10
- television in observation of, 11·37
- thickness gages using, 18·6
- thickness gaging with, 18·1–40
  - of coatings and walls, 24·35, 24·36
  - of different wave length, 18·11
  - system for, 18·8
- voltage maxima for steel of various thicknesses, 25·17
- wavelength of, for transmission thickness gages, 18·6
- in weld inspection, 25·1–28
- working distance for personnel subjected to, 26·6

X-Ray Spectrograph, principle of, 17·25

X-Ray Tube Kilovoltage, 19·46 (See also "Potential, Electric")
- in fluoroscopy, 19·15–16, 19·18

X-Ray Tubes
- anodes for, 14·27, 14·34
  - cooling system for, 14·33
  - hooded, to prevent random radiation, 14·34
  - rod-type, 14·41
  - rotating, 14·4, 14·30
- betatron-type, 14·11, 14·18
- cathodes for, 14·26, 14·35
- classification of, 14·3
- conditioning for, 14·35
- current control in, 18·8
- development of, 14·7
- dimensions of, 14·37
- direct pick-up, for closed-circuit television systems, 19·40–41
- electron-beam focusing, 14·9
- evacuation of, 14·35
- failures of, 14·36
- fine-focus, 14·32
- for flash or high-speed radiography, 20·46
- for fluoroscopy, 19·15–18
- focal spot of, 14·4, 14·29
  - measuring of, 14·32
  - reduction of, 14·37
- generation efficiency of, 14·3
- glass (borosilicate) for, 14·34
- heat dissipation in, 14·3
- hot-cathode, high-vacuum, 14·7–10
- housings for, 14·5, 14·23
- life of, 14·35
- line-focus, 14·30
- load limit of, 14·33
- manufacturing of, 14·34–35
- medium-voltage, 14·26–27
- for microradiography, 20·42
- multi-section high-vacuum, 14·9
  - linear-acceleration type, 14·10
- output of, 14·28
  - brightness compared with, in fluoroscopy, 19·17
- radiation emitted by, 20·3–5
- rating and life of, 14·35
- self-protected, 14·33
- self-rectified, current and voltage wave forms of, 14·23
- separately mounted, 14·25
- screen effect of, 14·29
- target materials in, 14·3
- targets (inclined) in, 14·4
- toroidal electromagnetic-type, 14·11

X-Ray Tubes (*Continued*)
  voltage, 19·46
    control in linearizing of thickness-gage output signals, 18·9
    current characteristics of, 14·28
    in fluoroscopy, 19·15–16, 19·18
    limits of, 14·33

Y

Yielding, of structures in strain-gage tests, recommendations concerning, 54·38
Yield Strength, of strain-gage-alloy wire, 54·9
Yokes
  for demagnetization, after magnetic-particle testing, 30·25
  electromagnetic hand-held, for magnetic-particle inspection, 31·2

Z

Zamak, electrical conductivity of, 42·16
Zero Readings, before strain-gage tests, 54·38–39
Zero Shift
  of foil strain gages, failure warning from large unaccounted-for, 54·26
  of strain gages
    effect of number of strain cycles on, 54·26
    prevention by temperature cycling, and effect of degree of cure of cement on, 54·24
  in strain-gage tests, choice of thermal expansion coefficient to minimize, 54·4–5
Ziljstra Eddy-Current Test Instrument, response characteristics of, 40·19
Zinc
  absorption coefficients (mass) for γ and X rays and photon energies of, 18·35, 27·21
  attenuation coefficients of, for γ and X rays, 27·21
  coatings on steel, determination of thickness of, 18·4
    radioisotope gaging of, 18·15
    X-ray fluorescence gaging of, 18·12
  effect on electrical conductivity
    of aluminum, 42·14
    of copper, 42·12
  electrical conductivity of, 42·16
  radiographic equivalence factors for, 20·14
Zinc Alloys, aluminum-magnesium, electrical conductivity *vs.* hardness of, 42·18
Zinc Cadmium Sulfide
  luminescence decay of screens of, 16·15
  spectrum (emission) of, 16·14
Zinc Iodide, X-ray barrier cells containing, 19·14, 19·15
Zinc Sulfide
  fluorescent screens, effective *vs.* peak kilovoltages of, 19·11
  spectrum (emission) of, 16·14
  in X-ray-intensifying screens, 16·17
Zirconium
  attenuation coefficients of, for γ and X rays, 27·24
  constant K value in ultrasonic resonance tests, 50·3
Zuschlag, for crack testing by eddy-current methods, 41·11

LIST OF SECTIONS

Alphabetical

	SECTION
Attenuation Coefficient Tables	27
Basic Test Methods	5
Brittle-Coating Tests	52
Double-Transducer Ultrasonic Tests	49
Eddy Current Cylinder Tests	37
Eddy Current Sphere and Sheet Tests	39
Eddy Current Test Automation	41
Eddy Current Test Equipment	40
Eddy Current Test Indications	42
Eddy Current Test Principles	36
Eddy Current Tube Tests	38
Electric Current Test Principles	35
Electrified-Particle Test Indications	29
Electrified-Particle Tests	28
Electronic Radiation Sources	14
Field and Maintenance Tests	3
Film Radiography	20
Filtered-Particle Tests	9
Fluoroscopy and X-Ray Image Devices	19
Fundamental Testing Principles	4
High Voltage Radiography	23
Isotope-Radiation Sources	15
Liquid-Penetrant Test Equipment	7
Liquid-Penetrant Test Indications	8
Liquid-Penetrant Test Principles	6
Magnetic-Field Test Equipment	34
Magnetic-Field Test Principles	33

NUMERICAL LIST APPEARS INSIDE FRONT COVER

LIST SECTIONS

betical

SECTION

Magnetic-Particle Test ent 31
Magnetic-Particle Test ions 32
Magnetic-Particle Test ples 30
Management and Appli of Tests 1
Natural Frequency Vibr ests 51
Nondestructive Testing ratories 2
Optical Projectors and ators 12
Photoelastic-Coating Te 53
Radiation and Particle 13
Radiation Detection and ding 16
Radiation Protection 26
Resistance Strain-Gage 54
Ultrasonic Contact Test 48
Ultrasonic Fields 45
Ultrasonic Immersion T ications 47
Ultrasonic Immersion T 46
Ultrasonic Resonance T 50
Ultrasonic Test Princip 43
Ultrasonic Transducers 44
Vision and Optics 10
Visual Inspection Equi 11
Xeroradiography 22
X-Ray and Isotope Ga 18
X-Ray Control of Weld 25
X-Ray Diffraction and scence 17
X-Ray Film Processin 21
X-Ray Interpretation 24

(Sections 1–27 appear i ; Sections 28–54 and Index appear
ol. II.)

UNIVERSAL LIBRARY

102 863

UNIVERSAL LIBRARY